Enantioselective Transformations of α- and β-Amino C–H Bonds Promoted by Cooperative Actions of Achiral and Chiral Lewis Acid Catalysts

Yejin Chang

A dissertation

submitted to the Faculty of

the department of Chemistry

in partial fulfillment

of the requirements for the degree of

Doctor of Philosophy

Boston College
Morrissey College of Arts and Sciences
Graduate School

June 2021

Enantioselective Transformations of α- and β-Amino C–H Bonds Promoted by Cooperative Actions of Achiral and Chiral Lewis Acid Catalysts

Yejin Chang

Advisor: Professor Masayuki Wasa, Ph.D.

Abstract

This dissertation describes the development of cooperative catalyst systems for the regio- and enantio-selective α- and β-amino C–H functionalization of *N*-alkylamines, inspired by the concepts of frustrated Lewis pairs (FLPs). Prior to this dissertation research, the development of effective and broadly applicable catalytic protocol to transform amino C–H bonds with high enantioselectivity remained as a formidable problem. In Chapter 1, the recent advances in the field of amino C–H functionalization through hydride transfer process that served as intellectual foundations for this dissertation research is presented. As highlighted in the first chapter, key challenges of amino C–H functionalization are: (1) unreactive nature of α, β- and/or γ-amino C–H bonds, (2) requirement for the use of precious metal-based catalysts and external oxidants under acidic/basic and harsh conditions, (3) use of directing groups for regioselectivity, and (4) poor functional group tolerance. Inspired by the unique capability of FLPs to activate otherwise unreactive molecules while disfavoring undesirable acid–base complexation, we have developed a protocol for enantioselective α-amino C–H functionalization of *N*-alkylamines, where chiral and achiral Lewis acid catalysts work cooperatively (Chapter 2). The application of the cooperative catalyst system comprising of $B(C_6F_5)_3$, a chiral Lewis acid, and a Brønsted base to the enantioselective β-amino C–H functionalization is described in Chapter 3.

Acknowledgements

First and foremost, I want to thank my advisor Professor Masayuki Wasa, for giving me an opportunity to join his group and participate in many exciting research projects that are presented in this dissertation. I would not be where I am today without his generous guidance and mentorship over the last five years. I have grown so much in all respects from the day I first stepped into Merkert Chemistry Center, and I deeply appreciate Professor Wasa for transforming me into an independent scientist. He was always open for discussion, and his infectious excitement and enthusiasm for chemistry encouraged me to move forward even in tough times. I am grateful for his patience and help as well as all the lessons I learned from him.

I would like to thank Professor Amir H. Hoveyda for his support and encouragement throughout my Ph.D. studies. Even though I was not in his research group, I was very fortunate to be able to join his group meetings and learn closely from him and his group members. He was always willing to share with us his insights and suggestions, which gave us an opportunity to further develop and polish our chemistry. One thing I will never forget is a piece of advice he gave me after my second year oral examination that has helped me during difficult times.

I am grateful to Professors Amir H. Hoveyda and James P. Morken for serving on my dissertation committee. I also want to thank Professor James P. Morken for his words of encouragement and thoughtful advice while I was exploring my options for the next step. I would like to express my gratitude to Professor Shih-Yuan Liu, for spending time with me to discuss mechanistic investigations. I learned so much from our Zoom meetings as well as countless emails that were filled with his thought-provoking questions.

I want to take this time to thank all the past and present Wasa group members for making my time in graduate school unforgettable. Dr. Jessica Chan, Dr. Min Cao, Ahmet Yesilcimen,

Yuyang Zhang, Bochao Zhang, Tanner Myers, Cunyuan Zhao, and Yuankai Wang are acknowledged for their collaboration on the research projects. I am grateful to Jessica, who has been a mentor, a friend, and a family. I was fortunate to have her next to my desk and my fume hood every day, both happy times and tough times. I want to thank Min for always being calm and helping me stay sane. As a classmate, we went through the major steps together during Ph.D. studies, and I was very lucky to have had Min by my side. Conversations with Ahmet were always enjoyable, whether it be chemistry-related or not. I would not have completed this journey if it were not for Jessica, Min, and Ahmet who were always there for me on rough days.

I want to thank all my friends who I met at Boston College. I would like to especially thank Dr. Katherine Grasso, Paul Hicks, Julia Falco and Dr. Yang Li for their support and friendship. We were able to spend time together and make lots of unforgettable memories over the five years. I am so proud of us all for what we have gone through and accomplished.

I would like to thank my fiancé, Allen, for his endless love and support. Every time I broke down, he pieced me back together and encouraged me to move forward. Thank you, Allen, and I cannot wait to begin our own journey together in Ithaca.

I want to express my appreciation to my family and close friends back in Korea, for their unconditional love and encouragement throughout this difficult process. My parents always reminded me that I am much stronger than what I think. Mom and Dad, thank you for believing in me. The paths I have taken are all because I aspire to be like you.

Lastly, I would like to dedicate this dissertation to my grandfather, who would be watching me from above with love. I hope I made him proud.

TABLE OF CONTENTS

Chapter One. Recent Advances in C–H Functionalization of *N*-Alkylamines **1**

1.1 Enzyme-Mediated Hydride Abstraction of Amines 5

1.2 Lewis Acid-Mediated Hydride Abstraction of Amines 7

1.2.1 Carbocation-Mediated Hydride Abstraction from *N*-Alkylamines 7

1.2.2 Organoborane-Mediated Hydride Abstraction from *N*-Alkylamines. 8

1.3 $(F_5C_6)_3B$-Catalyzed Transfer Hydrogenation/Dehydrogenation of Amines 11

1.4 $(F_5C_6)_3B$-Catalyzed α-Amino C–H Functionalization 13

1.5 $(F_5C_6)_3B$-Catalyzed β-Amino C–H Functionalization 16

1.5.1 C–Si Bond Formation 16

1.5.2 C–C Bond and C=C Bond Formation 18

1.6 $(F_5C_6)_3B$-Catalyzed C–N Bond Cleavage 20

1.7 Specific Aims of the Dissertation Research 23

Chapter Two. Enantioselective α-Amino C–H Functionalization through Cooperative Action of Chiral and Achiral Lewis Acid Catalysts **29**

2.1 Introduction 29

2.2 Background 31

2.3 Our Approach 34

2.4 $(F_5C_6)_3B$-Catalyzed α-Alkylation of *N*-Alkylamines Using Silicon Enolates 36

2.5 Union of *N*-Alkylamines and α,β-Unsaturated Compounds Through Cooperative Action of Chiral and Achiral Lewis Acid Catalysts 43

2.6 Conclusions and Future Outlook 55

Chapter Three. *β*-C–H Functionalization of *N*-Alkylamines through Cooperative Action of Lewis Acid and Brønsted Base Catalysts **57**

3.1 Introduction 57

3.2 Catalytic Deuterium Incorporation within Metabolically Stable *β*-Amino C–H Bonds of Drug Molecules 59

3.2.1 Background 62

3.2.2 Our Approach 65

3.2.3 Results and Discussion 66

3.2.4 Conclustions and Future Outlook. 76

3.3 Enantioselective *β*-Amino C–H Functionalization through Cooperative Action of Chiral and Achiral Lewis Acid Catalysts 77

3.3.1 Background 77

3.3.2 Our Approach 81

3.3.3 Results and Discussion – Method Development 83

3.3.4 Results and Discussion – Mechanistic Investigations 94

3.3.5 Conclustions and Future Outlook. 102

Appendix A. Experimental for Chapter 2 ..... **106**

Appendix B. Experimental for Section 3.2 ..... **377**

Appendix C. Experimental for Section 3.3 ..... **480**

Chapter One

Recent Advances in C–H Functionalization of *N*-Alkylamines

N-Alkylamines are ubiquitous in natural products, pharmaceuticals, polymers, as well as catalysts and ligands used in organic synthesis.[1] In particular, amines possessing stereogenic centers at α, β, and/or γ-positions can be found in approximately 40% of pharmaceuticals and 20% of agrochemicals.[1] Therefore, the synthesis of chiral amines with high enantiomeric purity represents one of the most essential and widely studied topics in organic synthesis.[2-3] Previously established approaches for the preparation of *N*-alkylamines in enantio- and/or diastereomerically-enriched forms include the resolution of *rac*-amines,[4] hydroamination,[5-6] reduction of imines or enamines,[7] and nucleophilic addition to imines.[8] A complementary strategy for the synthesis of enantio-enriched *N*-alkylamines involves stereoselective transformations of α, β, and/or γ-amino C–H bonds that are contained in prochiral amine substrates (Scheme 1.1).[9] Recent advances in the arena of C–H functionalization established that various organometallic complexes

[1] (a) McGrath, N. A.; Brichacek, M.; Njardarson, J. T. *J. Chem. Educ*. **2010**, *87*, 1348−1349. (b) Ghislieri, D.; Turner, N. J. *Top Catal.* **2014**, *57*, 284–300. (c) Schrittwieser, J. H.; Velikogne, S.; Kroutil, W. *Adv. Synth. Catal.*, **2015**, *357*, 1655–1685.

[2] (a) Chiral Amine Synthesis: Methods, Developments and Applications; Nugent, T. C., Ed.; Wiley-VCH Verlag GmbH & Co. KGaA: Weinheim, 2010, p 15–457. (b) Vardanyan, R. in Piperidine-Based Drug Discovery; Vardanyan, R., Ed.; Elsevier: 2017, p 147.

[3] (a) Campos, K. R.; Coleman, P. J.; Alvarez, J. C.; Dreher, S. D.; Garbaccio, R. M.; Terrett, N. K.; Tillyer, R. D.; Truppo, M. D.; Parmee, E. R. *Science* **2019**, *363*, eaat0805. (b) Trowbridge, A.; Walton, S. M.; Gaunt, M. J. *Chem. Rev.* **2020**, *120*, 2613–2692. (c) Yin, Q.; Shi, Y.; Wang, J.; Zhang, X. *Chem. Soc. Rev.* **2020**, *49*, 6141−6153.

[4] Wosinska-Hrydczuk, M.; Skarzewski, J. *Molecules* **2020**, *25*, 4907–4941.

[5] Huang, L.; Arndt, M.; Gooßen, K.; Heydt, H.; Gooßen, L. J. *Chem. Rev.* **2015**, *115*, 2596–2697.

[6] (a) Zhu, S.; Buchwald, S. L. *J. Am. Chem. Soc.* **2014**, *136*, 15913−15916. (b) Yang, Y.; Shi, S.-L.; Niu, D.; Liu, P.; Buchwald, S. L. *Science* **2015**, *349*, 62–66. (c) Roos, C. B.; Demaerel, J.; Graff, D. E.; Knowles, R. R. *J. Am. Chem. Soc.* **2020**, *142*, 5974–5979.

[7] Barrios-Rivera, J.; Xu, Y.; Wills, M.; Vyas, V. K. *Org. Chem. Front.* **2020**, *7*, 3312−3342.

[8] (a) Kobayashi, S.; Ishitani, H. *Chem. Rev.* **1999**, *99*, 1069−1094. (b) Kobayashi, S.; Mori, Y.; Fossey, J. S.; Salter, M. M. *Chem. Rev.* **2011**, *111*, 2626–2704.

[9] Cernak, T.; Dykstra, K. D.; Tyagarajan, S.; Vachal, P.; Krska, S. W. *Chem. Soc. Rev.*, **2016**, *45*, 546–576.

(e.g., Rh-, Pd-, Ir-, Pt-based complexes)[3b] promote efficient conversion of C(sp^3)–H bonds contained in a variety of *N*-alkylamines into C(sp^3)–C and C(sp^3)–heteroatom bonds.[10] Moreover, the use of chiral organometallic complexes allow for enantioselective synthesis of *N*-alkylamines from the prochiral substrates (Scheme 1.1A and 1.1B).[11] Highly attractive but less explored processes are those that enable enantioselective late-stage functionalization of bioactive amines (e.g., Scheme 1.1C).[3a]

Scheme 1.1. Regio- and Enantio-selective Functionalization of Amino C–H Bonds

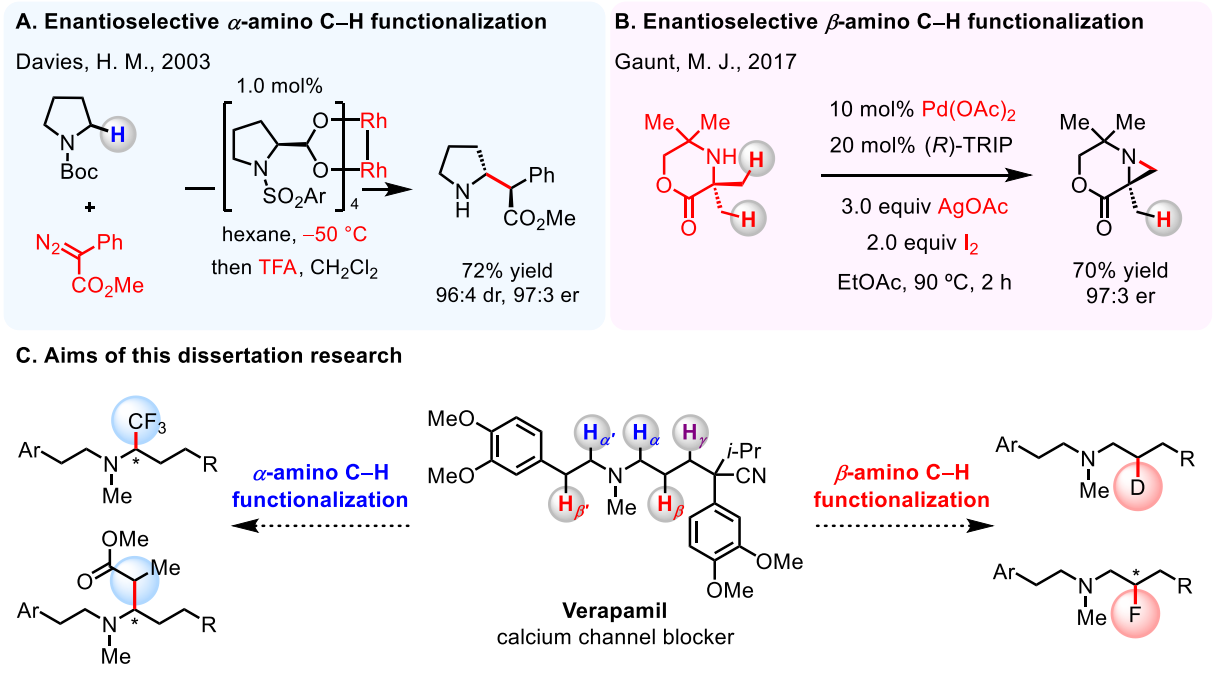

Despite the significant potentials of the stereoselective amino C–H functionalization strategy, there exist fundamental hurdles that need to be overcome in order for such methods to find practical applications. The challenges associated with the state-of-the-art include the following:

[10] Hong, B.; Luo, T.; Lei, X. *ACS Cent. Sci.*, **2020**, *6*, 622–635.
[11] (a) Davies, H. M.; Venkataramani, C.; Hansen, T.; Hopper, D. W. *J. Am. Chem. Soc.* **2003**, *125*, 6462–6468. (b) Smalley, A. P.; Cuthbertson, J. D.; Gaunt, M, J. *J. Am. Chem. Soc*. **2017**, *139*, 1412–1415.

1) α, β, and/or γ-amino C–H bonds are inherently unreactive; they have high bond dissociation energy (87–96 kcal/mol) and low acidity (pK_a = 45–60).[12-13]

2) For the cleavage of the poorly reactive amino C–H bonds, many methods rely on the use of highly reactive and precious metal-based catalysts, external oxidants to turn over the catalysts, and are performed under acidic/basic conditions under elevated temperatures (e.g., Scheme 1.1A and 1.1B).[11, 12c]

3) C–H Bonds are ubiquitous in bioactive amines; thus, the activation and functionalization of a specific C–H bond is a formidable problem. To achieve such regioselectivity, the preexisting methods can only be applied to substrates that possess appropriate functional groups that can serve as directing groups (e.g., Scheme 1.1B), or demand installation and removal of directing groups.[3b] Consequently, many of the amino C–H functionalization processes reported to date have poor functional group tolerance; the late-stage modification of bioactive compounds that possess various Lewis acid- and/or Lewis base-sensitive functional groups are not within the purview of the present state-of-the-art.[3,11]

The key aim of this dissertation research is to develop a powerful catalyst system which promotes regio- and stereo-selective transformations of α- and/or β-amino C–H bonds contained in various *N*-alkylamines (e.g., Scheme 1.1C). Furthermore, our goal is to devise methods that take place under mild and redox neutral conditions, while circumventing the use of precious metal-based catalysts and installation/removal of directing groups. Through the innovation of such novel catalysts, we aspire to address the critical unsolved problems listed above and achieve the late-

[12] (a) Lyons, T. W.; Sanford, M. S. *Chem. Rev*. **2010**, *110*, 1147-1169. (b) Baudoin, O. *Chem. Soc. Rev*. **2011**, *40*, 4902-4911. (c) Ohno, S.; Miyoshi, M.; Murai, K.; Arisawa, M. *Synthesis*, **2021**, doi:10.1055/a-1483-4575.

[13] (a) Wayner, D. D. M.; Clark, K. B.; Rauk, A.; Yu, D.; Armstrong, D. A. *J. Am. Chem. Soc.* **1997**, *119*, 8925–8932. (b) Lalevee, J.; Allonas, X.; Fouassier, J.-P. *J. Am. Chem. Soc.* **2002**, *124*, 9613–9621.

stage derivatization of bioactive amines and other industrially important *N*-alkylamines that contain an array of Lewis acid- and/or base-sensitive functional groups. Thus, an array of enantio- and diastereo-merically-pure amines that find applications in drug discovery, agrochemicals and materials chemistry, and are difficult to access through conventional synthetic methods, can be readily prepared.[14]

Below, a summary on the selected state-of-the-art methods in α- and β-amino C–H functionalization reactions that served as intellectual foundations of this dissertation research is provided. This chapter is focused on describing transformations of amino C–H bonds that proceed through intra- or inter-molecular hydride transfer process. Representative examples to be discussed in this chapter are as listed below:

1.1. Enzyme-Mediated Hydride Abstraction of Amines

1.2. Lewis Acid-Mediated Hydride Abstraction of Amines

Carbocation-Mediated Hydride Abstraction from *N*-Alkylamines

Organoborane-Mediated Hydride Abstraction from *N*-Alkylamines

1.3. $(F_5C_6)_3B$-Catalyzed Transfer Hydrogenation/Dehydrogenation of Amines

1.4. $(F_5C_6)_3B$-Catalyzed α-Amino C–H Functionalization

1.5. $(F_5C_6)_3B$-Catalyzed β-Amino C–H Functionalization

C–Si Bond Formation

C–C and C=C Bond Formation

1.6. $(F_5C_6)_3B$-Catalyzed C–N Bond Cleavage

[14] Börgel, J.; Ritter, T. *Chem* **2020**, *6*, 1877–1887.

1.1. Enzyme-Mediated Hydride Abstraction of Amines

An effective catalytic method to convert an *N*-alkylamine into an iminium ion through hydride abstraction can be found in enzymatic processes (e.g., Scheme 1.2).[15-16] Monoamine oxidases (MAOs) are flavoenzymes that are known to transform biogenic amines such as dopamine (**1.1**), adrenaline or serotonin into their corresponding imines (**1.2**).[15-16] The oxidation of an amine is proposed to proceed through hydride abstraction from **1.1** by the flavin's N5 atom which results in the formation of an iminium intermediate (**I→II**). Ensuing deprotonation of the iminium furnishes imine **1.2** (**II→III**) which then undergoes hydrolysis to afford aldehyde **1.3** and ammonia.

Scheme 1.2. Hydride Abstraction Mechanism for MAO-Catalyzed Oxidative Deamination

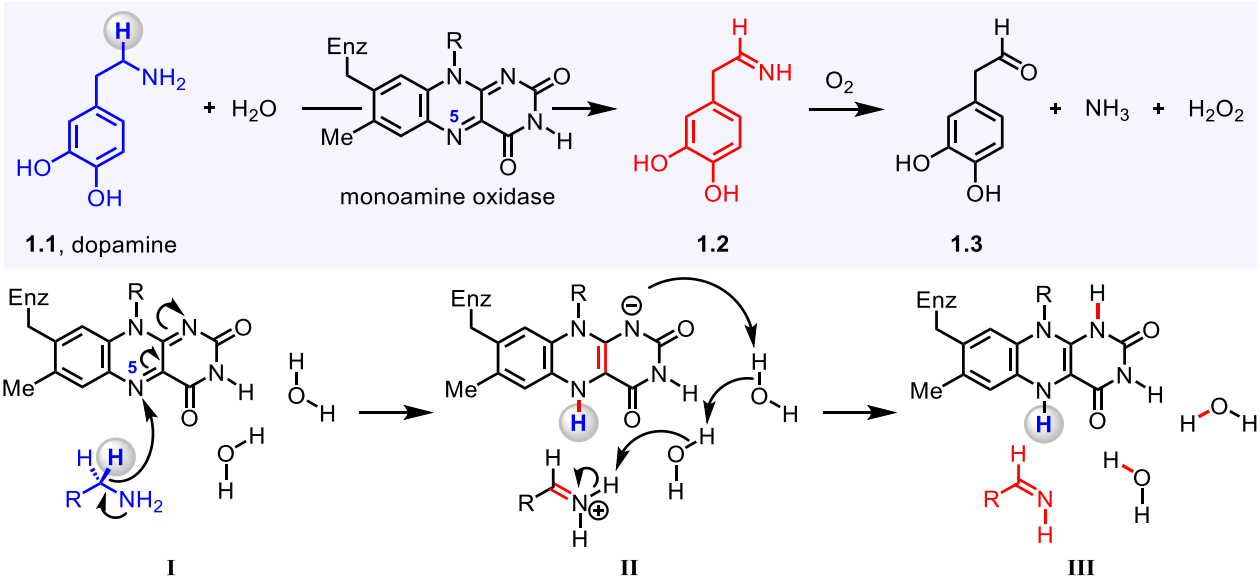

[15] (a) Fitzpatrick, P. F. *Archives of Biochemistry and Biophysics* **2010**, *493*, 13–25. (b) Vianello, R.; Repič, M.; Mavri, J. *Eur. J. Org. Chem*. **2012**, *36*, 7057–7065. (c) Maršavelski, A.; Vianello, R. *Chem. Eur. J.* **2017**, *23*, 2915–2925. (d) Maršavelski, A.; Petrović, D.; Bauer, P.; Vianello, R.; Kamerlin, S. C. L. *ACS Omega* **2018**, *3*, 3665–3674. (e) Tandarić, T.; Prah, A.; Stare, J.; Mavri, J.; Vianello, R. *Int. J. Mol. Sci*. **2020**, *21*, 6151–6163.

[16] (a) Segura-Aguilar, J.; Paris, I.; Munoz, P.; Ferrari, E.; Zecca, L.; Zucca, F. A. *J. Neurochem*, **2014**, *129*, 898–915. (b) Masato, A.; Plotegher, N.; Boassa, D.; Bubacco, L. *Molecular Neurodegeneration*, **2019**, doi:10.1186/s13024-019-0332-6.

Artificial methods to convert amines into iminium intermediates through hydride abstraction have also been investigated.[17] In the following sections, selected seminal reports on Lewis acid-mediated hydride abstraction of amines are described.

[17] (a) Ma, Y.; Lou, S.-J.; Hou, Z. *Chem. Soc. Rev.* **2021**, *50*, 1945−1967. (b) Basak, S.; Winfrey, L.; Kustiana, B. A.; Melen, R. L.; Morrill, L. C.; Pulis, A. P. *Chem. Soc. Rev.* **2021**, *50*, 3720−3737.

1.2. Lewis Acid-Mediated Hydride Abstraction of Amines

An array of *N*-alkylamines that contain electron-rich nitrogen centers and possess easily accessible α-C–H bonds are known to engage in Lewis acid-mediated hydride abstraction, generating an iminium cation.[18] Below are representative examples.

1.2.1. Carbocation-Mediated Hydride Abstraction from *N*-Alkylamines

In 1966, Damico and Broaddus reported that hydride abstraction occurs when tertiary amines are treated with a trityl cation (Scheme 1.3).[19] Specifically, the reaction of tribenzylamine (**1.4**) and tritylium tetrafluoroborate (**1.5**) gave an iminium salt **1.6** and triphenylmethane (**1.7**). However, further transformation of the iminium ion was not demonstrated in this report.

Scheme 1.3. Tritylium-Mediated Hydride Abstraction from Tertiary Amines

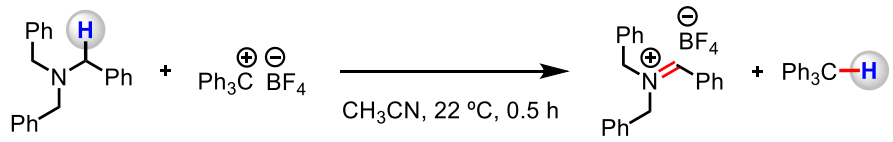

1.4, 16 mmol **1.5**, 1.0 equiv. **1.6**, 94% yield **1.7**, 89% yield

Lambert and coworkers developed a method for transforming an α-amino C–H bond into a C–CN bond which was mediated by a tropylium ion, a 6π-electron aromatic carbocation. The tropylium ion is responsible for converting amine **1.8** into an iminium salt **IV** (Scheme 1.4).[20] The iminium generated in this manner could react with KCN (**IV**→**V**) to afford an aminonitrile product **1.10**. This work demonstrated that the *N*-alkylamine-derived iminium ion formed through carbocation-mediated hydride abstraction can deliver α-substituted amine products upon its reaction with nucleophilic species.

---

[18] Meerwein, H.; Hederich, J.; Morschel, H.; Wunderlich, K. *Justus Liebigs Ann. Chem*. **1960**, *635*, 1–21.
[19] Damico, R.; Broaddus, C. D. *J. Org. Chem*. **1966**, *31*, 1607–1612.
[20] Allen, J. M.; Lambert, T. H. *J. Am. Chem. Soc*. **2011**, *133*, 1260–1262.

Scheme 1.4. *a*-Cyanation of Amines through Tropylium Ion-Mediated Hydride Abstraction

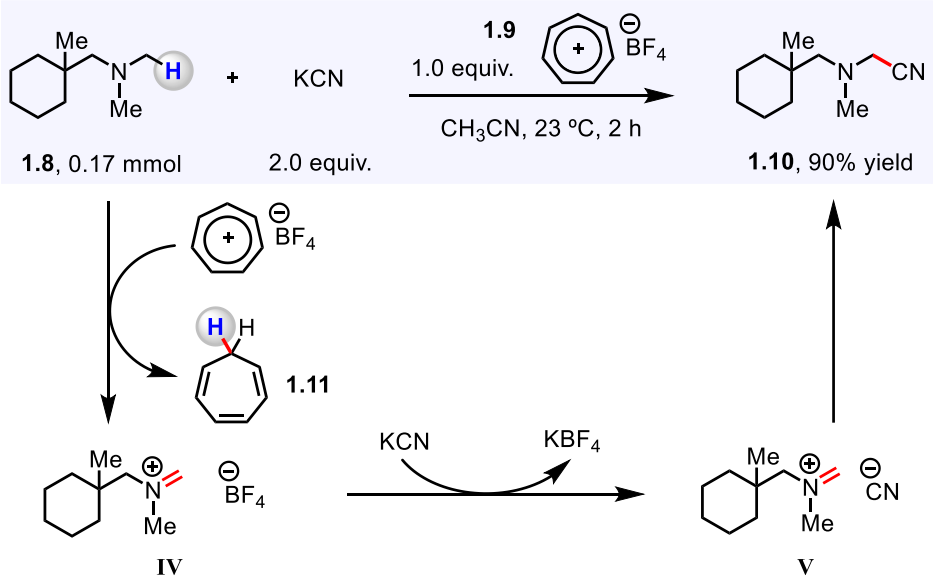

1.2.2. Organoborane-Mediated Hydride Abstraction from *N*-Alkylamines

In 2002, Santini and coworkers disclosed that when $B(C_6F_5)_3$ and *N,N*-dimethylaniline (**1.12**) were reacted in C_6D_6 at 22 ºC, an ion pair consisting of an iminium and a borohydride **1.13** can be generated (Scheme 1.5a).[21] Furthermore, the reaction of *N,N*-diethylaniline (**1.14**) and $B(C_6F_5)_3$ gave a zwitterionic species **1.15** together with an ionic complex of ammonium and borohydride **1.16** (Scheme 1.5b). In the latter process, iminium ion **VI** is generated upon $(F_5C_6)_3B$-mediated hydride abstraction of aniline **1.14**. Subsequently, deprotonation of iminium (**VI**) by another molecule of **1.14** affords an enamine intermediate (**VII**), which then reacts with $B(C_6F_5)_3$ to provide the zwitterionic product **1.15**. This seminal work elucidated that sterically encumbered and strongly Lewis acidic $B(C_6F_5)_3$ can promote hydride abstraction from *N*-alkylaniline derivatives, and also that the in situ-generated iminium ion can be deprotonated to afford enamines.

[21] Millot, N.; Santini, C. C.; Fenet, B.; Basset, J. M. *Eur. J. Inorg. Chem*. **2002**, *2002*, 3328−3335.

Scheme 1.5. $(F_5C_6)_3B$-Mediated Hydride Abstraction from Amine

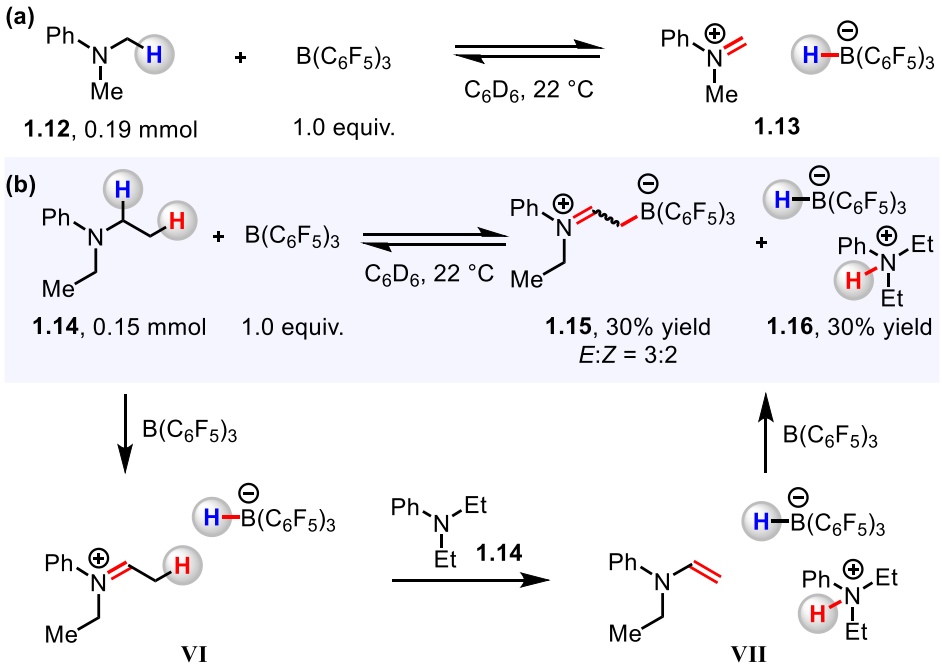

The group of Erker investigated intramolecular organoborane-mediated hydride abstraction, which occurs within a frustrated N/B Lewis pair **1.17** (Scheme 1.6).[22] The resulting zwitterionic intermediate **VIII** reacts with benzaldehyde to provide **1.18** containing iminium ion and boroalkoxide units. Thus, this work showed that the borohydride anion, which was generated in situ through hydride abstraction from an amine, could transfer the hydride to an appropriate electrophile.

Scheme 1.6. Hydride Abstraction within Intramolecular Frustrated N/B Lewis Pair

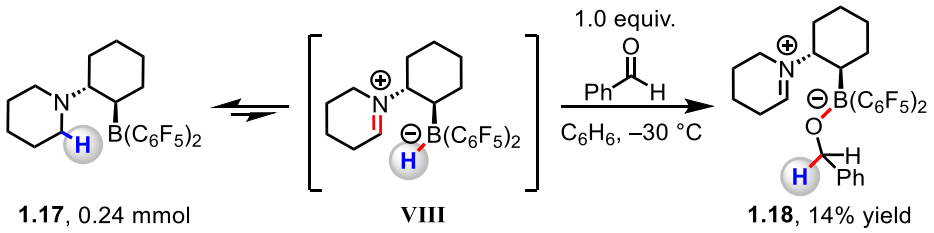

[22] Schwendemann, S.; Frohlich, R.; Kehr, G.; Erker, G. *Chem. Sci.* **2011**, *2*, 1842–1849.

In a subsequent work, Erker and coworkers achieved $(F_5C_6)_3B$-mediated Mannich-type reaction between *N,N*-dimethylaniline **1.19** and acetylenedicarboxylate **1.20** (Scheme 1.7).[23] This transformation is proposed to proceed through the reaction of **1.19** and 1.0 equivalent of $B(C_6F_5)_3$ to generate an iminium and a borohydride (**IX**). Ensuing borohydride reduction of **1.20** furnishes an allenoate (**X**), which undergoes C–C bond forming reaction with **1.19**-derived iminium ion to afford intermediate **XI**. Finally, a zwitterionic product **1.21** can be obtained upon isomerization of **XI**. Nonetheless, $(F_5C_6)_3B$-catalyzed variant of this process was not reported.

Scheme 1.7. $(F_5C_6)_3B$-Mediated Mannich-Type Reaction

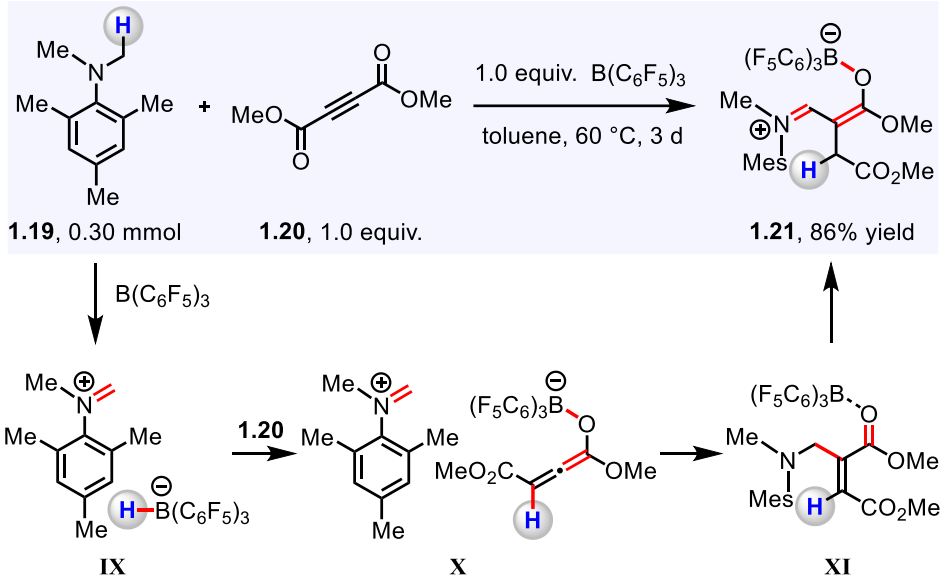

[23] Chen, G.-Q.; Kehr, G.; Daniliuc, C. G.; Bursch, M.; Grimme, S.; Erker, G. *Chem. Eur. J.* **2017**, *23*, 4723–4729.

1.3. $(F_5C_6)_3B$-Catalyzed Transfer Hydrogenation/Dehydrogenation of Amines

The ability of $B(C_6F_5)_3$ to abstract a hydride from *N*-alkylamines has found applications in catalytic processes involving transfer hydrogenation of imines as well as dehydrogenation of *N*-heterocycles.

The Stephan group demonstrated that $B(C_6F_5)_3$ can promote transfer hydrogenation of ketimine **1.22** using *i*-Pr_2NH as a source of hydride and proton (Scheme 1.8).[24] $(F_5C_6)_3B$-catalyzed hydride abstraction from *i*-Pr_2NH generates an ionic complex containing a borohydride and an iminium ion (**XII**). Deprotonation of the iminium by another equivalent of *i*-Pr_2NH affords an enamine and an ammonium ion (**XIII**). Imine **1.22** then undergoes sequential borohydride reduction and protonation by the ammonium ion to furnish sertraline **1.23**.

Scheme 1.8. $(F_5C_6)_3B$-Catalyzed Transfer Hydrogenation

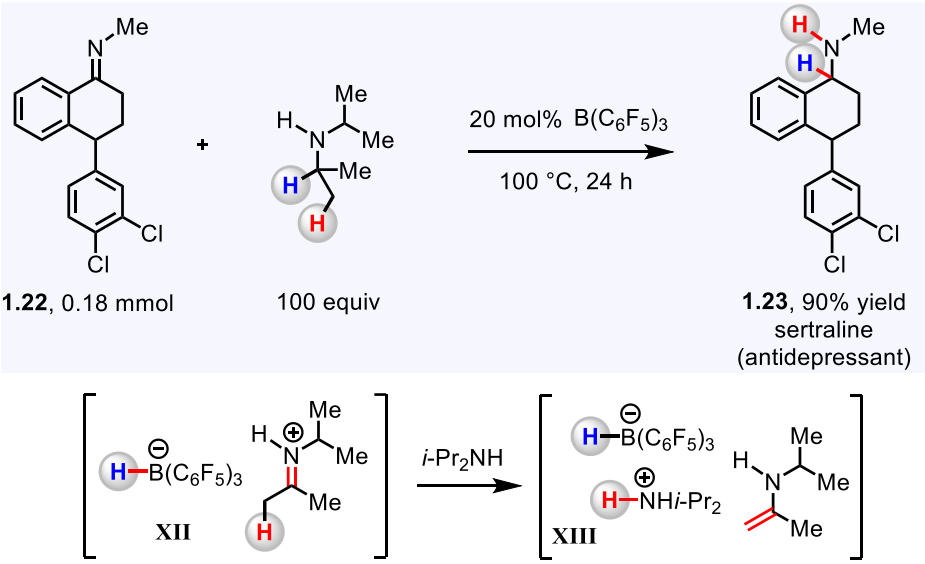

The group of Grimme and Paradies,[25] and that of Kanai[26] independently reported $(F_5C_6)_3B$-catalyzed dehydrogenation of *N*-heterocycles (Scheme 1.9); notably, these reactions can be

[24] Farrell, J. M.; Heiden, Z. M.; Stephan, D. W. *Organometallics* **2011**, *30*, 4497–4500.
[25] Maier, A. F. G.; Tussing, S.; Schneider, T.; Flörke, U.; Qu, Z.-W.; Grimme, S.; Paradies, J. *Angew. Chem., Int. Ed.* **2016**, *55*, 12219–12223.
[26] Kojima, M.; Kanai, M. *Angew. Chem., Int. Ed.* **2016**, *55*, 12224–12227.

performed in the absence of transition metal based-complexes and acceptors for H_2. The proposed mechanism involves $(F_5C_6)_3B$-catalyzed hydride abstraction of amine **1.24** to produce an ion pair of iminium and borohydride (**XIV**, Scheme 1.9a). Subsequent deprotonation of the iminium ion by a second molecule of Brønsted basic **1.24** affords indole **1.25**. The release of H_2 from an ionic complex of $[H–B(C_6F_5)_3]^-$ and protonated **1.24** regenerates $B(C_6F_5)_3$. In a related work, Kanai and co-workers reported $(F_5C_6)_3B$-catalyzed dehydrogenation of tetrahydroquinoline **1.26** for the synthesis of quinoline **1.27** (Scheme 1.9b). Despite these important advances in $(F_5C_6)_3B$-catalyzed hydride transfer processes, capturing of the iminium intermediate by nucleophilic entities to produce α-functionalized amines stood as an unsolved problem.

Scheme 1.9. $(F_5C_6)_3B$-Catalyzed Dehydrogenation of *N*-Heterocycle

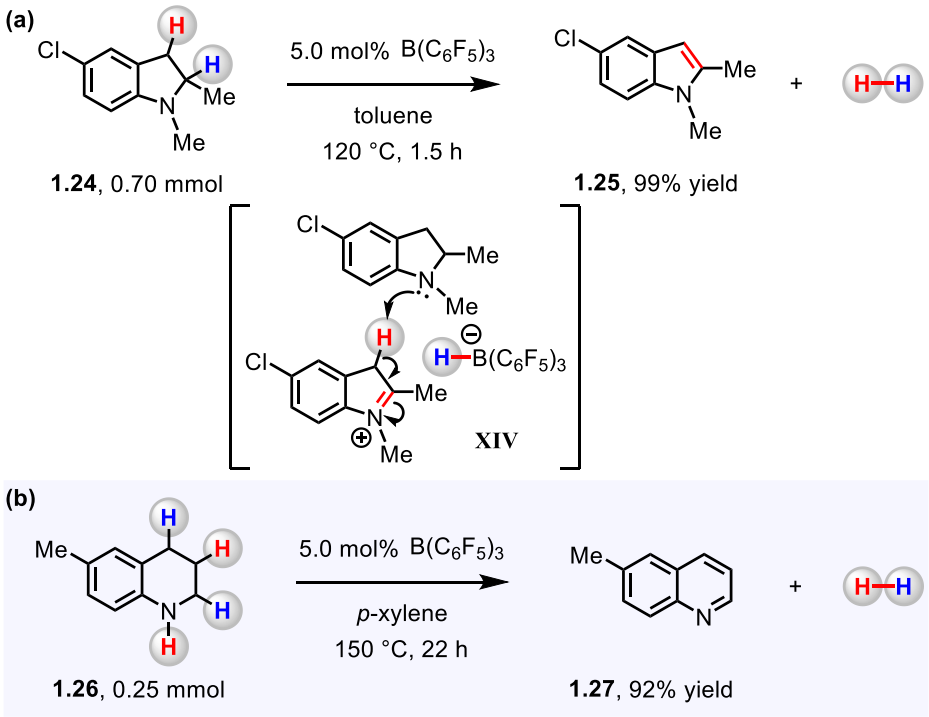

1.4. $(F_5C_6)_3B$-Catalyzed α-Amino C–H Functionalization

In this section, catalytic protocols for α-amino C–H functionalization via iminium promoted by $B(C_6F_5)_3$ will be discussed.

$(F_5C_6)_3B$-Catalyzed intramolecular transformations of alkene-substituted *N,N*-dialkylanilines through hydride abstraction were developed by the group of Grimme and Paradies,[27] and that of Wang,[28] independently (Scheme 1.10). After the $(F_5C_6)_3B$-mediated hydride abstraction from α-amino position of aniline **1.28**, the in situ generated iminium ion **XV** undergoes intramolecular C–C bond formation with the electron-rich alkene unit to afford a carbocation (**XVI**, Scheme 1.10a). Borohydride reduction of carbocation **XVI** provides ***rac*-1.29**.

Scheme 1.10. $(F_5C_6)_3B$-Catalyzed Intramolecular Reaction

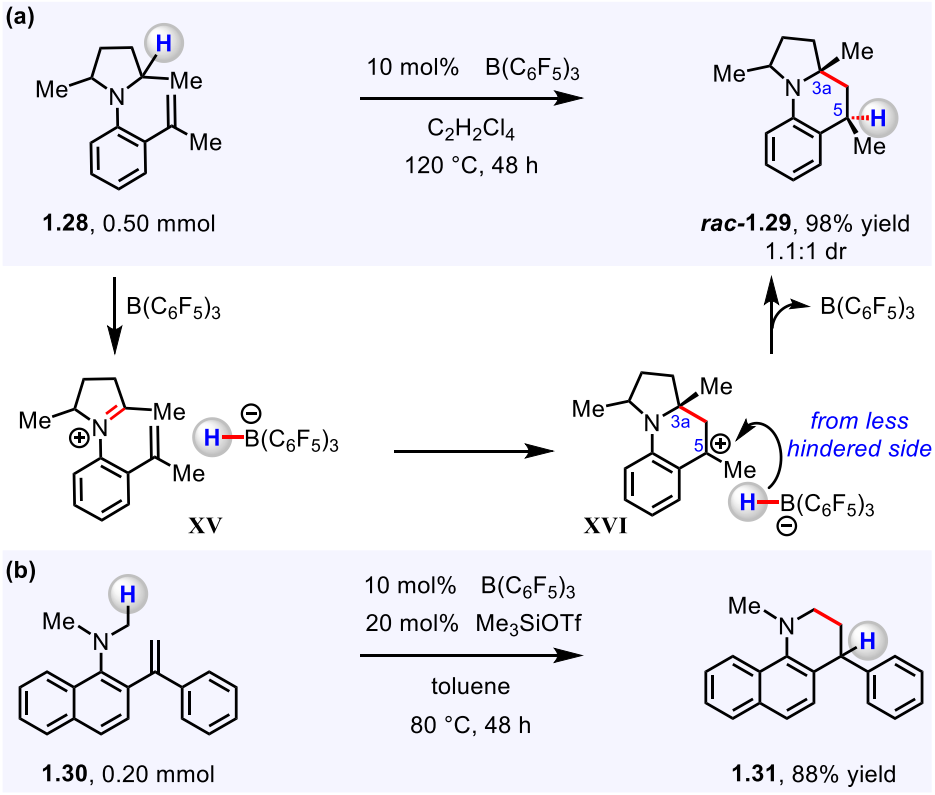

[27] Maier, A. F. G.; Tussing, S.; Zhu, H.; Wicker, G.; Tzvetkova, P.; Flörke, U.; Daniliuc, C. G.; Grimme, S.; Paradies, J. *Chem. Eur. J.* **2018**, *24*, 16287–16291.
[28] Tian, J. J.; Zeng, N. N.; Liu, N.; Tu, X. S.; Wang, X.-C. *ACS Catal*. **2019**, *9*, 295–300.

In Wang and co-workers' related study on intramolecular Mannich-type reaction for the synthesis of **1.31**, Me_3SiOTf was used as an additive to facilitate the turnover-limiting hydride transfer step (Scheme 1.10b).[28] It is proposed that hydride exchange between $[H–B(C_6F_5)_3]^-$ and Me_3SiOTf forms $[H–Si(OTf)Me_3]^-$, a better hydride donor, enhancing the reaction efficiency.

In 2021, the Wang group reported $(F_5C_6)_3B$-catalyzed intramolecular dehydrogenative cyclization of 2-cyclopropyl-*N,N*,-dimethylanilines (**1.32**, Scheme 1.11).[29] $B(C_6F_5)_3$ promotes cyclopropane ring opening to form **XVII**, which can be deprotonated by Barton's base to afford allylic borane (**XVIII**). $B(C_6F_5)_3$ can also abstract hydride from aniline unit, generating iminium-containing zwitterionic intermediate **XIX**, which undergoes cyclization to furnish the corresponding tetrahydroquinoline derivative **1.33**. Borohydride and protonated Barton's base (**XIX**) can release H_2 to regenerate the catalysts.

Scheme 1.11. $(F_5C_6)_3B$-Catalyzed Dehydrogenative Cyclization

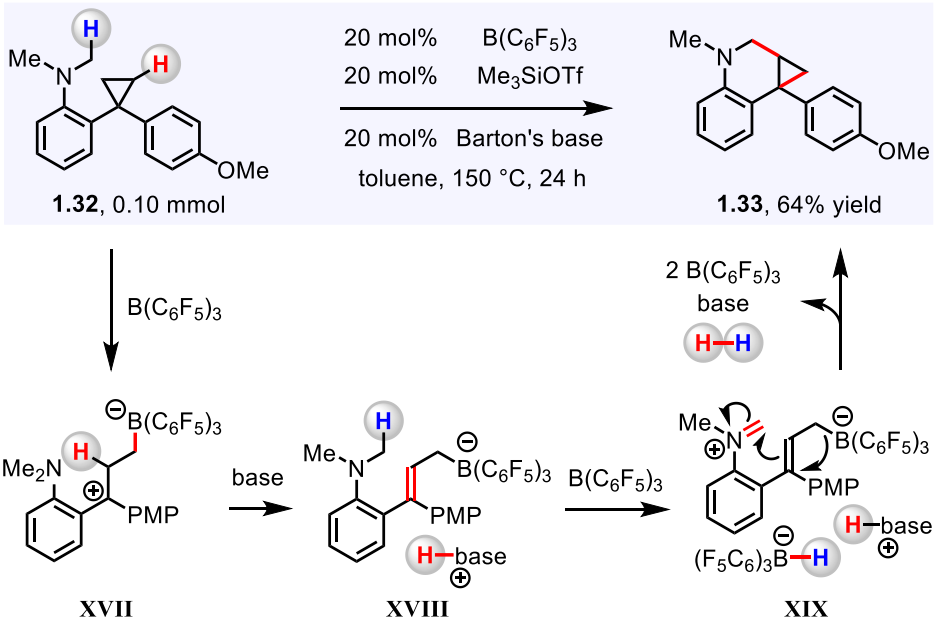

[29] Zhang, Z. Y.; Ren, J.; Zhang, M.; Xu, X.-F.; Wang, X.-C. *Chin. J. Chem*. **2021**, *39*, doi:10.1002/cjoc.202100056.

Paradies and co-workers developed an intramolecular cyclization of *o*-amino-substituted α,β-unsaturated ketones (**1.34**) through *endo*-1,7-hydride shift catalyzed by $B(C_6F_5)_3$ (Scheme 1.12).[30] It is proposed that hydride transfer is promoted by Lewis acid activation of the carbonyl moiety (**XX**) rather than $B(C_6F_5)_3$ abstracting a hydride from α-amino position of **1.34**. Ensuing intramolecular C–C bond forming reaction takes place between the boron–enolate and iminium ion (**XXI**) to produce a dihydroquinoline derivative **1.35**.

Scheme 1.12. $(F_5C_6)_3B$-Catalyzed 1,7-Hydride Transfer

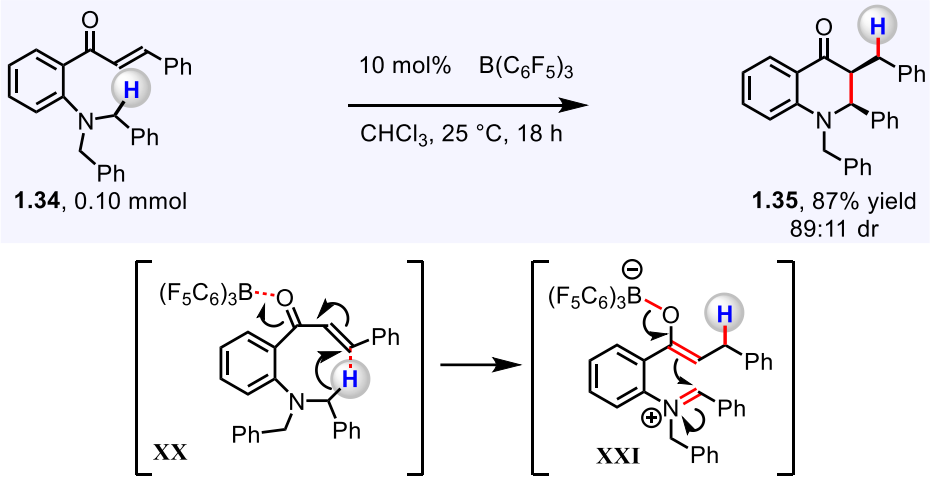

The literature precedents discussed above (Schemes 1.10–1.12) showed that the amine-derived iminium intermediate can be used to effect α-amino C–H alkylation processes. However, these methods have been confined to non-enantioselective intramolecular transformations of *N*-alklylaniline derivatives.

[30] Wicker, G.; Schoch, R.; Paradies, J. *Org. Lett.* **2021**, doi:10.1021/acs.orglett.1c01018

1.5. $(F_5C_6)_3B$-Catalyzed *β*-Amino C–H Functionalization

Direct transformation of less reactive *β*-amino C–H bond under redox- and pH-neutral conditions is a central challenge in catalysis.[7c] One of the emerging strategies to access the *β*-amino C–H bonds is $(F_5C_6)_3B/NR_3$-catalyzed conversion of *N*-alkylamines into enamine.[21] The enamine intermediate can then react with an appropriate electrophile to afford *β*-substituted amines.

1.5.1. C–Si Bond Formation

The Chang group developed a protocol for the synthesis of bridged sila-*N*-heterocycles (**1.37**) through silylation of *N*-aryl piperidines (**1.36**) with hydrosilanes, that is catalyzed by $B(C_6F_5)_3$ (Scheme 1.13).[31] After borane-mediated hydride abstraction of aniline **1.36**, the resultant

Scheme 1.13. $(F_5C_6)_3B$-Catalyzed Synthesis of Bridged Sila-*N*-Heterocycles from Piperidines

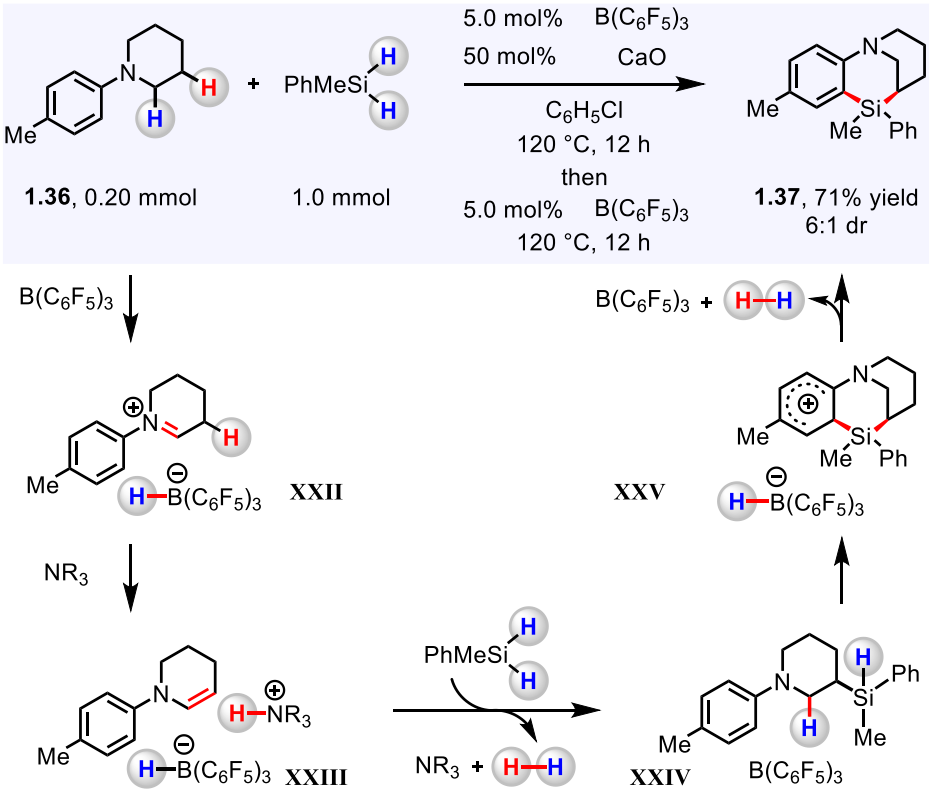

[31] Zhang, J.; Park, S.; Chang, S. *J. Am. Chem. Soc.* **2018**, *140*, 13209–13213.

iminium (**XXII**) can be deprotonated to form an enamine (**XXIII**). Following hydrosilylation of enamine **XXIII** gives *β*-silylated piperidine (**XXIV**), which undergoes intramolecular dehydrogenative sp^2 C−H silylation (**XXV**) to afford the bridged sila-*N*-heterocycle **1.37**.

In 2021, Oestreich and co-workers reported $(F_5C_6)_3B$-catalyzed *β*-amino C–H silylation of acyclic trialkylamines (**1.38**) to construct 4-silapiperidine derivatives (**1.39**, Scheme 1.14).[32] Sequential hydride abstraction and deprotonation of **1.38** affords an enamine (**XXVI**), which undergoes intermolecular C–Si bond forming reaction with $(F_5C_6)_3B$-activated hydrosilane (**XXVI→XXVII**). The resulting iminium ion can undergo isomerization (**XXVII→XXVIII**) and deprotonation to furnish an enamine intermediate (**XXIX**). Then, $(F_5C_6)_3B$-promoted intramolecular hydrosilylation and borohydride reduction provide the 4-silapiperidine **1.39**.

Scheme 1.14. $(F_5C_6)_3B$-Catalyzed *β,β'*-Silylation of Acyclic Tertiary Amines

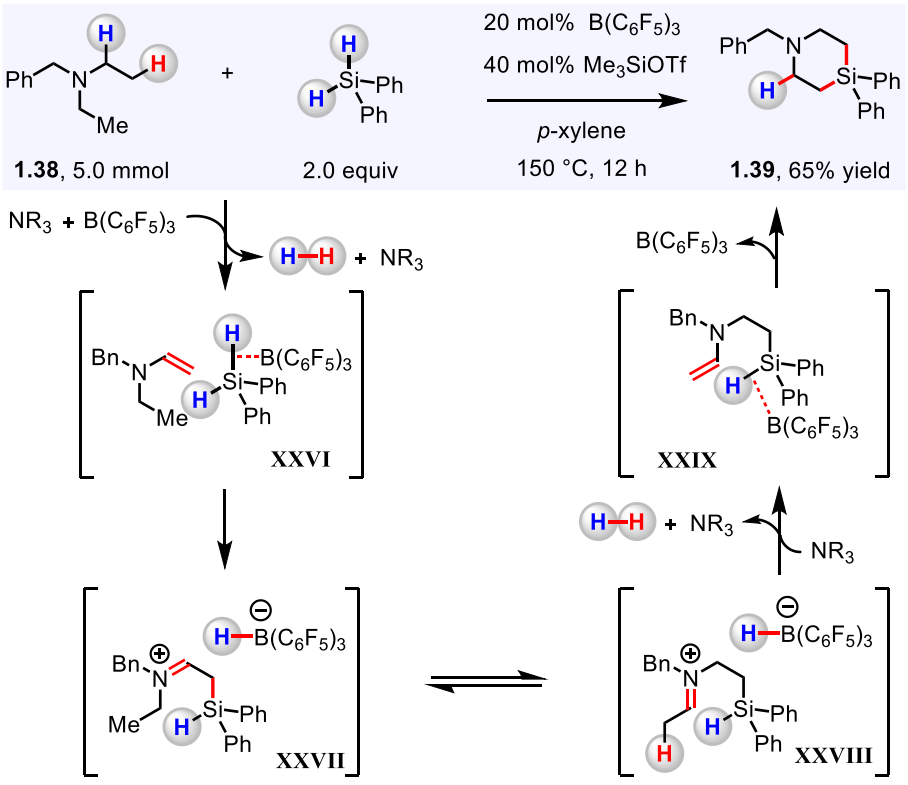

[32] Fang, H.; Xie, K.; Kemper, S.; Oestreich, M. *Angew. Chem., Int. Ed.* **2021**, 60, 8542–8546.

The studies described above (Schemes 1.13, 1.14) demonstrated that *β*-amino C–H bond can be converted into C–Si bond via the enamine that is generated in situ through consecutive $(F_5C_6)_3B$-promoted hydride abstraction and Brønsted base-mediated deprotonation.

1.5.2. C–C Bond and C=C Bond Formation

The groups of Yang, Zhao, and Ma disclosed intermolecular *β*-alkylation of acyclic tertiary amines (**1.40**) promoted by $B(C_6F_5)_3$ (Scheme 1.15).[33] This transformation involves conjugate addition of **1.40**-derived enamine (**XXX**) to *p*-quinone methide **1.41** that affords zwitterionic intermediate **XXXI**. The borohydride reduction and ammonium-mediated protonation of **XXXI** delivers the *β*-alkylation product **1.42** and regenerates the catalysts. Although $(F_5C_6)_3B$-catalyzed *β*-amino C–H alkylation was achieved, bulky 2,6-di-*t*-Bu substituents in *p*-quinone methide **1.41** was required and the amine substrate scope was confined to triethylamine (**1.40**) and its two analogues.

Scheme 1.15. $(F_5C_6)_3B$-Catalyzed *β*-Alkylation of Acyclic Tertiary Amines

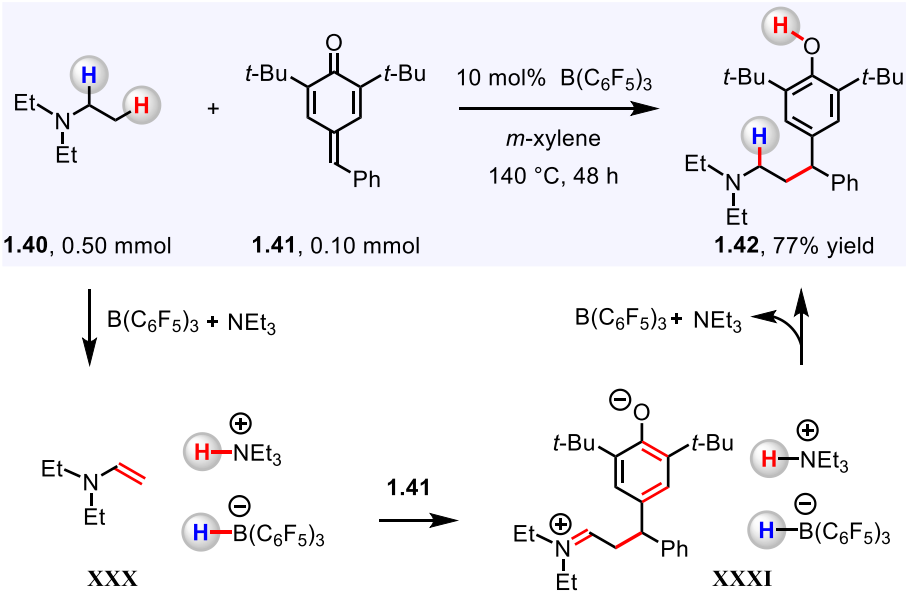

[33] Li, R.; Chen, Y.; Jiang, K.; Wang, F.; Lu, C.; Nie, J.; Chen, Z.; Yang, G.; Chen, Y.-C.; Zhao, Y. Ma, C. *Chem. Commun.* **2019**, *55*, 1217–1220.

Yang, Ma, and co-workers developed $(F_5C_6)_3B$-catalyzed union of *N*-aryl pyrrolidines (**1.43**) and isatins (**1.44**) for the synthesis of *β*-substituted pyrrolidines (**1.45**, Scheme 1.16).[34] The aniline **1.43**-derived enamine (**XXXII**) reacts with **1.44** to generate zwitterionic intermediate **XXXIII**. Subsequent protonation of alkoxide (**XXXIII**) by ammonium and dehydration would furnish a C=C bond (**XXXIV**). Upon borohydride reduction of the iminium ion (**XXXIV**), a pyrrolidine that bears exocyclic alkene (**1.45**) can be obtained.

Although these work demonstrated that redox-neutral *β*-functionalizations of *N*-alkylamines to construct a new C–C bond or C=C bond can be achieved, both transformations were confined to a narrow range of *N*-alkylamine substrates and electrophiles.

Scheme 1.16. $(F_5C_6)_3B$-Catalyzed *β*-Functionalization of *N*-Aryl Pyrrolidines with Isatins

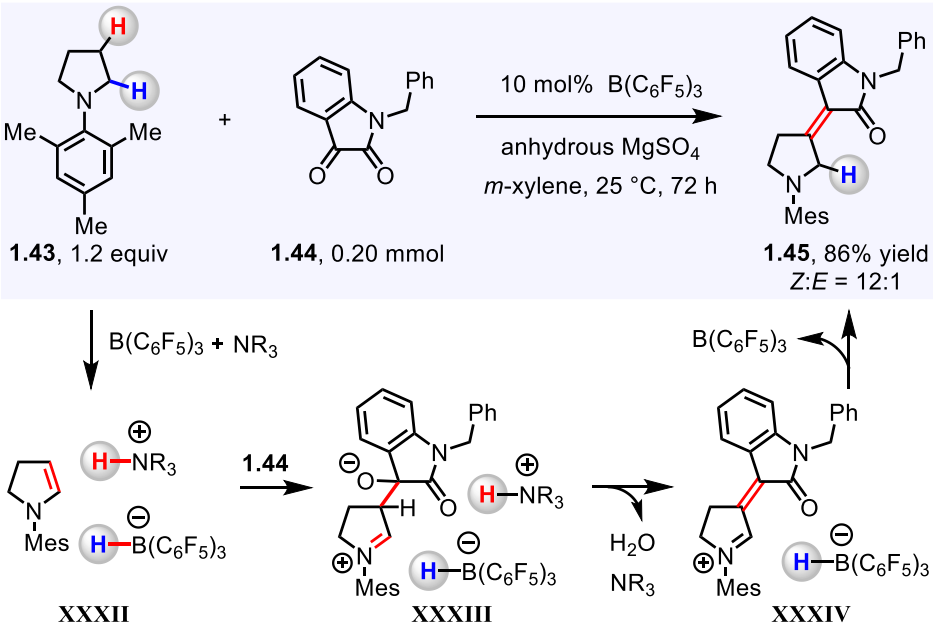

[34] Chen, Y.; Wan, H.-L.; Huang, Y.; Liu, S.; Wang, F.; Lu, C.; Nie, J.; Chen, Z.; Yang, G.; Ma, C. *Org. Lett.* **2020**, *22*, 7797–7803.

1.6. $(F_5C_6)_3B$-Catalyzed C–N Bond Cleavage

The deconstructive functionalization of amines has recently gained attention as a means to obtain products with complex structures that cannot be efficiently synthesized by other methods.[35] Accordingly, the strategies to cleave C–N bond in *N*-alkylamines involving $(F_5C_6)_3B$-catalyzed hydride abstraction have been investigated independently by several laboratories.

The Chang group reported $(F_5C_6)_3B$-catalyzed *cine*-silylative C–N cleavage of tertiary amines (**1.46**, Scheme 1.17).[36] This reaction proceeds by dehydrogenation of *N*-alkylamine to form an enamine intermediate (**XXXV**), which undergoes hydrosilylation promoted by $B(C_6F_5)_3$ to afford *β*-silylpiperidine (**XXXVI**). After the formation of 2-silazetidinium (**XXXVII**), *cis*-*β*-amino elimination takes place to form the intermediate **XXXVIII**. Finally, hydrosilylation of the terminal alkene unit provides the desired product **1.47**.

Scheme 1.17. $(F_5C_6)_3B$-Catalyzed C–N Bond Cleavage of Tertiary Amines

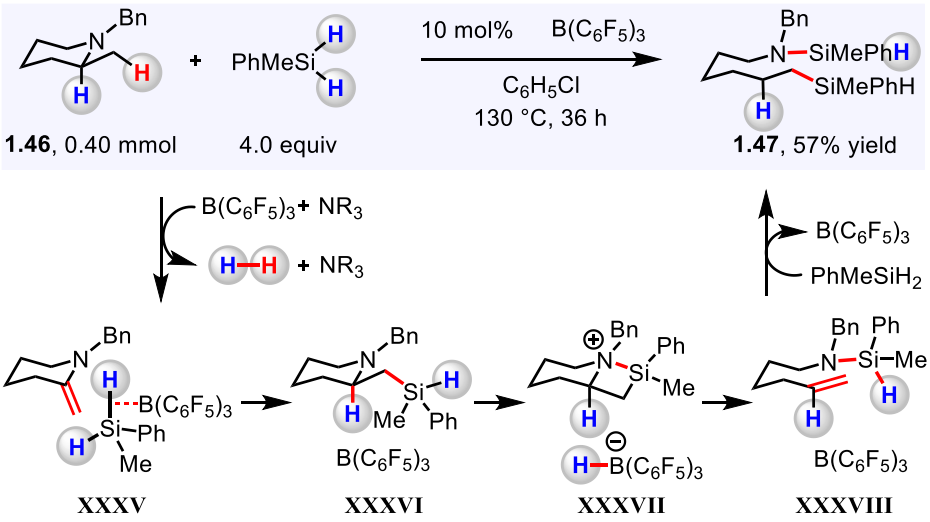

[35] (a) Roque, J. B.; Kuroda, Y.; Göttemann, L. T.; Sarpong, R. *Science* **2018**, *361*, 171–174. (b) Roque, J. B.; Kuroda, Y.; Göttemann, L. T.; Sarpong, R. *Nature* **2018**, *564*, 244–248.

[36] Zhang, J.; Chang, S. *J. Am. Chem. Soc.* **2020**, *142*, 12585–12590.

The groups of Melen, Morrill, and Pulis reported a method for direct C3 alkylation of indoles (**1.48**) using *N*-alkylanilines (**1.49**) as an alkylating reagent (Scheme 1.18).[37] The *N*-aryl pyrrolidine **1.49**-derived iminium ion reacts with a nucleophilic indole **1.48** to forge a new C–C bond (**XXXIX→XL**). Proton transfer enables the cleavage of C–N bond and generates a conjugated iminium ion (**XLI**), which is reduced by borohydride to furnish alkylated indole **1.50**. It was shown that *N*-alkylamines can serve as an alkylating reagent through $(F_5C_6)_3B$-catalyzed C–N bond cleavage.

Scheme 1.18. $(F_5C_6)_3B$-Catalyzed C3 Alkylation of Indoles

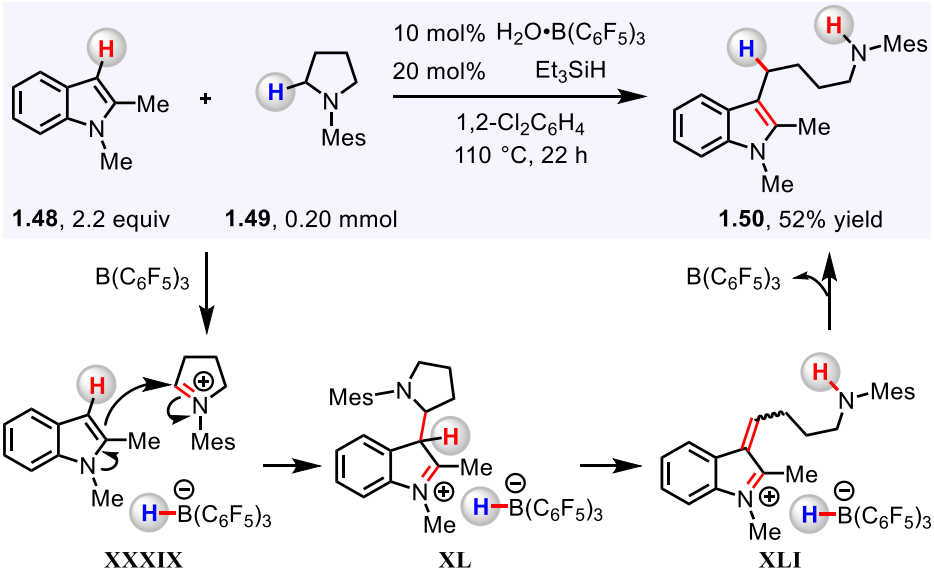

The Oestreich group developed a protocol for $(F_5C_6)_3B$-catalyzed reductive deamination of benzylic amines (e.g., **1.51**, Scheme 1.19).[38] $B(C_6F_5)_3$ promotes the Si–N bond forming reaction between *N*-alkylamine (**1.51**) and $PhSiH_3$, affording an ion pair consisting of a silylammonium and a borohydride (**XLII**). Upon the release of silazane **1.53**, benzylic carbocation (**XLIII**) is generated, which can then be reduced by a borohydride to deliver product **1.52**. This method was

[37] Basak, S.; Alvarez-Montoya, A.; Winfrey, L.; Melen, R. L.; Morrill, L. C.; Pulis, A. P. *ACS Catal.* **2020**, *10*, 4835–4840.
[38] Fang, H.; Oestreich, M. *Angew. Chem., Int. Ed.* **2020**, *59*, 11394–11398.

also applicable to the cleavage of C–N bonds contained in isocyanate, isothiocyanate, and thionyl imide.

Scheme 1.19. $(F_5C_6)_3B$-Catalyzed Reductive Deamination Using Hydrosilanes

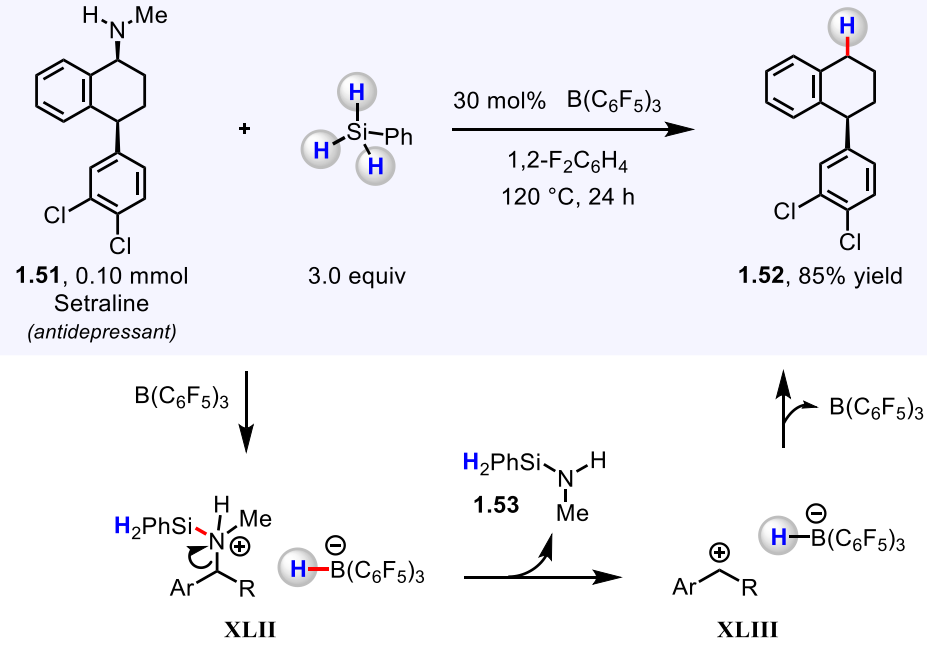

The approaches highlighted above (Schemes 1.17–1.19) demonstrated that $B(C_6F_5)_3$ can promote the cleavage of C–N bonds contained in *N*-alkylamines, however, application of such methods to more complex amine substrates remain as an unresolved problem.

1.7. Specific Aims of the Dissertation Research

Iminium ions have been utilized as highly versatile intermediates for stereoselective synthesis of *N*-alkylamines.[39-40] Iminiums have often been generated in a catalytic manner through condensation of primary or secondary amine catalysts with carbonyl molecules (**1.54→XLIV**, Scheme 1.20),[40a] protonation of imines by Brønsted acids (**1.55→XLIV**),[40b] and anion abstraction from α-haloamines or α-pseudohaloamines by hydrogen bond donors (**1.56→XLIV)**,[40c-d] among other approaches.[39] The processes highlighted in this chapter involving the organoborane-mediated hydride abstraction from *N*-alkylamines (e.g., Schemes 1.5−1.19) represent a complimentary strategy to furnish iminiums (**1.57→XLIV**, Scheme 1.20). Although there was no literature report on catalytic transformations of iminiums generated in this manner at the time this dissertation research was started in 2016, the organoborane- catalyzed hydride abstraction

Scheme 1.20. Catalytic Formation of Iminium Ion

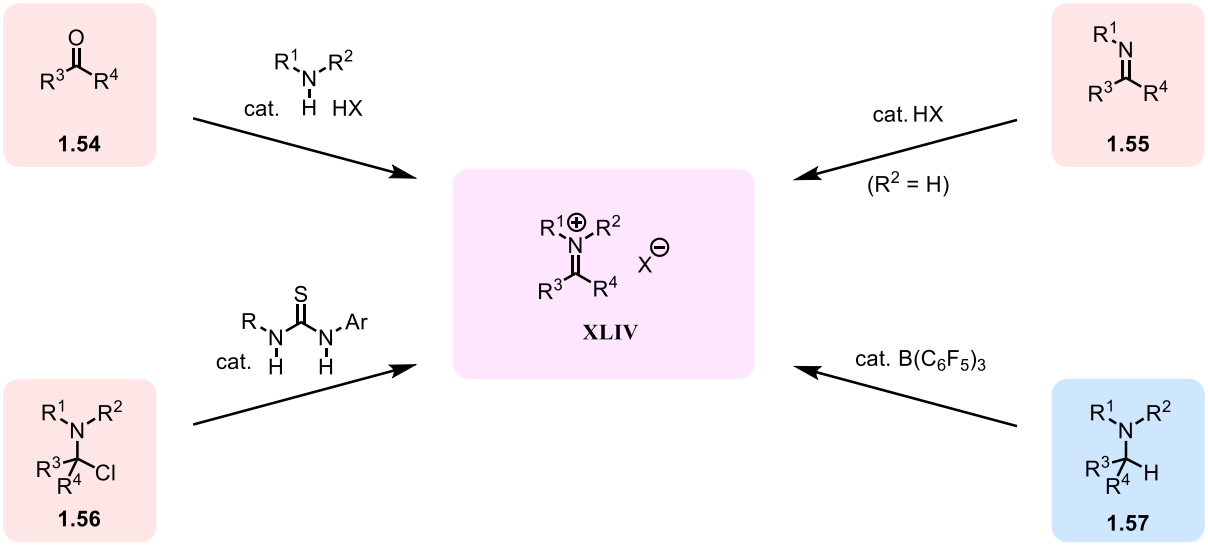

[39] Rostoll-Berenguer, J.; Blay, G.; Pedro, J. R.; Vila, C. *Adv. Synth. Catal*. **2021**, *363*, 602−628.

[40] (a) Erkkila, A.; Majander, I.; Pihko, P. M. *Chem. Rev*. **2007**, *107*, 5416–5470. (b) Yamanaka, M.; Itoh, J.; Fuchibe, K.; Akiyama, T. *J. Am. Chem. Soc*. **2007**, *129*, 6756–6764. (c) Wasa, M.; Liu, R.; Roche, S. P.; Jacobsen, E. N. *J. Am. Chem. Soc*. **2014**, *136*, 12872–12875. (d) Osberger, T. J.; Rogness, D. C.; Kohrt, J. T.; Stepan, A. F.; White, M. C. *Nature*, **2016**, *537*, 214–219.

approach holds the potential to offer the following distinctive advantages over the previously established methods (e.g., **1.54**, **1.55** or **1.56→XLIV**):

1) iminiums may be generated directly from a broad array of secondary and tertiary amines (vs a narrow scope of iminium intermediates that can be formed by reacting the primary and secondary amine catalysts and carbonyl compounds that must be able to undergo condensation readily, **1.54→XLIV**, Scheme 1.20).

2) cumbersome and wasteful preparation of aldimines and ketimines that are often required in the Brønsted acid-catalyzed processes can be circumvented (vs **1.55→XLIV**).

3) obviates the installation of halogen- or pseudo-halogen leaving groups (vs **1.56→XLIV**).

Thus, a significantly broader scope of iminium intermediates may be generated in a direct manner from *N*-alkylamines; particularly attractive would be processes in which α- and/or β-C–H bonds contained in N-based bioactive amines may be directly converted into different functional groups via the iminium formation (i.e., late-stage C–H functionalization, Scheme 1.21A–C).[14] Moreover, in comparison to C–H functionalization reactions that are catalyzed by precious metal-based complexes (c.f., Schemes 1.1A and 1.1B),[11] there may be significant benefits in implementing the organoborane-catalyzed hydride abstraction:

1) the catalysts to be used are based on sustainable elements.

2) does not require the installation/removal of directing groups; thus, is applicable to a broader scope of amines.

3) can be performed under pH neutral and oxidant-free conditions.

Based on the considerations as described above, we envisioned the development of enantio- and diastereo-selective α- and β-amino C–H functionalization processes that proceed through the organoborane-catalyzed hydride abstraction (Schemes 1.21A−C).

Scheme 1.21. Our Approach for Regio- and Enantioselective C–H Functionalization of *N*-Alkylamines to be Discussed in this Dissertation

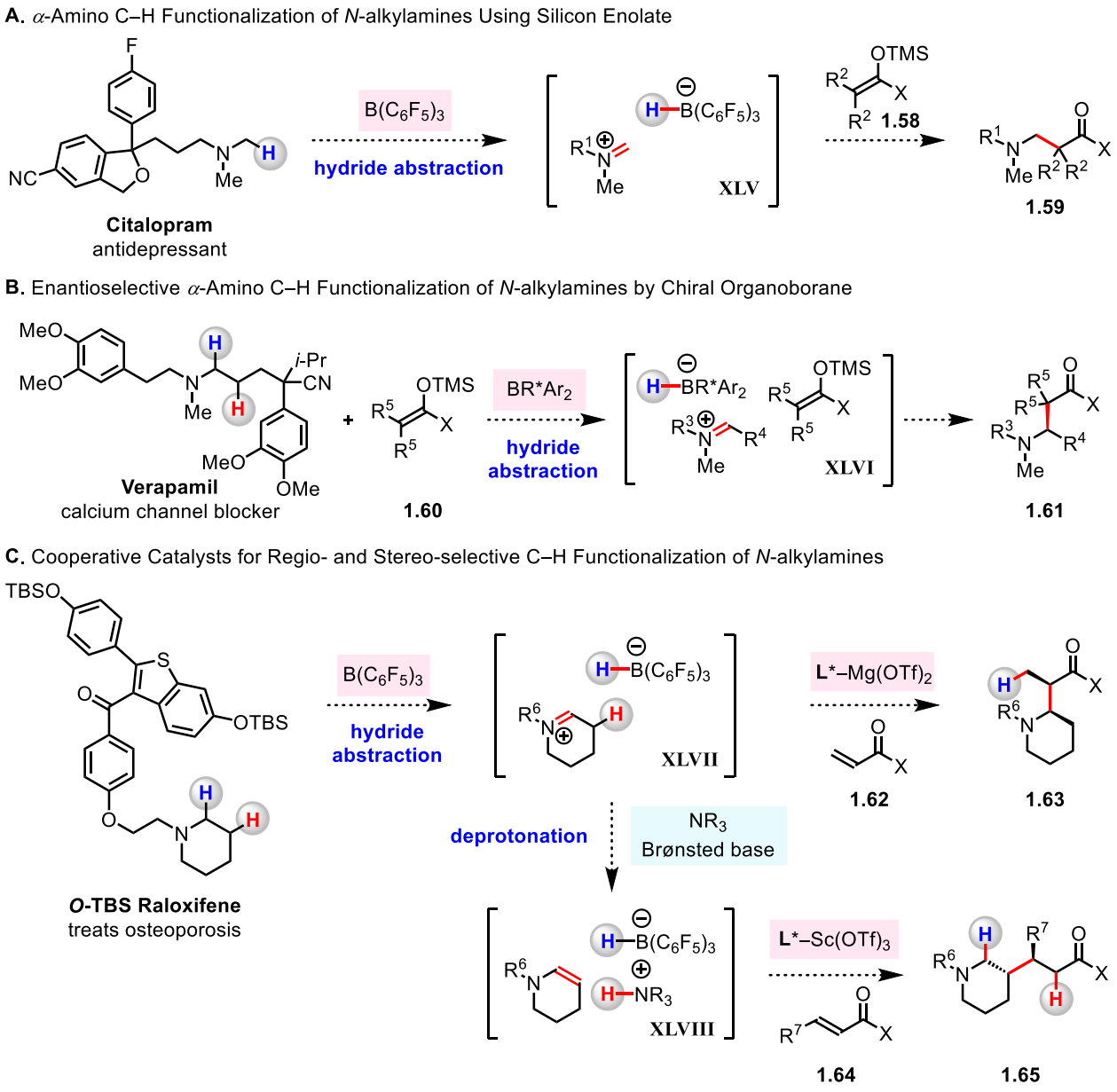

To begin our investigation, we decided to test the hypothesis that $B(C_6F_5)_3$ can catalyze reactions between various silicon enolates (**1.58**) and *N*-alkylamines, including N-based pharmaceuticals (e.g., citalopram, Scheme 1.21A), through their conversion into iminiums (**XLV**, Scheme 1.21A). It has previously been demonstrated that frustrated Lewis pairs (FLPs) consisting

of organoboranes and Lewis bases form relatively stable adducts with an array of small molecules such as amines (c.f., Scheme 1.5a, tertiary amine **1.12** and $B(C_6F_5)_3$ furnishes ammonium and borohydride complex **1.13**),[21] H_2,[41] CO_2[42] (Scheme 1.22), CO,[43] SO_2[44], and alkynes[45] among others. Therefore, development of $(F_5C_6)_3B$-catalyzed C–C bond forming reaction (Scheme 1.21) requires that $B(C_6F_5)_3$ abstracts a hydride from the substrate while overcoming undesirable catalyst deactivation through the formation of stable acid–base adducts with the amine unit as well as other Lewis acid-sensitive functional groups.[41-42] Furthermore, for the proposed transformation to be catalytic, we must find a way to let the in situ-generated $[H–B(C_6F_5)_3]^-$ release a hydride, thereby regenerating $B(C_6F_5)_3$; thus, an appropriate hydride acceptor must be identified.[46]

Scheme 1.22. Stoichiometric Activation of H_2 and CO_2 by FLP

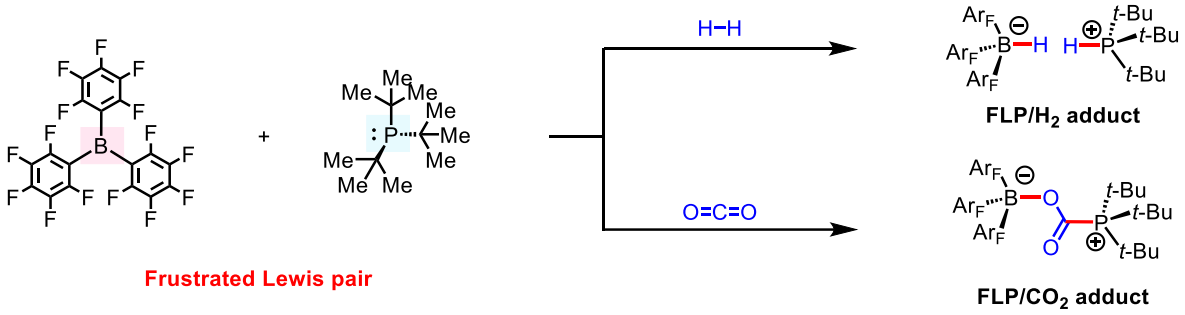

Our subsequent aim was to develop enantioselective organoborane-catalyzed α- and/or β-amino C–H functionalization reactions (Scheme 1.21B and C). The first transformation we envisioned to achieve was to use a chiral organoborane catalyst to promote enantioselective union of *N*-alkylamines and silicone enolates (Scheme 1.21B). This process requires that in situ-

[41] Welch, G. C.; San Juan, R. R.; Masuda, J. D.; Stephan, D. W. *Science*, **2006**, *314*, 1124−1126.
[42] Mömming, C. M.; Otten, E.; Kehr, G.; Fröhlich, R.; Grimme, S.; Stephan, D. W.; Erker, G. *Angew. Chem., Int. Ed.* **2009**, *48*, 6643−6646.
[43] Dobrovetsky, R.; Stephan, D. W. *J. Am. Chem. Soc.* **2013**, *135*, 4974–4977.
[44] Otten, E.; Neu, R. C.; Stephan, D. W. *J. Am. Chem. Soc.* **2009**, *131*, 9918–9919.
[45] Dureen, M. A.; Stephan, D. W. *J. Am. Chem. Soc.* **2009**, *131*, 8396–8397.
[46] Ilic, S.; Alherz, A.; Musgrave, C. B.; Glusac, K. D. *Chem. Soc. Rev*. **2018**, *47*, 2809−2836.

generated chiral borohydride, which is ionically bond to the iminium, controls enantioselectivity in the C–C bond forming step (**XLVI→1.61**).[47]

Another approach to achieve highly enantioselective α-amino C–H functionalization would be to implement a catalyst system consisting of an achiral organoborane and a chiral Lewis acid co-catalyst (Scheme 1.21C). Specifically, the B-based catalyst promotes the formation of iminiums while the chiral co-catalyst activates an appropriate pronucleophile (e.g., **1.62**); ensuing enantiodetermining C–C bond formation could afford the desired α-functionalized amines (e.g., **1.63**). Significant advantages of employing the cooperative Lewis acid/Lewis acid co-catalyst system are the following:

1) enables the generation of both nucleophilic and electrophilic partners from otherwise unreactive substrates.

2) either one or both of the catalysts can be chiral; various potential catalyst combinations are available for improving stereoselectivity.

3) both the reaction efficiency and stereoselectivity can be easily optimized by efficient evaluation of readily accessible Lewis acids and chiral ligands.

4) the enantioselective processes may be highly atom-economical as they generate no waste (vs the reactions in Scheme 1.21A and 1.21B that produce TMS−H as a byproduct).

Despite these desirable attributes of cooperative Lewis acid/Lewis acid catalysis, a fundamental challenge has to do with the difficulty in achieving highly enantioselective reactions by letting the achiral organoborane and chiral organometallic catalysts that may have potential overlapping functions play their independent roles.[48] In addition, functional group tolerance could

[47] Brak, K.; Jacobsen, E. N. *Angew. Chem., Int. Ed*. **2013**, *52*, 534−561.
[48] Romiti, F.; del Pozo, J.; Paioti, P. H. S.; Gonsales, S. A.; Li, X.; Hartrampf, F. W. W.; Hoveyda, A. H. *J. Am. Chem. Soc*. **2019**, *141*, 17952−17961.

be diminished in case the organometallic co-catalyst is not sterically and electronically "frustrated" against the Lewis basic moieties.

Should we find that the enantioselective α-amino C–H functionalization can be promoted by the cooperative functions of two Lewis acids, our next aim would be to achieve transformations of β-amino C–H bonds (Scheme 1.21C). Inspired by $(F_5C_6)_3B/NEt_2Ph$-mediated enamine forming reactions from NEt_2Ph reported by the Santini group (e.g., Scheme 1.5b, **VI→VII**),[21] we postulated that the *N*-alkylamine can be converted into an enamine intermediate (***O*-TBS raloxifene→XLVIII**) by deprotonation of the in situ-generated iminium (**XLVII**) by an appropriate Brønsted base catalyst. Ensuing stereoselective reaction of the enamine and an electrophile (e.g., α,β-unsaturated compound **1.64**), which is activated by the chiral Lewis acid, could deliver β-substituted amines (e.g., **1.65**).

Through the development of the cooperative catalyst systems, the main aim of this dissertation research is to address the critical unresolved problems of stereoselective amino C–H functionalization; that is to discover a highly functional group tolerant, efficient and stereoselective catalyst system that can be used to produce an array of structurally complex and synthetically valuable *N*-alkylamines that cannot be readily accessed by the conventional methods.

Chapter Two

Enantioselective α-Amino C–H Functionalization through Cooperative Action of Chiral and Achiral Lewis Acid Catalysts

2.1 Introduction

Amines that possess a stereogenic center at the α-position of the nitrogen atom are commonly found in pharmaceuticals, natural products, and catalysts used in enantioselective synthesis (Scheme 2.1).[1] Therefore, the development of catalytic processes for the preparation of enantiomerically enriched α-substituted amines is a crucial and widely investigated topic of research in chemical catalysis.[2] Particularly, direct functionalization of α-amino C–H bond has gained attention for its potential to be applied in the late-stage modification of various N-based molecules, which could provide rapid access to a library of structurally complex *N*-alkylamines that are difficult to prepare through conventional synthetic methods.[3-4]

Scheme 2.1. Enantio-enriched α-Substituted *N*-Alkylamines

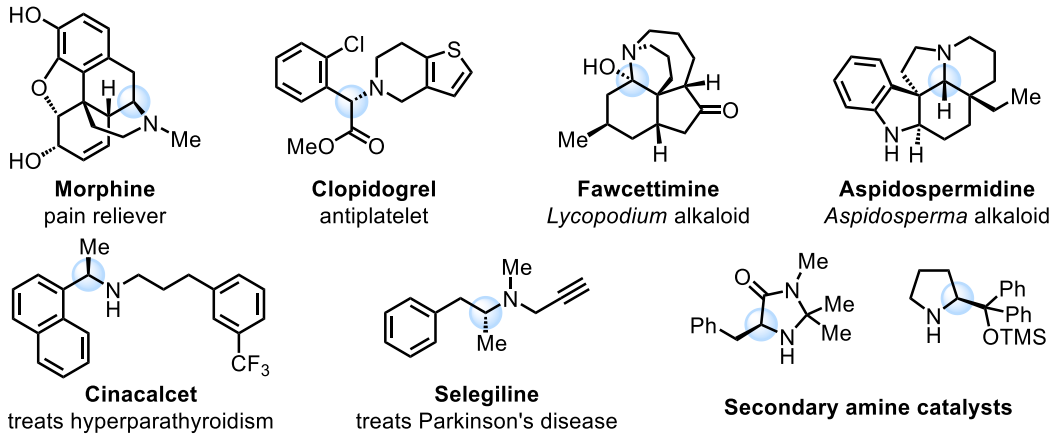

[1] (a) Linghu, X.; Kennedy-Smith, J. J.; Toste, F. D. *Angew. Chem., Int. Ed*. **2007**, *46*, 7671-7673. (b) Marino, J. P.; Rubio, M. B.; Cao, G.; de Dios, A. *J. Am. Chem. Soc*. **2002**, *124*, 13398-13399.
[2] Yin, Q.; Shi, Y.; Wang, J.; Zhang, X. *Chem. Soc. Rev.* **2020**, *49*, 6141–6153.
[3] Campos, K. *Chem. Soc. Rev*. **2007**, *36*, 1069–1084.
[4] Borgel, J.; Ritter, T. *Chem* **2020**, *6*, 1877–1887.

However, as discussed in Chapter 1, catalyst systems that could promote efficient, regio- and enantio-selective transformations of α-amino C–H bonds in *N*-alkylamines remain underdeveloped. The paucity of effective and broadly applicable catalyst systems originates from the following fundamental challenges:

1) unreactive nature of the α-amino C–H bonds.

2) the requirement for external oxidants and harsh reaction conditions.

3) the demand for directing groups; and their installation/removal for the molecule that does not contain a moiety to serve as a directing group.

In this chapter, we describe our studies aimed at overcoming the difficulties listed above and developing a broadly applicable and sustainable element-based catalyst system for enantioselective functionalization of otherwise unreactive α-amino C–H bond.

2.2 Background

Despite the difficulties associated with transformation of α-amino C–H bonds discussed above, synthesis of enantio-enriched α-substituted *N*-alkylamines through activation of amino C–H bond has been investigated by a number of groups. The previously reported protocols for α-C–H functionalization of *N*-alkylamines typically involve the formation of an iminium,[5] an α-amino radical,[6] or a metallacycle intermediate.[7] An alternative method for the activation and conversion of α-amino C–H bond was developed by the group of Davies (Scheme 2.2).[8] Through metal-carbenoid insertion into amino C–H bond of *N*-Boc pyrrolidine **2.1**, the β-amino carbonyl compound **2.3** was obtained. Although this method enabled highly selective transformation of amino C–H bonds, its application to late-stage modification could not be achieved due to the low functional group tolerance.

Scheme 2.2. α-Amino C–H Functionalization through Carbene Insertion

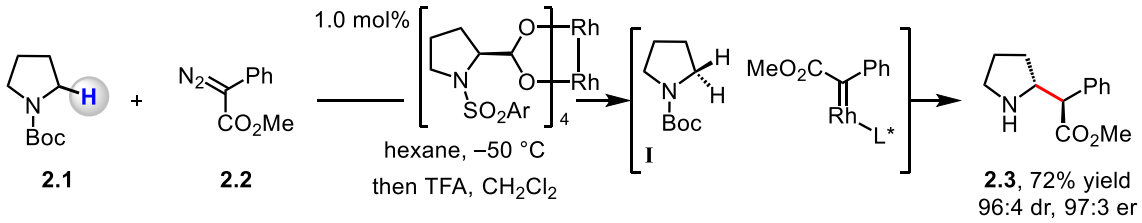

Campos and co-workers reported an enantioselective lithiation of *N*-Boc pyrrolidine and consecutive Negishi coupling for the synthesis of α-arylated amine (Scheme 2.3).[9] The reaction of N-Boc pyrrolidine **2.1** with *s*-BuLi and (–)-sparteine generates the enantio-enriched α-lithiated intermediate, which could be converted to organozinc halide (**II**) by ZnI_2. Ensuing Negishi

[5] Beatty, J. W.; Stephenson, C. R. J. *Acc. Chem. Res.* **2015**, *48*, 1474–1484.
[6] Nakajima, K.; Miyake, Y.; Nishibayashi, Y. *Acc. Chem. Res.* **2016**, *49*, 1946–1956.
[7] He, C.; Whitehurst, W. G.; Gaunt, M. J. *Chem* **2019**, *5*, 1031–1058.
[8] Davies, H. M. L.; Venkataramani, C.; Hansen, T.; Hopper, D. W. *J. Am. Chem. Soc.* **2003**, *125*, 6462–6468.
[9] Campos, K. R.; Klapars, A.; Waldman, J. H.; Dormer, P. G.; Chen, C.-Y. *J. Am. Chem. Soc.* **2006**, *128*, 3538–3539.

coupling with phenyl bromide affords the desired product **2.4**. As this method requires a stoichiometric amount of *s*-BuLi, amines that contain base-sensitive functional group cannot be tolerated in this catalyst system.

Scheme 2.3. Enantioselective Lithiation of *N*-Boc-Pyrrolidine and Negishi Coupling

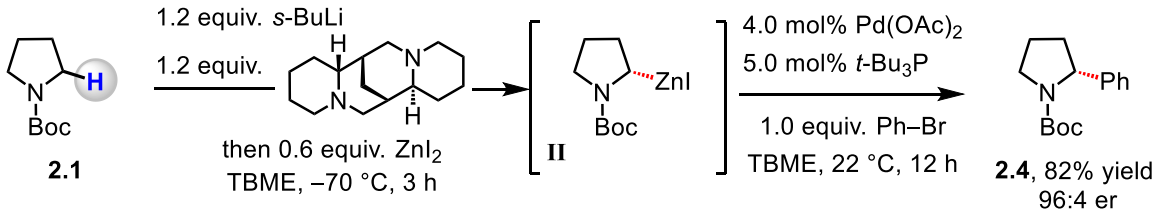

An enantioselective α-amino C–H functionalization of tetrahydroisoquinoline derivatives promoted by a combination of photoredox and *N*-heterocyclic carbene (NHC) catalysts was developed by the Rovis group (Scheme 2.4).[10] The Ru-based photocatalyst generates an iminium ion from N-alkylamine **2.5** while NHC catalyst promotes the formation of Breslow intermediate with an aldehyde (**III**). Ensuing stereoselective C–C bond forming reaction provides the α-substituted amine **2.7**. Major limitation of this method are the use of precious Ru-based catalyst as well as external oxidant.

Scheme 2.4. Cooperative *N*-Heterocyclic Carbene and Photoredox Catalysis

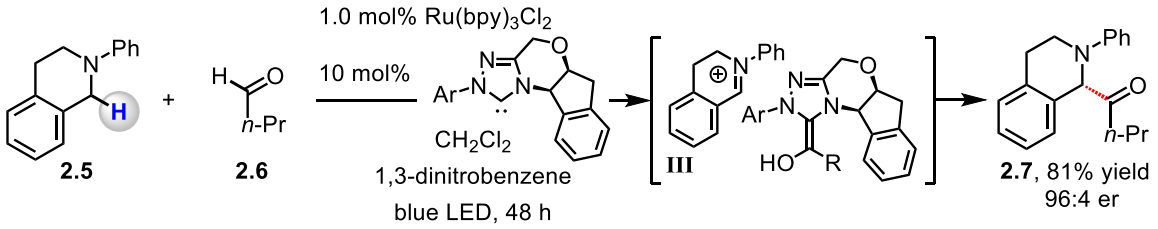

The group of Yu demonstrated the sulfur-directed C–H arylation of pyrrolidines promoted by a chiral Pd-based catalyst (Scheme 2.5).[11] This transformation is proposed to proceed via a five-

[10] DiRocco, D. A.; Rovis, T. *J. Am. Chem. Soc.* **2012**, *132*, 8094–8097.
[11] Jain, P.; Verma, P. Xia, G.; Yu, J.-Q. *Nat. Chem.* **2017**, *9*, 140–144.

membered palladacycle upon directed α-amino C–H activation (**IV**), which undergoes cross-coupling with $PhB(OH)_2$ affording α-arylated pyrrolidines **2.9**. In addition to the installation and removal of directing thionyl group, the use of stoichiometric oxidant and Pd-based catalyst are the limitation of this protocol.

Scheme 2.5. Directed α-Amino C–H Bond Functionalization Promoted by a Pd-Based Catalyst

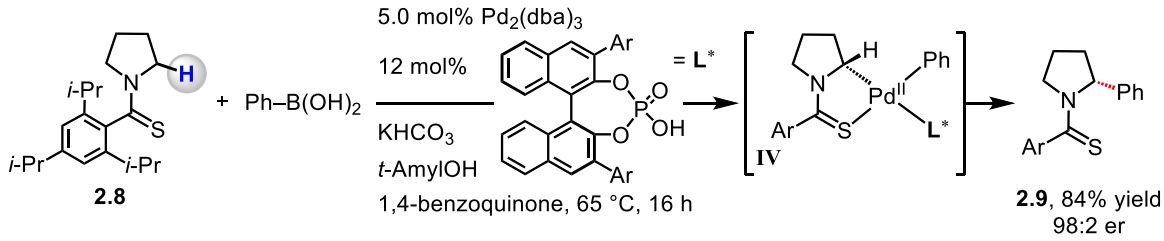

Despite the advances made in the field of enantioselective α-amino C–H functionalization, fundamental challenges still remain to be addressed for practical applications of the aforementioned methods. Therefore, we envisaged the development of a highly efficient, regio- and enantio-selective functionalizations of α-amino C–H bonds promoted by sustainable element-based catalysts.

2.3 Our Approach

As we contemplated ways to achieve α-amino C–H functionalization, we were inspired by the unique capability of frustrated Lewis pairs (FLPs) that could activate otherwise inert molecules.[12] As discussed in Chapter 1, it was demonstrated that hindered and strongly Lewis acidic organoborane could disfavor the formation of stable acid–base adduct with sterically encumbered amine and promote hydride abstraction from α-C–H bond, generating an ion pair of iminium and borohydride (e.g., **2.10**→**V**, Scheme 2.6).[13]

Based on the literature precedents, we envisioned the use of Lewis acidic organoborane to generate electrophilic iminium ion in situ, which can be trapped by an appropriate nucleophilic species such as silicon enolate (Scheme 2.6). Specifically, the organoborane catalyst could abstract hydride from amine **2.10** to form iminium ion and borohydride (**V**). The nucleophilic silicon enolate **2.11** could react with the iminium intermediate to forge a new α-amino C–C bond (**VI**). The β-amino carbonyl compound **2.12** can be obtained upon the release of environmentally benign Me_3Si–H as a single byproduct.

Scheme 2.6. Proposed Catalytic Cycle for Lewis Acid-Catalyzed Hydride Abstraction.

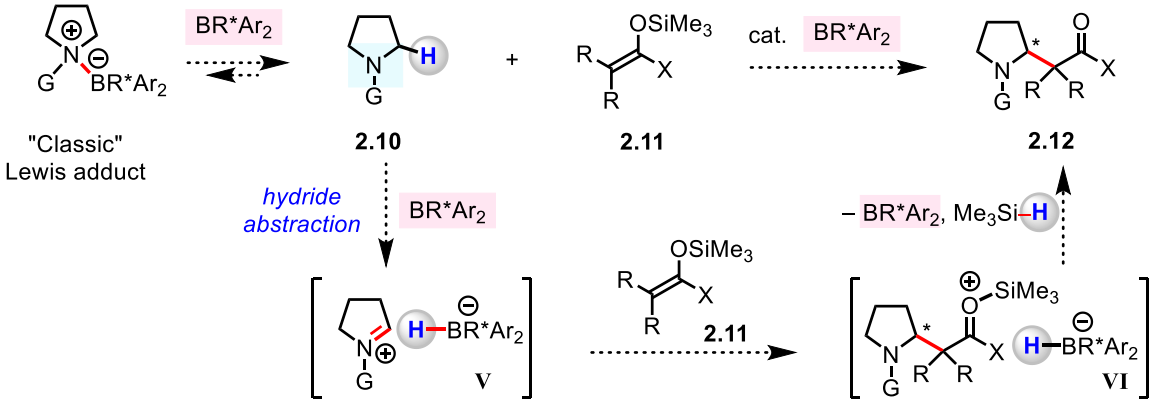

[12] Stephan, D. W.; Erker, G. *Angew. Chem., Int. Ed.* **2015**, *54*, 6400–6441.
[13] (a) Millot, N.; Santini, C. C.; Fenet, B.; Basset, J. M. *Eur. J. Inorg. Chem*. **2002**, *2002*, 3328−3335. (b) Schwendemann, S.; Frohlich, R.; Kehr, G.; Erker, G. *Chem. Sci.* **2011**, *2*, 1842–1849.

When we started our investigation, the use of an iminium ion in situ generated through borane-catalyzed hydride abstraction from *N*-alkylamines was confined to transfer hydrogenation of imines[14] and dehydrogenation of *N*-heterocycles.[15] The engagement of the versatile iminium intermediate in the context of amino C–H functionalization promoted by organoborane catalyst remained to be developed.

[14] Farrell, J. M.; Heiden, Z. M.; Stephan, D. W. *Organometallics* **2011**, *30*, 4497–4500.
[15] (a) Maier, A. F. G.; Tussing, S.; Schneider, T.; Flörke, U.; Qu, Z.-W.; Grimme, S.; Paradies, J. *Angew. Chem., Int. Ed.* **2016**, *55*, 12219–12223. (b) Kojima, M.; Kanai, M. *Angew. Chem., Int. Ed.* **2016**, *55*, 12224–12227.

2.4 $(F_5C_6)_3B$-Catalyzed α-Alkylation of *N*-Alkylamines Using Silicon Enolates

To first demonstrate the proof of concept that an organoborane can promote hydride abstraction from amines and the resulting iminium ion can react with silicon enolate, we evaluated various combinations of Lewis acid catalysts and *N*-alkylamine substrates. Based on the literature precedents,[10-11] we considered utilizing strongly Lewis acidic and hindered $B(C_6F_5)_3$ as a catalyst and examined its ability to convert *N,N*-dimethylanilines into corresponding β-amino carbonyl compounds via iminium ion (Table 2.1). The reaction of *N,N*-dimethylaniline (**2.13a**) and 1-methoxy-2-methyl-1-(trimethylsiloxy)propene (**2.11a**) in the presence of 20 mol% $B(C_6F_5)_3$ provided **2.14a** in 31% yield ($C_2H_4Cl_2$, 22 °C). We hypothesized that electron-donating substituents on the *N*-aryl group may enhance the reaction efficiency by increasing the hydride donor ability of the α-amino C–H bond as well as generating more stable iminium intermediate. While the reaction of electron-donating *para*-methoxy-substituted **2.13b** afforded **2.14b** in 25%

Table 2.1. Evaluation of *N*-Aryl Substituents[a,b]

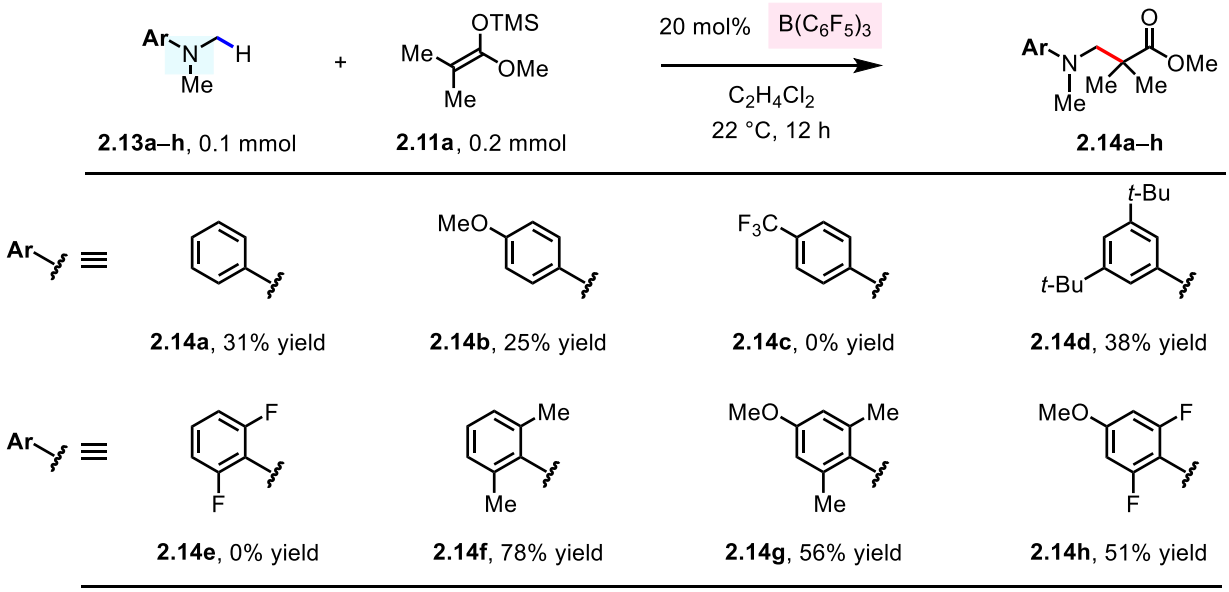

[a] Conditions: *N,N*-dimethylaniline (0.1 mmol), 1-methoxy-2-methyl-1-(trimethylsiloxy)propene (0.2 mmol), $B(C_6F_5)_3$ (20 mol%), dichloroethane (0.25 mL), under N_2, 22 °C, 12 h. [b] Yields were determined by ^1H NMR analysis of unpurified product mixtures with mesitylene as the internal standard. See Section 2.7 for details.

yield, none of the desired product was observed with electron-deficient *para*-trifluoromethylphenyl-substituted **2.13c**. With 3,5-di-*tert*-butyl-substituents, α-alkylation product **2.14d** was obtained in 38% yield.

To test whether more hindered amines could further disfavor the acid-base complexation and facilitate the hydride abstraction, we evaluated an array of *ortho*-disubstituted anilines. Whereas 2,6-difluoro-*N,N*-dimethylaniline (**2.13e**) gave none of the Mannich-type product, larger and more electron-rich *N,N,*2,6-tetramethylaniline (**2.13f**) resulted in the drastic improvement of reaction efficiency, providing **2.14f** in 78% yield. Encouraged by this result, we studied the reaction with 4-methoxy-*N,N*,2,6-tetramethylaniline (**2.13g**), which contains the *N*-aryl substituent that could be removed under oxidative conditions,[16] afforded the desired product **2.14g** in 56% yield. Through the use of less hindered and more electron-deficient 2,6-difluoro-4-methoxyphenyl-substituted **2.13h**, the corresponding β-amino carbonyl compound **2.14h** was obtained in 51% yield.

To further improve the reaction efficiency, we evaluated various reaction conditions using **2.14g** and **2.11a** as a model substrate (Table 2.2). In the absence of $B(C_6F_5)_3$, no desired product was obtained (entry 2). In some cases (entries 1 and 3–9), secondary amine **2.15g** was also obtained, likely through the cleavage of the C–N bond upon the reaction of in situ generated iminium ion with water. Among the *N*,*N*-dimethylanilines evaluated, only *ortho*- dimethyl-substituted **2.13f** and **2.13g** afforded the C–N cleaved byproducts. At lower catalyst loading of 10 mol%, **2.14g** was formed more selectively over **2.15g** in 71% and 22% yield, respectively (entry 3). Since the Mannich reaction involves ionic intermediates, we hypothesized more polar solvents could facilitate the reaction and evaluated the effect of ethereal solvents. In Et_2O with 10 mol%

[16] Jurberg, I. D.; Peng, B.; Wöstefeld, E.; Wasserloos, M.; Maulide, N. *Angew. Chem., Int. Ed.* **2012**, *51*, 1950–1953.

Table 2.2. Optimization of Reaction Conditions[a,b]

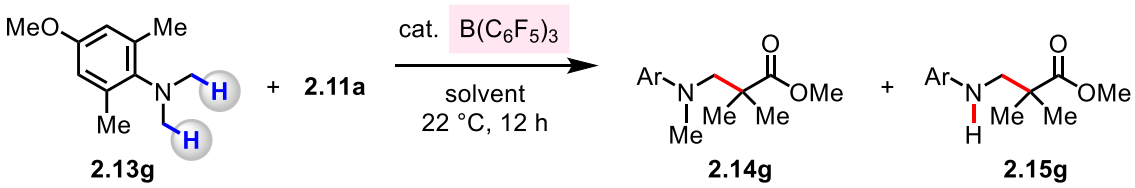

entry	Lewis acid	catalyst loading (mol%)	solvent	yield (%)	
				2.14g	**2.15g**
1	$B(C_6F_5)_3$	20	$C_2H_4Cl_2$	56	35
2	none	0	$C_2H_4Cl_2$	0	0
3	$B(C_6F_5)_3$	10	$C_2H_4Cl_2$	71	22
4	$B(C_6F_5)_3$	10	Et_2O	83	17
5	$B(C_6F_5)_3$	5.0	Et_2O	22	<5
6	$B(C_6F_5)_3$	10	THF	38	<5
7	$B(C_6F_5)_3$	10	toluene	75	21
8	$B(C_6F_5)_3$	10	benzene	81	16
9	$B(C_6F_5)_3$	5.0	benzene	>95	<5
10	BF_3•OEt_2	10	benzene	0	0
11	BPh_3	10	benzene	0	0

[a] Conditions: 4-methoxy-*N*,*N*,2,6-tetramethylaniline (0.1 mmol), 1-methoxy-2-methyl-1-(trimethylsiloxy)propene (0.2 mmol), Lewis acid, solvent (0.25 mL), under N_2, 22 °C, 12 h. [b] Yields were determined by ^{1}H NMR analysis of unpurified product mixtures with mesitylene as the internal standard. See Section 2.7 for details.

catalyst loading, **2.14g** was formed in an increased yield of 83%, but with 5.0 mol% $B(C_6F_5)_3$, the product yield diminished considerably (22% yield, entries 4–5). When THF was used as the solvent, **2.14g** was obtained in 38% yield (entry 6). Use of less polar aromatic hydrocarbons such as benzene and toluene as the solvent, **2.14g** was obtained in 81% and 75% yield, respectively (entries 7–8). When catalyst loading was lowered to 5.0 mol% in benzene, **2.14g** was obtained with high selectivity (<5% of **2.15g**) and in >95% yield (entry 9). The unique reactivity of $B(C_6F_5)_3$ has been demonstrated by the control experiments where less hindered BF_3•OEt_2 or less acidic BPh_3 proved to be ineffective (entries 10–11). These results are in line with our hypothesis that

strongly Lewis acidic and hindered $B(C_6F_5)_3$, along with sterically demanding and electron-rich *N*-alkylamines, represent the most effective catalyst/substrate combination.

With the optimal reaction conditions, we evaluated various *N*-alkylamines in the reaction with siliconenolate **2.11** (Table 2.3). With 5.0 mol% $B(C_6F_5)_3$, *N*,*N*-dimethyl-substituted **2.13g** afforded **2.14g** in 80% yield. *N*-Benzyl and *N*-cyclopropylmethyl-substituted anilines, **2.13i** and **2.13j**, gave the corresponding products in 64% and 56% yield, respectively. In these instances, α-amino methylene C–H bonds remained intact. α-Amino C–H bond of *N*-arylpyrrolidine **2.13k** was converted to a C–C bond by the use of 10 mol% $B(C_6F_5)_3$, affording **2.14k** in 90% yield. An

Table 2.3. Evaluation of *N*-Alkylamines[a,b]

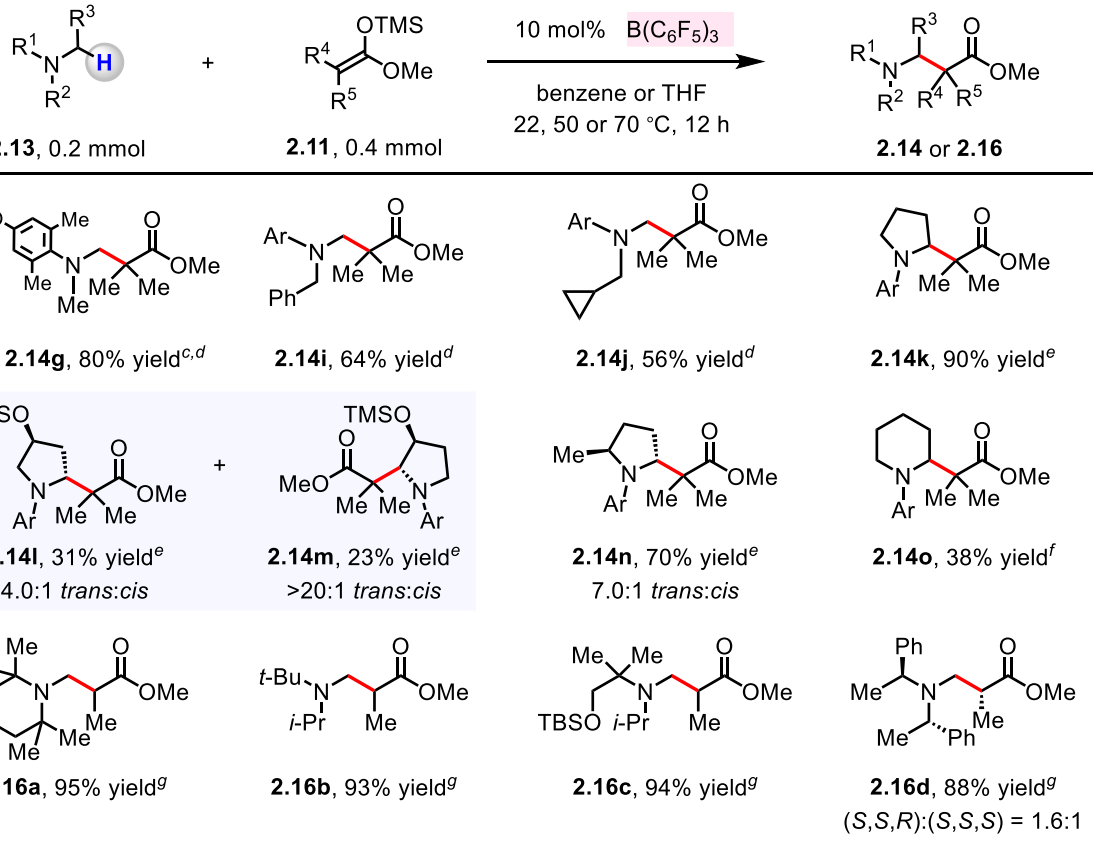

[a]Conditions: *N*,*N*-dialkylaniline (0.2 mmol), 1-methoxy-2-methyl-1-(trimethylsiloxy)propene (0.4 mmol), $B(C_6F_5)_3$, solvent (0.5 mL), under N_2, 22 °C, 12 h. [b] Yield of purified products. [c] $B(C_6F_5)_3$ (5.0 mol %) was used. [d] Benzene (0.5 mL) was used. [e] THF (0.5 mL) was used. [f] $B(C_6F_5)_3$ (10 mol%) and benzene (0.5 mL) were used and reaction was performed at 50 °C. [g] Benzene (0.5 mL) was used and reaction was performed at 70 °C.

unprotected hydroxyl group was tolerated in this reaction as 1-(4-Methoxy-2,6-dimethylphenyl)pyrrolidin-3-ol (**2.13l**), provided the α-alkylated products in their *O*-silylated forms of **2.14l** (31% yield, 4.0:1 *trans*:*cis*) and **2.14m** (23% yield, >20:1 *trans*:*cis*).[17] Reaction of α-methyl-substituted pyrrolidine furnished **2.14n** in 70% yield with *trans*:*cis* of 7.0:1. *N*-arylpiperidine **2.13o** was also a suitable substrate and **2.14o** was isolated in 38% yield with the elevated reaction temperature of 50 °C. *N*-aryl group was not a requirement as an array of trialkylamines were efficiently coupled with ((1-methoxyprop-1-en-1-yl)oxy)trimethylsilane (**2.11b**), leading to the formation of **2.16a**–**2.16d** (88%–95% yield). Reaction of methyl (*S*)-3-(bis((*S*)-1-phenylethyl)amino)-2-methylpropanoate with **2.11b** delivered **2.16d** as a 1.6:1 mixture of diastereomers, which were separated after flash silica gel column chromatography, providing the enantiomerically pure α-amino esters.

Then we moved on to the evaluation of various silicon enolates in the reaction with aniline (Table 2.4). Cyclopentyl- and cyclohexyl-substituted substrates reacted with **2.13g** to afford **2.14p** and **2.14q** in 73% and 79% yield, respectively. The less sterically hindered ketene acetal **2.11b** furnished **2.14r** in 66% yield. A broader range of ketene acetals proved to be applicable to reactions with *N*-arylpyrrolidine **2.13k**. α-Cycloalkylesters and methyl propionate could be incorporated, furnishing the corresponding 2-substituted pyrrolidine products **2.14s**–**2.14u** in 60% to >95% yield. Nucleophilic species derived from 3-methyldihydrofuran-2(3*H*)-one was found to be compatible and provided **2.14v** in 70% yield with 1.3:1 dr. In addition to silyl ketene acetals, trimethyl((1-(methylthio)vinyl)oxy)silane can give β-amino thioester **2.14w** (52% yield).

[17] After isolation by silica gel column chromatography, **2.14l** and **2.14m** were treated with an aqueous solution of 4.0 N HCl and characterized as their corresponding non-silylated compounds. See Section 2.7 for details.

Table 2.4. Evaluation of Various Silicon Enolates[a,b]

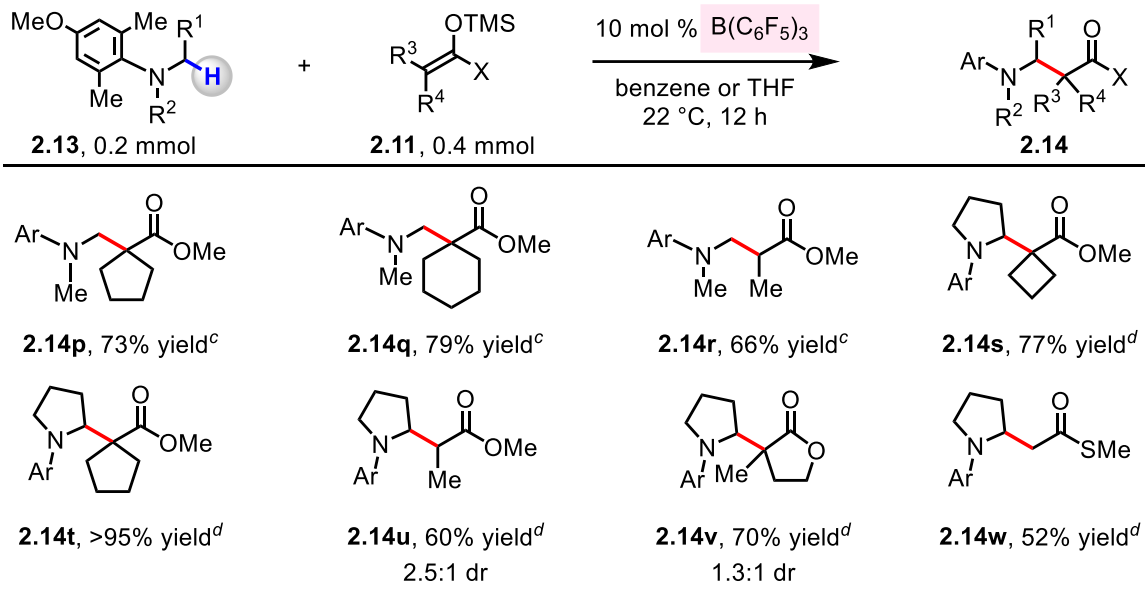

[a] Conditions: *N,N*-dialkylaniline (0.2 mmol), silicon enolate (0.4 mmol), $B(C_6F_5)_3$ (10 mol %), solvent, under N_2, 22 °C, 12 h. [b] Yield of purified products. [c] Benzene (0.5 mL) was used. [d] THF (0.5 mL) was used.

The catalytic protocol is scalable, as shown by the reaction of **2.13k** performed on a 1.0 mmol scale (Scheme 2.7). The *α*-alkylated product **2.14k** was obtained in 95% yield by the use of 5.0 mol% $B(C_6F_5)_3$. The 4-methoxy-2,6-dimethylphenyl group of **2.14k** could be readily removed under oxidative conditions to provide **2.19** in 97% yield.

Scheme 2.7. Scale-up Synthesis and Removal of *N*-Aryl Group

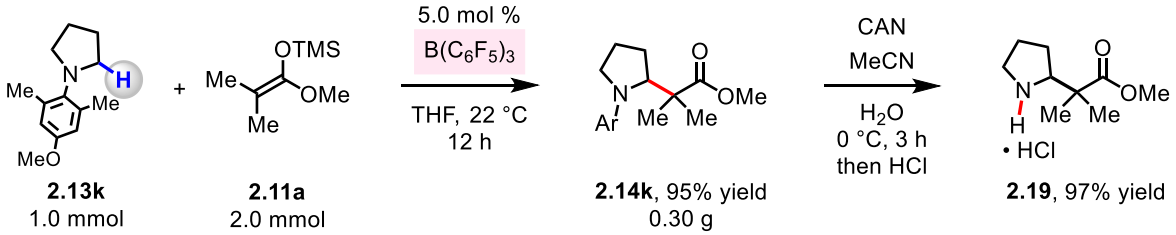

The utility of this method was demonstrated through the late-stage modification of bioactive *N*-alkylamines such as citalopram (antidepressant), atomoxetine (treatment for ADHD), and fluoxetine (antidepressant) (Table 2.5). *N*-Methyl C–H bonds of these drug compounds were

selectively functionalized to C–C bonds to afford synthetically useful amount of β-amino carbonyl compounds **2.18a** (23% yield, 0.30 g), **2.18b** (25% yield, 92 mg), and **2.18c** (27% yield, 113 mg).

Table 2.5. Late-Stage Functionalization of Bioactive Amines.

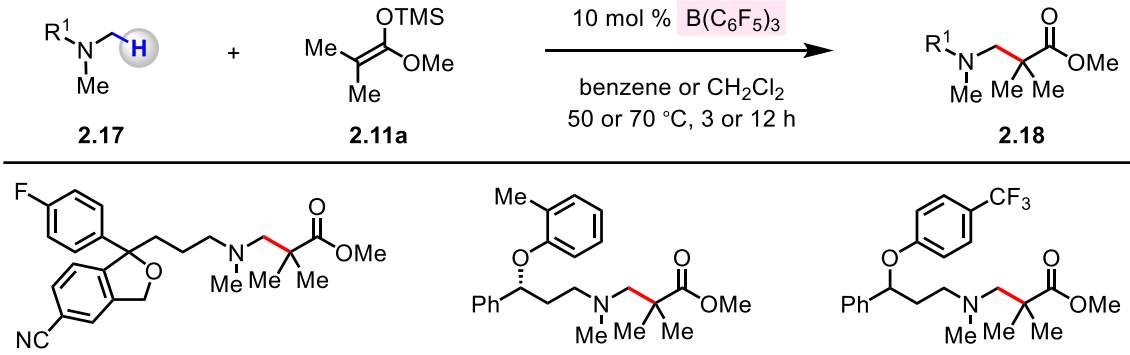

2.18a, **citalopram derivative**
0.30 g, 23% yield
(from 3.0 mmol of **2.17a**)

2.18b, **atomoxetine derivative**
92 mg, 25% yield
(from 1.0 mmol of **2.17b**)

2.18c, **fluoxetine derivative**
113 mg, 27% yield
(from 1.0 mmol of **2.17c**)

In summary, we have developed a catalytic protocol for the Mannich-type reaction of *N*-alkylamines catalyzed by $B(C_6F_5)_3$ in order to generate various β-amino carbonyl compounds. This method is applicable to the late-stage functionalization of various N-containing pharmaceuticals that contain α-C–H bonds. On the basis of our mechanistic hypotheses, development of an enantioselective variant of this transformation should be possible through the design of chiral Lewis acid catalysts.

2.5. Union of *N*-Alkylamines and α,β-Unsaturated Compounds Through Cooperative Action of Chiral and Achiral Lewis Acid Catalysts

Having demonstrated that $B(C_6F_5)_3$ can promote α-C–H alkylation of *N*-alkylamines via iminium ion through hydride abstraction, we envisioned the development of an enantioselective transformation based on this study. We first hypothesized that a chiral organoborane might be able to catalyze hydride abstraction from amine and the subsequent enantioselective C–C bond formation. However, when we prepared and evaluated chiral borane catalysts[18] for the union of **2.13k** and **2.11a**, no desired product (**2.14k**) was obtained (Scheme 2.8).

Scheme 2.8. Evaluation of chiral borane catalyst

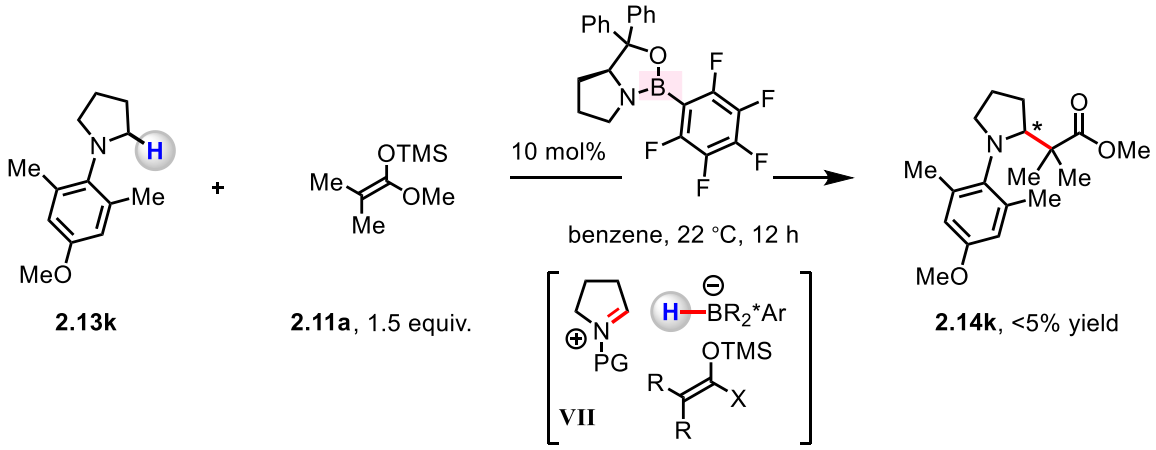

We postulated that the chiral organoboranes we evaluated were either not potent enough to abstract hydride from amine **2.13k**, or not sufficiently hindered to overcome acid–base complexation with the amine substrate. Furthermore, even if hydride abstraction from **2.13k** could take place to generate intermediate **VII**, it would be challenging to control the enantioselectivity by the in situ generated chiral borohydride, which is ionically bond to the iminium.[19]

[18] (a) Corey, E. J.; Helal, C. J. *Angew. Chem., Int. Ed*. **1998**, *37*, 1986–2012. (b) Meng, W.; Feng, X.; Du, H. *Acc. Chem. Res*. **2018**, *51*, 191–201.
[19] Brak, K.; Jacobsen, E. N. *Angew. Chem., Int. Ed*. **2013**, *52*, 534–561.

Since the approach utilizing chiral organoboranes for promoting the α-alkylation of amines was not successful, we envisioned the use of a chiral Lewis acid co-catalyst in combination with $B(C_6F_5)_3$. The cooperative catalyst system could enable the activation of both coupling partners and in situ generate the electrophilic and nucleophilic species, thus circumventing the wasteful pre-activation step. Furthermore, cooperative catalysts could enhance the reaction rate by bringing both nucleophilic and electrophilic coupling partners in close proximity. However, there are fundamental challenges that need to be overcome. Specifically, mutual quenching between acidic and basic components in an electrophile, a nucleophile, and catalysts might be problematic. To circumvent the acid–base complexation, a combination that exhibits high affinity (i.e., hard–hard or soft–soft pairing) are often avoided. Therefore, the existing cooperative catalyst systems have been limited to transformations involving weakly to moderately acidic and/or basic promoters, which confines the substrate scope to highly acid- or base-sensitive molecules. Development of potent cooperative two-catalyst systems that could overcome mutual quenching and facilitate reactions between otherwise inert substrates is an important unresolved problem in enantioselective catalysis.

To develop a catalytic protocol for enantioselective union of *N*-alkylamines and carbon-based nucleophiles, we envisioned the use of two independent Lewis acid catalysts for accomplishing separate tasks (Scheme 2.9). We premised that $B(C_6F_5)_3$ could abstract a hydride from amine **2.13** to generate an ion pair of borohydride and an iminium ion (**VIII**). Meanwhile, a chiral Lewis acid co-catalyst could activate the α,β-unsaturated compound (**2.20→IX**) to facilitate the borohydride reduction (**X**), furnishing the chiral enolate (**XI**). An ensuing stereoselective C–C bond forming reaction between the iminium ion and the enantio-enriched enolate would afford a β-amino carbonyl product (**2.21**).

Scheme 2.9. Proposed Catalytic Cycle for Cooperative Catalyst System

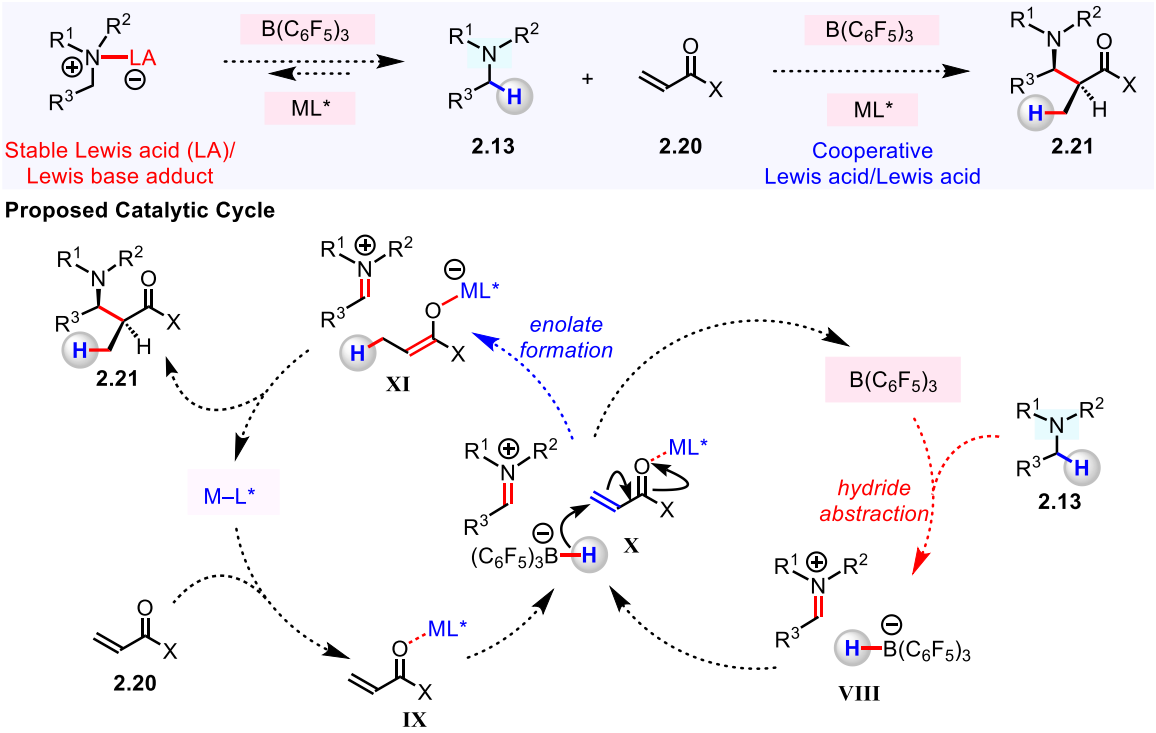

A major advantage of the proposed approach is that by evaluating various combinations of Lewis acids and chiral ligands, the reaction efficiency and stereoselectivity may be easily optimized (vs bifunctional catalysts that require tethering of different catalytic sites). To achieve this, the untethered Lewis acid catalysts must perform independently to activate each coupling partner without overlapping functions, as otherwise, stereoselectivity would suffer from the racemic background reaction.[20] The functionally similar $B(C_6F_5)_3$ and a chiral Lewis acid co-catalyst promoted enantioselective union of *N*-alkylamines and various α,β-unsaturated compounds is presented herein.

We first investigated whether a single Lewis acid $B(C_6F_5)_3$ can activate both coupling partners (Scheme 2.9, M–L* = $B(C_6F_5)_3$) to promote the Mannich-type reaction between N-

[20] Manville, N.; Alite, H.; Haeffner, F.; Hoveyda, A. H.; Snapper, M. L. *Nat. Chem.* **2013**, *5*, 768–774.

alkylamines and the α,β-unsaturated compounds (Table 2.6). The reaction between **2.13k** and **2.20a** in the presence of 5.0 mol% $B(C_6F_5)_3$ afforded **2.21a** in >95% yield as a separable mixture of diastereomers (entry 1, *anti*:*syn* = 2.3:1, Table 2.6). The di-substituted product **2.22** was obtained in less than 5% yield. In ethereal solvents, Et_2O and THF, **2.21a** was formed in 94% and 26% yield, respectively (entries 2–3). When the reaction was carried out in a relatively non-polar aromatic hydrocarbon, such as toluene and benzene, **2.21a** was obtained in 81% and >95% yield (entries 4–5); notably, **2.21a** was isolated in >95% yield in benzene in just 30 minutes (entry 6). When the catalyst loading was lowered to 2.5 mol%, longer reaction time was needed (48 h, **2.21a** in 84% yield; entry 7).[21] None of the desired product was formed in the absence of $B(C_6F_5)_3$ (entry

Table 2.6. Evaluation of Reaction Parameters

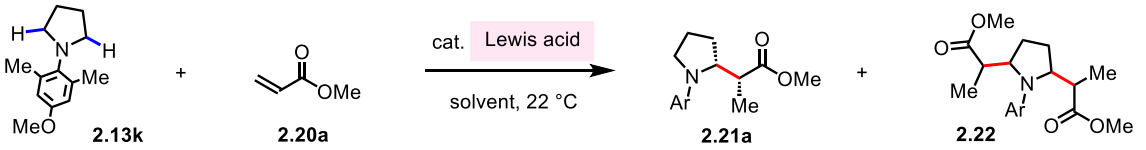

entry	Lewis acid	(mol%)	solvent	reaction time (h)	yield (%), *anti*:*syn* **2.21a**	yield (%) **2.22**
1	$B(C_6F_5)_3$	5.0	CH_2Cl_2	12	>95, 2.3:1	<5
2	$B(C_6F_5)_3$	5.0	Et_2O	12	94, 2.3:1	<5
3	$B(C_6F_5)_3$	5.0	THF	12	26, 1.9:1	<5
4	$B(C_6F_5)_3$	5.0	Toluene	12	81, 2.4:1	5
5	$B(C_6F_5)_3$	5.0	Benzene	12	>95, 2.4:1	<5
6	$B(C_6F_5)_3$	5.0	Benzene	0.5	>95, 2.4:1	<5
7	$B(C_6F_5)_3$	2.5	Benzene	48	84, 1.7:1	<5
8	none	0	Benzene	12	0	0
9	BF_3•OEt_2	5.0	Benzene	12	0	0
10	BPh_3	5.0	Benzene	12	0	0

[a] Conditions: 1-(4-Methoxy-2,6-dimethylphenyl)pyrrolidine (0.2 mmol), methyl acrylate (0.3 mmol), Lewis acid, solvent (0.3 mL), under N_2, 22 °C. [b] Yields were determined by ^{1}H NMR analysis of unpurified product mixtures with mesitylene as the internal standard. See Section 2.7 for details.

[21] The significant difference in reaction rate observed when the loading of $B(C_6F_5)_3$ is lowered from 5.0 mol% to 2.5 mol% suggests that the mechanism of the reaction proposed in Scheme 2.9 is not the complete picture. Formations of aggregates or other pre-organized states requiring multiple equivalents of $B(C_6F_5)_3$ or substrate may be involved. Kinetic and spectroscopic studies exhibited higher order dependence with respect to $B(C_6F_5)_3$ (see Section 2.7 for details).

8), or when the less hindered BF_3•OEt_2 or the less acidic BPh_3 were used (entries 9–10). These results are consistent with our hypothesis that hindered and highly acidic $B(C_6F_5)_3$ and sterically demanding and electron-rich *N*-alkylamines represent the most effective catalyst and substrate combination.

With the optimal reaction conditions, we evaluated the scope of the pronucleophiles using **2.13k** as the amine substrate to generate the corresponding *β*-amino carbonyl compounds (**2.21a**–**2.21h**, Table 2.7). The reaction with methyl acrylate (**2.20a**) and benzyl acrylate (**2.20b**) afforded **2.21a** and 2.21b in 97% and 91% yield, respectively. Isopropyl acrylate (**2.20c**) gave **2.21c** in 78% yield, while a more hindered *tert*-butyl acrylate did not afford the desired product. This result suggests that $B(C_6F_5)_3$ may not be capable of coordinating to more sterically encumbered acrylates. The less electrophilic thioacrylate (**2.20d**) was also suitable substrate, affording **2.21d** in 53% yield, and the use of acrylonitrile (**2.20e**) furnished **2.21e** in 50% yield. An *α*-quaternary carbon center-containing **2.21f** was obtained in 97% yield using methyl methacrylate (**2.20f**). With dimethyl acetylenedicarboxylate (**2.20g**), which can be converted to an allenolate nucleophile *in situ*, **2.21g** was furnished in 52% yield as a separable mixture of *E* and *Z* isomers (1:1.6). The use of *N*-phenylmaleimide (**2.20h**) furnished **2.21h** in >95% yield.

We then evaluated an array of cyclic and acyclic *N*-alkylamines. It was found that 3,3-dimethyl, 3-((*tert*-butyldimethylsilyl)oxy)-substituted *N*-aryl pyrrolidines (**2.13t** and **2.13u**), *N*-aryl piperidine (**2.13o**) and *N*-aryl azepane (**2.13v**) gave the corresponding products (**2.21i**–**2.21l**) in 63% to 95% yield. An acyclic 4-methoxy-*N,N*,2,6-tetramethylaniline (**2.13g**) can react with *N*-phenylmaleimide to provide **2.21m** in 62% yield. Trialkyl-substituted amines that lack the fused *N*-aryl group also underwent efficient transformation and were coupled with acrylates, leading to the formation of **2.21n**–**2.21p** (91% yield). The use of (*R*)-*N*-methyl-1-phenyl-*N*-((*R*)-1-

Table 2.7. Coupling of *N*-alkylamines and α,β-unsaturated compounds through $B(C_6F_5)_3$-catalyzed hydride abstraction

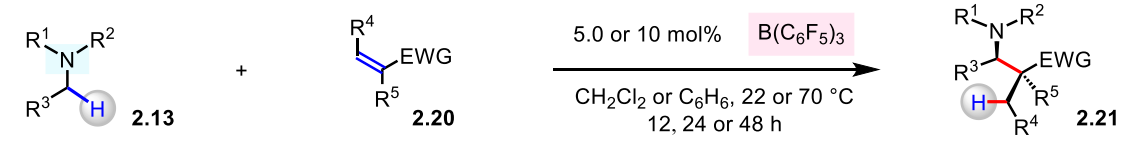

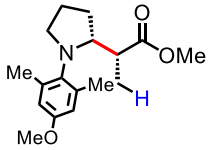

2.21a, 97% yield*
2.3:1 *anti*:*syn*

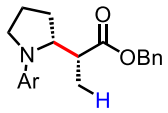

2.21b, 91% yield*
2.5:1 *anti*:*syn*

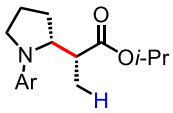

2.21c, 78% yield*
2.1:1 *anti*:*syn*

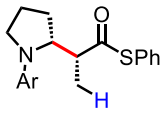

2.21d, 53% yield*
1.8:1 *anti*:*syn*

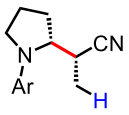

2.21e, 50% yield†
1.3:1 *anti*:*syn*

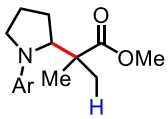

2.21f, 97% yield*

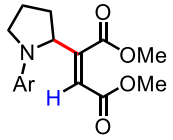

2.21g, 52% yield*
E:*Z* = 1:1.6

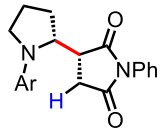

2.21h, 99% yield*
4.5:1 *anti*:*syn*

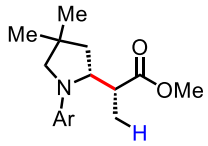

2.21i, 95% yield*
3.0:1 *anti*:*syn*

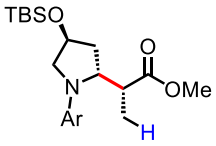

2.21j, 82% yield*
6.9:5.9:3.0:1 d.r.

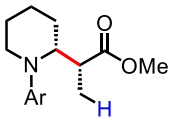

2.21k, 63% yield*
10:1 *anti*:*syn*

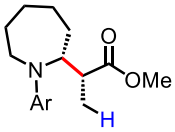

2.21l, 66% yield*
2.0:1 *anti*:*syn*

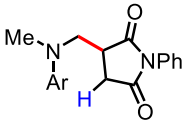

2.21m, 62% yield†

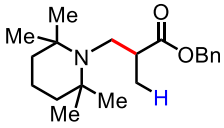

2.21n, 91% yield†

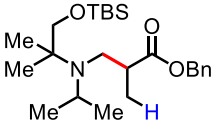

2.21o, 91% yield†

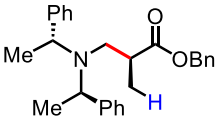

2.21p, 91% yield†
(*R*,*S*):(*R*,*R*) = 1.5:1

The values correspond to yields of isolated and purified products. Diastereomeric ratio (dr) values were determined by analysis of the unpurified product mixture through analysis of ^{1}H NMR spectra. *5.0 mol% of $B(C_6F_5)_3$ was used. † 10 mol% of $B(C_6F_5)_3$ was used. See Section 2.7 for details.

phenylethyl)ethan-1-amine (**2.13w**) with benzyl acrylate (**2.20b**) delivered **2.21p** as a 1.5:1 mixture of diastereomers which were separated through flash silica gel column chromatography to afford enantiomerically pure isomers.

Having demonstrated that $B(C_6F_5)_3$ is capable of generating both electrophilic and nucleophilic species *in situ*, we envisioned the incorporation of a chiral Lewis acid co-catalyst for

enantioselective transformation. With *N*-arylpyrrolidine **2.13k** and 3-acryloyloxazolidin-2-one **2.23a** as model substrates, we evaluated various combinations of Lewis acid and chiral ligands to find out that 10 mol% of $B(C_6F_5)_3$ and $(TfO)_2Mg$–**L1** can promote the coupling reaction affording **2.24a** in >95% yield with modest er of 80:20 and 68:32 for *anti* (major) and *syn* isomers, respectively (Scheme 2.10a). Control experiments with 10 mol% $B(C_6F_5)_3$ as the only catalyst demonstrated that $B(C_6F_5)_3$ not only promotes the desired hydride abstraction from amine **2.13k** but also activates the α,β-unsaturated *N*-acyloxazolidinone **2.23a** (**XIII**), providing ***rac*-2.24a** in 35% yield. To discourage carbonyl activation by the achiral co-catalyst $B(C_6F_5)_3$ (**XIII**), favoring

Scheme 2.10. Effect of Chiral Lewis Acid Co-catalysts on Enantioselective Coupling of an *N*-Alkylamine and *N*-Acryloyloxazolidinones

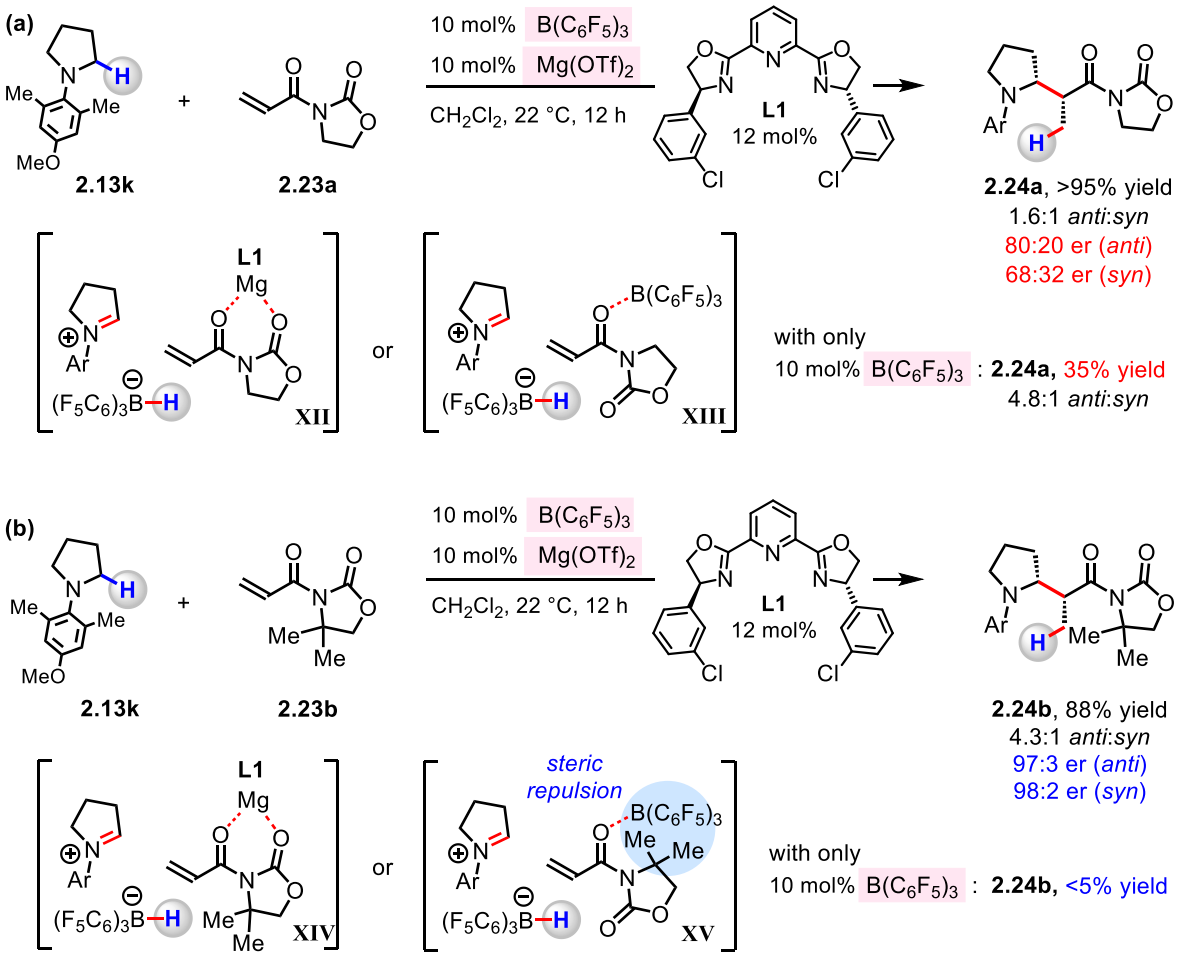

the involvement of **XII**, dimethyl oxazolidinone containing Michael acceptor **2.23b** was used in order to minimize the extent to which intermediates such as **XV** are formed (Scheme 2.10b). Indeed, the racemic background reaction was suppressed as ***rac*-2.24b** was produced in <5% yield with 10 mol% $B(C_6F_5)_3$ as the only catalyst, and **2.24b** was obtained in 88% yield with significantly improved enantioselectivity of up to 98:2 er.

Having identified that the use of a dimethyl oxazolidinone can suppress $(F_5C_6)_3B$-activation of α,β-unsaturated compound (Scheme 2.10b), other alkyl or aryl substituted oxazolidinones were evaluated with $B(C_6F_5)_3$ and $Mg(OTf)_2$/**L1** as the optimal catalyst combination (Table 2.8). Compared to dihydrogen- or dimethyl-substituted oxazolidinone-containing product, cyclohexyl-substituted **2.24c** was obtained with improved *anti*:*syn* ratio of 5.6:1. The enantiomerically pure *N*-acryloyloxazolidinones containing benzyl (**2.23d**) or phenyl

Table 2.8. Evaluation of Different Oxazolidinone Substrates

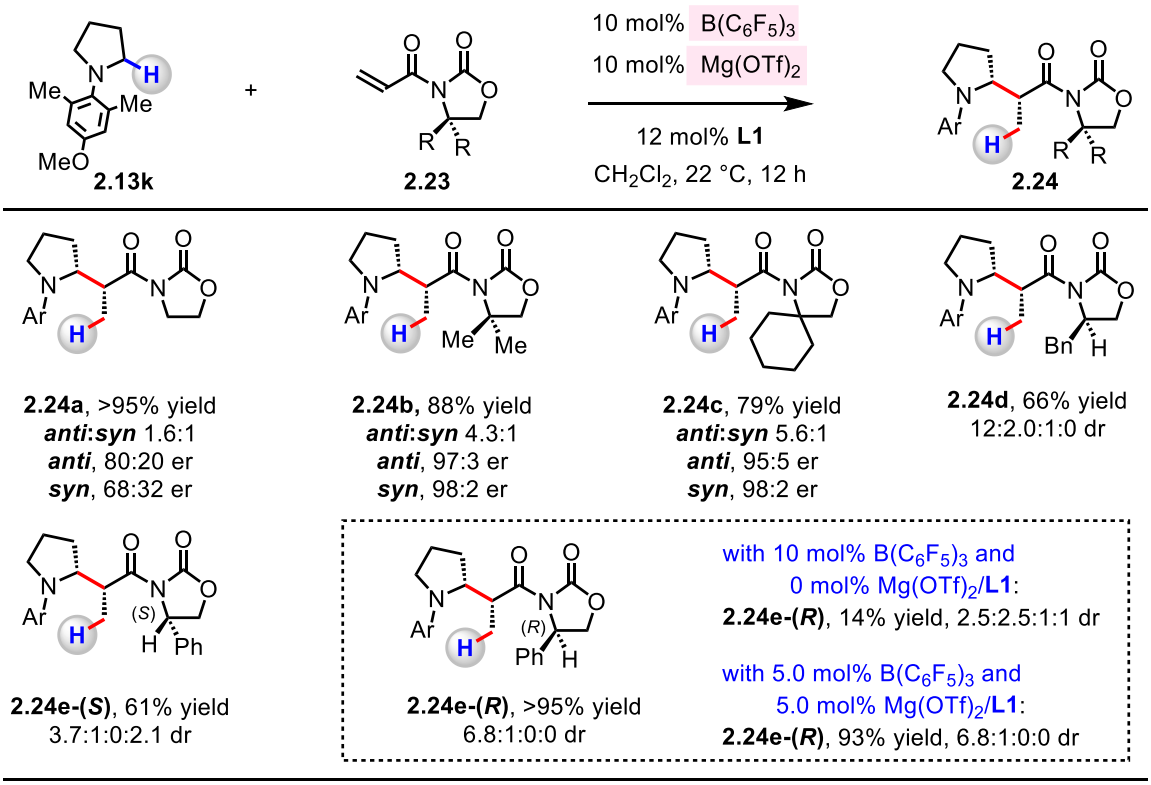

(**2.23e-(*S*)**, **2.23e-(*R*)**) moieties also underwent efficient reaction. (*R*)-3-Acryloyl-4-phenyloxazolidin-2-one (**2.23e-(*R*)**) represents the "matched" enantiomer with $Mg(OTf)_2$/**L1** combination to afford **2.24e-(*R*)** in >95% yield and 6.8:1:0:0 dr. When mismatching **2.23e-(*S*)** was used, **2.24e-(*S*)** was obtained in diminished yield and diastereoselectivity (61% yield, 3.7:1:0:2.1 dr). The use of the chiral co-catalyst in the diastereoselective reactions was important for both efficiency and stereoselectivity, as **2.24e-(*R*)** was produced in just 14% yield and 2.5:2.5:1:1 dr in its absence. When catalyst loadings of $B(C_6F_5)_3$ and $Mg(OTf)_2$/**L1** were reduced to 5.0 mol%, **2.24e-(*R*)** was obtained in comparable yield of 93% with retained diastereoselectivity.

This catalytic process is scalable; for instance, 5.0 mmol of **2.13k** was converted to **2.24e-(*R*)** in 6.7:1:0:0 dr (>95% conv.; Scheme 2.11a). The enantio-enriched diastereomers were isolated by flash silica gel column chromatography to afford the major isomer in 1.47 g (70% yield; minor diastereomer: 0.16 g, 8% yield). The major diastereomer was then converted to corresponding *β*-

Scheme 2.11. Synthesis of Enantio-enriched *α*-Substituted Amines

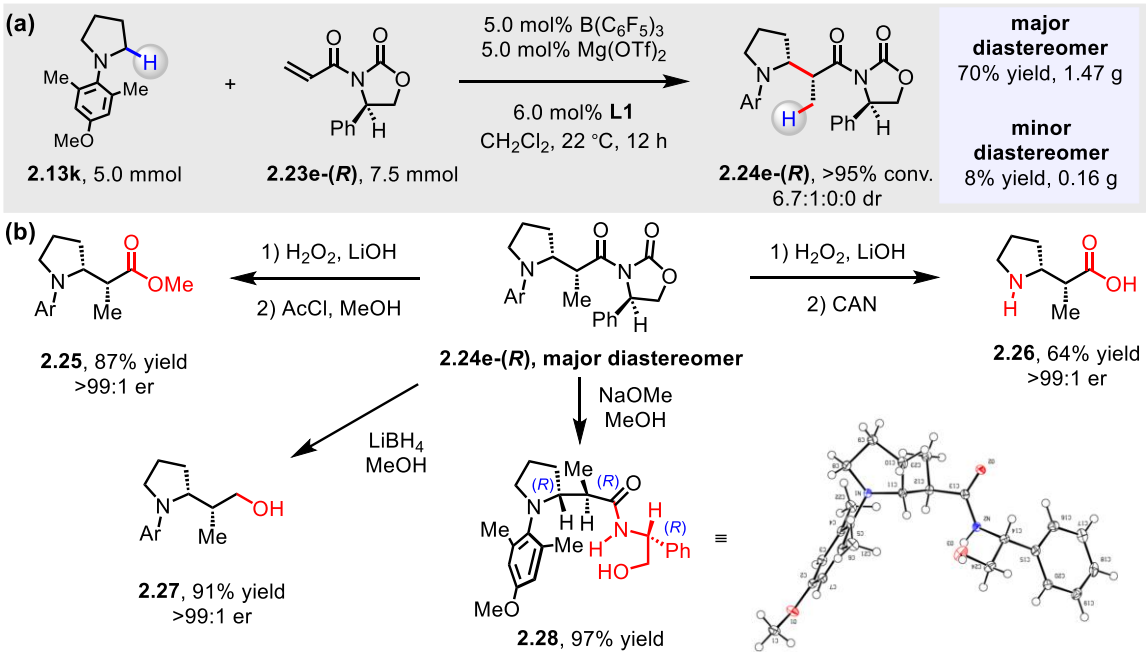

amino ester (**2.25**), *β*-amino acid (**2.26**), and *β*-amino alcohol (**2.27**) in 64–91% yield without erosion of er (Scheme 2.11b). Furthermore, by treating the major diastereomer of **2.24e-(*R*)** with NaOMe in methanol, **2.28** was obtained in 97% yield, which was analyzed by X-ray crystallography to reveal its absolute configuration to be (*R*,*R*,*R*).[22]

We applied this method for the synthesis of various enantiomerically enriched *N*-alkylamines (Table 2.9). Upon flash silica gel column chromatography, the diastereomers were converted into the corresponding benzyl ester (**2.29**), and HPLC analysis revealed that **2.24f**–**2.24h** were enantiopure isomers (>99:1 er). *N*-Substituted pyrrolidines were reacted with 3-acryloyl-4,4-

Table 2.9. Evaluation of *N*-Alkylamines

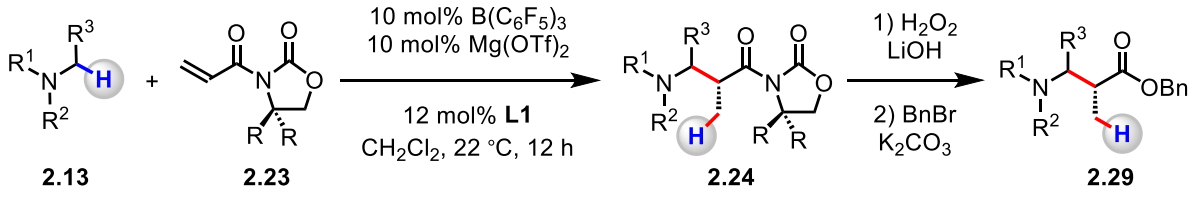

2.13 **2.23** **2.24** **2.29**

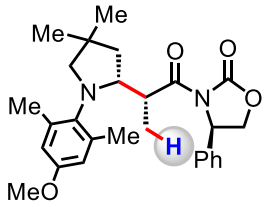

2.24f-major
58% yield, >99:1 er
2.24f-minor
17% yield, >99:1 er

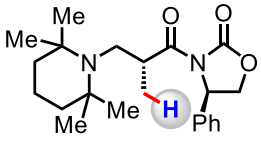

2.24g-major
47% yield, >99:1 er
2.24g-minor
24% yield, >99:1 er

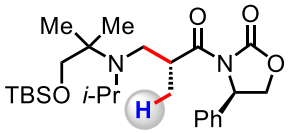

2.24h-major
74% yield, >99:1 er
2.24h-minor
10% yield, >99:1 er

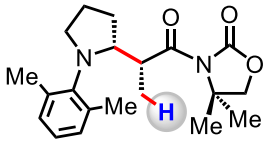

2.24i-*anti*
56% yield, 95:5 er
2.24i-*syn*
15% yield, 97:3 er

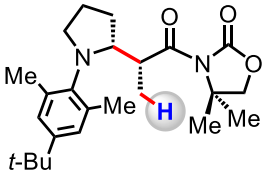

2.24j-*anti*
57% yield, 98:2 er
2.24j-*syn*
13% yield, 99:1 er

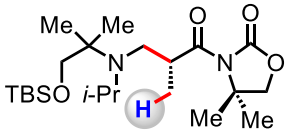

2.24k
46% yield, 95:5 er

[22] The absolute configuration of the minor diastereomer was determined as (*R*)-*N*-((*R*)-2-hydroxy-1-phenylethyl)-2-((*S*)-1-(4-methoxy-2,6-dimethylphenyl)pyrrolidin-2-yl)propanamide. See Section 2.7 for further details.

dimethyloxazolidin-2-one (**2.23b**) in the presence of catalytic amounts of $B(C_6F_5)_3$ and $Mg(OTf)_2$/**L1** to give *β*-amino carbonyl product **2.24i** and **2.24j** in 71% and 70% overall yield, respectively. An increase in enantioselectivity for both diastereomers was observed with more sterically hindered *para*-*t*-Bu-substituted **2.24j** (98:2 er (**2.24j-*anti***) and 99:1 er (**2.24j-*syn***)) compared to *para*-H-substituted **2.24i** (95:5 er (**2.24i-*anti***) and 97:3 er (**2.24i-*syn***)). Sterically congested trialkylamines such as **2.13r** also reacted with **2.23b** to afford **2.24k** in 46% yield with 95:5 er.

A stereochemical model for reaction of the *in situ* generated iminium ion with the **L1**–Mg–enolate complex was developed by density functional theory (DFT) studies (Figure 2.1).[23]

Figure 2.1. Stereochemical models to account for the observed sense of stereoselectivity.

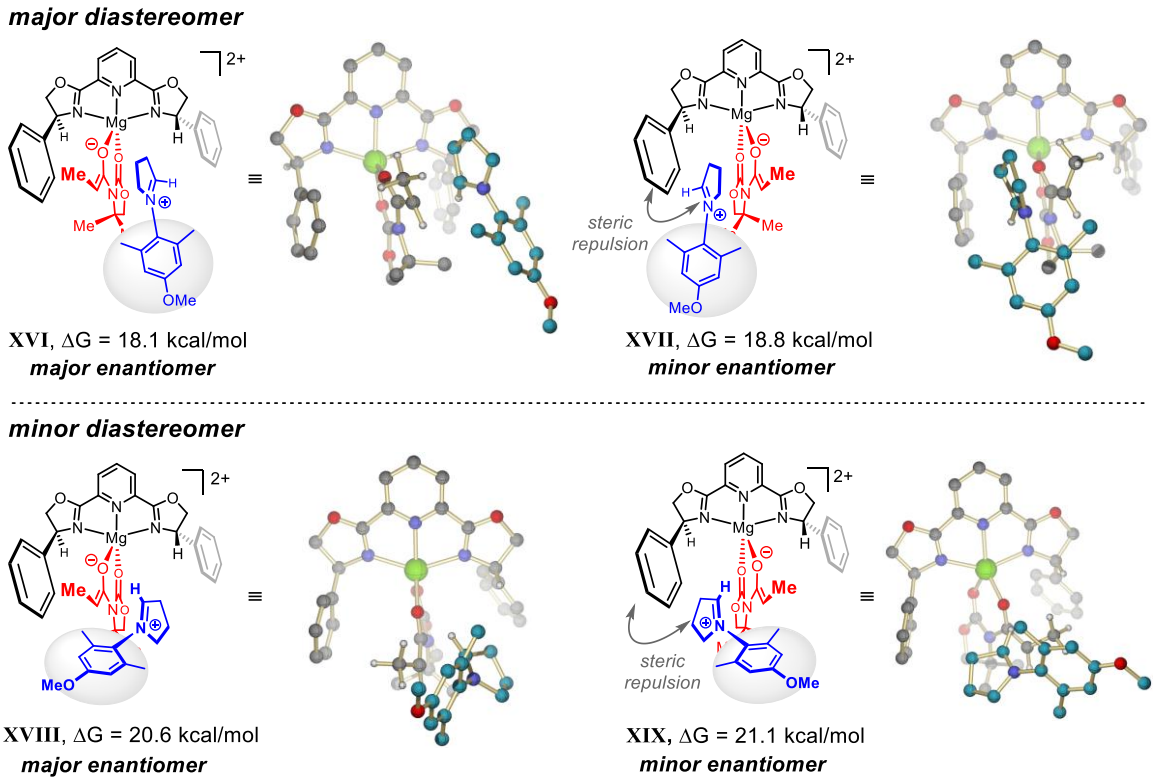

[23] Stereochemical model for reaction of **L3**–Mg–enolate complex with iminium ion; DFT studies were performed at the PBE0-D3BJ/def2TZVPP//M06L/DF-def2SVP level of theory in CH_2Cl_2 (SMD solvation model). See Section 2.7 for details. Abbreviations: **L3**, PyBOX ligand; SMD, solvation model based on density; ΔΔEdisp = ΔΔE(PBE0-D3BJ) – ΔΔE(PBE0).

These investigations suggest that the enantiomers of the major diastereomer are generated via **XVI** and **XVII** (ΔG = 18.1 and 18.8 kcal/mol, respectively), while the enantiomers of the minor diastereomer are probably formed via **XVIII** and **XIX** (ΔG = 20.6 and 21.1 kcal/mol respectively). High enantioselectivity for the major as well as the minor diastereomer is due to effective blocking of the *re* face of the Mg–enolate by steric repulsion (**XVII** and **XIX**). Nonetheless, we should note that highly accurate modeling of diastereoselectivity is difficult, and depends strongly on attenuation of dispersion interactions in solution.[24,25] It is possible that modes other than **XVI** and **XVIII** might similarly contribute to formation of the minor diastereomer (see Section 2.7 for details).

[24] Yang, L.; Adam, C.; Nichol, G. S.; Cockroft, S. L. *Nat. Chem*. **2013**, *5*, 1006–1010.
[25] Pollice, R.; Bot, M.; Kobylianskii, I. J.; Shenderovich, I.; Chen, P. *J. Am. Chem. Soc.* **2017**, *139*, 13126–13140.

2.6. Conclusions and Future Outlook

To summarize, we have developed a catalytic protocol for efficient and stereoselective Mannich-type reaction through the cooperative action of seemingly competitive Lewis acid catalysts, $B(C_6F_5)_3$ and a chiral Mg–PyBOX complex. We discovered that by proper tuning of structurally and electronically different Lewis acids and substrates, the ability of chiral and achiral Lewis acid catalysts to serve as a hydride acceptor from amines, or an activator of α,β-unsaturated compounds, can be adjusted. Therefore, enantioselective Mannich-type reactions between amines and α,β-unsaturated compounds were achieved without loss in enantioselectivity arising from any undesirable mode of activation by the achiral Lewis acid $B(C_6F_5)_3$.

The principles established in this work served as a conceptual framework for the development of transformations that demand independently operational Lewis acidic co-catalysts that may have overlapping functions. Based on this study, our group recently developed a catalytic protocol for enantioselective synthesis of *N*-propargylamines through α-amino C–H functionalization (Scheme 2.12).[26] This process is promoted through the concerted action of seemingly competitive Lewis acids, $B(C_6F_5)_3$ and a chiral organocopper complex. The reaction of *N*-alkylamine **2.13k** and trimethylsilylacetylene **2.29** with 10 mol% of $B(C_6F_5)_3$, a chiral Cu-based complex, and 1.0 equivalent of Ph_3COH afforded **2.30** in 75% yield with 95:5 er. Studies aimed at expanding the scope of hydride donors and pro-nucleophiles to achieve the late-stage regio- and stereo-selective α-amino C–H functionalization of bioactive compounds are currently ongoing in our laboratory.

[26] Chan, J. Z.; Yesilcimen, A.; Cao, M.; Zhang, Y.; Zhang, B.; Wasa, M. *J. Am. Chem. Soc.* **2020**, *142*, 16493–16505.

Scheme 2.12. Enantioselective α-Amino C–H Functionalization by $B(C_6F_5)_3$ and Cu–PyBOX

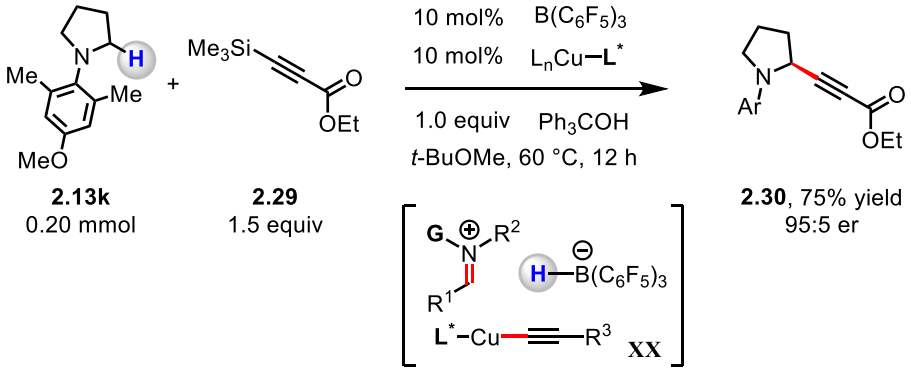

2.13k
0.20 mmol

2.29
1.5 equiv

2.30, 75% yield
95:5 er

Chapter Three

β-C–H Functionalization of *N*-Alkylamines through Cooperative Action of Lewis Acid and Brønsted Base Catalysts

3.1. Introduction

Despite the recent advances in activation of C–H bonds in *N*-alkylamines (**3.1**), catalytic strategies to functionalize *β*-amino C–H bonds remain underdeveloped, particularly in an enantioselective manner (Scheme 3.1).[1-2] One of the reason for this is that N-directed L_nPd-catalyzed *β*-amino C–H activation requires the formation of a strained four-membered

Scheme 3.1. Challenges Associated with *β*-Amino C–H Functionalization

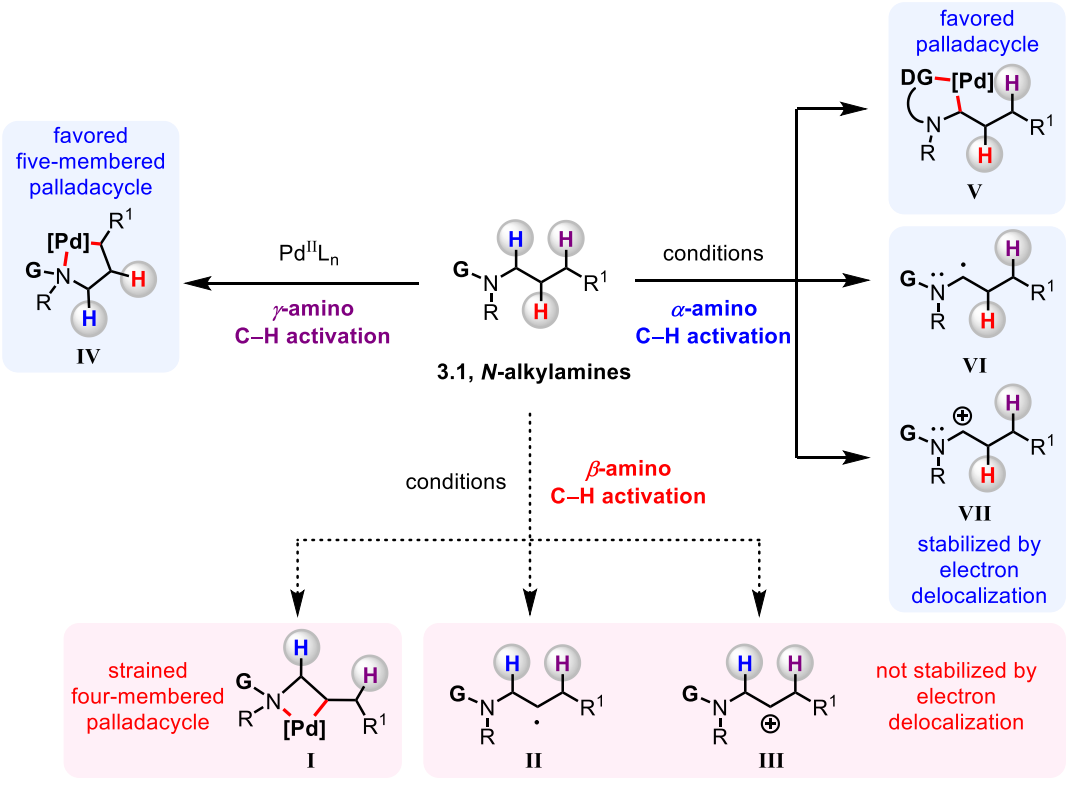

[1] (a) He, C.; Whitehurst, W. G.; Gaunt, M. J. *Chem*. **2019**, *5*, 1031−1058. (b) Trowbridge, A.; Walton, S. M.; Gaunt, M. J. *Chem. Rev*. **2020**, *120*, 2613−2692.
[2] Ohno, S.; Miyoshi, M.; Murai, K.; Arisawa, M. *Synthesis* **2021**, doi: 10.1055/a-1483-4575.

palladacycle **I** (vs a more favorable five-membered palladacycle **IV** formed by γ-amino C–H activation).[1] Moreover, the radical **II** or cationic intermediates **III** generated through activating β-amino C–H bonds are not stabilized by hyperconjugation (vs α-amino radical **VI** or carbocation **VII** generated by α-amino C–H activation) and thus are not readily accessible. Accordingly, the development of a general and broadly applicable catalyst system for regio- and enantio-selective transformations of β-amino C–H bonds that is applicable to late-stage functionalization of complex bioactive compounds represents an important research objective.

As described in Chapter 2, we have demonstrated that Lewis acidic $B(C_6F_5)_3$ abstracts a hydride from α-position of amines, thereby generating an iminium ion (**VIII**), which can be trapped by an appropriate nucleophile to provide α-substituted amines (Scheme 3.2). Based on the literature precedent,[3] we postulated that the iminium generated in situ can be deprotonated by a Brønsted base, furnishing an enamine intermediate (**IX**). Through the reaction between enamine and electrophilic species, activated by a chiral Lewis acid co-catalyst, we hypothesized that regio- and enantio-selective functionalization of β-amino C–H bonds can be achieved.

Scheme 3.2. Regioselective C–H Functionalization of *N*-Alkylamines

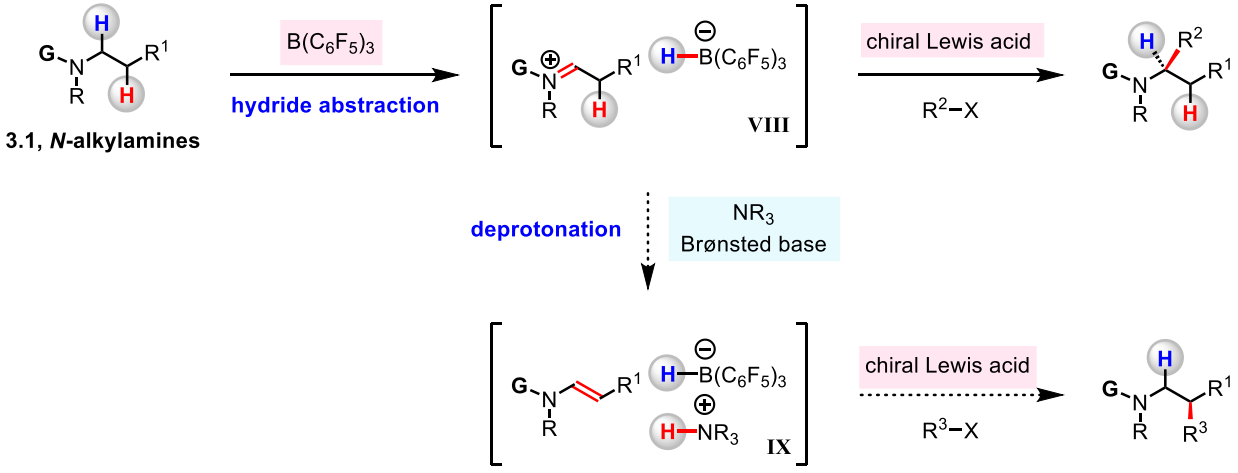

[3] Millot, N.; Santini, C. C.; Fenet, B.; Basset, J. M. *Eur. J. Inorg. Chem*. **2002**, *2002*, 3328−3335.

3.2. Catalytic Deuterium Incorporation within Metabolically Stable β-Amino C–H Bonds of Drug Molecules

Isotope labeling of bioactive compounds is a widely-applied strategy used in drug discovery.[4] It allows incorporation of additional mass or radioactive tag into a molecule without drastically changing its chemical structure or biological functions; these labeled compounds are applied to in vitro quantification of metabolites, which could assist elucidating metabolic pathway of drug molecules.[5] Furthermore, isotopically enriched molecules can be utilized in radioligand, protein and covalent binding assays to gain a better understanding of the pharmaceuticals' bioavailability and toxicity in vivo.[4]

Among various isotopes, hydrogen isotopes (deuterium and tritium) are often preferred as tracer nuclides. This is because: (i) hydrogens are ubiquitous in bioactive compounds, (ii) hydrogen isotope labeling reagents are readily available and (iii) hydrogen isotope can be detected with high sensitivity.[3-4] The hydrogen isotope incorporation into complex pharmaceuticals can be achieved through either a multistep synthesis, starting from commercially available isotope-enriched precursors,[6] or direct hydrogen isotope exchange (HIE) of C–H bonds in the drug molecules.[7-8] Although advances in C–H activation promoted by precious metal-based catalysts

---

[4] (a) Atzrodt, J.; Derdau, V.; Fey, T.; Zimmermann, J. *Angew. Chem., Int. Ed.* **2007***, 46,* 7744–7765. (b) Harbeson, S. L.; Tung, R. D. *MedChem News* **2014**, *2*, 8–22. (c) Atzrodt, J.; Derdau, V.; Kerr, W. J.; Reid, M. *Angew. Chem., Int. Ed.* **2018***, 57,* 1758–1784. (d) Atzrodt, J.; Derdau, V.; Kerr, W. J.; Reid, M. *Angew. Chem., Int. Ed.* **2018***, 57,* 3022–3047. (e) Pirali, T.; Serafini, M.; Cargnin, S.; Genazzani, A. A. *J. Med. Chem.* **2019**, *62*, 5276–5297.

[5] (a) Penner, N.; Klunk, L. J.; Prakash, C. *Biopharm. Drug Dispos.* **2009**, *30*, 185–203. (b) Miyoshi, S.; Mitsuoka, K.; Nishimura, S. A. in *Radioisotopes—Applications in Bio-Medical Science,* Singh, N., Ed.; InTech–Open Access Publisher, 2011; Chapter 5. (c) Iglesias, J.; Sleno, L.; Volmer, D. A. *Current Drug Metabolism* **2012**, *13*, 1213–1225.

[6] (a) Maltais, F.; Jung, Y. C.; Chen, M.; Tanoury, J.; Perni, R. B.; Mani, N.; Laitinen, L.; Huang, H.; Liao, S.; Gao, H.; Tsao, H.; Block, E.; Ma, C.; Shawgo, R. S.; Town, C.; Brummel, C. L.; Howe, D.; Pazhanisamy, S.; Raybuck, S.; Namchuk, M.; Bennani, Y. L. *J. Med. Chem*. **2009**, *52*, 7993–8001. (b) Allen, P. H.; Hickey, M. J.; Kingston, L. P.; Wilkinson, D. J. *J. Labelled Comp. Radiopharm*. **2010**, *53*, 731–738. (c) Lockey, W. J. S.; McEwen, A.; Cooke, R. *J. Labelled Comp. Radiopharm*. **2012**, *55*, 235–257. (d) Elmore, C. S.; Bragg, R. A. *Bioorg. Med. Chem. Lett.* **2015**, *25,* 167–171.

[7] Kang, Q.-K.; Shi, H. *Synlett* **2021**, *32*, doi: 10.1055/a-1354-0367.

[8] (a) Pieters, G.; Taglang, C.; Bonnefille, E.; Gutmann, T.; Puente, C.; Berthet, J.-C.; Dugave, C.; Chaudret, B.; Rousseau, B. *Angew. Chem., Int. Ed.* **2014**, *53*, 230–234. (b) Taglang, C.; Martinez-Prieto, L. M.; del Rosal, I.; Maron, L.; Poteau, R.; Philippot, K.; Chaudret, B.; Perato, S.; Lone, A. S.; Puente, C.; Dugave, C.; Rousseau, B.; Pieters, G.

enabled HIE involving aromatic C(sp^2)–H bonds, the HIE of C(sp^3)–H bonds remains as a difficult problem.[6-7] Furthermore, for identification and detection of drug metabolites, isotopes should be incorporated at a metabolically stable position in order to minimize the loss of the label.[3-4] However, metabolically stable C–H bonds are also often difficult to convert into C–D or C–T bonds using small-molecule catalysts.

As *N*-alkylamine moiety is prevalent in bioactive compounds,[9] there has been an increasing demand for the development of catalytic HIE process targeting amino C–H bonds.[10] Such methods would enable rapid access to a library of labeled N-containing drug analogues.[9] Particularly, catalytic HIE protocols involving α-amino C–H bonds have been developed by many groups including the work by the MacMillan group where the Ir-based photocatalyst promotes deuterium incorporation into bioactive amines (Scheme 3.3).[9d] However, as α-amino C–H bonds are labile

Scheme 3.3. Regioselective HIE of Amino C–H Bonds in Bioactive Compounds

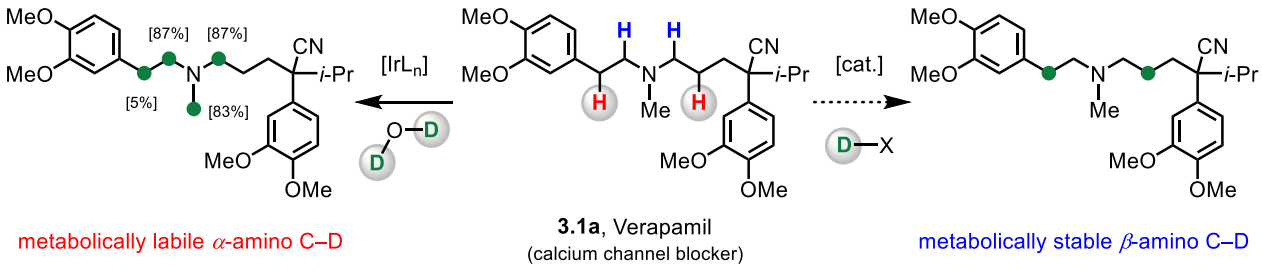

Angew. Chem., Int. Ed. **2015**, *54,* 10474–10477. (c) Yu, R. P.; Hesk, D.; Rivera, N.; Pelczer, I.; Chirik, P. J. *Nature* **2016**, *529*, 195–199. (d) Kerr, W. J.; Lindsay, D. M.; Reid, M.; Atzrodt, J.; Derdau, V.; Rojahn, P.; Weck, R. *Chem. Commun*. **2016**, *52*, 6669–6672. (e) Valero, M.; Weck, R.; Gussregen, S.; Atzrodt, J.; Derdau, Volker. *Angew. Chem., Int. Ed.* **2018**, *57*, 8159– 8163. (f) Kerr, W. J.; Mudd, R. J.; Reid, M.; Atzrodt, J.; Derdau, V. *ACS. Catal*. **2018**, *8*, 10895–10900. (g) Sawama, Y.; Nakano, A.; Matsuda, T.; Kawajiri, T.; Yamada, T.; Sajiki, H. *Org. Process Res. Dev.* **2019**, *23*, 648–653.

[9] McGrath, N. A.; Brichacek, M.; Njardarson, J. T. *J. Chem. Educ*. **2010**, *53*, 1348–1349.

[10] (a) Neubert, L.; Michalik, D.; Bahn, S.; Imm, S.; Neumann, H.; Atzrodt, J.; Derdau, V.; Holla, W.; Beller, M. *J. Am. Chem. Soc.* **2012**, *134*, 12239–12244. (b) Chatterjee, B.; Krishnakumar, V.; Gunanathan, C. *Org. Lett*. **2016**, *18*, 5892–5895. (c) Hale, L. V. A.; Szymczak, N. K. *J. Am. Chem. Soc.* **2016**, *138*, 13489–13492. (d) Loh, Y. Y.; Nagao, K.; Hoover, A. J.; Hesk, D.; Rivera, N. R.; Colletti, S. L.; Davies, I. W.; MacMillan, D. W. C. *Science* **2017**, *358*, 1182–1187

under physiological conditions,[11] α-labeled amine molecules may lose the isotope label during metabolic processes. Therefore, the development of methods for regioselective deuterium incorporation within metabolically stable β-amino C–H bonds (vs more reactive α- amino C–H bonds) contained in bioactive compounds would be highly desirable.

[11] (a) Markey, S. P. in Principles of Clinical Pharmacology, second ed., Atkinson, A.J.; Abernethy, D. R.; Daniels, C.E.; Dedrick, R.L.; Markey, S.P. Eds.; Academic Press, Burlington, 2007; Chapter 11. (b) Trager, W. F. in Comprehensive Medicinal Chemistry II, Taylor, J. B.; Triggle, D. J. Eds.; Elsevier, 2007; Volume 5.

3.2.1. Background

A great effort has been made to develop efficient catalytic methods for incorporation of hydrogen isotopes into amino C–H bonds over the last decade. The state-of-the-art examples of HIE of α-amino C–H bonds will be presented in this section.

The group of Beller developed a protocol for α,β-deuteration of tertiary amines utilizing a Ru-based Shvo's catalyst and protic deuterated solvents such as D_2O (Scheme 3.4).[9a] Upon heating by microwave in the presence of 10 mol% Shvo's catalyst, amine containing drug molecules including metoclopramide (**3.2**), underwent α,β-deuteration via enamine intermediate. Although selective deuterium incorporation into amino C–H bonds was achieved, the method required large excess of deuterium source and the substrate scope was limited to tertiary amines.

Scheme 3.4. α,β-Deuteration of Bioactive Amines Promoted by Ru-Based Catalyst

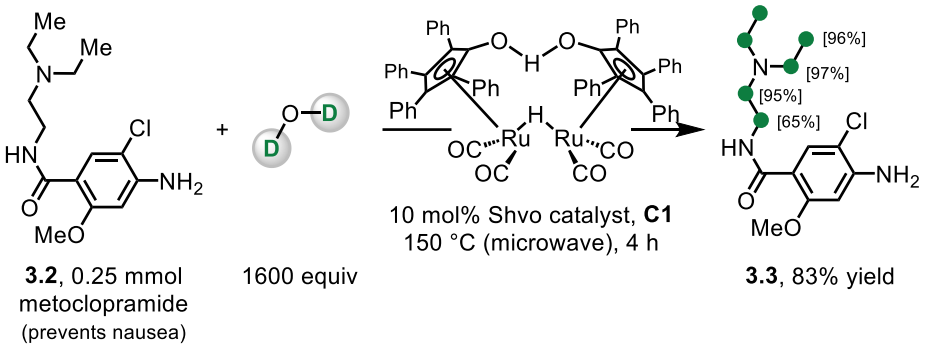

α-Deuteration of primary and secondary amines promoted by Ru-based catalyst was demonstrated by Gunanathan and coworkers (Scheme 3.5).[9b] A series of primary and secondary amines, such as sertraline (**3.4**), were reacted with 0.5–2.0 mol% of **C2** and D_2O to afford α-deuterated amines. The reaction proceeds through N–H activation by a cationic Ru complex to generate imine, followed by 1,3-deuteride transfer. Unlike Shvo's catalyst (**C1**, Scheme 2.1), **C2** did not promote deuteration of tertiary amines and the β-deuteration was only observed on linear

acyclic primary amines with <10% *d*-incorporation. In addition to amines, the potassium salt of amino acids also underwent α-deuteration selectively.

Scheme 3.5. α-Deuteration of Amines and Amino Acids Promoted by Ru-Based Catalyst

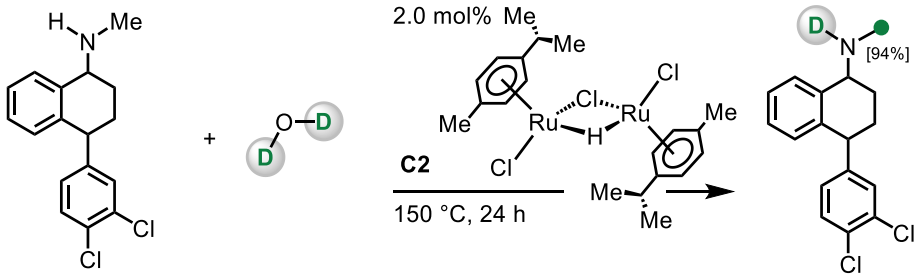

The MacMillan group has demonstrated that through a photoredox-mediated hydrogen atom transfer, selective installation of deuterium or tritium at α-amino C–H bonds of pharmaceuticals (**3.6**) can be achieved using isotopically labeled water (Scheme 3.6).[9d] Although this method uses an Ir-based catalyst, it is scalable and the functional group tolerance is high as shown by total 18 examples of N-containing bioactive compounds undergoing deuteration and tritiation.

Scheme 3.6. α-Deuteration of Bioactive Amines Promoted by Ir-Based Photoredox Catalyst

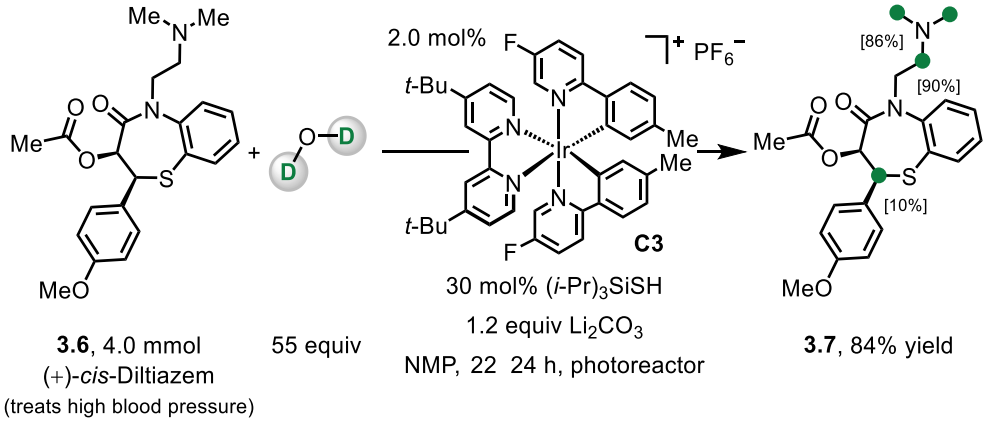

Current catalytic HIE protocols for bioactive amines developed by the groups of Beller, Gunanathan, and MacMillan involve isotope incorporation at α-amino C–H bond. We surmised that there still remains demand for a complimentary method where deuterium can be selectively installed at the metabolically stable β-amino position, as it could minimize the loss of isotope label. Therefore, we envisioned the development of a catalyst system that could selectively incorporate deuterium into β-C–H bonds in N-based pharmaceuticals using easily accessible deuterium source while circumventing the use of precious metal-based catalysts.

3.2.2. Our Approach

While contemplating ways to develop a protocol for selective *β*-amino C–H deuteration, we envisioned the use of cooperative catalyst system consisting of $B(C_6F_5)_3$ and a Brønsted base catalyst (Scheme 3.7). Based on previous stoichiometric reaction reported by Santini,[3] we hypothesized that $(F_5C_6)_3B$-catalyzed hydride abstraction from *N*-alkylamine would generate iminium ion in situ, which could be deprotonated by a Brønsted base co-catalyst furnishing enamine intermediate (**3.1→X→XI**). Concurrently, from Lewis acid-activated deuterium source, the base co-catalyst can promote dedeuteration (**3.8→XI**) to generate an electrophilic deuterating reagent [D–base]$^+$. The nucleophilic enamine then reacts with electrophilic deuterating reagent to forge a new C–D bond and the resultant iminium ion could undergo borohydride reduction affording the *β*-deuterated amine (**3.9**) while regenerating both acid and base catalysts.

Scheme 3.7. Proposed Catalytic Cycle for Deuterium Incorporation into *β*-Amino C–H Bonds

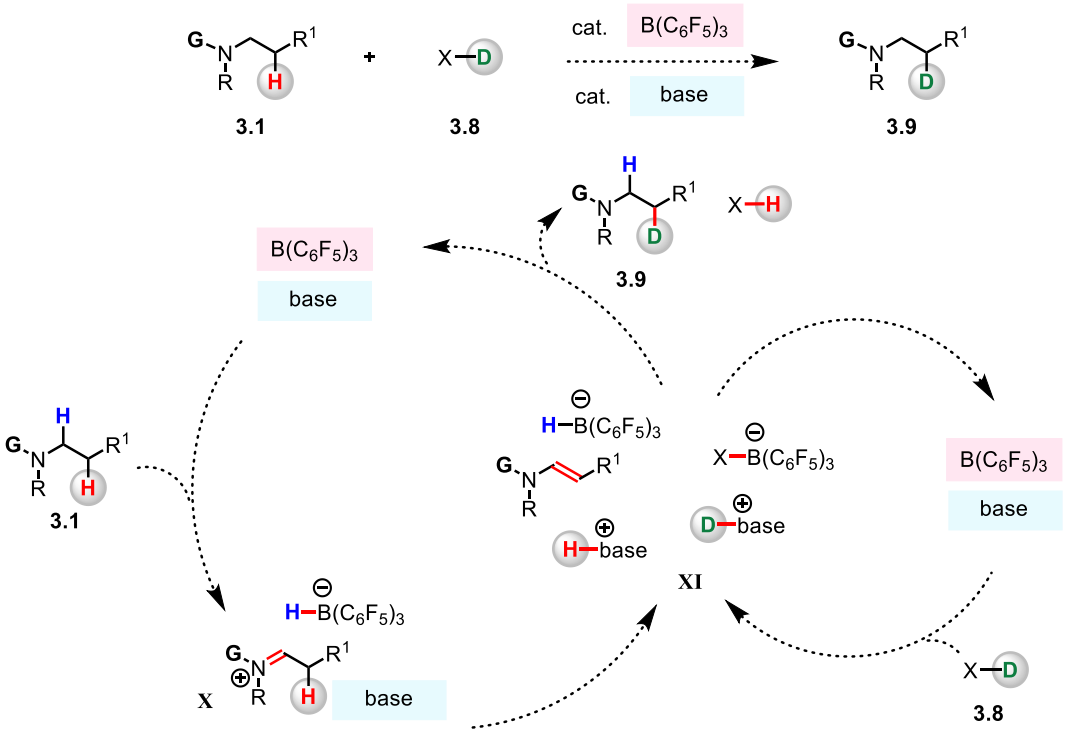

3.2.3. Results and Discussion

To begin our investigation, we set out to study whether $B(C_6F_5)_3$ can promote the *β*-selective deuteration of *N*-alkylamines (**3.1**) using D_2O since it is a commonly used *d*-source and its activation by $B(C_6F_5)_3$ has been demonstrated in the literature (Scheme 3.8).[12] When we treated *N*-aryl piperidine **3.1b** and D_2O with 10 mol% $B(C_6F_5)_3$, we were able to observe selective deuterium incorporation of 50% at the *β*-position of aniline (Scheme 3.8a). In this reaction, *N*-alkylamine substrate and/or product could serve as a Brønsted base and thus no external base catalyst was necessary. However, when trialkylamine substrates such as **3.1c** were evaluated, we did not observe any deuterium incorporation (Scheme 3.8b). We hypothesized that due to the higher basicity of trialkylamines (e.g., **3.1c**) relative to that of anilines (e.g., **3.1b**), $B(C_6F_5)_3$ may tend to form the borate and ammonium ion pair (**3.10**) in the presence of excess D_2O and the amine

Scheme 3.8. Deuteration of *β*-Amino C–H Bonds Using D_2O

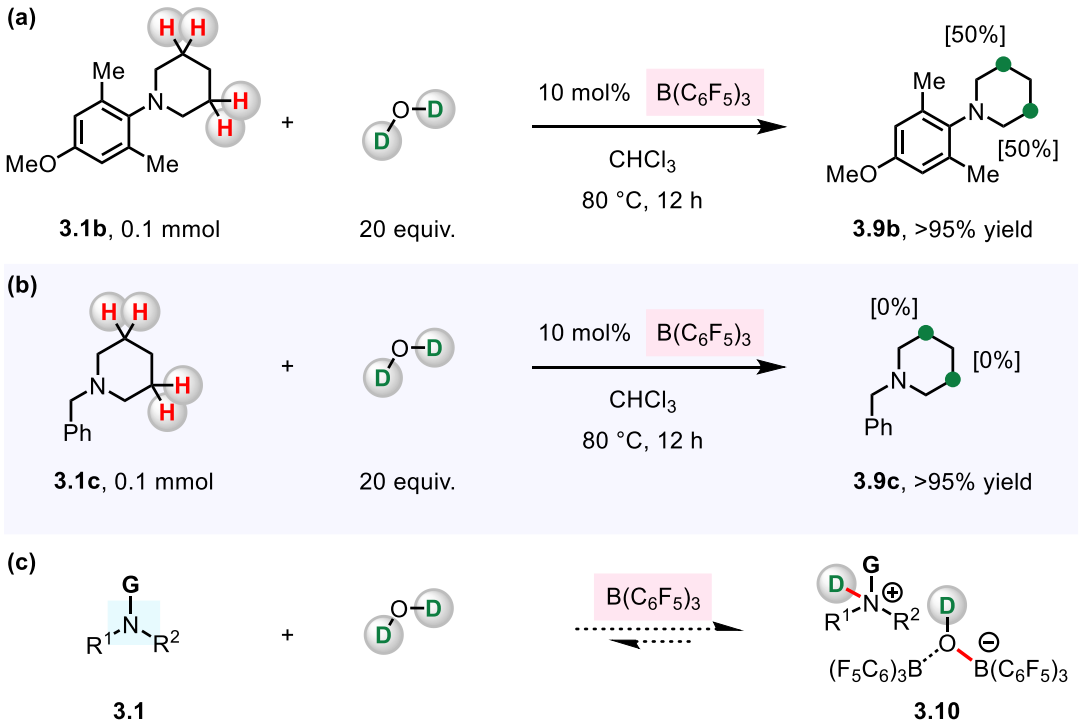

[12] For the use of D_2O and $B(C_6F_5)_3$, see: Li. W.; Wang, M.-M.; Hu, Y.; Werner, T. *Org. Lett.* **2017**, *19*, 5768–5771.

(Scheme 3.8c).[13] The formation of **3.10** could inhibit the $(F_5C_6)_3B$-catalyzed hydride abstraction and subsequent deprotonation, preventing the in situ generation of enamine intermediate. To overcome this issue, either less basic *N*-alkylamines such as **3.1a** or less base-sensitive *d*-source may be used. As our aim was to develop a general and broadly applicable deuteration method for bioactive amines, which often involve basic trialkylamine moiety, we decided to evaluate less acidic deuterium sources rather than compromising with the substrate scope.

Various *d*-alcohols, which contain less acidic deuteron than D_2O, were evaluated as deuterating reagent for HIE of *β*-amino C–H bonds using verapamil (**3.1a**, calcium channel blocker) as a representative substrate (Table 3.1). Similar to the discussion above, when **3.1a** was reacted with 6.8 equivalent of D_2O in the presence of 10 mol% $B(C_6F_5)_3$, no labeling was observed

Table 3.1. Evaluation of Alcohols as *d*-Source for *β*-Amino C–H Deuteration of Verapamil

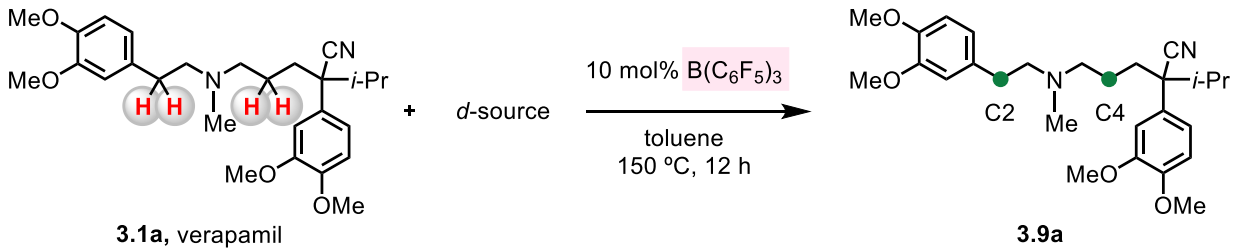

3.1a, verapamil
(calcium channel blocker)

3.9a

entry	*d*-source	equiv. of *d*-source	*d*-incorporation (%) [C2]	[C4]
1	D_2O	6.8	0	0
2	CH_3OD	6.8	14	20
3	$(CD_3)_2CDOD$	6.8	17	21
4	*t*-BuOD	6.8	63	58
5	*t*-BuOD	40.8	0	0

[13] Saverio, A. D.; Focante, F.; Camurati, I; Resconi, L.; Beringhelli, T.; D'Alfonso, G.; Donghi, D.; Maggioni, D.; Mercandelli, P.; Sironi, A. *Inorg. Chem*. **2005**, *44*, 5030–5041.

(entry 1). On the other hand, when *d*-labeled alcohols were used as *d*-source, we observed the conversion of *β*-amino C–H bonds into C–D bonds, consistent with our hypothesis (14-63% *d*-incorporation; entries 2–4). It should be noted that by using more sterically hindered *t*-BuOD, *d*-incorporation level drastically improved to 63% (vs 17% *d*-incorporation using $(CD_3)_2CDOD$). However, the use of larger equivalence (40.8 equivalent) of *t*-BuOD to further facilitate the labeling led to complete loss of reactivity (entry 5). We reasoned that the $(F_5C_6)_3B$-catalyzed hydride abstraction is outcompeted by $B(C_6F_5)_3$ interacting with large excess of Lewis basic alcohol and the deuteration process cannot take place. These results suggest that the ideal *d*-source that could prevent undesired acid–base complexation with $B(C_6F_5)_3$ should: (i) be less base-sensitive than D_2O or *d*-alcohol (ii) contain multiple accessible D atom per molecule so that large excess of *d*-source is not required.

Our group has previously demonstrated that cooperative Lewis acid and base catalysts can promote Mannich-type reaction of monocarbonyl compounds (e.g., **3.11a**) by activating less acidic *α*-carbonyl C–H bonds to in situ generate enolate and ammonium (**XII**; Scheme 3.9a).[14] Based on

Scheme 3.9. Deuteration of *β*-Amino C–H Bonds Using D_2O

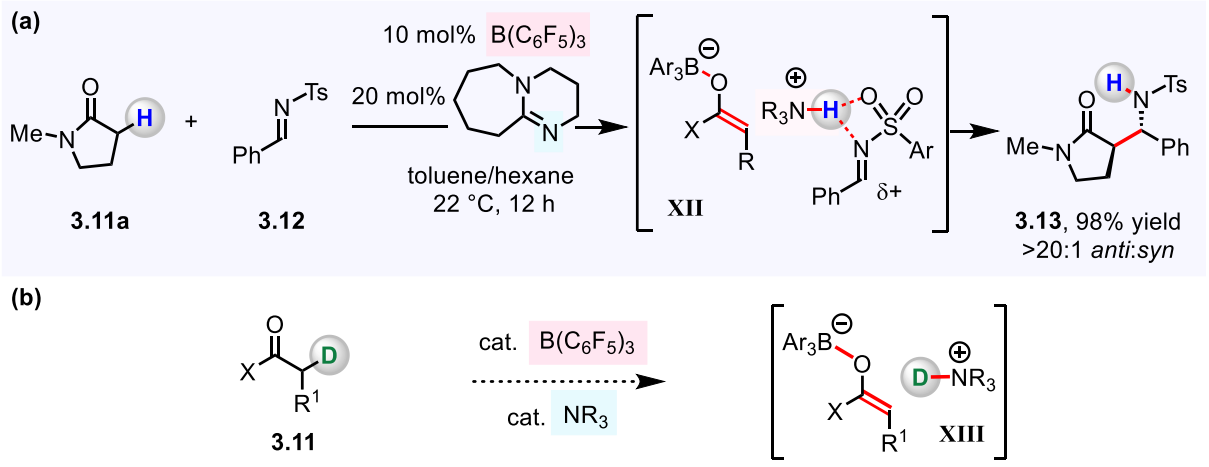

[14] Chan, J. Z.; Yao, W.; Hastings, B. T.; Lok, C. K.; Wasa, M. *Angew. Chem., Int. Ed.* **2016**, *55*, 13877–13881.

this study, we hypothesized that we could utilize α-deuterated monocarbonyl compounds **3.11** as *d*-source, which can contain multiple α-carbonyl C–D bonds with higher pK_a value compared to that of D_2O or alcohols (Scheme 3.9b). Through cooperative action of $B(C_6F_5)_3$ and Brønsted basic *N*- alkylamine, $[R_3N–D]^+$ can be generated in situ and serve as an electrophilic deuterating reagent (**XIII**).

Various α-deuterated ketones were prepared and evaluated as *d*-source for β-amino C–H deuteration of verapamil (**3.1a**; Table 3.2). Consistent with our hypothesis, when **3.1a** was treated with 6.8 equivalent of acetophenone-d_3 and 10 mol% $B(C_6F_5)_3$, we observed improved *d*-incorporation level of up to 79% (entry 1). We also tested cyclohexanone-d_4 but obtained **3.9a** with lower deuterium incorporation, probably due to its higher pK_a compared to acetophenone (entry 2). Finally, by using acetone-d_6, a readily accessible reagent that contains 6 D/molecule, we

Table 3.2. Evaluation of Ketones as *d*-Source for β-Amino C–H Deuteration of Verapamil

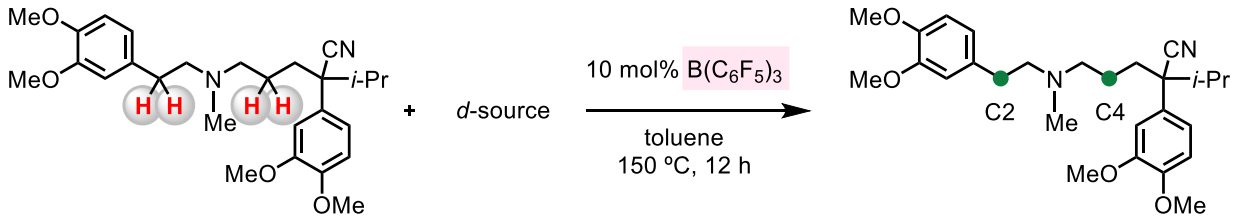

3.1a, verapamil (calcium channel blocker)

6.8 equiv.

3.9a

entry	*d*-source	D/molecule	*d*-incorporation (%) [C2]	[C4]
1	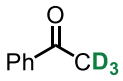	3	79	71
2	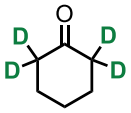	4	45	50
3	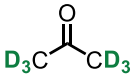	6	90	92

were able to obtain the product with >90% of *d*-incorporation (entry 3).

With acetone-d_6 as the optimal *d*-source, we then evaluated various reaction conditions in order to further improve the reaction efficiency (Table 3.3). It was found that only after 1 hour, we can observe similar level of reaction efficiency (entry 1). Although the *d*-incorporation level diminished, 5.0 mol% of $B(C_6F_5)_3$ was able to promote the *β*-selective deuteration of **3.1a** (entry 2). Deuterium incorporation drastically decreased to <35% at lower reaction temperature of 125 °C and 100 °C (entry 3–4). However, by reacting **3.1a** with two batches of 5.0 mol% of $B(C_6F_5)_3$

Table 3.3. Evaluation of Reaction Parameters[a,b,c]

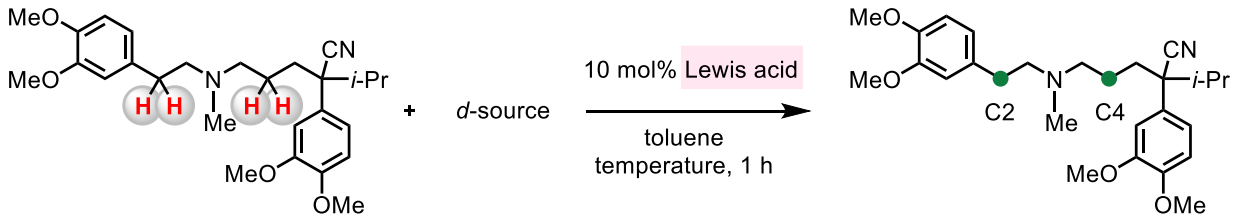

3.1a, verapamil
(calcium channel blocker)

3.9a

entry	Lewis acid (mol%)	temperature (°C)	*d*-incorporation (%) [C2]	[C4]
1	$B(C_6F_5)_3$ (10)	150	88	92
2	$B(C_6F_5)_3$ (5.0)	150	80	85
3	$B(C_6F_5)_3$ (5.0)	125	21	35
4	$B(C_6F_5)_3$ (5.0)	100	<5	7
5[d]	$B(C_6F_5)_3$ (5.0 x 2)	150	95	>98
6	none	150	0	0
7	BF_3•OEt_2 (5.0)	150	0	0
8	BPh_3 (5.0)	150	0	0

[a] Conditions: verapamil (**3.1a**, 0.1 mmol), acetone-d_6 (0.68 mmol), organoborane, toluene (0.4 mL), under N_2, 1 h. [b] Yield and deuterium incorporation level was determined by ^1H NMR analysis of unpurified reaction mixtures with mesitylene as the internal standard. [c] Green label indicates sites that are beta to N. [d] Conditions: verapamil (**3.1a**, 0.2 mmol), acetone-d_6 (1.36 mmol), $B(C_6F_5)_3$ (5.0 mol%), toluene (0.8 mL), under N_2, 150 °C, 1 h. Isolated and purified **3.9a** was reacted with acetone-d_6 (1.36 mmol), $B(C_6F_5)_3$ (5.0 mol%), toluene (0.8 mL), under N_2, 150 °C, 1 h.

and acetone-d_6 (6.8 equivalent), we were able to obtain **3.9a** with >95% labeling (entry 5). Without $B(C_6F_5)_3$ or when the less hindered BF_3 or the less Lewis acidic BPh_3 were used, no conversion of C–H bonds to C–D bonds was observed (entries 6–8). These findings are in line with our hypothesis that strongly acidic $B(C_6F_5)_3$ together with sterically demanding and electron-rich *N*-alkylamine constitute the most effective combination.

An array of acyclic bioactive compounds that contain β-amino C–H bonds (**3.1a**–**3.1j**) underwent efficient deuteration (Table 3.4). This catalytic method was found to be compatible with N-containing pharmaceuticals that contain Lewis acid-sensitive functional groups. In addition to the basic *N*-alkylamine moiety (**3.1a, 3.1d**–**3.1l**), cyano (**3.1a**), ether (**3.1a**, **3.1d**), ester (**3.1e**), amide (**3.1f**, **3.1g**, **3.1j**) and ketone (**3.1l**) were tolerated to afford the deuteration products **3.9a, 3.9d**–**3.9l** in 77 to >95% yield after isolation by flash column silica gel chromatography. Deuterium incorporation was achieved with high regioselectivity for β-amino C–H bonds. In addition, acidic α-carbonyl C–H bonds were converted to C–D bonds under the standard reaction conditions (**3.9g**, **3.9j**, **3.9l**) based on ^{1}H NMR spectra analysis of crude reaction mixtures. However, in case of **3.9j**, α-carbonyl C–D bonds underwent D–H exchange during purification by silica gel column chromatography.

For substrates that possess electronically and sterically disparate β-amino C–H bonds (**3.1a**, **3.1d**, **3.1e**, **3.1h**, **3.1i**, **3.1j**, **3.1l**), different levels of deuterium labeling was observed. With verapamil **3.1a**, deuteration of non-benzylic C4–H bonds was more efficient compared to benzylic C2–H (Table 3.3, entries 1-5). In case of clomiphene **3.1d** and dicyclomine **3.1e**, C2'–H bonds of *N*-ethyl groups underwent more efficient deuteration (90%) than C1–H bonds (15 and 23%). Although this protocol is highly functional group tolerant, HIE was more efficient with substrates bearing a protecting group as shown by the examples of lidocaine (**3.1f**) and cinacalcet (**3.1h**).

Table 3.4. Deuteration of Acyclic β-Amino C–H Bonds[a,b,c]

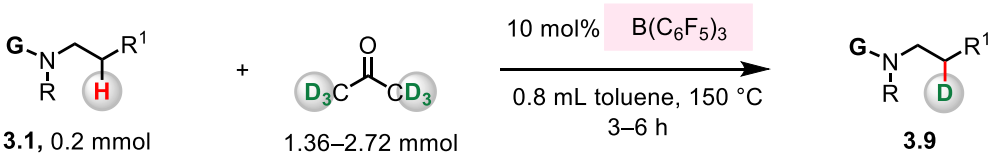

3.1, 0.2 mmol + 1.36–2.72 mmol → **3.9**

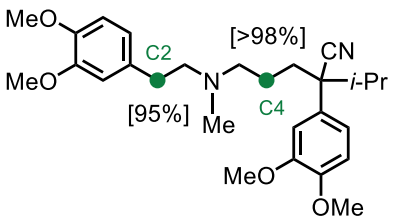

3.9a, verapamil
(calcium channel blocker)
92% yield[d]

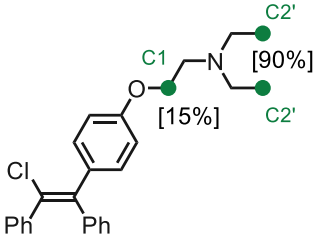

3.9d, clomiphene
(ovulatory stimulant)
>95% yield

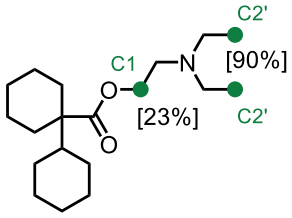

3.9e, dicyclomine
(anticholinergics)
>95% yield

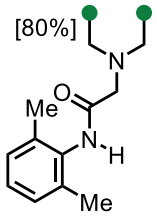

3.9f, lidocaine
(local anesthetic)
>95% yield

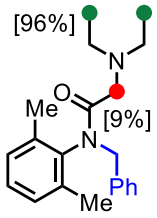

3.9g, *N*-Bn lidocaine
(local anesthetic)
>95% yield[d]

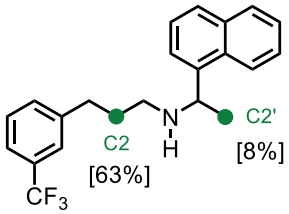

3.9h, cinacalcet
(calcimimetic)
>95% yield

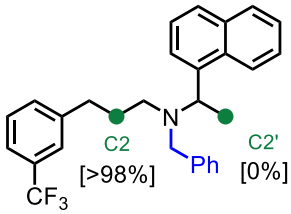

3.9i, *N*-Bn cinacalcet
(calcimimetic)
>95% yield[d]

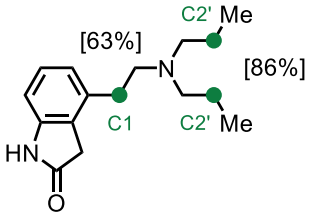

3.9j, ropinirole
(Parkinson's disease)
77% yield[e]

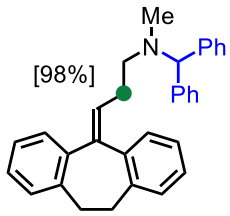

3.9k, *N*-Bzh nortriptyline
(antidepressant)
>95% yield[d]

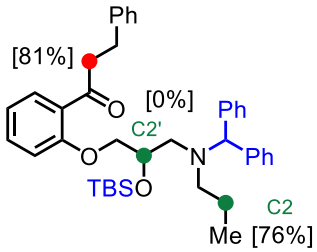

3.9l, *N*-Bzh, *O*-TBS propafenone
(antiarrhythmic agent)
92% yield

[a] Conditions: *N*-alkylamine (3.1, 0.2 mmol), acetone-d_6 (1.36 mmol), $B(C_6F_5)_3$ (10 mol%), toluene (0.8 mL), under N_2, 150 °C, 3 h. [b] Yield of isolated and purified product. Deuterium incorporation level was determined by ^1H NMR analysis of the isolated and purified product. [c] Green label indicates sites that are beta to N. Red label is used for any other sites that undergo deuteration. Blue color indicates protecting groups. [d] Conditions: *N*-alkylamine (3.1, 0.2 mmol), acetone-d_6 (1.36 mmol), $B(C_6F_5)_3$ (5.0 mol%), toluene (0.8 mL), under N_2, 150 °C, 3 h. After the filtration of the crude reaction mixture through a pad of silica gel and removal of volatiles, acetone-d_6 (1.36 mmol), $B(C_6F_5)_3$ (5.0 mol%), and toluene (1.0 mL) were added under N_2, and then heated at 150 °C, 3 h. [e] The reaction was carried out in two batches, using 10 mol% of $B(C_6F_5)_3$ in the first batch, and 5.0 mol% in the second.

While 80% of β-C–H bonds of lidocaine **3.1f** was converted to C–D bonds to give **3.9f**, deuteration of *N*-benzyl-protected lidocaine **3.1g** proceeded more efficiently to afford **3.9g** with 96% labeling. Cinacalcet **3.1h**, which contains secondary amine moiety, afforded **3.9h** (63% [C2] and 8% [C2']) under the standard conditions, when *N*-benzyl-protected cinacalcet **3.1f** was obtained with >98% of β-amino C2–H bonds labeled. With less sterically hindered secondary amine-containing nortriptyline **3.1k** and propafenone **3.1l**, *N*-benzhydryl group was installed to furnish **3.9k** and **3.9l**. Silyl protection of the secondary alcohol also improved the efficiency of deuteration in the case of propafenone **3.1l**.

Deuteration of β-C–H bonds in various cyclic bioactive amines was successful (Table 3.5; **3.1m**–**3.1u**). An array of heterocycles including piperidine (**3.1m**–**3.1s**), 1,4-diazepane (**3.1t**), piperazine (**3.1u**), thiophene (**3.1m**, **3.1n**), indanone (**3.1o**), benzodioxole (**3.1q**, **3.1r**), benzothiophene (**3.1s**), as well as benzoimidazole (**3.1t**) were tolerated to afford the corresponding labeled products in 85 to >95% yield. Enolizable α-carbonyl C–H bonds in clopidogrel **3.1m**, prasugrel **3.1n**, and donepezil **3.1o** underwent efficient deuteration, but acidic α-keto C–D bond of **3.9n** was converted to C–H bond during purification by silica gel chromatography. Less acidic α-carbonyl C–H bond in bupivacaine **3.1p** was not deuterated. When both acyclic and cyclic β-amino C–H bonds were present (**3.1p** and **3.1s**), labeling of the cyclic C–H bond was more efficient (>90% vs ≤29% for the acyclic C–H). For paroxetine, more hindered *N*-benzhydryl-protected **3.9r** was obtained with higher *d*-incorporation level (92%) compared to *N*-benzyl-protected **3.9q** (76%). Furthermore, the tertiary C3–H bond remained intact for both **3.9q** and **3.9r**. Deuteration of 1,4-diazepane-containing emedastine **3.1t** took place at C2–H (33%) and C6–H (61%) bonds. All eight C–H bonds of piperazine in *O*-TBS-dropropizine **3.1u** underwent efficient deuteration providing **3.9u** (>86%).

Table 3.5. Deuteration of Cyclic *β*-Amino C–H Bonds[a,b,c]

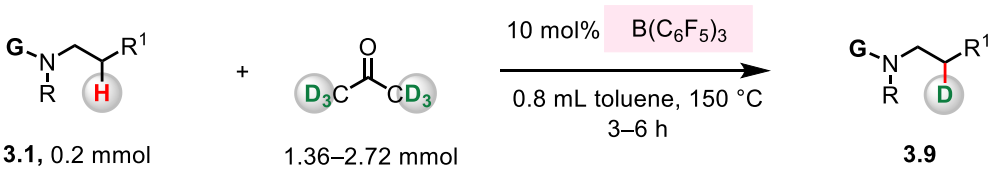

3.1, 0.2 mmol + 1.36–2.72 mmol → **3.9**

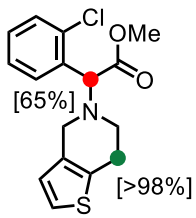

3.9m, clopidogrel (antiaggregant)
94% yield[d]

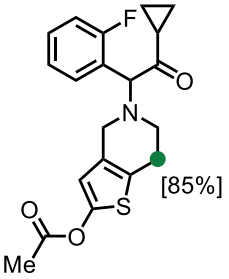

3.9n, prasugrel (antiaggregant)
85% yield[e]

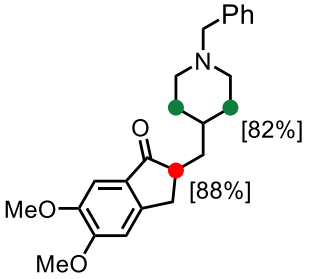

3.9o, donepezil (anti-Alzheimer)
>95% yield

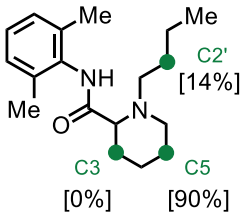

3.9p, bupivacaine (local anesthetic)
>95% yield

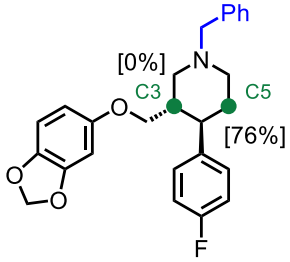

3.9q, *N*-Bn paroxetine
(antidepressant)
>95% yield

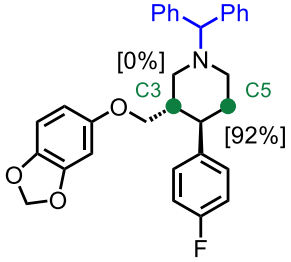

3.9r, *N*-Bzh paroxetine
(antidepressant)
95% yield

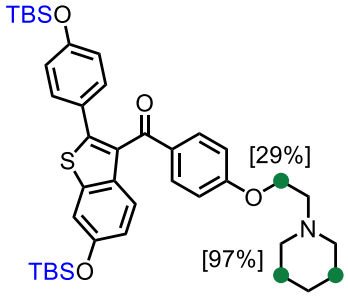

3.9s, *O*-TBS raloxifene
(treats osteoporosis)
>95% yield

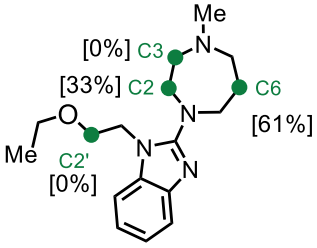

3.9t, emedastine
(antihistamine)
88% yield

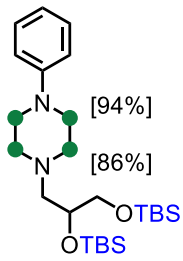

3.9u, *O*-TBS dropropizine
(cough suppressant)
94% yield[d]

[a] Conditions: *N*-alkylamine (3.1, 0.2 mmol), acetone-d_6 (1.36 mmol), $B(C_6F_5)_3$ (10 mol%), toluene (0.8 mL), under N_2, 150 °C, 3 h. [b] Yield of isolated and purified product. Deuterium incorporation level was determined by ^1H NMR analysis of the isolated and purified product. [c] Green label indicates sites that are beta to N. Red label is used for any other sites that undergo deuteration. Blue color indicates protecting groups. [d] Conditions: *N*-alkylamine (3.1, 0.2 mmol), acetone-d_6 (1.36 mmol), $B(C_6F_5)_3$ (5.0 mol%), toluene (0.8 mL), under N_2, 150 °C, 3 h. After the filtration of the crude reaction mixture through a pad of silica gel and removal of volatiles, acetone-d_6 (1.36 mmol), $B(C_6F_5)_3$ (5.0 mol%), and toluene (1.0 mL) were added under N_2, and then heated at 150 °C, 3 h. [e] The reaction was carried out in two batches, using 10 mol% of $B(C_6F_5)_3$ in the first batch, and 5.0 mol% in the second.

The protocol is scalable as demonstrated by the gram scale reaction of verapamil **3.1a** (1.4 g, 3.0 mmol; Scheme 3.10). By treating **3.1a** with 5.0 mol% $B(C_6F_5)_3$, 20.4 mmol of acetone-d_6, followed by filtration through a pad of silica gel and repeating the aforementioned procedure, **3.9a** was obtained in 95% yield (2.9 mmol, 1.3 g) with >93% *d*-incorporation.

Scheme 3.10. Scale-Up Experiment

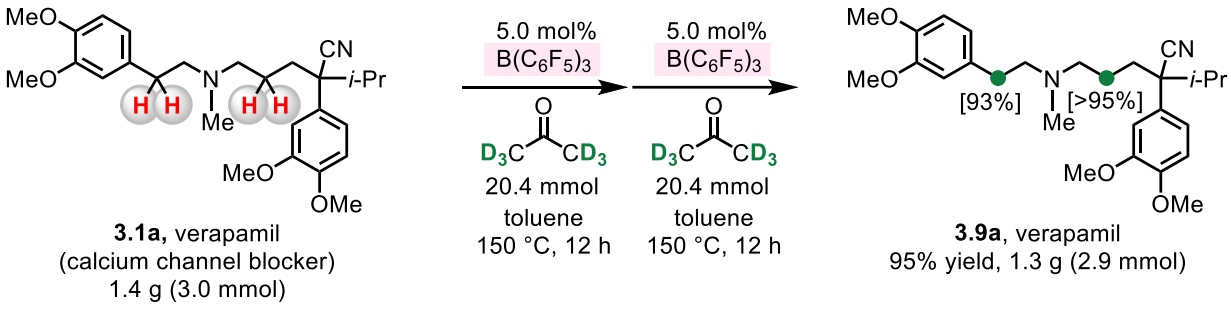

3.1a, verapamil
(calcium channel blocker)
1.4 g (3.0 mmol)

3.9a, verapamil
95% yield, 1.3 g (2.9 mmol)

3.2.4. Conclusions and Future Outlook

In summary, we have developed an efficient and regioselective HIE protocol for *β*-amino C–H bonds in various bioactive compounds through cooperative action of $B(C_6F_5)_3$ and *N*-alkylamine. We have demonstrated that N-containing pharmaceuticals can be converted to the corresponding enamine intermediate, which can react with an electrophilic deuterating agent that is in situ generated from readily accessible acetone-d_6.

The principles outlined above provide a new rational basis for the development of processes applicable to the late-stage stereoselective *β*-amino C–H functionalization of bioactive amines.

3.3. Enantioselective β-Amino C–H Functionalization through Cooperative Action of Chiral and Achiral Lewis Acid Catalysts

As discussed in Section 3.1, there is a paucity of catalyst systems that could promote the regio- and stereo-selective β-C–H functionalization of *N*-alkylamines.[1-2] This is mainly due to the poorly reactive nature of the β-amino C–H bond, which would require the formation of the radical or cationic intermediates (**II** or **III**, Scheme 3.1) that cannot be stabilized by hyperconjugation, or a strained four-membered metallacycle (**I**, Scheme 3.1). Therefore, the development of an efficient and enantioselective catalyst system for the synthesis of β-substituted N-alkylamines through C–H functionalization remains as an important unsolved problem.

3.3.1. Background

Despite the aforementioned challenges associated with β-amino C–H functionalization, there exist few literature precedents for the synthesis of enantiomerically enriched β-substituted amines through activation of β-amino C–H bond.[15-16] The Gaunt group disclosed a Pd-catalyzed enantioselective C–H activation protocol to afford enantio-enriched aziridines **3.15** using chiral phosphoric acid as a ligand (Scheme 3.11).[11b] This transformation is proposed to proceed via a four-membered cyclopalladation complex (**XIV**) through secondary amine-directed stereoselective C–H activation. However, this method is limited to sterically hindered amines such as tetramethyl-morpholinone derivatives in order to overcome the undesired mutual quenching between acidic catalyst and basic amine moiety. Furthermore, the poor functional group tolerance

[15] Ohno, S.; Miyoshi, M.; Murai, K.; Arisawa, M. *Synthesis* **2021**, doi: 10.1055/a-1483-4575.
[16] (a) He, J.; Li, S.; Deng, Y.; Fu, H.; Laforteza, B. N.; Spangler, J. E.; Homs, A.; Yu, J.-Q. *Science* **2014**, *343*, 1216–1220. (b) Smalley, A. P.; Cuthbertson, J. D.; Gaunt, M, J. *J. Am. Chem. Soc*. **2017**, *139*, 1412–1415. (c) Su, B.; Lee, T.; Hartwig, J. F. *J. Am. Chem. Soc*. **2018**, *140*, 18032–18038. (d) Lin, W.; Zhang, K.-F.; Baudoin, O. *Nat. Catal.* **2019**, *2*, 882–888.

of this catalyst system due to the requirement for stoichiometric oxidant limits its application to the late-stage functionalization of complex molecules.

Scheme 3.11. Enantioselective C–H Activation of Aliphatic Amines Promoted by a Pd-Based Catalyst

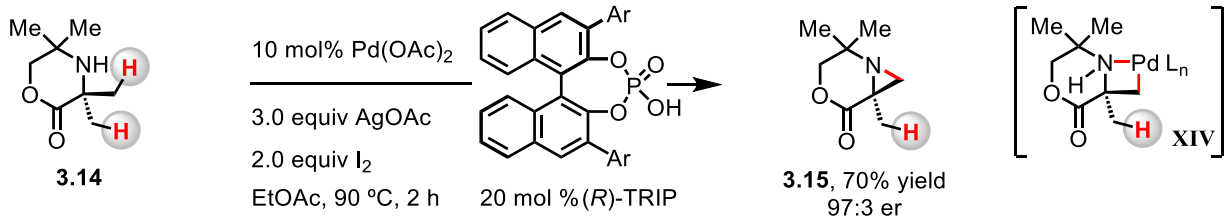

Hartwig and coworkers demonstrated enantioselective β-C–H silylation of (silylmethyl)amine **3.16** for the synthesis of silicon-containing pyrrolidines derivatives **3.17** promoted by an Ir-based catalyst (Scheme 3.12).[11c] The incorporation of a methylene linker between the silyl group and the nitrogen center prevents the activation of a weaker α-C–H bond as it would lead to a strained four-membered azasiletidine; instead, a rare β-selective C–H bond functionalization is achieved to generate a more stable five-membered metallacycle intermediate. The limitation of this method includes the use of precious Ir-based catalyst and cryogenic conditions. Moreover, the substrates that contain functional groups that are prone to reduction may not be tolerated in this catalyst system involving the use of silane-containing substrate and Ir-based catalyst.

Scheme 3.12. β-Selective C–H Silylation of Aliphatic Amines Promoted by an Ir-Based Catalyst

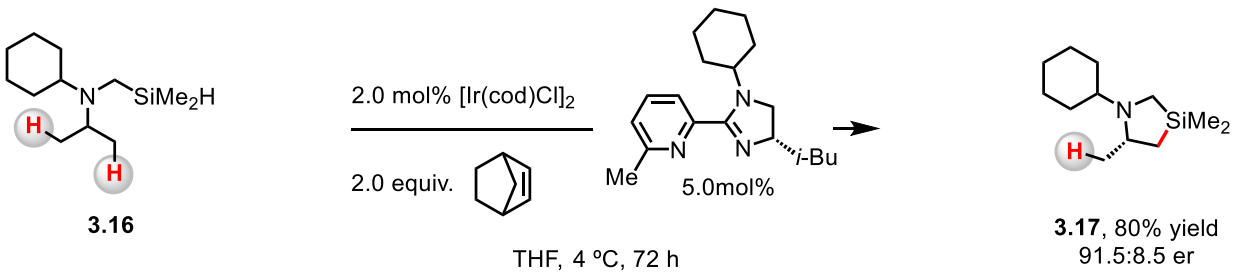

The group of Baudoin reported a regiodivergent enantioselective C–H functionalization of Boc-1,3-oxazinanes **3.18** (Scheme 3.13).[11d] This one-pot reaction proceeds through sparteine-mediated enantioselective lithiation of Boc-1,3-oxazinane **3.18** and transmetallation to zinc to afford **3.19**. Following migratory Negishi coupling of organozinc species with an organic electrophile such as phenyl bromide furnishes *β*-substituted amine product **3.20**, which can be converted to an enantio-enriched *β*^{3}-amino acid. However, due to the demand for stoichiometric amounts of *s*-BuLi and (+)-sparteine, this method is not functional group tolerant. Furthermore, this method has a confined substrate scope of sterically hindered Boc-1,3-oxazinanes to overcome the undesired acid–base complexation.

Scheme 3.13. Enantioselective *β*-C–H Functionalization of Boc-1,3-oxazinanes

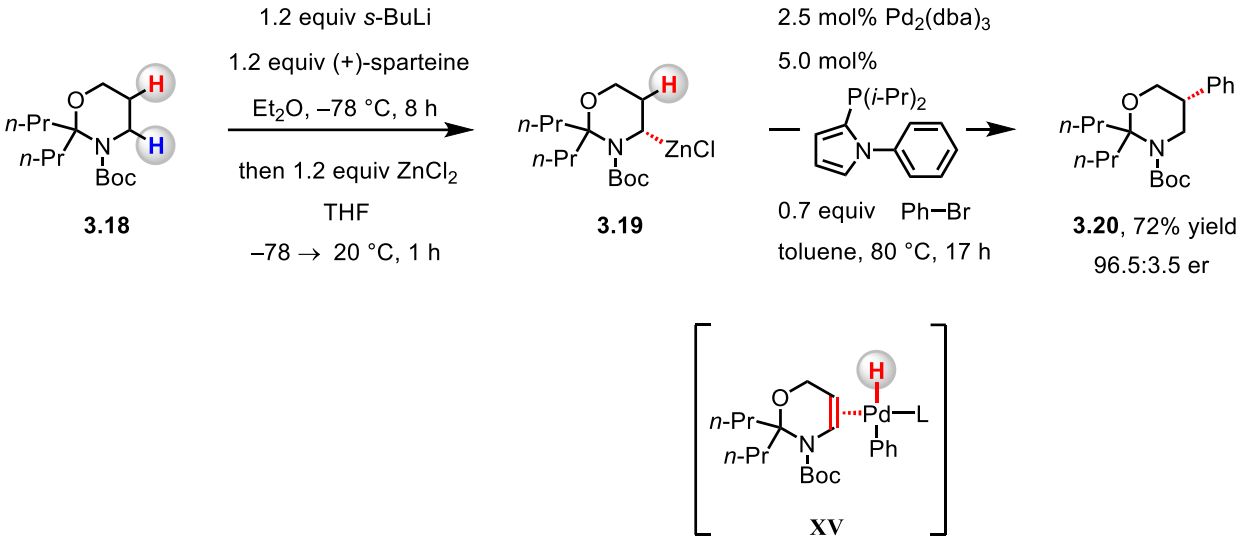

As summarized above, the literature precedents on enantioselective methods for *β*-amino C–H functionalization require the use of precious Pd- or Ir-based catalysts. Moreover, the use of stoichiometric oxidant (AgOAc, I_2, and/or IOAc) or base (*s*-BuLi) would be problematic with substrates that contain oxidant- and/or base-sensitive functional groups. As a consequence, application of these methods to the late stage modification of bioactive amines would be

challenging (Scheme 3.14a). To address these fundamental limitations, we envisioned the development of an enantioselective and sustainable element-based catalyst system that is applicable to the late-stage β-C–H functionalization of bioactive amines under mild and redox-neutral conditions (Scheme 3.14b).

Scheme 3.14. Enantioselective β-amino C–H Functionalization

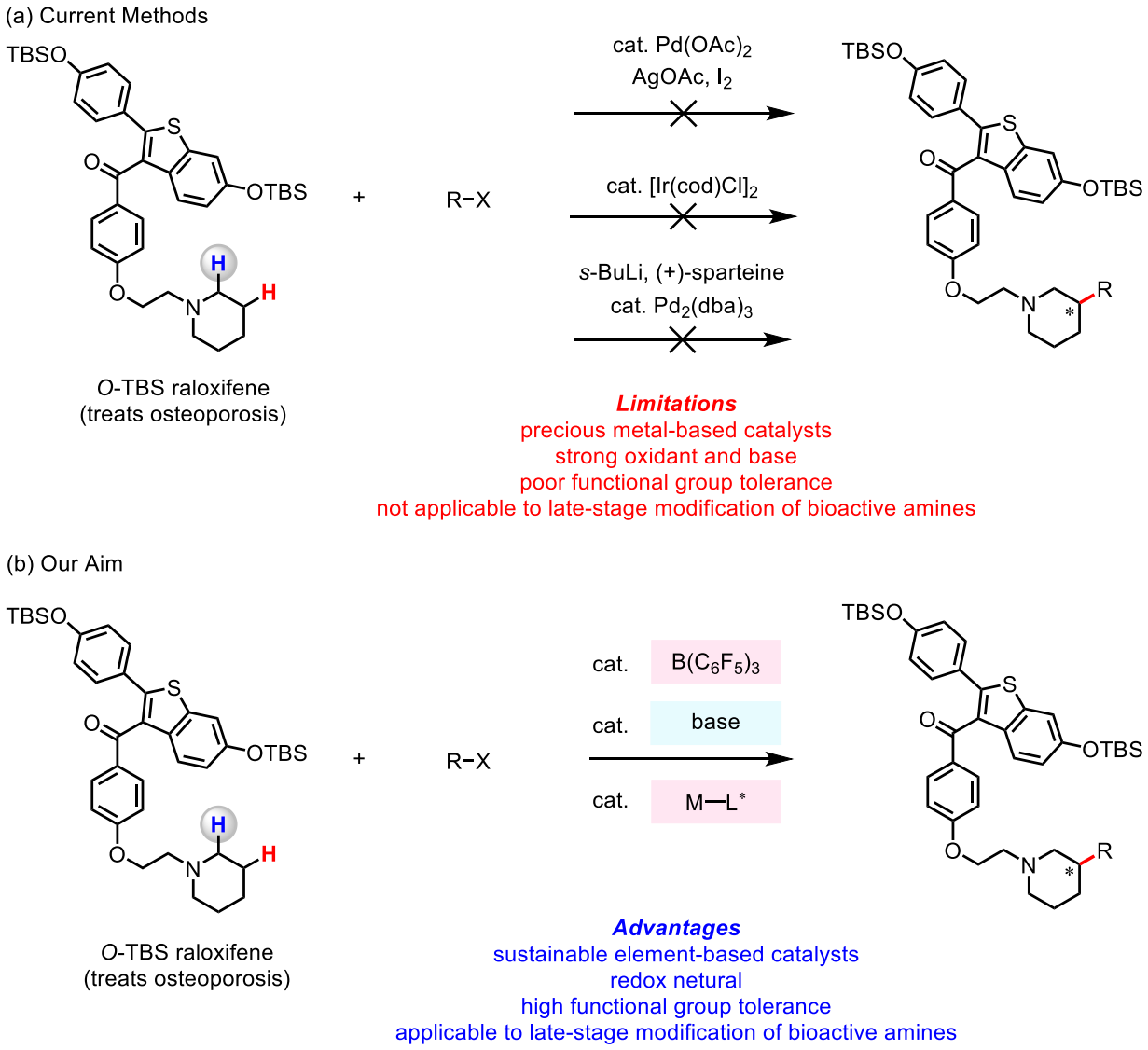

3.3.2. Our Approach

As described in Section 2.5, we have demonstrated that separate and independently operational Lewis acid co-catalysts whose functions might easily overlap and the simultaneous use of which might initially seem to have a negative impact on enantioselectivity can, in fact, promote highly enantioselective process. Furthermore, in Section 3.2, we disclosed that through cooperative function of Lewis acidic $B(C_6F_5)_3$ and a Brønsted basic *N*-alkylamine, enamine can be generated in situ from the corresponding N-containing pharmaceuticals. It was also shown that the resultant enamine intermediate can react with an appropriate electrophilic species to regioselectively modify *β*-C–H bond contained in structurally complex bioactive amines.

Based on these previous studies, we envisioned the development of a catalytic protocol for the late-stage stereoselective *β*-amino C–H functionalization of N-based drug molecules through the use of a cooperative catalyst system consisting of $B(C_6F_5)_3$, a Brønsted base catalyst, and a chiral Lewis acid co-catalyst ($M–L^*$, Scheme 3.15). We propose that $B(C_6F_5)_3$ could abstract hydride from *N*-alkylamine **3.21** to give an ion pair consisting of an iminium and a borohydride (**XVI**). The iminium ion could be deprotonated by a Brønsted base to afford enamine **XVII**. The reaction between the nucleophilic enamine (**XVII**) and the chiral Lewis acid-activated *α*,*β*-unsaturated compound (**XVIII**) would forge a new C–C bond in a stereoselective manner to furnish zwitterionic intermediate **XIX**. Ensuing protonation and reduction of **XIX** would provide *β*-alkylation product **3.23**.

By using the untethered and independently operational catalyst system, we could easily optimize the reaction efficiency and stereoselectivity through evaluation of Lewis acids, chiral ligands and base co-catalysts. Nonetheless, the major challenge we need to overcome is the potential mutual quenching between the acidic and basic components of catalysts, substrates, and

the product. Moreover, the achiral Lewis acid $B(C_6F_5)_3$ could have overlapping function with the chiral Lewis acid and promote racemic background reaction by activating the electrophile **3.22** ($M–L^*$= $B(C_6F_5)_3$; **XVIII**). Therefore, we need to develop a potent cooperative catalyst system that could overcome these fundamental challenges and promote the enantioselective *β*-amino C–H functionalization of *N*-alkylamines.

Scheme 3.15. Direct Enantioselective *β*-C–H Functionalization of Amines through Cooperative Actions of $B(C_6F_5)_3$ and Chiral Lewis Acid Co-catalyst

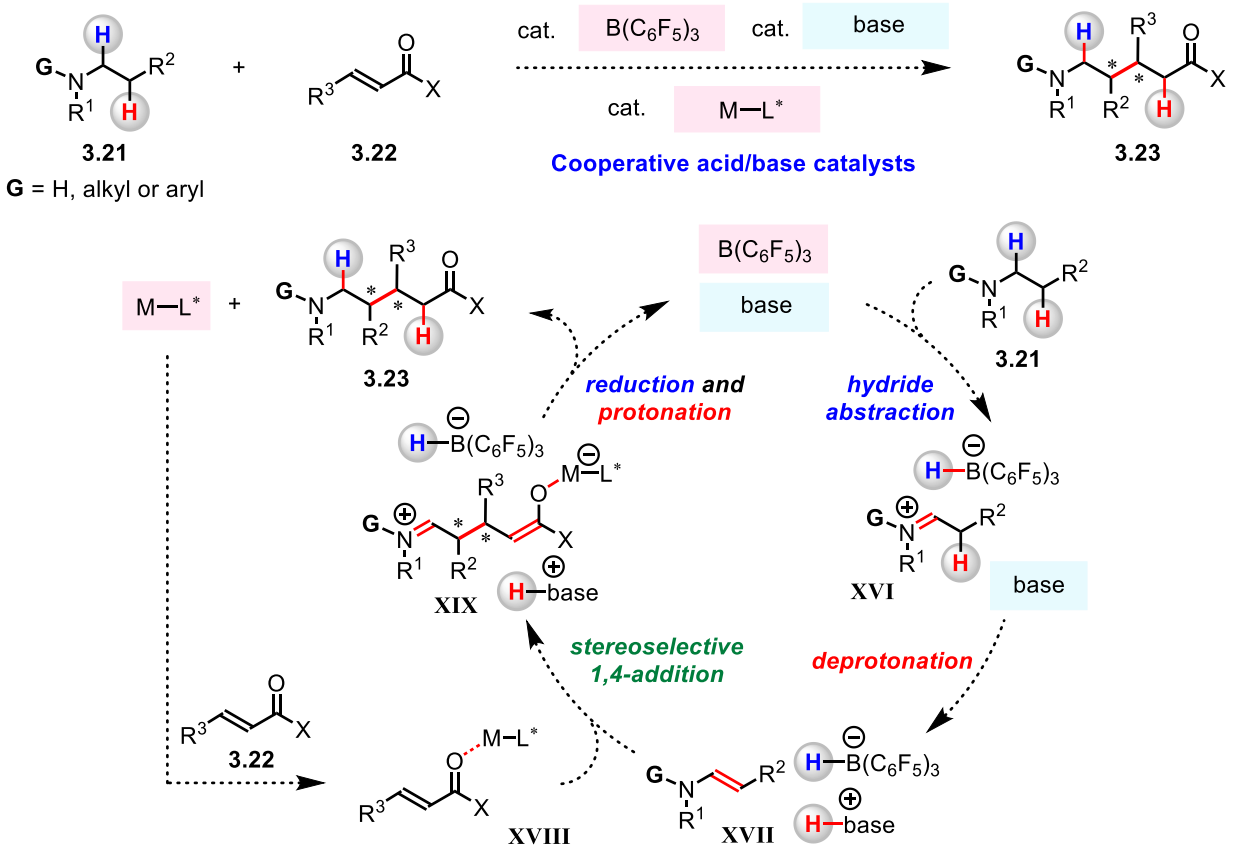

3.3.3. Results and Discussion – Method Development

We began our investigation by examining if $B(C_6F_5)_3$ could activate both *N*,*N*-dibenzylethanamine (**3.21a**) and diisopropyl fumarate (**3.22a**) to promote the *β*-amino C–H alkylation affording **3.23a** (Table 3.6). When **3.21a** was reacted with **3.22a** under the presence of 10 mol% $B(C_6F_5)_3$ and 10 mol% triethylamine, 2,2,6,6-tetramethylpiperidine (TMP) or 1,8-diazabicyclo[5.4.0]undec-7-ene (DBU), **3.23a** was obtained in 50%, 25%, and <5% yield, respectively (entries 1–3). When the reaction was conducted without any external base catalyst, the desired product **3.23a** was furnished in 73% yield (entry 4); suggesting Brønsted basic **3.21a** and/or **3.23a** could mediate the deprotonation of iminium intermediate for generation of enamine (**XVI→XVII**, Scheme 3.15). It should be noted that the formation of **3.24** was also observed (entried 1–6), probably through the reaction between enolate (**XIX**, Scheme 3.15) and **3.22a**, followed by intramolecular cyclization. To improve the selectivity and suppress formation of **3.24**,

Table 3.6. Evaluation of Various Reaction Parameters[a,b,c]

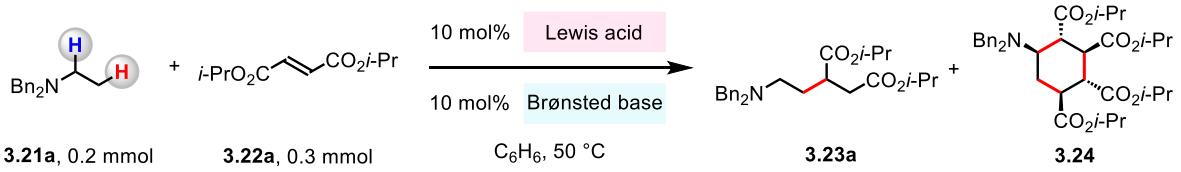

3.21a, 0.2 mmol **3.22a**, 0.3 mmol **3.23a** **3.24**

entry	Lewis acid	Brønsted base	time (h)	yield of **3.23a** (%)	yield of **3.24** (%)
1	$B(C_6F_5)_3$	Et_3N	3	50	23
2	$B(C_6F_5)_3$	TMP	3	25	29
3	$B(C_6F_5)_3$	DBU	3	<5	<5
4	$B(C_6F_5)_3$	none	3	73	25
5[d]	$B(C_6F_5)_3$	none	3	54	5
6[d]	$B(C_6F_5)_3$	none	12	91	7
7	none	none	12	0	0
8	BCl_3	none	12	0	0
9	BPh_3	none	12	0	0

[a] Conditions: *N*,*N*-dibenzylethanamine (**3.21a**, 0.2 mmol), diisopropyl fumarate (**3.22a**, 0.3 mmol), Lewis acid, Brønsted base, C_6H_6 (0.2 mL), under N_2, 50 °C. [b] Yield was determined by ^1H NMR analysis of unpurified reaction mixtures with *m*-xylene as the internal standard. [c] The structure and relative configuration of **3.24** were established by nuclear Overhauser effect spectroscopy (NOESY) studies. [d] 0.8 mL of C_6H_6 was used.

we carried out the transformation in lower concentration (entries 5–6). Although we were able to observe **3.24** in only 5% yield, the overall reaction efficiency decreased and the desired **3.23a** was also obtained in lower yield of 54% (vs 73% in entry 4). When the reaction was run for 12 hours, **3.23a** was furnished in 91% yield. None of the product was formed without $B(C_6F_5)_3$, or when less hindered BCl_3 or less acidic BPh_3 were used (entries 7–9). These results point to the fact that strongly Lewis acidic and hindered $B(C_6F_5)_3$ together with sterically demanding and electron-rich *N*-alkylamines represent the most effective catalyst–substrate combination.

With the optimal reaction conditions, we went on to evaluate various *N*-alkylamines using diisopropyl fumarate **3.22a** (Table 3.7). An array of acyclic amines was found to be suitable for this transformation, providing corresponding *β*-substituted amines (**3.23a**–**3.23h**). While reaction of *N*,*N*-dibenzylethanamine and **3.22a** afforded **3.23a** in 88% yield, *N*,*N*-dibenzylpropan-1-amine afforded **3.23b** and **3.23c** in 58% and 33% yield, respectively. Compound **3.23c** is likely generated through intramolecular Mannich-type reaction between an iminium ion and enolate (**XIX**, Scheme 3.15). With the more sizeable *N*,*N*-dibenzyl-2-methylpropan-1-amine, **3.23d** was obtained as the only product (69% yield), which may be due to acceleration of the Mannich-process by the Thorpe-Ingold effect.

N-Benzhydryl-substituted secondary amines containing an N–H group were suitable substrates, giving **3.23e**–**3.23g** in 66–93% yield. However, when a secondary amine that bears a more hindered trityl group (e.g., *N*-tritylethanamine), none of the desired product was obtained; this may be attributed to rapid substrate decomposition. Furthermore, with less hindered *N*-benzylethanamine, the formation of $(F_5C_6)_3B$–amine adduct likely competes with Lewis acid-catalyzed hydride abstraction, affording the desired *β*-alkylation product in <5% yield. From the reaction of enantio-enriched **3.21xx**, **3.23h** was furnished in 90% yield as a 1.4:1 mixture of

Table 3.7. *β*-Alkylation of Different *N*-Alkylamines[a,b,c]

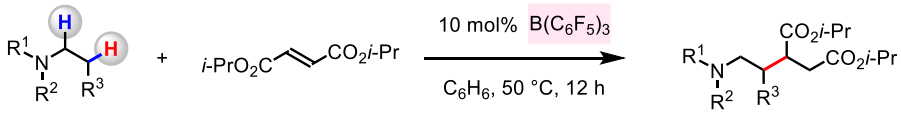

3.21 + **3.22a** → **3.23**

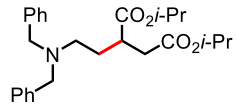 **3.23a**, 88% yield	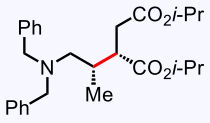 **3.23b**, 58% yield[c] 1.3:1 dr	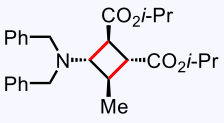 **3.23c**, 33% yield[c] >20:1 dr	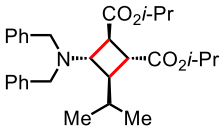 **3.23d**, 69% yield[c] >20:1 dr
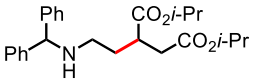 **3.23e**, 93% yield	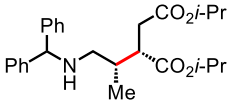 **3.23f**, 66% yield[c] 1.1:1 dr	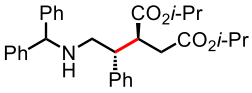 **3.23g**, 87% yield[c] 2.1:1 dr	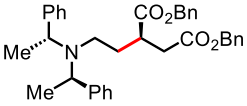 **3.23h**, 90% yield[d] (*R*,*R*,*R*):(*R*,*R*,*S*) = 1.4:1
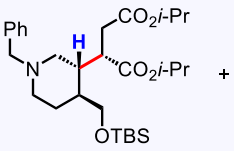 **3.23i**, 74% yield[e] 1.1:1 dr	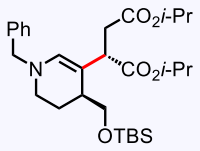 **3.23j**, 26% yield[e] 1.4:1 dr	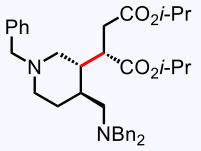 **3.23k**, 51% yield[e] 1.8:1 dr	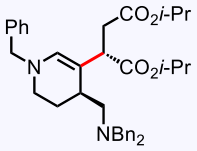 **3.23l**, 47% yield[e] 1.7:1 dr
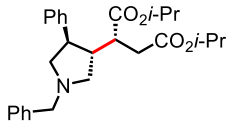 **3.23m**, 90% yield[e] 1.6:1 dr	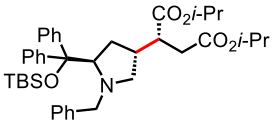 **3.23n**, 56% yield[e] 2.5:1 dr	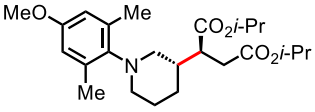 **3.23o**, 89% yield[e] 1.3:1 dr	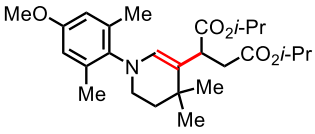 **3.23p**, 93% yield

The values correspond to yields of isolated and purified products. [a] Conditions: *N*-alkylamine (**3.21**, 0.2 mmol), diisopropyl fumarate (**3.22a**, 0.3–0.4 mmol), $B(C_6F_5)_3$ (10 mol%), C_6H_6, under N_2, 50 °C. [b] Yield of isolated and purified product. The dr values were determined by ^1H NMR analysis of the unpurified reaction mixtures. [c] The structure and relative configuration of **3.23b**, **3.23f**, and **3.23g** were assigned in analogy. The stereochemistry of **3.23c** and **3.23d** was assigned in analogy and also by NOESY studies. [d] The absolute configuration of **3.23h** was determined based on the specific rotation of the derivative. [e] The structure and absolute configuration of **3.23i** and **3.23n** was established by X-ray crystallographic analysis. The stereochemistry of **3.23j–m, 3.23o** was assigned in analogy and also by NOESY studies. See Section 3.4.2 for details.

chromatographically separable diastereomers, allowing us to secure the amino ester in enantiomerically pure form.

A range of compounds that contain a 4-substituted piperidine moiety, which is prevalent in pharmaceuticals, proved to be compatible pro-nucleophiles. The union of *N*-benzyl-4-(((*tert*-butyldimethylsilyl)oxy)methyl)piperidine and **3.22a** afforded a mixture of **3.23i** and enamine **3.23j** in 74% and 26% yield, respectively. The reaction of *N*,*N*-dibenzyl-1-(1-benzylpiperidin-4-yl)methanamine and **3.22a** gave **3.23k** and **3.23l** in 51% and 47% yield, respectively. The enamine product (e.g., **3.23j**) may be produced through intramolecular deprotonation of iminium ion by the enolate moiety within the zwitterionic intermediate (**XIX**, Scheme 3.15). Alternatively, protonation of enolate in **XIX** by the ammonium ion, followed by deprotonation of the resulting iminium intermediate by the amine may provide enamine product. In both pathways, regeneration of reactive catalysts from borohydride and ammonium ion likely proceeds through reduction of **3.22a**; indeed, the formation of diisopropyl succinate was observed.

As indicated by synthesis of **3.23m** and **3.23n**, chiral pyrrolidines may be used as starting materials. While the reaction involving less hindered 1-(4-methoxy-2,6-dimethylphenyl) piperidine provided **3.23o** as the only product in 89% yield, with the bulkier 4,4-dimethyl-substituted piperidine, enamine **3.23p** was obtained in 93% yield.[24]

The functional group tolerance of this protocol was demonstrated by the late-stage modification of bioactive amines, which afforded corresponding *β*-functionalized amines (**3.23q**–**3.23t**; Table 3.8). The piperidine moiety in raloxifine (antidepressant), risperidone (anti-psychotic) and paroxetine (anti-Alzheimer) was readily altered, showing that not only the basic *N*-alkylamine moieties but also a ketone (**3.23q**), a benzothiophene (**3.23q**), an ether (**3.23q**, **3.23s**), a pyrimidinone (**3.23r**) and benzoisoxazole (**3.23s**) can be tolerated in our catalyst system. Risperidone, possessing more sterically hindered *β*-amino C–H bonds furnished enamine **3.23r** in 32% yield and only <5% of the product derived from alkylation of acyclic *β*-amino C–H bond (H

Table 3.8. *β*-Alkylation of Various N-Containing Pharmaceuticals[a,b,c]

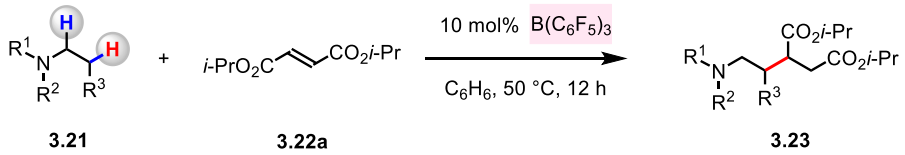

3.21 + 3.22a → 3.23

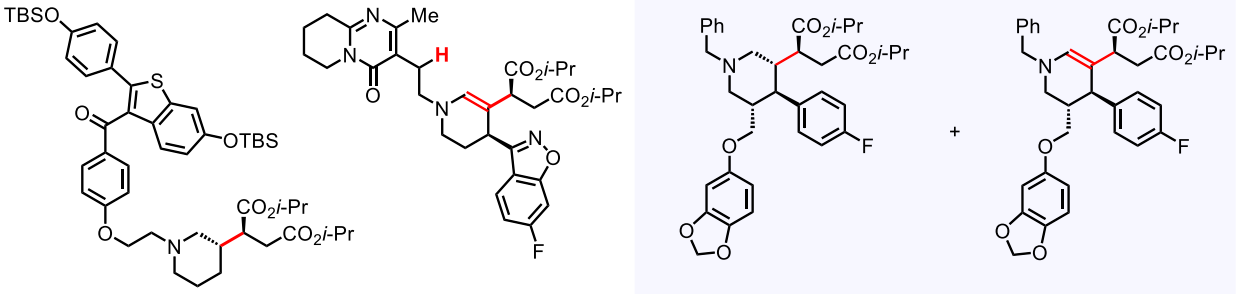

3.23q, **raloxifene derivative**
80% yield, 2.5:1 dr

3.23r, **risperidone derivative**
32% yield, 1.7:1 dr

3.23s, **paroxetine derivative**
39% yield, 2.3:1 dr

3.23t, **paroxetine derivative**
14% yield, 1.9:1 dr

The values correspond to yields of isolated and purified products. [a] Conditions: *N*-alkylamine (**3.21**, 0.2 mmol), diisopropyl fumarate (**3.22a**, 0.3–0.4 mmol), $B(C_6F_5)_3$ (10 mol%), C_6H_6, under N_2, 50 °C. [b] Yield of isolated and purified product. The dr values were determined by ^1H NMR analysis of the unpurified reaction mixtures. [c] The structure and relative configuration of **3.23q**–**r** were assigned in analogy. The stereochemistry of **3.23s**–**t** was assigned in analogy and also by NOESY studies. See Section 3.4.2 for details.

labelled in red) was be observed (^1H NMR analysis). The process involving *N*-benzyl paroxetine afforded **3.23s** and **3.23t** in 39% and 14% yield, respectively.

Mono- and di-carbonyl-substituted alkenes proved to be suitable substrates (Table 3.9). Using dibenzyl fumarate, we were able to isolate **3.23u** in 79% yield; <10% cyclobutane product was observed (vs **3.23b** and **3.23c**, 58% and 33% yield, respectively; Table 3.7). Methyl-4,4,4-trifluorobut-2-enoate was converted to **3.23v** in 74% yield as a single diastereomer. The reaction of *N*,*N*-dibenzylpropan-1-amine with benzyl acrylate gave **3.23w** exclusively in 75% yield. Finally, *N*-phenylmaleimide afforded the corresponding product **3.23x** in 49% yield.

Having demonstrated that $B(C_6F_5)_3$ can promote union of *N*-alkylamines and *α*,*β*-unsaturated compounds, we aimed to develop a catalytic protocol for highly stereoselective *β*-amino C–H functionalization. We first chose the prolinol derivative **3.21k** and (*S*,*E*)-4-phenyl-3-(4,4,4-trifluorobut-2-enoyl)oxazolidin-2-one **3.25a** as model substrates for diastereoselective

Table 3.9. *β*-Alkylation of Amines with Different Electrophiles[a,b]

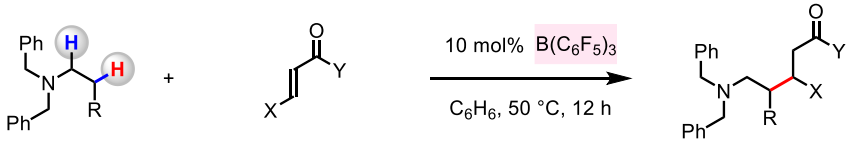

3.21 3.22 3.23

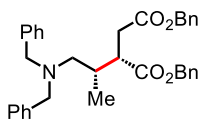

3.23u, 79% yield[c]
2.5:1 dr

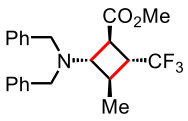

3.23v, 74% yield[c]
>20:1 dr

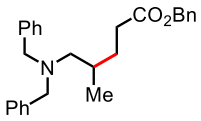

3.23w, 75% yield[d]

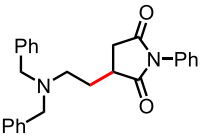

3.23x 49% yield

[a] Conditions: *N*-alkylamine (0.2 mmol), *α,β*-unsaturated molecule, $B(C_6F_5)_3$ (10 mol%), benzene, under N_2, 50 °C. For the detailed conditions, see Section 3.4. [b] Yield of isolated and purified product. The dr values were determined by ^1H NMR analysis of the unpurified product mixtures. [c] The relative configuration of **3.23u** and **3.23v** were assigned in analogy to that determined for **3.23b** and **3.23d.** [d] 5.0 mol% of $B(C_6F_5)_3$ was used.

transformation (Scheme 3.16). We hypothesized that the use of enantio-enriched electrophile may provide the product with diastereoselectivity and reacted **3.21k** and **3.25a** in the presence of $B(C_6F_5)_3$, however, the product **3.26a** was formed in <5% yield (Scheme 3.16a). This could be because $B(C_6F_5)_3$ does not sufficiently activate **3.25a** as it was shown to facilitate the in situ generation enamine intermediate (*β*-alkylation product **3.23n** was obtained from $(F_5C_6)_3B$-catalyzed reaction of **3.21k** and **3.22a**). We wondered if a Lewis acid co-catalyst could activate **3.25a** and promote diastereoselective *β*-amino alkylation. After evaluation of various Lewis acids, it was found that the use of 10 mol% ZnI_2 as a co-catalyst can afford **3.26a** in 82% yield as a single diastereomer. The presence of HBPin as an additive affected the diastereoselectivity, as **3.26a** was produced in 67% yield and 10:1 dr without HBPin.

We then started our investigation on enantioselective *β*-amino C–H alkylation reaction using achiral substrates **3.21q** and **3.25b**, through cooperative function of $B(C_6F_5)_3$ and a chiral organometallic co-catalyst (Scheme 3.16b). After extensive evaluation of metal-ligand complex, we found out that a complex of **L1**–$Mg(ClO_4)_2$ can promote *β*-amino C–H alkylation of **3.21q**

Scheme 3.16. Stereoselective *β*-C–H Functionalization of *N*-Alkylamines through Cooperative Actions of $B(C_6F_5)_3$ and a Lewis Acid Co-catalyst

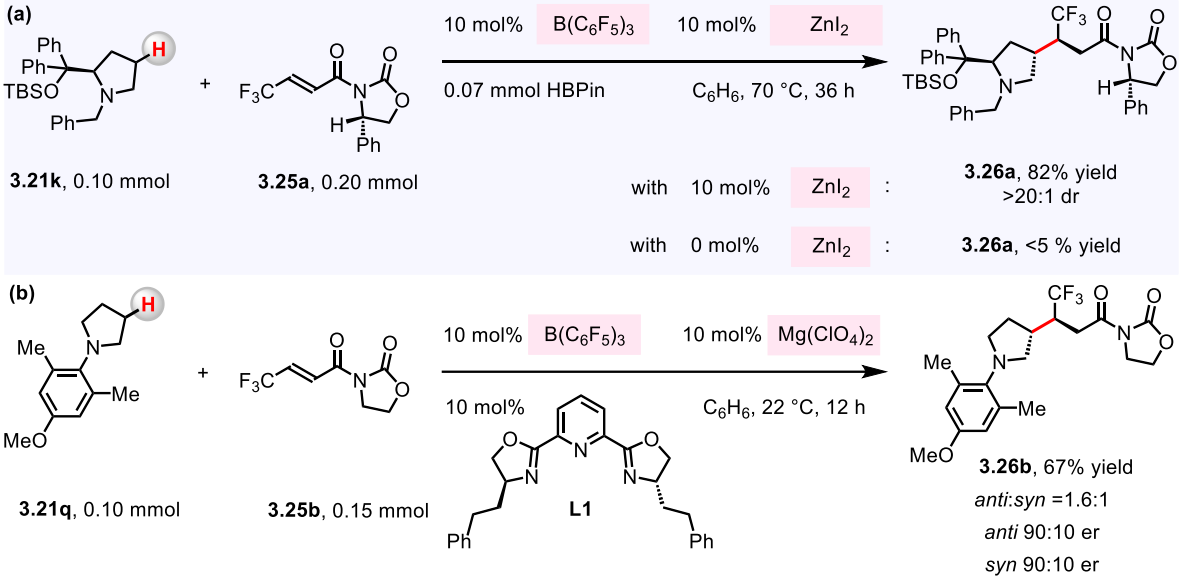

affording **3.26b** in 67% yield (1.6:1 dr, 90:10 er). However, it was the highest efficiency or enantioselectivity we could obtain for the reaction between **3.21q** and **3.25b**.

In an effort to achieve highly enantioselective *β*-C–H functionalization of *N*-alkylamines, we evaluated various combinations of chiral Lewis acid co-catalysts and *α*,*β*-unsaturated compounds possessing different auxiliaries (Table 3.10). It was found that 1-(4-methoxyphenyl)pyrrolidine **3.21r** can be coupled with 2-acryloylpyrazolidinone derivative **3.25c** in the presence of 10 mol% of $B(C_6F_5)_3$ and chiral bisoxazoline ligand–$Sc(OTf)_3$ complex. When Ph–BOX, Ph–DBFOX and Ph–PyBOX ligands (e.g., **L2**–**L4**) were tested, **3.26c** was obtained with low enantioselectivity (58:42–50:50 er). However, after evaluation of alkyl-substituted PyBOX ligands (e.g., **L5**–**L8**), **3.26c** was obtained in 72% yield, 2.7:1 dr and up to 98:2 er, using (*S*)-*i*-Bu–PyBOX (**L8**). Yield of **3.26c** was improved to 85% when **L9** and **L10** were used, however, **L10** was a superior ligand as **3.26c** was obtained with higher enantioselectivity of up to 98:2 er.

Table 3.10. Evaluation of Chiral Ligands[a,b]

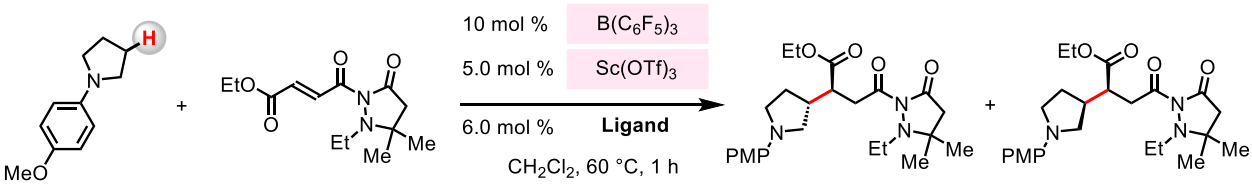

3.21r, 0.20 mmol | **3.25c**, 0.30 mmol | **(*R*,*S*)-3.26c** | **(*S*,*S*)-3.26c**

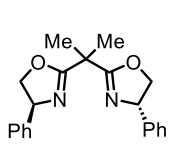

L2

3.26c, 57% yield
R*,*S*:*S*,*S = 2.0:1
R*,*S, 50:50 er
S*,*S, 50:50 er

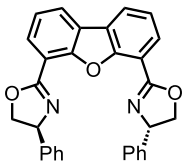

L3

3.26c, 46% yield
R*,*S*:*S*,*S = 2.0:1
R*,*S, 51:49 er
S*,*S, 50:50 er

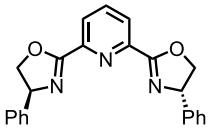

L4

3.26c, 72% yield
R*,*S*:*S*,*S = 5.0:1
R*,*S, 53:47 er
S*,*S, 58:42 er

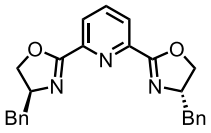

L5

3.26c, 60% yield
R*,*S*:*S*,*S = 2.0:1
R*,*S, 85:15 er
S*,*S, 80:20 er

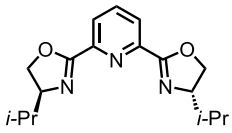

L6

3.26c, 80% yield
R*,*S*:*S*,*S = 4.0:1
R*,*S, 95:5 er
S*,*S, 94:6 er

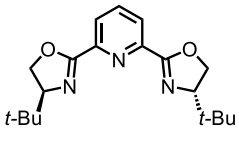

L7

3.26c, 85% yield
R*,*S*:*S*,*S = 1.7:1
R*,*S, 92:8 er
S*,*S, 93:7 er

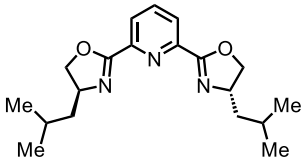

L8

3.26c, 72% yield
R*,*S*:*S*,*S = 2.7:1
R*,*S, 98:2 er
S*,*S, 98:2 er

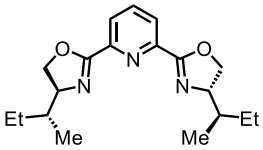

L9

3.26c, 85% yield
R*,*S*:*S*,*S = 2.4:1
R*,*S, 92:8 er
S*,*S, 92:8 er

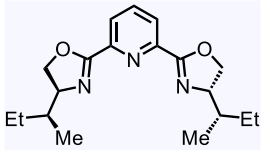

L10

3.26c, 85% yield
R*,*S*:*S*,*S = 2.0:1
R*,*S, 97:3 er
S*,*S, 98:2 er

Yield and diastreomeric ratio (dr) values were determined by the ^{1}H NMR analysis of unpurified reaction mixtures with mesitylene as the internal standard. Enantiomeric ratio (er) values were determined by the HPLC analysis of isolated and purified product. Conditions: *N*-arylpyrrolidine (**3.21r**, 0.20 mmol), *α,β*-unsaturated compound (**3.25c**, 0.30 mmol), $B(C_6F_5)_3$ (10 mol%), $Sc(OTf)_3$ (5.0 mol%), ligand (6.0 mol%), CH_2Cl_2 (2.0 mL), under N_2, 60 °C, 1 h. See Section 3.4.2 for details.

Having found the optimal combination of **L**–$Sc(OTf)_3$ complex and auxiliary, we explored the scope of *α,β*-unsaturated compounds and *N*-alkylamines for the enantioselective transformation (Table 3.11). Electrophiles possessing ester, ketone, or CF_3 substituent underwent efficient reaction with 1-(4-methoxyphenyl)pyrrolidine (**3.21r**) to furnish corresponding *β*-alkylated products (**3.26c**–**3.26f**) in 62–83% yield with 95:5–98:2 er. *N*-Substituents of the pyrazolidinone unit were found to affect stereoselectivity as the reaction of **3.21r** with **3.25c** and **3.25d** afforded **3.26c** (2.0:1 dr, up to 98:2 er) and **3.26d** (3.0:1, up to 95:5 er), respectively.

Table 3.11. Enantioselective *β*-Functionalization of *N*-Alkylamines [a,b]

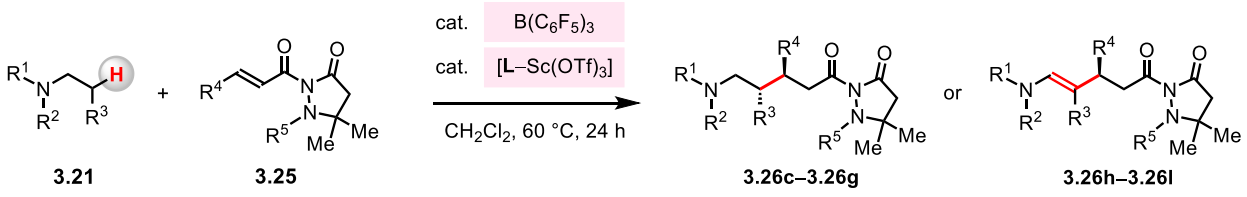

3.21 + **3.25** → **3.26c–3.26g** or **3.26h–3.26l**

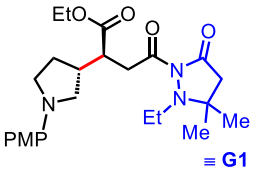

3.26c, 80% yield
(*R*,*S*):(*S*,*S*) = 2.0:1
(*R*,*S*) 97:3 er
(*S*,*S*) 98:2 er

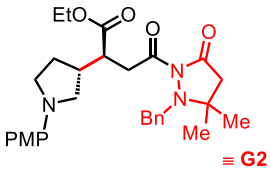

3.26d, 83% yield[b]
(*R*,*S*):(*S*,*S*) = 3.0:1
(*R*,*S*) 95:5 er
(*S*,*S*) 95:5 er

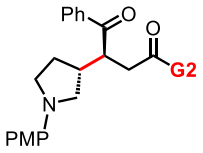

3.26e, 78% yield[b]
(*R*,*S*):(*S*,*S*) = 3.5:1
(*R*,*S*) 95:5 er
(*S*,*S*) 95:5 er

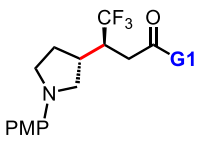

3.26f, 62% yield
(*R*,*S*):(*S*,*S*) = 6.7:1
(*R*,*S*) 96:4 er
(*S*,*S*) 96:4 er

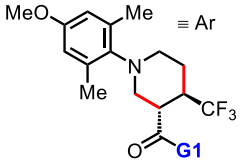

3.26g, 67% yield[c,d]
(*S*,*R*):(*R*,*R*) = >20:1
(*S*,*R*) 95:5 er

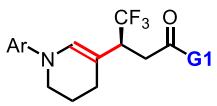

3.26h, 95% yield
95:5 er

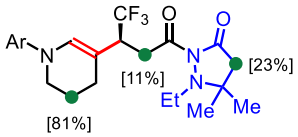

3.26h-*d*, 84% yield
95:5 er

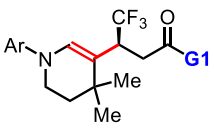

3.26i, 74% yield[e]
93:7 er

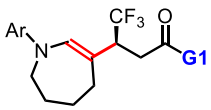

3.26j, 78% yield
96:4 er

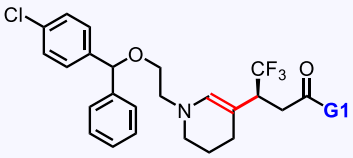

3.26k, **cloperastine derivative**
53% yield
1.0:1 dr, 90:10 er[c,e,f]

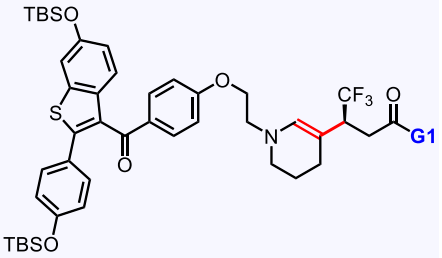

3.26l, **raloxifene derivative**
57% yield
95:5 er[c,e,f]

[a] Conditions: *N*-alkylamine (**3.21**, 0.10 mmol), *α*,*β*-unsaturated compound (**3.25**, 0.15 mmol), $B(C_6F_5)_3$ (10 mol%), $(TfO)_3Sc$/**L10** (10 mol%), CH_2Cl_2 (1.0 mL), under N_2, 60 °C, 1–36 h. [b] 10 mol% of $(TfO)_3Sc$/**L6** was used. [c] 20 mol% of $B(C_6F_5)_3$ was used. [d] 20 mol% of $(TfO)_3Sc$/**L10** was used. [e] The reaction was performed at 80 °C. [f] 10 mol% of $(TfO)_3Sc$/**L8** was used. See Section 3.4.2 for details.

When acyclic *N*-ethyl-4-methoxy-*N*,2,6-trimethylaniline **3.21s** was treated with F_3C-substituted **3.25f** (Scheme 3.17), *N*-arylpiperidine derivative **3.26g** was obtained in 67% yield (>20:1 dr, 95:5 er). The plausible mechanism for generation of **3.26g** involves *β*-amino C–H alkylation of **3.21s** by **3.25f** furnishing a zwitterionic intermediate containing an iminium and an enolate (**XX**), which could isomerize to **XXI**; ensuing intramolecular Mannich-type reaction would afford **3.26g**.

Scheme 3.17. Sequential *β*-alkylation and Mannich-type reaction for synthesis of piperidine derivative **3.26g**

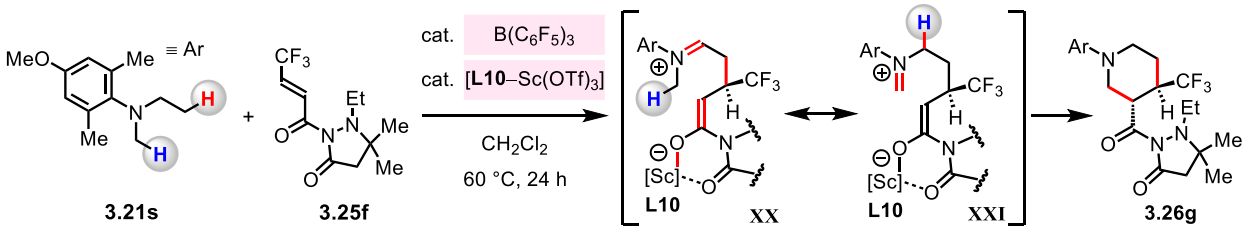

The *β*-alkylation of *N*-arylpiperidines or *N*-arylazapene using **3.25f** provided products as enamines **3.26h**–**3.26j** in 74–95% yield and 93:7–96:4 er (Table 3.11). The reaction of *N*-arylpiperidine-3,3,5,5-d_4 **3.21l-*d*** (0.10 mmol) and **3.25f** (0.20 mmol) afforded **3.26h-*d*** (84% yield, 95:5 er) and **3.27f-*d*** (0.08 mmol; Scheme 3.18). The D/H exchange at C5 position of **3.26h-*d*** (>95% in **3.21l-*d*** → 81% in **3.26h-*d***) and incorporation of deuterium at enolizable *α*-carbonyl positions in **3.26h-*d*** and **3.27f-*d*** was observed by the ^{1}H NMR analyses, indicating that $[(F_5C_6)_3B–H]^-$ $[base–D]^+$ formed in situ reacts with **3.25f** to produce **3.27f-*d***, to regenerate $B(C_6F_5)_3$ (vs through the release of H–D).

Scheme 3.18. Incorporation Deuterium into Enolizable Positions of **3.26h-*d***

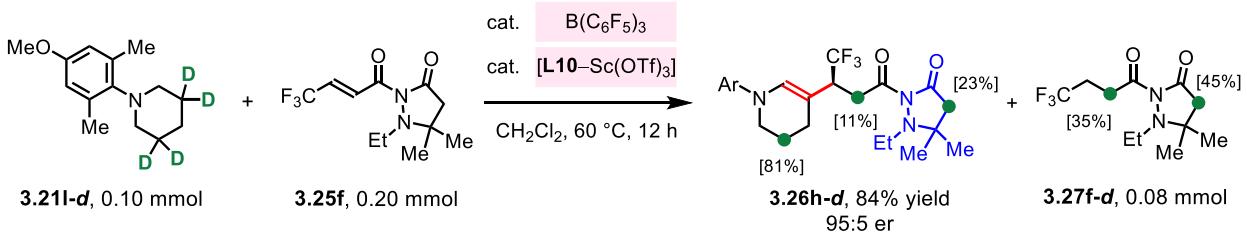

This protocol is highly functional group tolerant as shown by the conversion of *β*-Amino C–H bonds in bioactive trialkylamines such as cloperastine **3.21u** and raloxifene derivative **3.21n**, which afforded enamines **3.26k** and **3.26l** in 53% yield (90:10 er) and 57% yield (95:5 er), respectively (Table 3.11).

The scalability of this method was demonstrated by the reaction of 4.0 mmol of *N*-arylpiperidine **3.21l** and **3.25f** with 10 mol% $B(C_6F_5)_3$ and **L10**–$Sc(OTf)_3$, which delivered the corresponding product **3.26h** in 95% yield (1.9 g; Scheme 3.19).

Scheme 3.19. Scalability of Enantioselective *β*-Amino C–H Alkylation

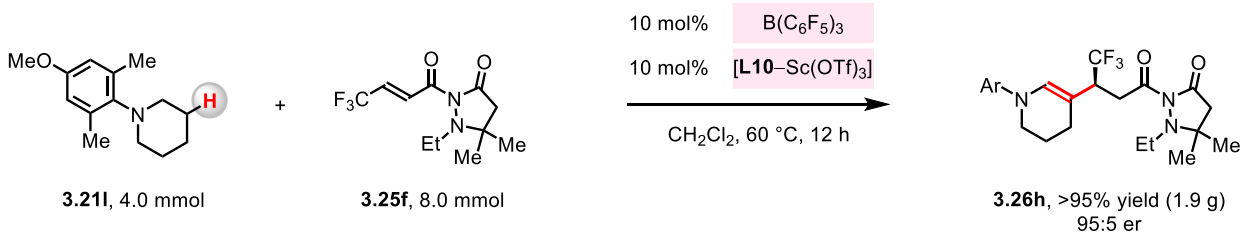

By treating **3.26f** with LiSEt followed by reduction of the resulting thioester, alcohol **3.28** was obtained in 95% yield (Scheme 3.20a). After the conversion of **3.28** into the corresponding carbamate **3.29**, absolute configuration was determined through the X-ray crystallographic analysis (see Section 3.4 for details). Enamine product **3.26h**, obtained by enantioselective *β*-alkylation, could serve as versatile intermediates (Scheme 3.20b) as hydrogenation of **3.26h** by a chiral Ir-based complex afforded **3.30** in 83% yield with 5.0:1 dr,[26] while fluorocyanation of **3.26h** using NFSI and TMSCN furnished **3.31** in 88% yield with 4.0:1 dr.[27]

Scheme 3.20. Modification of *β*-Alkylated Amine Products

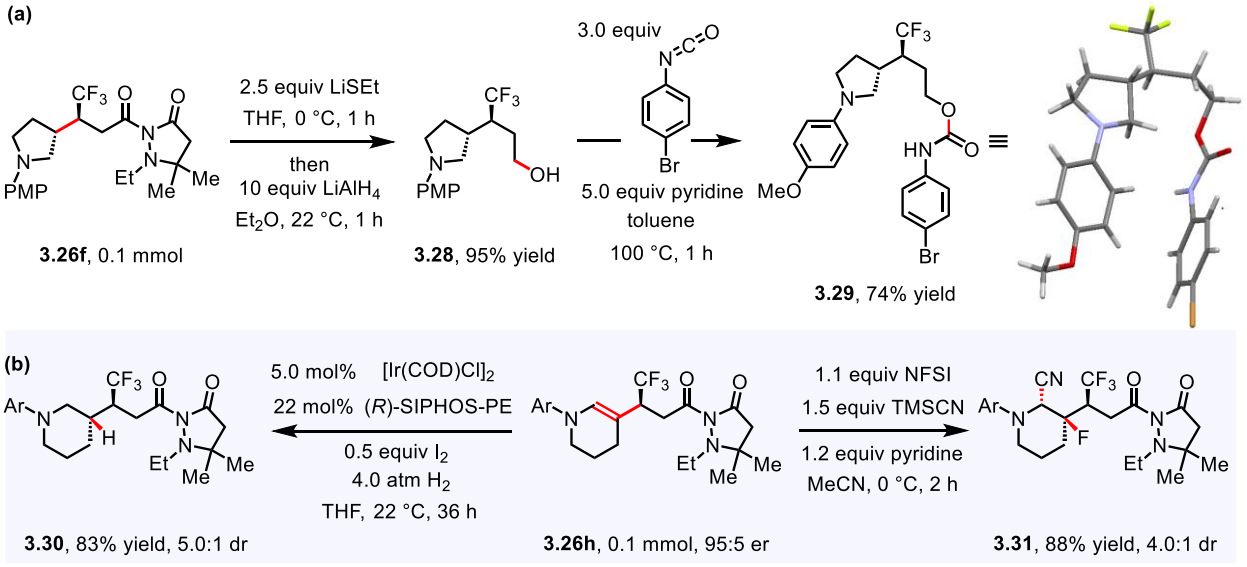

3.3.4. Results and Discussion – Mechanistic Investigations

Having demonstrated that cooperative catalyst system consisting of $B(C_6F_5)_3$, chiral Lewis acid, and Brønsted base can promote the functionalization of β-amino C–H bonds, we designed and carried out investigations to shed light on the mechanism of the catalytic process. The mechanistic studies include: (i) determination of reaction orders (Figure 3.1), (ii) kinetic isotope effect (KIE) studies (Scheme 3.21), and (iii) determination of Hammett ρ values (Scheme 3.24). Based on the results obtained from mechanistic investigations, we propose a revised catalytic cycle for catalytic β-C–H alkylation reaction (Scheme 3.22).

We began our investigation by performing the initial kinetic experiments for the reaction of *N*-arylpyrrolidine **3.21r** and α,β-unsaturated compound **3.25g** to determine the reaction order of each species (Figure 3.1). The reaction rate was found to have: (i) a second-order dependence on $B(C_6F_5)_3$ concentration (Figure 3.1a), (ii) a zero-order dependence on the concentration of **L6**–$Sc(OTf)_3$ complex (Figure 3.1b), (iii) a first-order dependence on concentration of amine **3.21r** (Figure 3.1c), and (iv) a reverse first-order dependence on the concentration of electrophile **3.25g** (Figure 3.1d). The independence of the reaction rate on the initial concentration of **L6**–$Sc(OTf)_3$ implies that turnover-limiting step is prior to the enantioselective C–C bond formation between in situ generated enamine and [**L6**–$Sc(OTf)_3$]-activated **3.25g** (Scheme 3.15, **XXVI** → **XXVII**); thus, either the hydride abstraction or the deprotonation step is likely turnover-limiting.

To determine whether the cleavage of α- or β-amino C–H bond is involved in the turnover-limiting step, we carried out independent KIE experiments (Scheme 3.21). From the independent rate measurements involving **3.21r**and **3.21r-*d*$_\alpha$** (Scheme 3.21a), $k_H/k_D = 1.28 \pm 0.07$ was observed. On the other hand, the reaction rate comparison between **3.21r** and **3.21r-*d*$_\beta$** (Scheme 3.21b) disclosed that **3.21r** reacts 2.5 times faster than **3.21r-*d*$_\beta$** ($k_H/k_D = 2.50 \pm 0.13$). These results

Figure 3.1. Determination of Reaction Orders

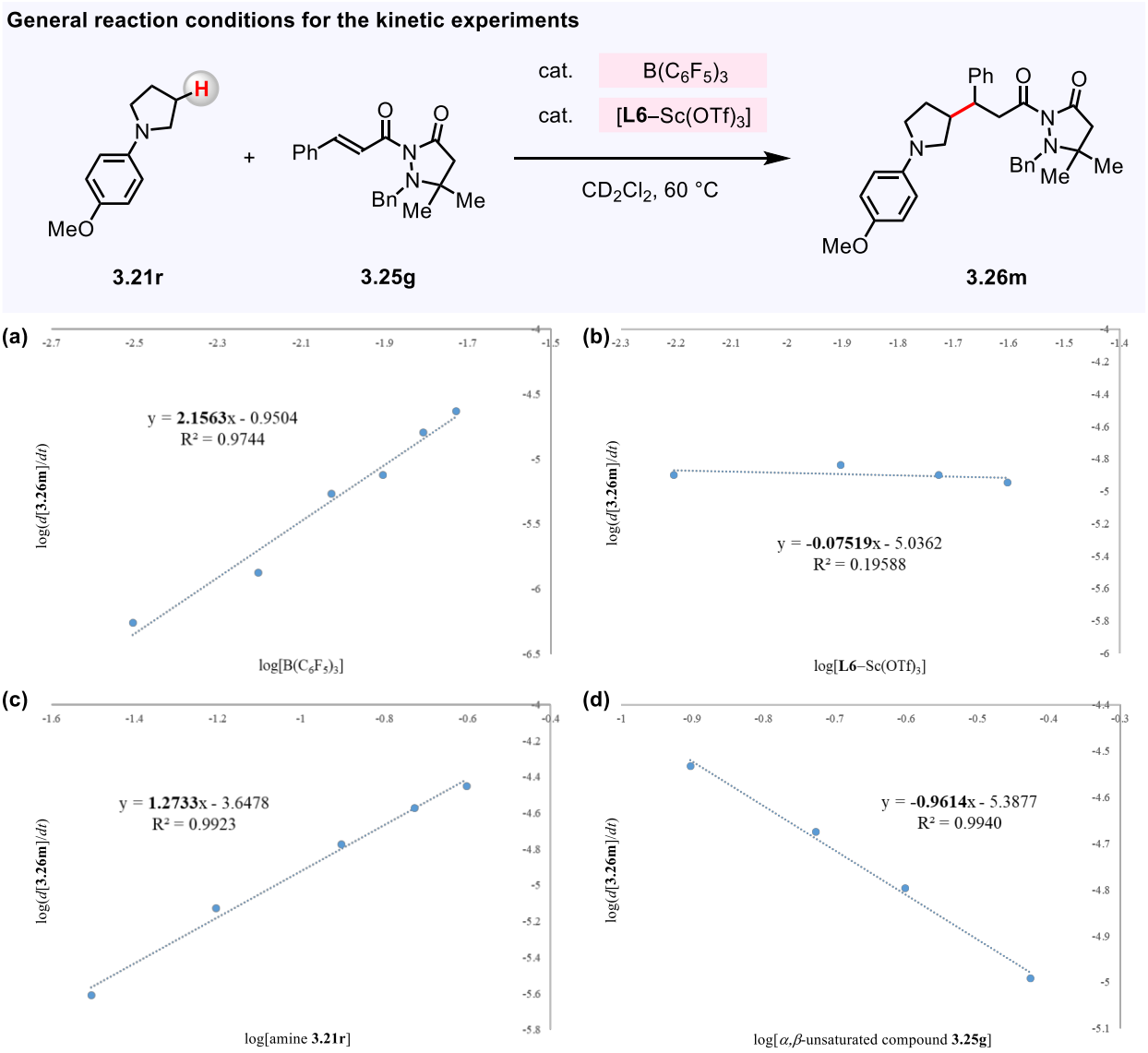

suggest that the turnover-limiting step is the deprotonation step involving cleavage of α-imino C–H or C–D bonds (Scheme 3.15, **XVI**→**XVII**) and that $(F_5C_6)_3B$-catalyzed hydride abstraction is reversible.

We hypothesized that the reverse first-order dependence on the concentration of **3.25g** is due to the catalyst resting state consisting of **3.25g** and $B(C_6F_5)_3$. Indeed, the ^{19}F NMR analysis of the reaction mixture supports the formation of [**3.25g**–$B(C_6F_5)_3$] (**XXII**, Scheme 3.22).

Scheme 3.21. Kinetic Isotope Effect Studies

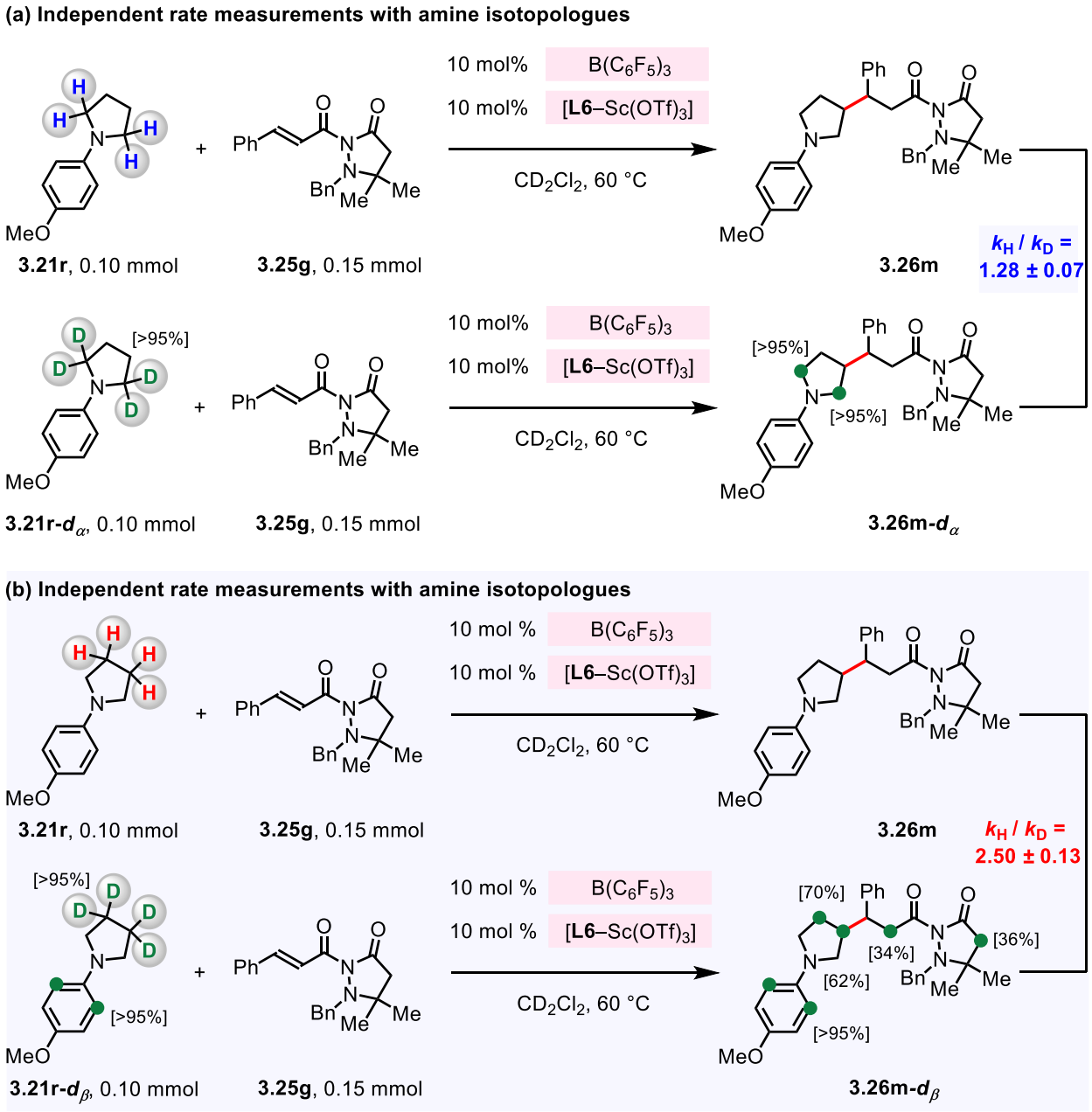

Meanwhile, the second-order dependence on $B(C_6F_5)_3$ concentration indicates that there are two $B(C_6F_5)_3$ involved in the turnover-limiting step; thus, second-order dependence on the concentration of electrophile **3.25g** is expected**.** However, the reverse first-order dependence we observed suggests that one electrophile **3.25g** is involved in the turnover-limiting step. Furthermore, the first-order dependence on the concentration of amine **3.21r** implies that the

Scheme 3.22. A Revised Catalytic Cycle Consistent with the Results of Mechanistic Investigations

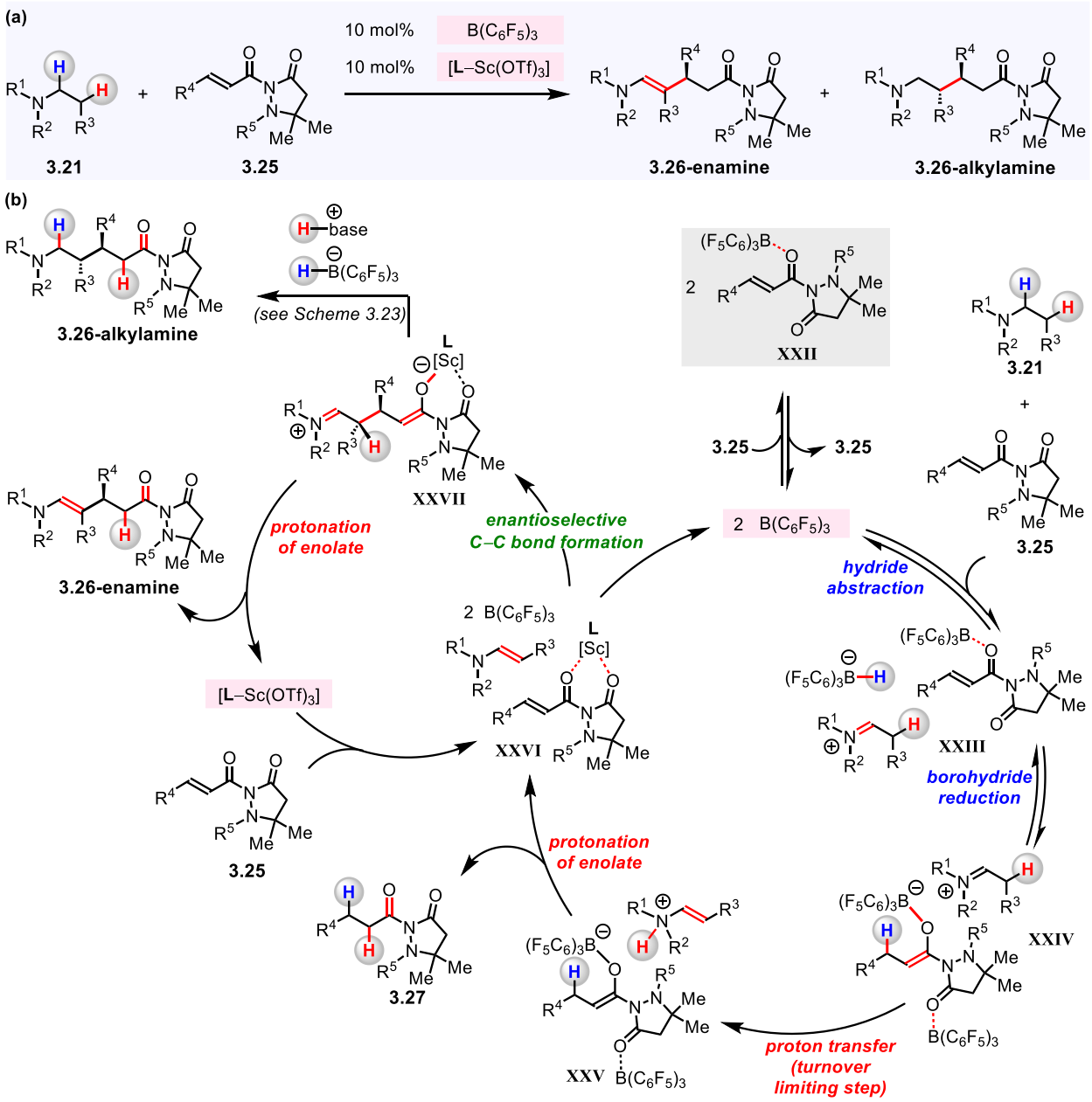

deprotonation of iminium (Scheme 3.15, **XVI→XVII**) is not mediated by the *N*-alkylamine substrate.

Based on the results discussed above, we propose a revised catalytic cycle that is consistent with the kinetic data we obtained from the mechanistic studies (Scheme 3.22). The reaction is proposed to proceed through the release of $B(C_6F_5)_3$ from the catalyst resting state (**XXII**),

followed by hydride abstraction from **3.21** to generate an ion pair consisting of an iminium and a borohydride (**XXIII**). Borohydride could then reduce $(F_5C_6)_3B$-activated **3.25** to furnish a $(F_5C_6)_3B$–enolate (**XXIII→XXIV**).[17] Ensuing isomerization of the iminium into an enammonium (**XXIV→XXV**) is likely the turnover-limiting step (see the Hammett studies, and Section 3.4).[18] Protonation of $(F_5C_6)_3B$–enolate would release $B(C_6F_5)_3$, **3.27**, and the enamine intermediate (**XXV→XXVI**). The reaction between the nucleophilic enamine and [**L**–$Sc(OTf)_3$]-activated electrophile **3.25** would forge a new C–C bond in an enantioselective manner affording a zwitterionic intermediate **XXVII**. To close the catalytic cycle, proton transfer within **XXVII** delivers **3.26-enamine** and regenerates **L**–$Sc(OTf)_3$. Alternatively, borohydride reduction of the iminium and protonation of the enolate in **XXVII** could furnish **3.26-alkylamine**.

As shown in Tables 3.7, 3.8, and 3.11, the *β*-alkylated amine products were obtained either as an enamine, an *N*-alkylamine, or a mixture of the two (e.g., **3.23i** and **3.23j**, Table 3.7). Therefore, we wanted to study the origin of enamine and *N*-alkylamine products. Specifically, whether the *N*-alkylamine product was formed by transfer hydrogenation of **XXVII** (**XXVII→3.26-alkylamine**, Scheme 3.22), or through reduction of enamines (**3.26-enamine→3.26-alkylamine**). The progress of $(F_5C_6)_3B$-catalyzed reaction between *N*-arylpiperidine **3.21l** and **3.22a** was monitored (Scheme 3.23a), which gives a mixture of *N*-alkylamine **3.23o** (57% yield) and enamine **3.32** (29% yield) under the concentration of 1.0 M (vs the process in 0.25 M, which selectively affords **3.23o**; Table 3.7). There was minimal transformation of **3.32** into **3.23o** as the concentration of **3.32** mostly unchanged once the reaction

[17] Chen, G. Q.; Kehr, G.; Daniliuc, C. G.; Bursch, M.; Grimme, S.; Erker, G. *Chem. Eur. J.* **2017**, *23*, 4723–4729.
[18] (a) Sorgi, K. L.; Maryanoff, C. A.; McComsey, D. F.; Graden, D. W.; Maryanoff, B. E. *J. Am. Chem. Soc.* **1990**, *112*, 3567–3579. (b) Han, J.; Lu, Z.; Flach, A. L.; Paton, R. S.; Hammond, G. B.; Xu, B. *Chem. Eur. J.* **2015**, *21*, 11687–11691. (c) Ashley, M. A.; Hirschi, J. S.; Izzo, J. A.; Vetticatt, M. J. *J. Am. Chem. Soc*. **2016**, *138*, 1756–1759.

was complete (2 h; Scheme 3.23b). These results are consistent with our hypothesis that **3.26-alkylamine** (Scheme 3.22) is formed by transfer hydrogenation of **XXVII** without the intermediacy of **3.26-enamine**. However, the source of proton and hydride has not yet been identified.

Scheme 3.23. Origin of Enamine and *N*-Alkylamine Products

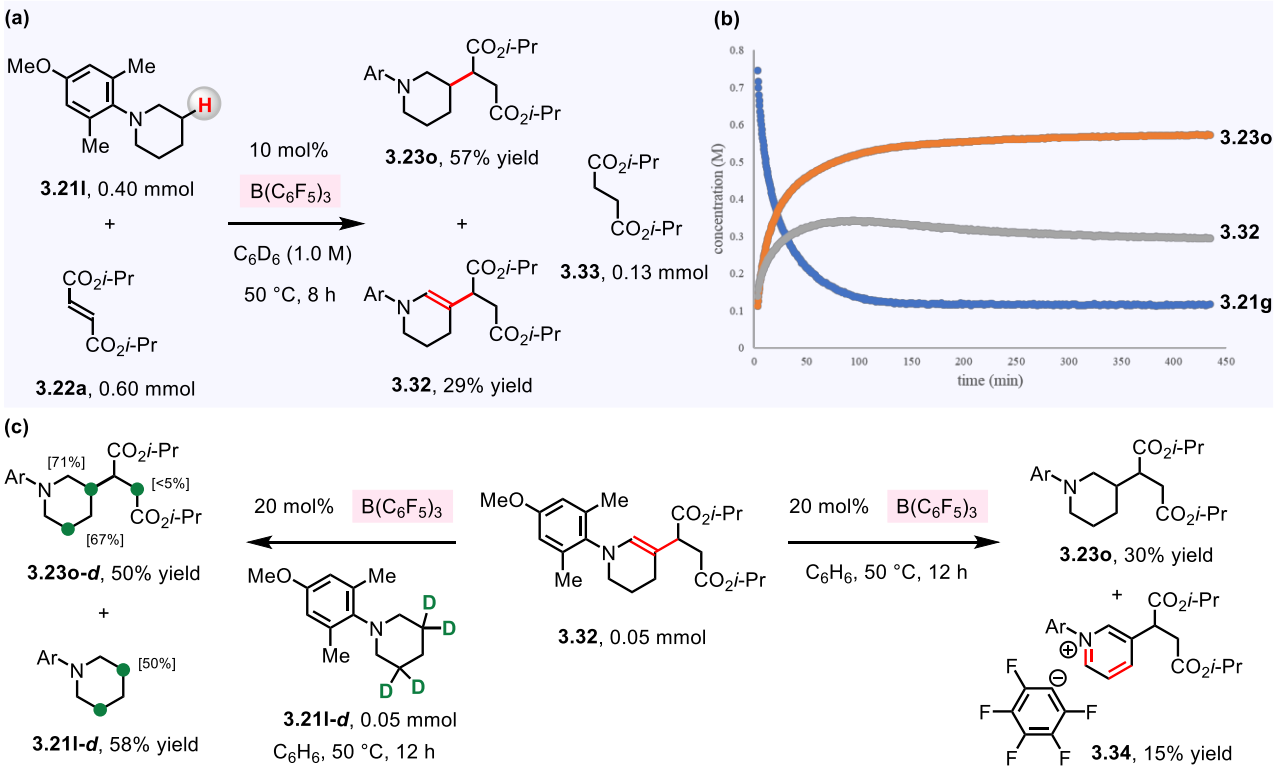

To probe further if, and under precisely what conditions **3.32** can be converted to **3.23o**, we investigated the transformation of **3.32** in the presence of 20 mol% $B(C_6F_5)_3$ (C_6H_6, 12 h; Scheme 3.23c). We were able to observe 30% conversion of **3.32** to **3.23o** as well as 15% of [pyridinium]$^+$[C_6F_5]$^-$ (**3.34**). Furthermore, by treating **3.32** with *N*-arylpiperidine-3,3,5,5-d_4 ***3.21l-d***, ***3.23o-d*** was obtained in 50% yield; there was significant D/H exchange in both ***3.23o-d*** (at **C3** and **C5** positions, 71% and 67%, respectively) and recovered ***3.21l-d***. These data suggest that $B(C_6F_5)_3$ can catalyze transfer hydrogenation of **3.32** in the presence of another molecule of **3.32**

and/or **3.21l-*d*** serving as sources of H^+ (or D^+) and hydride. Nonetheless, under the standard conditions for $(F_5C_6)_3B$-catalyzed β-C–H alkylation reaction (Schemes 3.22 and 3.23a), in situ generated $[(F_5C_6)_3B–H]^-[base–H]^+$ (derived from the reaction of $B(C_6F_5)_3$ and *N*-alkylamine **3.21**) reacts with either a highly reactive zwitterionic intermediate (**XXVII→3.26-alkylamine**) or $(F_5C_6)_3B$-activated α,β-unsaturated compounds (**XXIII→XXIV→XXV→3.27**). Therefore, transfer hydrogenation of the relatively unreactive enamine **3.32** to give **3.23o** is likely outcompeted by these more facile processes.

We carried out Hammett studies to gain further insight regarding the turnover-limiting step of this catalytic transformation (Scheme 3.24). It was found that the reaction rate has a strong dependence on the electronic properties of the *N*-alkylamines; *N*-arylpyrrolidine derivatives (**3.21**) possessing electron-donating substituents reacted with higher efficiency ($\rho = –4.9$, Schemes 3.24a and 3.24c). The large negative ρ value supports the proposed mechanism (Scheme 3.22) where $B(C_6F_5)_3$ abstracts a hydride from *N*-arylpyrrolidine **3.21** into an *N*-aryl iminium cation (**3.21→XXIII**), and its isomerization into an enammonium species (**XXIII→XXIV→XXV**); these processes take place at or prior to the turnover-limiting step.

Meanwhile, the reaction rate was less dependent of the electronic properties of α,β-unsaturated compounds **3.25** and those involving electron-withdrawing groups reacted more rapidly ($\rho = 0.92$, Schemes 3.24b and 3.24d). This result is consistent with the proposed catalytic cycle that borohydride reduction of **3.25** furnishes a boron–enolate intermediate (Scheme 3.22; **XXIII→XXIV**), which also occurs at or prior to the turnover-limiting step.

Scheme 3.24. Hammett Studies

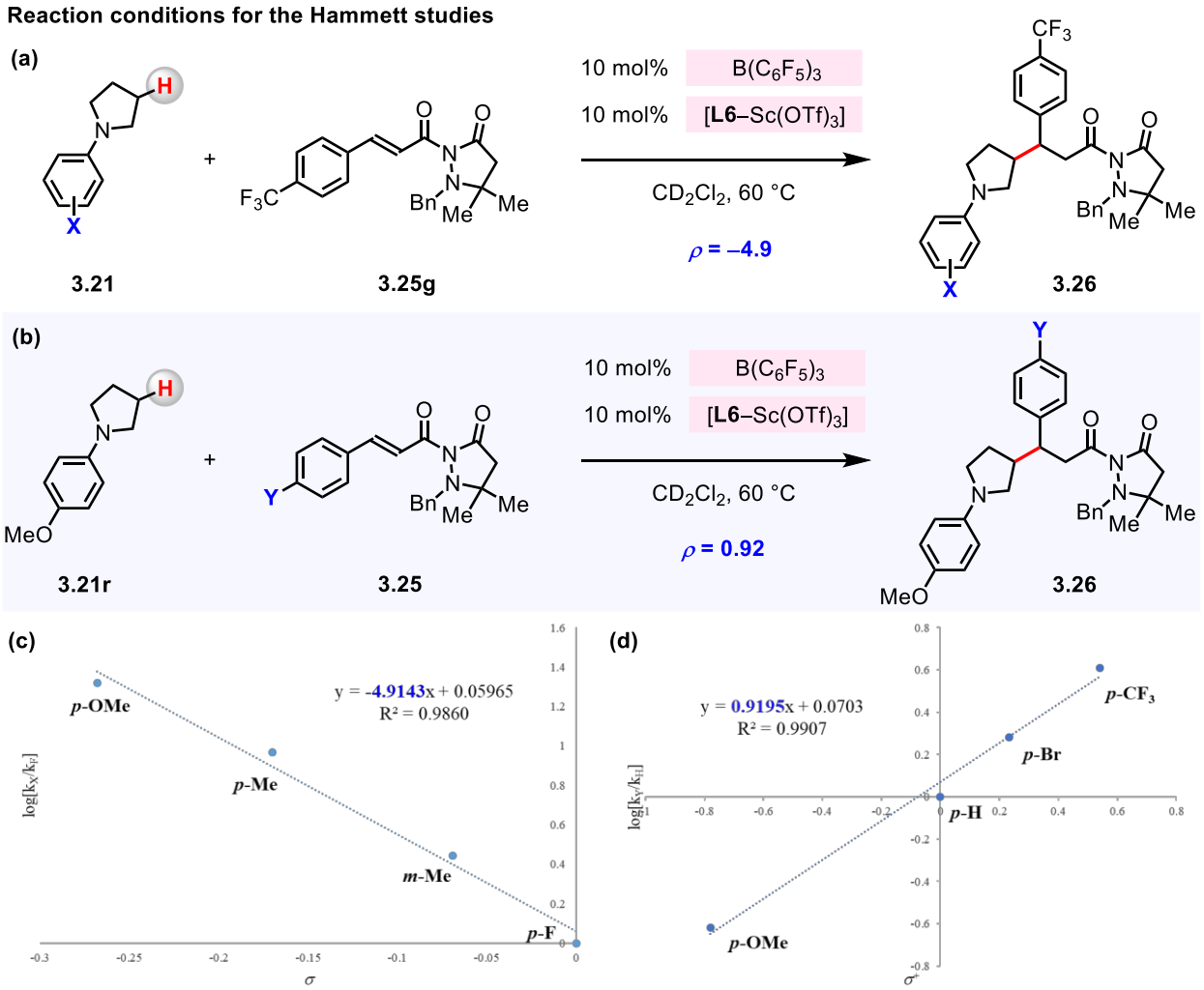

3.3.5. Conclusions and Future Outlook

We have demonstrated that the cooperative actions of $B(C_6F_5)_3$ and an appropriate Brønsted base can convert a broad array of N-based pharmaceuticals into enamines. We have successfully developed the reaction of in situ generated enamines with D^+ as well as Michael acceptors.[19-20] By incorporation of a chiral organometallic catalyst, enantioselective β-amino C–H alkylation was also achieved.

Despite the advances we have achieved, these work also unveiled key shortcomings of our approach.

1) scope of compatible transformations is narrow

2) functional group tolerance remains to be modest; less hindered basic moieties (e.g., alcohols, primary amines) needed appropriate protections.

3) modest reaction efficiency and enantioselectivity (e.g., **3.26k**, Table 3.11).

These problems originate from the fact that our organoborane/chiral Lewis acid co-catalyst system is not generally applicable enough to promote efficient and enantioselective union of otherwise poorly reactive pronucleophiles and electrophiles.

In the future work, our group will continue to investigate novel catalyst systems capable of converting various molecules into electrophilic and/or nucleophilic intermediates through Lewis acid-catalyzed hydride abstraction (Scheme 3.25). Some of the representative processes include the activation of ethers **3.36**, thioethers **3.37** and alkenes **3.38** into the corresponding carbocations (**XXX**, **XXXII**, and **XXXIV**); trapping of these carbocations with different nucleophiles may allow access to a broad array of α-substituted compounds. Alternatively, nucleophilic

[19] Chang, Y.; Yesilcimen, A.; Cao, M.; Zhang, Y.; Zhang, B.; Chan, J. Z.; Wasa, M. *J. Am. Chem. Soc*. **2019**, *141*, 14570–14575.

[20] Chang, Y.; Cao, M.; Chan, J. Z.; Zhao, C.; Wang, Y.; Yang, R.; Wasa, M. *J. Am. Chem. Soc*. **2021**, *143*, 2441–2455.

intermediates (**XXXI**, **XXXIII**, and **XXXV**) generated through deprotonation of the carbocations can be used to produce a wide range of *β*-substituted molecules. To address the issue of functional group tolerance, further investigation must be performed to discover Lewis acid and base catalysts that are more sterically and electronically "frustrated" against the acidic and basic moieties. Our studies (c.f., Schemes 2.12 and 3.24) indicate that various metal–ligand complexes (e.g., L_nSc–PyBoX, L_nCu–bisphosphine) are moderately tolerant of acid-sensitive functional groups; identification of other organometallic complexes that promote more efficient hydride abstraction and/or activation of coupling partners could lead to drastic expansion in the substrate scope as well as functional group tolerance. Furthermore, the in-situ generated intermediates generated by hydride abstraction from amines, ethers, thioethers and alkenes (e.g., **XXVIII**–**XXXV**, Scheme 3.25A–D) can be trapped by nucleophilic and/or electrophilic partners that are generated by organometallic catalysis (Scheme 3.25E), [21 - 22] photocatalysis (Scheme 3.25E), [23 - 24] and electrocatalysis (Scheme 3.25G). [25 - 26] Through these future work, our aim is to address the fundamental limitations associated with enantioselective late-stage C–H functionalization reactions.

[21] He, J.; Wasa, M.; Chan, K. S. L.; Shao, Q.; Yu, J.-Q. *Chem. Rev*. **2017**, *117*, 8754–8786.
[22] Ozawa, F.; Kubo, A.; Hayashi, T. *J. Am. Chem. Soc*. **1991**, *113*, 1417–1419.
[23] (a) Romero, N. A.; Nicewicz, D. A. *Chem. Rev*. **2016**, *116*, 10075–10166. (b) Shaw, M. H.; Twilton, J.; MacMillan, D. W. C. *J. Org. Chem*. **2016**, *81*, 6898–6926.
[24] Nagib, D. A.; Scott, M. E.; MacMillan, D. W. C. *J. Am. Chem. Soc*. **2009**, *131*, 10875–10877.
[25] Yan, M.; Kawamata, Y.; Baran, P. S. *Chem. Rev*. **2017**, *117*, 13230–13319. (b) Liu, J.; Lu, L.; Wood, D.; Lin, S. *ACS Cent. Sci*. **2020**, *6*, 1317–1340.
[26] Song, L.; Fu, N.; Ernst, B. G.; Lee, W. H.; Frederick, M. O.; DiStasio Jr., R. A.; Lin, S. *Nat. Chem*. **2020**, *12*, 747–754.

Scheme 3.25. Cooperative Catalyst Systems for Selective Late-Stage C–H Functionalization

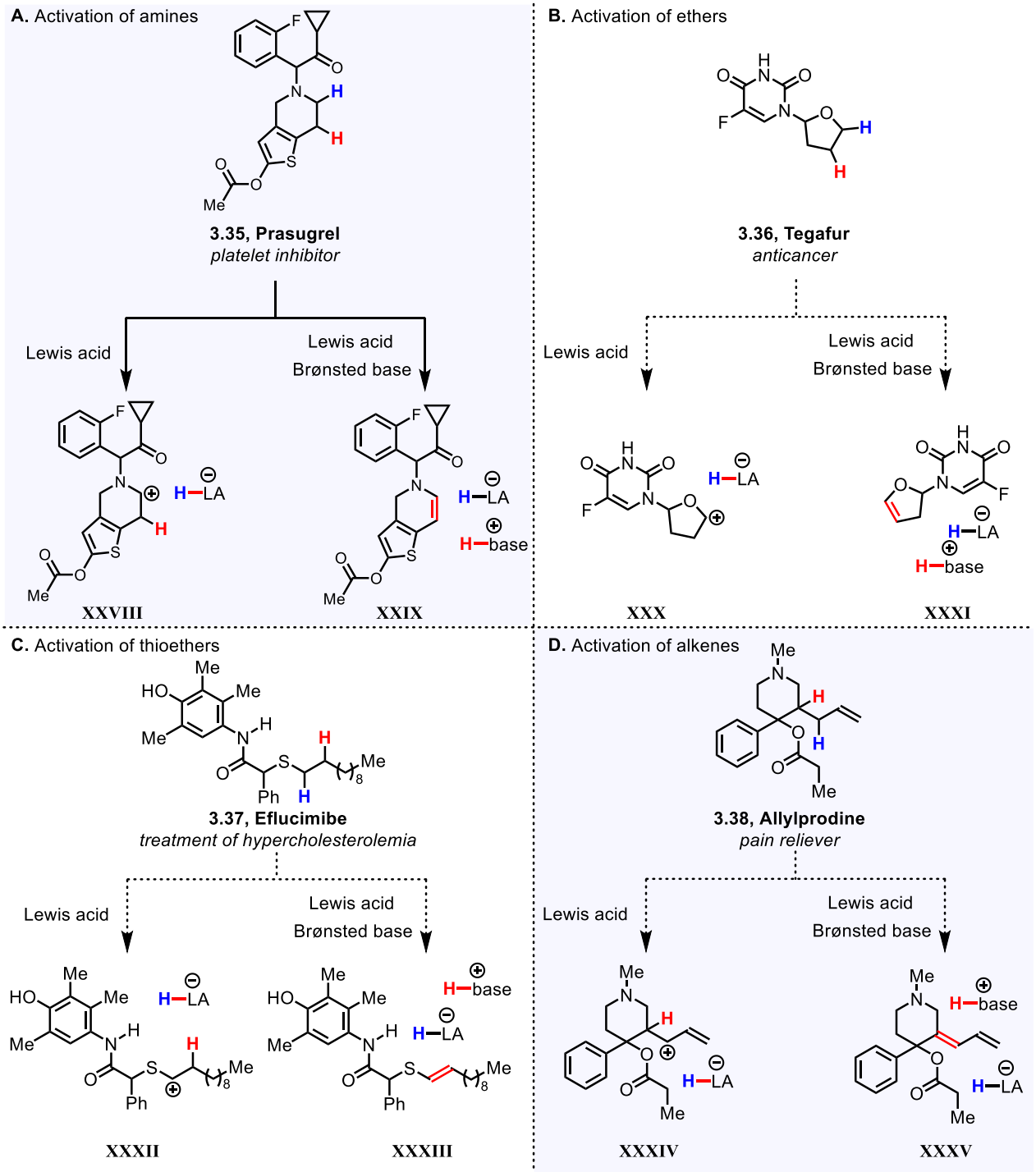

Scheme 3.25. Cooperative Catalyst Systems for Selective Late-Stage C–H Functionalization (Continued)

E Cooperative FLP/organometallic catalysis

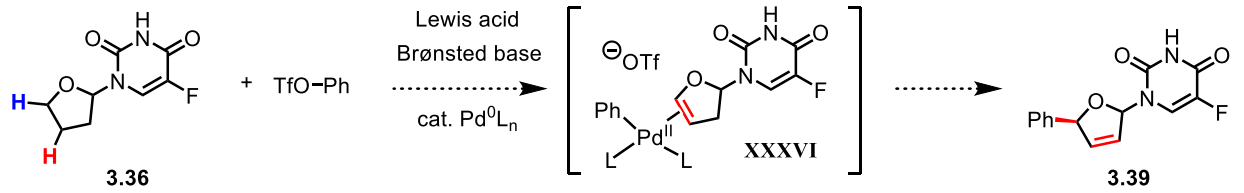

3.36 3.39

F Cooperative FLP/photocatalysis

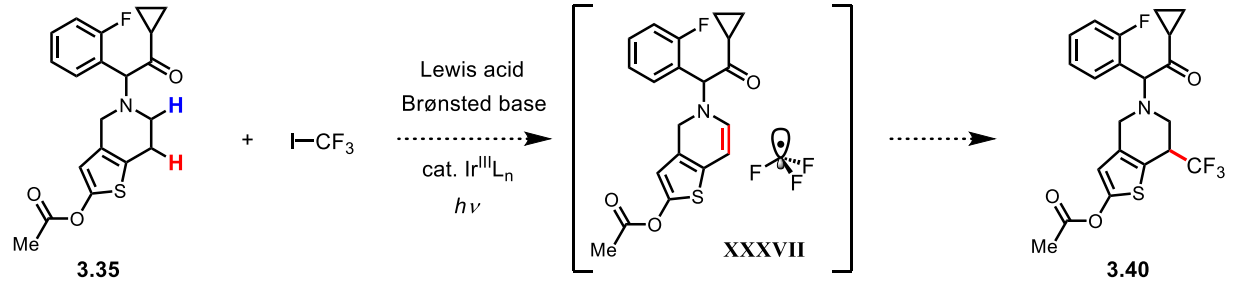

3.35 3.40

G Cooperative FLP/electrocatalysis

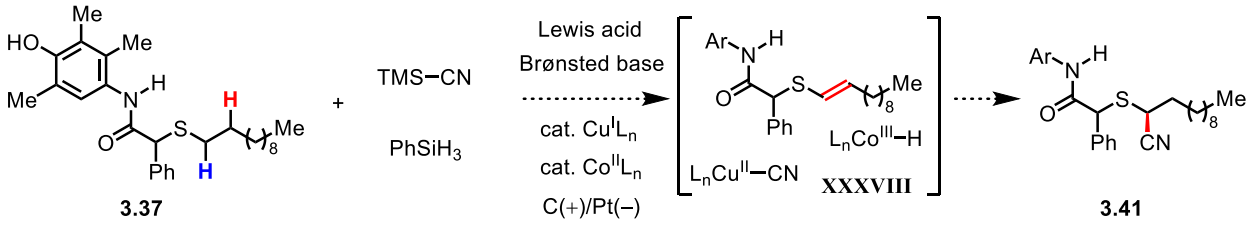

3.37 3.41

Appendix A. Experimental for Chapter 2

General experimental procedures

All reactions were performed in standard, dry glassware fitted with rubber septa under an inert atmosphere of nitrogen unless otherwise described. Stainless steel syringes or cannulae were used to transfer air- and moisture-sensitive liquids. Reported concentrations refer to solution volumes at room temperature. Evaporation and concentration *in vacuo* were performed using house vacuum (ca. 40 mm Hg). Column chromatography was performed with SiliaFlash® 60 (40–63 micron) silica gel from Silicycle. Thin layer chromatography (TLC) was used for reaction monitoring and product detection using pre-coated glass plates covered with 0.20 mm silica gel with fluorescent indicator; visualization by UV light (λ_{ex} = 254 nm) or $KMnO_4$ stain.

Materials

Reagents were purchased in reagent grade from commercial suppliers and used without further purification, unless otherwise described. Amines and silicon enolates were prepared according to the procedures reported previously.[1-22] Tris(pentafluorophenyl)borane and ((1-methoxy-2-methylprop-1-en-1-yl)oxy)trimethylsilane were purchased from TCI and used without further purification. H_2O, in synthetic procedures, refers to distilled water.

Instrumentation

Proton nuclear magnetic resonance (^{1}H NMR) spectra and proton-decoupled carbon nuclear magnetic resonance (^{13}C {^{1}H} NMR) spectra were recorded at 25 °C (unless stated otherwise) on Inova 600 (600 MHz), Varian Unity/Inova 500 (500 MHz) or Oxford AS400 (400 MHz) spectrometers at the Boston College nuclear magnetic resonance facility. Chemical shifts for protons are reported in parts per million downfield from tetramethylsilane and are referenced to 0 ppm. Chemical shifts for carbon are reported in parts per million downfield from tetramethylsilane

and are referenced to the carbon resonances of the solvent. The solvent peak was referenced to 77.0 ppm for ^{13}C for $CDCl_3$. Benzotrifluoride was used as an external standard for ^{19}F NMR and referenced to –63.7 ppm. Data are represented as follows: chemical shift, integration, multiplicity (br = broad, s = singlet, d = doublet, t = triplet, q = quartet, m = multiplet), coupling constants in Hertz (Hz).

Infrared spectra were recorded on a Bruker FT-IR Alpha (ATR mode) spectrophotometer. Data are represented as follows: frequency of absorption (cm^{-1}).

High-resolution mass spectrometry was performed on a JEOL AccuTOF-DART (positive mode) at the Mass Spectrometry Facility, Boston College.

Abbreviations used

Bn = benzyl, Boc = *tert*-butoxycarbonyl, DART = direct analysis in real time, DCE = 1,2-dichloroethane, DCM = dichloromethane, DIPEA = diisopropylethylamine, DMF = *N,N*-dimethylformamide, dr = diastereomeric ratio, er = enantiomeric ratio, ESI = electrospray ionization, Et_2O = diethyl ether, EtOAc = ethyl acetate, HR = high-resolution, KOH = potassium hydroxide, LC = liquid chromatography, $MgSO_4$ = magnesium sulfate, MS = mass spectrometry, NA = not applicable, PTLC = preparatory thin-layer chromatography, TBME = *tert*-butyl methyl ether, TBS = *tert*-butyldimethylsilyl, Tf = trifluromethanesulfonate, THF = tetrahydrofuran, TLC = thin-layer chromatography, TMS = trimethylsilane, TOF = time-of-flight.

A1. Substrate Preparation

Preparation of Amine Substrates

Table S2.1A. List of Amine Substrates

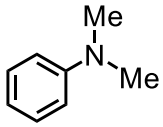 **2.13a**	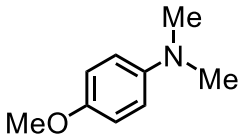 **2.13b**	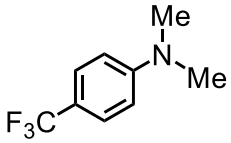 **2.13c**
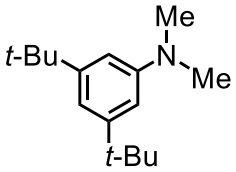 **2.13d**	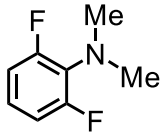 **2.13e**	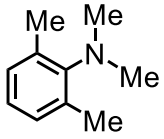 **2.13f**
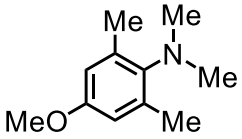 **2.13g**	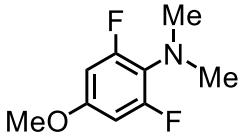 **2.13h**	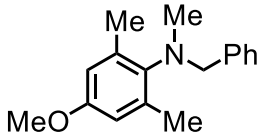 **2.13i**
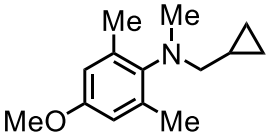 **2.13j**	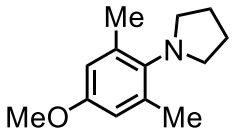 **2.13k**	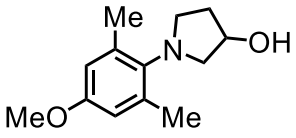 **2.13l**
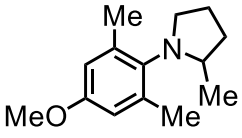 **2.13n**	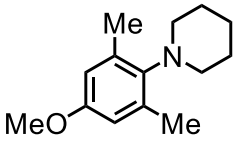 **2.13o**	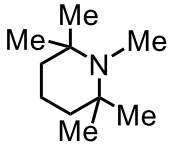 **2.13p**
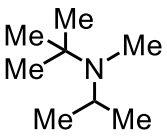 **2.13q**	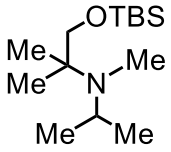 **2.13r**	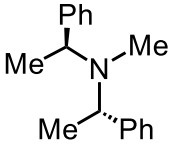 **2.13s**

Table S2.1B. List of Amine Substrates

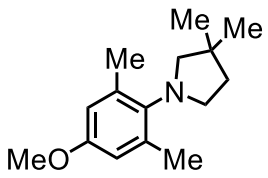	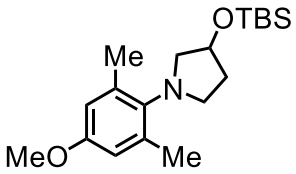	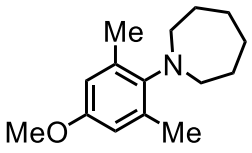
2.13t	**2.13u**	**2.13v**
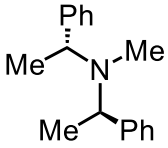	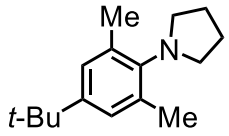	
2.13w	**2.13x**	
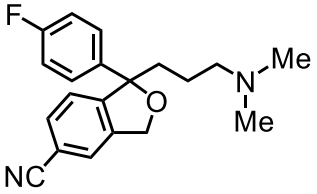	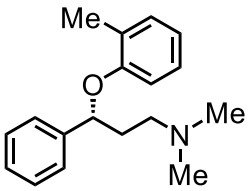	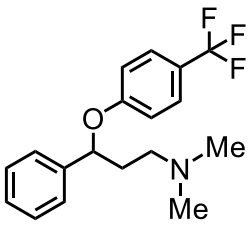
2.17a	**2.17b**	**2.17c**

Amines **2.13a**, **2.13p** and **2.13q** were obtained from commercial sources and used without further purification. Substrates **2.13b-2.13f**,[1] **2.13g**,[2-7] **2.13h**[1], **2.13i**,[7] **2.13j**,[8] **2.13k**,[9] **2.13l**,[10-12] **2.13n**,[13] **2.13o**,[9] **2.13r**,[14-16] and **2.13s**,[17-18] were prepared accordingly to the literature procedures. Amine **2.17a** was obtained commercially as the HBr salt and was treated with NaOH (1.0 M aqueous solution) before use. Amines **2.17b**[1] and **2.17c**[1] were prepared accordingly to the literature procedures. The spectroscopic data for the newly synthesized molecules (**2.13e**, **2.13g**, **2.13h**, **2.13i,** **2.13j**, **2.13k**, **2.13l**, **2.13n**, **2.13o**, **2.13r**, **2.13s**, **2.17b**, and **2.17c**) are described as the following.

General Procedure for the Methylation of Amines

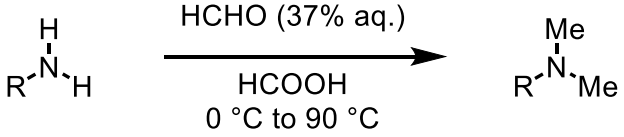

Amines **2.13b**-**2.13f**, **2.13h**, **2.17b** and **2.17c** were prepared following a known procedure.[1] A solution of amine and formaldehyde (37% aq. solution, 6.0 equiv.) was cooled to 0 °C. To the reaction mixture, formic acid (10 equiv.) was added dropwise. The reaction mixture was then warmed to 90 °C for 2 hours. Upon completion, NaOH (1M aq. solution) was added at 0 °C until the pH of the aqueous layer was 12. The organic material was then extracted with Et_2O (3 x 15 mL). The combined organic layers were dried ($MgSO_4$), filtered, and concentrated *in vacuo*. The unpurified product mixture was subjected to silica gel chromatography.

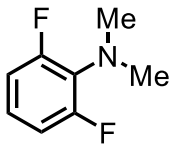

2.13e

2,6-Difluoro-*N,N*-dimethylaniline (2.13e)

2,6-Difluoro-*N,N*-dimethylaniline was prepared on a 5.0 mmol scale using the General Procedure for the Methylation of Amines to afford a colorless liquid (560 mg, 71%). **^{1}H NMR** (500 MHz, $CDCl_3$) δ 6.91 (ddt, J = 9.1, 7.5, 5.9 Hz, 1H), 6.82 (ddd, J = 9.8, 8.2, 1.1 Hz, 2H), 2.88 (t, J = 1.7 Hz, 6H).

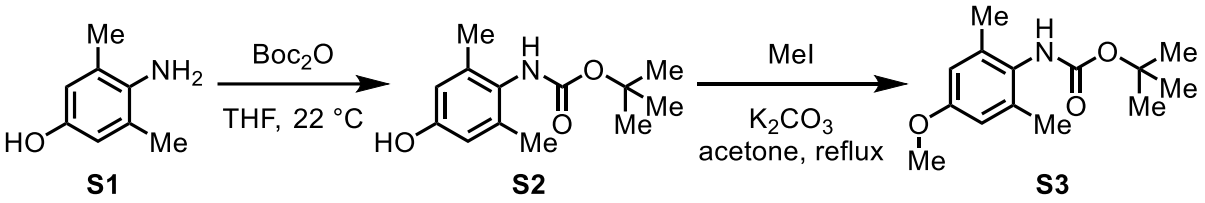

***tert*-Butyl (4-hydroxy-2,6-dimethylphenyl)carbamate (S2)**: *tert*-Butyl (4-hydroxy-2,6-dimethylphenyl)carbamate was prepared following a known procedure.[2] To a solution of 4-amino-3,5-dimethylphenol (**S1**, 10.0 g, 72.9 mmol) in THF (200 mL), was added di-*tert*-butyl dicarbonate (16.7 mL, 72.9 mmol) in a dropwise manner. The reaction mixture was allowed to stir at 22 °C for 12 hours. Upon completion, the reaction mixture was concentrated and used without further purification. The spectroscopic data of **S2** matched those reported by Nam.[3]

***tert*-Butyl (4-methoxy-2,6-dimethylphenyl)carbamate (S3)**: *tert*-Butyl (4-methoxy-2,6-dimethylphenyl)carbamate was prepared following a known procedure.[4] Carbamate **S2** (8.6 g, 36.4 mmol) was dissolved in acetone (50 mL). To the solution was added potassium carbonate (6.1 g, 54.6 mmol) and iodomethane (2.3 mL, 36.4 mmol), dropwise. The reaction mixture was heated to reflux and allowed to stir for 12 hours. Upon completion (monitored by TLC), the reaction was quenched with a saturated aqueous solution of KOH (50 mL), extracted with Et_2O (3 x 50 mL), dried ($MgSO_4$), and concentrated *in vacuo*. The unpurified product mixture was subjected to silica gel chromatography to afford a colorless solid (5.9 g, 65% yield). **^{1}H NMR** (400 MHz, $CDCl_3$) δ 6.60 (s, 2H), 3.76 (s, 3H), 2.24 (s, 6H), 1.49 (s, 9H).

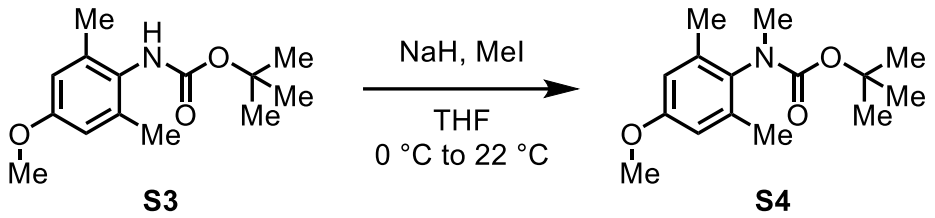

S3 **S4**

***tert*-Butyl (4-methoxy-2,6-dimethylphenyl)(methyl)carbamate (S4):** *tert*-Butyl (4-methoxy-2,6-dimethylphenyl)(methyl)carbamate was prepared following a known procedure.[5] Carbamate **S3** (8.5 g, 33.9 mmol) was dissolved in THF (30 mL). The solution was cooled to 0 °C, sodium hydride (60% oil dispersion, 1.6 g, 40.7 mmol) was added and allowed to stir for 10 minutes. Subsequently, iodomethane (2.5 mL, 40.7 mmol) was added dropwise at 0 °C. The reaction mixture was allowed to stir at 22 °C for 2 hours. Upon completion of the reaction (monitored by TLC), water was slowly added to the reaction mixture, extracted with EtOAc (3 x 20 mL), dried ($MgSO_4$) and concentrated *in vacuo*. The unpurified product mixture was subjected to silica gel chromatography (5% EtOAc/hexanes) to give the product as a colorless solid (8.5 g, 95%). **^{1}H NMR** (400 MHz, $CDCl_3$) δ 6.59–6.57 (m, 2H), 3.77–3.75 (m, 3H), 3.04 (s, 3H), 2.17– 2.15 (m, 6H), 1.32 (s, 9H).

General Procedure for the Removal of *N*-Boc Protection Group[5]

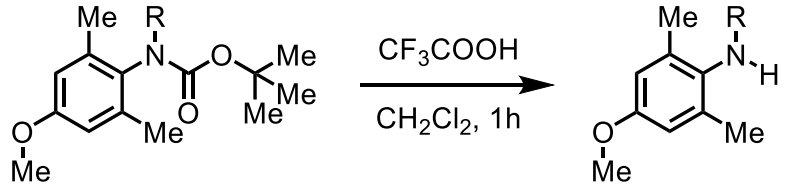

S3, R = H
S4, R = Me

S5, R = H
S6, R = Me

To a solution of carbamate **S3** or **S4** in DCM (0.3 M), CF_3COOH (5.0 equiv.) was added dropwise at 22 °C. The reaction mixture was allowed to stir for 1 hour. Upon completion of the reaction (monitored by TLC), aqueous $NaHCO_3$ was added until the solution was alkaline, extracted with

DCM, dried ($MgSO_4$), filtered, and concentrated. The unpurified product mixture was subjected to silica gel chromatography (5% EtOAc/hexanes) to give the product as a yellow liquid. The spectroscopic data of **S5** matched those reported by Organ.[6]

4-Methoxy-*N*,2,6-trimethylaniline (S6): ^{1}H NMR (500 MHz, $CDCl_3$) δ 6.58 (s, 2H), 3.74 (s, 3H), 2.72 (s, 1H), 2.68 (s, 3H), 2.29 (s, 6H).

General Procedure A for the Alkylation of Amine S6

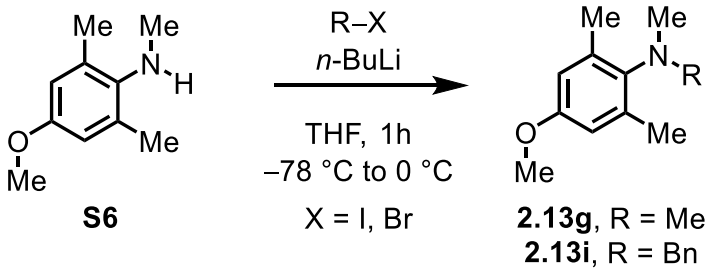

Amines **2.13g** and **2.13i** were prepared following a known procedure.[7] To a solution of 4-methoxy-*N*,2,6-trimethylaniline (**S6)** in THF (0.5 M) at –78 °C, was added *n*-BuLi (2.5 M, 1.0 equiv.), dropwise. The reaction mixture was allowed to stir for 10 minutes, whereupon the respective alkylhalide (1.0 equiv.) was added dropwise at –78 °C. The reaction mixture was then allowed to warm to 0 °C. Upon completion of the reaction (monitored by TLC), the unpurified product mixture was concentrated *in vacuo* and purified by silica gel chromatography (2% EtOAc/hexanes).

General Procedure B for the Alkylation of Amine S6

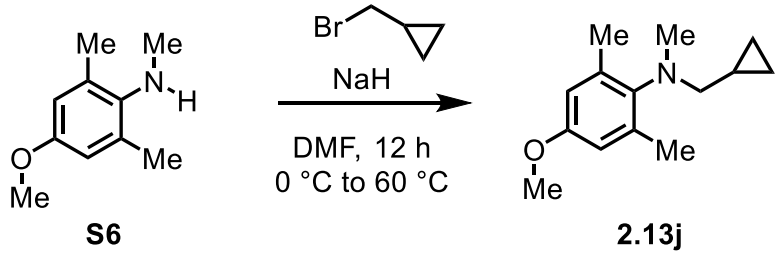

Amine **2.13j** was prepared following a known procedure.[8] To a solution of 4-methoxy-*N*,2,6-trimethylaniline (**S6)** in DMF (1 M) at 0 °C, was added sodium hydride (1.2 equiv.). The mixture was warmed to 60 °C to stir for 15 minutes then allowed to cool to 0 °C, whereupon the alkylhalide (1.2 equiv.) was added dropwise. The reaction mixture was warmed to 60 °C and stirred for 12 hours. The unpurified product mixture was then cooled to 0 °C, water was added slowly, extracted with EtOAc, dried ($MgSO_4$), concentrated *in vacuo*, and was purified by silica gel chromatography (2% EtOAc/hexanes).

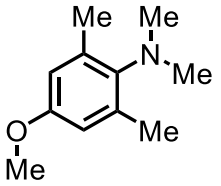

2.13g

4-Methoxy-*N,N*,2,6-tetramethylaniline (2.13g)

4-Methoxy-*N,N*,2,6-tetramethylaniline was synthesized using General Procedure A on a 10.0 mmol scale to afford a colorless liquid (765 mg, 43%). **^{1}H NMR** (400 MHz, $CDCl_3$) δ 6.54 (s, 2H), 3.75 (s, 3H), 2.79 (s, 6H), 2.28 (s, 6H).

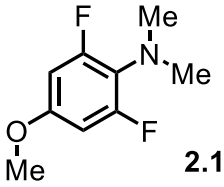

2.13h

2,6-Difluoro-4-methoxy-*N,N*-dimethylaniline (2.13h)

2,6-Difluoro-4-methoxy-*N,N*-dimethylaniline was prepared on a 5.0 mmol scale following the General Procedure for the Methylation of Amines to afford a colorless liquid (860 mg, 92%). **^{1}H NMR** (400 MHz, $CDCl_3$) δ 6.46 – 6.37 (m, 2H), 3.74 (s, 3H), 2.81 (t, J = 1.3 Hz, 6H).

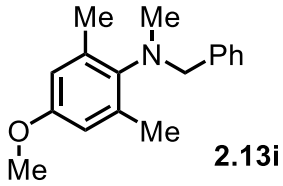

2.13i

***N*-Benzyl-4-methoxy-*N*,2,6-trimethylaniline (2.13i)**

N-Benzyl-4-methoxy-*N*,2,6-trimethylaniline was synthesized using General Procedure A on a 3.1 mmol scale to afford a colorless oil (408 mg, 52%). **^{1}H NMR** (500 MHz, $CDCl_3$) δ 7.41 – 7.37 (m, 2H), 7.33 (t, *J* = 7.5 Hz, 2H), 7.25 (m, 1H), 6.56 (s, 2H), 4.14 (s, 3H), 3.76 (s, 3H), 2.65 (s, 2H), 2.35 (s, 6H).

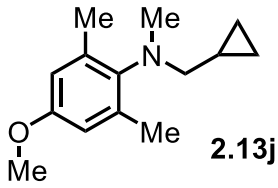

2.13j

***N*-(Cyclopropylmethyl)-4-methoxy-*N*,2,6-trimethylaniline (2.13j)**

N-(Cyclopropylmethyl)-4-methoxy-*N*,2,6-trimethylaniline was synthesized using General Procedure B on a 3.0 mmol scale to give the product as a colorless liquid (346 mg, 53%). **^{1}H NMR** (400 MHz, $CDCl_3$) δ 6.54 (s, 2H), 3.75 (s, 3H), 2.81 (m, 5H), 2.27 (s, 6H), 0.95 – 0.82 (m, 1H), 0.45 – 0.39 (m, 2H), 0.11 – 0.02 (m, 2H).

Procedure for Synthesizing Amine 2.13k and 2.13o

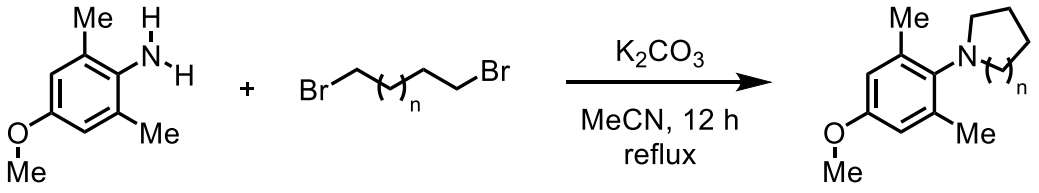

S5 n = 1 or 2 **2.13k**, n = 1 **2.13o**, n = 2

1-(4-Methoxy-2,6-dimethylphenyl)pyrrolidine (2.13k)

1-(4-Methoxy-2,6-dimethylphenyl)pyrrolidine was prepared using a known procedure.[9] A mixture of aniline **S5** (1.0 g, 6.6 mmol), K_2CO_3 (2.7 g, 19.8 mmol), and 1,4-dibromobutane (1.2 mL, 9.9 mmol) in acetonitrile (10 mL) was heated to reflux for 12 hours. Upon completion, the reaction mixture was quenched with H_2O, extracted with EtOAc (3 x 25 mL), dried ($MgSO_4$), filtered, and concentrated *in vacuo*. The unpurified product mixture was subjected to silica gel chromatography (3% EtOAc/hexanes) to give the product as a yellow liquid (1.1 g, 82%). **^{1}H NMR** (500 MHz, $CDCl_3$) δ 6.58 (s, 2H), 3.75 (s, 3H), 3.20 – 3.08 (m, 4H), 2.23 (s, 6H), 1.99 – 1.90 (m, 4H).

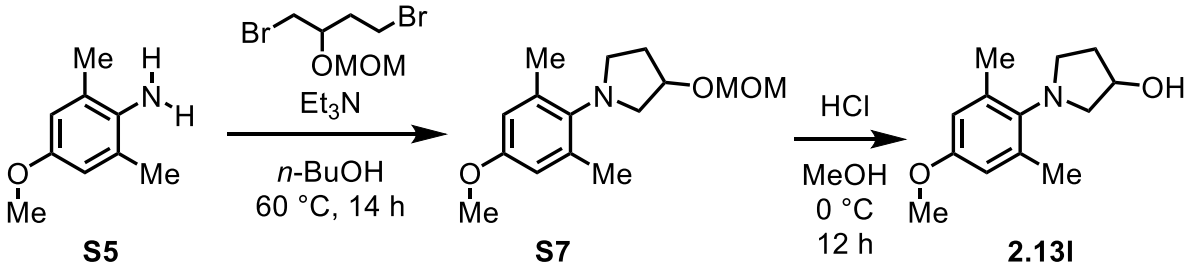

1-(4-Methoxy-2,6-dimethylphenyl)-3-(methoxymethoxy)pyrrolidine (S7)

1-(4-Methoxy-2,6-dimethylphenyl)-3-(methoxymethoxy)pyrrolidine was synthesized using a known procedure.[10] 1,4-dibromo-2-(methoxymethoxy)butane was prepared following the literature procedure using chloromethyl methyl ether.[11] To a solution of aniline **S5** (500 mg, 3.3 mmol) in *n*-butanol (5 mL) was added 1,4-dibromo-2-(methoxymethoxy)butane (1.0 g, 3.63 mmol) and triethylamine (1.4 mL, 9.9 mmol). The solution was then allowed to heat at 80 °C for 14 hours. The reaction mixture was diluted with H_2O (10 mL) and extracted with EtOAc (3 x 10 mL). The combined organic layer was washed with brine (1 x 20 mL), dried ($MgSO_4$), and concentrated *in vacuo*. The unpurified product mixture was subjected to silica gel chromatography to afford **S7** as a colorless liquid (263 mg, 30%). **^{1}H NMR** (500 MHz, $CDCl_3$) δ 6.57 (s, 2H), 4.75 – 4.69 (m, 2H),

4.44 – 4.36 (m, 1H), 3.75 (s, 3H), 3.47 – 3.39 (m, 2H), 3.39 (s, 3H), 3.21 – 3.09 (m, 2H), 2.25 (s, 6H), 2.24 – 2.12 (m, 1H), 2.11 – 2.00 (m, 1H).

1-(4-Methoxy-2,6-dimethylphenyl)pyrrolidin-3-ol (2.13l)

1-(4-Methoxy-2,6-dimethylphenyl)pyrrolidin-3-ol was obtained by the deprotection of the MOM protecting group of **S7** following the literature procedure.[12] To a solution of amine **S7** (100 mg, 0.4 mmol) in MeOH (1 mL) at 0 °C was added 10 M HCl (0.8 mL), dropwise. The reaction was allowed to stir for 12 hours at room temperature, whereupon the reaction mixture was concentrated *in vacuo*. The resulting residue was basified with saturated aqueous solution of K_2CO_3 until alkaline. The solution was then extracted with EtOAc (3 x 15 mL) and the combined organic layers were dried ($MgSO_4$), filtered, and concentrated *in vacuo.* The unpurified product mixture was subjected to silica gel chromatography (15% EtOAc/hexanes) to afford the product as a colorless liquid (70 mg, 78%). **^{1}H NMR** (500 MHz, $CDCl_3$) δ 6.52 (s, 2H), 4.45 (s, 1H), 3.70 (s, 3H), 3.43 – 3.39 (m, 1H), 3.11 – 3.06 (m, 1H), 3.01 – 2.97 (m, 1H), 2.20 (s, 6H), 2.18 – 2.10 (m, 1H), 1.94 – 1.87 (m, 1H), 1.76 (s, 1H).

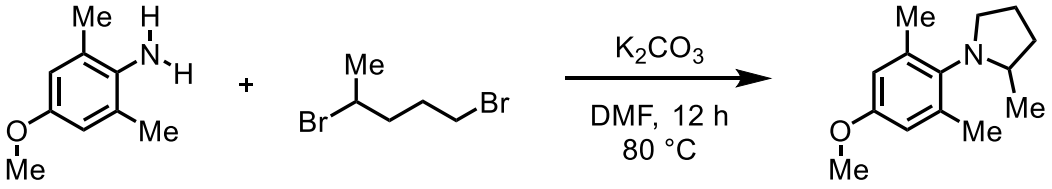

S5 **2.13n**

1-(4-Methoxy-2,6-dimethylphenyl)-2-methylpyrrolidine (2.13n)

1-(4-Methoxy-2,6-dimethylphenyl)-2-methylpyrrolidine was prepared using a known procedure.[13] To a solution of aniline **S5** (650 mg, 4.3 mmol) in DMF (5 mL) was added K_2CO_3 (654 mg, 4.7 mmol) and 1,4-dibromopentane (0.6 mL, 4.7 mmol). The reaction mixture was stirred under reflux

for 12 hours. After cooling the reaction mixture to room temperature, the mixture was quenched with H_2O (10 mL) and extracted with EtOAc (3 x 10 mL). The combined organic layers were dried ($MgSO_4$), filtered, and concentrated *in vacuo*. The unpurified product mixture was subjected to silica gel chromatography (2% EtOAc/hexanes) to afford **2.13n** as a colorless liquid (593 mg, 63%). **^{1}H NMR** (500 MHz, $CDCl_3$) δ 6.57 (s, 2H), 3.75 (s, 3H), 3.59 – 3.51 (m, 1H), 3.27 (td, *J* = 7.9, 5.0 Hz, 1H), 3.05 (td, *J* = 8.1, 6.2 Hz, 1H), 2.24 (s, 6H), 2.14 – 2.03 (m, 1H), 2.02 – 1.81 (m, 2H), 1.59 – 1.46 (m, 1H), 0.91 (d, *J* = 6.0 Hz, 3H).

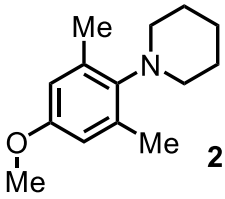

2.13o

1-(4-Methoxy-2,6-dimethylphenyl)piperidine (2.13o)

1-(4-Methoxy-2,6-dimethylphenyl)piperidine was prepared using a known procedure[9] on 1.0 mmol scale, using 1,5-dibromopentane. The product was obtained as a white solid (165 mg, 75%). **^{1}H NMR** (500 MHz, $CDCl_3$) δ 6.52 (s, 2H), 3.74 (s, 3H), 2.98 (t, *J* = 5.1 Hz, 4H), 2.29 (s, 6H), 1.65 – 1.58 (m, 4H), 1.58 – 1.51 (m, 2H).

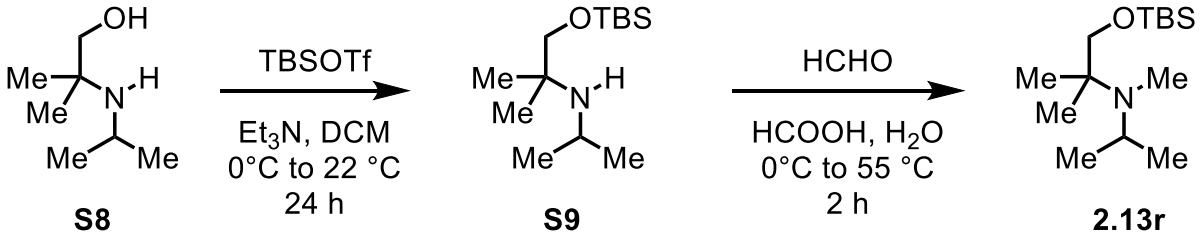

S8 **S9** **2.13r**

1-((*tert*-Butyldimethylsilyl)oxy)-*N*-isopropyl-2-methylpropan-2-amine (S8) 1-((*tert*-Butyldimethylsilyl)oxy)-*N*-isopropyl-2-methylpropan-2-amine was prepared following a known

procedure.[14] To a solution of 2-(isopropylamino)-2-methylpropan-1-ol[15] (20 mmol), and triethylamine (26 mmol) in DCM (50 mL) at 0 °C was added *tert*-butyldimethylsilyl trifluoromethanesulfonate (26 mmol) dropwise. The reaction mixture was allowed to stir at 22 °C for 24 hours. Upon completion, the reaction was quenched with H_2O (20 mL), the organic phase was separated and the aqueous phase was extracted with DCM (3 × 50 mL). The combined organic phases were dried ($MgSO_4$), filtered, and concentrated *in vacuo*. The unpurified product mixture was subjected to silica gel chromatography (5% Et_3N/hexanes) to afford **S9** as a colorless oil (4.68 g, 19.08 mmol, 95%). **^{1}H NMR** (400 MHz, $CDCl_3$) δ 3.32 (s, 2H), 2.87 (m, 1H), 1.04 (d, J = 6.3 Hz, 6H), 1.01 (s, 6H), 0.89 (s, 9H), 0.04 (s, 6H).

1-((*tert*-Butyldimethylsilyl)oxy)-*N*-isopropyl-*N*,2-dimethylpropan-2-amine (2.13r)

1-((*tert*-Butyldimethylsilyl)oxy)-*N*-isopropyl-*N*,2-dimethylpropan-2-amine was prepared following a known procedure.[16] A 37% aq. solution of formaldehyde (1.6 g, 22 mmol) was added to a mixture of 1-((*tert*-butyldimethylsilyl)oxy)-*N*-isopropyl-2-methylpropan-2-amine **S9** (4.43 g, 18.1 mmol) and 88% formic acid (1.8 g, 39 mmol) at 0 °C. The reaction mixture was kept at 55 °C for 2 hours. Upon completion (monitored by TLC), the reaction was quenched with 8.0 M KOH (10 mL), extracted with Et_2O (3 x 50 mL), dried ($MgSO_4$), and concentrated *in vacuo*. The unpurified product mixture was subjected to silica gel chromatography (2% Et_3N/hexanes) to afford **2.13r** as a colorless oil (3.2 g, 68% yield). **^{1}H NMR** (600 MHz, $CDCl_3$) δ 3.43 (s, 2H), 3.31 (hept, J = 6.6 Hz, 1H), 2.21 (s, 3H), 1.05 (s, 6H), 1.00 (d, J = 6.8 Hz, 6H), 0.89 (s, 9H), 0.03 (s, 6H).

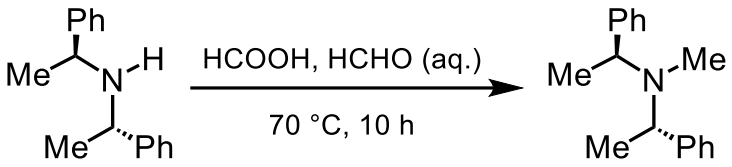

S10 **2.13s**

(*S*)-*N*-Methyl-1-phenyl-*N*-((*S*)-1-phenylethyl)ethan-1-amine (2.13s)

(*S*)-*N*-Methyl-1-phenyl-*N*-((*S*)-1-phenylethyl)ethan-1-amine was prepared following a known procedure.[17] A 37% aq. solution of formaldehyde (17.6 mmol) was added to a mixture of (*S*)-bis((*S*)-1-phenylethyl)amine **S10** (1.0 g, 4.4 mmol) and 88% formic acid (8.8 mmol) at 0 °C. The reaction mixture was kept at 70 °C for 10 hours. Upon completion (monitored by TLC), the reaction was basified with 1 M NaOH, extracted with EtOAc (3 x 40 mL), dried ($MgSO_4$), and concentrated *in vacuo*. The unpurified product mixture was subjected to silica gel chromatography (2% Et_3N/hexanes) to afford **2.13s** as a colorless oil (0.9 g, 94% yield). **^{1}H NMR** (500 MHz, $CDCl_3$) δ 7.40 – 7.30 (m, 7H), 7.26 – 7.21 (m, 2H), 3.82 (q, *J* = 6.8 Hz, 2H), 2.00 (s, 3H), 1.33 (d, *J* = 6.8 Hz, 6H).[18]

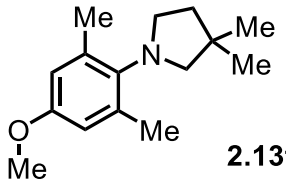

2.13t

1-(4-Methoxy-2,6-dimethylphenyl)-3,3-dimethylpyrrolidine (2.13t)

1-(4-Methoxy-2,6-dimethylphenyl)-3,3-dimethylpyrrolidine was synthesized using the General Procedure for Cyclic Amine Substrates on a 5.9 mmol scale, using 1,4-dibromo-2,2-dimethylbutane. The product was obtained as a colorless liquid (1.2 g, 88%). **^{1}H NMR** (600 MHz, $CDCl_3$) δ 6.57 (s, 2H), 3.75 (s, 3H), 3.25 (t, *J* = 6.9 Hz, 2H), 2.90 (s, 2H), 2.24 (s, 6H), 1.73 (t, *J* = 6.9 Hz, 2H), 1.18 (s, 6H).

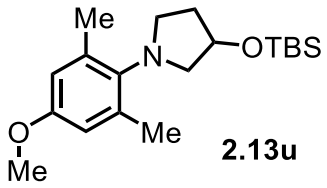

2.13u

3-((*tert*-Butyldimethylsilyl)oxy)-1-(4-methoxy-2,6-dimethylphenyl)pyrrolidine (2.13u)

3-((*tert*-Butyldimethylsilyl)oxy)-1-(4-methoxy-2,6-dimethylphenyl)pyrrolidine was synthesized using the General Procedure for Cyclic Amine Substrates on a 16.5 mmol scale, using *tert*-butyl((1,4-dibromobutan-2-yl)oxy)dimethylsilane. The product was obtained as a colorless liquid (4.9 g, 89%). **^{1}H NMR** (500 MHz, $CDCl_3$) δ 6.57 (s, 2H), 4.48 (tt, *J* = 5.2, 3.5 Hz, 1H), 3.75 (s, 3H), 3.41 – 3.35 (m, 2H), 3.08 (td, *J* = 7.8, 4.1 Hz, 1H), 3.02 (dd, *J* = 8.9, 3.1 Hz, 1H), 2.25 (s, 6H), 2.12 – 2.04 (m, 1H), 1.92 – 1.85 (m, 1H), 0.90 (s, 9H), 0.09 (s, 3H), 0.07 (s, 3H).

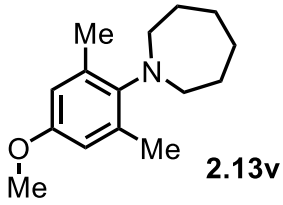

2.13v

1-(4-Methoxy-2,6-dimethylphenyl)azepane (2.13v)

1-(4-Methoxy-2,6-dimethylphenyl)azepane was prepared using the General Procedure for Cyclic Amine Substrates on 4.7 mmol scale, using 1,6-dibromohexane. The product was obtained as a colorless oil (371 mg, 34%). **^{1}H NMR** (500 MHz, $CDCl_3$) δ 6.56 (s, 2H), 3.75 (s, 3H), 3.09 – 3.01 (m, 4H), 2.29 (s, 6H), 1.70 (s, 8H).

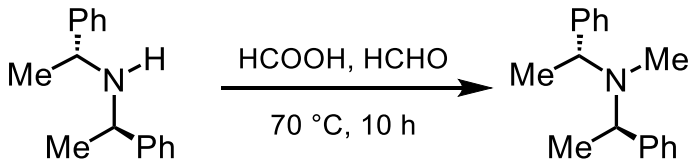

S11 **1t**

(*R*)-*N*-Methyl-1-phenyl-*N*-((*R*)-1-phenylethyl)ethan-1-amine (2.13w)

(*R*)-*N*-Methyl-1-phenyl-*N*-((*R*)-1-phenylethyl)ethan-1-amine (**2.13w**) was prepared following a known procedure.[7] A 37% aq. solution of formaldehyde (4.4 mmol) was added to a mixture of (*R*)-bis((*R*)-1-phenylethyl)amine **S11** (0.54 g, 2.2 mmol) and 88% formic acid (8.8 mmol) at 0 °C. The reaction mixture was kept at 70 °C for 10 hours. Upon completion (monitored by TLC), the reaction was basified with 1 M NaOH, extracted with EtOAc (3 x 40 mL), dried ($MgSO_4$), and concentrated *in vacuo*. The crude reaction mixture was purified by silica gel chromatography (hexanes/Et_3N = 50:1) to afford a colorless oil (440 mg, 84% yield). **^{1}H NMR** (500 MHz, $CDCl_3$) δ 7.40 – 7.30 (m, 7H), 7.26 – 7.21 (m, 2H), 3.82 (q, *J* = 6.8 Hz, 2H), 2.00 (s, 3H), 1.33 (d, *J* = 6.8 Hz, 6H).[8]

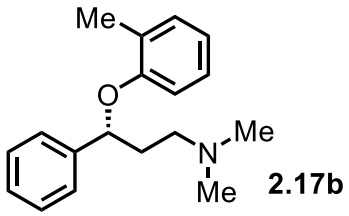

2.17b

(*R*)-*N,N*-Dimethyl-3-phenyl-3-(*o*-tolyloxy)propan-1-amine (2.17b)

(*R*)-*N,N*-Dimethyl-3-phenyl-3-(*o*-tolyloxy)propan-1-amine was prepared following the General Procedure for Methylation of Amines on a 8.8 mmol scale. The unpurified product mixture was subjected to silica gel chromatography (4% MeOH/DCM) and was obtained as a colorless liquid (2.3 g, 97% yield). **^{1}H NMR** (500 MHz, $CDCl_3$) δ 7.41 – 7.28 (m, 4H), 7.28 – 7.19 (m, 1H), 7.13

– 7.06 (m, 1H), 6.99 – 6.90 (m, 1H), 6.76 (td, *J* = 7.4, 1.1 Hz, 1H), 6.62 (d, *J* = 8.2 Hz, 1H), 5.22 (dd, *J* = 8.2, 4.7 Hz, 1H), 2.45 (t, *J* = 7.3 Hz, 2H), 2.31 (s, 3H), 2.23 (s, 6H), 2.21 – 2.12 (m, 1H), 2.05 – 1.92 (m, 1H).

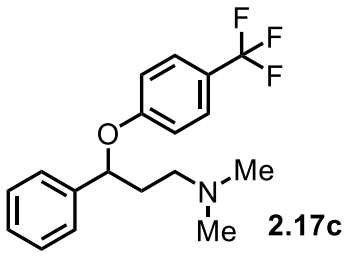

2.17c

***N,N*-Dimethyl-3-phenyl-3-(4-(trifluoromethyl)phenoxy)propan-1-amine (2.17c)**

N,N-Dimethyl-3-phenyl-3-(4-(trifluoromethyl)phenoxy)propan-1-amine was prepared following the General Procedure for Methylation of Amines on a 7.3 mmol scale. The unpurified product mixture was subjected to silica gel chromatography (2% MeOH/DCM) and was obtained as a colorless liquid (2.2 g, 95% yield). **^{1}H NMR** (500 MHz, $CDCl_3$) δ 7.42 (d, *J* = 8.6 Hz, 2H), 7.37 – 7.30 (m, 4H), 7.29 – 7.25 (m, 1H), 6.91 (d, *J* = 8.6 Hz, 2H), 5.28 (dd, *J* = 8.2, 5.0 Hz, 1H), 2.50 – 2.37 (m, 2H), 2.24 (s, 6H), 2.22 – 2.14 (m, 1H), 1.98 (tt, *J* = 13.9, 5.7 Hz, 1H).

Preparation of Silicon Enolate Substrates

Table S2.2. Silicon Enolate Substrates

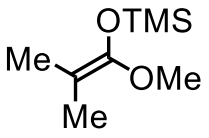	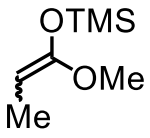	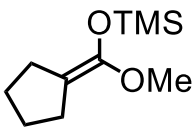	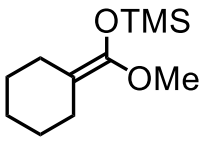
2.11a	**2.11b**	**2.11c**	**2.11d**
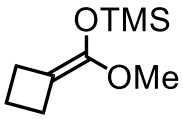	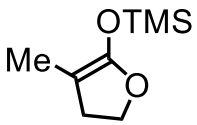	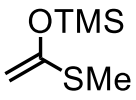	
2.11e	**2.11f**	**2.11g**	

Silicon enolate molecule **2.11a** was obtained from commercial sources. Substrates **2.11b**,[19] **2.11c**,[20] **2.11d**,[20] **2.11e**,[20] **2.11f**,[21] and **2.11g**[22] were prepared accordingly to the procedures previously reported in the literatures.

General Procedure for Preparation of Silicon Enolates

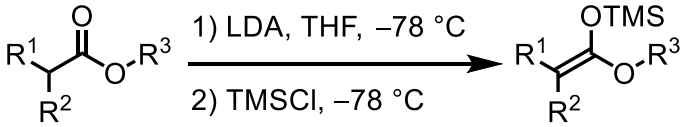

To a solution of diisopropylamine (1.25 equiv.) in THF, *n*-BuLi (2.5 M in hexanes, 1.2 equiv.) was added dropwise at −78 °C and the solution was stirred for 15 minutes. A solution of ester in THF was added dropwise at −78 °C and the solution was stirred for 1 hour. Subsequently, TMSCl (1.2 equiv.) was added slowly at −78 °C, the reaction mixture was warmed up to 22 °C and was stirred until the completion of the reaction (monitored by ^{1}H NMR). The reaction mixture was diluted with ice-cold pentane and the resulting suspension was filtered through a pad of Celite. The filtrate

was concentrated under vacuum and the resulting crude mixture was purified by distillation under reduced pressure to give the corresponding silicon enolate.

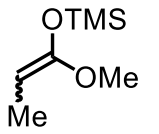

2.11b

((1-Methoxyprop-1-en-1-yl)oxy)trimethylsilane (2.11b)

((1-Methoxyprop-1-en-1-yl)oxy)trimethylsilane was synthesized following the general procedure at 20.0 mmol scale and was kept at −78 °C until the reaction was complete. The product was obtained as colorless liquid (*E*/*Z* = 7:1). The NMR spectroscopic data were in agreement with those reported in the literature.[19]

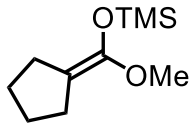

2.11c

(Cyclopentylidene(methoxy)methoxy)trimethylsilane (2.11c)

(Cyclopentylidene(methoxy)methoxy)trimethylsilane was synthesized following the general procedure on 7.7 mmol scale. The product was obtained as colorless liquid. The NMR spectroscopic data were in agreement with those reported in the literature.[20]

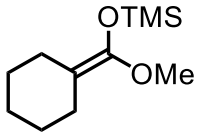

2.11d

(Cyclohexylidene(methoxy)methoxy)trimethylsilane (2.11d)

(Cyclohexylidene(methoxy)methoxy)trimethylsilane was synthesized following the general procedure at 10.0 mmol scale. The product was obtained as colorless liquid. The NMR spectroscopic data were in agreement with those reported in the literature.[20]

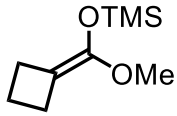

2.11e

(Cyclobutylidene(methoxy)methoxy)trimethylsilane (2.11e)

(Cyclobutylidene(methoxy)methoxy)trimethylsilane was synthesized following the general procedure at 8.7 mmol scale. The product was obtained as colorless liquid (OSi/CSi=6:1). The NMR spectroscopic data were in agreement with those reported in the literature.[20]

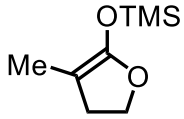

2.11f

Trimethyl((3-methyl-4,5-dihydrofuran-2-yl)oxy)silane (2.11f)

Trimethyl((3-methyl-4,5-dihydrofuran-2-yl)oxy)silane was synthesized following the general procedure at 10.0 mmol scale. The product was obtained as colorless liquid. The NMR spectroscopic data were in agreement with those reported in the literature.[22]

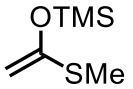

2.11g

Trimethyl((1-(methylthio)vinyl)oxy)silane (2.11g)

Trimethyl((1-(methylthio)vinyl)oxy)silane was synthesized following the general procedure at 10.0 mmol scale and was kept at −78 °C until the reaction was complete (1 hour). The filtrate was concentrated under vacuum and the resulting crude oil was purified by distillation under reduced pressure (40 °C, 40 mmHg), to give trimethyl((1-(methylthio)vinyl)oxy)silane as colorless liquid. **^{1}H NMR** (400 MHz, $CDCl_3$) δ 4.39 (d, *J* = 2.2 Hz, 1H), 4.22 (d, *J* = 2.2 Hz, 1H), 2.22 (s, 3H), 0.26 (s, 9H).

Preparation of α,β-Unsaturated Substrates

Table S2.3. α,β-Unsaturated Substrates.

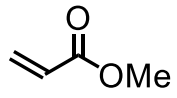	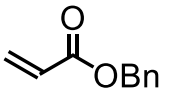	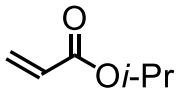	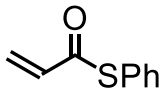
2.20a	**2.20b**	**2.20c**	**2.20d**
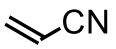	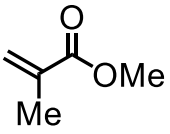	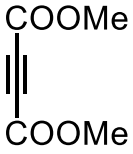	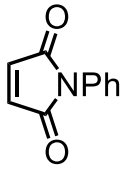
2.20e	**2.20f**	**2.20g**	**2.20h**
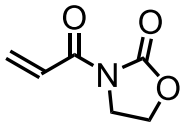	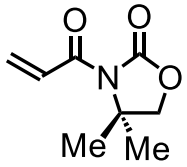	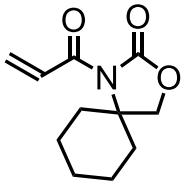	
2.23a	**2.23b**	**2.23c**	
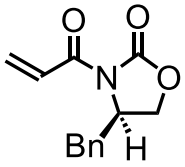	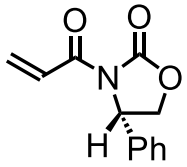	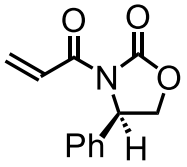	
2.23d	**2.23e-(*S*)**	**2.23e-(*R*)**	

α,β-Unsaturated molecules **2.20a**, **2.20b**, and **2.20e–2.20h** were obtained from commercial sources. Substrates **2.20c**,[14] **2.20d**,[15] **2.23a**,[16] **2.23b**,[17] **2.23c**,[17] **2.23d**,[16] **2.23e-(*S*)**,[16] and **2.23e-(*R*)**[16] were prepared accordingly to the procedures previously reported in the literatures.

A2. Optimization Studies

$B(C_6F_5)_3$-Catalyzed Mannich-type Reaction

Experimental Procedure for the Optimization of Solvent (Table S2.4)

To a 15 mL oven-dried sealed tube equipped with a magnetic stir bar was added amine **2.13k** (0.1 mmol), $B(C_6F_5)_3$ (0.01 mmol), ((1-methoxy-2-methylprop-1-en-1-yl)oxy)trimethylsilane **2.11a** (0.2 mmol), and solvent (0.25 mL) under a nitrogen atmosphere. The reaction mixture was stirred for 12 hours at 22 °C. Upon completion, the reaction mixture was concentrated *in vacuo*. The product yield was determined by the ^{1}H NMR analysis of the unpurified product mixtures using mesitylene as the internal standard. The unpurified product mixture was subjected to PTLC using 20% EtOAc in hexanes as the eluent to give **2.14k**.

Table S2.4. Evaluation of Solvents for Cyclic Amine Substrate **2.14k**

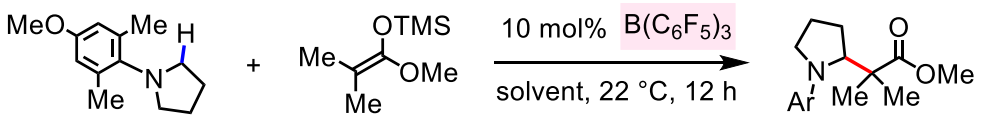

2.13k **2.11a** **2.14k**

Entry	Solvent	yield (%)
1	CH_2Cl_2	46
2	Toluene	76
3	Benzene	78
4	TBME	90
5	THF	93

Reaction of Different *N,N*-Dialkylanilines with Silicon Enolate 2.11a (Table S2.5)

To a 15 mL oven-dried sealed tube equipped with a magnetic stir bar was added *N,N*-dialkylaniline (0.2 mmol), $B(C_6F_5)_3$ (0.02 mmol), ((1-methoxy-2-methylprop-1-en-1-yl)oxy)trimethylsilane **2.11a** (0.4 mmol), and DCE (0.5 mL) under a nitrogen atmosphere. The reaction mixture was allowed to stir for 12 hours at 22 °C. Upon completion, the reaction mixture was concentrated *in vacuo*. The ^{1}H NMR analysis of the unpurified product mixtures revealed that there was no product formation and >90% of the starting amine was observed using mesitylene as the internal standard.

Table S2.5. Evaluation of *N,N*-Dialkylanilines

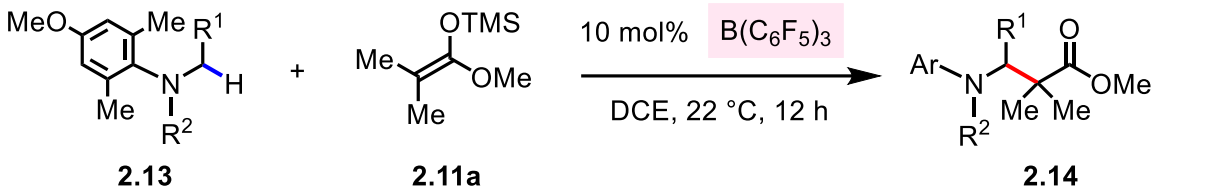

2.13 **2.11a** **2.14**

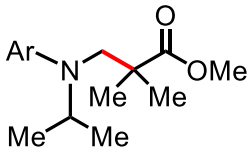

2.14aa, 10% yield

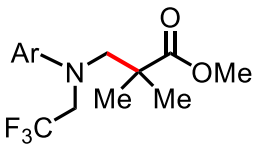

2.14ba, 0% yield

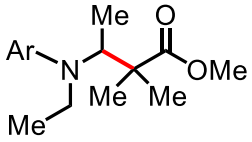

2.14ca, 0% yield

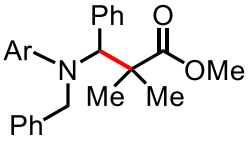

2.14da, 0% yield

Reaction of *N,N*-Dimethylaniline with Different Silicon Enolates (Table S2.6)

To a 15 mL oven-dried sealed tube equipped with a magnetic stir bar was added *N,N*-methylaniline (0.2 mmol), $B(C_6F_5)_3$ (0.02 mmol), silicon enolate **2** (0.4 mmol), and benzene (0.5 mL) under a nitrogen atmosphere. The reaction mixture was allowed to stir for 12 hours at 22 °C. Upon completion, the reaction mixture was concentrated *in vacuo*. The ^{1}H NMR analysis of the unpurified product mixtures revealed that there was no product formation and >90% of **2.13g** was observed using mesitylene as the internal standard.

Table S2.6. Evaluation of Silicon Enolates

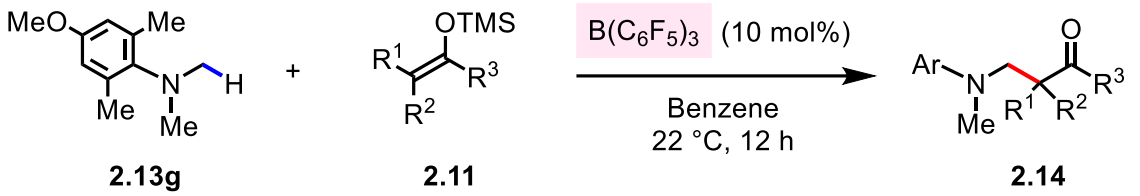

2.13g **2.11** **2.14**

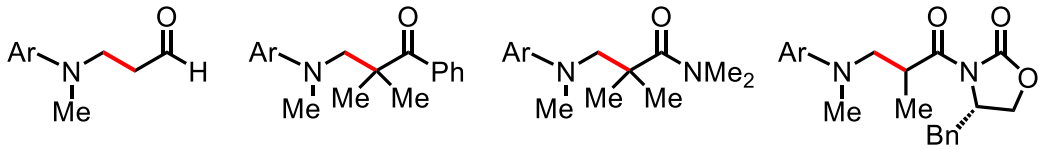

2.14ga, 0% yield | **2.14gb**, 0% yield | **2.14gc**, 0% yield | **2.14gd**, 0% yield

Experimental Procedure for the Optimization of the Amine Protecting Group (Table S2.7)

An oven-dried sealed tube equipped with a magnetic stir bar was used. Amine **2.13** (0.20 mmol), methyl acrylate **2.20a** (0.24 mmol), $B(C_6F_5)_3$ (0.01 mmol), and benzene (0.2 mL) were added to the reaction vessel under nitrogen atmosphere. The reaction mixture was stirred at 22 °C for 12 h. Upon completion, the reaction mixture was concentrated *in vacuo*. The product yield was determined by the ^{1}H NMR analysis of the unpurified product mixture using mesitylene as the internal standard.

Table S2.7. Evaluation of Amine Protecting Group.

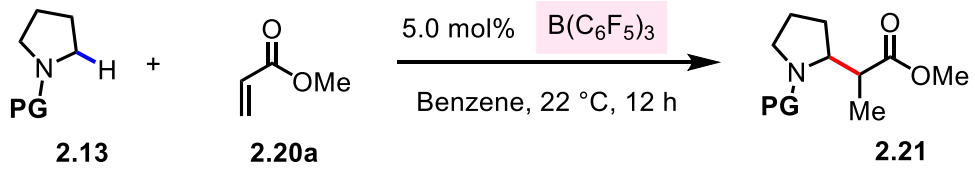

2.13 **2.20a** **2.21**

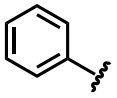	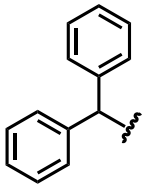	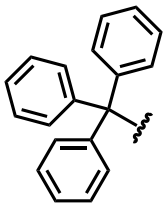
2.21-PG1 <10% yield	**2.21-PG2** <10% yield	**2.21-PG3** <10% yield
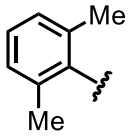	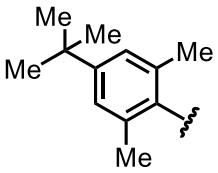	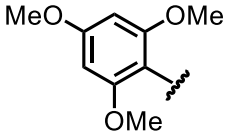
2.21-PG4 >95% yield	**2.21-PG5** 92% yield	**2.21-PG6** <10% yield
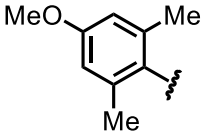		
2.21-PG7 >95% yield		

[a] Conditions: **2.13** (0.2 mmol), **2.20a** (0.24 mmol), $B(C_6F_5)_3$ (5.0 mol%), benzene (0.2 mL), under N_2, 22 °C, 12 h. [b] The yield was determined by ^{1}H NMR analysis of the unpurified product mixture using mesitylene as the internal standard.

Experimental Procedure for the Optimization of the 1,2,2,6,6-Pentamethylpiperidine Substrate (Table S2.8)

An oven-dried sealed tube equipped with a magnetic stir bar was used. Amine **2.13p** (0.20 mmol), benzyl acrylate **2.20b** (0.24 mmol), $B(C_6F_5)_3$, and solvent (0.4 mL) were added to the reaction vessel under nitrogen atmosphere. The reaction mixture was stirred under nitrogen atmosphere for 12 h. Upon completion, the reaction mixture was concentrated *in vacuo*. The product yield was determined by the ^1H NMR analysis of the unpurified product mixture using mesitylene as the internal standard.

Table S2.8. Evaluation of Substrate **2.13p**.

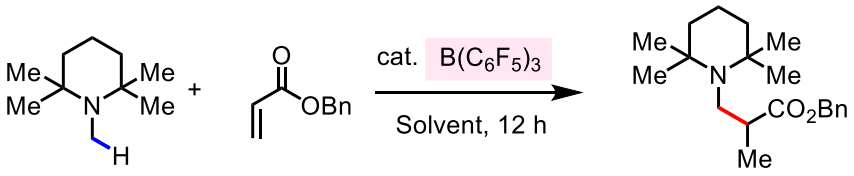

2.13p **2.20b** **2.21pb**

entry	Temp (°C)	$B(C_6F_5)_3$ (mol%)	Solvent	**2.21pb** (%)
1	22	5	DCM	< 5
2	22	5	Benzene	< 5
3	22	10	Benzene	85
4	70	10	Benzene	99

[a] Conditions: **2.13p** (0.2 mmol), **2.20b** (0.24 mmol), $B(C_6F_5)_3$ (cat.), solvent (0.4 mL), under N_2, 12 h. [b] The yield was determined by ^1H NMR analysis of the unpurified product mixture using mesitylene as the internal standard.

Experimental Procedure for the Optimization of the Lewis Acid Co-Catalyst (Table S2.9)

An oven-dried sealed tube equipped with a magnetic stir bar was used. 1-(4-Methoxy-2,6-dimethylphenyl)pyrrolidine **2.13k** (0.10 mmol), 3-acryloyloxazolidin-2-one **2.23a** (0.12 mmol), $B(C_6F_5)_3$ (0.01 mmol), Lewis acid co-catalyst (0.01 mmol) and DCM (0.3 mL) were added to the reaction vessel under nitrogen atmosphere. The reaction mixture was stirred at 22 °C for 12 h. Upon completion, the reaction mixture was filtered through silica gel and concentrated *in vacuo*. The product yield was determined by the ^{1}H NMR analysis of the unpurified product mixture using mesitylene as the internal standard.

Table S2.9. Evaluation of Co-Catalyst.

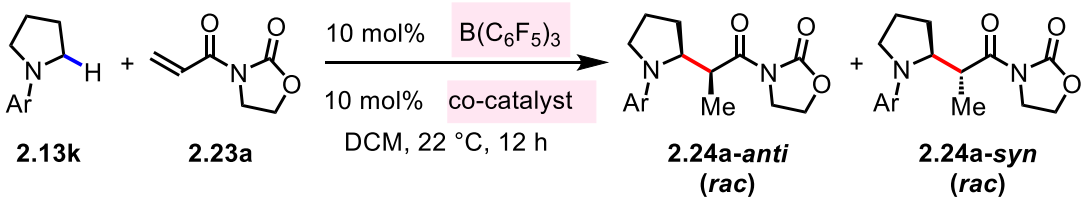

2.13k + **2.23a** → **2.24a-*anti*** (***rac***) + **2.24a-*syn*** (***rac***)

entry	co-catalyst	yield (%)	***anti:syn***
1	None	35	3.2:1
2	CuOTf·Toluene	86	2.6:1
3	$Ni(OTf)_2$	31	4.2:1
4	$Mg(OTf)_2$	38	3.8:1

[a] Conditions: **2.13k** (0.1 mmol), **2.23a** (0.12 mmol), $B(C_6F_5)_3$ (10 mol%), cocatalyst (10 mol%), DCM (0.3 mL), under N_2, 22 °C, 12 h. [b] The yield was determined by ^{1}H NMR analysis of the unpurified product mixture using mesitylene as the internal standard.

Experimental Procedure for the Optimization of the Metal with L3 (Table S2.10)

An oven-dried sealed tube equipped with a magnetic stir bar was used. To this tube were added Lewis acid co-catalyst (0.01 mmol), 2,6-bis((*R*)-4-phenyl-4,5-dihydrooxazol-2-yl)pyridine **L3** (0.012 mmol), and DCM (0.2 mL) under nitrogen atmosphere. The mixture was stirred for 20 min at 22 °C. Subsequently, 3-acryloyloxazolidin-2-one **2.23a** (0.12 mmol), 1-(4-methoxy-2,6-dimethylphenyl)pyrrolidine **2.13k** (0.10 mmol), $B(C_6F_5)_3$ (0.01 mmol) and DCM (0.1 mL) were added to the reaction vessel, and the resulting mixture was stirred at 22 °C for 12 h. Upon completion, the reaction mixture was filtered through a plug of silica gel and concentrated *in vacuo*. The product yield and *anti:syn* ratio were determined by the ^{1}H NMR analysis of the unpurified product mixture using mesitylene as the internal standard. The Mannich product was purified and isolated by preparative TLC (4:1 hexanes/EtOAc). The er value of each diastereomer was determined by HPLC analysis of the isolated product.

Table S2.10. Evaluation of Metal with **L3**.

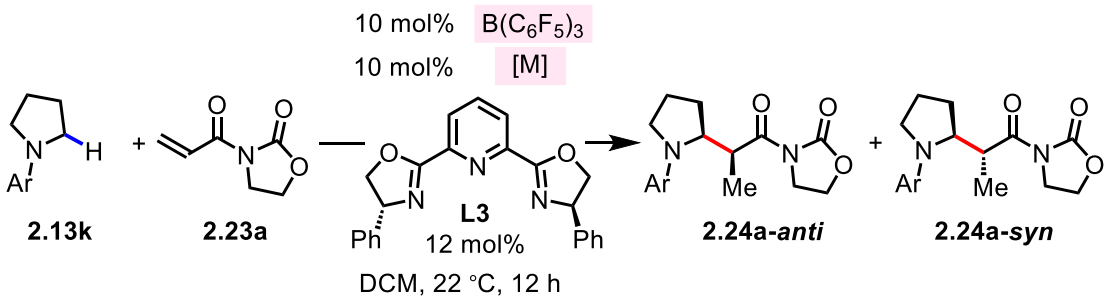

entry	[M]	yield (%)	***anti*:*syn***	enantiomeric ratio	
				2.24a-*anti*	**2.24a-*syn***
1	None(without **L3**)	35	4.8:1	NA	NA
2	None(with **L3**)	<5	NA	NA	NA
3	CuOTf Toluene	71	3.2:1	50:50	50:50
4	$Zn(OTf)_2$	15	1:1	50:50	50:50
5	$Mg(ClO_4)_2$	40	3.4:1	50:50	50:50
6	$Sc(OTf)_3$	<5	NA	NA	NA
7	$Ni(BF_4)_2\ H_2O$	<5	NA	NA	NA
8	$Fe(ClO_4)_3\ H_2O$	<5	NA	NA	NA
9	$Mg(OTf)_2$	66	2.3:1	72:28	75:25

[a] Conditions: **2.13k** (0.1 mmol), **2.23a** (0.12 mmol), $B(C_6F_5)_3$ (10 mol%), [M] (10 mol%), **L3** (12 mol%), DCM (0.3 mL), under N_2, 22 °C, 12 h. [b] The yield and *anti:syn* ratio were determined by ^1H NMR analysis of the unpurified product mixture using mesitylene as the internal standard.

Experimental Procedure for the Optimization of PyBOX Ligand (Table S2.11)

An oven-dried sealed tube equipped with a magnetic stir bar was used. To this tube were added $Mg(OTf)_2$ (0.01 mmol), ligand (0.012 mmol), DCM (0.2 mL) under nitrogen atmosphere. The mixture was stirred for 20 min at 22 °C. Subsequently, 3-acryloyl-4,4-dimethyloxazolidin-2-one **2r** (0.12 mmol), 1-(4-methoxy-2,6-dimethylphenyl)pyrrolidine **1a** (0.10 mmol), $B(C_6F_5)_3$ (0.01 mmol), and DCM (0.1 mL) were added to the reaction vessel, and the resulting mixture was stirred at 22 °C for 12 h. Upon completion, the reaction mixture was filtered through a pad of silica gel and concentrated *in vacuo*. The product yield and *anti:syn* ratio were determined by the ^1H NMR analysis of the unpurified product mixture using mesitylene as the internal standard. The Mannich product was purified and isolated by preparative TLC (4:1 hexanes/EtOAc). The er values of each diastereomer was determined by HPLC analysis of the isolated product.

Table S2.11. Evaluation of Chiral Ligand.

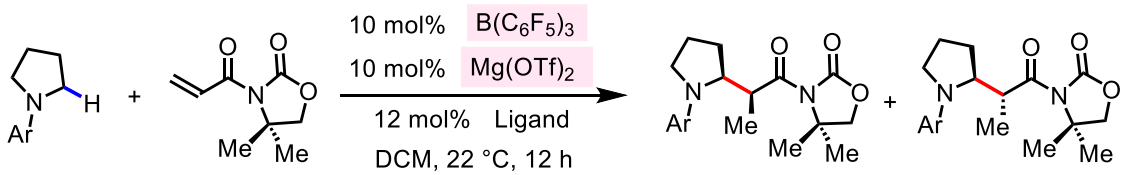

2.13k **2.23b** **2.24b-*anti*** **2.24b-*syn***

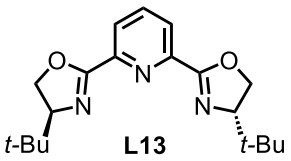

2.24b, <5% yield

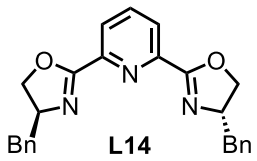

2.24b, 39% yield
anti*:*syn 4.5:1
anti, 34:66 er
syn, 28:72 er

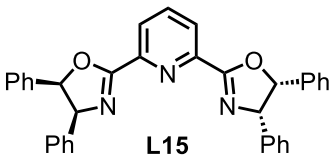

2.24b, <5% yield

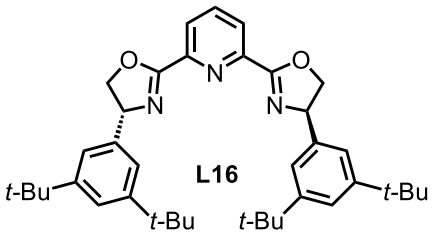

2.24b, <5% yield

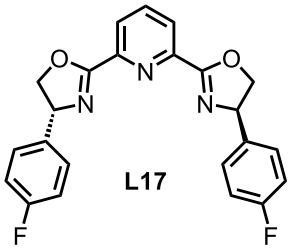

2.24b, 26% yield
anti*:*syn 3.3:1
anti, 93:7 er
syn, 94:6 er

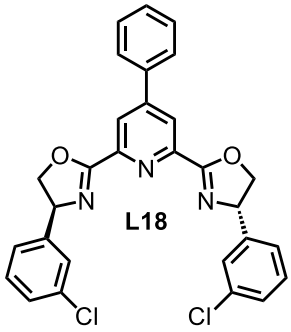

2.24b,<5% yield

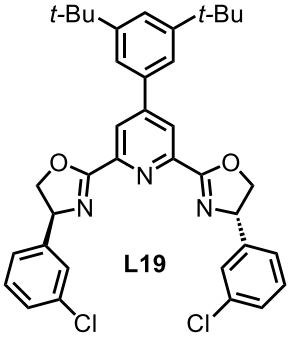

2.24b,<5% yield

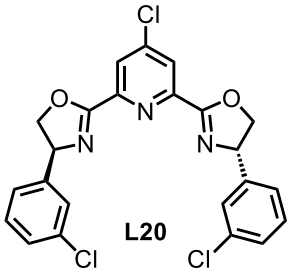

2.24b, 69% yield
anti*:*syn 4.3:1
anti, 4:96 er
syn, 3:97 er

[a] Conditions: **2.13k** (0.1 mmol), **2.23b** (0.12 mmol), $B(C_6F_5)_3$ (10 mol%), $Mg(OTf)_2$ (10 mol%), Ligand (12 mol%), DCM (0.3 mL), under N_2, 22 °C, 12 h. [b] The yield was determined by ^1H NMR analysis of the unpurified product mixture using mesitylene as the internal standard.

A3. General Procedures

General Procedure for the $(F_5C_6)_3B$-Catalyzed Mannich Reaction Using Silicon Enolate (Tables 2.2-2.5)

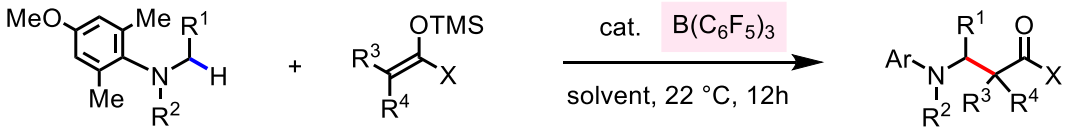

2.13 or **2.17** **2.11** **2.14, 2.16** or **2.18**

An oven-dried sealed tube equipped with a magnetic stir bar was used. To this tube were added amine (0.2 mmol), $B(C_6F_5)_3$ (0.01 mmol or 0.02 mmol), silicon enolate **2.11** (0.4 mmol), and solvent (0.5 mL) under nitrogen atmosphere. The reaction mixture was allowed to stir for 12 hours at 22 °C. Upon completion, the reaction mixture was diluted with DCM, concentrated *in vacuo* and purified by silica gel column chromatography, typically using ethyl ether in hexanes as the eluent.

Procedure for a 1.0 mmol Scale Reaction (Scheme 2.7)

An oven-dried sealed tube equipped with a magnetic stir bar was used. To this tube were added amine **2.13k** (0.2 g, 1.0 mmol), $B(C_6F_5)_3$ (26 mg, 0.05 mmol), ((1-methoxy-2-methylprop-1-en-1-yl)oxy)trimethylsilane **2.11a** (0.3 g, 2.0 mmol), and THF (2.5 mL) under nitrogen atmosphere. The reaction mixture was allowed to stir for 12 hours at 22 °C. The unpurified product mixture was subjected to silica gel chromatography (3% Et_2O/hexanes) to afford **2.14k** as a colorless liquid (0.3 g, 97%).

Procedure for Deprotection of *N*-Aryl Group

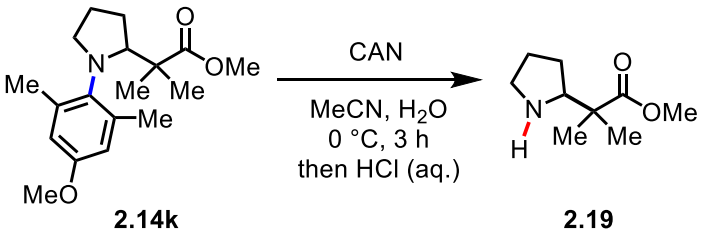

2.14k **2.19**

The deprotection of *N*-aryl group was performed following the literature procedure.[23] To a solution of **2.14k** (61 mg, 0.2 mmol) in MeCN (2.0 mL) at 0 °C was added a solution of ceric ammonium nitrate (548 mg, 1.0 mmol) in H_2O (3.3 mL), dropwise. The reaction mixture was allowed to stir at 0 °C for 1 hour, whereupon the mixture was cooled to 22 °C and stirred for 3 hours. Upon completion (monitored by TLC), the reaction mixture was quenched with 1.0 M NaOH until the pH of the solution was 10; and the crude product was extracted with DCM (3 x 15 mL). The combined organic layers were concentrated *in vacuo*, whereupon the resulting oil was acidified with 4.0 N HCl (4 mL) and extracted again with DCM (3 x 5 mL). The *aqueous* layer was then concentrated *in vacuo* to obtain a solid residue. To the unpurified product mixture was added DCM, and the resulting suspension was filtered through Celite and concentrated to afford a brown residue which was characterized as the HCl salt of **2.19** (40 mg, 97%). Upon treatment of the salt with K_2CO_3 (aqueous) and extraction with DCM (3 x 10 mL), the free base **2.19** was obtained as a brown oil (27 mg, 79% yield from **2.19•HCl**). The spectroscopic data of **2.19** matched those reported by Sekiya.[24]

General Procedures for the Stereoselective Coupling of *N*-Alkylamines and *α,β*-Unsaturated Molecules

General Procedure for $(F_5C_6)_3B$-Catalyzed Racemic Mannich Reactions

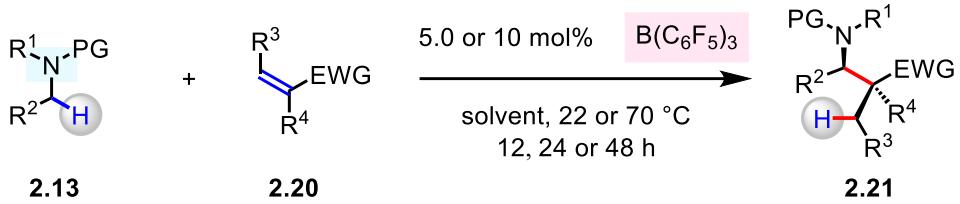

2.13 **2.20** **2.21**

To a 15 mL oven-dried sealed tube was added amine **2.13** (0.2 mmol, 1 equiv.), *α,β*-unsaturated compound **2.20** (0.24 mmol, 1.2 equiv.), a catalytic amount of $B(C_6F_5)_3$ and solvent under nitrogen atmosphere. The reaction mixture was stirred at either 22 °C or 70 °C for 12 to 48 hours. Upon completion, the reaction mixture was diluted with EtOAc, concentrated *in vacuo* and purified by silica gel column chromatography.

General Procedure for Stereoselective Mannich Reactions

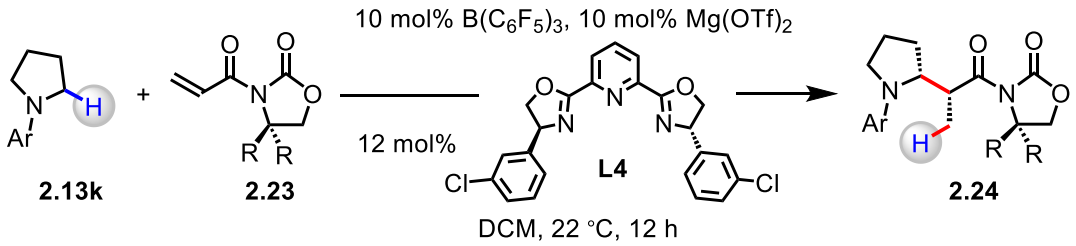

2.13k **2.23** **L4** **2.24**

An oven-dried sealed tube equipped with a magnetic stir bar was used. To this tube were added $Mg(OTf)_2$ (0.02 mmol), ligand **L4** (0.024 mmol), DCM (0.2 mL) under nitrogen atmosphere. The mixture was stirred for 20 min at 22 °C, then oxazolidinone substrate **2.23** (0.30 mmol), 1-(4-methoxy-2,6-dimethylphenyl)pyrrolidine **2.13k** (0.20 mmol), $B(C_6F_5)_3$ (0.02 mmol), and DCM (0.1 mL) were added to the vessel. The reaction mixture was stirred at 22 °C for 12 h. Upon completion, the crude mixture was filtered through a pad of silica gel and concentrated *in vacuo*.

The Mannich product was purified and isolated by silica gel column chromatography. The *anti*:*syn* ratio was determined by ^{1}H NMR analysis of the crude reaction mixture. The er values of each diastereomer was determined by HPLC analysis of the isolated product.

Procedure for Large Scale Reaction

We carried out the following studies in order to determine the absolute configuration of enantioenriched products **2.24a–2.24d**, **2.24e-(S)**, and **2.24e-(*R*)** and the relative configuration of products **2.21a** to **2.21p** and **2.24a** to **2.24l**. We first obtained product **2.24e-(*R*)** in 1.68 g by the following procedure.

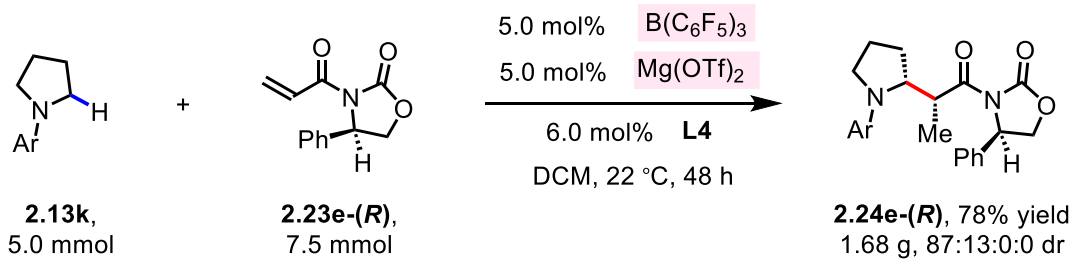

To a 35 mL oven-dried sealed tube was added $Mg(OTf)_2$ (0.25 mmol), ligand **L4** (0.30 mmol), DCM (10 mL) under nitrogen atmosphere. The mixture was stirred for 30 min at 22 °C, then (*R*)-3-acryloyl-4-phenyloxazolidin-2-one **2.24e-(*R*)** (1.3 g, 6.0 mmol), 1-(4-methoxy-2,6-dimethylphenyl)pyrrolidine **2.13k** (1.02 g, 5.0 mmol), $B(C_6F_5)_3$ (0.25 mmol), and DCM (5.0 mL) were added to the vessel. The reaction mixture was stirred at 22 °C for 48 h. Upon completion, the solvent was removed *in vacuo.* The *anti*:*syn* ratio was determined to be 87:13 by ^{1}H NMR analysis of the crude reaction mixture. Purification by silica gel column chromatography using 4:1 hexanes:Et_2O gave the product as a colorless solid as a mixture of diastereomers (1.68 g, 78% yield). Further purification was carried out by silica gel column chromatography using 4:1 hexanes:Et_2O to obtain the major diastereomer in 1.41 g as a colorless oil.

We then subjected **2.24e-(*R*)** to the following derivatization studies which yielded **2.25–2.28**.

Procedure for Determination of the Absolute Configuration

The absolute configuration of **2.24e-(*R*)** was determined by X-ray crystallographic analysis of **2.28**.

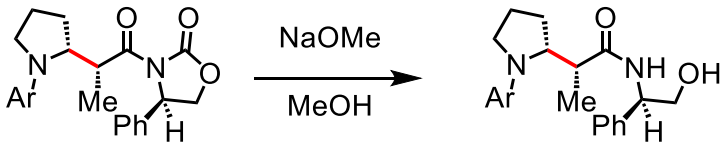

2.24e-(*R*)-*anti* **2.28**, 97% yield

(*R*)-*N*-((*R*)-2-Hydroxy-1-phenylethyl)-2-((*R*)-1-(4-methoxy-2,6-dimethylphenyl)pyrrolidin-2-yl)propanamide (2.28)

(*R*)-*N*-((*R*)-2-Hydroxy-1-phenylethyl)-2-((*R*)-1-(4-methoxy-2,6-dimethylphenyl)pyrrolidin-2-yl)propanamide (**2.28**) was synthesized following a known procedure.[21] A solution of **2.24e-(*R*)-*anti*** (590 mg, 1.4 mmol) in MeOH (3.5 mL) was chilled to 0 °C, whereupon NaOMe (827 mg, 15.3 mmol) was added portionwise. The reaction was allowed to stir for 1 h, whereupon the reaction was quenched with aq. NH_4Cl (3 mL). The aqueous layer was extracted with EtOAc (3 x 5 mL). The combined organic layers were dried ($MgSO_4$), filtered, and concentrated *in vacuo*. The crude product was purified by silica gel chromatography (3:1 hexanes:EtOAc) to afford **2.28** as a crystalline solid (393 mg, 97% yield). The solid material was recrystallized in 19:1 hexanes:isopropanol to obtain a crystal for X-ray crystallography. The X-ray crystallographic analysis revealed that the absolute configuration of **2.28** is (*R,R,R*), see SI Section 7. The Mannich product **2.24e-(*R*)-*syn*** was also subjected to these reaction conditions, but was obtained as a colorless oil.

^{1}H NMR (600 MHz, $CDCl_3$) δ 7.32 (t, *J* = 7.5 Hz, 2H), 7.29 – 7.25 (m, 1H), 7.20 – 7.17 (m, 2H), 6.59 (d, *J* = 3.0 Hz, 1H), 6.56 (d, *J* = 3.1 Hz, 1H), 5.89 (d, *J* = 6.3 Hz, 1H), 4.74 (td, *J* = 6.0, 3.6 Hz, 1H), 3.92 (dt, *J* = 7.1, 5.4 Hz, 1H), 3.75 (s, 3H), 3.63 (tdd, *J* = 10.7, 8.9, 7.2, 3.6 Hz, 2H), 3.26

(dt, J = 8.4, 5.9 Hz, 1H), 2.98 (q, J = 7.6 Hz, 1H), 2.89 (d, J = 6.1 Hz, 1H), 2.29 (s, 3H), 2.25 (s, 3H), 2.17 (qd, J = 6.9, 5.1 Hz, 1H), 2.07 (dq, J = 11.7, 7.5, 7.1 Hz, 1H), 1.93 – 1.83 (m, 3H), 1.13 (d, J = 7.0 Hz, 3H); **^{13}C NMR** (151 MHz, $CDCl_3$) δ 178.9, 159.4, 142.8, 141.8, 141.6, 140.4, 131.5, 130.5, 129.3, 117.3, 115.7, 69.5, 65.5, 59.2, 57.9, 55.3, 49.1, 31.6, 27.8, 22.3, 22.2, 16.7; **IR** (neat) 3383, 3305, 2952, 1644, 1602, 1601, 1512, 1492, 1466, 1261, 1154,1068, 700 cm^{-1}; **HRMS** (DART) m/z Calcd for $C_{26}H_{33}N_2O_4$ (MH^+): 274.1596; found: 274.1588.

Procedures for the Derivatization of Enantioenriched Mannich Products

Compounds **2.24e-(*R*)-*anti***, **2.24e-(*R*)-*syn***, and **2.24b** could be converted into the corresponding methyl esters (**2.25-*anti*** or **2.25-*syn***).

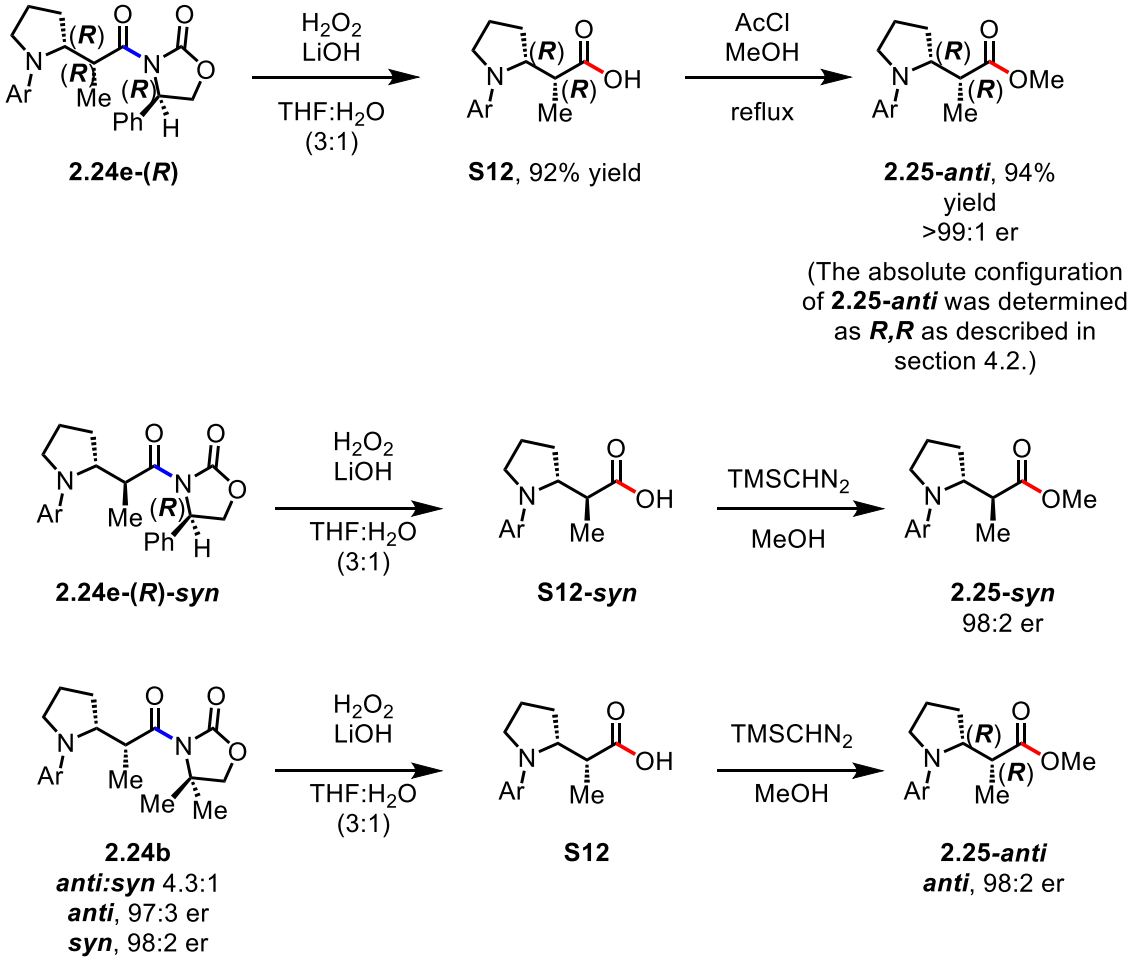

(*R*)-2-((*R*)-1-(4-Methoxy-2,6-dimethylphenyl)pyrrolidin-2-yl)propanoic acid (S12)

(*R*)-2-((*R*)-1-(4-Methoxy-2,6-dimethylphenyl)pyrrolidin-2-yl)propanoic acid was prepared by following a known procedure.[19] To a solution of Mannich product **2.24b-(*R*)-*anti*** (169 mg, 0.4 mmol) in THF:H_2O (3:1, 4.8 mL) at 0 °C was added H_2O_2 (30% v/v, 0.16 mL, 1.6 mmol) and 2.0 M LiOH (0.28 mL, 0.56 mmol), dropwise. The mixture was stirred at 22 °C for 5 h, whereupon the reaction was quenched with $NaHSO_3$. The crude mixture was then concentrated *in vacuo*, then diluted with EtOAc (10 mL), H_2O (10 mL), and 1.0 M NaOH (5 mL). The organic layer was

separated and the aqueous layer was extracted with EtOAc (3 x 15 mL). Subsequently, the aqueous layer was acidified with 6.0 M HCl (3 mL) and extracted with EtOAc (3 x 15 mL). The combined organic layers were washed with brine (20 mL), dried ($MgSO_4$), filtered. and concentrated *in vacuo* to afford **S12** as a colorless solid (102 mg, 92%) which was used without further purification. **^{1}H NMR** (600 MHz, $CDCl_3$) δ 6.66 – 6.40 (m, 1H), 3.92 (dt, *J* = 9.0, 4.9 Hz, 1H), 3.71 (s, 3H), 3.34 (td, *J* = 7.9, 3.9 Hz, 1H), 3.02 (q, *J* = 8.1 Hz, 1H), 2.39 (m, 1H), 2.29 (s, 3H), 2.25 (s, 3H), 2.16 – 2.06 (m, 1H), 2.02 – 1.89 (m, 1H), 1.87 – 1.78 (m, 1H), 1.12 (d, *J* = 7.1 Hz, 3H).

Methyl (*R*)-2-((*R*)-1-(4-methoxy-2,6-dimethylphenyl)pyrrolidin-2-yl)propanoate (2.25-*anti*)

Methyl (*R*)-2-((*R*)-1-(4-methoxy-2,6-dimethylphenyl)pyrrolidin-2-yl)propanoate was prepared by following a known procedure.[22] Acetyl chloride (0.14 mL, 2.0 mmol) was added dropwise to a solution of propanoic acid **S12** (111 mg, 0.4 mmol) in MeOH (1.8 mL). The reaction mixture was heated at reflux for 12 h. The reaction mixture was concentrated *in vacuo*, then saturated K_2CO_3 (6 mL) was added at 0 °C. The aqueous layer was extracted with DCM (3 x 10 mL) and the combined organic layers were washed with brine (15 mL), dried ($MgSO_4$), filtered, and concentrated *in vacuo*. The crude product was purified by silica gel column chromatography (50:1 Hexanes: Et_2O) to afford **2.25** as a colorless oil (110 mg, 94% yield). **HPLC** (Chiralpak IC then Chiralcel OJ-H; 1%/ 99% hexane/isopropanol, 0.5 mL/min; **2.25-*anti*:** tr = 33.1 min (major), 42.1 min (minor); >99:1 er.

```
Acq. Operator   : SYSTEM                          Seq. Line :   2
Acq. Instrument : Wasa_LC1                         Location :   41
Injection Date  : 12/7/2017 9:33:45 PM                Inj :   1
                                                 Inj Volume : 8.000 µl
Method          : C:\Chem32\1\Data\JOE 2017-12-07 19-50-57\column2 1% IPA 99% hexane 50min-0.
                  5mL.M (Sequence Method)
Last changed    : 12/7/2017 7:50:58 PM by SYSTEM
Method Info     : Column2 50min-1% iPrOH 99% hexane-0.5mL
```

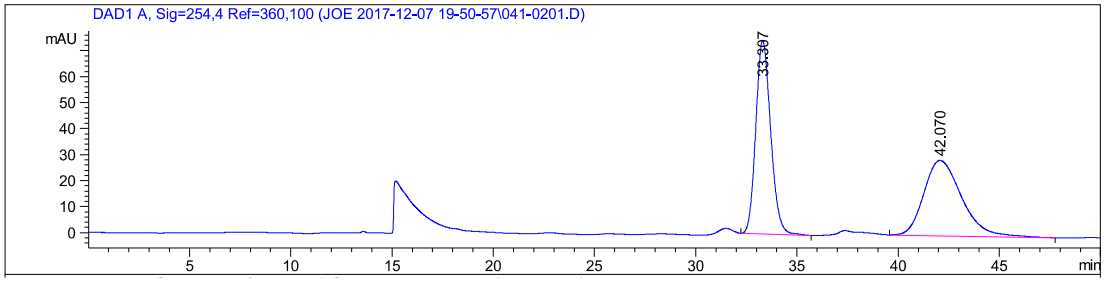

Signal 1: DAD1 A, Sig=254,4 Ref=360,100

Peak #	RetTime [min]	Type	Width [min]	Area [mAU*s]	Height [mAU]	Area %
1	33.307	BB	0.7908	3803.36499	74.34589	50.3094
2	42.070	BB	1.9461	3756.58228	28.98495	49.6906

```
Acq. Operator   : SYSTEM                          Seq. Line :   3
Acq. Instrument : Wasa_LC1                         Location :   51
Injection Date  : 12/7/2017 10:24:43 PM               Inj :   1
                                                 Inj Volume : 8.000 µl
Method          : C:\Chem32\1\Data\JOE 2017-12-07 19-50-57\column2 1% IPA 99% hexane 50min-0.
                  5mL.M (Sequence Method)
Last changed    : 12/7/2017 7:50:58 PM by SYSTEM
Method Info     : Column2 50min-1% iPrOH 99% hexane-0.5mL
```

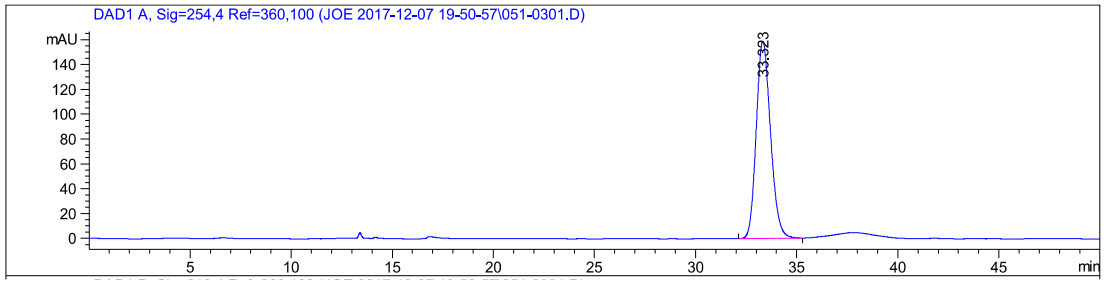

Signal 1: DAD1 A, Sig=254,4 Ref=360,100

Peak #	RetTime [min]	Type	Width [min]	Area [mAU*s]	Height [mAU]	Area %
1	33.323	BB	0.7542	7793.69141	158.89992	100.0000

2.24e-(*R*)-*syn* and **2.24b** were subjected to analogous conditions to afford **2.25-*syn*** and **2.25-*anti***.[23]

2.24b was carried through as a mixture of diastereomers.

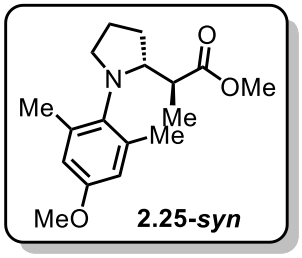

2.25-*syn* from **2.24e-(*R*)-*syn*: HPLC** (Chiralpak IC then Chiralcel OJ-H; 1%/ 99% hexanes/isopropanol, 0.5 mL/min; tr = 30.9 min (major), 32.6 min (minor); 98:2 er.

```
Acq. Operator   : SYSTEM                          Seq. Line :   3
Acq. Instrument : Wasa_LC1                         Location :   42
Injection Date  : 10/28/2017 4:40:15 PM                Inj :   1
                                                  Inj Volume : 8.000 µl
Method          : C:\Chem32\1\Data\JOE 2017-10-28 14-56-02\column2 1% IPA 99% hexane 50min-0.
                  5mL.M (Sequence Method)
Last changed    : 10/28/2017 2:56:04 PM by SYSTEM
Method Info     : Column2 50min-1% iPrOH 99% hexane-0.5mL
```

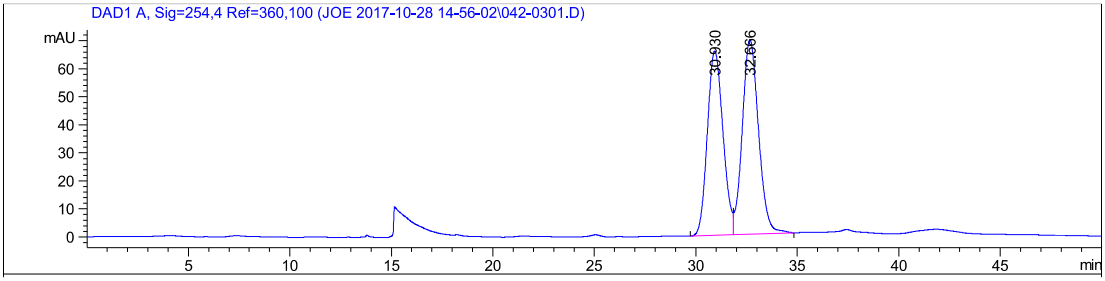

Signal 1: DAD1 A, Sig=254,4 Ref=360,100

Peak #	RetTime [min]	Type	Width [min]	Area [mAU*s]	Height [mAU]	Area %
1	30.930	BV	0.8350	3518.35767	65.67362	47.7326
2	32.666	VB	0.8595	3852.61475	69.41617	52.2674

```
Acq. Operator   : SYSTEM                          Seq. Line :   2
Acq. Instrument : Wasa_LC1                         Location :   21
Injection Date  : 10/30/2017 9:45:42 PM                Inj :   1
                                                 Inj Volume : 8.000 µl
Method          : C:\Chem32\1\Data\JOE 2017-10-30 20-52-54\column2 1% IPA 99% hexane 50min-0.
                  5mL.M (Sequence Method)
Last changed    : 10/30/2017 8:52:56 PM by SYSTEM
Method Info     : Column2 50min-1% iPrOH 99% hexane-0.5mL
```

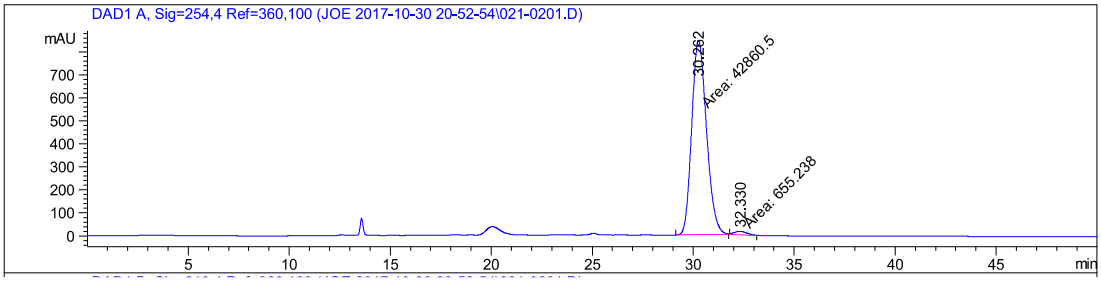

Signal 1: DAD1 A, Sig=254,4 Ref=360,100

Peak #	RetTime [min]	Type	Width [min]	Area [mAU*s]	Height [mAU]	Area %
1	30.262	MM	0.8462	4.28605e4	844.14630	98.4942
2	32.330	MM	0.7432	655.23840	14.69504	1.5058

Product **2.25**, derived from **2.24b**, was isolated as a mixture of diastereomers. The following is the HPLC trace for the mixture of **2.25-*anti*** and **2.25-*syn*.**

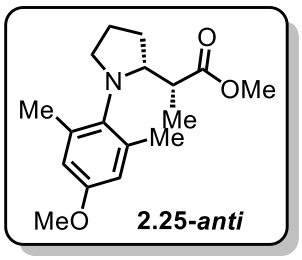

2.25-*anti* (from 2.24b): HPLC (Chiralpak IC then Chiralcel OJ-H; 1%/ 99% hexanes/isopropanol, 0.5 mL/min; **2.25-*anti*:** tr = 33.3 min (major), 42.0 min (minor); 98:2 er.

```
Acq. Operator   : SYSTEM                          Seq. Line :   2
Acq. Instrument : Wasa_LC1                        Location :   11
Injection Date  : 10/11/2017 4:19:51 PM               Inj :   1
                                                 Inj Volume : 2.000 µl
Method          : C:\Chem32\1\Data\JOE 2017-10-11 15-27-57\column2 1% IPA 99% hexane 50min-0.
                  5mL.M (Sequence Method)
Last changed    : 10/11/2017 3:27:59 PM by SYSTEM
Method Info     : Column2 50min-1% iPrOH 99% hexane-0.5mL
```

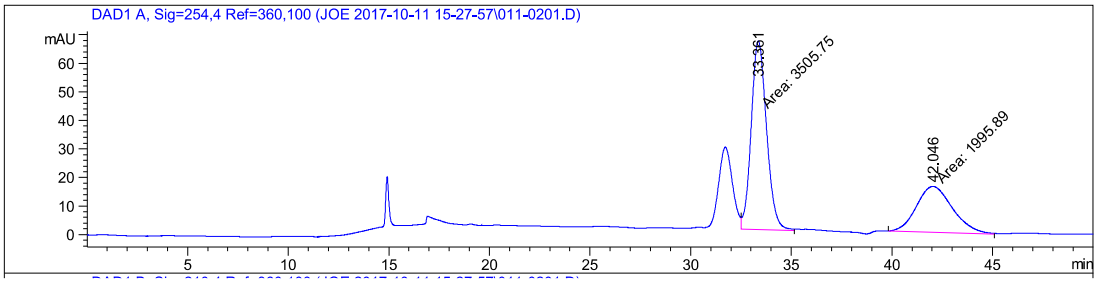


```
Signal 1: DAD1 A, Sig=254,4 Ref=360,100

Peak RetTime Type  Width     Area      Height     Area
  #   [min]        [min]   [mAU*s]     [mAU]       %
----|-------|----|-------|----------|----------|--------|
   1  33.361 FM    0.8837 3505.75146   66.12045  63.7219
   2  42.046 MM    2.0717 1995.89001   16.05654  36.2781
```

```
Acq. Operator   : SYSTEM                          Seq. Line :   3
Acq. Instrument : Wasa_LC1                         Location :   15
Injection Date  : 10/27/2017 6:16:42 PM               Inj :   1
                                                  Inj Volume : 8.000 µl
Method          : C:\Chem32\1\Data\JOE 2017-10-27 16-32-53\column2 1% IPA 99% hexane 50min-0.
                  5mL.M (Sequence Method)
Last changed    : 10/27/2017 4:32:55 PM by SYSTEM
Method Info     : Column2 50min-1% iPrOH 99% hexane-0.5mL
```

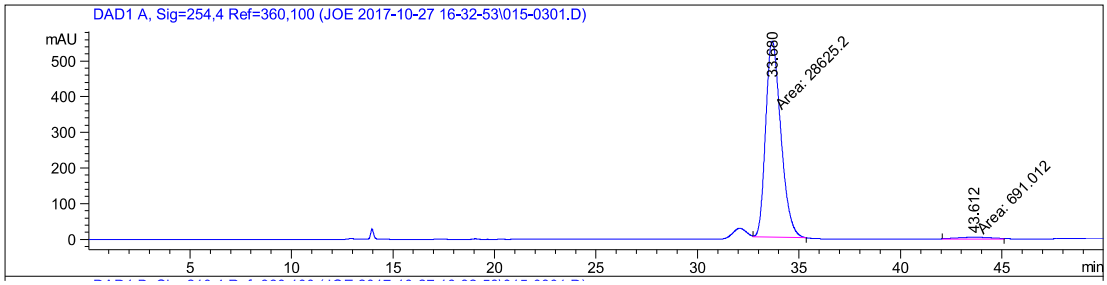

Signal 1: DAD1 A, Sig=254,4 Ref=360,100

Peak #	RetTime [min]	Type	Width [min]	Area [mAU*s]	Height [mAU]	Area %
1	33.680	MM	0.8687	2.86252e4	549.18225	97.6429
2	43.612	MM	2.0869	691.01215	5.51856	2.3571

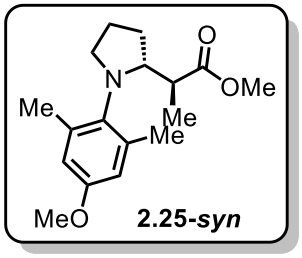

2.25-*syn* (from 2.24b): HPLC (Chiralpak IC then Chiralcel OJ-H; 1%/ 99% hexanes/isopropanol, 0.5 mL/min; tr = 33.4 min (major), 31.7 min (minor); >99:1 er.

```
Acq. Operator   : SYSTEM                          Seq. Line :   2
Acq. Instrument : Wasa_LC1                         Location :   11
Injection Date  : 10/11/2017 4:19:51 PM                 Inj :   1
                                                 Inj Volume : 2.000 µl
Method          : C:\Chem32\1\Data\JOE 2017-10-11 15-27-57\column2 1% IPA 99% hexane 50min-0.
                  5mL.M (Sequence Method)
Last changed    : 10/11/2017 3:27:59 PM by SYSTEM
Method Info     : Column2 50min-1% iPrOH 99% hexane-0.5mL
```

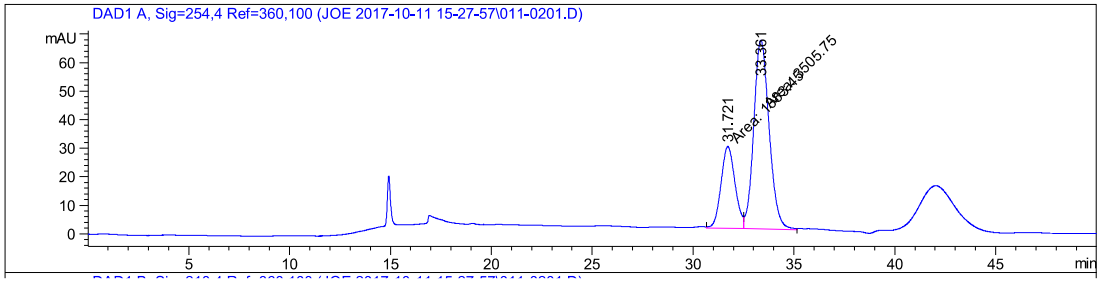

Signal 1: DAD1 A, Sig=254,4 Ref=360,100

Peak #	RetTime [min]	Type	Width [min]	Area [mAU*s]	Height [mAU]	Area %
1	31.721	MF	0.8048	1383.45337	28.65113	28.2961
2	33.361	FM	0.8837	3505.75146	66.12045	71.7039

```
Acq. Operator   : SYSTEM                          Seq. Line :   3
Acq. Instrument : Wasa_LC1                         Location :   15
Injection Date  : 10/27/2017 6:16:42 PM                 Inj :   1
                                                 Inj Volume : 8.000 µl
Method          : C:\Chem32\1\Data\JOE 2017-10-27 16-32-53\column2 1% IPA 99% hexane 50min-0.
                  5mL.M (Sequence Method)
Last changed    : 10/27/2017 4:32:55 PM by SYSTEM
Method Info     : Column2 50min-1% iPrOH 99% hexane-0.5mL
```

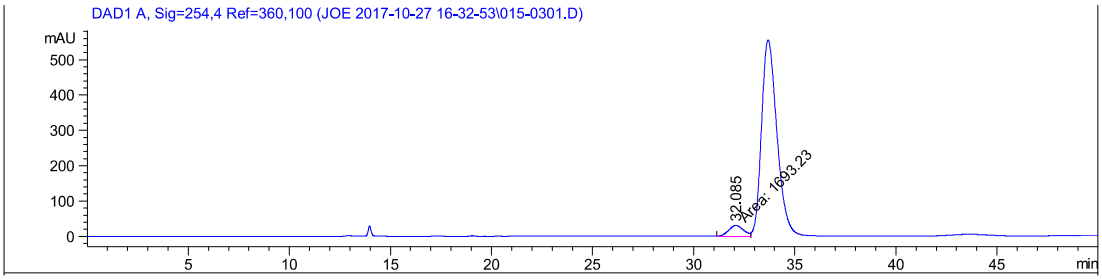

Signal 1: DAD1 A, Sig=254,4 Ref=360,100

Peak #	RetTime [min]	Type	Width [min]	Area [mAU*s]	Height [mAU]	Area %
1	32.085	MM	0.8934	1693.23450	31.58757	100.0000

By comparing the HPLC traces of **2.25-*anti*** and **2.25-*syn*** prepared as above, we determined that the absolute configuration of **2.24b-*anti*** is (*R,R*).

Procedure for the Removal of the Chiral Auxiliary to obtain Amino Alcohol 2.27

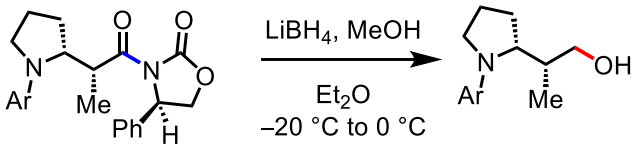

2.24e-(*R*)-*anti* **2.27**, 91% yield

(*R*)-2-((*R*)-1-(4-Mmethoxy-2,6-dimethylphenyl)pyrrolidin-2-yl)propan-1-ol (2.27)

(*R*)-2-((*R*)-1-(4-Mmethoxy-2,6-dimethylphenyl)pyrrolidin-2-yl)propan-1-ol (**2.27**) was prepared using a known procedure.[24] A solution of $LiBH_4$ in THF (2M, 0.15 mL, 0.3 mmol) was added to a solution of imide **2.24e-(*R*)-*anti*** (85 mg, 0.2 mmol) in Et_2O (2.0 mL) under N_2 atmosphere at –20 °C. Subsequently, MeOH (0.3 mmol) was added dropwise at –20 °C. The reaction mixture was then allowed to stir at 0 °C for 1 h. Upon completion of the reaction (monitored by TLC), aq. $NaHCO_3$ (2 mL) was added slowly and was extracted with EtOAc (3 x 5 mL). The combined organic layers were dried ($MgSO_4$), filtered, and concentrated *in vacuo*. The crude product was purified by silica gel column chromatography (3:1 Hexanes: Et_2O) to afford **2.27**as a colorless solid (48 mg, 91% yield).

^{1}H NMR (600 MHz, $CDCl_3$) δ 6.58 (s, 1H), 6.53 (s, 1H), 3.74 (s, 3H), 3.70 – 3.59 (m, 1H), 3.49 – 3.33 (m, 2H), 3.27 (ddd, *J* = 11.7, 5.7, 3.6 Hz, 1H), 2.98 (q, *J* = 7.8 Hz, 1H), 2.30 (s, 3H), 2.24 (s, 3H), 2.01 – 1.84 (m, 3H), 1.82 – 1.67 (m, 1H), 1.57 (dt, *J* = 6.5, 3.3 Hz, 1H), 1.30 (s, 1H), 0.90 (dd, *J* = 6.9, 1.1 Hz, 3H); **^{13}C NMR** (151 MHz, $CDCl_3$) δ 156.4, 140.3, 138.6, 137.7, 114.7, 113.2, 66.7, 62.1, 55.1, 52.4, 40.2, 27.3, 25.5, 19.6, 19.3, 12.2; **HPLC** (Chiralpak AD-H; 2.5%/ 98.5% hexane/isopropanol, 0.5 mL/min; **2.27:** tr = 29.6 min (minor), 33.4 min (major); >99:1 er.

```
Acq. Operator   : SYSTEM                          Seq. Line :   2
Acq. Instrument : Wasa_LC1                         Location :   3
Injection Date  : 1/9/2018 8:29:07 PM                 Inj :   1
                                                 Inj Volume : 4.000 µl
Method          : C:\Chem32\1\Data\JOE 2018-01-09 19-25-54\column1 2.5% IPA 97.5% hex 60min-0
                  .5mL.M (Sequence Method)
Last changed    : 1/9/2018 7:25:56 PM by SYSTEM
Method Info     : Washing 40min-2.5% iPrOH 97.5% hexane-0.5mL
```

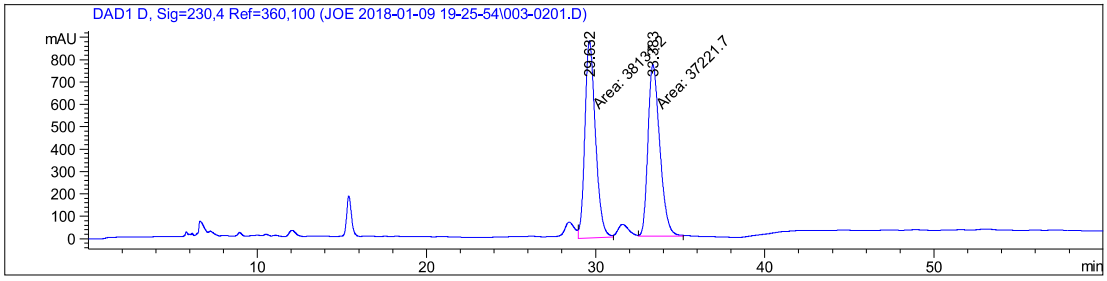

Signal 4: DAD1 D, Sig=230,4 Ref=360,100

Peak #	RetTime [min]	Type	Width [min]	Area [mAU*s]	Height [mAU]	Area %
1	29.632	MM	0.7208	3.81312e4	881.72113	50.6034
2	33.383	MM	0.8097	3.72217e4	766.20929	49.3966

```
Acq. Operator   : SYSTEM                          Seq. Line :   1
Acq. Instrument : Wasa_LC1                         Location :   51
Injection Date  : 1/10/2018 10:26:15 AM               Inj :   1
                                                 Inj Volume : 4.000 µl
Method          : C:\Chem32\1\Data\JOE 2018-01-10 10-23-59\column1 2.5% IPA 97.5% hex 60min-0
                  .5mL.M (Sequence Method)
Last changed    : 1/10/2018 10:24:01 AM by SYSTEM
Method Info     : Washing 40min-2.5% iPrOH 97.5% hexane-0.5mL
```

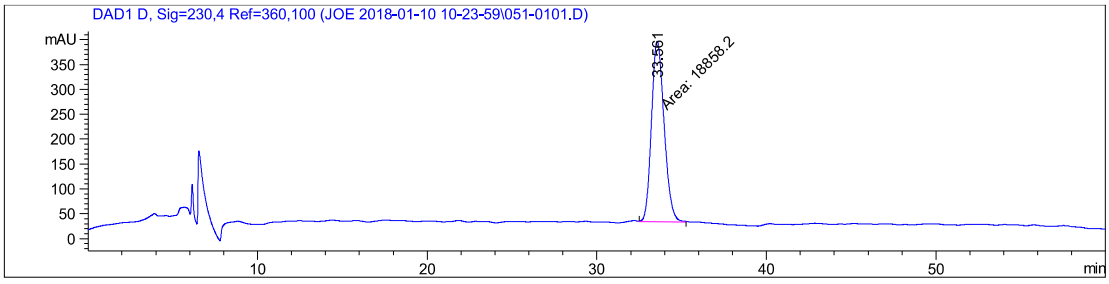

Signal 4: DAD1 D, Sig=230,4 Ref=360,100

Peak #	RetTime [min]	Type	Width [min]	Area [mAU*s]	Height [mAU]	Area %
1	33.561	MM	0.8663	1.88582e4	362.82062	100.0000

Procedure for the Removal of the *para*-Methoxyphenyl Group

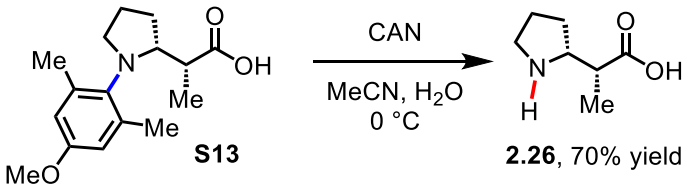

(*R*)-2-((*R*)-Pyrrolidin-2-yl)propanoic acid (2.26)

(*R*)-2-((*R*)-Pyrrolidin-2-yl)propanoic acid (**2.26**) was prepared using a known procedure.[25] A solution of ceric ammonium nitrate (CAN, 548 mg, 1.0 mmol) in H_2O (3.3 mL, 0.30 M to CAN) was added to a solution of propanoic acid **S13** (55.5 mg, 0.20 mmol) in MeCN (2.0 mL) at 0 °C under N_2 atmosphere. The mixture was stirred at 0 °C for 1 h, whereupon the reaction was diluted with EtOAc (2.0 mL) then concentrated *in vacuo* to remove volatile side products and solvent (H_2O was evaporated by azeotropic distillation with toluene). The solid residue was then filtered over a pad of Celite using EtOAc as the eluent. The filtrate was concentrated to afford **2.26** as a solid (19.9 mg, 70% yield). **^{1}H NMR** (500 MHz, D_2O) δ 3.75 (q, J = 9.1 Hz, 1H), 3.36 (dt, J = 19.6, 11.4 Hz, 2H), 2.90 (ddt, J = 13.5, 8.5, 4.1 Hz, 1H), 2.33 (td, J = 7.6, 7.1, 3.8 Hz, 1H), 2.17 – 2.07 (m, 1H), 2.01 (dt, J = 14.0, 8.4 Hz, 1H), 1.84 – 1.70 (m, 1H), 1.35 (dd, J = 7.2, 2.0 Hz, 3H).

Experimental Procedure for the Control Experiments with (*R*)-3-acryloyl-4-phenyloxazolidin-2-one

An oven-dried sealed tube equipped with a magnetic stir bar was used. Amine **2.13k** (0.20 mmol), (*R*)-3-acryloyl-4-phenyloxazolidin-2-one **2.23e-(*R*)** (0.24 mmol), $B(C_6F_5)_3$ (0.02 mmol), and DCM (0.3 mL) were added under nitrogen atmosphere. The reaction mixture was stirred at 22 °C for 12 h. Upon completion, the reaction mixture was concentrated *in vacuo*. The product yield was determined by the ^{1}H NMR analysis of the crude product using mesitylene as the internal standard.

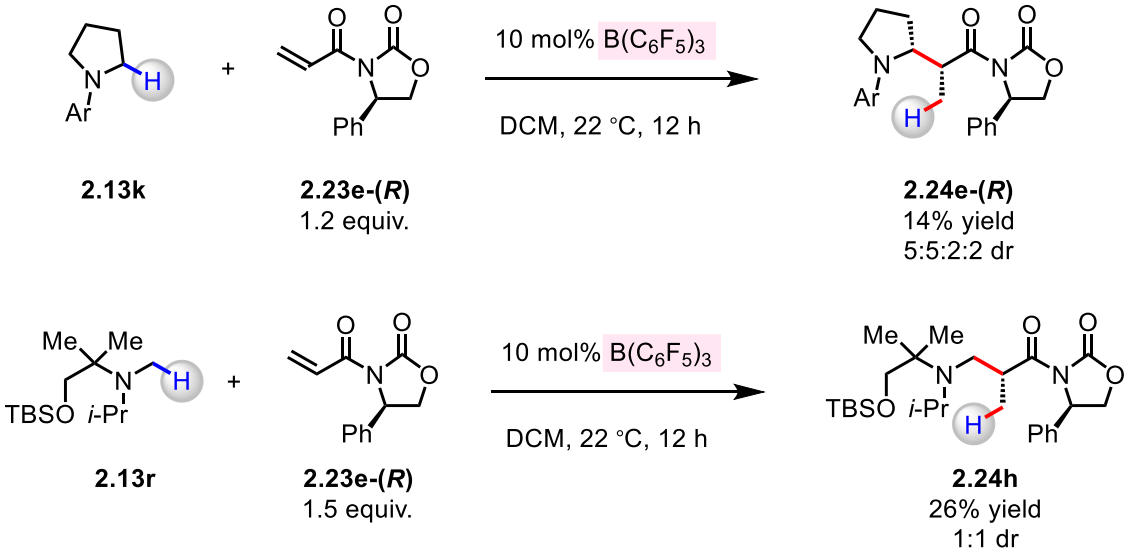

A4. Density Functional Theory (DFT) Calculations

DFT computations[26] were performed with the Gaussian 09 suite of programs.[27] Geometries were optimized with the M06L[28] functional and the def2-SVP basis set[29] in conjunction with the corresponding Coulomb fitting basis set to speed up calculations (denoted DF; density fitting).[30] An ultrafine integration grid was applied. The effect of a polar reaction medium (dichloromethane, DCM) was approximated by means of an integral equation formalism variant of the polarizable continuum model (IEFPCM).[31] Stationary points were probed through vibrational analysis and Gibbs free energy corrections were performed under standard conditions (298.15 K, 1.0 atm). Additionally, we probed the performance of various density functionals through single-point energy calculations at the geometries optimized with the level described above by means of the SMD[32] solvation model with DCM as solvent and the larger def2-TZVPP basis set.[29] Since the correct density functional is not known we tested several state of the art approaches that have been developed over the past decade, all of which are have been designed to account for dispersion:[26,33] M06L,[28] M06,[28] MN15,[26i] ωB97XD[34] and PBE0-D3BJ.[26b,35] Additionally, results with the corresponding parent functionals ωB97X and PBE0[26b] are included. In the manuscript we only report the M06L/def2-TZVPP$_{DCM(SMD)}$//M06L/DF-def2-SVP$_{DCM(IEFPCM)}$ energies and the comparison of other density functionals is provided in Figures S4-S12. Images of computed geometries are shown in Figures S1–S3 and a file for convenient viewing of computed geometries with the program Mercury 3.3 is appended as separate "coordinates.xyz" file.[36]

Challenges and simplifications

(a) All transition state calculations have been carried out in absence of the triflate counterions, rendering the overall charge of the transition state structures +2 (Figure S1). Furthermore,

the solvent has been approximated by a contiuum and it is assumed that the M06L/DF-def2-SVP$_{DCM(IEFPCM)}$ optimized structures are an appropriate reflection of the geometry in solution. Nonetheless, the exact solution geometry is likely unknown.

(b) Initial scans of the potential energy surface have revealed a very flat region for C–C distances between 2.2 and 2.6 Å and attempts to locate a transition state were unsuccessful in most instances. We hence decided to perform a number of constrained optimizations in 0.03–0.10 Å intervals (Figures S4–S8), including the assessment of thermal corrections to the free energy (G_{corr}; see Figure S4c). The largest energy values from Figures S4–S8 have been used in the comparsion of various density functionals (Figures S9–S12).

(c) The stereochemical model under investigation resembles molecular balance experiments designed to assess the contribution of dispersion interactions in solution.[37,38] The challenge here lies in the accurate comparison of two kinds of molecular assemblies: that is, in some structures dispersion is a dominant contributor to the interaction energy (for example, **IX'** and **X'**; Figure S1), whereas dispersion interactions are much less pronounced in alternative geometries (for example, **XI** and **XII**; Figure S1).

(d) Accurate electronic energies are likely not sufficient in assessing the relative energies of **IX–XII**. Equally important are thermal/entropic contributions ($G_{corr} = \Delta G - \Delta E$; see Figure S4c). The large G_{corr}-values for **IX'** and **X'** (22–23 kcal/mol) are expected and are likely the result from significantly reduced vibrational freedom due to the close alignment between the aryl ring of the substrate and the ligand. It is, however, much less clear why the G_{corr}-values for structures **IX**, **X**, **XI** and **XII** fluctuate between 17–20 kcal/mol. We assume an error bar of 1–2 kcal/mol, particularly since G_{corr}-values for the immediate sphere of solvent molecules, which has not been explicitly modeled, are unknown.

(e) To assess the error due to basis set incompleteness associated with the def2-TZVPP basis set we performed additional single point calculations with M06L/DF-def2-QZVPP$_{DCM(SMD)}$. The energies relative to the separate iminium ion and Z-enolate complex increased by less than 0.3 kcal/mol, suggesting that the def2-TZVPP basis set is of sufficient quality.

The stereochemical model

An extended stereochemical model (than the one provided in the manuscript) for reaction of **L3**–Mg-enolate complex with the *in situ* generated iminium ion is shown in Figure S1 and the computed electronic (ΔE) and free energies (ΔE) at the M06L/DF-def2-TZVPP$_{DCM(SMD)}$//M06L/DF-def2-SVP$_{DCM(IEFPCM)}$ level of theory are provided in Figure S2. In addition to the four modes shown in the manuscript (**IX–XII**), we considered two additional modes that lead to the minor diastereomer (i.e., **IX'** and **X'**), wherein the iminium ion is approaching the enolate nucleophile with its aryl ring pointing up. It appears that accurate determination of free energy values is challenging and will strongly depend on the attenuation of dispersion interactions in solution.[37,38] For instance, we find that functionals accounting for dispersion (e.g., M06–L) clearly favor pathway **IX'** over **XI** electronically (ΔE values), particularly with the small def2-SVP basis set applied during geometry optimization (−8.8 vs −5.0 kcal/mol; grey curve in Figure S2). While correcting for basis set incompleteness reduces the energy difference to 2.0 kcal/mol (−3.3 vs −1.3 kcal/mol; red curve in Figure S2), it is only after addition of thermal corrections (ΔG = ΔE + G_{corr}) when **XI** becomes the most favorable mode of addition (19.1 vs 18.1 kcal/mol; blue curve in Figure S2).

Steric influence of the *para*-substituent on the substrate on diastereoselectivity

Based on these large fluctuations in the relative energy between pathways **IX'** and **XI** we decided to test experimentally the influence of substituent R on diastereoselectivity (Figure S3a). We hypothesized that increasing the size of R would lead to destabilization of mode **IX'** and result in an increase in d.r. We indeed observed a minor effect when R is altered from H to *tert*-butyl (3.8:1.0 vs 4.6:1.0 d.r.), although this change is likely too small to render **IX'** the major pathway for generation of the minor diastereomer. In addition to these experimental trends we investigated the effect of a more sizable *tert*-butyl group on the relative energy between **IX'** and **XI** computationally (labeled as **IX'**$_{t\text{-Bu}}$ and **XI**$_{t\text{-Bu}}$; Figure S3b). While the electronic energy (ΔE) of **IX'** is 2.0 kcal/mol lower than for **XI** (R = OMe), **IX'**$_{t\text{-Bu}}$ is destabilized by 0.8 kcal/mol relative to **XI**$_{t\text{-Bu}}$. A side view of the corresponding transition state structures for **IX'** and **IX'**$_{t\text{-Bu}}$ illustrates the significantly increased steric demand in the latter structure. This is reflected in the longer distance between C^2 on the substrate and C^1 on the ligand in **IX'**$_{t\text{-Bu}}$ (3.65 Å; Figure S2), as opposed to **IX'** (3.15 Å).

On the basis of these results we propose that the minor diastereomer is generated through a combination of pathways **IX'** and **IX**, with **IX** likely being favored, otherwise a much more pronounced effect on diastereoselectivity would be expected.

Comparison of results with various density functionals

A comparison of electronic energies (ΔE) with a range of density functionals is provided in Figures S9–S10, the corresponding free energy values are shown in Figures S11–S12. Various state of the art methods (M06L, M06, MN15, ωB97XD and PBE0-D3BJ) yield similar electronic energies relative to the separate iminium ion and Z-enolate complex (Figure S9–S10), while ΔE-

values are significantly larger with density functionals that do not properly account for dispersion (ωB97X and PBE0). It is worth mentioning that the electronic energy of **IX'** is predicted to be lower than that of **XI** by approximately 3 kcal/mol with functionals M06L, M06, MN15, ωB97XD and PBE0-D3BJ (Figure S10), whereas **IX'** is destabilized relative to **XI** by approximately 3 kcal/mol with ωB97X and PBE0 (Figure S9). These data indicate that dispersion terms (D) contribute about 6 kcal/mol to the stabilization of **IX'** relative to **XI**. After addition of thermal contributions (G_{corr}; cf. Figure S4c) the energy values for **IX'** and **XI** are of similar magnitude with functionals M06L, M06, MN15, ωB97XD and PBE0-D3BJ (Figure S12). Based on these results and considering the expected error bar associated with densitiy functionals (>1–2 kcal/mol),[26] we chose to report the single point energies with M06-L, which is also the method used during geometry optimization.

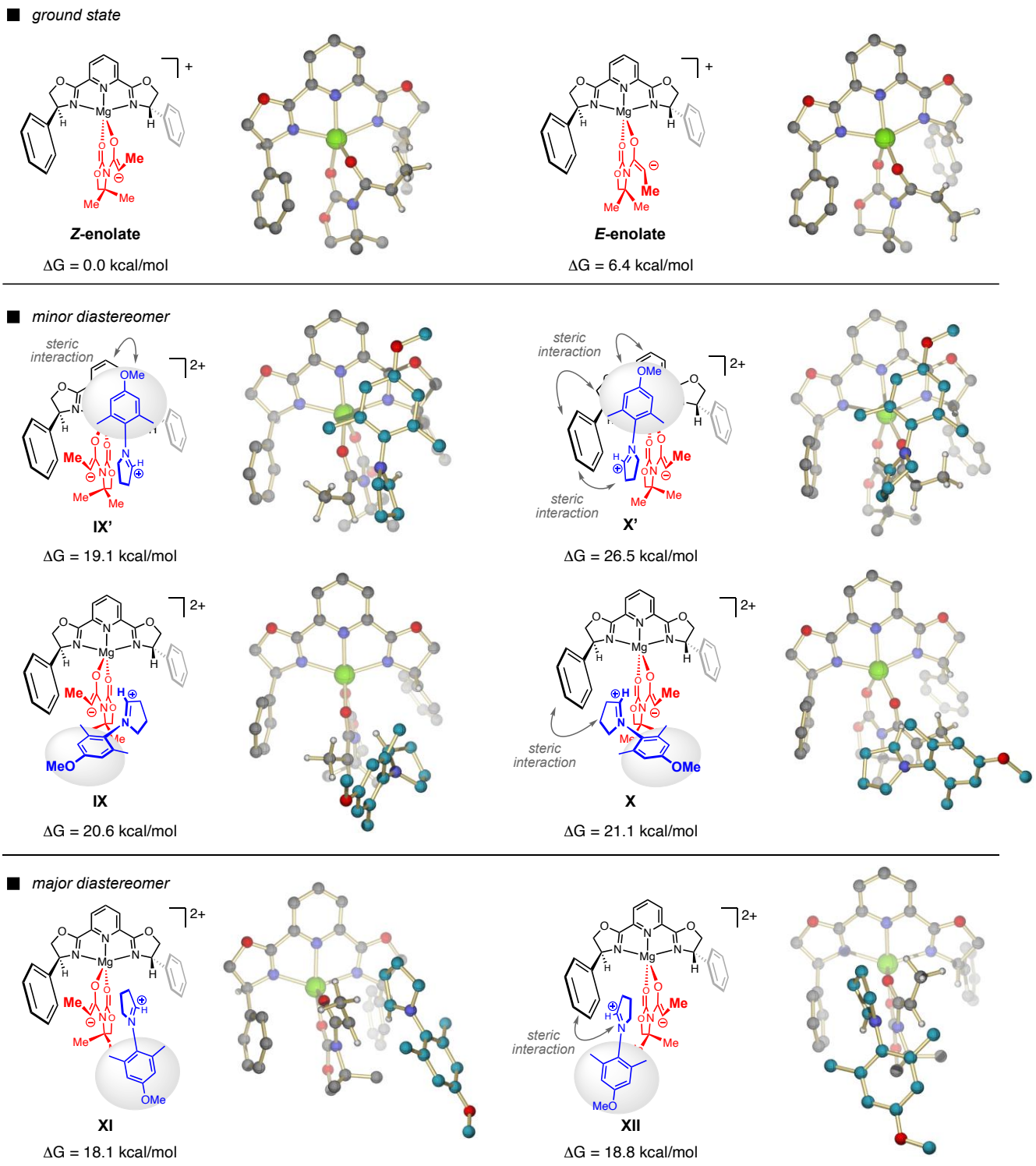

Figure S1. Geometries of computed structures [M06L/DF-def2-SVP$_{DCM(IEFPCM)}$] including free energy values obtained at the M06L/DF-def2-TZVPP$_{DCM(SMD)}$//M06L/DF-def2-SVP$_{DCM(IEFPCM)}$ level of theory; the C–C distance between the electrophilic carbon on the iminium and the nucleophilic carbon on the enolate has been constrained to 2.3 Å.

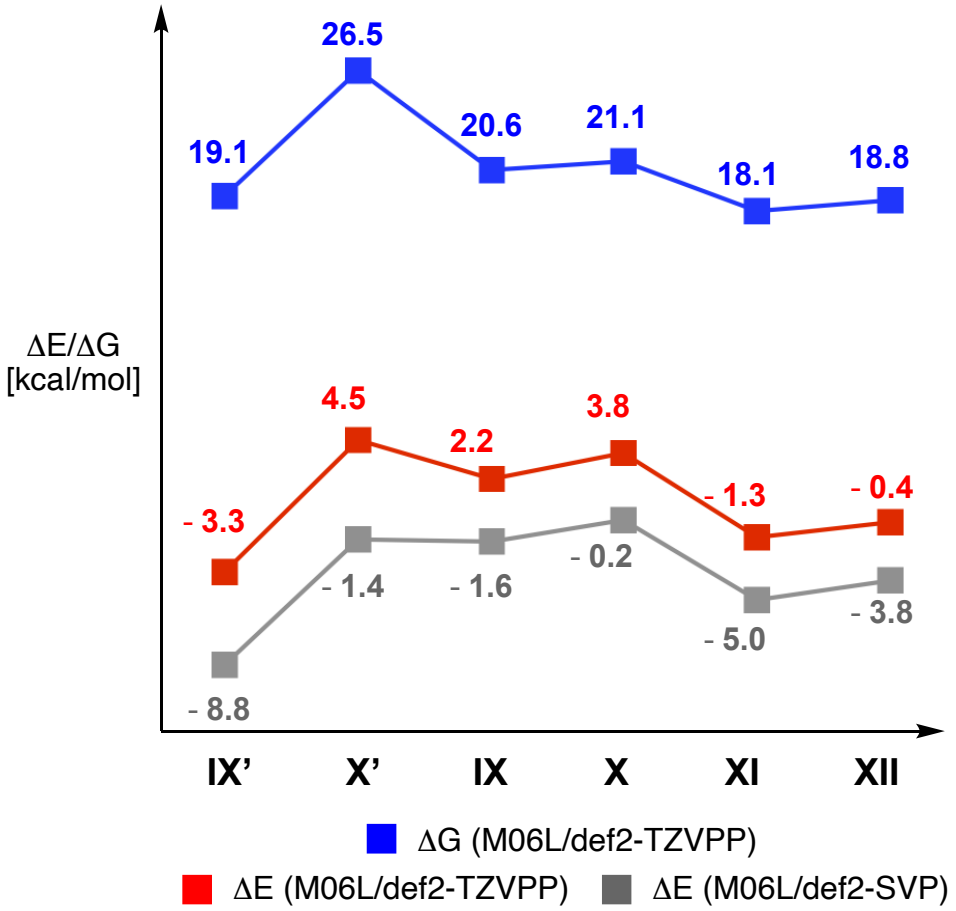

Figure S2. Comparison of electronic and free energies for transition states **IX'–XII** obtained at the M06L/DF-def2-TZVPP$_{DCM(SMD)}$//M06L/DF-def2-SVP$_{DCM(IEFPCM)}$ level of theory.

a Experimentally observed influence of the size of the *para* substituent on the substrate on diastereoselectivity

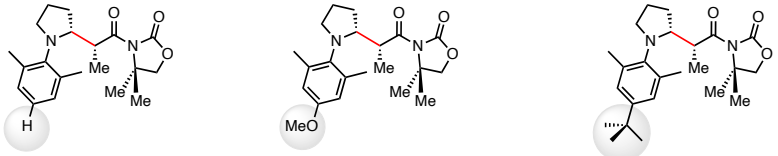

72% yield
anti:syn 3.8:1.0
anti, 95:5 er
syn, 97:3 er

88% yield
anti:syn 4.3:1.0
anti, 97:3 er
syn, 98:2 er

39% yield
anti:syn 4.6:1.0
anti, 97:3 er
syn, 98:2 er

minor increase in d.r.

b Computationally investigated influence of a *tert*-butyl group in *para* position of the substrate on diastereoselectivity

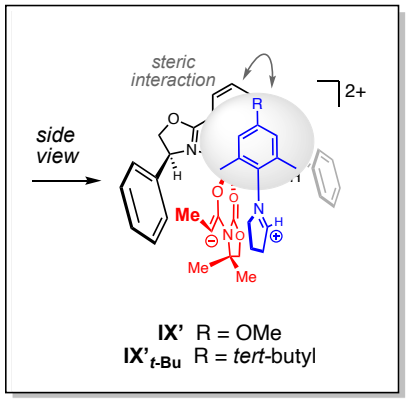

IX' R = OMe
IX'$_{t\text{-Bu}}$ R = *tert*-butyl

Carbon atoms used to determine the C^1- C^2 distance:

C^1 carbon atom on oxazole ring between O and N

C^2 carbon atom in para position of the aryl group on the substrate

a structure of **IX'** (R = OMe)

front view

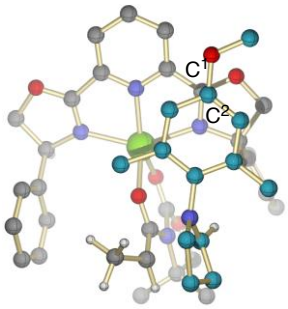

side view

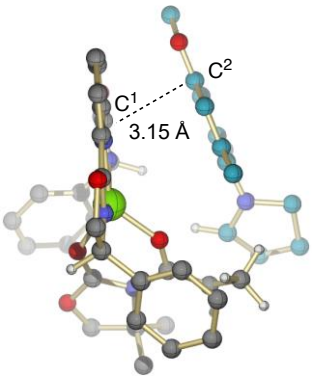

energy relative to **XI**
ΔE: - 2.0 kcal/mol
ΔG: 1.0 kcal/mol

b structure of **IX'$_{t\text{-Bu}}$** (R = *tert*-butyl)

front view

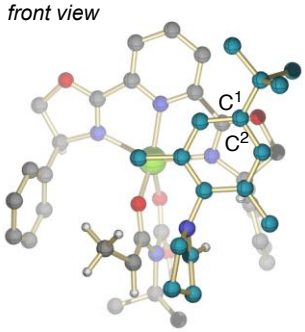

side view

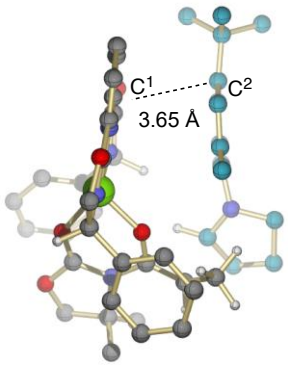

energy relative to **XI$_{t\text{-Bu}}$**
ΔE: 0.8 kcal/mol
ΔG: 3.8 kcal/mol

Figure S3. Influence of the para-substituent on the substrate on the relative energy between **IX'** and **XI**; electronic and free energies have been assessed at the M06L/DF-def2-TZVPP$_{DCM(SMD)}$//M06L/DF-def2-SVP$_{DCM(IEFPCM)}$ level of theory; the C–C distance between the electrophilic carbon on the iminium and the nucleophilic carbon on the enolate has been constrained to 2.3 Å.

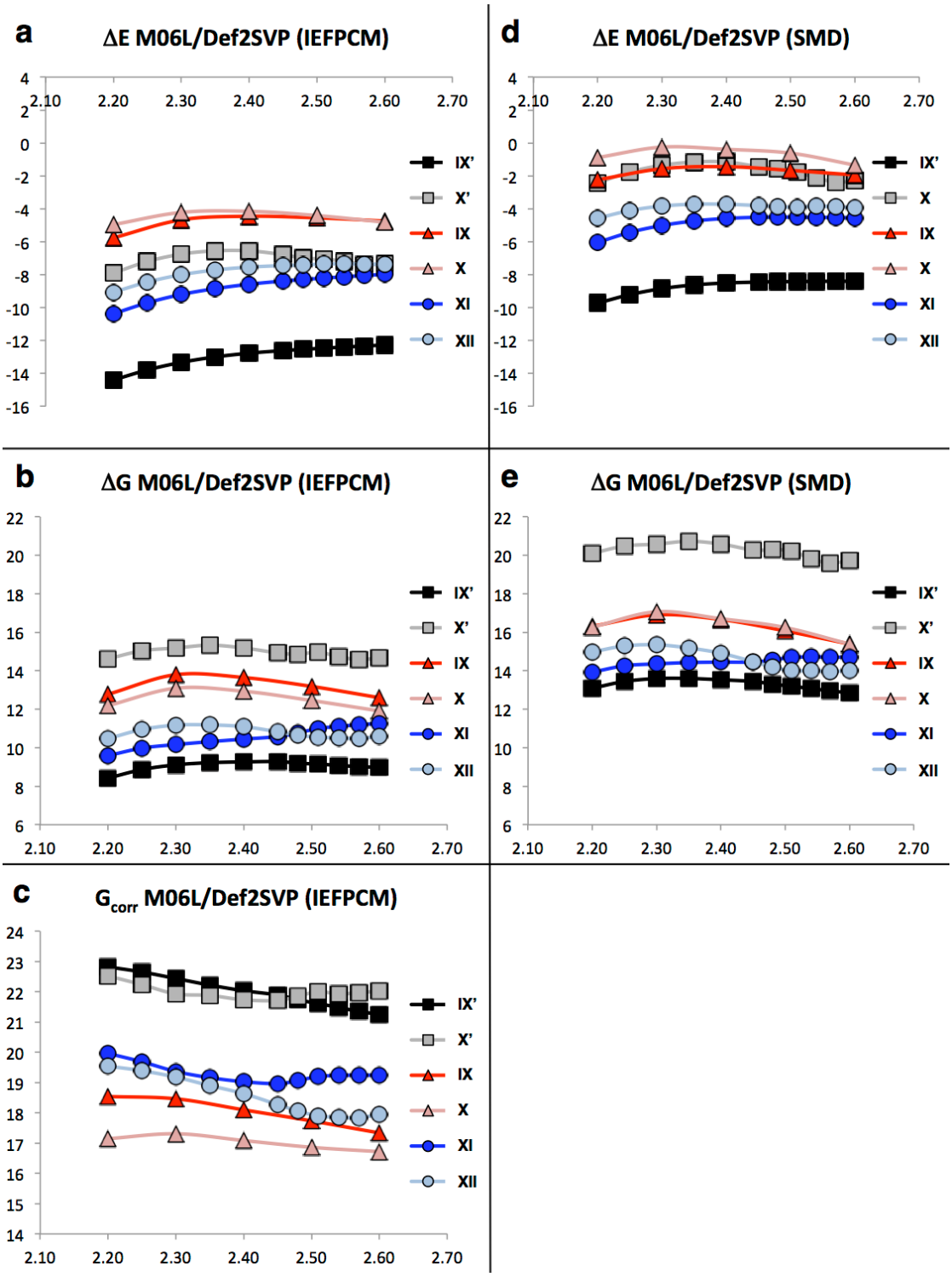

Figure S4. (a) Electronic energies (ΔE), **(b)** free energies (ΔG) and **(c)** thermal corrections to the free energy (G_{corr}) at the level of optimization [M06L/DF-def2-$SVP_{DCM(IEFPCM)}$] as a function of the C–C distance [Å] and **(d,e)** single point energies with the SMD solvation model [M06L/DF-def2-$SVP_{DCM(SMD)}$]; $\Delta G = \Delta E + G_{corr}$.

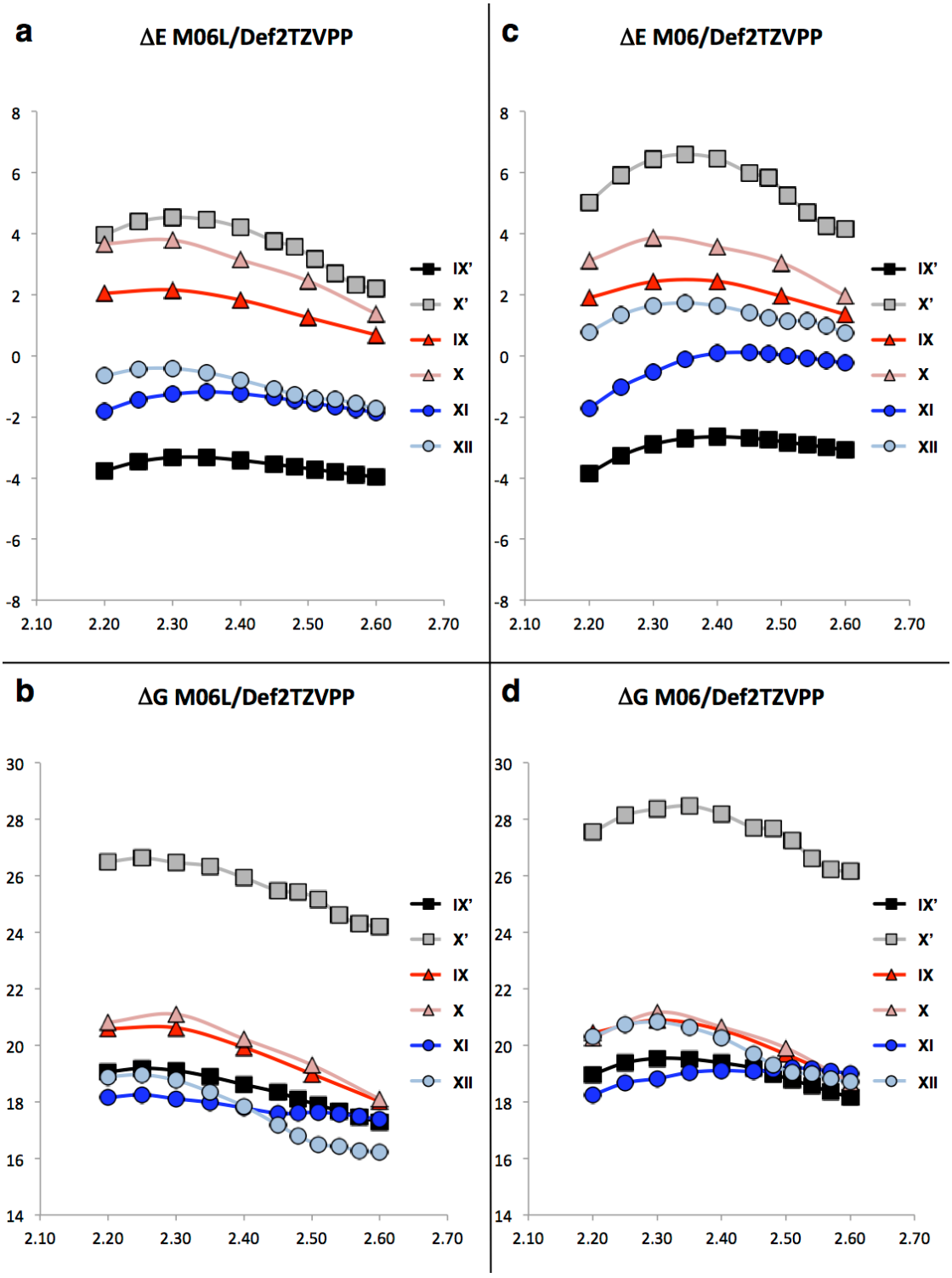

Figure S5. (a,b) Single point electronic energies (ΔE) and free energies (ΔG) at the M06L/DF-def2-TZVPP$_{DCM(SMD)}$ level as a function of the C–C distance [Å]; **(c,d)** single point electronic energies (ΔE) and free energies (ΔG) at the M06/def2-TZVPP$_{DCM(SMD)}$ level as a function of the C–C distance [Å]; $\Delta G = \Delta E + G_{corr}$.

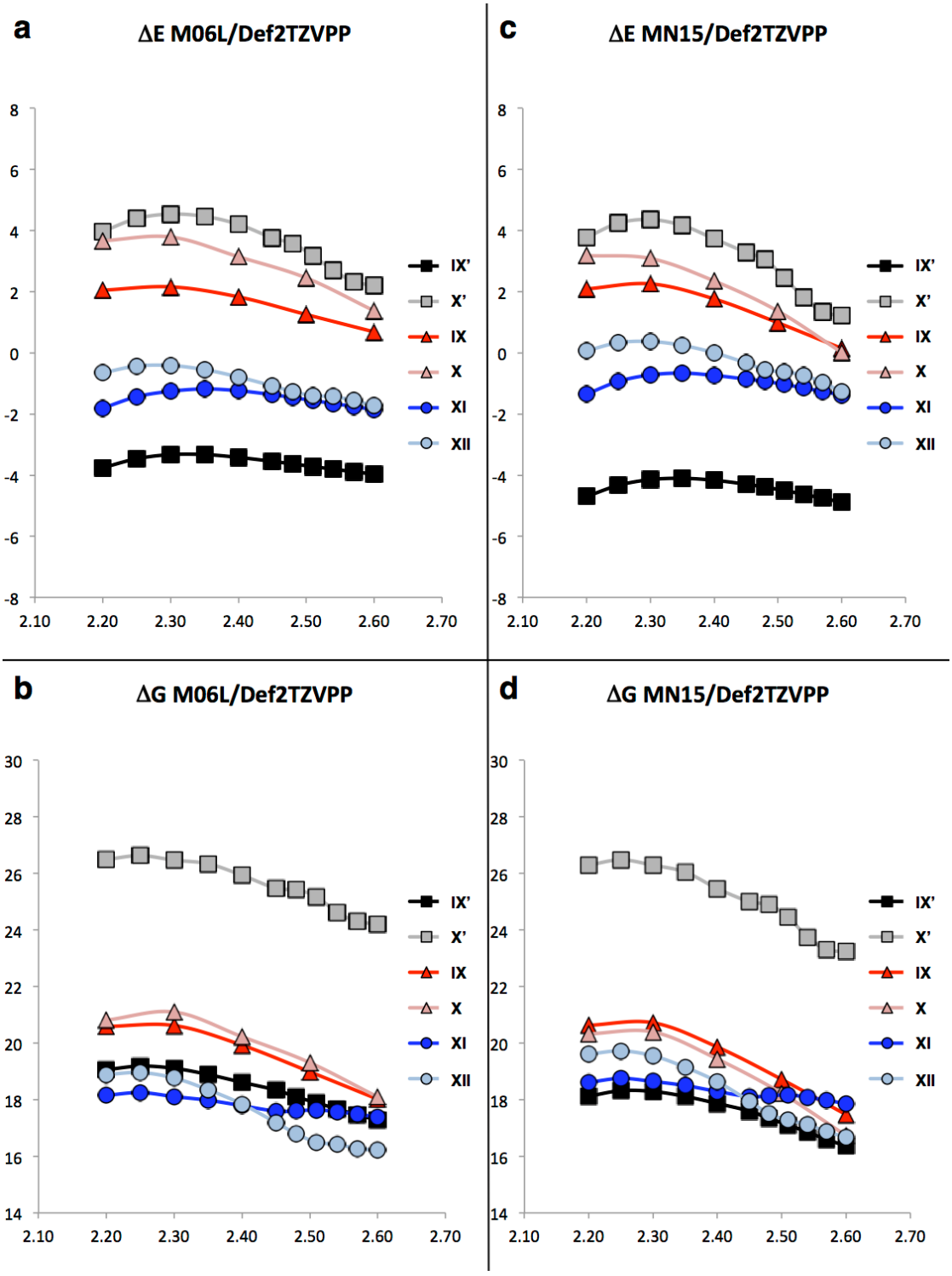

Figure S6. (a,b) Single point electronic energies (ΔE) and free energies (ΔG) at the M06L/DF-def2-TZVPP$_{DCM(SMD)}$ level as a function of the C–C distance [Å]; **(c,d)** single point electronic energies (ΔE) and free energies (ΔG) at the MN15/def2-TZVPP$_{DCM(SMD)}$ level as a function of the C–C distance [Å]; $\Delta G = \Delta E + G_{corr}$.

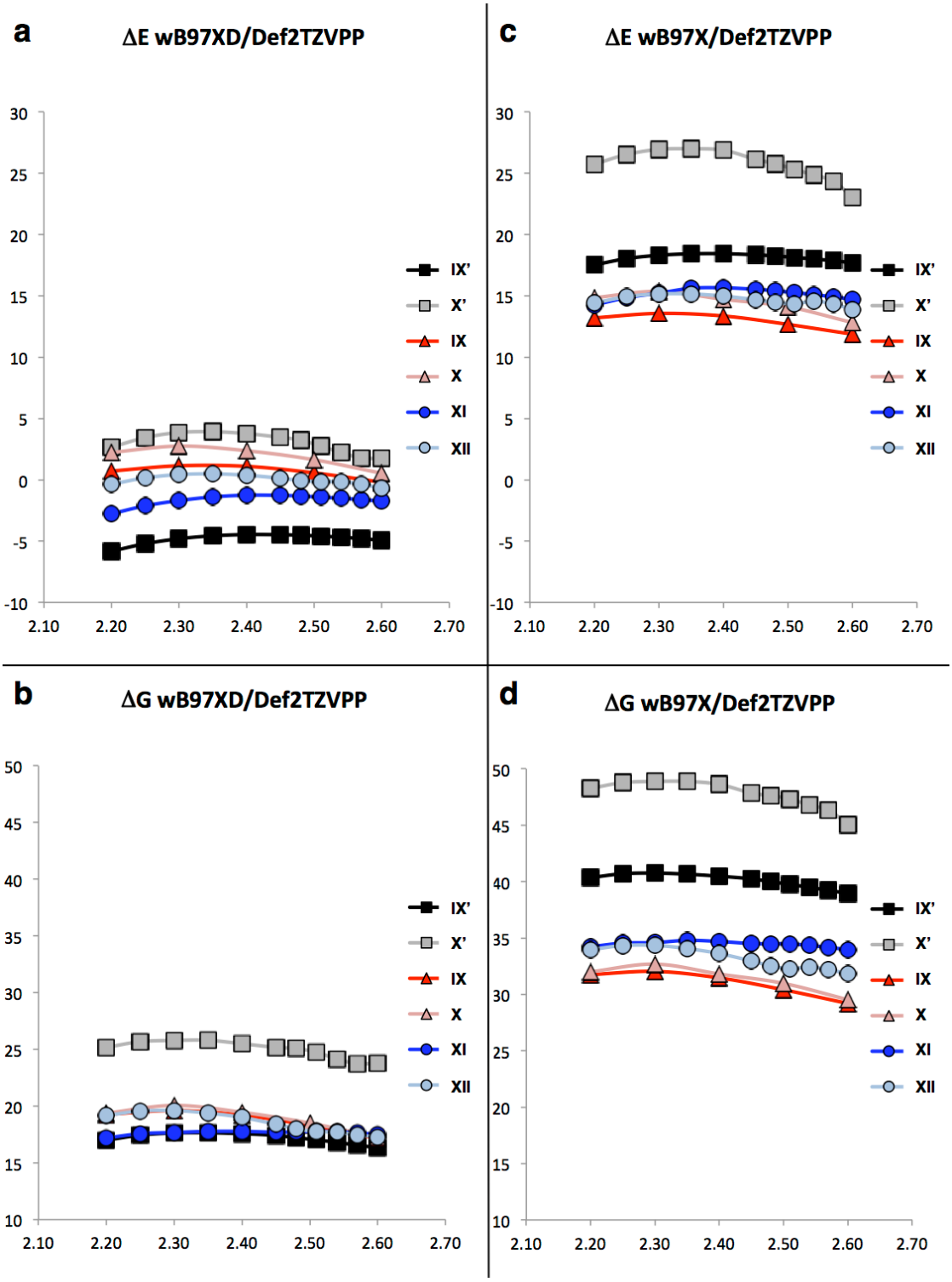

Figure S7. (a,b) Single point electronic energies (ΔE) and free energies (ΔG) at the ωB97XD/DF-def2-TZVPP$_{DCM(SMD)}$ level as a function of the C–C distance [Å]; **(c,d)** single point electronic energies (ΔE) and free energies (ΔG) at the ωB97X/def2-TZVPP$_{DCM(SMD)}$ level as a function of the C–C distance [Å]; $\Delta G = \Delta E + G_{corr}$.

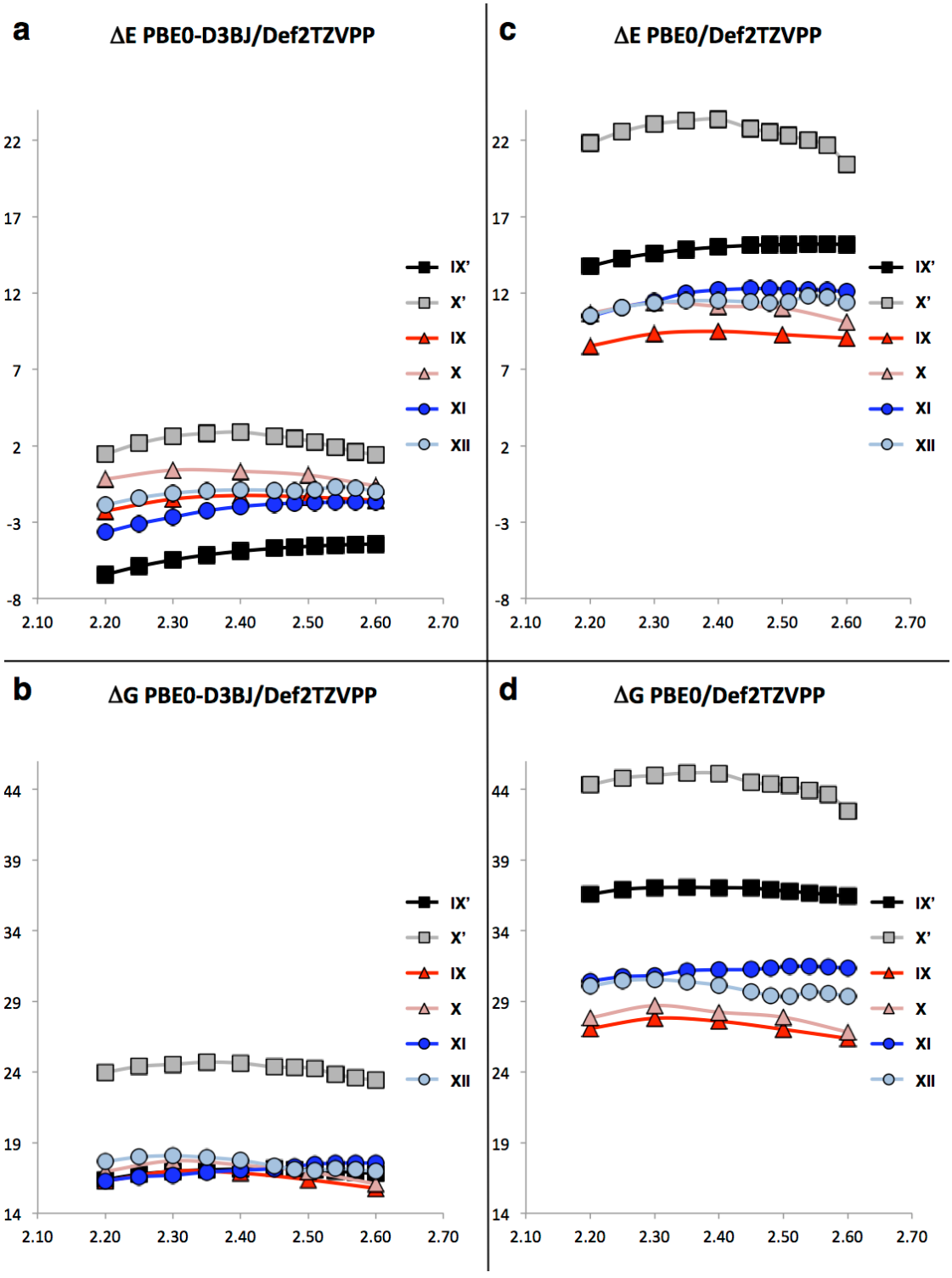

Figure S8. (a,b) Single point electronic energies (ΔE) and free energies (ΔG) at the PBE0-D3BJ/DF-def2-TZVPP$_{DCM(SMD)}$ level as a function of the C–C distance [Å]; **(c,d)** single point electronic energies (ΔE) and free energies (ΔG) at the PBE0/def2-TZVPP$_{DCM(SMD)}$ level as a function of the C–C distance [Å]; $\Delta G = \Delta E + G_{corr}$.

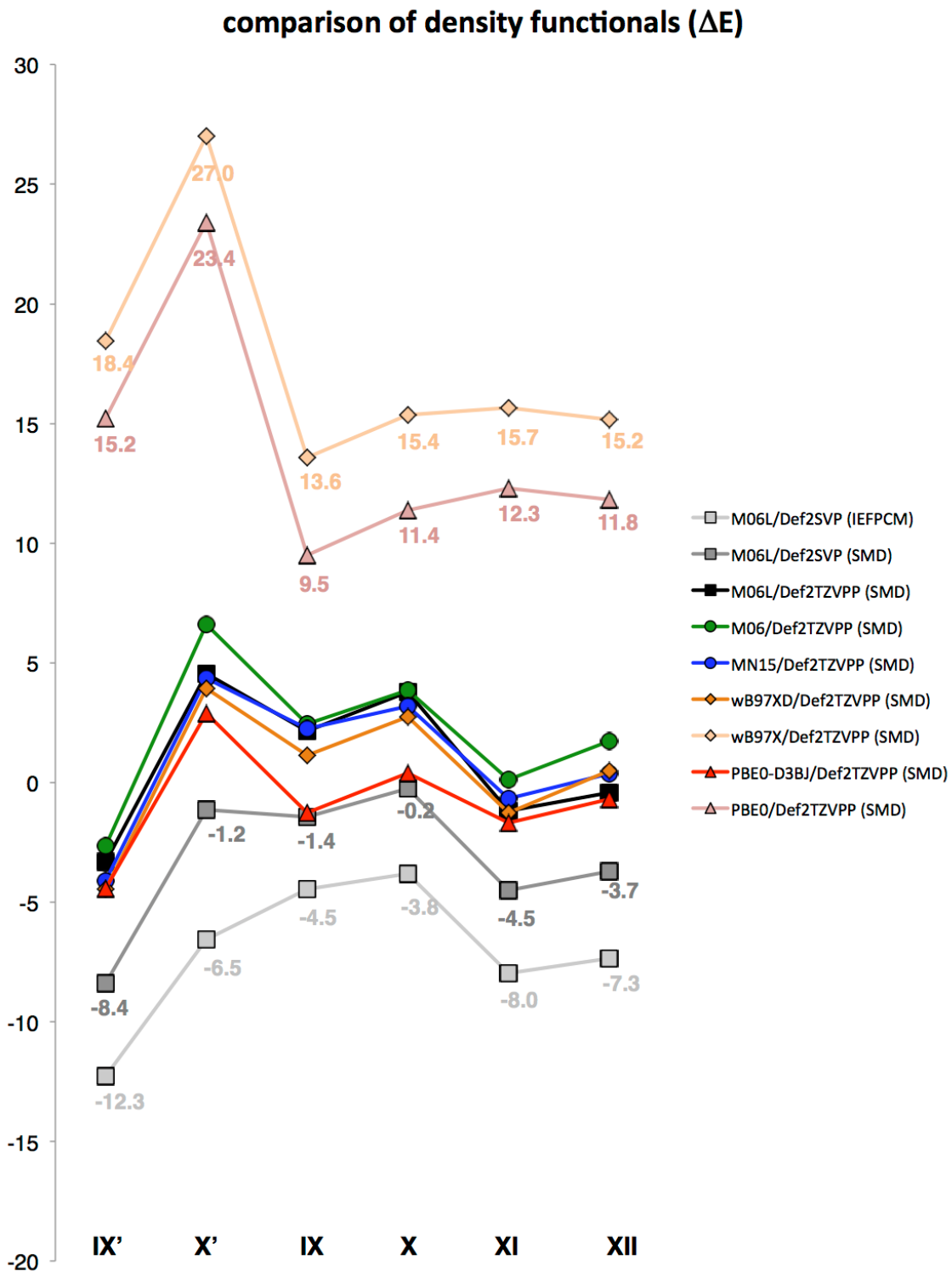

Figure S9. Comparison of electronic energies (ΔE in kcal/mol) for **IX'–XII** obtained with several density functionals; the maximum values from the corresponding graphs in Figures S4–S8 have been used.

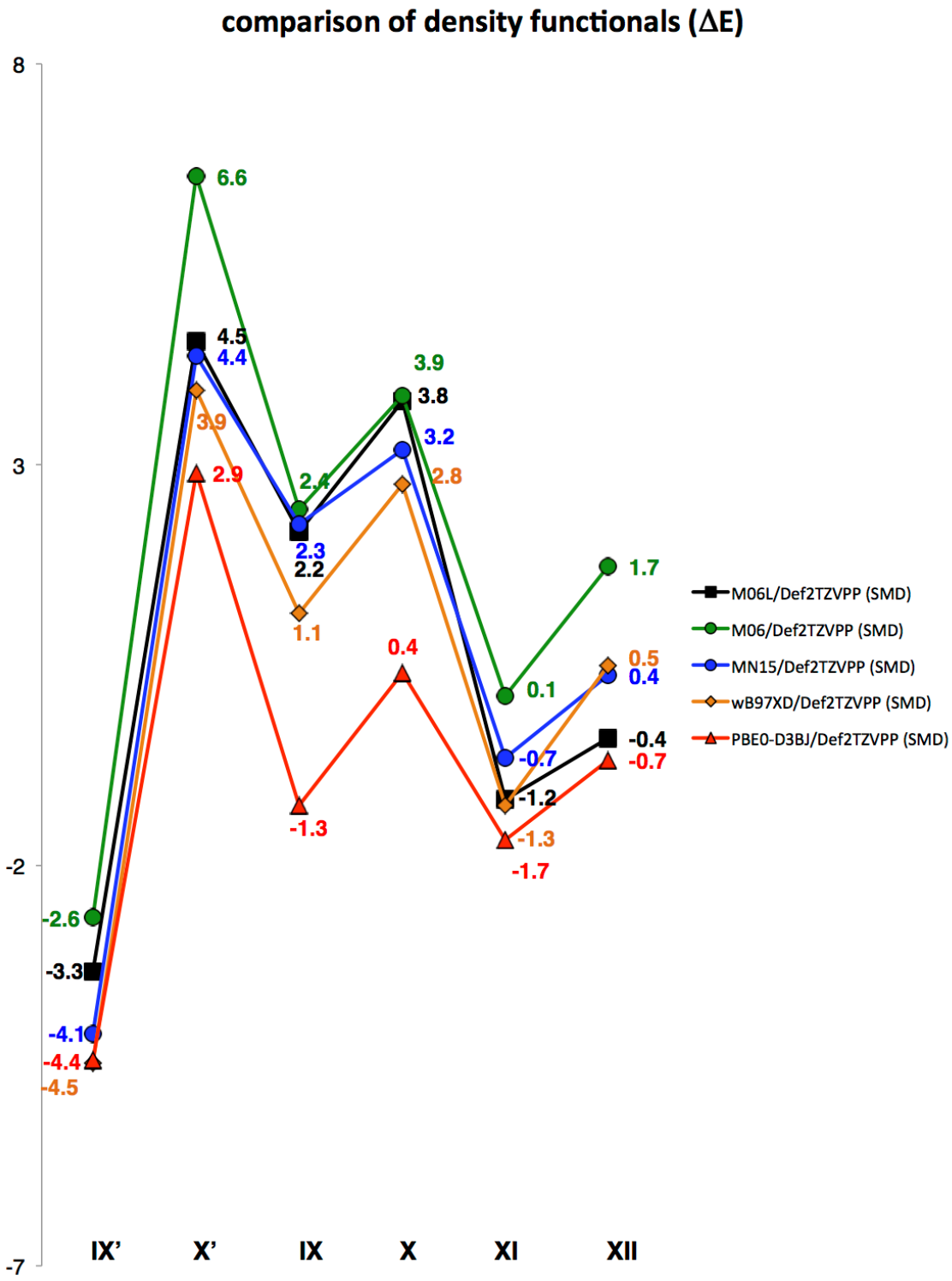

Figure S10. Comparison of electronic energies (ΔE in kcal/mol) for **IX'–XII** obtained with several density functionals; expansion of the energy range between –7 and 8 kcal/mol in Figure S9.

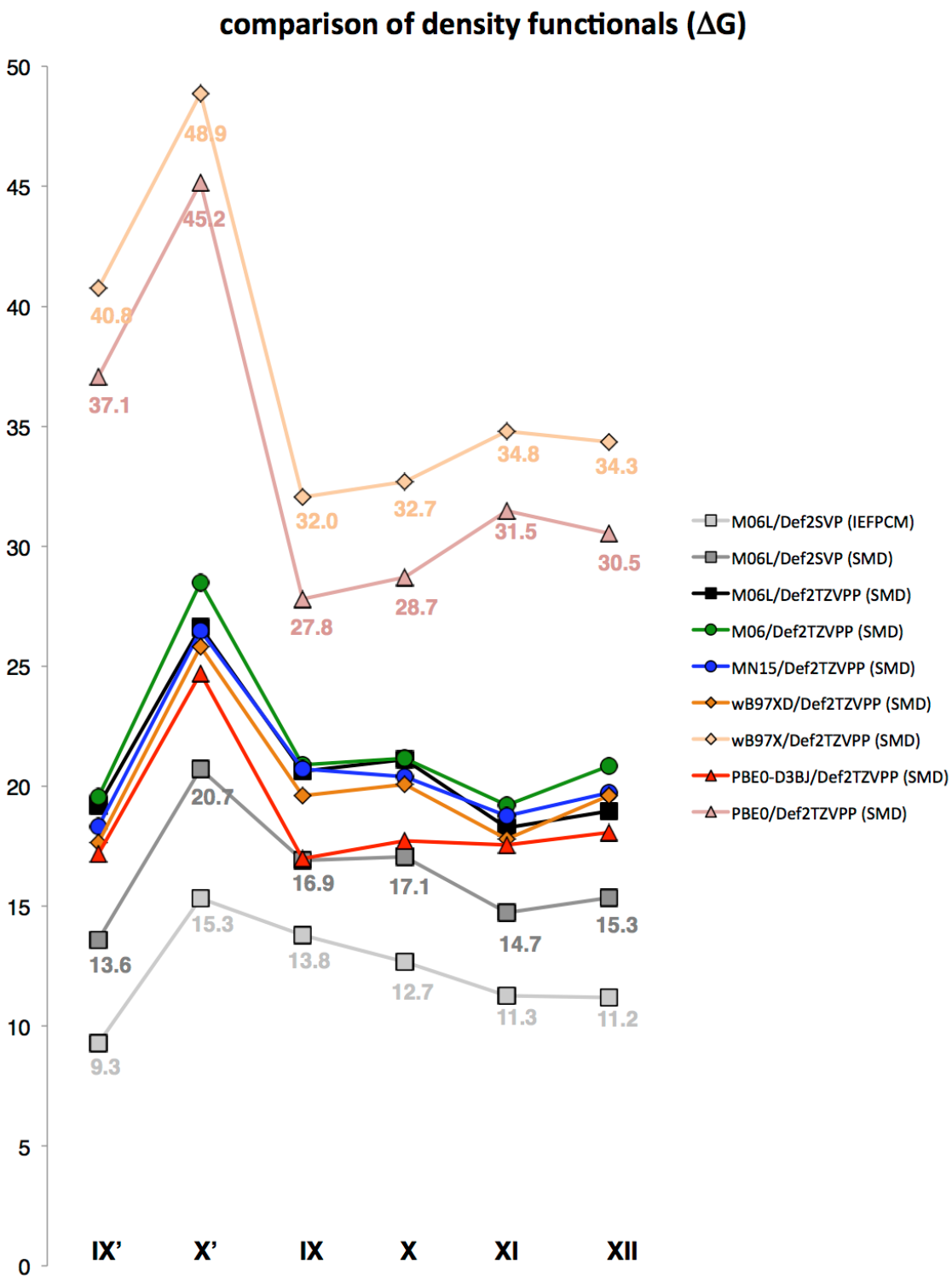

Figure S11. Comparison of free energies (ΔG in kcal/mol) for **IX'–XII** obtained with several density functionals; the maximum values from the corresponding graphs in Figures S4–S8 have been used.

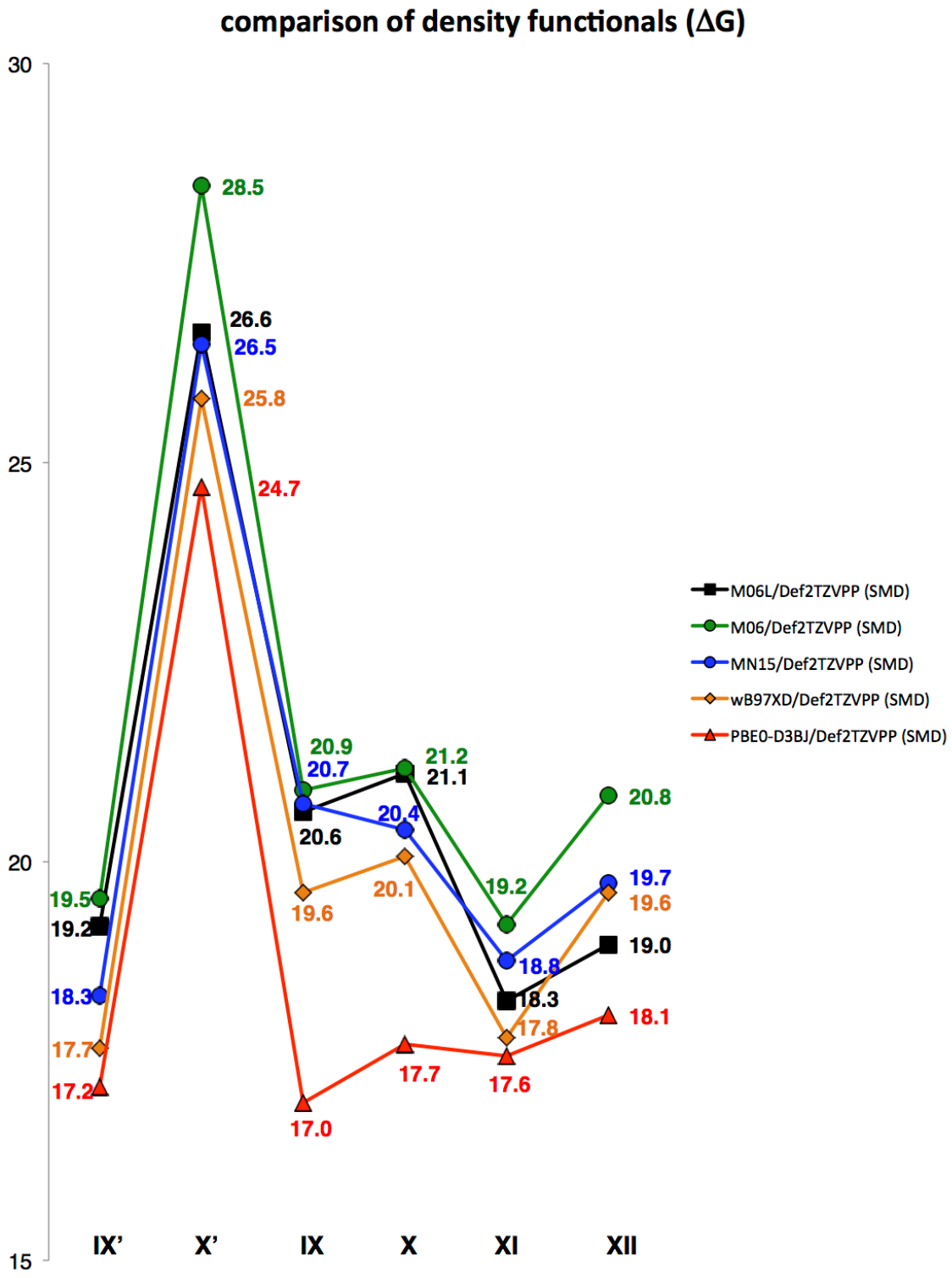

Figure S12. Comparison of free energies (ΔG in kcal/mol) for **IX'–XII** obtained with several density functionals; expansion of the energy range between 15 and 30 kcal/mol in Figure S11.

A5. Analytical Data

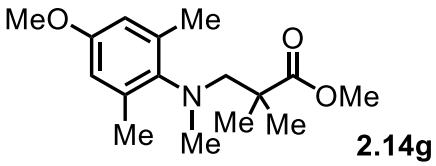

2.14g

Methyl 3-((4-methoxy-2,6-dimethylphenyl)(methyl)amino)-2,2-dimethylpropanoate (2.14g)

Substrate **2.13g** was reacted with ((1-methoxy-2-methylprop-1-en-1-yl)oxy)trimethylsilane **2.11a** following the general procedure using benzene as the solvent and 5 mol% $B(C_6F_5)_3$. After purification by column chromatography (3% ethyl ether in hexanes), **2.14g** was obtained as a colorless liquid (44.7 mg, 80%). **^{1}H NMR** (600 MHz, $CDCl_3$) δ 6.53 (s, 2H), 3.73 (s, 3H), 3.52 (s, 3H), 3.17 (s, 2H), 2.69 (s, 3H), 2.26 (s, 6H), 1.16 (s, 6H); **^{13}C NMR** (151 MHz, $CDCl_3$) δ 178.1, 156.2, 144.2, 137.5, 113.7, 67.2, 55.2, 51.4, 45.3, 43.9, 23.7, 19.3; **IR** (neat) ν 2948, 2837, 2790, 1729, 1602, 1484, 1468, 1433, 1286, 1192, 1154, 1140, 1063, 983, 855 cm^{-1}; **HRMS** (DART) Calcd for $C_{16}H_{26}NO_3$ (MH^+): 280.1913; found: 280.1902.

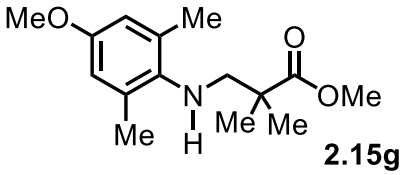

2.15g

Methyl 3-((4-methoxy-2,6-dimethylphenyl)amino)-2,2-dimethylpropanoate (2.15g)

^{1}H NMR (400 MHz, $CDCl_3$) δ 6.45 (s, 2H), 4.39 (s, 1H), 3.52 (s, 3H), 3.16 (s, 2H), 2.69 (s, 3H), 2.23 (s, 6H), 1.16 (s, 6H); **^{13}C NMR** (126 MHz, $CDCl_3$) δ 178.2, 152.1, 144.2, 137.8, 115.1, 67.2, 51.4, 45.4, 43.9, 23.7, 19.1; **IR** (neat) ν 3402, 2949, 2927, 2792, 1707, 1609, 1592, 1467, 1390, 1289, 1239, 1196, 1163, 1095, 1026, 856 cm^{-1}; **HRMS** (DART) Calcd for $C_{15}H_{24}NO_3$ (MH^+): 266.1756; found: 266.1744.

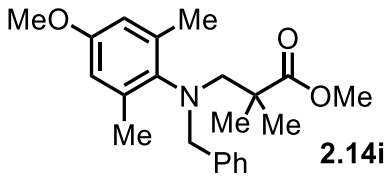

2.14i

Methyl 3-(benzyl(4-methoxy-2,6-dimethylphenyl)amino)-2,2-dimethylpropanoate (2.14i)

Substrate **2.13i** was reacted with ((1-methoxy-2-methylprop-1-en-1-yl)oxy)trimethylsilane **2.11a** following the general procedure using benzene as the solvent. After purification by column chromatography (2% ethyl ether in hexanes), **2.14i** was obtained as a colorless liquid (45.5 mg, 64%). **^{1}H NMR** (500 MHz, $CDCl_3$) δ 7.23 – 7.19 (m, 3H), 7.06 – 7.00 (m, 2H), 6.48 (s, 2H), 4.00 (s, 2H), 3.73 (s, 3H), 3.42 (s, 3H), 3.25 (s, 2H), 2.05 (s, 6H), 1.12 (s, 6H); **^{13}C NMR** (126 MHz, $CDCl_3$) δ 177.9, 156.1, 141.1, 138.7, 138.1, 129.9, 127.9, 127.0, 113.8, 63.3, 60.4, 55.1, 51.3, 44.9, 23.9, 19.8; **IR** (neat) ν 3027, 2948, 2837, 1732, 1602, 1470, 1455, 1314, 1261, 1194, 1152, 1069, 861, 701 cm^{-1}; **HRMS** (DART) Calcd for $C_{22}H_{30}NO_3$ (MH^+): 356.2226; found: 356.2238.

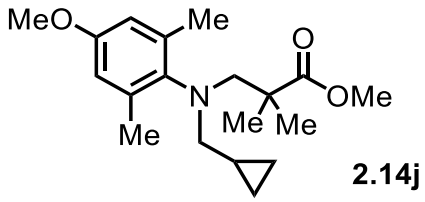

2.14j

Methyl 3-((cyclopropylmethyl)(4-methoxy-2,6-dimethylphenyl)amino)-2,2-dimethylpropanoate (2.14j)

Substrate **2.13j** was reacted with ((1-methoxy-2-methylprop-1-en-1-yl)oxy)trimethylsilane **2.11a** following the general procedure using benzene as the solvent. After purification by column chromatography (3% ethyl ether in hexanes), **2.14j** was obtained as a colorless liquid (35.8 mg, 56%). **^{1}H NMR** (600 MHz, $CDCl_3$) δ 6.52 (s, 2H), 3.73 (s, 3H), 3.42 (s, 3H), 3.27 (s, 2H), 2.79 (d, J = 6.9 Hz, 2H), 2.31 (s, 6H), 1.15 (s, 6H), 0.85 – 0.77 (m, 1H), 0.35 – 0.31 (m, 2H), -0.06 – -0.10 (m, 2H); **^{13}C NMR** (151 MHz, $CDCl_3$) δ 178.0, 156.1, 142.2, 138.1, 113.7, 65.1, 62.0, 55.1, 51.3, 45.1, 23.8, 23.7, 19.9, 10.5, 3.7; **IR** (neat) ν 2947, 2837, 1730, 1602, 1468, 1389, 1314, 1259, 1192, 1153, 1069, 855 cm^{-1}; **HRMS** (DART) Calcd for $C_{19}H_{30}NO_3$ (MH^+): 320.2226; found: 320.2236.

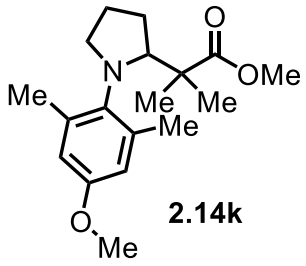

2.14k

Methyl 2-(1-(4-methoxy-2,6-dimethylphenyl)pyrrolidin-2-yl)-2-methylpropanoate (2.14k)

Substrate **2.13k** was reacted with ((1-methoxy-2-methylprop-1-en-1-yl)oxy)trimethylsilane **2.11a** following the general procedure, using THF as the solvent. After purification by column chromatography (5% ethyl ether in hexanes) **2.14k** was obtained as a colorless liquid (55.0 mg, 90%). **^{1}H NMR** (600 MHz, $CDCl_3$) δ 6.56 – 6.51 (m, 2H), 4.05 (dd, J_1 = 9.4 Hz, J_2 = 2.0 Hz, 1H), 3.73 (s, 3H), 3.30 – 3.28 (m, 1H), 3.07 (s, 3H), 2.92 – 2.88 (m, 1H), 2.29 (s, 3H), 2.25 (s, 3H), 2.13 – 2.05 (m, 1H), 1.91 – 1.81 (m, 3H), 1.11 (s, 3H), 1.08 (s, 3H); **^{13}C NMR** (151 MHz, $CDCl_3$) δ 177.8, 156.1, 139.9, 139.8, 136.8, 114.6, 112.9, 66.8, 55.1, 54.5, 50.9, 47.7, 27.6, 25.6, 23.2, 19.7, 19.6, 19.4; **IR** (neat) ν 2948, 2836, 1732, 1603, 1466, 1315, 1253, 1192, 1129, 1070, 839 cm^{-1}; **HRMS** (DART) Calcd for $C_{18}H_{28}NO_3$ (MH^+): 306.2069; found: 306.2067.

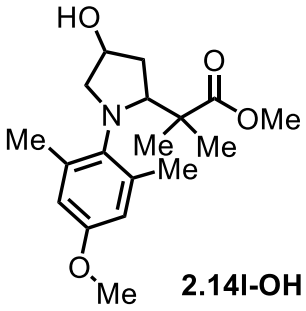

2.14l-OH

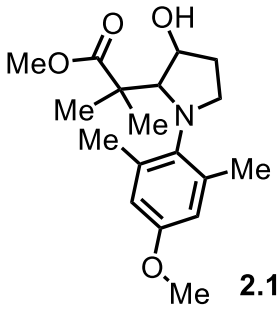

2.14m-OH

Methyl 2-(hydroxy-1-(4-methoxy-2,6-dimethylphenyl)pyrrolidin-2-yl)-2-methylpropanoate (2.14l-OH, 2.14m-OH)

Substrate **2.13l** was reacted with ((1-methoxy-2-methylprop-1-en-1-yl)oxy)trimethylsilane **2.11a** following the general procedure using THF as the solvent. ^{1}H NMR analysis of the unpurified reaction mixture revealed that **2.14l** and **2.14m** were obtained in the ratio of 2.5:1. The diastereomeric ratio (dr) of **2.14l** was 4:1 and the dr of **2.14m** was >20:1. After purification by column chromatography (3% ethyl ether in hexanes), **2.14l** and **2.14m** were separated to give pure **2.14l** (24.2 mg, 31% yield) and **2.14m** (18.3 mg, 23% yield). The isolated and purified products were treated with 4.0 N HCl for 24 hours to give the desilylated products that are characterized as below. The relative configuration of the pyrrolidine substituents for **2.14l-OH** and **2.14m-OH** was assigned *anti* based on NOESY experiments (See SI Section 5 for NOE spectra).

Major regioisomer (2.14l-OH): ^{1}H NMR (500 MHz, $CDCl_3$) δ 6.57 – 6.48 (m, 2H), 4.55 – 4.35 (m, 1H), 4.34 – 4.05 (m, 1H), 3.77 – 3.68 (m, 3H), 3.64 – 3.57 (m, 1H), 3.28 – 3.01 (m, 3H), 2.88 – 2.80 (m, 1H), 2.40 – 2.19 (m, 6H), 2.14 – 1.93 (m, 2H), 1.70 – 1.54 (m, 1H), 1.13 – 0.93 (m, 6H); **^{13}C NMR** (126 MHz, $CDCl_3$) δ 177.8, 177.3, 156.5, 156.3, 139.9, 139.6, 138.4, 138.4, 137.3, 136.9, 114.9, 114.7, 113.2, 113.0, 70.7, 70.5, 66.8, 65.9, 63.3, 62.0, 55.2, 51.4, 51.1, 46.9, 46.7, 36.7, 36.6, 24.2, 23.5, 21.0, 20.0, 19.50, 19.46; **IR** (neat) ν 3418, 2947, 2837, 1730, 1602, 1469, 1315, 1267, 1193, 1134, 1069, 990, 854 cm^{-1}; **HRMS** (DART) Calcd for $C_{18}H_{28}NO_4$ (MH^+): 322.2018; found: 322.2024.

Minor regioisomer (2.14m-OH): ^{1}**H NMR** (500 MHz, $CDCl_3$) δ 6.57 – 6.49 (m, 2H), 4.31 (d, *J* = 5.1 Hz, 1H), 4.05 (s, 1H), 3.73 (s, 3H), 3.32 – 3.20 (m, 2H), 3.14 (s, 3H), 2.40 (s, 3H), 2.29 (s, 3H), 2.06 – 1.97 (m, 1H), 1.81 (dd, *J* = 13.2, 5.5 Hz, 1H), 1.69 (br, 1H), 1.18 (s, 3H), 1.05 (s, 3H); ^{13}**C NMR** (151 MHz, $CDCl_3$) δ177.4, 156.3, 139.8, 138.1, 137.4, 114.7, 113.1, 75.8, 75.3, 55.2, 52.2, 51.2, 46.1, 34.0, 22.6, 20.8, 19.7, 19.5; **IR** (neat) ν 3485, 2948, 2835, 1732, 1603, 1469, 1314, 1256, 1192, 1154, 1131, 1071, 991, 856 cm^{-1}; **HRMS** (DART) Calcd for $C_{18}H_{28}NO_4$ (MH^+): 322.2018; found: 322.2016.

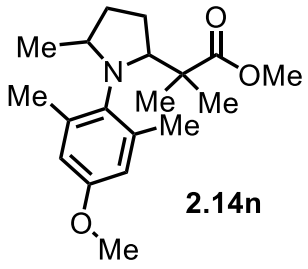

2.14n

Methyl 2-(-1-(4-methoxy-2,6-dimethylphenyl)-5-methylpyrrolidin-2-yl)-2-methylpropanoate (2.14n)

Substrate **2.13n** was reacted with ((1-methoxy-2-methylprop-1-en-1-yl)oxy)trimethylsilane **2.11a** following the general procedure, using THF as the solvent. ^{1}H NMR analysis of the crude material revealed that the diastereomeric ratio was 7:1. After purification by column chromatography (4% ethyl ether in hexanes) **2.14n** was obtained as a colorless liquid (44.7 mg, 70%) as a mixture of diastereomers. The relative configuration of the pyrrolidine substituents was assigned *anti* based on NOESY experiments.

^{1}H NMR (500 MHz, $CDCl_3$) δ 6.51 (d, J = 6.1 Hz, 2H), 4.20 – 4.14 (m, 1H), 3.76 – 3.70 (m, 4H), 3.05 (s, 3H), 2.26 (s, 3H), 2.24 (s, 3H), 2.16 – 2.05 (m, 2H), 1.80 – 1.70 (m, 1H), 1.55 – 1.46 (m, 1H), 1.09 (s, 3H), 1.04 (s, 3H), 0.71 (d, J = 6.4 Hz, 3H); **^{13}C NMR** (126 MHz, $CDCl_3$) δ 177.7, 155.6, 139.4, 137.8, 136.8, 113.9, 112.9, 67.3, 57.5, 55.1, 51.0, 47.8, 33.8, 25.5, 23.3, 20.6, 20.0, 19.7, 19.5; **IR** (neat) ν 2956, 2873, 2836, 1731, 1602, 1467, 1371, 1303, 1256, 1192, 1155, 1131, 1070, 854 cm^{-1}; **HRMS** (DART) Calcd for $C_{19}H_{30}NO_3$ (MH^+): 320.2226; found: 320.2236.

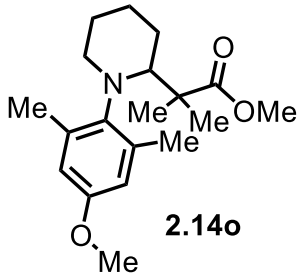

2.14o

Methyl -2-(1-(4-methoxy-2,6-dimethylphenyl)piperidin-2-yl)-2-methylpropanoate (2.14o)

Substrate **2.13o** was reacted with ((1-methoxy-2-methylprop-1-en-1-yl)oxy)trimethylsilane **2.11a** following the general procedure using benzene as the solvent; the reaction mixture was heated at 50 °C. After purification by column chromatography (5% ethyl ether in hexanes), **2.14o** was obtained as a colorless liquid (24.3 mg, 38%). **^{1}H NMR** (600 MHz, $CDCl_3$) δ 6.55 (d, *J* = 3.1 Hz, 1H), 6.44 (d, *J* = 3.1 Hz, 1H), 3.81 – 3.76 (m, 1H), 3.73 (s, 3H), 3.23 (s, 3H), 3.07 – 2.99 (m, 1H), 2.99 – 2.91 (m, 1H), 2.35 (s, 3H), 2.32 (s, 3H), 1.82 – 1.72 (m, 2H), 1.59 – 1.47 (m, 4H), 1.06 (m, 6H); **^{13}C NMR** (151 MHz, $CDCl_3$) δ 177.9, 155.9, 142.4, 138.6, 137.9, 114.5, 113.4, 61.4, 55.1, 52.2, 51.3, 48.3, 26.2, 25.7, 24.4, 22.9, 20.9, 20.6, 19.7; **IR** (neat) ν 2934, 2854, 2836, 1731, 1601, 1466, 1388, 1255, 1233, 1171, 1133, 1069, 917, 854 cm^{-1}; **HRMS** (ESI) Calcd for $C_{19}H_{30}NO_3$ (MH^+): 320.2226; found: 320.2228.

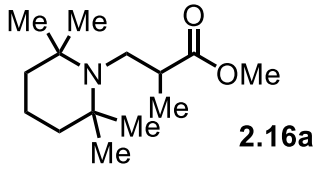

2.16a

Methyl 2-methyl-3-(2,2,6,6-tetramethylpiperidin-1-yl)propanoate (2.16a)

Substrate **2.13p** was reacted with ((1-methoxyprop-1-en-1-yl)oxy)trimethylsilane **2.11b** following the general procedure using THF as the solvent at 70 °C. After purification by column chromatography (2.5% triethylamine in hexanes), **2.16a** was obtained as a colorless liquid (45.8 mg, 95%). **^{1}H NMR** (600 MHz, $CDCl_3$) δ 3.65 (s, 3H), 2.86 (dd, *J* = 15.4, 7.4 Hz, 1H), 2.57 (h, *J* = 7.1 Hz, 1H), 2.45 (dd, *J* = 15.5, 5.4 Hz, 1H), 1.52 (br, 2H), 1.44 – 1.36 (m, 4H), 1.11 (d, *J* = 7.3 Hz, 3H), 1.01 (s, 6H), 0.95 (s, 6H); **^{13}C NMR** (151 MHz, $CDCl_3$) δ 177.8, 54.6, 51.2, 48.9, 44.2, 41.3, 17.8, 16.1; **IR** (neat) ν 2966, 2927, 2874, 1736, 1464, 1434, 1379, 1365, 1256, 1168 cm^{-1}; **HRMS** (ESI) Calcd for $C_{14}H_{28}NO_2$ (MH^+): 242.2042; found: 242.2117.

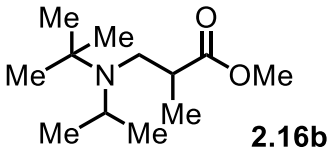

2.16b

Methyl 3-(*tert*-butyl(isopropyl)amino)-2-methylpropanoate (2.16b)

Substrate **2.13q** was reacted with ((1-methoxyprop-1-en-1-yl)oxy)trimethylsilane **2.11b** following the general procedure using THF as the solvent at 70 °C. After purification by column chromatography (2.5% triethylamine in hexanes), **2.16b** was obtained as a colorless liquid (40.1 mg, 93%). **^{1}H NMR** (600 MHz, $CDCl_3$) δ 3.66 (s, 3H), 3.29 – 3.19 (m, 1H), 2.84 (dd, *J* = 14.5, 7.7 Hz, 1H), 2.65 – 2.52 (m, 1H), 2.49 (dd, *J* = 14.4, 6.8 Hz, 1H), 1.10 (d, *J* = 6.9 Hz, 3H), 1.07 (s, 9H), 1.01 (d, *J* = 6.7 Hz, 3H), 0.94 (d, *J* = 6.8 Hz, 3H); **^{13}C NMR** (151 MHz, $CDCl_3$) δ 177.4, 55.6, 51.2, 47.0, 46.6, 43.0, 28.6, 22.7, 15.2; **IR** (neat) ν 2959, 2928, 2864, 2178, 1738, 1707, 1457, 1387, 1376, 1249, 1168, 1138, 1112 cm^{-1}; **HRMS** (ESI) Calcd for $C_{12}H_{26}NO_2$ (MH^+): 216.1885; found: 216.1961.

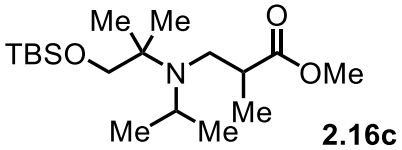

2.16c

Methyl 3-((1-((*tert*-butyldimethylsilyl)oxy)-2-methylpropan-2-yl)(isopropyl)amino)-2-methylpropanoate (2.16c)

Substrate **2.13r** was reacted with ((1-methoxyprop-1-en-1-yl)oxy)trimethylsilane **2.11b** following the general procedure using THF as the solvent at 70 °C. After purification by column chromatography (2% triethylamine in hexanes), **2.16c** was obtained as a colorless liquid (64.9 mg, 94%). **^{1}H NMR** (600 MHz, $CDCl_3$) δ 3.65 (s, 3H), 3.40 – 3.34 (m, 2H), 3.26 (dt, *J* = 12.8, 7.0 Hz, 1H), 2.96 (dd, *J* = 14.6, 7.8 Hz, 1H), 2.65 (dd, *J* = 15.0, 7.2 Hz, 1H), 2.57 (h, *J* = 7.0 Hz, 1H), 1.08 (d, *J* = 7.0 Hz, 3H), 1.05 (s, 6H), 1.02 (d, *J* = 6.8 Hz, 3H), 0.96 (d, *J* = 6.7 Hz, 3H), 0.89 (s, 9H), 0.03 (s, 6H); **^{13}C NMR** (151 MHz, $CDCl_3$) δ 177.3, 69.6, 59.3, 51.1, 47.3, 46.4, 42.9, 25.8, 24.3, 22.8, 18.2, 15.1, -5.6; **IR** (neat) ν 2954, 2929, 2884, 2857, 1737, 1462, 1360, 1250, 1197, 1165, 1086, 835, 774 cm^{-1}; **HRMS** (ESI) Calcd for $C_{18}H_{40}NO_3Si$ (MH^+): 346.2699; found: 346.2778.

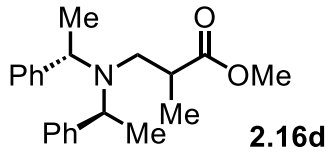

2.16d

Methyl 3-(bis((*S*)-1-phenylethyl)amino)-2-methylpropanoate (2.16d)

Substrate **2.13s** was reacted with ((1-methoxyprop-1-en-1-yl)oxy)trimethylsilane **2.11b** following the general procedure using THF as the solvent at 70 °C. By ^{1}H NMR analysis of the unpurified reaction mixture, the diastereomeric ratio was determined to be 1.6:1. After purification by column chromatography (2% triethylamine in hexanes), **2.16d** was obtained as a colorless liquid (57.3 mg, 88%). Diastereomers were separated chromatographically: **2.16d-(*S,S,R*)** (35.3 mg, 54%) and **2.16d-(*S,S,S*)** (22.0 mg, 34%).[25]

2.16d-(*S*, *S, R*):

^{1}H NMR (500 MHz, $CDCl_3$) δ 7.35 – 7.24 (m, 8H), 7.24 – 7.18 (m, 2H), 3.86 (q, *J* = 6.9 Hz, 2H), 3.68 (s, 3H), 3.06 (ddd, *J* = 13.9, 8.2, 1.4 Hz, 1H), 2.53 – 2.41 (m, 1H), 2.36 (ddd, *J* = 13.8, 6.4, 1.5 Hz, 1H), 1.35 (dd, *J* = 6.9, 1.5 Hz, 6H), 0.87 (dd, *J* = 6.9, 1.5 Hz, 3H); **^{13}C NMR** (151 MHz, $CDCl_3$) δ 176.9, 144.4, 128.0, 127.9, 126.6, 58.4, 51.3, 50.1, 41.4, 18.8, 15.1; **IR** (neat) ν 2969, 2934, 1736, 1452, 1371, 1196, 1177, 1150, 758, 700 cm^{-1}; **HRMS** (ESI) Calcd for $C_{21}H_{28}NO_2$ (MH^+): 326.4240; found: 326.2121; $[\alpha]^{25}_D$ = –33.5° (c = 0.4, EtOH).

2.16d-(*S, S*, *S*):

^{1}H NMR (500 MHz, $CDCl_3$) δ 7.32 – 7.23 (m, 8H), 7.23 – 7.17 (m, 2H), 3.95 (q, *J* = 6.9 Hz, 2H), 3.46 (s, 3H), 2.76 (dd, *J* = 7.5, 2.4 Hz, 2H), 2.59 (q, *J* = 7.1 Hz, 1H), 1.44 – 1.33 (m, 6H), 1.11 (dd, *J* = 6.9, 0.8 Hz, 3H); **^{13}C NMR** (151 MHz, $CDCl_3$) δ 176.3, 144.4, 127.9, 127.9, 126.5, 57.5, 51.3, 49.5, 40.5, 17.8, 15.4; **IR** (neat) ν 2968, 2946, 1735, 1493, 1451, 1196, 1180, 1152, 699 cm^{-}

[1]; **HRMS** (ESI) Calcd for $C_{21}H_{28}NO_2$ (MH^+): 326.4240; found: 326.2120; $[\alpha]^{25}_D = -2.1°$ (c = 0.3, EtOH).

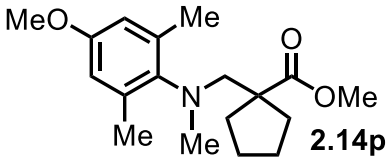

2.14p

Methyl 1-(((4-methoxy-2,6-dimethylphenyl)(methyl)amino)methyl)cyclopentane-1-carboxylate (2.14p)

Substrate **2.13g** was reacted with (cyclopentylidene(methoxy)methoxy)trimethylsilane **2.11c** following the general procedure using benzene as the solvent. After purification by column chromatography (3% ethyl ether in hexanes), **2.14p** was obtained as a colorless liquid (44.6 mg, 73%). **^{1}H NMR** (500 MHz, $CDCl_3$) δ 6.52 (s, 2H), 3.73 (s, 3H), 3.55 (s, 3H), 3.26 (s, 2H), 2.69 (s, 3H), 2.25 (s, 6H), 2.16 – 2.04 (m, 2H), 1.67 – 1.46 (m, 6H); **^{13}C NMR** (151 MHz, $CDCl_3$) δ 178.0, 156.2, 143.8, 137.8, 113.7, 65.1, 56.7, 55.2, 51.4, 43.2, 34.4, 25.0, 19.3; **IR** (neat) ν 2948, 2870, 2837, 2794, 1729, 1602, 1484, 1434, 1272, 1192, 1154, 1063, 854 cm^{-1}; **HRMS** (DART) Calcd for $C_{18}H_{28}NO_3$ (MH^+): 306.2069; found: 306.2076.

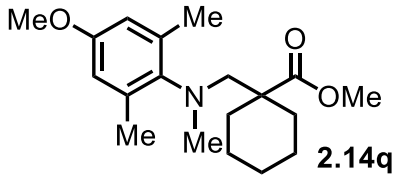

2.14q

Methyl 1-(((4-methoxy-2,6-dimethylphenyl)(methyl)amino)methyl)cyclohexane-1-carboxylate (2.14q)

Substrate **2.13g** was reacted with (cyclohexylidene(methoxy)methoxy)trimethylsilane **2.11d** following the general procedure using benzene as the solvent. After purification by column chromatography (4% ethyl ether in hexanes), **2.14q** was obtained as a colorless liquid (50.5 mg, 79%). **^{1}H NMR** (500 MHz, $CDCl_3$) δ 6.52 (s, 2H), 3.73 (s, 3H), 3.55 (s, 3H), 3.17 (s, 2H), 2.65 (s, 3H), 2.27 (s, 6H), 2.13 – 2.04 (m, 2H), 1.59 – 1.49 (m, 3H), 1.40 – 1.28 (m, 2H), 1.24 – 1.15 (m, 3H); **^{13}C NMR** (126 MHz, $CDCl_3$) δ 176.9, 156.1, 144.4, 137.4, 113.7, 67.7, 55.1, 51.2, 49.9, 43.8, 32.6, 26.0, 23.0, 19.4; **IR** (neat) ν 2934, 2853, 2792, 1730, 1602, 1451, 1372, 1298, 1156, 1133, 1095, 1064, 1035, 988, 854, 832 cm^{-1}; **HRMS** (DART) Calcd for $C_{19}H_{30}NO_3$ (MH^+): 320.2226; found: 320.2221.

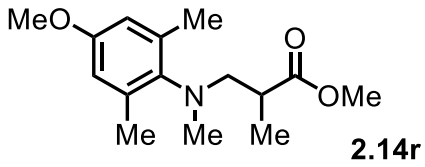

2.14r

Methyl 3-((4-methoxy-2,6-dimethylphenyl)(methyl)amino)-2-methylpropanoate (2.14r)

Substrate **2.13g** was reacted with ((1-methoxyprop-1-en-1-yl)oxy)trimethylsilane **2.11b** following the general procedure using benzene as the solvent. After purification by column chromatography (5% ethyl acetate in hexanes), **2.14r** was obtained as a colorless liquid (35.0 mg, 66%). **^{1}H NMR** (600 MHz, $CDCl_3$) δ 6.52 (s, 2H), 3.74 (s, 3H), 3.65 (s, 3H), 3.32 – 3.25 (m, 1H), 3.07 – 3.00 (m, 1H), 2.74 – 2.65 (m, 4H), 2.25 (s, 3H), 2.21 (s, 3H), 1.13 (d, J = 7.0 Hz, 3H); **^{13}C NMR** (151 MHz, $CDCl_3$) δ 176.7, 156.4, 142.5, 138.3, 138.2, 113.8, 113.6, 60.1, 55.2, 51.5, 41.0, 40.3, 19.4, 19.1, 15.4; **IR** (neat) ν 2949, 2838, 2799, 1736, 1602, 1485, 1458, 1435, 1379, 1304, 1254, 1194, 1155, 1063, 987, 854, 834 cm^{-1}; **HRMS** (DART) Calcd for $C_{15}H_{24}NO_3$ (MH^+): 266.1756; found: 266.1755.

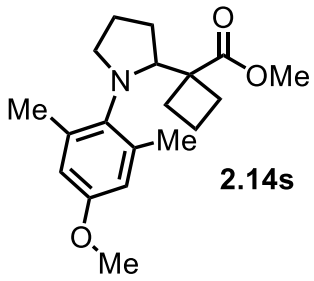

2.14s

Methyl 1-(1-(4-methoxy-2,6-dimethylphenyl)pyrrolidin-2-yl)cyclobutane-1-carboxylate (2.14s)

Substrate **2.13k** was reacted with (cyclobutylidene(methoxy)methoxy)trimethylsilane **2.11e** following the general procedure using THF as the solvent. After purification by column chromatography (5% ethyl ether in hexanes), **2.14s** was obtained as a colorless liquid (48.9 mg, 77%). **^{1}H NMR** (500 MHz, $CDCl_3$) δ 6.56 – 6.50 (m, 2H), 4.07 (dd, J_1 = 8.6 Hz, J_2 = 3.8 Hz, 1H), 3.73 (s, 3H), 3.33 – 3.24 (m, 4H), 2.94 (q, J = 7.8 Hz, 1H), 2.41 – 2.29 (m, 1H), 2.26 (s, 3H), 2.24 (s, 3H), 2.21 – 1.98 (m, 5H), 1.93 – 1.67 (m, 4H); **^{13}C NMR** (151 MHz, $CDCl_3$) δ 177.2, 156.4, 140.8, 139.0, 137.4, 114.4, 112.8, 64.8, 55.1, 54.1, 52.4, 51.3, 28.4, 28.1, 25.6, 25.2, 19.5, 19.0, 15.7; **IR** (neat) ν 2947, 2836, 1727, 1602, 1481, 1464, 1434, 1316, 1266, 1209, 1193, 1153, 1116, 1069, 854 cm^{-1}; **HRMS** (DART) Calcd for $C_{19}H_{28}NO_3$ (MH^+): 318.2069; found: 318.2080.

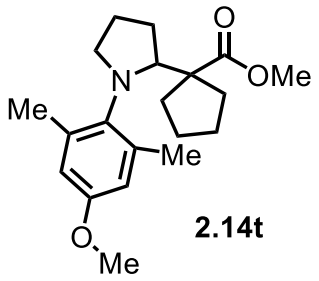

2.14t

Methyl 1-(1-(4-methoxy-2,6-dimethylphenyl)pyrrolidin-2-yl)cyclopentane-1-carboxylate (2.14t)

Substrate **2.13k** was reacted with (cyclopentylidene(methoxy)methoxy)trimethylsilane **2.11c** following the general procedure using THF as the solvent. After purification by column chromatography (5% ethyl ether in hexanes), **2.14t** was obtained as a colorless liquid (66.0 mg, >95%). **^{1}H NMR** (600 MHz, $CDCl_3$) δ 6.58 – 6.50 (m, 2H), 4.13 (dd, J_1 = 9.2 Hz, J_2 = 2.6 Hz, 1H), 3.73 (s, 3H), 3.32 – 3.18 (m, 4H), 2.90 (q, J = 7.4 Hz, 1H), 2.29 (s, 3H), 2.23 (s, 3H), 2.19 – 2.09 (m, 2H), 1.93 – 1.81 (m, 4H), 1.60 – 1.48 (m, 6H); **^{13}C NMR** (151 MHz, $CDCl_3$) δ 177.6, 156.2, 140.2, 139.5, 137.0, 114.5, 112.8, 66.0, 60.5, 55.1, 54.4, 51.2, 34.1, 31.4, 28.8, 25.3, 25.2, 25.1, 19.6, 19.1; **IR** (neat) ν 2947, 2872, 2835, 1726, 1602, 1463, 1433, 1370, 1316, 1255, 1228, 1192, 1151, 1121, 1068, 853, 834 cm^{-1}; **HRMS** (DART) Calcd for $C_{20}H_{30}NO_3$ (MH^+): 332.2226; found: 332.2222.

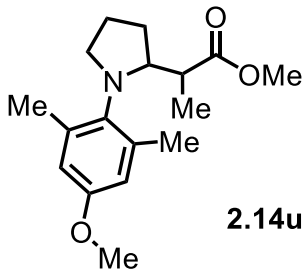

2.14u

Methyl 2-(1-(4-methoxy-2,6-dimethylphenyl)pyrrolidin-2-yl)propanoate (2.14u)

Substrate **2.13k** was reacted with ((1-methoxyprop-1-en-1-yl)oxy)trimethylsilane **2.11b** following the general procedure using THF as the solvent. ^{1}H NMR analysis of the unpurified reaction mixture revealed that the diastereomeric ratio was 2.5:1. After purification by column chromatography (5% ethyl ether in hexanes), **2.14u** was obtained as a colorless liquid (34.9 mg, 60%) as a mixture of diastereomers. The diastereomers were isolated by PTLC (10% ether in hexanes): major diastereomer (16.0 mg, 27% yield), minor diastereomer (12.2 mg, 21% yield).[25]

2.14u-major: ^{1}H NMR (400 MHz, $CDCl_3$) δ 6.59 – 6.50 (m, 2H), 3.92 – 3.84 (m, 1H), 3.74 (s, 3H), 3.34 – 3.24 (m, 4H), 3.02 – 2.94 (m, 1H), 2.40 – 2.31 (m, 1H), 2.27 (s, 3H), 2.24 (s, 3H), 2.12 – 2.02 (m, 1H), 1.97 – 1.86 (m, 2H), 1.82 – 1.72 (m, 1H), 1.11 (d, J = 7.0 Hz, 3H); **^{13}C NMR** (151 MHz, $CDCl_3$) δ 176.1, 156.6, 140.7, 138.5, 137.4, 114.4, 112.9, 62.7, 55.2, 52.7, 51.1, 45.2, 29.0, 25.0, 19.5, 19.2, 13.5; **IR** (neat) ν 2948, 2838, 1733, 1602, 1484, 1465, 1374, 1318, 1273, 1194, 1154, 1117, 1067, 855 cm^{-1}; **HRMS** (ESI) Calcd for $C_{17}H_{26}NO_3$ (MH^+): 292.1912; found: 292.1908.

2.14u-minor: ^{1}H NMR (500 MHz, $CDCl_3$) δ 6.59 – 6.52 (m, 2H), 3.87 – 3.81 (m, 1H), 3.74 (s, 3H), 3.44 (s, 3H), 3.30 – 3.24 (m, 1H), 2.96 – 2.88 (m, 1H), 2.49 – 2.41 (m, 1H), 2.29 (s, 3H), 2.23 (s, 3H), 2.17 – 2.08 (m, 1H), 1.96 – 1.84 (m, 3H), 1.01 (d, J = 7.0 Hz, 3H); **^{13}C NMR** (151 MHz,

$CDCl_3$) δ 175.9, 156.4, 140.3, 138.8, 137.2, 114.5, 113.0, 63.6, 55.2, 53.4, 51.1, 45.9, 29.8, 25.1, 19.4, 19.1, 13.8; **HRMS** (ESI) Calcd for $C_{17}H_{26}NO_3$ (MH^+): 292.1912; found: 292.1911.

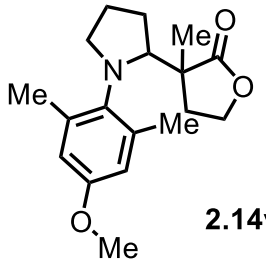

2.14v

3-(1-(4-Methoxy-2,6-dimethylphenyl)pyrrolidin-2-yl)-3-methyldihydrofuran-2(3*H*)-one (2.14v)

Substrate **2.13k** was reacted with trimethyl((3-methyl-4,5-dihydrofuran-2-yl)oxy)silane **2.11f** following the general procedure using THF as the solvent. ^{1}H NMR analysis of the unpurified reaction mixture revealed that the diastereomeric ratio was 1.3:1. After purification by column chromatography (10% ethyl ether in hexanes), **2.14v** was obtained as a colorless liquid (42.8 mg, 70%). Diastereomers were separated chromatographically; major diastereomer (23.9 mg, 39%) and minor diastereomer (18.9 mg, 31%).

2.14v-major: ^{1}H NMR (400 MHz, $CDCl_3$) δ 6.55 (s, 2H), 4.12 – 4.04 (m, 2H), 3.87 (t, J = 6.1 Hz, 1H), 3.74 (s, 3H), 3.39 – 3.31 (m, 1H), 3.00 – 2.91 (m, 1H), 2.38 – 2.27 (m, 4H), 2.25 (s, 3H), 2.20 – 2.13 (m, 2H), 2.00 – 1.88 (m, 2H), 1.78 – 1.69 (m, 1H), 1.26 (s, 3H); **^{13}C NMR** (151 MHz, $CDCl_3$) δ 180.8, 156.5, 139.9, 139.2, 136.5, 114.9, 113.3, 64.7, 64.0, 55.1, 54.5, 48.2, 32.1, 27.6, 25.8, 19.5, 19.3, 19.1; **IR** (neat) ν 2962, 2912, 2836, 1767, 1603, 1482, 1466, 1371, 1317, 1255, 1193, 1154, 1070, 1031, 854 cm^{-1}; **HRMS** (DART) Calcd for $C_{18}H_{26}NO_3$ (MH^+): 304.1913; found: 304.1924.

2.14v-minor: ^{1}H NMR (600 MHz, $CDCl_3$) δ 6.60 – 6.53 (m, 2H), 4.27 – 4.16 (m, 2H), 3.94 (dd, J_1 = 8.8 Hz, J_2 = 3.9 Hz, 1H), 3.75 (s, 3H), 3.37 – 3.32 (m, 1H), 2.99 – 2.93 (m, 1H), 2.55 – 2.48

(m, 1H), 2.30 (s, 3H), 2.29 – 2.22 (m, 4H), 2.00 – 1.89 (m, 3H), 1.79 – 1.73 (m, 1H), 0.94 (s, 3H); **^{13}C NMR** (126 MHz, $CDCl_3$) δ 181.2, 156.5, 140.4, 139.1, 136.4, 114.8, 113.4, 65.5, 65.2, 55.1, 54.7, 48.9, 31.2, 29.5, 25.6, 22.6, 19.8, 19.2; **HRMS** (ESI) Calcd for $C_{18}H_{26}NO_3$ (MH^+): 304.1913; found: 304.1915.

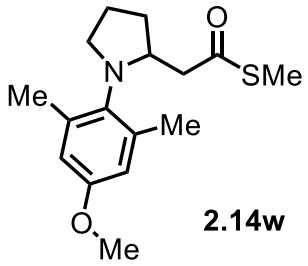

2.14w

***S*-Methyl 2-(1-(4-methoxy-2,6-dimethylphenyl)pyrrolidin-2-yl)ethanethioate (2.14w)**

Substrate **2.13k** was reacted with trimethyl((1-(methylthio)vinyl)oxy)silane **2.11g** following the general procedure using THF as the solvent. After purification by column chromatography (5% ethyl acetate in hexanes), **2.14w** was obtained as a colorless liquid (30.5 mg, 52%). **^{1}H NMR** (400 MHz, $CDCl_3$) δ 6.57 (br, 2H), 3.95 – 3.88 (m, 1H), 3.75 (s, 3H), 3.28 – 3.22 (m, 1H), 3.06 – 2.99 (m, 1H), 2.58 (dd, J_1 = 14.3 Hz, J_2 = 4.4 Hz, 1H), 2.48 (dd, J_1 = 14.3, J_2 = 9.2 Hz, 1H), 2.24 (s, 6H), 2.23 – 2.13 (m, 4H), 2.03 – 1.86 (m, 2H), 1.79 – 1.70 (m, 1H); **^{13}C NMR** (151 MHz, $CDCl_3$) δ 198.4, 156.8, 140.7, 138.9, 136.4, 114.3, 113.0, 58.7, 55.2, 51.4, 50.6, 31.9, 24.5, 19.2, 11.5; **IR** (neat) ν 2953, 2872, 2836, 1685, 1603, 1483, 1370, 1319, 1269, 1193, 1154, 1069, 1018, 855 cm^{-1}; **HRMS** (ESI) Calcd for $C_{16}H_{24}NO_2S$ (MH^+): 294.1527; found: 294.1530.

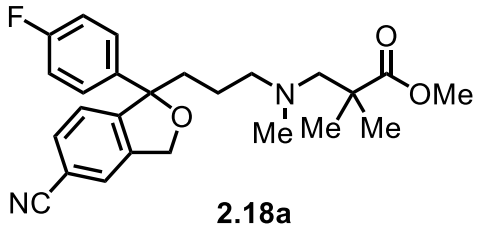

2.18a

Methyl 3-((3-(5-cyano-1-(4-fluorophenyl)-1,3-dihydroisobenzofuran-1-yl)propyl) (methyl)amino)-2,2-dimethylpropanoate (2.18a)

Substrate **2.17a** was reacted with ((1-methoxy-2-methylprop-1-en-1-yl)oxy)trimethylsilane **2.11a** following the general procedure on a 3.0 mmol scale using benzene as the solvent at 70 °C. After purification by column chromatography (20% ethyl acetate in hexanes), **2.18a** was obtained as a colorless liquid (301.9 mg, 23%).

^{1}H NMR (500 MHz, $CDCl_3$) δ 7.63 – 7.56 (m, 1H), 7.50 (s, 1H), 7.46 – 7.34 (m, 3H), 7.01 (t, J = 8.7 Hz, 2H), 5.17 (q, J = 12.9 Hz, 2H), 3.59 (s, 3H), 2.44 (s, 2H), 2.34 (t, J = 7.0 Hz, 2H), 2.18 (ddd, J = 14.2, 11.4, 4.7 Hz, 1H), 2.08 (s, 4H), 1.45 – 1.32 (m, 1H), 1.29 – 1.18 (m, 1H), 1.12 (s, 6H); **^{13}C NMR** (126 MHz, $CDCl_3$) δ 178.1, 162.0 (d, $J_{C\text{-}F}$ = 246.1 Hz), 149.6, 140.3, 139.7 (d, $J_{C\text{-}F}$ = 3.1 Hz), 131.8, 126.7 (d, $J_{C\text{-}F}$ = 8.0 Hz), 125.2, 122.7, 118.6, 115.3 (d, $J_{C\text{-}F}$ = 21.1 Hz), 111.6, 91.2, 71.3, 67.4, 59.5, 51.5, 44.1, 43.6, 38.7, 23.9, 23.8, 22.0; **^{19}F NMR** (470 MHz, $CDCl_3$) δ -116.48 (tt, J = 8.4, 5.0 Hz); **IR** (neat) ν 2950, 2847, 2788, 2229, 1725, 1506, 1460, 1271, 1224, 1193, 1149, 1049, 1033, 834 cm^{-1}; **HRMS** (ESI) Calcd for $C_{25}H_{30}FN_2O_3$ (MH^+): 425.2235; found: 425.2232.

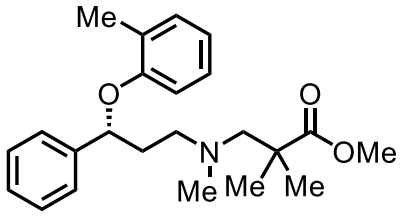

2.18b

Methyl (*R*)-2,2-dimethyl-3-(methyl(3-phenyl-3-(o-tolyloxy)propyl)amino)propanoate (2.18b)

Substrate **2.17b** was reacted with ((1-methoxy-2-methylprop-1-en-1-yl)oxy)trimethylsilane **2.11a** following the general procedure on a 1.0 mmol scale using DCM as the solvent. After purification by column chromatography (15% ethyl acetate in hexanes), **2.18b** was obtained as a colorless liquid (91.9 mg, 25%).

^{1}H NMR (500 MHz, $CDCl_3$) δ 7.36 – 7.26 (m, 4H), 7.26 – 7.19 (m, 1H), 7.09 (d, J = 7.3 Hz, 1H), 6.94 (t, J = 7.9 Hz, 1H), 6.75 (t, J = 7.4 Hz, 1H), 6.59 (d, J = 8.2 Hz, 1H), 5.19 (dd, J = 8.5, 4.3 Hz, 1H), 3.58 (s, 3H), 2.59 (t, J = 7.3 Hz, 2H), 2.51 (t, J = 1.8 Hz, 2H), 2.31 (s, 3H), 2.21 (s, 3H), 2.11 (dq, J = 14.4, 7.2 Hz, 1H), 2.00 – 1.88 (m, 1H), 1.18 – 1.07 (m, 6H); **^{13}C NMR** (151 MHz, $CDCl_3$) δ 180.8, 158.7, 145.0, 133.1, 131.2, 130.0, 129.6, 129.1, 128.4, 122.7, 115.4, 80.4, 69.7, 58.9, 54.2, 54.2, 46.6, 39.5, 26.6, 26.5, 19.2; **IR** (neat) ν 2949, 2847, 1727, 1601, 1491, 1453, 1305, 1270, 1237, 1192, 1149, 1119, 1047, 747, 700 cm^{-1}; **HRMS** (ESI) Calcd for $C_{23}H_{32}NO_3$ (MH^+): 370.2383; found: 370.2372; $[\alpha]^{25}_D$ = –4.6° (c = 1.0, $CHCl_3$).

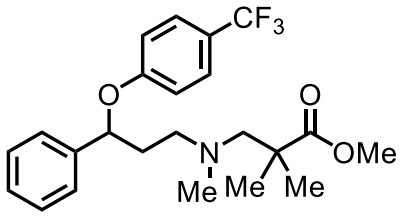

2.18c

Methyl 2,2-dimethyl-3-(methyl(3-phenyl-3-(4-(trifluoromethyl)phenoxy)propyl) amino)propanoate (2.18c)

Substrate **2.17c** was reacted with ((1-methoxy-2-methylprop-1-en-1-yl)oxy)trimethylsilane **2.11a** following the general procedure on 1.0 mmol scale using DCM as the solvent. After purification by column chromatography (15% ethyl acetate in hexanes), **2.18c** was obtained as a colorless liquid (113 mg, 27%).

^{1}H NMR (500 MHz, $CDCl_3$) δ 7.42 (d, J = 8.5 Hz, 2H), 7.32 (d, J = 4.3 Hz, 4H), 7.25 (d, J = 3.4 Hz, 1H), 6.89 (d, J = 8.5 Hz, 2H), 5.25 (dd, J = 8.5, 4.4 Hz, 1H), 3.59 (d, J = 1.1 Hz, 3H), 2.67 – 2.45 (m, 4H), 2.21 (s, 3H), 2.16 – 2.01 (m, 1H), 2.01 – 1.86 (m, 1H), 1.12 (d, J = 7.4 Hz, 6H); **^{13}C NMR** (151 MHz, $CDCl_3$) δ 178.1, 160.7, 141.4, 128.7, 127.7, 125.8, 126.7 (q, $J_{C\text{-}F}$ = 3.8 Hz), 124.4 (q, $J_{C\text{-}F}$ = 271.1 Hz), 122.6 (q, $J_{C\text{-}F}$ = 32.7 Hz), 115.7, 78.3, 67.1, 55.8, 51.6, 43.92, 43.91, 36.9, 24.0, 23.8; **^{19}F NMR** (470 MHz, $CDCl_3$) δ -62.53; **IR** (neat) ν 2970, 1727, 1614, 1517, 1455, 1325, 1250, 1177, 1158, 1110, 1067, 1044, 835, 701 cm^{-1}; **HRMS** (ESI) Calcd for $C_{23}H_{29}F_3NO_3$ (MH^+): 424.2100; found: 424.2092.

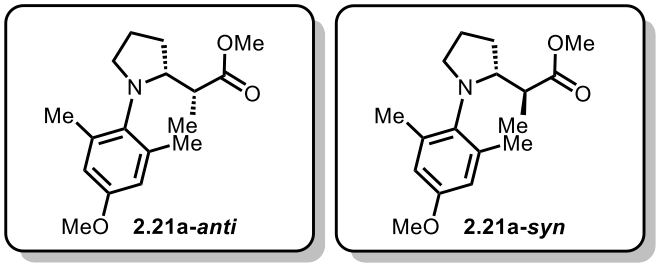

Methyl 2-(1-(4-methoxy-2,6-dimethylphenyl)pyrrolidin-2-yl)propanoate (2.21a)

1-(4-Methoxy-2,6-dimethylphenyl)pyrrolidine **2.13k** (0.2 mmol, 1 equiv.) was reacted with methyl acrylate **2.20a** (0.24 mmol, 1.2 equiv.) following the General Procedure using $B(C_6F_5)_3$ (5.0 mol%), benzene (0.2 mL) as the solvent and was carried out for 12 h at 22 °C. ^{1}H NMR analysis of the crude material revealed that **2.21a-*anti*** and **2.21a-*syn*** were obtained in the ratio of 2.3:1. After purification by column chromatography (hexanes: EtOAc = 20:1), **2.21a** was obtained as a mixture of diastereomers (56 mg, 97%). Further purification was carried out by PTLC using hexanes: DCM = 5:1 as the eluent to separate **2.21a-*anti*** and **2.21a-*syn***.

2.21a-*anti*: ^{1}H NMR (600 MHz, $CDCl_3$) δ 6.56 (d, J = 3.0 Hz, 1H), 6.53 (d, J = 3.0 Hz, 1H), 3.88 (q, J = 6.4 Hz, 1H), 3.74 (s, 3H), 3.31 – 3.28 (m, 4H), 2.98 (q, J = 7.7 Hz, 1H), 2.36 (p, J = 6.8 Hz, 1H), 2.27 (s, 3H), 2.24 (s, 3H), 2.07 (dq, J = 12.4, 7.5 Hz, 1H), 1.96 – 1.87 (m, 2H), 1.77 (dq, J = 12.8, 6.1 Hz, 1H), 1.11 (d, J = 7.0 Hz, 3H); **^{13}C NMR** (151 MHz, $CDCl_3$) δ176.2, 156.6, 140.7, 138.5, 137.5, 114.4, 112.9, 62.8, 55.2, 52.7, 51.1, 45.2, 29.1, 25.0, 19.5, 19.3, 13.5; **IR** (neat) 2947, 1733, 1061, 1484, 1464, 1434, 1319, 1260, 1194, 1154, 1066 cm^{-1}; **HRMS** (DART) m/z Calcd for $C_{17}H_{26}NO_3$ (MH^+): 292.1913; found: 292.1921.

2.21a-*syn*: ^{1}H NMR (600 MHz, $CDCl_3$) δ 6.57 (d, J = 3.1 Hz, 1H), 6.54 (d, J = 2.8 Hz, 1H), 3.88 – 3.81 (m, 1H), 3.74 (s, 3H), 3.44 (s, 3H), 3.27 (td, J = 8.1, 7.5, 2.8 Hz, 1H), 2.92 (td, J = 8.5, 6.6

Hz, 1H), 2.45 (ddd, J = 7.0, 5.6, 1.4 Hz, 1H), 2.29 (s, 3H), 2.23 (s, 3H), 2.15 – 2.08 (m, 1H), 1.97 – 1.84 (m, 3H), 1.01 (dd, J = 7.0, 1.4 Hz, 3H); **^{13}C NMR** (151 MHz, $CDCl_3$) δ 175.9, 156.4, 140.3, 138.9, 137.2, 114.5, 113.0, 63.6, 55.2, 53.4, 51.1, 45.9, 29.8, 25.1, 19.4, 19.1, 13.8; **IR** (neat) 2948, 1733, 1602, 1483, 1463, 1318, 1257, 1193, 1154, 1068cm^{-1}; **HRMS** (DART) m/z Calcd for $C_{17}H_{26}NO_3$ (MH^+): 292.1913; found: 292.1919.

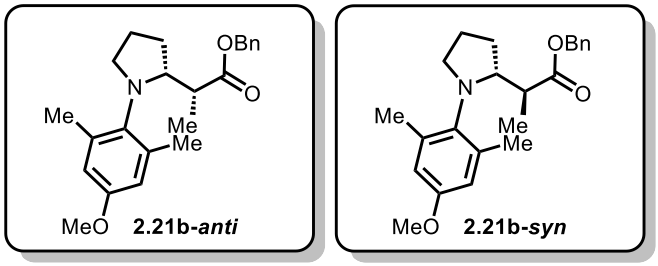

Benzyl 2-(1-(4-methoxy-2,6-dimethylphenyl)pyrrolidin-2-yl)propanoate (2.21b)

1-(4-Methoxy-2,6-dimethylphenyl)pyrrolidine **2.13k** (0.1 mmol, 1.0 equiv.) was reacted with benzyl acrylate **2.20b** (0.24 mmol, 1.2 equiv.) following the General Procedure using $B(C_6F_5)_3$ (5.0 mol%), benzene (0.2 mL) as the solvent and was carried out for 12 h at 22 °C. ^{1}H NMR analysis of the crude material revealed that **2.21b-*anti*** and **2.21b-*syn*** were obtained in the ratio of 2.5:1. After purification by column chromatography (hexanes: EtOAc = 30:1), **3c** was obtained as a mixture of diastereomers (67 mg, 91%). Further purification was carried out by PTLC using hexanes: DCM = 5:1 as the eluent to separate **2.21b-*anti*** and **2.21b-*syn***.

2.21b-*anti*: ^{1}H NMR (600 MHz, $CDCl_3$) δ 7.34 – 7.28 (m, 3H), 7.24 – 7.19 (m, 2H), 6.54 (d, J = 3.1 Hz, 1H), 6.51 (d, J = 3.1 Hz, 1H), 4.77 – 4.62 (m, 2H), 3.95 – 3.91 (m, 1H), 3.72 (s, 3H), 3.30 (ddd, J = 8.4, 7.0, 4.8 Hz, 1H), 2.98 (dt, J = 8.4, 7.4 Hz, 1H), 2.42 (p, J = 6.8 Hz, 1H), 2.26 (s, 3H), 2.21 (s, 3H), 2.09 – 2.02 (m, 1H) 1.96 – 1.85 (m, 2H), 1.80 – 1.74 (m, 1H), 1.14 (d, J = 7.0 Hz, 3H); **^{13}C NMR** (151 MHz, $CDCl_3$) δ178.2, 159.2, 143.3, 141.2, 140.1, 138.9, 131.0, 130.5, 130.5, 117.1, 115.6, 68.4, 65.4, 57.8, 55.3, 47.9, 31.6, 27.7, 22.1, 22.0, 16.1; **IR** (neat) 2944, 2878, 2837, 1731, 1602, 1483, 1464, 1318, 1263, 1192, 1154, 1068, 697 cm^{-1}; **HRMS** (DART) m/z Calcd for $C_{23}H_{30}NO_3$ (MH^+): 368.2226; found: 368.2237.

2.21b-*syn*: ^{1}H NMR (600 MHz, $CDCl_3$) δ 7.37 – 7.27 (m, 5H), 6.56 (d, *J* = 3.1 Hz, 1H), 6.51 (d, *J* = 3.1 Hz, 1H), 4.95 (d, *J* = 12.3 Hz, 1H), 4.71 (d, *J* = 12.3 Hz, 1H), 3.88 (ddd, *J* = 8.2, 5.5, 2.8 Hz, 1H), 3.73 (s, 3H), 3.33 – 3.20 (m, 1H), 2.91 (td, *J* = 8.6, 6.6 Hz, 1H), 2.50 (qd, *J* = 7.0, 5.5 Hz, 1H), 2.27 (s, 3H), 2.20 (s, 3H), 2.16 – 2.07 (m, 1H), 1.94 – 1.84 (m, 3H), 1.04 (d, *J* = 7.0 Hz, 3H); **^{13}C NMR** (151 MHz, $CDCl_3$) δ 175.3, 156.4, 140.4, 139.0, 137.2, 136.1, 128.4, 128.2, 128.0, 114.5, 113.1, 65.9, 63.7, 55.2, 53.5, 46.1, 29.9, 25.2, 19.4, 19.2, 13.7; **IR** (neat) 2940, 1731, 1602, 1483, 1463, 1256, 1192, 1154, 1068, 698 cm^{-1}; **HRMS** (DART) m/z Calcd for $C_{23}H_{30}NO_3$ (MH^+): 368.2226; found: 368.2239.

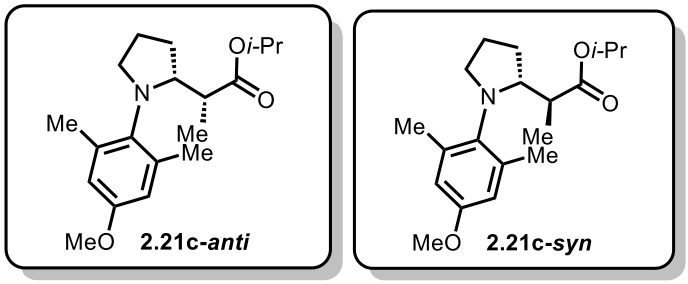

Isopropyl 2-(1-(4-methoxy-2,6-dimethylphenyl)pyrrolidin-2-yl)propanoate (2.21c)

1-(4-Methoxy-2,6-dimethylphenyl)pyrrolidine **2.13k** (0.2 mmol, 1.0 equiv.) was reacted with isopropyl acrylate **2.20c** (0.24 mmol, 1.2 equiv.) following the General Procedure using $B(C_6F_5)_3$ (5.0 mol%), benzene (0.2 mL) as the solvent and was carried out for 12 h at 22 °C. ^{1}H NMR analysis of the crude material revealed that **2.21c-*anti*** and **2.21c-*syn*** were obtained in the ratio of 2.1:1. After purification by column chromatography (hexanes: Et_2O = 32:1), **2.21c** was obtained as a mixture of diastereomers (50 mg, 78%). Further purification was carried out by PTLC using hexanes: Et_2O = 9:1 as the eluent to separate **2.21c-*anti*** and **2.21c-*syn***.

2.21c-*anti*: ^{1}H NMR (500 MHz, $CDCl_3$) δ 6.57 – 6.55 (m, 1H), 6.54 (d, *J* = 2.8 Hz, 1H), 4.65 (hept, *J* = 6.2 Hz, 1H), 3.91 (dt, *J* = 7.7, 5.4 Hz, 1H), 3.74 (s, 3H), 3.29 (ddd, *J* = 8.4, 6.8, 4.6 Hz, 1H), 2.98 (q, *J* = 7.6 Hz, 1H), 2.35 – 2.29 (m, 1H), 2.27 (s, 3H), 2.25 (s, 3H), 2.07 – 1.99 (m, 1H), 1.96 – 1.88 (m, 2H), 1.83 – 1.77 (m, 1H), 1.11 (dd, *J* = 7.1, 0.6 Hz, 3H), 1.08 (d, *J* = 6.3 Hz, 3H), 1.05 (d, *J* = 6.2 Hz, 3H); **^{13}C NMR** (126 MHz, $CDCl_3$) δ175.2, 156.6, 140.5, 138.5, 137.6, 114.5, 113.0, 67.1, 62.4, 55.1, 52.6, 44.8, 28.4, 25.1, 21.6, 21.5, 19.5, 19.3, 12.8; **IR** (neat) 2973, 1731, 1602, 1481, 1464, 1371, 1317, 1260, 1153, 1105, 1067, 854, 698 cm^{-1}; **HRMS** (DART) m/z Calcd for $C_{19}H_{30}NO_3$ (MH^+): 320.2226; found: 320.2221.

2.21c-*syn*: ^{1}H NMR (600 MHz, $CDCl_3$) δ 6.57 (d, *J* = 3.0 Hz, 1H), 6.53 (d, *J* = 3.0 Hz, 1H), 4.82 (hept, *J* = 6.3 Hz, 1H), 3.78 (ddd, *J* = 8.6, 6.0, 2.9 Hz, 1H), 3.74 (s, 3H), 3.27 (td, *J* = 7.9, 2.6 Hz, 1H), 2.92 (td, *J* = 8.6, 6.5 Hz, 1H), 2.43 – 2.36 (m, 1H), 2.32 (s, 3H), 2.23 (s, 3H), 2.17 – 2.09 (m, 1H), 1.98 – 1.91 (m, 1H), 1.91 – 1.85 (m, 2H), 1.16 (d, *J* = 6.3 Hz, 3H), 1.08 (d, *J* = 6.3 Hz, 3H), 0.97 (d, *J* = 6.9 Hz, 3H); **^{13}C NMR** (151 MHz, $CDCl_3$) δ 175.1, 156.4, 140.3, 139.3, 137.2, 114.5, 113.0, 67.1, 63.8, 55.1, 53.5, 46.7, 30.1, 25.2, 21.8, 21.5, 19.3, 19.3, 14.2; **IR** (neat) 2974, 1723, 1603, 1464, 1317, 1255, 1153, 1107, 1068, 854 cm^{-1}; **HRMS** (DART) m/z Calcd for $C_{19}H_{30}NO_3$ (MH^+): 320.2226; found: 320.2216.

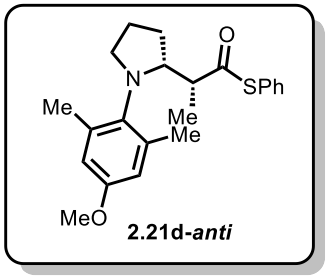

***S*-Phenyl 2-(1-(4-methoxy-2,6-dimethylphenyl)pyrrolidin-2-yl)propanethioate (2.21d)**

1-(4-Methoxy-2,6-dimethylphenyl)pyrrolidine **2.13k** (0.2 mmol, 1.0 equiv.) was reacted with *S*-phenyl prop-2-enethioate **2.20d** (0.24 mmol, 1.2 equiv.) following the General Procedure using $B(C_6F_5)_3$ (5.0 mol%), benzene (0.2 mL) as the solvent and was carried out for 12 h at 22 °C. ^{1}H NMR analysis of the crude material revealed that **2.21d-*anti*** and **2.21d-*syn*** were obtained in the ratio of 1.8:1. After purification by column chromatography (hexanes: Et_2O = 30:1), **2.21d** was obtained as a mixture of diastereomers (39 mg, 53%). **^{1}H NMR** (500 MHz, $CDCl_3$) δ 7.36 – 7.29 (m, 3H), 7.16 – 7.11 (m, 2H), 6.59 (s, 1H), 6.55 (s, 1H), 4.06 (dt, *J* = 7.3, 5.7 Hz, 1H), 3.76 (s, 3H), 3.33 (ddd, *J* = 8.4, 6.9, 4.9 Hz, 1H), 3.00 (q, *J* = 7.6 Hz, 1H), 2.70 – 2.62 (m, 1H), 2.32 (s, 3H), 2.25 (s, 3H), 2.11 – 1.98 (m, 1H), 1.97 – 1.88 (m, 2H), 1.86 – 1.80 (m, 1H), 1.22 (d, *J* = 7.0 Hz, 3H); **^{13}C NMR** (151 MHz, $CDCl_3$) δ200.0, 156.8, 140.6, 138.8, 137.2, 134.5, 129.1, 129.0, 128.8, 114.5, 113.2, 62.6, 55.1, 53.5, 52.5, 28.9, 25.0, 19.6, 19.5, 13.74; **HRMS** (DART) m/z Calcd for $C_{22}H_{27}NO_2S$ (MH^+): 370.1835; found: 370.1833.

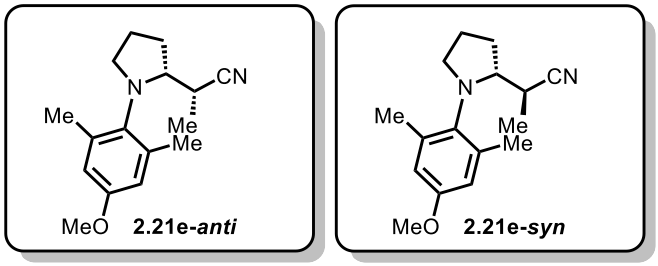

2-(1-(4-Methoxy-2,6-dimethylphenyl)pyrrolidin-2-yl)propanenitrile (2.21e)

1-(4-Methoxy-2,6-dimethylphenyl)pyrrolidine **2.13k** (0.2 mmol, 1.0 equiv.) was reacted with acrylonitrile **2.20e** (0.5 mmol, 2.5 equiv.) following the General Procedure using $B(C_6F_5)_3$ (10 mol%), benzene (0.4 mL) as the solvent and was carried out for 48 h at 70 °C. ^{1}H NMR analysis of the crude material revealed that **2.21e-*anti*** and **2.21e-*syn*** were obtained in the ratio of 1.3:1. After purification by column chromatography (hexanes: Et_2O = 10:1), **2.21e** was obtained as a mixture of diastereomers (25.9 mg, 50%). Further purification was carried out by PTLC using hexanes: Et_2O = 20:1 as the eluent to separate **2.21e-*anti*** and **2.21e-*syn***.

2.21e-*anti*: **^{1}H NMR** (600 MHz, $CDCl_3$) δ 6.60 (d, *J* = 3.0 Hz, 1H), 6.56 (d, *J* = 3.0 Hz, 1H), 3.80 – 3.72 (m, 4H), 3.36 (td, *J* = 8.0, 2.5 Hz, 1H), 3.02 (td, *J* = 8.9, 6.6 Hz, 1H), 2.53 (qd, *J* = 7.2, 3.5 Hz, 1H), 2.34 (s, 3H), 2.28 – 2.23 (m, 1H), 2.22 (s, 3H), 2.14 – 2.09 (m, 1H), 2.01 – 1.90 (m, 2H), 1.18 (d, *J* = 7.3 Hz, 3H); **^{13}C NMR** (151 MHz, $CDCl_3$) δ 156.9, 140.3, 137.8, 137.2, 122.7, 114.8, 113.3, 63.3, 55.2, 53.6, 32.3, 29.7, 25.3, 19.4, 19.2, 14.0; **IR** (neat) 2951, 2242, 2228, 1603, 1483, 1464, 1318, 1262, 1192, 1154, 1068, 837 cm^{-1}; **HRMS** (DART) m/z Calcd for $C_{16}H_{23}N_2O$ (MH^+): 259.1810; found: 259.1807.

2.21e-*syn*: ^{1}H NMR (600 MHz, $CDCl_3$) δ 6.62 (d, *J* = 3.0 Hz, 1H), 6.56 (d, *J* = 3.0 Hz, 1H), 3.76 (s, 3H), 3.46 (dt, *J* = 8.0, 3.9 Hz, 1H), 3.35 (td, *J* = 7.8, 3.2 Hz, 1H), 3.10 – 3.02 (m, 1H), 2.56 (qd,

J = 7.3, 3.7 Hz, 1H), 2.39 (s, 3H), 2.30 – 2.24 (m, 1H), 2.23 – 2.17 (m, 4H), 2.04 (td, *J* = 8.3, 3.9 Hz, 1H), 1.97 (dq, *J* = 11.2, 3.7 Hz, 1H), 1.15 (d, *J* = 7.3 Hz, 3H); **^{13}C NMR** (151 MHz, $CDCl_3$) δ 157.1, 141.3, 138.0, 136.3, 122.8, 114.8, 113.2, 64.7, 55.2, 52.5, 31.7, 28.3, 24.7, 19.2, 19.1, 15.6; **IR** (neat) 2951, 2837, 2239, 1602, 1544, 1483, 1464, 1318, 1267, 1192, 1155, 1067, 858 cm^{-1}; **HRMS** (DART) m/z Calcd for $C_{16}H_{23}N_2O$ (MH^+): 259.1810; found: 259.1816.

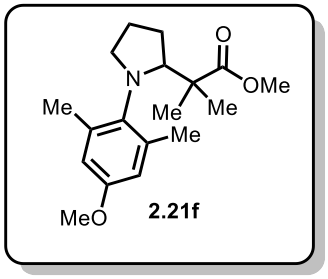

Methyl 2-(1-(4-methoxy-2,6-dimethylphenyl)pyrrolidin-2-yl)-2-methylpropanoate (2.21f)

1-(4-Methoxy-2,6-dimethylphenyl)pyrrolidine **2.13k** (0.2 mmol, 1.0 equiv.) was reacted with methyl methacrylate **2.20f** (0.24 mmol, 1.2 equiv.) following the General Procedure using $B(C_6F_5)_3$ (10 mol%), benzene (0.4 mL) as the solvent and was carried out for 24 h at 70 °C.

After purification by column chromatography (hexanes: Et_2O = 40:1), **2.21f** was obtained as a colorless oil (59.1 mg, 97%).

^{1}H NMR (600 MHz, $CDCl_3$) δ 6.54 (q, *J* = 3.1 Hz, 2H), 4.05 (dd, *J* = 9.4, 2.2 Hz, 1H), 3.73 (s, 3H), 3.29 (ddd, *J* = 9.1, 6.9, 2.5 Hz, 1H), 3.07 (s, 3H), 2.90 (td, *J* = 8.9, 6.8 Hz, 1H), 2.29 (s, 3H), 2.25 (s, 3H), 2.13 – 2.05 (m, 1H), 1.92 – 1.80 (m, 3H), 1.11 (s, 3H), 1.08 (s, 3H); **^{13}C NMR** (151 MHz, $CDCl_3$) δ 177.8, 156.1, 139.9, 139.8, 136.8, 114.6, 112.9, 66.8, 55.1, 54.5, 50.9, 47.7, 27.6, 25.6, 23.2, 19.7, 19.6, 19.4; **IR** (neat) 2947, 2836, 1731, 1602, 1466, 1315, 1253, 1191, 1128, 1069, 839 cm^{-1}; **HRMS** (DART) Calcd for $C_{18}H_{28}NO_3$ (MH^+): 306.2069; found: 306.2067.

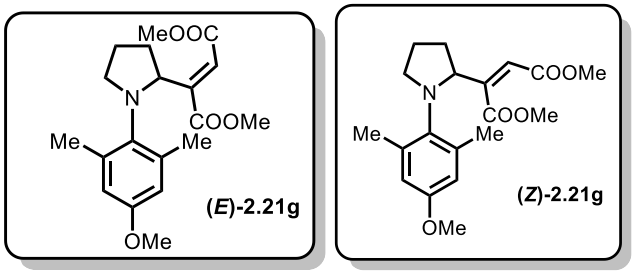

Dimethyl 2-(1-(4-methoxy-2,6-dimethylphenyl)pyrrolidin-2-yl)fumarate (2.21g)

1-(4-Methoxy-2,6-dimethylphenyl)pyrrolidine **2.13k** (0.2 mmol, 1.0 equiv.) was reacted with dimethyl but-2-ynedioate **2.20g** (0.24 mmol, 1.2 equiv.) following the General Procedure using $B(C_6F_5)_3$ (10 mol%), benzene (0.4 mL) as the solvent and was carried out for 24 h at 70 °C. ^{1}H NMR analysis of the crude material revealed that *(E)*-**2.21g** and *(Z)*-**2.21g** were obtained in the ratio of 1:1.6. After purification by column chromatography (hexanes: Et_2O = 5:1), (*E*)-**2.21g** was obtained as yellow liquid (29.8 mg, 21%) and (*Z*)-**2.21g** was obtained as colorless liquid (42.5 mg, 31%). The relative configuration was assigned based on NOESY experiments (see SI Section 7 for NOE spectra).

(E)-**2.21g: ^{1}H NMR** (600 MHz, $CDCl_3$) δ 6.51 (s, 2H), 6.27 (s, 1H), 5.50 (dd, *J* = 9.6, 4.2 Hz, 1H), 3.77 (s, 3H), 3.72 (s, 3H), 3.61 (s, 3H), 3.44 – 3.39 (m, 1H), 3.06 – 3.00 (m, 1H), 2.47 – 2.41 (m, 1H), 2.35 – 2.09 (m, 8H), 2.06 – 1.95 (m, 1H); **^{13}C NMR** (126 MHz, $CDCl_3$) δ167.8, 165.8, 156.5, 152.4, 138.0, 124.8, 114.5, 113.0, 58.6, 55.1, 53.9, 51.9, 51.6, 32.0, 25.9, 19.1; **IR** (neat) 2951, 2848, 1729, 1603, 1434, 1256, 1206, 1154, 1114, 1069, 855 cm^{-1}; **HRMS** (DART) m/z Calcd for $C_{19}H_{26}NO_5$ (MH^+): 348.1811; found: 348.1822.

(Z)-**2.21g**: **^{1}H NMR** (600 MHz, $CDCl_3$) δ 6.55 (s, 2H), 5.99 (d, *J* = 1.1 Hz, 1H), 4.35 – 4.28 (m, 1H), 3.77 (d, *J* = 1.7 Hz, 3H), 3.74 (d, *J* = 1.7 Hz, 3H), 3.67 (d, *J* = 1.8 Hz, 3H), 3.41 – 3.37 (m,

1H), 3.01 (dt, *J* = 10.2, 7.8 Hz, 1H), 2.32 – 2.28 (m, 7H), 2.16 – 2.09 (m, 1H), 2.04 – 1.95 (m, 1H)；**^{13}C NMR** (151 MHz, $CDCl_3$) δ1168.7, 165.7, 156.7, 153.8, 137.3, 119.0, 114.1, 113.5, 64.3, 55.1, 53.0, 52.2, 51.7, 31.9, 24.7, 19.6; **IR** (neat) 2950, 2838, 1724, 1602, 1434, 1316, 1255, 1193, 1153, 1067, 854 cm^{-1}; **HRMS** (DART) m/z Calcd for $C_{19}H_{26}NO_5$ (MH^+): 348.1811; found: 348.1810.

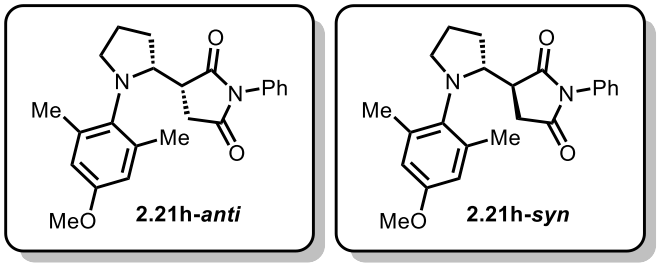

1-(4-Methoxy-2,6-dimethylphenyl)-1'-phenyl-[2,3'-bipyrrolidine]-2',5'-dione (2.21h)

1-(4-Methoxy-2,6-dimethylphenyl)pyrrolidine **2.13k** (0.2 mmol, 1.0 equiv.) was reacted with 1-phenyl-1*H*-pyrrole-2,5-dione **2.20h** (0.24 mmol, 1.2 equiv.) following the General Procedure using $B(C_6F_5)_3$ (5.0 mol%), benzene (0.2 mL) as the solvent and was carried out for 12 h at 22 °C. ^{1}H NMR analysis of the crude material revealed that **2.21h-*anti*** and **2.21h-*syn*** were obtained in the ratio of 4.5:1. After purification by column chromatography (hexanes: EtOAc = 5:1), **2.21h** was obtained as a mixture of diastereomers (75 mg, 99%). Further purification was carried out by PTLC to separate **2.21h-*anti*** and **2.21h-*syn***.

2.21h-*anti*: ^{1}H NMR (500 MHz, $CDCl_3$) δ 7.46 (t, *J* = 7.7 Hz, 2H), 7.41 – 7.35 (m, 1H), 7.27 – 7.22 (m, 2H), 6.62 – 6.56 (m, 2H), 4.31 (td, *J* = 6.8, 4.0 Hz, 1H), 3.76 (s, 3H), 3.38 – 3.30 (m, 1H), 3.16 – 3.07 (m, 1H), 2.98 – 2.93 (m, 1H), 2.89 (dd, *J* = 18.8, 4.0 Hz, 1H), 2.71 (dd, *J* = 18.8, 9.2 Hz, 1H), 2.32 (s, 3H), 2.26 (s, 3H), 2.14 – 1.98 (m, 3H), 1.64 (dt, *J* = 11.2, 6.6 Hz, 1H); **^{13}C NMR** (101 MHz, $CDCl_3$) δ 177.8, 176.4, 157.0, 139.8, 138.3, 135.6, 131.9, 129.1, 128.6, 126.4, 114.9, 113.4, 60.8, 55.2, 51.8, 43.2, 30.7, 26.3, 24.6, 19.8, 18.9; **IR** (neat) 2946, 1711, 1599, 1498, 1384, 1181, 1154, 692 cm^{-1}; **HRMS** (DART) m/z Calcd for $C_{23}H_{27}N_2O_3$ (MH^+): 379.2022; found: 379.2039.

2.21h-*syn*: ^{1}H NMR (500 MHz, $CDCl_3$) δ 7.34 – 7.27 (m, 3H), 6.79 – 6.74 (m, 2H), 6.55 – 6.49 (m, 2H), 4.53 (td, *J* = 7.0, 2.9 Hz, 1H), 3.72 (s, 3H), 3.44 (dt, *J* = 8.8, 6.2 Hz, 1H), 3.12 (dd, *J* = 18.1, 4.8 Hz, 1H), 3.07 – 2.96 (m, 2H), 2.78 (dd, *J* = 18.1, 9.5 Hz, 1H), 2.35 – 2.27 (m, 4H), 2.25 (s, 3H), 2.04 – 1.95 (m, 2H), 1.89 – 1.80 (m, 1H); **^{13}C NMR** (126 MHz, $CDCl_3$) δ 177.4, 176.3, 156.9, 139.0, 138.2, 137.0, 131.7, 128.7, 128.2, 126.3, 115.2, 113.4, 59.4, 55.1, 54.1, 45.6, 31.7, 29.9, 24.7, 20.3, 18.8; **IR** (neat) 2951, 1709, 1600, 1499, 1382, 1180, 1068, 694 cm^{-1}; **HRMS** (DART) m/z Calcd for $C_{23}H_{27}N_2O_3$ (MH^+): 379.2022; found: 379.2036.

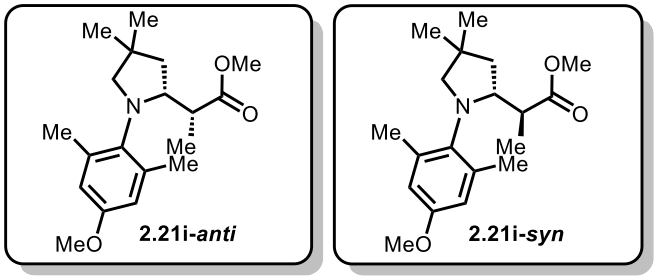

Methyl 2-(1-(4-methoxy-2,6-dimethylphenyl)-4,4-dimethylpyrrolidin-2-yl)propanoate (2.21i)

1-(4-Methoxy-2,6-dimethylphenyl)-3,3-dimethylpyrrolidine **2.13t** (0.2 mmol, 1.0 equiv.) was reacted with methyl acrylate **2.20a** (0.24 mmol, 1.2 equiv.) following the General Procedure using $B(C_6F_5)_3$ (5.0 mol%), benzene (0.2 mL) as the solvent and was carried out for 12 h at 22 °C. ^{1}H NMR analysis of the crude material revealed that **2.21i-*anti*** and **2.21i-*syn*** were obtained in the ratio of 3.0:1. After purification by column chromatography (hexanes: Et_2O = 65:1), **2.21i-*anti*** was obtained as a white solid (44.9 mg, 70%), **2.21i-*syn*** was obtained as a colorless oil (15.6 mg, 24%).

2.21i-*anti*: ^{1}H NMR (600 MHz, $CDCl_3$) δ 6.55 (d, *J* = 3.0 Hz, 1H), 6.48 (d, *J* = 3.0 Hz, 1H), 4.05 (q, *J* = 7.9, 7.4 Hz, 1H), 3.73 (d, *J* = 1.0 Hz, 3H), 3.11 (s, 3H), 3.08 (d, *J* = 8.3 Hz, 1H), 2.82 (d, *J* = 8.3 Hz, 1H), 2.36 (p, *J* = 6.9 Hz, 1H), 2.29 (s, 3H), 2.29 (s, 3H), 1.81 (dd, *J* = 12.2, 6.8 Hz, 1H), 1.52 (dd, *J* = 12.2, 8.0 Hz, 1H), 1.20 (s, 3H), 1.15 (s, 3H), 1.02 (d, *J* = 7.0 Hz, 3H). **^{13}C NMR** (151 MHz, $CDCl_3$) δ 176.1, 156.5, 140.5, 139.3, 135.7, 114.1, 113.0, 66.0, 61.9, 55.1, 51.0, 45.3, 44.7, 36.3, 29.4, 28.6, 19.7, 19.4, 14.7; **IR** (neat) 2950, 1734, 1602, 1482, 1465, 1269, 1193, 1154, 854 cm^{-1}; **HRMS** (DART) m/z Calcd for $C_{19}H_{30}NO_3$ (MH^+): 320.2226; found: 320.2241.

2.21i-*syn*: ^{1}H NMR (600 MHz, $CDCl_3$) δ 6.57 (d, *J* = 3.0 Hz, 1H), 6.50 (d, *J* = 3.0 Hz, 1H), 3.90 (q, *J* = 7.1 Hz, 1H), 3.75 (s, 3H), 3.57 (s, 3H), 3.03 (d, *J* = 8.4 Hz, 1H), 2.82 (d, *J* = 8.4 Hz, 1H),

2.54 (p, *J* = 7.0 Hz, 1H), 2.28 (s, 3H), 2.27 (s, 3H), 1.88 (dd, *J* = 12.6, 7.7 Hz, 1H), 1.67 (dd, *J* = 12.6, 6.3 Hz, 1H), 1.22 (s, 3H), 1.12 (s, 3H), 0.87 (dd, *J* = 6.9, 0.8 Hz, 3H); **^{13}C NMR** (151 MHz, $CDCl_3$) δ 176.0, 156.4, 139.8, 137.8, 137.3, 114.4, 113.3, 66.5, 63.1, 55.1, 51.2, 46.0, 44.7, 36.8, 29.2, 28.4, 19.8, 19.4, 15.4; **IR** (neat) 2951, 1735, 1603, 1483, 1465, 1256, 1192, 1155, 1069, 855 cm^{-1}; **HRMS** (DART) m/z Calcd for $C_{19}H_{30}NO_3$ (MH^+): 320.2226; found: 320.2240.

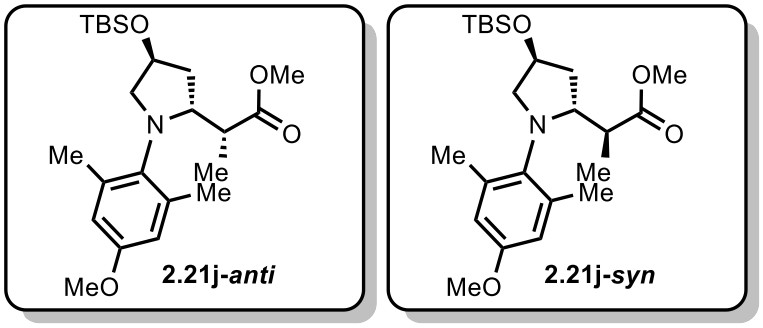

Methyl 2-(4-((*tert*-butyldimethylsilyl)oxy)-1-(4-methoxy-2,6-dimethylphenyl)pyrrolidin-2-yl)propanoate (2.21j)

3-((*tert*-Butyldimethylsilyl)oxy)-1-(4-methoxy-2,6-dimethylphenyl)pyrrolidine **2.13u** (0.2 mmol, 1.0 equiv.) was reacted with methyl acrylate **2.20a** (0.24 mmol, 1.2 equiv.) following the General Procedure using $B(C_6F_5)_3$ (5.0 mol%), benzene (0.2 mL) as the solvent and was carried out for 12 h at 22 °C. ^{1}H NMR analysis of the crude material revealed that **2.21j-*anti***, **2.21j-*anti'*** and **2.21j-*syn***, **2.21j-*syn'*** were obtained in the ratio of 6.9:5.9:3.0:1. After purification by column chromatography (hexanes: Et_2O = 13:1), **2.21j** was obtained as a mixture of diastereomers (69 mg, 82%). Further purification was carried out by PTLC to separate **2.21j-*anti*** and **2.21j-*syn***. The relative configuration of the pyrrolidine substituents was assigned *anti* based on NOESY experiments.

2.21j-*anti*: ^{1}H NMR (600 MHz, $CDCl_3$) δ 6.56 (d, *J* = 3.0 Hz, 1H), 6.53 (d, *J* = 3.1 Hz, 1H), 4.41 (t, *J* = 4.7 Hz, 1H), 4.09 – 4.04 (m, 1H), 3.74 (s, 3H), 3.55 (dd, *J* = 9.2, 5.2 Hz, 1H), 3.47 (s, 3H), 2.81 (dd, *J* = 9.2, 3.6 Hz, 1H), 2.42 (qd, *J* = 6.9, 5.1 Hz, 1H), 2.33 (s, 3H), 2.23 (s, 3H), 2.06 (ddd, *J* = 12.6, 7.0, 5.6 Hz, 1H), 1.98 (ddd, *J* = 12.1, 7.1, 4.3 Hz, 1H), 0.97 (d, *J* = 7.0 Hz, 3H), 0.89 (s, 9H), 0.08 (s, 3H), 0.04 (s, 3H); **^{13}C NMR** (151 MHz, $CDCl_3$) δ 175.7, 156.5, 140.1, 138.0, 137.6, 114.4, 112.9, 70.9, 62.0, 61.8, 55.1, 51.1, 44.5, 39.1, 25.8, 19.3, 19.1, 18.1, 14.1, -4.75, -4.81.; **IR**

(neat) 2951, 2929, 2856, 1735, 1603, 1464, 1318, 1253, 1154, 1068, 1024, 832, 774 cm^{-1}; **HRMS** (DART) m/z Calcd for $C_{23}H_{40}NO_4Si$ (MH^+): 422.2727; found: 422.2724.

2.21j-*syn*: ^{1}H NMR (600 MHz, $CDCl_3$) δ 6.54 (s, 1H), 6.52 (s, 1H), 4.38 (dp, *J* = 5.1, 2.6 Hz, 1H), 4.14 (q, *J* = 7.3 Hz, 1H), 3.73 (s, 3H), 3.60 (dd, *J* = 9.5, 4.9 Hz, 1H), 3.18 (s, 3H), 2.83 (d, *J* = 9.5 Hz, 1H), 2.34 (s, 3H), 2.32 – 2.27 (m, 1H), 2.25 (s, 3H), 1.97 (ddd, *J* = 12.6, 6.3, 2.8 Hz, 1H), 1.78 – 1.72 (m, 1H), 1.06 (d, *J* = 7.0 Hz, 3H), 0.89 (s, 9H), 0.08 (s, 3H), 0.04 (s, 3H); **^{13}C NMR** (151 MHz, $CDCl_3$) δ 176.0, 156.6, 140.6, 139.6, 136.2, 114.2, 112.7, 70.8, 62.0, 60.9, 55.1, 51.0, 45.3, 39.7, 25.8, 19.2, 19.0, 18.0, 14.2, -4.77, -4.81; **IR** (neat) 2952, 2928, 2856, 1737, 1604, 1465, 1319, 1258, 1155, 1069, 1028, 853, 775 cm^{-1}; **HRMS** (DART) m/z Calcd for $C_{23}H_{40}NO_4Si$ (MH^+): 422.2727; found: 422.2741.

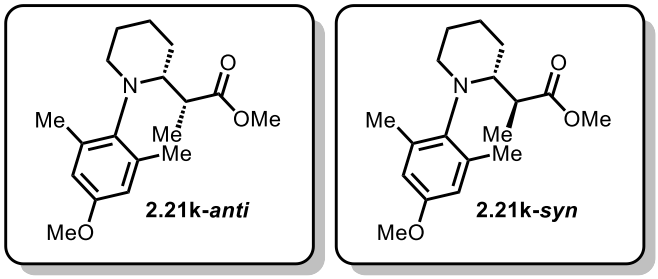

Methyl 2-(1-(4-methoxy-2,6-dimethylphenyl)piperidin-2-yl)propanoate (2.21k)

1-(4-Methoxy-2,6-dimethylphenyl)piperidine **2.13o** (0.2 mmol, 1.0 equiv.) was reacted with methyl acrylate **2.20a** (0.24 mmol, 1.2 equiv.) following the General Procedure using $B(C_6F_5)_3$ (5.0 mol%), benzene (0.2 mL) as the solvent and was carried out for 12 h at 22 °C. ^{1}H NMR analysis of the crude material revealed that **2.21k-*anti*** and **2.21k-*syn*** were obtained in the ratio of 10:1.0. After purification by column chromatography (hexanes: Et_2O = 19:1), **2.21k** was obtained as a mixture of diastereomers (39 mg, 63%). Further purification was carried out by PTLC using DCM: hexanes = 3:2 as the eluent to separate **2.21k-*anti*** and **2.21k-*syn***.

2.21k-*anti*: ^{1}H NMR (600 MHz, $CDCl_3$) δ 6.60 (d, *J* = 3.0 Hz, 1H), 6.43 (d, *J* = 3.0 Hz, 1H), 3.73 (s, 3H), 3.67 (dt, *J* = 9.7, 3.3 Hz, 1H), 3.60 (s, 3H), 3.10 – 3.04 (m, 1H), 2.84 – 2.79 (m, 1H), 2.44 (qd, *J* = 7.0, 3.6 Hz, 1H), 2.37 (s, 3H), 2.30 (s, 3H), 1.89 – 1.83 (m, 1H), 1.62 – 1.56 (m, 2H), 1.48 – 1.34 (m, 3H), 0.86 (d, *J* = 7.0 Hz, 3H); **^{13}C NMR** (151 MHz, $CDCl_3$) δ 175.8, 156.4, 139.4, 139.2, 138.4, 114.3, 113.5, 59.6, 55.0, 52.4, 51.5, 41.1, 27.3, 26.7, 24.9, 20.0, 19.1, 9.7; **IR** (neat) 2922, 2851, 1736, 1602, 1481, 1464, 1211, 1169, 1151, 1111, 1069, 855 cm^{-1}; **HRMS** (DART) m/z Calcd for $C_{18}H_{28}NO_3$ (MH^+): 306.2069; found: 306.2078.

2.21k-*syn*: ^{1}H NMR (600 MHz, $CDCl_3$) δ 6.60 (d, *J* = 3.0 Hz, 1H), 6.44 (d, *J* = 3.0 Hz, 1H), 3.75 (s, 3H), 3.49 (s, 3H), 3.23 (dt, *J* = 10.6, 2.9 Hz, 1H), 3.00 (td, *J* = 11.7, 3.1 Hz, 1H), 2.84 (dd, *J* =

11.9, 3.8 Hz, 1H), 2.53 (qd, *J* = 7.3, 3.3 Hz, 1H), 2.26 (s, 3H), 2.22 (s, 3H), 1.89 (dt, *J* = 12.8, 4.1 Hz, 1H), 1.84 – 1.79 (m, 1H), 1.66 – 1.50 (m, 3H), 1.33 (tdt, *J* = 12.8, 9.0, 3.9 Hz, 1H), 1.08 (d, *J* = 7.2 Hz, 3H); **^{13}C NMR** (151 MHz, $CDCl_3$) δ175.2, 156.4, 140.3, 140.1, 137.6, 113.8, 113.4, 62.8, 55.1, 52.7, 51.0, 40.5, 27.9, 26.7, 25.2, 20.0, 19.3, 15.7; **HRMS** (DART) m/z Calcd for $C_{18}H_{28}NO_3$ (MH^+): 306.2069; found: 306.207.

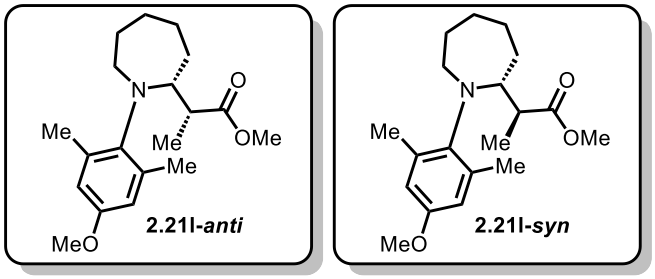

Methyl 2-(1-(4-methoxy-2,6-dimethylphenyl)azepan-2-yl)propanoate (2.21l)

1-(4-Methoxy-2,6-dimethylphenyl)azepane **2.13v** (0.2 mmol, 1.0 equiv.) was reacted with methyl acrylate **2.20a** (0.24 mmol, 1.2 equiv.) following the General Procedure using $B(C_6F_5)_3$ (5.0 mol%), benzene (0.2 mL) as the solvent and was carried out for 12 h at 22 °C. ^{1}H NMR analysis of the crude material revealed that **2.21l-*anti*** and **2.21l-*syn*** were obtained in the ratio of 2.0:1.0. After purification by column chromatography (hexanes: Et_2O = 32:1), **2.21l** was obtained as a mixture of diastereomers (42 mg, 66%). Further purification was carried out by PTLC using DCM: hexanes = 3:2 as the eluent to seperate **2.21l-*anti*** and **2.21l-*syn***.

2.21l-*anti*: ^{1}H NMR (500 MHz, $CDCl_3$) δ 6.59 – 6.55 (m, 2H), 3.79 (dt, *J* = 10.0, 4.3 Hz, 1H), 3.74 (s, 3H), 3.46 (s, 3H), 3.31 (ddd, *J* = 14.8, 9.9, 1.4 Hz, 1H), 3.15 – 3.07 (m, 1H), 2.45 (qd, *J* = 7.0, 4.1 Hz, 1H), 2.39 (s, 3H), 2.26 (s, 3H), 1.94 – 1.86 (m, 1H), 1.84 – 1.61 (m, 5H), 1.51 (dtt, *J* = 13.8, 9.2, 2.1 Hz, 1H), 1.44 – 1.33 (m, 1H), 1.13 (d, *J* = 7.0 Hz, 3H); **^{13}C NMR** (126 MHz, $CDCl_3$) δ 176.2, 155.9, 141.4, 138.7, 137.9, 114.3, 113.8, 62.1, 55.2, 53.1, 51.3, 43.9, 32.3, 30.0, 29.3, 26.3, 20.4, 20.0, 12.1; **IR** (neat) 2923, 2849, 1731, 1602, 1481, 1433, 1309, 1253, 1196, 1162, 1069, 853 cm^{-1}; **HRMS** (DART) m/z Calcd for $C_{19}H_{30}NO_3$ (MH^+): 320.2226; found: 320.2231.

2.21l-*syn*: ^{1}H NMR (600 MHz, $CDCl_3$) δ 6.57 (dd, *J* = 22.4, 3.1 Hz, 2H), 3.74 (s, 3H), 3.50 (s, 3H), 3.46 – 3.38 (m, 2H), 3.01 (dd, *J* = 15.1, 5.6 Hz, 1H), 2.50 (qd, *J* = 7.1, 3.2 Hz, 1H), 2.38 (s,

3H), 2.29 (s, 3H), 2.01 – 1.91 (m, 2H), 1.86 – 1.68 (m, 3H), 1.58 (dt, J = 13.9, 4.7 Hz, 1H), 1.48 – 1.40 (m, 1H), 1.33 (qt, J = 12.1, 3.9 Hz, 1H), 0.99 (d, J = 7.1 Hz, 3H); **^{13}C NMR** (151 MHz, $CDCl_3$) δ 176.0, 155.6, 141.6, 138.8, 137.0, 114.1, 114.0, 64.7, 55.1, 52.1, 51.0, 44.3, 32.5, 30.8, 30.1, 26.6, 20.6, 19.8, 14.9; **IR** (neat) 2925, 2851, 1732, 1602, 1482, 1411, 1308, 1254, 1196, 1164, 1070, 853 cm^{-1}; **HRMS** (DART) m/z Calcd for $C_{19}H_{30}NO_3$ (MH^+): 320.2226; found: 320.2211.

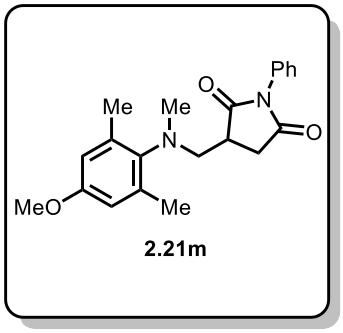

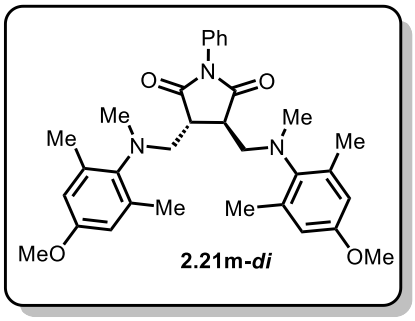

3-(((4-Methoxy-2,6-dimethylphenyl)(methyl)amino)methyl)-1-phenylpyrrolidine-2,5-dione (2.21m)

4-Methoxy-*N,N*,2,6-tetramethylaniline **2.13g** (0.2 mmol, 1.0 equiv.) was reacted with 1-phenyl-1*H*-pyrrole-2,5-dione **2.20h** (0.24 mmol, 1.2 equiv.) following the General Procedure using $B(C_6F_5)_3$ (10 mol%), benzene (0.2 mL) as the solvent and was carried out for 24 h at 70 °C. After purification by column chromatography (hexanes: EtOAc = 4:1), **2.21m** was obtained as a white solid (44 mg, 62%), **2.21m-*di*** was obtained as a white solid (14 mg, 27%).

2.21m: ^{1}H NMR (600 MHz, $CDCl_3$) δ 7.46 (t, *J* = 7.7 Hz, 2H), 7.40 – 7.36 (m, 1H), 7.26 – 7.23 (m, 2H), 6.56 (s, 2H), 3.75 (s, 3H), 3.69 (dd, *J* = 13.2, 4.1 Hz, 1H), 3.36 (dd, *J* = 13.2, 8.4 Hz, 1H), 3.09 (tt, *J* = 8.8, 4.5 Hz, 1H), 2.94 – 2.81 (m, 2H), 2.78 (s, 3H), 2.31 (s, 3H), 2.29 (s, 3H); **^{13}C NMR** (151 MHz, $CDCl_3$) δ 180.6, 178.7, 159.4, 144.3, 140.7, 140.5, 134.6, 131.8, 131.2, 129.0, 116.8, 116.7, 60.0, 57.9, 44.6, 44.0, 36.3, 22.1, 22.0; **IR** (neat) 2929, 2849, 1710, 1599, 1499, 1384, 1177, 1063, 756, 696 cm^{-1}; **HRMS** (DART) m/z Calcd for $C_{21}H_{25}N_2O_3$ (MH^+): 353.1865; found: 353.187.

3,4-Bis(((4-methoxy-2,6-dimethylphenyl)(methyl)amino)methyl)-1-phenylpyrrolidine-2,5-dione (2.21m-*di*): ^{1}H NMR (600 MHz, $CDCl_3$) δ 7.48 – 7.44 (m, 2H), 7.40 – 7.36 (m, 1H), 7.22

(dt, J = 8.4, 1.2 Hz, 2H), 6.51 (d, J = 3.0 Hz, 2H), 6.48 (d, J = 3.0 Hz, 2H), 3.73 (s, 6H), 3.56 (dd, J = 13.5, 5.3 Hz, 2H), 3.40 (dd, J = 13.5, 3.5 Hz, 2H), 3.01 (t, J = 4.1 Hz, 2H), 2.64 (s, 6H), 2.24 (s, 6H), 2.21 (s, 6H); **^{13}C NMR** (151 MHz, $CDCl_3$) δ 181.0, 159.3, 145.1, 140.3, 139.9, 134.8, 131.8, 131.1, 129.0, 117.0, 116.5, 59.5, 57.8, 48.3, 45.0, 22.2, 21.9; **IR** (neat) 2960, 2921, 1710, 1600, 1485, 1368, 1315, 1191, 1154, 1063 cm^{-1}; **HRMS** (DART) m/z Calcd for $C_{32}H_{40}N_3O_4$ (MH^+): 530.3019; found: 530.3021.

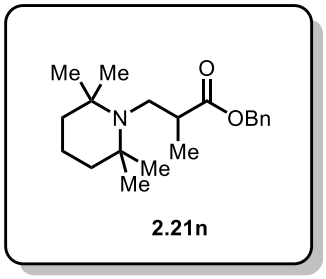

2.21n

Benzyl 2-methyl-3-(2,2,6,6-tetramethylpiperidin-1-yl)propanoate (2.21n)

1,2,2,6,6-Pentamethylpiperidine **2.13p** (0.2 mmol, 1.0 equiv.) was reacted with benzyl acrylate **2c** (0.24 mmol, 1.2 equiv.) following the General Procedure using $B(C_6F_5)_3$ (10 mol%), benzene (0.4 mL) as the solvent and was carried out for 12 h at 70 °C. After purification by column chromatography (hexanes: EtOAc = 10:1), **2.21n** was obtained as a colorless oil (57.8 mg, 91%).

^{1}H NMR (600 MHz, $CDCl_3$) δ 7.40 – 7.28 (m, 5H), 5.16 – 5.04 (m, 2H), 2.89 (dd, *J* = 15.4, 7.5 Hz, 1H), 2.64 (td, *J* = 7.5, 5.8 Hz, 1H), 2.48 (dd, *J* = 15.4, 5.6 Hz, 1H), 1.51 (s, 2H), 1.38 (dd, *J* = 6.7, 4.4 Hz, 4H), 1.13 (d, *J* = 7.1 Hz, 3H), 1.01 (s, 6H), 0.95 (s, 6H); **^{13}C NMR** (126 MHz, $CDCl_3$) δ177.1, 136.3, 128.4, 128.0, 128.0, 65.8, 54.6, 48.9, 44.2, 41.3, 17.8, 16.1; **IR** (neat) 2965, 2927, 1733, 1456, 1379, 1364, 1256, 1164, 696 cm^{-1}; **HRMS** (DART) m/z Calcd for $C_{20}H_{32}NO_2$ (MH^+): 318.2433; found: 318.2443.

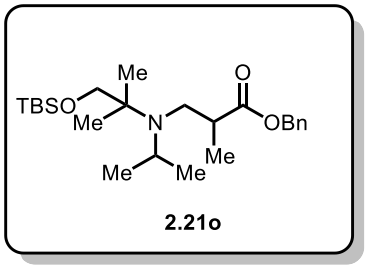

Benzyl 3-((1-((*tert*-butyldimethylsilyl)oxy)-2-methylpropan-2-yl)(isopropyl)amino)-2-methylpropanoate (2.21o)

1-((*tert*-Butyldimethylsilyl)oxy)-*N*-isopropyl-*N*,2-dimethylpropan-2-amine **2.13r** (0.2 mmol, 1.0 equiv.) was reacted with benzyl acrylate **2.20b** (0.24 mmol, 1.2 equiv.) following the General Procedure using $B(C_6F_5)_3$ (10 mol%) and 0.2 mL benzene as the solvent and was carried out for 12 h at 22 °C.. After purification by column chromatography (hexanes: Et_3N = 49:1), **2.21o** was obtained as a colorless oil (76.6 mg, 91%).

^{1}H NMR (500 MHz, $CDCl_3$) δ 7.37 – 7.26 (m, 5H), 5.14 – 5.05 (m, 2H), 3.39 – 3.33 (m, 2H), 3.25 (qd, *J* = 8.2, 7.5, 5.3 Hz, 1H), 3.04 – 2.97 (m, 1H), 2.70 – 2.59 (m, 2H), 1.09 (dt, *J* = 6.7, 1.6 Hz, 3H), 1.01 (d, *J* = 9.7 Hz, 9H), 0.95 (dt, *J* = 6.7, 1.5 Hz, 3H), 0.87 (t, *J* = 1.5 Hz, 9H); **^{13}C NMR** (126 MHz, $CDCl_3$) δ176.7, 136.4, 128.4, 128.0, 127.9, 69.6, 65.7, 59.3, 47.4, 46.4, 42.9, 25.9, 24.32, 24.28, 18.2, 15.2, -5.6; **IR** (neat) 2956, 2929, 2856, 1734, 1461, 1250, 1156, 1085, 834, 773, 667 cm^{-1}; **HRMS** (DART) m/z Calcd for $C_{24}H_{44}NO_3Si$ (MH^+): 422.309; found: 422.3102.

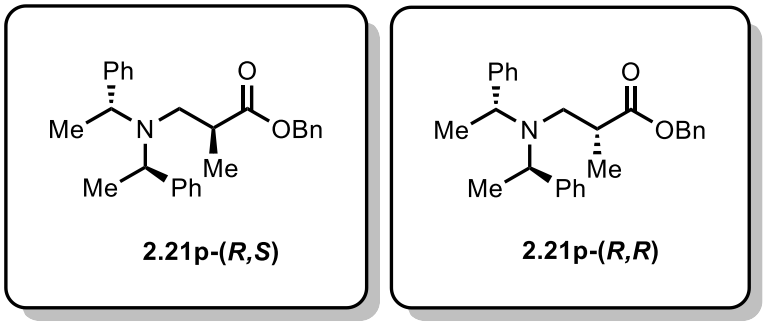

Benzyl 3-(bis((*R*)-1-phenylethyl)amino)-2-methylpropanoate (2.21p)

(*R*)-*N*-Methyl-1-phenyl-*N*-((*R*)-1-phenylethyl)ethan-1-amine **2.13w** (0.2 mmol, 1 equiv.) was reacted with benzyl acrylate **2.20b** (0.24 mmol, 1.2 equiv.) following the General Procedure using $B(C_6F_5)_3$ (10 mol%), DCM (0.4 mL) as the solvent and was carried out for 12 h at 70 °C. ^{1}H NMR analysis of the crude material revealed that **2.21p-(*R*,*S*)** and **2.21p-(*R*,*R*)** were obtained in the ratio of 1.5:1.0. After purification by column chromatography (hexanes: Et_2O = 30:1), **2.21p** was obtained as a colorless oil (72.5 mg, 91%). Further purification was carried out by PTLC using Et_2O: hexanes = 1:9 as the eluent to separate **2.21p-(*R*,*S*)** and **2.21p-(*R*,*R*)**.

2.21p-(*R*,*S*): ^{1}H NMR (500 MHz, $CDCl_3$) δ 7.41 – 7.31 (m, 4H), 7.28 – 7.18 (m, 6H), 5.19 – 5.07 (m, 2H), 3.84 (q, *J* = 6.9 Hz, 2H), 3.10 (dd, *J* = 14.0, 8.3 Hz, 1H), 2.52 (q, *J* = 7.1 Hz, 1H), 2.36 (dd, *J* = 14.0, 6.2 Hz, 1H), 1.33 (d, *J* = 6.9 Hz, 6H), 0.90 (d, *J* = 6.9 Hz, 3H); **^{13}C NMR** (126 MHz, $CDCl_3$) δ176.4, 144.4, 136.2, 128.5, 128.14, 128.06, 128.0, 127.9, 126.6, 66.0, 58.4, 50.1, 41.6, 18.9, 15.2; **IR** (neat) 2971, 1731, 1492, 1452, 1174, 1144, 748, 695 cm^{-1}; **HRMS** (DART) m/z Calcd for $C_{27}H_{32}NO_2$ (MH^+): 402.2433; found: 402.2451.

2.21p-(*R*,*R*): ^{1}H NMR (500 MHz, $CDCl_3$) δ 7.33 (dd, *J* = 12.7, 6.9 Hz, 2H), 7.28 – 7.23 (m, 6H), 7.19 (q, *J* = 4.9, 4.5 Hz, 2H), 4.97 (d, *J* = 12.5 Hz, 1H), 4.83 (d, *J* = 12.5 Hz,1H), 3.94 (q, *J* = 6.9 Hz, 2H), 2.80 (qd, *J* = 13.8, 7.2 Hz, 2H), 2.62 (h, *J* = 7.0 Hz, 1H), 1.37 (d, *J* = 6.8 Hz, 6H), 1.13

(d, J = 6.9 Hz, 3H); **^{13}C NMR** (126 MHz, $CDCl_3$) δ 175.8, 144.4, 136.3, 128.4, 127.94, 127.92, 126.6, 65.8, 57.7, 49.7, 40.7, 18.0, 15.4; **IR** (neat) 2970, 1732, 1492, 1452, 1356, 1218, 1177, 751, 698 cm^{-1}; **HRMS** (DART) m/z Calcd for $C_{27}H_{32}NO_2$ (MH^+): 402.2433; found: 402.2442.

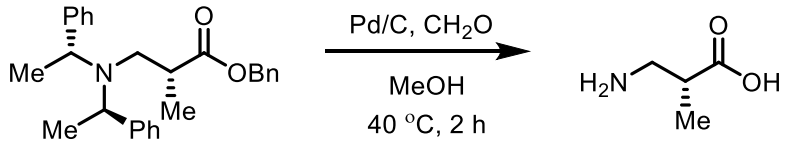

2.21p-(*R,R*)

The minor diastereomer was obtained from three reactions following the General Procedure using $B(C_6F_5)_3$ (10 mol%), DCM (0.6 mL) as the solvent and was carried out for 12 h at 70 °C on 0.6 mmol scale. The derivatization of the minor diastereomer was performed based on the literature previously reported.[18] The minor diastereomer (190 mg, 0.47 mmol) was dissolved in a solution of 4.4% formic acid in MeOH (9.4 mL), whereupon Pd-C (10 mol%, 162 mg) was added. The reaction mixture was then heated at 40 °C for 2 h. Upon cooling, the suspension was filtered through a pad of Celite and the mixture was concentrated to remove the solvent and volatile side products to obtain the product as a colorless oil (48 mg, >95% yield). $[\alpha]^{25}_D = -4.8°$ (c = 1.0, H_2O). Based on the observed optical rotation value, the absolute configuration of the minor diastereomer was assigned as **2.21p-(*R,R*)**.

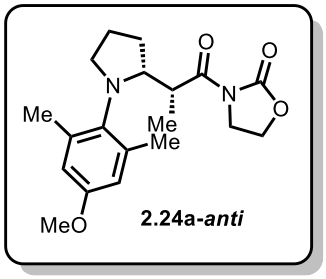

3-(2-(1-(4-Methoxy-2,6-dimethylphenyl)pyrrolidin-2-yl)propanoyl)oxazolidin-2-one (2.24a)

1-(4-Methoxy-2,6-dimethylphenyl)pyrrolidine **2.13k** was reacted with 3-acryloyloxazolidin-2-one **2.23a** following the General Procedure for Stereoselective Mannich Reactions. The ^{1}H NMR analysis of the crude material revealed **2.24a** was obtained in >95% yield as a mixture of diastereomers; the ratio of **2.24a-*anti*** and **2.24a-*syn*** was determined to be 1.6:1. $[\alpha]^{25}_{D} = -18.2°$ (c = 1.0, EtOH). The absolute configuration of **2.24a-*anti*** was assigned in analogy (see SI Section 4).

^{1}H NMR (600 MHz, $CDCl_3$) δ 6.55 (d, *J* = 2.9 Hz, 1H), 6.49 (d, *J* = 3.0 Hz, 1H), 4.20 (td, *J* = 9.0, 4.8 Hz, 1H), 4.04 – 3.99 (m, 2H), 3.73 (s, 3H), 3.68 (dd, *J* = 8.0, 6.7 Hz, 1H), 3.60 (dt, *J* = 10.5, 9.1 Hz, 1H), 3.32 (q, *J* = 7.5 Hz, 1H), 3.13 (ddd, *J* = 10.4, 9.2, 4.8 Hz, 1H), 2.99 (td, *J* = 8.4, 4.6 Hz, 1H), 2.27 (s, 3H), 2.22 (s, 3H), 2.14 – 2.08 (m, 1H), 2.01 – 1.94 (m, 1H), 1.93 – 1.86 (m, 1H), 1.77 – 1.71 (m, 1H), 1.12 (d, *J* = 6.9 Hz, 3H); **^{13}C NMR** (151 MHz, $CDCl_3$) δ176.4, 156.7, 153.0, 141.1, 140.8, 136.8, 113.7, 112.4, 62.8, 61.7, 55.2, 51.7, 42.9, 42.6, 30.8, 24.4, 19.4, 19.1, 15.6; **IR** (neat) 2962, 2837, 1775, 1695, 1601, 1478, 1384, 1267, 1221, 1194, 1154, 1066 cm^{-1}; **HRMS** (DART) m/z Calcd for $C_{19}H_{27}N_2O_4$ (MH^+): 347.1971; found: 347.1964. **HPLC** (Chiralpak IA; 10%/ 90% hexane/ isopropanol, 1.0 mL/min; **2.24a-*anti*:** tr = 6.8 min (major), 6.2 min (minor); 80:20 er; **2.24a-*syn***: 8.4 min (major), 7.6 min (minor) 68:32 er).

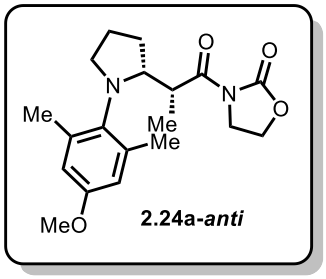


```
Acq. Operator    : SYSTEM                          Seq. Line :   2
                                                    Location :   11
Injection Date   : 6/17/2017 6:58:53 PM                Inj :   1
Acq. Method      : column1 10% IPA 90% hexane 60min-1.0mL.M
Analysis Method  : C:\Chem32\1\Data\JOE 2017-06-17 18-41-04\column1 10% IPA 90% hexane 60min-1
                   .0mL.M (Sequence Method)
Last changed     : 6/17/2017 6:41:05 PM by SYSTEM
Method Info      : Washing 60min-10% iPrOH 90% hexane-1.0mL
```

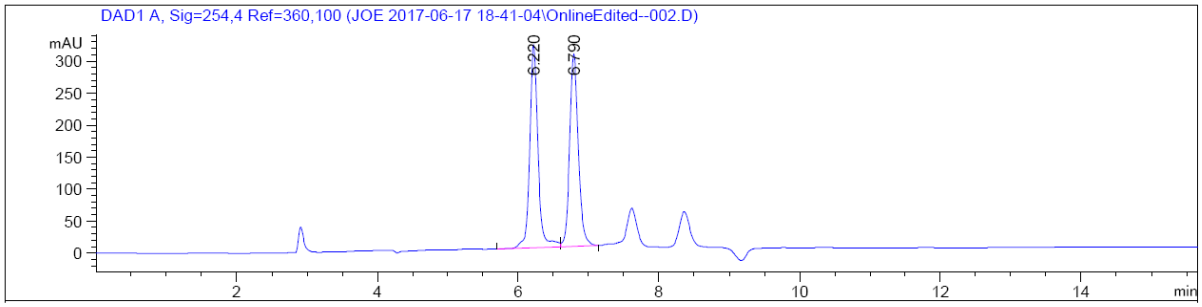

Signal 1: DAD1 A, Sig=254,4 Ref=360,100

Peak #	RetTime [min]	Type	Width [min]	Area [mAU*s]	Height [mAU]	Area %
1	6.220	BV R	0.1227	2598.01807	317.40524	50.1526
2	6.790	VB	0.1303	2582.20337	300.33380	49.8474

```
Acq. Operator   : SYSTEM                          Seq. Line :   2
Acq. Instrument : Wasa_LC1                         Location :   81
Injection Date  : 12/4/2017 3:14:54 PM                Inj :   1
                                                 Inj Volume : 4.000 µl
Method          : C:\Chem32\1\Data\JOE 2017-12-04 14-42-57\column1 10% IPA 90% hexane 30min-1
                  .0mL.M (Sequence Method)
Last changed    : 12/4/2017 2:42:59 PM by SYSTEM
Method Info     : Washing 30min-10% iPrOH 90% hexane-1.0mL

Additional Info : Peak(s) manually integrated
```

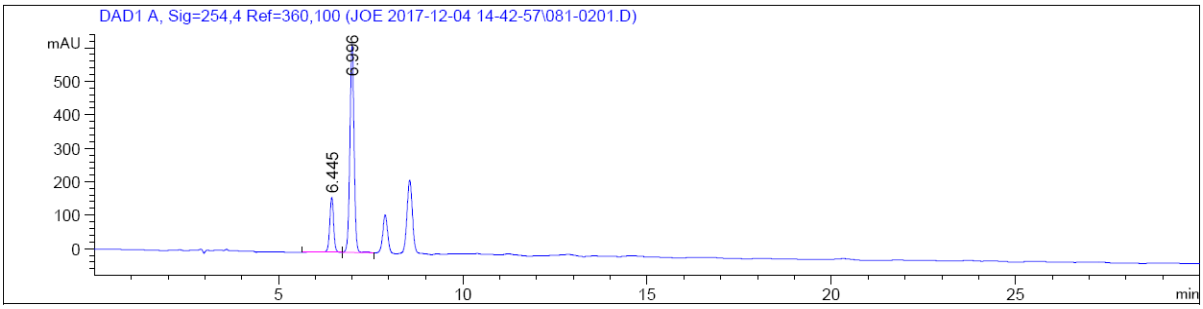

Signal 1: DAD1 A, Sig=254,4 Ref=360,100

Peak #	RetTime [min]	Type	Width [min]	Area [mAU*s]	Height [mAU]	Area %
1	6.445	VB R	0.1153	1247.11548	163.76060	19.9504
2	6.996	BV R	0.1234	5003.96973	619.55853	80.0496

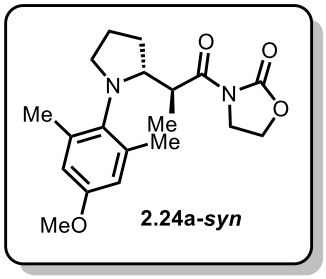


```
Acq. Operator    : SYSTEM                          Seq. Line :   2
                                                    Location :   11
Injection Date   : 6/17/2017 6:58:53 PM                Inj :   1
Acq. Method      : column1 10% IPA 90% hexane 60min-1.0mL.M
Analysis Method  : C:\Chem32\1\Data\JOE 2017-06-17 18-41-04\column1 10% IPA 90% hexane 60min-1
                   .0mL.M (Sequence Method)
Last changed     : 6/17/2017 6:41:05 PM by SYSTEM
Method Info      : Washing 60min-10% iPrOH 90% hexane-1.0mL
```

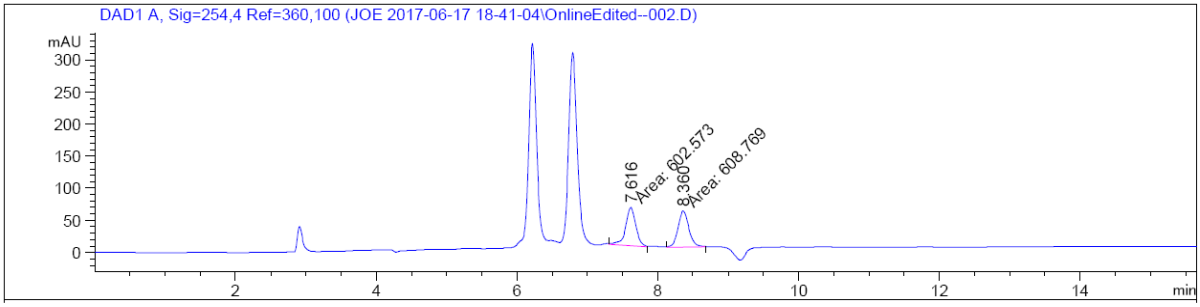

Signal 1: DAD1 A, Sig=254,4 Ref=360,100

Peak #	RetTime [min]	Type	Width [min]	Area [mAU*s]	Height [mAU]	Area %
1	7.616	MM	0.1688	602.57312	59.48536	49.7443
2	8.360	MM	0.1794	608.76910	56.56682	50.2557

```
Acq. Operator    : SYSTEM                          Seq. Line :   2
Acq. Instrument  : Wasa_LC1                         Location :   81
Injection Date   : 12/4/2017 3:14:54 PM                Inj :   1
                                                  Inj Volume : 4.000 µl
Method           : C:\Chem32\1\Data\JOE 2017-12-04 14-42-57\column1 10% IPA 90% hexane 30min-1
                   .0mL.M (Sequence Method)
Last changed     : 12/4/2017 2:42:59 PM by SYSTEM
Method Info      : Washing 30min-10% iPrOH 90% hexane-1.0mL
```

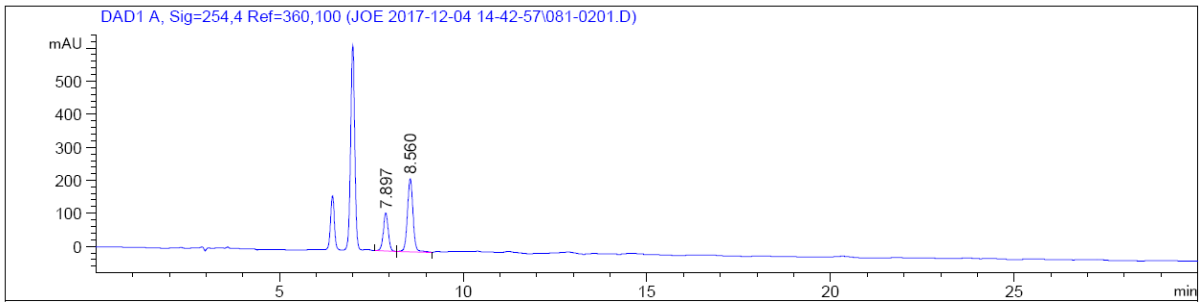

Signal 1: DAD1 A, Sig=254,4 Ref=360,100

Peak #	RetTime [min]	Type	Width [min]	Area [mAU*s]	Height [mAU]	Area %
1	7.897	BB	0.1432	1078.82910	115.25144	31.6807
2	8.560	BB	0.1625	2326.48999	221.55330	68.3193

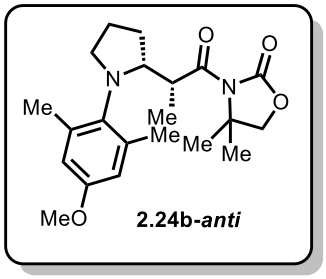

3-(2-(1-(4-Methoxy-2,6-dimethylphenyl)pyrrolidin-2-yl)propanoyl)-4,4-dimethyloxazolidin-2-one (2.24b)

1-(4-Methoxy-2,6-dimethylphenyl)pyrrolidine **2.13k** was reacted with 3-acryloyl-4,4-dimethyloxazolidin-2-one **2.23b** following the General Procedure for Stereoselective Mannich Reactions. The ^{1}H NMR analysis of the crude material revealed **2.24b** was obtained in 88% yield as a mixture of diastereomers; the ratio of **2.24b-*anti*** and **2.24b-*syn*** was determined to be 4.3:1. $[\alpha]^{25}_{D} = -31.1°$ (c = 1.0, EtOH).

^{1}H NMR (500 MHz, $CDCl_3$) δ 6.53 – 6.50 (m, 2H), 4.02 (q, *J* = 6.7 Hz, 1H), 3.84 (d, *J* = 8.3 Hz, 1H), 3.74 (d, *J* = 8.4 Hz, 1H), 3,73 – 3.71 (m, 4H), 3.30 (ddd, *J* = 8.4, 7.2, 5.6 Hz, 1H), 2.97 (td, *J* = 7.9, 6.1 Hz, 1H), 2.26 (s, 3H), 2.24 (s, 3H), 2.10 (dtd, *J* = 11.8, 7.0, 5.9 Hz, 1H), 2.01 – 1.88 (m, 2H), 1.87 – 1.80 (m, 1H), 1.37 (s, 3H), 1.12 (d, *J* = 7.0 Hz, 3H), 1.10 (s, 3H); **^{13}C NMR** (126 MHz, $CDCl_3$) δ 177.1, 156.7, 153.5, 140.6, 139.5, 137.6, 114.4, 112.8, 74.7, 61.8, 55.1, 54.0, 52.5, 44.2, 29.9, 25.1, 24.4, 24.1, 19.4, 15.0; **IR** (neat) 2963, 2836, 1773, 1698, 1602, 1481, 1376, 1303, 1176, 1154, 1071, 765 cm^{-1}; **HRMS** (DART) m/z Calcd for $C_{21}H_{31}N_2O_4$ (MH^+): 375.2284; found: 375.2292. **HPLC** (Chiralpak IC; 2.5%/ 97.5% hexane/ isopropanol, 0.5 mL/min; **2.24b-*anti*:** tr = 25.1 min (major), 19.3 min (minor); 97:3 er; **2.24b-*syn***: 22.1 min (major), 20.9 min (minor) 98:2 er).

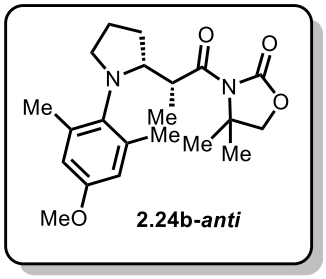


```
Acq. Operator    : SYSTEM                          Seq. Line :   2
Acq. Instrument  : Wasa_LC1                         Location :   1
Injection Date   : 8/7/2017 11:53:09 PM                Inj :   1
                                                  Inj Volume : 4.000 µl
Method           : C:\Chem32\1\Data\JOE 2017-08-07 23-36-08\column1 2.5% IPA 97.5% hex 40min-0
                   .5mL.M (Sequence Method)
Last changed     : 8/7/2017 11:36:10 PM by SYSTEM
Method Info      : Washing 40min-2.5% iPrOH 97.5% hexane-0.5mL
```

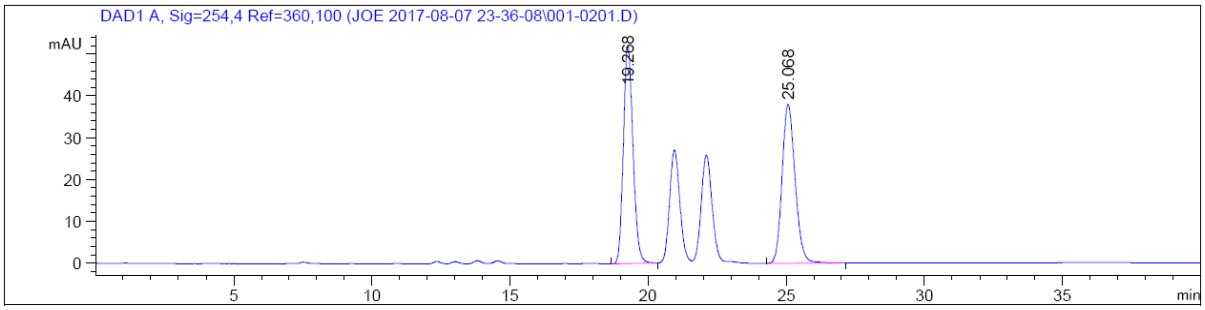

Signal 1: DAD1 A, Sig=254,4 Ref=360,100

Peak #	RetTime [min]	Type	Width [min]	Area [mAU*s]	Height [mAU]	Area %
1	19.268	BB	0.3750	1255.30591	52.11531	50.1904
2	25.068	BB	0.5073	1245.78149	37.91677	49.8096

Acq. Operator : SYSTEM Seq. Line : 4
Acq. Instrument : Wasa_LC1 Location : 12
Injection Date : 8/9/2017 10:38:27 PM Inj : 1
Inj Volume : 4.000 µl
Method : C:\Chem32\1\Data\JOE 2017-08-09 21-23-42\column1 2.5% IPA 97.5% hex 40min-0.5mL.M (Sequence Method)
Last changed : 8/9/2017 9:23:43 PM by SYSTEM
Method Info : Washing 40min-2.5% iPrOH 97.5% hexane-0.5mL

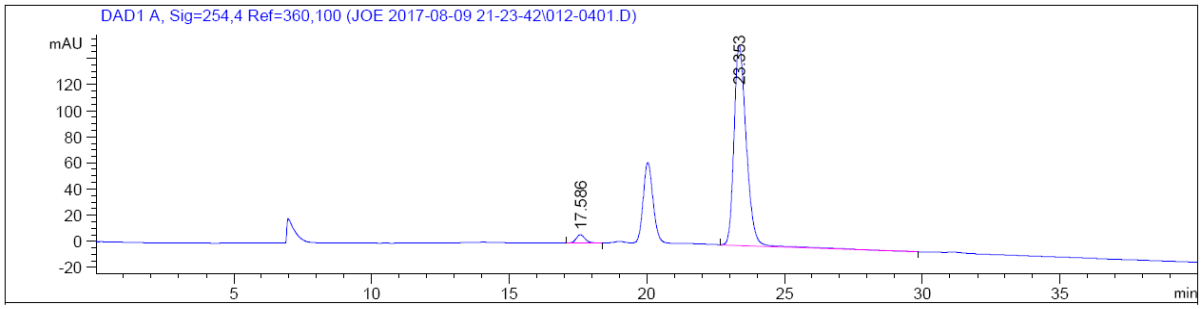

Signal 1: DAD1 A, Sig=254,4 Ref=360,100

Peak #	RetTime [min]	Type	Width [min]	Area [mAU*s]	Height [mAU]	Area %
1	17.586	BB	0.3424	139.11646	6.28083	2.8199
2	23.353	BB	0.4809	4794.23730	153.27171	97.1801

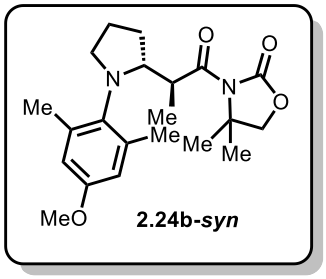


```
Acq. Operator    : SYSTEM                          Seq. Line :   2
Acq. Instrument  : Wasa_LC1                         Location :   1
Injection Date   : 8/7/2017 11:53:09 PM                 Inj :   1
                                                  Inj Volume : 4.000 µl
Method           : C:\Chem32\1\Data\JOE 2017-08-07 23-36-08\column1 2.5% IPA 97.5% hex 40min-0
                   .5mL.M (Sequence Method)
Last changed     : 8/7/2017 11:36:10 PM by SYSTEM
Method Info      : Washing 40min-2.5% iPrOH 97.5% hexane-0.5mL
```

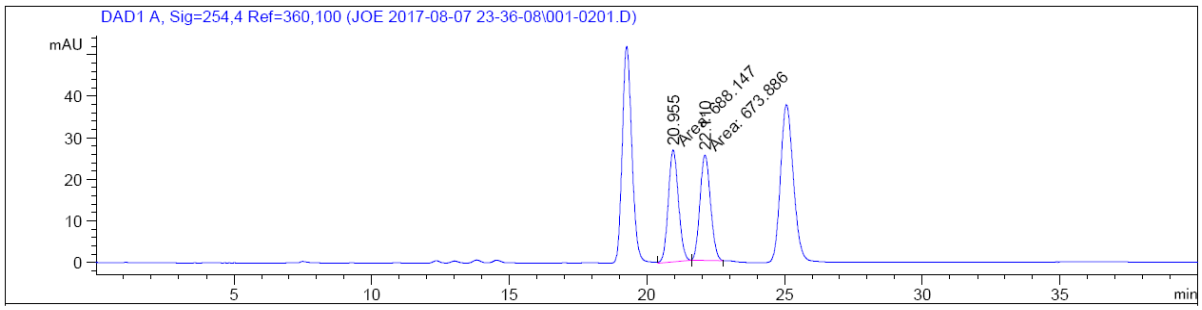

Signal 1: DAD1 A, Sig=254,4 Ref=360,100

Peak #	RetTime [min]	Type	Width [min]	Area [mAU*s]	Height [mAU]	Area %
1	20.955	MM	0.4269	688.14746	26.86458	50.5235
2	22.110	MM	0.4435	673.88586	25.32295	49.4765

```
Acq. Operator   : SYSTEM                          Seq. Line :   4
Acq. Instrument : Wasa_LC1                         Location :   12
Injection Date  : 8/9/2017 10:38:27 PM                Inj :   1
                                                 Inj Volume : 4.000 µl
Method          : C:\Chem32\1\Data\JOE 2017-08-09 21-23-42\column1 2.5% IPA 97.5% hex 40min-0
                  .5mL.M (Sequence Method)
Last changed    : 8/9/2017 9:23:43 PM by SYSTEM
Method Info     : Washing 40min-2.5% iPrOH 97.5% hexane-0.5mL
```

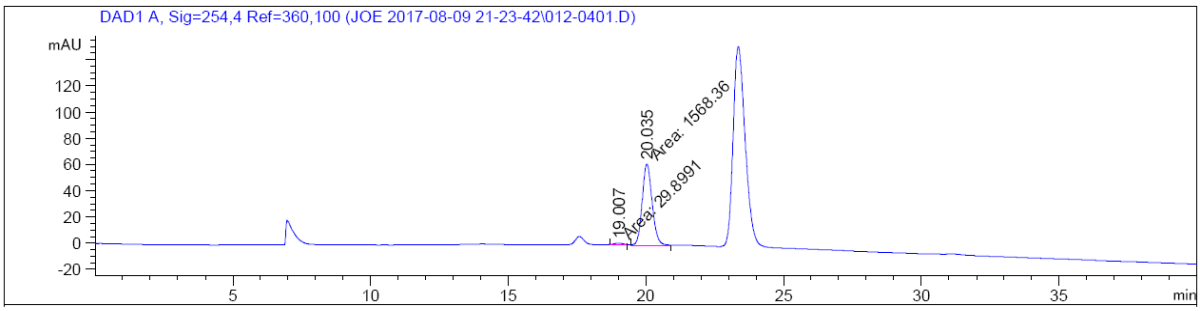

Signal 1: DAD1 A, Sig=254,4 Ref=360,100

Peak #	RetTime [min]	Type	Width [min]	Area [mAU*s]	Height [mAU]	Area %
1	19.007	MM	0.3936	29.89911	1.26620	1.8707
2	20.035	MM	0.4209	1568.36365	62.10253	98.1293

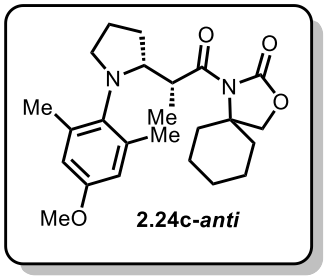

1-(2-(1-(4-Methoxy-2,6-dimethylphenyl)pyrrolidin-2-yl)propanoyl)-3-oxa-1-azaspiro[4.5]decan-2-one (2.24c)

1-(4-Methoxy-2,6-dimethylphenyl)pyrrolidine **2.13k** was reacted with 1-acryloyl-3-oxa-1-azaspiro[4.5]decan-2-one **2.23c** following the General Procedure for Stereoselective Mannich Reactions. The ^{1}H NMR analysis of the crude material revealed **2.24c** was obtained in 79% yield as a mixture of diastereomers; the ratio of **2.24c-*anti*** and **2.24c-*syn*** was determined to be 5.6:1. $[\alpha]^{25}_{D} = -47.5°$ (c = 1.0, EtOH). The absolute configuration of **2.24c-*anti*** was assigned in analogy

^{1}H NMR (600 MHz, $CDCl_3$) δ6.52 (t, *J* = 2.8 Hz, 2H), 4.07 (d, *J* = 8.5 Hz, 1H), 3.99 (q, *J* = 6.6 Hz, 1H), 3.87 (dd, *J* = 8.5, 1.1 Hz, 1H), 3.75 (t, *J* = 6.8 Hz, 1H), 3.71 (s, 3H), 3.29 (td, *J* = 7.8, 5.5 Hz, 1H), 2.97 (td, *J* = 8.0, 6.5 Hz, 1H), 2.25 (s, 3H), 2.24 (s, 3H), 2.17 – 2.06 (m, 2H), 1.97 – 1.89 (m, 2H), 1.85 (ddd, *J* = 11.3, 7.4, 5.7 Hz, 1H), 1.76 – 1.69 (m, 1H), 1.66 – 1.62 (m, 1H), 1.57 – 1.53 (m, 1H), 1.49 – 1.45 (m, 1H), 1.18 – 1.08 (m, 7H), 1.07 – 1.01 (m, 1H); **^{13}C NMR** (151 MHz, $CDCl_3$) δ 177.6, 156.7, 154.0, 140.5, 139.3, 137.6, 114.3, 112.9, 71.3, 63.9, 61.9, 55.1, 52.6, 44.3, 31.9, 31.2, 29.7, 25.2, 24.0, 22.9, 22.8, 19.4, 19.2, 14.8; **IR** (neat) 2929, 2860, 1771, 1698, 1602, 1482, 1456, 1375, 1318, 1262, 1224, 1157, 1071 cm^{-1}; **HRMS** (DART) m/z Calcd for $C_{24}H_{35}N_2O_4$ (MH^+): 415.2597; found: 415.2594. **HPLC** (Chiralcel IA; 2.5%/ 97.5% hexane/ isopropanol, 0.5 mL/min; **3s-*anti*:** tr = 12.6 min (major), 14.7 min (minor); 95:5 er; **3s-*syn***: 13.4 min (major), 16.9 min (minor) 98:2 er).

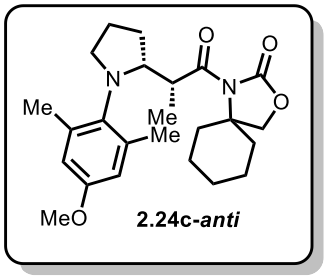


```
Acq. Operator   : SYSTEM                          Seq. Line :   2
                                                   Location :   11
Injection Date  : 7/22/2017 4:42:06 PM                 Inj :   1
Acq. Method     : column1 2.5% IPA 97.5% hex 40min-0.5mL.M
Analysis Method : C:\Chem32\1\Data\JOE 2017-07-22 16-24-18\column1 2.5% IPA 97.5% hex 40min-0
                  .5mL.M (Sequence Method)
Last changed    : 7/22/2017 4:24:19 PM by SYSTEM
Method Info     : Washing 40min-2.5% iPrOH 97.5% hexane-0.5mL
```

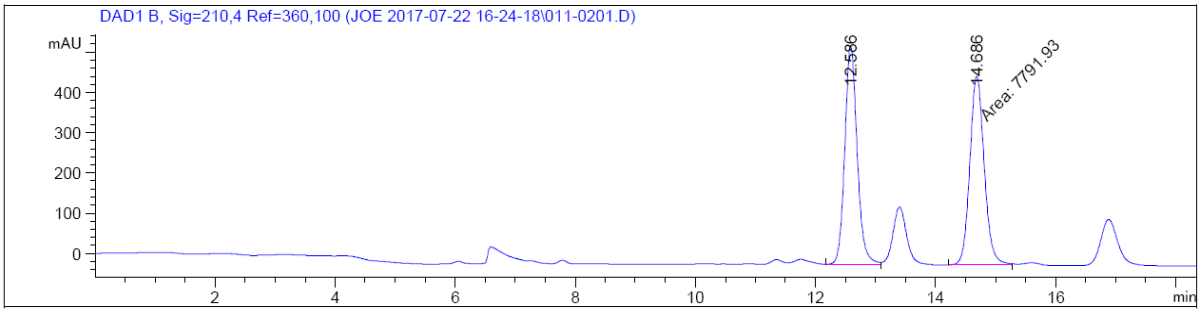

Signal 2: DAD1 B, Sig=210,4 Ref=360,100

Peak #	RetTime [min]	Type	Width [min]	Area [mAU*s]	Height [mAU]	Area %
1	12.586	BV	0.2193	7810.43555	544.58679	50.0593
2	14.686	MM	0.2769	7791.93359	469.04736	49.9407

```
Acq. Operator    : SYSTEM                          Seq. Line :   2
Acq. Instrument  : Wasa_LC1                         Location :   1
Injection Date   : 7/31/2017 3:20:09 PM                 Inj :   1
                                                 Inj Volume : 4.000 µl
Method           : C:\Chem32\1\Data\JOE 2017-07-31 15-02-20\column1 2.5% IPA 97.5% hex 40min-0
                   .5mL.M (Sequence Method)
Last changed     : 7/31/2017 3:02:21 PM by SYSTEM
Method Info      : Washing 40min-2.5% iPrOH 97.5% hexane-0.5mL
```

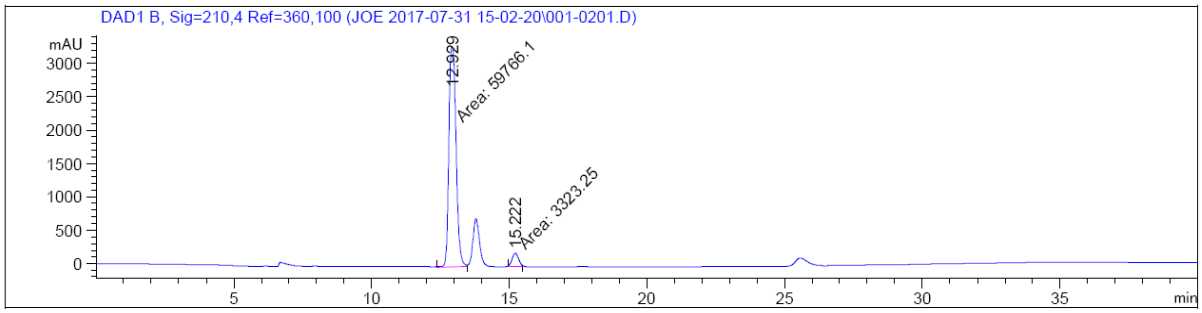

Signal 2: DAD1 B, Sig=210,4 Ref=360,100

Peak #	RetTime [min]	Type	Width [min]	Area [mAU*s]	Height [mAU]	Area %
1	12.929	MM	0.3012	5.97661e4	3306.89624	94.7325
2	15.222	MM	0.2748	3323.25269	201.53804	5.2675

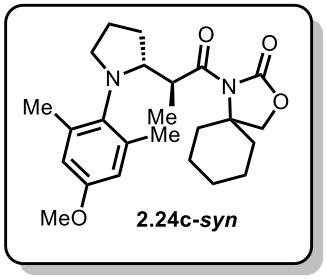


```
Acq. Operator   : SYSTEM                          Seq. Line :   2
                                                   Location :   11
Injection Date  : 7/22/2017 4:42:06 PM                Inj :   1
Acq. Method     : column1 2.5% IPA 97.5% hex 40min-0.5mL.M
Analysis Method : C:\Chem32\1\Data\JOE 2017-07-22 16-24-18\column1 2.5% IPA 97.5% hex 40min-0
                  .5mL.M (Sequence Method)
Last changed    : 7/22/2017 4:24:19 PM by SYSTEM
Method Info     : Washing 40min-2.5% iPrOH 97.5% hexane-0.5mL
```

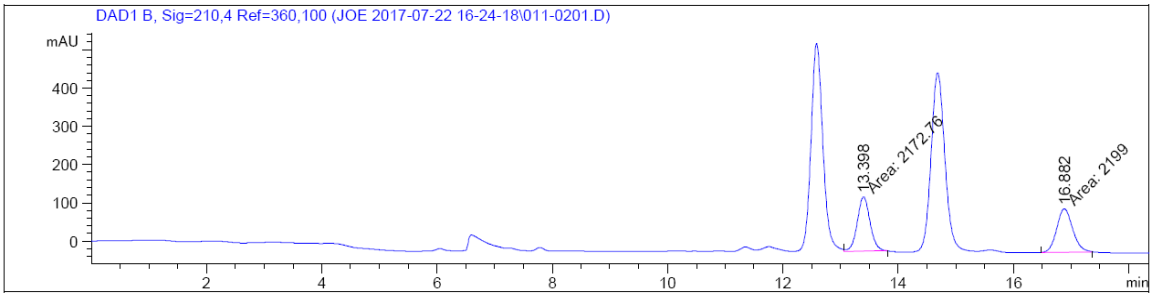

Signal 2: DAD1 B, Sig=210,4 Ref=360,100

Peak #	RetTime [min]	Type	Width [min]	Area [mAU*s]	Height [mAU]	Area %
1	13.398	MM	0.2555	2172.76001	141.74721	49.6999
2	16.882	MM	0.3208	2199.00220	114.25597	50.3001

Acq. Operator : SYSTEM Seq. Line : 2
Acq. Instrument : Wasa_LC1 Location : 1
Injection Date : 7/31/2017 3:20:09 PM Inj : 1
Inj Volume : 4.000 µl
Method : C:\Chem32\1\Data\JOE 2017-07-31 15-02-20\column1 2.5% IPA 97.5% hex 40min-0.5mL.M (Sequence Method)
Last changed : 7/31/2017 3:02:21 PM by SYSTEM
Method Info : Washing 40min-2.5% iPrOH 97.5% hexane-0.5mL

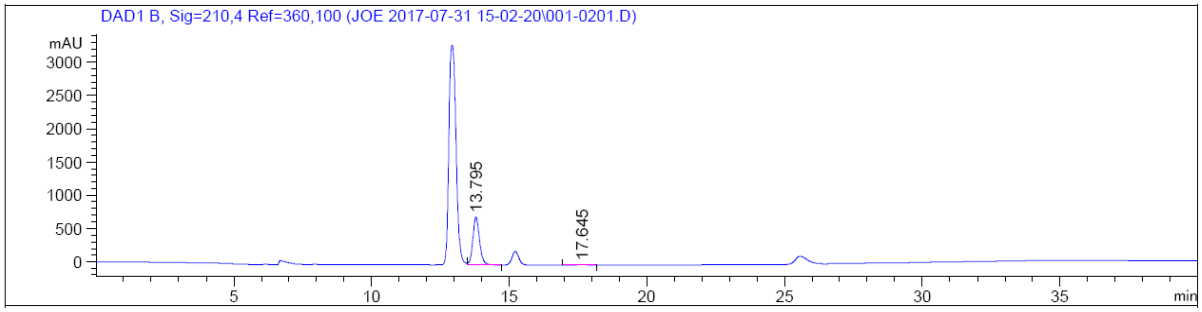

Signal 2: DAD1 B, Sig=210,4 Ref=360,100

Peak #	RetTime [min]	Type	Width [min]	Area [mAU*s]	Height [mAU]	Area %
1	13.795	VB	0.2598	1.22359e4	721.54706	98.0554
2	17.645	BB	0.3192	242.66100	11.73826	1.9446

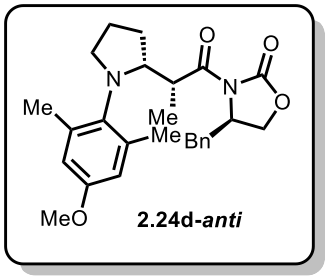

(4*R*)-4-Benzyl-3-(2-(1-(4-methoxy-2,6-dimethylphenyl)pyrrolidin-2-yl)propanoyl)oxazolidin-2-one (2.24d)

1-(4-Methoxy-2,6-dimethylphenyl)pyrrolidine **2.13k** was reacted with (*R*)-3-acryloyl-4-benzyloxazolidin-2-one **2.23d** following the General Procedure for Stereoselective Mannich Reactions. The ^{1}H NMR analysis of the crude material revealed **2.24d** was obtained in 66% yield as a mixture of diastereomers; the ratio of diastereomers was determined to be 12:2:1:0.

^{1}H NMR (500 MHz, $CDCl_3$) δ 7.32 – 7.22 (m, 3H), 7.10 – 7.04 (m, 2H), 6.50 (s, 2H), 4.05 (td, *J* = 8.2, 5.9 Hz, 1H), 3.93 (dd, *J* = 8.3, 1.5 Hz, 1H), 3.85 – 3.75 (m, 2H), 3.68 (s, 3H), 3.66 – 3.59 (m,1H), 3.32 (q, *J* = 7.5 Hz, 1H), 3.03 – 2.97 (m, 2H), 2.62 (dd, *J* = 13.5, 8.7 Hz, 1H), 2.26 (s, 3H), 2.24 (s, 3H), 2.16 – 2.09 (m, 1H), 2.01 – 1.89 (m, 2H), 1.74 (dq, *J* = 11.0, 8.4 Hz, 1H), 1.17 (d, *J* = 6.9 Hz, 3H); **^{13}C NMR** (151 MHz, $CDCl_3$) δ 178.7, 159.4, 155.5, 143.80, 143.76, 139.4, 138.0, 132.0, 131.4, 129.8, 116.3, 115.2, 68.5, 65.2, 57.8, 54.2, 45.6, 40.3, 33.6, 27.1, 22.1, 21.8, 18.5; **IR** (neat) 2959, 2923, 2852, 1776, 1692, 1601, 1481, 1383, 1210, 1154, 1067, 703 cm^{-1}; **HRMS** (DART) m/z Calcd for $C_{26}H_{33}N_2O_4$ (MH^+): 437.244; found: 437.2436.

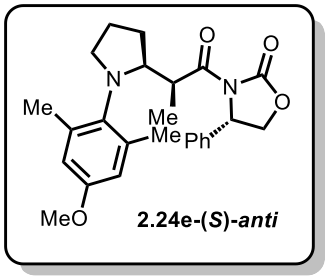

(4*S*)-3-(2-(1-(4-Methoxy-2,6-dimethylphenyl)pyrrolidin-2-yl)propanoyl)-4-phenyloxazolidin-2-one (2.24e-(*S*))

1-(4-Methoxy-2,6-dimethylphenyl)pyrrolidine **2.13k** was reacted with (*S*)-3-acryloyl-4-phenyloxazolidin-2-one **2.23e-(*S*)** following the General Procedure for Stereoselective Mannich Reactions. The ^{1}H NMR analysis of the crude material revealed **2.24e-(*S*)** was obtained in 61% yield as a mixture of diastereomers; the ratio of diaseteromers was determined to be 3.6:2.1:1:0.

^{1}H NMR (600 MHz, $CDCl_3$) δ 7.38 – 7.29 (m, 3H), 7.21 – 7.17 (m, 2H), 6.53 (s, 2H), 5.31 (dd, *J* = 8.8, 3.8 Hz, 1H), 4.57 (t, *J* = 8.8 Hz, 1H), 4.18 (dd, *J* = 8.9, 3.9 Hz, 1H), 3.87 (dt, *J* = 7.1, 4.5 Hz, 1H), 3.75 (s, 3H), 3.70 – 3.65 (m, 1H), 3.23 (ddd, *J* = 8.5, 6.9, 3.4 Hz, 1H), 2.97 (q, *J* = 8.1 Hz, 1H), 2.24 (s, 3H), 2.19 (s, 3H), 1.85 – 1.79 (m, 2H), 1.76 – 1.72 (m, 2H), 1.19 (d, *J* = 6.9 Hz, 3H); **^{13}C NMR** (151 MHz, $CDCl_3$) δ175.6, 156.5, 153.0, 140.3, 139.2, 138.2, 137.5, 129.0, 128.5, 126.0, 114.6, 113.0, 69.6, 61.8, 57.7, 55.0, 52.8, 42.8, 27.2, 25.7, 19.30, 19.25, 11.4; **IR** (neat) 2955, 2835, 1777, 1699, 1602, 1480, 1457, 1382, 1316, 1262, 1194, 1153, 699 cm^{-1}; **HRMS** (DART) m/z Calcd for $C_{25}H_{31}N_2O_4$ (MH^+): 423.2284; found: 423.2267.

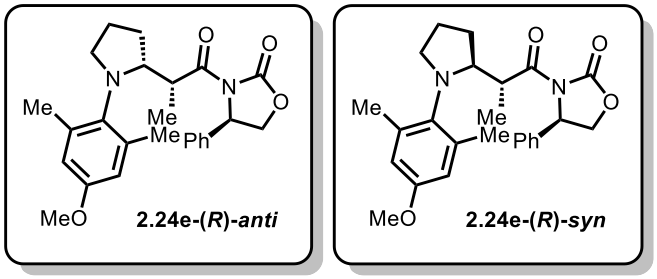

(*R*)-3-((*R*)-2-((*R*)-1-(4-methoxy-2,6-dimethylphenyl)pyrrolidin-2-yl)propanoyl)-4-phenyloxazolidin-2-one (2.24e-(*R*))

1-(4-Methoxy-2,6-dimethylphenyl)pyrrolidine **2.13k** was reacted with (*R*)-3-acryloyl-4-phenyloxazolidin-2-one **2.23e-(*R*)** following the General Procedure for Stereoselective Mannich Reactions. The ^{1}H NMR analysis of the crude material revealed **2.24e-(*R*)** was obtained in >95% yield as a mixture of diastereomers; the ratio of **2.24e-(*R*)-*anti*** and **2.24e-(*R*)-*syn*** was determined to be 87:13. $[\alpha]^{25}_{D}$ = –160.8° (c = 1.0, EtOH). The absolute configurations of **2.24e-(*R*)-*anti*** and **2.24e-(*R*)-*syn*** were assigned as described in SI Section 4.

2.24e-(*R*)-*anti*: ^{1}H NMR (600 MHz, $CDCl_3$) δ 7.29 (t, *J* = 7.4 Hz, 2H), 7.26 – 7.23 (m, 1H), 7.06 (d, *J* = 7.5 Hz,2H), 6.60 (d, *J* = 3.0 Hz, 1H), 6.54 (d, *J* = 3.0 Hz, 1H), 4.56 (dd, *J* = 8.4, 2.4 Hz, 1H), 4.27 (t, *J* = 8.4 Hz, 1H), 4.03 – 3.94 (m, 2H), 3.77 (s, 3H), 3.71 (q, *J* = 7.3 Hz, 1H), 3.33 (q, *J* = 7.5 Hz, 1H), 3.01 (td, *J* = 8.4, 4.6 Hz, 1H), 2.31 (s, 3H), 2.21 (s, 3H), 2.13 – 2.04 (m, 1H), 2.10 – 2.05 (m, 1H), 1.92 – 1.86 (m, 1H), 1.74 – 1.68 (m, 1H), 1.07 (d, *J* = 6.9 Hz, 3H); **^{13}C NMR** (151 MHz, $CDCl_3$) δ 175.2, 156.8, 153.2, 141.3, 141.2, 139.5, 136.7, 129.0, 128.2, 125.1, 113.8, 112.4, 69.8, 62.4, 57.4, 55.2, 51.5, 42.7, 30.7, 24.4, 19.4, 19.2, 15.6; **IR** (neat) 2962, 2836, 1776, 1698, 1600, 1479, 1456, 1380, 1193, 1153, 699 cm^{-1}; **HRMS** (DART) m/z Calcd for $C_{25}H_{31}N_2O_4$ (MH^+): 423.2284; found: 423.2282.

2.24e-(*R*)-*syn*: ^{1}H NMR (600 MHz, $CDCl_3$) δ 7.33 – 7.29 (m, 2H), 7.28 – 7.24 (m, 1H), 7.16 – 7.12 (m, 2H), 6.59 (d, *J* = 3.1 Hz, 1H), 6.54 (d, *J* = 3.1 Hz, 1H), 4.70 (dd, *J* = 8.4, 2.9 Hz, 1H), 4.37 (t, *J* = 8.5 Hz, 1H), 4.13 – 4.03 (m, 2H), 3.81 – 3.70 (m, 4H), 3.35 – 3.26 (m, 1H), 2.95 – 2.85 (m, 1H), 2.31 (s, 3H), 2.28 – 2.19 (m, 4H), 2.03 – 1.94 (m, 1H), 1.91 – 1.85 (m, 1H), 1.84 – 1.80 (m, 1H), 1.00 (d, *J* = 6.8 Hz, 3H); **^{13}C NMR** (126 MHz, $CDCl_3$) δ 175.0, 156.4, 153.5, 140.7, 139.5, 139.4, 137.0, 129.0, 128.4, 125.5, 114.4, 113.0, 70.0, 62.5, 57.9, 55.2, 53.6, 44.6, 30.9, 25.3, 19.4, 19.3, 12.6; **IR** (neat) 2957, 2835, 1774, 1701, 1602, 1479, 1457, 1380, 1317, 1193, 1042, 698 cm^{-1}; **HRMS** (DART) m/z Calcd for $C_{25}H_{31}N_2O_4$ (MH^+): 423.2284; found: 423.2291.

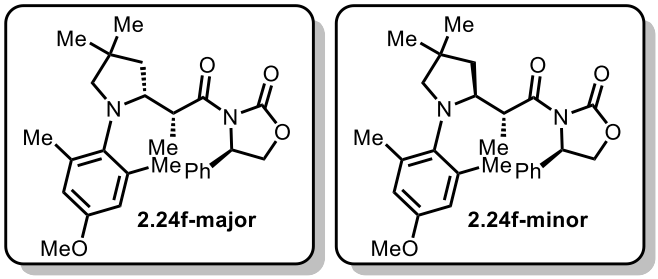

(4*R*)-3-(2-(1-(4-Methoxy-2,6-dimethylphenyl)-4,4-dimethylpyrrolidin-2-yl)propanoyl)-4-phenyloxazolidin-2-one (2.24f)

1-(4-Methoxy-2,6-dimethylphenyl)-3,3-dimethylpyrrolidine **2.13t** was reacted with (*R*)-3-acryloyl-4-phenyloxazolidin-2-one **2.23e-(*R*)** following the General Procedure for Stereoselective Mannich Reactions. ^{1}H NMR analysis of the crude material revealed that **2.24f-major** and **2.24f-minor** were obtained in the ratio of 58:17:0:0. After purification by column chromatography (hexanes: Et_2O = 17:3 then 15:5), **2.24f-major** (52 mg, 58%) and **2.24f-minor** (15 mg, 17%) were obtained as single diastereomers. The absolute configurations of **2.24f-major** and **2.24f-minor** were assigned as described in SI Section 4.

2.24f-major: ^{1}H NMR (500 MHz, $CDCl_3$) δ7.34 – 7.20 (m, 3H), 7.08 – 7.02 (m, 2H), 6.60 (d, *J* = 3.0 Hz, 1H), 6.53 (d, *J* = 3.0 Hz, 1H), 4.45 (dd, *J* = 8.4, 2.2 Hz, 1H), 4.23 – 4.11 (m, 2H), 4.01 – 3.93 (m, 1H), 3.81 – 3.71 (m, 4H), 3.17 (d, *J* = 7.9 Hz, 1H), 2.80 (d, *J* = 7.9 Hz, 1H), 2.33 (s, 3H), 2.24 (s, 3H), 1.78 (dd, *J* = 11.6, 5.5 Hz, 1H), 1.56 (dd, *J* = 11.7, 9.7 Hz, 1H), 1.19 (s, 3H), 1.17 (s, 3H), 1.00 (d, *J* = 6.9 Hz, 3H); **^{13}C NMR** (126 MHz, $CDCl_3$) δ175.0, 156.8, 153.2, 142.5, 141.5, 139.6, 135.7, 129.0, 128.2, 125.1, 113.7, 112.5, 69.7, 65.1, 61.9, 57.4, 55.3, 46.2, 42.6, 36.7, 29.2, 28.4, 19.7, 19.3, 16.1; **IR** (neat) 2953, 2863, 2836, 1780, 1698, 1600, 1481, 1380, 1196, 1154, 702 cm^{-1}; **HRMS** (DART) m/z Calcd for $C_{27}H_{35}N_2O_4$ (MH^+): 451.2597; found: 451.2612; $[\alpha]^{25}_D$ = –152.7° (c = 1.0, EtOH).

2.24f-minor: **^{1}H NMR** (500 MHz, $CDCl_3$) δ7.41 – 7.30 (m, 3H), 7.16 – 7.11 (m, 2H), 6.48 (d, *J* = 3.1 Hz, 1H), 6.40 (d, *J* = 3.0 Hz, 1H), 5.27 (dd, *J* = 8.8, 4.0 Hz, 1H), 4.57 (t, *J* = 8.8 Hz, 1H), 4.18 (ddd, *J* = 12.5, 8.8, 5.2 Hz, 2H), 3.81 (t, *J* = 6.6 Hz, 1H), 3.73 (s, 3H), 3.03 (d, *J* = 8.4 Hz, 1H), 2.76 (d, *J* = 8.4 Hz, 1H), 2.25 (s, 6H), 1.50 (dd, *J* = 12.3, 8.6 Hz, 1H), 1.24 – 1.18 (m, 1H), 1.12 (s, 3H), 1.05 (s, 3H), 1.01 (d, *J* = 6.9 Hz, 3H); **^{13}C NMR** (151 MHz, $CDCl_3$) δ175.6, 156.3, 153.1, 139.4, 139.04, 139.01, 135.5, 129.0, 128.5, 126.1, 114.4, 113.3, 69.6, 65.9, 60.1, 57.9, 55.0, 42.7, 41.1, 36.0, 29.5, 28.8, 19.7, 19.4, 12.7; **IR** (neat) 2952, 2920, 2850, 1779, 1702, 1481, 1381, 1319, 1193, 1067, 700 cm^{-1}; **HRMS** (DART) m/z Calcd for $C_{27}H_{35}N_2O_4$ (MH^+): 451.2597; found: 451.2613.

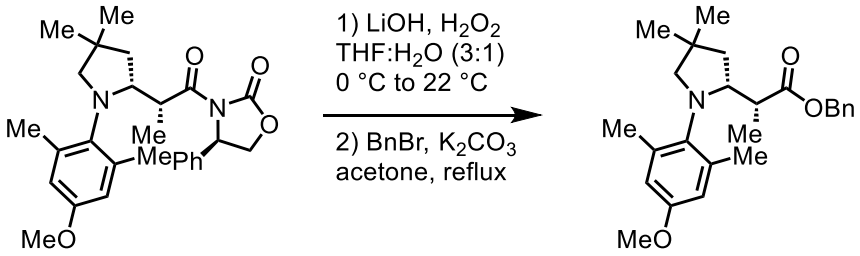

2.24f-major was transformed into the corresponding benzyl ester **2.29-major** following previously reported literatures.[19,20]

(*R*)-2-((*R*)-1-(4-Methoxy-2,6-dimethylphenyl)-4,4-dimethylpyrrolidin-2-yl)propanoic acid

(*R*)-2-((*R*)-1-(4-Methoxy-2,6-dimethylphenyl)-4,4-dimethylpyrrolidin-2-yl)propanoic acid was prepared by following a known procedure.[19] To a solution of Mannich product **2.24f-major** (90 mg, 0.2 mmol) in THF:H_2O (3:1, 2.4 mL) at 0 °C was added H_2O_2 (30% v/v, 0.02 mL, 0.8 mmol) and 2.0 M LiOH (0.14 mL, 0.28 mmol), dropwise. The mixture was stirred at 22 °C for 5 h, whereupon the reaction was quenched with $NaHSO_3$. The crude mixture was then concentrated *in*

vacuo, then diluted with EtOAc (2 mL), H_2O (2 mL), and 1 M NaOH (2 mL). The organic layer was separated and the aqueous layer was extracted with EtOAc (3 x 5 mL). Subsequently, the aqueous layer was acidified with 6 M HCl (2 mL) and extracted with EtOAc (3 x 5 mL). The combined organic layers were washed with brine (10 mL), dried ($MgSO_4$), filtered. and concentrated *in vacuo* to afford (*R*)-2-((*R*)-1-(4-Methoxy-2,6-dimethylphenyl)-4,4-dimethylpyrrolidin-2-yl)propanoic acid as a yellow solid (60 mg, 98%) which was used without further purification.

Benzyl (*R*)-2-((*R*)-1-(4-methoxy-2,6-dimethylphenyl)-4,4-dimethylpyrrolidin-2-yl)propanoate (2.29-major)

Benzyl (*R*)-2-((*R*)-1-(4-methoxy-2,6-dimethylphenyl)-4,4-dimethylpyrrolidin-2-yl)propanoate was prepared by following a known procedure.[20] Benzyl bromide (0.12 mL, 1.0 mmol) was added dropwise to a mixture of (*R*)-2-((*R*)-1-(4-Methoxy-2,6-dimethylphenyl)-4,4-dimethylpyrrolidin-2-yl)propanoic acid (61 mg, 0.2 mmol) and K_2CO_3 (28 mg, 0.2 mmol) in acetone (1.0 mL). The reaction mixture was heated at reflux for 12 h. The reaction mixture was filtered through a pad of celite and the solvent was evaporated by rotary evaporation. The crude product was purified by silica gel column chromatography (19:1 Hexanes: Et_2O) to afford **2.29-major** as a colorless oil (74 mg, 93% yield).

^{1}H NMR (500 MHz, $CDCl_3$) δ7.31 (qd, *J* = 7.7, 4.0 Hz, 3H), 7.20 (d, *J* = 7.2 Hz, 2H), 6.51 (d, *J* = 3.0 Hz, 1H), 6.47 (d, *J* = 3.1 Hz, 1H), 4.61 – 4.38 (m, 2H), 4.10 (q, *J* = 7.6 Hz, 1H), 3.70 (s, 3H), 3.12 – 3.02 (m, 1H), 2.87 – 2.77 (m, 1H), 2.48 – 2.38 (m, 1H), 2.29 (s, 3H), 2.27 (s, 3H), 1.82 – 1.75 (m, 1H), 1.52 (dd, *J* = 12.2, 8.1 Hz, 1H), 1.21 – 1.18 (m, 3H), 1.14 (d, *J* = 1.3 Hz, 3H), 1.05

(dd, J = 7.0, 1.4 Hz, 3H); **^{13}C NMR** (151 MHz, $CDCl_3$) δ175.5, 156.5, 140.5, 139.4, 136.2, 135.7, 128.3, 127.80, 127.75, 114.2, 113.0, 66.0, 65.7, 61.9, 55.1, 45.3, 44.6, 36.3, 29.4, 28.6, 19.7, 19.5, 14.7; **HPLC** (Chiralpak AD-H; 1%/ 99% hexane/isopropanol, 0.5 mL/min; **5v-major:** tr = 11.4 min (minor), 12.1 min (major); >99:1 er.

```
Acq. Operator   : SYSTEM                          Seq. Line :   2
Acq. Instrument : Wasa_LC1                         Location :   1
Injection Date  : 1/9/2018 6:20:24 PM                   Inj :   1
                                                Inj Volume : 4.000 µl
Method          : C:\Chem32\1\Data\JOE 2018-01-09 17-17-31\column1 1% IPA 99% hex 20min-0.5mL
                  .M (Sequence Method)
Last changed    : 1/9/2018 5:17:33 PM by SYSTEM
Method Info     : Column 1 20min-1% iPrOH 99% hexane-0.5mL
```

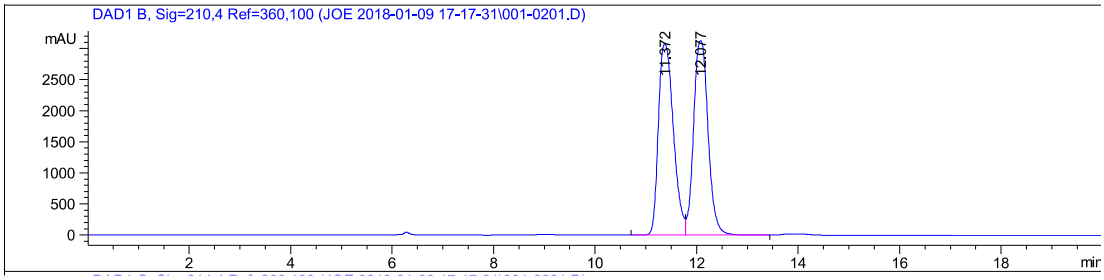

Signal 2: DAD1 B, Sig=210,4 Ref=360,100

Peak #	RetTime [min]	Type	Width [min]	Area [mAU*s]	Height [mAU]	Area %
1	11.372	BV	0.3234	6.31420e4	3076.77075	50.4308
2	12.077	VB	0.3114	6.20631e4	3129.58765	49.5692

```
Acq. Operator   : SYSTEM                          Seq. Line :   3
Acq. Instrument : Wasa_LC1                         Location :   2
Injection Date  : 1/19/2018 1:53:28 PM                  Inj :   1
                                                Inj Volume : 4.000 µl
Method          : C:\Chem32\1\Data\JOE 2018-01-19 12-09-44\column1 1% IPA 99% hex 40min-0.5mL
                  .M (Sequence Method)
Last changed    : 1/19/2018 12:09:46 PM by SYSTEM
Method Info     : Column 1 40min-1% iPrOH 99% hexane-0.5mL
```

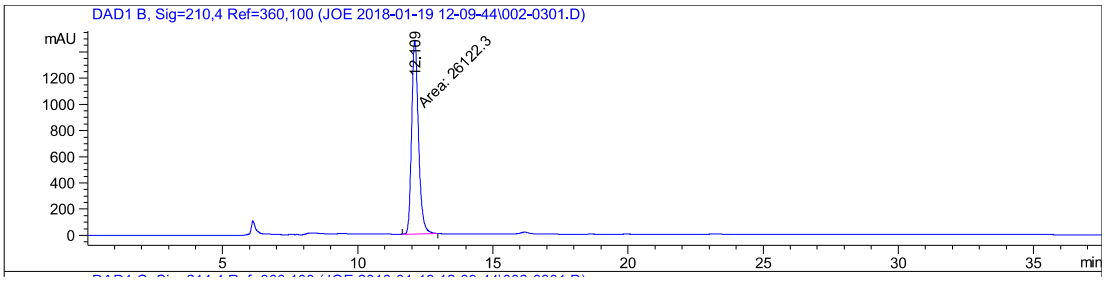

Signal 2: DAD1 B, Sig=210,4 Ref=360,100

Peak #	RetTime [min]	Type	Width [min]	Area [mAU*s]	Height [mAU]	Area %
1	12.109	MM	0.2945	2.61223e4	1478.15210	100.0000

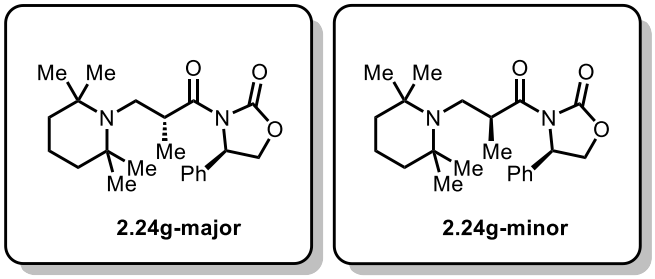

(4*R*)-3-(2-Methyl-3-(2,2,6,6-tetramethylpiperidin-1-yl)propanoyl)-4-phenyloxazolidin-2-one (2.24g)

1,2,2,6,6-Pentamethylpiperidine **2.13p** was reacted with (*R*)-3-acryloyl-4-phenyloxazolidin-2-one **2.23e-(*R*)** following the General Procedure for Stereoselective Mannich Reactions at 60 °C. ^{1}H NMR analysis of the crude material revealed that **2.24g-major** and **2.24g-minor** were obtained in the ratio of 2.0:1. After purification by PTLC (hexanes: EtOAc: Et_3N = 16:4:1), **2.24g-major** (35 mg, 47%) and **2.24g-minor** (28 mg, 24%) were obtained as single diastereomers.

2.24g-major: ^{1}H NMR (500 MHz, $CDCl_3$) δ7.37 (t, *J* = 7.0 Hz, 2H), 7.33 (d, *J* = 6.8 Hz, 1H), 7.29 – 7.25 (m, 2H), 5.44 – 5.36 (m, 1H), 4.69 – 4.60 (m, 1H), 4.23 (ddd, *J* = 8.9, 3.4, 1.6 Hz, 1H), 4.03 (p, *J* = 6.8 Hz, 1H), 2.95 (dd, *J* = 15.5, 6.5 Hz, 1H), 2.49 (dd, *J* = 15.5, 5.8 Hz, 1H), 1.51 (d, *J* = 5.9 Hz, 2H), 1.39 (dd, *J* = 8.5, 4.6 Hz,4H), 1.10 (d, *J* = 7.1 Hz,3H), 1.03 (s, 6H), 0.97 (s, 6H); **^{13}C NMR** (126 MHz, $CDCl_3$) δ177.6, 153.3, 139.4, 129.1, 128.5, 125.6, 69.6, 57.8, 54.6, 47.8, 41.4, 41.3, 17.8, 16.4; **IR** (neat) 2963, 2926, 1780, 1699, 1381, 1320, 1242, 1197, 1042, 761 cm^{-1}; **HRMS** (DART) m/z Calcd for $C_{22}H_{33}N_2O_3$ (MH^+): 373.2491; found: 373.2504; $[\alpha]^{25}_D = -107.9°$ (c = 0.3, EtOH).

2.24g-minor: ^{1}H NMR (500 MHz, $CDCl_3$) δ7.40 – 7.30 (m, 5H), 5.45 (dd, *J* = 8.9, 4.0 Hz, 1H), 4.67 (dd, *J* = 9.6, 8.2 Hz, 1H), 4.31 – 4.24 (m, 1H), 3.97 (q, *J* = 6.8 Hz, 1H), 2.90 (dd, *J* = 15.4,

6.3 Hz, 1H), 2.37 (dd, *J* = 15.4, 6.3 Hz, 1H), 1.47 (s, 2H), 1.32 (t, *J* = 6.0 Hz, 4H), 1.16 (dd, *J* = 7.1, 1.3 Hz, 3H), 0.96 (s, 6H), 0.78 (s, 6H); **^{13}C NMR** (151 MHz, $CDCl_3$) δ177.7, 153.4, 139.3, 129.0, 128.6, 126.3, 69.5, 57.9, 54.6, 47.5, 41.6, 41.4, 17.8, 16.4; **IR** (neat) 2964, 2925, 2872, 1777, 1700, 1457, 1380, 1319, 1196, 1044, 949, 699 cm^{-1}; **HRMS** (DART) m/z Calcd for $C_{22}H_{33}N_2O_3$ (MH^+): 373.2491; found: 373.2474.

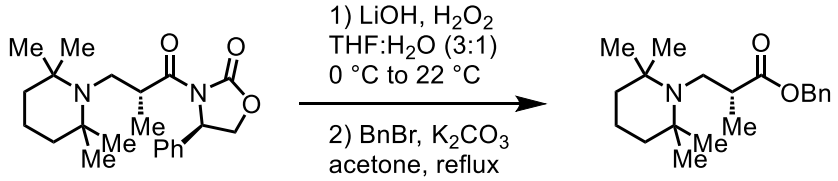

2.24g-major **2.30**, 83% yield
>99:1 er

2.24g-major was transformed into the corresponding benzyl ester **2.30** following previously reported literatures.[19,20] **HPLC** (Chiralcel OD-H; 2.5%/ 97.5% hexane/ isopropanol, 0.3 mL/min; **2.30:** tr = 12.6 min (major), 13.3 min (minor); >99:1 er.

```
Acq. Operator   : SYSTEM                        Seq. Line :   3
Acq. Instrument : Wasa_LC1                       Location :   51
Injection Date  : 1/24/2018 1:20:46 PM               Inj :   1
                                               Inj Volume : 4.000 µl
Method          : C:\Chem32\1\Data\JOE 2018-01-24 11-57-03\column1 2.5%IPA 97.5% hexane 40min
                  -0.3mL.M (Sequence Method)
Last changed    : 1/24/2018 11:57:04 AM by SYSTEM
Method Info     : Column1 40min-2.5% iPrOH 97.5% hexane-0.3mL
```

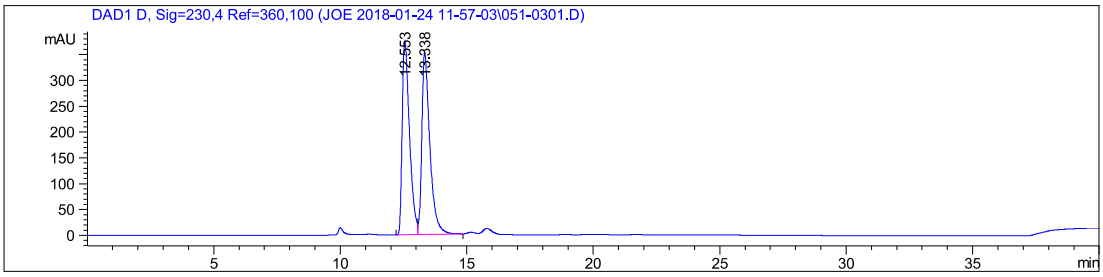

Signal 4: DAD1 D, Sig=230,4 Ref=360,100

Peak #	RetTime [min]	Type	Width [min]	Area [mAU*s]	Height [mAU]	Area %
1	12.553	BV	0.2982	7523.91992	374.85226	49.2105
2	13.338	VB	0.3294	7765.33203	351.95917	50.7895

Acq. Operator : SYSTEM Seq. Line : 2
Acq. Instrument : Wasa_LC1 Location : 52
Injection Date : 1/25/2018 5:34:58 PM Inj : 1
Inj Volume : 8.000 µl
Method : C:\Chem32\1\Data\JOE 2018-01-25 17-02-55\column1 2.5% IPA 97.5% hex 30min-0.3mL.M (Sequence Method)
Last changed : 1/25/2018 5:02:57 PM by SYSTEM
Method Info : Washing 40min-2.5% iPrOH 97.5% hexane-0.5mL

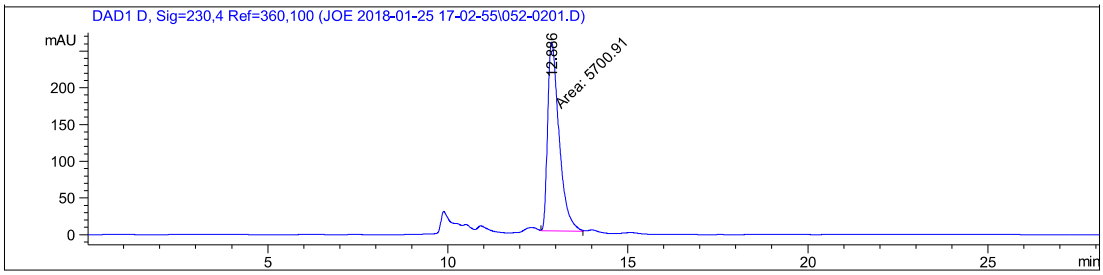

Signal 4: DAD1 D, Sig=230,4 Ref=360,100

Peak #	RetTime [min]	Type	Width [min]	Area [mAU*s]	Height [mAU]	Area %
1	12.886	MM	0.3695	5700.90869	257.16043	100.0000

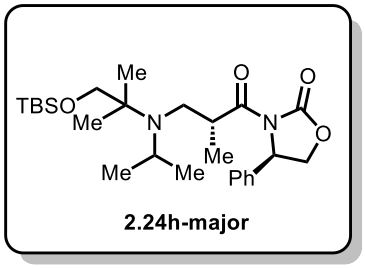

(4*R*)-3-(3-((1-((*tert*-Butyldimethylsilyl)oxy)-2-methylpropan-2-yl)(isopropyl)amino)-2-methylpropanoyl)-4-phenyloxazolidin-2-one (2.24h)

1-((*tert*-Butyldimethylsilyl)oxy)-*N*-ethyl-*N*-isopropyl-2-methylpropan-2-amine **2.13r** was reacted with (*R*)-3-acryloyl-4-phenyloxazolidin-2-one **2.23e-(*R*)** following the General Procedure for Stereoselective Mannich Reactions. ^{1}H NMR analysis of the crude material revealed that **2.24h-major** and **2.24h-minor** were obtained in the ratio of 7.4:1. After purification by silica gel column chromatography (hexanes: Et_3N = 50:1 then 19:1), **2.24h-major** (71 mg, 70%) and **2.24h-minor** (9 mg, 10%) were obtained as single diastereomers.

2.24h-major*:* **^{1}H NMR** (600 MHz, $CDCl_3$) δ 7.37 (dd, *J* = 8.2, 6.7 Hz, 2H), 7.33 (d, *J* = 7.1 Hz, 1H), 7.29 – 7.27 (m, 2H), 5.42 (dd, *J* = 8.5, 3.2 Hz, 1H), 4.64 (t, *J* = 8.7 Hz, 1H), 4.23 (dd, *J* = 8.8, 3.3 Hz, 1H), 3.99 (h, *J* = 7.0 Hz, 1H), 3.43 – 3.34 (m, 2H), 3.27 (p, *J* = 6.7 Hz, 1H), 3.03 (dd, *J* = 14.8, 7.3 Hz, 1H), 2.68 (dd, *J* = 14.8, 6.6 Hz, 1H), 1.06 (d, *J* = 7.2 Hz, 9H), 1.01 (d, *J* = 6.7 Hz, 3H), 0.98 (d, *J* = 6.7 Hz, 3H), 0.89 (s, 9H), 0.02 (d, *J* = 1.3 Hz, 6H); **^{13}C NMR** (151 MHz, $CDCl_3$) δ179.8, 156.0, 142.1, 131.8, 131.2, 128.3, 72.3, 72.2, 62.1, 60.4, 49.2, 49.0, 42.8, 28.5, 26.8, 26.8, 20.8, 18.1, -2.9; **IR** (neat) 2956, 2925, 2854, 1781, 1702, 1459, 1381, 1195, 1086, 1044, 836, 774 cm^{-1}; **HRMS** (DART) m/z Calcd for $C_{26}H_{45}N_2O_4Si$ (MH^+): 477.3147; found: 477.3171; $[\alpha]^{25}_D$ = –60.9° (c = 0.8, EtOH).

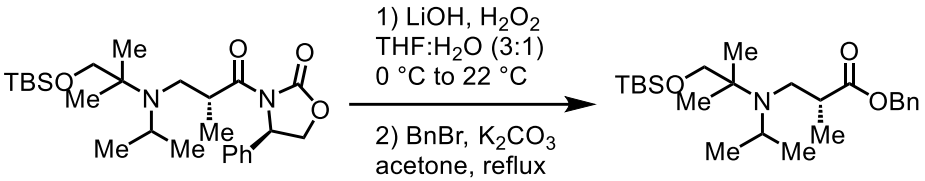

2.24h-major

2.31, 87% yield
>99:1 er

2.24h-major was transformed into the corresponding benzyl ester **2.31** following previously reported literatures.[19,20] **HPLC** (Chiralcel OD-H; 0.5%/ 99.5% hexane/ isopropanol, 1.0 mL/min; **2.31:** tr = 8.5 min (minor), 9.6 min (major); >99:1 er.

```
Acq. Operator   : SYSTEM                          Seq. Line :   3
Acq. Instrument : Wasa_LC1                         Location :   31
Injection Date  : 1/22/2018 4:55:37 PM                Inj :   1
                                                  Inj Volume : 4.000 µl
Method          : C:\Chem32\1\Data\JOE 2018-01-22 15-32-04\column1 0.5% IPA 99.5% hex 40min-1
                  .0mL.M (Sequence Method)
Last changed    : 1/22/2018 3:32:06 PM by SYSTEM
Method Info     : Column1 40min-0.5% iPrOH 99.5% hexane-1.0mL
```

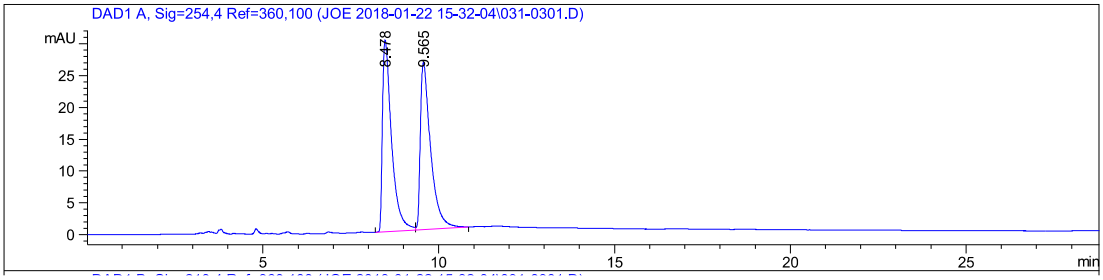

Signal 1: DAD1 A, Sig=254,4 Ref=360,100

Peak #	RetTime [min]	Type	Width [min]	Area [mAU*s]	Height [mAU]	Area %
1	8.478	BV	0.2633	540.04773	30.10438	50.2350
2	9.565	VB	0.3001	534.99445	26.21741	49.7650

```
Acq. Operator   : SYSTEM                          Seq. Line :   1
Acq. Instrument : Wasa_LC1                         Location :   32
Injection Date  : 1/22/2018 5:27:21 PM                 Inj :   1
                                                 Inj Volume : 4.000 µl
Method          : C:\Chem32\1\Data\JOE 2018-01-22 17-26-19\column1 0.5% IPA 99.5% hex 40min-1
                  .0mL.M (Sequence Method)
Last changed    : 1/22/2018 5:26:21 PM by SYSTEM
Method Info     : Column1 40min-0.5% iPrOH 99.5% hexane-1.0mL
```

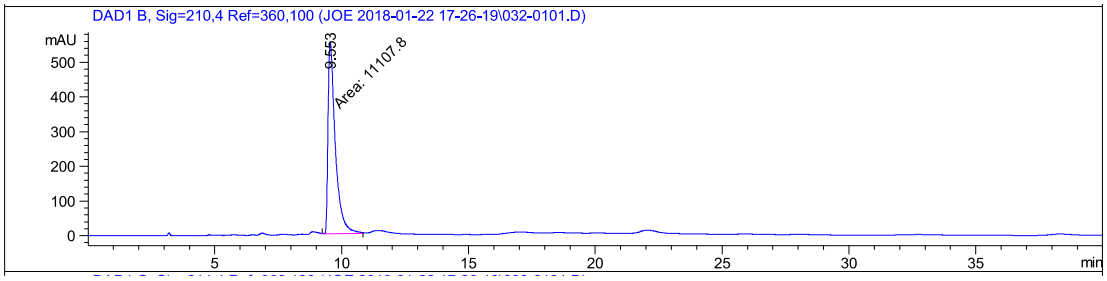

Signal 2: DAD1 B, Sig=210,4 Ref=360,100

Peak #	RetTime [min]	Type	Width [min]	Area [mAU*s]	Height [mAU]	Area %
1	9.553	MM	0.3346	1.11078e4	553.30640	100.0000

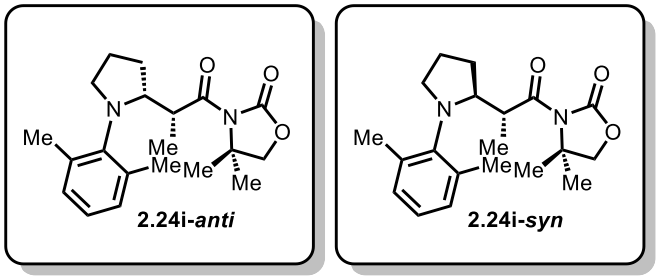

3-(2-(1-(2,6-dimethylphenyl)pyrrolidin-2-yl)propanoyl)-4,4-dimethyloxazolidin-2-one (2.24i)

1-(2,6-dimethylphenyl)pyrrolidine **2.13y** was reacted with 3-acryloyl-4,4-dimethyloxazolidin-2-one **2.23b** following the General Procedure for Stereoselective Mannich Reactions. The ^{1}H NMR analysis of the crude material revealed that **2.24i-anti** and **2.24i-syn** were obtained in the ratio of 3.8:1. After purification by column chromatography (hexanes: Et_2O = 19:1 then 9:1), **2.24i-anti** (39 mg, 56%) and **2.24i-syn** (10 mg, 15%) were obtained as single diastereomers. The absolute configurations of **2.24i-anti** and **2.24i-syn** were assigned in analogy.

2.24i-anti: **^{1}H NMR** (600 MHz, $CDCl_3$) δ 6.98 – 6.89 (m, 3H), 4.09 (q, *J* = 6.7 Hz, 1H), 3.83 (d, *J* = 8.2 Hz, 1H), 3.78 – 3.70 (m, 2H), 3.34 (ddd, J = 8.2, 7.0, 5.4 Hz, 1H), 2.96 (td, *J* = 7.9, 6.2 Hz, 1H), 2.27 (d, J = 1.9 Hz, 6H), 2.13 (dq, J = 12.0, 6.7 Hz, 1H), 2.02 – 1.82 (m, 3H), 1.35 (s, 3H), 1.12 (d, J = 6.9 Hz, 3H), 1.04 (s, 3H); **^{13}C NMR** (151 MHz, $CDCl_3$) δ 177.0, 153.6, 144.8, 139.1, 138.0, 129.4, 127.9, 125.2, 74.7, 61.7, 60.3, 52.5, 44.5, 29.8, 25.3, 24.4, 24.1, 19.3, 19.0, 15.0; **IR** (neat) 2965, 2874, 1774, 1699, 1466, 1374, 1304, 1219, 1176, 1085, 1035, 766 cm^{-1} ; **HRMS** (DART) m/z Calcd for $C_{20}H_{28}N_2O_3$ (MH^+): 345.2172; found: 345.2181; $[\alpha]^{25}_D$ = –36.2° (c = 0.8, EtOH); **HPLC** (Chiralcel IC; 5.0%/ 95.0% *n*-butanol/ hexanes, 0.2 mL/min; tr = 27.3 min (minor), 30.4 min (major); 89:11 er.

2.24i-syn: **^{1}H NMR** (500 MHz, $CDCl_3$) δ 6.98 (t, J = 8.1 Hz, 2H), 6.92 (t, J = 7.4 Hz, 1H), 4.04 (ddd, J = 8.9, 6.5, 2.7 Hz, 1H), 3.90 (d, J = 8.3 Hz, 1H), 3.82 (d, J = 8.3 Hz, 1H), 3.75 (q, J = 6.7 Hz, 1H), 3.36 (td, J = 7.9, 2.8 Hz, 1H), 2.89 (td, J = 8.9, 6.7 Hz, 1H), 2.35 (s, 3H), 2.27 (s, 1H), 2.25 (s, 3H), 2.09 – 1.96 (m, 1H), 1.95 – 1.84 (m, 1H), 1.75 (ddt, J = 12.9, 6.7, 2.9 Hz, 1H), 1.45 (s, 3H), 1.17 (s, 3H), 1.00 (d, J = 6.7 Hz, 3H); **^{13}C NMR** (151 MHz, $CDCl_3$) δ 177.1, 153.9, 146.9, 139.0, 135.5, 129.6, 128.3, 124.8, 74.9, 63.3, 60.5, 53.7, 46.5, 31.7, 25.5, 24.6, 23.9, 19.3, 19.1, 13.6; **IR** (neat) 2965, 2874, 1774, 1699, 1466, 1374, 1304, 1219, 1176, 1085, 1035, 766 cm^{-1}; **HRMS** (DART) m/z Calcd for $C_{20}H_{28}N_2O_3$ (MH^+): 345.2172; found: 345.2181; **HPLC** (Chiralcel IC; 5.0%/ 95.0% *n*-butanol/ hexanes, 0.5 mL/min; tr = 10.5 min (minor), 11.7 min (major); 93:7 er

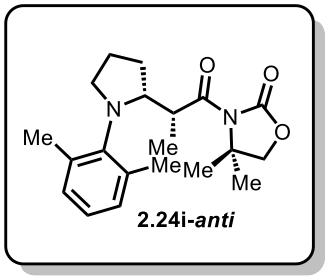


```
Acq. Operator   : SYSTEM                        Seq. Line :   1
Acq. Instrument : Wasa_LC1                       Location :   1
Injection Date  : 6/21/2018 12:30:35 AM              Inj :   1
                                               Inj Volume : 6.000 µl
Acq. Method     : C:\Chem32\1\Data\JOE 2018-06-21 00-28-47\column2 5.0%BuOH 95% hex 60min-0.
                  2mL.M
```

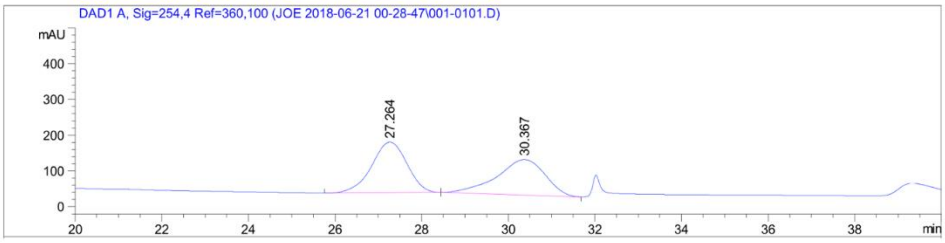


```
Signal 1: DAD1 A, Sig=254,4 Ref=360,100

Peak RetTime Type  Width     Area      Height     Area
  #   [min]        [min]   [mAU*s]     [mAU]       %
----|-------|----|-------|----------|----------|--------|
   1  27.264 BB    0.8812 8043.24463  141.49239  51.0721
   2  30.367 BB    1.1558 7705.54541   99.46435  48.9279
```

```
Acq. Operator   : SYSTEM                          Seq. Line :   2
Acq. Instrument : Wasa_LC1                         Location :   3
Injection Date  : 6/21/2018 1:04:03 PM                Inj :   1
                                                Inj Volume : 6.000 µl
Acq. Method     : C:\Chem32\1\Data\JOE 2018-06-21 12-31-11\column2 5.0%BuOH 95% hex 60min-0.
                  2mL.M
```

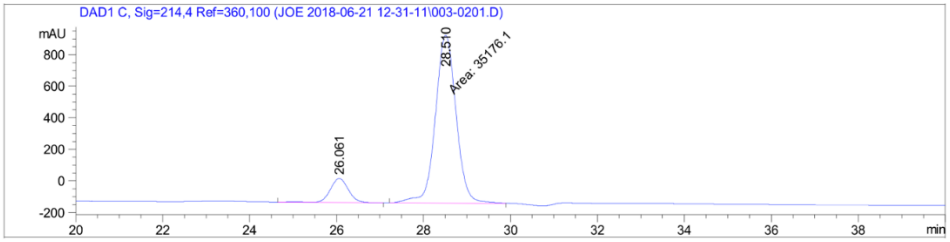

Signal 3: DAD1 C, Sig=214,4 Ref=360,100

Peak #	RetTime [min]	Type	Width [min]	Area [mAU*s]	Height [mAU]	Area %
1	26.061	VB R	0.4427	4418.16357	152.59972	11.1586
2	28.510	MM	0.5518	3.51761e4	1062.52637	88.8414

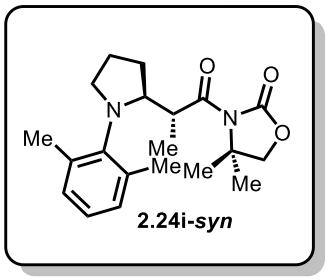


```
Acq. Operator   : SYSTEM                          Seq. Line :   3
Acq. Instrument : Wasa_LC1                         Location :   2
Injection Date  : 6/21/2018 2:32:30 AM                Inj :   1
                                                Inj Volume : 6.000 µl
Acq. Method     : C:\Chem32\1\Data\JOE 2018-06-21 00-28-47\column2 5.0%BuOH 95% hex 20min-0.
                  5mL.M
```

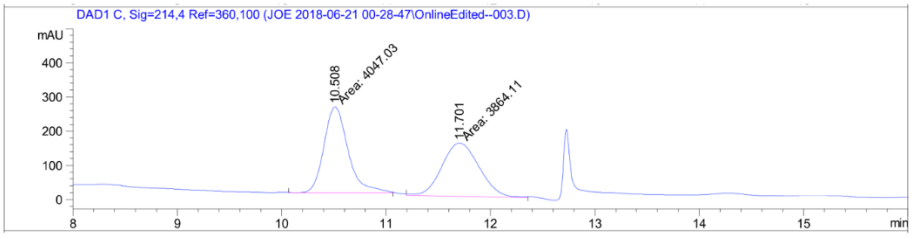

Signal 3: DAD1 C, Sig=214,4 Ref=360,100

Peak #	RetTime [min]	Type	Width [min]	Area [mAU*s]	Height [mAU]	Area %
1	10.508	MM	0.2688	4047.02881	250.90140	51.1561
2	11.701	MM	0.4140	3864.10767	155.56763	48.8439

```
Acq. Operator   : SYSTEM                          Seq. Line :   4
Acq. Instrument : Wasa_LC1                         Location :   4
Injection Date  : 6/21/2018 2:53:28 AM                Inj :   1
                                                 Inj Volume : 6.000 µl
Acq. Method     : C:\Chem32\1\Data\JOE 2018-06-21 00-28-47\column2 5.0%BuOH 95% hex 20min-0.
                  5mL.M
```

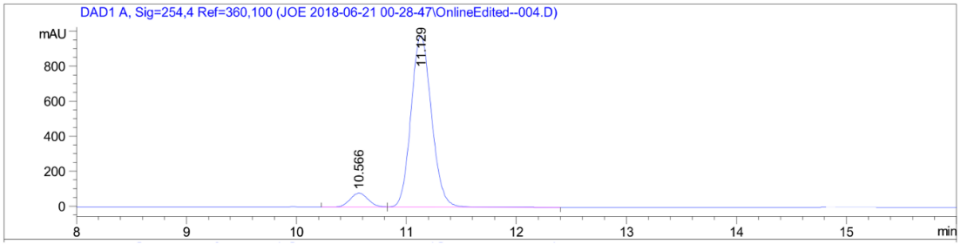

Signal 1: DAD1 A, Sig=254,4 Ref=360,100

Peak #	RetTime [min]	Type	Width [min]	Area [mAU*s]	Height [mAU]	Area %
1	10.566	BV	0.1815	936.54675	80.62458	6.8448
2	11.129	VB	0.2014	1.27461e4	982.07147	93.1552

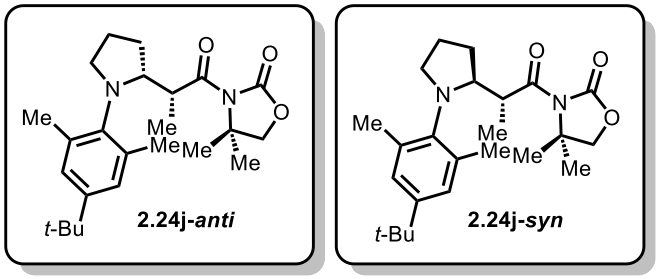

3-(2-(1-(4-(tert-Butyl)-2,6-dimethylphenyl)pyrrolidin-2-yl)propanoyl)-4,4-dimethyloxazolidin-2-one (2.24j)

1-(4-(tert-Butyl)-2,6-dimethylphenyl)pyrrolidine **2.13z** was reacted with 3-acryloyl-4,4-dimethyloxazolidin-2-one **2.23b** following the General Procedure for Stereoselective Mannich Reactions. The ^{1}H NMR analysis of the crude material revealed that **2.24j-anti** and **2.24j-syn** were obtained in the ratio of 4.4:1. After purification by column chromatography (hexanes: Et_2O = 19:1 then 9:1), **2.24j-anti** (46 mg, 57%) and **2.24j-syn** (10 mg, 13%) were obtained as single diastereomers. The absolute configurations of **2.24j-anti** and **2.24j-syn** were assigned in analogy.

2.24j-anti: **^{1}H NMR** (500 MHz, $CDCl_3$) δ 6.99 – 6.91 (m, 2H), 4.10 (q, J = 6.8 Hz, 1H), 3.83 (dd, J = 8.2, 1.0 Hz, 1H), 3.77 – 3.67 (m, 2H), 3.38 – 3.26 (m, 1H), 2.99 – 2.89 (m, 1H), 2.26 (d, J = 3.0 Hz, 6H), 2.17 – 2.08 (m, 1H), 1.90 (dddd, J = 27.8, 23.7, 12.1, 6.6 Hz, 3H), 1.34 (s, 3H), 1.25 (d, J = 1.0 Hz, 9H), 1.12 (dd, J = 7.0, 1.0 Hz, 3H), 0.98 (s, 3H); **^{13}C NMR** (126 MHz, $CDCl_3$) δ 177.1, 153.6, 147.4, 142.1, 138.2, 137.1, 126.3, 124.9, 74.7, 61.7, 60.2, 52.8, 44.7, 34.0, 31.5, 30.2, 25.2, 24.4, 24.2, 19.6, 19.2, 15.34; **IR** (neat) 2963, 2871, 1774, 1700, 1483, 1459, 1373, 1305, 1221, 1176, 1084, 766 cm^{-1} ; **HRMS** (DART) m/z Calcd for $C_{24}H_{36}N_2O_3$ (MH^+): 401.2799; found: 401.2789; $[\alpha]^{25}_D$ = –40.6° (c = 1.0, EtOH).

2.24j-syn: **^{1}H NMR** (500 MHz, $CDCl_3$) δ 7.05 – 6.87 (m, 2H), 4.06 (ddd, J = 8.4, 5.4, 2.4 Hz, 1H), 3.87 (d, J = 8.3 Hz, 1H), 3.73 (dd, J = 12.8, 7.4 Hz, 2H), 3.41 – 3.28 (m, 1H), 2.89 (ddd, J = 9.5, 8.5, 6.5 Hz, 1H), 2.34 (s, 3H), 2.32 – 2.25 (m, 1H), 2.22 (s, 3H), 2.09 – 1.94 (m, 1H), 1.94 – 1.84 (m, 1H), 1.78 (ddt, J = 12.6, 7.2, 2.7 Hz, 1H), 1.42 (s, 3H), 1.25 (s, 9H), 1.06 (d, J= 6.7 Hz, 3H), 1.00 (s, 3H); **^{13}C NMR** (151 MHz, $CDCl_3$) δ 176.8, 154.0, 147.4, 144.0, 138.3, 134.5, 126.4, 125.3, 74.9, 63.2, 60.5, 54.1, 46.4, 34.0, 31.6, 31.4, 25.5, 24.6, 24.4, 23.6, 19.5, 12.7; **IR** (neat) 2963, 2871, 1774, 1700, 1483, 1459, 1373, 1305, 1221, 1176, 1084, 766 cm^{-1} ; **HRMS** (DART) m/z Calcd for $C_{24}H_{36}N_2O_3$ (MH^+): 401.2799; found: 401.2789; **HPLC** (Chiralpak IA then OJ-H; 1.0%/ 99.0% isopropanol/ hexanes, 0.1 mL/min; tr = 103.3 min (major), 108.1 min (minor); 98:2 er.

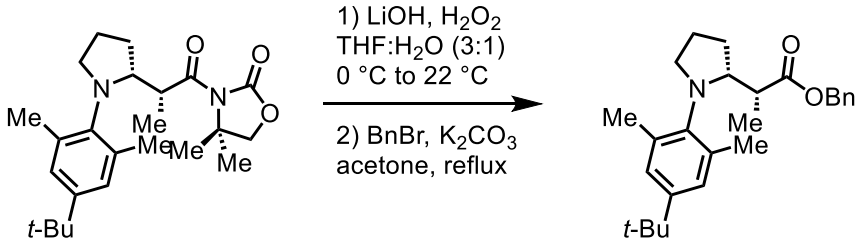

2.24j-*anti* **2.32-*anti***, 91% yield >99:1 er

2.24j-anti was transformed into the corresponding benzyl ester **2.32-anti** following previously reported literatures.[19,20]

^{1}H NMR (500 MHz, CDCl3) δ 7.34 – 7.27 (m, 3H), 7.21 – 7.18 (m, 2H), 7.00 (d, J = 2.4 Hz, 1H), 6.96 (d, J = 2.4 Hz, 1H), 4.65 (d, J = 12.5 Hz, 1H), 4.54 (d, J = 12.5 Hz, 1H), 3.98 (td, J = 6.9, 5.3 Hz, 1H), 3.39 – 3.29 (m, 1H), 3.00 (q, J = 7.7 Hz, 1H), 2.43 (p, J = 6.9 Hz, 1H), 2.29 (s, 3H), 2.24 (s, 3H), 2.07 (dq, J = 12.1, 7.6 Hz, 1H), 1.98 – 1.85 (m, 2H), 1.84 – 1.73 (m, 1H), 1.25 (s, 9H), 1.13 (d, J = 7.0 Hz, 3H); **IR** (neat) 2959, 2924, 2869, 2359, 2158, 1720, 1553, 1482, 1455, 1361, 1222, 1151, 1109, 732, 696 cm-1 ; **HRMS** (DART) m/z Calcd for $C_{26}H_{36}NO_2$ (MH^+): 394.2741;

found: 394.2733; $[\alpha]^{25}_{D}$ = −38.9° (c = 0.5, EtOH); HPLC (Chiralpak OJ-H; 1.0%/ 99.0% isopropanol/ hexanes, 0.5 mL/min; tr = 7.3 min (minor), 8.3 min (major); 91:9 er.

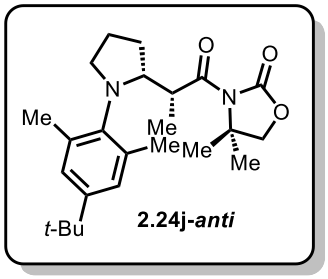


```
Acq. Operator    : SYSTEM                          Seq. Line :   1
Acq. Instrument  : Wasa_LC1                         Location :   31
Injection Date   : 6/21/2018 10:27:23 PM               Inj :   1
                                                  Inj Volume : 8.000 µl
Acq. Method      : C:\Chem32\1\Data\JOE 2018-06-21 22-25-30\column1 1% IPA 99% hex 40min-0.5mL
                   .M
```

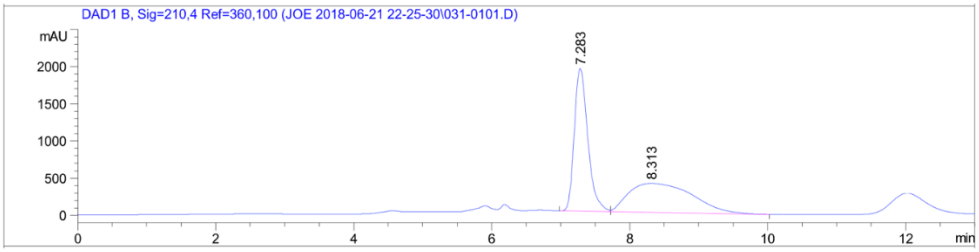

Signal 2: DAD1 B, Sig=210,4 Ref=360,100

Peak #	RetTime [min]	Type	Width [min]	Area [mAU*s]	Height [mAU]	Area %
1	7.283	BV	0.2095	2.62151e4	1917.36487	50.9982
2	8.313	VB	1.0825	2.51889e4	390.51810	49.0018

```
Acq. Operator    : SYSTEM                          Seq. Line :   2
Acq. Instrument  : Wasa_LC1                         Location :   32
Injection Date   : 6/21/2018 11:08:21 PM               Inj :   1
                                                  Inj Volume : 8.000 µl
Acq. Method      : C:\Chem32\1\Data\JOE 2018-06-21 22-25-30\column1 1% IPA 99% hex 40min-0.5mL
                   .M
```

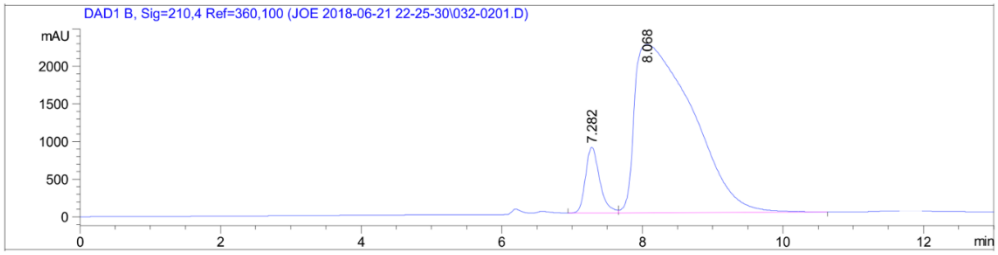

Signal 2: DAD1 B, Sig=210,4 Ref=360,100

Peak #	RetTime [min]	Type	Width [min]	Area [mAU*s]	Height [mAU]	Area %
1	7.282	BV	0.2137	1.23096e4	877.13251	8.7194
2	8.068	VB	0.8255	1.28865e5	2238.84619	91.2806

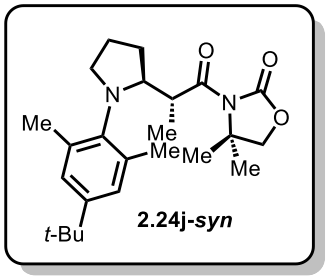


```
Acq. Operator   : SYSTEM                        Seq. Line :   2
Acq. Instrument : Wasa_LC1                       Location :   1
Injection Date  : 6/23/2018 7:08:43 PM               Inj :   1
                                               Inj Volume : 4.000 µl
Method          : C:\Chem32\1\Data\JOE 2018-06-23 18-06-37\column1 1% IPA 99% hex 150min-0.
                  1mL.M (Sequence Method)
Last changed    : 6/23/2018 6:06:40 PM by SYSTEM
Method Info     : column1 1% IPA 99% hex-150min-0.1mL
```

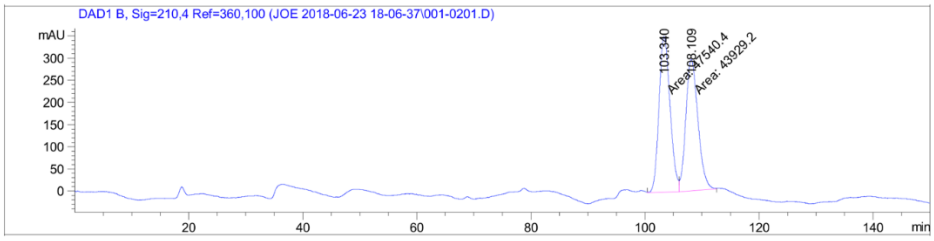

Signal 2: DAD1 B, Sig=210,4 Ref=360,100

Peak #	RetTime [min]	Type	Width [min]	Area [mAU*s]	Height [mAU]	Area %
1	103.340	MM	2.2579	4.75404e4	350.91858	51.9740
2	108.109	MM	2.4702	4.39292e4	296.39090	48.0260

```
Acq. Operator   : SYSTEM                        Seq. Line :   3
Acq. Instrument : Wasa_LC1                       Location :   2
Injection Date  : 6/23/2018 9:39:38 PM               Inj :   1
                                               Inj Volume : 4.000 µl
Method          : C:\Chem32\1\Data\JOE 2018-06-23 18-06-37\column1 1% IPA 99% hex 150min-0.
                  1mL.M (Sequence Method)
Last changed    : 6/23/2018 6:06:40 PM by SYSTEM
Method Info     : column1 1% IPA 99% hex-150min-0.1mL
```

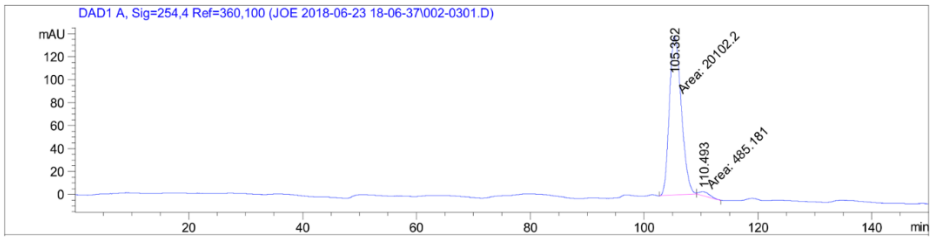

Signal 1: DAD1 A, Sig=254,4 Ref=360,100

Peak #	RetTime [min]	Type	Width [min]	Area [mAU*s]	Height [mAU]	Area %
1	105.362	MM	2.4176	2.01022e4	138.58492	97.6433
2	110.493	MM	2.1680	485.18082	3.72993	2.3567

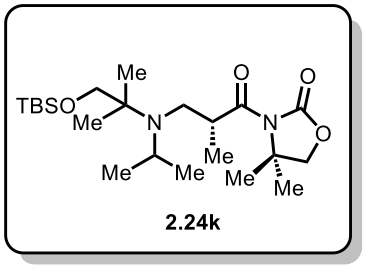

3-(3-((1-((tert-Butyldimethylsilyl)oxy)-2-methylpropan-2-yl)(isopropyl)amino)-2-methylpropanoyl)-4,4-dimethyloxazolidin-2-one (2.24k)

1-((tert-Butyldimethylsilyl)oxy)-*N*-ethyl-*N*-isopropyl-2-methylpropan-2-amine **2.13r** was reacted with 3-acryloyl-4,4-dimethyloxazolidin-2-one **2.23b** following the General Procedure for Stereoselective Mannich Reactions. After purification by silica gel column chromatography (hexanes: Et_3N = 98.5 : 1.5), **2.24k** (40 mg, 46%) was obtained as a colorless oil.

^{1}H NMR (400 MHz, $CDCl_3$) δ 4.03 – 3.91 (m, 2H), 3.81 (h, J = 6.9 Hz, 1H), 3.37 (s, 2H), 3.26 (h, J = 6.7 Hz, 1H), 3.13 (dd, J = 14.4, 7.8 Hz, 1H), 2.64 (dd, J = 14.4, 6.6 Hz, 1H), 1.56 (d, J = 7.3 Hz, 6H), 1.09 (d, J = 6.8 Hz, 3H), 1.07 – 0.99 (m, 12H), 0.88 (s, 9H), 0.01 (s, 6H); ^{13}C NMR (151 MHz, $CDCl_3$) δ 178.8, 153.9, 75.0, 69.4, 60.6, 59.4, 46.9, 46.3, 41.1, 25.8, 24.8, 24.3, 24.2, 23.5, 22.2, 18.2, 15.5, -5.6; IR (neat) 2958, 2930, 2888, 2857, 1780, 1705, 1467, 1387, 1362, 1304, 1252, 1087, 837, 774 cm^{-1}; HRMS (DART) m/z Calcd for $C_{22}H_{44}N_2O_4Si$ (MH^+): 429.3143; found: 429.3133; $[\alpha]^{25}_D = -7.3°$ (c = 1.0, EtOH).

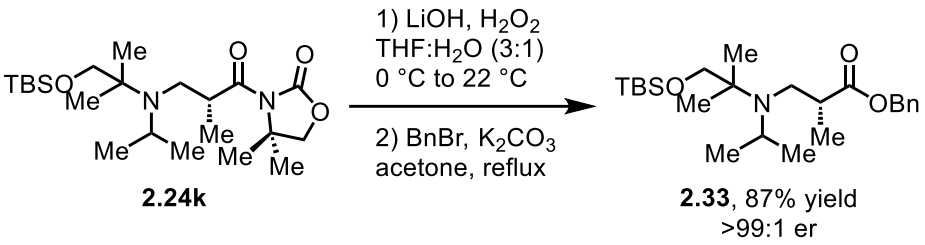

2.24k was transformed into the corresponding benzyl ester **2.33** following previously reported literatures.[19,20] **HPLC** (Chiralcel OD-H; 0.5%/ 99.5% n-butanol/ hexanes, 1.0 mL/min; 4c: tr = 6.5 min (minor), 12.0 min (major); 96:4 er.

```
Acq. Operator   : SYSTEM                          Seq. Line :   4
Acq. Instrument : Wasa_LC1                         Location :   31
Injection Date  : 6/19/2018 11:06:37 PM                Inj :   1
                                                  Inj Volume : 4.000 µl
Acq. Method     : C:\Chem32\1\Data\JOE 2018-06-19 21-01-56\column1 0.5% nBuOH 99.5% hex 40min
                  -1.0mL.M
Last changed    : 6/19/2018 9:01:59 PM by SYSTEM
Analysis Method : C:\Chem32\1\Data\JOE 2018-06-19 21-01-56\column1 0.5% nBuOH 99.5% hex 40min
                  -1.0mL.M (Sequence Method)
```

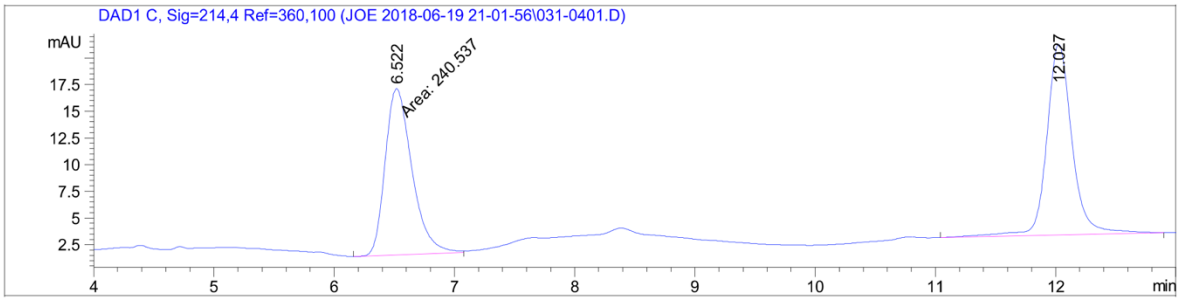

Signal 3: DAD1 C, Sig=214,4 Ref=360,100

Peak #	RetTime [min]	Type	Width [min]	Area [mAU*s]	Height [mAU]	Area %
1	6.522	MM	0.2577	240.53671	15.55946	47.8882
2	12.027	BB	0.2228	261.75095	17.87901	52.1118

```
Acq. Operator   : SYSTEM                          Seq. Line :   3
Acq. Instrument : Wasa_LC1                         Location :   32
Injection Date  : 6/19/2018 10:25:42 PM               Inj :   1
                                                 Inj Volume : 4.000 µl
Acq. Method     : C:\Chem32\1\Data\JOE 2018-06-19 21-01-56\column1 0.5% nBuOH 99.5% hex 40min
                  -1.0mL.M
Last changed    : 6/19/2018 9:01:59 PM by SYSTEM
Analysis Method : C:\Chem32\1\Data\JOE 2018-06-19 21-01-56\column1 0.5% nBuOH 99.5% hex 40min
                  -1.0mL.M (Sequence Method)
```

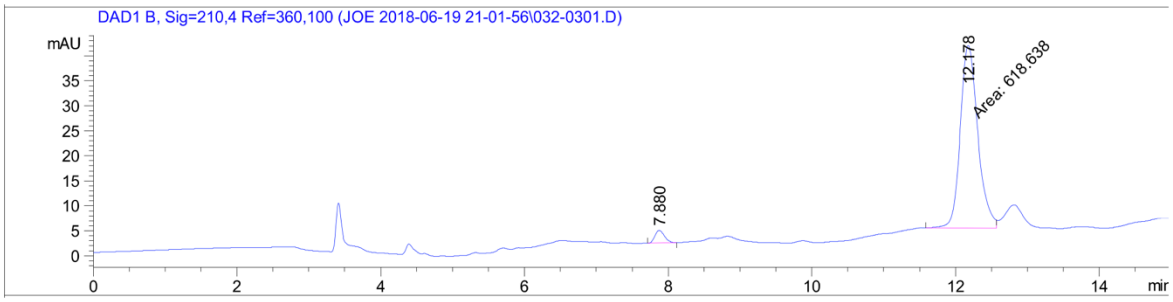

Signal 2: DAD1 B, Sig=210,4 Ref=360,100

Peak #	RetTime [min]	Type	Width [min]	Area [mAU*s]	Height [mAU]	Area %
1	7.880	BB	0.1410	22.67528	2.51915	3.5358
2	12.178	MF	0.2820	618.63849	36.55745	96.4642

A6. References

(1) Flock, A. M.; Krebs, A.; Bolm, C. Ephedrine- and Pseudoephedrine-Derived Thioureas in Asymmetric Michael Additions of Keto Esters and Diketones to Nitroalkenes. *Synlett.* **2010**, *8*, 1219-1222.

(2) Burgy, G.; Tahtouh, T.; Durieu, E.; Foll-Josselin, B.; Limanton, E.; Meijer, L.; Carreaux, F.; Bazurea, J. P. Chemical synthesis and biological validation of immobilized protein kinase inhibitory Leucettines. *Eur. J. Med. Chem.* **2013**, *62*, 728-737.

(3) Nam, K.-H.; Kim, H.; Choi, H. K.; Yeo, H.; Goh, M.; Yu, J.; Hahn, J. R.; Han, H.; Ku, B.-C.; You. N.-H. Thermomechanical and optical properties of molecularly controlled polyimides derived from ester derivatives. *Polymer* **2017**, *108*, 502-512.

(4) Noël, S.; Hoegy, F.; Rivault, F.; Rognan, D.; Schalk, I. J.; Mislin, G. L. A. Synthesis and biological properties of thiazole-analogues of pyochelin, a siderophore of *Pseudomonas aeruginosa. Bioorg. Med. Chem. Lett.* **2014**, *24*, 132-135.

(5) Youn, S. W. and Kim, Y. H. Pd(II)/Ag(I)-Promoted One-Pot Synthesis of Cyclic Ureas from (Hetero)Aromatic Amines and Isocyanates. *Org. Lett.* **2016**, *18*, 6140-6143.

(6) Lombardi, C.; Day, J.; Chandrasoma, N.; Mitchell, D.; Rodriguez, M. J.; Farmer, J. L.; Organ, M. G. Selective Cross-Coupling of (Hetero)aryl Halides with Ammonia To Produce Primary Arylamines using Pd-NHC Complexes. *Organometallics* **2017**, *36*, 251-254.

(7) Do, H.-Q.; Daugulis, O. An Aromatic Glaser−Hay Reaction. *J. Am. Chem. Soc.* **2009**, *131*, 17052-17053.

(8) Palani, V. P.; Chen, J.; Hoye, T. R. Reactions of Hexadehydro-Diels–Alder (HDDA)-Derived Benzynes with Thioamides: Synthesis of Dihydrobenzothiazino-Heterocyclics. *Org. Lett.* **2016**, *18*, 6312-6315.

(9) Shen, H.; Zhang, X.; Liu, Q.; Pan, J.; Hu, W.; Xiong, Y.; Zhu, X. Direct oxidative cyanation of tertiary amines promoted by in situ generated hypervalent iodine(III)-CN intermediate. *Tetrahedron Lett.* **2015**, *56*, 5628-5631.

(10) Lee, H.; Kim, K.-H.; Jeong, S. Discovery of a novel class of 2-aminopyrimidines as CDK1 and CDK2 inhibitors. *Bioorg. Med. Chem. Lett.* **2011**, *21*, 4203-4205.

(11) Dhanjee, H.; Minehan, T. G. Indium-mediated allylation of aldehydes, ketones and sulfonimines with 2-(alkoxy)allyl bromides. *Tetrahedron Lett.* **2010**, *51*, 5609-5612.

(12) Marson, C. M.; Melling, R. C.; Coles, S. J.; Hursthouse, M. B. Synthesis of (3*S*,3*S*′,4*S*,4*S*′)-1,1′-ethylenedipyrrolidine-3,3′,4,4′-tetraol and related diamino diols: donor–acceptor hydrogen-bonding motifs of the C_2 symmetric 3,4-dihydroxypyrrolidine unit. *Tetrahedron: Asymmetry* **2005**, *16*, 2799-2809.

(13) Joe, C. L.; Doyle, A. Direct Acylation of C(sp^3)−H Bonds Enabled by Nickel and Photoredox Catalysis. *Angew. Chem., Int. Ed.* **2016**, *55*, 4040-4043.

(14) Collins, K. D.; Rühling, A.; Lied, F.; Glorius, F. Rapid Assessment of Protecting-Group Stability by Using a Robustness Screen. *Chem*. *Eur*. *J*. **2014**, *20*, 3800-3805.

(15) Benson, Jr, O.; Demirdji, S. H.; Haltiwanger, R. C.; Koch, T. H. *N*-Alkyl-5,5-dimethyl-2-oxomorpholin-3-yl radicals. Characterization and reaction with molecular oxygen. *J*. *Am*. *Chem*. *Soc*. **1991**, *113*, 8879-8886.

(16) Brown, H. C.; Kanth, J. V. B.; Dalvi, P. V.; Zaidlewicz, M. Molecular Addition Compounds. 15. Synthesis, Hydroboration, and Reduction Studies of New, Highly Reactive *tert*-Butyldialkylamine−Borane Adducts. *J*. *Org*. *Chem*. **1994**, *64*, 6263-6274.

(17) Rao, R.; Shewalkar, M. P.; Nandipati, R.; Yadav, J. S.; Khagga, M.; Shinde, D. B. General Strategy for Large-Scale Synthesis of (+)-Rivastigmine and (+)-NPS R-568. *Synth. Commun*. **2012**, *42*, 589-598.

(18) Simov, B. P.; Wuggenig, F.; Mereiter, K.; Andres, H.; France, J.; Schnelli, P.; Hammerschmidt, F. Direct Chemical Synthesis of Chiral Methanol of 98% ee and Its Conversion to [$^{2}H_{1}$,^{3}H]Methyl Tosylate and [$^{2}H_{1}$,^{3}H-Methyl]Methionine. *J. Am. Chem. Soc.* **2005**, *127*, 13934-13940.

(19) Huang, Z.; Liu, Z.; Zhou, J. An Enantioselective, Intermolecular α-Arylation of Ester Enolates To Form Tertiary Stereocenters. *J. Am. Chem. Soc.* **2011**, *133*, 15882-15885.

(20) Martin, A.; Vors, J.-P.; Baudoin, O. Synthesis of Conformationally Constrained Esters and Amines by Pd-Catalyzed α-Arylation of Hindered Substrates. *ACS Catal.* **2016**, *6*, 3941-3945.

(21) Peifer, M.; Berger, R.; Shurtleff, V. W.; Conrad, J. C.; MacMillan, D. W. C. A General and Enantioselective Approach to Pentoses: A Rapid Synthesis of PSI-6130, the Nucleoside Core of Sofosbuvir. *J. Am. Chem. Soc.* **2014**, *136*, 5900-5903.

(22) Zhou, F. and Yamamoto, H. A Powerful Chiral Phosphoric Acid Catalyst for Enantioselective Mukaiyama–Mannich Reactions. *Angew. Chem., Int. Ed*. **2016**, *55*, 8970-8974.

(23) Jurberg, I. D.; Peng, B.; Wöstefeld, E.; Wasserloos, M.; Maulide, N. Intramolecular Redox‐Triggered C–H Functionalization. *Angew. Chem., Int. Ed.* **2012**, *51*, 1950-1953.

(24) Ikeda, K.; Achiwa, K.; Sekiya, M. Trifluoromethanesulfonic Acid-Promoted Reaction of Hexahydro-1, 3, 5-triazines. Introduction of a Secondary Aminomethyl Grouping into

Carboxylates at the α-Position through Ketene Silyl Acetals. *Chem. Pharm. Bull.* **1986**, *34*, 1579-1583.

A7. NMR Spectra

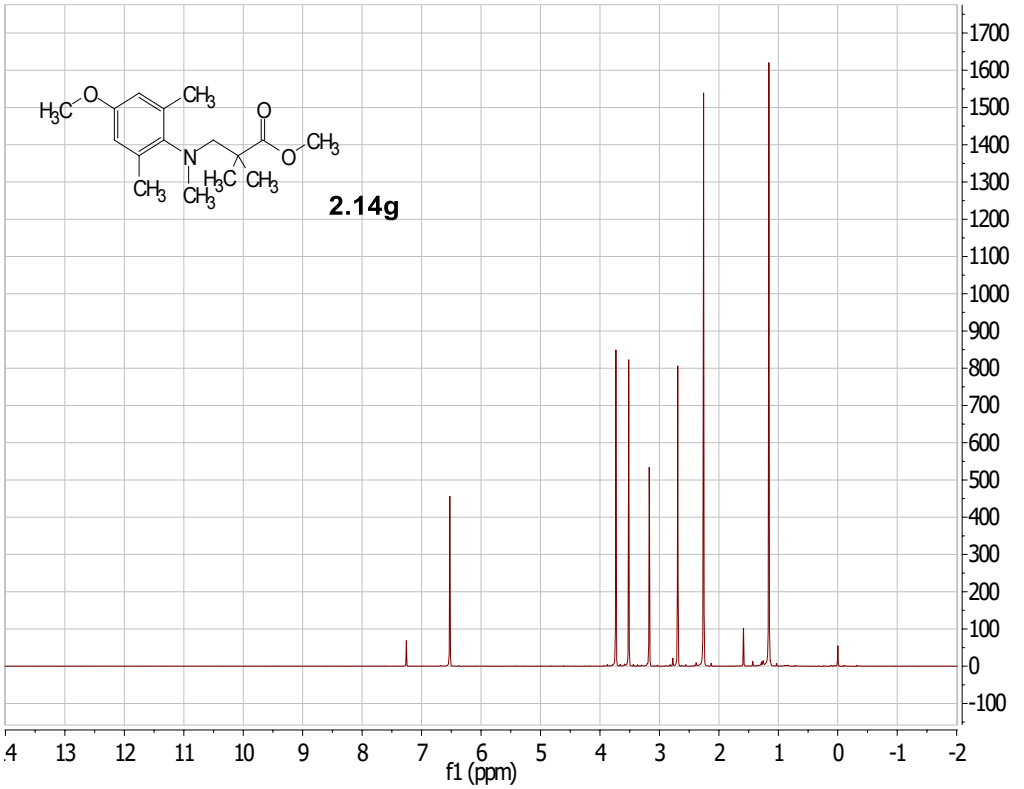

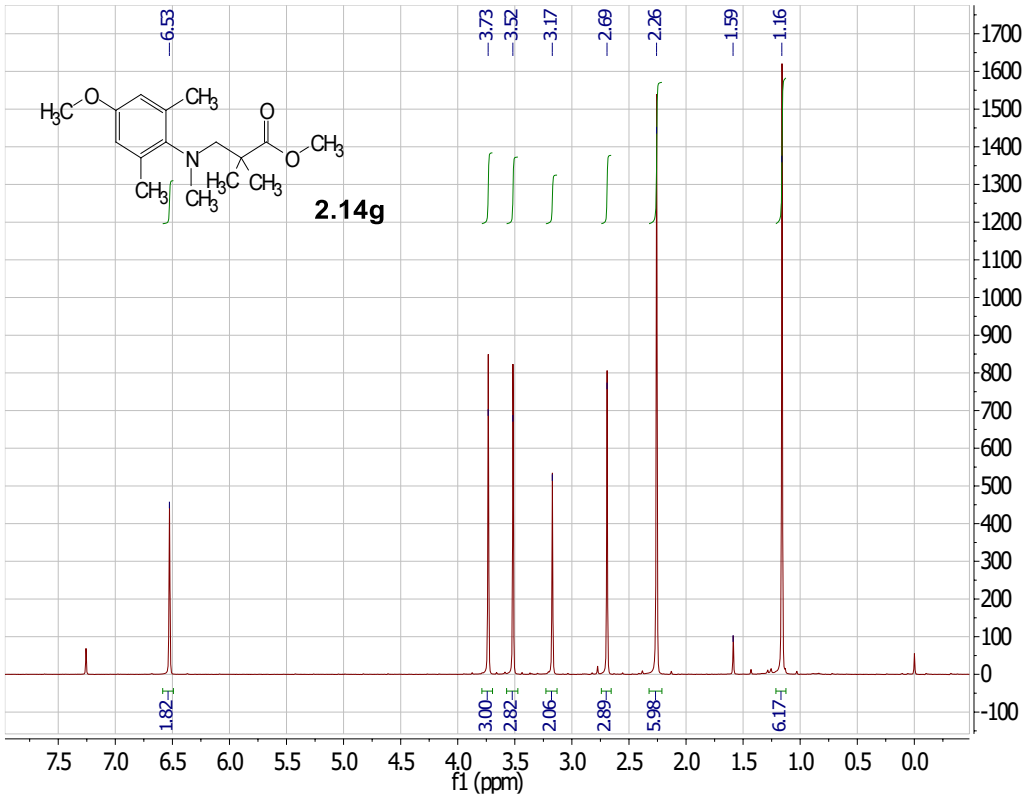

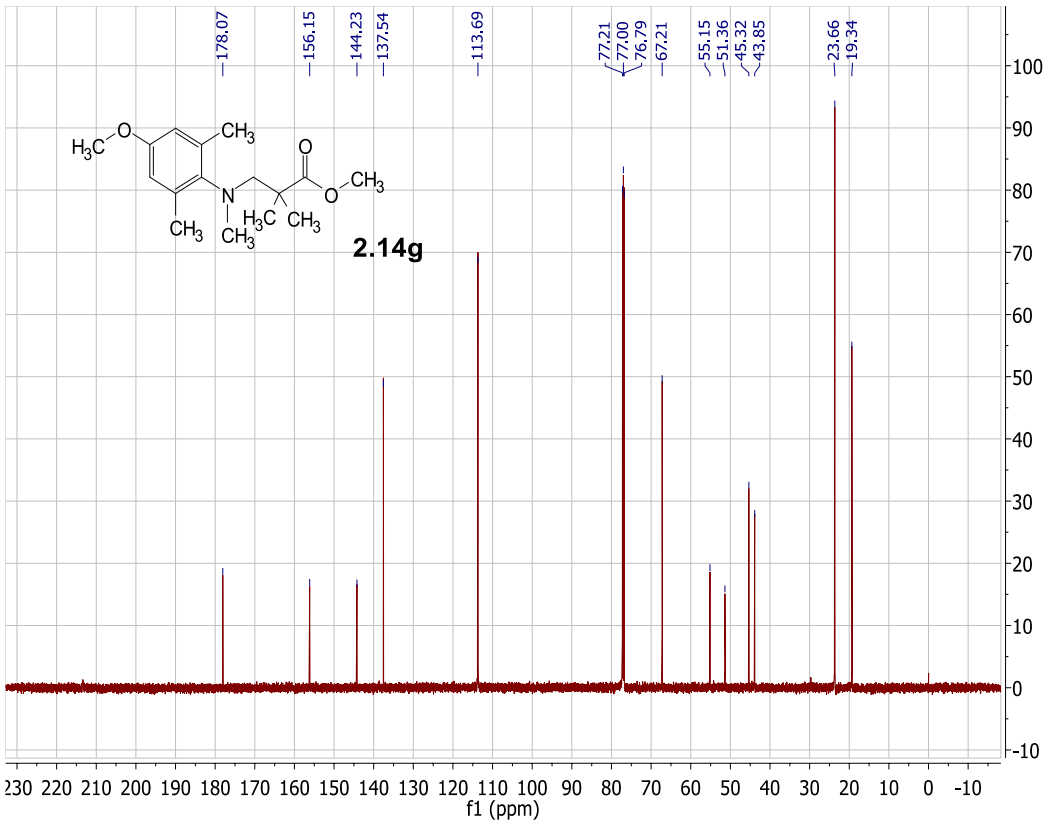
178.07
156.15
144.23
137.54
113.69
77.21
77.00
76.79
67.21
55.15
51.36
45.32
43.85
23.66
19.34
2.14g
f1 (ppm)

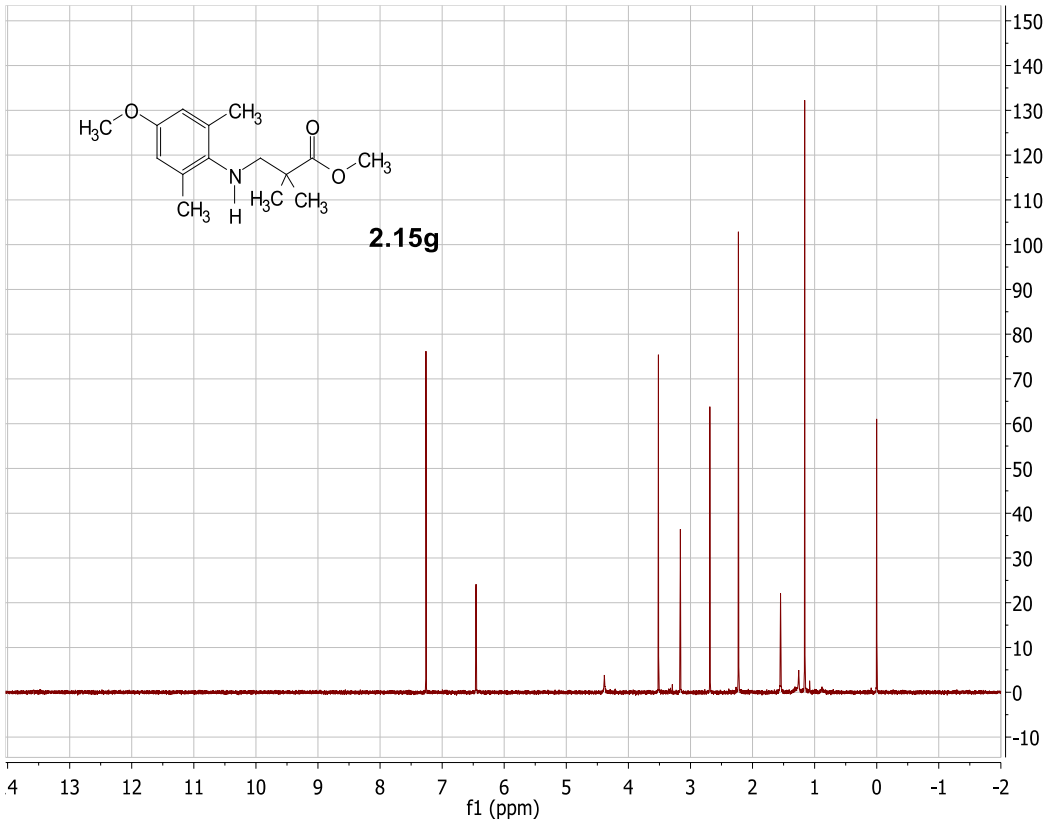
2.15g
f1 (ppm)

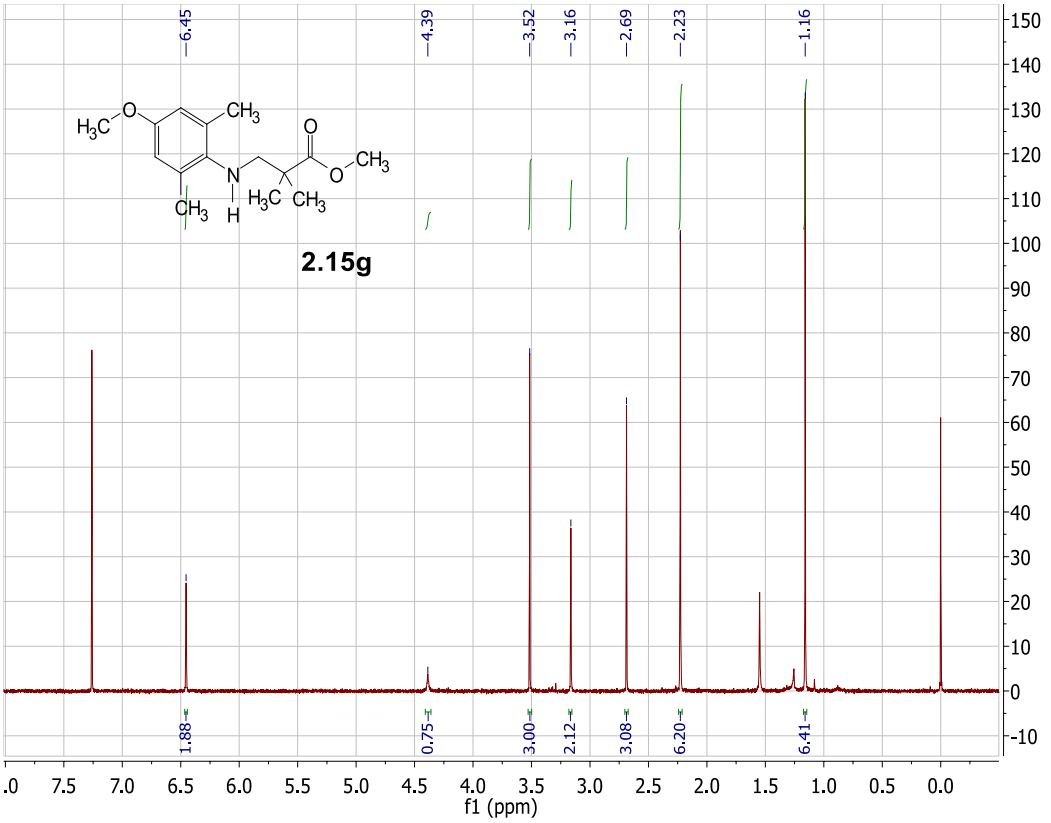
6.45
4.39
3.52
3.16
2.69
2.23
1.16
2.15g
1.88
0.75
3.00
2.12
3.08
6.20
6.41
f1 (ppm)

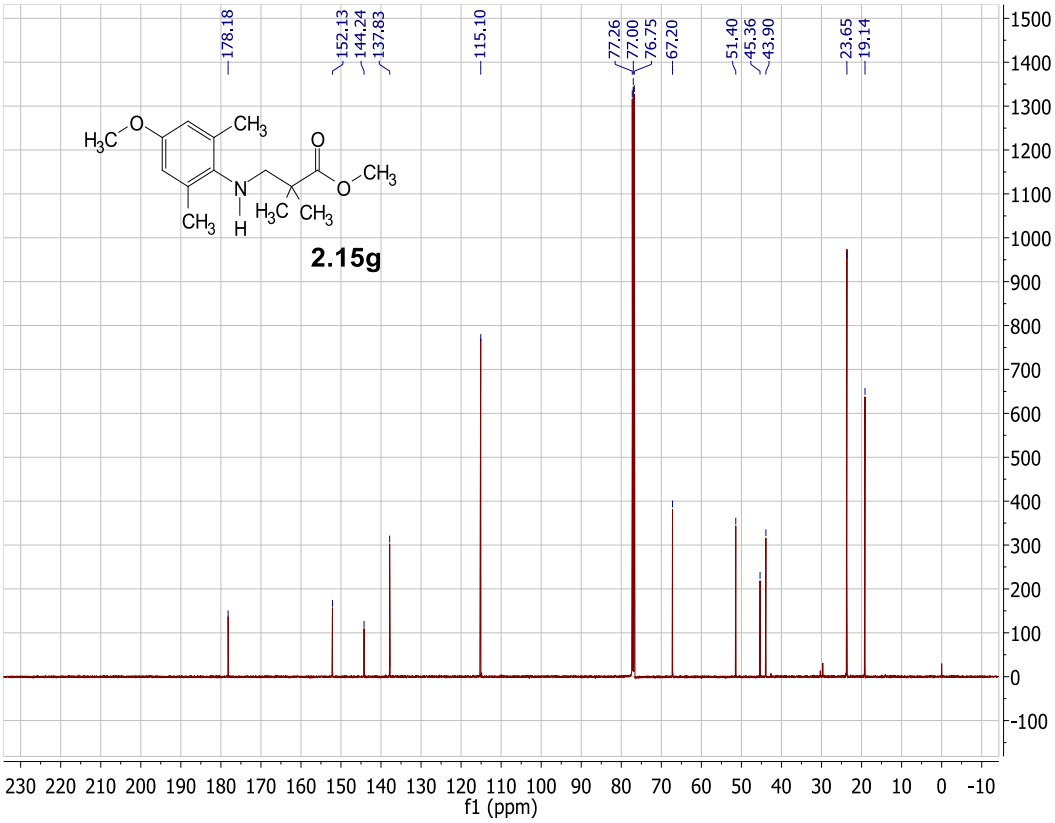
178.18
152.13
144.24
137.83
115.10
77.26
77.00
76.75
67.20
51.40
45.36
43.90
23.65
19.14
2.15g
f1 (ppm)

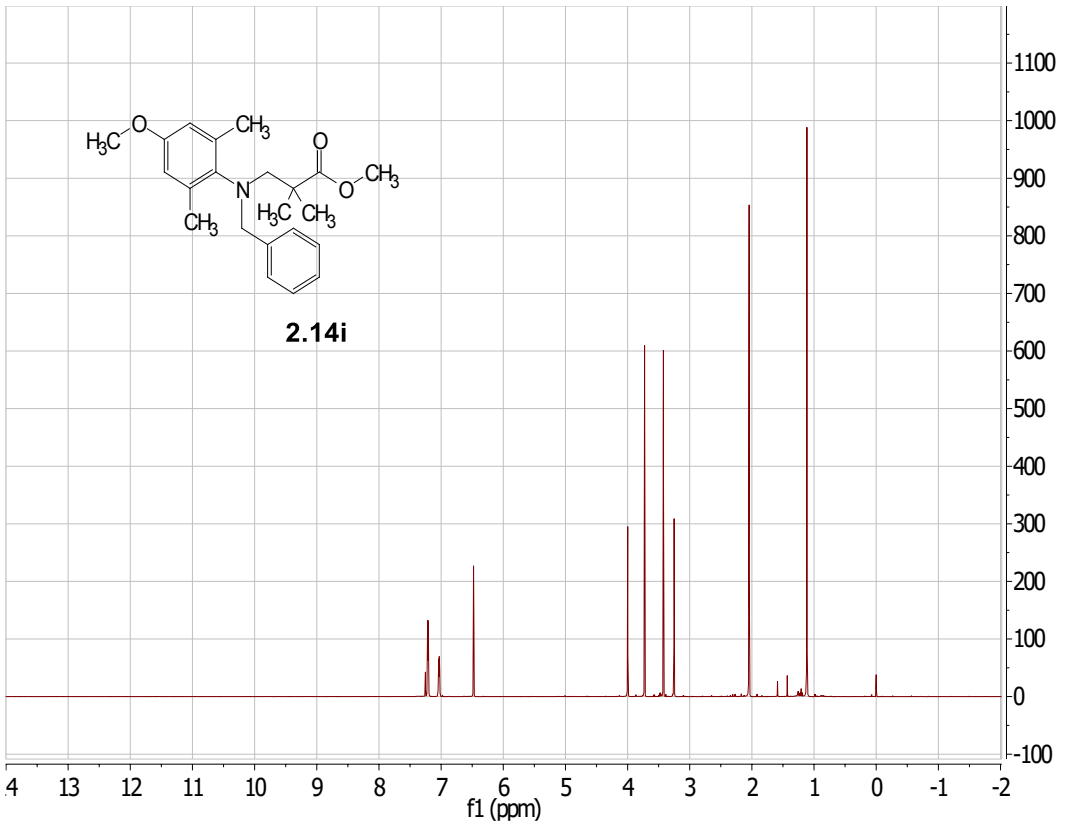
2.14i
f1 (ppm)

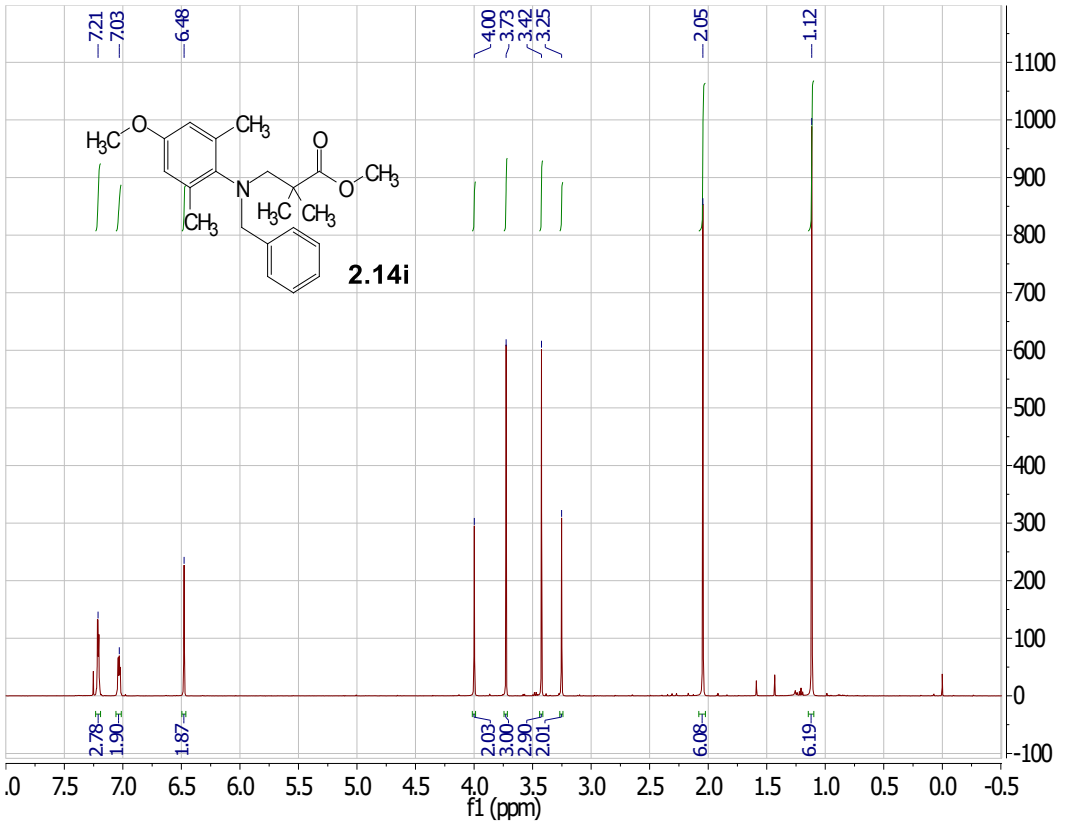
7.21
7.03
6.48
4.00
3.73
3.42
3.25
2.05
1.12
2.14i
2.78
1.90
1.87
2.03
3.00
2.90
2.01
6.08
6.19
f1 (ppm)

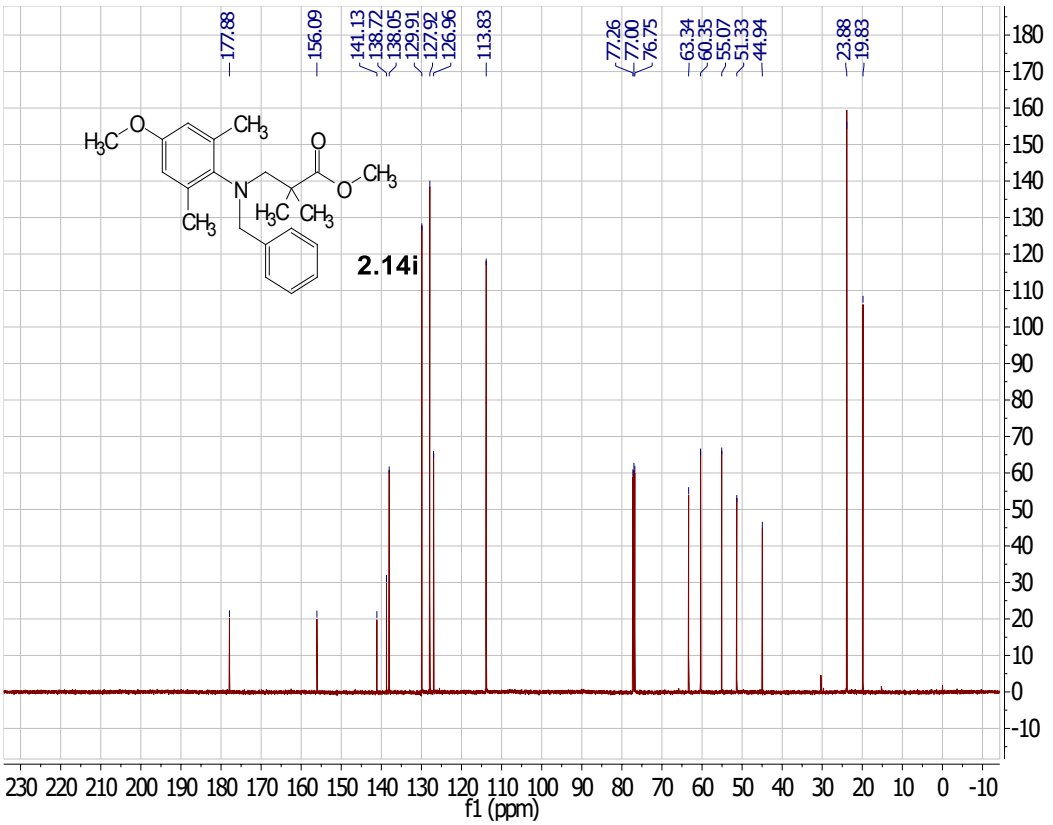
177.88
156.09
141.13
138.72
138.05
129.91
127.92
126.96
113.83
77.26
77.00
76.75
63.34
60.35
55.07
51.33
44.94
23.88
19.83
2.14i
f1 (ppm)

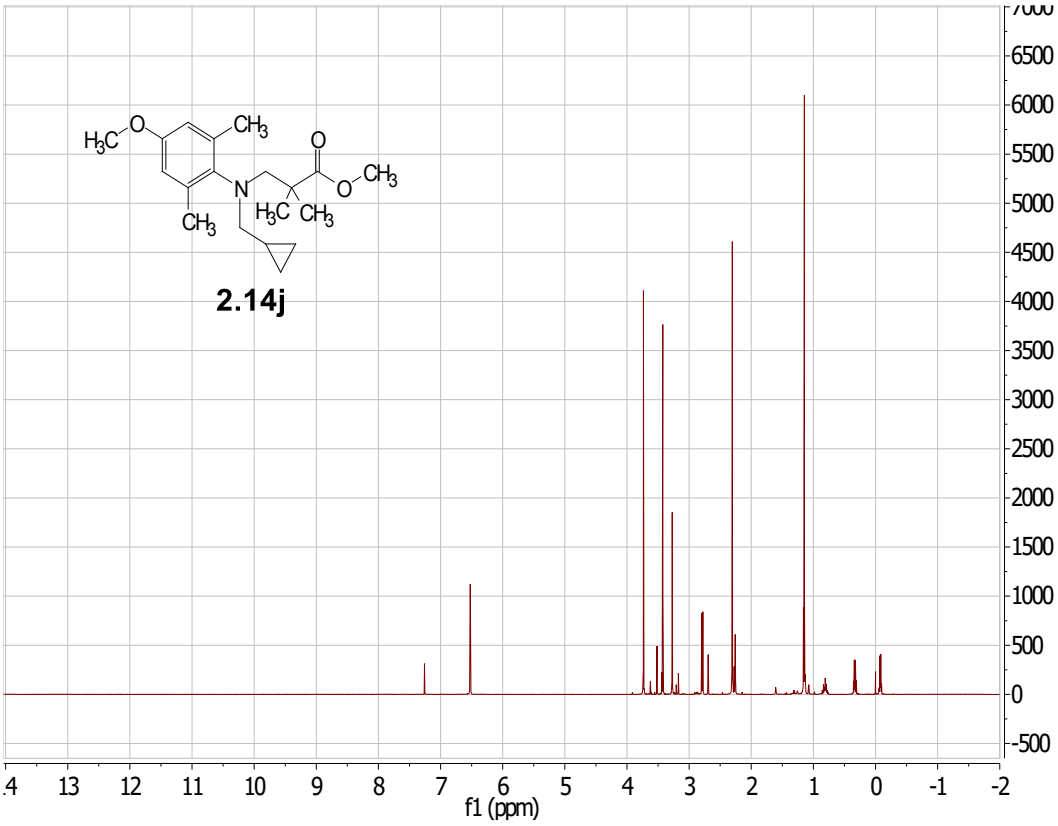
2.14j
f1 (ppm)

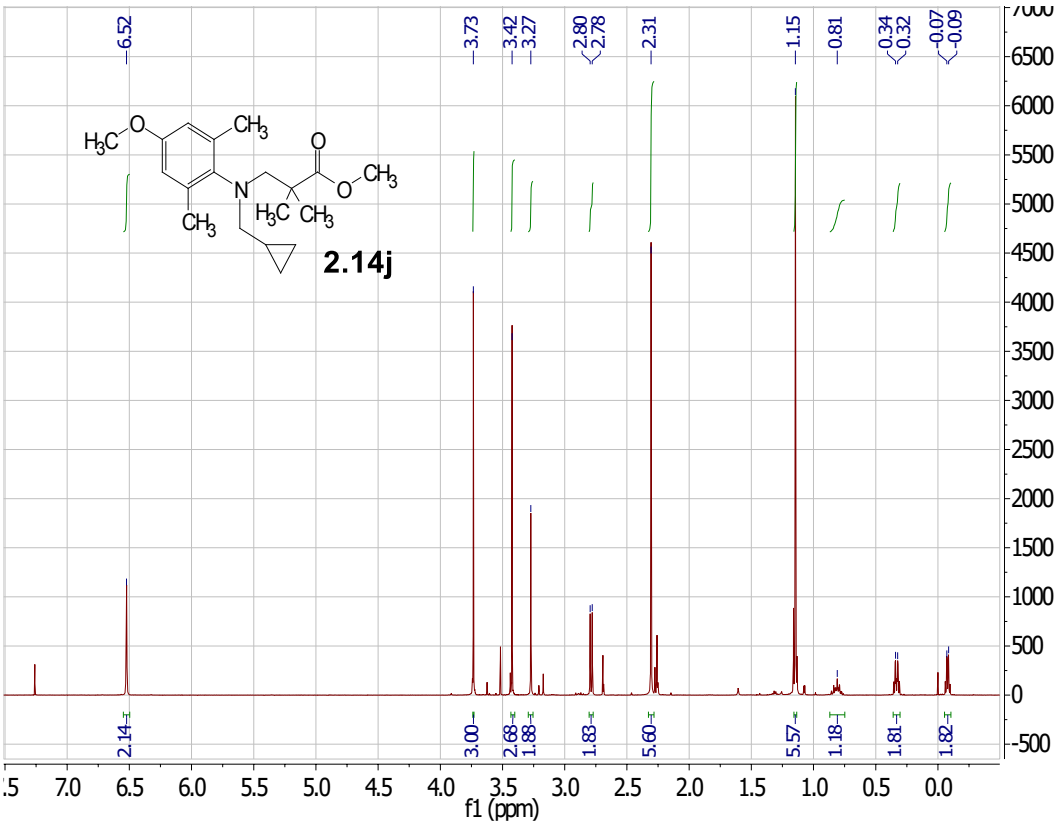
6.52
3.73
3.42
3.27
2.80
2.78
2.31
1.15
0.81
0.34
0.32
0.07
0.09
2.14
3.00
2.68
1.88
1.83
5.60
5.57
1.18
1.81
1.82
2.14j
f1 (ppm)

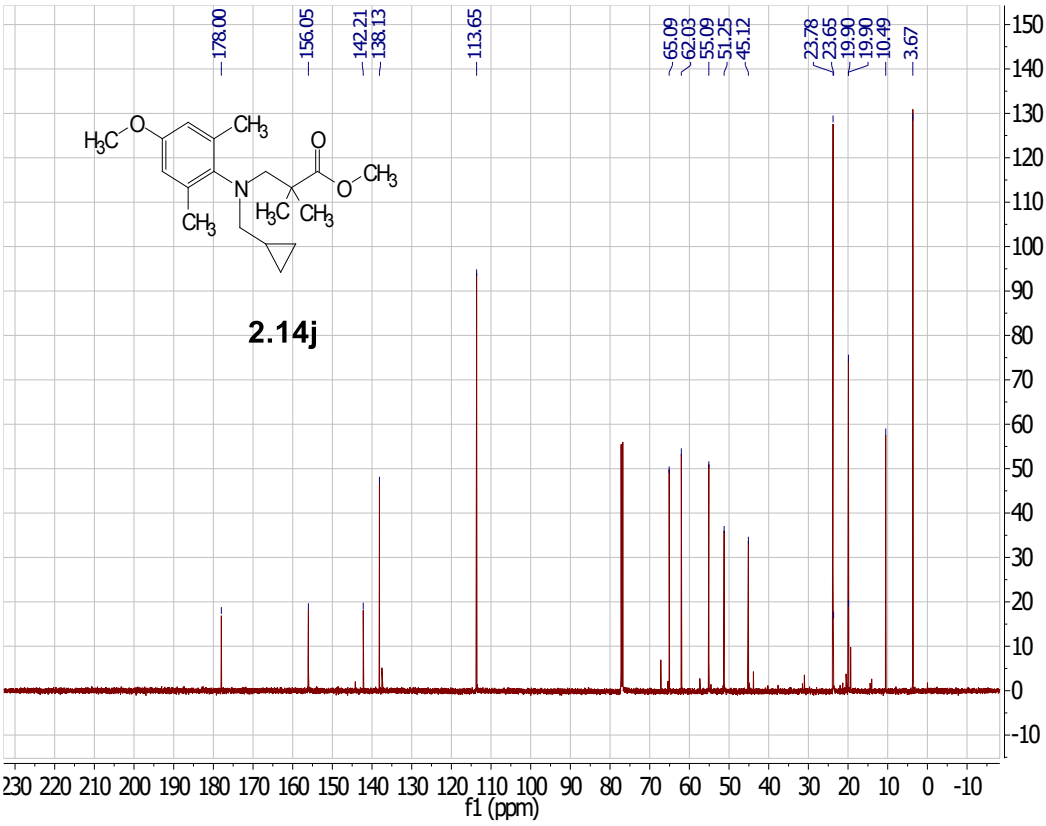
178.00
156.05
142.21
138.13
113.65
65.09
62.03
55.09
51.25
45.12
23.78
23.65
19.90
19.90
10.49
3.67
2.14j
f1 (ppm)

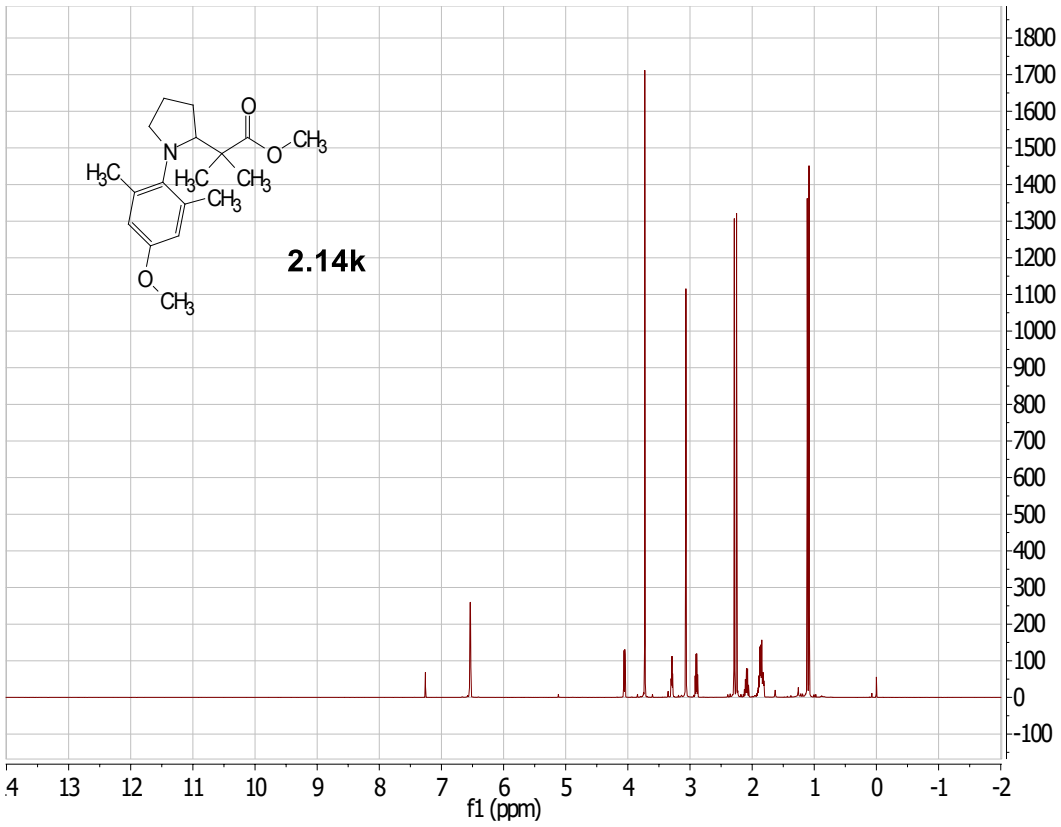
2.14k
f1 (ppm)

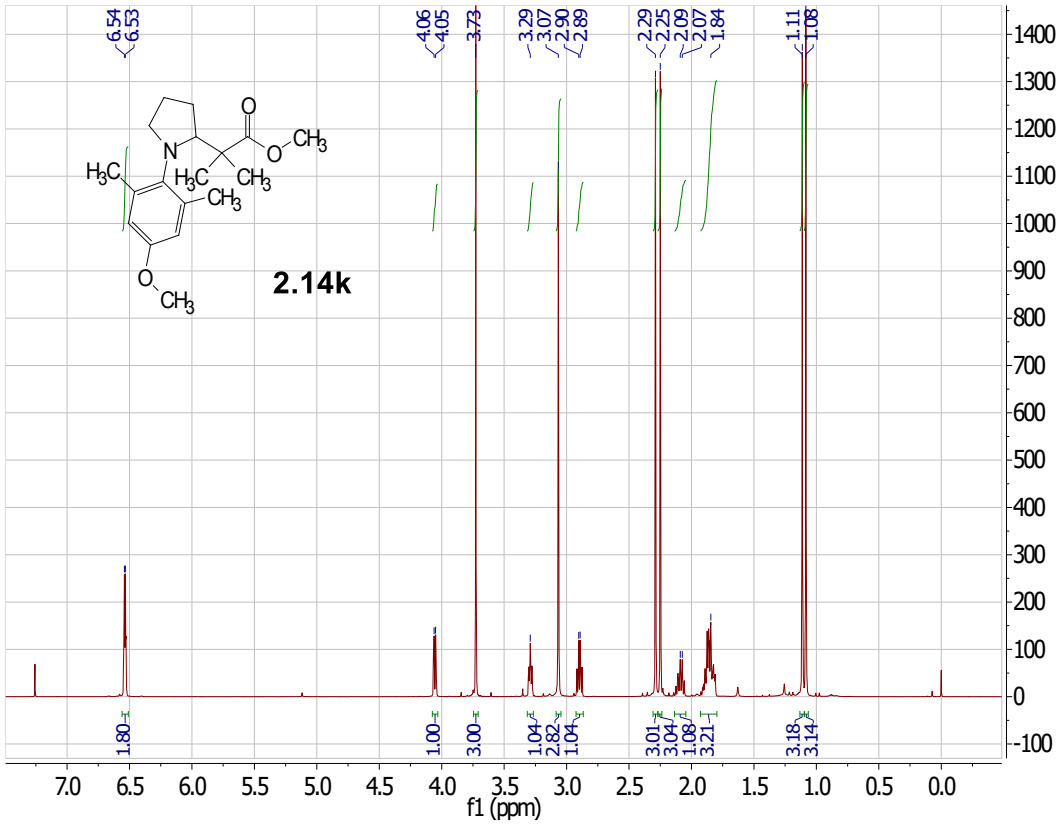
6.54
6.53
4.06
4.05
3.73
3.29
3.07
2.90
2.89
2.29
2.25
2.09
2.07
1.84
1.11
1.08
2.14k
1.80
1.00
3.00
1.04
2.82
1.04
3.01
3.04
1.08
3.21
3.18
3.14
f1 (ppm)

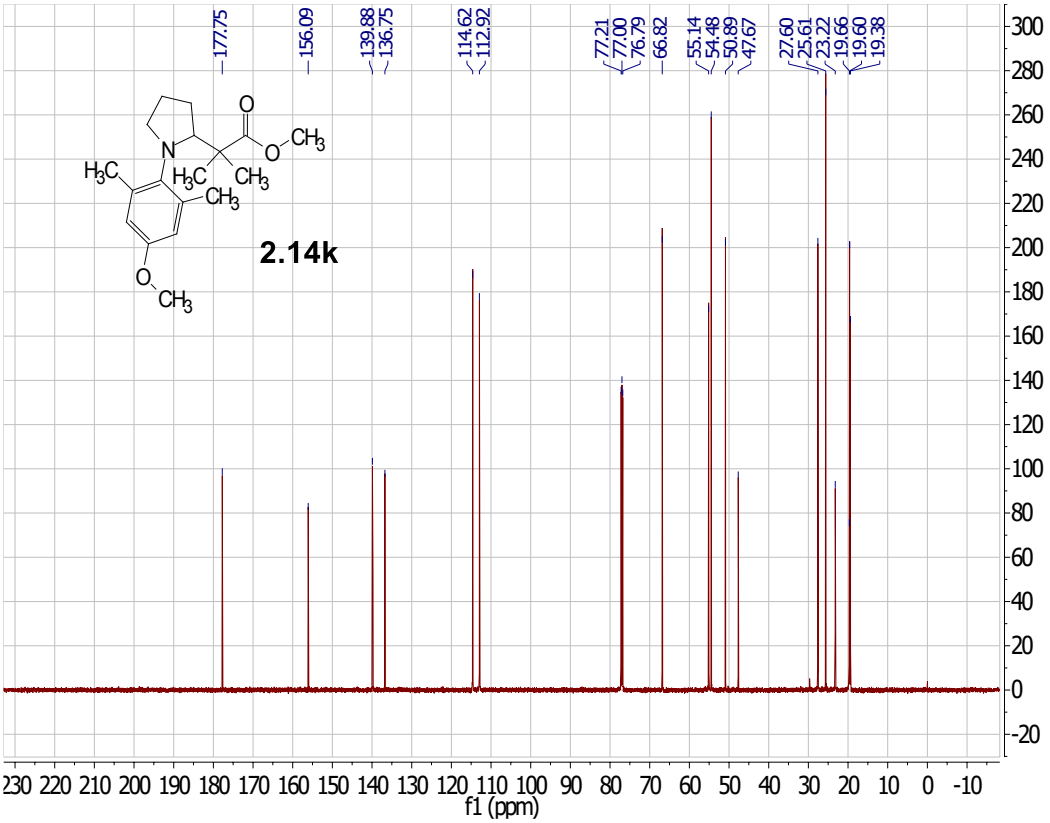
177.75
156.09
139.88
136.75
114.62
112.92
77.21
77.00
76.79
66.82
55.14
54.48
50.89
47.67
27.60
25.61
23.22
19.66
19.60
19.38
2.14k
f1 (ppm)

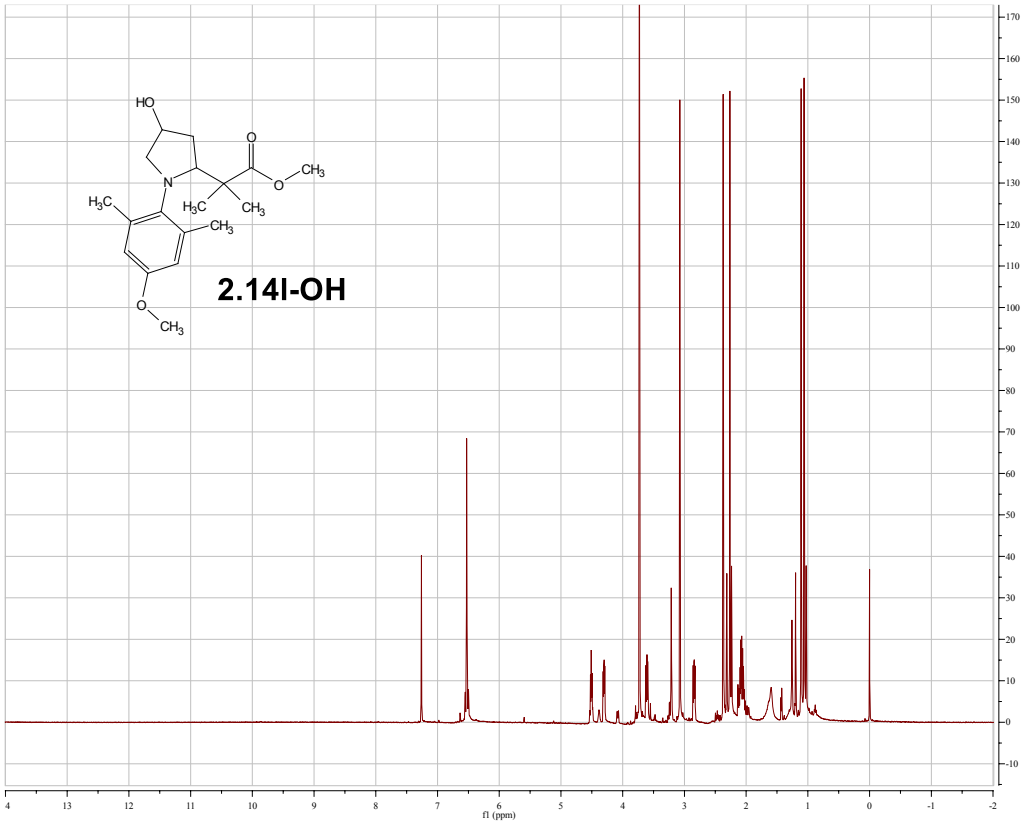
2.14l-OH
f1 (ppm)

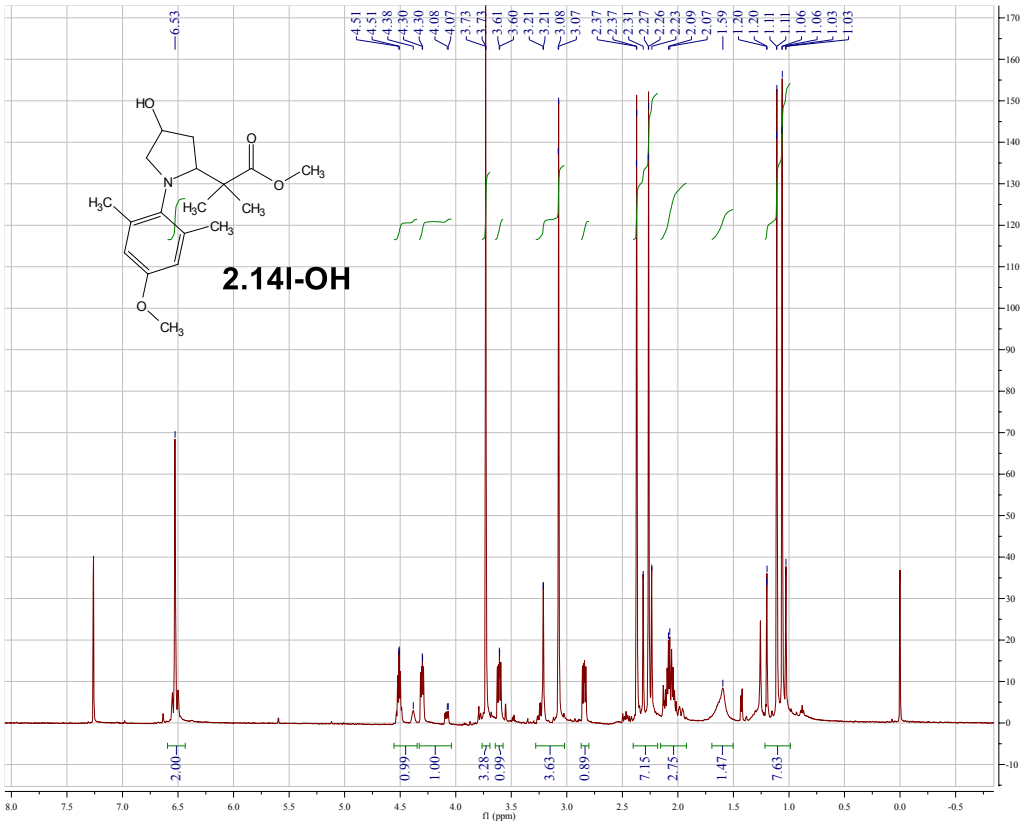
2.14l-OH
f1 (ppm)

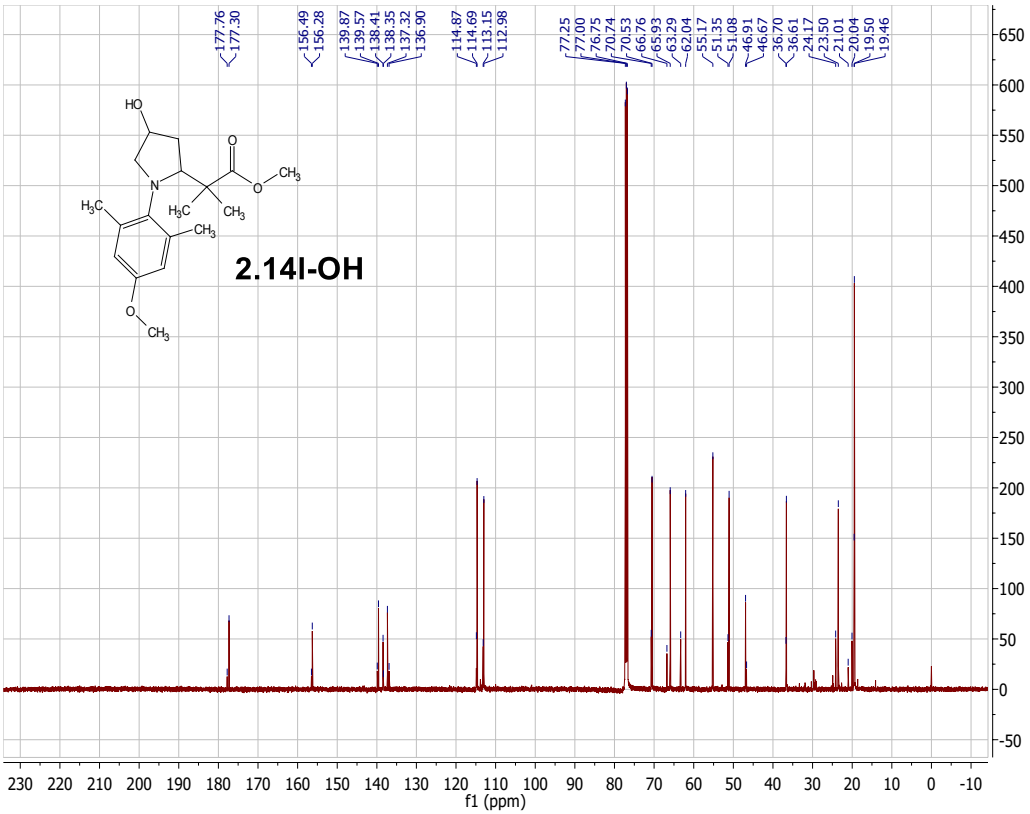
2.14l-OH
f1 (ppm)

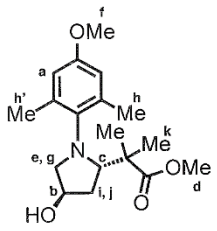

2.14l-OH

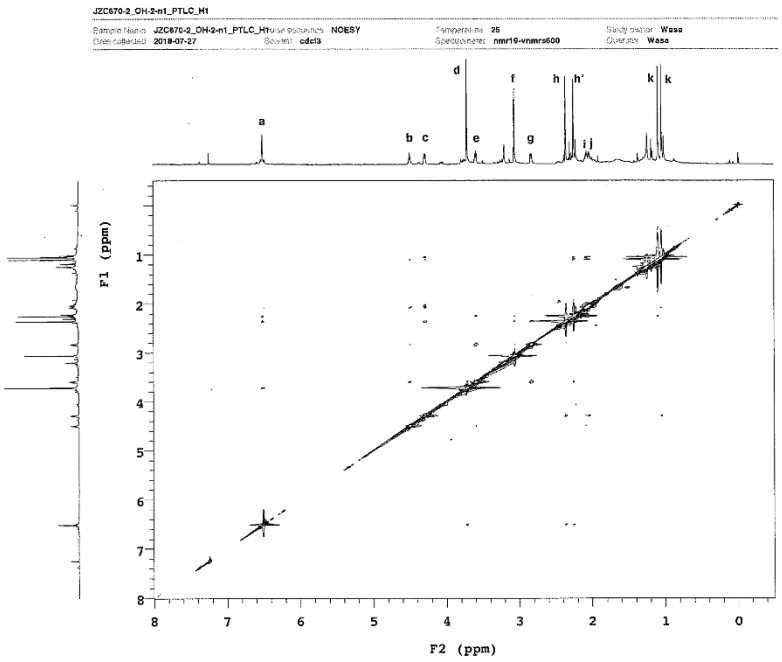

Data file /home/AllWasa/Yujin/JZC670-2_OH_SINAUTOEF3-2_OH-2-n1_PTLC_NOESY_19h.fid

Plot date 2018-07-28

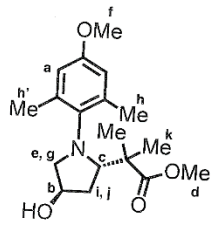

2.14l-OH

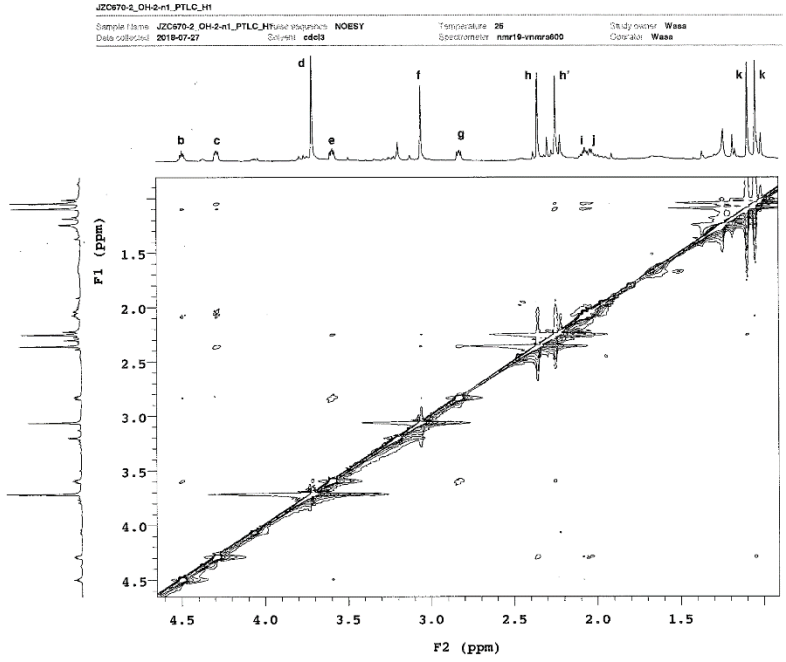

Data file /home/AllWasa/Yujin/JZC670-2_OH_SINAUTOEF3-2_OH-2-n1_PTLC_NOESY_19h.fid

Plot date 2018-07-28

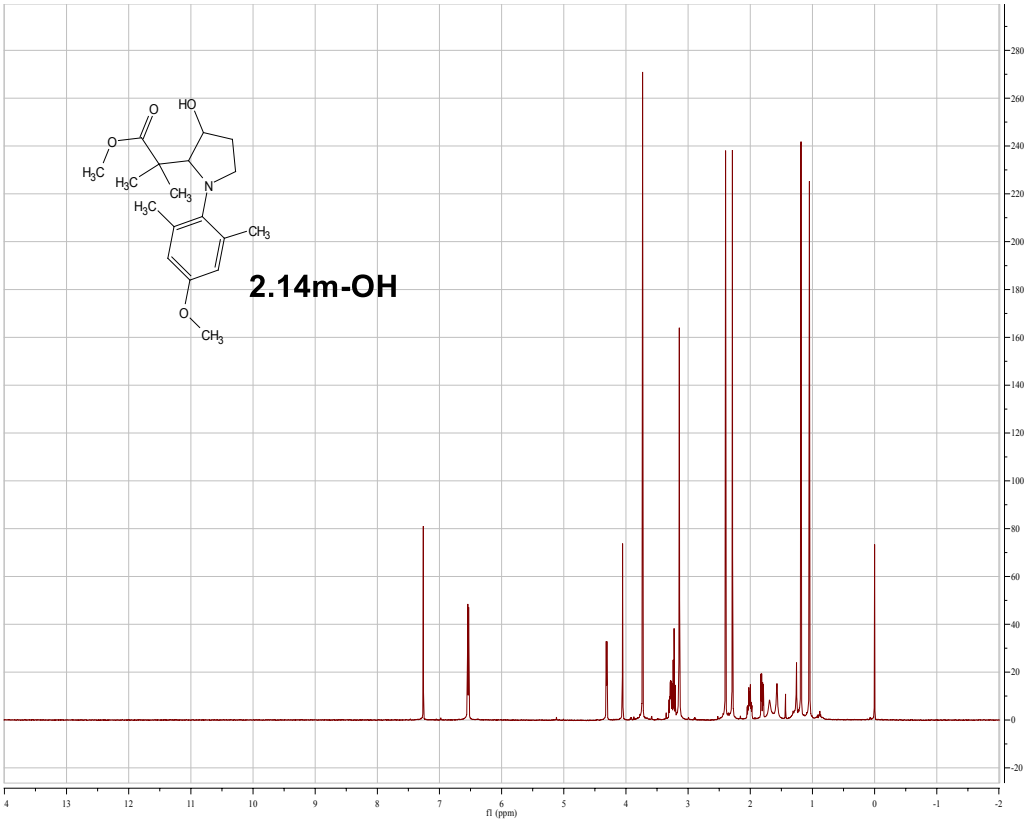
2.14m-OH
f1 (ppm)

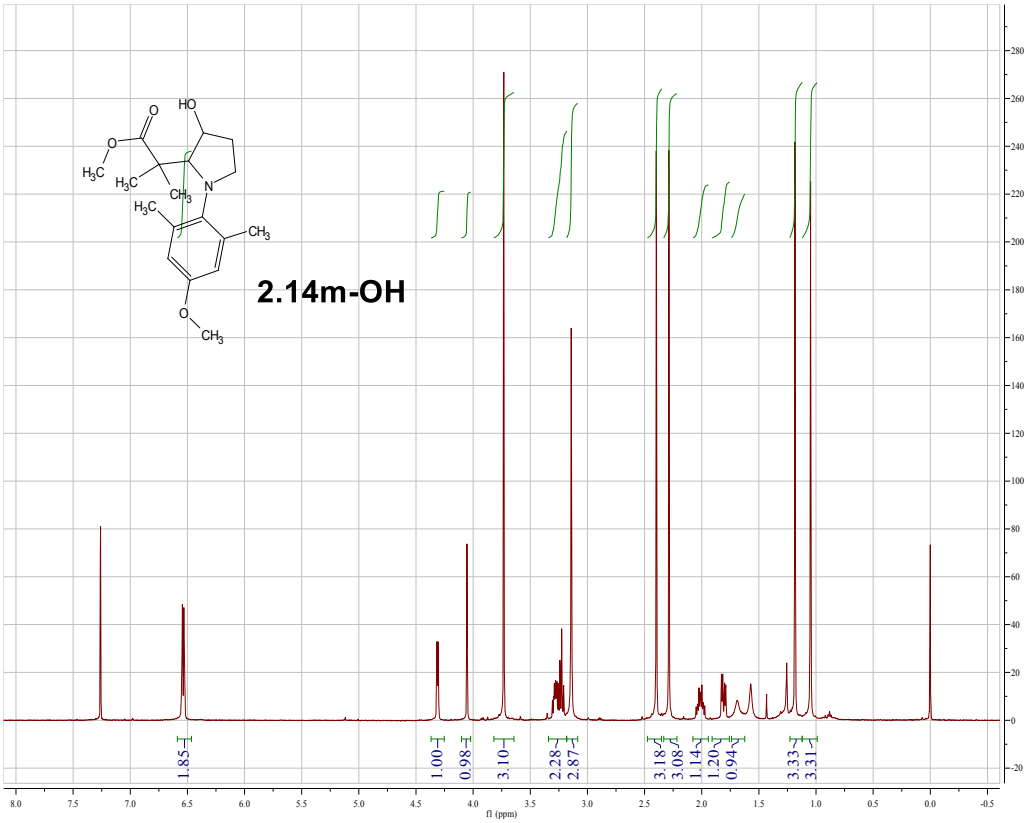
2.14m-OH
1.85
1.00
0.98
3.10
2.28
2.87
3.18
3.08
1.14
1.20
0.94
3.33
3.31
f1 (ppm)

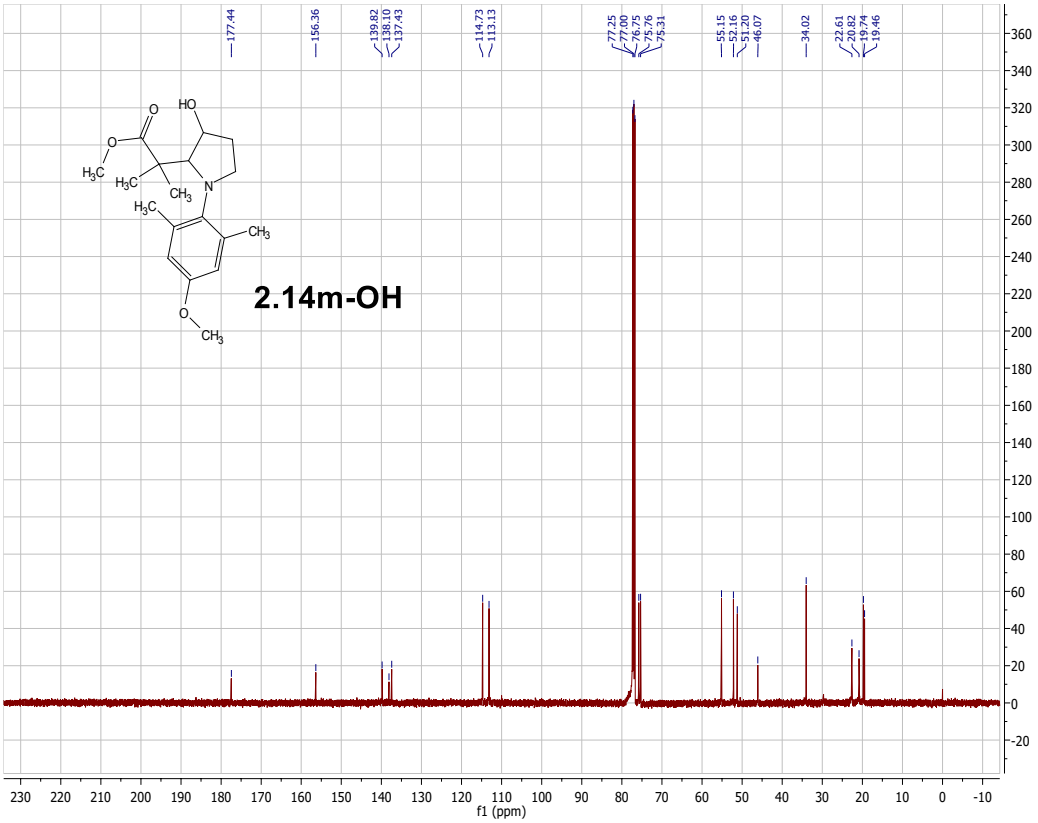

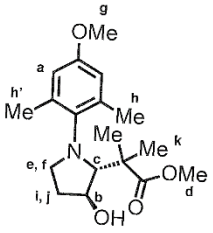

2.14m-OH

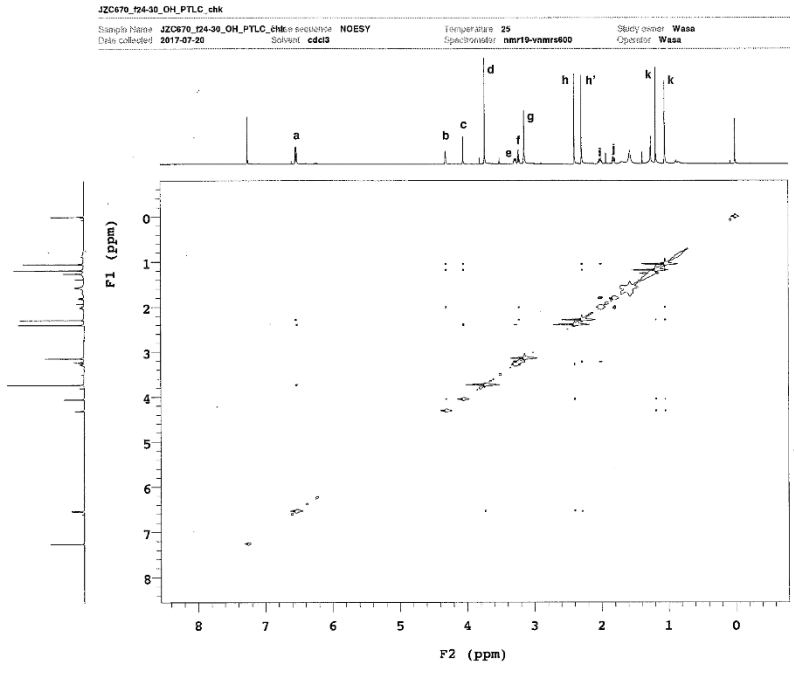

Data file /home/ALL/Wasa/Jessica/TJa_group/was_NOESY_07212017.fid

Plot date 2017-07-21

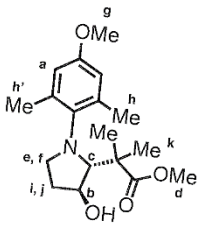
g
OMe
a
h'
Me
h
Me
Me
N
e, f
c
Me
k
OMe
i, j
b
OH
O
d

2.14m-OH

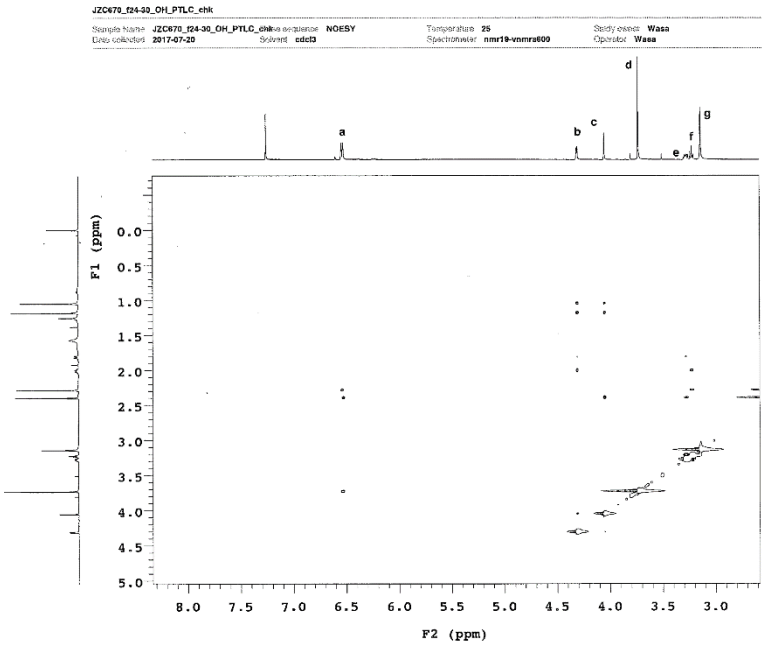
JZC670_f24-30_OH_PTLC_chk
Sample Name JZC670_f24-30_OH_PTLC_chk
Pulse sequence NOESY
Temperature 25
Study name Wasa
Data collected 2017-07-20
Solvent cdcl3
Spectrometer nmr19-vnmrs600
Operator Wasa
a
b
c
d
e
f
g
F1 (ppm)
F2 (ppm)

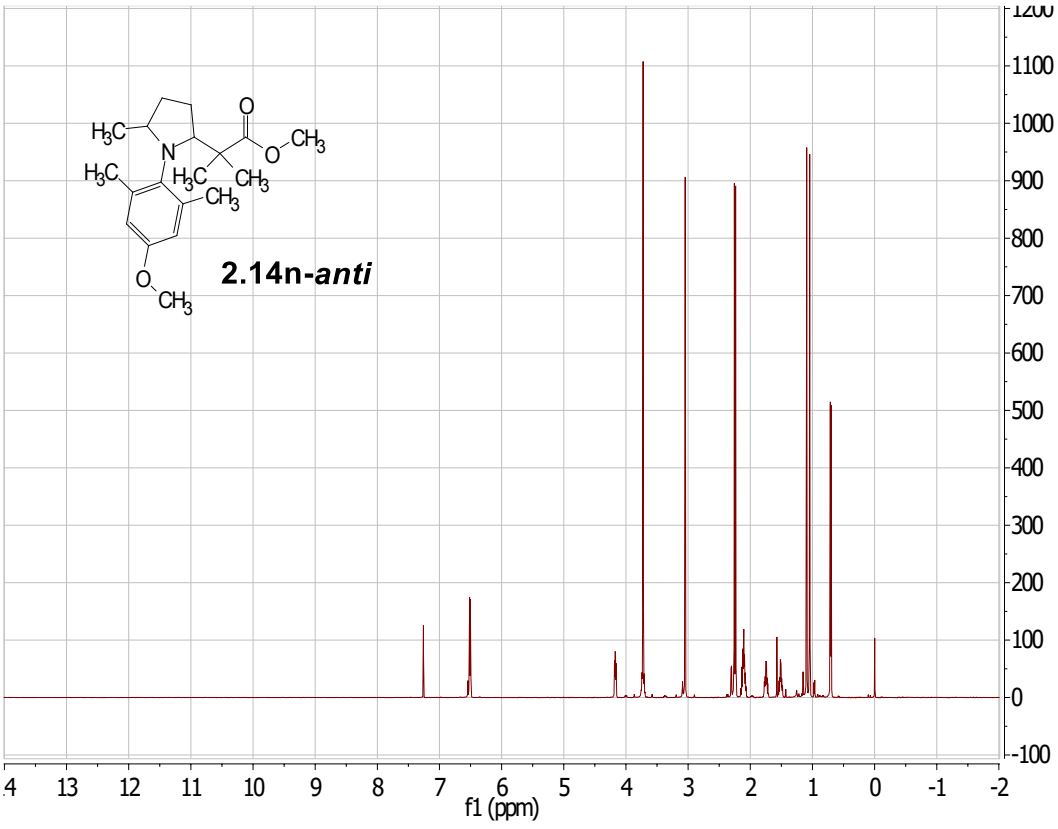
2.14n-*anti*
f1 (ppm)

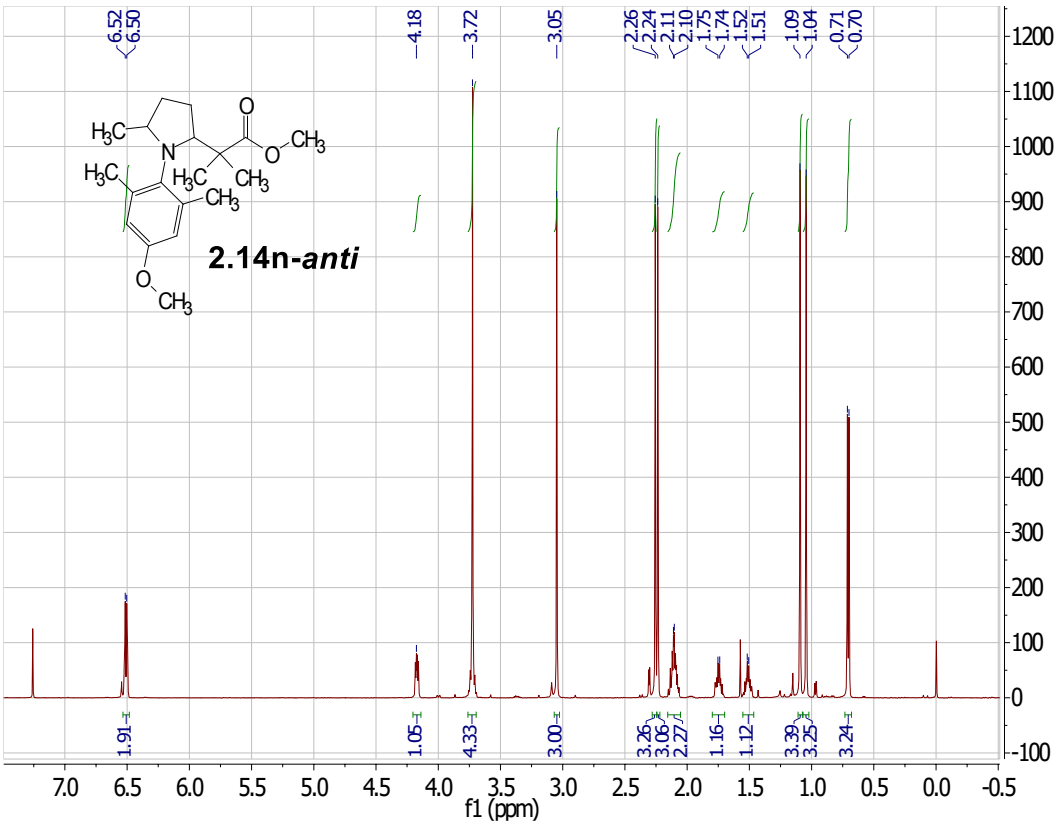
6.52
6.50
4.18
3.72
3.05
2.26
2.24
2.11
2.10
1.75
1.74
1.52
1.51
1.09
1.04
0.71
0.70
2.14n-anti
1.91
1.05
4.33
3.00
3.26
3.06
2.27
1.16
1.12
3.39
3.25
3.24
f1 (ppm)

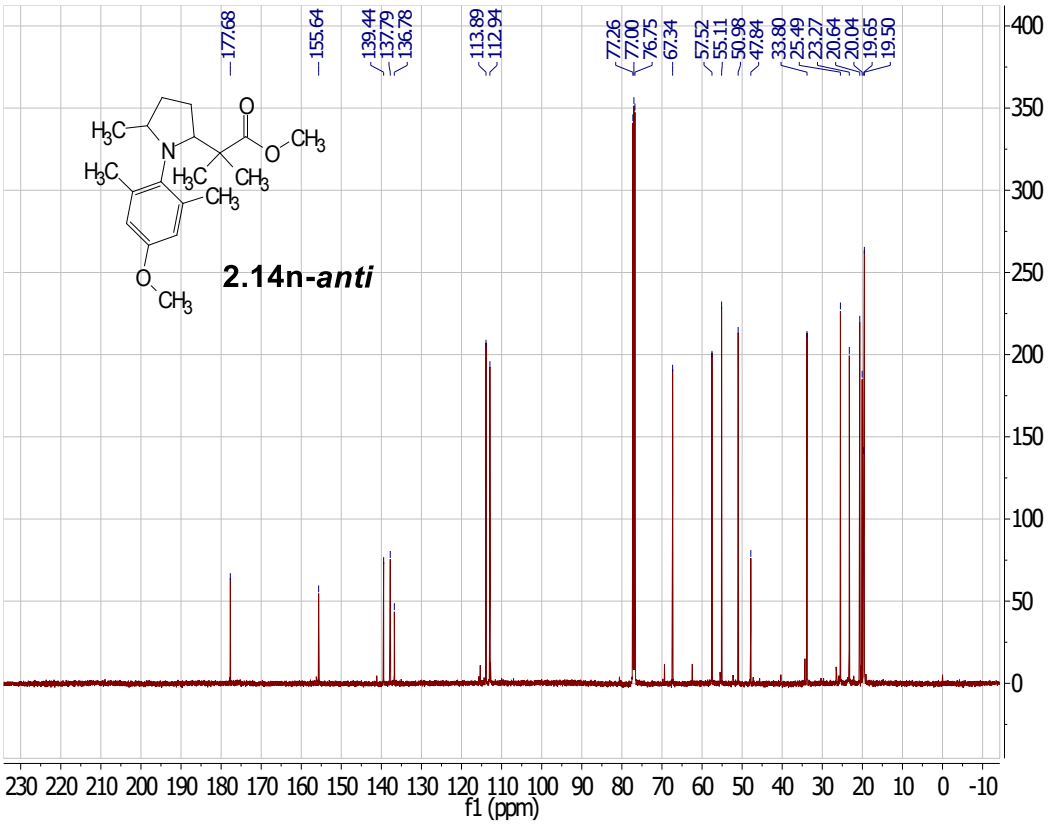
177.68
155.64
139.44
137.79
136.78
113.89
112.94
77.26
77.00
76.75
67.34
57.52
55.11
50.98
47.84
33.80
25.49
23.27
20.64
20.04
19.65
19.50
2.14n-anti
f1 (ppm)

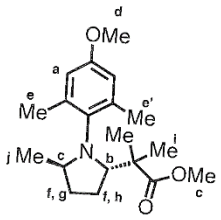

2.14n-*anti*

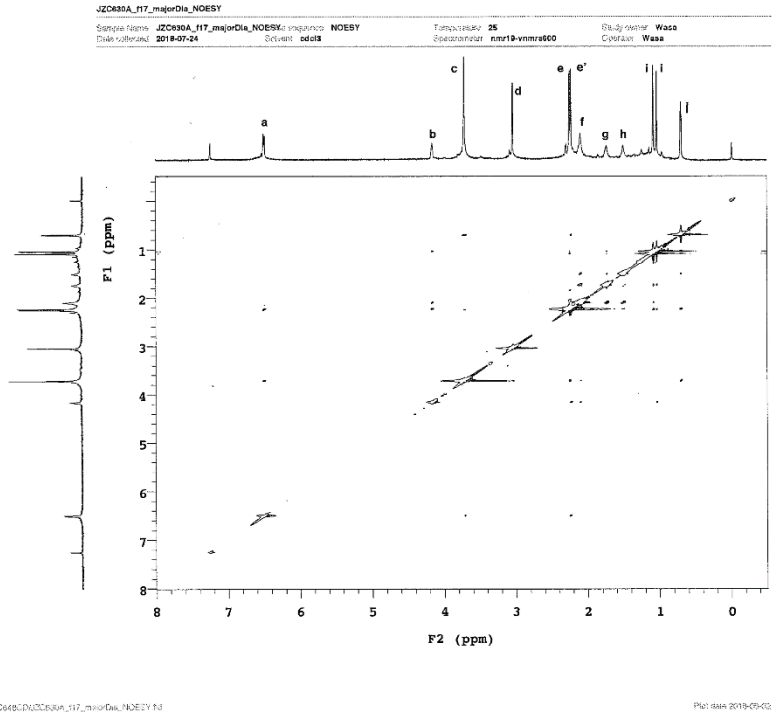

Data file /home/NMRWaste/Yelin/JZC648CDCl3/JZC630A_f17_majorDia_NOESY.fid

Plot date 2018-09-02

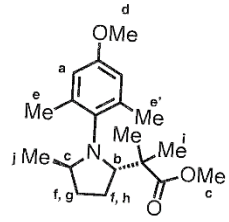

2.14n-*anti*

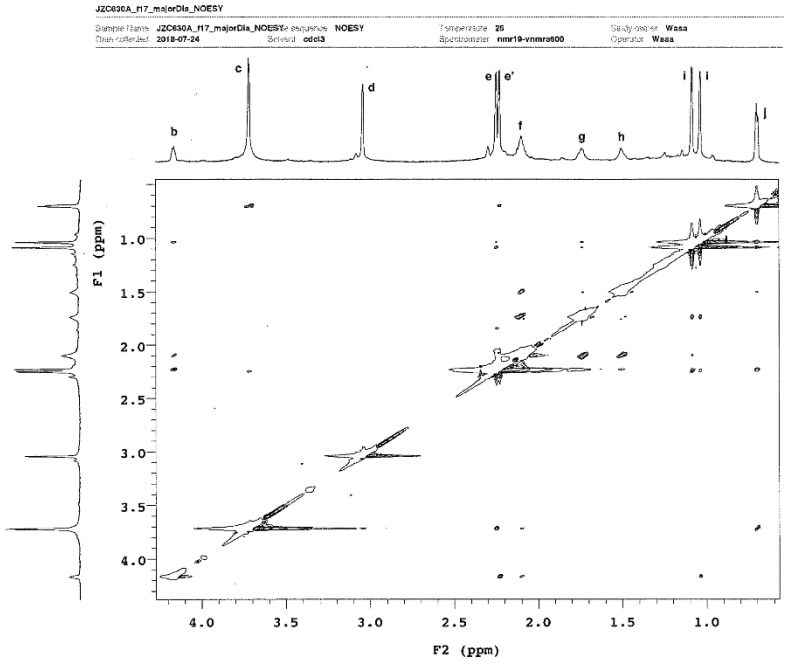

Data file /home/NMRWaste/Yelin/JZC648CDCl3/JZC630A_f17_majorDia_NOESY.fid

Plot date 2018-09-02

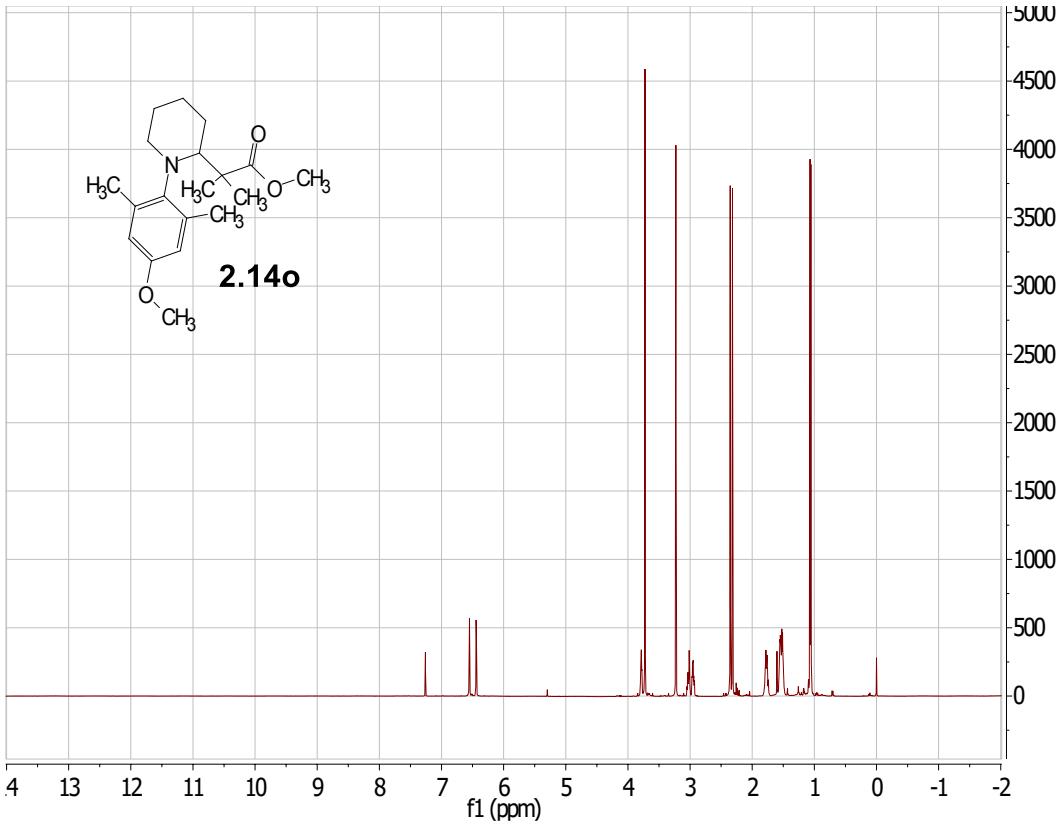
2.14o
f1 (ppm)

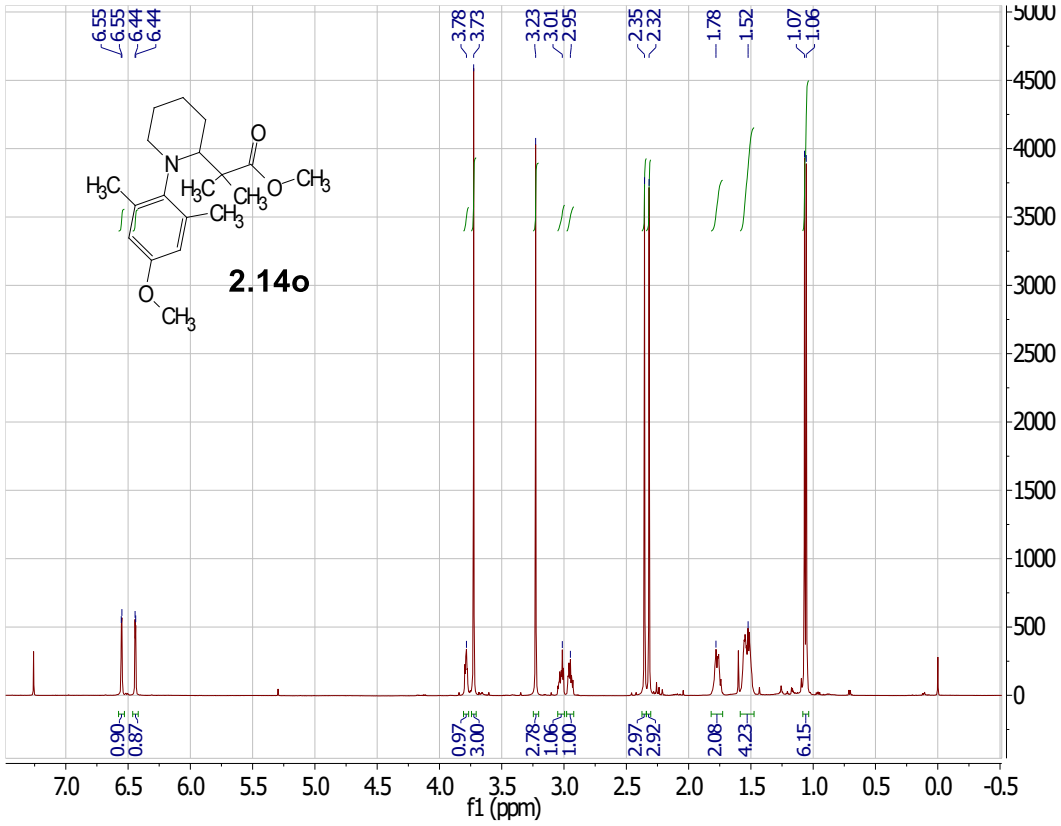
6.55
6.55
6.44
6.44
3.78
3.73
3.23
3.01
2.95
2.35
2.32
1.78
1.52
1.07
1.06
2.14o
0.90
0.87
0.97
3.00
2.78
1.06
1.00
2.97
2.92
2.08
4.23
6.15
f1 (ppm)

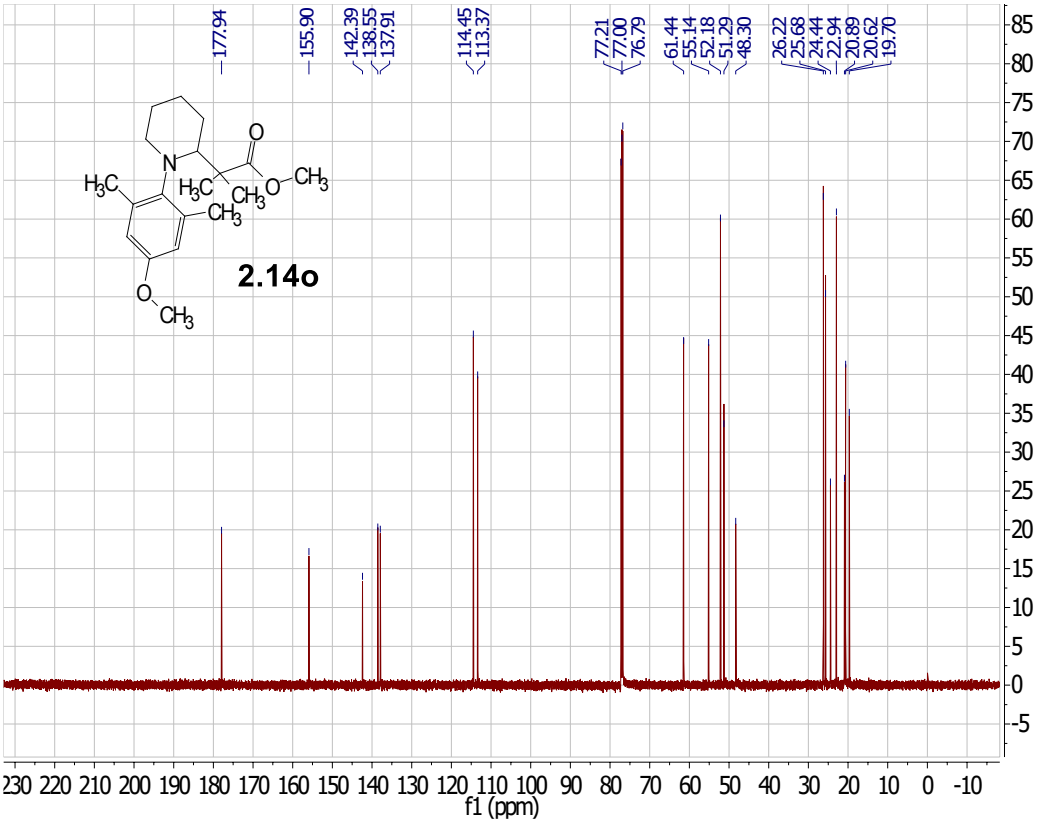
177.94
155.90
142.39
138.55
137.91
114.45
113.37
77.21
77.00
76.79
61.44
55.14
52.18
51.29
48.30
26.22
25.68
24.44
22.94
20.89
20.62
19.70
2.14o
f1 (ppm)

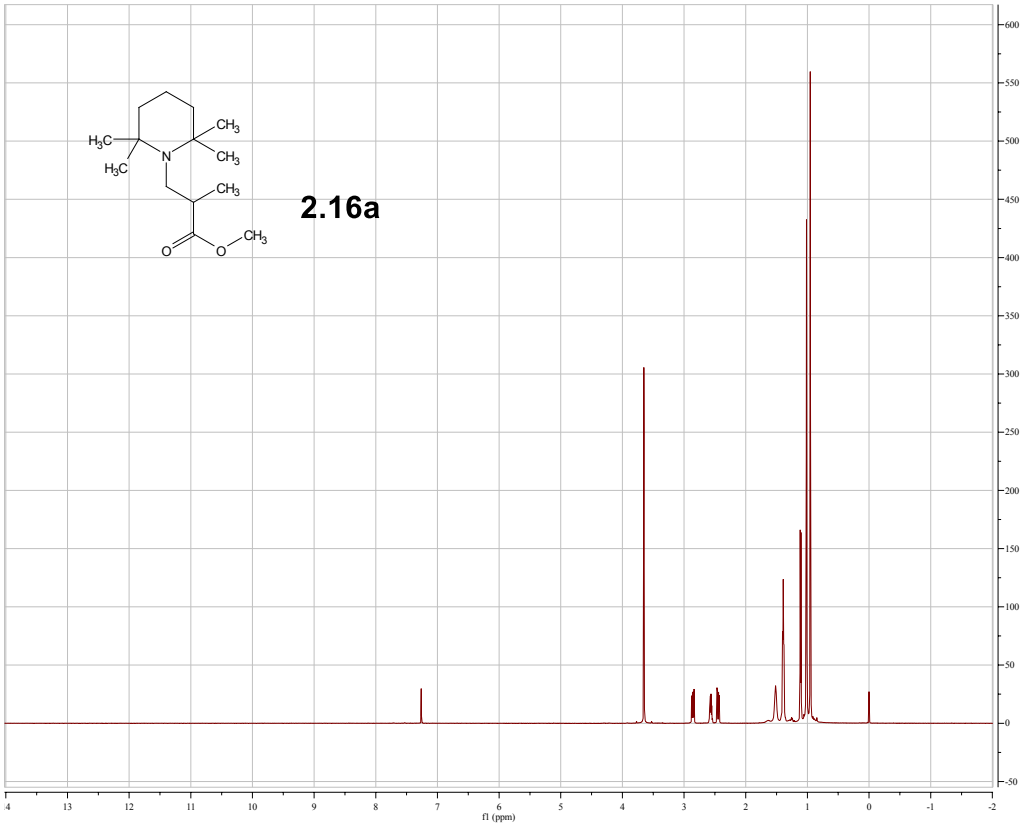
2.16a
f1 (ppm)

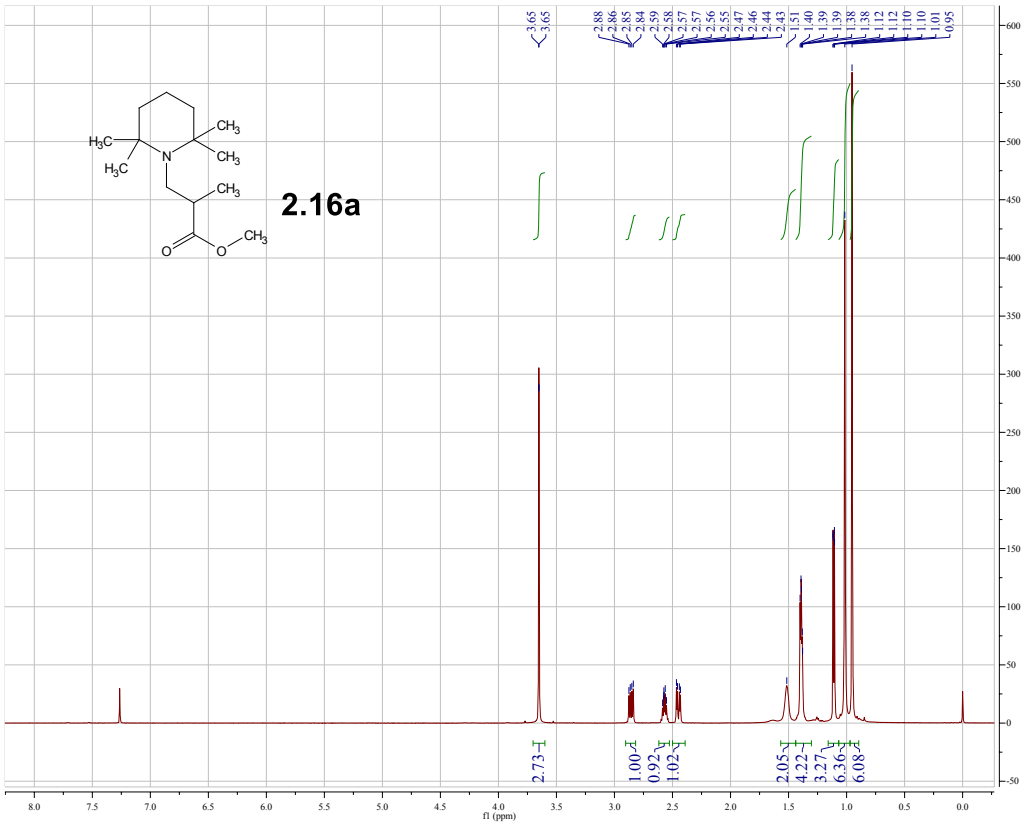
2.16a
3.65
3.65
2.88
2.86
2.85
2.84
2.59
2.58
2.57
2.57
2.56
2.55
2.47
2.46
2.44
2.43
1.51
1.40
1.39
1.39
1.38
1.38
1.12
1.12
1.10
1.10
1.01
0.95
2.73
1.00
0.92
1.02
2.05
4.22
3.27
6.36
6.08
f1 (ppm)

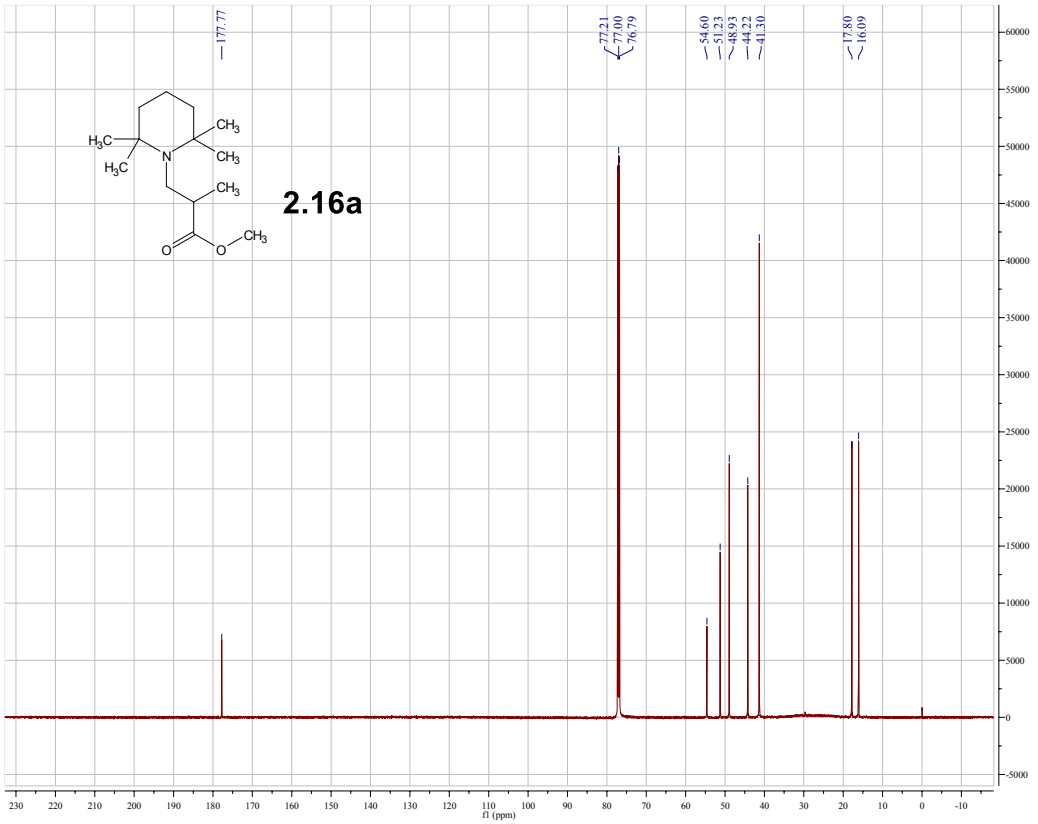
2.16a
177.77
77.21
77.00
76.79
54.60
51.23
48.93
44.22
41.30
17.80
16.09
f1 (ppm)

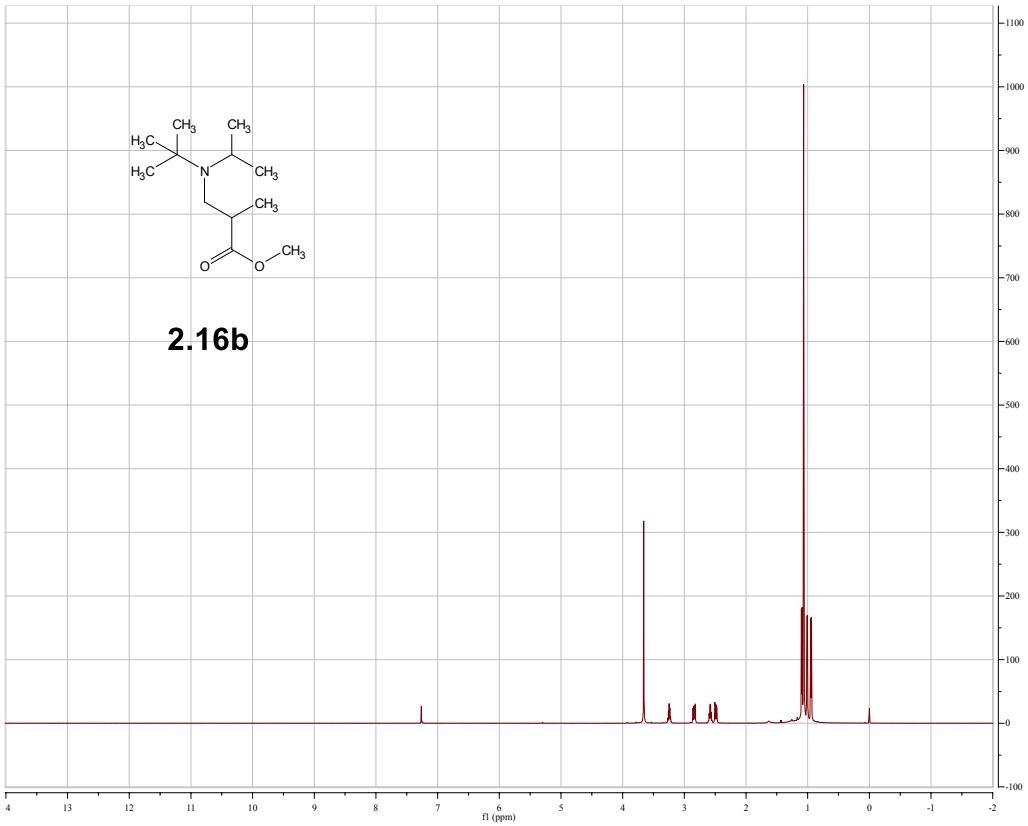
2.16b
f1 (ppm)

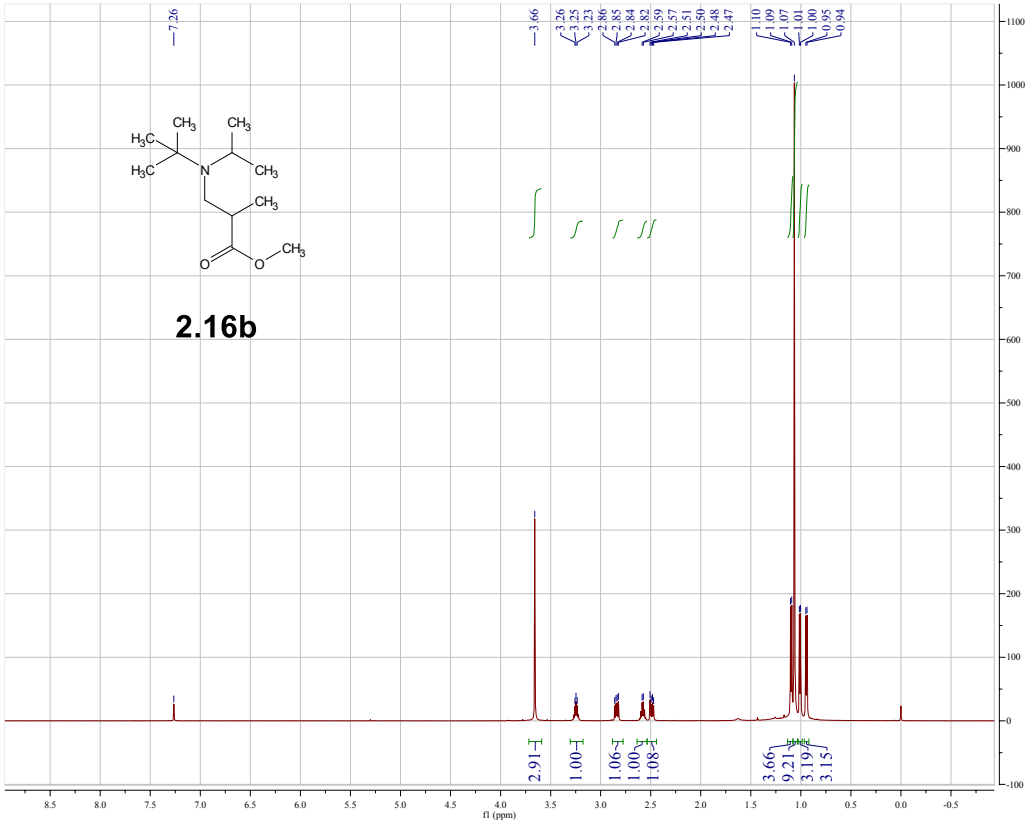
7.26
3.66
3.26
3.25
3.23
2.86
2.85
2.84
2.82
2.59
2.57
2.51
2.50
2.48
2.47
1.10
1.09
1.07
1.01
1.00
0.95
0.94
2.16b
2.91
1.00
1.06
1.00
1.08
3.66
9.21
3.19
3.15
f1 (ppm)

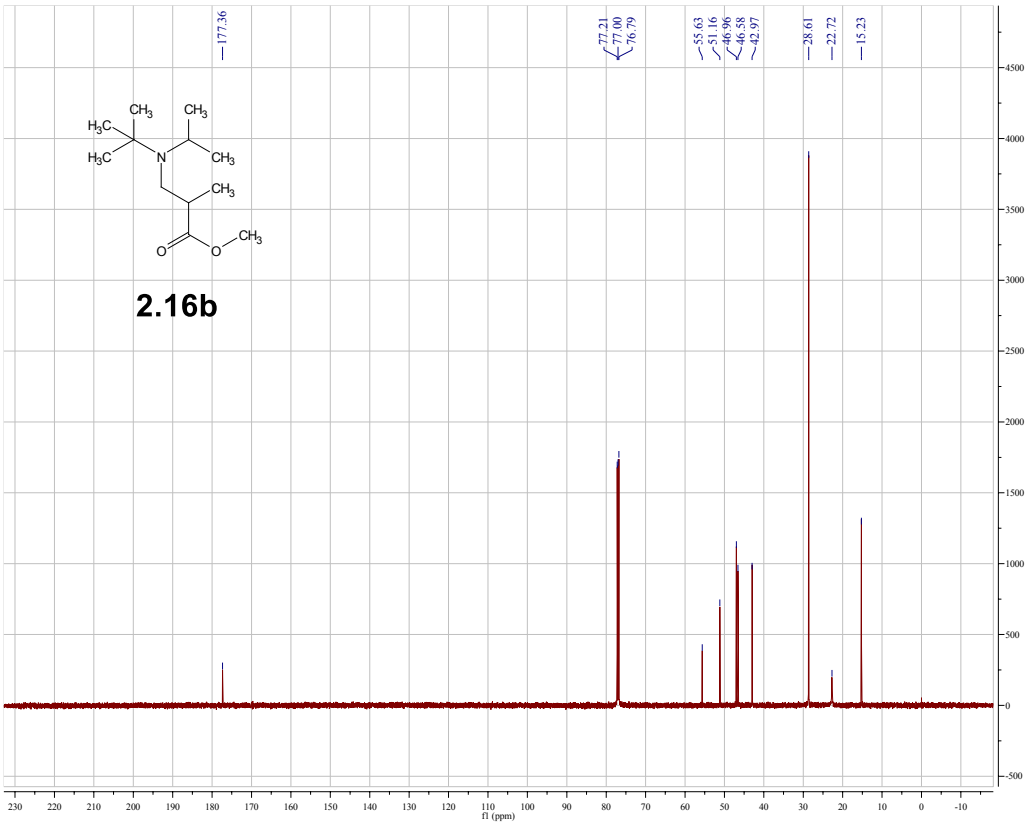
177.36
77.21
77.00
76.79
55.63
51.16
46.96
46.58
42.97
28.61
22.72
15.23
f1 (ppm)

2.16b

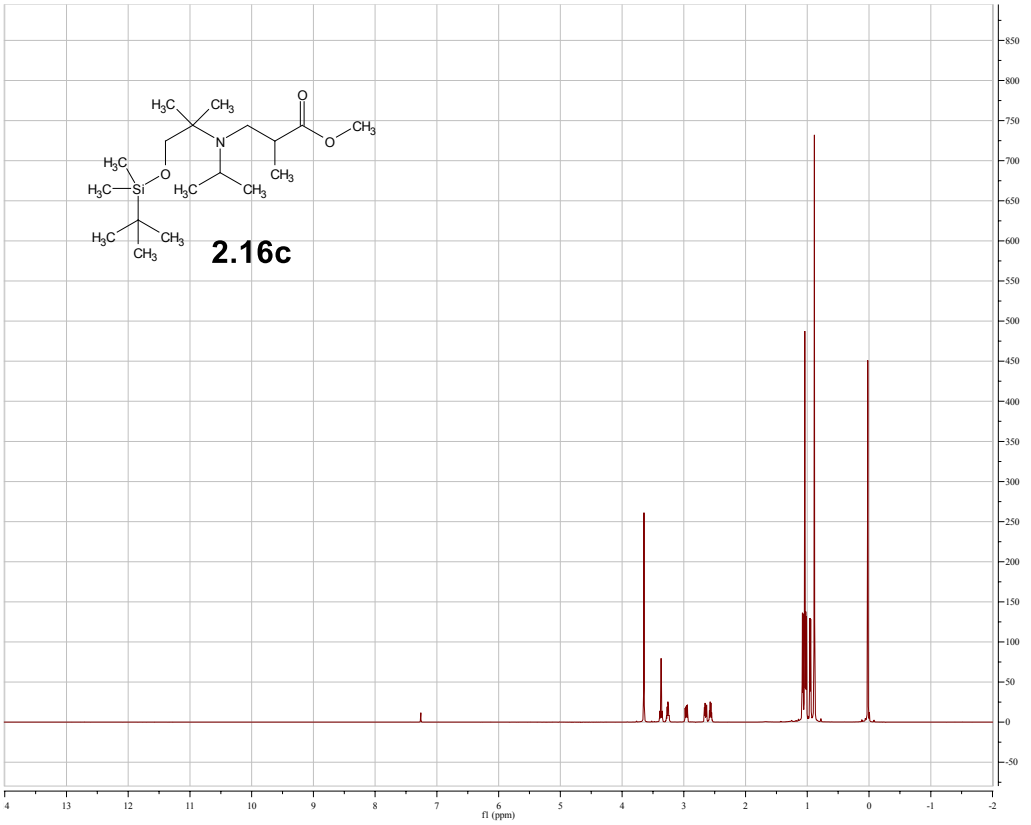
f1 (ppm)

2.16c

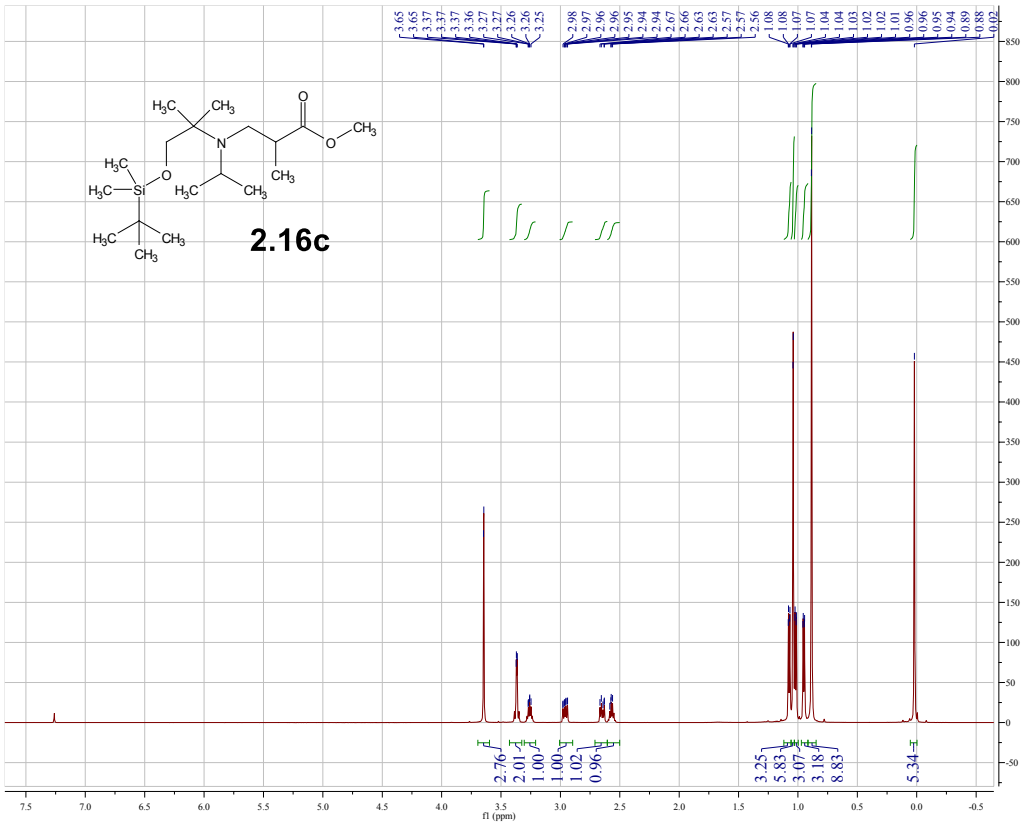
2.16c
f1 (ppm)

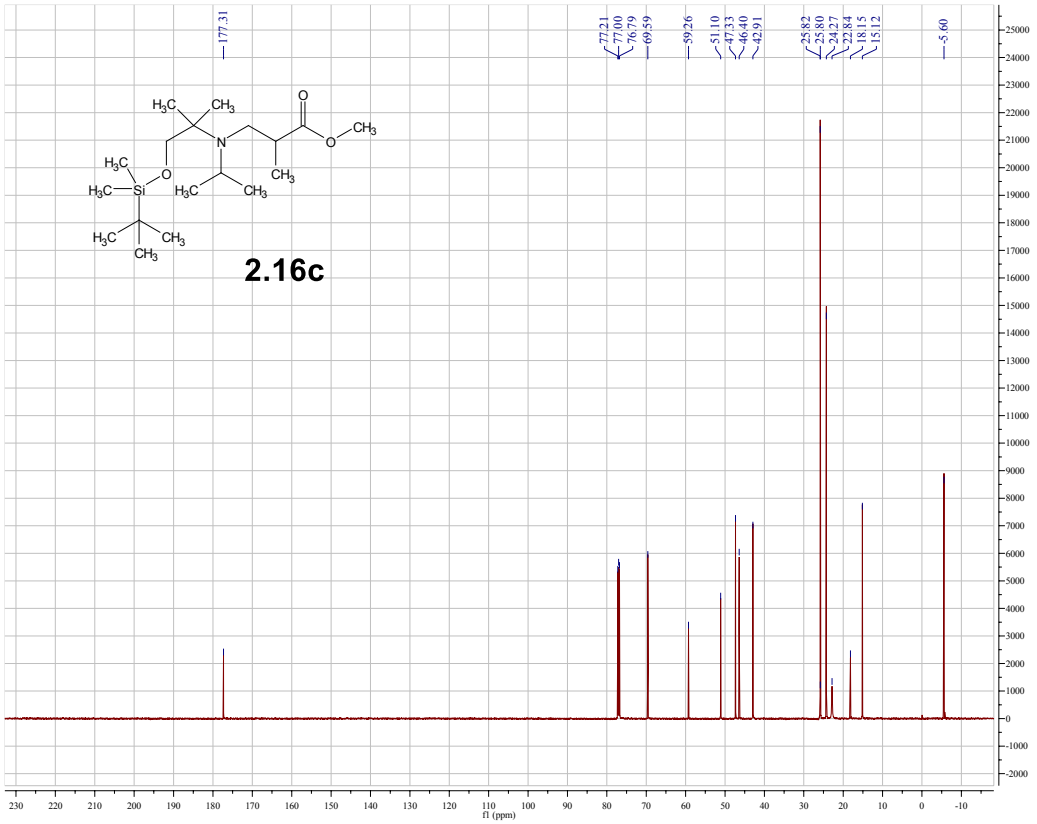
2.16c
f1 (ppm)

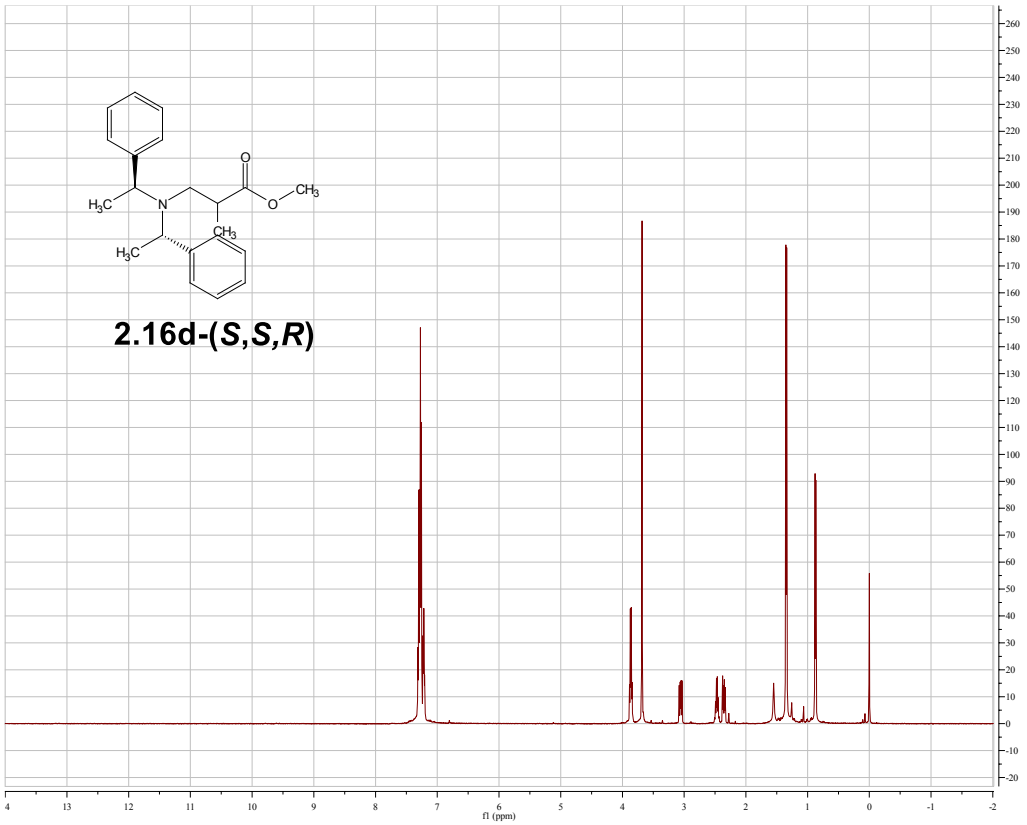
2.16d-(S,S,R)
f1 (ppm)

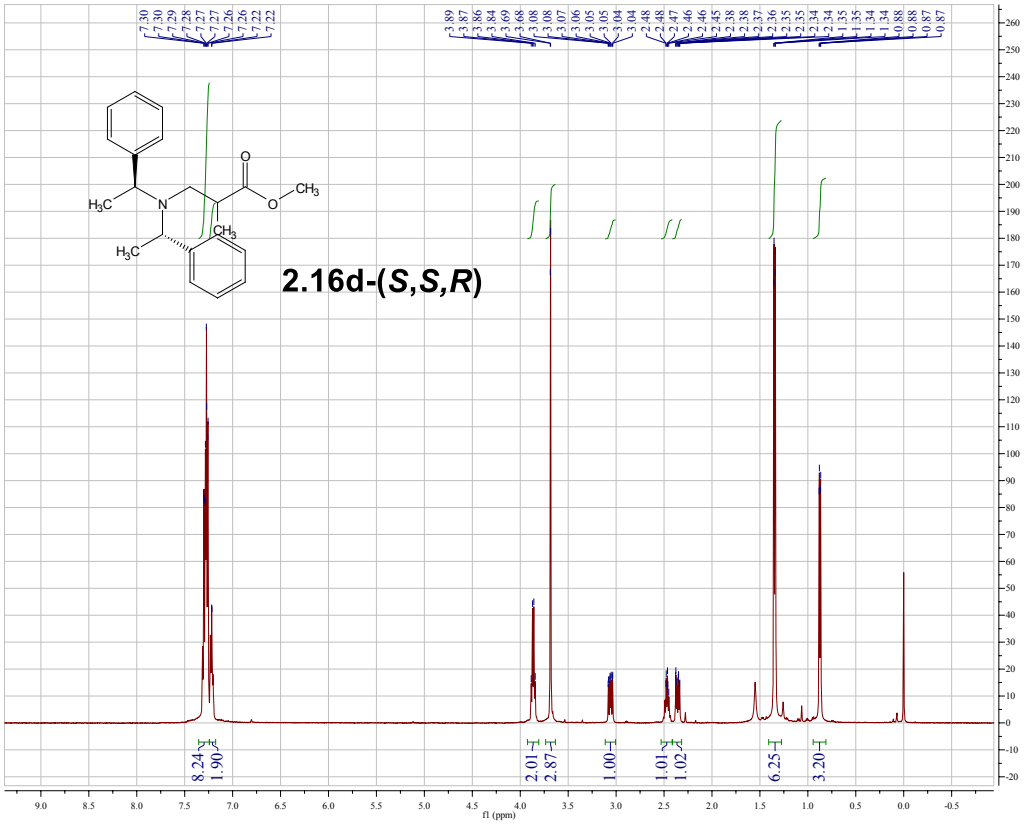
2.16d-(S,S,R)
8.24
1.90
2.01
2.87
1.00
1.01
1.02
6.25
3.20
f1 (ppm)

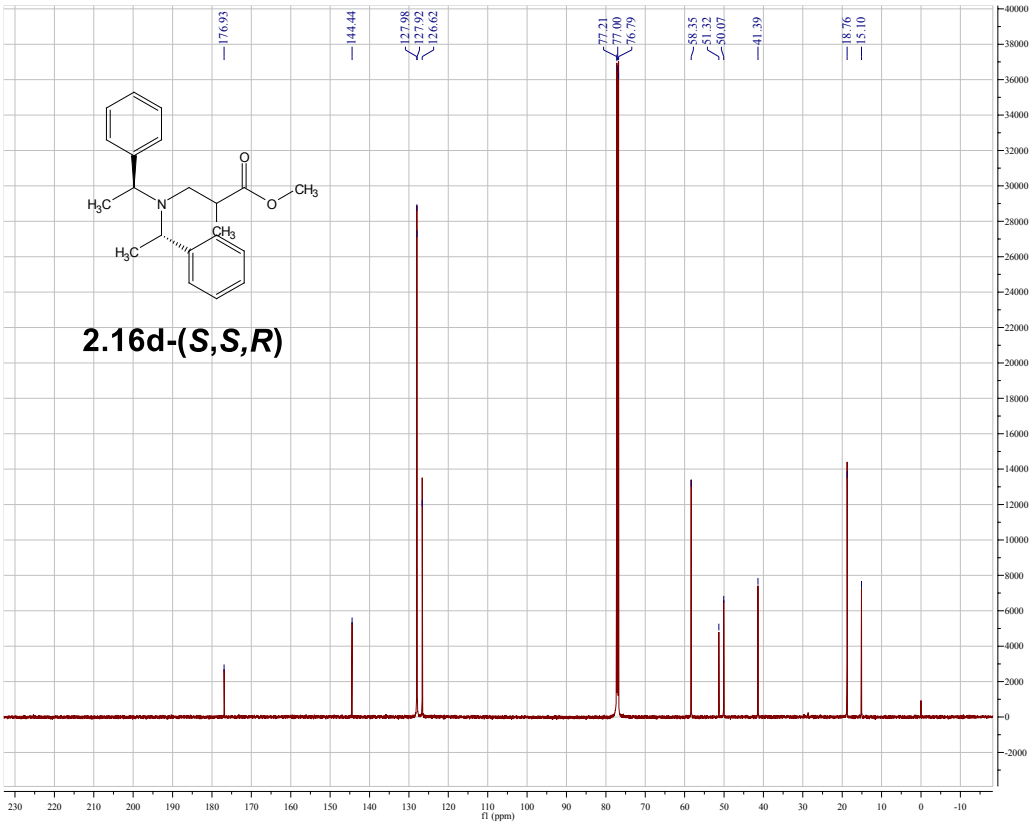

2.16d-(*S*,*S*,*R*)

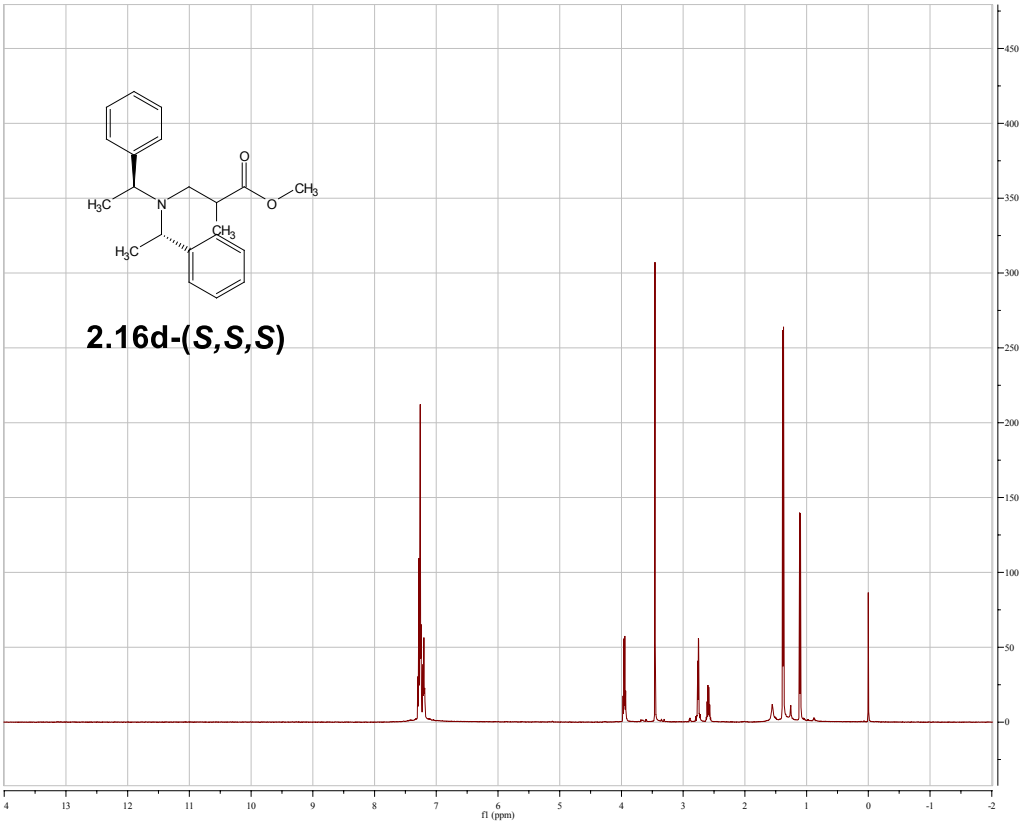

2.16d-(*S*,*S*,*S*)

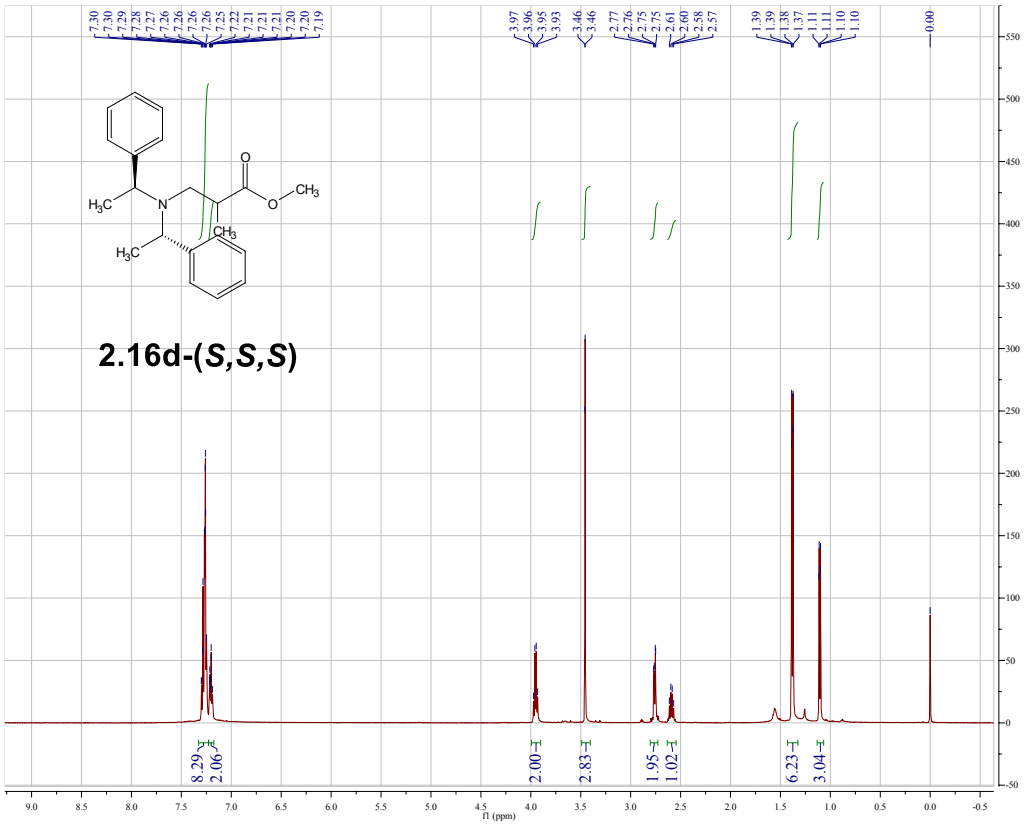
2.16d-(S,S,S)

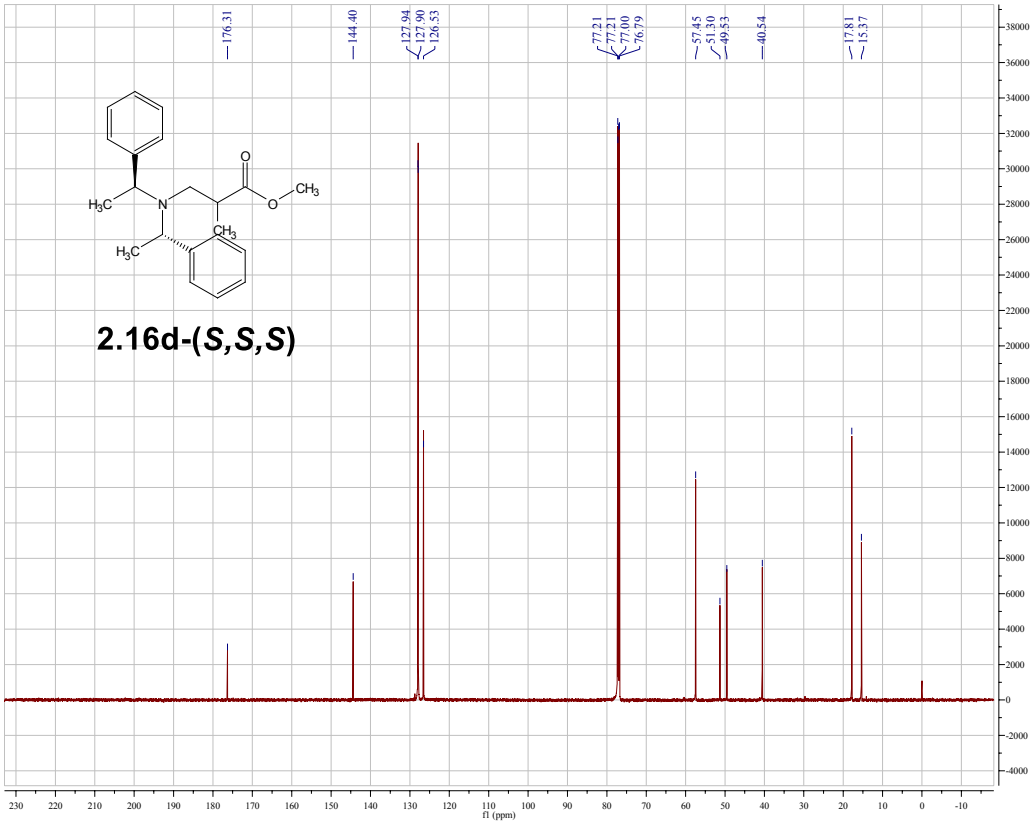
2.16d-(S,S,S)

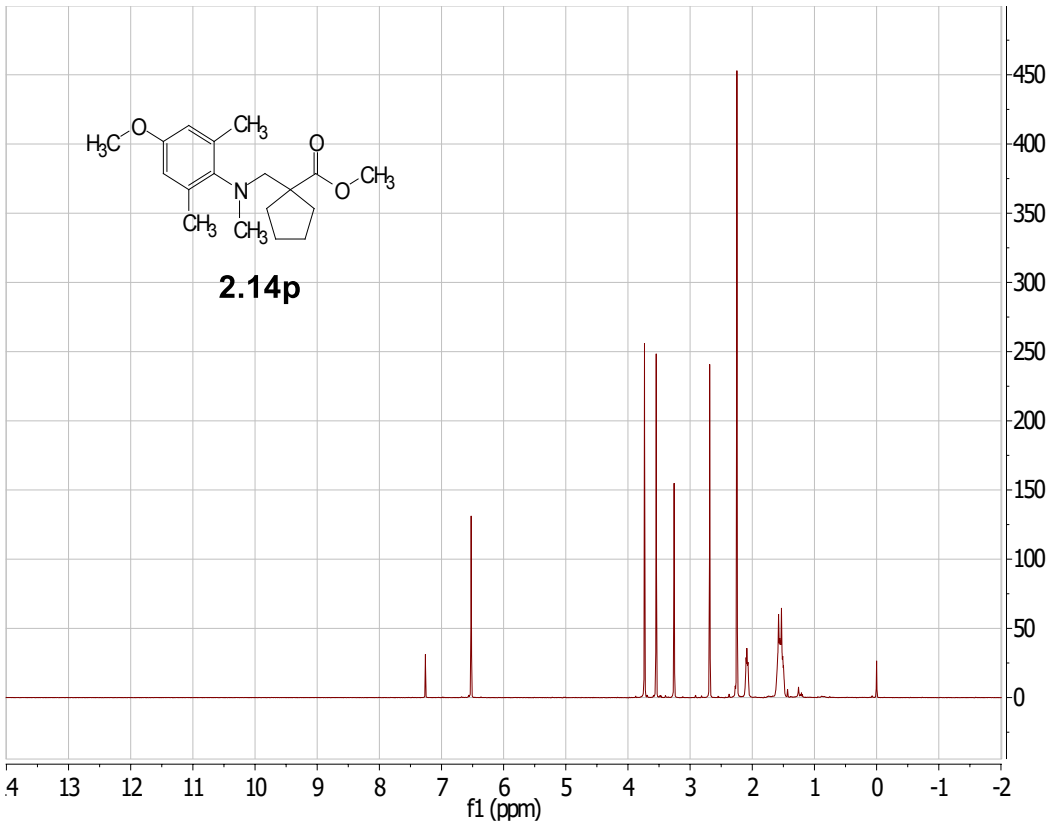
2.14p
f1 (ppm)

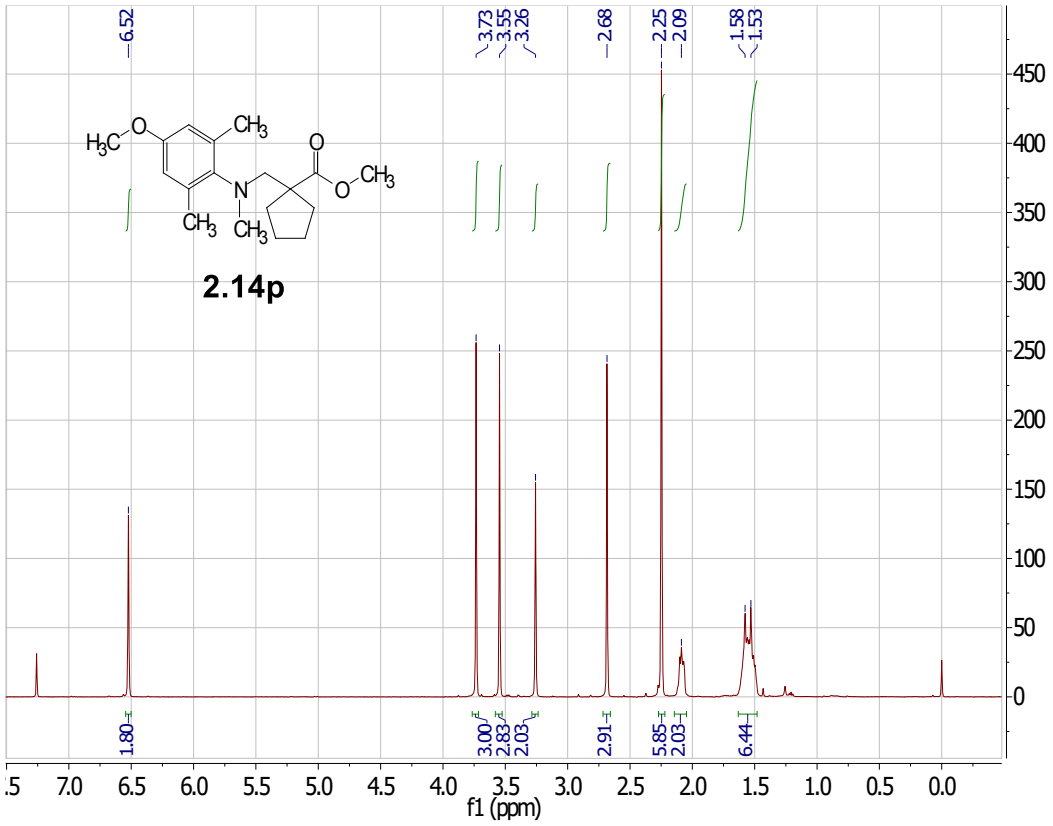
6.52
3.73
3.55
3.26
2.68
2.25
2.09
1.58
1.53
2.14p
1.80
3.00
2.83
2.03
2.91
5.85
2.03
6.44
f1 (ppm)

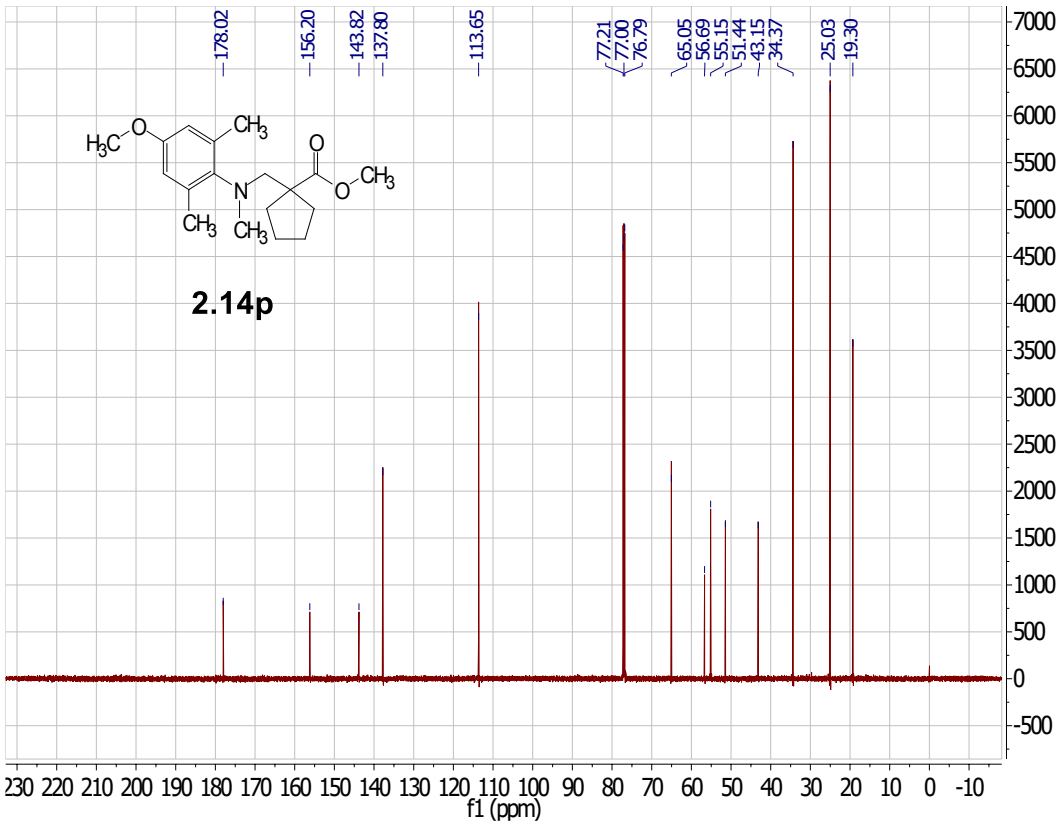
178.02
156.20
143.82
137.80
113.65
77.21
77.00
76.79
65.05
56.69
55.15
51.44
43.15
34.37
25.03
19.30
2.14p
f1 (ppm)

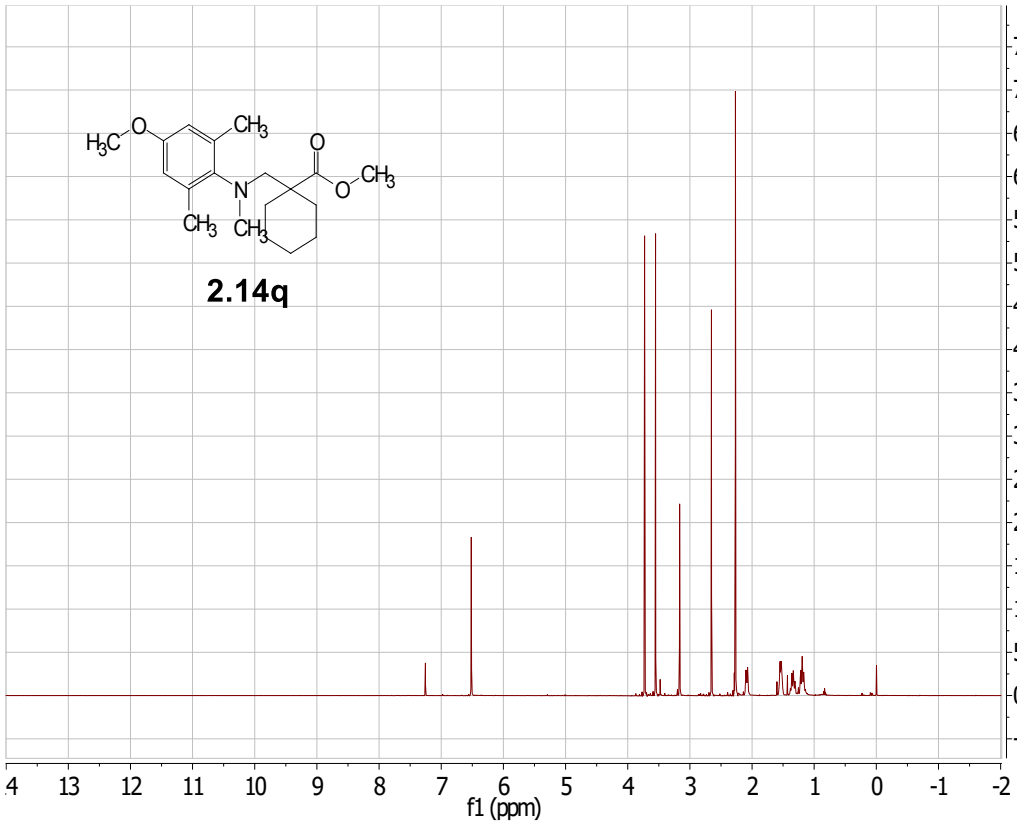
2.14q
f1 (ppm)

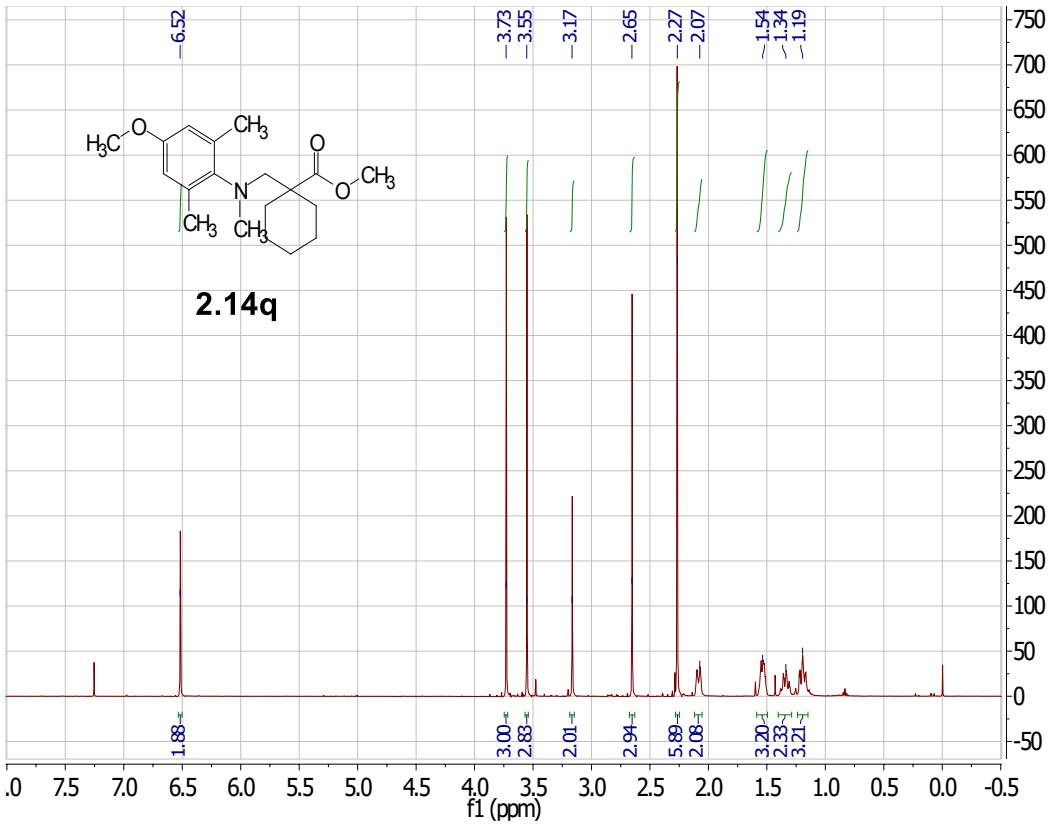
6.52
3.73
3.55
3.17
2.65
2.27
2.07
1.54
1.34
1.19
2.14q
1.88
3.00
2.83
2.01
2.94
5.89
2.08
3.20
2.33
3.21
f1 (ppm)

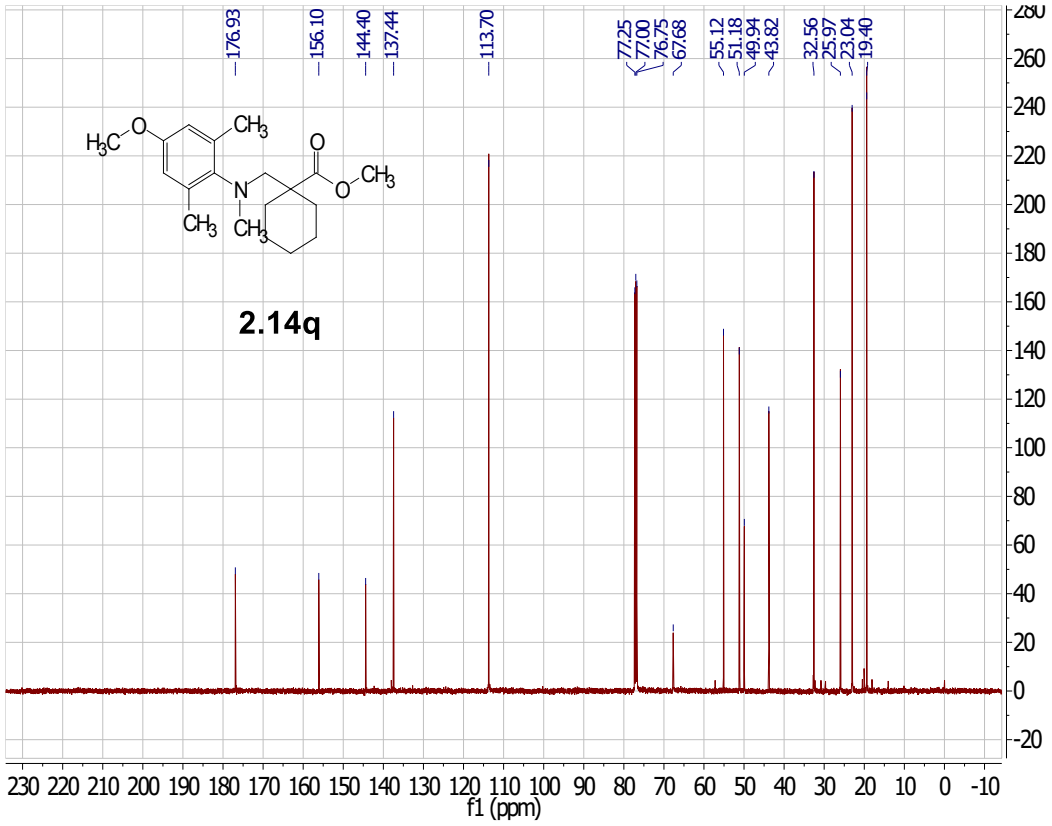
176.93
156.10
144.40
137.44
113.70
77.25
77.00
76.75
67.68
55.12
51.18
49.94
43.82
32.56
25.97
23.04
19.40
2.14q
f1 (ppm)

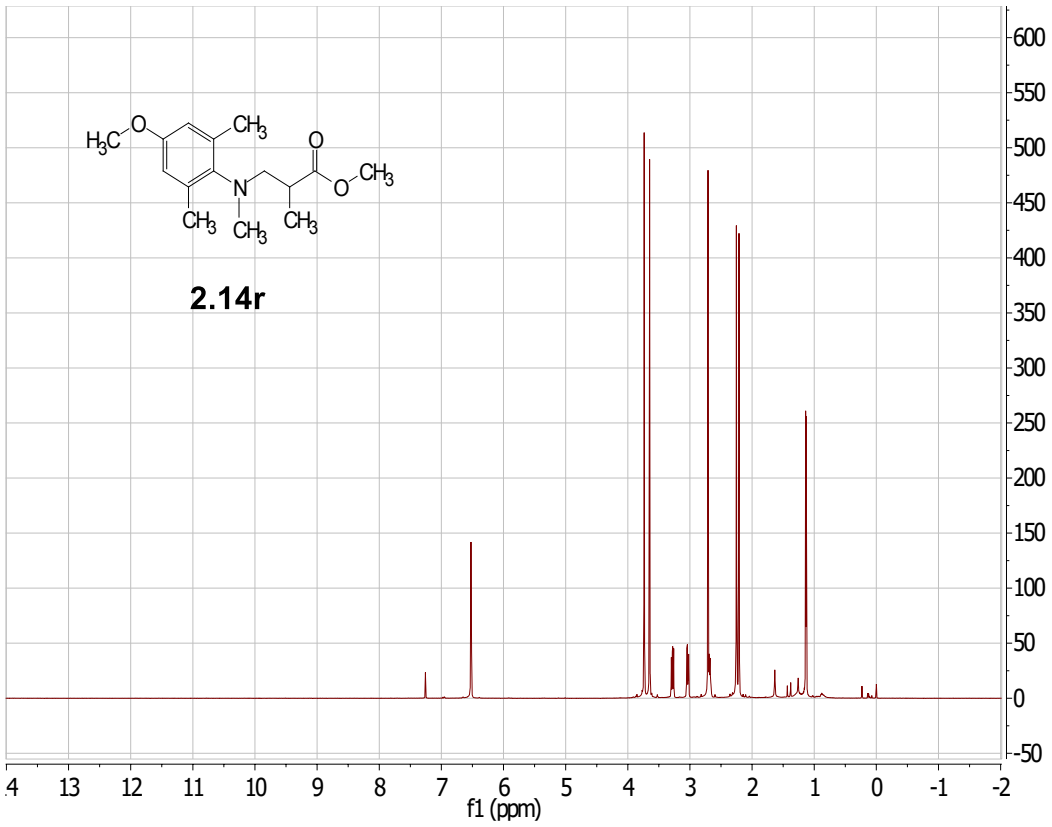
2.14r
f1 (ppm)

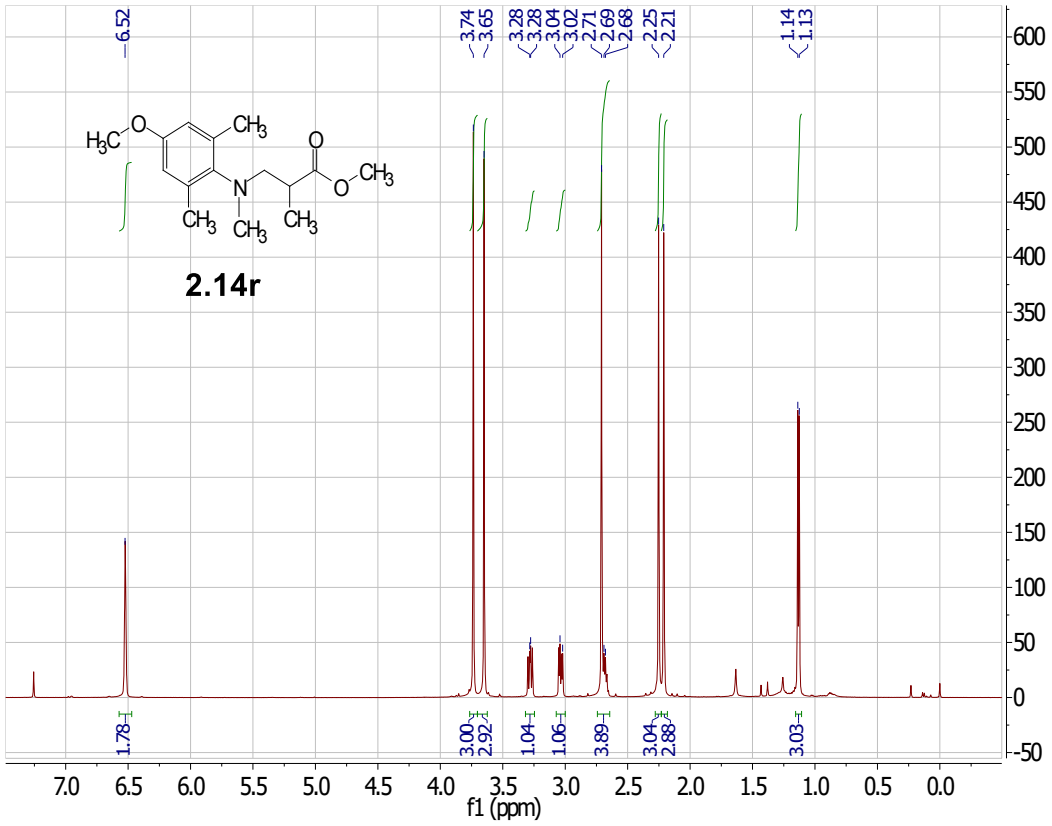
6.52
3.74
3.65
3.28
3.28
3.04
3.02
2.71
2.69
2.68
2.25
2.21
1.14
1.13
2.14r
1.78
3.00
2.92
1.04
1.06
3.89
3.04
2.88
3.03
f1 (ppm)

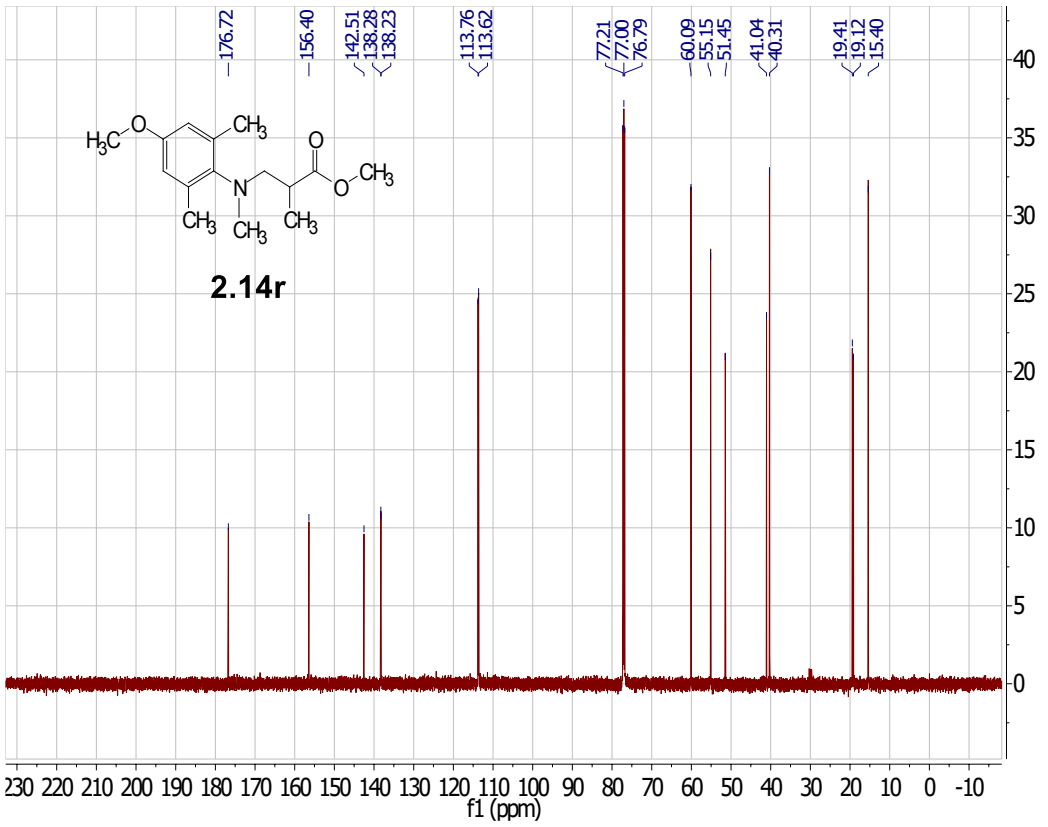
176.72
156.40
142.51
138.28
138.23
113.76
113.62
77.21
77.00
76.79
60.09
55.15
51.45
41.04
40.31
19.41
19.12
15.40
2.14r
f1 (ppm)

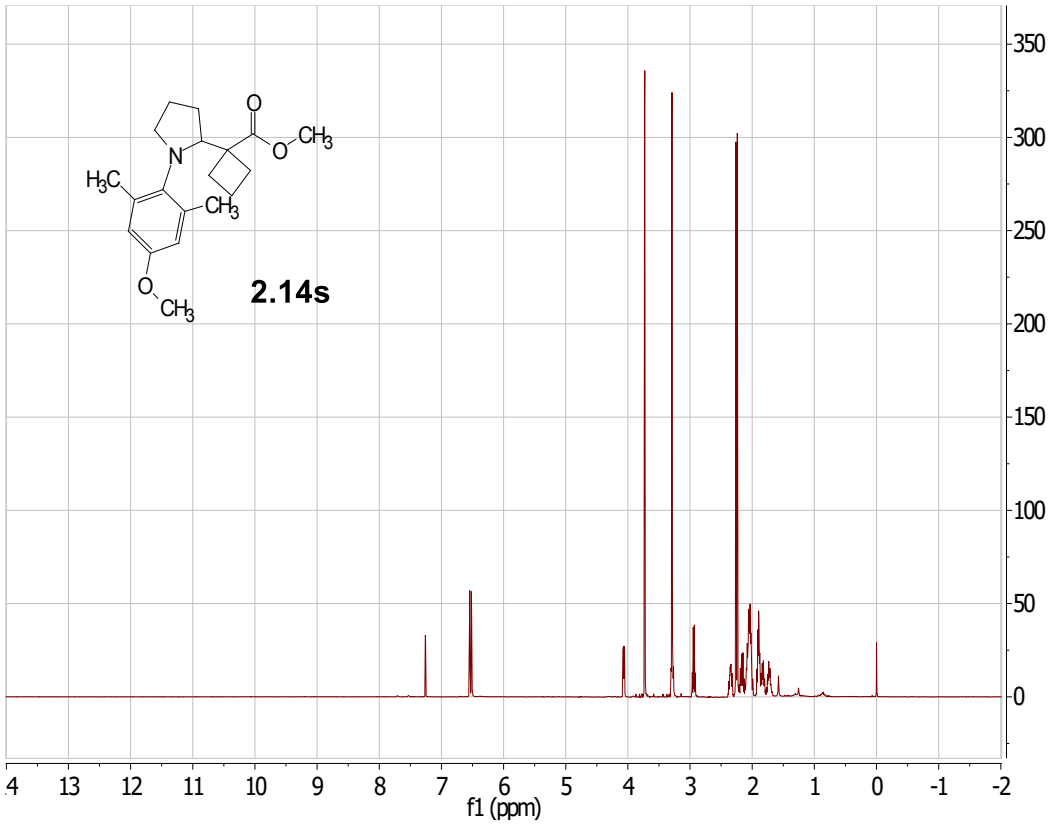
2.14s
f1 (ppm)

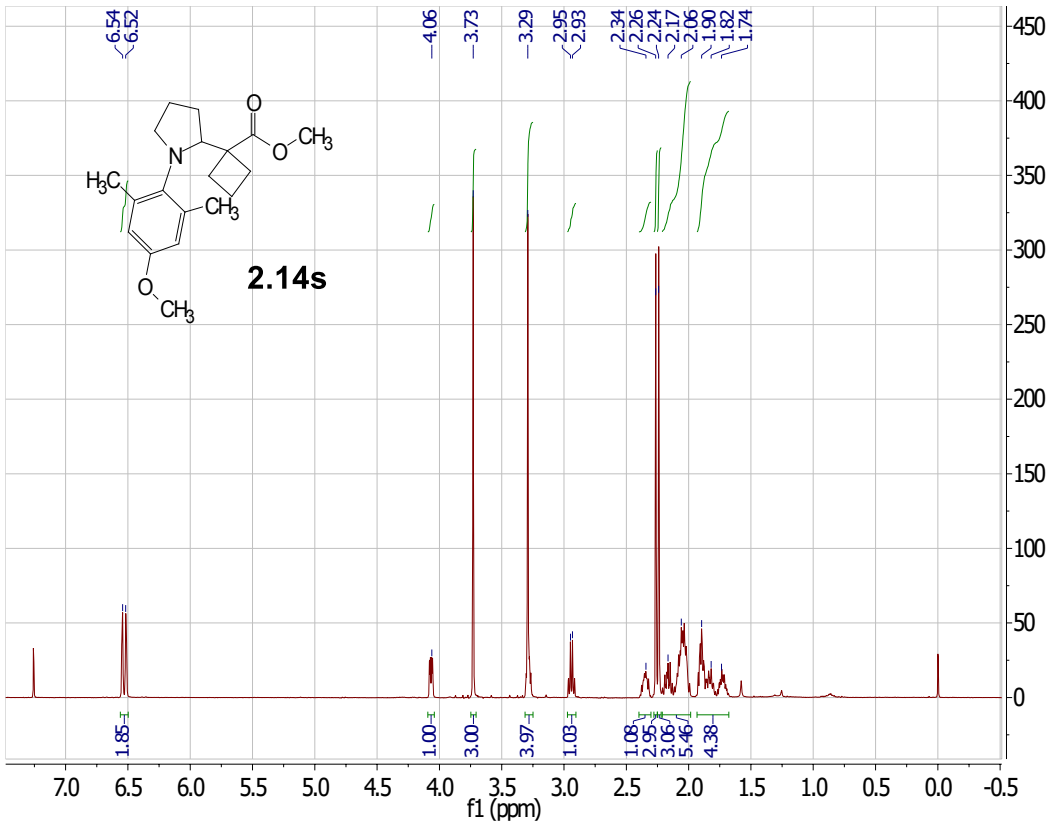
6.54
6.52
4.06
3.73
3.29
2.95
2.93
2.34
2.26
2.24
2.17
2.06
1.90
1.82
1.74
2.14s
1.85
1.00
3.00
3.97
1.03
1.08
2.95
3.06
5.46
4.38
f1 (ppm)

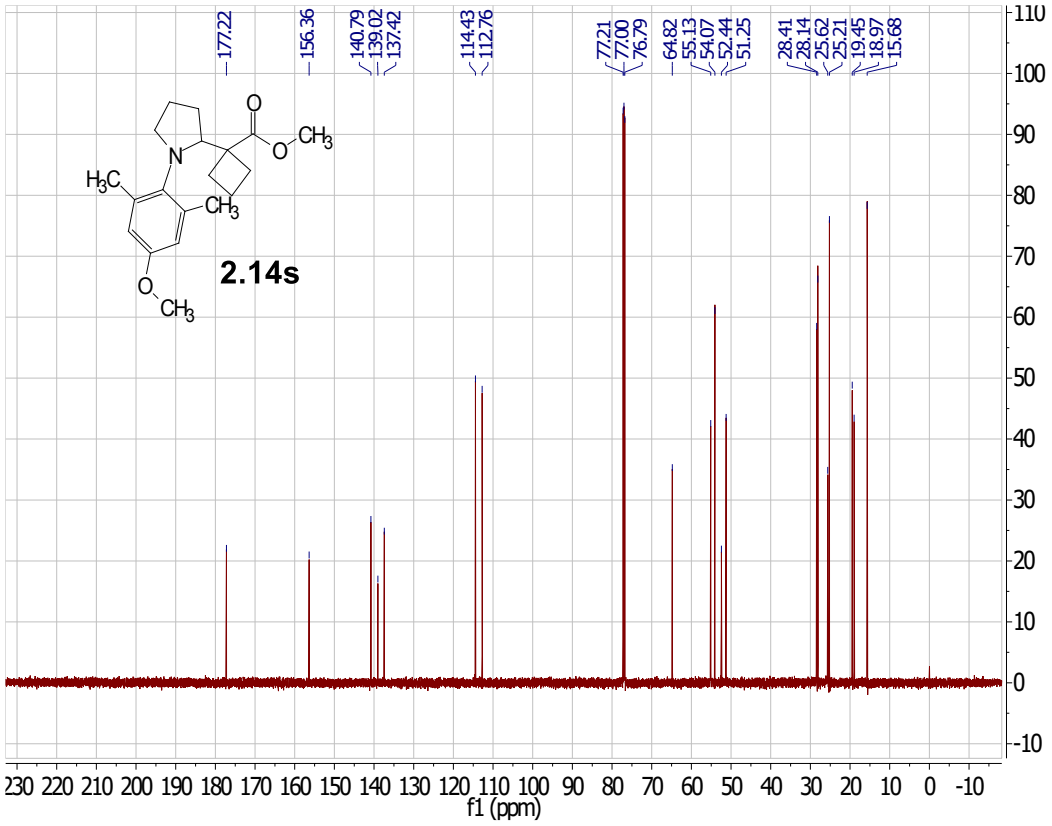
177.22
156.36
140.79
139.02
137.42
114.43
112.76
77.21
77.00
76.79
64.82
55.13
54.07
52.44
51.25
28.41
28.14
25.62
25.21
19.45
18.97
15.68
2.14s
f1 (ppm)

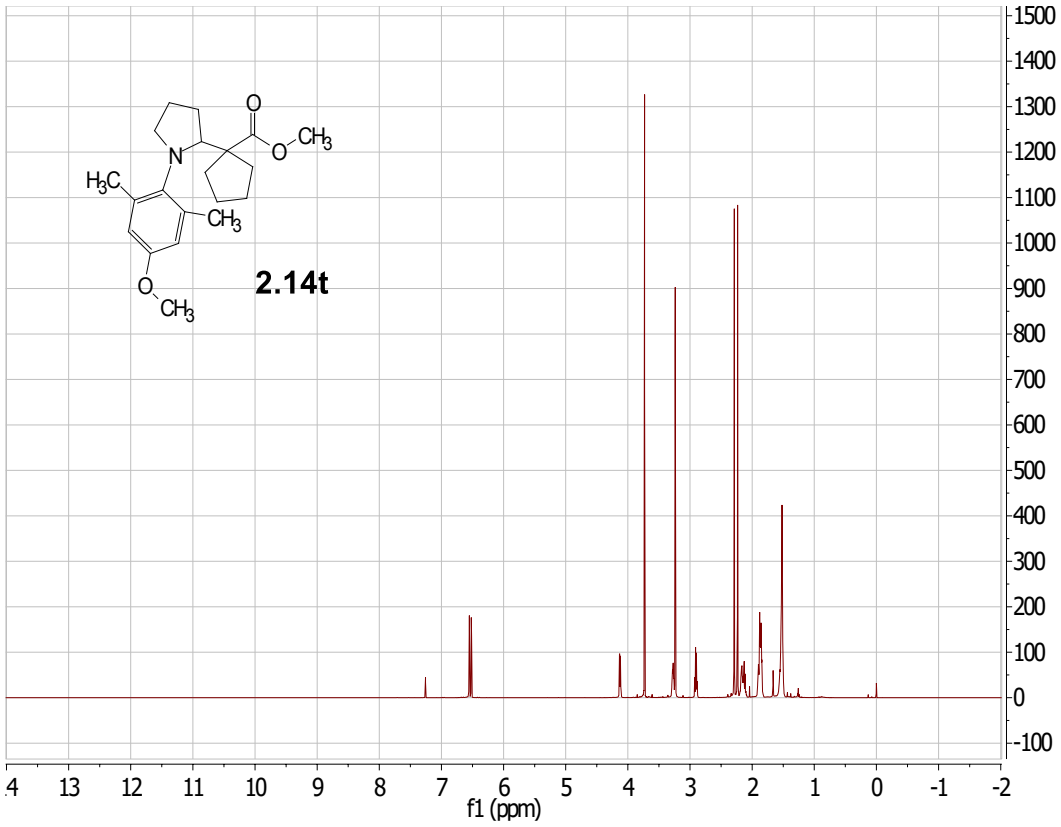
2.14t
f1 (ppm)

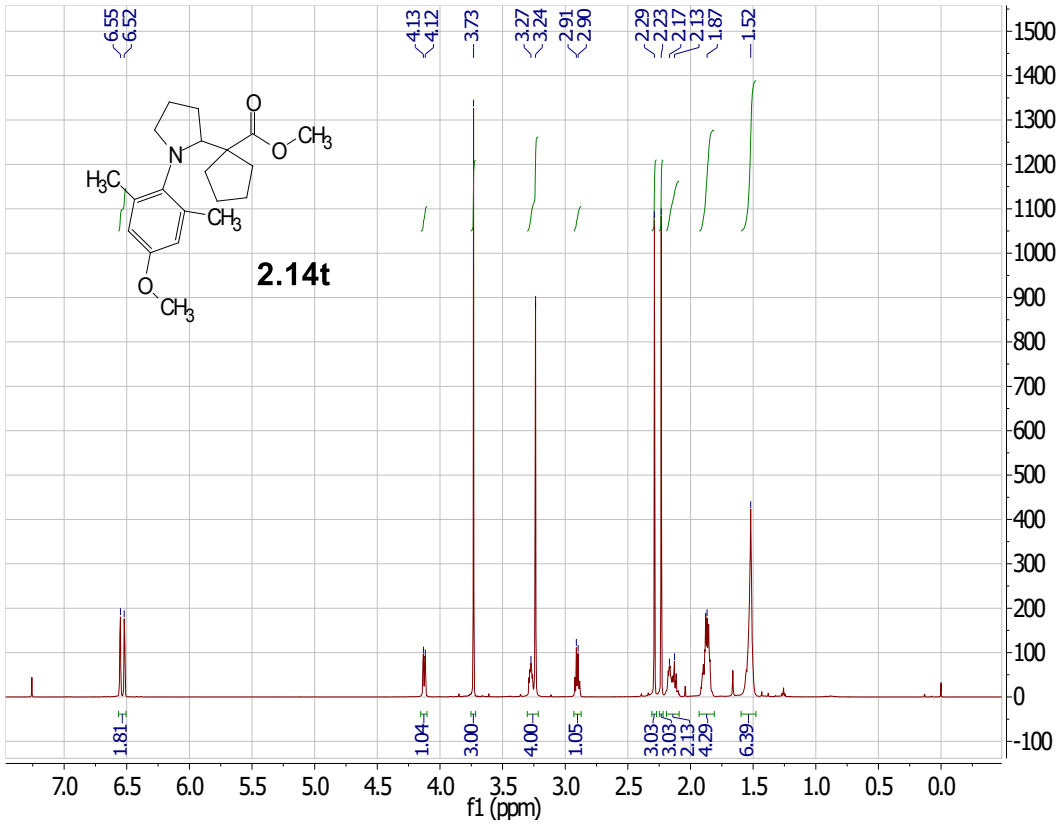
6.55
6.52
4.13
4.12
3.73
3.27
3.24
2.91
2.90
2.29
2.23
2.17
2.13
1.87
1.52
2.14t
1.81
1.04
3.00
4.00
1.05
3.03
3.03
2.13
4.29
6.39
f1 (ppm)

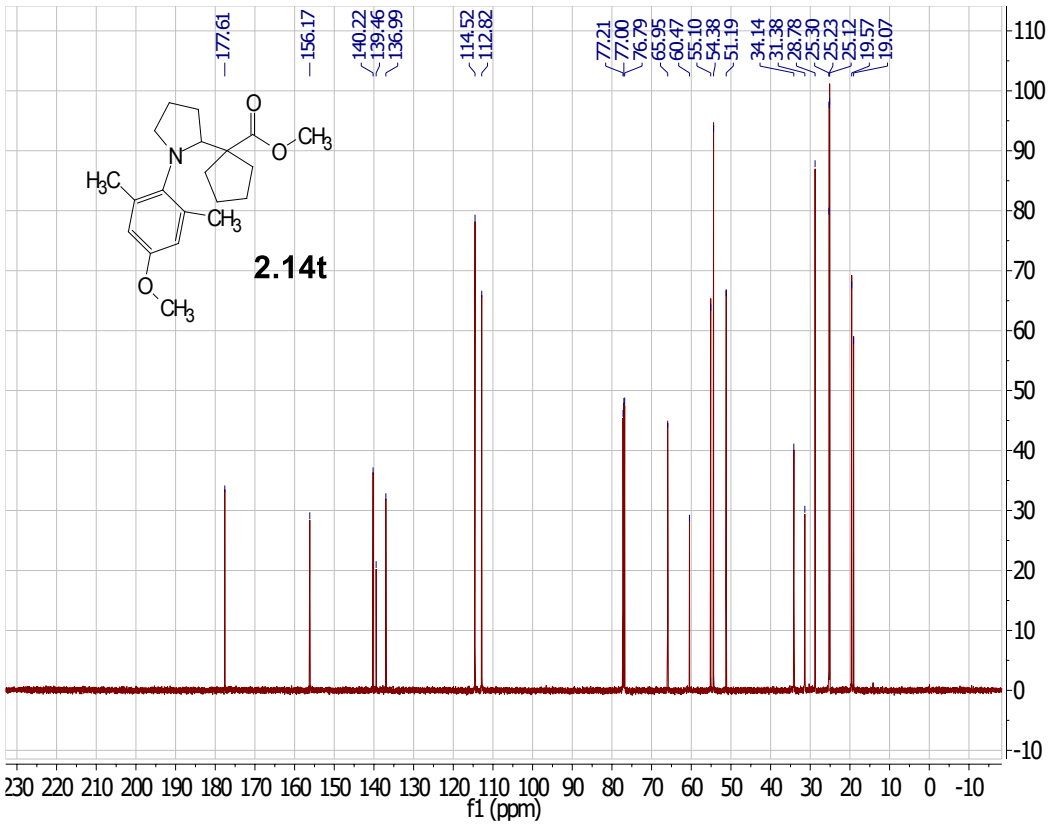
177.61
156.17
140.22
139.46
136.99
114.52
112.82
77.21
77.00
76.79
65.95
60.47
55.10
54.38
51.19
34.14
31.38
28.78
25.30
25.23
25.12
19.57
19.07
2.14t
f1 (ppm)

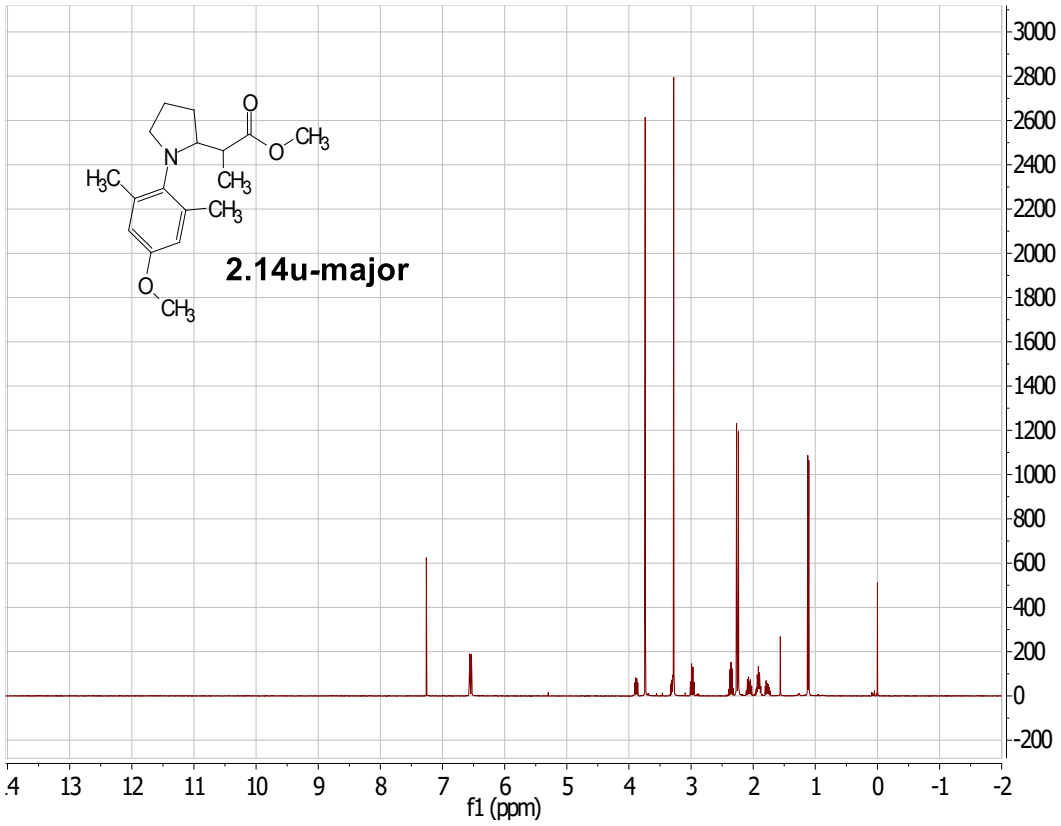
2.14u-major
f1 (ppm)

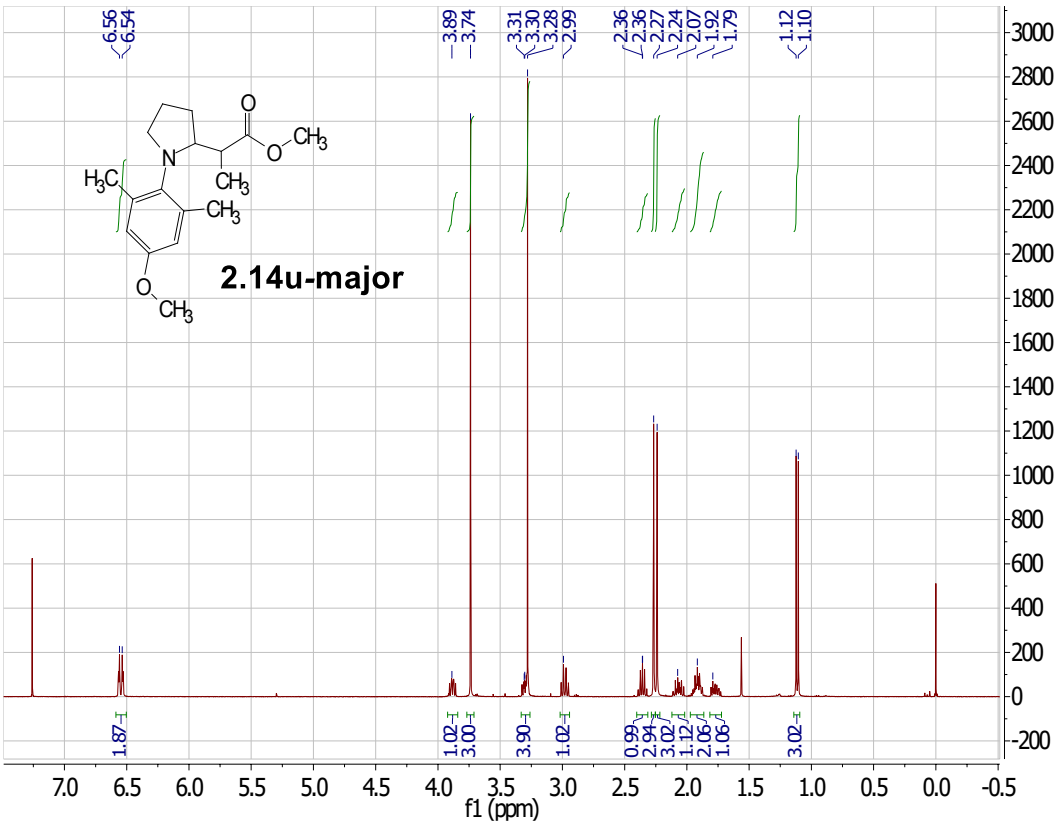
6.56
6.54
3.89
3.74
3.31
3.30
3.28
2.99
2.36
2.36
2.27
2.24
2.07
1.92
1.79
1.12
1.10
2.14u-major
1.87
1.02
3.00
3.90
1.02
0.99
2.94
3.02
1.12
2.06
1.06
3.02
f1 (ppm)

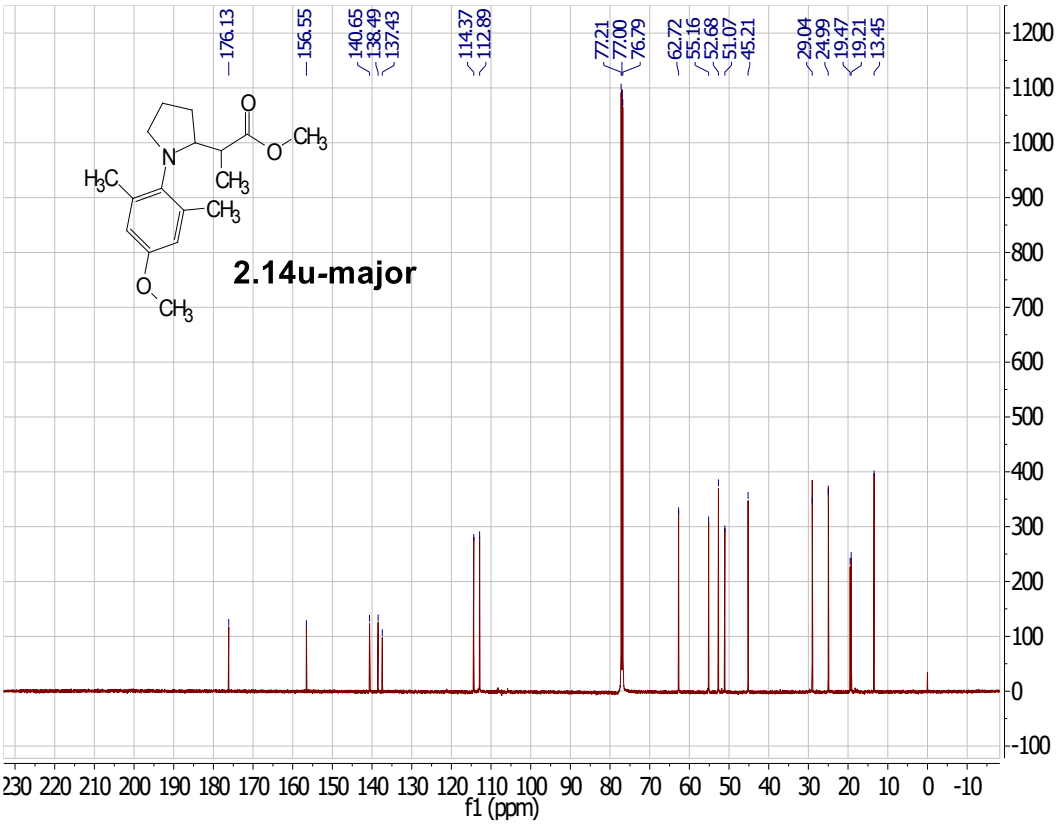
176.13
156.55
140.65
138.49
137.43
114.37
112.89
77.21
77.00
76.79
62.72
55.16
52.68
51.07
45.21
29.04
24.99
19.47
19.21
13.45
2.14u-major
f1 (ppm)

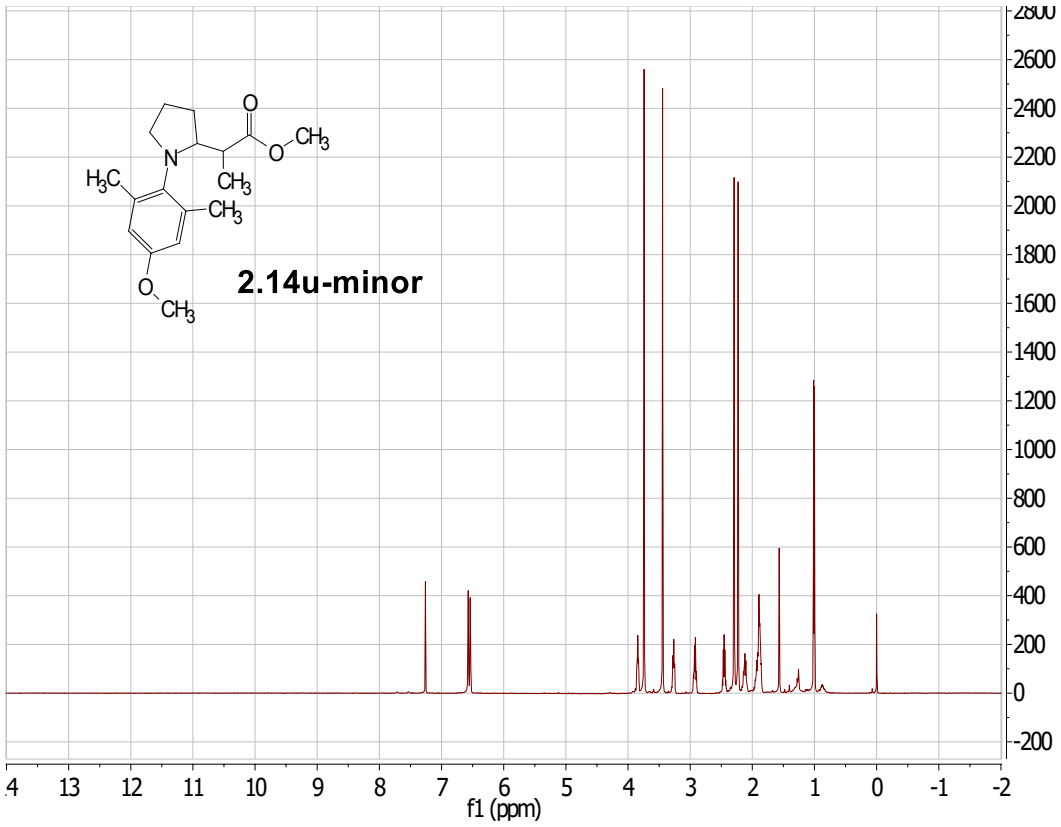
2.14u-minor
f1 (ppm)

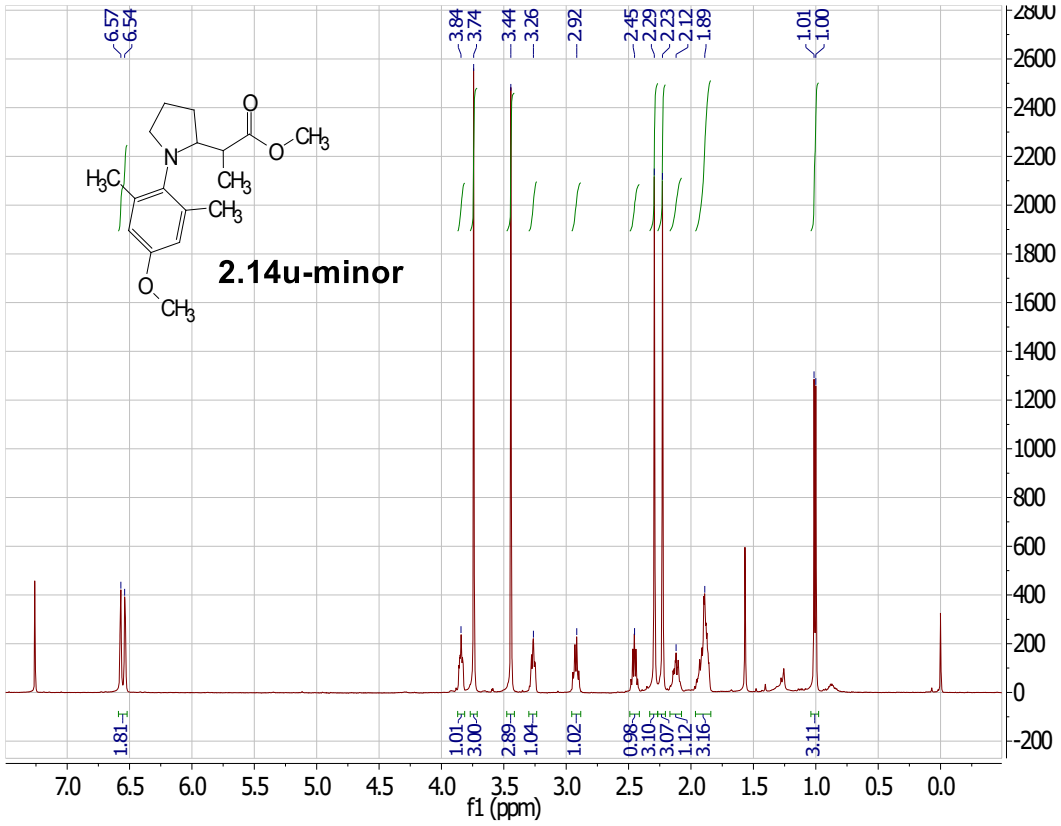
6.57
6.54
3.84
3.74
3.44
3.26
2.92
2.45
2.29
2.23
2.12
1.89
1.01
1.00
2.14u-minor
1.81
1.01
3.00
2.89
1.04
1.02
0.98
3.10
3.07
1.12
3.16
3.11
f1 (ppm)

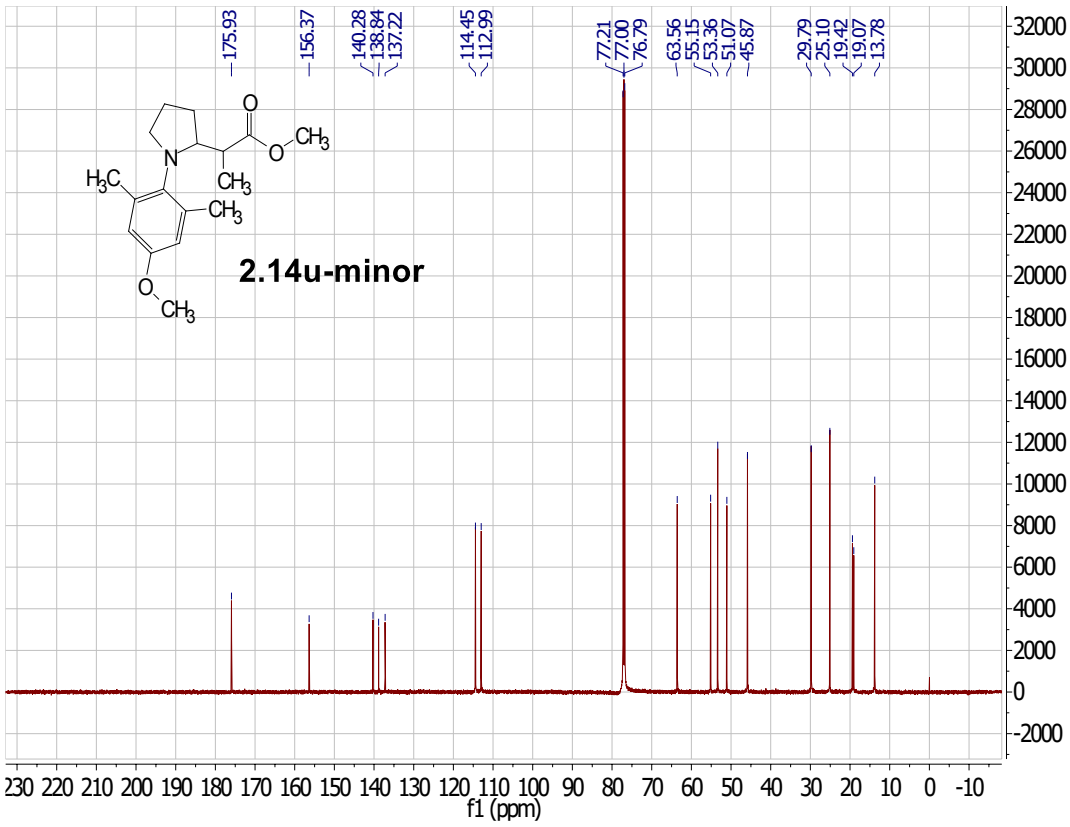
175.93
156.37
140.28
138.84
137.22
114.45
112.99
77.21
77.00
76.79
63.56
55.15
53.36
51.07
45.87
29.79
25.10
19.42
19.07
13.78
2.14u-minor
f1 (ppm)

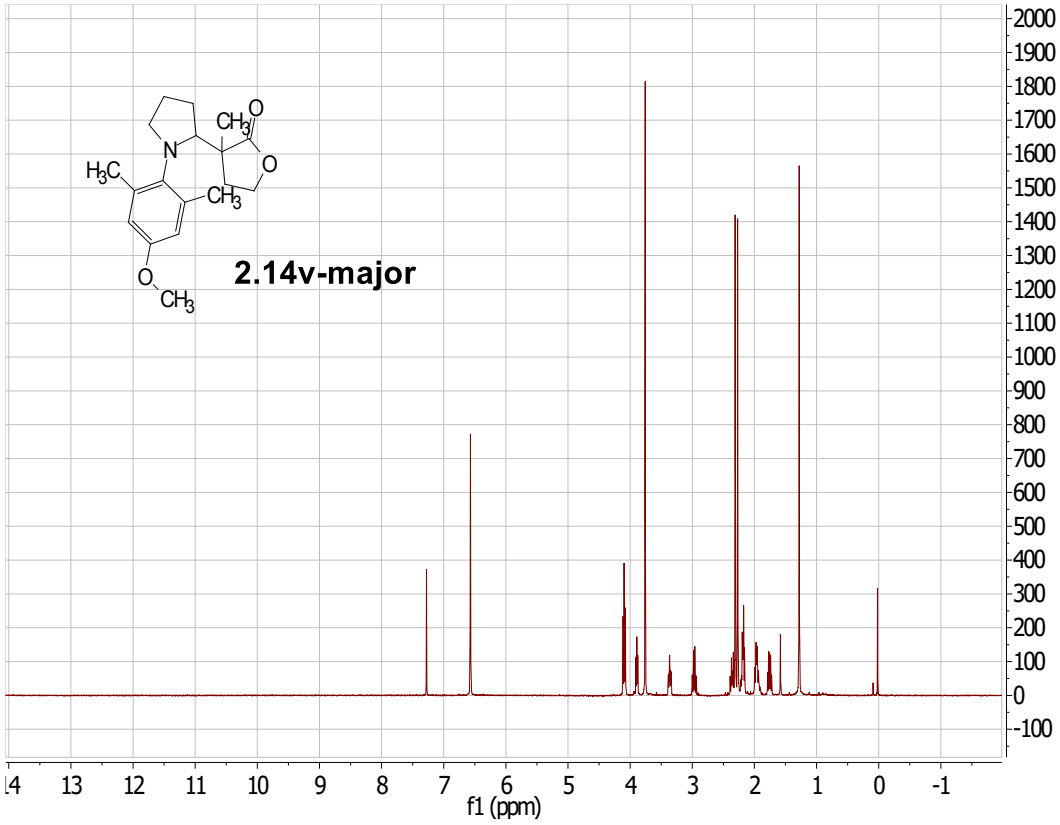
2.14v-major
f1 (ppm)

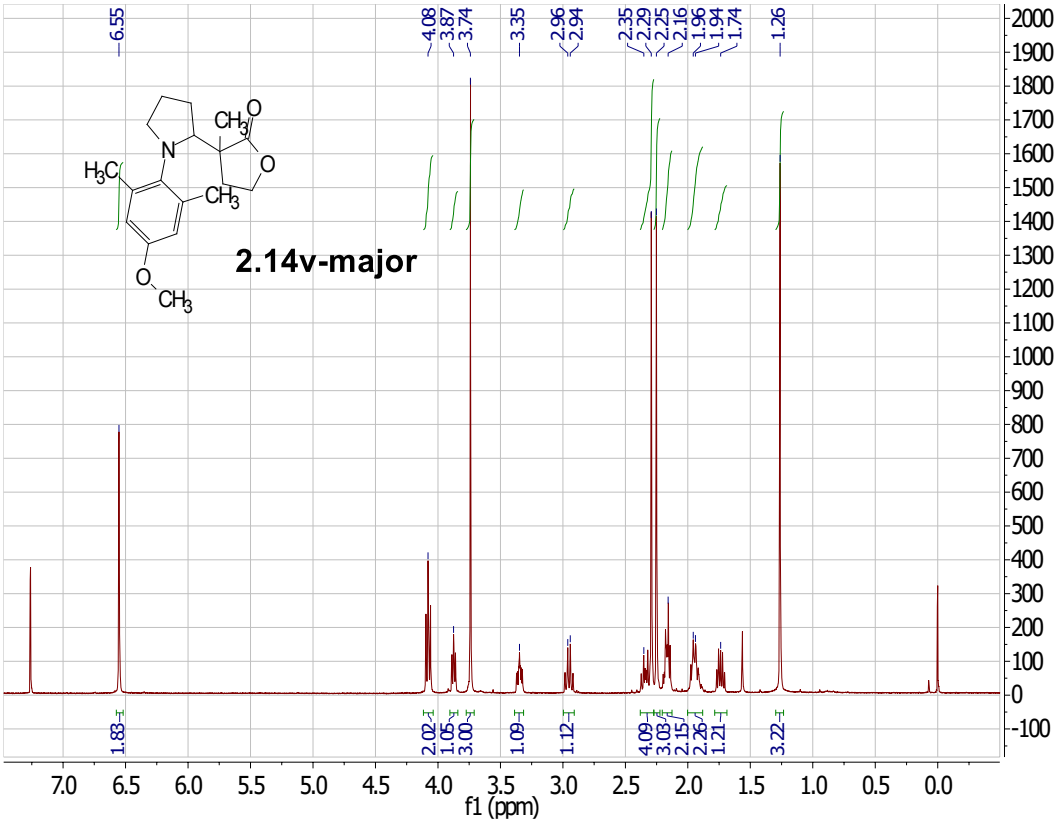
6.55
4.08
3.87
3.74
3.35
2.96
2.94
2.35
2.29
2.25
2.16
1.96
1.94
1.74
1.26
2.14v-major
1.83
2.02
1.05
3.00
1.09
1.12
4.09
3.03
2.15
2.26
1.21
3.22
f1 (ppm)

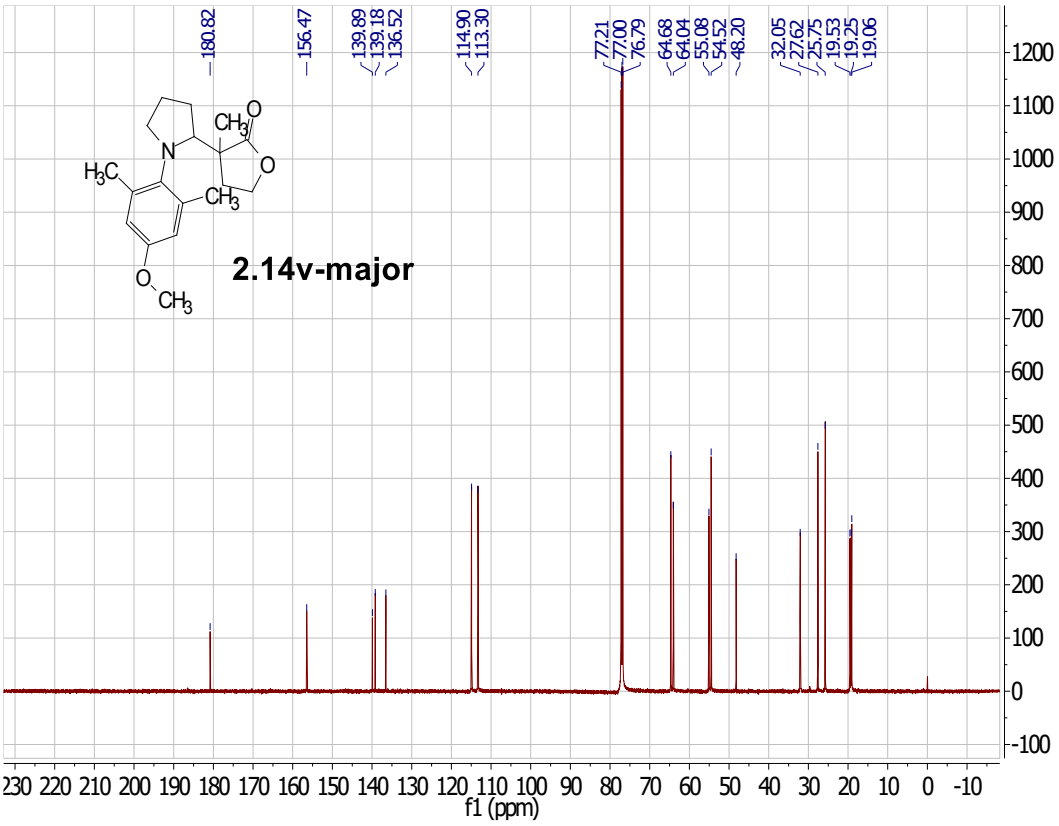
180.82
156.47
139.89
139.18
136.52
114.90
113.30
77.21
77.00
76.79
64.68
64.04
55.08
54.52
48.20
32.05
27.62
25.75
19.53
19.25
19.06
2.14v-major
f1 (ppm)

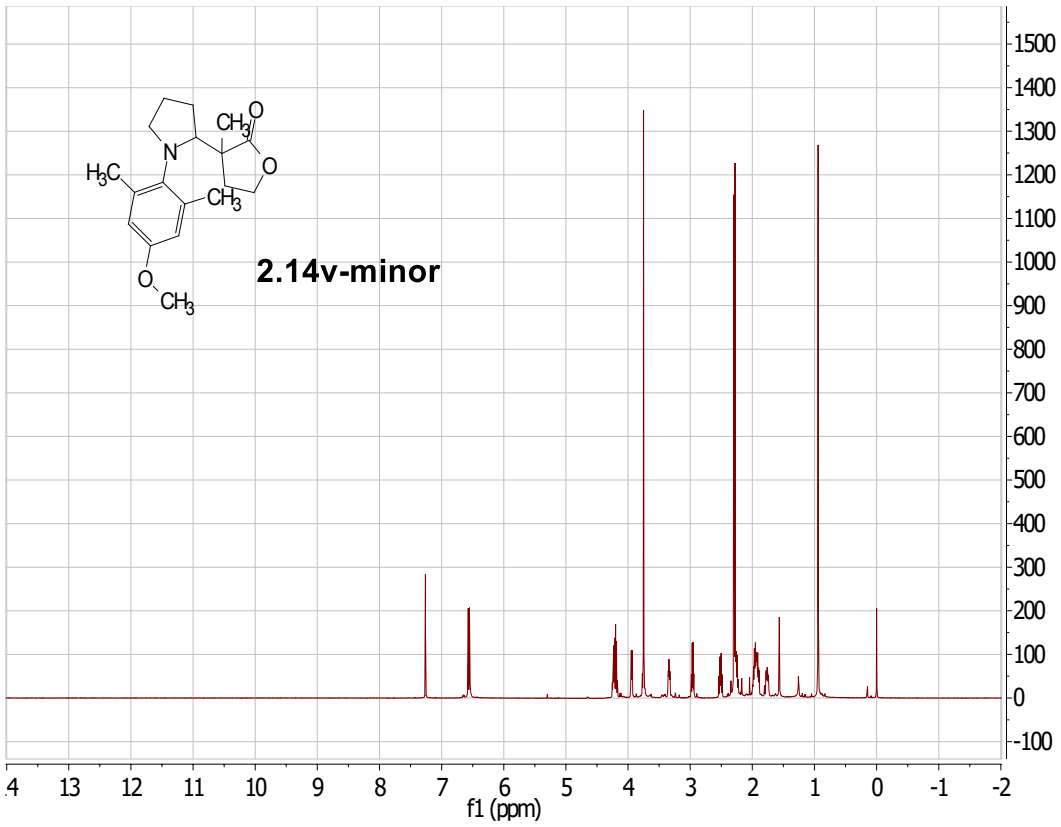
2.14v-minor
f1 (ppm)

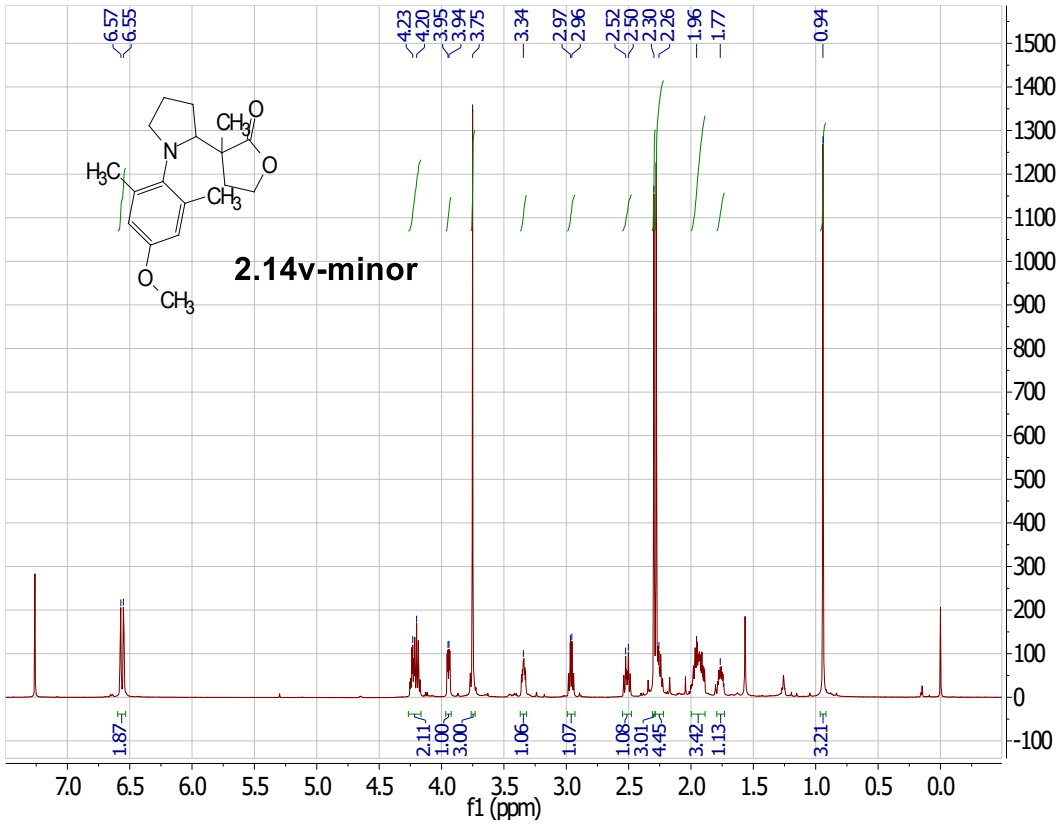
6.57
6.55
4.23
4.20
3.95
3.94
3.75
3.34
2.97
2.96
2.52
2.50
2.30
2.26
1.96
1.77
0.94
2.14v-minor
f1 (ppm)

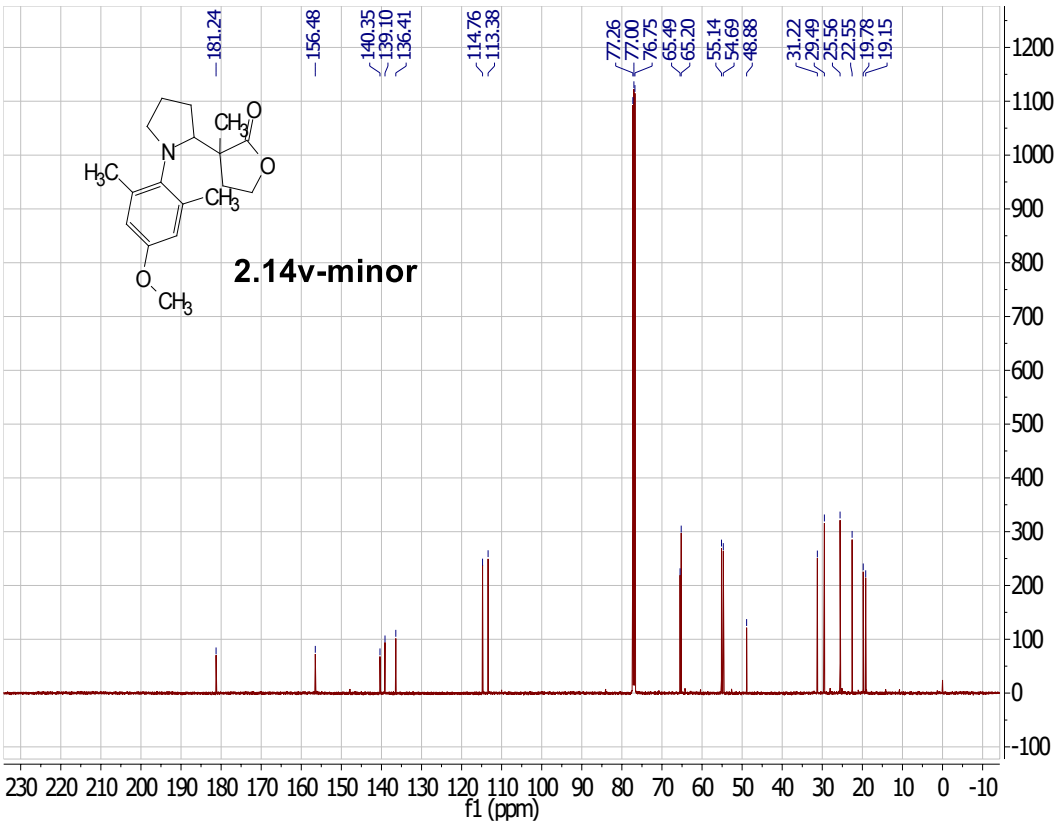
181.24
156.48
140.35
139.10
136.41
114.76
113.38
77.26
77.00
76.75
65.49
65.20
55.14
54.69
48.88
31.22
29.49
25.56
22.55
19.78
19.15
2.14v-minor
f1 (ppm)

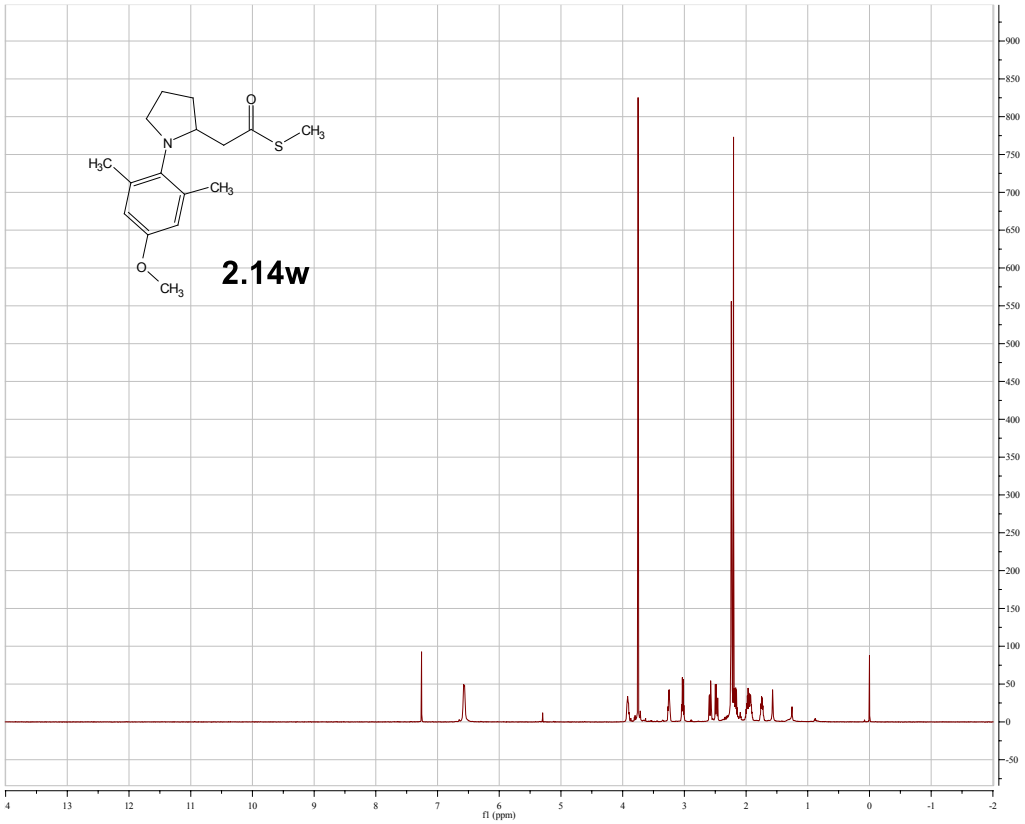
2.14w
f1 (ppm)

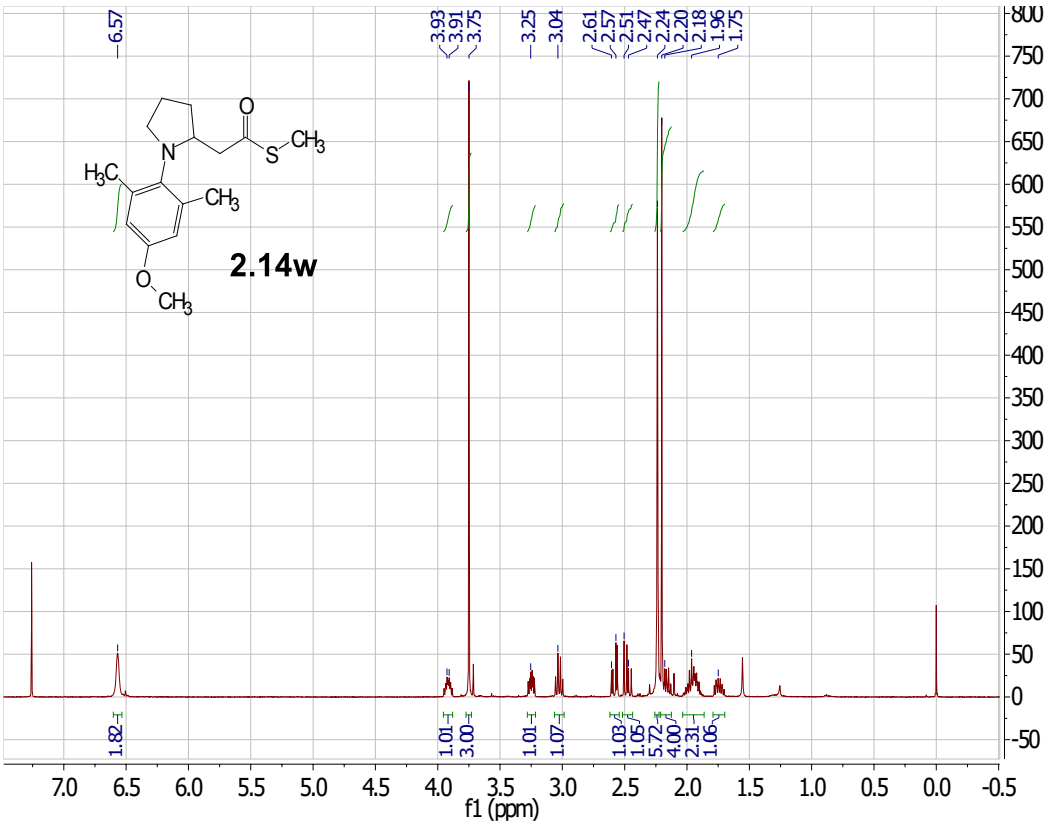
6.57
3.93
3.91
3.75
3.25
3.04
2.61
2.57
2.51
2.47
2.24
2.20
2.18
1.96
1.75
2.14w
1.82
1.01
3.00
1.01
1.07
1.03
1.05
5.72
4.00
2.31
1.06
f1 (ppm)

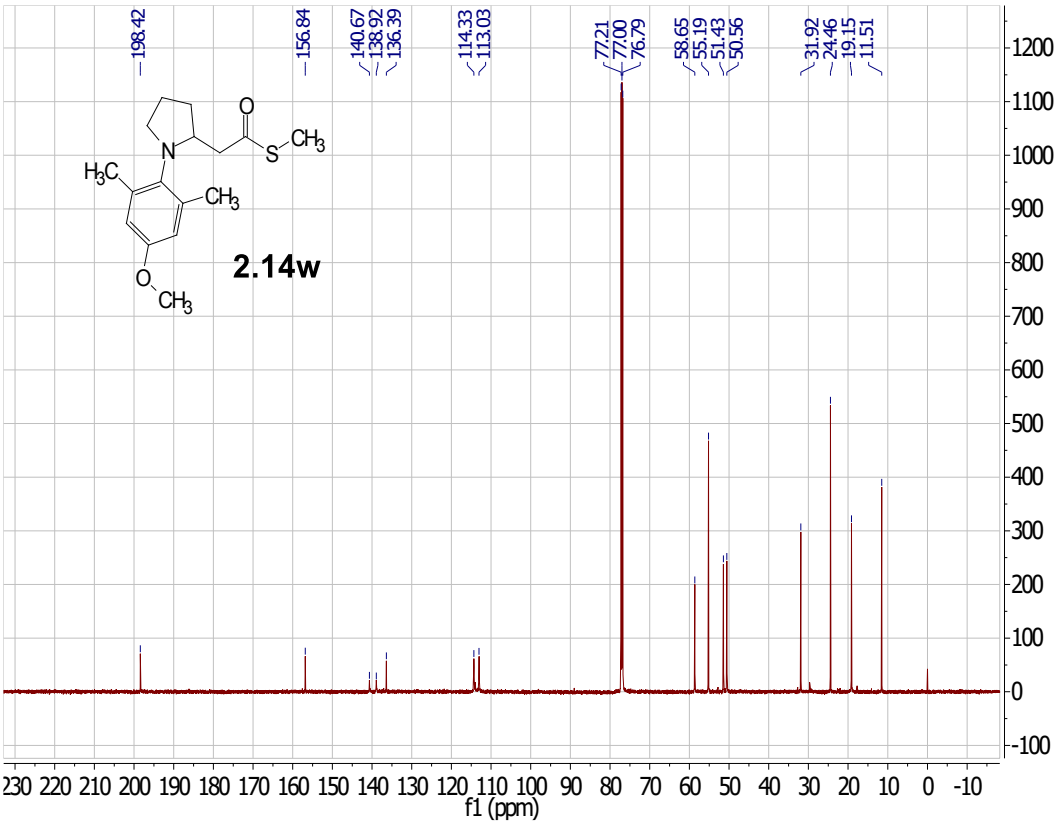
198.42
156.84
140.67
138.92
136.39
114.33
113.03
77.21
77.00
76.79
58.65
55.19
51.43
50.56
31.92
24.46
19.15
11.51
2.14w
f1 (ppm)

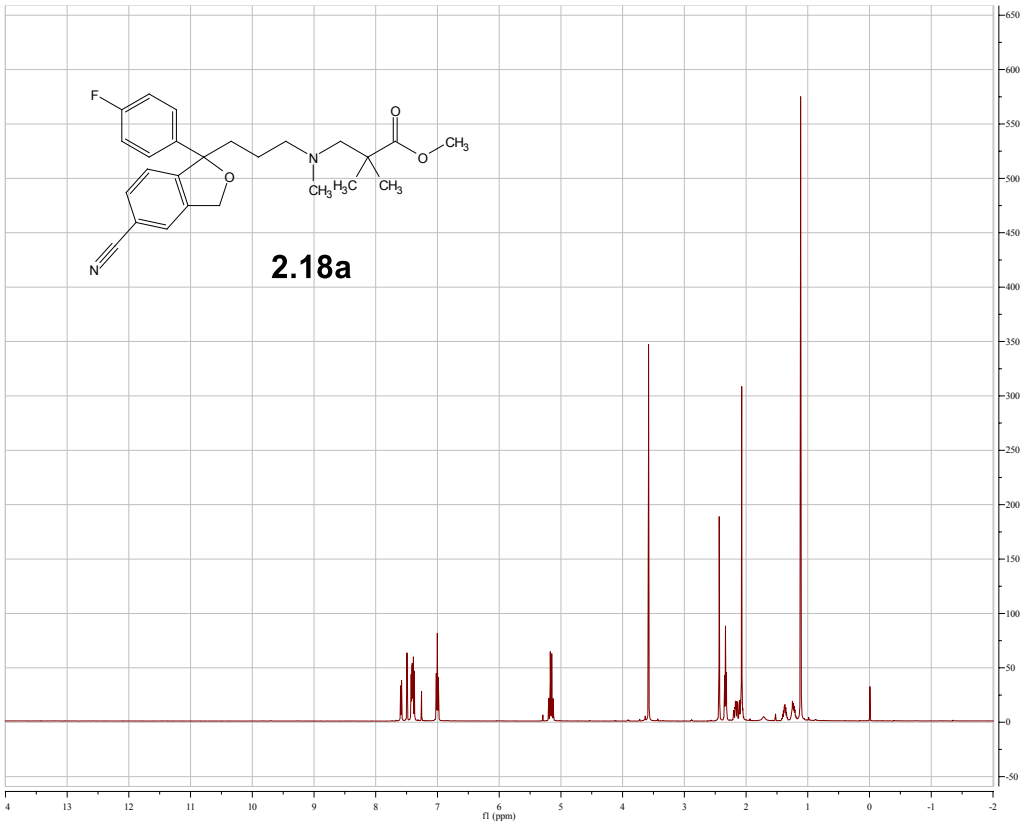
F
O
O
CH3
N
CH3
H3C
CH3
O
N
2.18a
f1 (ppm)

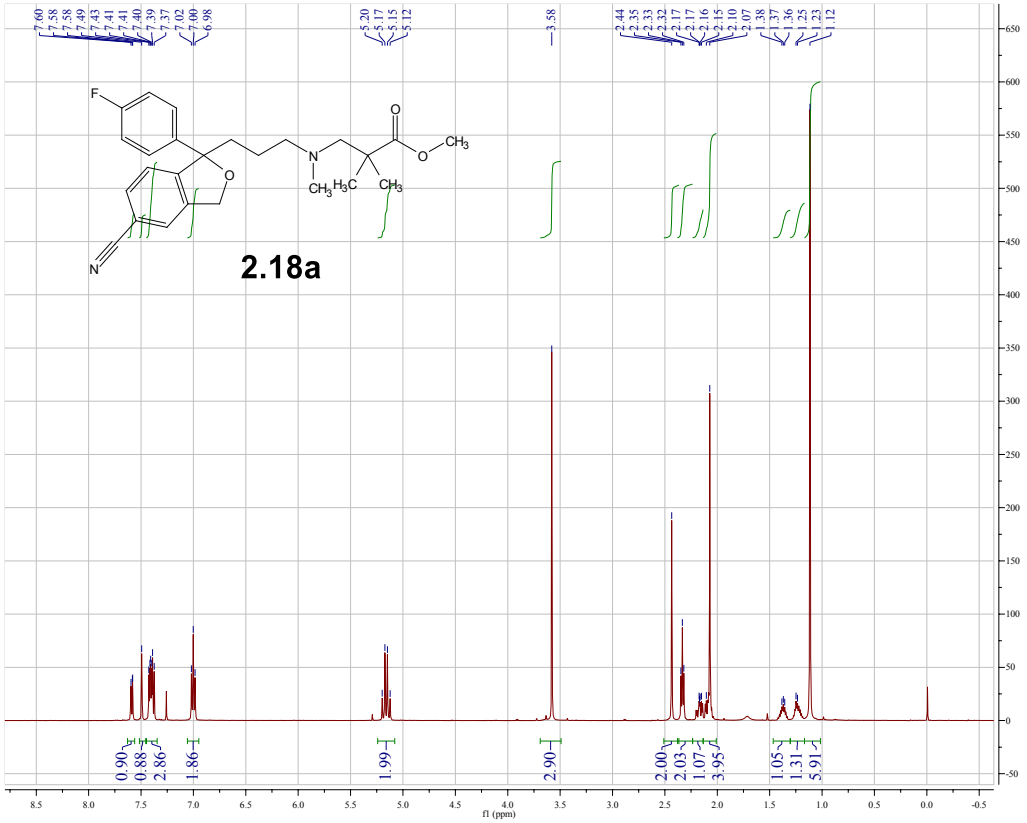
7.60
7.58
7.58
7.49
7.43
7.41
7.41
7.40
7.39
7.37
7.02
7.00
6.98
5.20
5.17
5.15
5.12
3.58
2.44
2.35
2.33
2.32
2.17
2.17
2.16
2.15
2.10
2.07
1.38
1.37
1.36
1.25
1.23
1.12
F
O
O
CH3
N
CH3
H3C
CH3
O
N
2.18a
0.90
0.88
2.86
1.86
1.99
2.90
2.00
2.03
1.07
3.95
1.05
1.31
5.91
f1 (ppm)

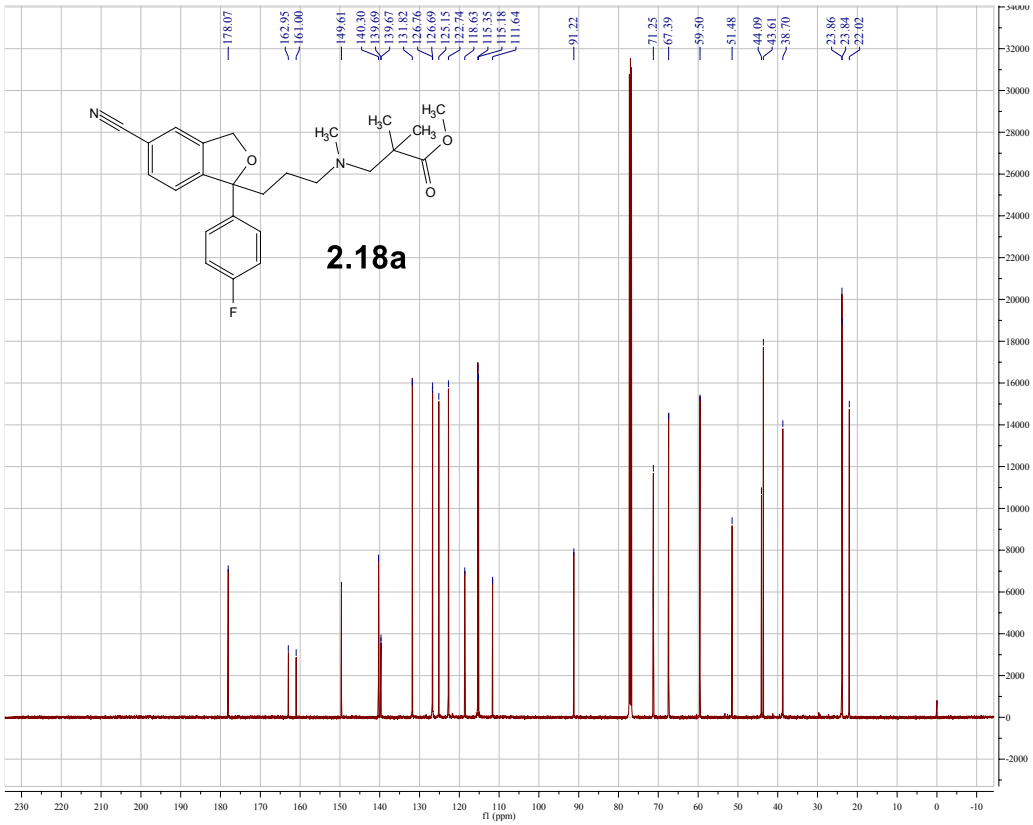
178.07
162.95
161.00
149.61
140.30
139.69
139.67
131.82
126.76
126.69
125.15
122.74
118.63
115.35
115.18
111.64
91.22
71.25
67.39
59.50
51.48
44.09
43.61
38.70
23.86
23.84
22.02
N
O
N
O
O
F
H3C
H3C
CH3
H3C
2.18a
f1 (ppm)

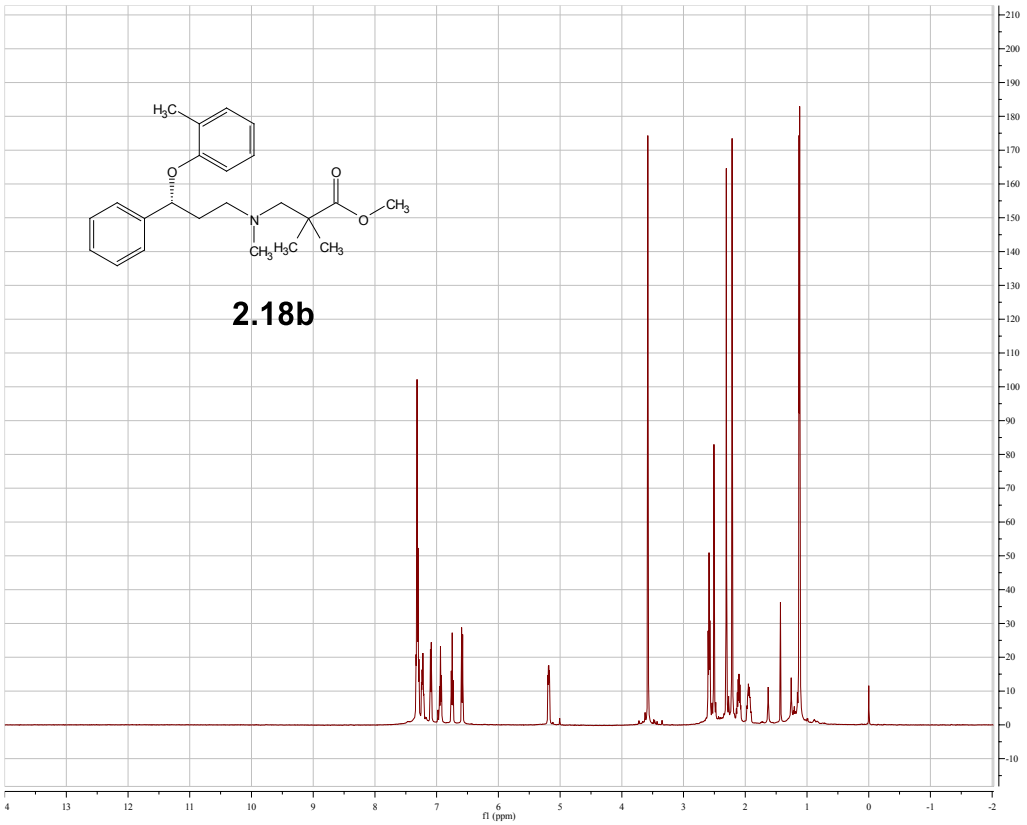
2.18b
f1 (ppm)

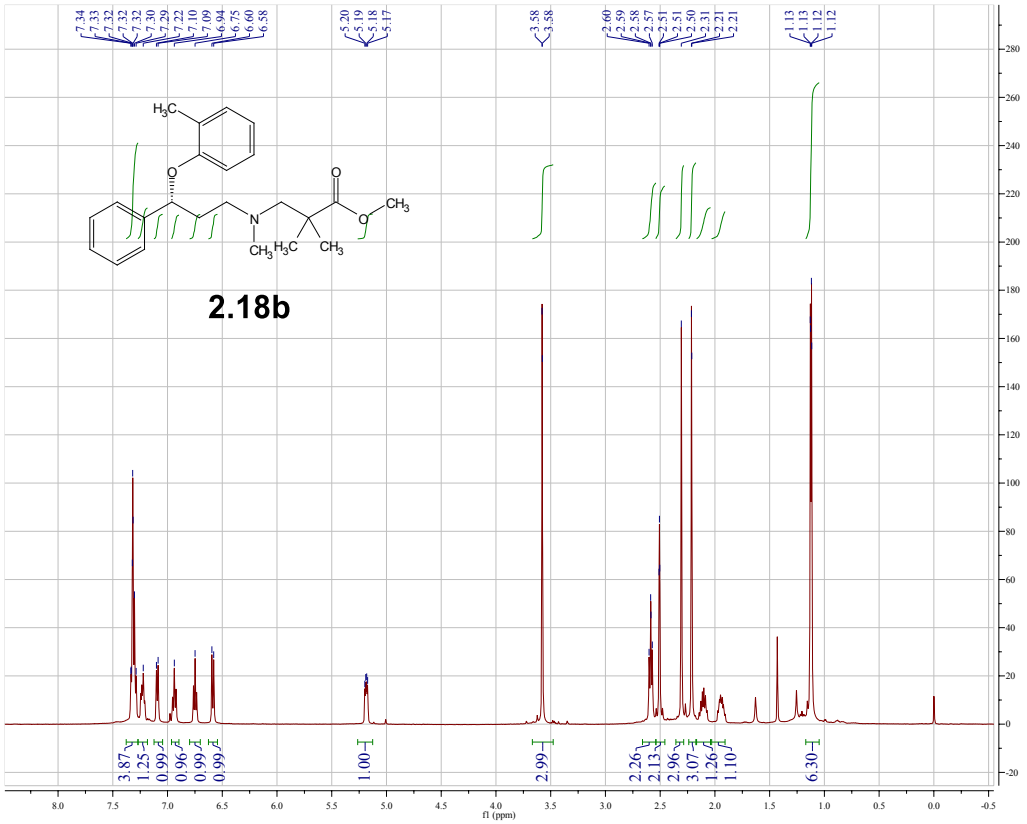
7.34
7.33
7.32
7.32
7.32
7.30
7.29
7.22
7.10
7.09
6.94
6.75
6.60
6.58
5.20
5.19
5.18
5.17
3.58
3.58
2.60
2.59
2.58
2.57
2.51
2.51
2.50
2.31
2.21
2.21
1.13
1.13
1.12
1.12
2.18b
3.87
1.25
0.99
0.96
0.99
0.99
1.00
2.99
2.26
2.13
2.96
3.07
1.26
1.10
6.30
f1 (ppm)

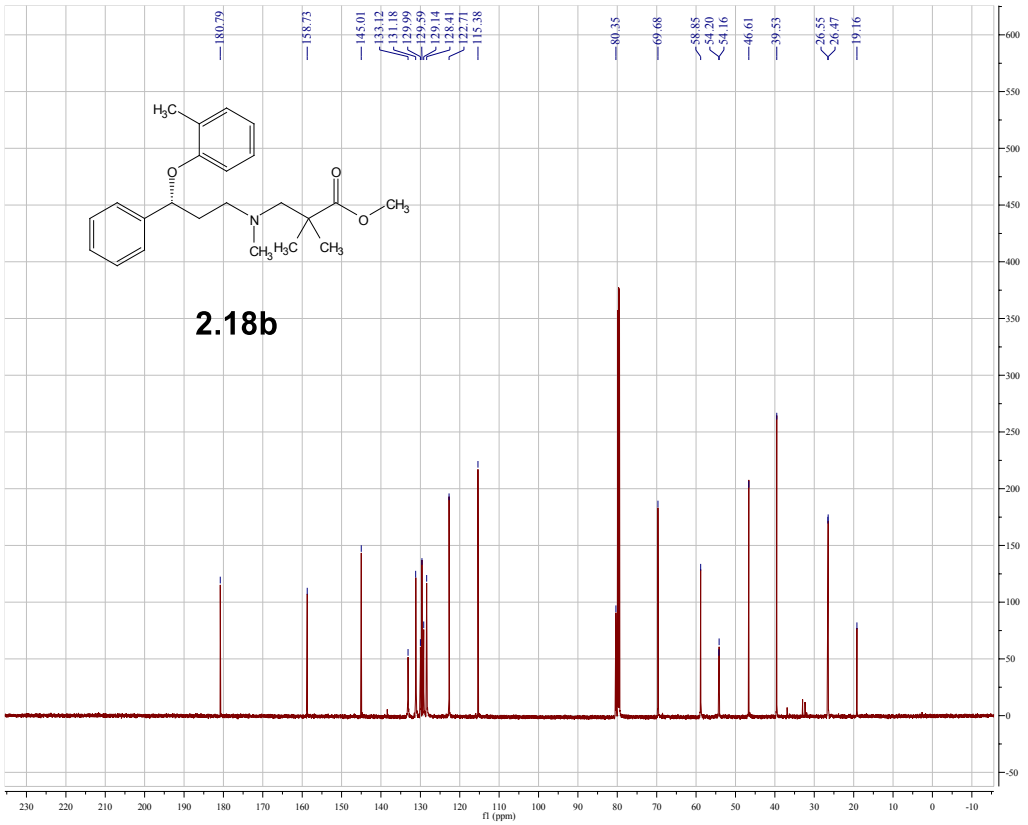
180.79
158.73
145.01
133.12
131.18
129.99
129.59
129.14
128.41
122.71
115.38
80.35
69.68
58.85
54.20
54.16
46.61
39.53
26.55
26.47
19.16
2.18b
f1 (ppm)

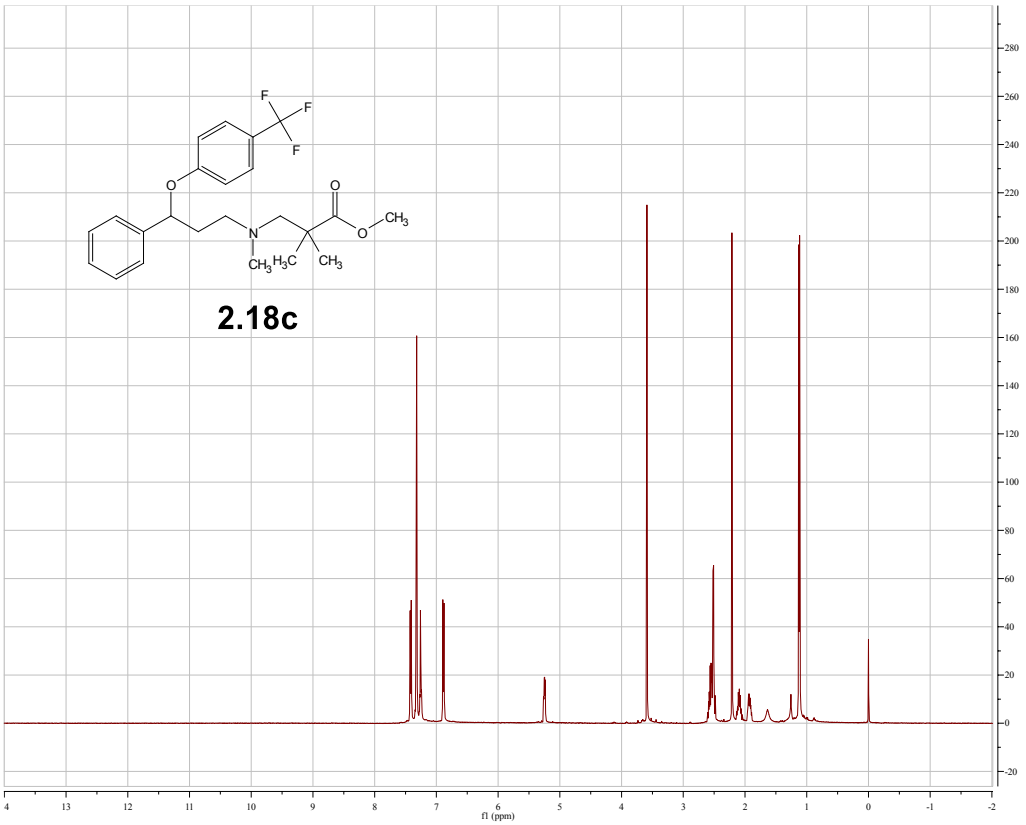
2.18c
f1 (ppm)

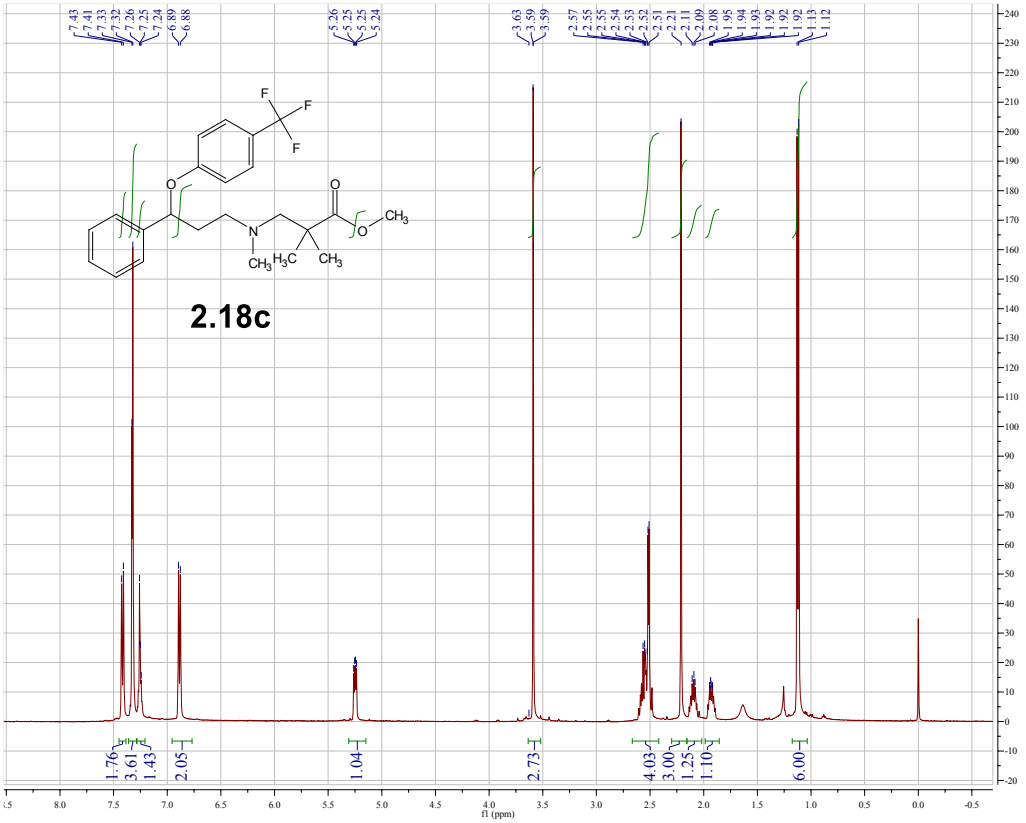
2.18c
f1 (ppm)

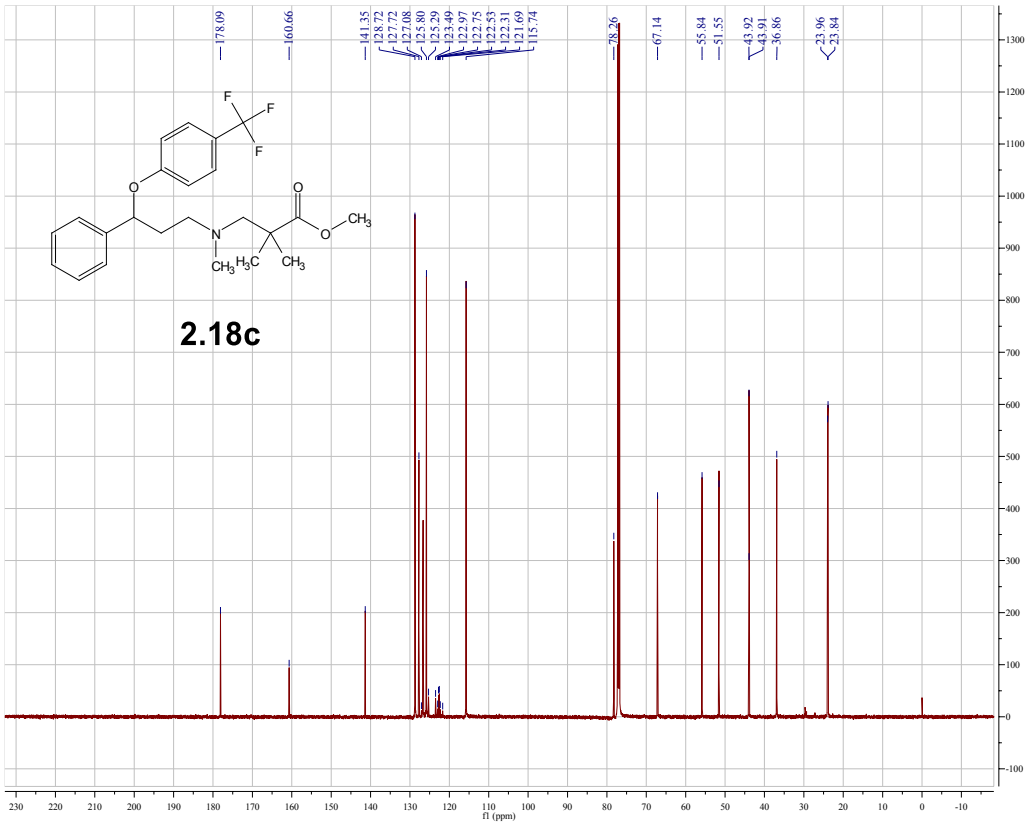
178.09
160.66
141.35
128.72
127.72
127.08
125.80
125.29
123.49
122.97
122.75
122.53
122.31
121.69
115.74
78.26
67.14
55.84
51.55
43.92
43.91
36.86
23.96
23.84
F
F
F
O
N
O
O
CH3
CH3
H3C
CH3
2.18c
f1 (ppm)

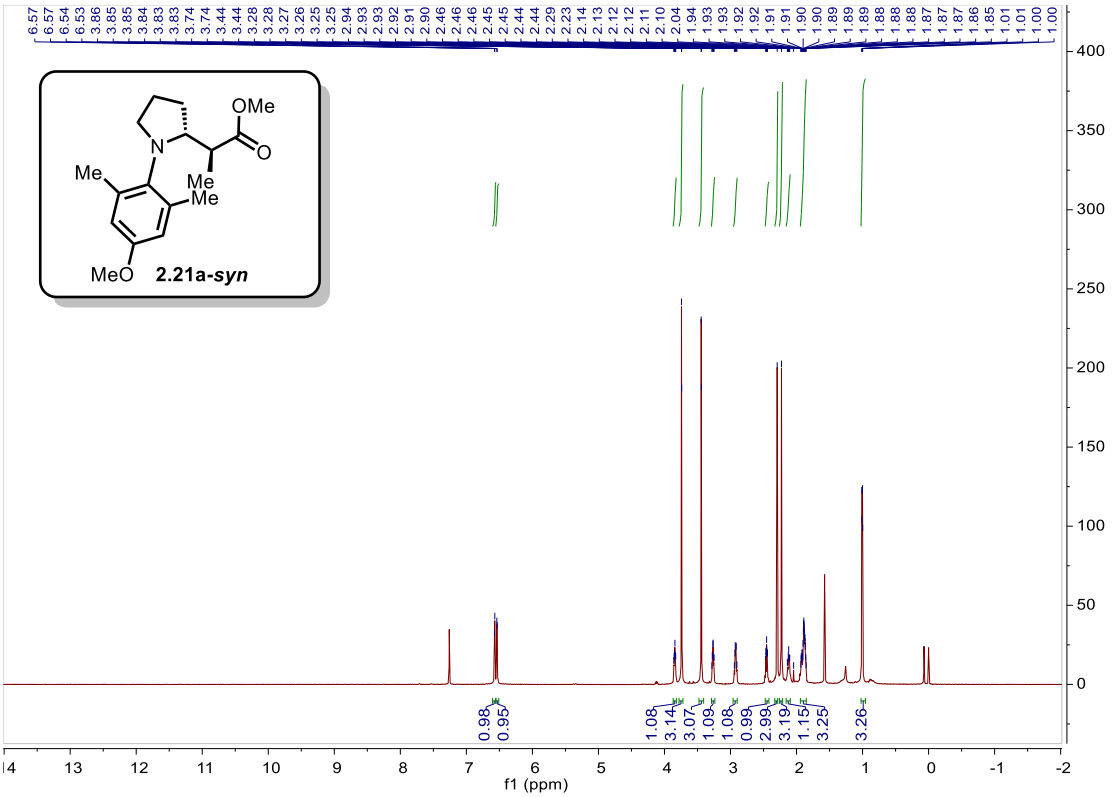
OMe
O
N
Me
Me
Me
MeO
2.21a-syn
f1 (ppm)

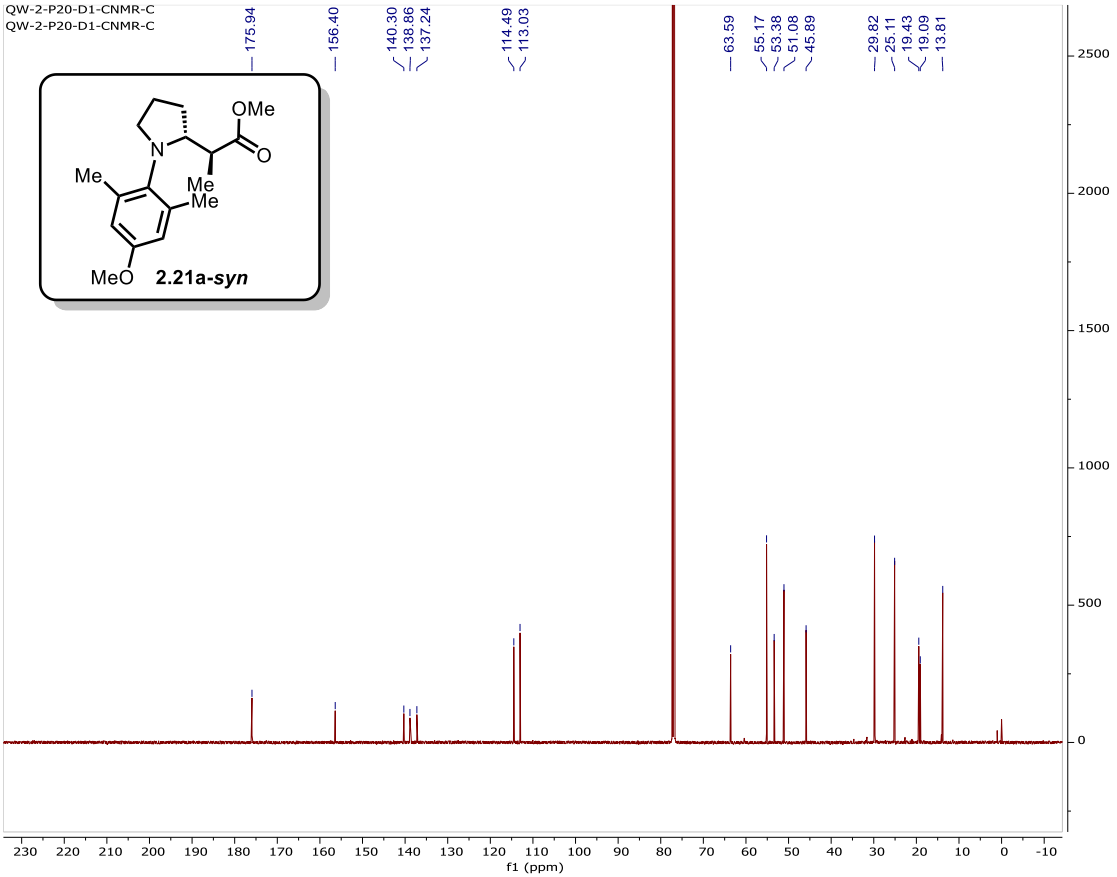
QW-2-P20-D1-CNMR-C
QW-2-P20-D1-CNMR-C
OMe
O
N
Me
Me
Me
MeO
2.21a-syn
f1 (ppm)

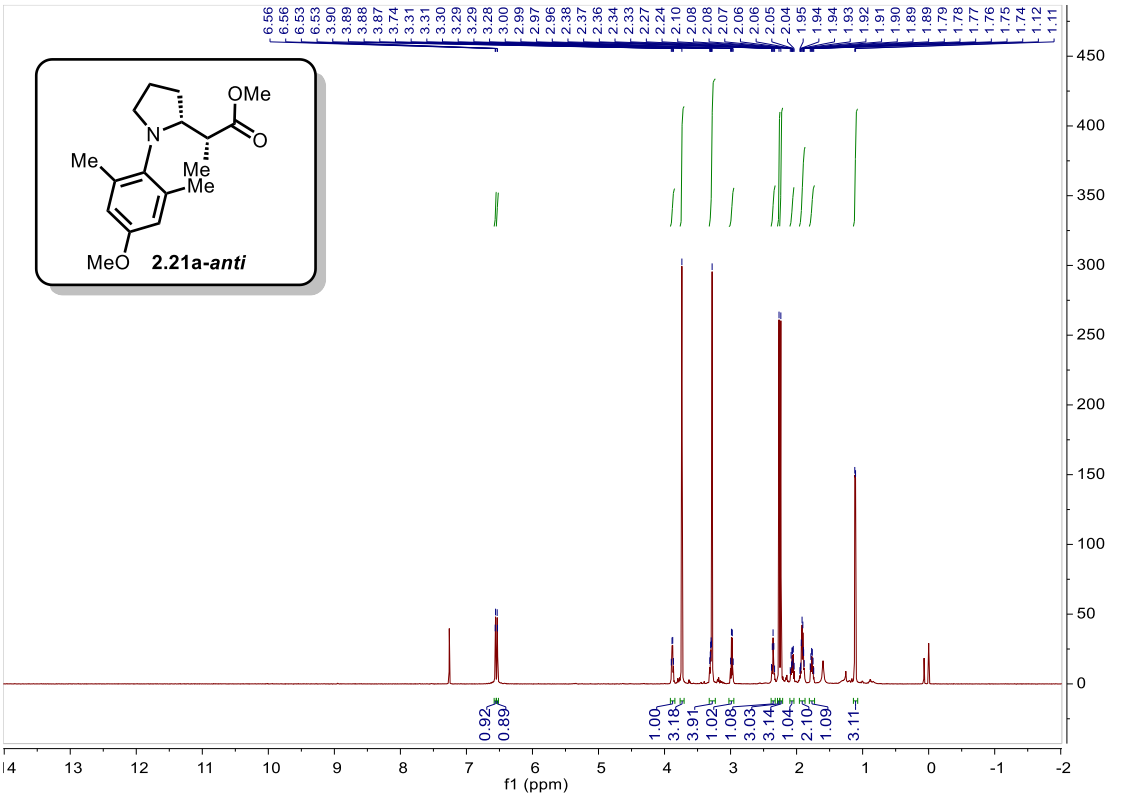
OMe
O
N
Me
Me
Me
MeO
2.21a-anti
f1 (ppm)

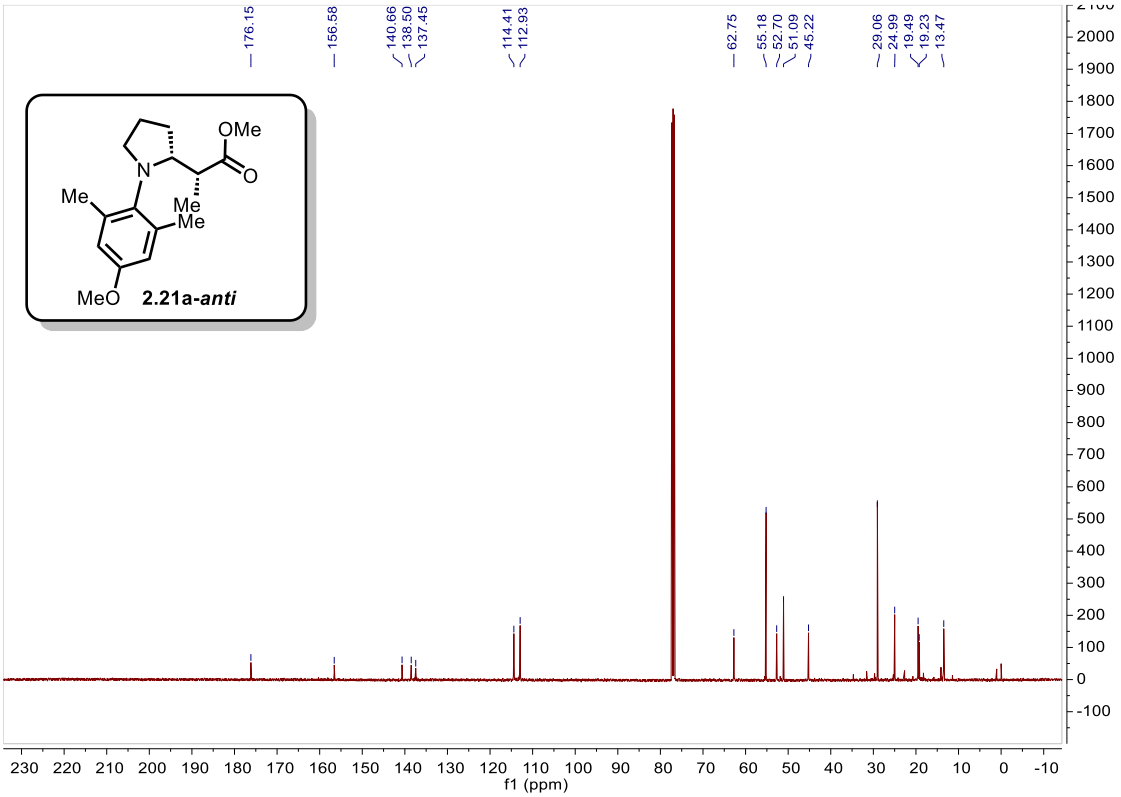
OMe
O
N
Me
Me
Me
MeO
2.21a-anti
f1 (ppm)

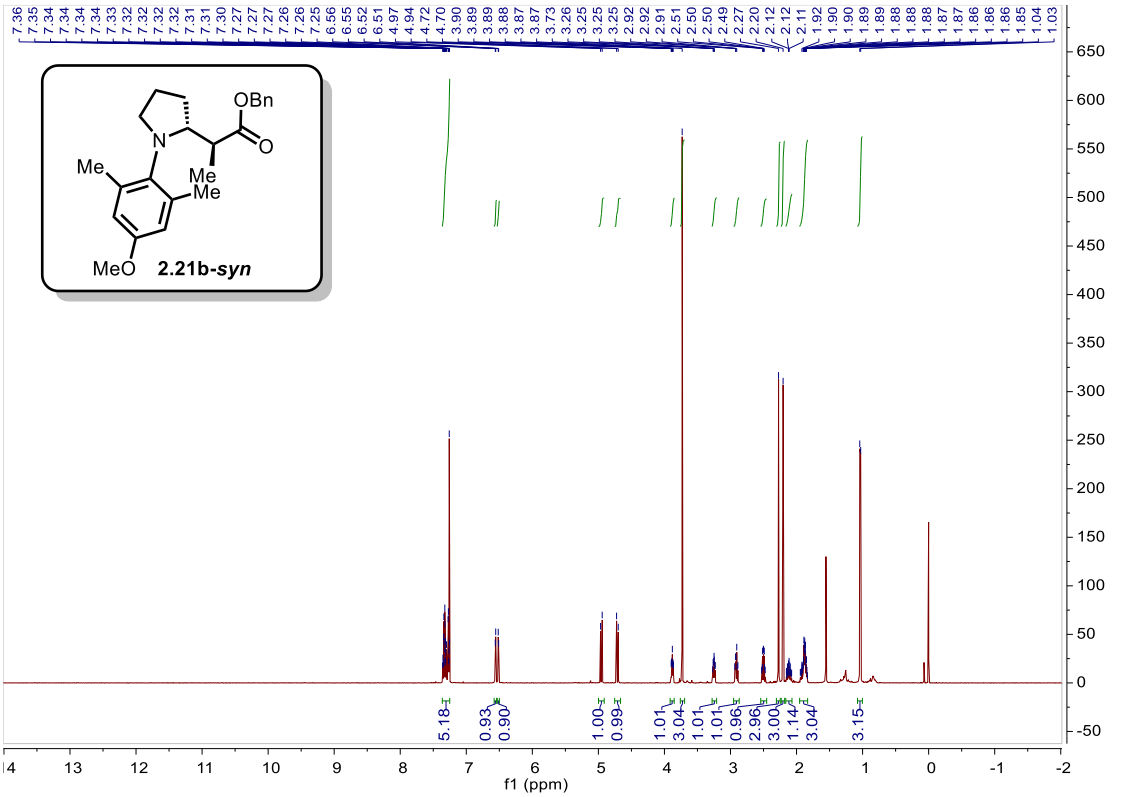
OBn
N
O
Me
Me
Me
MeO
2.21b-syn
f1 (ppm)

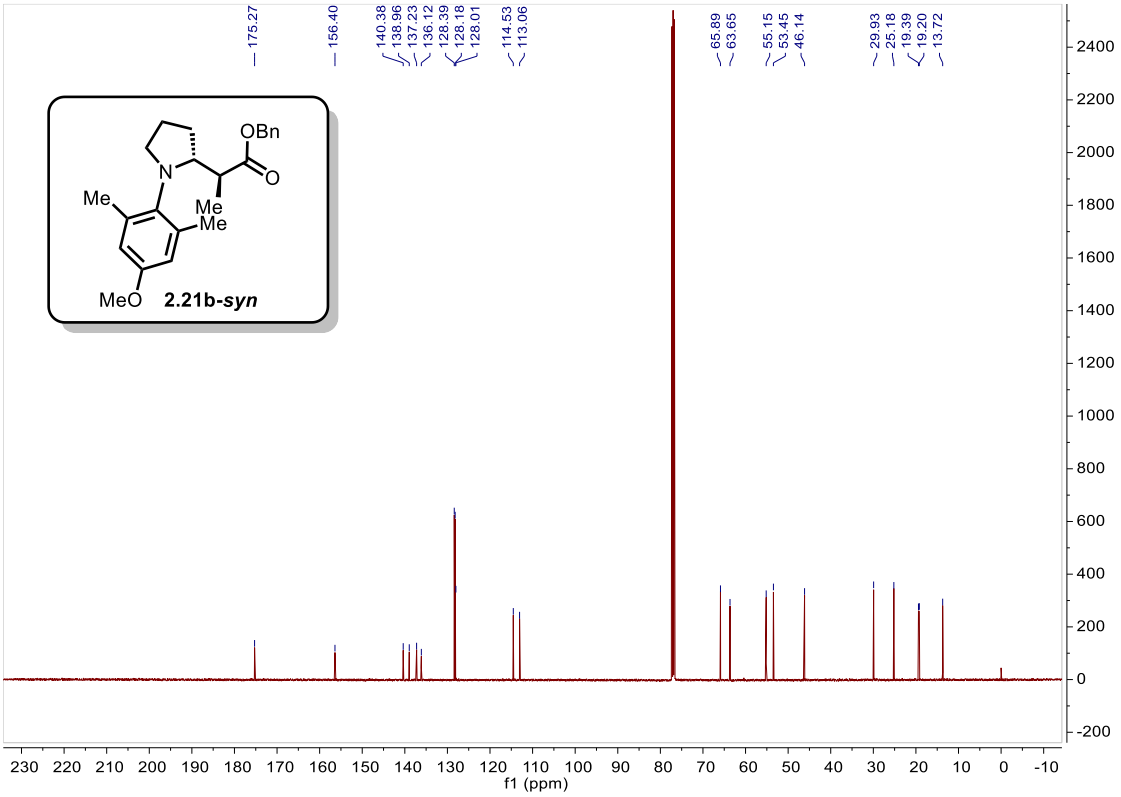
OBn
N
O
Me
Me
Me
MeO
2.21b-syn
f1 (ppm)

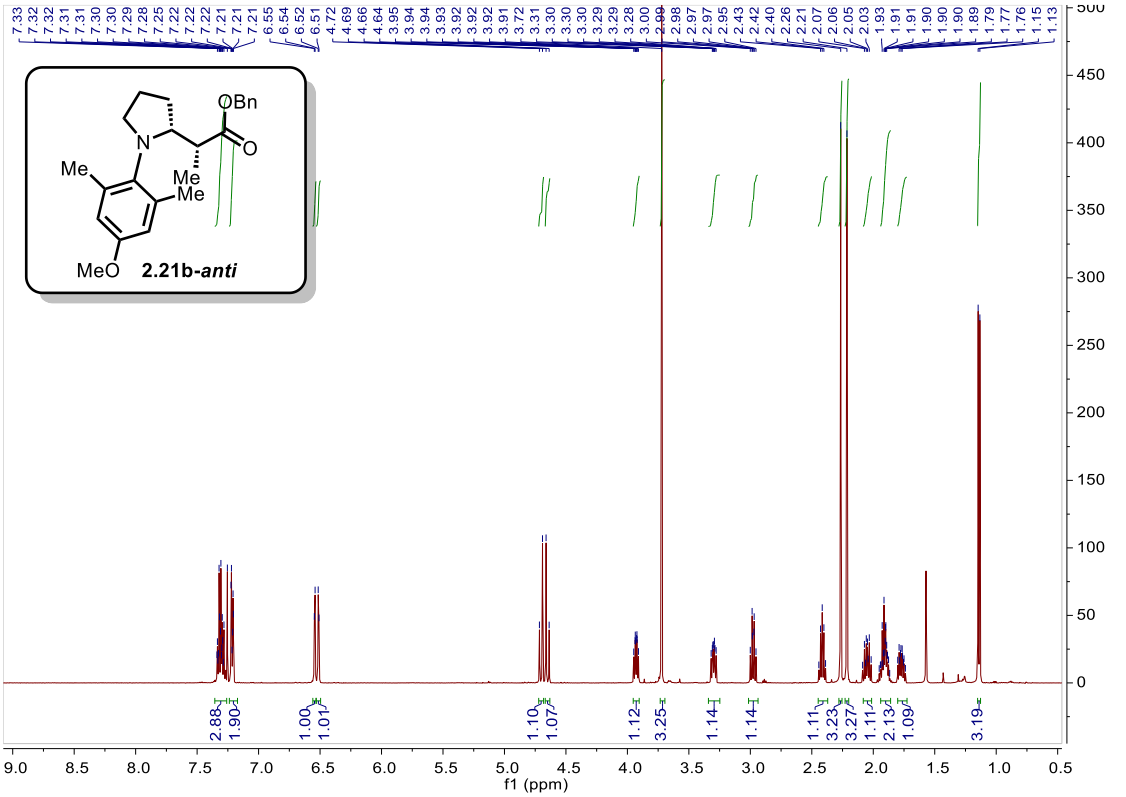
OBn
O
N
Me
Me
Me
MeO
2.21b-anti
f1 (ppm)

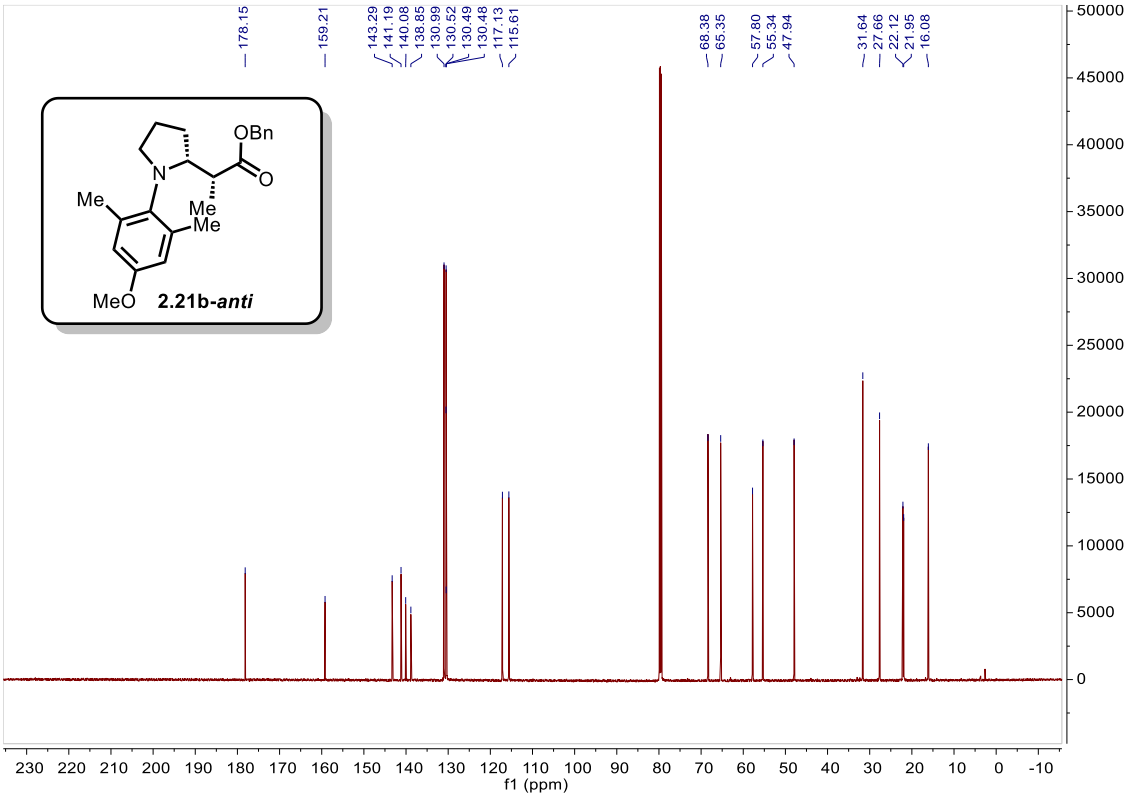
178.15
159.21
143.29
141.19
140.08
138.85
130.99
130.52
130.49
130.48
117.13
115.61
68.38
65.35
57.80
55.34
47.94
31.64
27.66
22.12
21.95
16.08
OBn
O
N
Me
Me
Me
MeO
2.21b-anti
f1 (ppm)

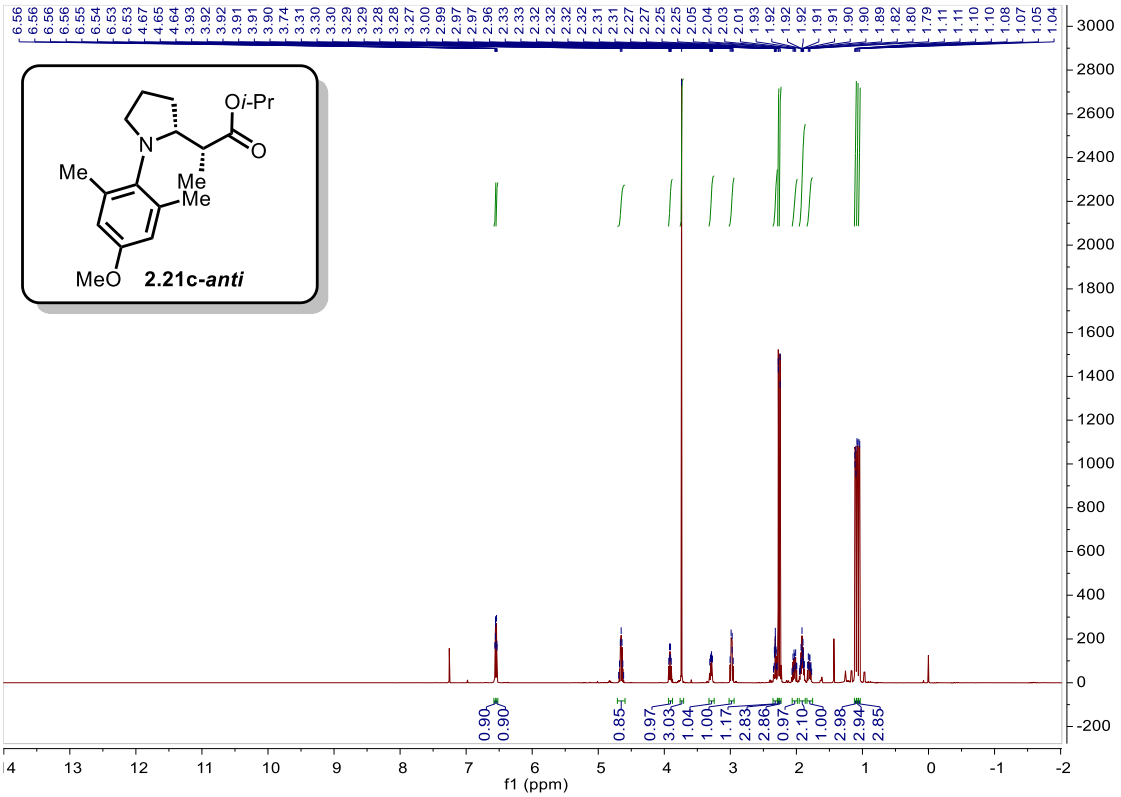
O*i*-Pr
N
O
Me
Me
Me
MeO
2.21c-*anti*
f1 (ppm)

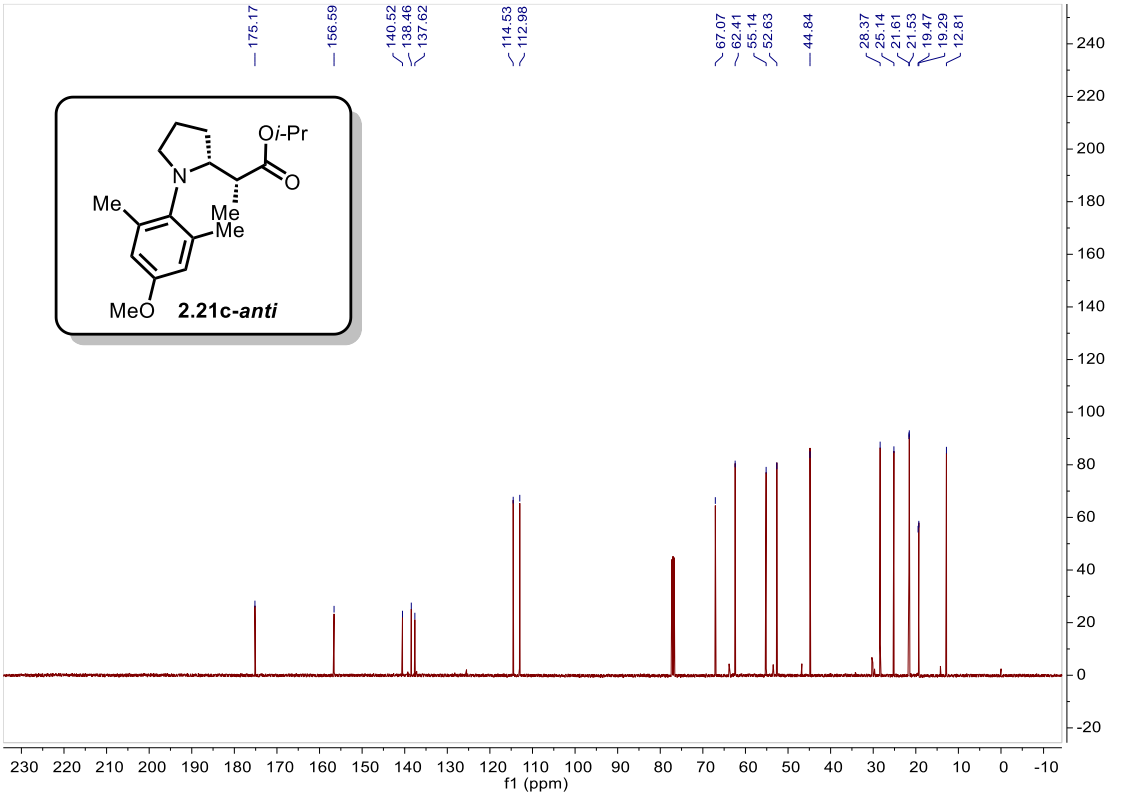
O*i*-Pr
N
O
Me
Me
Me
MeO
2.21c-*anti*
f1 (ppm)

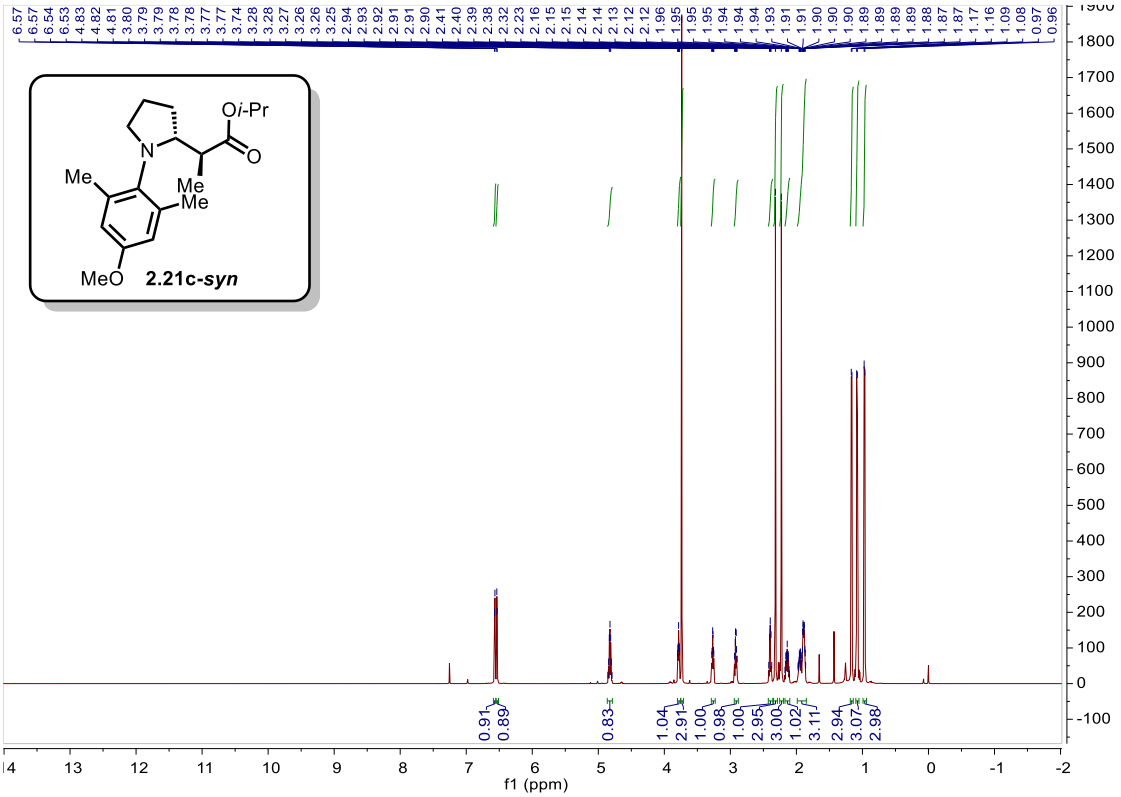
O*i*-Pr
O
N
Me
Me
Me
MeO
2.21c-*syn*
f1 (ppm)

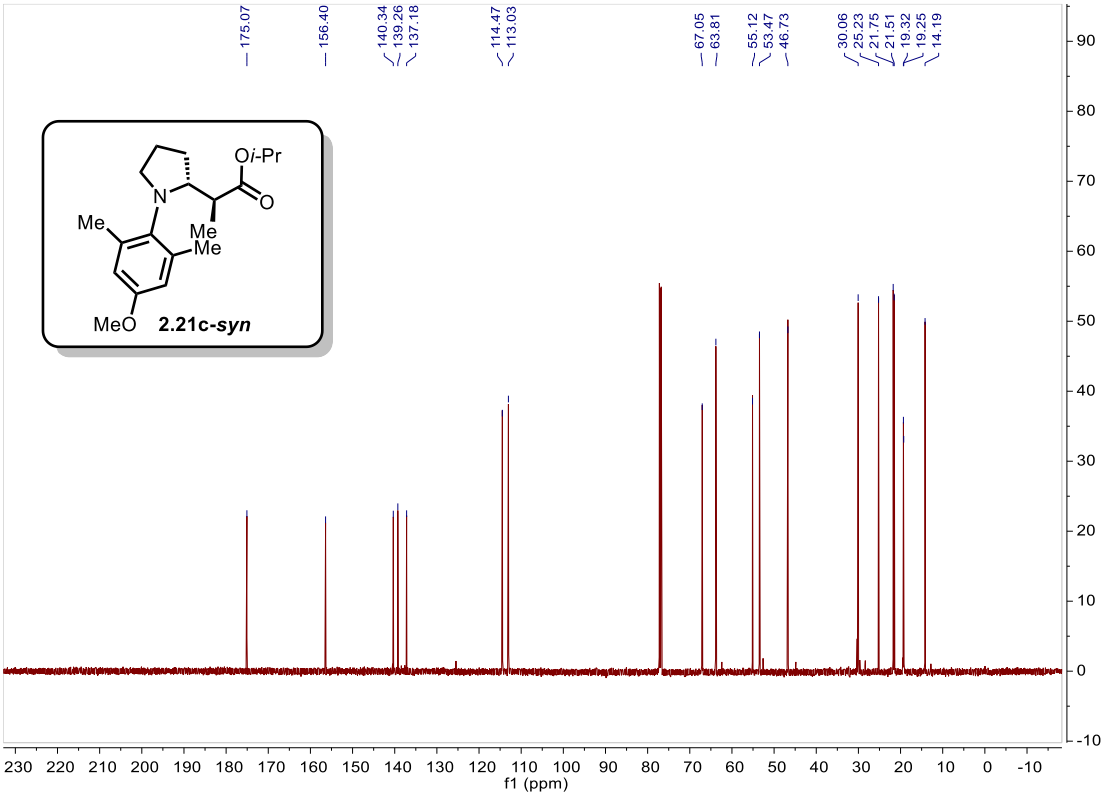
O*i*-Pr
O
N
Me
Me
Me
MeO
2.21c-*syn*
f1 (ppm)

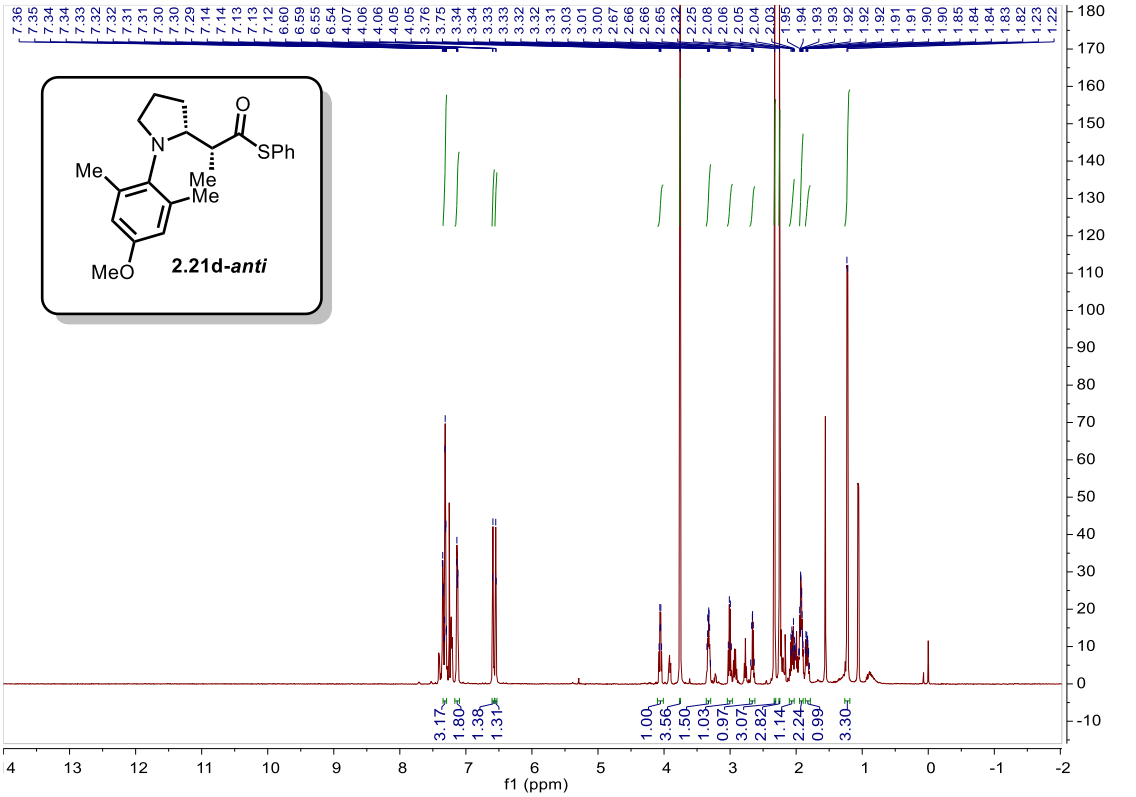
2.21d-*anti*
f1 (ppm)

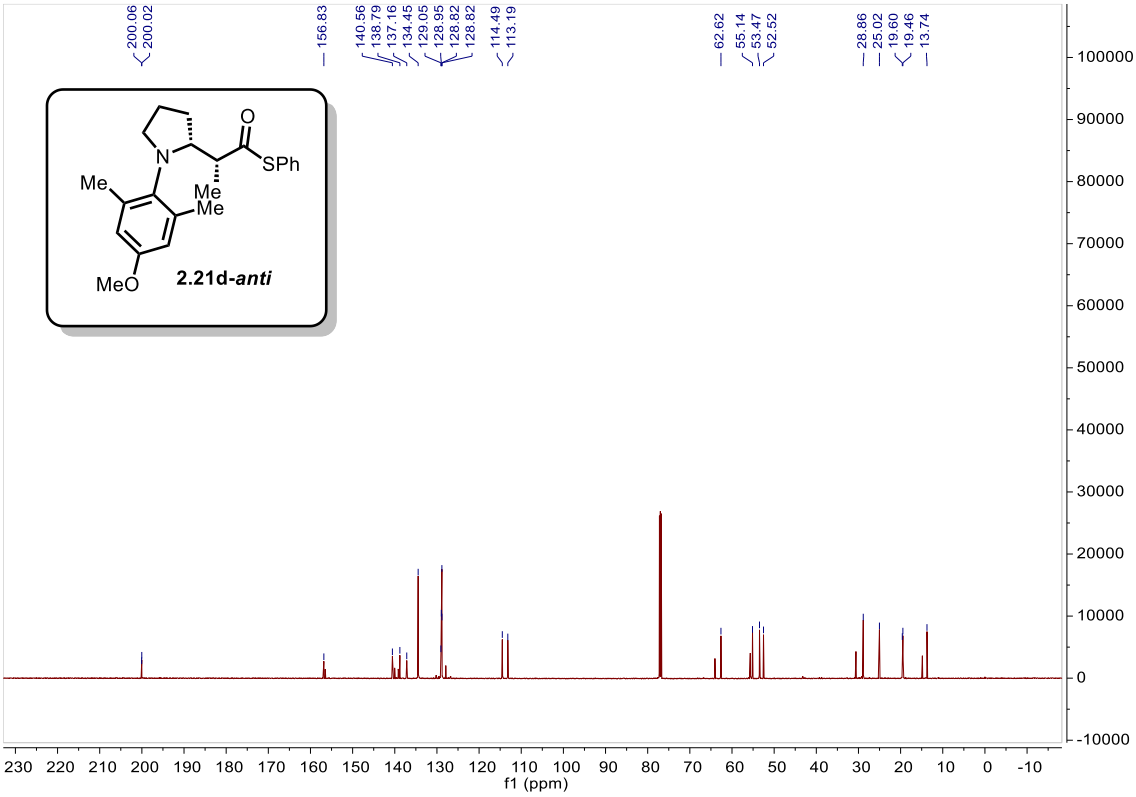
2.21d-*anti*
f1 (ppm)

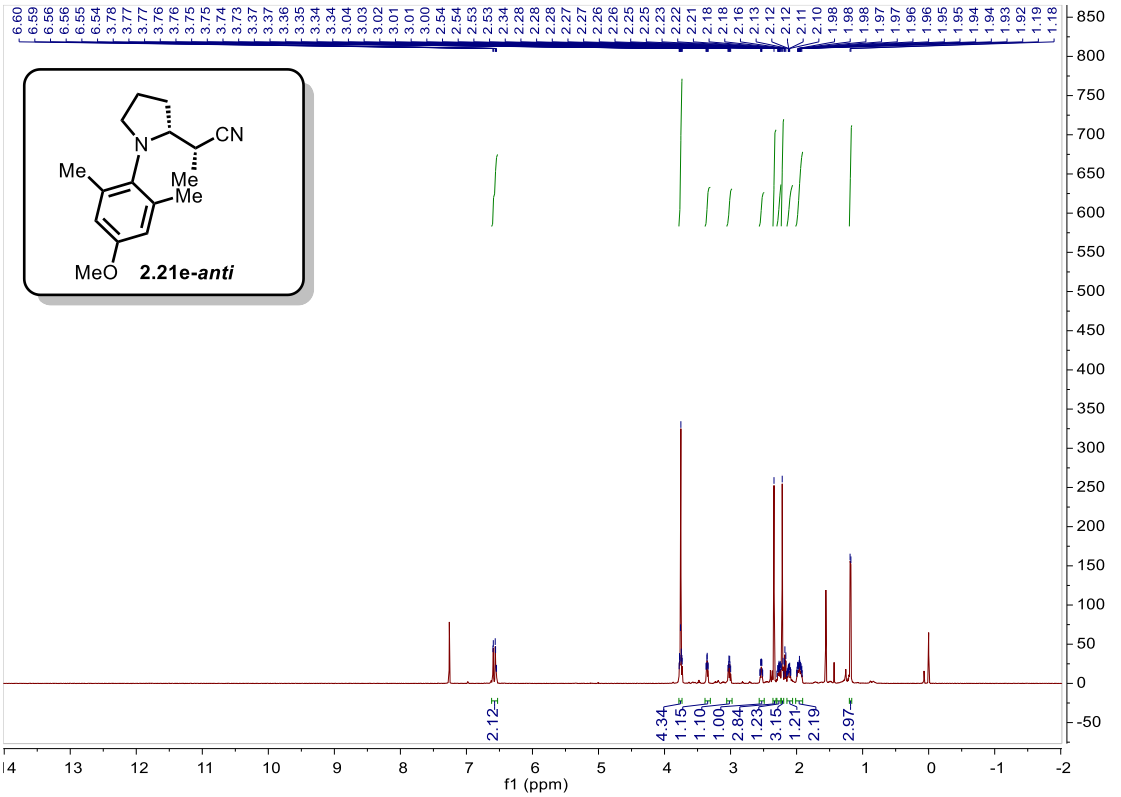
6.60 6.59 6.56 6.56 6.55 6.54 3.78 3.77 3.77 3.76 3.76 3.75 3.75 3.74 3.73 3.37 3.36 3.35 3.34 3.34 3.04 3.03 3.02 3.01 3.01 3.00 2.54 2.54 2.53 2.53 2.34 2.28 2.28 2.28 2.27 2.27 2.26 2.26 2.25 2.25 2.23 2.22 2.21 2.18 2.18 2.16 2.13 2.12 2.12 2.11 2.10 1.98 1.98 1.97 1.97 1.96 1.96 1.95 1.95 1.94 1.94 1.93 1.92 1.19 1.18
N
CN
Me
Me
Me
MeO
2.21e-anti
2.12
4.34
1.15
1.10
1.00
2.84
1.23
3.15
1.21
2.19
2.97
f1 (ppm)

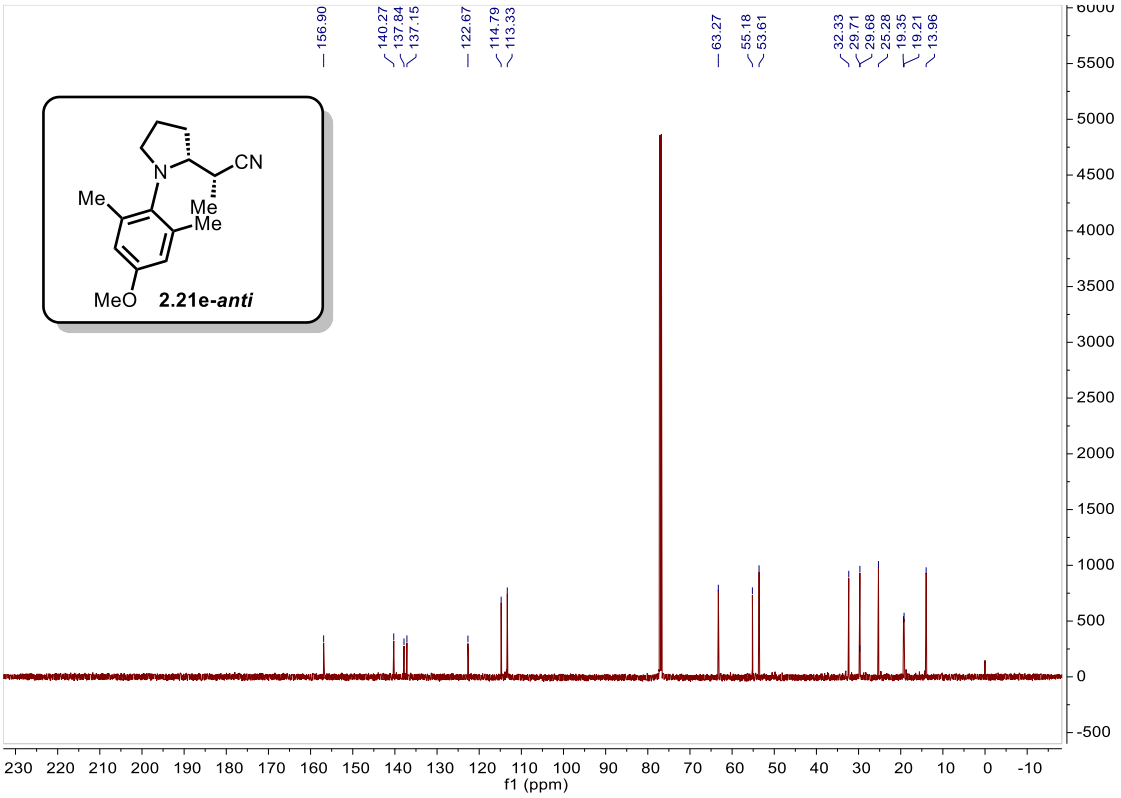
156.90
140.27
137.84
137.15
122.67
114.79
113.33
63.27
55.18
53.61
32.33
29.71
29.68
25.28
19.35
19.21
13.96
N
CN
Me
Me
Me
MeO
2.21e-anti
f1 (ppm)

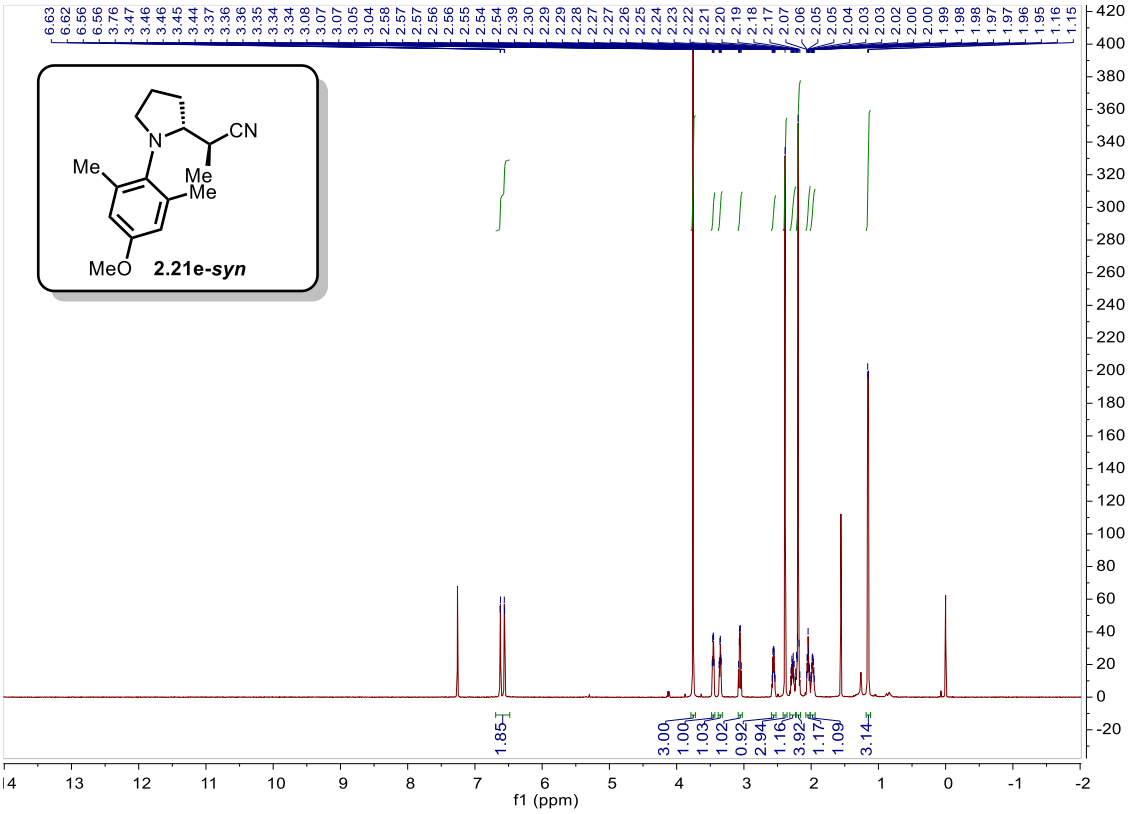
6.63 6.62 6.56 6.56 6.56 3.76 3.47 3.46 3.46 3.45 3.44 3.37 3.36 3.36 3.35 3.34 3.34 3.08 3.07 3.07 3.05 3.04 2.58 2.57 2.57 2.56 2.56 2.55 2.54 2.54 2.39 2.30 2.29 2.29 2.28 2.27 2.27 2.26 2.25 2.24 2.23 2.22 2.21 2.20 2.19 2.18 2.17 2.07 2.06 2.05 2.05 2.04 2.03 2.03 2.02 2.00 2.00 1.99 1.98 1.98 1.97 1.97 1.96 1.95 1.16 1.15
CN
Me
Me
Me
MeO
2.21e-syn
1.85
3.00
1.00
1.03
1.02
0.92
2.94
1.16
3.92
1.17
1.09
3.14
f1 (ppm)

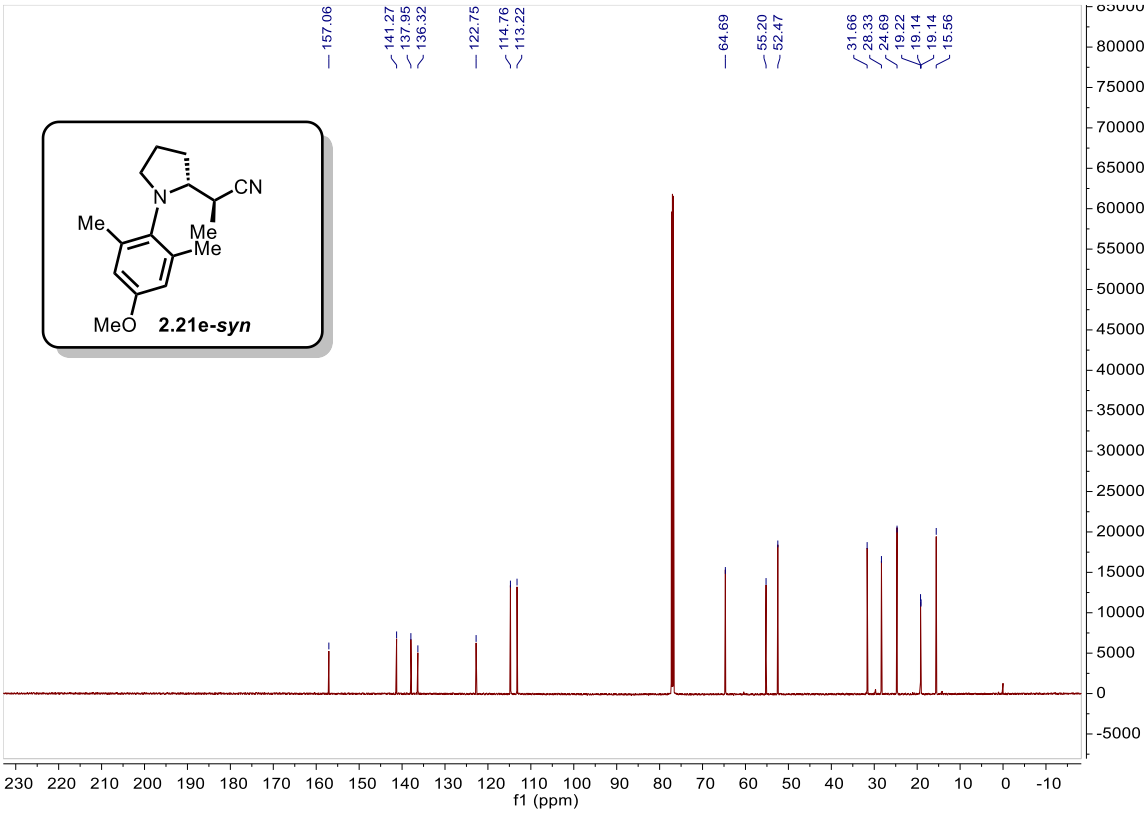
157.06
141.27
137.95
136.32
122.75
114.76
113.22
64.69
55.20
52.47
31.66
28.33
24.69
19.22
19.14
19.14
15.56
CN
Me
Me
Me
MeO
2.21e-syn
f1 (ppm)

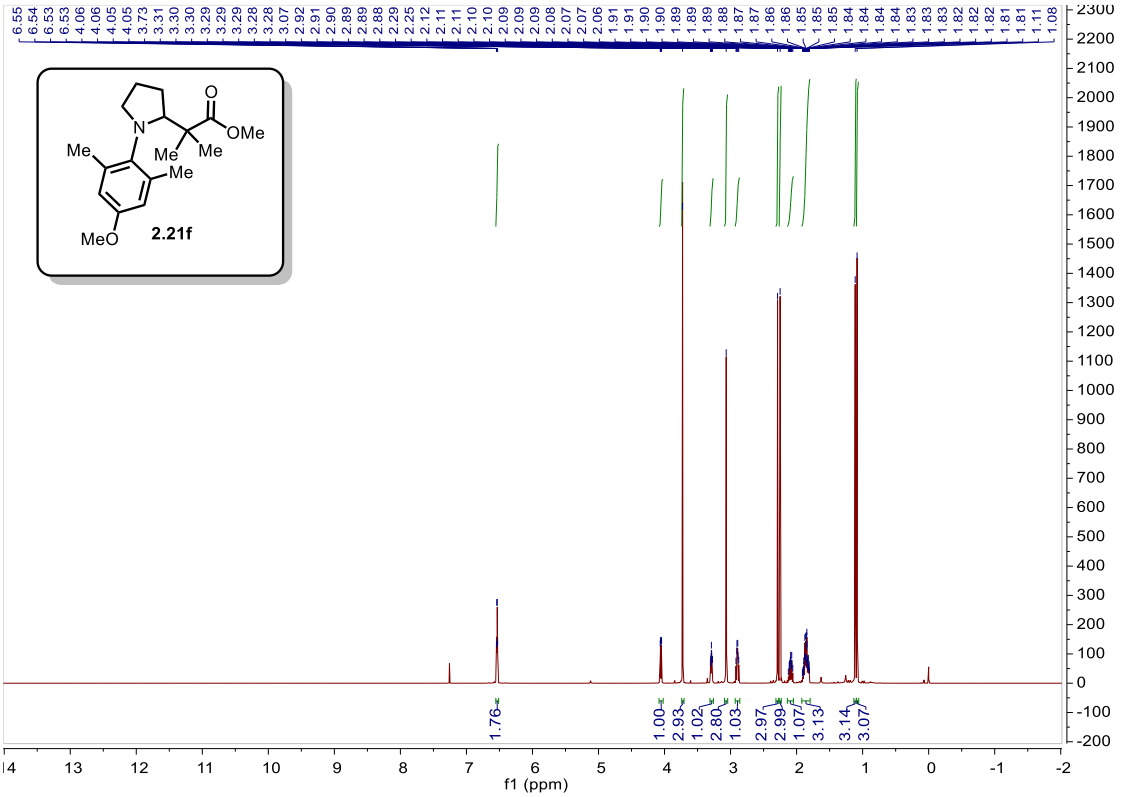
2.21f
f1 (ppm)

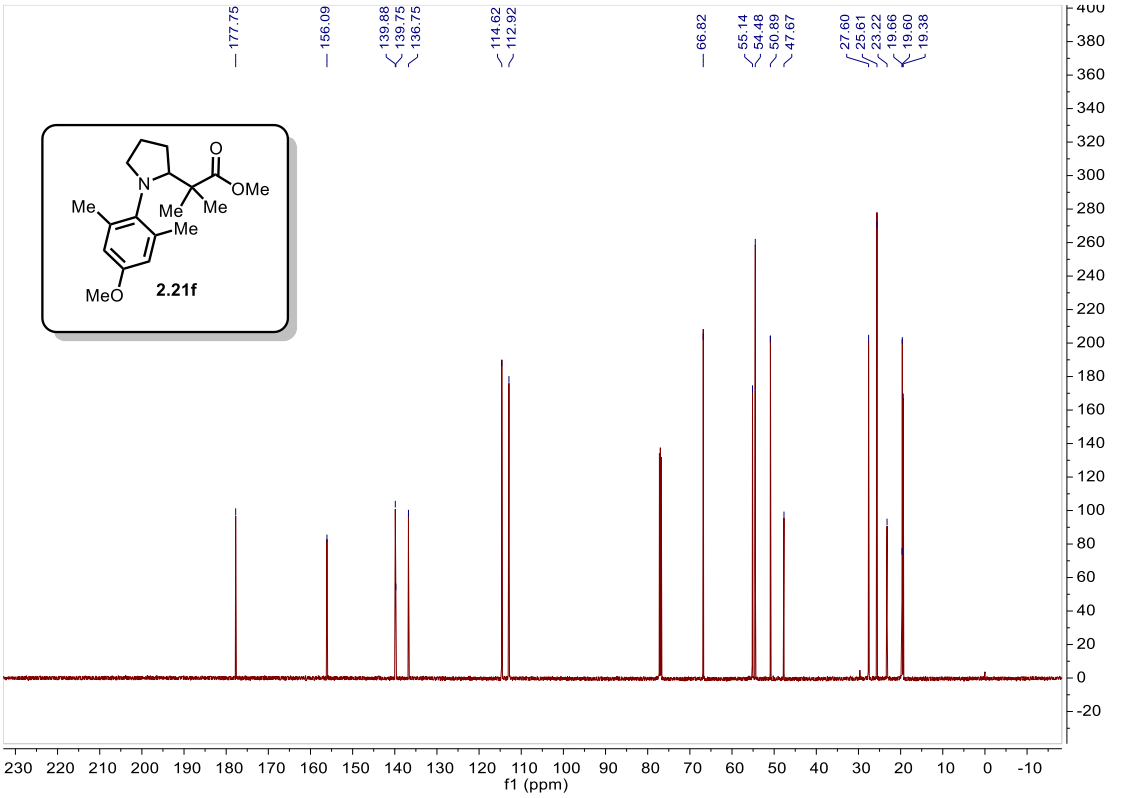
2.21f
f1 (ppm)

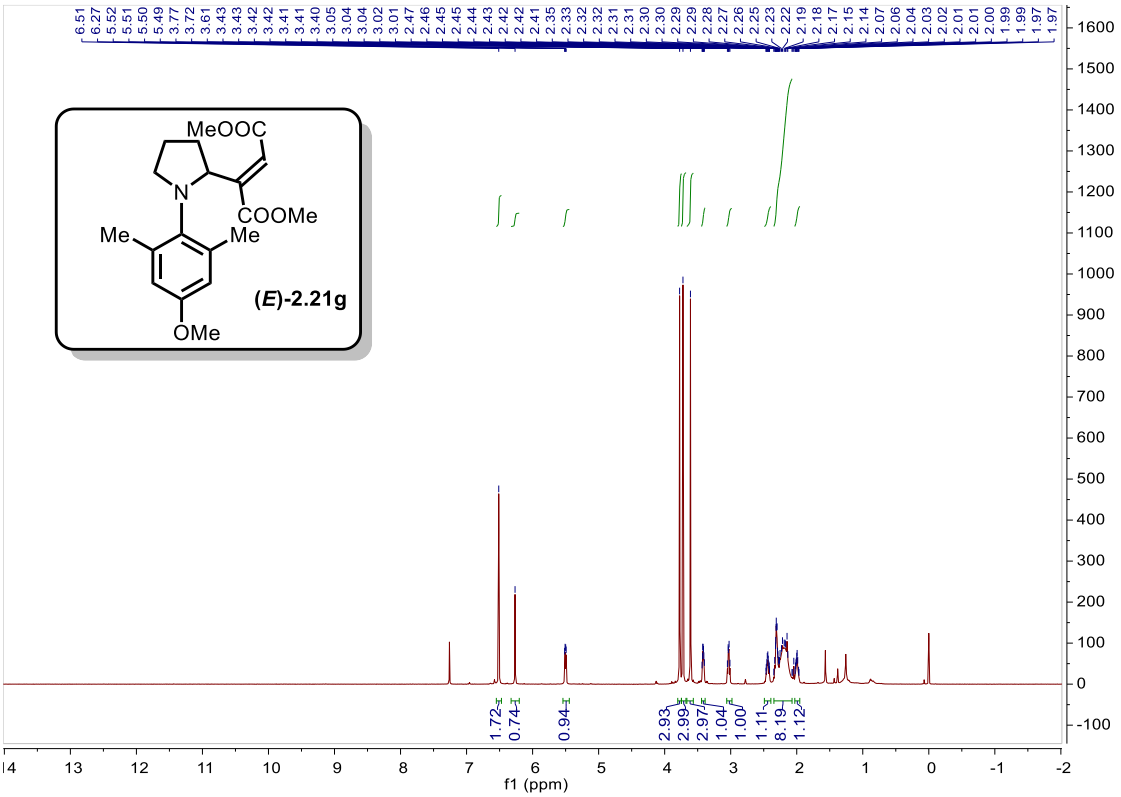
MeOOC
COOMe
Me
Me
OMe
(E)-2.21g
f1 (ppm)

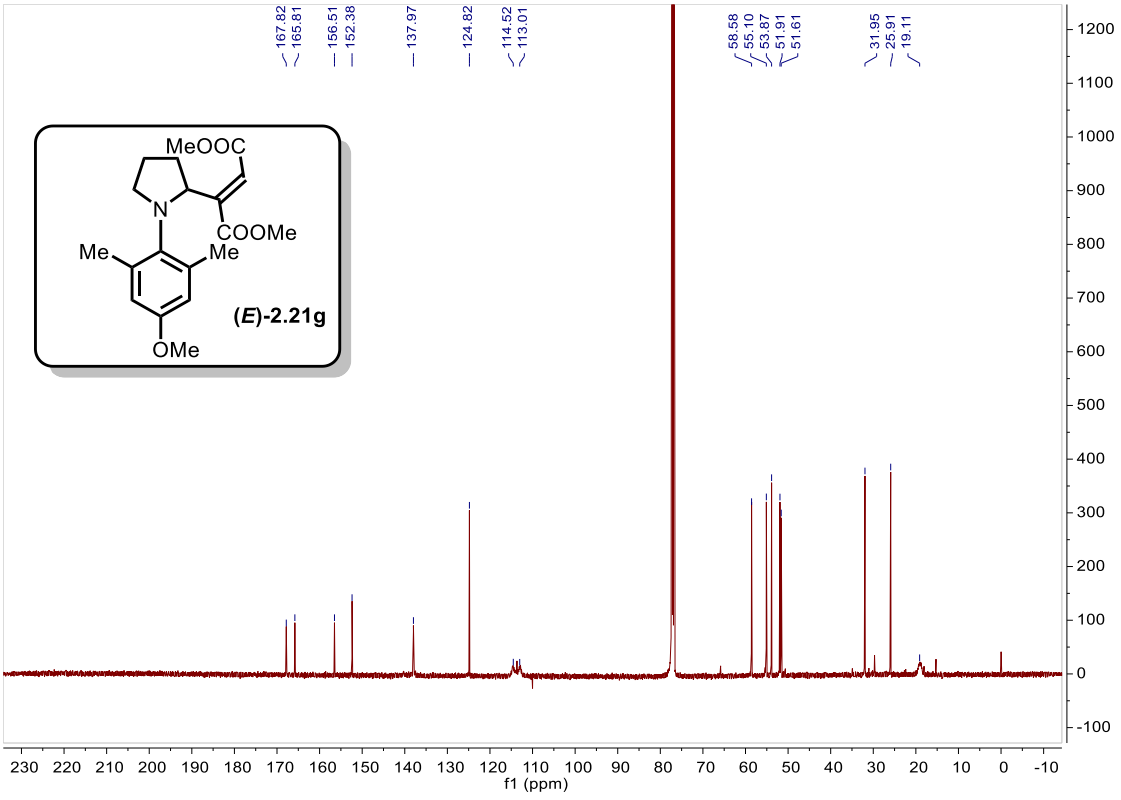
MeOOC
COOMe
Me
Me
OMe
(E)-2.21g
f1 (ppm)

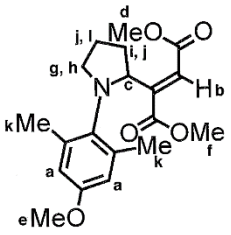

(*E*)-2.21g

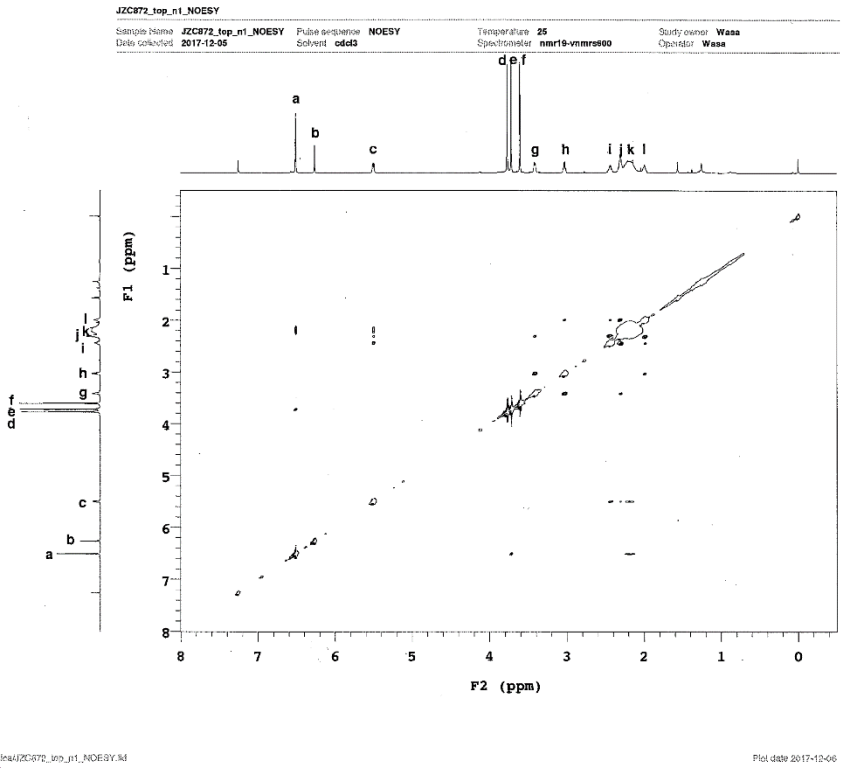

Data file /home/ALL/Wasa/Jessica/JZC872_top_n1_NOESY.fid

Plot date 2017-12-06

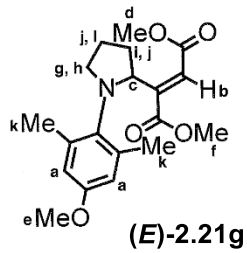

(*E*)-2.21g

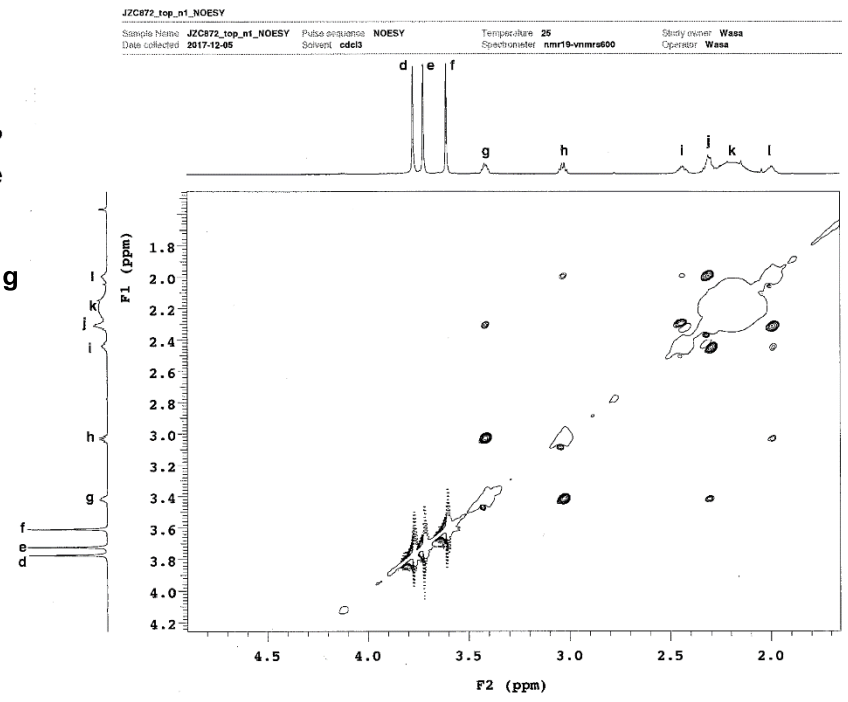

Data file /home/ALL/Wasa/Jessica/JZC872_top_n1_NOESY.fid

Plot date 2017-12-06

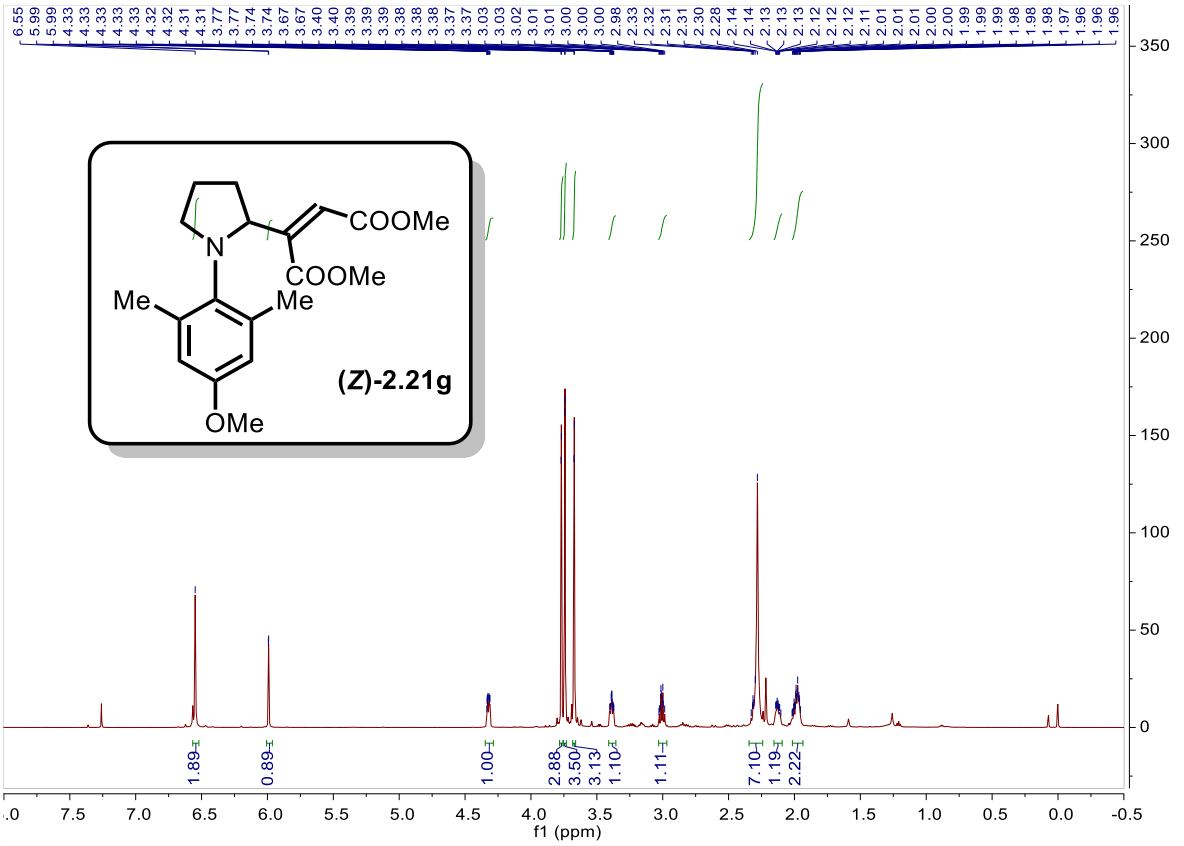
COOMe
COOMe
Me
Me
OMe
(Z)-2.21g
f1 (ppm)

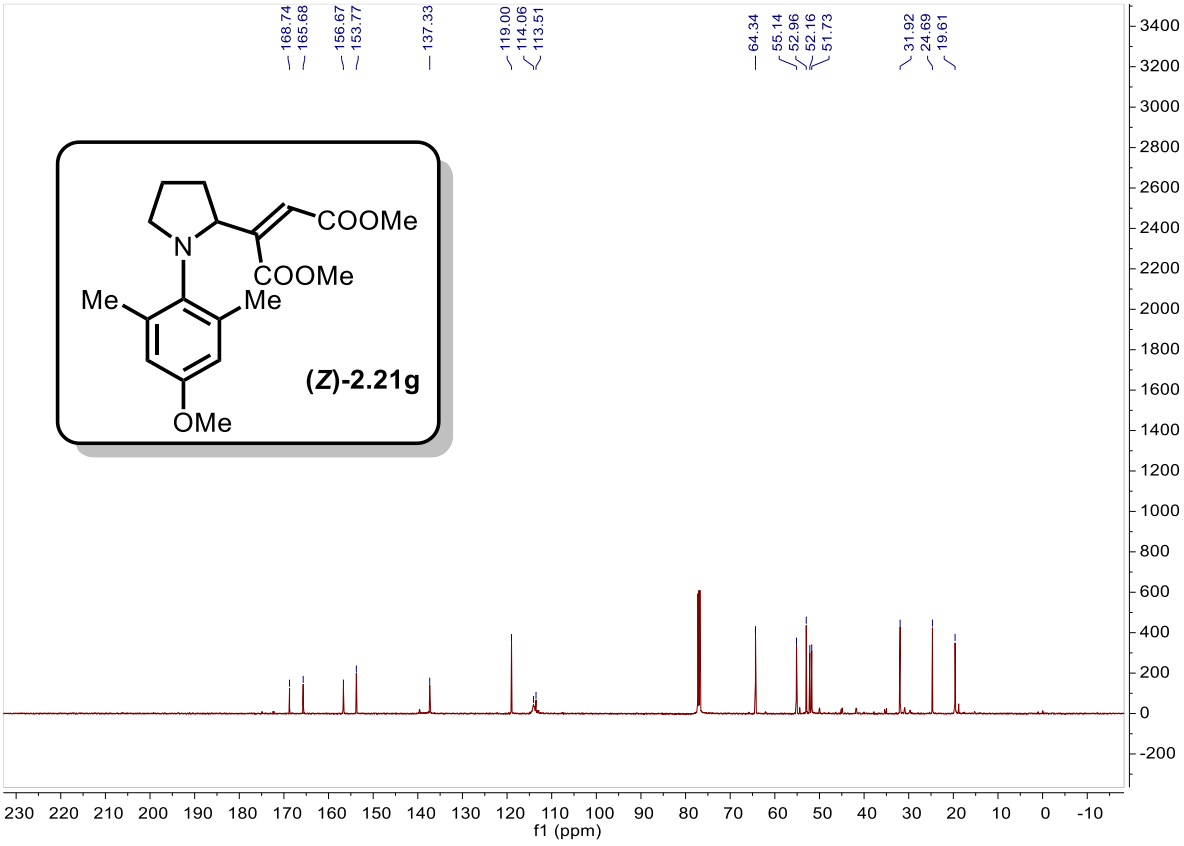
COOMe
COOMe
Me
Me
OMe
(Z)-2.21g
f1 (ppm)

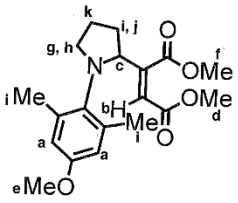

(*Z*)-2.21g

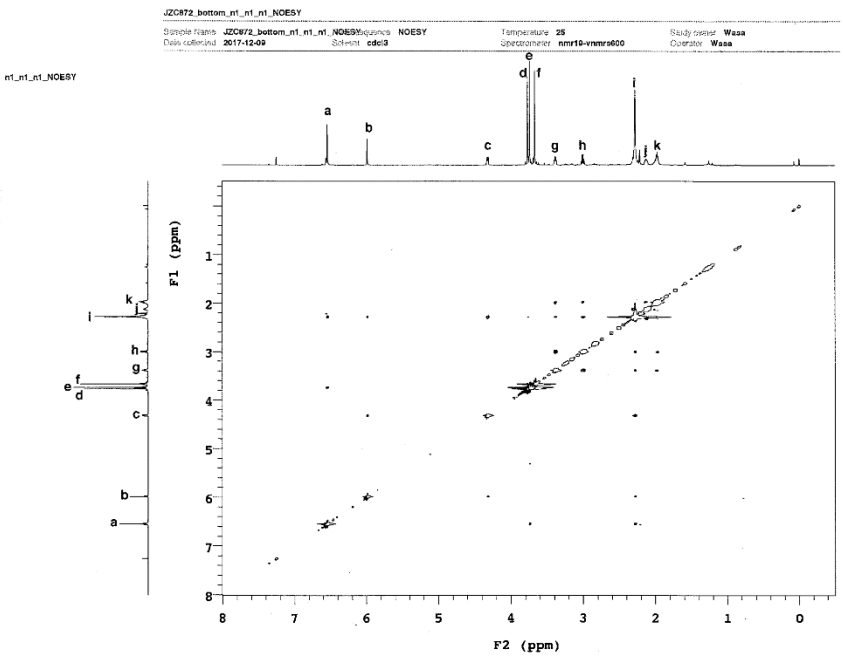
JZC872_bottom_n1_n1_n1_NOESY
F1 (ppm)
F2 (ppm)

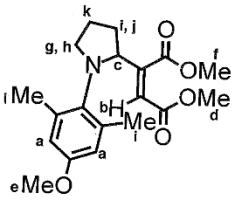

(*Z*)-2.21g

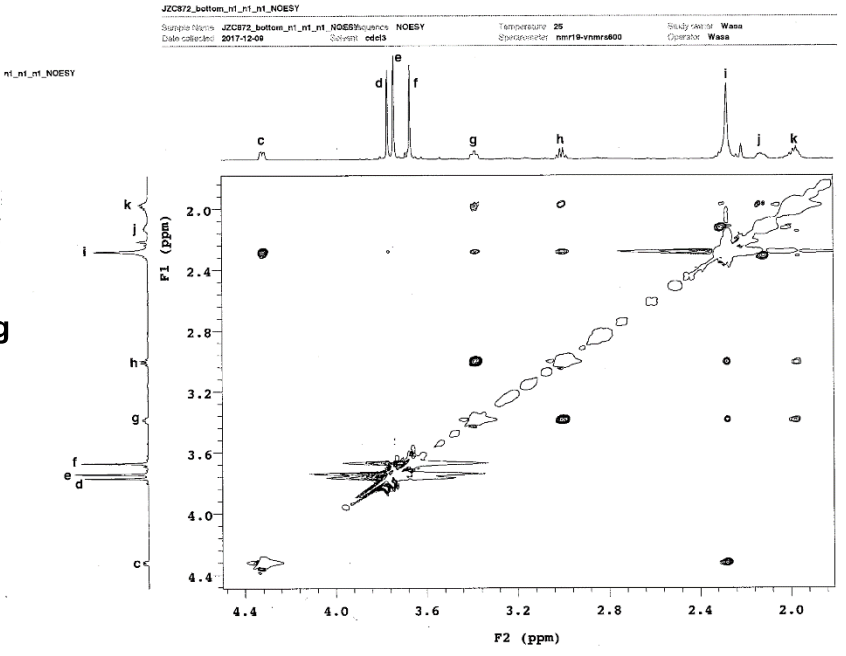
JZC872_bottom_n1_n1_n1_NOESY
F1 (ppm)
F2 (ppm)

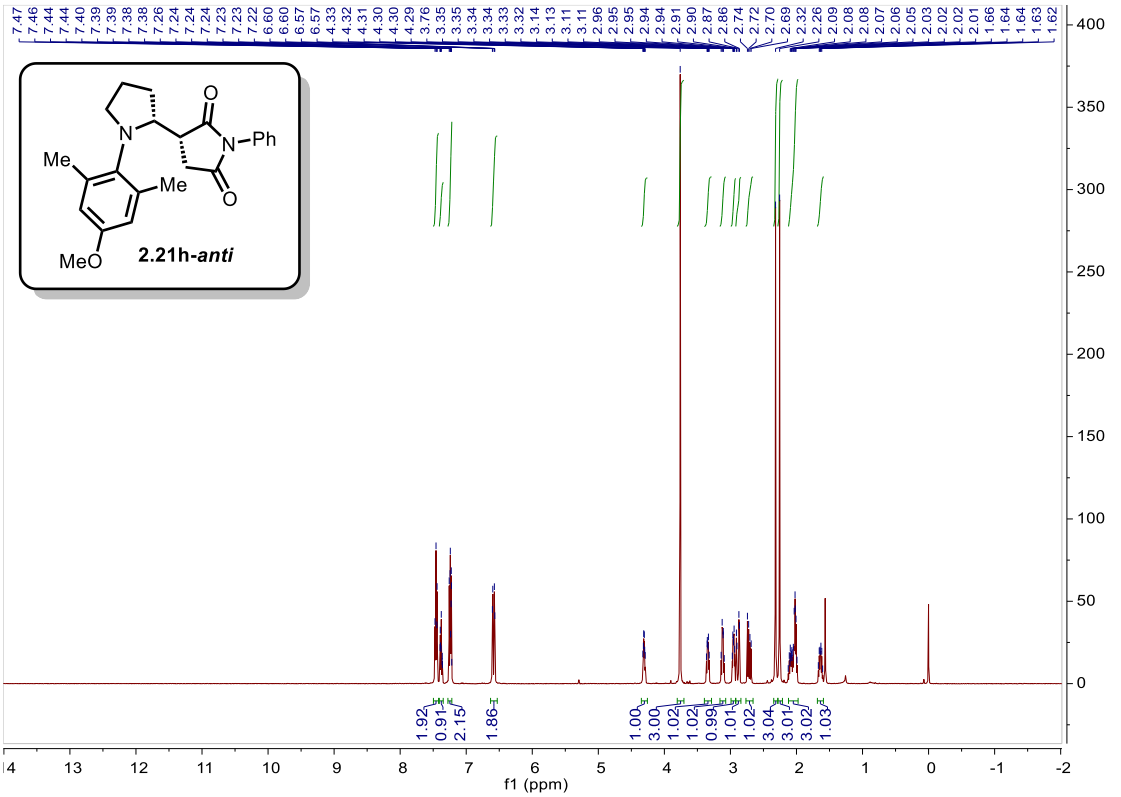
2.21h-anti
f1 (ppm)

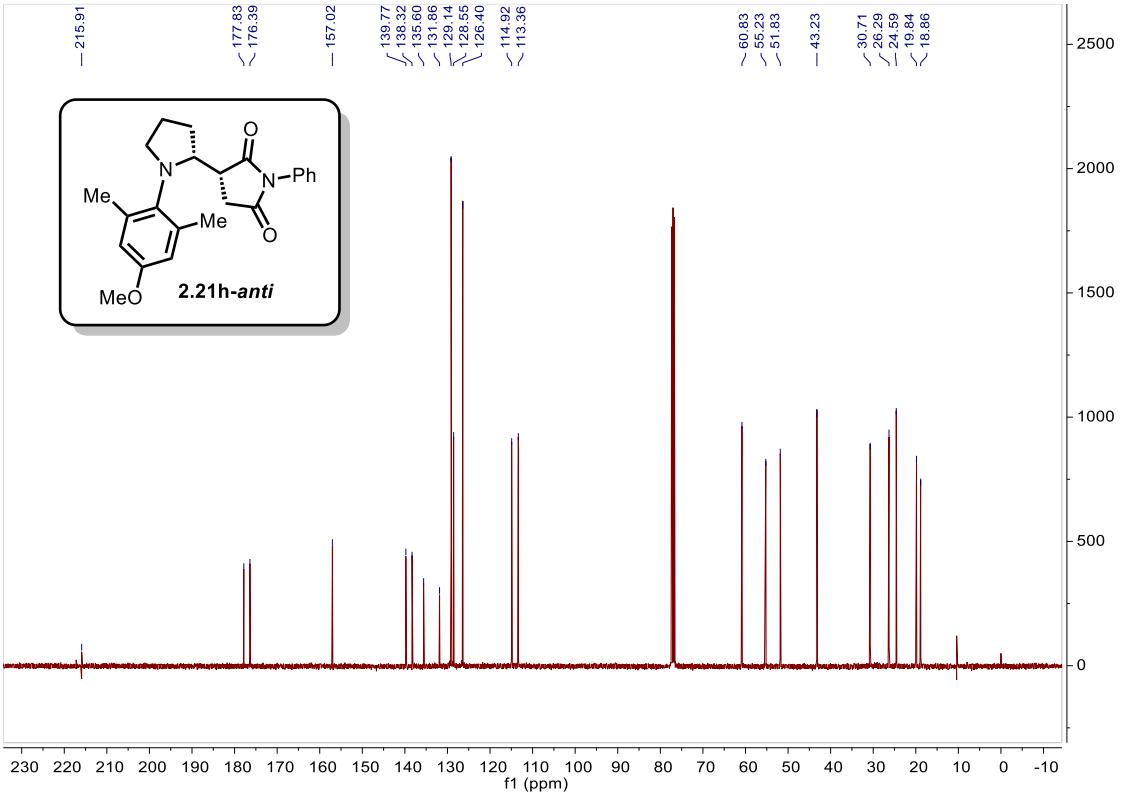
2.21h-anti
f1 (ppm)

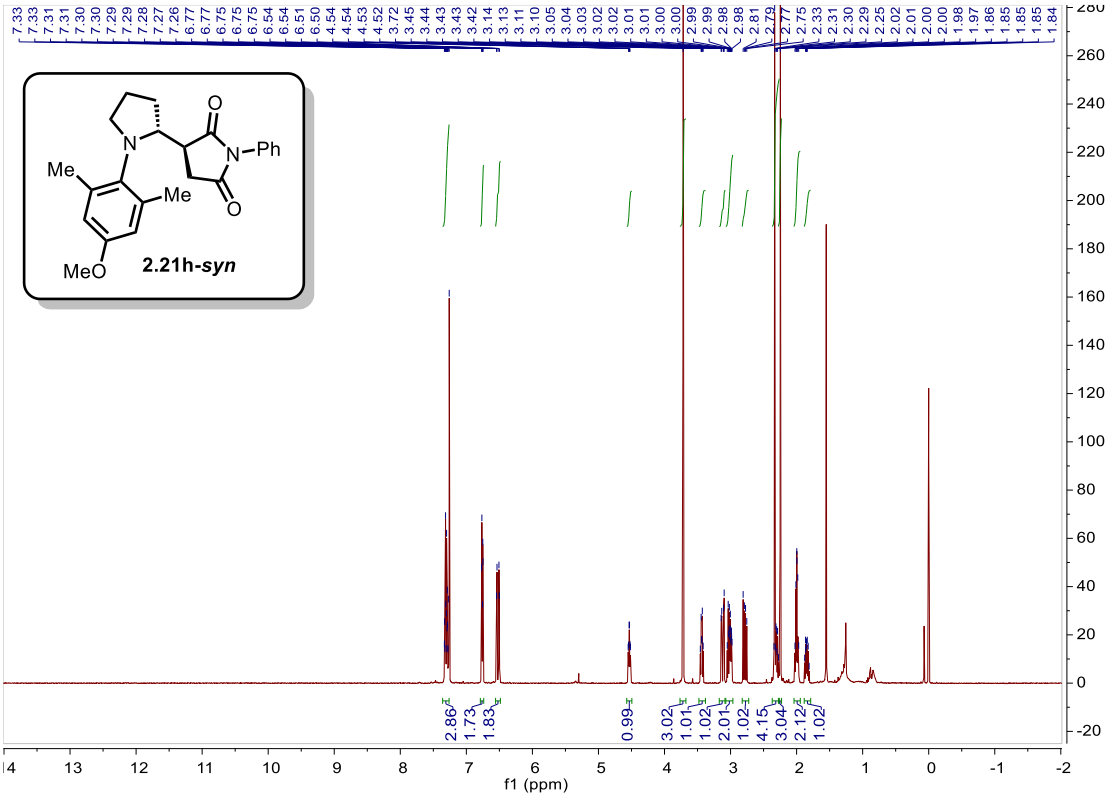
Me
Me
MeO
N
O
N-Ph
O
2.21h-syn
f1 (ppm)

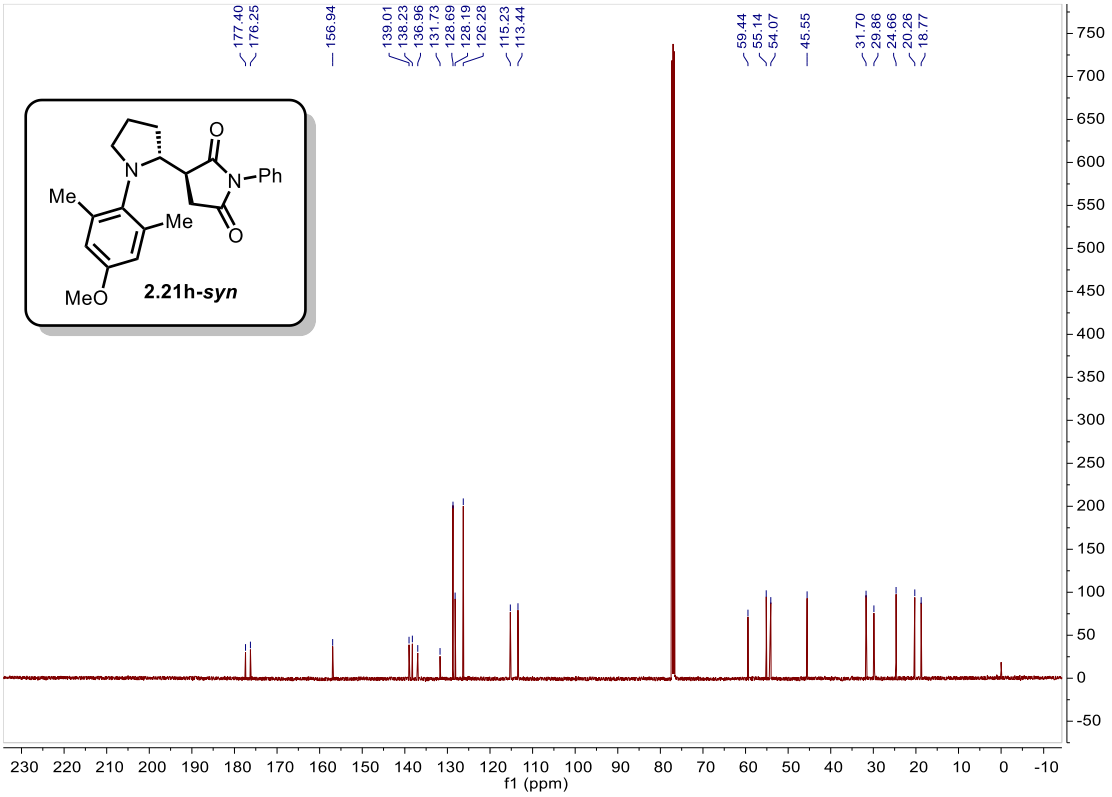
Me
Me
MeO
N
O
N-Ph
O
2.21h-syn
f1 (ppm)

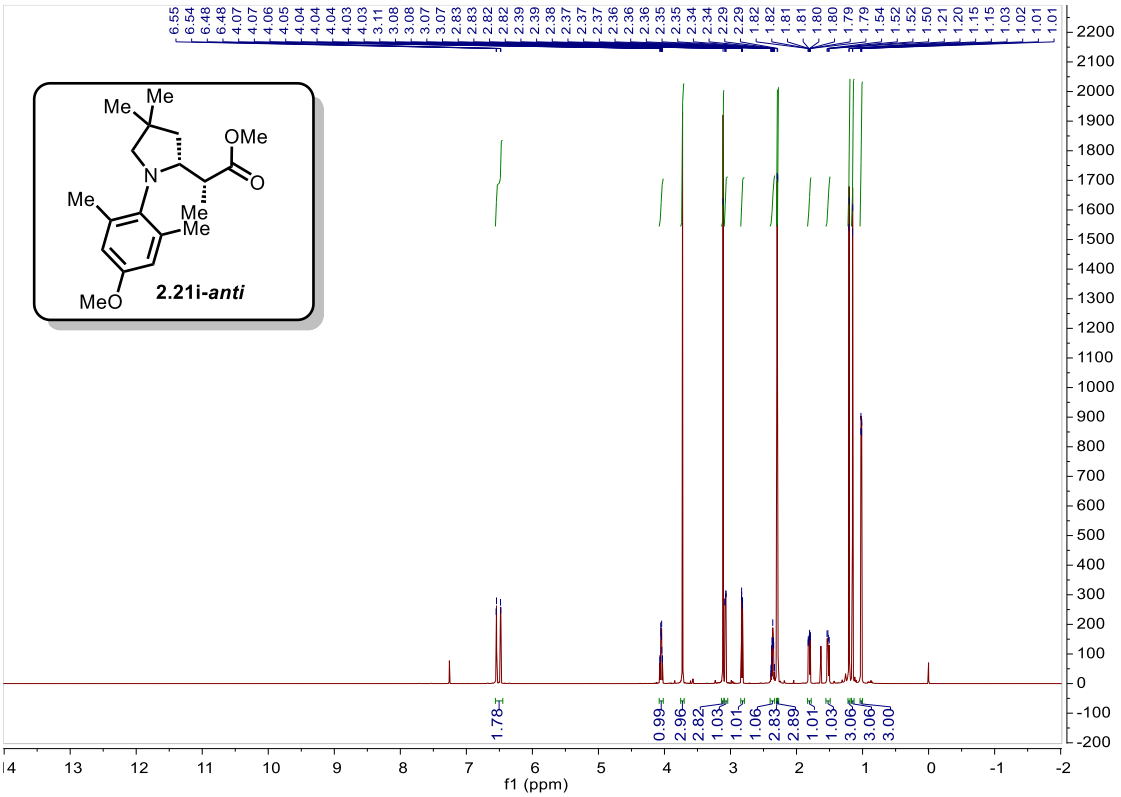
2.21i-anti
f1 (ppm)

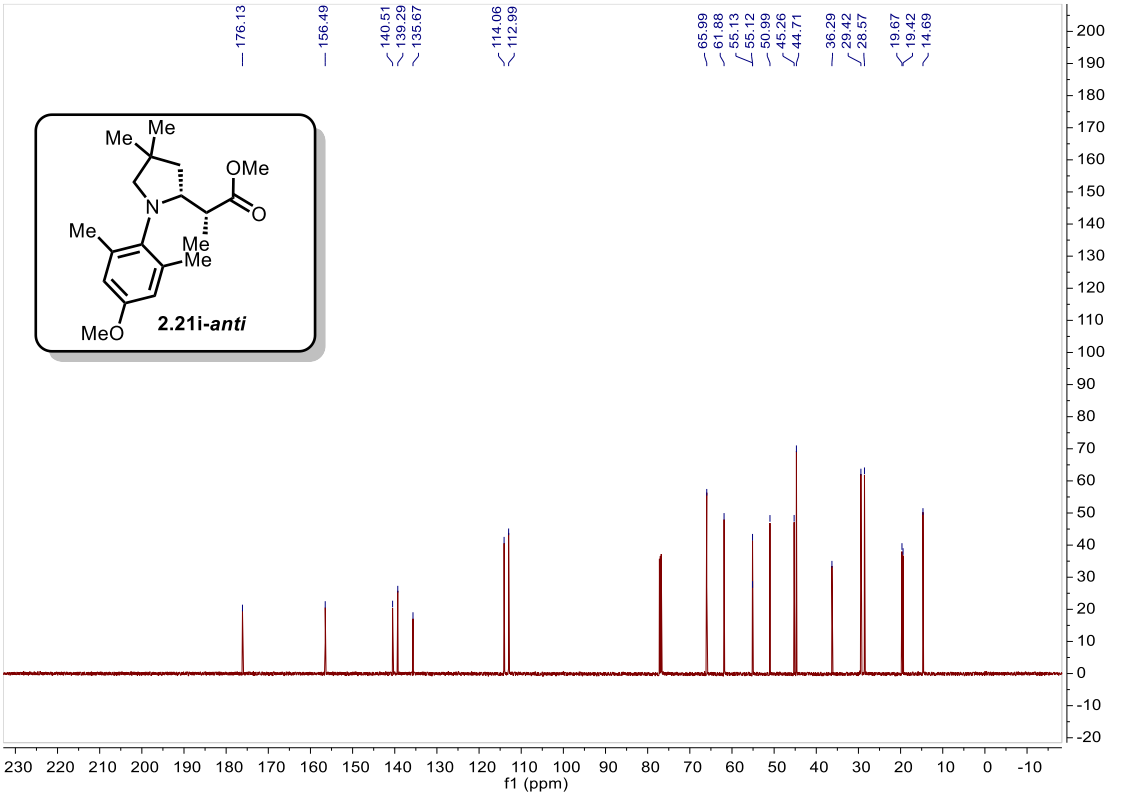
2.21i-anti
f1 (ppm)

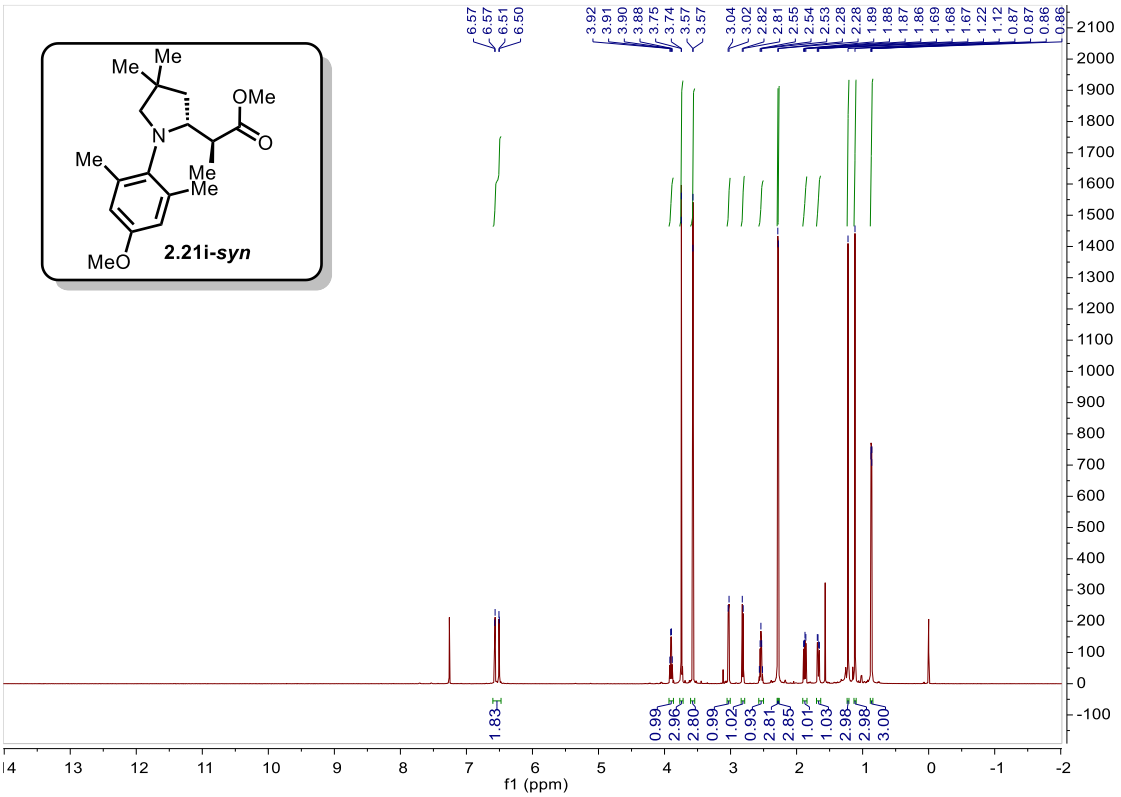
Me
Me
OMe
N
O
Me
Me
Me
MeO
2.21i-syn
6.57
6.57
6.51
6.50
3.92
3.91
3.90
3.88
3.75
3.74
3.57
3.57
3.04
3.02
2.82
2.81
2.55
2.54
2.53
2.28
2.28
1.89
1.88
1.87
1.86
1.69
1.68
1.67
1.22
1.12
0.87
0.87
0.86
0.86
1.83
0.99
2.96
2.80
0.99
1.02
0.93
2.81
2.85
1.01
1.03
2.98
2.98
3.00
f1 (ppm)

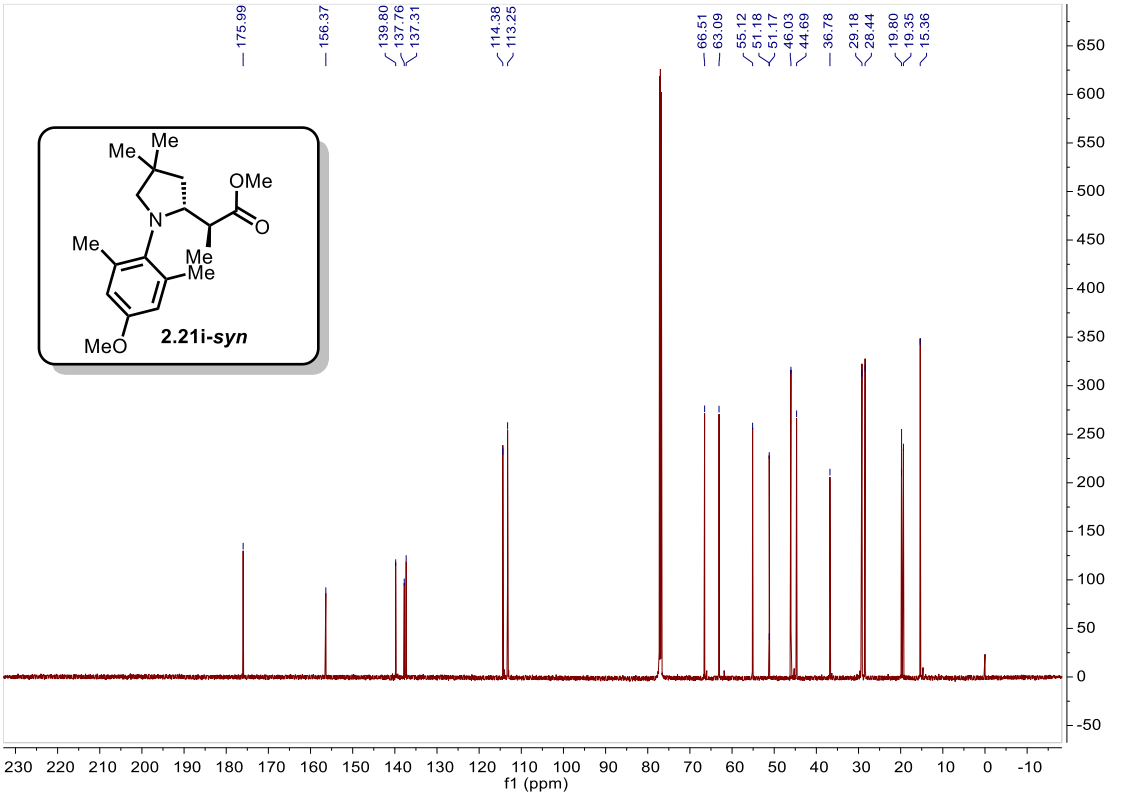
Me
Me
OMe
N
O
Me
Me
Me
MeO
2.21i-syn
175.99
156.37
139.80
137.76
137.31
114.38
113.25
66.51
63.09
55.12
51.18
51.17
46.03
44.69
36.78
29.18
28.44
19.80
19.35
15.36
f1 (ppm)

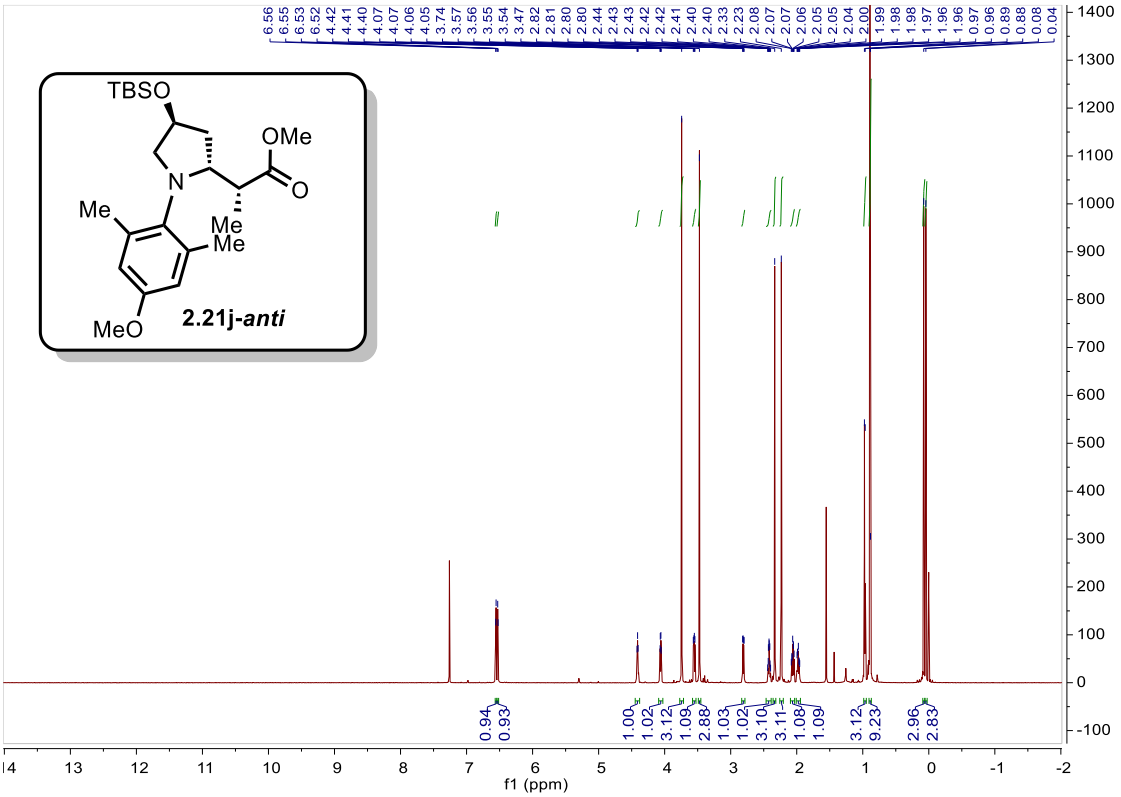
TBSO
OMe
N
O
Me
Me
Me
MeO
2.21j-anti
f1 (ppm)

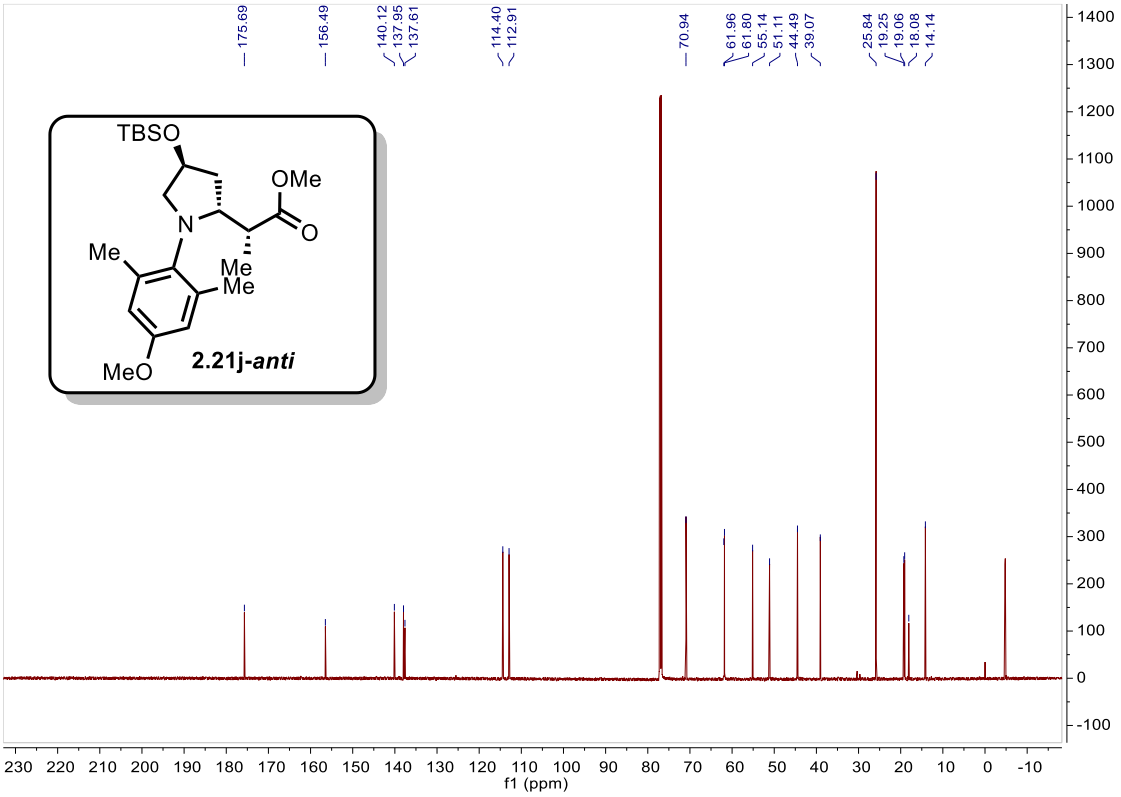
TBSO
OMe
N
O
Me
Me
Me
MeO
2.21j-anti
f1 (ppm)

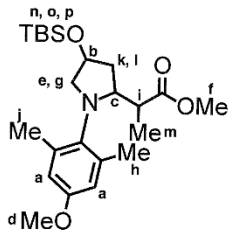

2.21j-*anti*

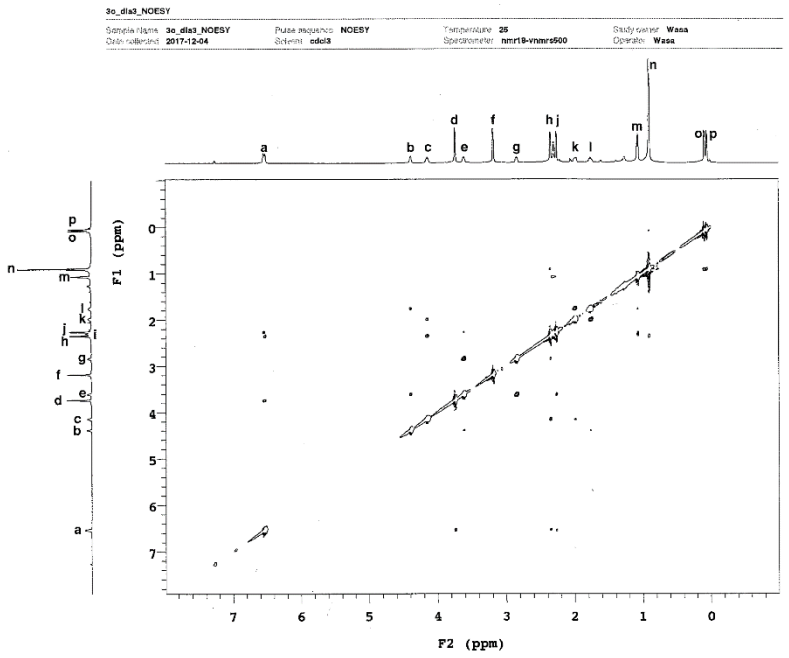

Data file /home/AIMWasa/Yeljin/3o_dia3_NOESY.fid

Plot date 2017-12-05

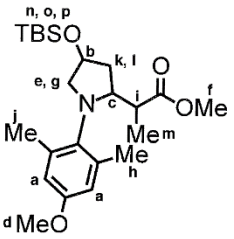

2.21j-*anti*

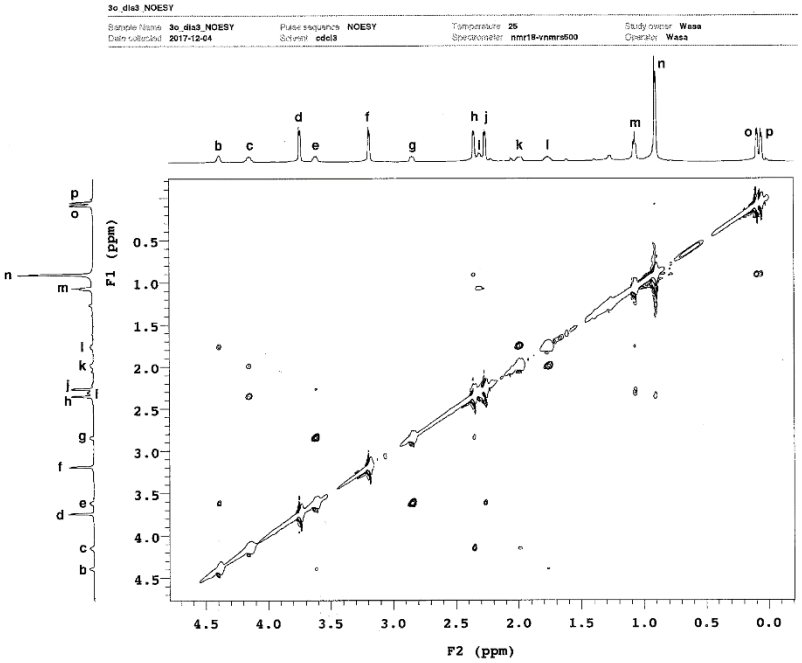

Data file /home/AIMWasa/Yeljin/3o_dia3_NOESY.fid

Plot date 2017-12-05

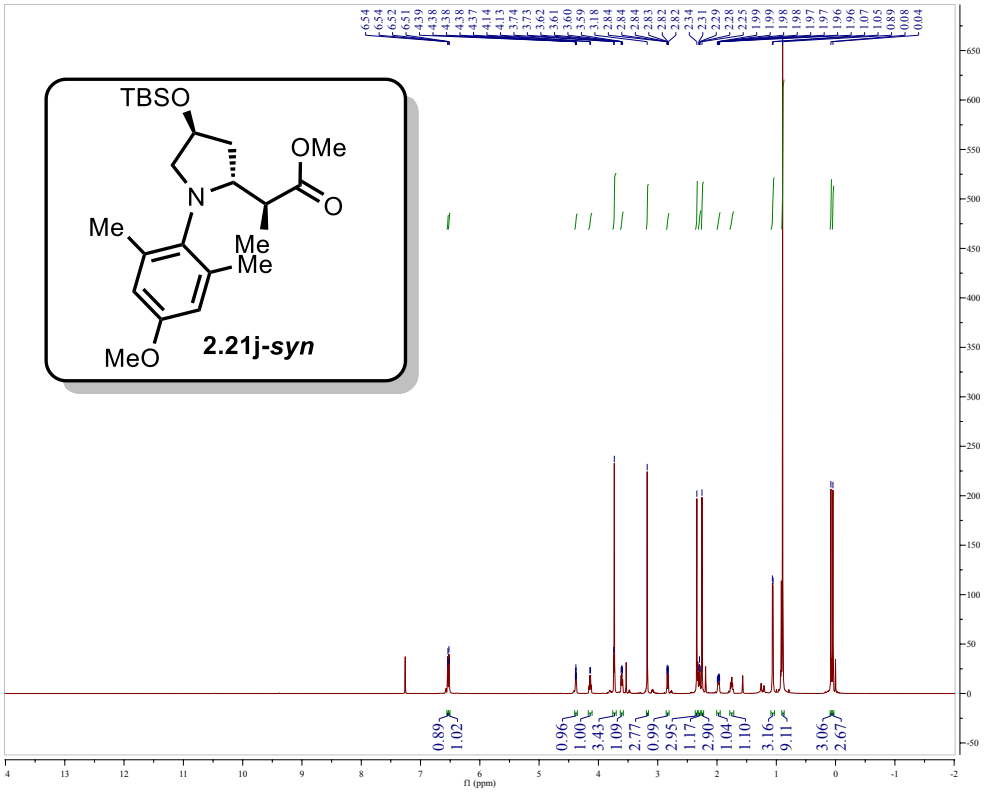
TBSO
OMe
N
O
Me
Me
Me
MeO
2.21j-syn

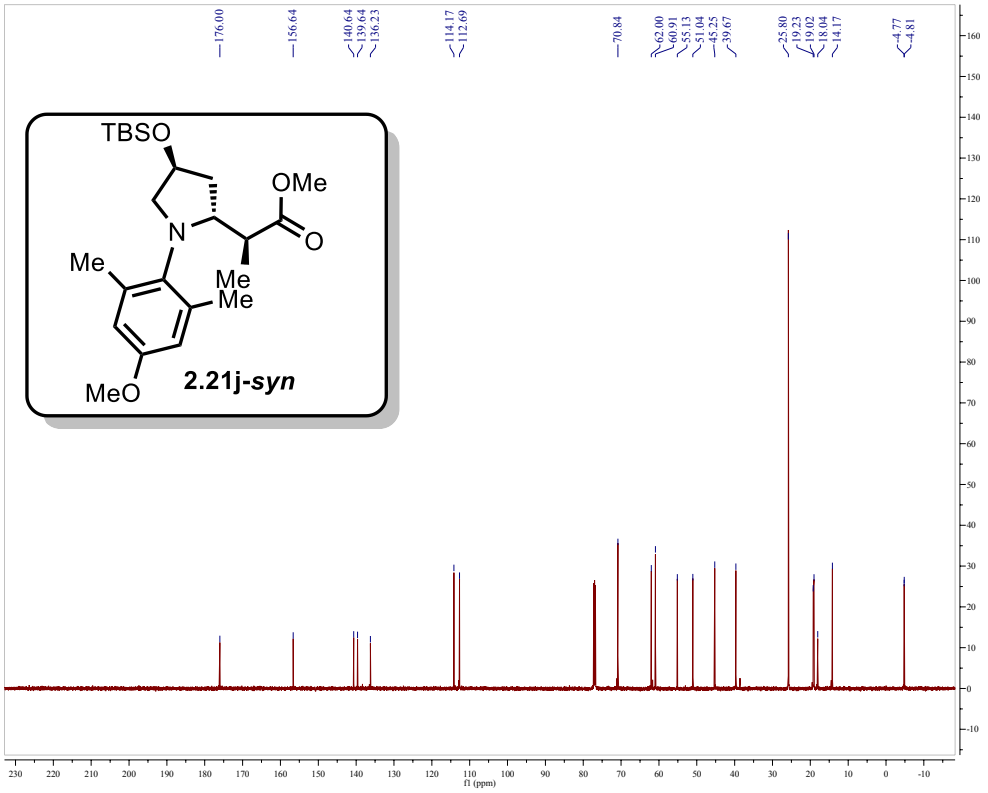
TBSO
OMe
N
O
Me
Me
Me
MeO
2.21j-syn

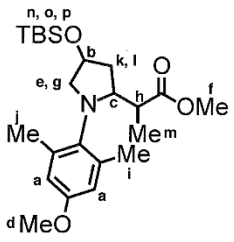

2.21j-*syn*

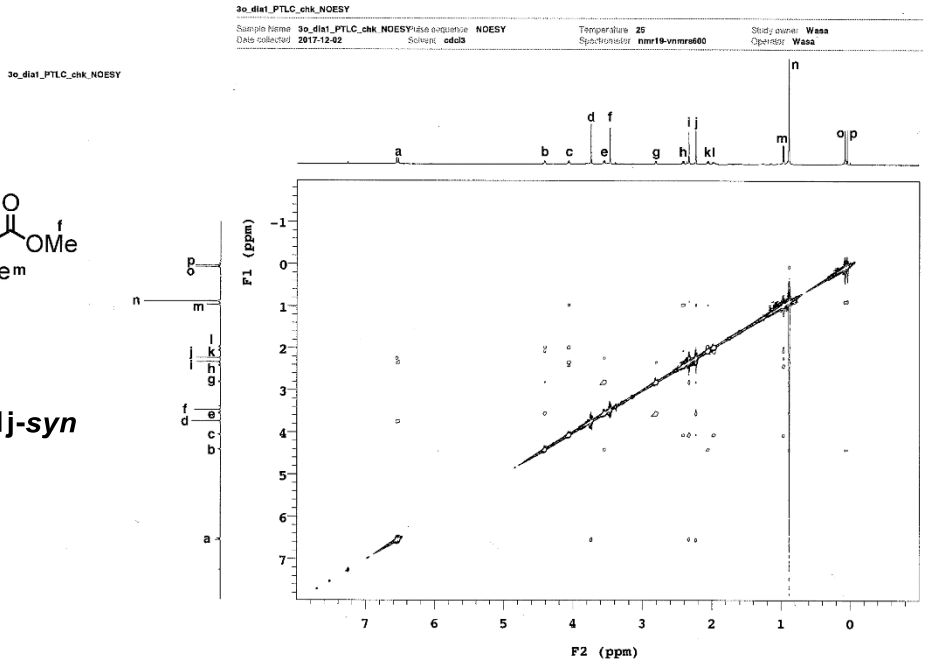

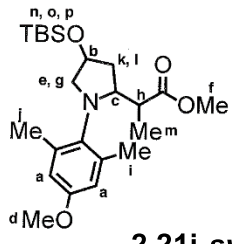

2.21j-*syn*

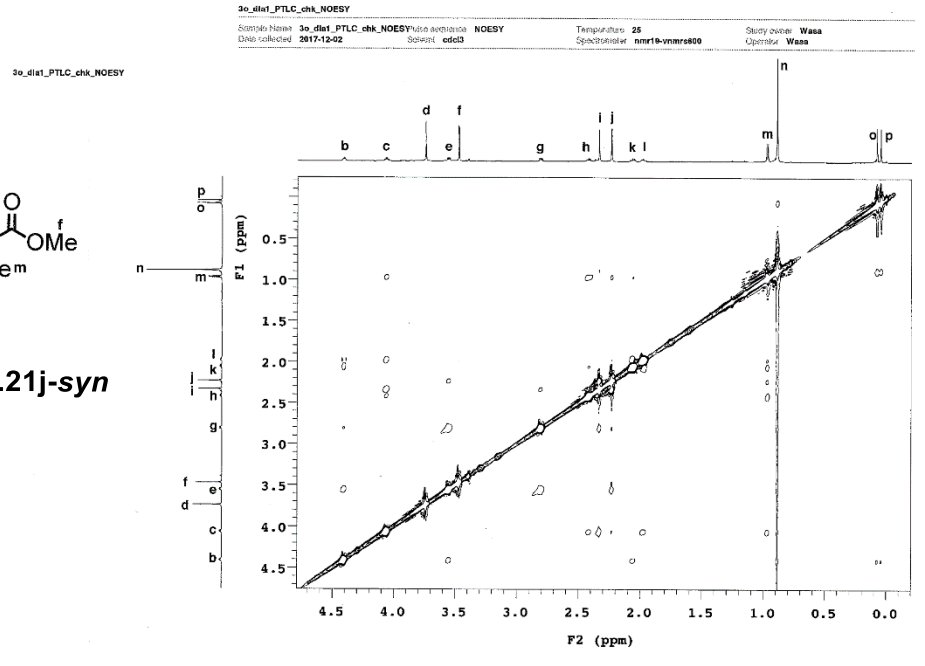

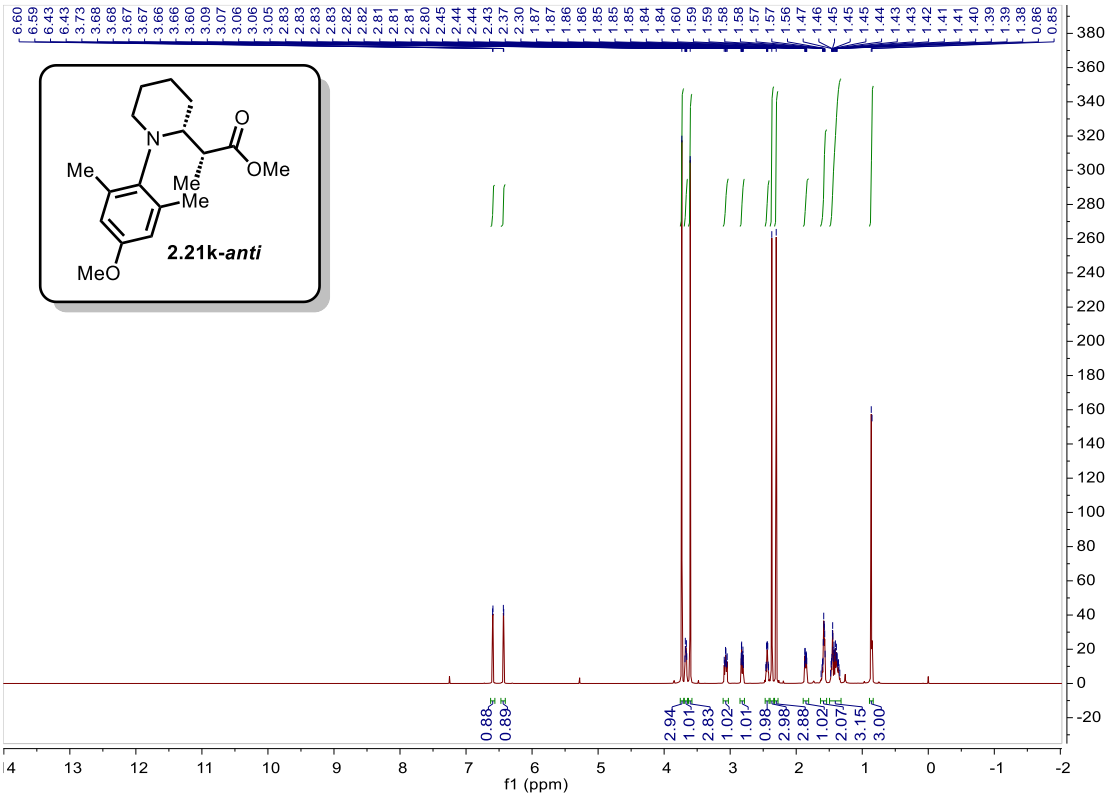
2.21k-anti
f1 (ppm)

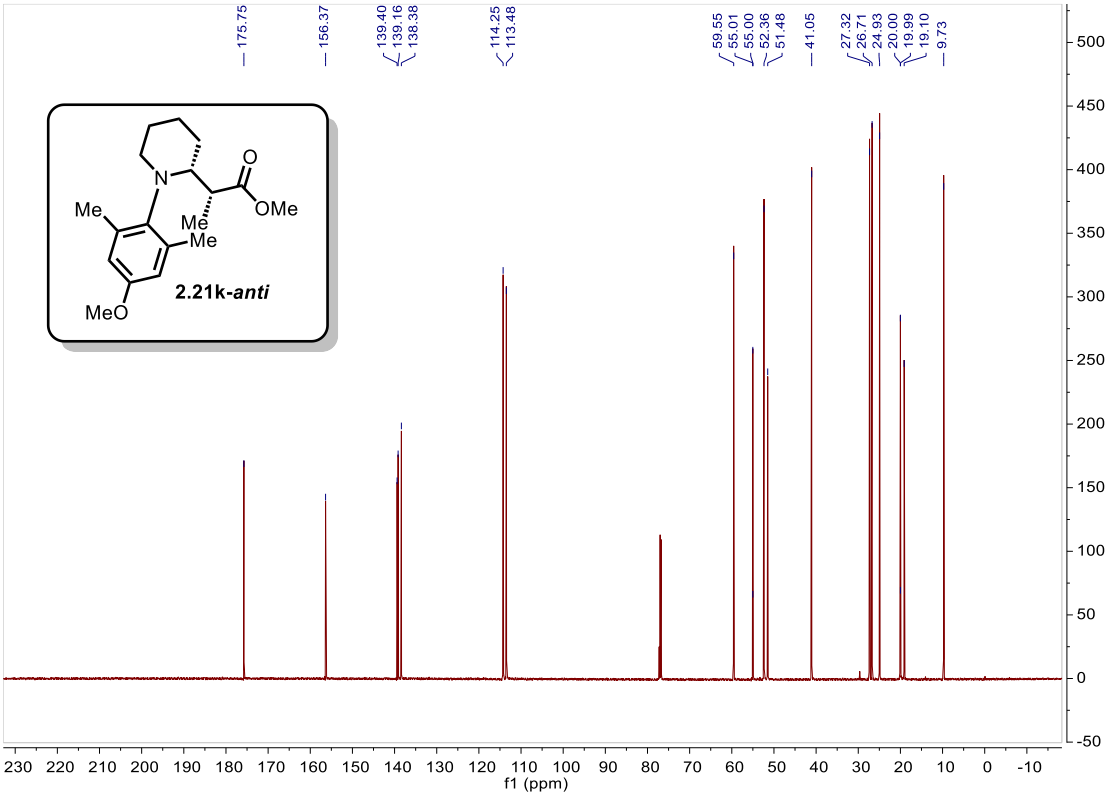
2.21k-anti
f1 (ppm)

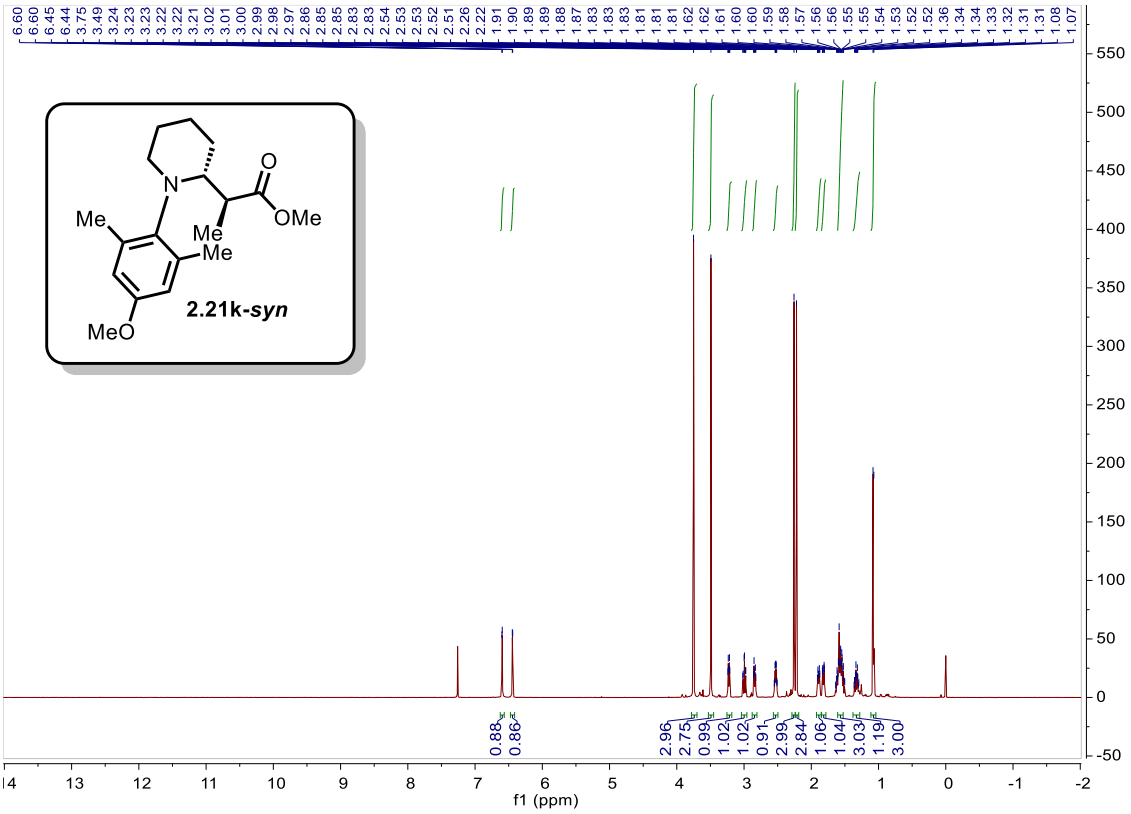
2.21k-syn
f1 (ppm)

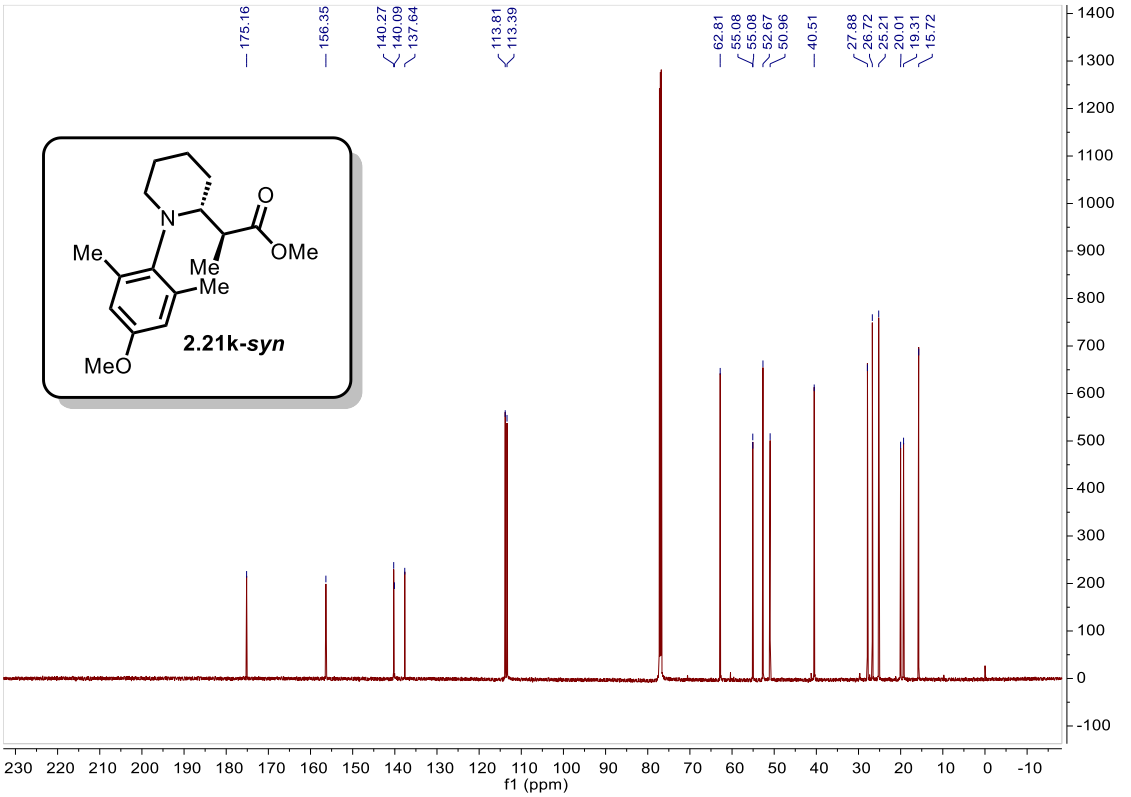
2.21k-syn
f1 (ppm)

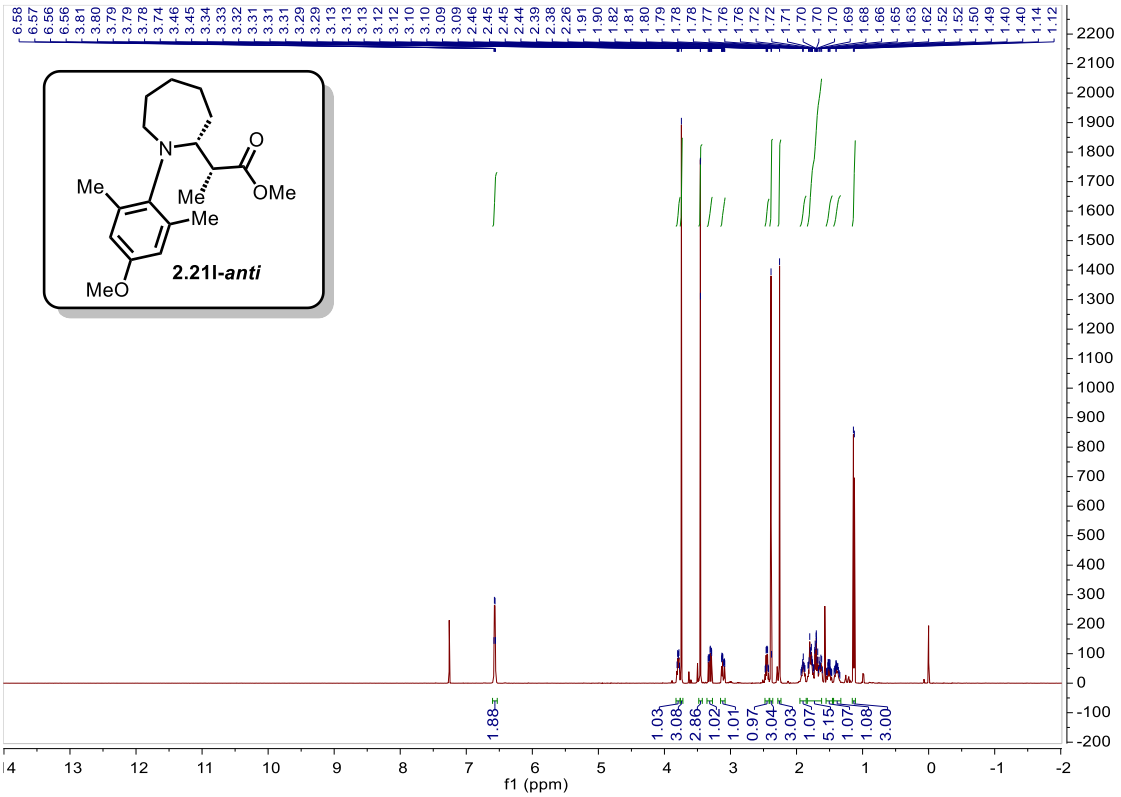
2.21l-*anti*
f1 (ppm)

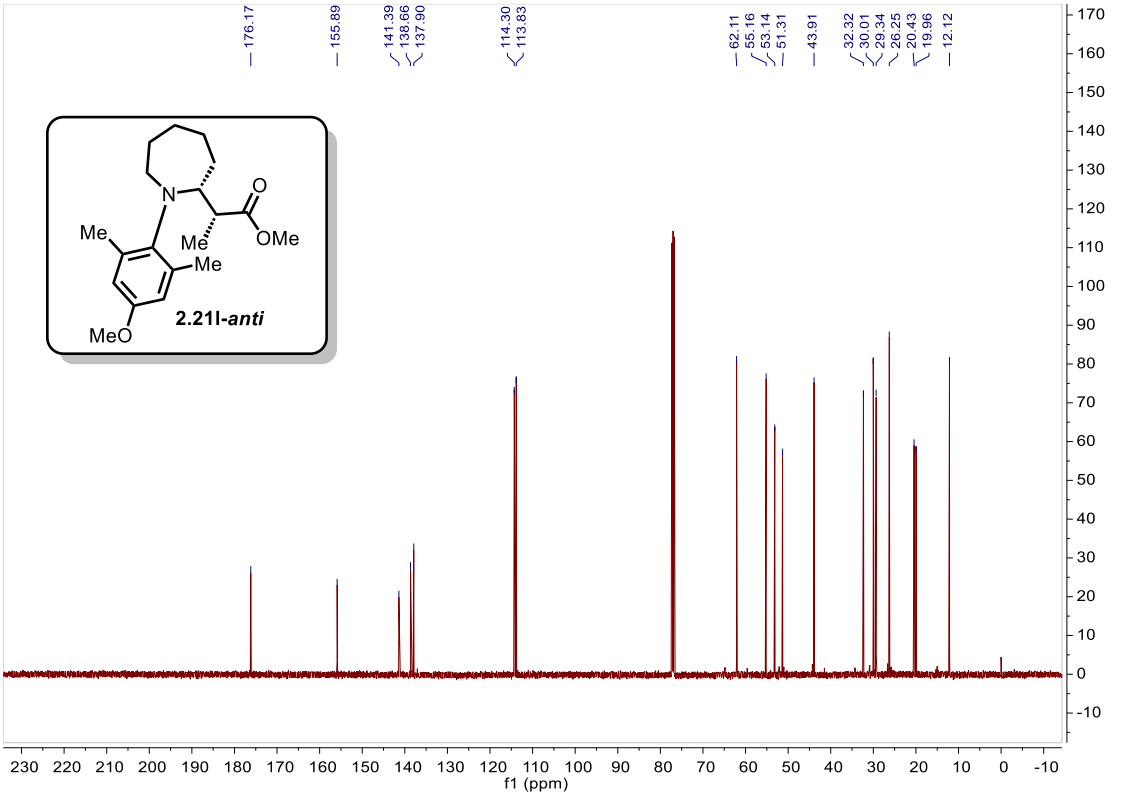
2.21l-*anti*
f1 (ppm)

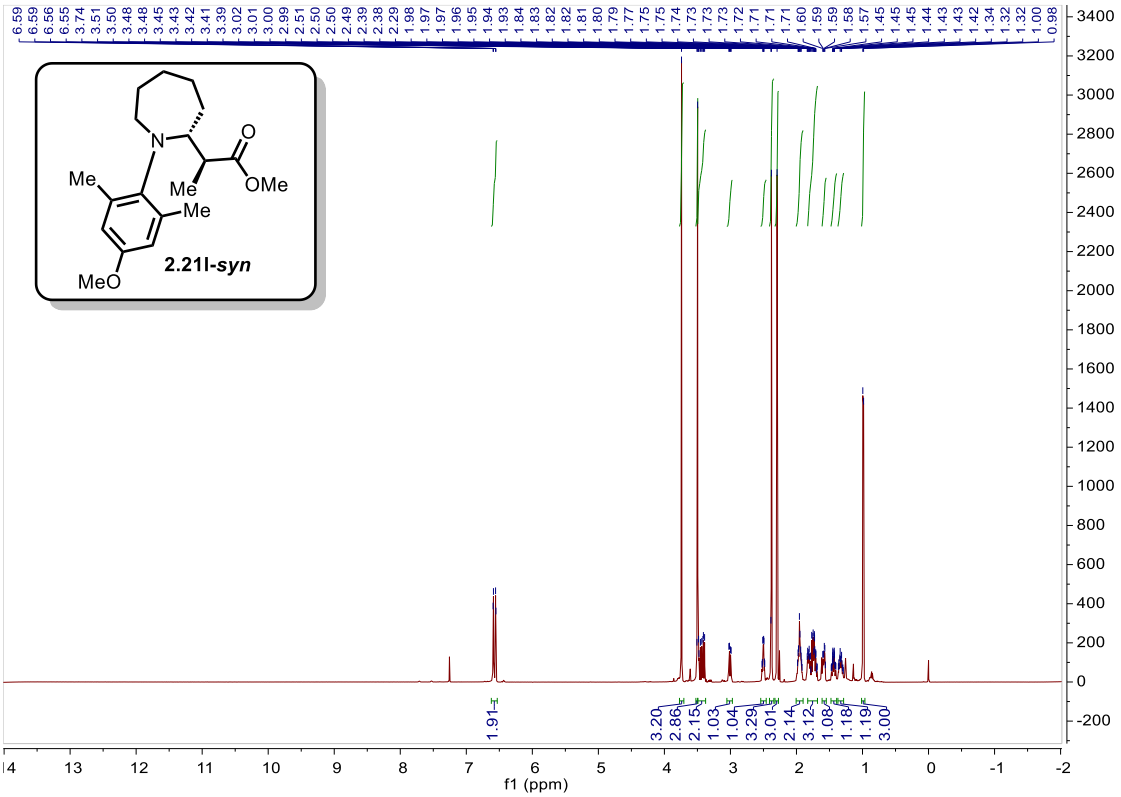
2.21l-syn
f1 (ppm)

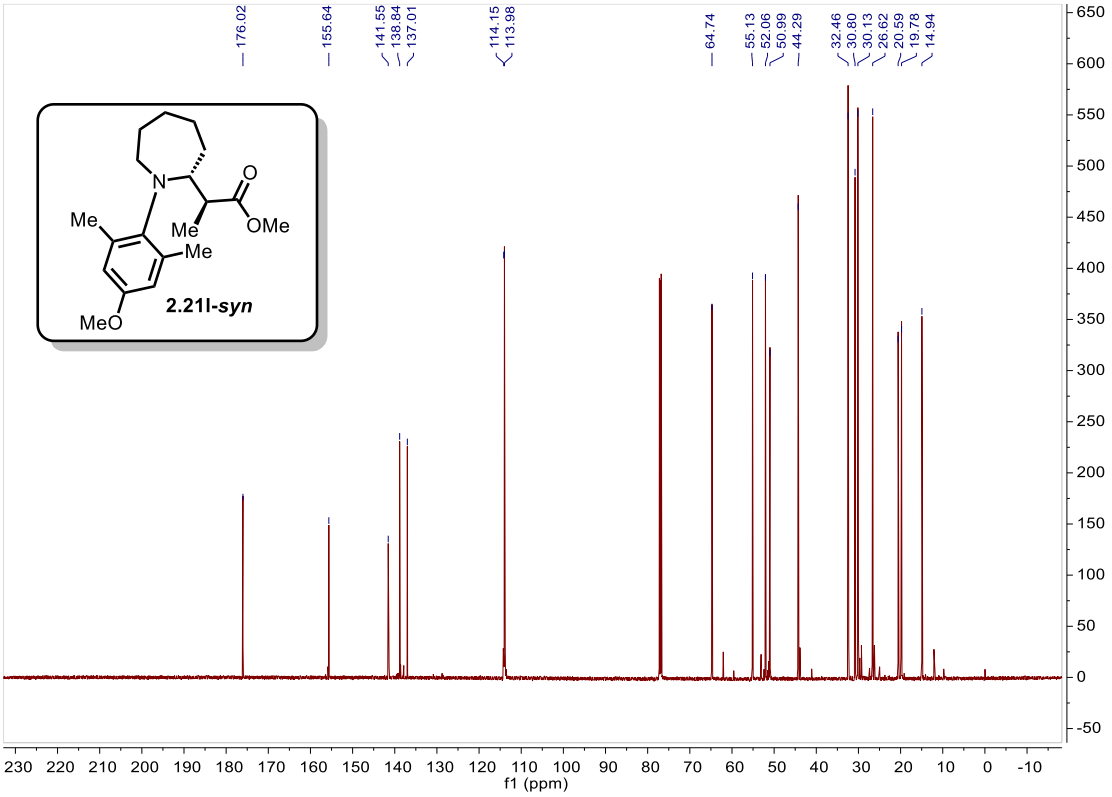
2.21l-syn
f1 (ppm)

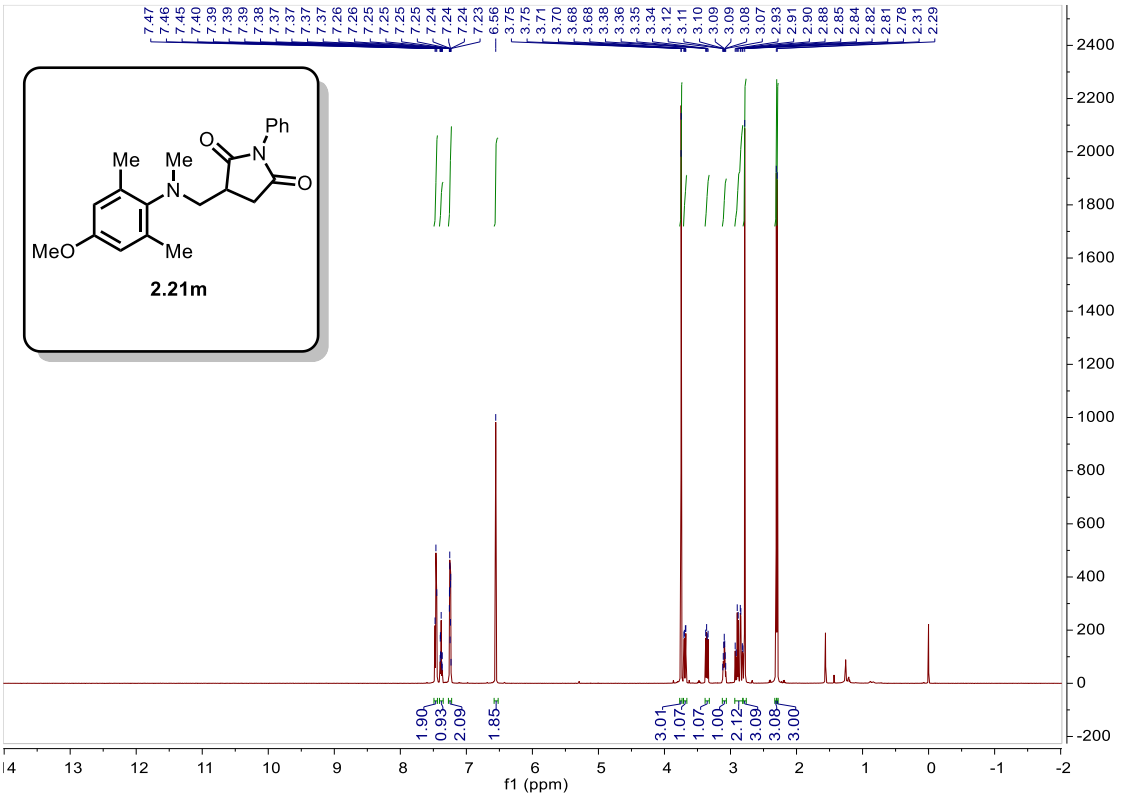
7.47 7.46 7.45 7.40 7.39 7.39 7.39 7.38 7.37 7.37 7.37 7.37 7.26 7.26 7.25 7.25 7.25 7.25 7.24 7.24 7.24 7.23 6.56
3.75 3.75 3.71 3.70 3.68 3.68 3.38 3.36 3.35 3.34 3.12 3.11 3.10 3.09 3.09 3.08 3.07 2.93 2.91 2.90 2.88 2.85 2.84 2.82 2.81 2.78 2.31 2.29
Ph
O
N
O
Me
Me
N
MeO
Me
2.21m
1.90 0.93 2.09 1.85 3.01 1.07 1.07 1.00 2.12 3.09 3.08 3.00
f1 (ppm)

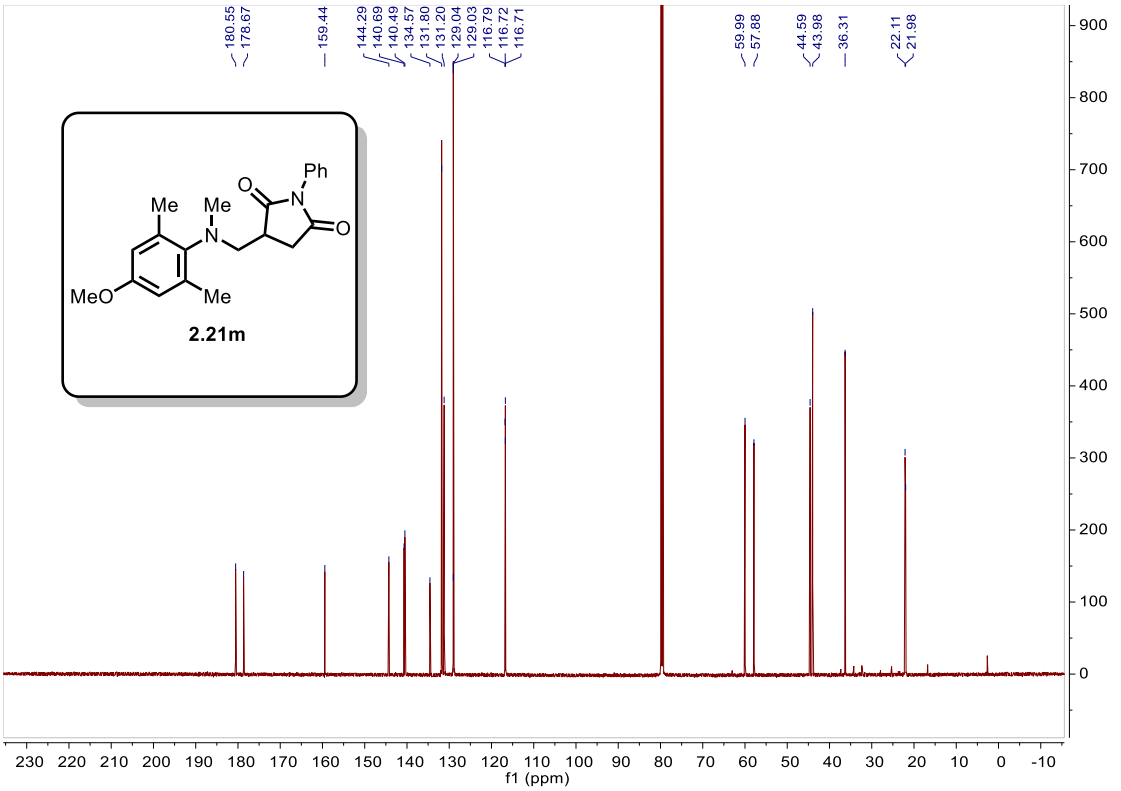
180.55 178.67 159.44 144.29 140.69 140.49 134.57 131.80 131.20 129.04 129.03 116.79 116.72 116.71
59.99 57.88 44.59 43.98 36.31 22.11 21.98
Ph
O
N
O
Me
Me
N
MeO
Me
2.21m
f1 (ppm)

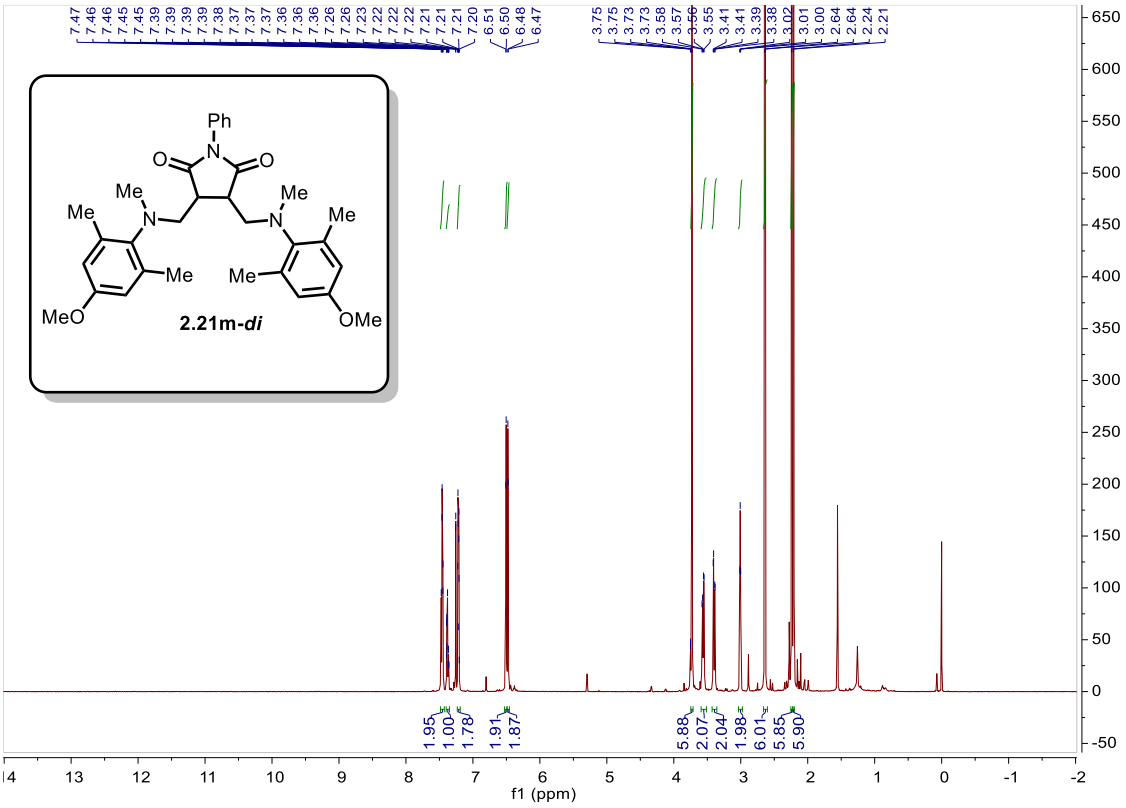
7.47 7.46 7.46 7.45 7.45 7.39 7.39 7.39 7.39 7.38 7.37 7.37 7.37 7.36 7.36 7.36 7.26 7.23 7.22 7.22 7.21 7.21 7.21 7.20 6.51 6.50 6.48 6.47
3.75 3.75 3.73 3.73 3.58 3.57 3.56 3.55 3.41 3.41 3.39 3.38 3.02 3.01 3.00 2.64 2.64 2.24 2.21
Ph
N
O
O
Me
Me
N
N
Me
Me
Me
Me
MeO
OMe
2.21m-di
1.95 1.00 1.78 1.91 1.87 5.88 2.07 2.04 1.98 6.01 5.85 5.90
f1 (ppm)

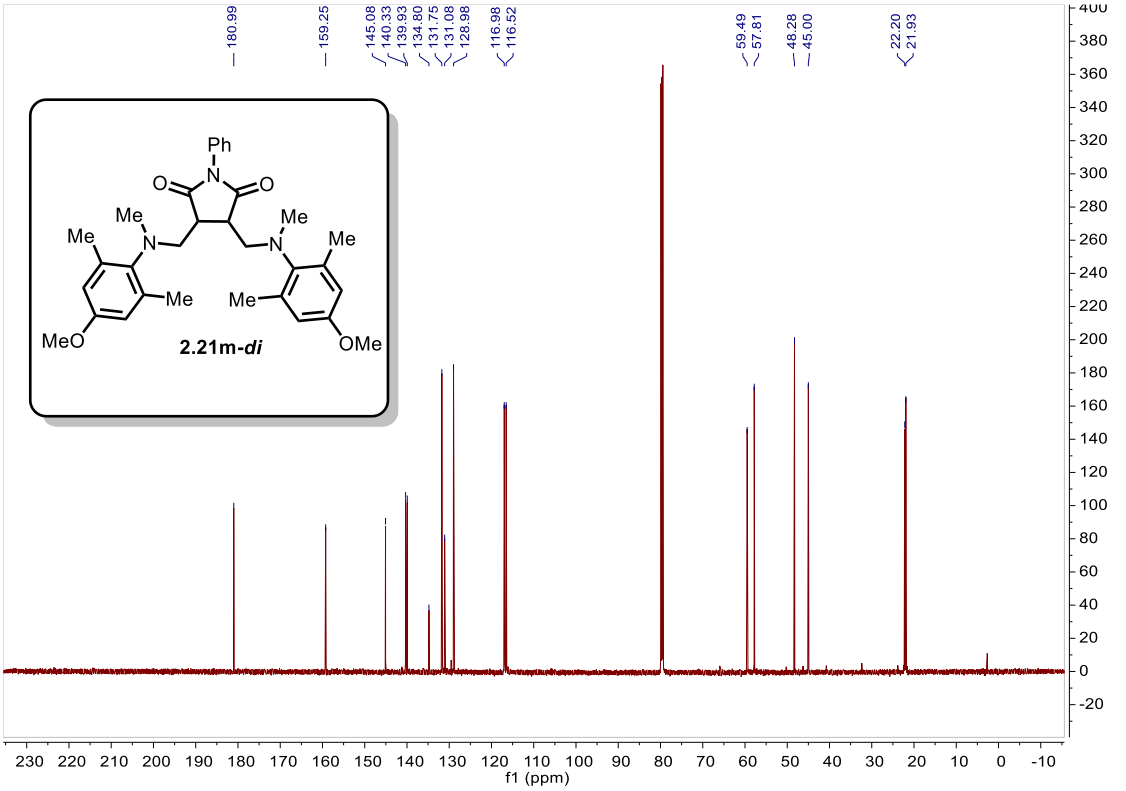
180.99 159.25 145.08 140.33 139.93 134.80 131.75 131.08 128.98 116.98 116.52 59.49 57.81 48.28 45.00 22.20 21.93
Ph
N
O
O
Me
Me
N
N
Me
Me
Me
Me
MeO
OMe
2.21m-di
f1 (ppm)

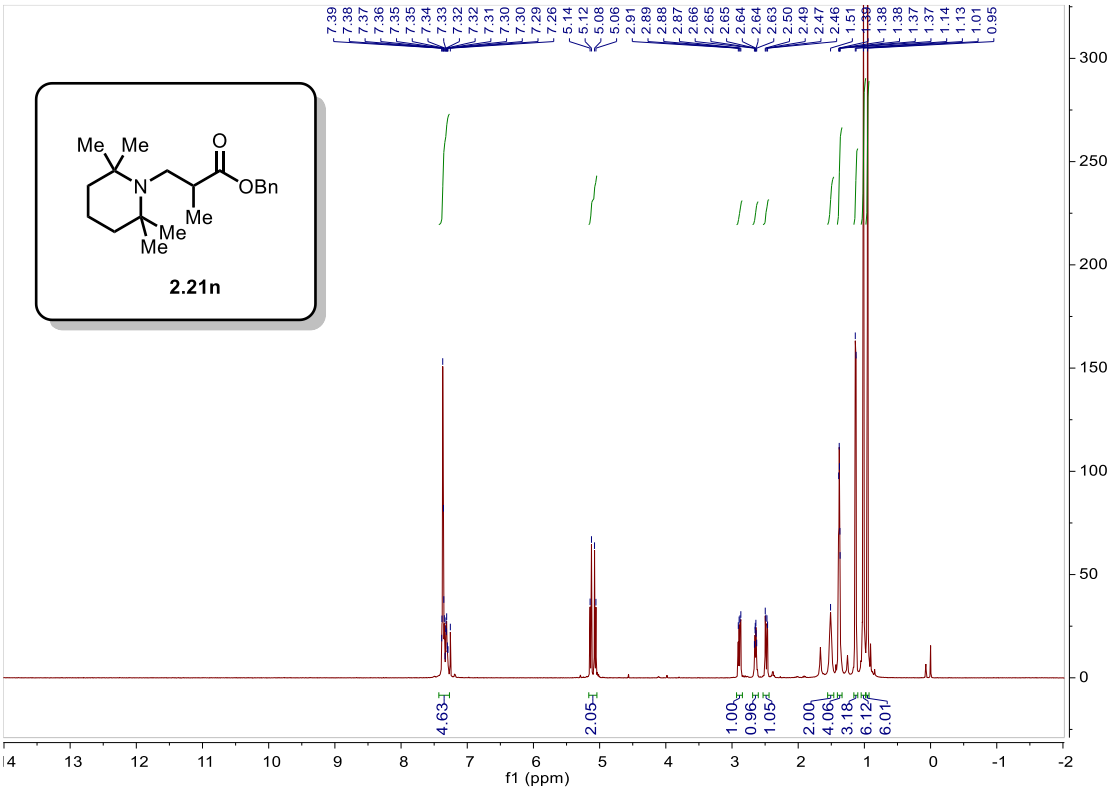
Me Me
O
N
OBn
Me
Me
Me
2.21n
f1 (ppm)

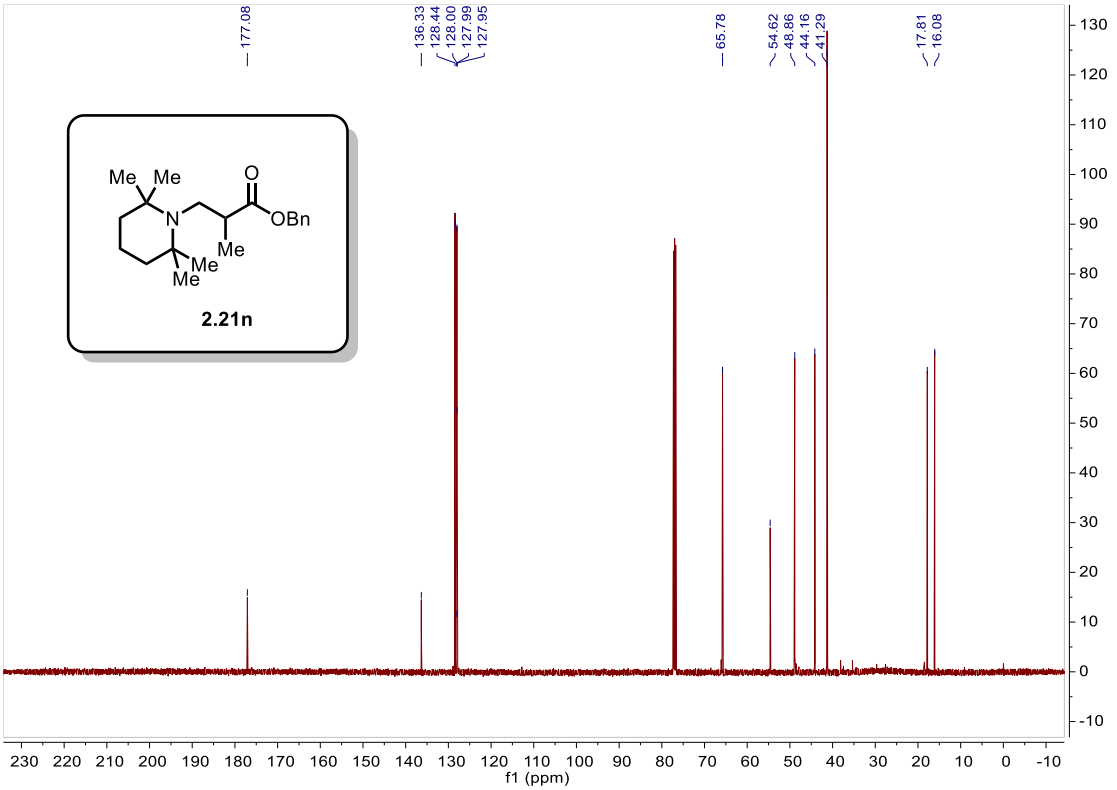
Me Me
O
N
OBn
Me
Me
Me
2.21n
f1 (ppm)

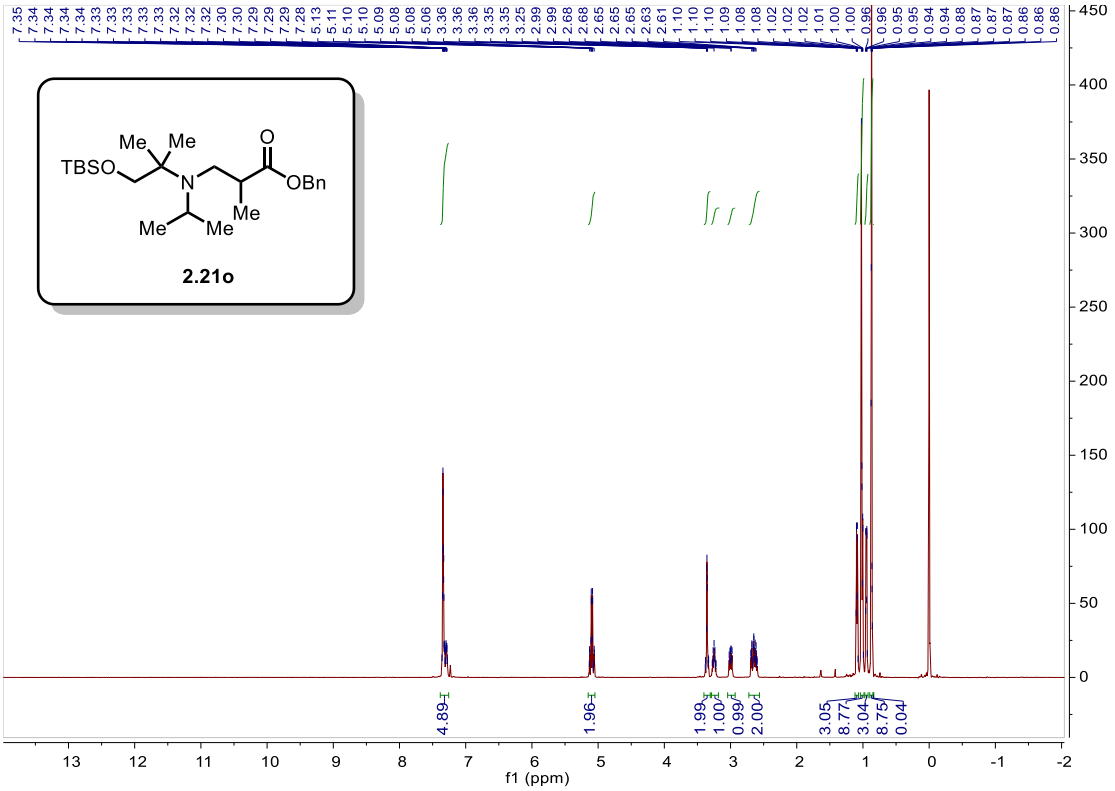
Me
Me
O
TBSO
N
OBn
Me
Me
Me
2.21o
f1 (ppm)

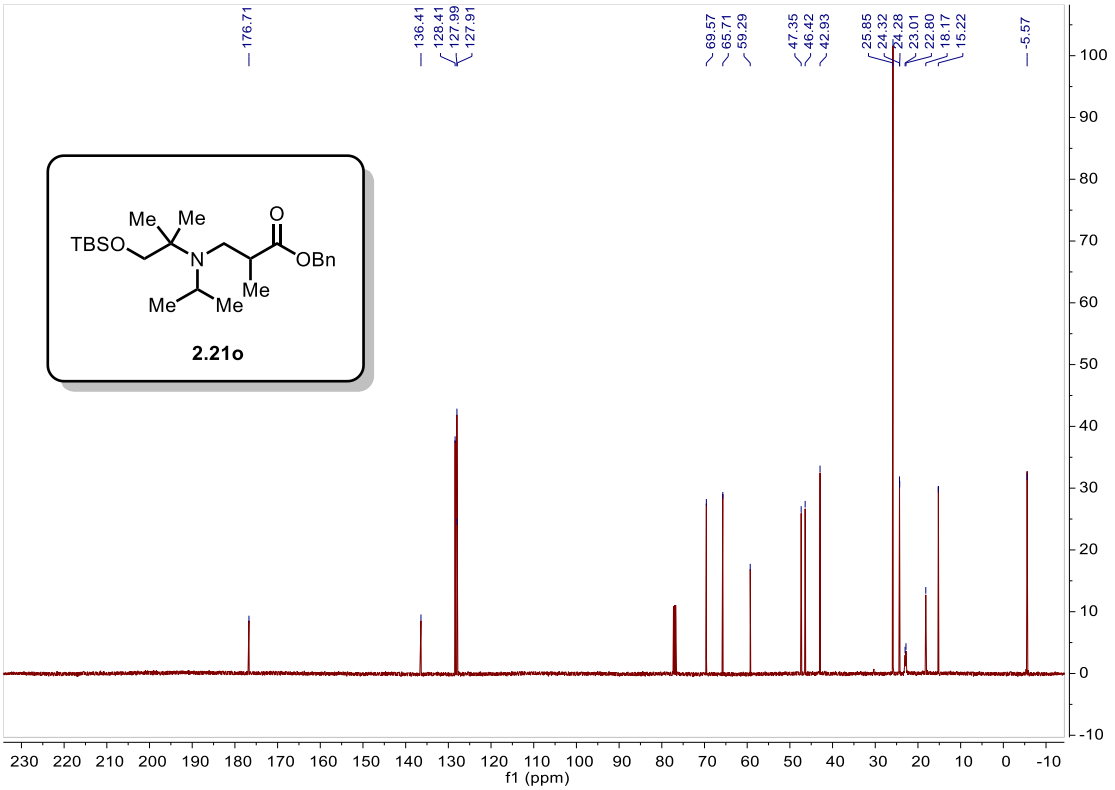
Me
Me
O
TBSO
N
OBn
Me
Me
Me
2.21o
f1 (ppm)

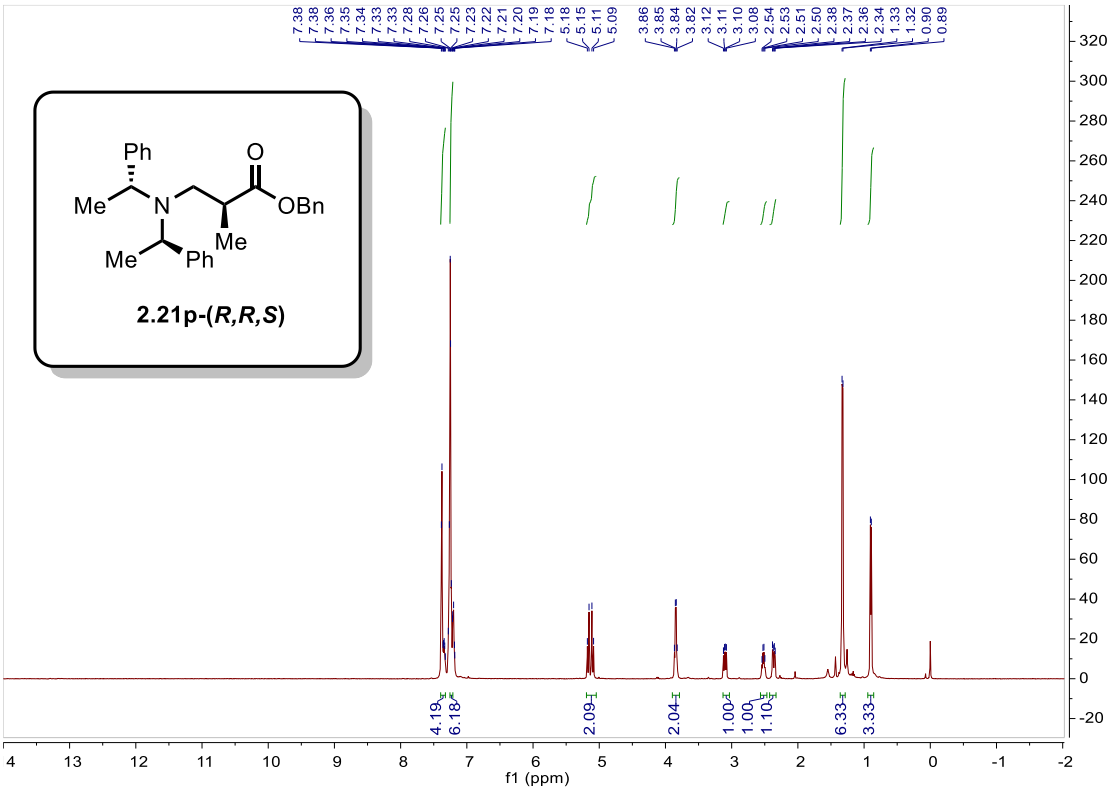
Ph
O
Me
N
OBn
Me
Me
Ph
2.21p-(R,R,S)
f1 (ppm)

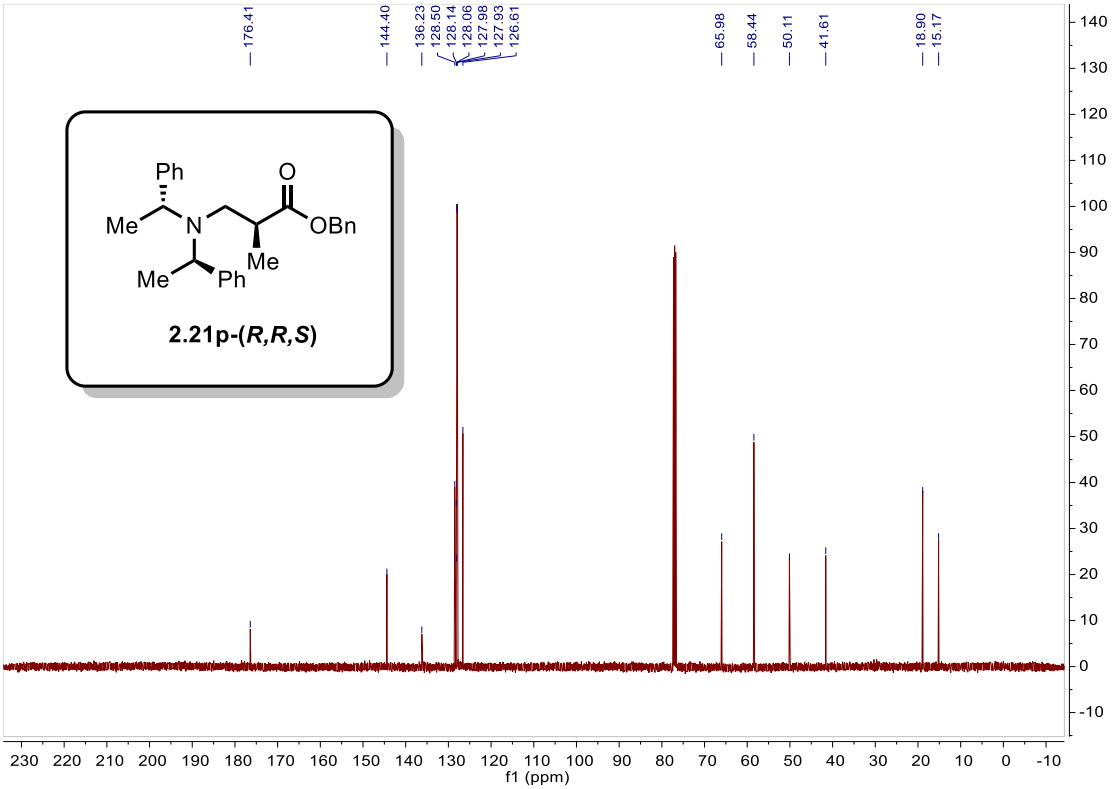
Ph
O
Me
N
OBn
Me
Me
Ph
2.21p-(R,R,S)
f1 (ppm)

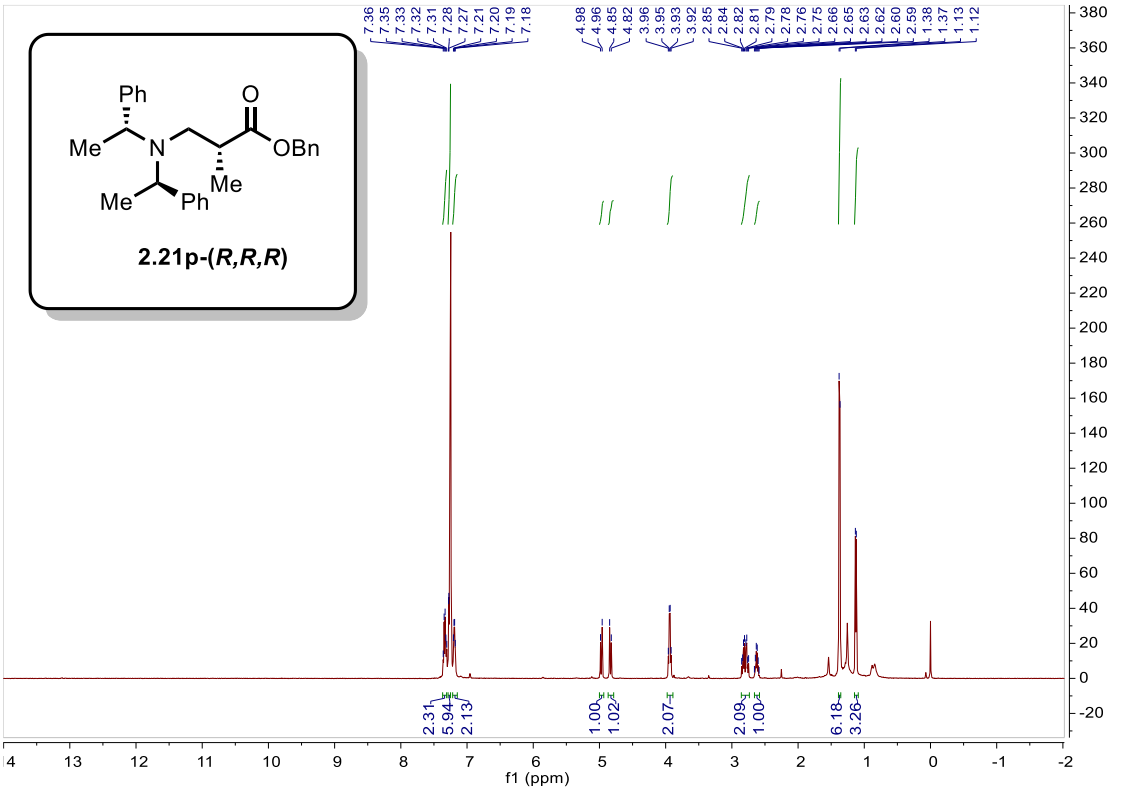
Ph
O
Me
N
OBn
Me
Me
Ph
2.21p-(R,R,R)
f1 (ppm)

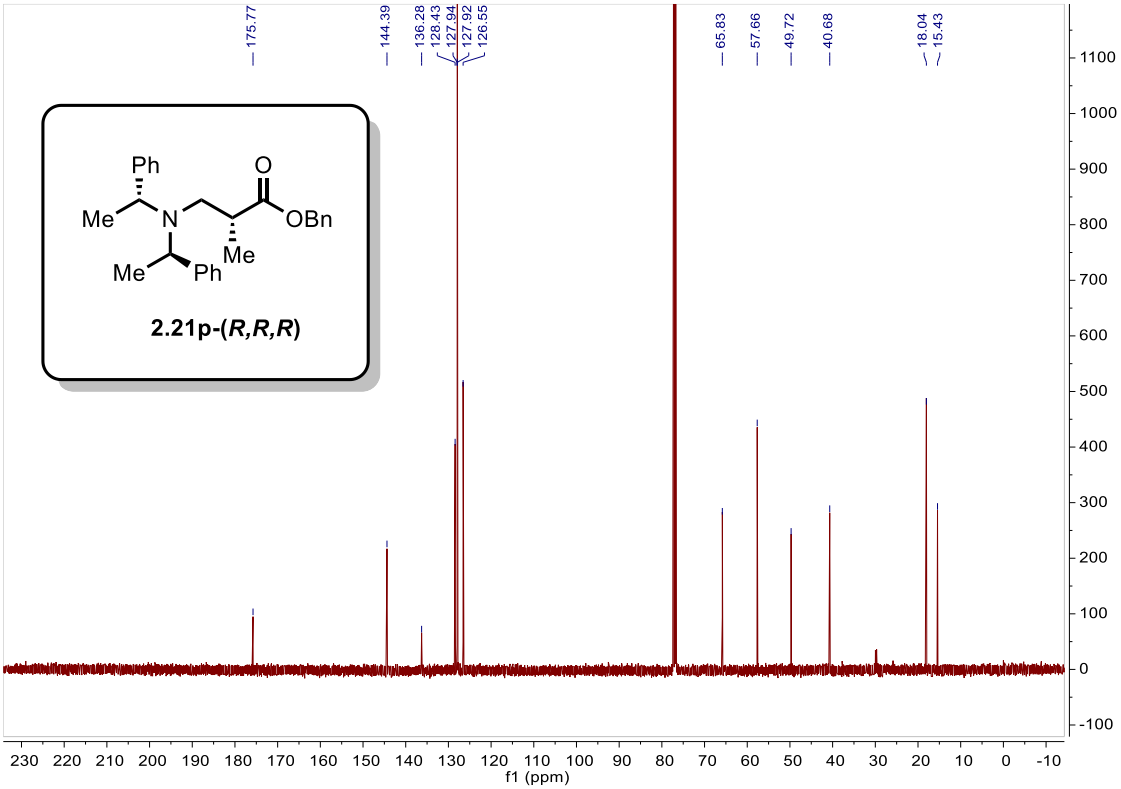
Ph
O
Me
N
OBn
Me
Me
Ph
2.21p-(R,R,R)
f1 (ppm)

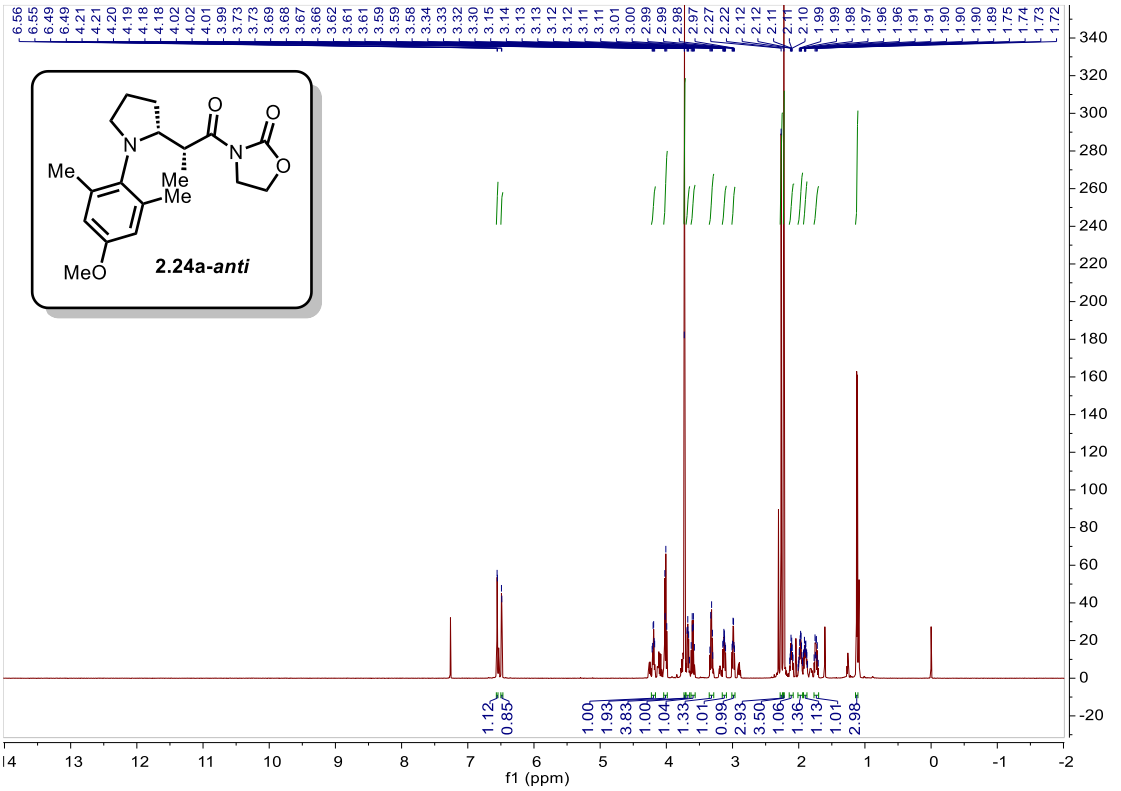
2.24a-anti
f1 (ppm)

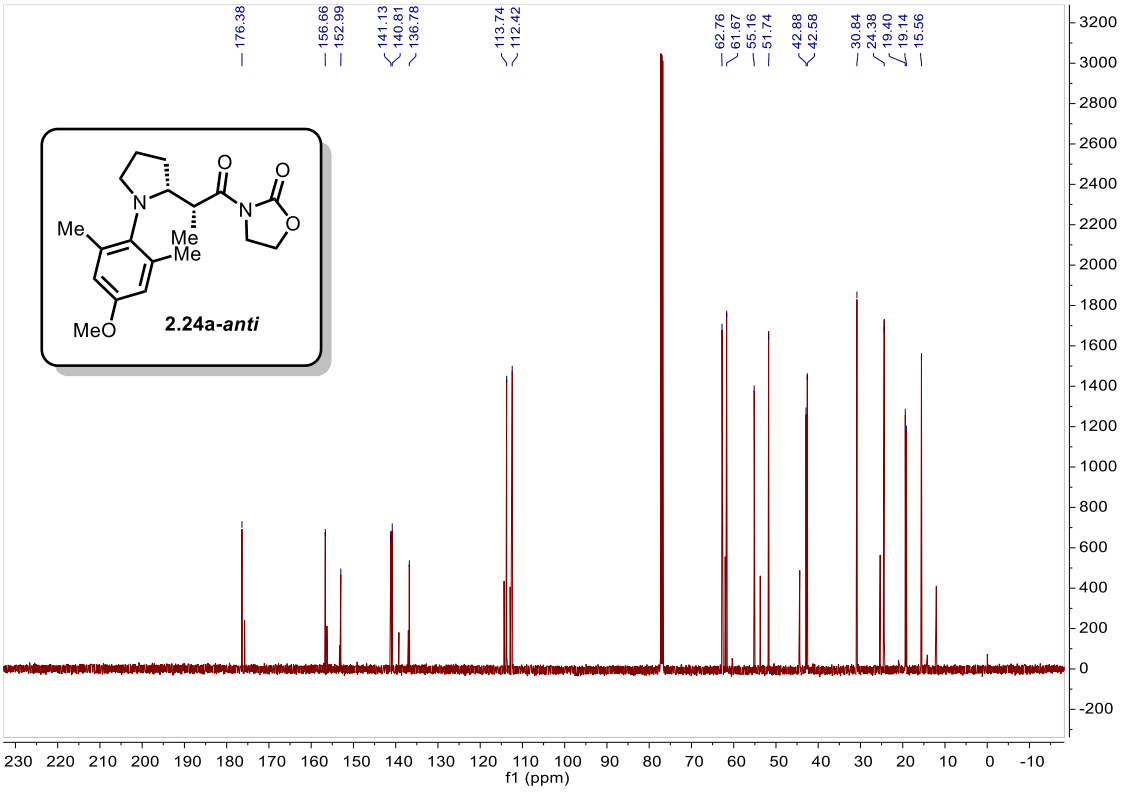
2.24a-anti
f1 (ppm)

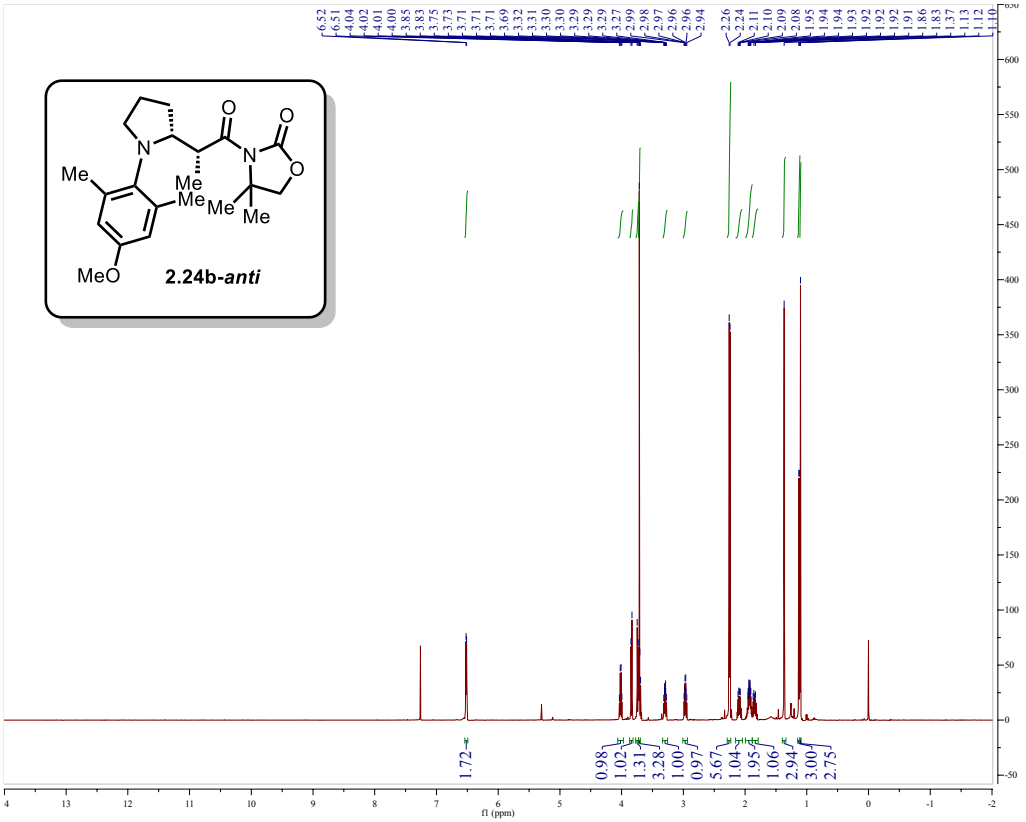
2.24b-*anti*

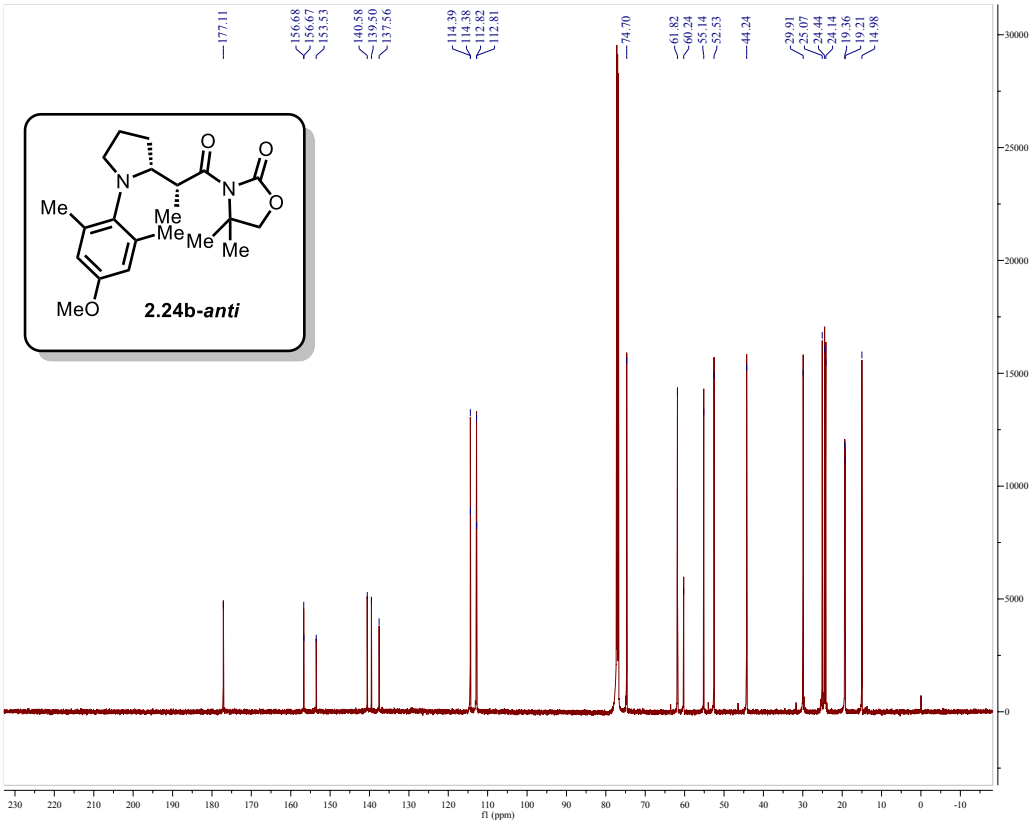
2.24b-*anti*

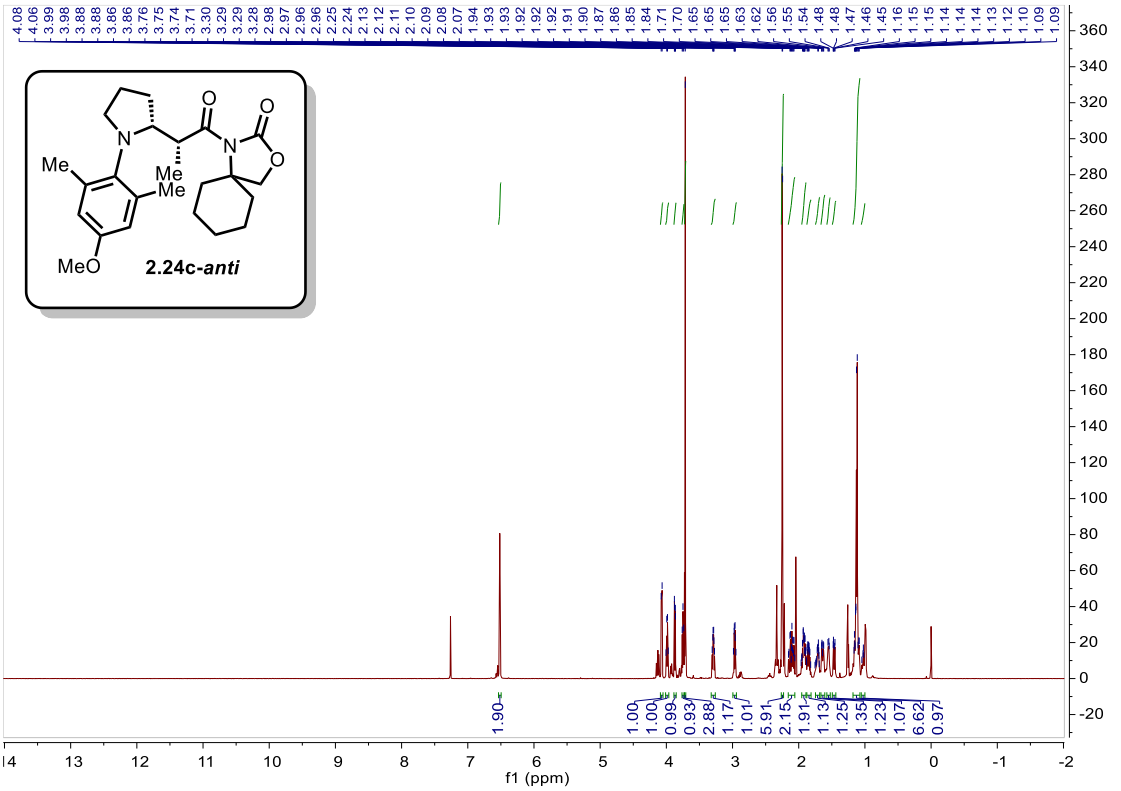
2.24c-*anti*
f1 (ppm)

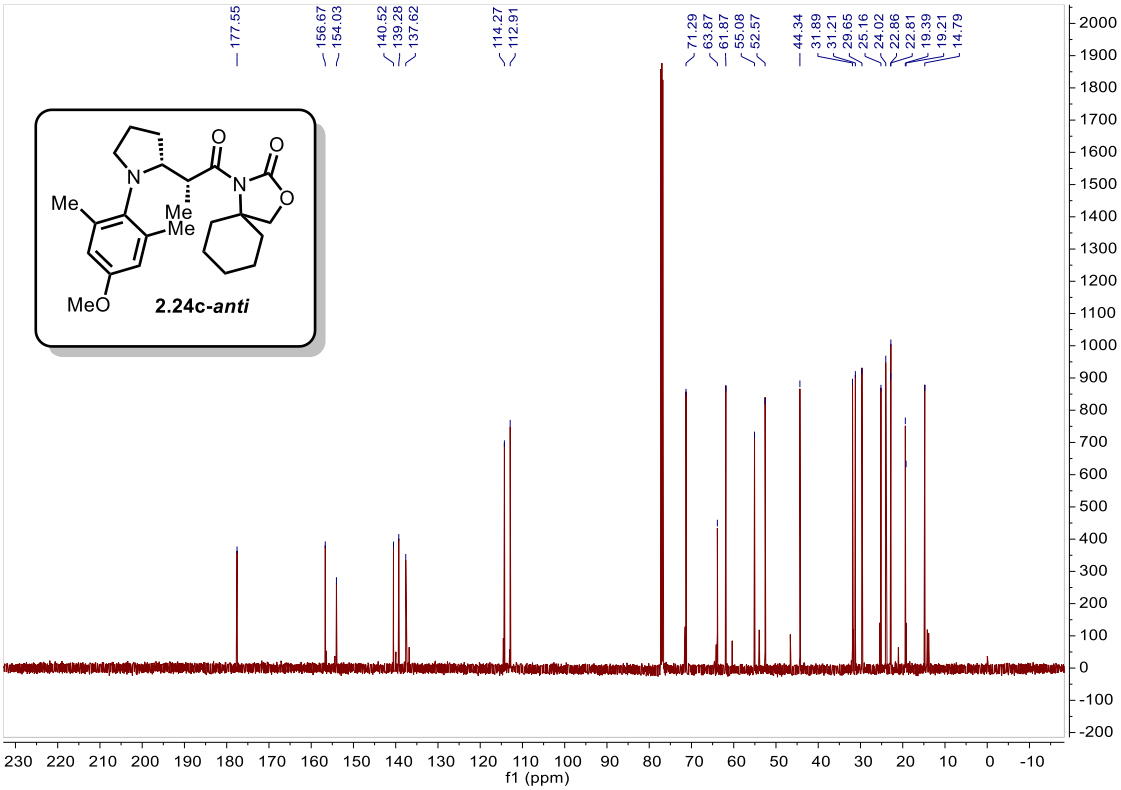
2.24c-*anti*
f1 (ppm)

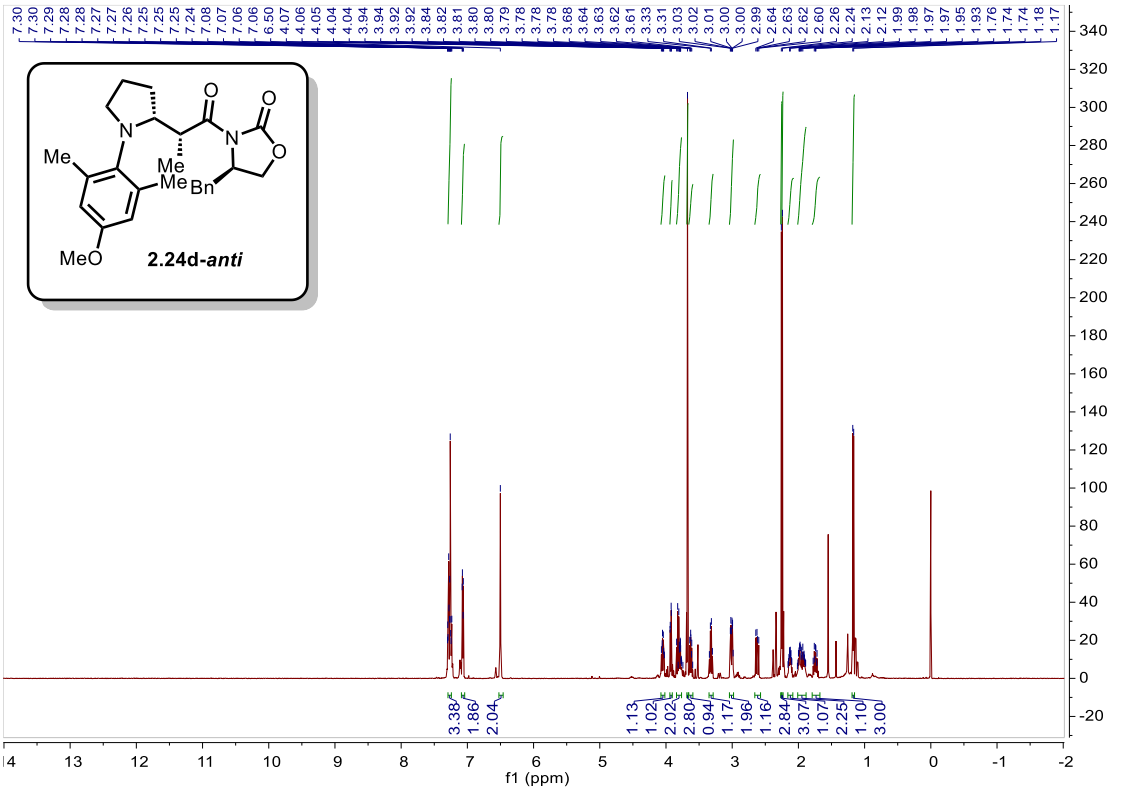
2.24d-*anti*
f1 (ppm)

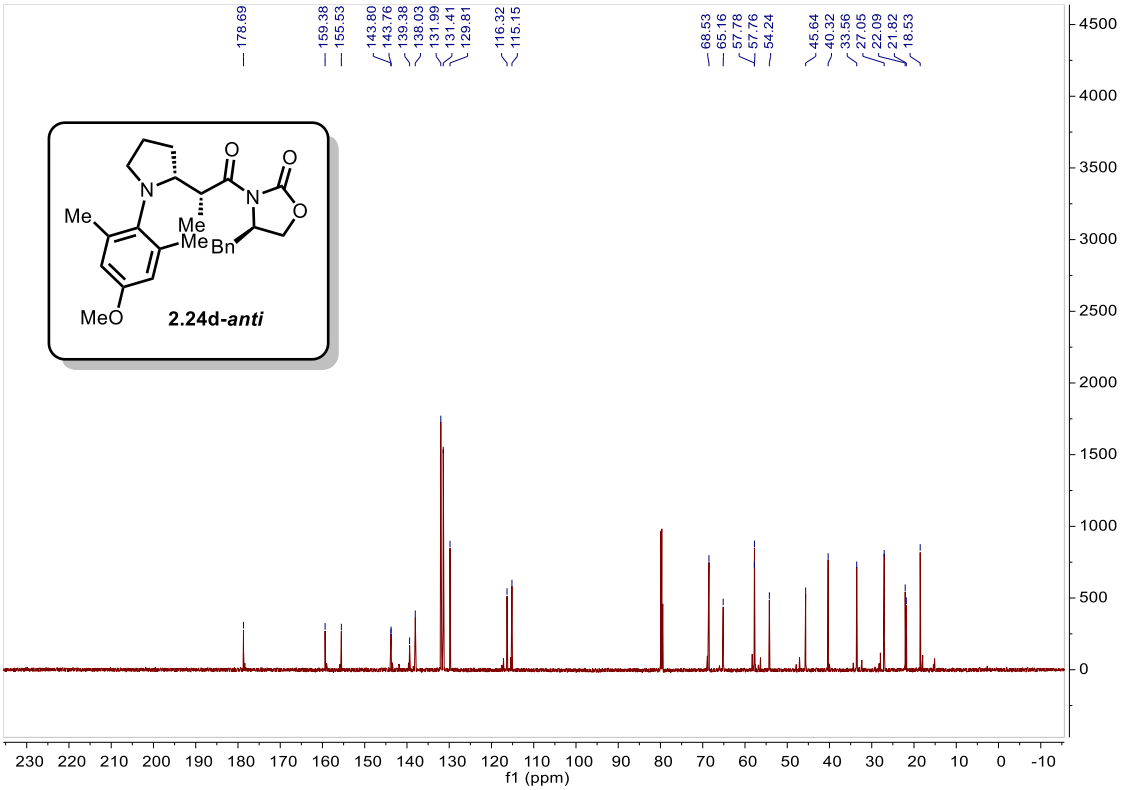
2.24d-*anti*
f1 (ppm)

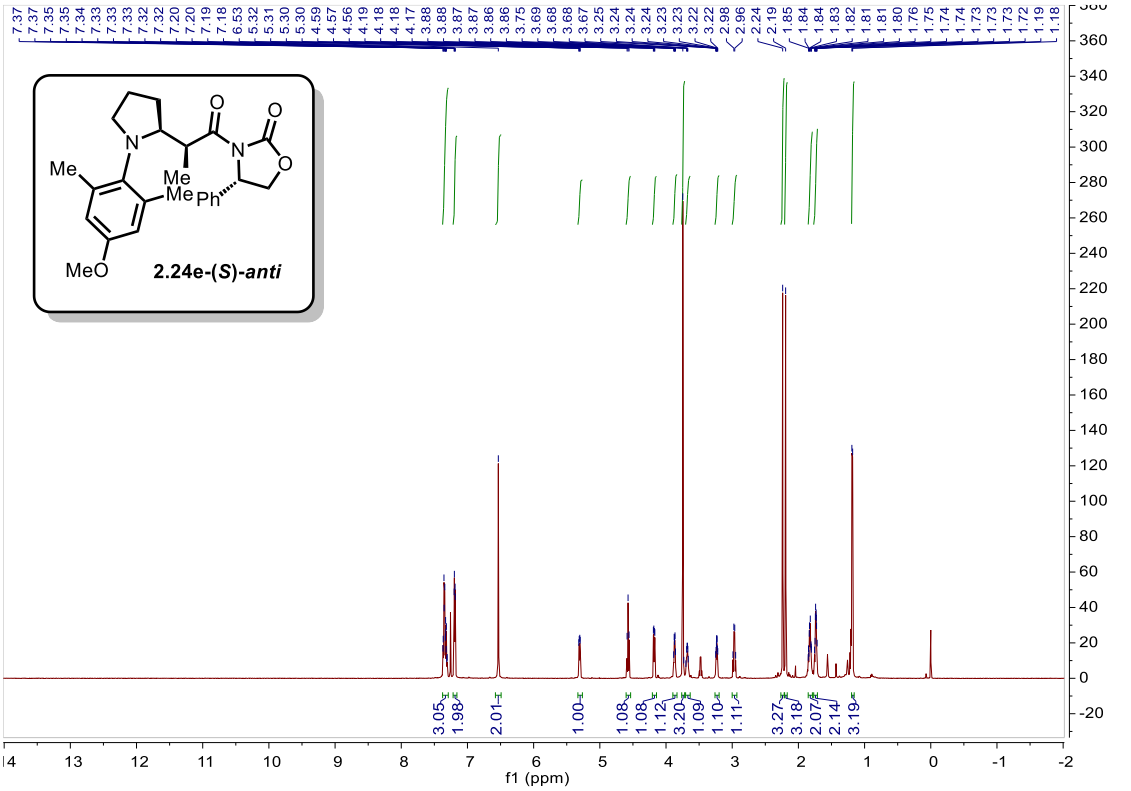
2.24e-(S)-anti
f1 (ppm)

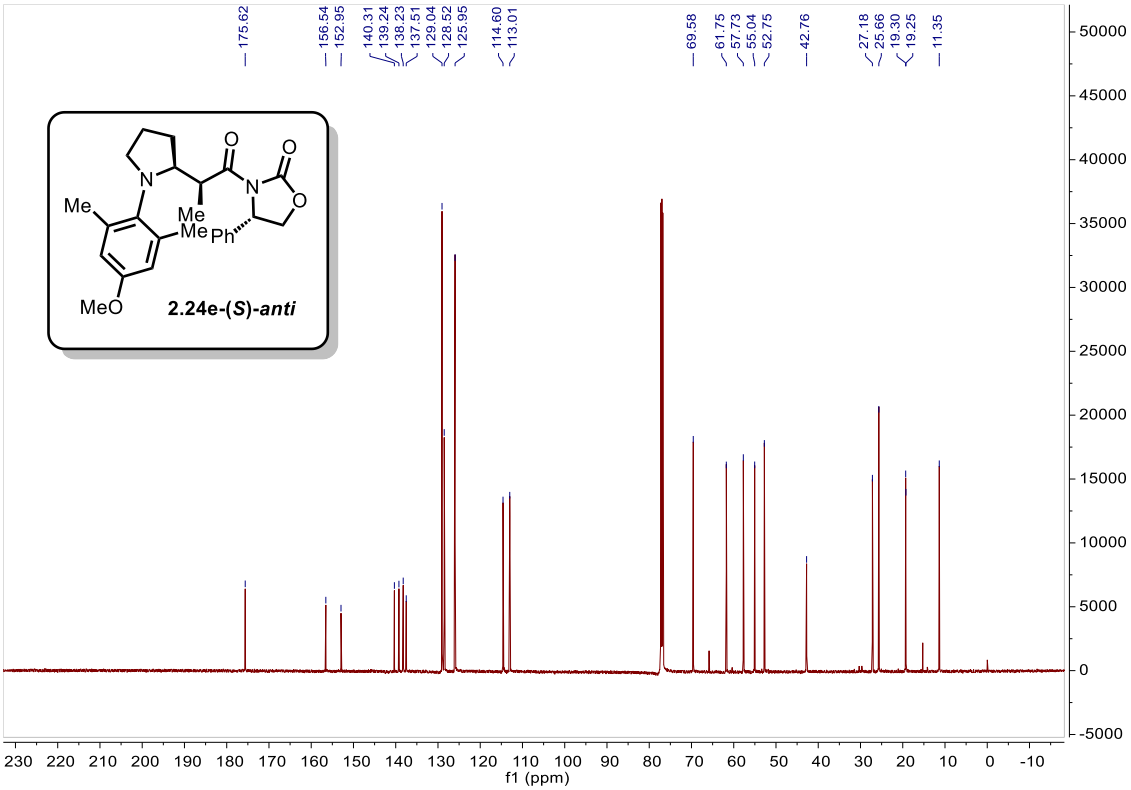
2.24e-(S)-anti
f1 (ppm)

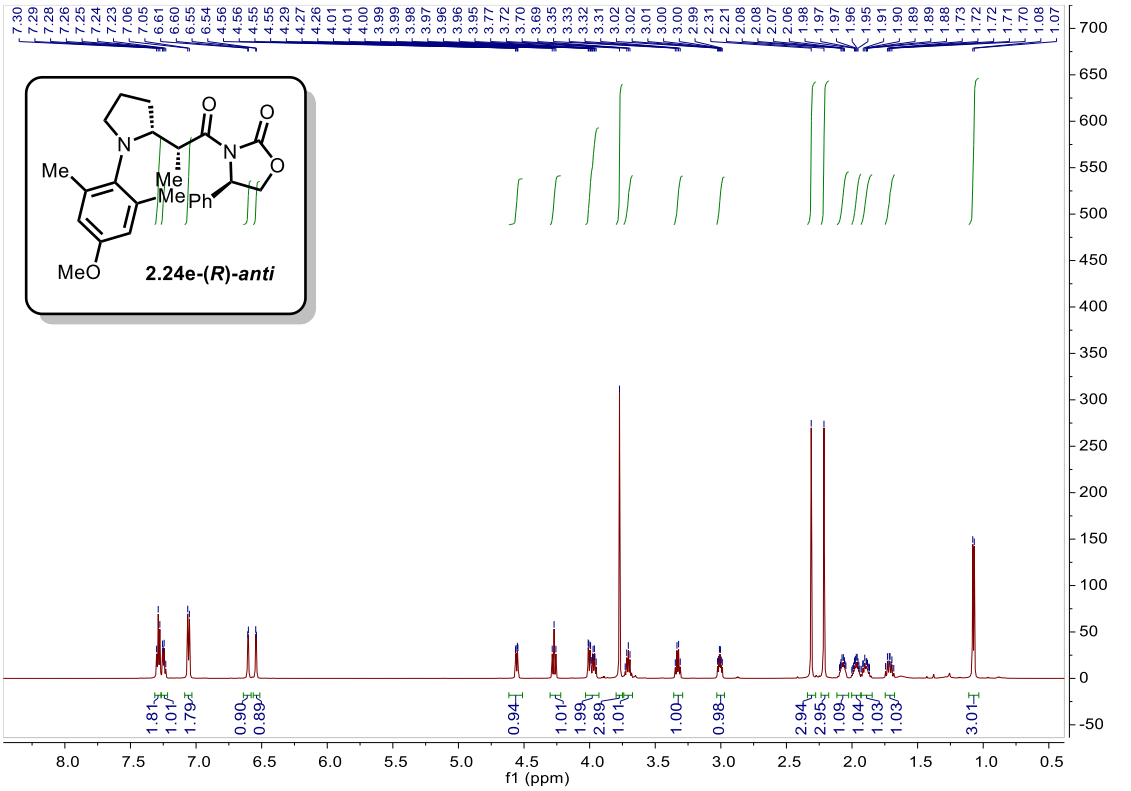
2.24e-(R)-anti

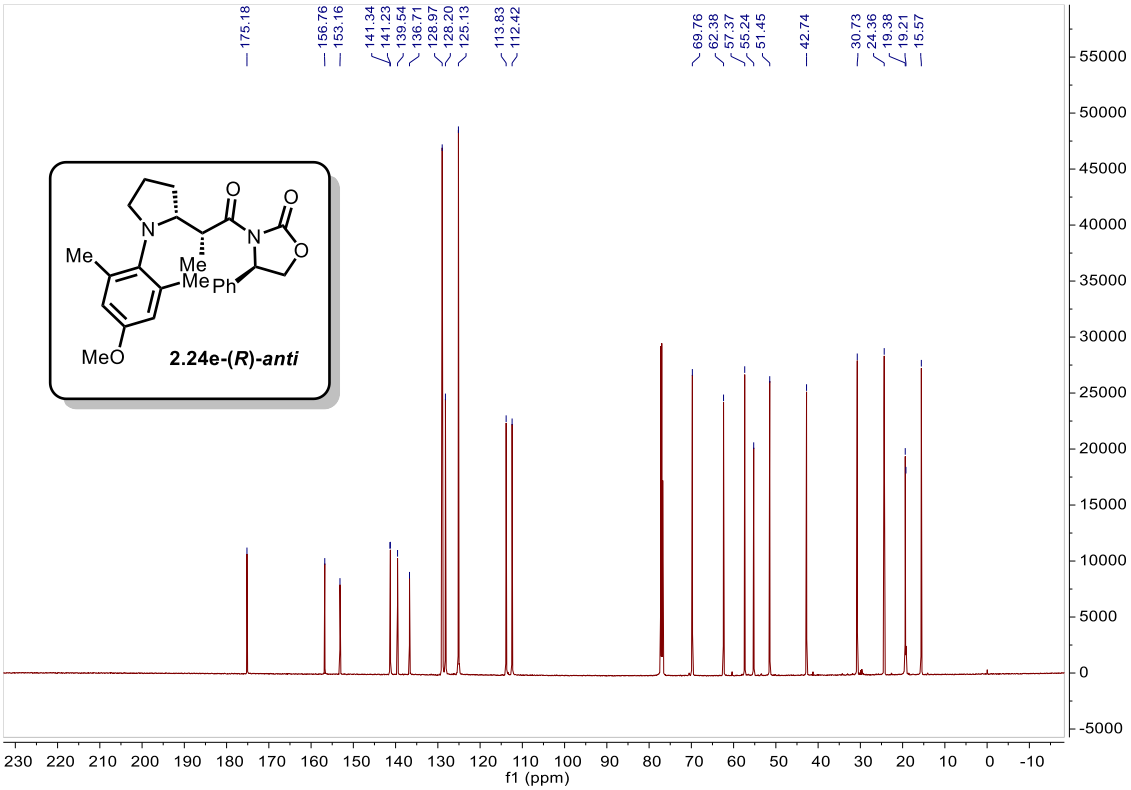
2.24e-(R)-anti

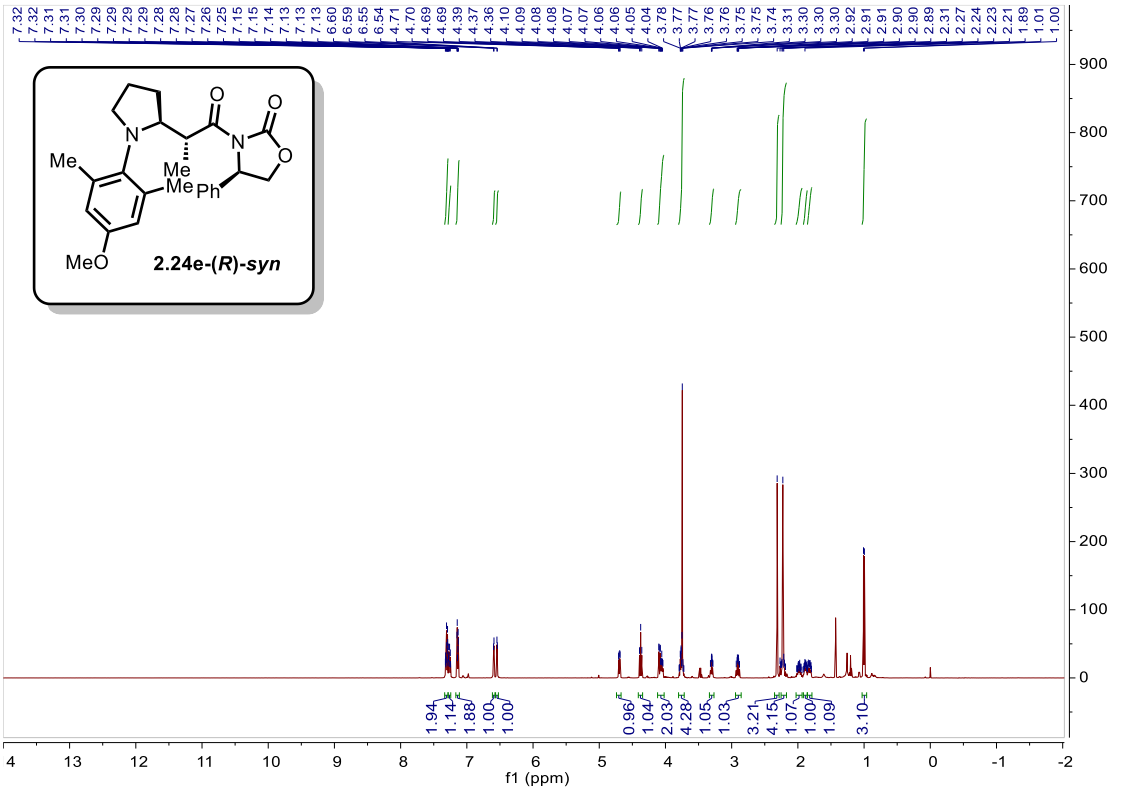
2.24e-(R)-syn
f1 (ppm)

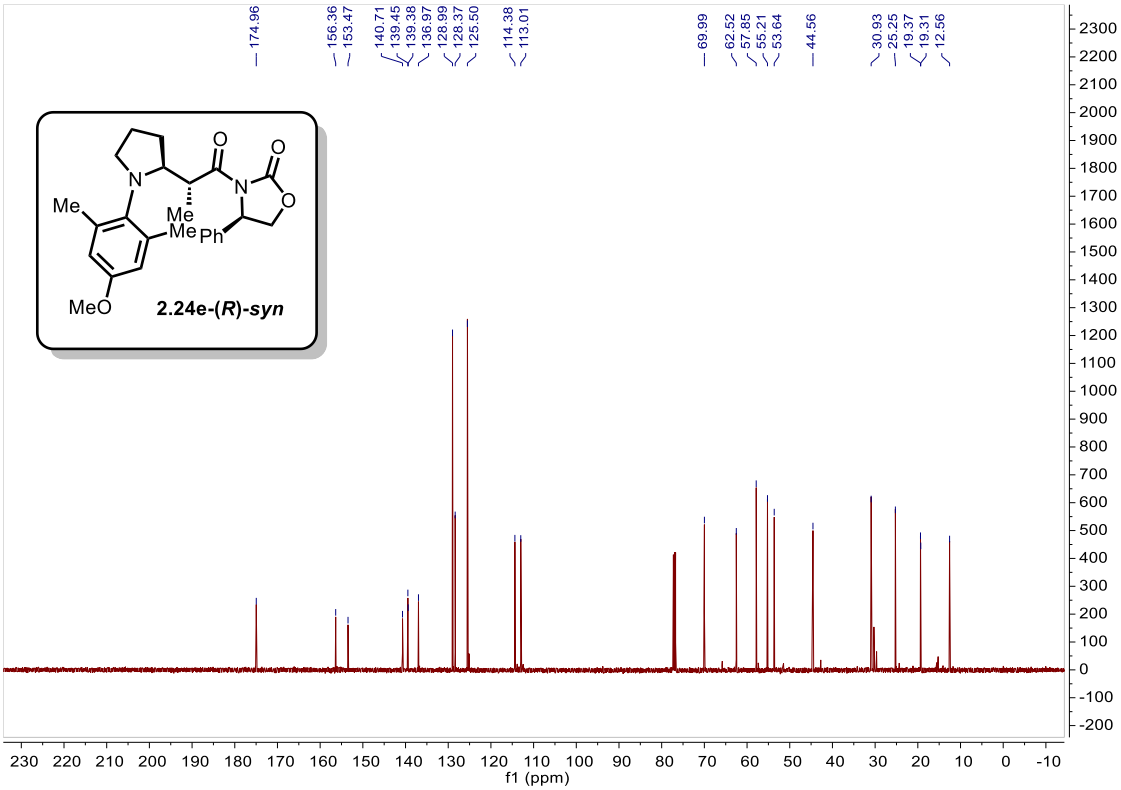
2.24e-(R)-syn
f1 (ppm)

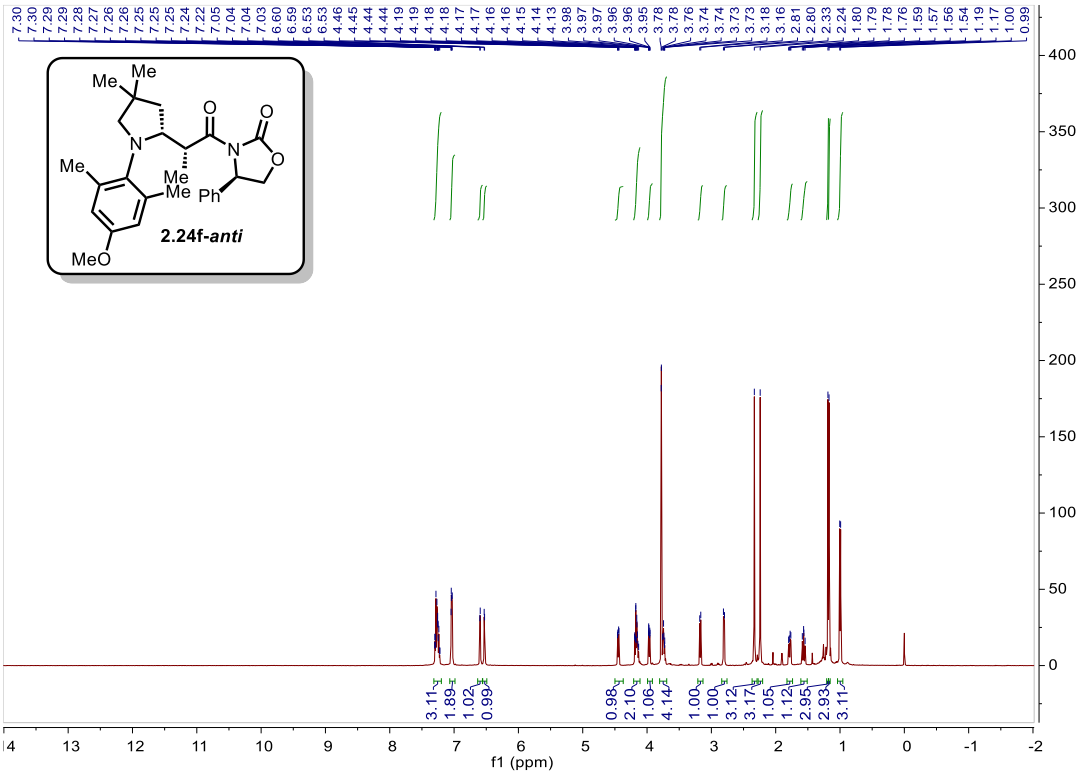
2.24f-anti
f1 (ppm)

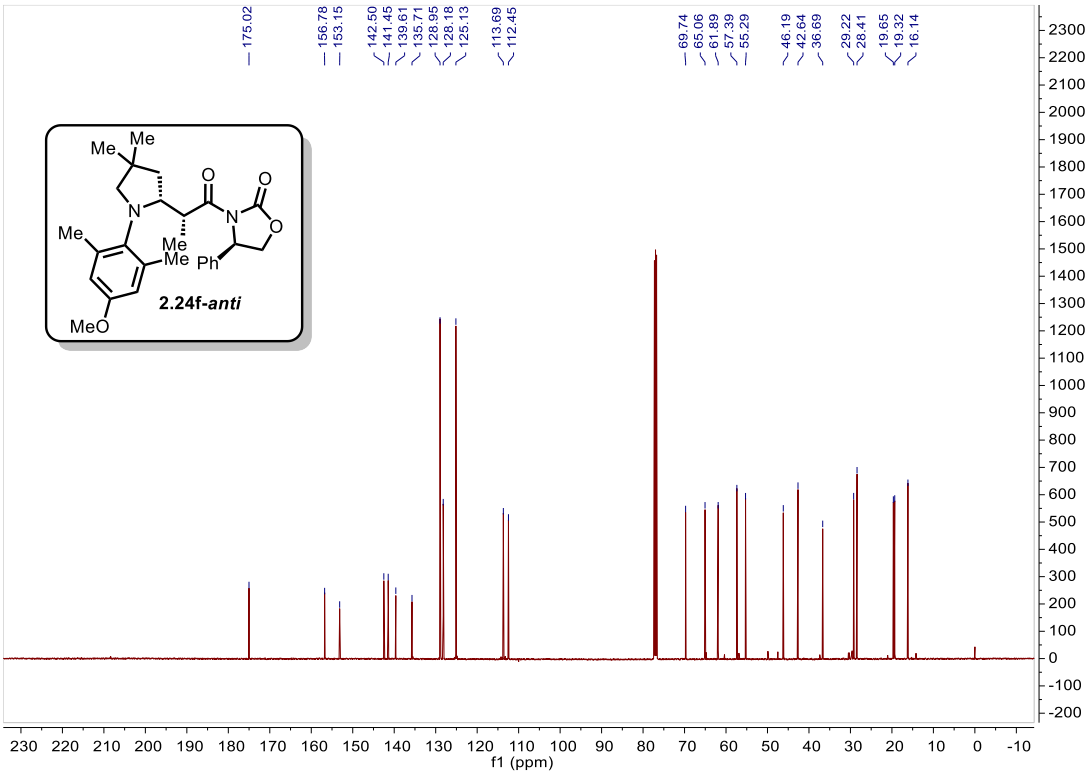
2.24f-anti
f1 (ppm)

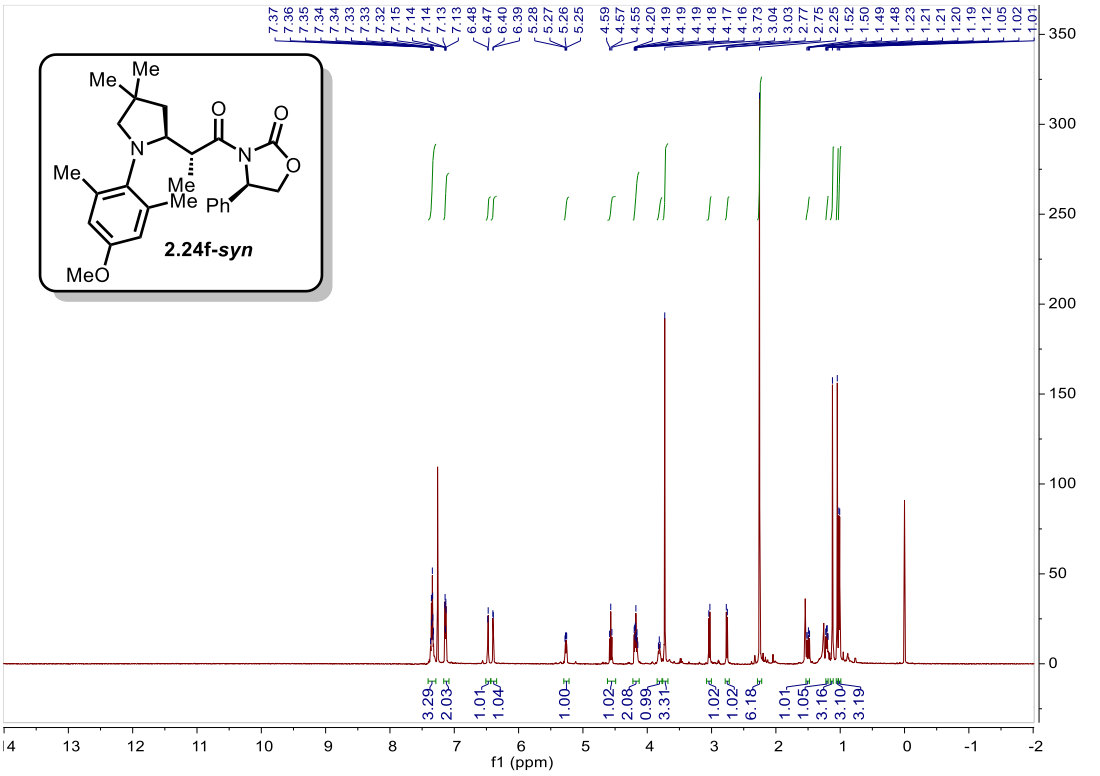
2.24f-syn
f1 (ppm)

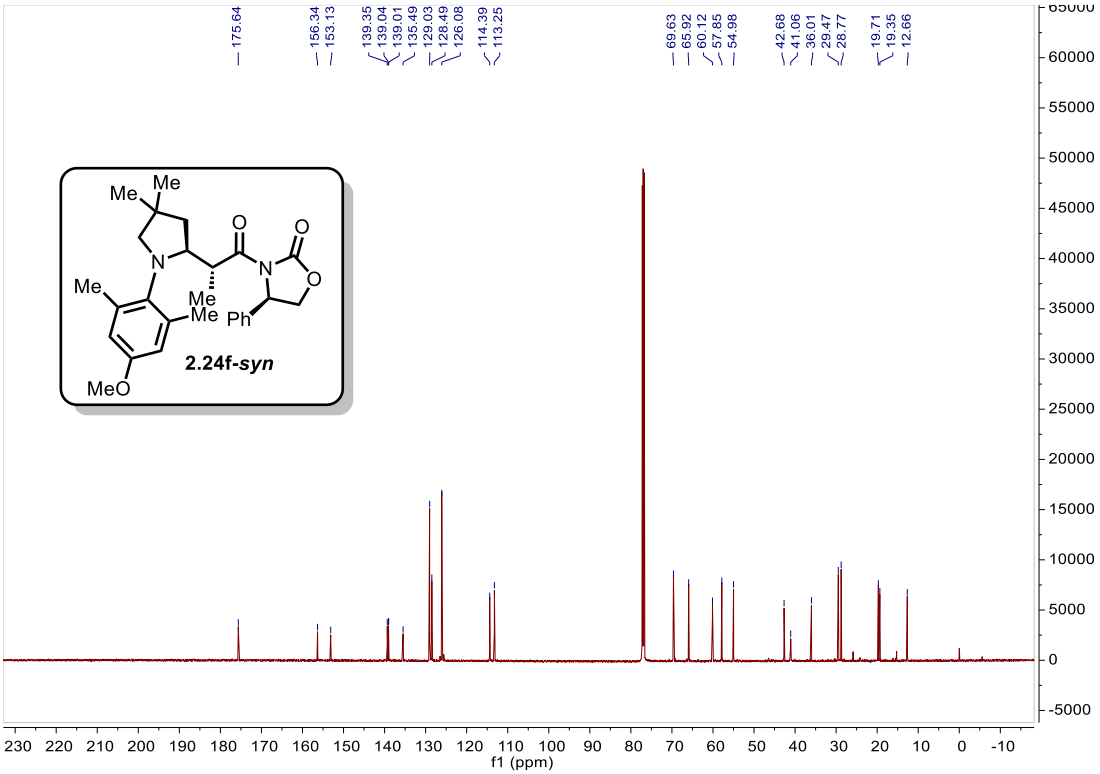
2.24f-syn
f1 (ppm)

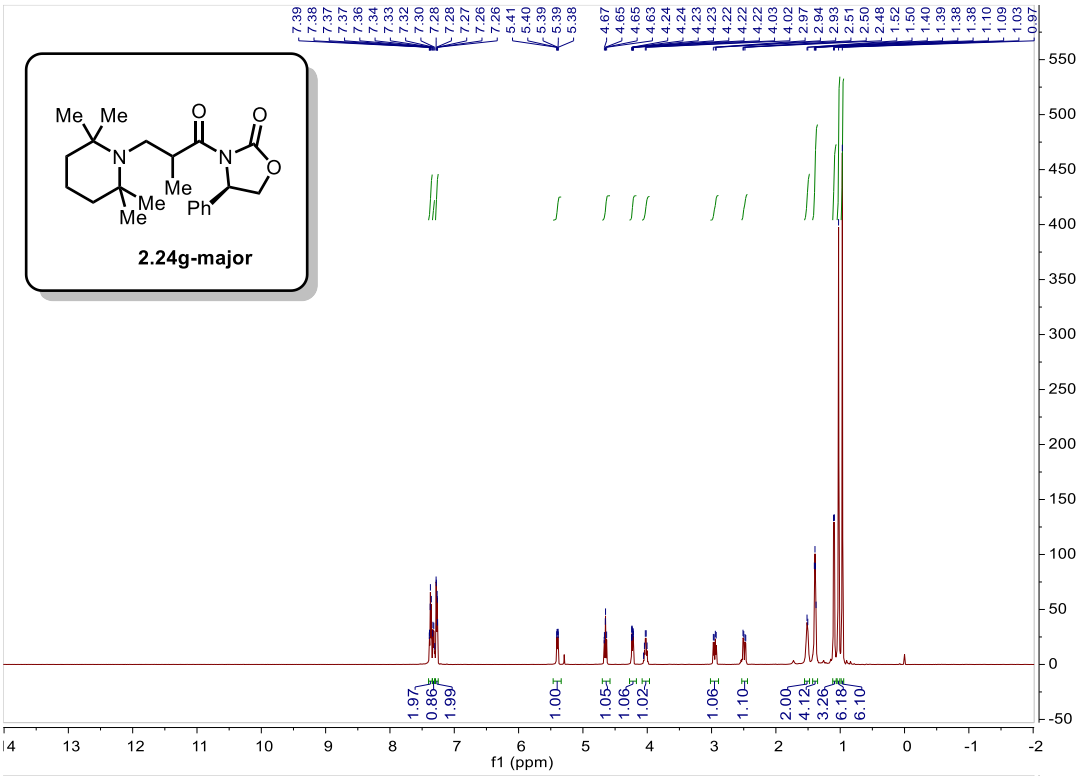
Me Me
O
O
N
N
O
Me
Me
Me
Ph
2.24g-major
f1 (ppm)

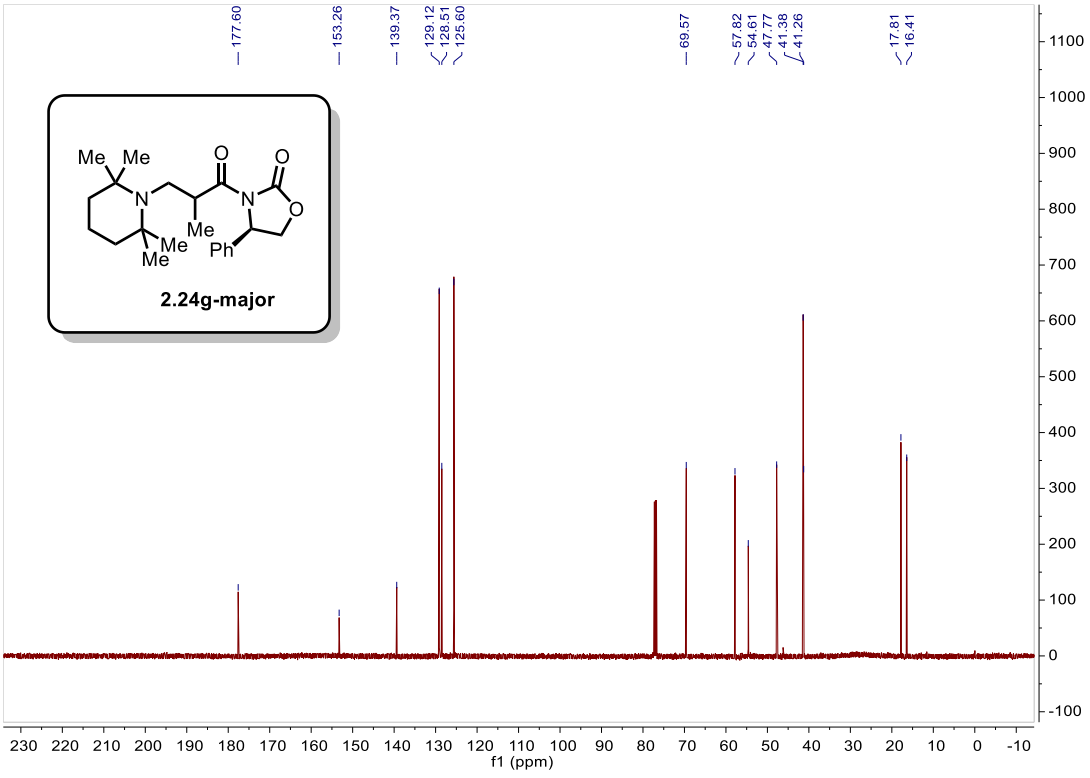
Me Me
O
O
N
N
O
Me
Me
Me
Ph
2.24g-major
f1 (ppm)

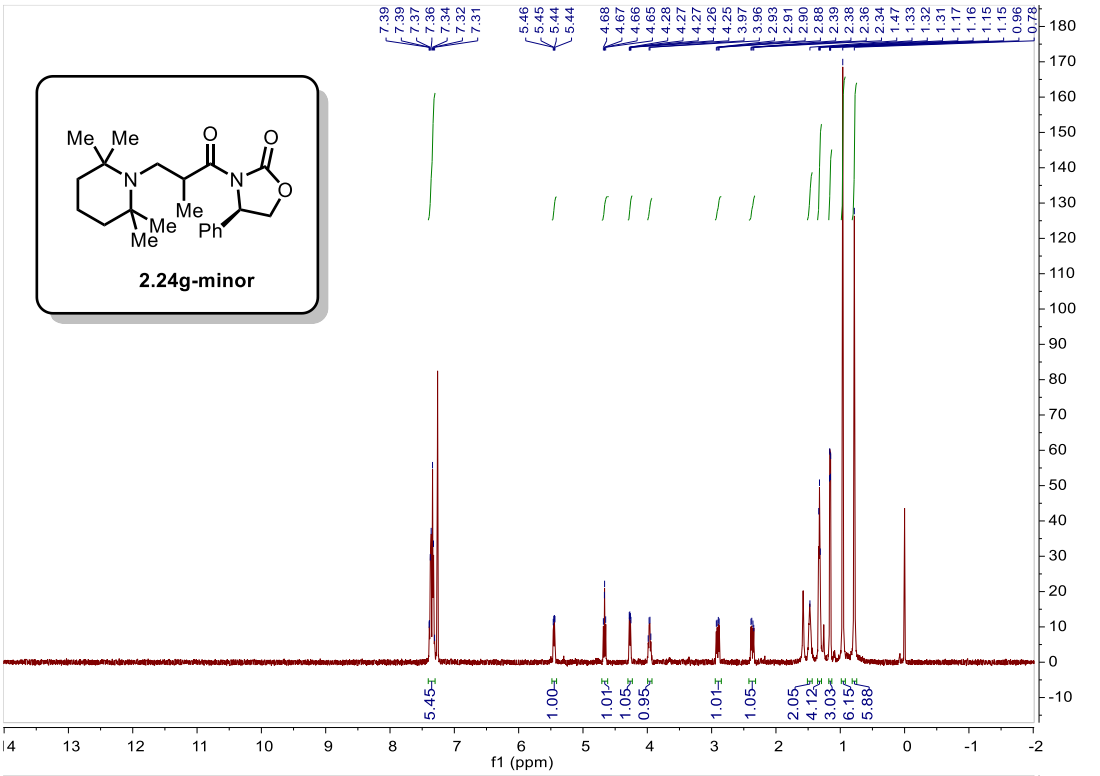
2.24g-minor
f1 (ppm)

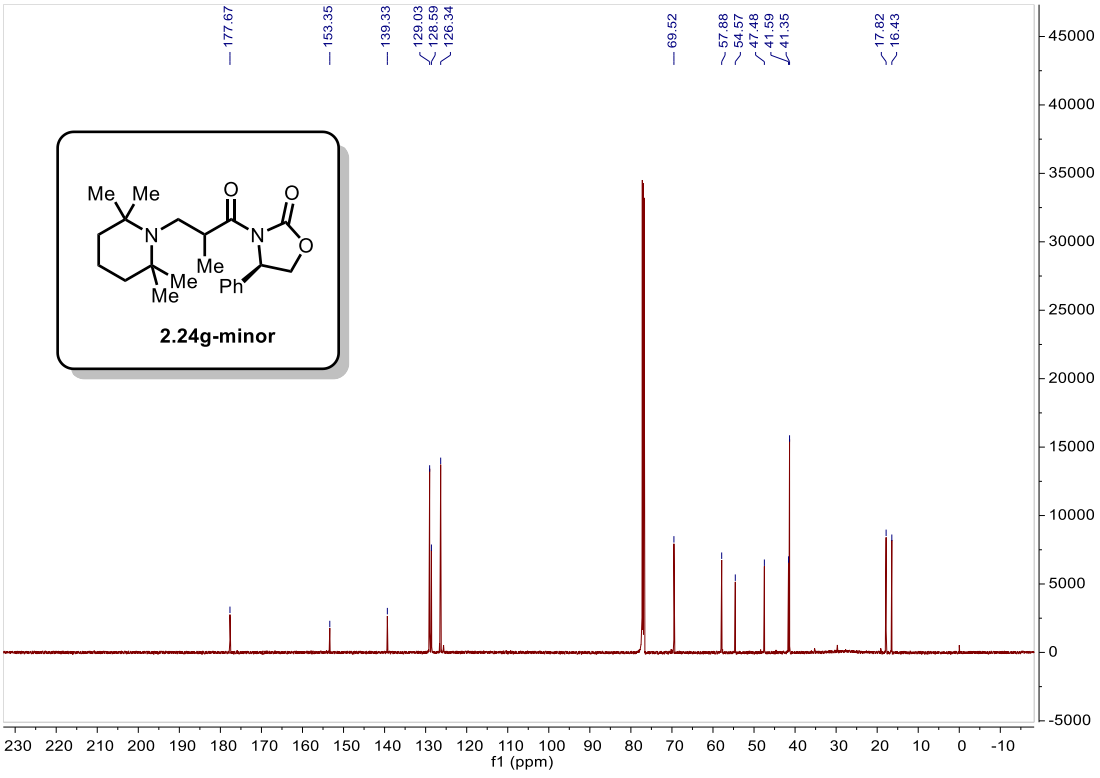
2.24g-minor
f1 (ppm)

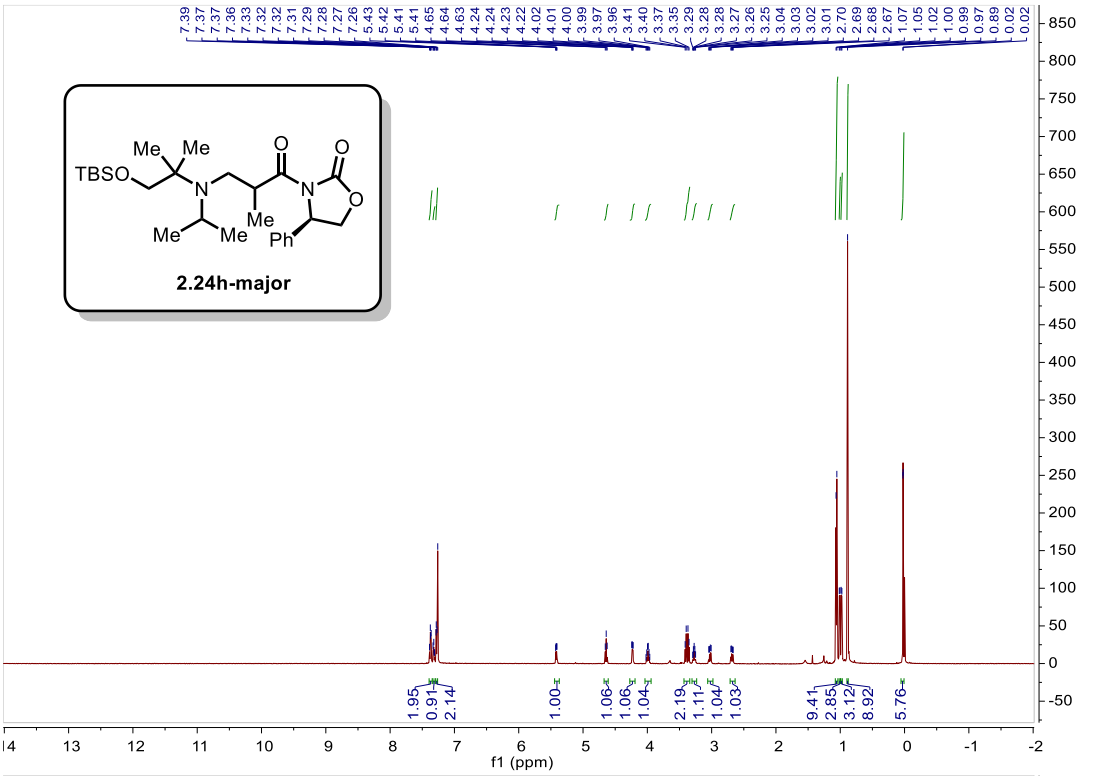
Me
Me
TBSO
O
O
N
N
O
Me
Me
Me
Ph
2.24h-major
f1 (ppm)

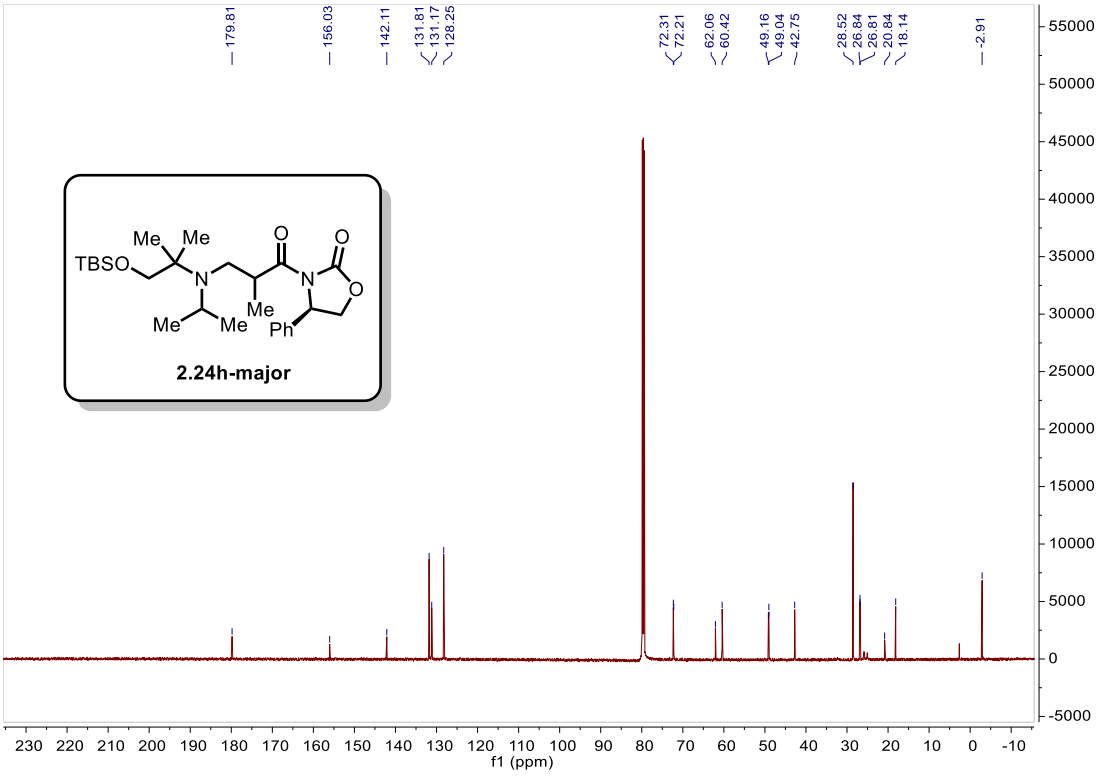
Me
Me
TBSO
O
O
N
N
O
Me
Me
Me
Ph
2.24h-major
f1 (ppm)

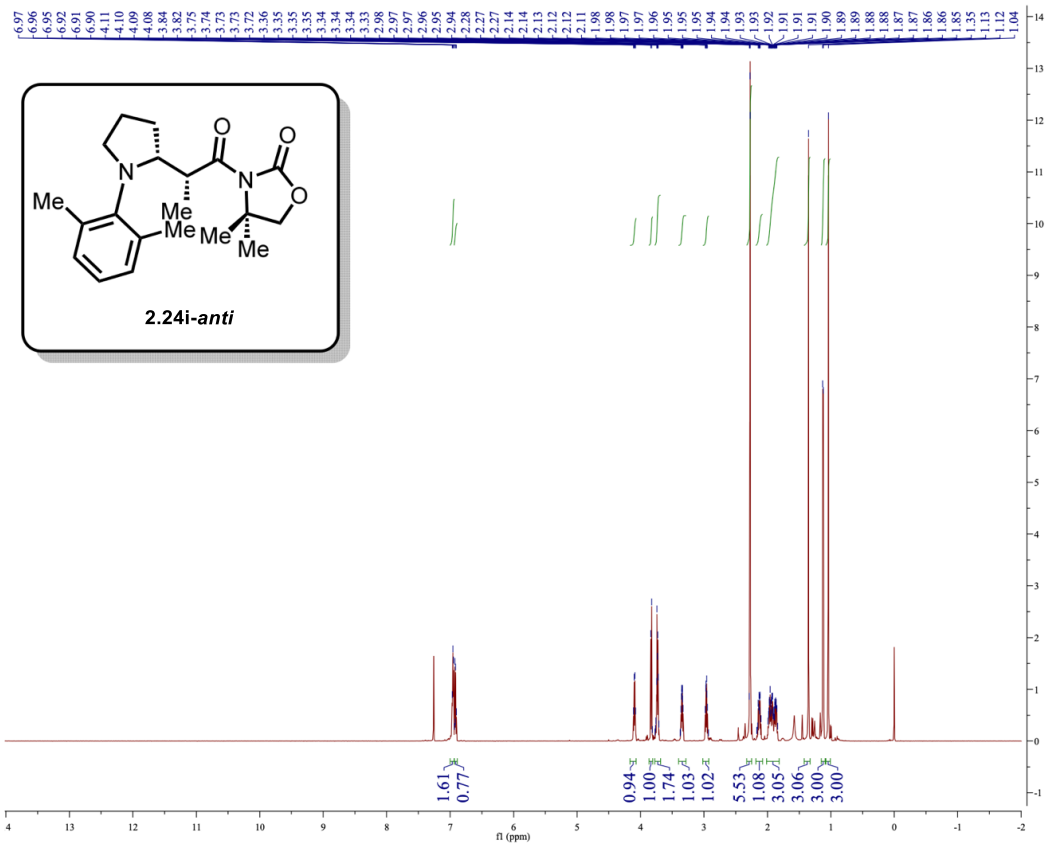
2.24i-*anti*
1.61
0.77
0.94
1.00
1.74
1.03
1.02
5.53
1.08
3.05
3.06
3.00
3.00
f1 (ppm)

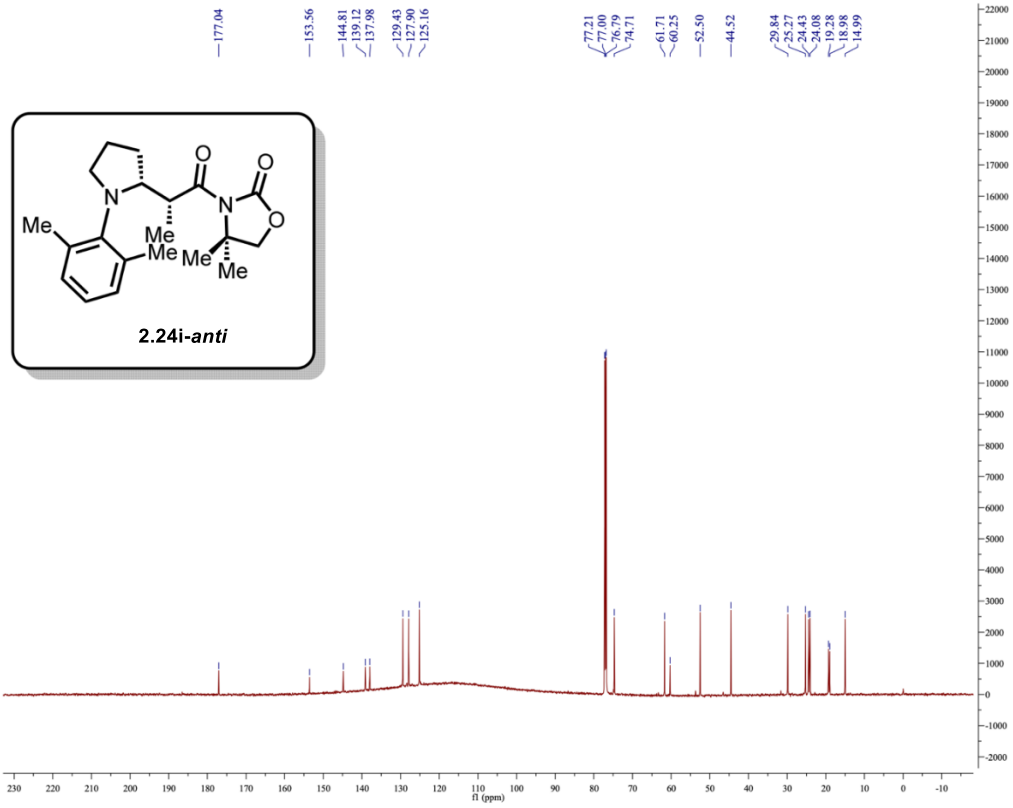
177.04
153.56
144.81
139.12
137.98
129.43
127.90
125.16
77.21
77.00
76.79
74.71
61.71
60.25
52.50
44.52
29.84
25.27
24.43
24.08
19.28
18.98
14.99
2.24i-*anti*
f1 (ppm)

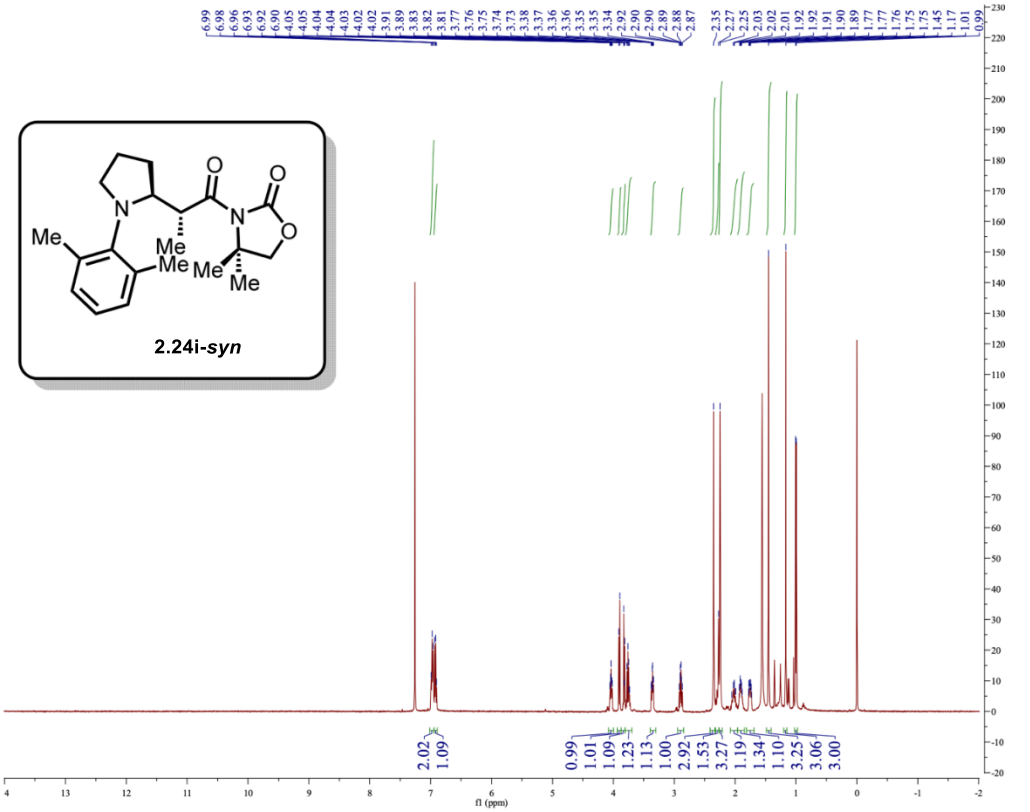
2.24i-*syn*

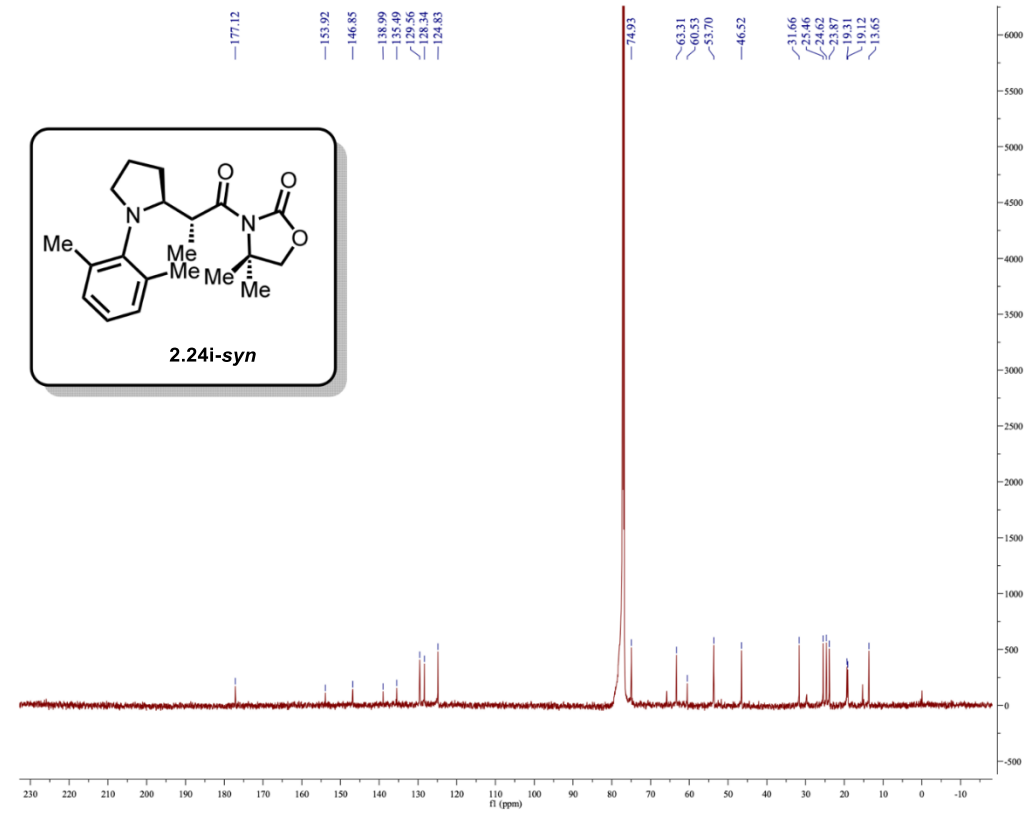
2.24i-*syn*

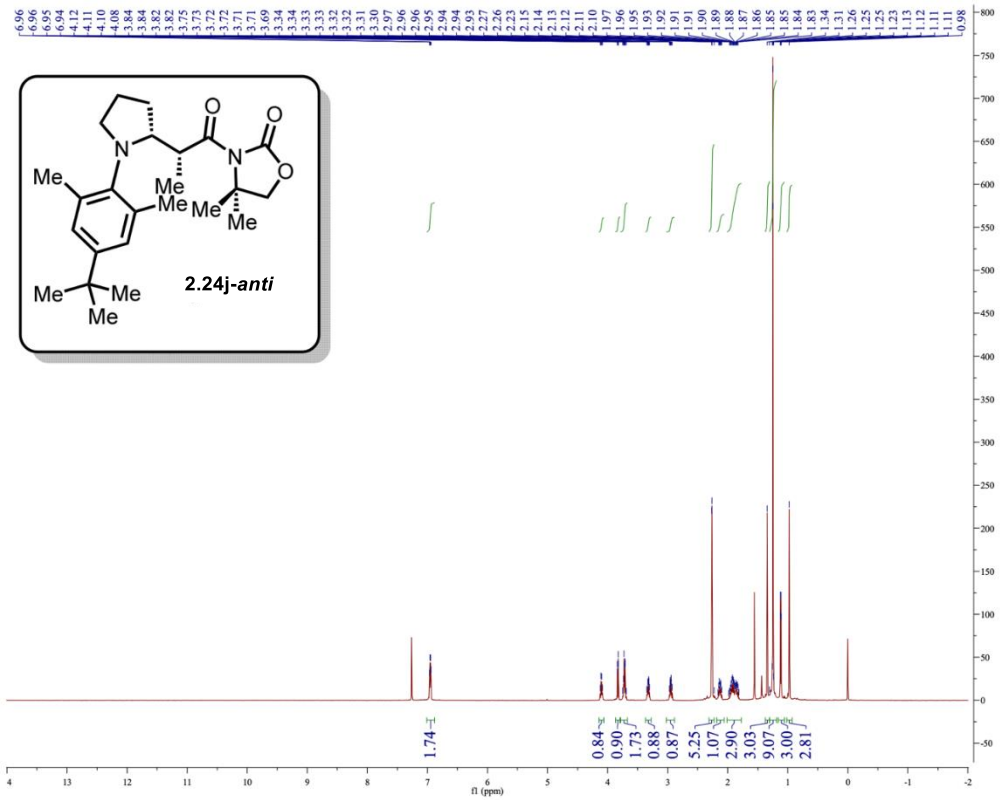
2.24j-*anti*
1.74
0.84
0.90
1.73
0.88
0.87
5.25
1.07
2.90
3.03
9.07
3.00
2.81
f1 (ppm)

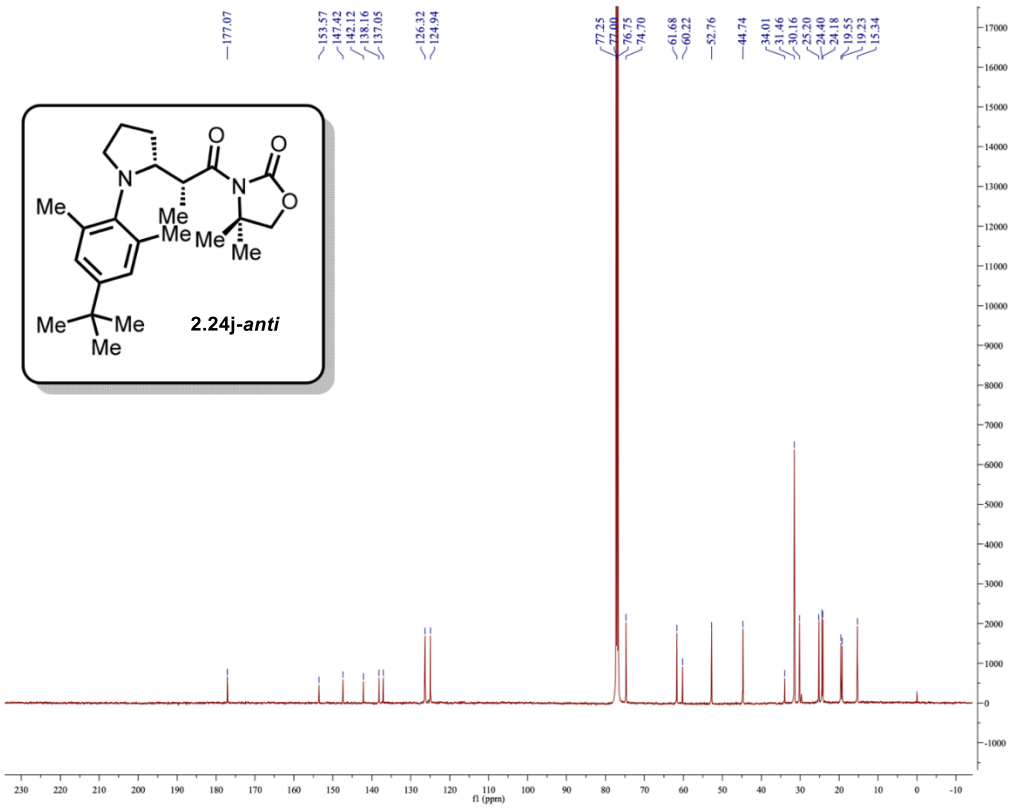
2.24j-*anti*
177.07
153.57
147.42
142.12
138.16
137.05
126.32
124.94
77.25
77.00
76.75
74.70
61.68
60.22
52.76
44.74
34.01
31.46
30.16
25.20
24.40
24.18
19.55
19.23
15.34
f1 (ppm)

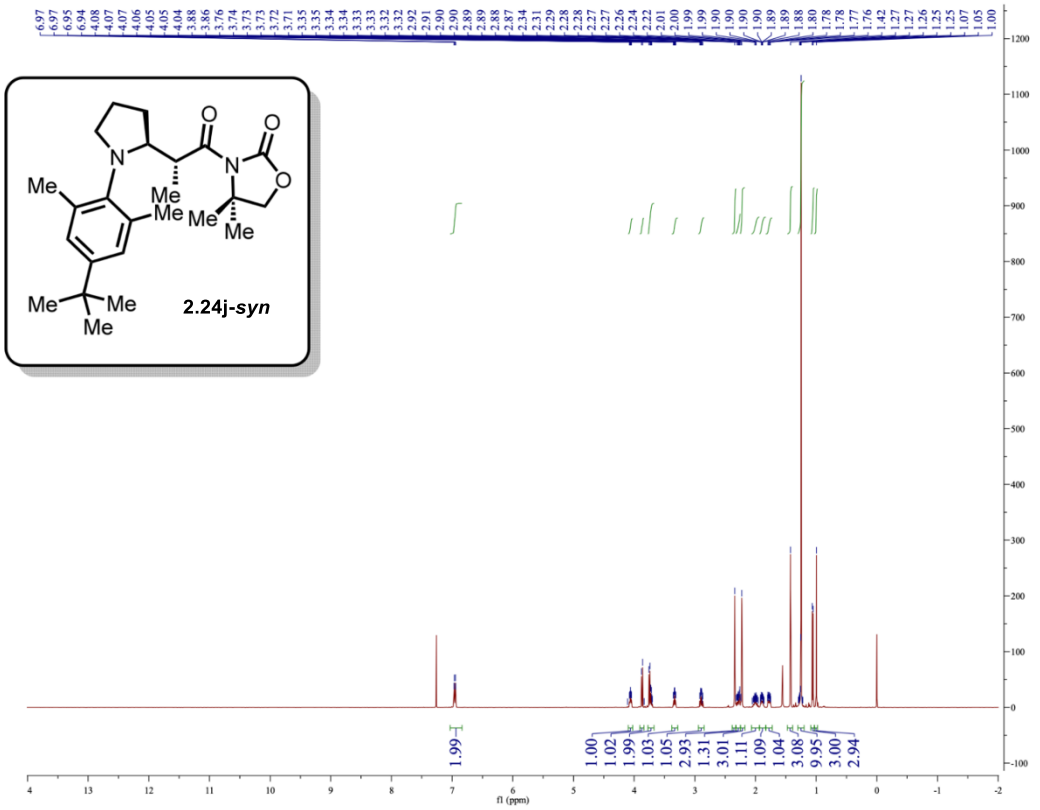
Me
Me
Me
Me
Me
Me
Me
Me
2.24j-*syn*

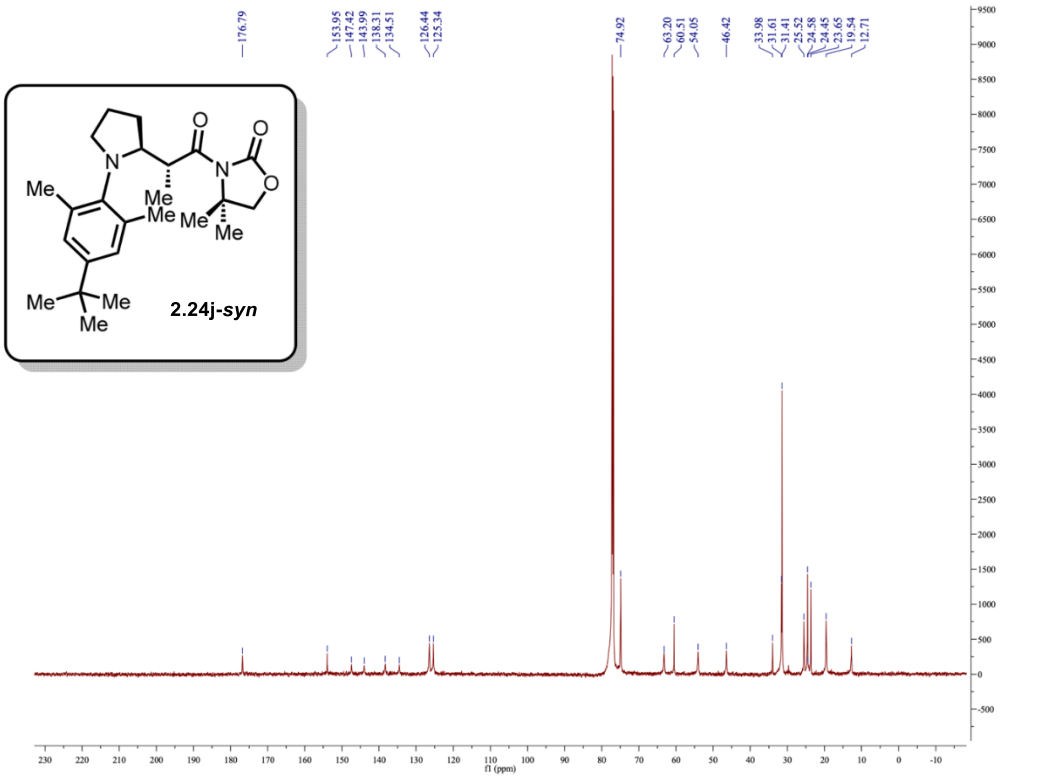
Me
Me
Me
Me
Me
Me
Me
Me
2.24j-*syn*

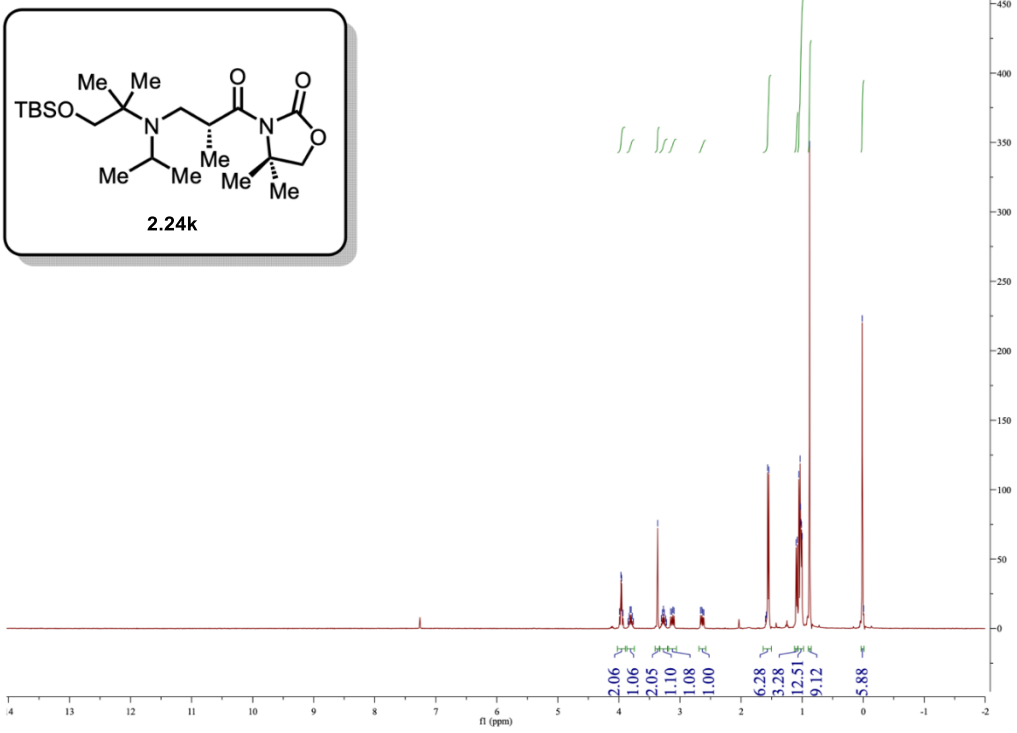
TBSO
Me
Me
N
O
O
N
O
Me
Me
Me
Me
Me
2.24k
f1 (ppm)

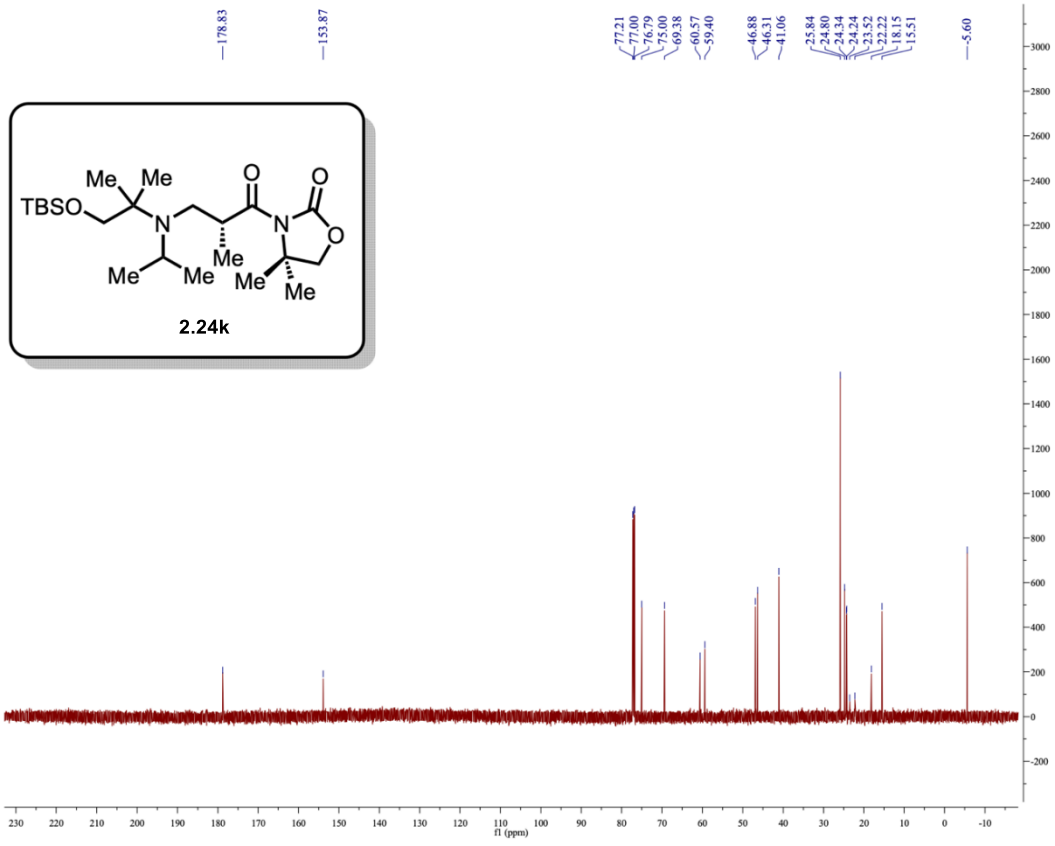
TBSO
Me
Me
N
O
O
N
O
Me
Me
Me
Me
Me
2.24k
f1 (ppm)

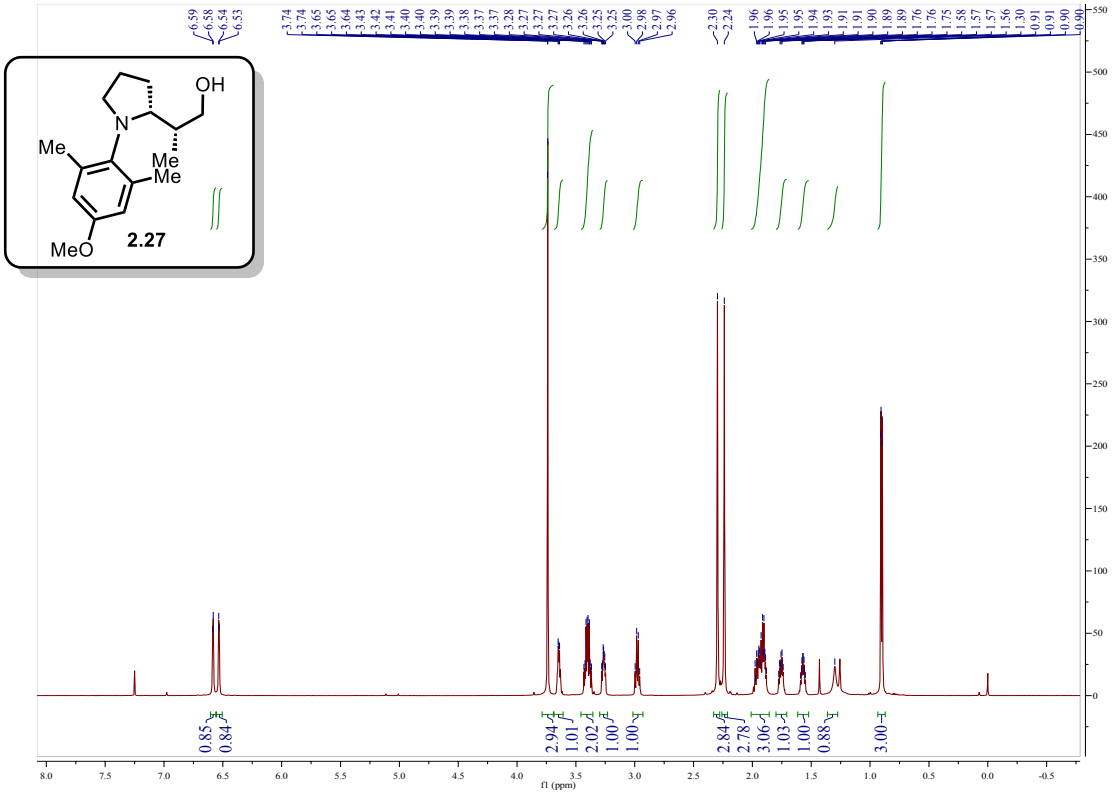
OH
N
Me
Me
Me
MeO
2.27

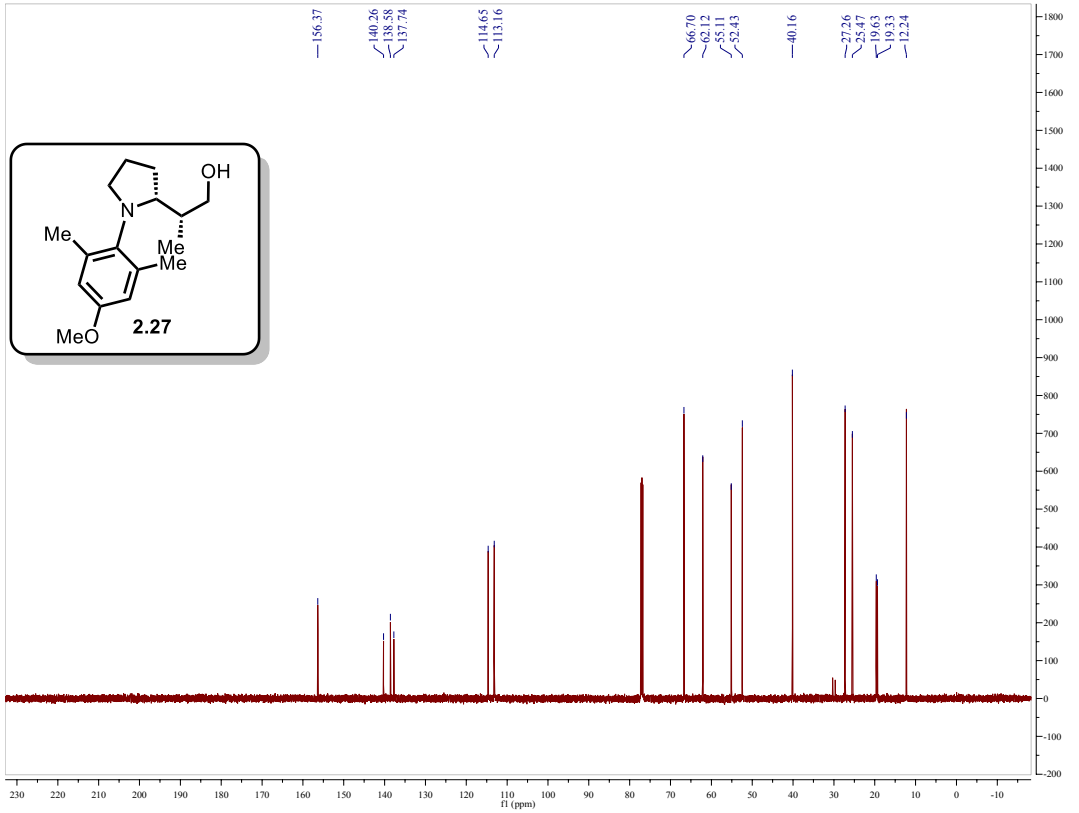
OH
N
Me
Me
Me
MeO
2.27

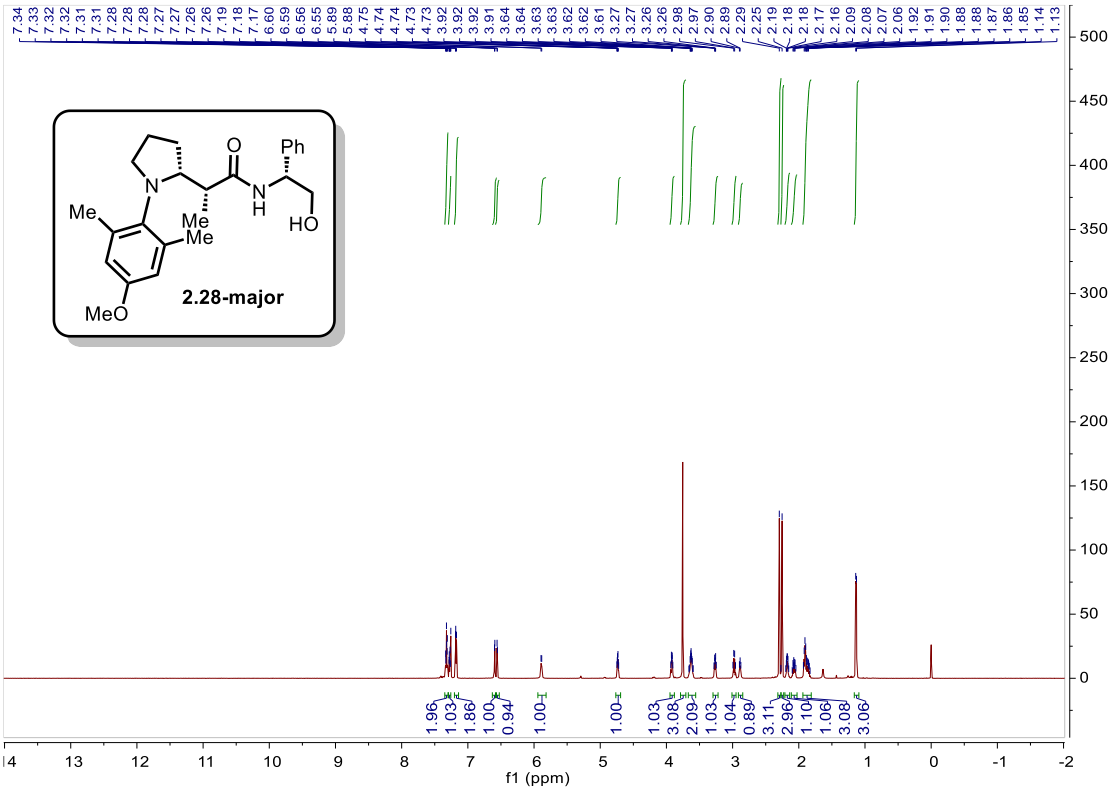
2.28-major
f1 (ppm)

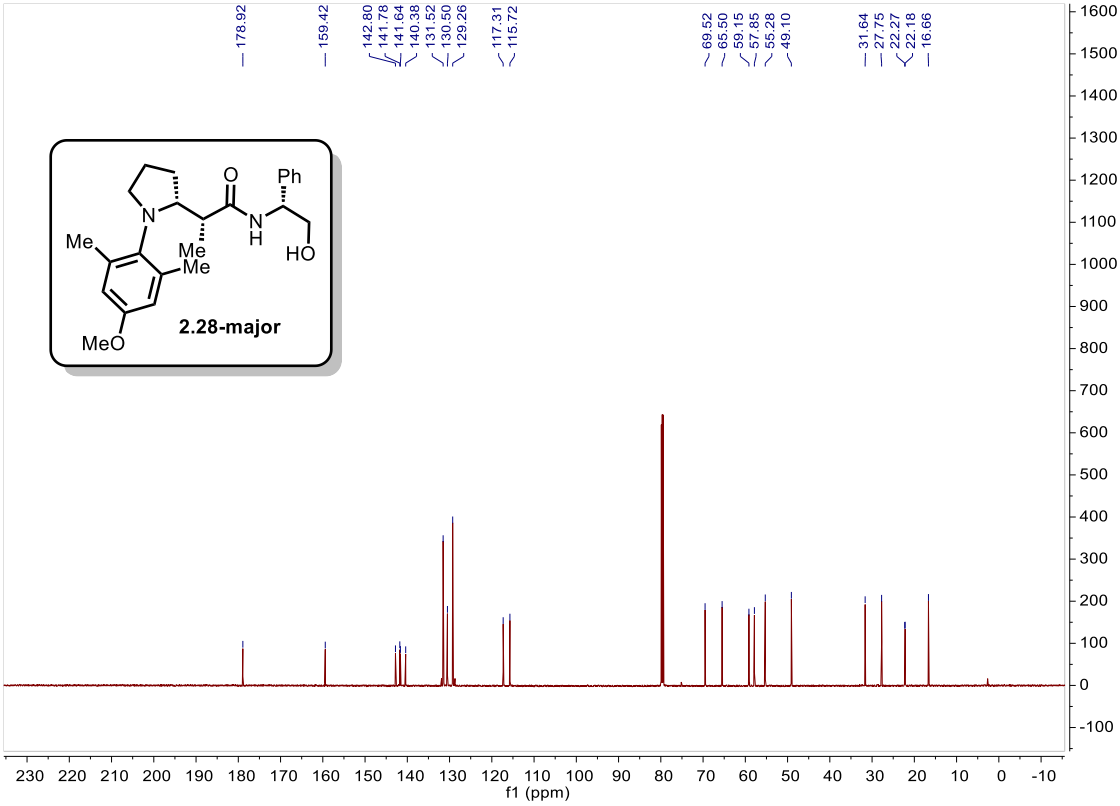
2.28-major
f1 (ppm)

A8. X-Ray Crystallography Data of 2.28-major and 2.28-minor

X-Ray Crystallography Data of 2.28-major

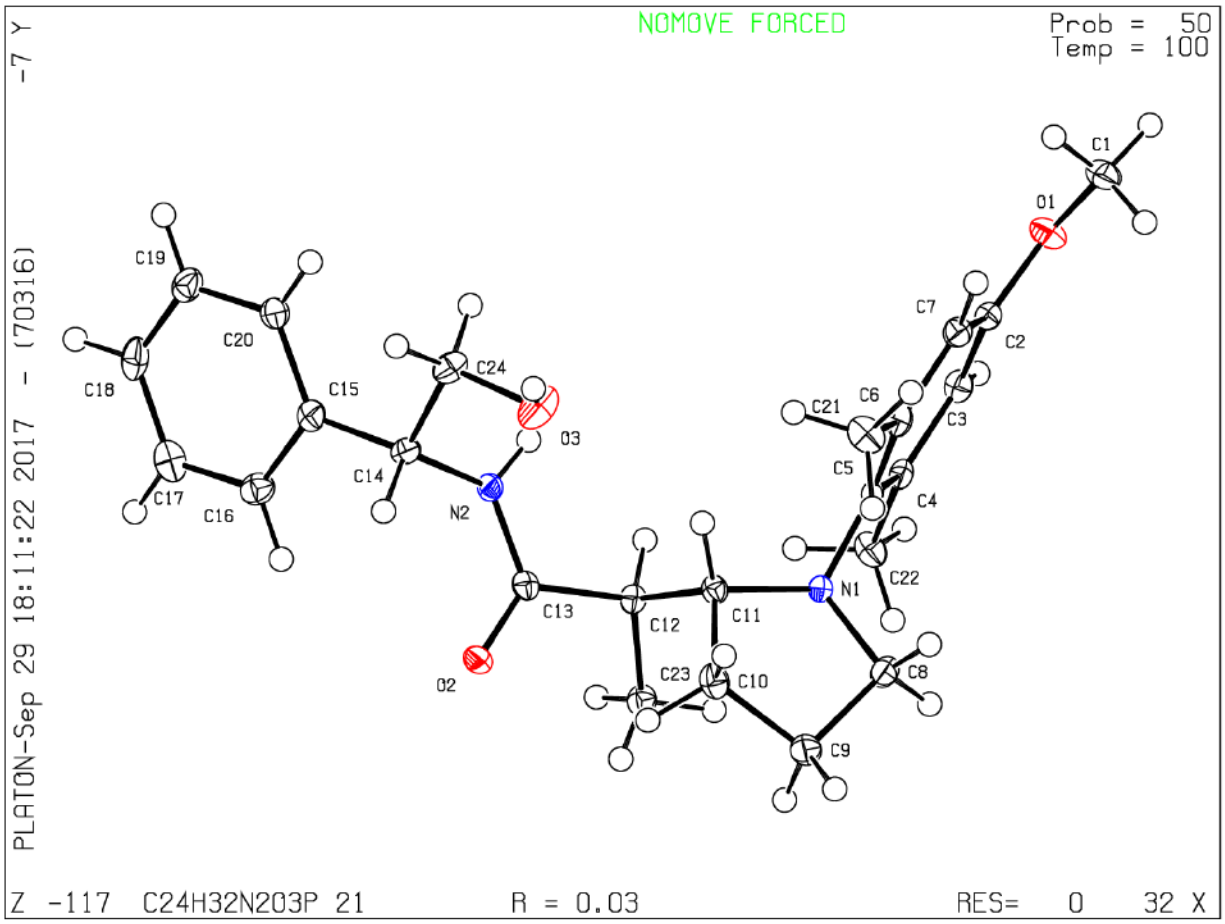

Table S2.12. Crystal data and structure refinement for $C_{24}H_{32}N_2O_3$.

Identification code	$C_{24}H_{32}N_2O_3$	
Empirical formula	C24 H32 N2 O3	
Formula weight	396.51	
Temperature	100(2) K	
Wavelength	1.54178 Å	
Crystal system	Monoclinic	
Space group	$P2_1$	
Unit cell dimensions	a = 9.6090(4) Å	a= 90°.

	b = 8.9512(4) Å	b= 101.0730(10)°.
	c = 12.4737(5) Å	g = 90°.
Volume	1052.92(8) $Å^3$	
Z	2	
Density (calculated)	1.251 Mg/m^3	
Absorption coefficient	0.653 mm^{-1}	
F(000)	428	
Crystal size	0.560 x 0.460 x 0.280 mm^3	
Theta range for data collection	3.611 to 66.644°.	
Index ranges	-11<=h<=11, -10<=k<=10, -14<=l<=14	
Reflections collected	19999	
Independent reflections	3701 [R(int) = 0.0307]	
Completeness to theta = 66.644°	99.2 %	
Absorption correction	Semi-empirical from equivalents	
Max. and min. transmission	0.7528 and 0.6460	
Refinement method	Full-matrix least-squares on F^2	
Data / restraints / parameters	3701 / 3 / 274	
Goodness-of-fit on F^2	1.062	
Final R indices [I>2sigma(I)]	R1 = 0.0265, wR2 = 0.0684	
R indices (all data)	R1 = 0.0265, wR2 = 0.0684	
Absolute structure parameter	0.00(4)	
Extinction coefficient	n/a	
Largest diff. peak and hole	0.202 and -0.152 $e.Å^{-3}$	

X-Ray Crystallography Data of 2.28-minor

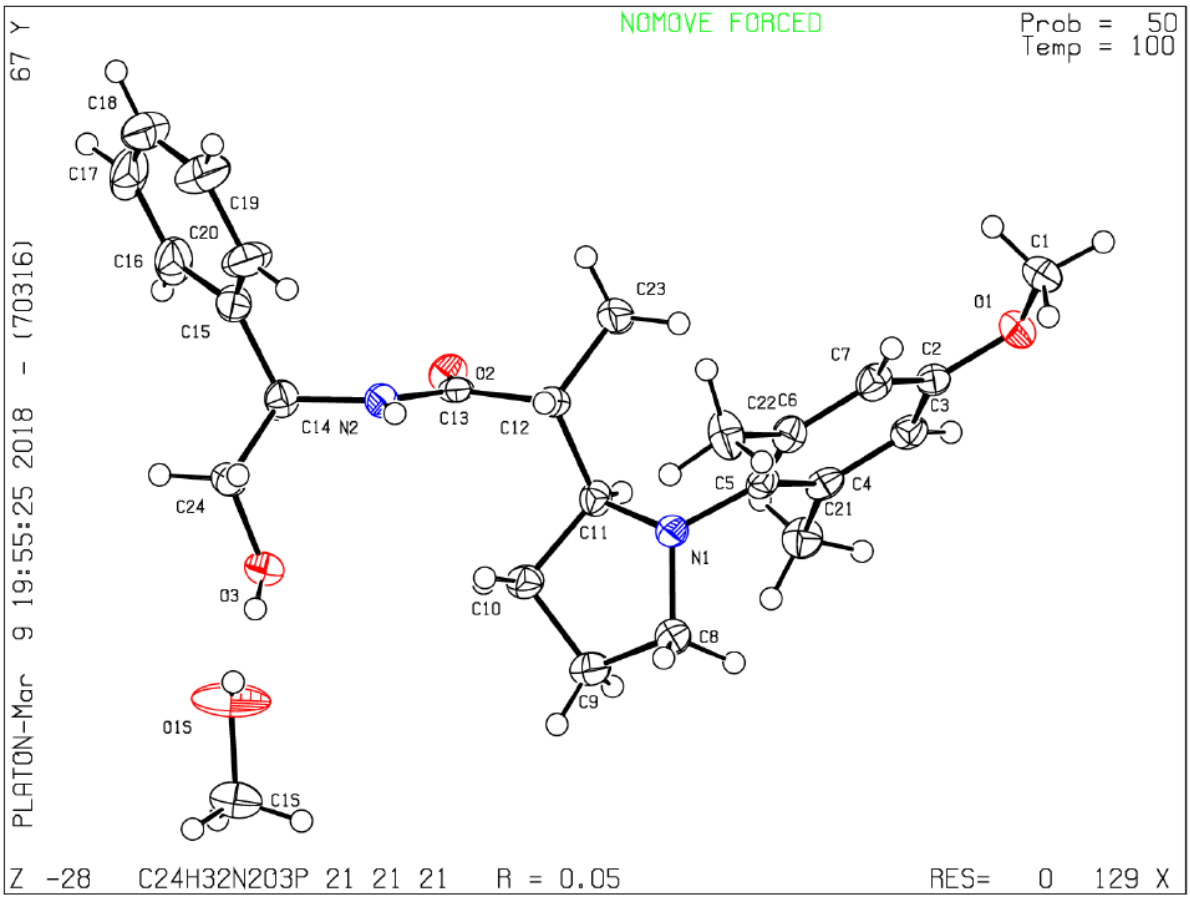

Table S2.13. Crystal data and structure refinement for $C_{24}H_{32}N_2O_3(CH_3OH)$.

Identification code	$C_{24}H_{32}N_2O_3(CH_3OH)$	
Empirical formula	C25 H36 N2 O4	
Formula weight	428.56	
Temperature	100(2) K	
Wavelength	1.54178 Å	
Crystal system	Orthorhombic	
Space group	$P2_12_12_1$	
Unit cell dimensions	a = 7.8167(3) Å	α= 90°.
	b = 15.1723(5) Å	β= 90°.

	c = 20.1325(7) Å γ = 90°.
Volume	2387.66(15) $Å^3$
Z	4
Density (calculated)	1.192 Mg/m^3
Absorption coefficient	0.642 mm^{-1}
F(000)	928
Crystal size	0.420 x 0.120 x 0.080 mm^3
Theta range for data collection	3.648 to 66.655°.
Index ranges	-9<=h<=9, -18<=k<=18, -23<=l<=23
Reflections collected	16235
Independent reflections	4210 [R(int) = 0.0707]
Completeness to theta = 66.655°	100.0 %
Absorption correction	Semi-empirical from equivalents
Max. and min. transmission	0.7533 and 0.5967
Refinement method	Full-matrix least-squares on F^2
Data / restraints / parameters	4210 / 3 / 291
Goodness-of-fit on F^2	1.026
Final R indices [I>2sigma(I)]	R1 = 0.0461, wR2 = 0.1154
R indices (all data)	R1 = 0.0574, wR2 = 0.1232
Absolute structure parameter	0.4(2)
Extinction coefficient	n/a
Largest diff. peak and hole	0.329 and -0.277 $e.Å^{-3}$

Appendix B. Experimental for Section 3.2

General Experimental Procedures

All reactions were performed in standard, oven-dried glassware fitted with rubber septa under an inert atmosphere of nitrogen unless otherwise described. Stainless steel syringes or cannulas were used to transfer air- and moisture-sensitive liquids. Reported concentrations refer to solution volumes at room temperature. Evaporation and concentration *in vacuo* were performed using house vacuum (ca. 40 mm Hg). Column chromatography was performed with SiliaFlash® 60 (40–63 micron) silica gel from Silicycle. Thin layer chromatography (TLC) was used for reaction monitoring and product detection using pre-coated glass plates covered with 0.25 mm silica gel with fluorescent indicator; visualization by UV light (λ_{ex} = 254 nm) or $KMnO_4$ stain.

Materials

Reagents were purchased in reagent grade from commercial suppliers and used without further purification, unless otherwise described. Amines were prepared according to the procedures reported previously[1-6]. Tris(pentafluorophenyl)borane was purchased from TCI and used without further purification. Acetone-d_6 was purchased from Cambridge Isotope Laboratory and used without further purification. H_2O, in synthetic procedures, refers to distilled water.

Instrumentation

Proton nuclear magnetic resonance (^{1}H NMR) spectra and proton-decoupled carbon nuclear magnetic resonance (^{13}C {^{1}H} NMR) spectra were recorded at 25 °C (unless stated otherwise) on Inova 600 (600 MHz) or Varian Unity/Inova 500 (500 MHz) or Oxford AS400 (400 MHz) spectrometers at the Boston College nuclear magnetic resonance facility. Chemical shifts for protons are reported in parts per million downfield from tetramethylsilane and are referenced to 0 ppm. Chemical shifts for carbon are reported in parts per million downfield from tetramethylsilane

and are referenced to the carbon resonances of the solvent. The peak positions are quoted to one decimal place unless they are indistinguishable. The solvent peak was referenced to 77.0 ppm for ^{13}C for $CDCl_3$. Benzotrifluoride was used as an external standard for ^{19}F NMR and referenced to -63.7 ppm. Data are represented as follows: chemical shift, integration, multiplicity (br = broad, s = singlet, d = doublet, t = triplet, q = quartet, m = multiplet), coupling constants in Hertz (Hz). Infrared spectra were recorded on a Bruker FT-IR Alpha (ATR mode) spectrophotometer. Data are represented as follows: frequency of absorption (cm^{-1}).

Optical rotations were measured using a 1 mL cell with a 5 cm path length on a Rudolph Research Analytical Autopol IV Polarimeter. Infrared spectra were recorded on a Bruker FT-IR Alpha (ATR mode) spectrophotometer. Data are represented as follows: frequency of absorption (cm^{-1}). High-resolution mass spectrometry was performed on a JEOL AccuTOF-DART (positive mode) at the Mass Spectrometry Facility, Boston College.

Determination of Deuterium Content

The amount of incorporated deuterium in a sample was quantified by mass spectrometry and by the decrease of ^1H NMR integral intensities at the specified positions compared to the starting material. Integral intensities were calibrated against hydrogen signals that do not undergo H/D-exchange. Mass spectrometry quantification was performed by subtraction of the mean molecular masses of the product and substrate isotopologue clusters in order to eliminate the contribution of the natural isotope abundance to the total mass. The mean molecular masses were calculated as the sum of the relative signal intensities of a given isotopologue multiplied with the corresponding m/z values derived from the mass spectrum.

Abbreviations Used

Bn = benzyl, Bzh= benzhydryl, DART = direct analysis in real time, DCM = dichloromethane, Et_3N = trimethylamine, Et_2O = diethyl ether, EtOAc = ethyl acetate, HR = high-resolution, LC = liquid chromatography, MS = mass spectrometry, PTLC = preparative thin layer chromatography, TBS = *tert*-butyldimethylsilyl, Tf = trifluromethanesulfonate, THF = tetrahydrofuran, TOF = time-of-flight.

B1. Substrate Preparation

Preparation of Amine Substrates

Table S3.1. List of Acyclic Amine Substrates

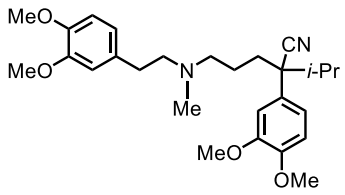	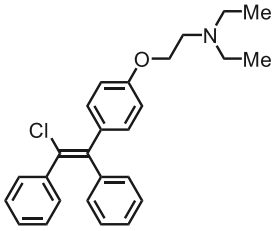	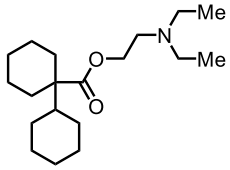
3.1a, verapamil	**3.1d**, clomiphene	**3.1e**, dicyclomine
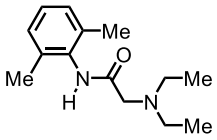	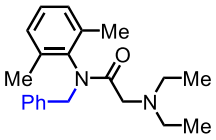	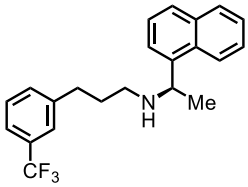
3.1f, lidocaine	**3.1g**, *N*-Bn lidocaine	**3.1h**, cinacalcet
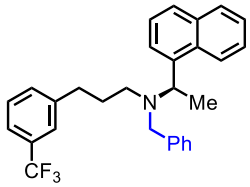	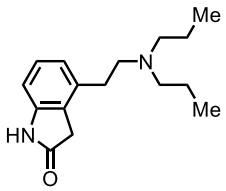	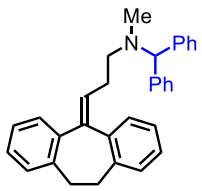
3.1i, *N*-Bn cinacalcet	**3.1j**, ropinirole	**3.1k**, *N*-Bzh nortriptyline
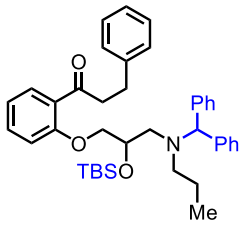		
3.1l, *N*-Bzh, *O*-TBS propafenone		

Amines **3.1a, 3.1d**, **3.1e**, **3.1h** and **3.1j** were obtained from free-basing commercially available amine salts and used without further purification.[1] Amine **3.1f** was obtained from commercial source and used without further purification. Amines **3.1g**,[2] **3.1i**,[3] **3.1k**[4] and **3.1l**[5] were prepared according to the literature procedures. The spectroscopic data are provided below.

Table S3.2. List of Cyclic Amine Substrates

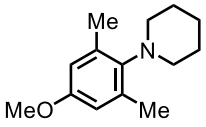

3.1b

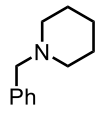

3.1c

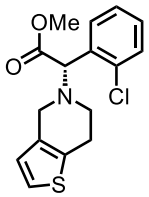

3.1m, clopidogrel

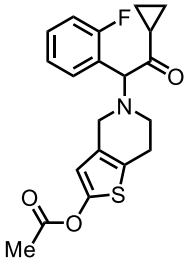

3.1n, prasugrel

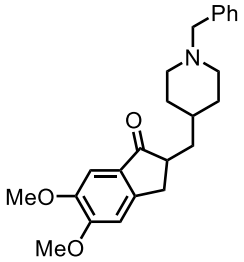

3.1o, donepezil

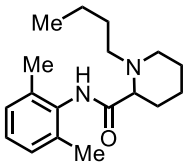

3.1p, bupivacaine

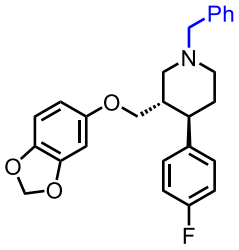

3.1q, *N*-Bn paroxetine

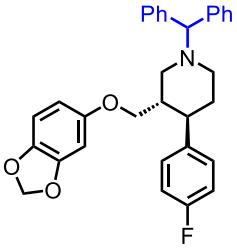

3.1r, *N*-Bzh paroxetine

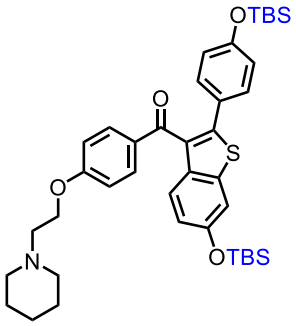

3.1s, *O*-TBS raloxifene

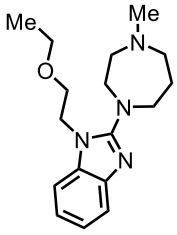

3.1t, emedastine

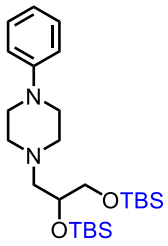

3.1u, *O*-TBS dropropizine

Amines **3.1b**, **3.1c**, **3.1q**,[3] **3.1r**,[4] **3.1s**,[5] and **3.1u**[6] were prepared according to the literature procedures. The spectroscopic data are provided below. Amines **3.1m**-**3.1p** were obtained from commercial source and used without further purification. Amine **3.1t** was obtained from free-basing commercially available amine salt and used without further purification.[1]

General Procedure for the Free-Basing Amine Salts[1]

To a 250 mL Erlenmeyer flask was added amine salt and DCM. 2.0 M NaOH (*aq*.) was added dropwise to the stirred solution until pH paper indicated that the aqueous layer is basic. The aqueous layer was extracted with DCM and the combined organic layers were dried with $MgSO_4$, filtered, and concentrated *in vacuo*. The resulting amine was used without further purification.

General Procedure A for the Alkylation of Amines[3]

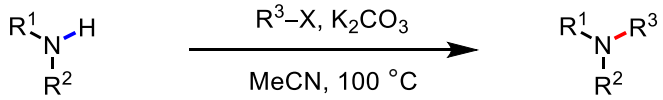

Amines **3.1i**, **3.1k** and **3.1q** were prepared by the alkylation of secondary amines. To a solution of amine (1.0 equiv.) and K_2CO_3 (5.0 equiv.) in MeCN was added alkyl halide (1.5 equiv.). The reaction mixture was then allowed heated to 100 °C for 12 hours. Upon completion (monitored by TLC), H_2O was added and the organic material was extracted with EtOAc. The combined organic layers were dried over $MgSO_4$, filtered, and concentrated *in vacuo*. The unpurified product mixture was subjected to silica gel chromatography.

General Procedure B for the Alkylation of Amines[4]

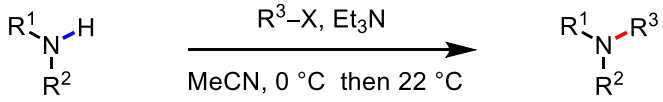

Amines **3.1l** and **3.1r** were prepared by the alkylation of secondary amines. To a solution of amine (1.0 equiv.) and alkyl halide (1.1 equiv.) in MeCN, Et_3N (3.0 equiv.) was added at 0 °C. The reaction mixture was then warmed up to 22 °C and allowed to stir for 12 hours. Upon completion (monitored by TLC), H_2O was added and the organic material was extracted with EtOAc. The

combined organic layers were dried over $MgSO_4$, filtered, and concentrated *in vacuo*. The unpurified product mixture was subjected to silica gel chromatography.

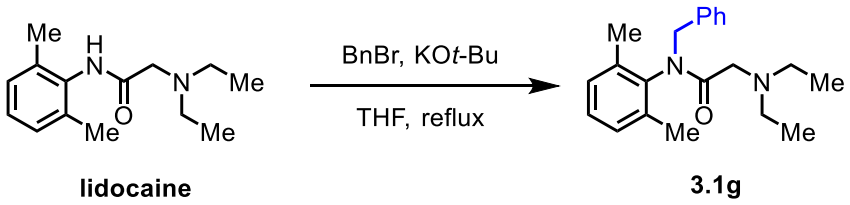

lidocaine **3.1g**

_N_-Bn lidocaine (3.1g)

N-Bn lidocaine was prepared following a known procedure.[2] To a solution of lidocaine (3.0 g, 12.8 mmol) in THF (45 mL) was added benzyl bromide (1.8 mL, 15.4 mmol). To the reaction mixture, KO*t*-Bu (2.9 g, 25.6 mmol) was then added portionwise and the reaction mixture was allowed to stir at reflux for 48 hours. The reaction mixture was then cooled and concentrated *in vacuo* to remove THF. To the mixture was added H_2O and was extracted with EtOAc. The combined organic layers were then dried over $MgSO_4$, filtered, and concentrated *in vacuo*. The unpurified product mixture was then subjected to silica gel column chromatography (MeOH:DCM = 1:99) to afford **3.1g** as a yellow liquid (2.5 g, 60%).

^{1}H NMR (600 MHz, $CDCl_3$) δ 7.25 – 7.16 (m, 5H), 7.12 (d, J = 7.5 Hz, 1H), 7.04 (d, J = 7.5 Hz, 2H), 4.73 (s, 2H), 2.80 (s, 2H), 2.57 (q, J = 7.1 Hz, 4H), 1.87 (s, 6H), 0.91 (t, J = 7.1 Hz, 6H); **^{13}C NMR** (151 MHz, $CDCl_3$) δ 170.6, 139.0, 137.1, 136.3, 128.9, 128.2, 128.0, 127.5, 54.6, 51.7, 47.4, 17.8, 12.0; **IR** (neat) 2964, 2926, 1653, 1466, 1453, 1400, 1385, 1258, 1242, 1195, 1078, 773, 743, 699 cm^{-1}.

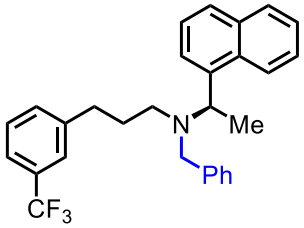

_N_-Bn cinacalcet (3.1i)

_N_-Bn cinacalcet was prepared following a General Procedure A for the Alkylation of Amines using cinacalcet hydrochloride (1.0 g, 2.5 mmol) and benzyl bromide. The unpurified product mixture was then subjected to silica gel column chromatography (EtOAc:hexanes = 1:4) to afford **3.1i** as a colorless liquid (0.9 g, 82%).

^{1}H NMR (600 MHz, $CDCl_3$) δ 8.26 (d, J = 8.0 Hz, 1H), 7.83 (d, J = 7.7 Hz, 1H), 7.74 (d, J = 8.1 Hz, 1H), 7.56 (d, J = 7.1 Hz, 1H), 7.50 – 7.38 (m, 3H), 7.35 (d, J = 7.6 Hz, 1H), 7.24 (t, J = 7.8 Hz, 6H), 7.12 (s, 1H), 6.96 (d, J = 7.4 Hz, 1H), 4.75 – 4.62 (m, 1H), 3.72 (d, J = 13.8 Hz, 1H), 3.63 (d, J = 13.8 Hz, 1H), 2.60 (s, 2H), 2.33 (d, J = 14.0 Hz, 1H), 2.26 (d, J = 13.9 Hz, 1H), 1.53 (d, J = 6.8 Hz, 5H); **^{13}C NMR** (126 MHz, $CDCl_3$) δ 143.4, 140.6, 140.0, 134.0, 132.1, 131.6, 130.5, 130.2, 129.0, 128.5, 128.4, 128.1, 127.6, 126.7, 125.33, 125.28, 125.0, 124.9, 124.6, 122.3, 56.4, 55.8, 49.8, 33.2, 29.0, 14.3; **^{19}F NMR** (470 MHz, $CDCl_3$) δ -62.40 (d, J = 3.0 Hz); **IR** (neat) 2968, 2939, 1492, 1327, 1160, 1120, 1072, 797, 778, 699 cm^{-1}.

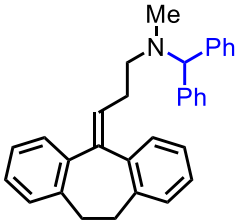

_N_-Bzh nortriptyline (3.1k)

N-Bzh nortriptyline was prepared following a General Procedure A for the Alkylation of Amines using nortriptyline hydrochloride (2.0 g, 6.7 mmol) and (bromomethylene)dibenzene. The unpurified product mixture was then subjected to silica gel column chromatography (Et_2O:hexanes = 1:49) to afford **3.1k** as a yellow liquid (2.2 g, 77%).

^{1}H NMR (500 MHz, $CDCl_3$) δ 7.35 (d, *J* = 7.6 Hz, 4H), 7.23 (dd, *J* = 8.3, 6.9 Hz, 5H), 7.20 – 7.09 (m, 7H), 7.09 – 7.05 (m, 1H), 7.02 (dd, *J* = 5.3, 3.8 Hz, 1H), 5.82 (t, *J* = 7.5 Hz, 1H), 4.31 (s, 1H), 3.30 (s, 2H), 2.94 (s, 1H), 2.71 (s, 1H), 2.46 (d, *J* = 8.7 Hz, 2H), 2.32 (dd, *J* = 15.7, 8.4 Hz, 2H), 2.07 (s, 3H); **^{13}C NMR** (126 MHz, $CDCl_3$) δ 143.20, 143.17, 141.4, 140.1, 139.4, 137.0, 129.9, 129.8, 129.0, 128.5, 128.3, 127.9, 127.3, 126.9, 126.7, 125.9, 125.7, 75.6, 55.0, 40.2, 33.7, 32.0, 27.2; **IR** (neat) 3061, 3020, 1485, 1451, 1278, 1079, 756, 743, 704 cm^{-1}.

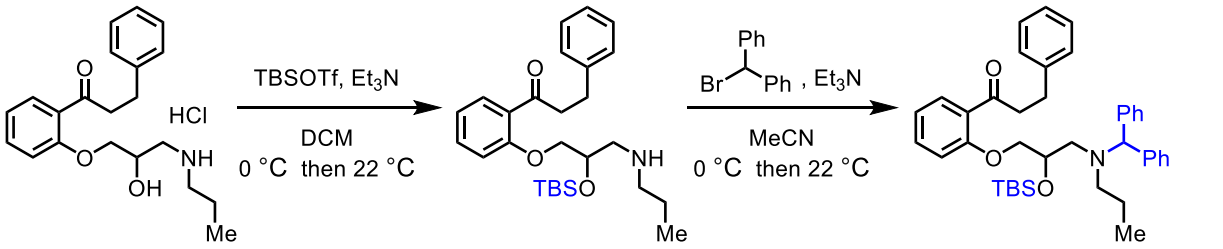

_O_-TBS propafenone

_O_-TBS propafenone was prepared following the known procedure.[5] To a solution of propafenone HCl (2.0 g, 5.29 mmol) in DCM at 0 °C, imidazole (5.0 equiv.) was added, followed by the dropwise addition of TBSCl (1.3 equiv.). After the addition, the reaction mixture was allowed to warm to 22 °C and stirred for 12 hours. Upon completion (monitored by TLC), H_2O was added and the organic material was then extracted with DCM. The combined organic layers were dried over $MgSO_4$, filtered, and concentrated *in vacuo*. The unpurified product mixture was subjected to silica gel column chromatography (MeOH:DCM = 1:19) to afford _O_-TBS propafenone as a colorless liquid (2.0 g, 83%).

_N_-Bzh, _O_-TBS propafenone (3.1l)

_N_-Bzh, _O_-TBS propafenone was prepared following the General Procedure B for the Alkylation of Amines using _O_-TBS propafenone (2.0 g, 4.4 mmol) and (bromomethylene)dibenzene. The unpurified product mixture was subjected to silica gel column chromatography (Et_2O:hexanes = 1:19) to afford **3.1l** as a colorless liquid (2.2 g, 81%).

^{1}H NMR (600 MHz, $CDCl_3$) δ 7.72 (d, J = 9.5 Hz, 1H), 7.47 – 7.40 (m, 1H), 7.25 (dd, J = 25.5, 8.1 Hz, 6H), 7.14 (dt, J = 15.4, 7.7 Hz, 9H), 7.03 – 6.92 (m, 2H), 4.82 (s, 1H), 4.18 (dd, J = 9.5, 3.8 Hz, 1H), 4.10 (dd, J = 9.5, 3.3 Hz, 1H), 3.92 (d, J = 4.3 Hz, 1H), 3.36 – 3.16 (m, 1H), 3.08 –

2.99 (m, 1H), 2.98 – 2.84 (m, 2H), 2.79 (dd, J = 13.5, 9.0 Hz, 1H), 2.55 (dd, J = 13.5, 4.7 Hz, 1H), 2.45 (d, J = 6.0 Hz, 2H), 1.43 (d, J = 7.4 Hz, 2H), 0.79 (s, 9H), 0.71 (t, J = 7.3 Hz, 3H), -0.06 (s, 3H), -0.09 (s, 3H); **^{13}C NMR** (126 MHz, $CDCl_3$) δ 201.2, 158.2, 142.1, 141.7, 141.5, 133.3, 130.5, 128.8, 128.7, 128.4, 128.3, 128.2, 128.2, 128.1, 126.91, 126.88, 125.7, 120.5, 112.3, 71.2, 70.5, 69.9, 54.2, 54.0, 45.4, 30.0, 25.7, 19.4, 17.9, 11.7, -4.7, -4.8; **IR** (neat) 2953, 2926, 1671, 1595, 1578, 1469, 1248, 1110, 838, 752, 698 cm^{-1}.

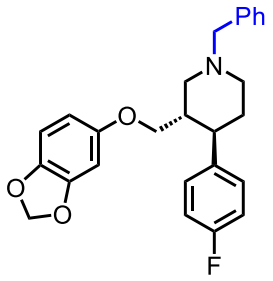

_N_-Bn paroxetine (3.1q)

_N_-Bn paroxetine was prepared following the General Procedure A for the Alkylation of Amines using paroxetine hydrochloride (3.0 g, 8.2 mmol) and benzyl bromide. The unpurified product was subjected to silica gel column chromatography (EtOAc:hexanes = 1:9) to afford **3.1q** as a white solid (2.9 g, 84%).

^{1}H NMR (500 MHz, $CDCl_3$) δ 7.40 – 7.30 (m, 4H), 7.25 (s, 1H), 7.16 (dd, J = 8.6, 5.5 Hz, 2H), 6.96 (t, J = 8.7 Hz, 2H), 6.61 (d, J = 8.4 Hz, 1H), 6.31 (d, J = 2.5 Hz, 1H), 6.10 (dd, J = 8.5, 2.5 Hz, 1H), 5.87 (s, 2H), 3.64 (d, J = 13.1 Hz, 1H), 3.59 – 3.50 (m, 2H), 3.44 (d, J = 6.9 Hz, 1H), 3.04 – 2.96 (m, 1H), 2.55 – 2.42 (m, 1H), 2.27 – 2.14 (m, 1H), 2.12 – 2.01 (m, 2H), 1.90 – 1.73 (m, 2H); **^{13}C NMR** (126 MHz, $CDCl_3$) δ 162.4, 160.5, 154.4, 148.1, 141.5, 139.9, 139.8, 138.3, 129.2, 128.9, 128.8, 128.2, 127.0, 115.4, 115.2, 107.8, 105.6, 101.0, 98.0, 69.7, 63.4, 57.6, 53.8, 44.1, 42.2, 34.4; **^{19}F NMR** (470 MHz, $CDCl_3$) δ -116.71 (d, J = 7.5 Hz); **IR** (neat) 2912, 1602, 1506, 1485, 1221, 1181, 1132, 1036, 933, 831, 781, 738 cm^{-1}.

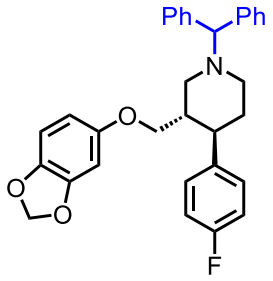

_N_-Bzh paroxetine (3.1r)

_N_-Bzh paroxetine was prepared following the General Procedure B for the Alkylation of Amines using paroxetine hydrochloride (3.0 g, 8.2 mmol), (bromomethylene)dibenzene. The unpurified product was subjected to silica gel column chromatography (Et_2O:hexanes = 1:9) to afford **3.1r** as a white solid (3.5 g, 86%).

^{1}H NMR (500 MHz, $CDCl_3$) δ 7.52 – 7.35 (m, 4H), 7.28 (t, J = 7.5 Hz, 4H), 7.17 (dt, J = 8.5, 6.4 Hz, 5H), 6.96 (t, J = 8.6 Hz, 2H), 6.57 (d, J = 8.5 Hz, 1H), 6.21 (d, J = 2.5 Hz, 1H), 6.01 (dd, J = 8.5, 2.5 Hz, 1H), 5.85 (d, J = 0.9 Hz, 2H), 4.37 (s, 1H), 3.50 (dd, J = 9.5, 2.9 Hz, 1H), 3.38 (dd, J = 9.5, 6.7 Hz, 1H), 3.23 (dd, J = 11.4, 2.9 Hz, 1H), 3.08 – 2.89 (m, 1H), 2.47 (dd, J = 11.6, 4.2 Hz, 1H), 2.22 (s, 1H), 2.06 – 1.81 (m, 3H), 1.77 (d, J = 3.6 Hz, 1H); **^{13}C NMR** (126 MHz, $CDCl_3$) δ 162.5, 160.5, 154.3, 148.1, 142.81, 142.78, 141.5, 140.1, 140.0, 128.9, 128.8, 128.44, 128.43, 128.1, 127.9, 126.9, 115.4, 115.2, 107.8, 105.7, 101.0, 98.1, 76.1, 69.6, 56.0, 52.5, 44.2, 42.5, 34.6; **^{19}F NMR** (470 MHz, $CDCl_3$) δ -116.74 (ddd, J = 14.0, 8.9, 5.3 Hz); **IR** (neat) 2912, 1506, 1485, 1466, 1336, 1268, 1222, 1037, 815, 705 cm^{-1}.

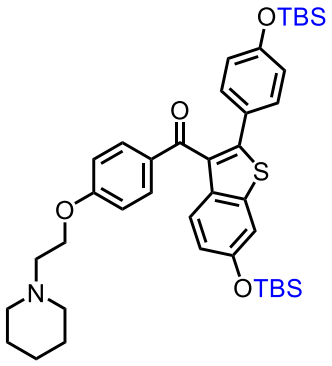

_O_-TBS raloxifene (3.1s)

O-TBS raloxifene was prepared following the known procedure.[5] To a solution of raloxifene HCl (2.0 g, 3.9 mmol) in DCM at 0 °C, imidazole (5.0 equiv.) was added, followed by the dropwise addition of TBSCl (2.6 equiv.). After the addition, the reaction mixture was allowed to warm to 22 °C and stirred for 12 hours. Upon completion (monitored by TLC), H_2O was added and the organic material was then extracted with DCM. The combined organic layers were dried over $MgSO_4$, filtered, and concentrated *in vacuo*. The unpurified product mixture was then subjected to silica gel column chromatography (MeOH:DCM = 1:49) to afford **3.1s** as a colorless liquid (2.0 g, 73%). **^{1}H NMR** (500 MHz, $CDCl_3$) δ 7.73 (d, J = 8.8 Hz, 2H), 7.56 (s, 1H), 7.32 – 7.22 (m, 3H), 6.89 (s, 1H), 6.73 (d, J = 8.9 Hz, 2H), 6.66 (d, J = 8.6 Hz, 2H), 4.05 (t, J = 6.0 Hz, 2H), 2.72 (t, J = 6.0 Hz, 2H), 2.47 (s, 4H), 1.58 (p, J = 5.6 Hz, 4H), 1.46 – 1.39 (m, 2H), 1.01 (s, 9H), 0.93 (s, 9H), 0.23 (s, 6H), 0.12 (s, 6H); **^{13}C NMR** (126 MHz, $CDCl_3$) δ 193.1, 162.9, 156.1, 153.5, 143.3, 139.9, 134.5, 132.3, 130.6, 130.5, 130.3, 126.8, 124.0, 120.3, 119.2, 114.0, 112.1, 66.1, 57.7, 55.1, 25.9, 25.7, 25.6, 24.1, 18.24, 18.19, -4.4, -4.5; **IR** (neat) 2927, 2891, 1596, 1464, 1255, 1164, 943, 909, 837, 780 cm^{-1}.

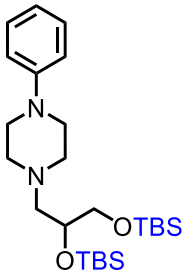

***O*-TBS dropropizine (3.1u)**

O-TBS dropropizine was prepared following the known procedure.[6] To a solution of dropropizine (1.2 g, 5.0 mmol) in DCM at 0 °C, Et_3N (2.6 equiv.) was added, followed by the dropwise addition of TBSOTf (2.6 equiv.). After the addition, the reaction mixture was allowed to warm to 22 °C and stirred for 12 hours. Upon completion (monitored by TLC), H_2O was added and the organic material was then extracted with DCM. The combined organic layers were dried over $MgSO_4$, filtered, and concentrated *in vacuo*. The unpurified product mixture was then subjected to silica gel column chromatography (MeOH:DCM = 1:99) to afford **3.1u** as a colorless liquid (1.6 g, 69%). **^{1}H NMR** (600 MHz, $CDCl_3$) δ 7.25 (dd, *J* = 8.8, 7.2 Hz, 2H), 6.95 – 6.88 (m, 2H), 6.83 (d, *J* = 7.3 Hz, 1H), 3.80 (d, *J* = 5.1 Hz, 1H), 3.61 (dd, *J* = 10.0, 5.7 Hz, 1H), 3.53 (dd, *J* = 10.0, 5.6 Hz, 1H), 3.17 (t, *J* = 5.0 Hz, 4H), 2.72 – 2.64 (m, 2H), 2.64 – 2.57 (m, 2H), 2.50 (dd, *J* = 13.0, 4.8 Hz, 1H), 2.38 (dd, *J* = 13.0, 6.1 Hz, 1H), 0.90 (d, *J* = 5.1 Hz, 18H), 0.09 (d, *J* = 7.5 Hz, 6H), 0.06 (d, *J* = 1.8 Hz, 6H); **^{13}C NMR** (126 MHz, $CDCl_3$) δ 151.5, 129.0, 119.4, 115.9, 71.8, 66.2, 62.0, 54.3, 49.2, 26.0, 25.9, 18.4, 18.2, -4.4, -4.5, -5.26, -5.34; **IR** (neat) 2925, 2853, 1598, 1500, 1460, 1229, 1107, 1082, 989, 829, 772 cm^{-1}.

Preparation of α-Deuterated Ketone Substrates

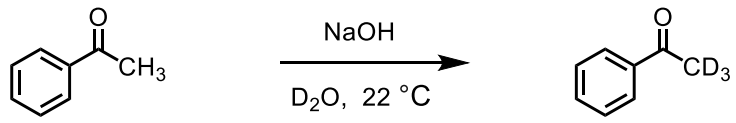

acetophenone **acetophenone-d_3**

Acetophenone-d_3

Acetophenone-d_3 was synthesized following the known procedure.[7] Acetophenone (5.8 g, 48 mmol), NaOH (0.16 g, 4.0 mmol) and D_2O (32 mL) was allowed to stir at 22 °C for 24 hours under nitrogen. The reaction mixture was diluted with diethyl ether. The aqueous layer was extracted with diethyl ether. The combined organic layer was dried over $MgSO_4$, filtered and concentrated *in vacuo*. The unpurified product mixture was subjected to silica gel column chromatography using hexanes as elute to afford the acetophenone-d_3 as colorless liquid (4.9 g, 97%D, 84% yield). The spectroscopic data matched those reported by Zhou.[7]

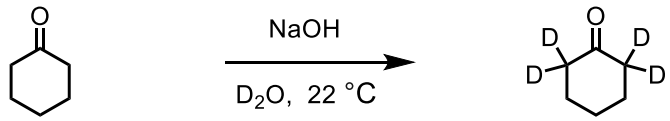

cyclohexanone **cyclohexa-1-one-2,2,6,6,-d_4**

Cyclohexan-1-one-2,2,6,6-d_4

Cyclohexan-1-one-2,2,6,6-d_4 was synthesized following the known procedure.[7] Cyclohexanone (5.2 mL, 50 mmol), NaOH (0.16 g, 1.0 mmol) and D_2O (32 mL) was allowed to stir at 22 °C for 24 hours under nitrogen. The reaction mixture was diluted with diethyl ether. The aqueous layer was extracted with diethyl ether. The combined organic layer was dried over $MgSO_4$, filtered and concentrated *in vacuo*. The unpurified product mixture was distilled (40 mmHg, 40 °C) to afford

the cyclohexan-1-one-2,2,6,6-d_4 as colorless liquid (4.0 g, 95%D, 78% yield). The spectroscopic data matched those reported by Chang.[8]

B2. Optimization Studies

Evaluation of Reaction Conditions for $B(C_6F_5)_3$-Catalyzed β-Deuteration Involving Verapamil

Experimental Procedure for the Evaluation of Reaction Parameters (see Table 3.3 in the Manuscript)

To a 15 mL oven-dried pressure vessel was added verapamil **3.1a** (0.1 mmol), Lewis acid (5.0 mol% or 10 mol%), Brønsted base (10 mol%), toluene (0.4 mL), and acetone-d_6 (0.68 mmol) under a nitrogen atmosphere. The reaction mixture was allowed to stir for 1 hour at 100 °C, 125 °C, or 150 °C. Upon completion, the reaction mixture was concentrated *in vacuo*. The product yield and deuterium incorporation rate were determined by the ^{1}H NMR analysis of the unpurified product mixtures using mesitylene as the internal standard.

Experimental Procedure for the Evaluation of Solvents (see Table S3.3)

To a 15 mL oven-dried pressure vessel was added verapamil **3.1a** (0.1 mmol), $B(C_6F_5)_3$ (10 mol%), solvent (0.4 mL), and acetone-d_6 (6.8 equiv.) under a nitrogen atmosphere. The reaction mixture was allowed to stir for 1 hour at 150 °C. Upon completion, the reaction mixture was concentrated *in vacuo*. The product yield and deuterium incorporation rate were determined by the ^{1}H NMR analysis of the unpurified product mixtures using mesitylene as the internal standard.

Table S3.3. Evaluation of Solvents Involving Verapamil **3.1a**

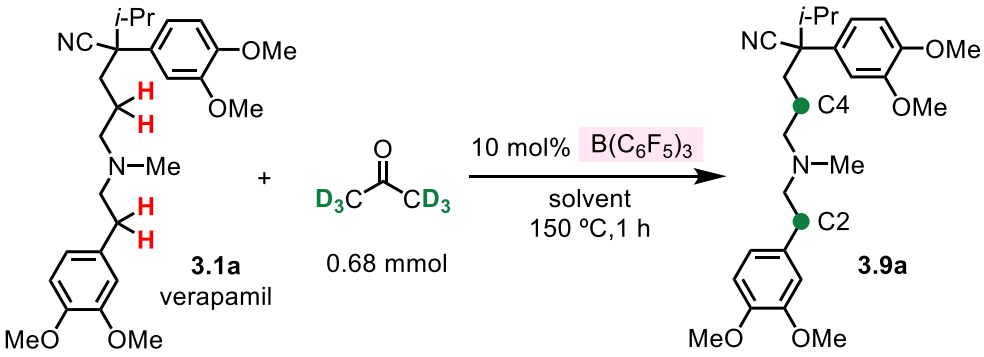

entry	solvent	*d*-incorporation (%)	
		[C2]	[C4]
1	toluene	90	92
2	benzene	84	91
3	$ClCH_2CH_2Cl$	78	90
4	$CHCl_3$	71	85
5	Et_2O	14	24
6	THF	<5	<5

Conditions: verapamil (**3.1a**, 0.1 mmol), $B(C_6F_5)_3$ (10 mol%), solvent (0.4 mL), acetone-d_6 (0.68 mmol) under N_2, 150 ºC. Yield and deuterium incorporation rate was determined by ^1H NMR analysis of unpurified reaction mixtures with mesitylene as the internal standard.

Experimental Procedure for the Evaluation of Deuterium Sources (see Table S3.4)

To a 15 mL oven-dried pressure vessel was added verapamil **3.1a** (0.1 mmol), $B(C_6F_5)_3$ (10 mol%), toluene (0.4 mL), and *d*-source (6.8 equiv. or 40.8 equiv.) under a nitrogen atmosphere. The reaction mixture was allowed to stir for 12 hours at 150 °C. Upon completion, the reaction mixture was concentrated *in vacuo*. The product yield and deuterium incorporation rate were determined by the ^1H NMR analysis of the unpurified product mixtures using mesitylene as the internal standard.

Table S3.4. Evaluation of Deuterium Sources Involving Verapamil **3.1a**

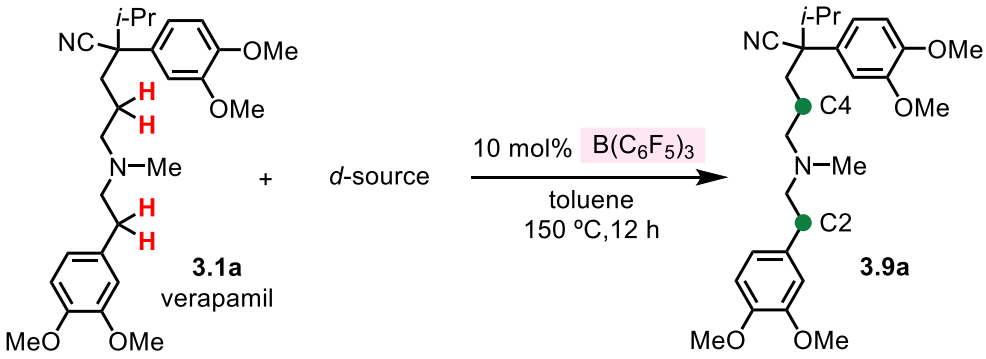

entry	*d*-source	equiv. (D equiv.)	*d*-incorporation (%) [C2]	[C4]
1	acetone-d_6	6.8 (40.8)	90	92
2	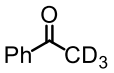	6.8 (20.4)	79	71
3	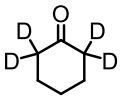	6.8 (27.2)	45	50
4	CH_3OD	6.8 (6.8)	14	20
5	$(CD_3)_2CDOD$	6.8 (6.8)	17	21
6	*t*-BuOD	6.8 (6.8)	63	58
7	*t*-BuOD	40.8 (40.8)	0	0

Conditions: verapamil (**3.1a**, 0.1 mmol), $B(C_6F_5)_3$ (10 mol%), toluene (0.4 mL), *d*-source under N_2, 150 °C. Yield and deuterium incorporation rate was determined by ^1H NMR analysis of unpurified reaction mixtures with mesitylene as the internal standard.

Experimental Procedure for the Evaluation of Acetone-d_6 Equivalence (see Table S3.5)

To a 15 mL oven-dried pressure vessel was added verapamil **3.1a** (0.3 mmol), $B(C_6F_5)_3$ (2.5 mol%), toluene (1.2 mL), and acetone-d_6 (2.0–10 equiv.) under a nitrogen atmosphere. The reaction mixture was allowed to stir for 1 hour at 150 °C. Upon completion, the reaction mixture was concentrated *in vacuo*. The product yield and deuterium incorporation rate were determined by the ^{1}H NMR analysis of the unpurified product mixtures using mesitylene as the internal standard.

Table S3.5. Evaluation of Acetone-d_6 Equivalence Involving Verapamil **3.1a**

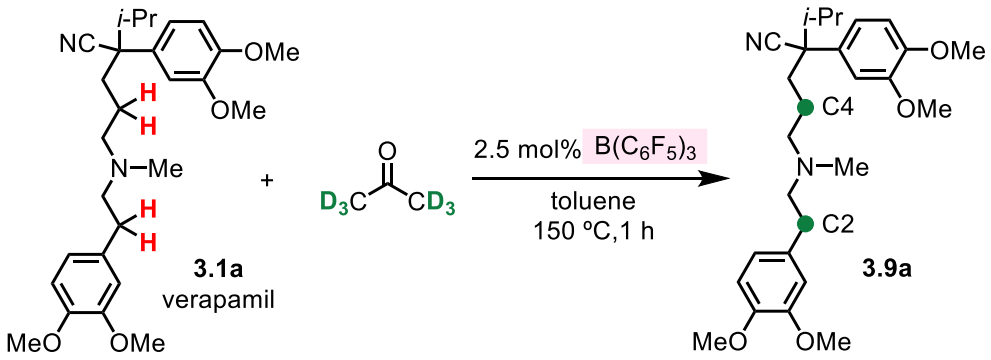

entry	equiv. of acetone-d_6	*d*-incorporation (%)	
		[C2]	[C4]
1	2.0	47	60
2	4.0	72	82
3	6.8	80	86
4	10	70	85

Conditions: verapamil (**3.1a**, 0.3 mmol), $B(C_6F_5)_3$ (2.5 mol%), toluene (1.2 mL), acetone-d_6 under N_2, 150 ºC. Yield and deuterium incorporation rate was determined by ^{1}H NMR analysis of unpurified reaction mixtures with mesitylene as the internal standard.

B3. General Procedures for *β*-Deuteration of *N*-Alkylamines

General Procedure A for the *β*-Deuteration of *N*-Alkylamines (See Tables 3.4–3.5 in the Manuscript)

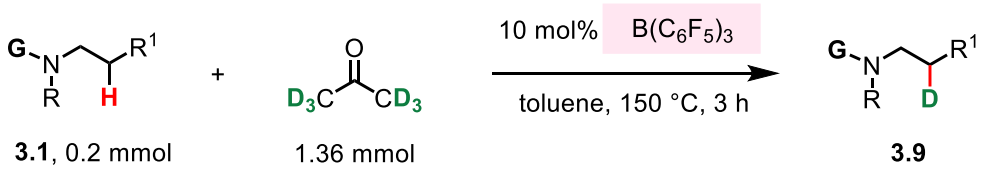

To a 15 mL oven-dried pressure vessel was added amine **3.1** (0.2 mmol), $B(C_6F_5)_3$ (10 mol%), toluene (0.8 mL), and acetone-d_6 (1.36 mmol, 6.8 equiv.) under a nitrogen atmosphere. The reaction mixture was allowed to stir for 3 hours at 150 °C. Upon completion, the reaction mixture was concentrated *in vacuo* and purified by silica gel column chromatography.

General Procedure B for the *β*-Deuteration of *N*-Alkylamines (See Tables 3.4–3.5 in the Manuscript)

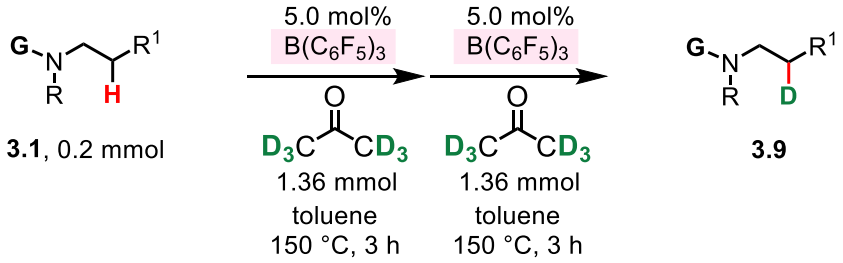

To a 15 mL oven-dried pressure vessel was added amine **3.1** (0.2 mmol), $B(C_6F_5)_3$ (5.0 mol%), toluene (0.8 mL), and acetone-d_6 (1.36 mmol, 6.8 equiv.) under a nitrogen atmosphere. The reaction mixture was allowed to stir for 3 hours at 150 °C. After the purification by silica gel column chromatography and removal of volatiles, $B(C_6F_5)_3$ (5.0 mol%), toluene (0.8 mL), and acetone-d_6 (1.36 mmol, 6.8 equiv.) were added under a nitrogen atmosphere and was allowed to

stir for 3 hours at 150 °C. Upon completion, the reaction mixture was concentrated *in vacuo* and purified by silica gel column chromatography.

General Procedure C for the *β*-Deuteration of *N*-Alkylamines (See Tables 3.4–3.5 in the Manuscript)

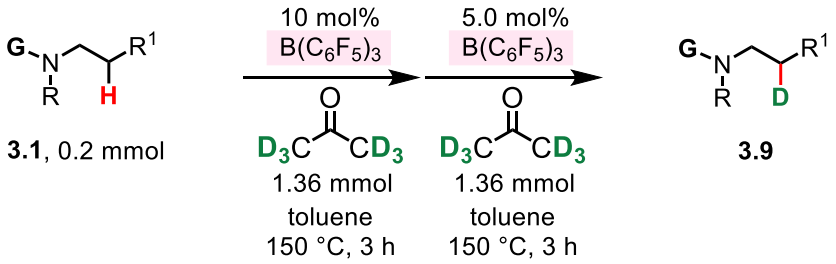

To a 15 mL oven-dried pressure vessel was added amine **3.1** (0.2 mmol), $B(C_6F_5)_3$ (10 mol%), toluene (0.8 mL), and acetone-d_6 (1.36 mmol, 6.8 equiv.) under a nitrogen atmosphere. The reaction mixture was allowed to stir for 3 hours at 150 °C. After the purification by silica gel column chromatography and removal of volatiles, $B(C_6F_5)_3$ (5.0 mol%), toluene (0.8 mL), and acetone-d_6 (1.36 mmol, 6.8 equiv.) were added under a nitrogen atmosphere and was allowed to stir for 3 hours at 150 °C. Upon completion, the reaction mixture was concentrated *in vacuo* and purified by silica gel column chromatography.

Procedure for Scale-Up Reaction (See Scheme 3.10 in the Manuscript)

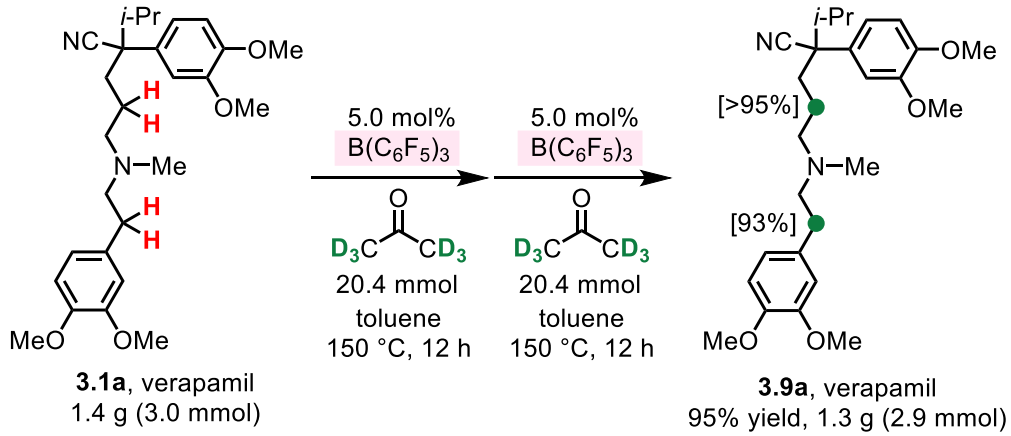

3.1a, verapamil
1.4 g (3.0 mmol)

3.9a, verapamil
95% yield, 1.3 g (2.9 mmol)

To a 100 mL oven-dried Schlenk flask was added amine **3.1a** (3.0 mmol), $B(C_6F_5)_3$ (5.0 mol%), toluene (12 mL), and acetone-d_6 (20.4 mmol, 6.8 equiv.) under a nitrogen atmosphere. The reaction mixture was allowed to stir for 12 hours at 150 °C. After the purification by silica gel column chromatography and removal of volatiles, $B(C_6F_5)_3$ (5.0 mol%), toluene (12 mL), and acetone-d_6 (20.4 mmol, 6.8 equiv.) were added under a nitrogen atmosphere and was allowed to stir for 12 hours at 150 °C. Upon completion, the reaction mixture was concentrated *in vacuo* and purified by silica gel column chromatography (MeOH:DCM = 1:49) to afford **3.9a** as a yellow liquid (1.29 g, 95%).

B4. Analytical Data and Spectra

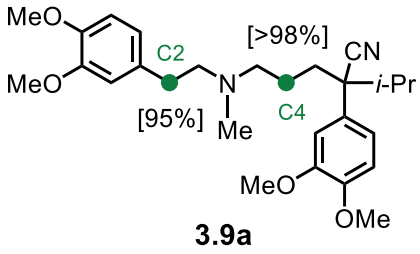

3.9a

Verapamil, 3.9a

Verapamil **3.1a** was reacted with acetone-d_6 following the General Procedure B. After purification by column chromatography (MeOH:DCM = 1:49), **3.9a** was obtained as a yellow liquid (84 mg, 92%).

Deuterium incorporation: 3.86 D/molecule (^{1}H NMR), 4.11 D/molecule [HRMS (DART)]

^{1}H NMR (600 MHz, $CDCl_3$) δ 6.91 (dd, J = 8.4, 2.2 Hz, 1H), 6.88 – 6.81 (m, 2H), 6.79 (d, J = 7.9 Hz, 1H), 6.69 (d, J = 7.8 Hz, 2H), 3.94 – 3.76 (m, 12H), 2.73 – 2.60 (m, 0.11H, 95%D), 2.56 – 2.46 (m, 2H), 2.44 – 2.29 (m, 2H), 2.20 (s, 3H), 2.15 – 1.99 (m, 2H), 1.84 (d, J = 13.7 Hz, 1H), 1.58 – 1.49 (m, 0.02H, 99%D), 0.79 (d, J = 6.7 Hz, 3.05H, 98%D); **^{13}C NMR** (151 MHz, $CDCl_3$) δ 148.9, 148.7, 148.2, 147.2, 132.5, 130.5, 121.3, 120.4, 118.6, 111.9, 111.2, 111.0, 109.5, 59.0, 56.5, 55.9, 55.8, 55.73, 55.71, 53.2, 41.7, 37.8, 35.2, 32.1, 22.3, 18.8, 18.5; **IR** (neat) 2933, 1512, 1460, 1411, 1258, 1237, 1162, 1141, 1024, 804, 764 cm^{-1}.

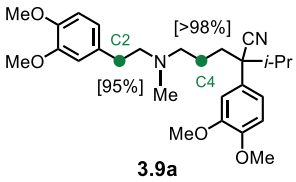
MeO
MeO
C2
[95%]
N
Me
[>98%]
C4
CN
i-Pr
MeO
OMe

3.9a

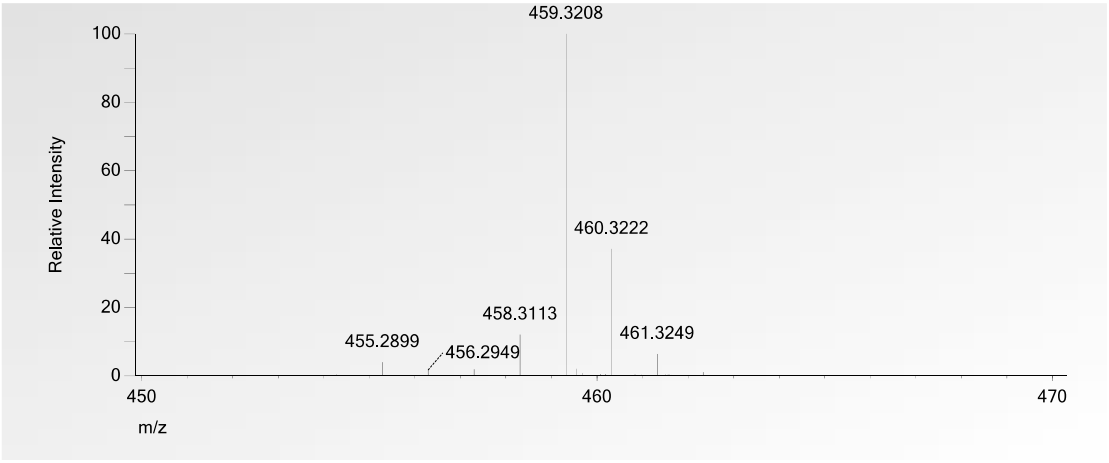
459.3208
100
80
60
40
20
0
Relative Intensity
460.3222
458.3113
461.3249
455.2899
456.2949
450
460
470
m/z

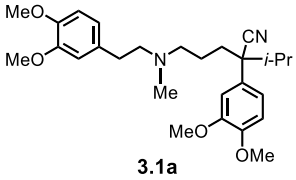
MeO
MeO
N
Me
CN
i-Pr
MeO
OMe

3.1a

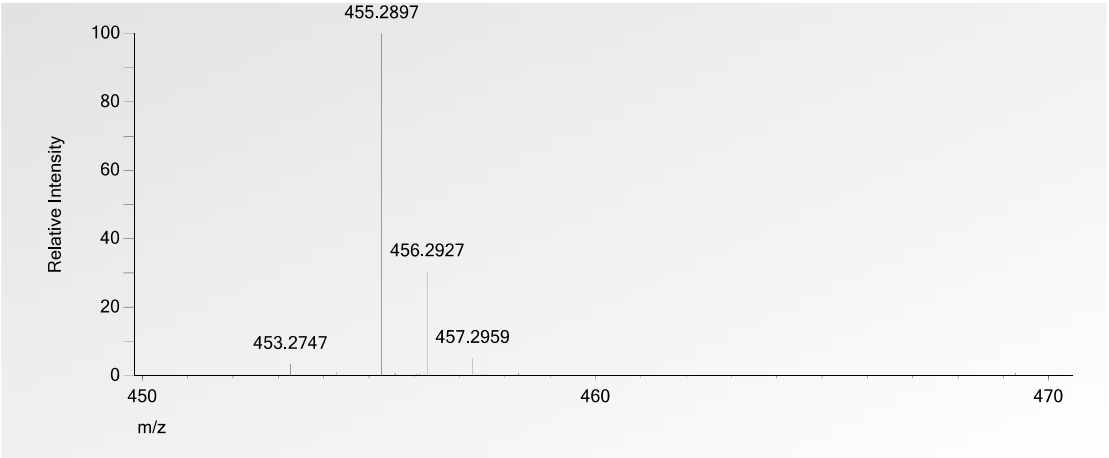
455.2897
100
80
60
40
20
0
Relative Intensity
456.2927
453.2747
457.2959
450
460
470
m/z

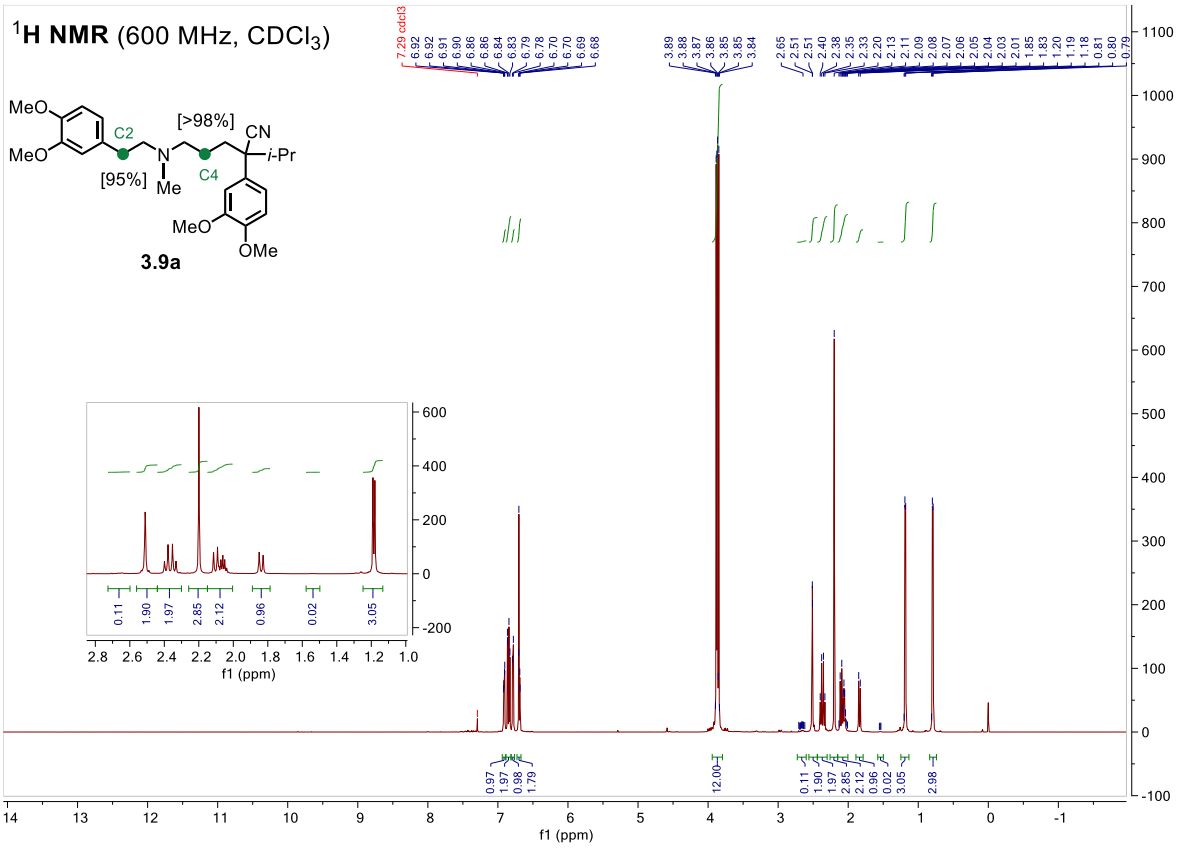
^{1}H NMR (600 MHz, $CDCl_3$)
MeO
MeO
C2
[95%]
N
Me
[>98%]
C4
CN
i-Pr
MeO
OMe
3.9a
f1 (ppm)

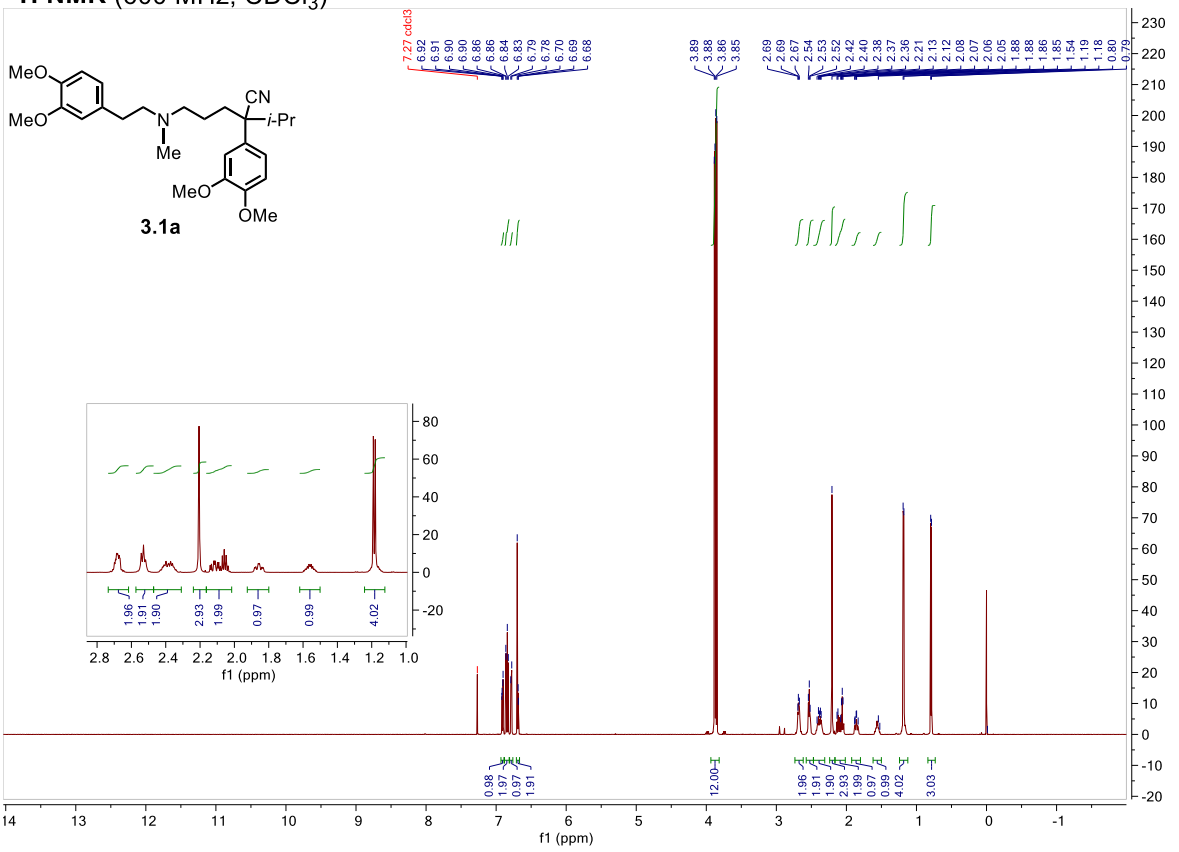
^{1}H NMR (600 MHz, $CDCl_3$)
MeO
MeO
N
Me
CN
i-Pr
MeO
OMe
3.1a
f1 (ppm)

^{13}C NMR (151 MHz, $CDCl_3$)

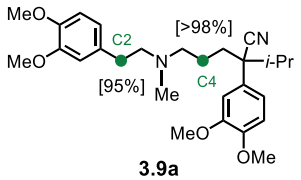

3.9a

^{13}C NMR (126 MHz, $CDCl_3$)

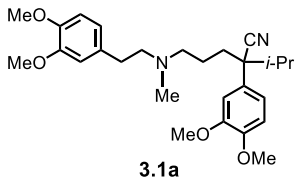

3.1a

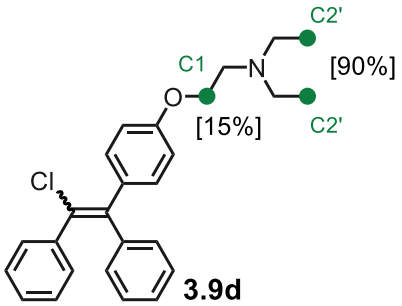

3.9d

Clomiphene, 3.9d

Clomiphene **3.1d** was reacted with acetone-d_6 following the General Procedure A. After purification by column chromatography (MeOH:DCM = 1:19), **3.9d** was obtained as a colorless liquid (78 mg, 96%).

Deuterium incorporation: 5.70 D/molecule (^{1}H NMR), 6.89 D/molecule [HRMS (DART)]

^{1}H NMR (600 MHz, $CDCl_3$) δ 7.44 – 7.26 (m, 6H), 7.22 – 7.13 (m, 3H), 7.11 – 6.93 (m, 1H), 6.87 (dd, *J* = 26.9, 8.7 Hz, 2H), 6.61 (d, *J* = 8.8 Hz, 2H), 4.16 – 3.93 (m, 1.71H, 15%D), 3.00 – 2.81 (m, 2H), 2.67 (d, *J* = 34.3 Hz, 4H), 1.13 – 0.98 (m, 0.61H, 90%D); **^{13}C NMR** (151 MHz, $CDCl_3$) δ 158.0, 157.6, 142.1, 141.3, 139.9, 139.8, 139.6, 134.3, 133.5, 132.5, 131.8, 131.2, 130.6, 130.0, 129.9, 129.8, 129.7, 129.3, 129.0, 128.1, 128.0, 127.8, 127.4, 126.9, 113.9, 113.9, 66.9, 66.0, 60.3, 51.6, 51.5, 51.4, 51.3, 47.62, 47.56, 10.8; **IR** (neat) 2940, 2806, 1603, 1505, 1244, 1174, 1153, 1029, 758, 745, 695 cm^{-1}.

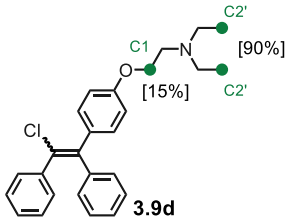
C2'
C1
N
[90%]
O
[15%]
C2'
Cl

3.9d

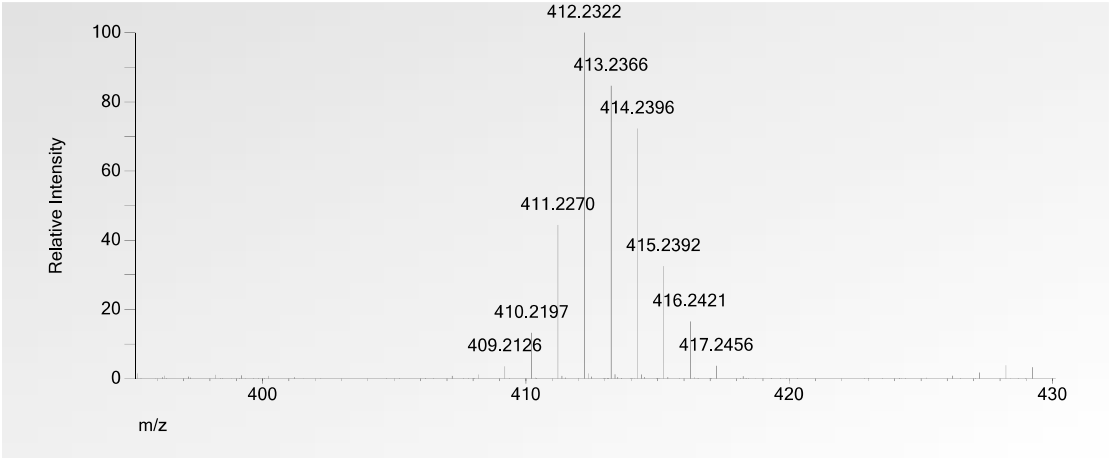
412.2322
413.2366
414.2396
411.2270
415.2392
416.2421
410.2197
409.2126
417.2456
Relative Intensity
m/z
100
80
60
40
20
0
400
410
420
430

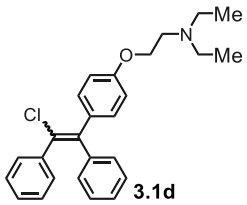
Me
N
Me
O
Cl

3.1d

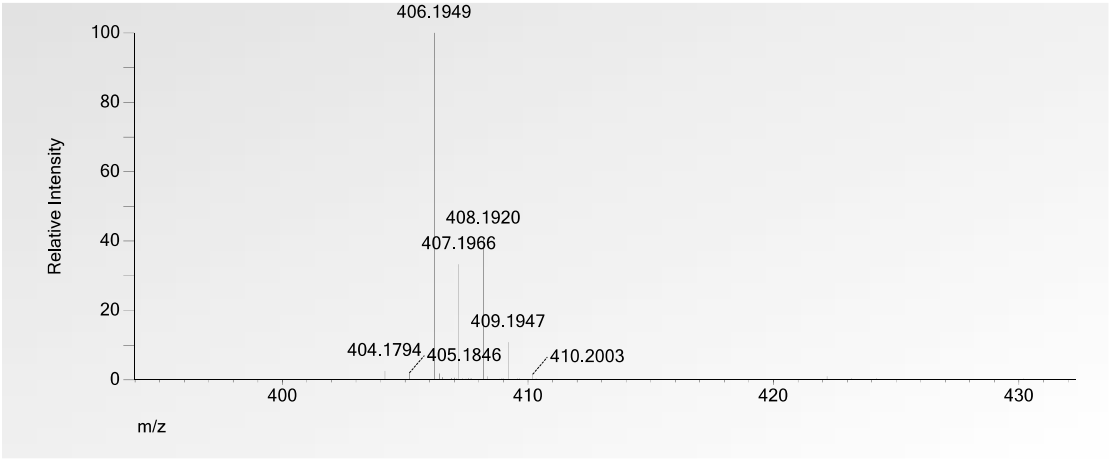
406.1949
408.1920
407.1966
409.1947
404.1794
405.1846
410.2003
Relative Intensity
m/z
100
80
60
40
20
0
400
410
420
430

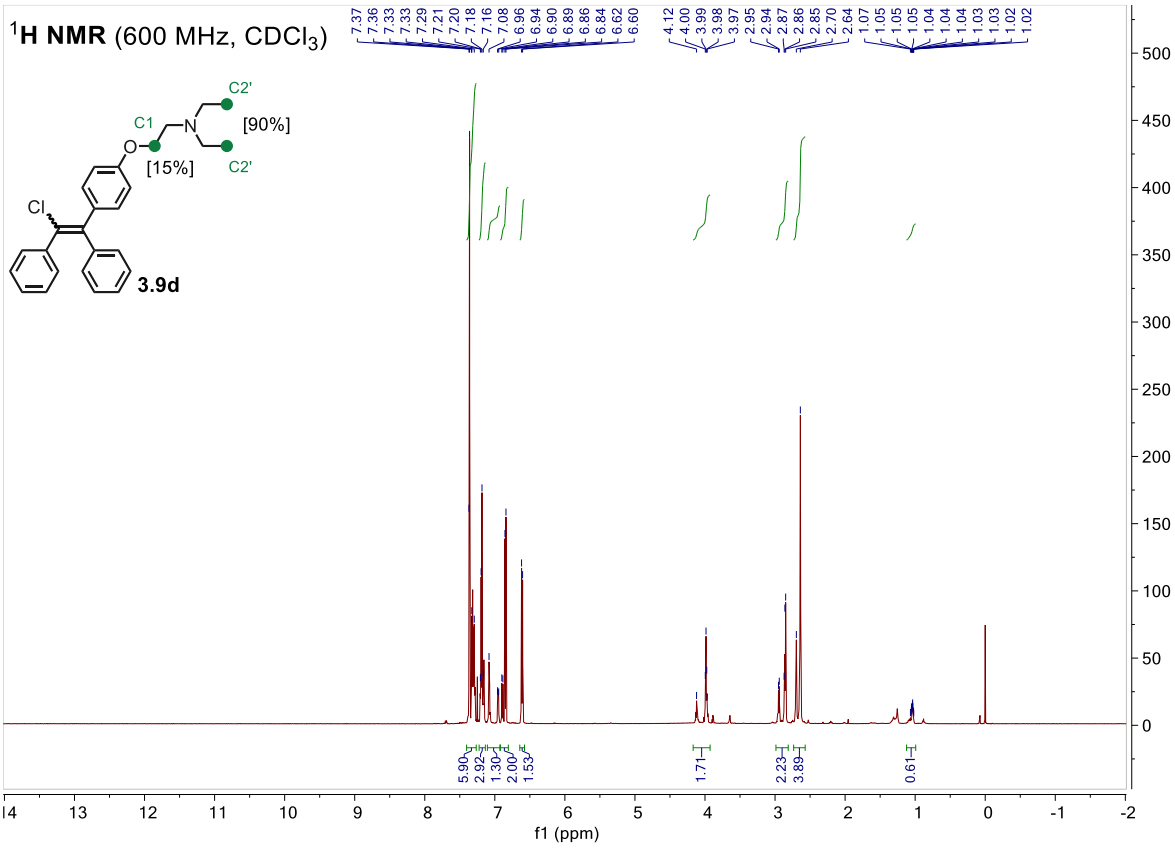
^{1}H NMR (600 MHz, $CDCl_3$)
C2'
C1
N
[90%]
O
[15%]
C2'
Cl
3.9d
f1 (ppm)

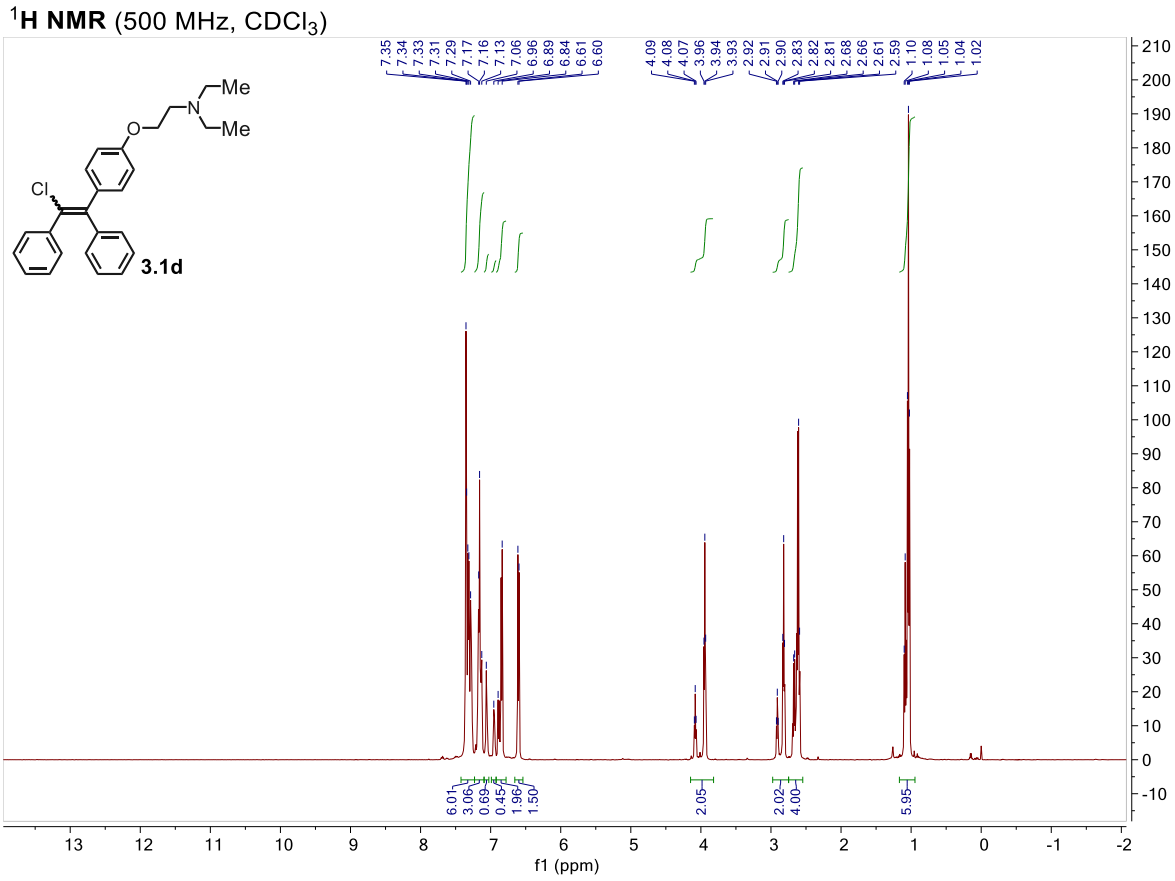
^{1}H NMR (500 MHz, $CDCl_3$)
Me
N
Me
O
Cl
3.1d
f1 (ppm)

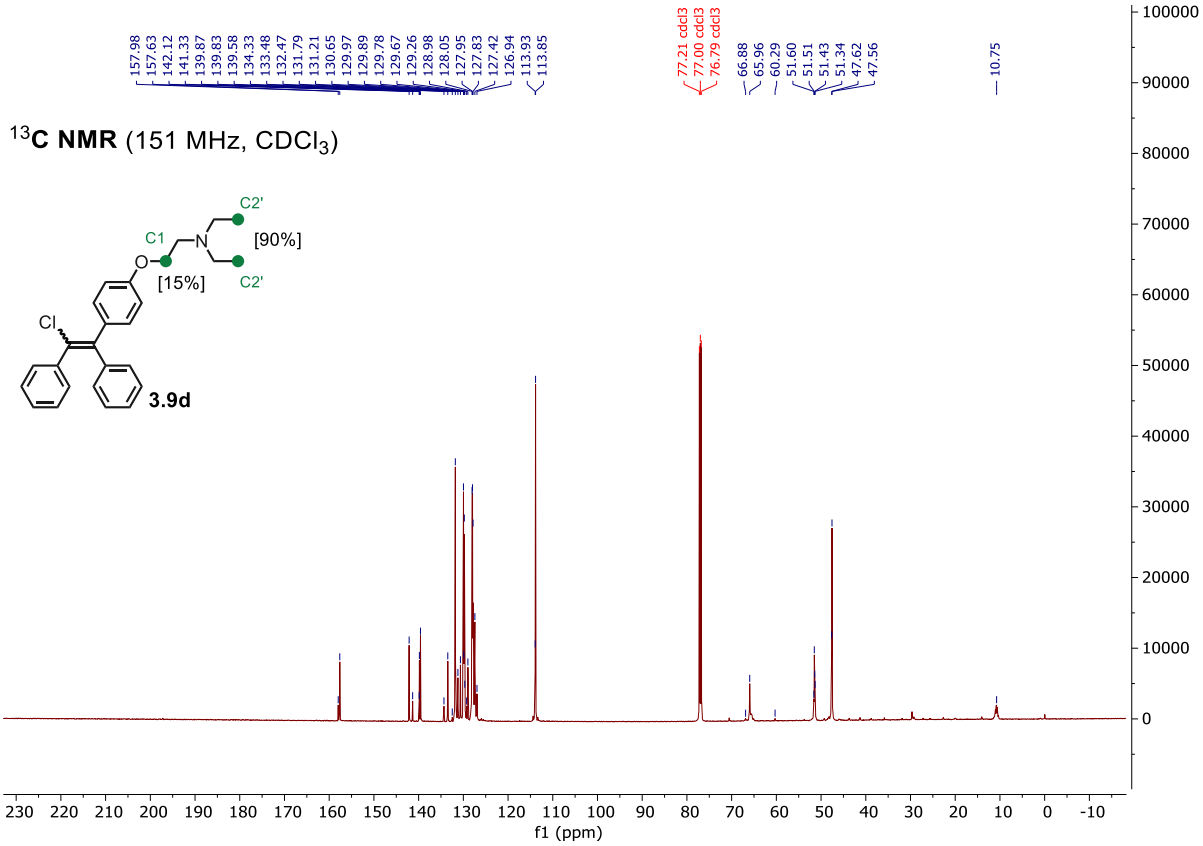
157.98
157.63
142.12
141.33
139.87
139.83
139.58
134.33
133.48
132.47
131.79
131.21
130.65
129.97
129.89
129.78
129.67
129.26
128.98
128.05
127.95
127.83
127.42
126.94
113.93
113.85
77.21 cdcl3
77.00 cdcl3
76.79 cdcl3
66.88
65.96
60.29
51.60
51.51
51.43
51.34
47.62
47.56
10.75
13C NMR (151 MHz, CDCl3)
C2'
C1
N
O
[90%]
[15%]
C2'
Cl
3.9d
100000
90000
80000
70000
60000
50000
40000
30000
20000
10000
0
230 220 210 200 190 180 170 160 150 140 130 120 110 100 90 80 70 60 50 40 30 20 10 0 -10
f1 (ppm)

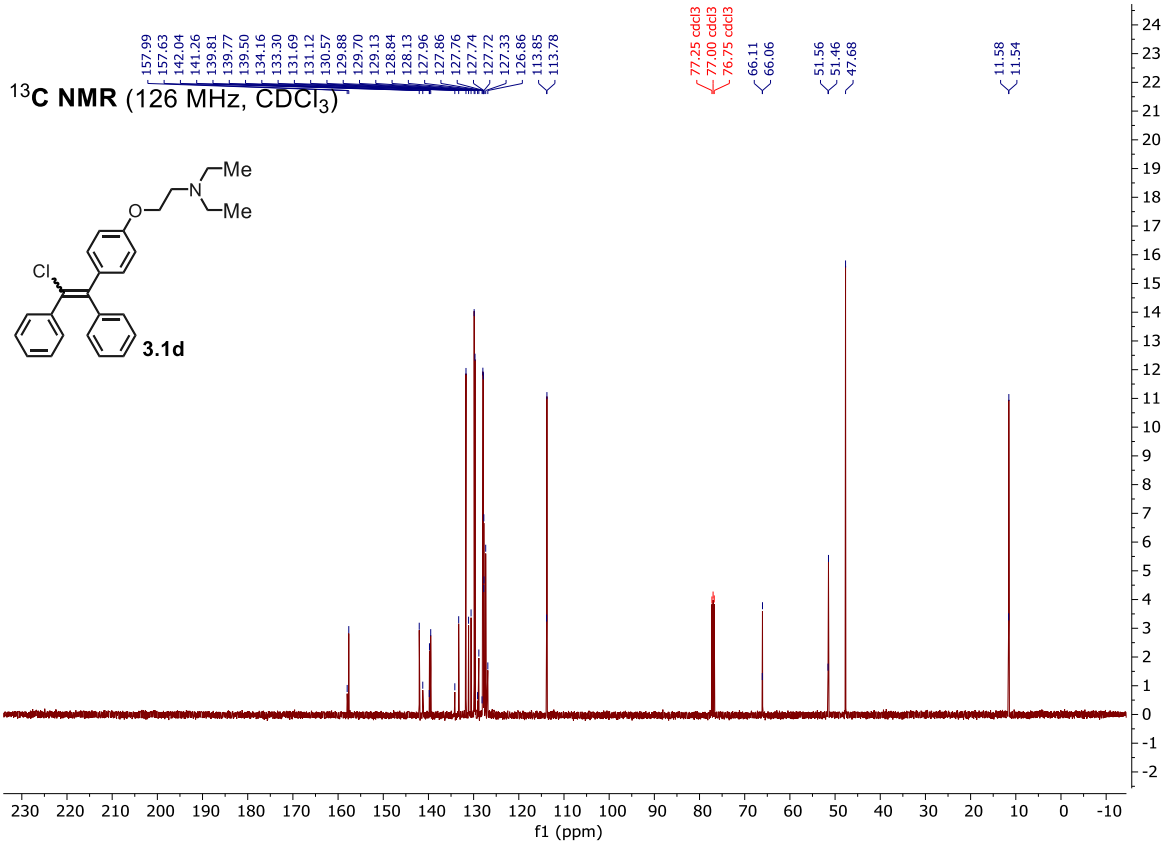
157.99
157.63
142.04
141.26
139.81
139.77
139.50
134.16
133.30
131.69
131.12
130.57
129.88
129.70
129.13
128.84
128.13
127.96
127.86
127.76
127.74
127.72
127.33
126.86
113.85
113.78
77.25 cdcl3
77.00 cdcl3
76.75 cdcl3
66.11
66.06
51.56
51.46
47.68
11.58
11.54
13C NMR (126 MHz, CDCl3)
Me
N
Me
O
Cl
3.1d
24
23
22
21
20
19
18
17
16
15
14
13
12
11
10
9
8
7
6
5
4
3
2
1
0
-1
-2
230 220 210 200 190 180 170 160 150 140 130 120 110 100 90 80 70 60 50 40 30 20 10 0 -10
f1 (ppm)

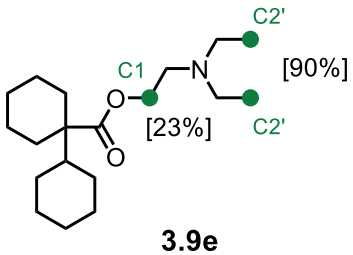

3.9e

Dicyclomine, 3.9e

Dicyclomine **3.1e** was reacted with acetone-d_6 following the General Procedure A. After purification by column chromatography (MeOH:DCM = 1:49), **3.9e** was obtained as a colorless liquid (60 mg, 97%).

Deuterium incorporation: 5.86 D/molecule (^{1}H NMR), 5.50 D/molecule [HRMS (DART)]

^{1}H NMR (600 MHz, $CDCl_3$) δ 4.17 (t, J = 6.3 Hz, 1.55H, 23%D), 2.73 (t, J = 6.5 Hz, 2H), 2.58 (d, J = 7.0 Hz, 4H), 2.06 (d, J = 12.4 Hz, 2H), 1.75 (m, 2H), 1.69 (d, J = 12.9 Hz, 2H), 1.66 – 1.54 (m, 4H), 1.37 – 1.24 (m, 3H), 1.23 – 1.06 (m, 6H), 1.06 – 1.02(m, 0.59H, 90%D), 1.02 – 0.93 (m, 2H); **^{13}C NMR** (151 MHz, $CDCl_3$) δ 176.2, 77.2, 77.0, 76.8, 62.0, 51.1, 50.7, 47.3, 46.8, 31.5, 31.4, 27.8, 27.7, 27.0, 26.6, 26.04, 26.00, 23.75, 11.21; **IR** (neat) 2923, 2850, 1720, 1449, 1207, 1194, 1171, 1156, 1125, 1101, 1049 cm^{-1}.

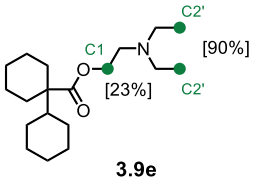
C2'
C1
N
[90%]
O
[23%]
C2'
O

3.9e

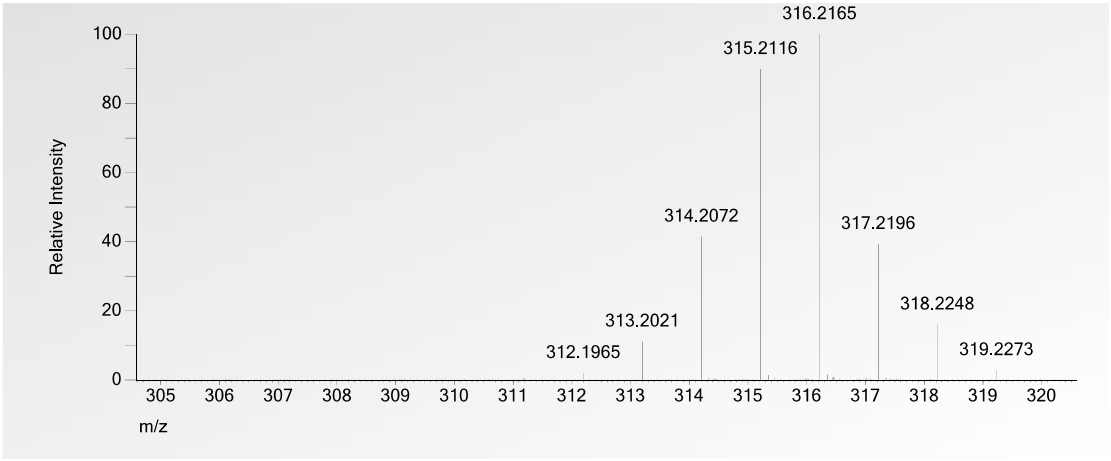
316.2165
315.2116
314.2072
317.2196
318.2248
313.2021
312.1965
319.2273
Relative Intensity
m/z

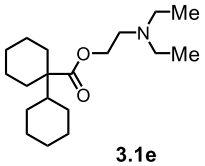
Me
N
Me
O
O

3.1e

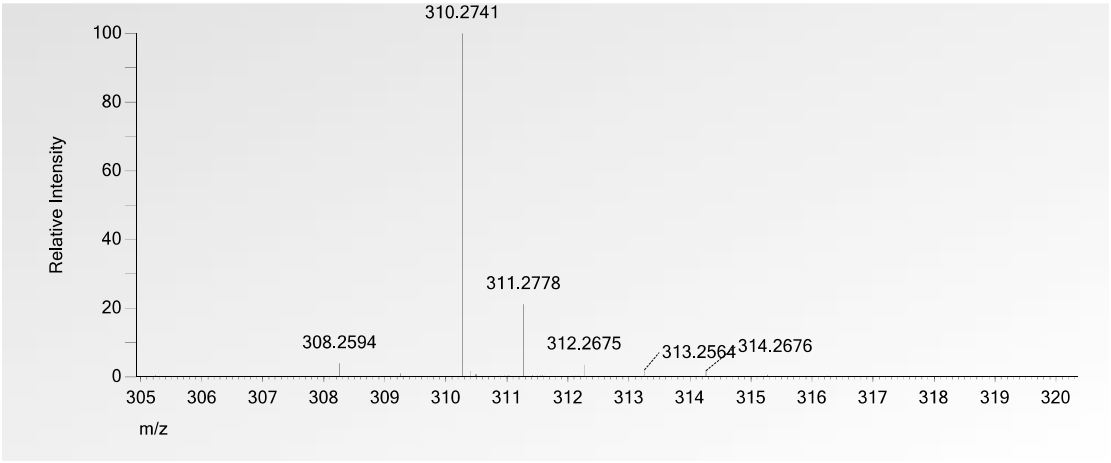
310.2741
311.2778
308.2594
312.2675
313.2564
314.2676
Relative Intensity
m/z

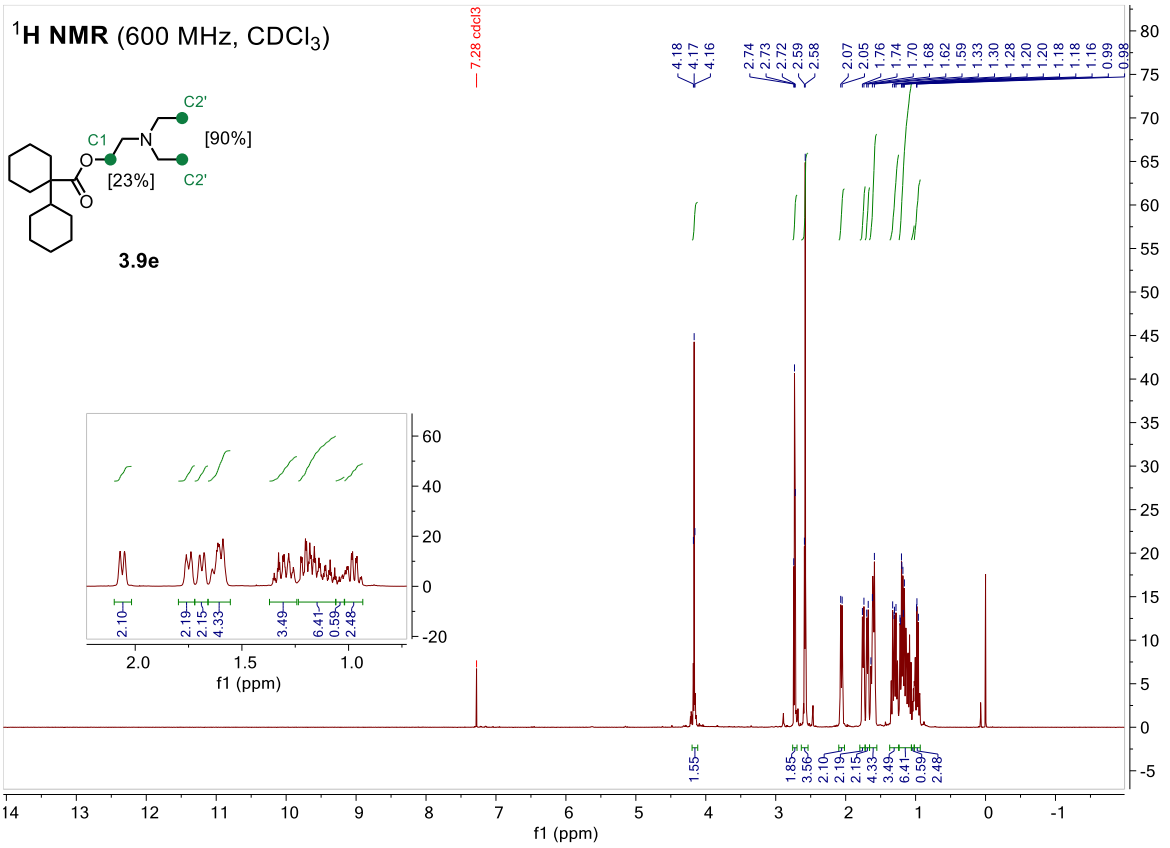
^{1}H NMR (600 MHz, $CDCl_3$)
C2'
C1
N
[90%]
O
[23%]
C2'
O
3.9e
7.28 cdcl3
4.18
4.17
4.16
2.74
2.73
2.72
2.59
2.58
2.07
2.05
1.76
1.74
1.70
1.68
1.62
1.59
1.33
1.30
1.28
1.20
1.18
1.16
0.99
0.98
2.10
2.19
2.15
4.33
3.49
6.41
0.59
2.48
f1 (ppm)
1.55
1.85
3.56
2.10
2.19
2.15
4.33
3.49
6.41
0.59
2.48
f1 (ppm)

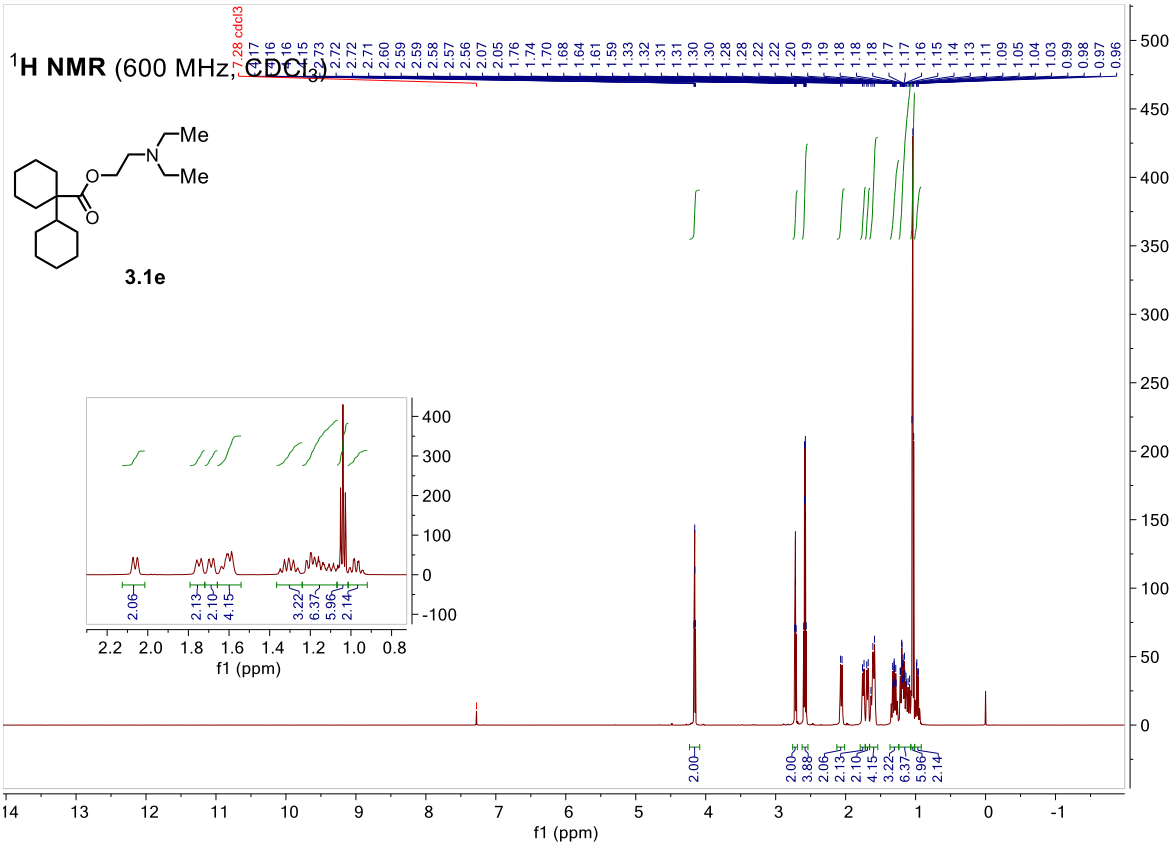
^{1}H NMR (600 MHz, $CDCl_3$)
Me
N
Me
O
O
3.1e
7.28 cdcl3
2.06
2.13
2.10
4.15
3.22
6.37
5.96
2.14
f1 (ppm)
2.00
2.00
3.88
2.06
2.13
2.10
4.15
3.22
6.37
5.96
2.14
f1 (ppm)

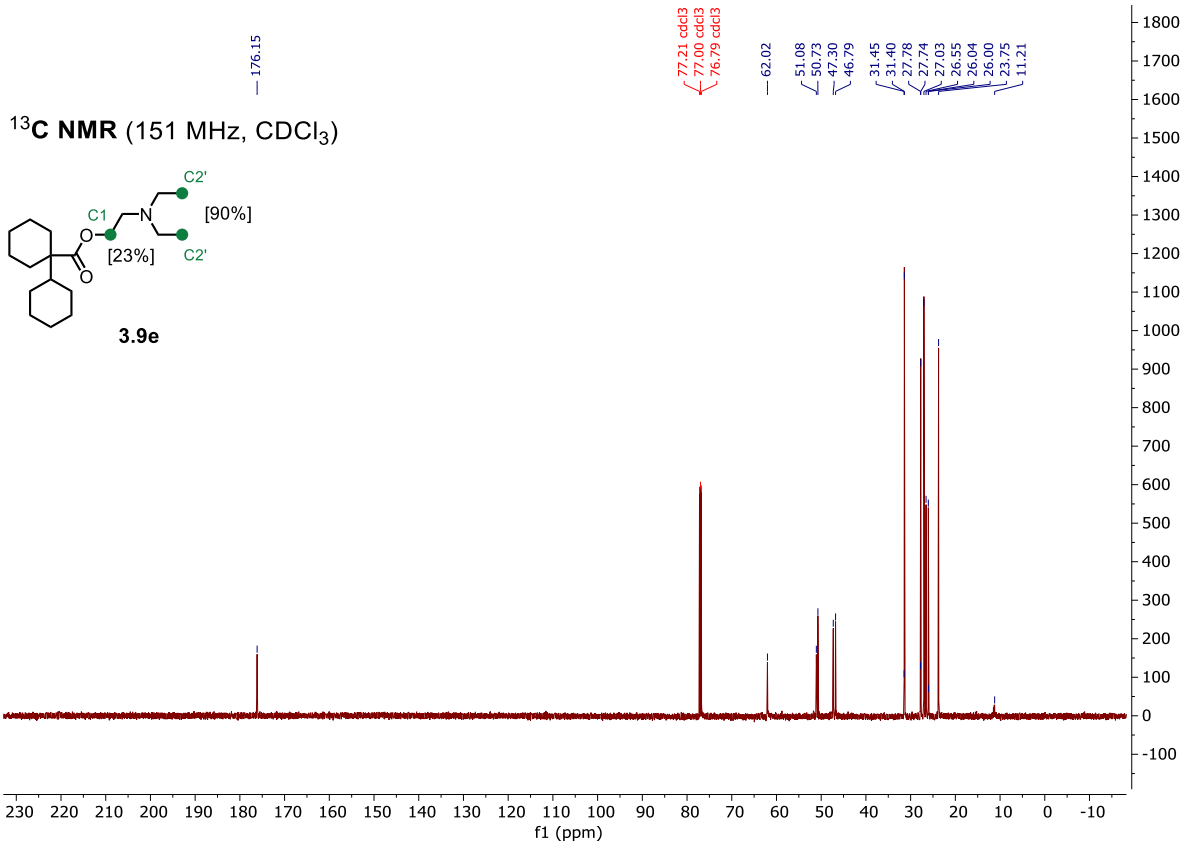
176.15
77.21 cdcl3
77.00 cdcl3
76.79 cdcl3
62.02
51.08
50.73
47.30
46.79
31.45
31.40
27.78
27.74
27.03
26.55
26.04
26.00
23.75
11.21
13C NMR (151 MHz, CDCl3)
C2'
C1
N
[90%]
O
[23%]
C2'
O
3.9e
f1 (ppm)

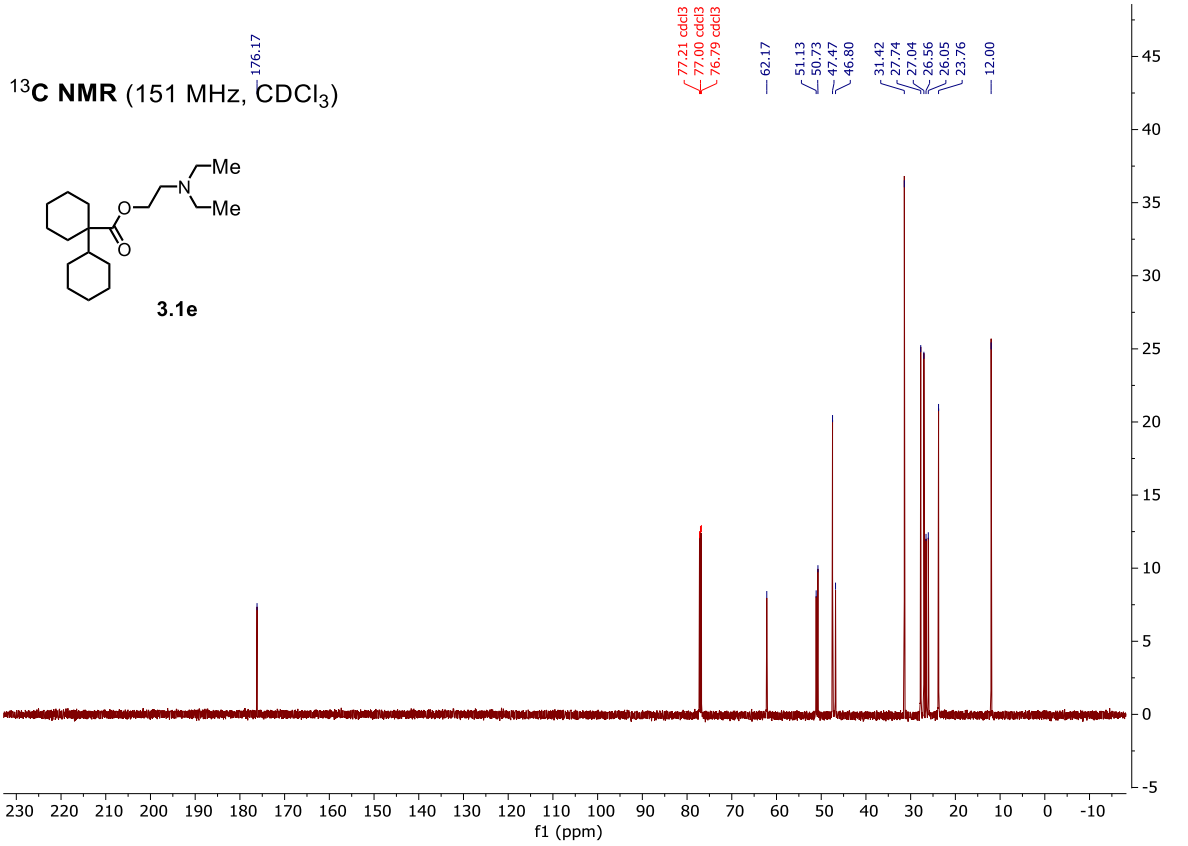
176.17
77.21 cdcl3
77.00 cdcl3
76.79 cdcl3
62.17
51.13
50.73
47.47
46.80
31.42
27.74
27.04
26.56
26.05
23.76
12.00
13C NMR (151 MHz, CDCl3)
Me
N
Me
O
O
3.1e
f1 (ppm)

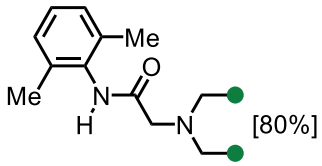

3.9f

Lidocaine, 3.9f

Lidocaine **3.1f** was reacted with acetone-d_6 following the General Procedure A. After purification by column chromatography (MeOH:DCM = 1:49), **3.9f** was obtained as a white solid (46 mg, 99%).

Deuterium incorporation: 4.80 D/molecule (^{1}H NMR), 4.78 D/molecule [HRMS (DART)]

^{1}H NMR (500 MHz, $CDCl_3$) δ 8.91 (s, 1H), 7.08 (s, 3H), 3.21 (s, 2H), 2.77 – 2.54 (m, 4H), 2.23 (s, 6H), 1.23 – 1.01 (m, 1.23H, 80%D); **^{13}C NMR** (126 MHz, $CDCl_3$) δ 170.1, 134.9, 133.9, 128.0, 126.9, 57.4, 48.82, 48.76, 48.7, 48.6, 18.4, 11.9; **IR** (neat) 3265, 2936, 2818, 2219, 1684, 1491, 1284, 1163, 1051, 767 cm^{-1}.

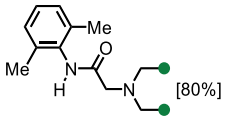
Me
Me
O
N
H
N
[80%]

3.9f

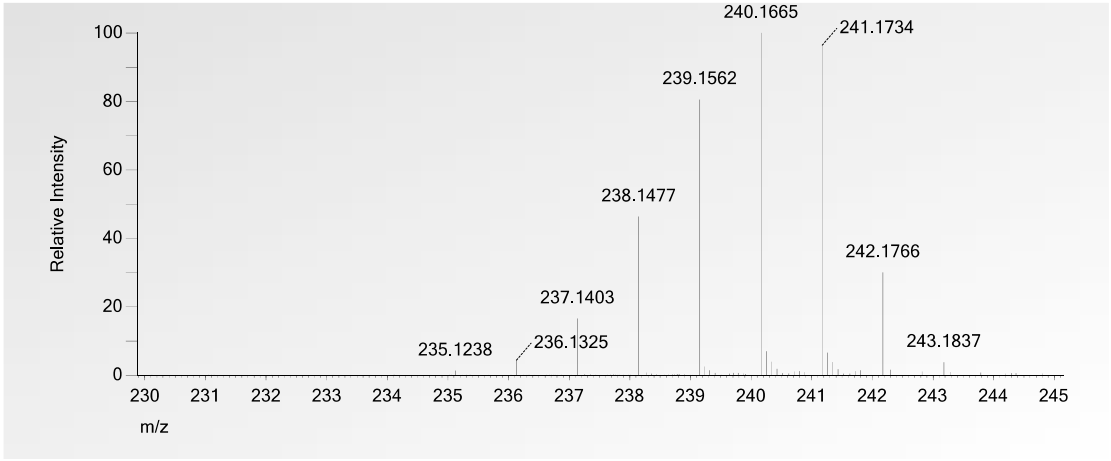
240.1665
241.1734
239.1562
238.1477
242.1766
237.1403
235.1238
236.1325
243.1837
Relative Intensity
m/z

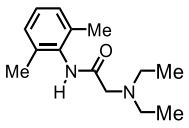
Me
Me
O
N
H
N
Me
Me

3.1f

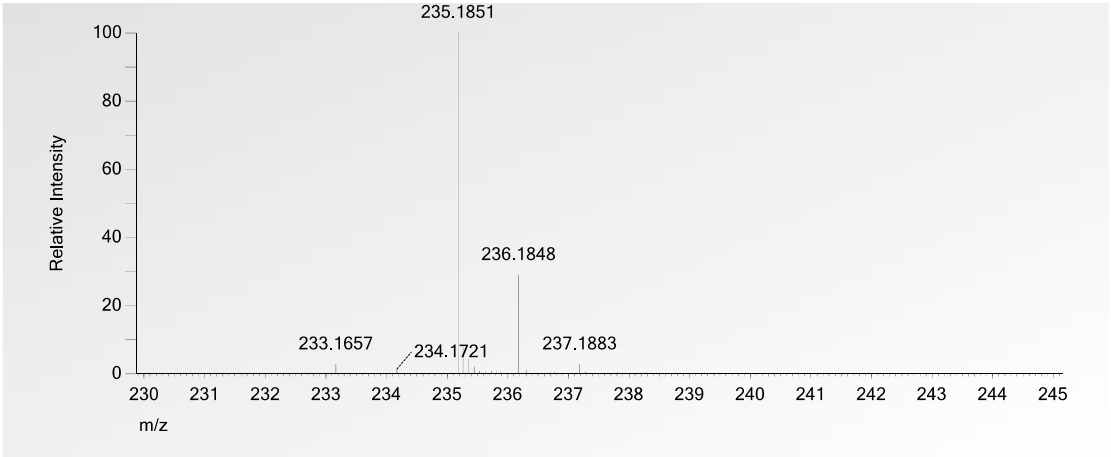
235.1851
236.1848
233.1657
234.1721
237.1883
Relative Intensity
m/z

^{1}H NMR (500 MHz, $CDCl_3$)

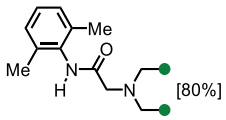

3.9f

^{1}H NMR (600 MHz, $CDCl_3$)

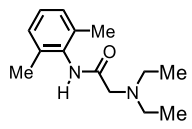

3.1f

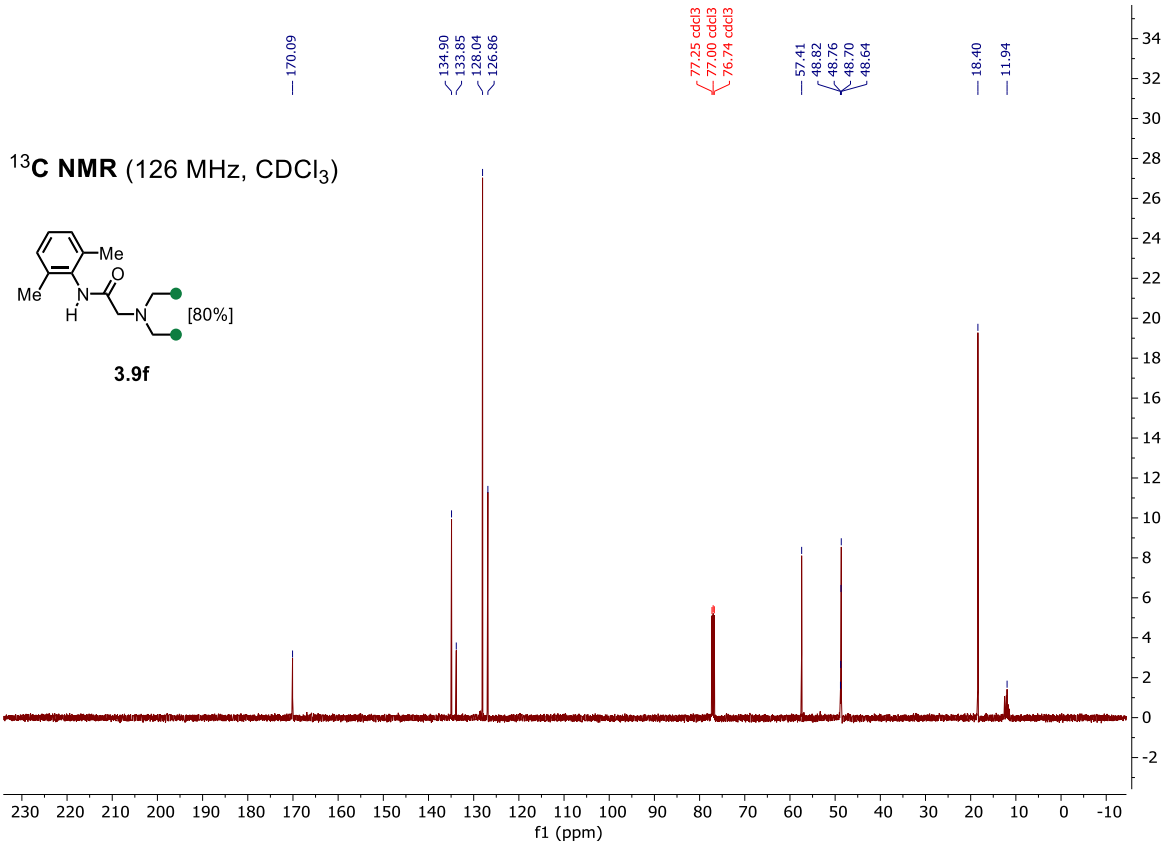
170.09
134.90
133.85
128.04
126.86
77.25 cdcl3
77.00 cdcl3
76.74 cdcl3
57.41
48.82
48.76
48.70
48.64
18.40
11.94
13C NMR (126 MHz, CDCl3)
Me
Me
N
H
O
N
[80%]
3.9f
f1 (ppm)

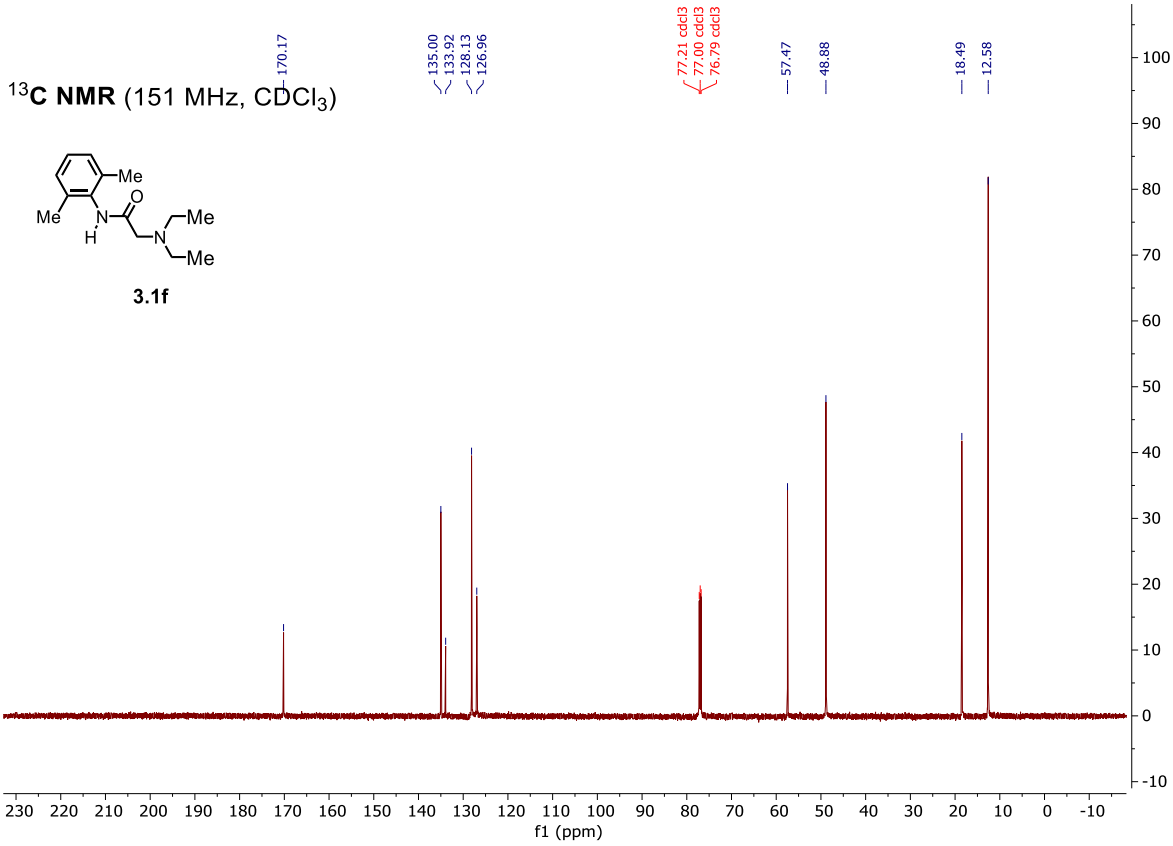
170.17
135.00
133.92
128.13
126.96
77.21 cdcl3
77.00 cdcl3
76.79 cdcl3
57.47
48.88
18.49
12.58
13C NMR (151 MHz, CDCl3)
Me
Me
N
H
O
N
Me
Me
3.1f
f1 (ppm)

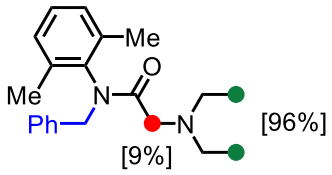

3.9g

_N_-Bn lidocaine, 3.9g

N-Bn lidocaine **3.1g** was reacted with acetone-d_6 **2** following the General Procedure B. After purification by column chromatography (MeOH:DCM = 1:49), **3.9g** was obtained as a yellow liquid (62 mg, 96%).

Deuterium incorporation: 6.18 D/molecule (^{1}H NMR), 6.26 D/molecule [HRMS (DART)]

^{1}H NMR (500 MHz, $CDCl_3$) δ 7.22 (s, 5H), 7.13 (dd, *J* = 8.0, 7.0 Hz, 1H), 7.04 (d, *J* = 7.6 Hz, 2H), 4.73 (s, 1.82H, 9%D), 2.81 (s, 2H), 2.57 (s, 4H), 1.87 (s, 6H), 0.88 (s, 0.22H, 96%D); **^{13}C NMR** (126 MHz, $CDCl_3$) δ 170.4, 138.9, 137.1, 136.3, 130.2, 129.0, 128.3, 128.1, 127.6, 54.6, 51.8, 47.3, 17.9, 11.0; **IR** (neat) 2926, 1650, 1460, 1400, 1242, 1141, 1078, 773, 743, 700 cm^{-1}.

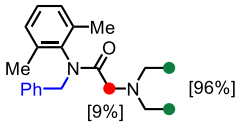
Me
Me
N
O
Ph
N
[96%]
[9%]

3.9g

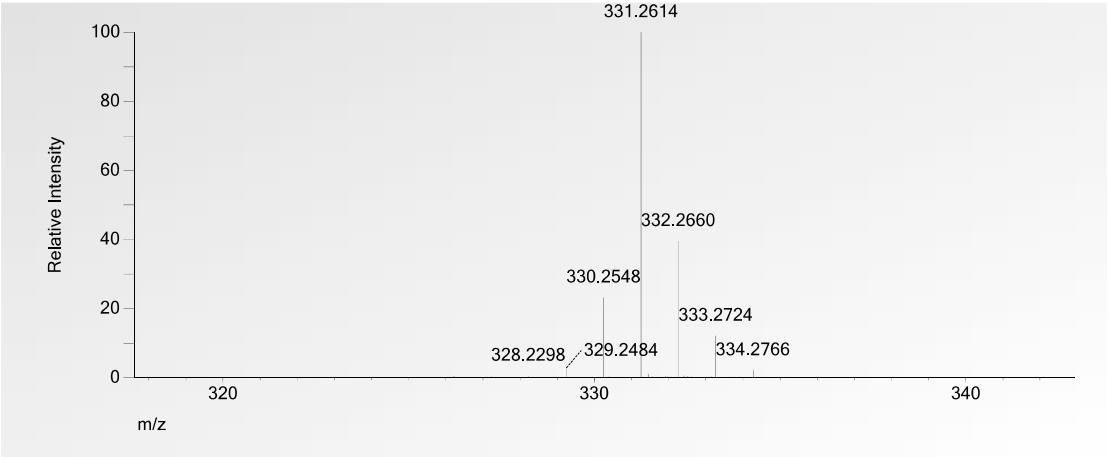
331.2614
100
80
60
40
20
0
Relative Intensity
332.2660
330.2548
333.2724
328.2298
329.2484
334.2766
320
330
340
m/z

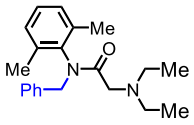
Me
Me
N
O
Ph
N
Me
Me

3.1g

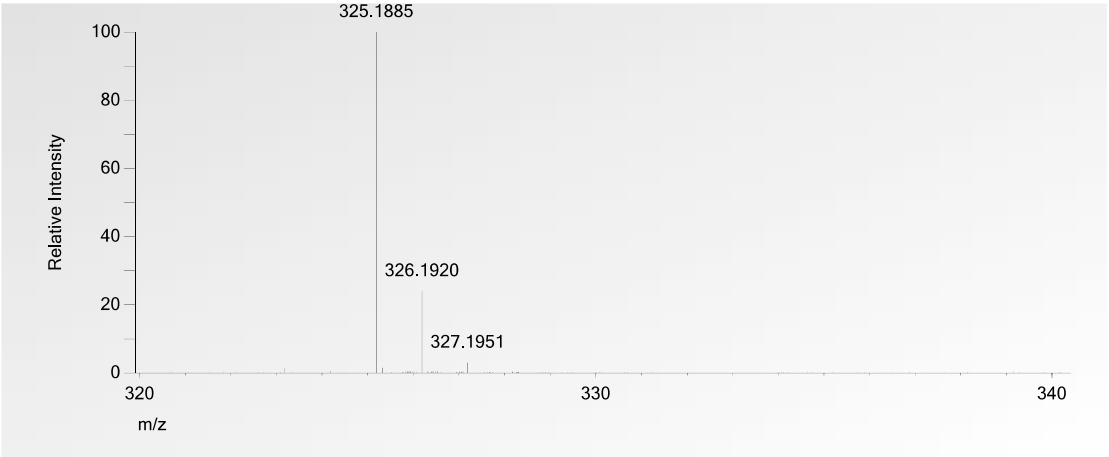
325.1885
100
80
60
40
20
0
Relative Intensity
326.1920
327.1951
320
330
340
m/z

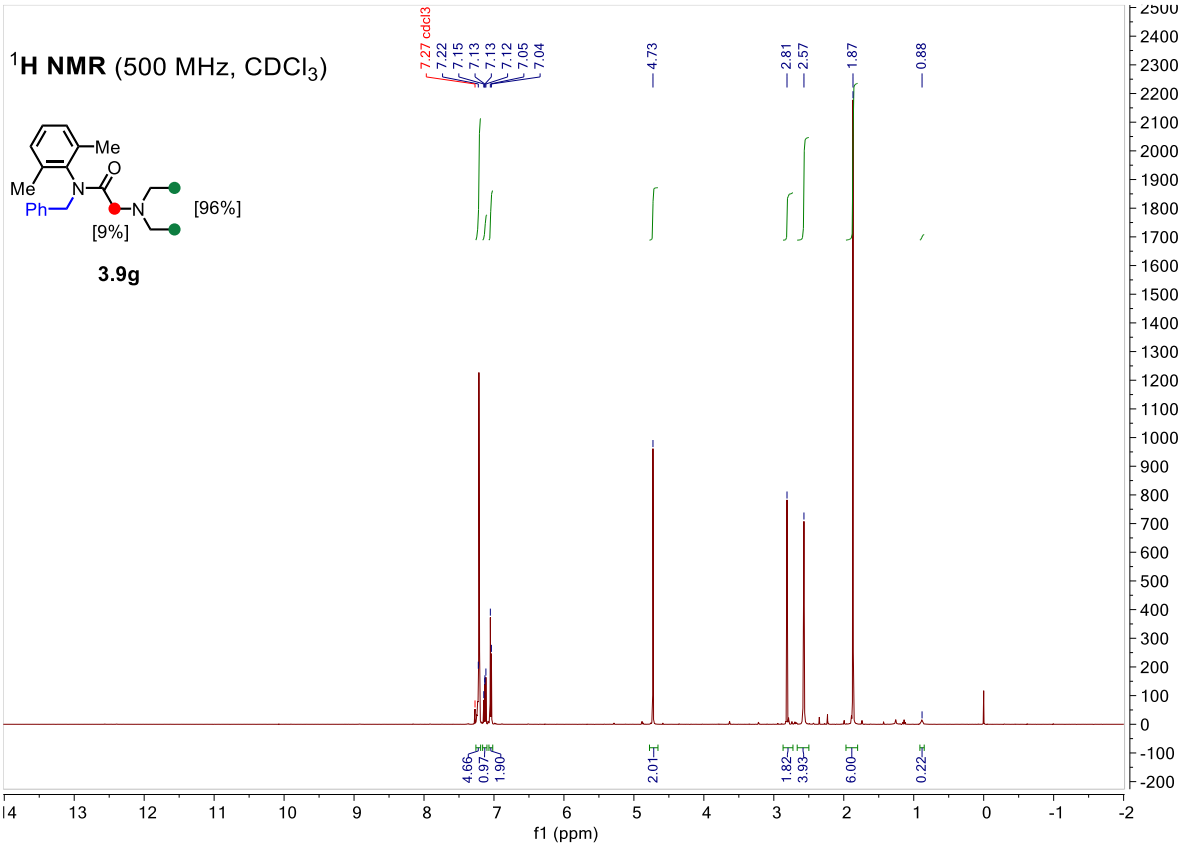
^{1}H NMR (500 MHz, CDCl$_3$)
Me
Me
N
O
Ph
N
[9%]
[96%]
3.9g
7.27 cdcl3
7.22
7.15
7.13
7.13
7.12
7.05
7.04
4.73
2.81
2.57
1.87
0.88
4.66
0.97
1.90
2.01
1.82
3.93
6.00
0.22
f1 (ppm)

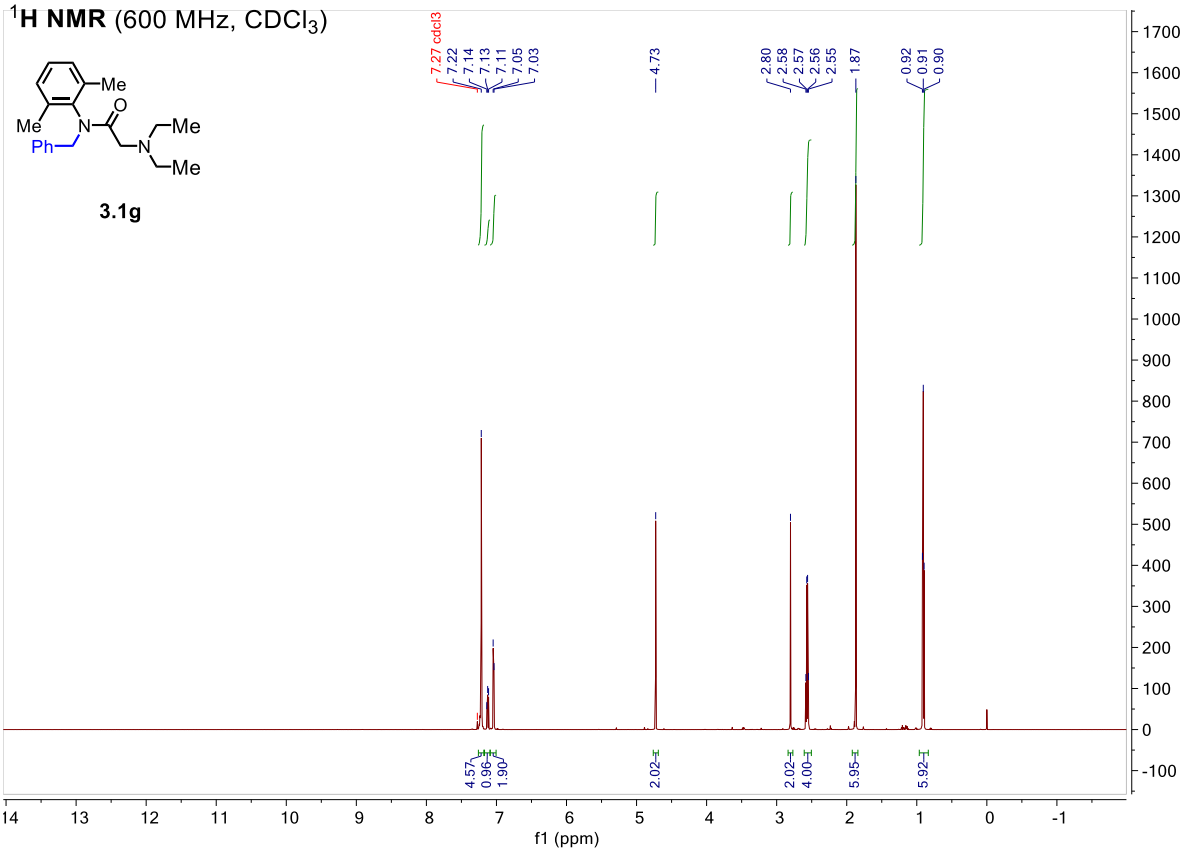
^{1}H NMR (600 MHz, CDCl$_3$)
Me
Me
N
O
Ph
N
Me
Me
3.1g
7.27 cdcl3
7.22
7.14
7.13
7.11
7.05
7.03
4.73
2.80
2.58
2.57
2.56
2.55
1.87
0.92
0.91
0.90
4.57
0.96
1.90
2.02
2.02
4.00
5.95
5.92
f1 (ppm)

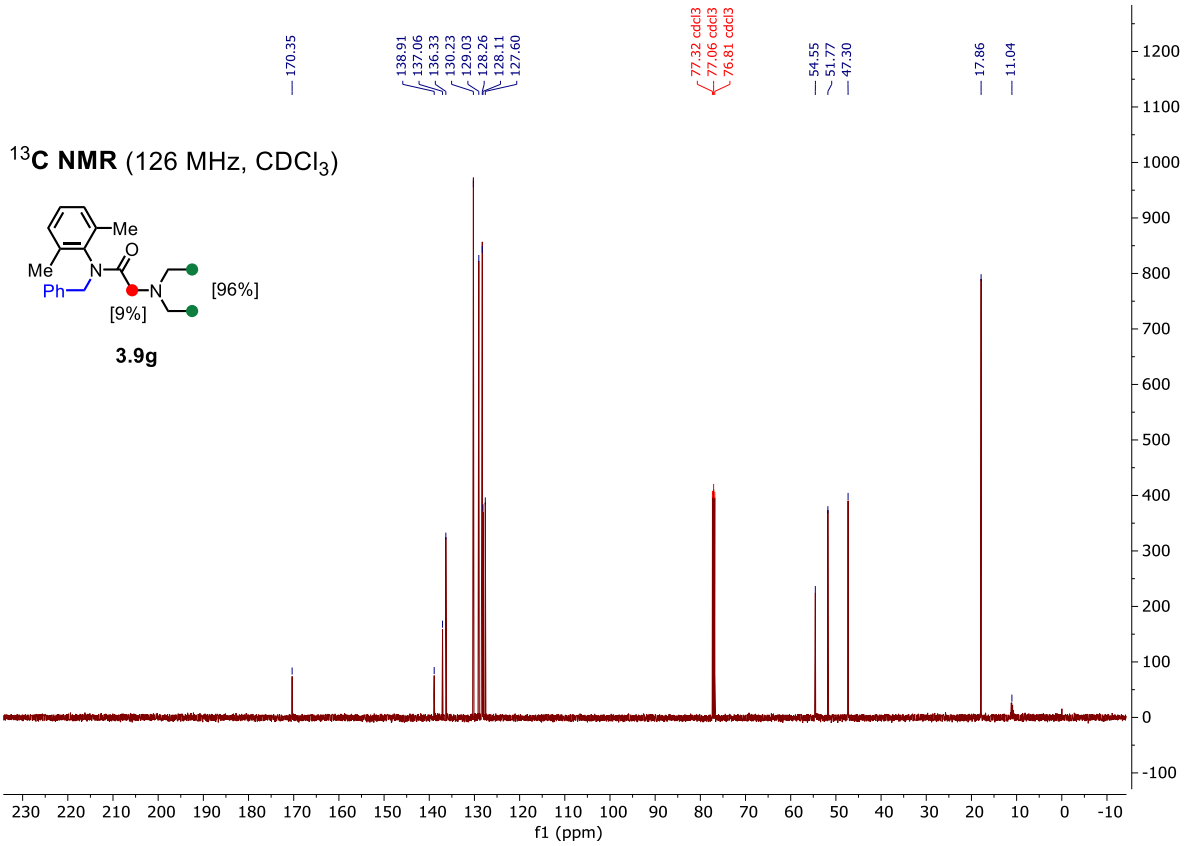
170.35
138.91
137.06
136.33
130.23
129.03
128.26
128.11
127.60
77.32 cdcl3
77.06 cdcl3
76.81 cdcl3
54.55
51.77
47.30
17.86
11.04
13C NMR (126 MHz, CDCl3)
Me
Me
Ph
O
N
N
[96%]
[9%]
3.9g
f1 (ppm)

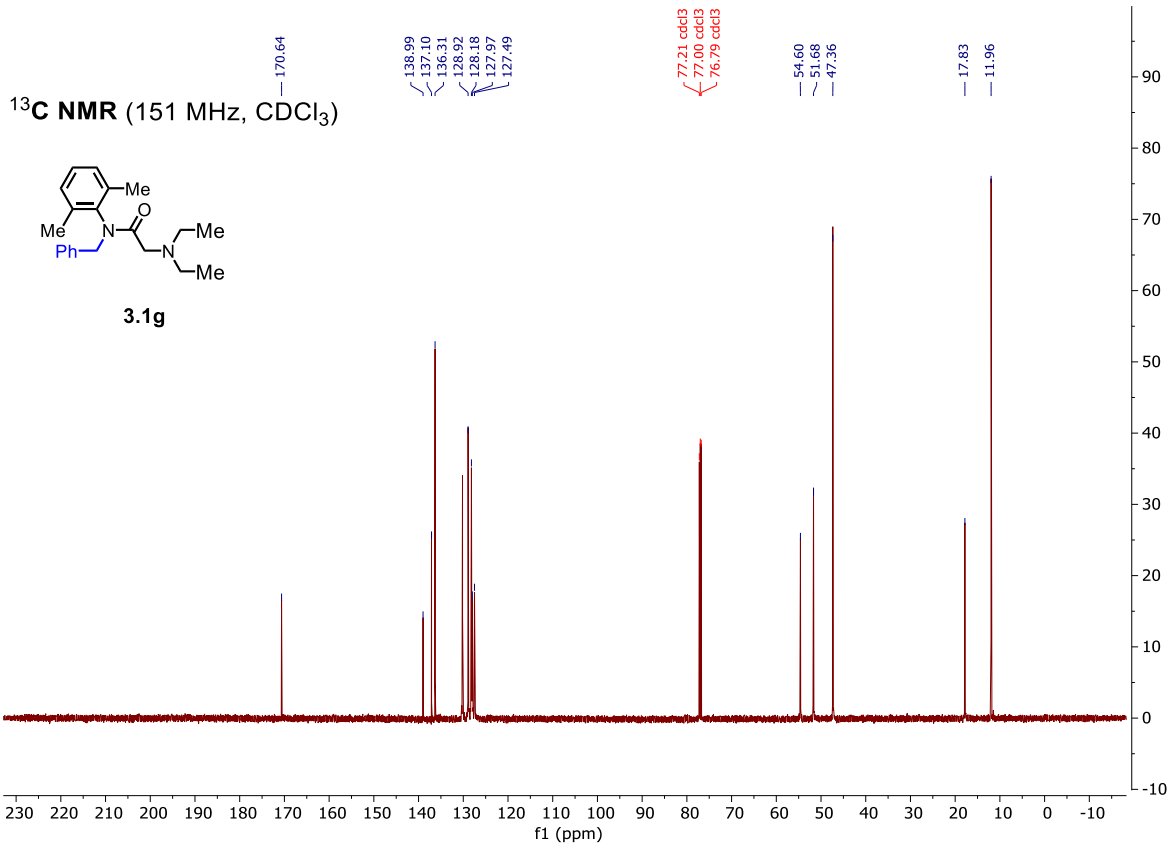
170.64
138.99
137.10
136.31
128.92
128.18
127.97
127.49
77.21 cdcl3
77.00 cdcl3
76.79 cdcl3
54.60
51.68
47.36
17.83
11.96
13C NMR (151 MHz, CDCl3)
Me
Me
Ph
O
N
N
Me
Me
3.1g
f1 (ppm)

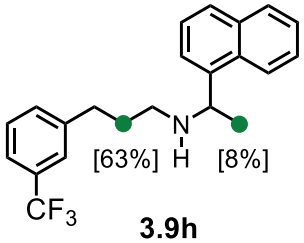

3.9h

Cinacalcet, 3.9h

Cinacalcet **3.1h** was reacted with acetone-d_6 following the General Procedure A. After purification by column chromatography (MeOH:DCM = 1:19), **3.9h** was obtained as a yellow liquid (69 mg, 97%).

Deuterium incorporation: 1.50 D/molecule (^{1}H NMR), 1.52 D/molecule [HRMS (DART)]

^{1}H NMR (500 MHz, CD_3OD) δ 8.01 (d, J = 8.5 Hz, 1H), 7.72 (d, J = 8.1 Hz, 1H), 7.61 (d, J = 8.2 Hz, 1H), 7.47 (d, J = 7.2 Hz, 1H), 7.40 – 7.26 (m, 5H), 7.20 (dt, J = 16.2, 7.6 Hz, 2H), 4.54 (q, J = 6.5 Hz, 1H), 2.43 (ddd, J = 38.2, 16.0, 8.0 Hz, 4H), 1.75 – 1.57 (m, 0.75H, 63%D), 1.34 (d, J = 6.7 Hz, 2.72H, 8%D); **^{13}C NMR** (126 MHz, $CDCl_3$) δ 143.1, 141.1, 134.0, 131.79, 131.78, 131.4, 131.0, 130.7, 130.5, 130.2, 129.04, 129.03, 128.7, 127.3, 125.8, 125.7, 125.41, 125.37, 125.11, 125.08, 125.05, 125.0, 123.2, 122.9, 122.8, 122.71, 122.68, 122.65, 122.6, 53.8, 47.2, 33.3, 31.8, 23.6; **^{19}F NMR** (470 MHz, $CDCl_3$) δ -62.47; **IR** (neat) 2923, 1448, 1326, 1198, 1160, 1119, 1072, 798, 777, 701, 659 cm^{-1}; $[\alpha]^{25}_{D}$ = +19.1° (c = 1.0, CH_2Cl_2 labeled), $[\alpha]^{25}_{D}$ = +28.3° (c = 1.0, CH_2Cl_2 unlabeled).

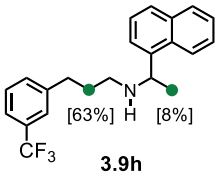
[63%]
H
[8%]
CF3

3.9h

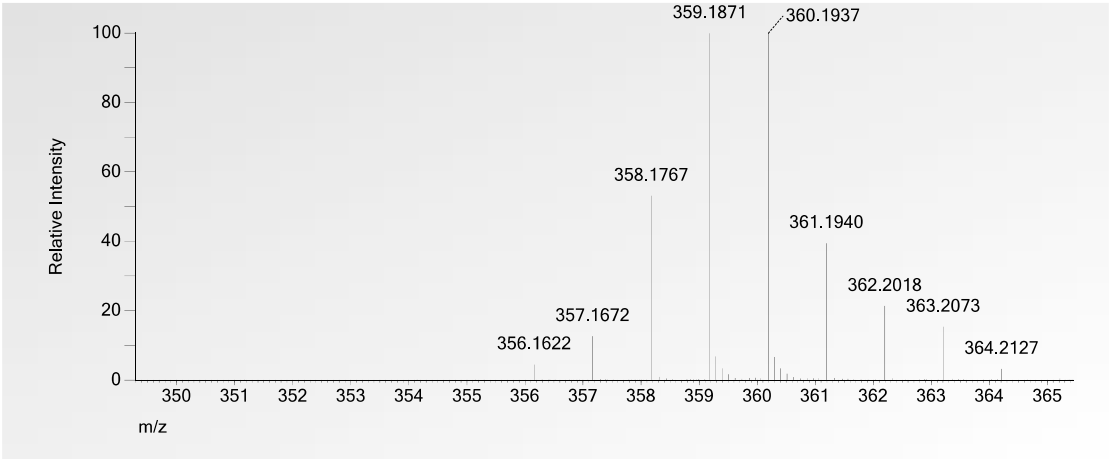
359.1871
360.1937
358.1767
361.1940
362.2018
363.2073
357.1672
356.1622
364.2127
Relative Intensity
m/z

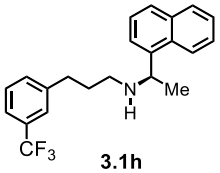
Me
H
CF3

3.1h

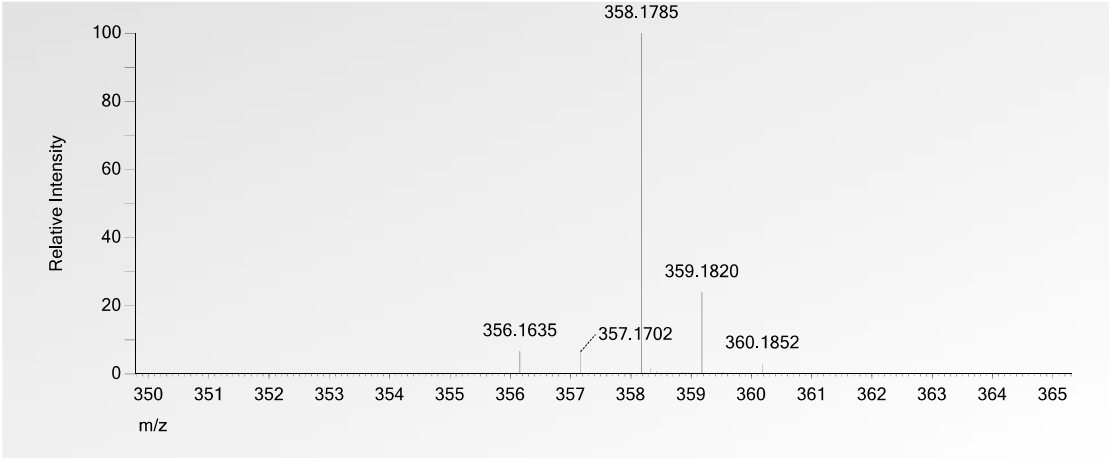
358.1785
359.1820
356.1635
357.1702
360.1852
Relative Intensity
m/z

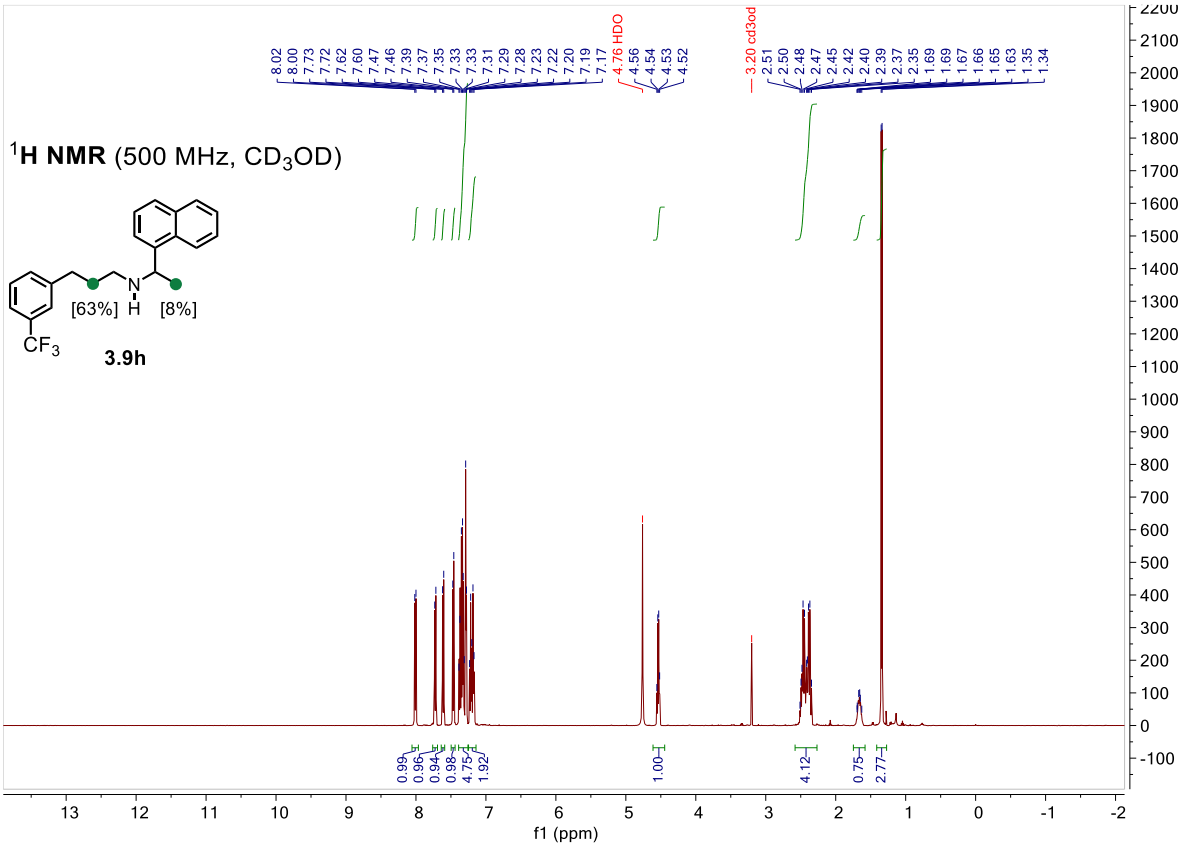
1H NMR (500 MHz, CD3OD)
[63%] H [8%]
CF3
3.9h
4.76 HDO
3.20 cd3od
f1 (ppm)

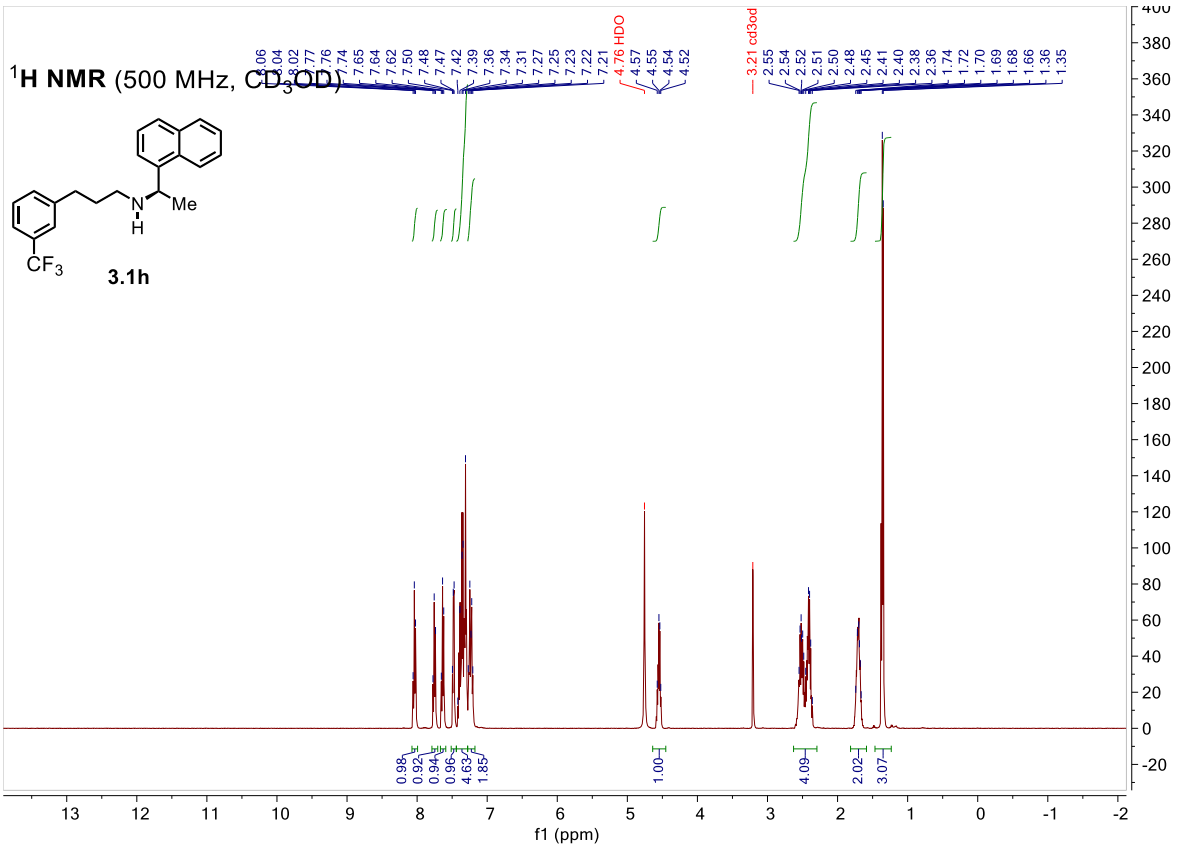
1H NMR (500 MHz, CD3OD)
N
H
Me
CF3
3.1h
4.76 HDO
3.21 cd3od
f1 (ppm)

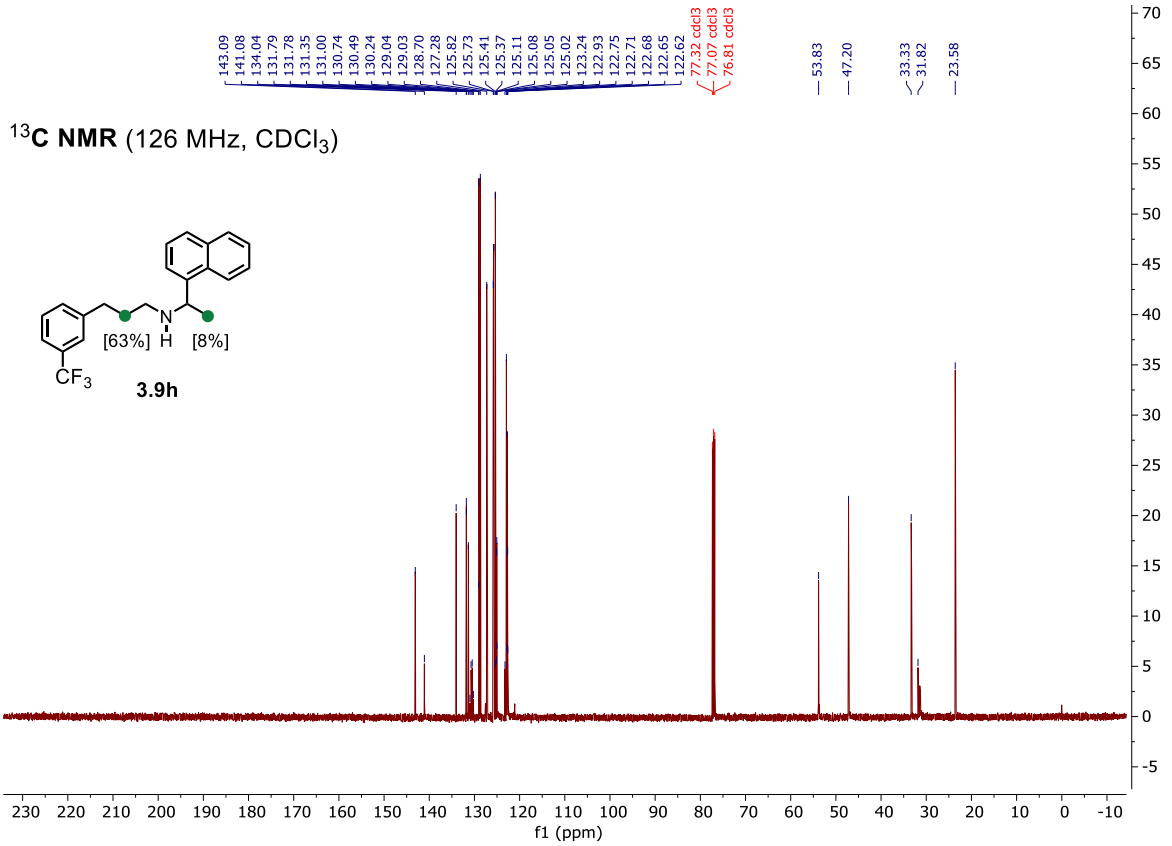
143.09
141.08
134.04
131.79
131.78
131.35
131.00
130.74
130.49
130.24
129.04
129.03
128.70
127.28
125.82
125.73
125.41
125.37
125.11
125.08
125.05
125.02
123.24
122.93
122.75
122.71
122.68
122.65
122.62
77.32 cdcl3
77.07 cdcl3
76.81 cdcl3
53.83
47.20
33.33
31.82
23.58
13C NMR (126 MHz, CDCl3)
[63%]
[8%]
3.9h
f1 (ppm)

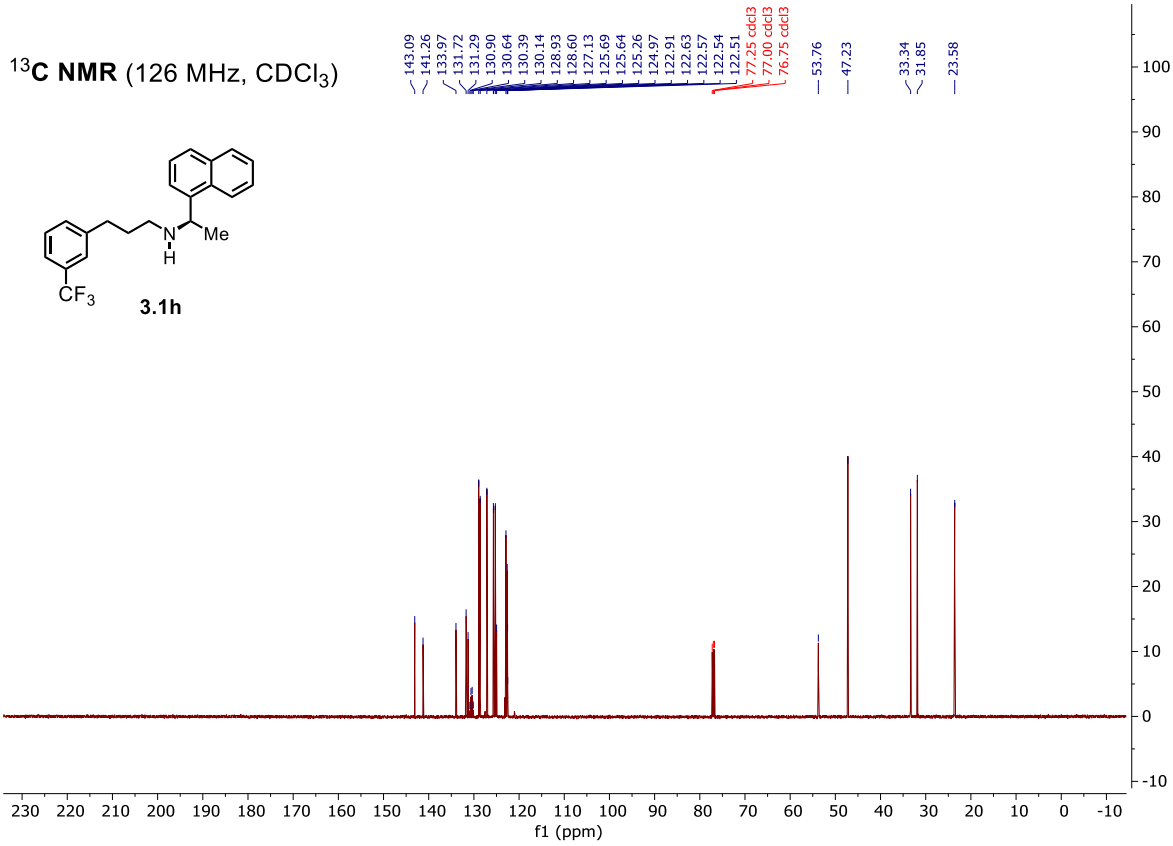
143.09
141.26
133.97
131.72
131.29
130.90
130.64
130.39
130.14
128.93
128.60
127.13
125.69
125.64
125.26
124.97
122.91
122.63
122.57
122.54
122.51
77.25 cdcl3
77.00 cdcl3
76.75 cdcl3
53.76
47.23
33.34
31.85
23.58
13C NMR (126 MHz, CDCl3)
Me
3.1h
f1 (ppm)

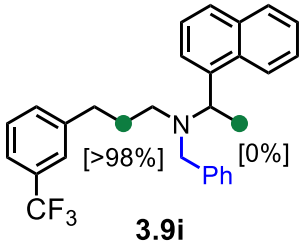

3.9i

***N*-Bn cinacalcet, 3.9i**

N-Bn cinacalcet **3.1i** was reacted with acetone-d_6 following the General Procedure B. After purification by column chromatography (Et_2O:hexanes = 1:9), **3.9i** was obtained as a yellow liquid (88 mg, 98%).

Deuterium incorporation: 1.99 D/molecule (^{1}H NMR), 2.28 D/molecule [HRMS (DART)]

^{1}H NMR (600 MHz, $CDCl_3$) δ 8.26 (d, *J* = 8.0 Hz, 1H), 7.83 (d, *J* = 7.7 Hz, 1H), 7.74 (d, *J* = 8.1 Hz, 1H), 7.56 (d, *J* = 7.1 Hz, 1H), 7.50 – 7.38 (m, 3H), 7.35 (d, *J* = 7.6 Hz, 1H), 7.24 (t, *J* = 7.8 Hz, 6H), 7.12 (s, 1H), 6.96 (d, *J* = 7.4 Hz, 1H), 4.75 – 4.62 (m, 1H), 3.72 (d, *J* = 13.8 Hz, 1H), 3.63 (d, *J* = 13.8 Hz, 1H), 2.60 (s, 2H), 2.33 (d, *J* = 14.0 Hz, 1H), 2.26 (d, *J* = 13.9 Hz, 1H), 1.63 (d, *J* = 6.3 Hz, 0.02H, >98%D), 1.53 (d, *J* = 6.8 Hz, 3H); **^{13}C NMR** (126 MHz, $CDCl_3$) δ 143.4, 140.6, 140.0, 134.0, 132.1, 131.59, 131.58, 130.5, 130.2, 129.0, 128.6, 128.4, 128.2, 128.1, 127.6, 126.7, 125.4, 125.33, 125.28, 125.0, 124.89, 124.85, 124.83, 124.80, 124.6, 123.2, 122.4, 122.33, 122.30, 122.27, 56.4, 55.8, 49.7, 33.1, 28.2, 14.4; **^{19}F NMR** (564 MHz, $CDCl_3$) δ -62.49; **IR** (neat) 2858, 1449, 1331, 1197, 1159, 1118, 1097, 797, 778, 733, 699 cm^{-1}; $[\alpha]^{25}_{D}$ = -28.5° (c = 1.0, CH_2Cl_2 labeled), $[\alpha]^{25}_{D}$ = -39.2° (c = 1.0, CH_2Cl_2 unlabeled).

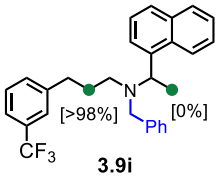
[>98%]
N
Ph
[0%]
CF3

3.9i

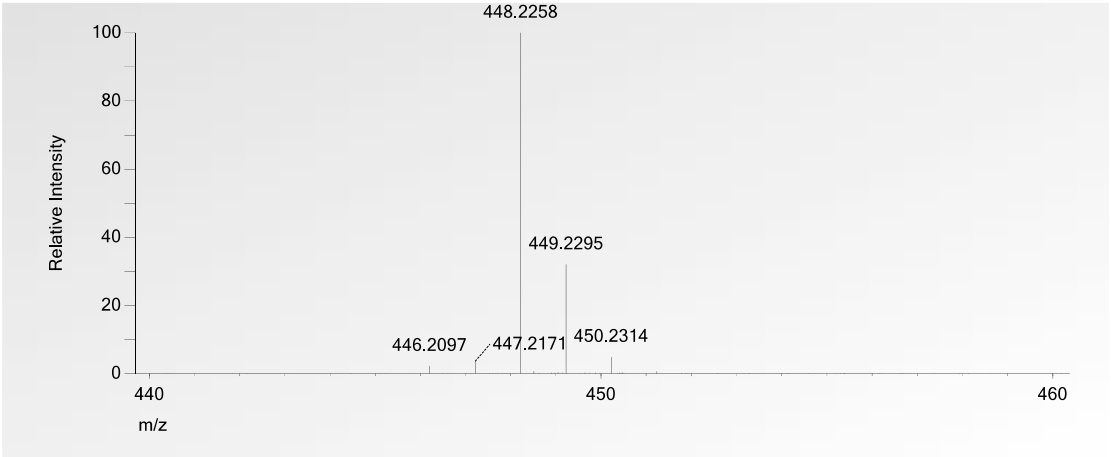
448.2258
449.2295
446.2097
447.2171
450.2314
Relative Intensity
m/z
100
80
60
40
20
0
440
450
460

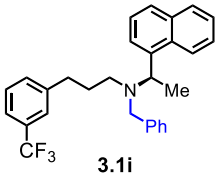
N
Me
Ph
CF3

3.1i

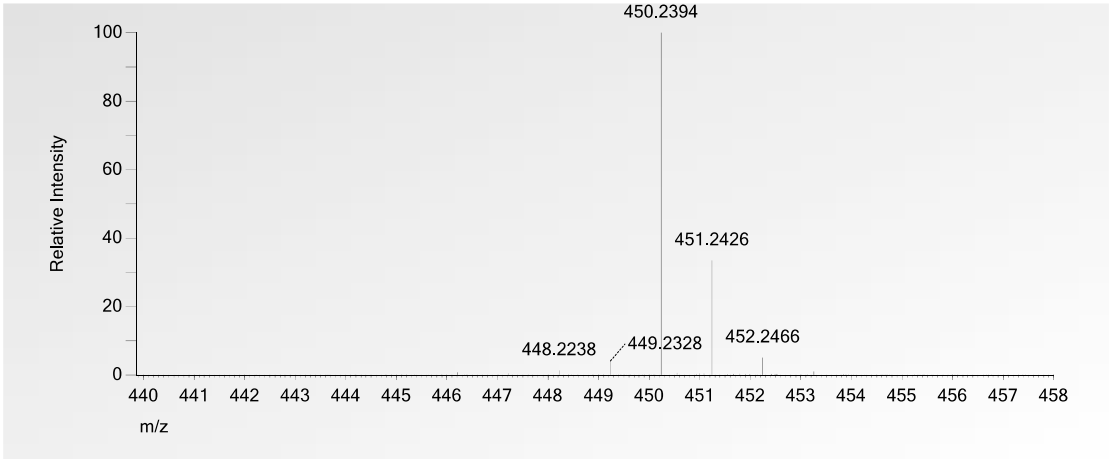
450.2394
451.2426
448.2238
449.2328
452.2466
Relative Intensity
m/z
100
80
60
40
20
0
440
441
442
443
444
445
446
447
448
449
450
451
452
453
454
455
456
457
458

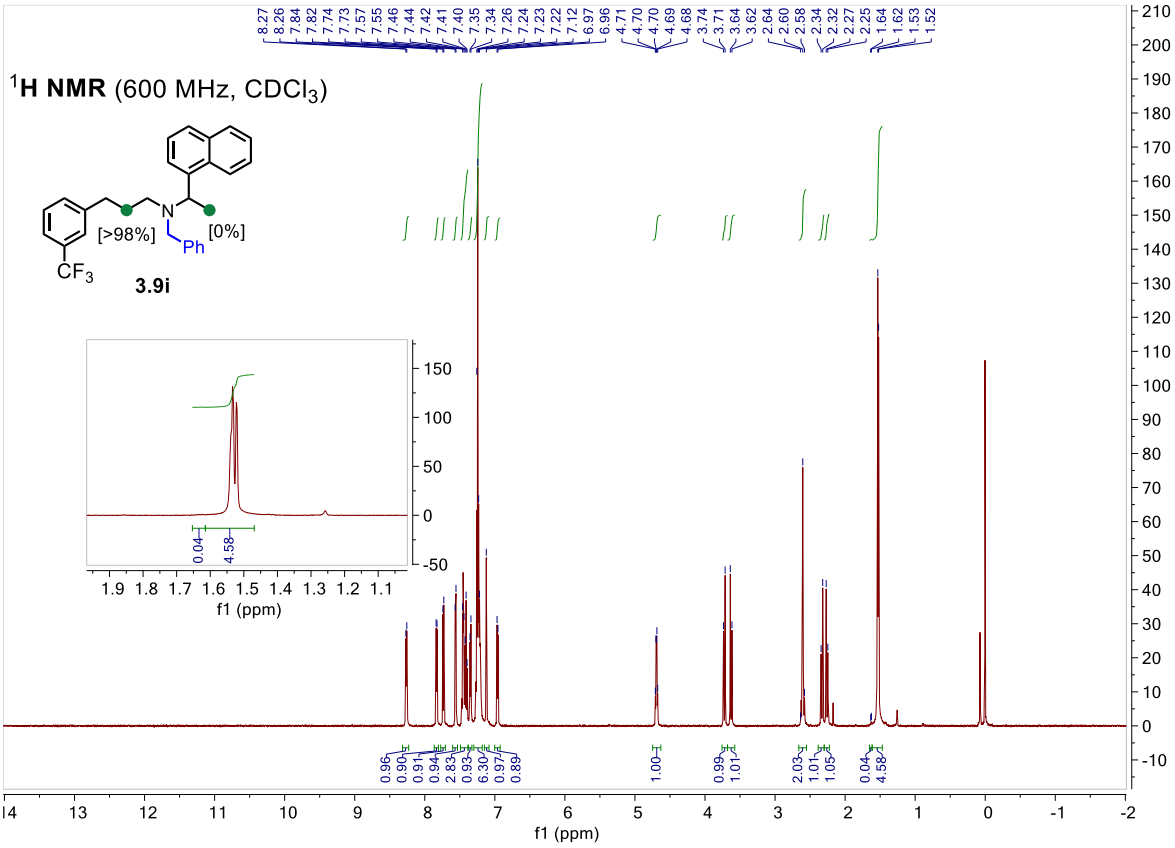
^{1}H NMR (600 MHz, CDCl$_3$)
[>98%]
[0%]
Ph
CF$_3$
3.9i
f1 (ppm)

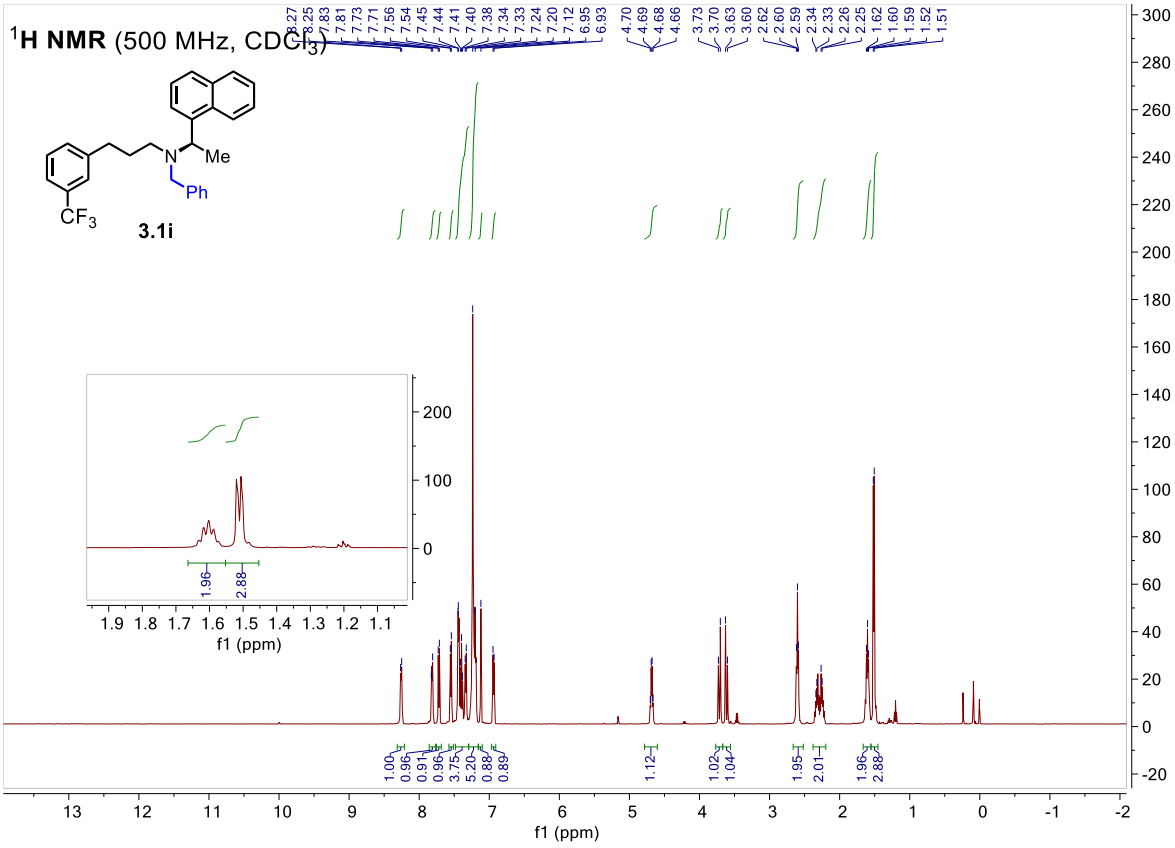
^{1}H NMR (500 MHz, CDCl$_3$)
N
Me
Ph
CF$_3$
3.1i
f1 (ppm)

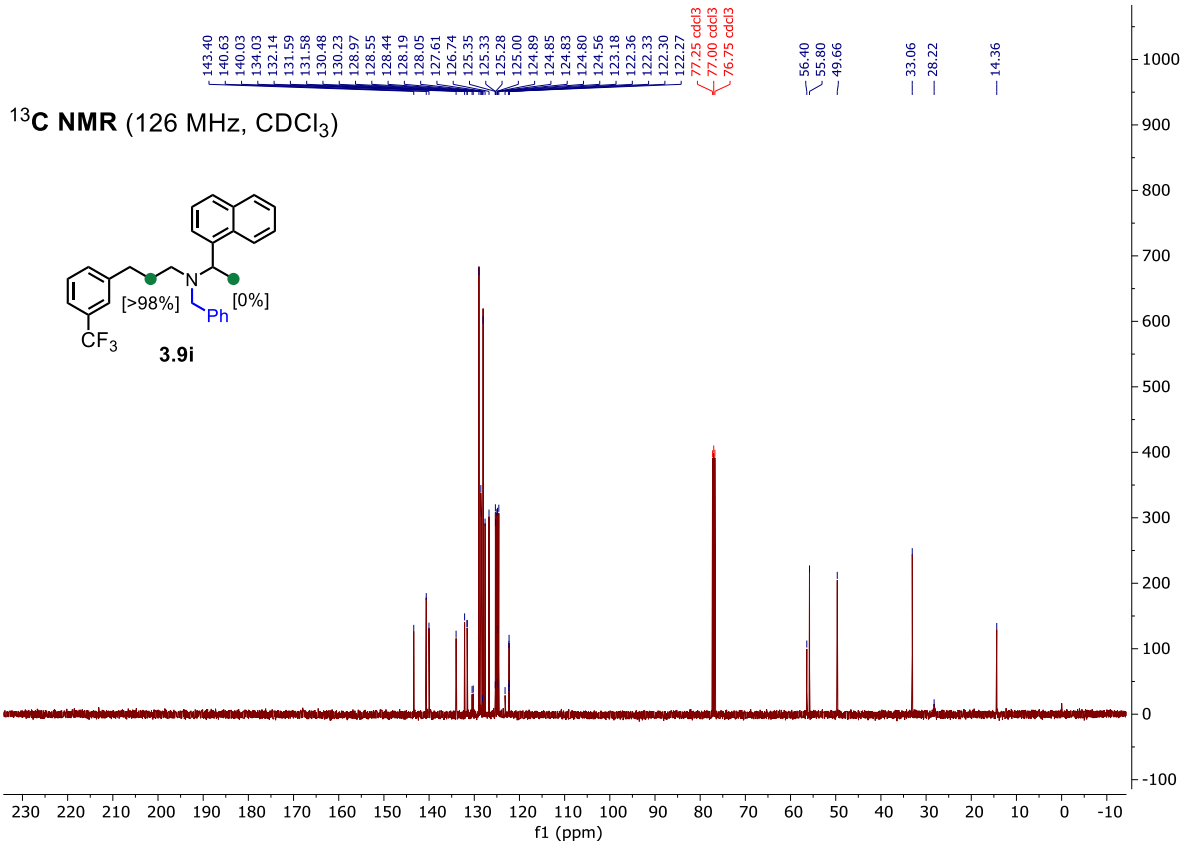
143.40
140.63
140.03
134.03
132.14
131.59
131.58
130.48
130.23
128.97
128.55
128.44
128.19
128.05
127.61
126.74
125.35
125.33
125.28
125.00
124.89
124.85
124.83
124.80
124.56
123.18
122.36
122.33
122.30
122.27
77.25 cdcl3
77.00 cdcl3
76.75 cdcl3
56.40
55.80
49.66
33.06
28.22
14.36
13C NMR (126 MHz, CDCl3)
[>98%]
[0%]
N
Ph
CF3
3.9i
f1 (ppm)

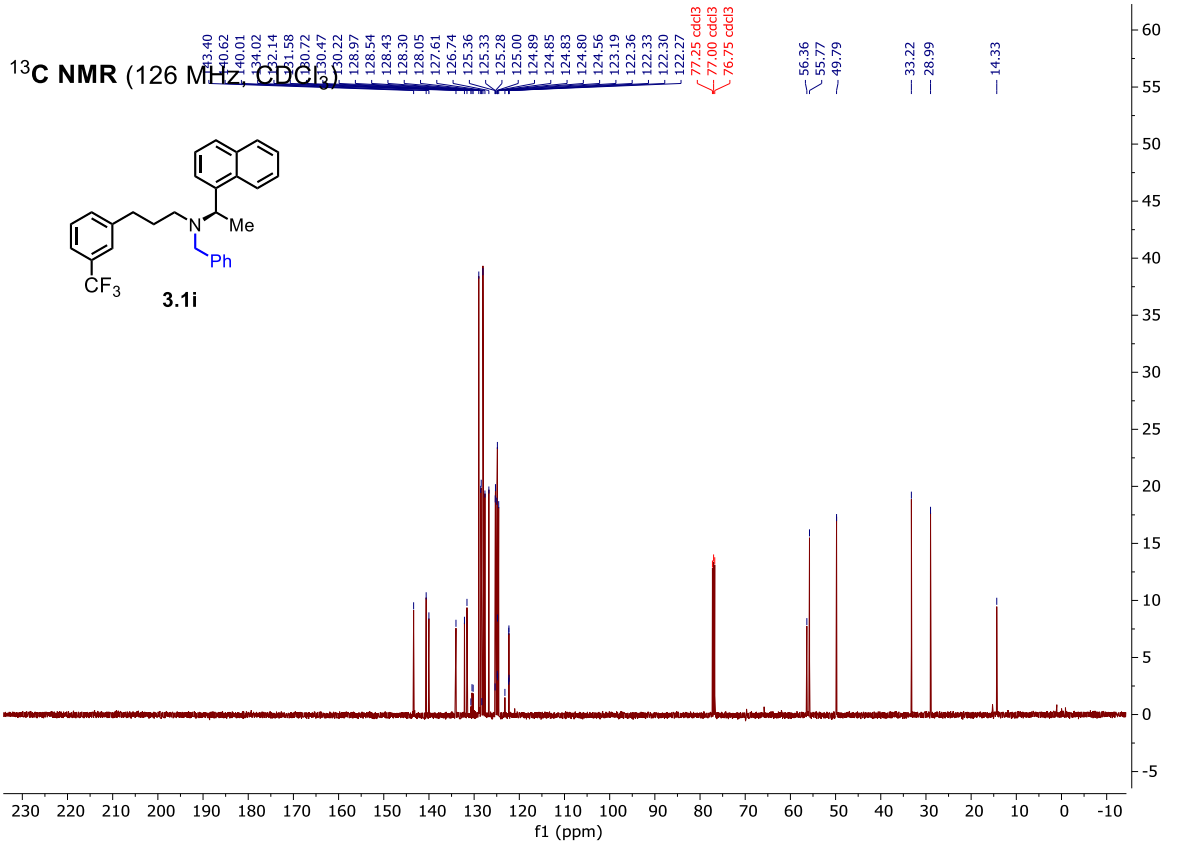
143.40
140.62
140.01
134.02
132.14
131.58
130.72
130.47
130.22
128.97
128.54
128.43
128.30
128.05
127.61
126.74
125.36
125.33
125.28
125.00
124.89
124.85
124.83
124.80
124.56
123.19
122.36
122.33
122.30
122.27
77.25 cdcl3
77.00 cdcl3
76.75 cdcl3
56.36
55.77
49.79
33.22
28.99
14.33
13C NMR (126 MHz, CDCl3)
N
Me
Ph
CF3
3.1i
f1 (ppm)

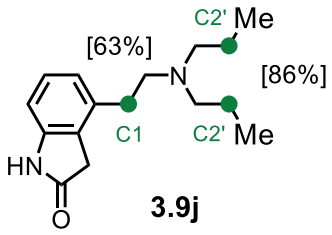

3.9j

Ropinirole, 3.9j

Ropinirole **3.1j** was reacted with acetone-d_6 following the General Procedure C. After purification by column chromatography (MeOH:DCM = 1:24), **3.9j** was obtained as a white solid (40 mg, 77%).

Deuterium incorporation: 4.70 D/molecule (^{1}H NMR), 5.24 D/molecule [HRMS (DART)]

^{1}H NMR (500 MHz, $CDCl_3$) δ 9.22 (s, 1H), 7.14 (t, J = 7.7 Hz, 1H), 6.84 (d, J = 7.8 Hz, 1H), 6.75 (d, J = 7.7 Hz, 1H), 3.49 (s, 2H), 2.71 (d, J = 5.1 Hz, 2.74H, 63%D), 2.50 (s, 4H), 1.55 – 1.44 (m, 0.58H, 86%D), 0.89 (d, J = 8.5 Hz, 6H); **^{13}C NMR** (126 MHz, $CDCl_3$) δ 177.6, 142.5, 136.8, 128.1, 128.0, 124.0, 122.8, 107.6, 55.9, 55.8, 54.13, 54.07, 54.0, 35.1, 30.5, 19.3, 11.9, 11.8, 11.7; **IR** (neat) 2952, 2928, 2799, 1701, 1615, 1601, 1453, 1254, 762, 719 cm^{-1}.

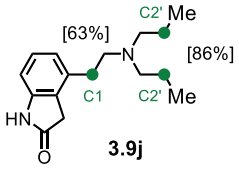
[63%]
C2' Me
N
[86%]
C1
C2' Me
HN
O

3.9j

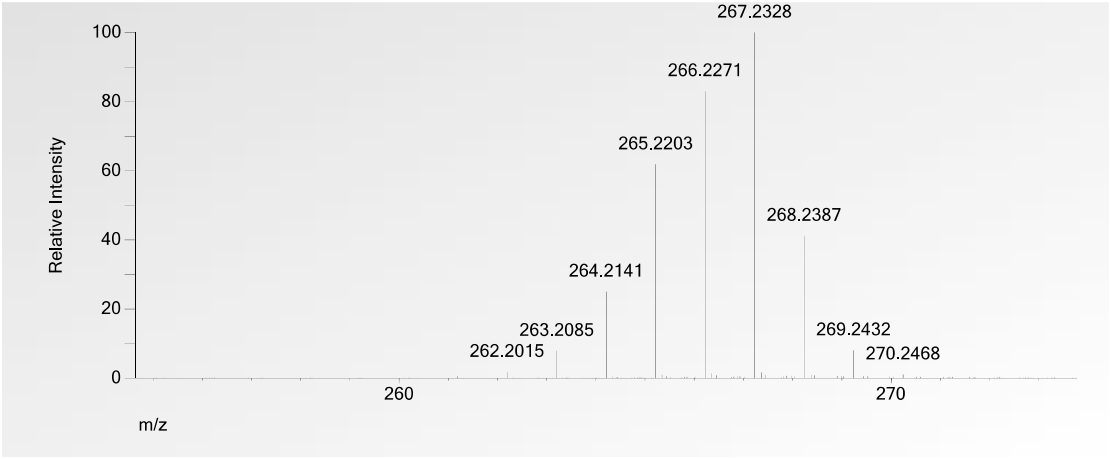
267.2328
266.2271
265.2203
268.2387
264.2141
263.2085
262.2015
269.2432
270.2468
100
80
60
40
20
0
Relative Intensity
260
270
m/z

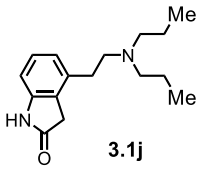
Me
N
Me
HN
O

3.1j


261.2059
262.2016
259.1829
260.1859
263.2044
100
80
60
40
20
0
Relative Intensity
260
270
m/z

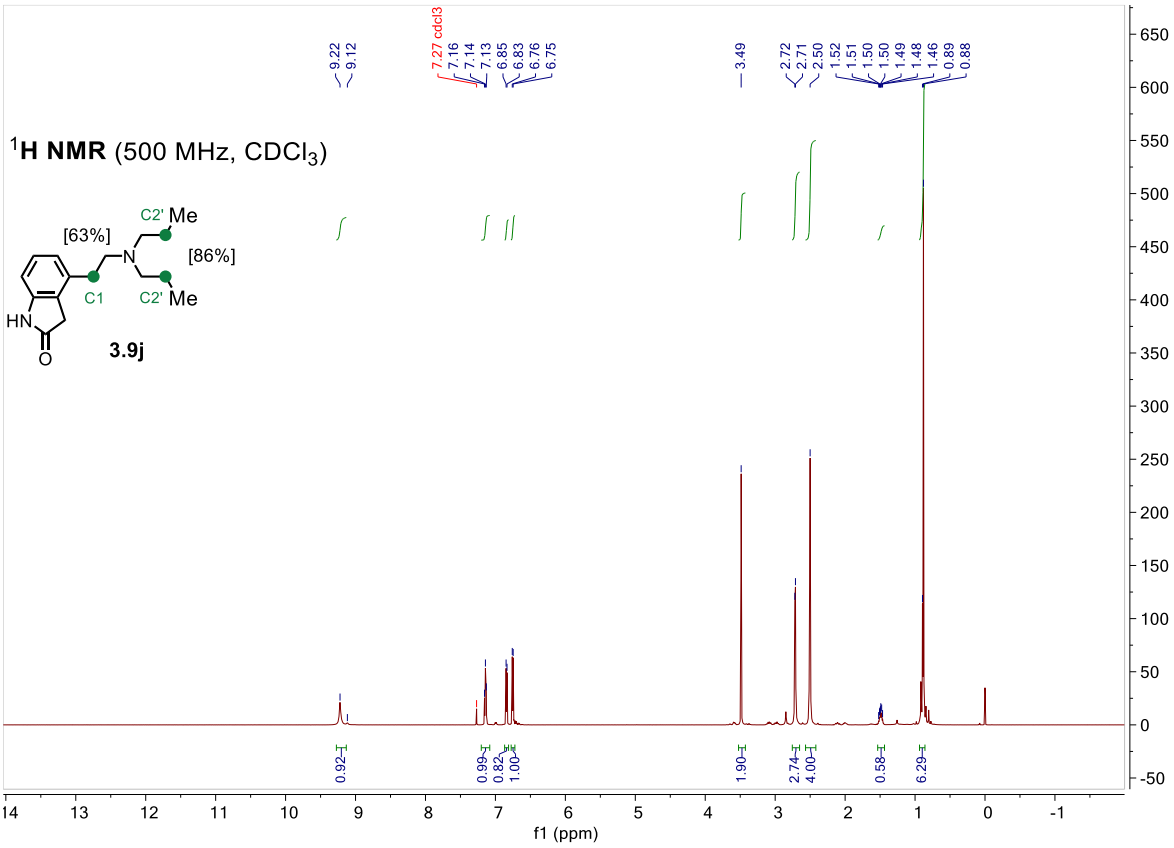
1H NMR (500 MHz, CDCl3)
[63%]
[86%]
C2' Me
C2' Me
C1
HN
O
3.9j
9.22
9.12
7.27 cdcl3
7.16
7.14
7.13
6.85
6.83
6.76
6.75
3.49
2.72
2.71
2.50
1.52
1.51
1.50
1.50
1.49
1.48
1.46
0.89
0.88
0.92
0.99
0.82
1.00
1.90
2.74
4.00
0.58
6.29
f1 (ppm)

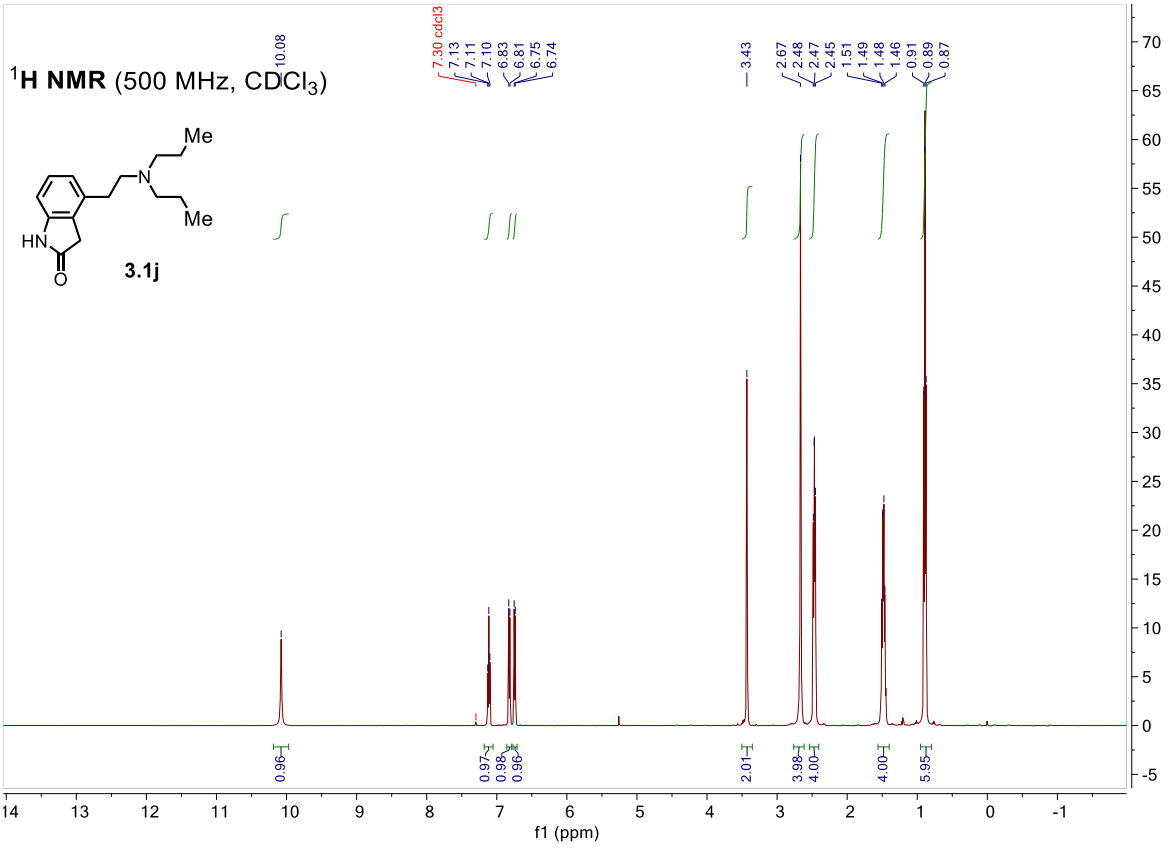
1H NMR (500 MHz, CDCl3)
Me
Me
HN
O
3.1j
10.08
7.30 cdcl3
7.13
7.11
7.10
6.83
6.81
6.75
6.74
3.43
2.67
2.48
2.47
2.45
1.51
1.49
1.48
1.46
0.91
0.89
0.87
0.96
0.97
0.98
0.96
2.01
3.98
4.00
4.00
5.95
f1 (ppm)

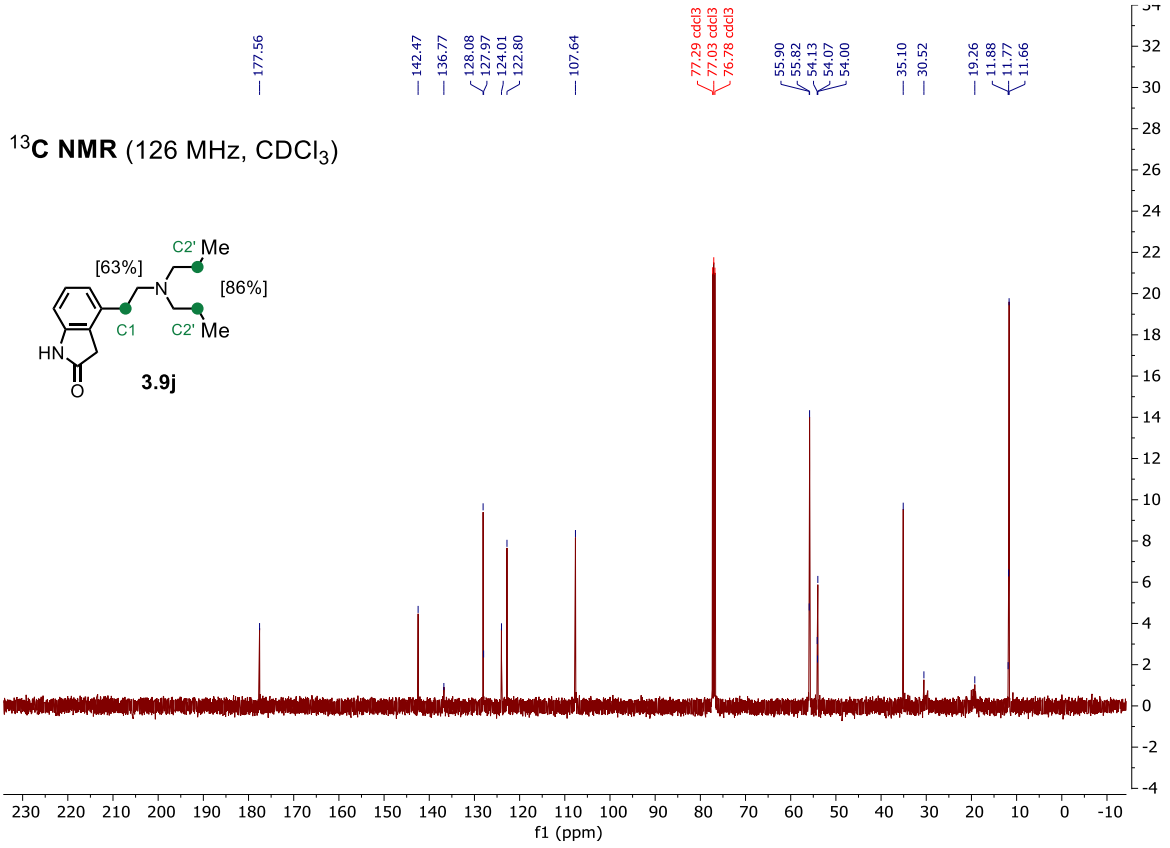
177.56
142.47
136.77
128.08
127.97
124.01
122.80
107.64
77.29 cdcl3
77.03 cdcl3
76.78 cdcl3
55.90
55.82
54.13
54.07
54.00
35.10
30.52
19.26
11.88
11.77
11.66
13C NMR (126 MHz, CDCl3)
[63%]
C2' Me
N
[86%]
C1
C2' Me
HN
O
3.9j
f1 (ppm)

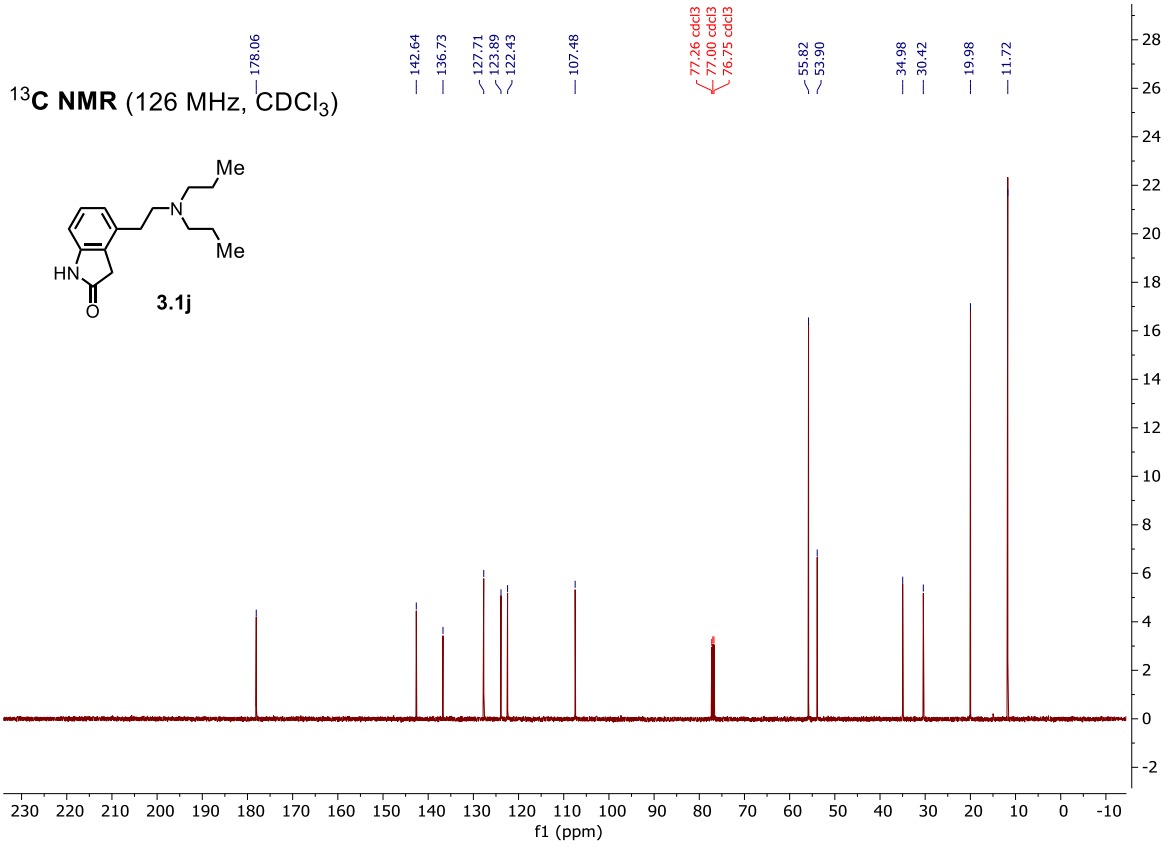
178.06
142.64
136.73
127.71
123.89
122.43
107.48
77.26 cdcl3
77.00 cdcl3
76.75 cdcl3
55.82
53.90
34.98
30.42
19.98
11.72
13C NMR (126 MHz, CDCl3)
Me
N
Me
HN
O
3.1j
f1 (ppm)

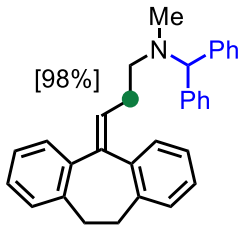

3.9k

***N*-Bzh nortriptyline, 3.9k**

N-Bzh nortriptyline **3.1k** was reacted with acetone-d_6 following the General Procedure B. After purification by column chromatography (Et_2O:hexanes = 1:9), **3.9k** was obtained as a yellow liquid (83 mg, 96%).

Deuterium incorporation: 1.96 D/molecule (^{1}H NMR), 2.34 D/molecule [HRMS (DART)]

^{1}H NMR (500 MHz, $CDCl_3$) δ 7.35 (d, *J* = 7.6 Hz, 4H), 7.22 (dd, *J* = 8.4, 6.8 Hz, 5H), 7.20 – 7.09 (m, 7H), 7.09 – 7.04 (m, 1H), 7.03 (s, 1H), 5.81 (s, 1H), 4.30 (s, 1H), 3.27 (dt, *J* = 32.1, 23.1 Hz, 2H), 2.94 (s, 1H), 2.71 (s, 1H), 2.44 (d, *J* = 5.3 Hz, 2H), 2.30 (d, *J* = 7.5 Hz, 0.04H, 98%D), 2.07 (s, 3H); **^{13}C NMR** (126 MHz, $CDCl_3$) δ 143.3, 141.5, 140.2, 139.4, 137.1, 130.0, 129.8, 128.6, 128.4, 128.0, 127.3, 126.9, 126.8, 126.0, 125.7, 75.7, 54.9, 40.3, 33.8, 32.1; **IR** (neat) 3020, 2784, 1485, 1451, 1265, 1028, 1012, 924, 756, 742, 704 cm^{-1}.

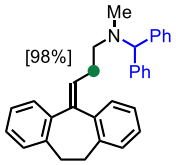
Me
N
Ph
Ph
[98%]

3.9k

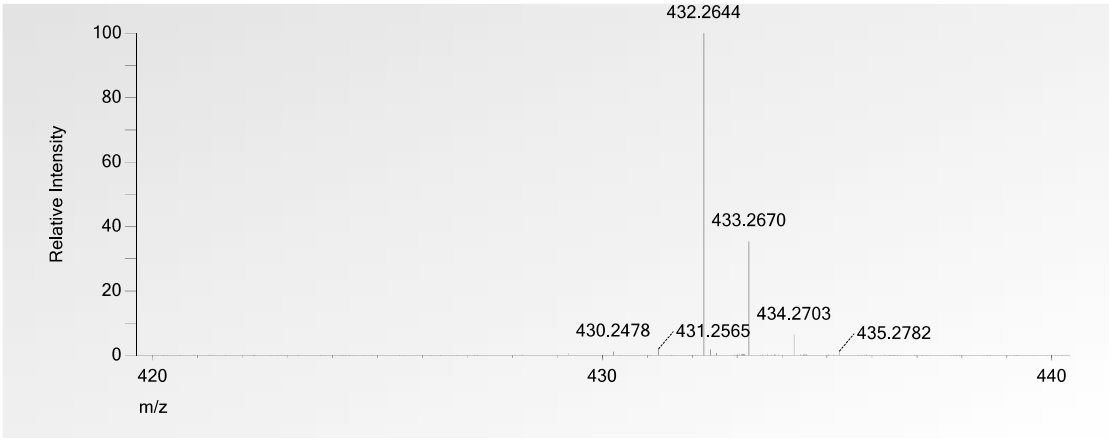
432.2644
433.2670
434.2703
430.2478
431.2565
435.2782
Relative Intensity
100
80
60
40
20
0
420
430
440
m/z

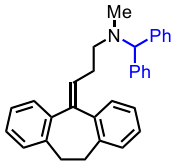
Me
N
Ph
Ph

3.1k

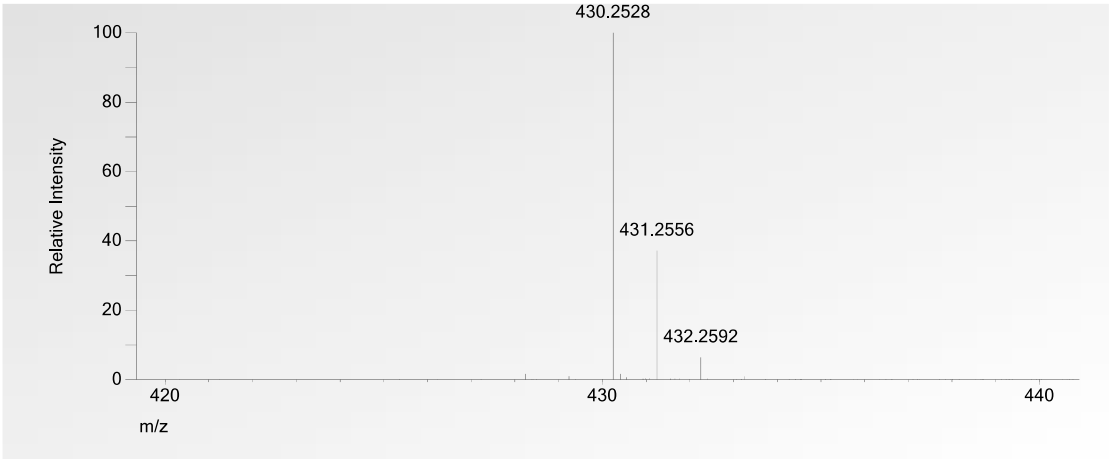
430.2528
431.2556
432.2592
Relative Intensity
100
80
60
40
20
0
420
430
440
m/z

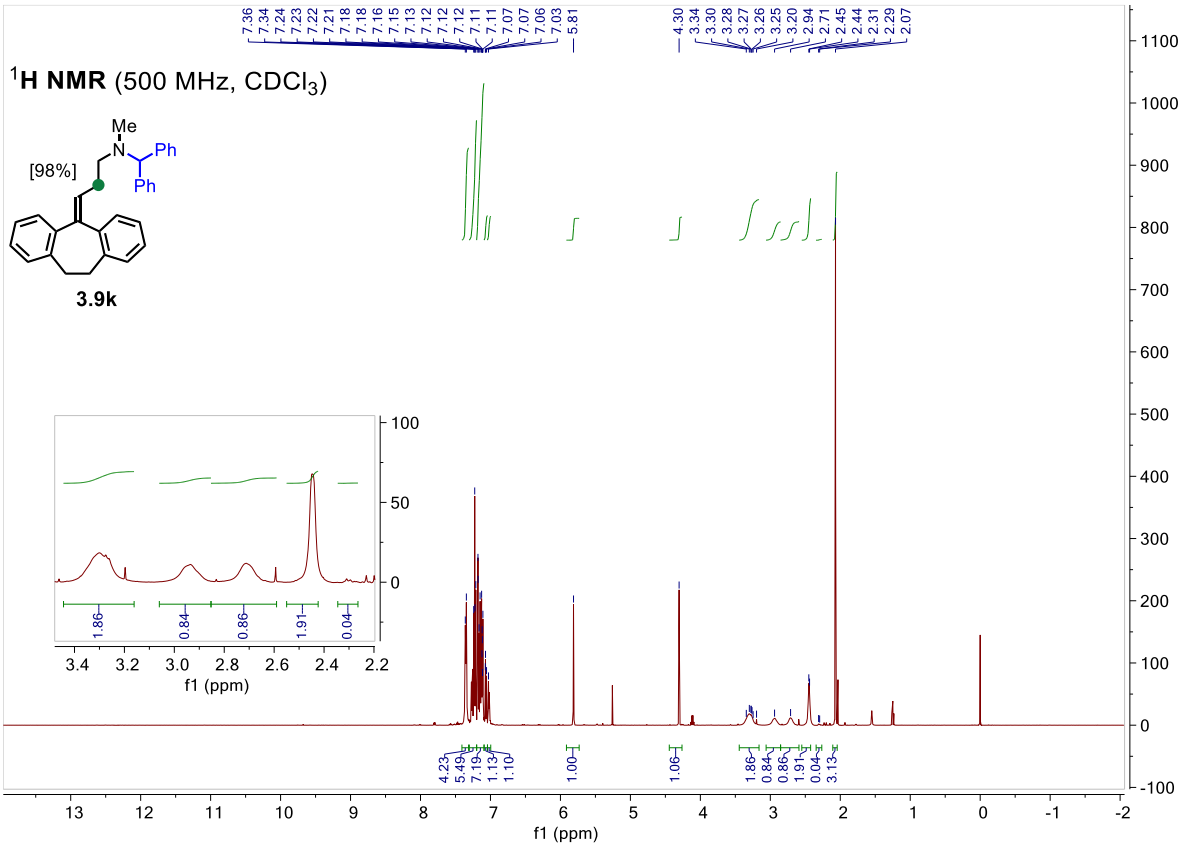
1H NMR (500 MHz, CDCl3)
Me
N
Ph
Ph
[98%]
3.9k
f1 (ppm)

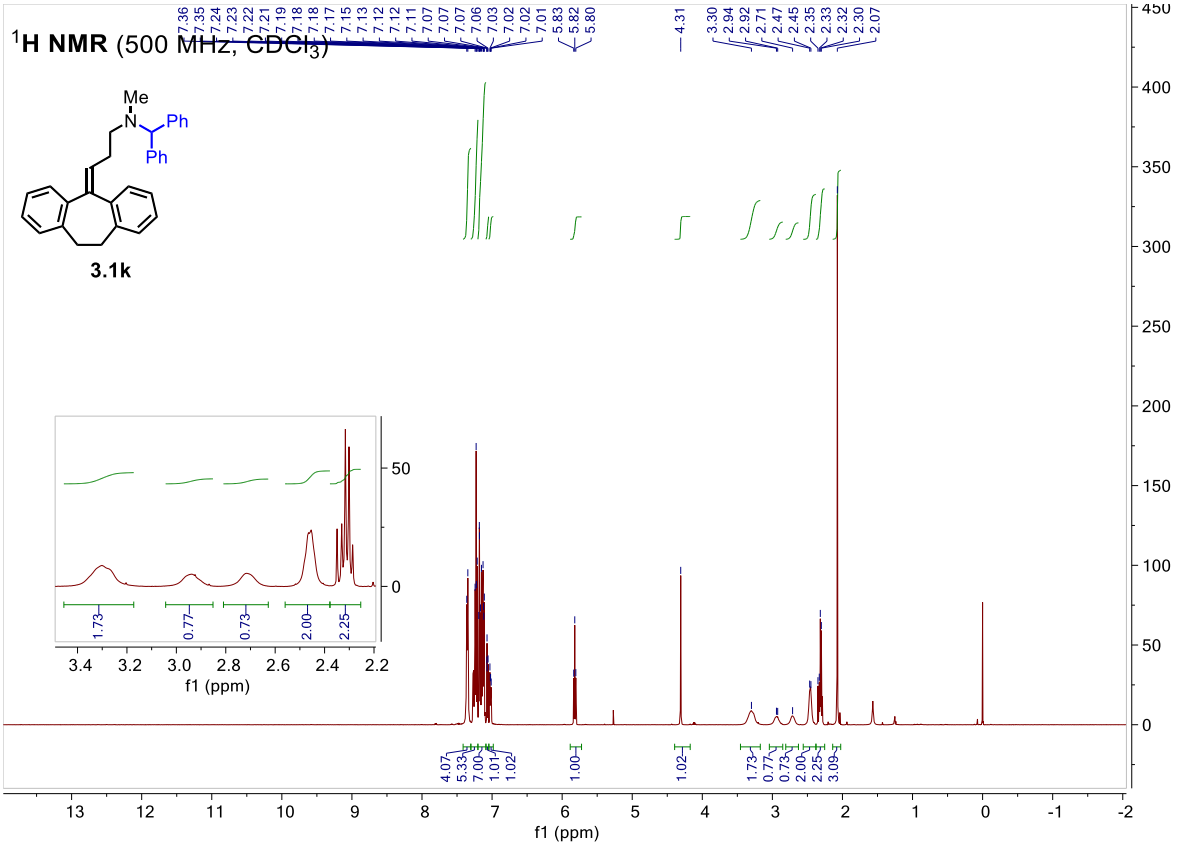
1H NMR (500 MHz, CDCl3)
Me
N
Ph
Ph
3.1k
f1 (ppm)

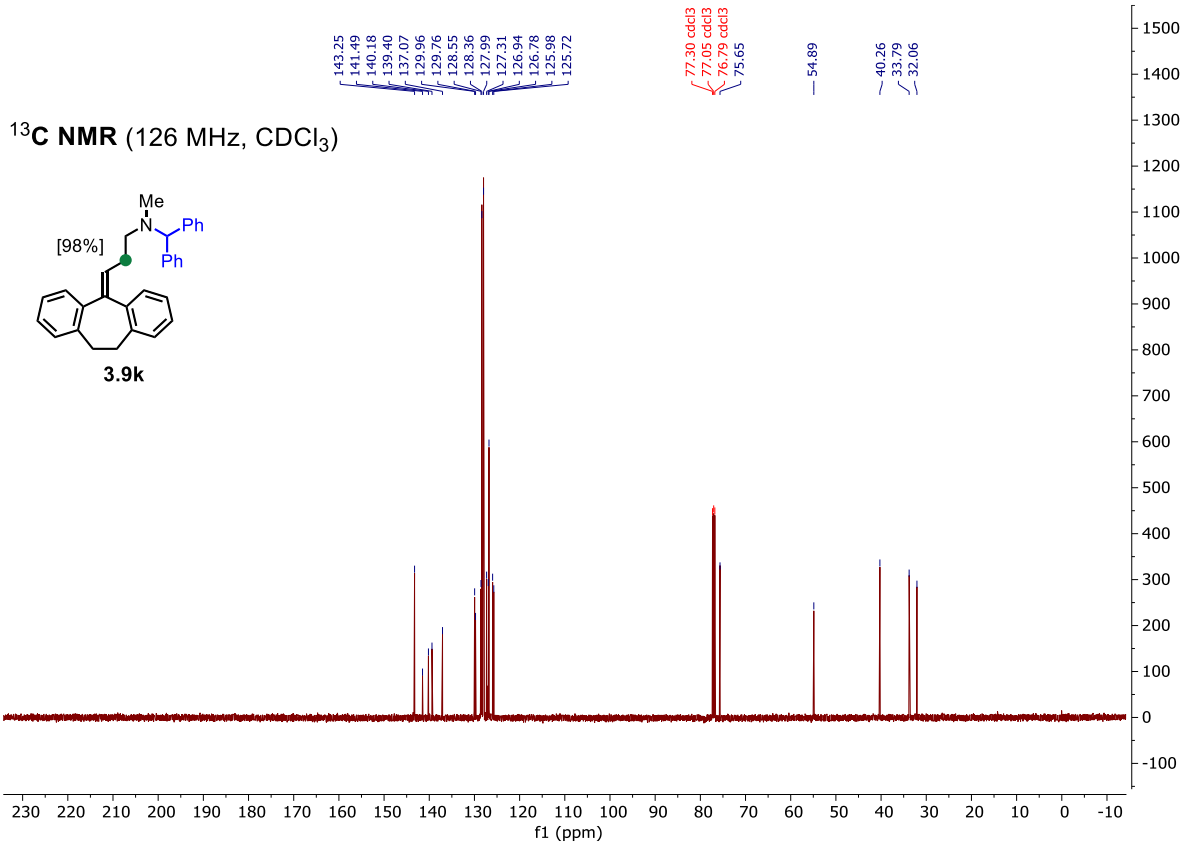
143.25
141.49
140.18
139.40
137.07
129.96
129.76
128.55
128.36
127.99
127.31
126.94
126.78
125.98
125.72
77.30 cdcl3
77.05 cdcl3
76.79 cdcl3
75.65
54.89
40.26
33.79
32.06
13C NMR (126 MHz, CDCl3)
Me
N
Ph
Ph
[98%]
3.9k
f1 (ppm)

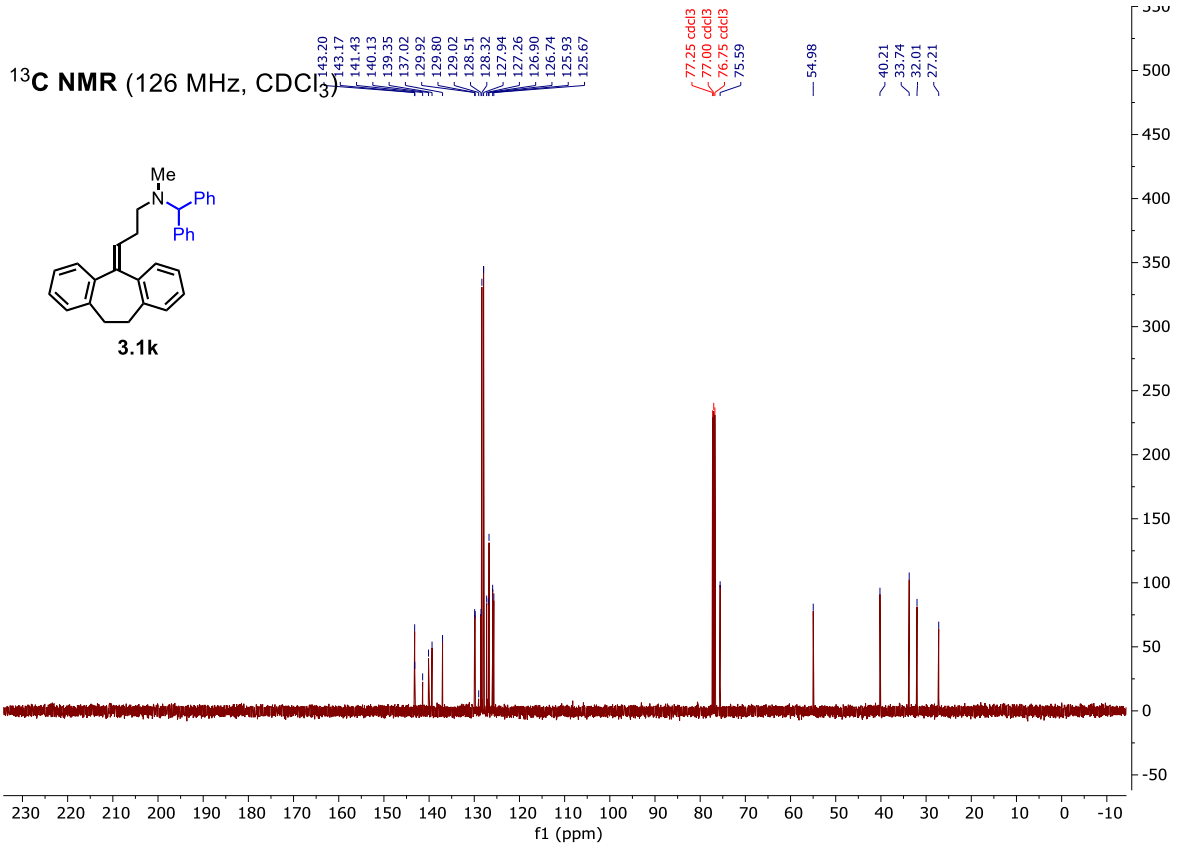
143.20
143.17
141.43
140.13
139.35
137.02
129.92
129.80
129.02
128.51
128.32
127.94
127.26
126.90
126.74
125.93
125.67
77.25 cdcl3
77.00 cdcl3
76.75 cdcl3
75.59
54.98
40.21
33.74
32.01
27.21
13C NMR (126 MHz, CDCl3)
Me
N
Ph
Ph
3.1k
f1 (ppm)

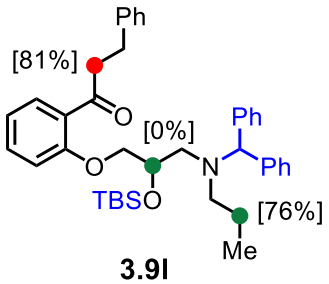

3.9l

***N*-Bzh, *O*-TBS propafenone, 3.9l**

N-Bzh, *O*-TBS propafenone **3.1l** was reacted with acetone-d_6 following the General Procedure A. After purification by column chromatography (Et_2O:hexanes = 1:9), **3.9l** was obtained as a yellow liquid (114 mg, 92%).

Deuterium incorporation: 3.14 D/molecule (^{1}H NMR), 3.51 D/molecule [HRMS (DART)]

^{1}H NMR (600 MHz, $CDCl_3$) δ 7.72 (d, *J* = 9.4 Hz, 1H), 7.47 – 7.40 (m, 1H), 7.27 (d, *J* = 7.1 Hz, 2H), 7.23 (d, *J* = 7.6 Hz, 4H), 7.20 – 7.08 (m, 9H), 6.99 (dd, *J* = 15.9, 8.8 Hz, 2H), 4.81 (s, 1H), 4.18 (d, *J* = 3.8 Hz, 1H), 4.11 (d, *J* = 3.3 Hz, 1H), 3.92 (dd, *J* = 8.7, 4.3 Hz, 1H), 3.35 – 3.18 (m, 0.19H, 81%D), 3.11 – 2.97 (m, 0.24H, 76%D), 2.91 (d, *J* = 11.4 Hz, 2H), 2.79 (dd, *J* = 13.5, 8.9 Hz, 1H), 2.55 (dd, *J* = 13.5, 4.6 Hz, 1H), 2.51 – 2.38 (m, 2H), 1.50 – 1.35 (m, 0.50H, 76%D), 0.79 (s, 9H), 0.75 – 0.66 (m, 3H), -0.06 (s, 3H), -0.09 (s, 3H); **^{13}C NMR** (151 MHz, $CDCl_3$) δ 201.4, 201.3, 158.2, 142.1, 141.7, 141.5, 133.3, 130.5, 128.8, 128.7, 128.5, 128.4, 128.3, 128.22, 128.16, 128.1, 126.92, 126.89, 125.7, 120.5, 112.3, 71.2, 70.5, 69.9, 54.2, 53.9, 45.0, 29.9, 25.7, 19.0, 17.9, 11.5, -4.7, -4.8; **IR** (neat) 2950, 2926, 1669, 1595, 1470, 1293, 1248, 1113, 833, 747, 699 cm^{-1}.

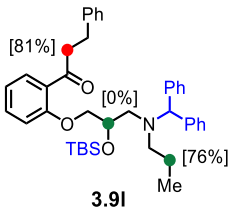
Ph
[81%]
O
[0%]
Ph
Ph
O
N
TBSO
[76%]
Me

3.9l

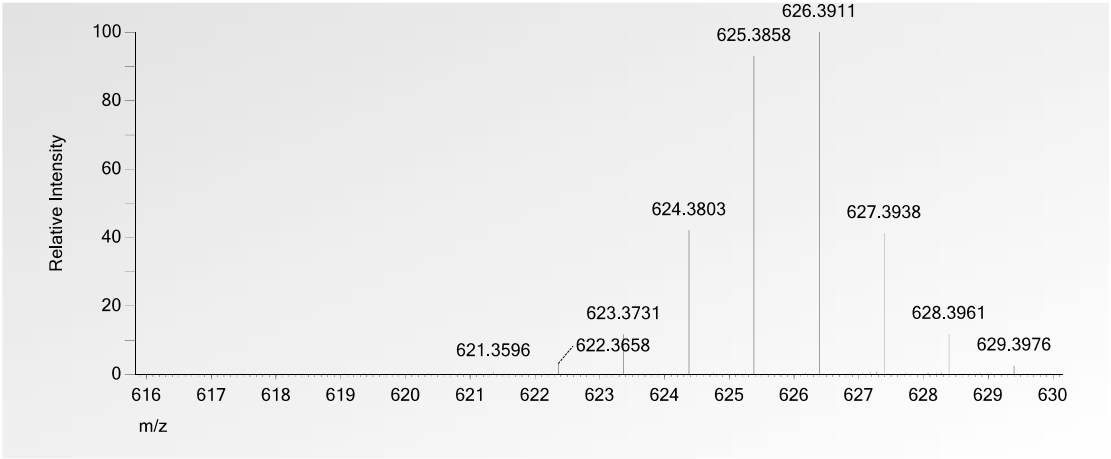
626.3911
625.3858
624.3803
627.3938
623.3731
628.3961
621.3596
622.3658
629.3976
Relative Intensity
m/z

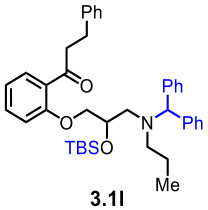
Ph
O
Ph
Ph
O
N
TBSO
Me

3.1l

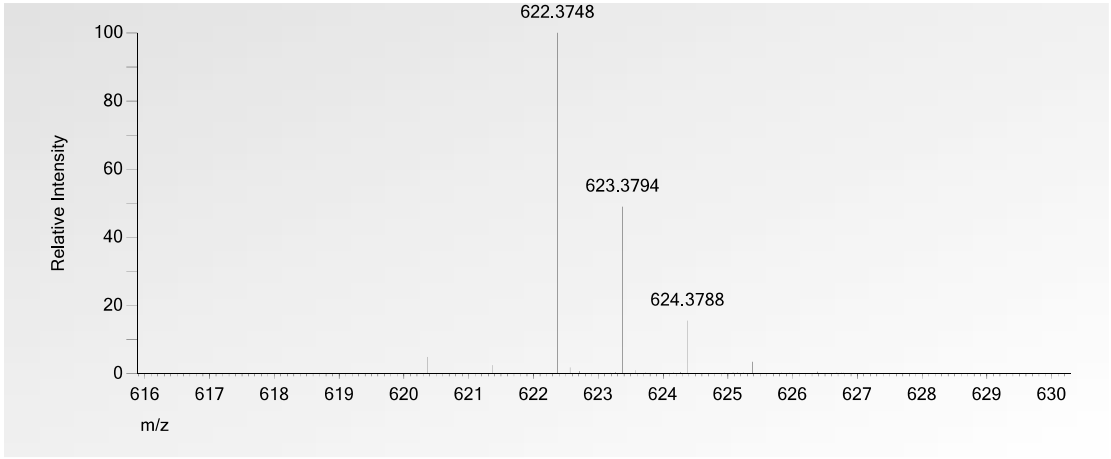
622.3748
623.3794
624.3788
Relative Intensity
m/z

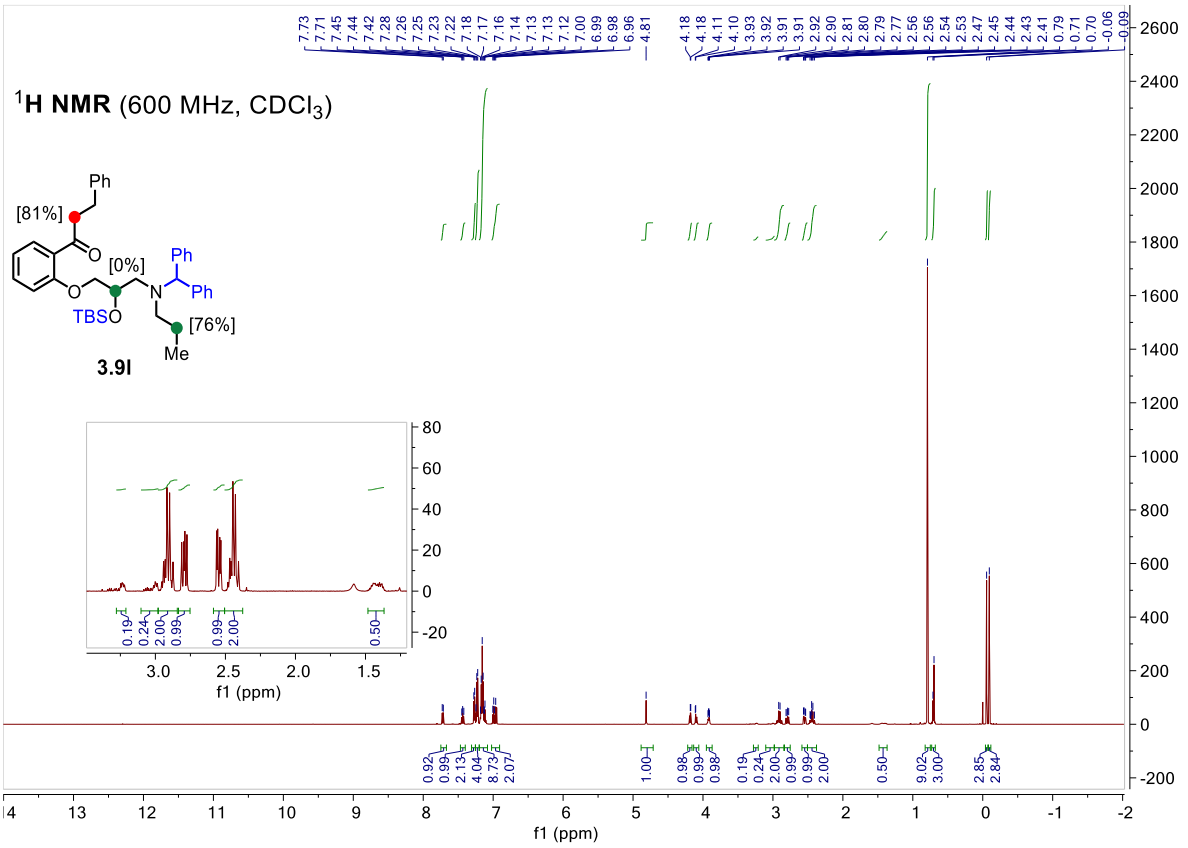
1H NMR (600 MHz, CDCl3)
Ph
[81%]
O
[0%]
Ph
Ph
N
TBSO
[76%]
Me
3.9l
f1 (ppm)

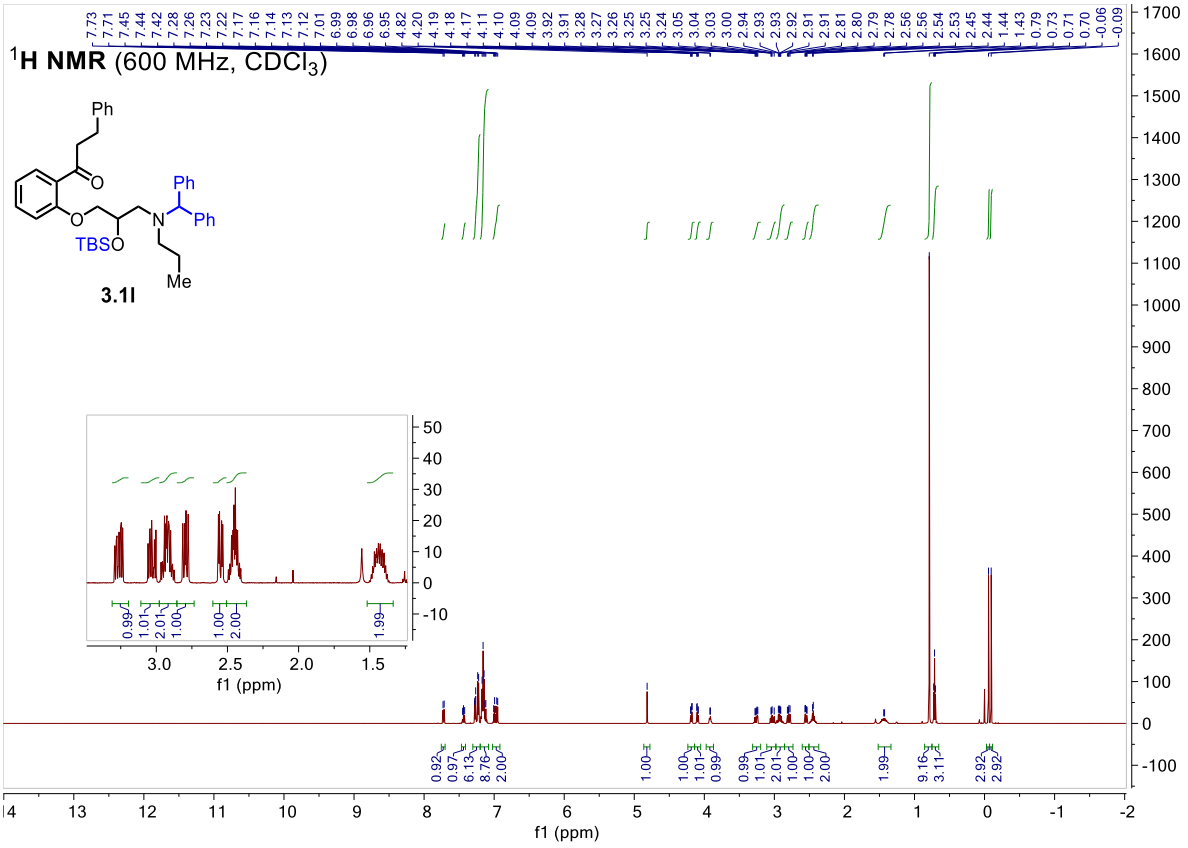
1H NMR (600 MHz, CDCl3)
Ph
O
Ph
Ph
N
TBSO
Me
3.1l
f1 (ppm)

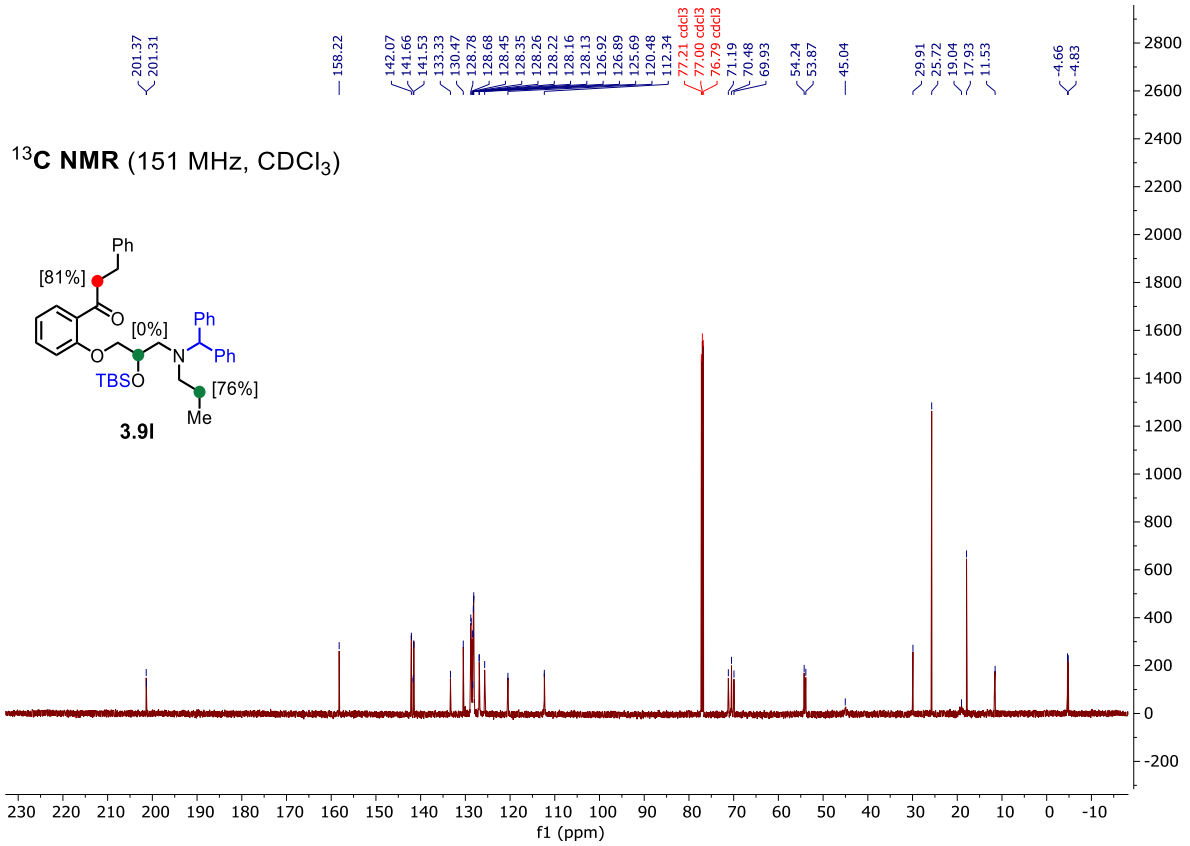
201.37
201.31
158.22
142.07
141.66
141.53
133.33
130.47
128.78
128.68
128.45
128.35
128.26
128.22
128.16
128.13
126.92
126.89
125.69
120.48
112.34
77.21 cdcl3
77.00 cdcl3
76.79 cdcl3
71.19
70.48
69.93
54.24
53.87
45.04
29.91
25.72
19.04
17.93
11.53
-4.66
-4.83
13C NMR (151 MHz, CDCl3)
Ph
[81%]
O
[0%]
Ph
O
N
Ph
TBSO
[76%]
Me
3.9l
f1 (ppm)

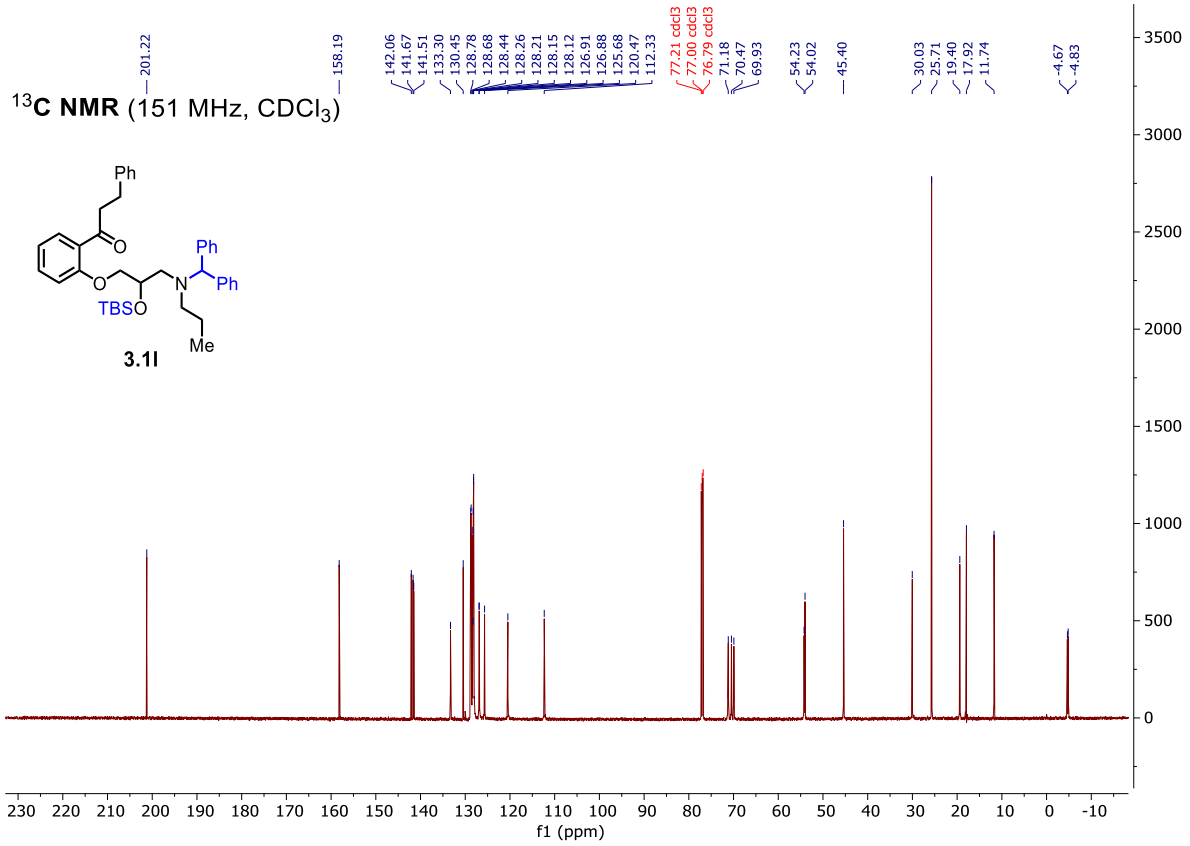
201.22
158.19
142.06
141.67
141.51
133.30
130.45
128.78
128.68
128.44
128.26
128.21
128.15
128.12
126.91
126.88
125.68
120.47
112.33
77.21 cdcl3
77.00 cdcl3
76.79 cdcl3
71.18
70.47
69.93
54.23
54.02
45.40
30.03
25.71
19.40
17.92
11.74
-4.67
-4.83
13C NMR (151 MHz, CDCl3)
Ph
O
Ph
O
N
Ph
TBSO
Me
3.1l
f1 (ppm)

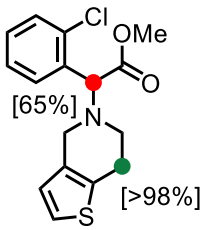

3.9m

Clopidogrel, 3.9m

Clopidogrel **3.1m** was reacted with acetone-d_6 following the General Procedure B. After purification by column chromatography (Et_2O:hexanes = 1:9), **3.9m** was obtained as a colorless liquid (61 mg, 94%).

Deuterium incorporation: 2.65 D/molecule (^{1}H NMR), 2.88 D/molecule [HRMS (DART)]

^{1}H NMR (500 MHz, $CDCl_3$) δ 7.70 (d, J = 7.4 Hz, 1H), 7.40 (d, J = 7.5 Hz, 1H), 7.36 – 7.18 (m, 2H), 7.11 – 7.00 (m, 1H), 6.75 – 6.59 (m, 1H), 4.92 (d, J = 2.0 Hz, 0.35H, 65%D), 3.79 – 3.70 (m, 4H), 3.63 (d, J = 14.2 Hz, 1H), 2.88 (s, 2.00H, >98%D); **^{13}C NMR** (126 MHz, $CDCl_3$) δ 171.3, 134.7, 133.8, 133.4, 133.1, 130.0, 129.8, 129.4, 127.15, 125.24, 122.8, 67.9, 52.1, 50.70, 50.65, 48.2, 48.1, 25.1; **IR** (neat) 2947, 1735, 1469, 1431, 1245, 1140, 1105, 1064, 752, 704 cm^{-1}; $[\alpha]^{25}_D$ = 0.7° (c = 1.0, CH_2Cl_2 labeled), $[\alpha]^{25}_D$ = 15.0° (c = 1.0, CH_2Cl_2 unlabeled).

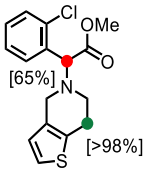
Cl
OMe
O
[65%]
N
S
[>98%]

3.9m

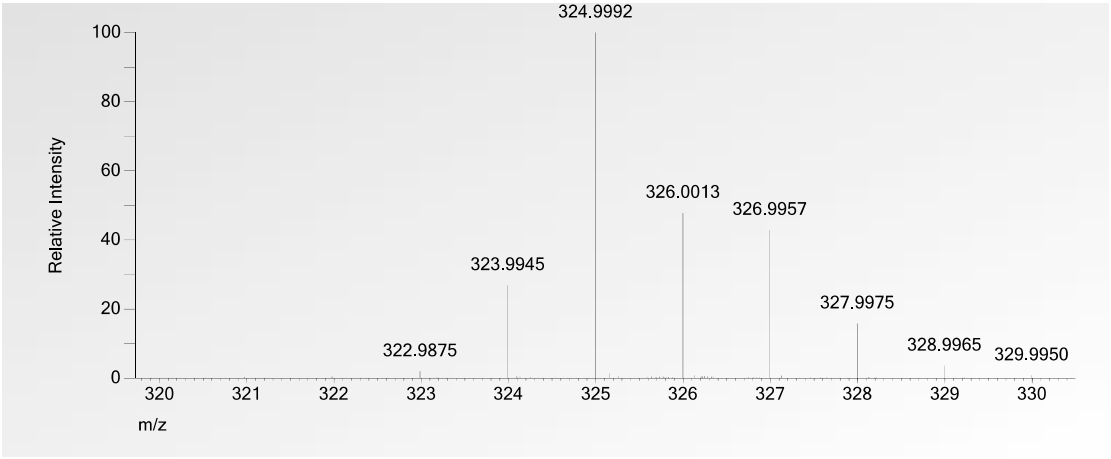
324.9992
326.0013
326.9957
323.9945
327.9975
322.9875
328.9965
329.9950
Relative Intensity
m/z

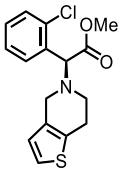
Cl
OMe
O
N
S

3.1m

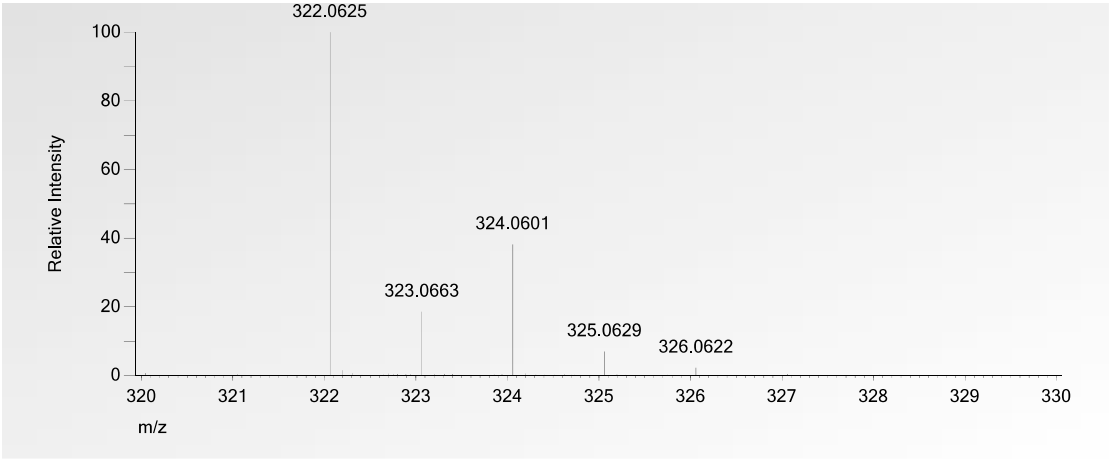
322.0625
324.0601
323.0663
325.0629
326.0622
Relative Intensity
m/z

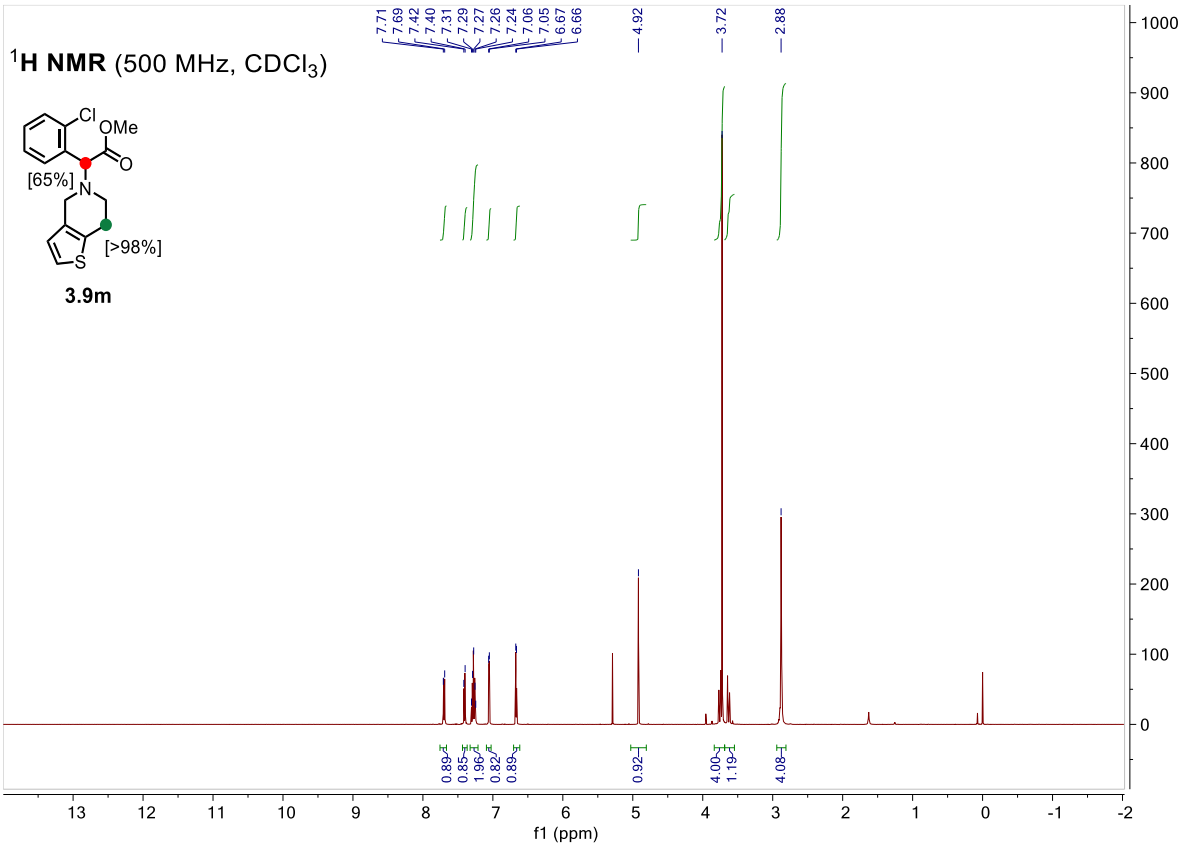
1H NMR (500 MHz, CDCl3)
Cl
OMe
O
[65%]
N
[>98%]
S
3.9m
7.71
7.69
7.42
7.40
7.31
7.29
7.27
7.26
7.24
7.06
7.05
6.67
6.66
4.92
3.72
2.88
0.89
0.85
1.96
0.82
0.89
0.92
4.00
1.19
4.08
f1 (ppm)

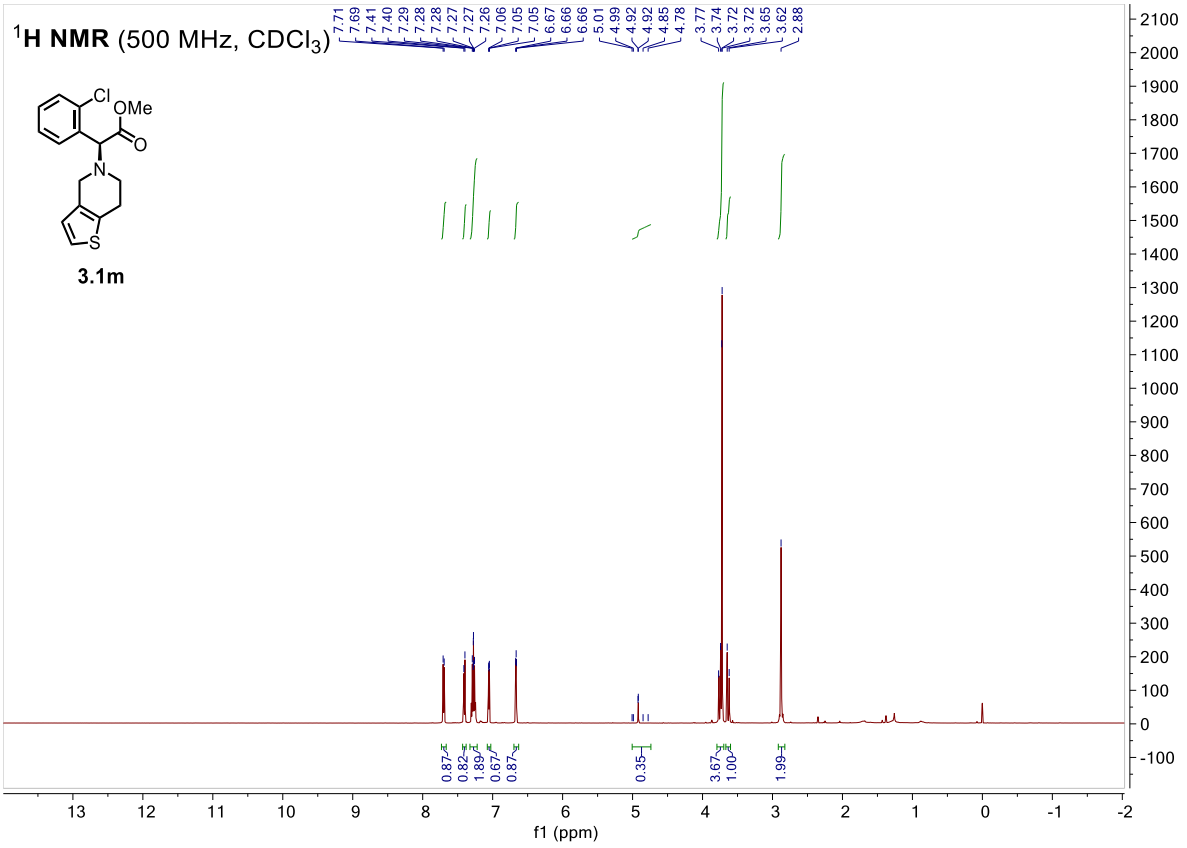
1H NMR (500 MHz, CDCl3)
Cl
OMe
O
N
S
3.1m
7.71
7.69
7.41
7.40
7.29
7.28
7.28
7.27
7.27
7.26
7.06
7.05
7.05
6.67
6.66
6.66
5.01
4.99
4.92
4.92
4.85
4.78
3.77
3.74
3.72
3.72
3.65
3.62
2.88
0.87
0.82
1.89
0.67
0.87
0.35
3.67
1.00
1.99
f1 (ppm)

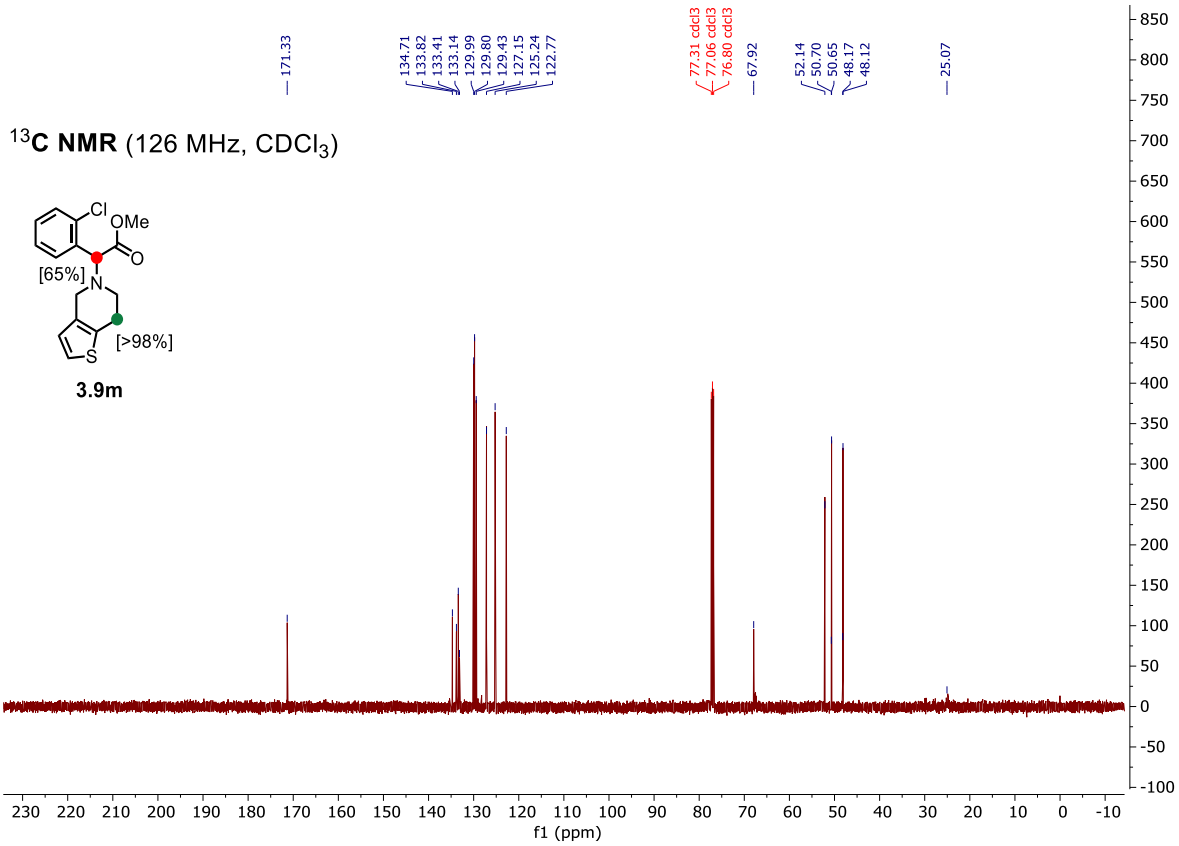
171.33
134.71
133.82
133.41
133.14
129.99
129.80
129.43
127.15
125.24
122.77
77.31 cdcl3
77.06 cdcl3
76.80 cdcl3
67.92
52.14
50.70
50.65
48.17
48.12
25.07
13C NMR (126 MHz, CDCl3)
Cl
OMe
O
[65%]
N
[>98%]
S
3.9m
f1 (ppm)

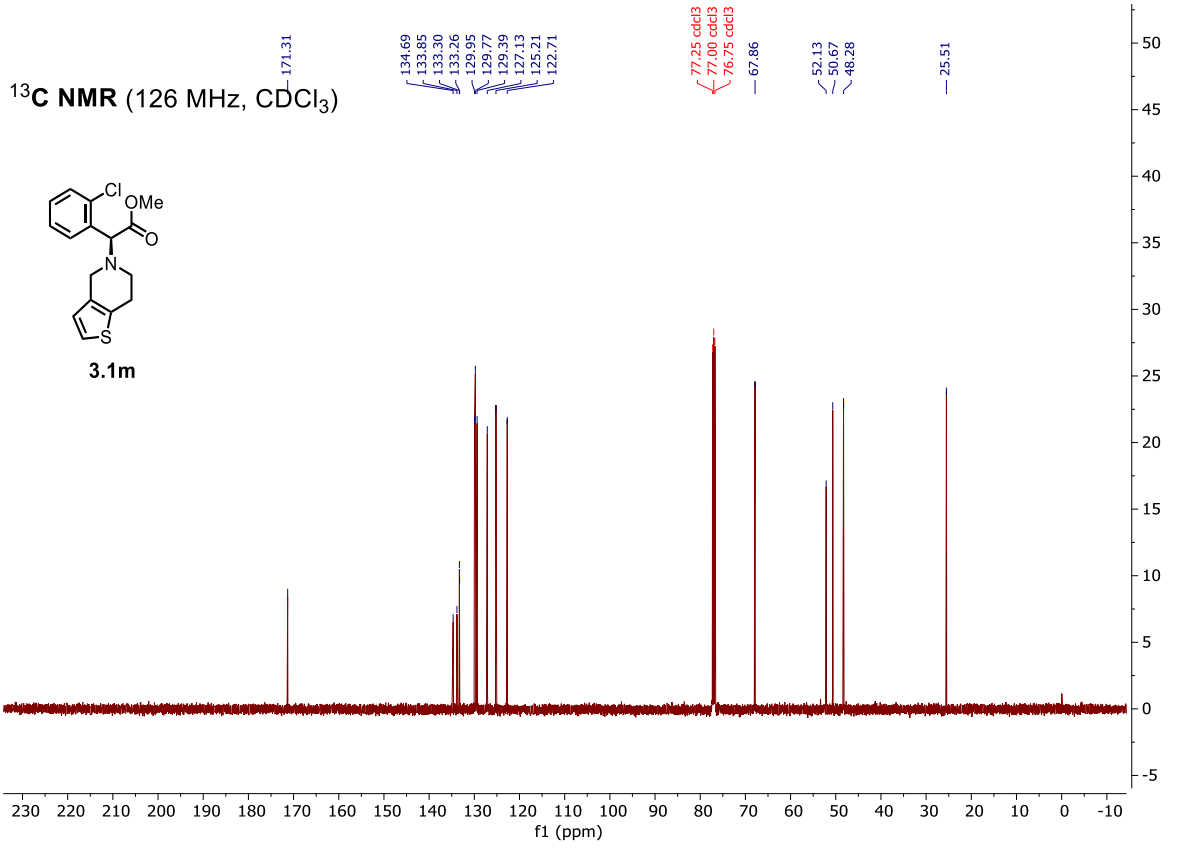
171.31
134.69
133.85
133.30
133.26
129.95
129.77
129.39
127.13
125.21
122.71
77.25 cdcl3
77.00 cdcl3
76.75 cdcl3
67.86
52.13
50.67
48.28
25.51
13C NMR (126 MHz, CDCl3)
Cl
OMe
O
N
S
3.1m
f1 (ppm)

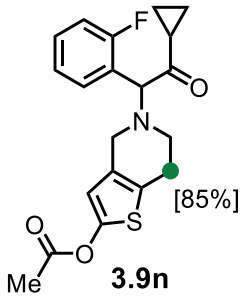

3.9n

Prasugrel, 3.9n

Prasugrel **3.1n** was reacted with acetone-d_6 following the General Procedure C. After purification by column chromatography (Et_2O:hexanes = 1:19), **3.9n** was obtained as a white solid (64 mg, 85%).

Deuterium incorporation: 1.70 D/molecule (^{1}H NMR), 1.99 D/molecule [HRMS (DART)]

^{1}H NMR (600 MHz, $CDCl_3$) δ 7.47 (s, 1H), 7.31 (s, 1H), 7.17 (s, 1H), 7.11 (s, 1H), 6.26 (s, 1H), 4.83 (s, 1H), 3.63 – 3.43 (m, 2H), 2.89 (d, J = 11.5 Hz, 1H), 2.75 (d, J = 11.4 Hz, 1.30H, 85%D), 2.25 (s, 4H), 1.03 (dd, J = 26.7, 2.8 Hz, 2H), 0.85 (d, J = 2.7 Hz, 2H); **^{13}C NMR** (151 MHz, $CDCl_3$) δ 207.6, 167.7, 162.1, 160.5, 149.5, 130.6, 129.9, 129.8, 129.5, 125.6, 124.37, 124.35, 122.1, 122.0, 115.9, 115.7, 112.00, 111.96, 71.61, 71.56, 50.50, 50.48, 50.46, 48.3, 25.0, 20.7, 18.3, 12.1, 11.5; **^{19}F NMR** (564 MHz, $CDCl_3$) δ -114.68 – -118.69 (m); **IR** (neat) 1776, 1758, 1698, 1486, 1454, 1369, 1191, 1086, 1037, 1008, 903, 759 cm^{-1}.

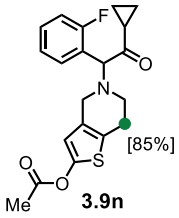
F
O
N
[85%]
S
O
O
Me

3.9n

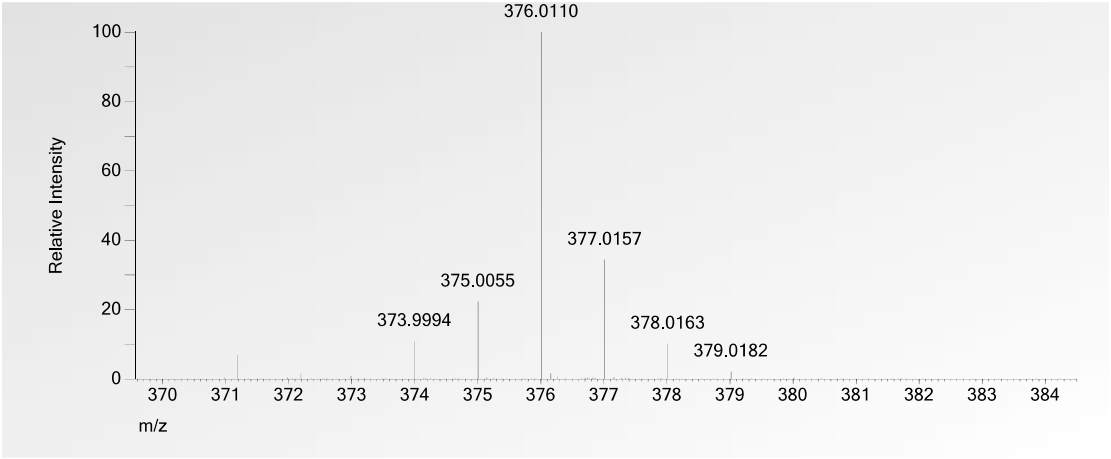
376.0110
377.0157
375.0055
373.9994
378.0163
379.0182
Relative Intensity
m/z
100
80
60
40
20
0
370
371
372
373
374
375
376
377
378
379
380
381
382
383
384

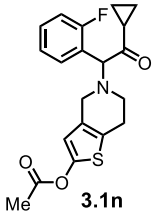
F
O
N
S
O
O
Me

3.1n

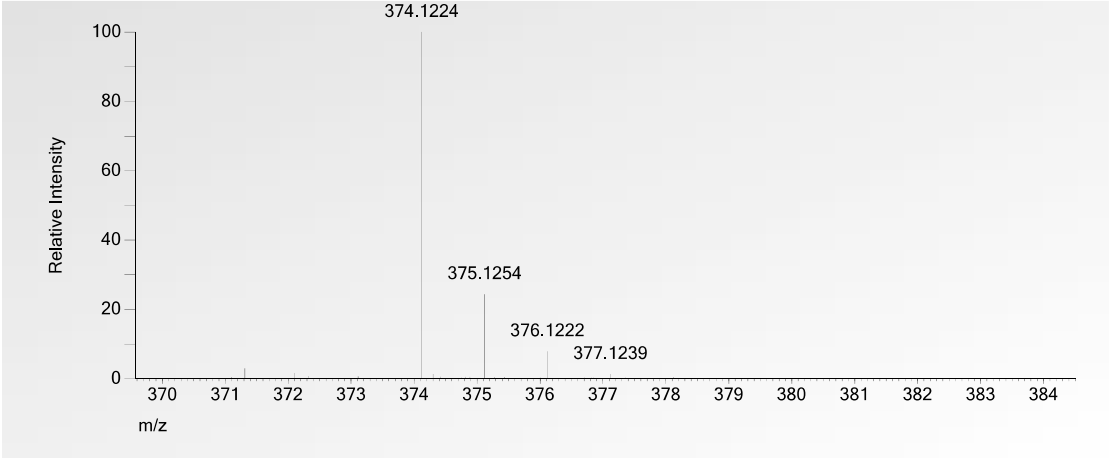
374.1224
375.1254
376.1222
377.1239
Relative Intensity
m/z
100
80
60
40
20
0
370
371
372
373
374
375
376
377
378
379
380
381
382
383
384

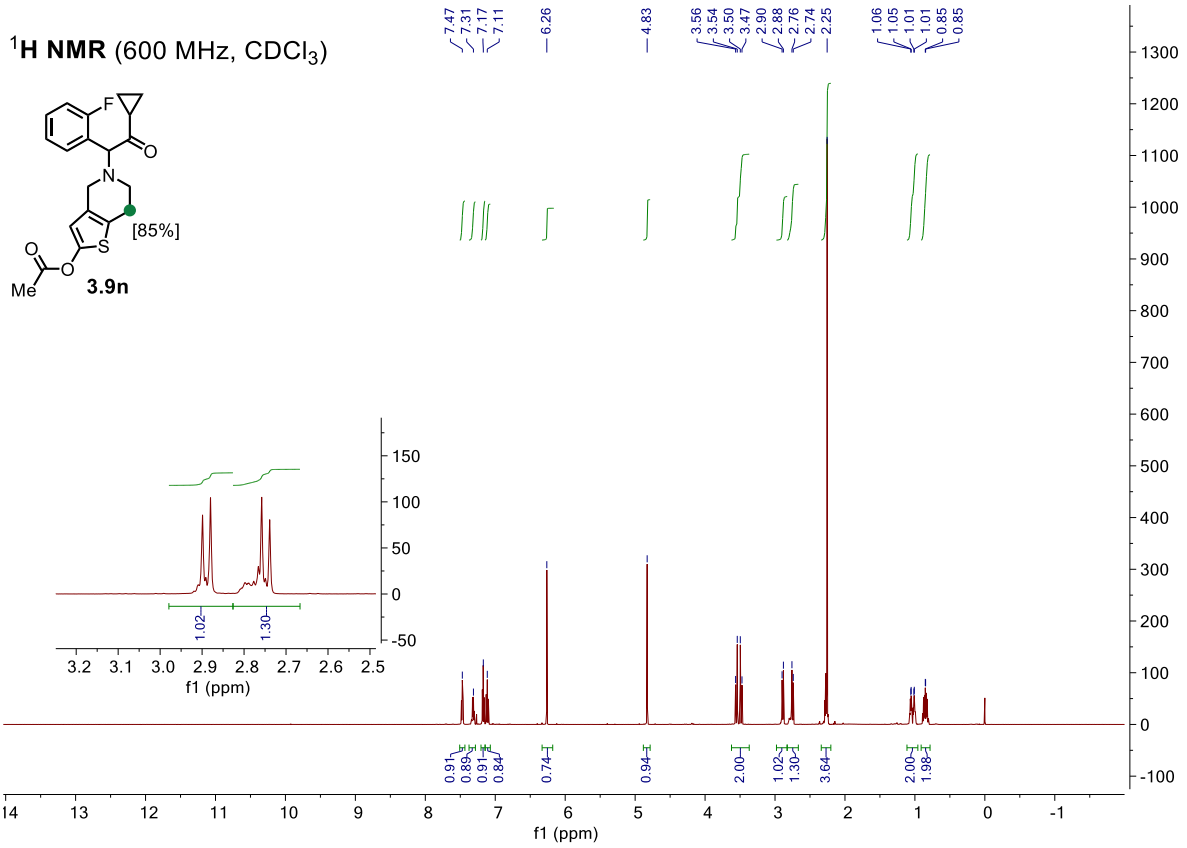
1H NMR (600 MHz, CDCl3)
[85%]
3.9n
f1 (ppm)

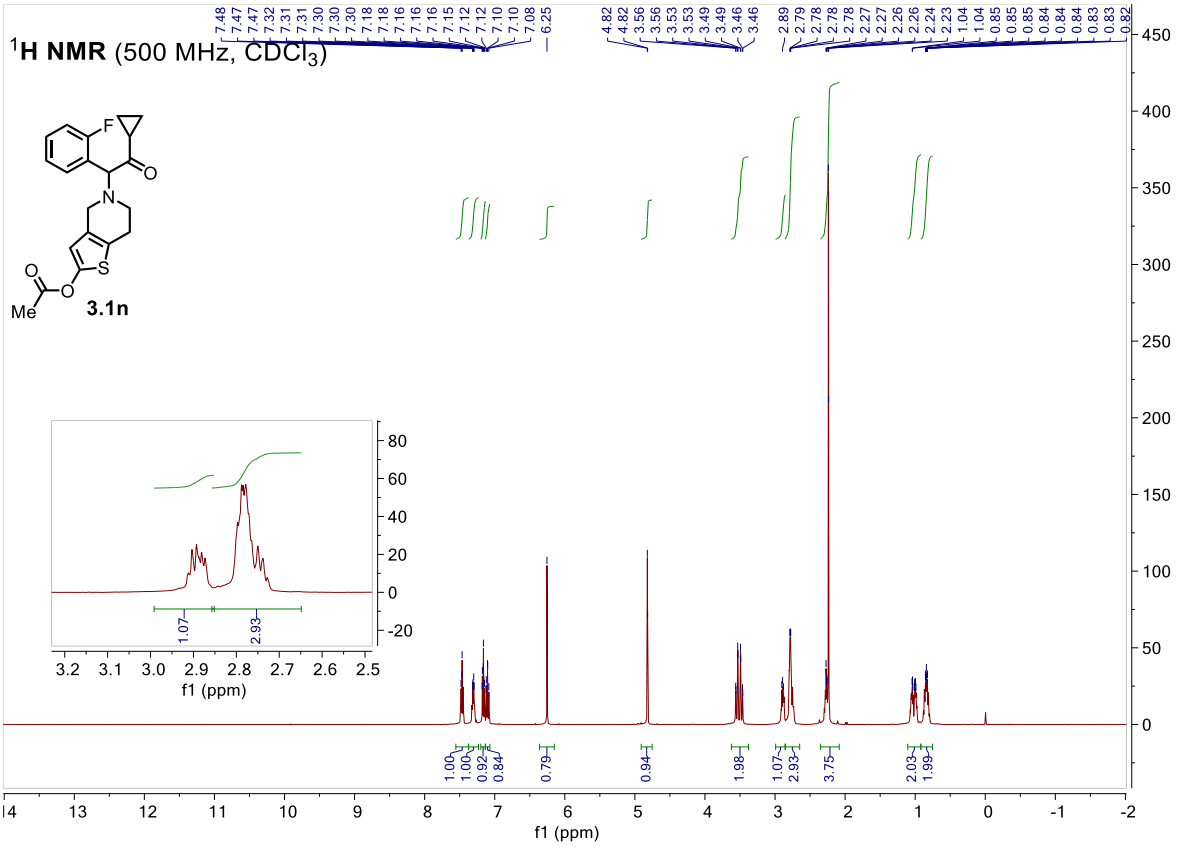
1H NMR (500 MHz, CDCl3)
3.1n
f1 (ppm)

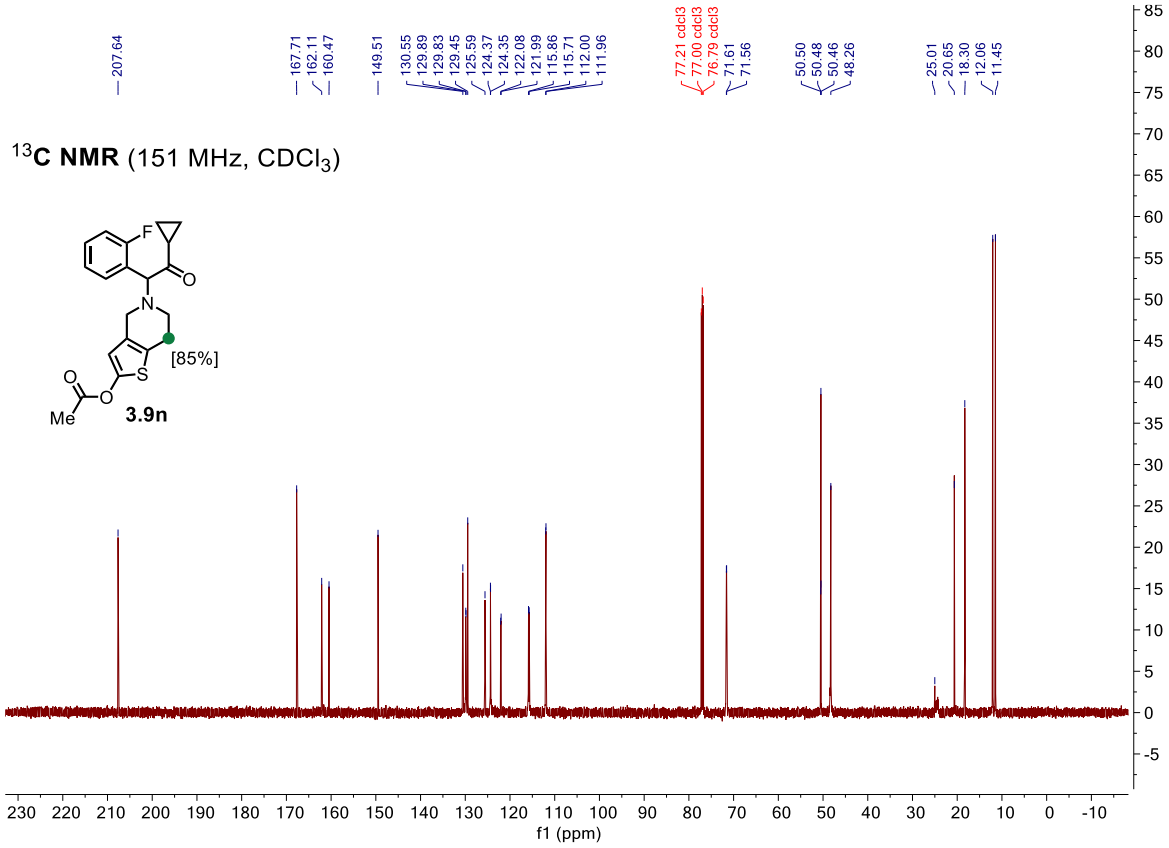
207.64
167.71
162.11
160.47
149.51
130.55
129.89
129.83
129.45
125.59
124.37
124.35
122.08
121.99
115.86
115.71
112.00
111.96
77.21 cdcl3
77.00 cdcl3
76.79 cdcl3
71.61
71.56
50.50
50.48
50.46
48.26
25.01
20.65
18.30
12.06
11.45
13C NMR (151 MHz, CDCl3)
F
O
N
S
O
O
Me
[85%]
3.9n
f1 (ppm)

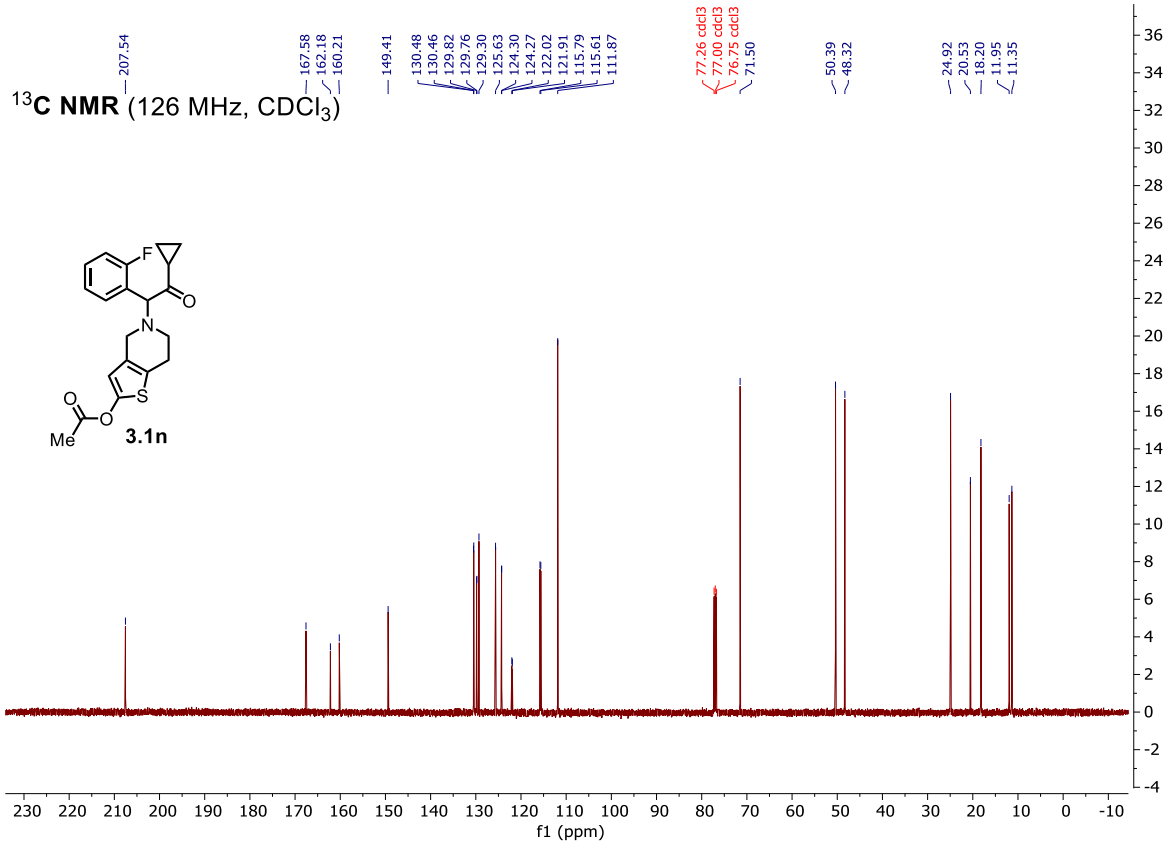
207.54
167.58
162.18
160.21
149.41
130.48
130.46
129.82
129.76
129.30
125.63
124.30
124.27
122.02
121.91
115.79
115.61
111.87
77.26 cdcl3
77.00 cdcl3
76.75 cdcl3
71.50
50.39
48.32
24.92
20.53
18.20
11.95
11.35
13C NMR (126 MHz, CDCl3)
F
O
N
S
O
O
Me
3.1n
f1 (ppm)

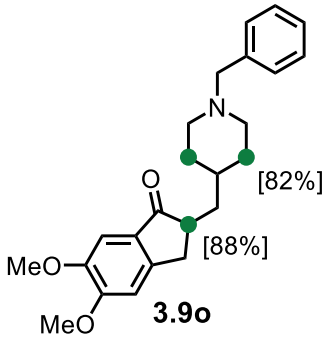

3.9o

Donepezil, 3.9o

Donepezil **3.1o** was reacted with acetone-d_6 following the General Procedure A. After purification by column chromatography (MeOH:DCM = 1:49), **3.9o** was obtained as a white solid (74 mg, 98%).

Deuterium incorporation: 5.04 D/molecule (^{1}H NMR), 4.17 D/molecule [HRMS (DART)]

^{1}H NMR (600 MHz, $CDCl_3$) δ 7.39 (d, *J* = 7.5 Hz, 2H), 7.34 (t, *J* = 7.4 Hz, 2H), 7.30 (d, *J* = 7.1 Hz, 1H), 7.16 (s, 1H), 6.85 (s, 1H), 3.96 (s, 3H), 3.90 (s, 3H), 3.67 (s, 2H), 3.24 (d, *J* = 16.9 Hz, 1H), 3.02 (d, *J* = 10.6 Hz, 2H), 2.68 (d, *J* = 16.9 Hz, 1.12H, 88%D), 2.15 (s, 2H), 1.89 (dd, *J* = 13.8, 7.6 Hz, 1H), 1.78–1.70 (m, 0.25H, 88%D), 1.59 (s, 1H), 1.56–1.44 (m, 0.49H, 75%D), 1.43 – 1.32 (m, 1H); **^{13}C NMR** (151 MHz, $CDCl_3$) δ 207.6, 155.5, 149.4, 148.7, 136.2, 129.7, 129.2, 128.4, 127.6, 107.3, 104.3, 62.7, 56.0, 53.1, 45.2, 38.3, 33.3; **IR** (neat) 2913, 1691, 1590, 1499, 1454, 1310, 1269, 1247, 1218, 1114, 727 cm^{-1}.

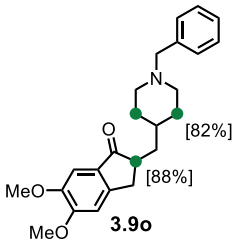
N
O
[82%]
[88%]
MeO
MeO

3.9o

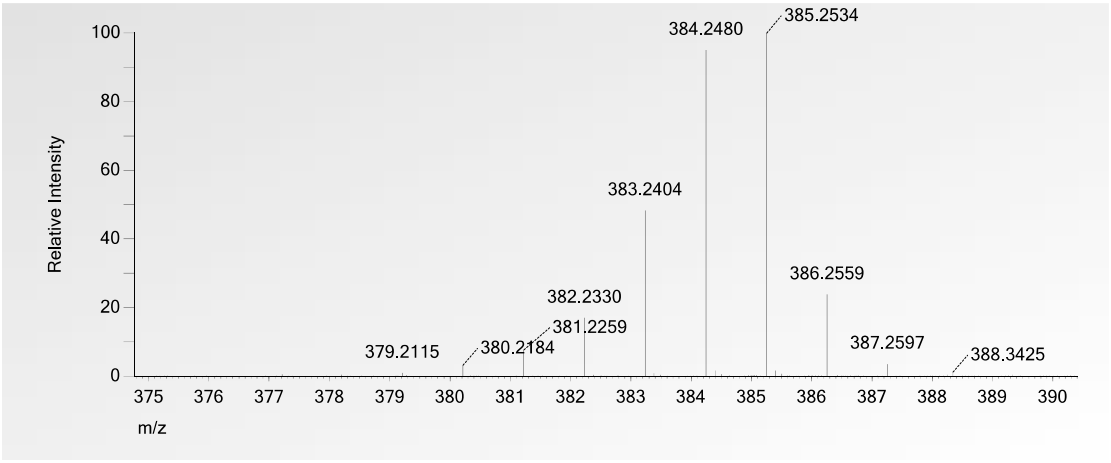
Relative Intensity
m/z
384.2480
385.2534
383.2404
386.2559
382.2330
381.2259
379.2115
380.2184
387.2597
388.3425

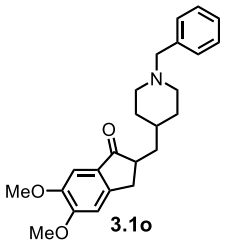
N
O
MeO
MeO

3.1o

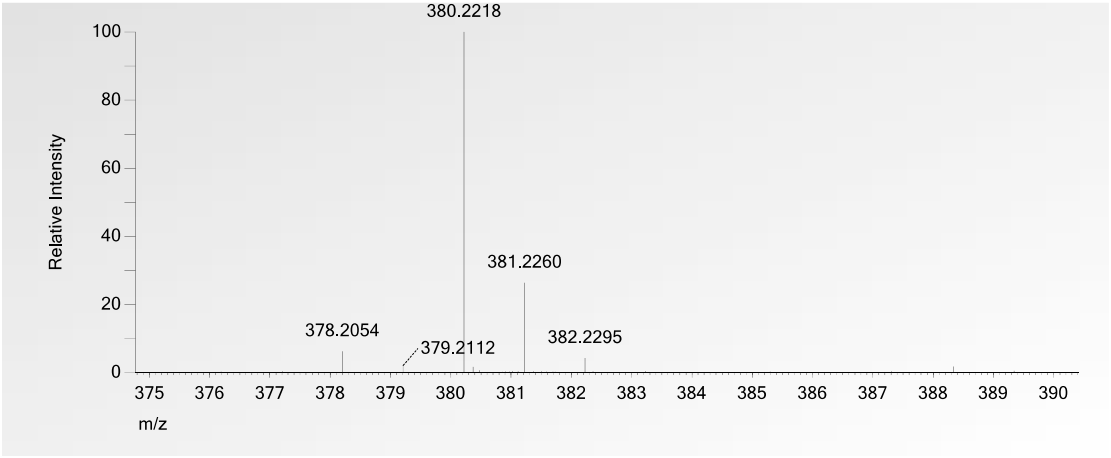
Relative Intensity
m/z
380.2218
381.2260
378.2054
379.2112
382.2295

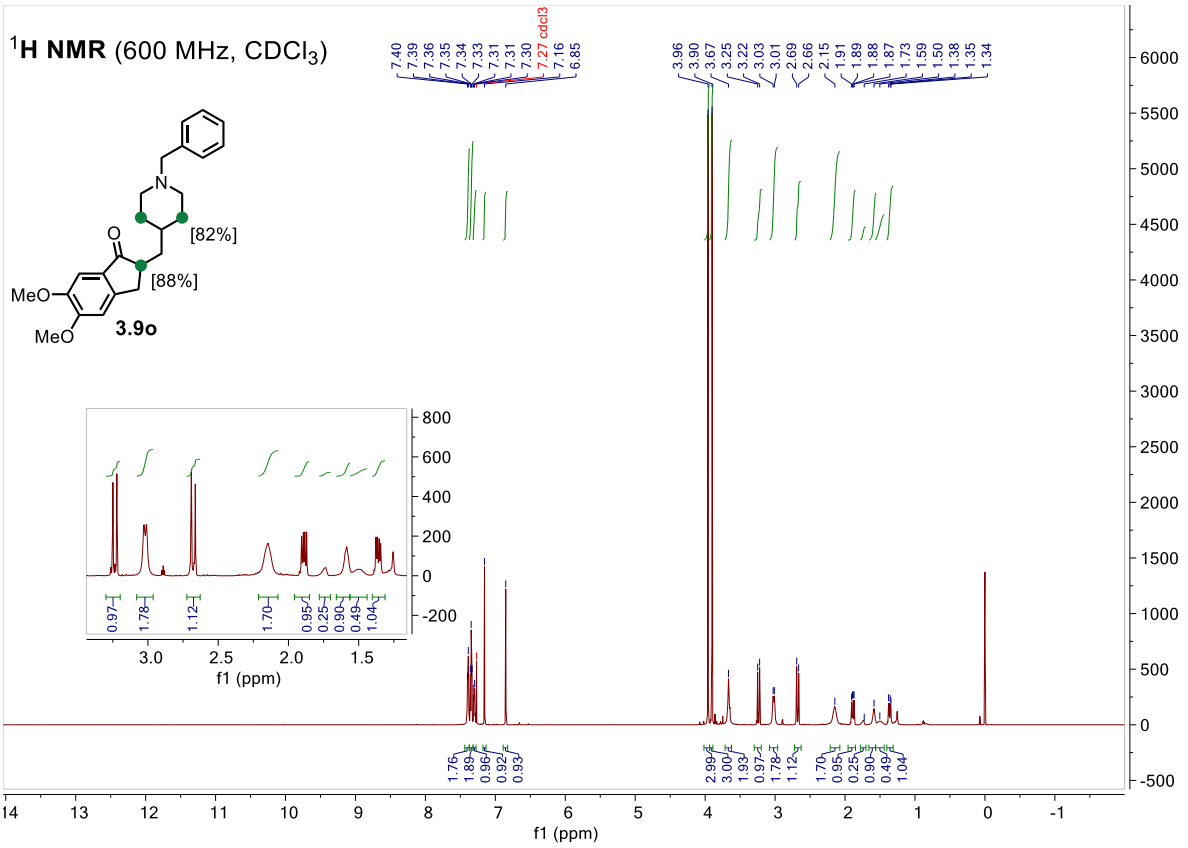
1H NMR (600 MHz, CDCl3)
[82%]
[88%]
MeO
MeO
3.9o
f1 (ppm)

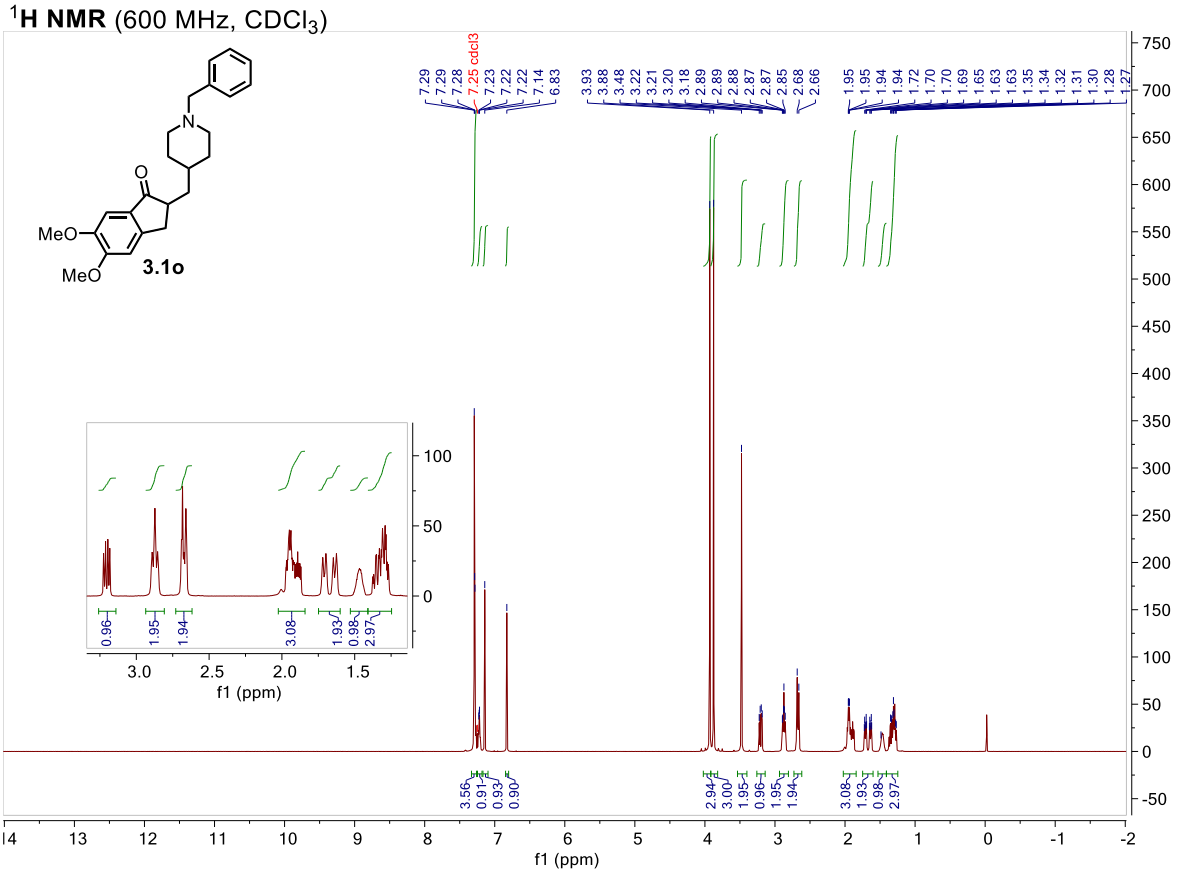
1H NMR (600 MHz, CDCl3)
MeO
MeO
3.1o
f1 (ppm)

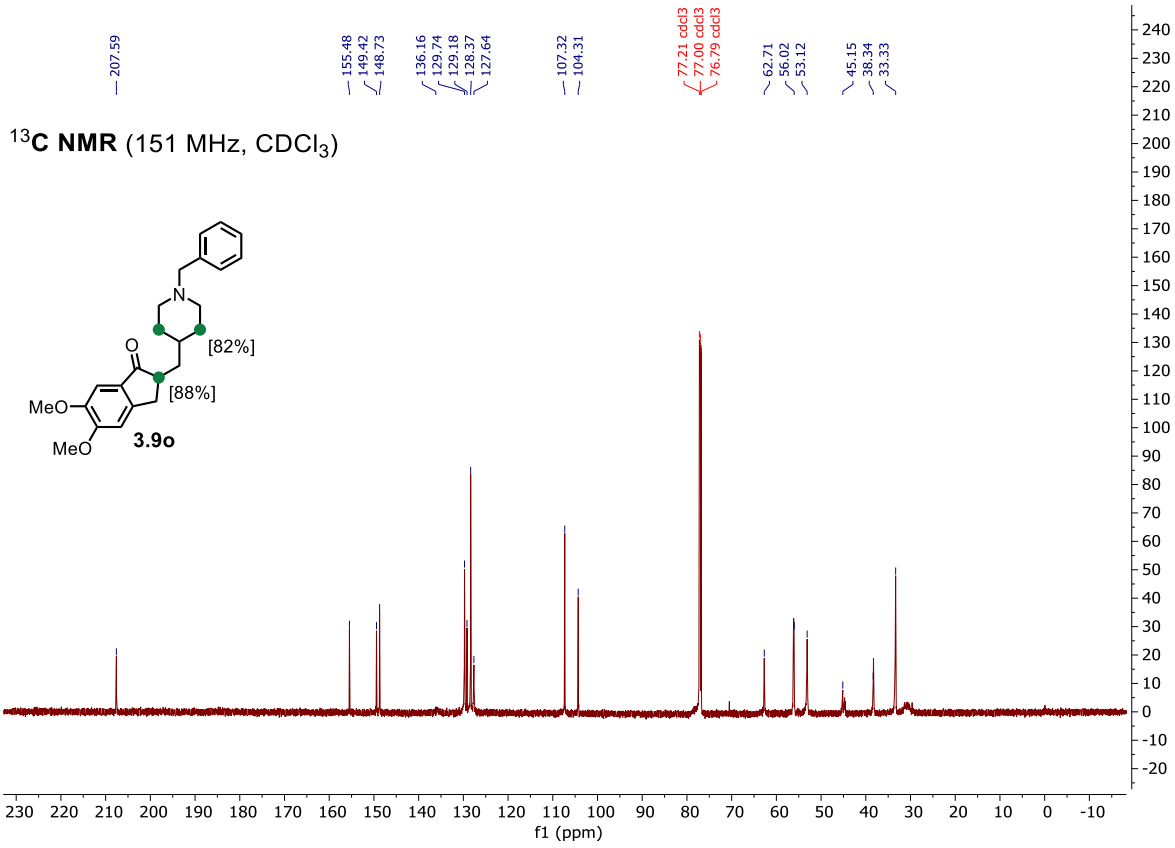
207.59
155.48
149.42
148.73
136.16
129.74
129.18
128.37
127.64
107.32
104.31
77.21 cdcl3
77.00 cdcl3
76.79 cdcl3
62.71
56.02
53.12
45.15
38.34
33.33
13C NMR (151 MHz, CDCl3)
[82%]
[88%]
MeO
MeO
3.9o
f1 (ppm)

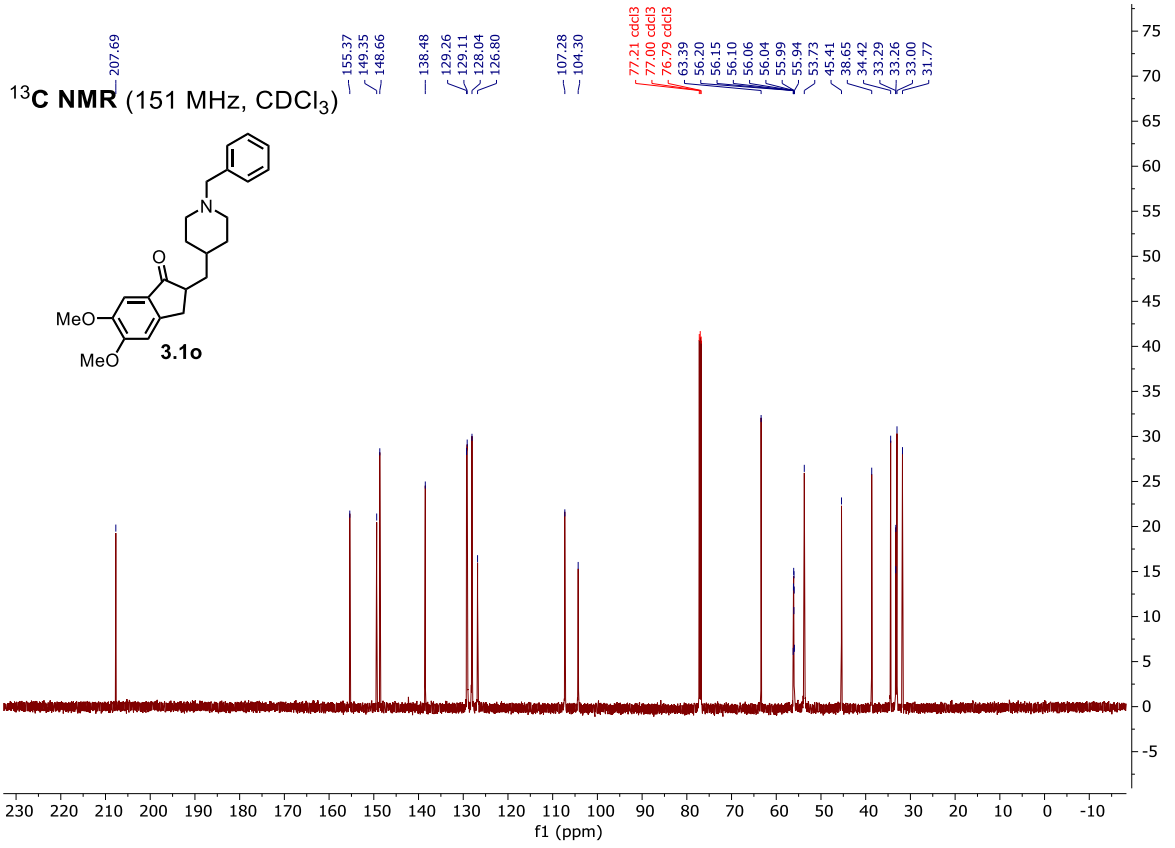
207.69
155.37
149.35
148.66
138.48
129.26
129.11
128.04
126.80
107.28
104.30
77.21 cdcl3
77.00 cdcl3
76.79 cdcl3
63.39
56.20
56.15
56.10
56.06
56.04
55.99
55.94
53.73
45.41
38.65
34.42
33.29
33.26
33.00
31.77
13C NMR (151 MHz, CDCl3)
MeO
MeO
3.1o
f1 (ppm)

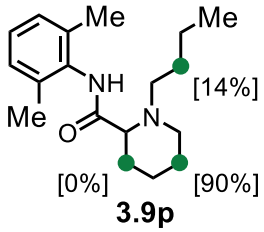

3.9p

Bupivacaine, 3.9p

Bupivacaine **3.1p** was reacted with acetone-d_6 following the General Procedure A. After purification by column chromatography (MeOH:DCM = 1:49), **3.9p** was obtained as a white solid (55 mg, 96%).

Deuterium incorporation: 2.08 D/molecule (^{1}H NMR), 2.83 D/molecule [HRMS (DART)]

^{1}H NMR (600 MHz, $CDCl_3$) δ 8.25 (s, 1H), 7.06 (d, J = 5.5 Hz, 3H), 3.18 (d, J = 11.6 Hz, 1H), 2.92 (d, J = 9.3 Hz, 1H), 2.86 – 2.74 (m, 1H), 2.31 – 2.17 (m, 7H), 2.11 – 2.01 (m, 2H), 1.77 – 1.66 (m, 2.2H, 80%D), 1.65 – 1.54 (m, 0.86H, 14%D), 1.54 – 1.39 (m, 0.85H, 15%D and >98%D), 1.41 – 1.24 (m, 3H), 0.91 (t, J = 7.4 Hz, 3H); **^{13}C NMR** (151 MHz, $CDCl_3$) δ 172.7, 135.2, 133.6, 128.2, 127.0, 68.3, 57.4, 57.3, 51.5, 51.4, 30.4, 29.5, 23.9, 23.1, 20.6, 20.5, 20.4, 18.6, 14.0; **IR** (neat) 3224, 2952, 2927, 2855, 1650, 1513, 1463, 1228, 1097, 764 cm^{-1}.

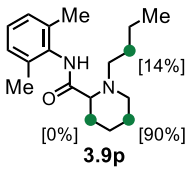
Me
Me
NH
[14%]
Me
O
N
[0%]
[90%]

3.9p

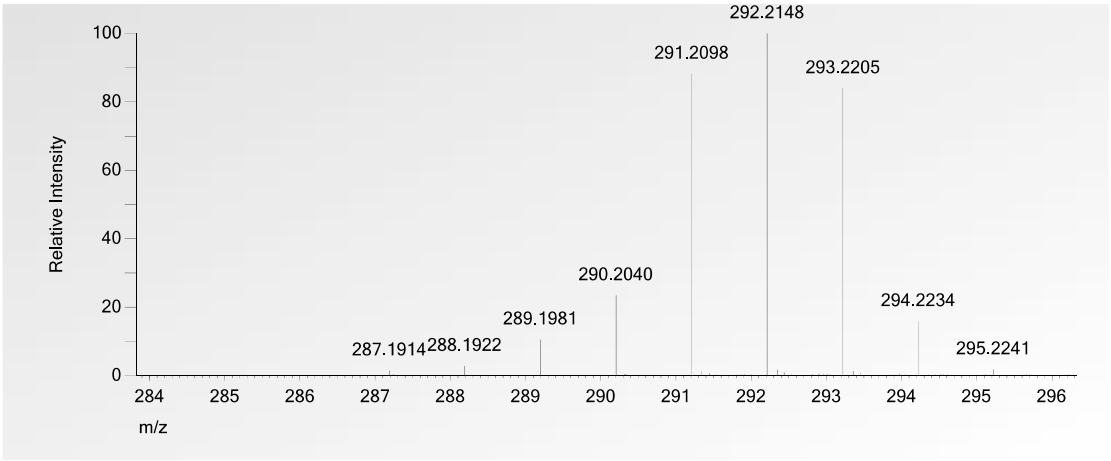
292.2148
291.2098
293.2205
290.2040
294.2234
289.1981
287.1914
288.1922
295.2241
Relative Intensity
m/z

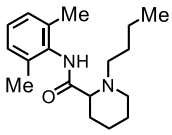
Me
Me
NH
Me
O
N

3.1p

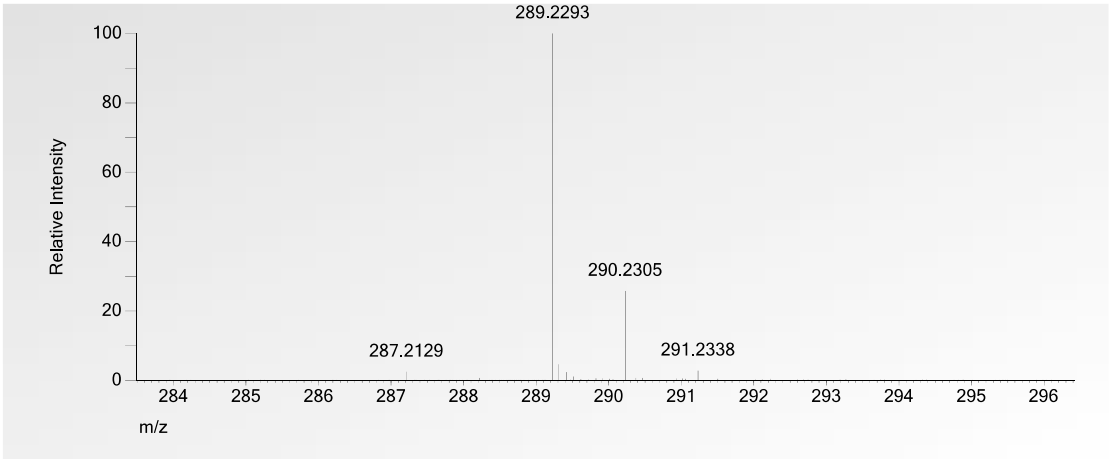
289.2293
290.2305
287.2129
291.2338
Relative Intensity
m/z

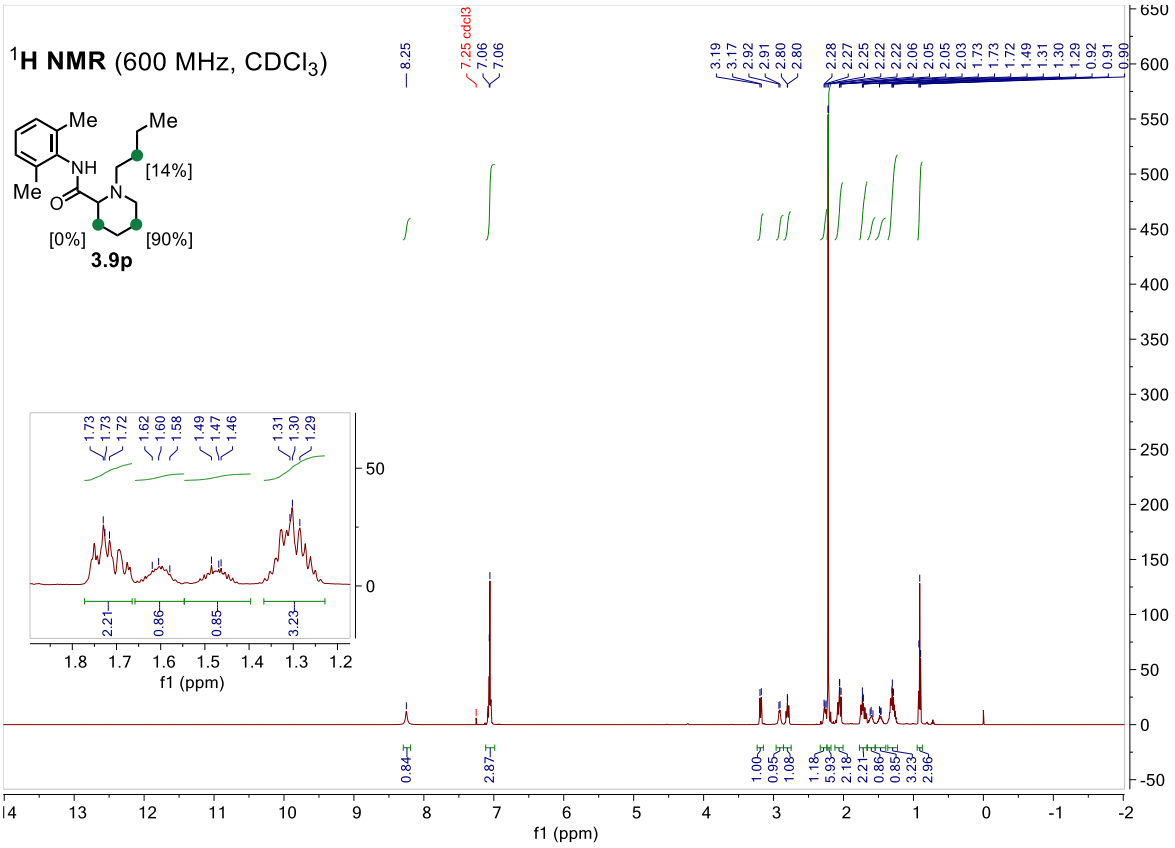
1H NMR (600 MHz, CDCl3)
Me
Me
NH
Me
O
N
[14%]
[0%]
[90%]
3.9p
f1 (ppm)

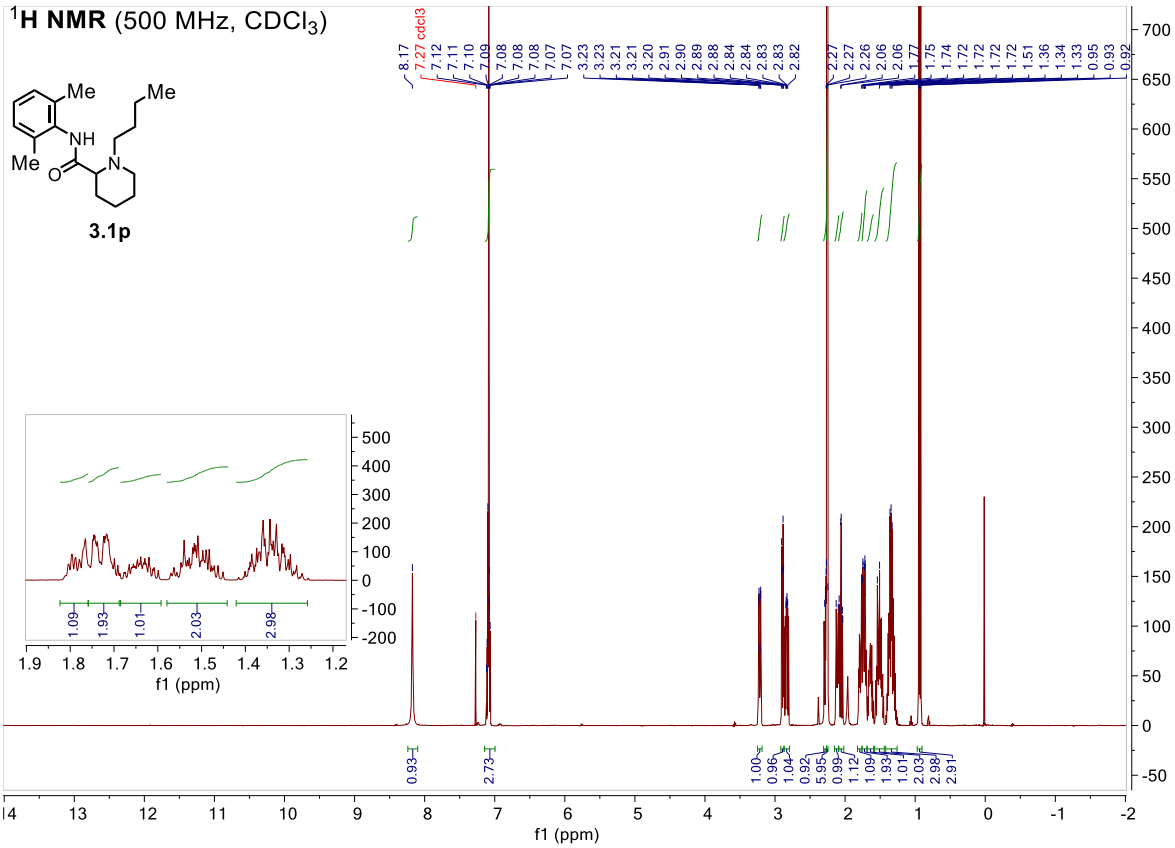
1H NMR (500 MHz, CDCl3)
Me
Me
NH
Me
O
N
3.1p
f1 (ppm)

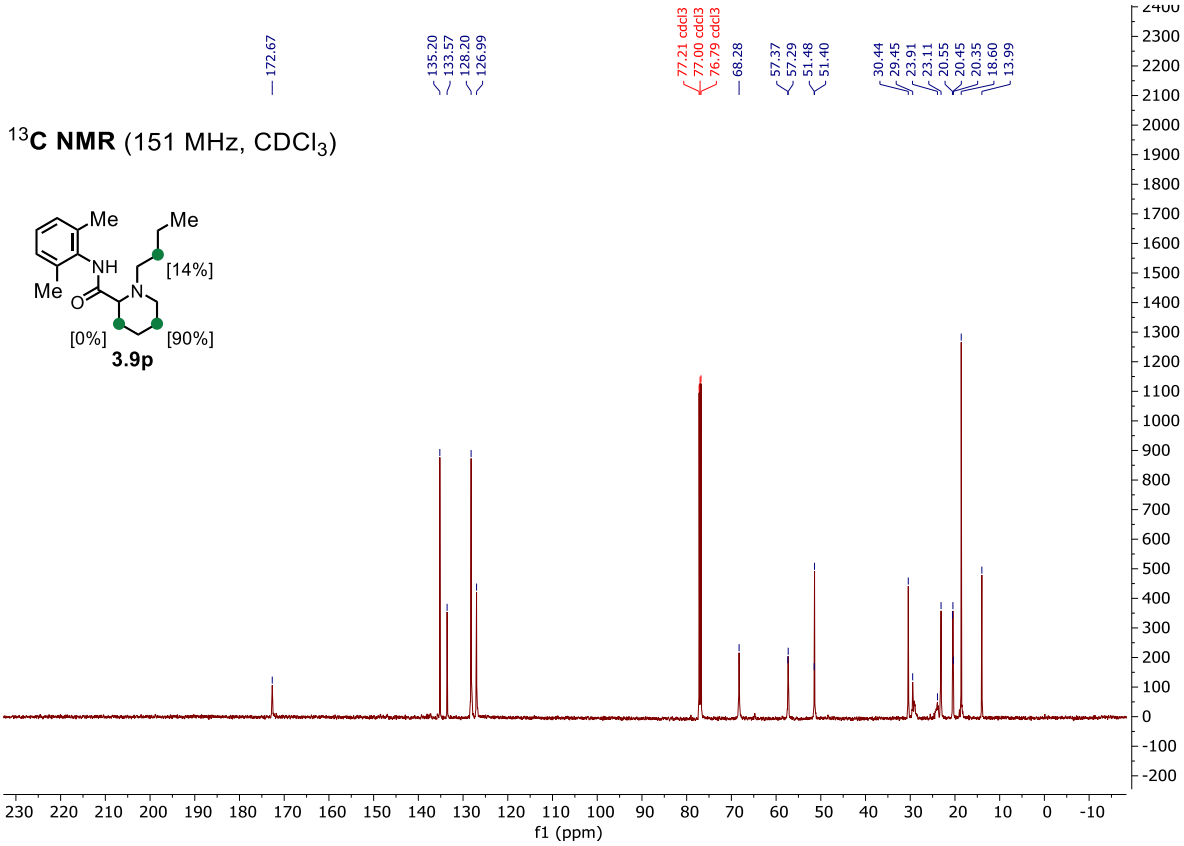
172.67
135.20
133.57
128.20
126.99
77.21 cdcl3
77.00 cdcl3
76.79 cdcl3
68.28
57.37
57.29
51.48
51.40
30.44
29.45
23.91
23.11
20.55
20.45
20.35
18.60
13.99
13C NMR (151 MHz, CDCl3)
Me
Me
NH
Me
O
N
[14%]
[0%]
[90%]
3.9p
f1 (ppm)

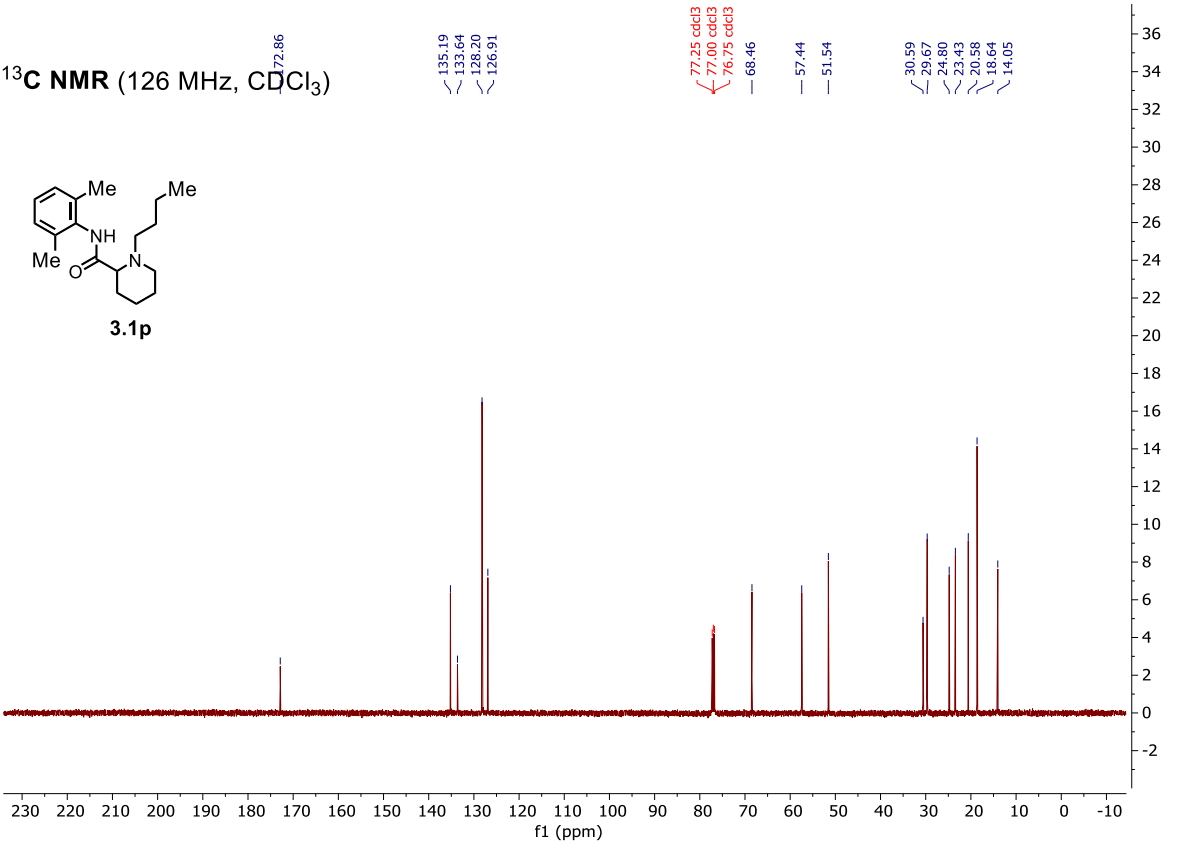
172.86
135.19
133.64
128.20
126.91
77.25 cdcl3
77.00 cdcl3
76.75 cdcl3
68.46
57.44
51.54
30.59
29.67
24.80
23.43
20.58
18.64
14.05
13C NMR (126 MHz, CDCl3)
Me
Me
NH
Me
O
N
3.1p
f1 (ppm)

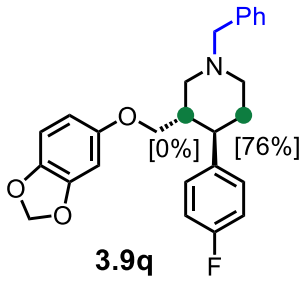

3.9q

***N*-Bn paroxetine, 3.9q**

N-Bn paroxetine **3.1q** was reacted with acetone-d_6 following the General Procedure A. After purification by column chromatography (Et_2O:hexanes = 1:9), **3.9q** was obtained as a white solid (82 mg, 98%).

Deuterium incorporation: 1.52 D/molecule (^{1}H NMR), 1.85 D/molecule [HRMS (DART)]

^{1}H NMR (500 MHz, $CDCl_3$) δ 7.44 – 7.30 (m, 4H), 7.30 – 7.21 (m, 1H), 7.15 (ddd, *J* = 7.1, 5.3, 2.7 Hz, 2H), 7.04 – 6.87 (m, 2H), 6.61 (dd, *J* = 8.5, 1.6 Hz, 1H), 6.31 (t, *J* = 2.1 Hz, 1H), 6.10 (d, *J* = 8.5 Hz, 1H), 5.86 (d, *J* = 1.7 Hz, 2H), 3.64 (dd, *J* = 13.2, 1.6 Hz, 1H), 3.59 – 3.49 (m, 2H), 3.43 (s, 1H), 3.31 – 3.17 (m, 1H), 2.97 (d, *J* = 11.2 Hz, 1H), 2.46 (d, *J* = 11.1 Hz, 1H), 2.20 (dd, *J* = 7.5, 3.3 Hz, 1H), 2.14 – 2.00 (m, 2H), 1.92 – 1.73 (m, 0.49H, 76%D); **^{13}C NMR** (151 MHz, $CDCl_3$) δ 162.5, 160.5, 154.4, 148.1, 141.5, 139.88, 139.86, 138.3, 129.2, 128.9, 128.8, 128.2, 127.0, 115.4, 115.3, 107.8, 105.6, 101.1, 98.0, 69.7, 63.4, 57.6, 53.7, 44.0, 42.2, 34.4; **^{19}F NMR** (564 MHz, $CDCl_3$) δ -116.68 (td, J = 8.8, 4.5 Hz); **IR** (neat) 2895, 2799, 1506, 1486, 1466, 1451, 1222, 1181, 1090, 1037, 830, 744, 705 cm^{-1}; $[\alpha]^{25}_D$ = -27.3° (c = 1.0, CH_2Cl_2 labeled), $[\alpha]^{25}_D$ = -44.9° (c = 1.0, CH_2Cl_2 unlabeled).

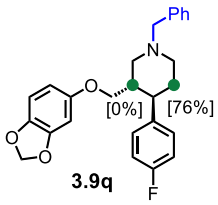
Ph
N
O
[0%]
[76%]
O
O
F

3.9q

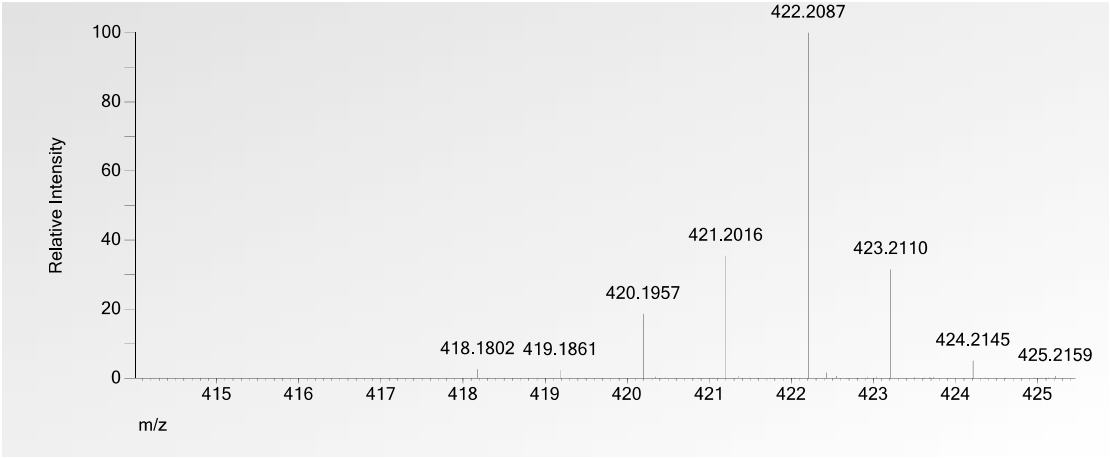
422.2087
100
80
60
40
20
0
Relative Intensity
421.2016
423.2110
420.1957
418.1802
419.1861
424.2145
425.2159
415
416
417
418
419
420
421
422
423
424
425
m/z

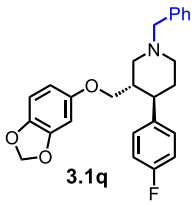
Ph
N
O
O
O
F

3.1q

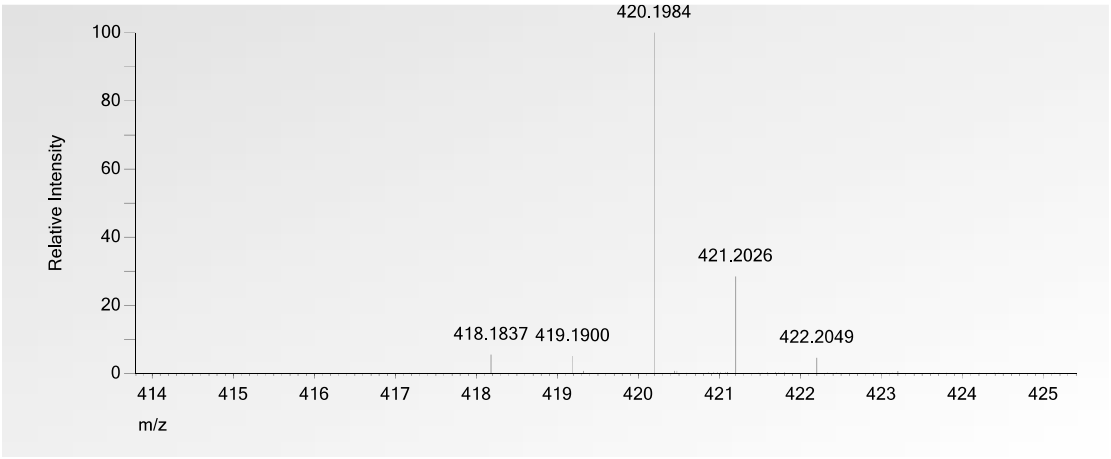
420.1984
100
80
60
40
20
0
Relative Intensity
421.2026
418.1837
419.1900
422.2049
414
415
416
417
418
419
420
421
422
423
424
425
m/z

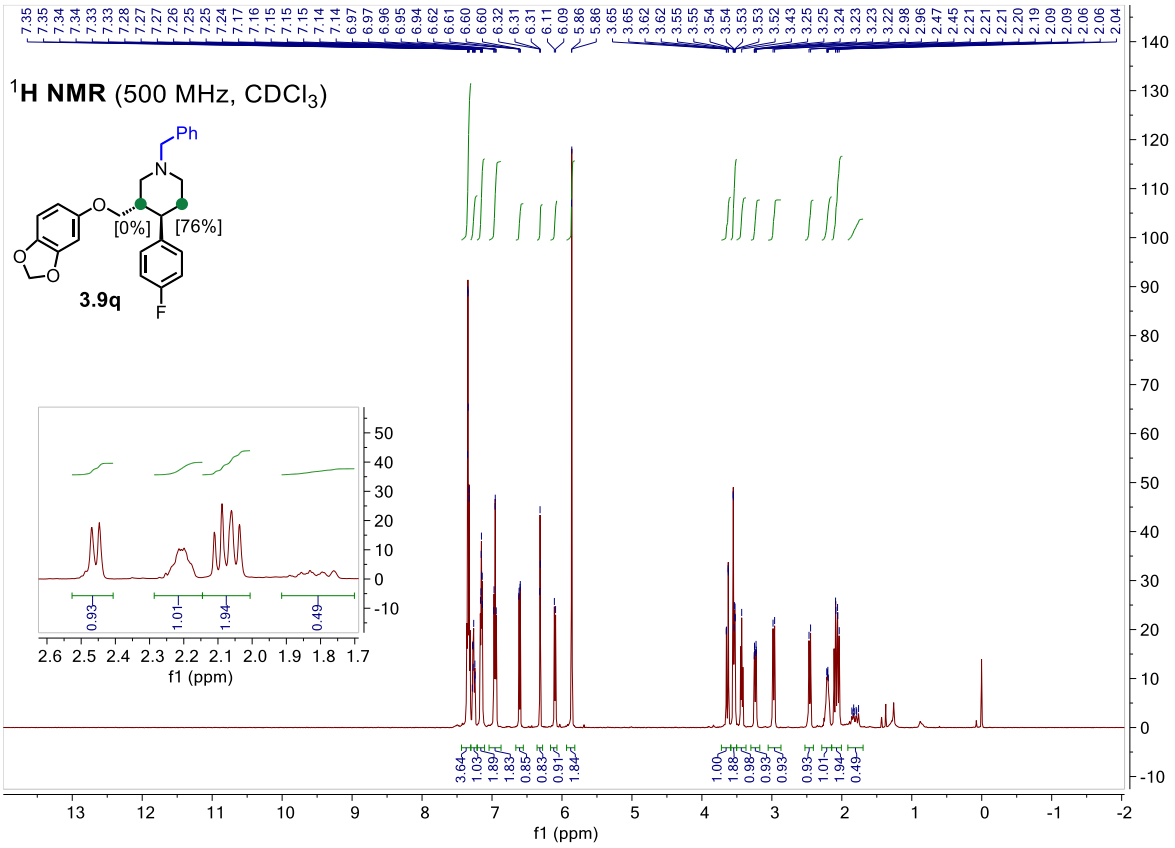
1H NMR (500 MHz, CDCl3)
Ph
N
O
[0%]
[76%]
O
O
F
3.9q
f1 (ppm)

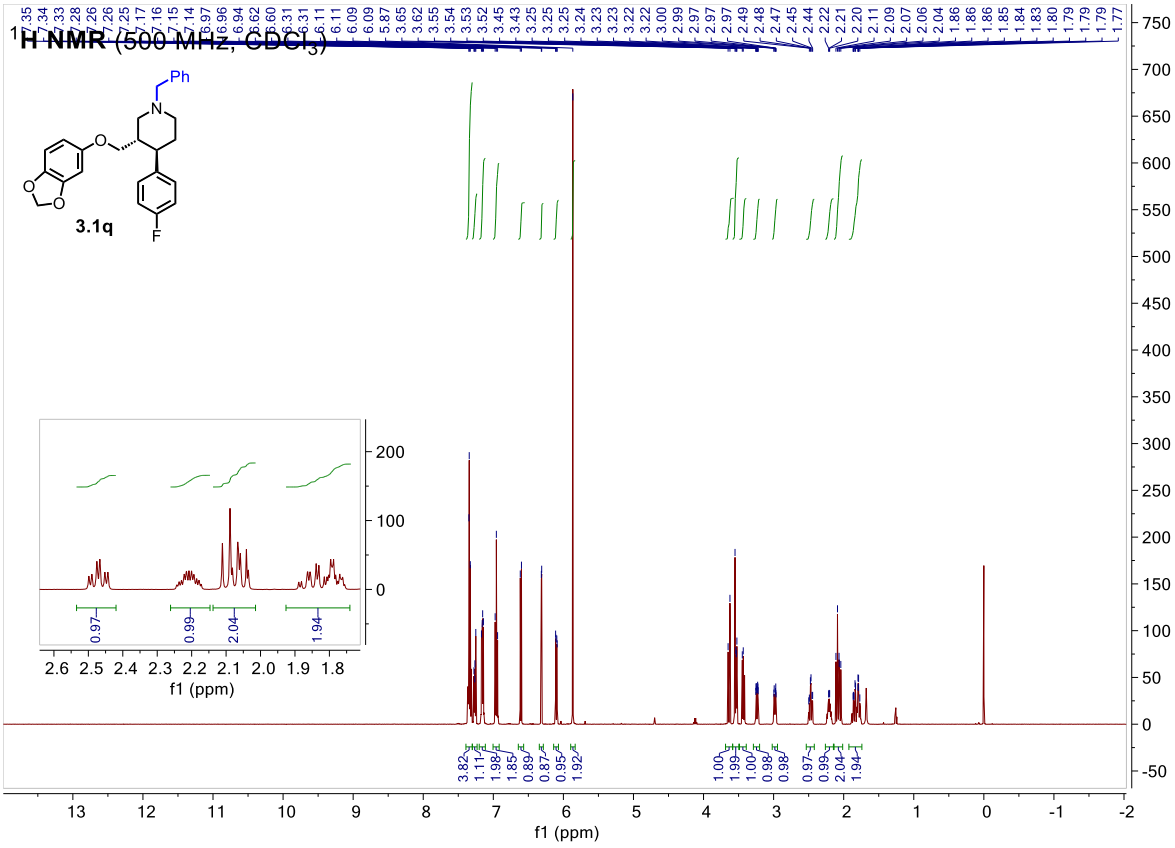
1H NMR (500 MHz, CDCl3)
Ph
N
O
O
O
F
3.1q
f1 (ppm)

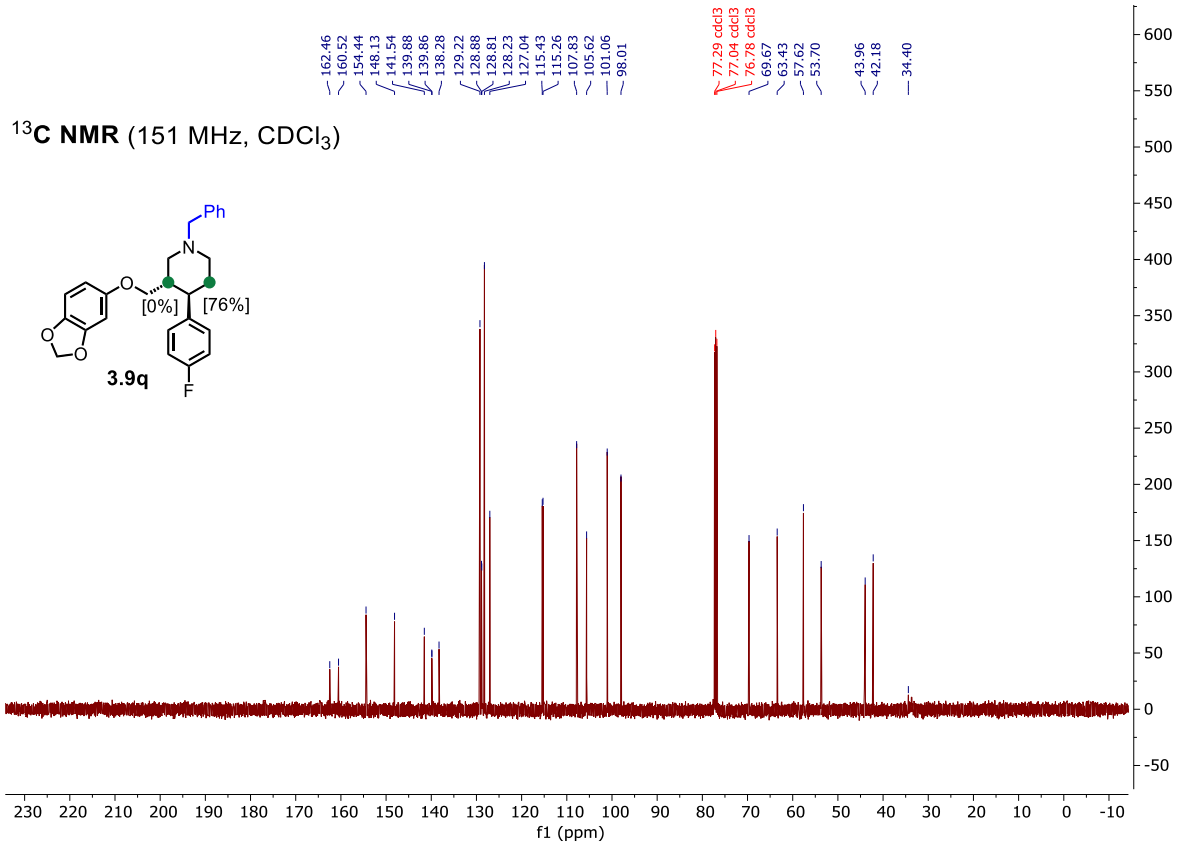
13C NMR (151 MHz, CDCl3)
Ph
N
O
[0%]
[76%]
O
O
F
3.9q
162.46
160.52
154.44
148.13
141.54
139.88
139.86
138.28
129.22
128.88
128.81
128.23
127.04
115.43
115.26
107.83
105.62
101.06
98.01
77.29 cdcl3
77.04 cdcl3
76.78 cdcl3
69.67
63.43
57.62
53.70
43.96
42.18
34.40
f1 (ppm)

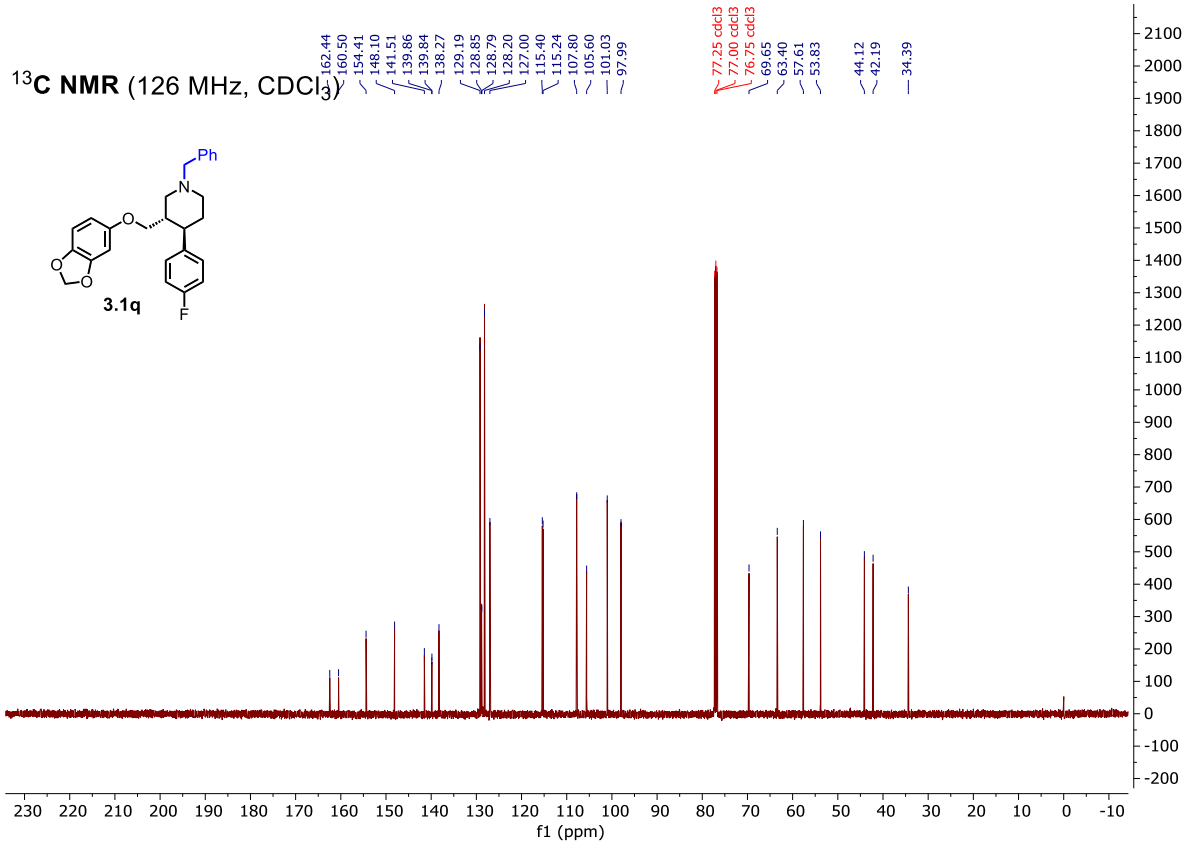
13C NMR (126 MHz, CDCl3)
Ph
N
O
O
O
F
3.1q
162.44
160.50
154.41
148.10
141.51
139.86
139.84
138.27
129.19
128.85
128.79
128.20
127.00
115.40
115.24
107.80
105.60
101.03
97.99
77.25 cdcl3
77.00 cdcl3
76.75 cdcl3
69.65
63.40
57.61
53.83
44.12
42.19
34.39
f1 (ppm)

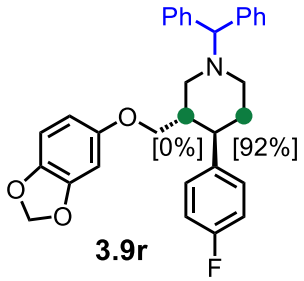

3.9r

***N*-Bzh Paroxetine, 3.9r**

N-Bzh paroxetine **3.1r** was reacted with acetone-d_6 following the General Procedure A. After purification by column chromatography (Et_2O:hexanes = 1:9), **3.9r** was obtained as a colorless liquid (94 mg, 95%).

Deuterium incorporation: 1.88 D/molecule (^{1}H NMR), 2.09 D/molecule [HRMS (DART)]

^{1}H NMR (500 MHz, $CDCl_3$) δ 7.52 – 7.37 (m, 4H), 7.28 (t, *J* = 7.7 Hz, 4H), 7.23 – 7.08 (m, 4H), 6.96 (d, *J* = 8.7 Hz, 2H), 6.57 (d, *J* = 8.4 Hz, 1H), 6.21 (d, *J* = 2.4 Hz, 1H), 6.01 (dd, *J* = 8.5, 2.5 Hz, 1H), 5.84 (s, 2H), 4.36 (s, 1H), 3.49 (d, *J* = 2.9 Hz, 1H), 3.39 (d, *J* = 6.8 Hz, 1H), 3.23 (ddd, *J* = 11.4, 3.6, 2.1 Hz, 1H), 2.97 (s, 1H), 2.47 (d, *J* = 11.2 Hz, 1H), 2.21 (dt, *J* = 7.2, 3.5 Hz, 1H), 1.94 (d, *J* = 11.3 Hz, 2H), 1.89 – 1.84 (m, 0.08H, 92%D), 1.75 – 1.71 (m, 0.08H, 92%D); **^{13}C NMR** (126 MHz, $CDCl_3$) δ 162.47, 160.52, 154.3, 148.1, 142.82, 142.79, 141.5, 140.08, 140.05, 128.91, 128.85, 128.5, 128.4, 128.1, 128.0, 126.9, 115.4, 115.2, 107.8, 105.8, 101.0, 98.1, 76.1, 69.6, 56.0, 52.42, 52.35, 44.2, 44.1, 42.5, 33.9; **^{19}F NMR** (564 MHz, $CDCl_3$) δ -116.80 (tt, J = 8.8, 5.2 Hz); **IR** (neat) 2895, 2799, 1506, 1486, 1466, 1222, 1182, 1037, 830, 705 cm^{-1}; $[\alpha]^{25}_D$ = -36.5 ° (c = 1.0, CH_2Cl_2 labeled), $[\alpha]^{25}_D$ = -43.4° (c = 1.0, CH_2Cl_2 unlabeled).

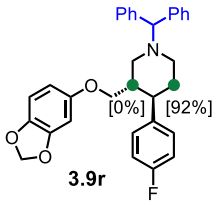
Ph
Ph
N
O
[0%]
[92%]
O
O
F

3.9r

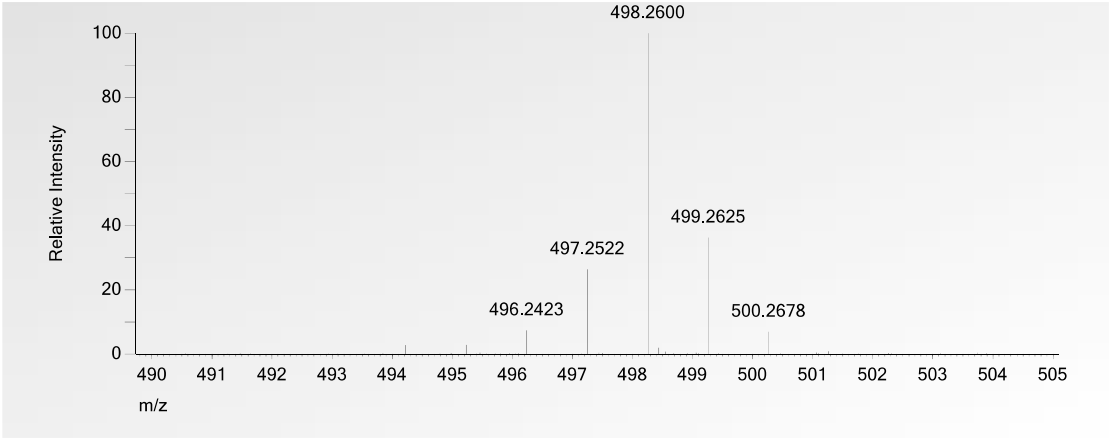
498.2600
100
80
60
40
20
0
Relative Intensity
499.2625
497.2522
496.2423
500.2678
490
491
492
493
494
495
496
497
498
499
500
501
502
503
504
505
m/z

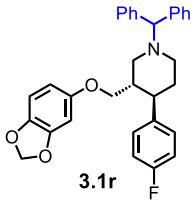
Ph
Ph
N
O
O
O
F

3.1r

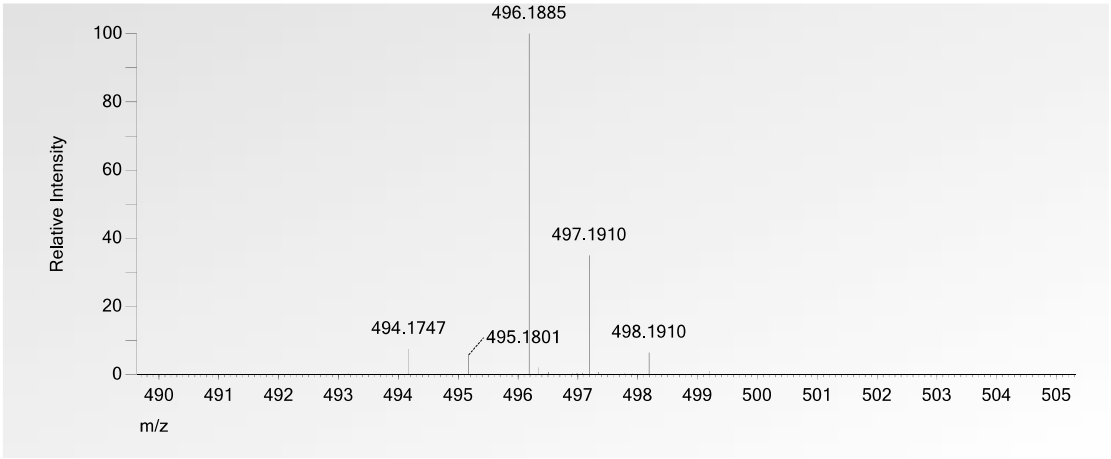
496.1885
100
80
60
40
20
0
Relative Intensity
497.1910
494.1747
495.1801
498.1910
490
491
492
493
494
495
496
497
498
499
500
501
502
503
504
505
m/z

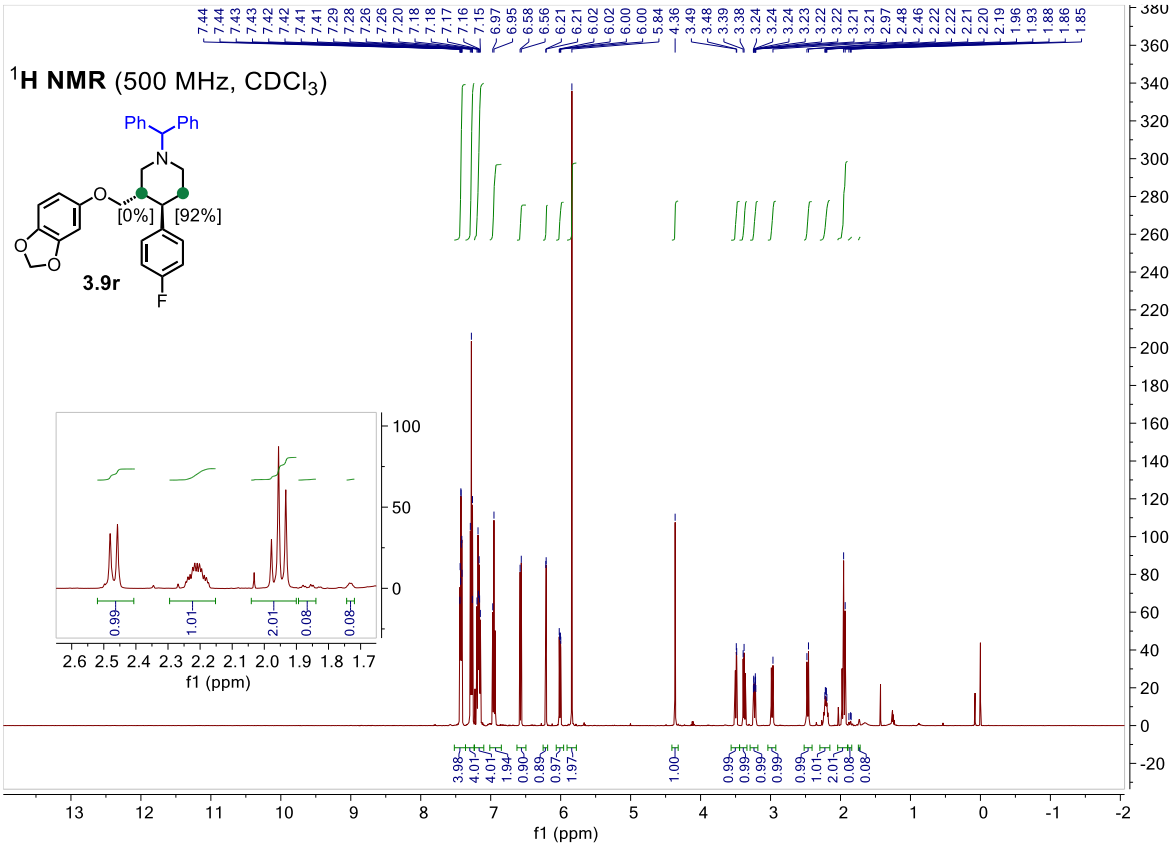
1H NMR (500 MHz, CDCl3)
Ph
Ph
N
O
[0%]
[92%]
3.9r
F
f1 (ppm)

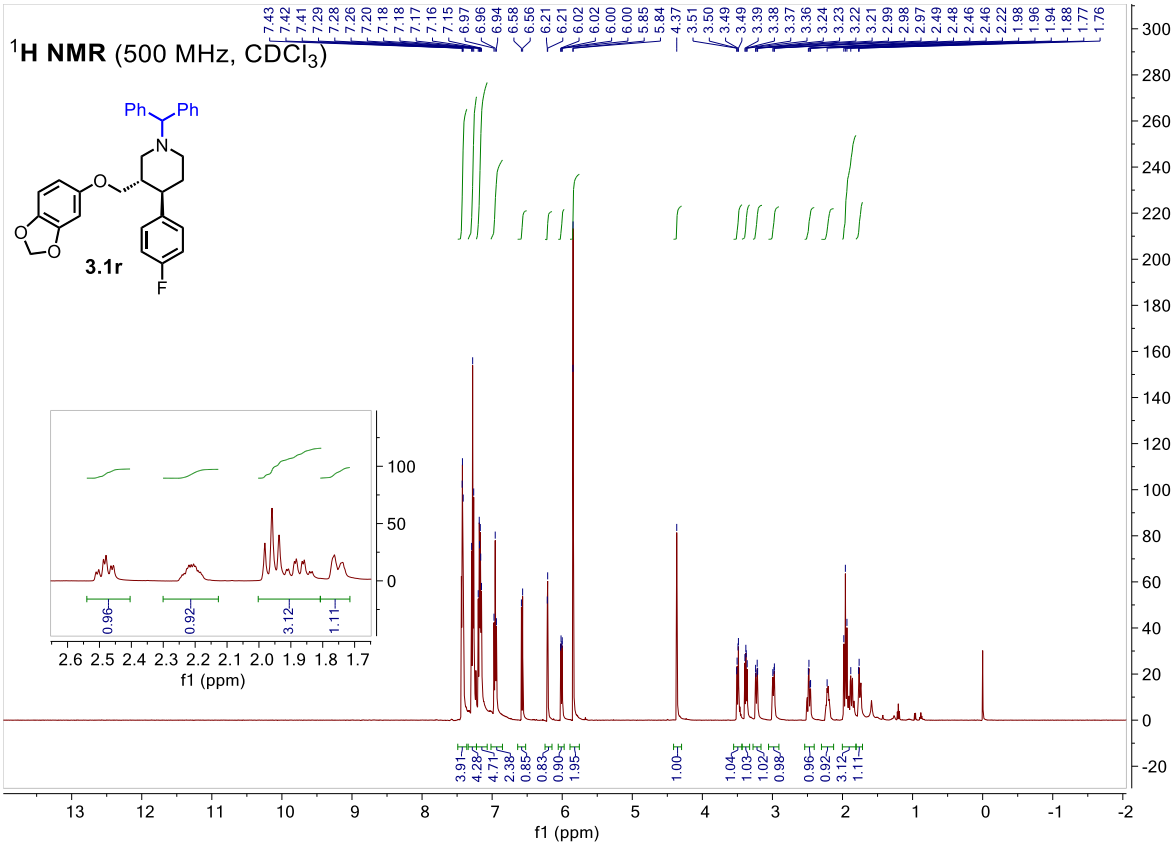
1H NMR (500 MHz, CDCl3)
Ph
Ph
N
O
3.1r
F
f1 (ppm)

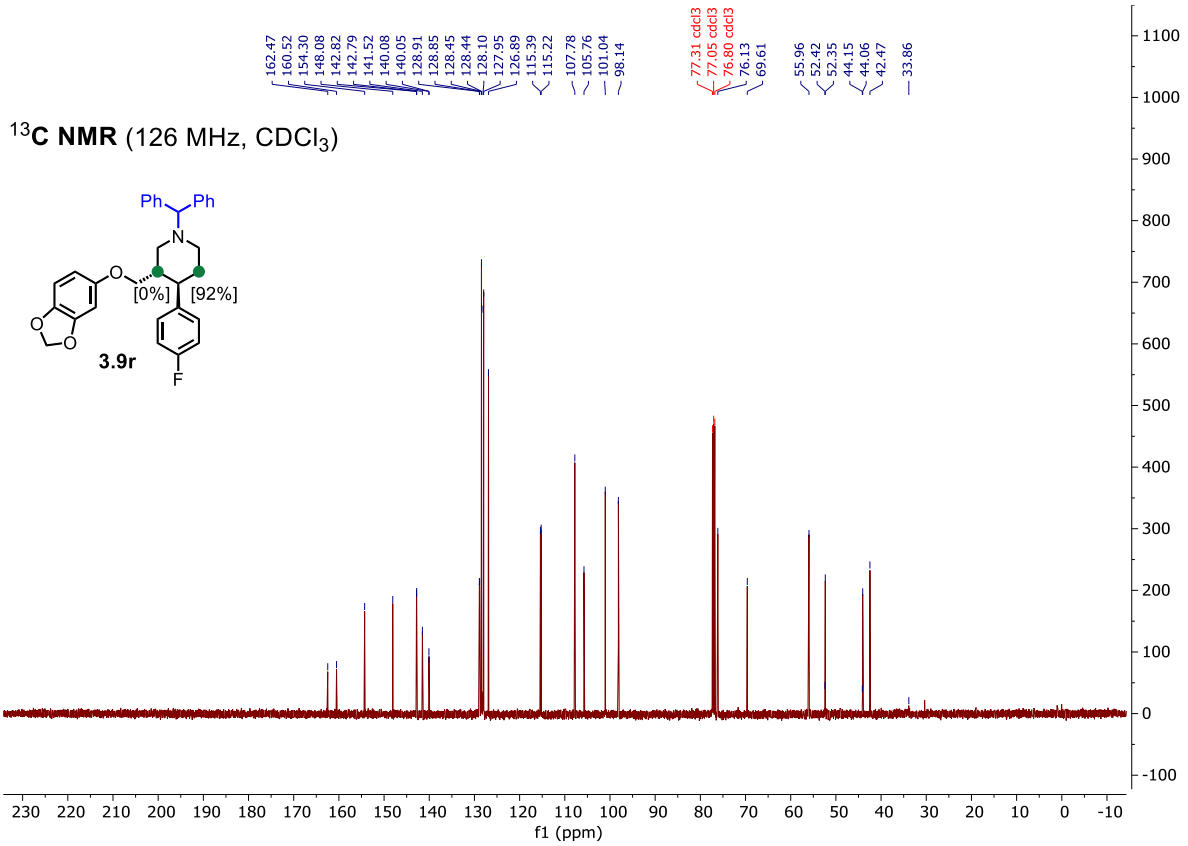
162.47
160.52
154.30
148.08
142.82
142.79
141.52
140.08
140.05
128.91
128.85
128.45
128.44
128.10
127.95
126.89
115.39
115.22
107.78
105.76
101.04
98.14
77.31 cdcl3
77.05 cdcl3
76.80 cdcl3
76.13
69.61
55.96
52.42
52.35
44.15
44.06
42.47
33.86
13C NMR (126 MHz, CDCl3)
Ph
Ph
N
O
[0%]
[92%]
O
O
3.9r
F
f1 (ppm)

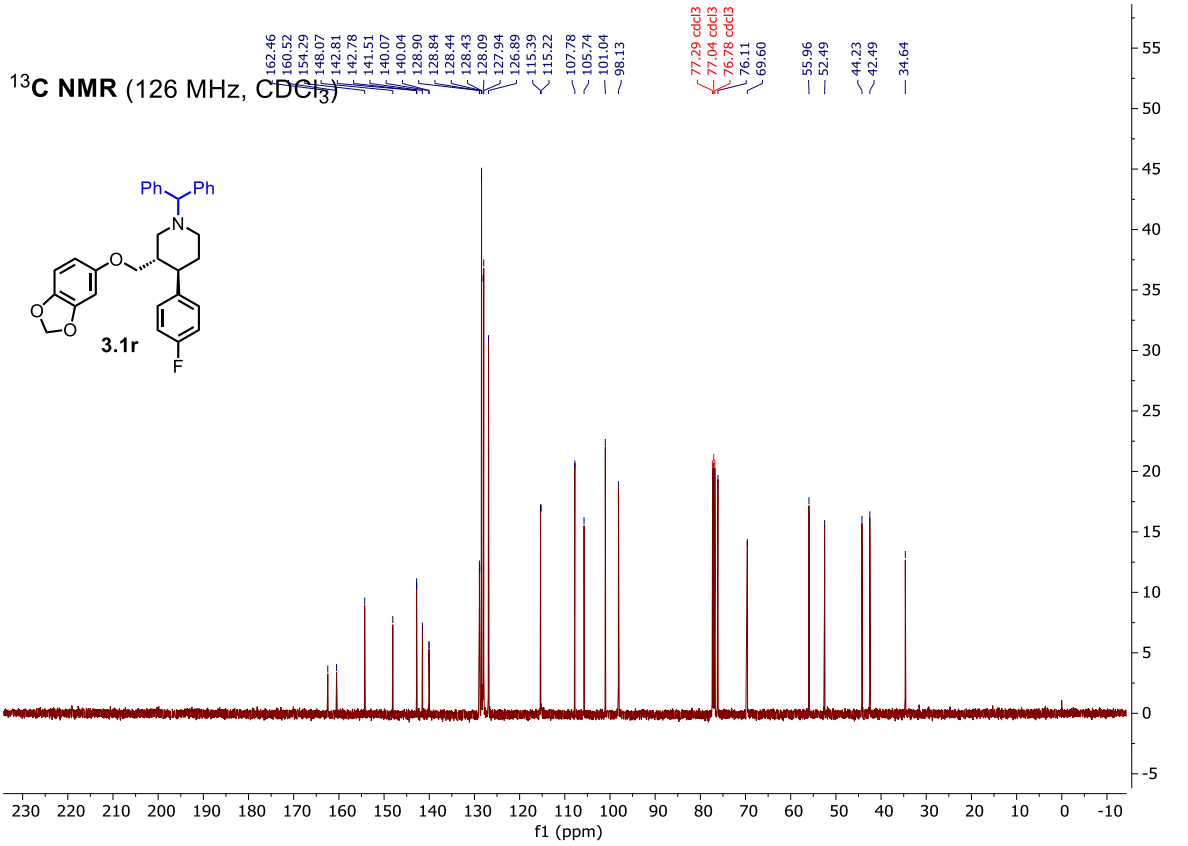
162.46
160.52
154.29
148.07
142.81
142.78
141.51
140.07
140.04
128.90
128.84
128.44
128.43
128.09
127.94
126.89
115.39
115.22
107.78
105.74
101.04
98.13
77.29 cdcl3
77.04 cdcl3
76.78 cdcl3
76.11
69.60
55.96
52.49
44.23
42.49
34.64
13C NMR (126 MHz, CDCl3)
Ph
Ph
N
O
O
O
3.1r
F
f1 (ppm)

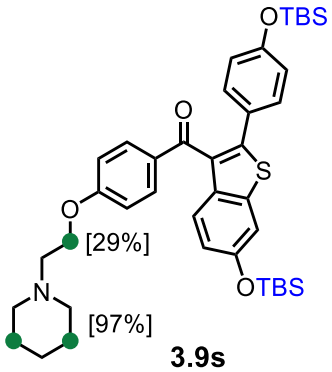

3.9s

***O*-TBS raloxifene, 3.9s**

O-TBS raloxifene **3.1s** was reacted with acetone-d_6 following the General Procedure A. After purification by column chromatography (MeOH:DCM = 1:49), **3.9s** was obtained as a yellow liquid (136 mg, 97%).

Deuterium incorporation: 4.46 D/molecule (^{1}H NMR), 5.08 D/molecule [HRMS (DART)]

^{1}H NMR (600 MHz, $CDCl_3$) δ 7.72 (d, *J* = 8.9 Hz, 2H), 7.57 (d, *J* = 8.7 Hz, 1H), 7.33 – 7.22 (m, 3H), 6.88 (dd, *J* = 8.8, 2.2 Hz, 1H), 6.72 (d, *J* = 9.0 Hz, 2H), 6.66 (d, *J* = 8.6 Hz, 2H), 4.05 (s, 1.42H, 29%D), 2.77 – 2.70 (m, 2H), 2.46 (s, 4H), 1.62 – 1.51 (m, 0.14H, 97%D), 1.40 (s, 2H), 1.01 (s, 9H), 0.93 (s, 9H), 0.23 (s, 6H), 0.12 (s, 6H); **^{13}C NMR** (151 MHz, $CDCl_3$) δ 193.0, 162.8, 156.0, 153.4, 143.3, 139.8, 134.4, 132.2, 130.5, 130.4, 130.3, 130.2, 126.7, 123.92, 123.90, 120.2, 119.18, 119.16, 113.9, 112.03, 112.00, 66.0, 54.81, 54.81, 25.64, 25.57, 25.0, 23.7, 23.6, 18.2, 18.1, -4.4, -4.5; **IR** (neat) 2927, 1595, 1463, 1252, 1164, 939, 907, 827, 779, 734 cm^{-1}.

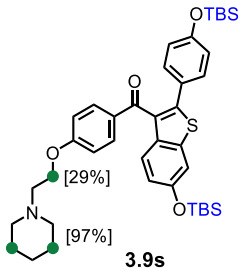
OTBS
O
S
O
[29%]
N
[97%]
OTBS

3.9s

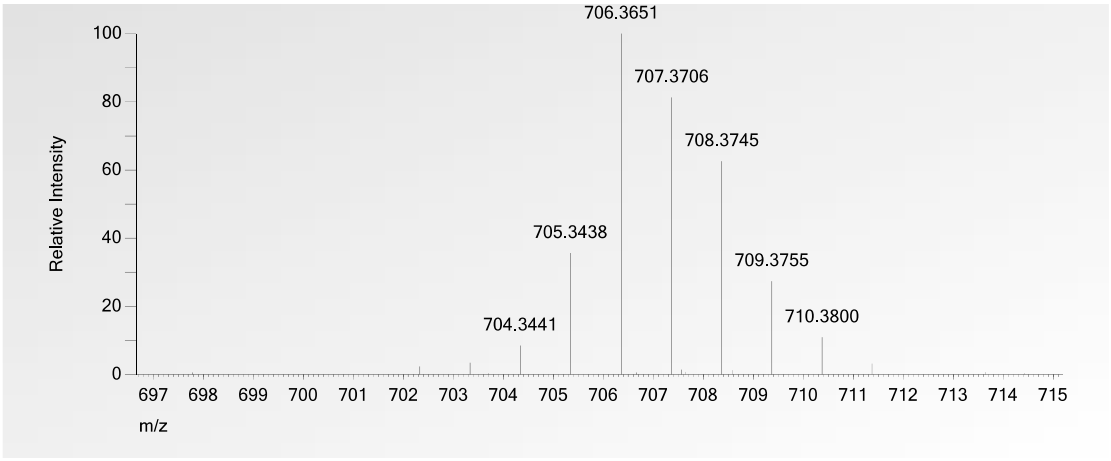
706.3651
707.3706
708.3745
705.3438
709.3755
710.3800
704.3441
Relative Intensity
m/z

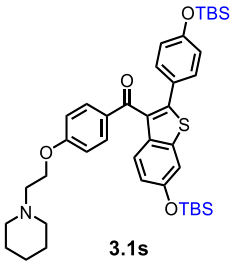
OTBS
O
S
O
N
OTBS

3.1s

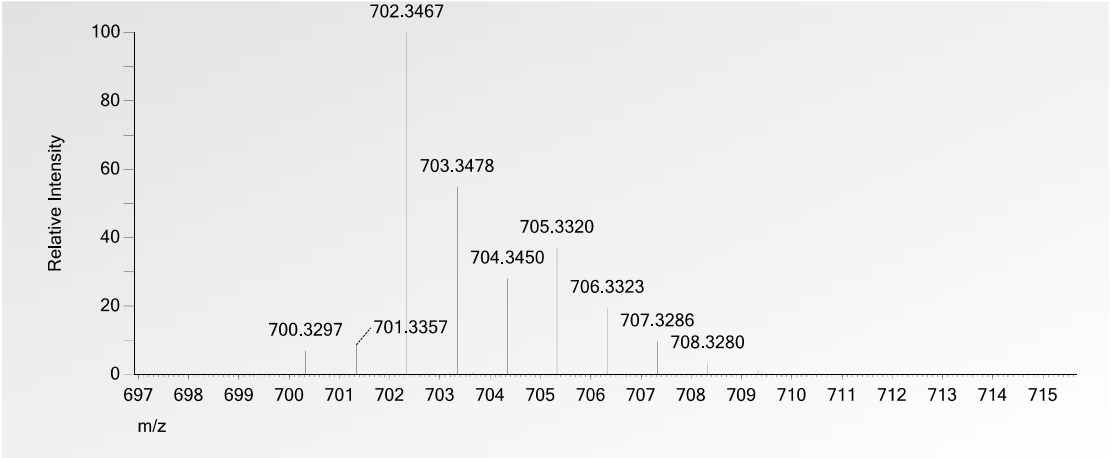
702.3467
703.3478
705.3320
704.3450
706.3323
707.3286
708.3280
700.3297
701.3357
Relative Intensity
m/z

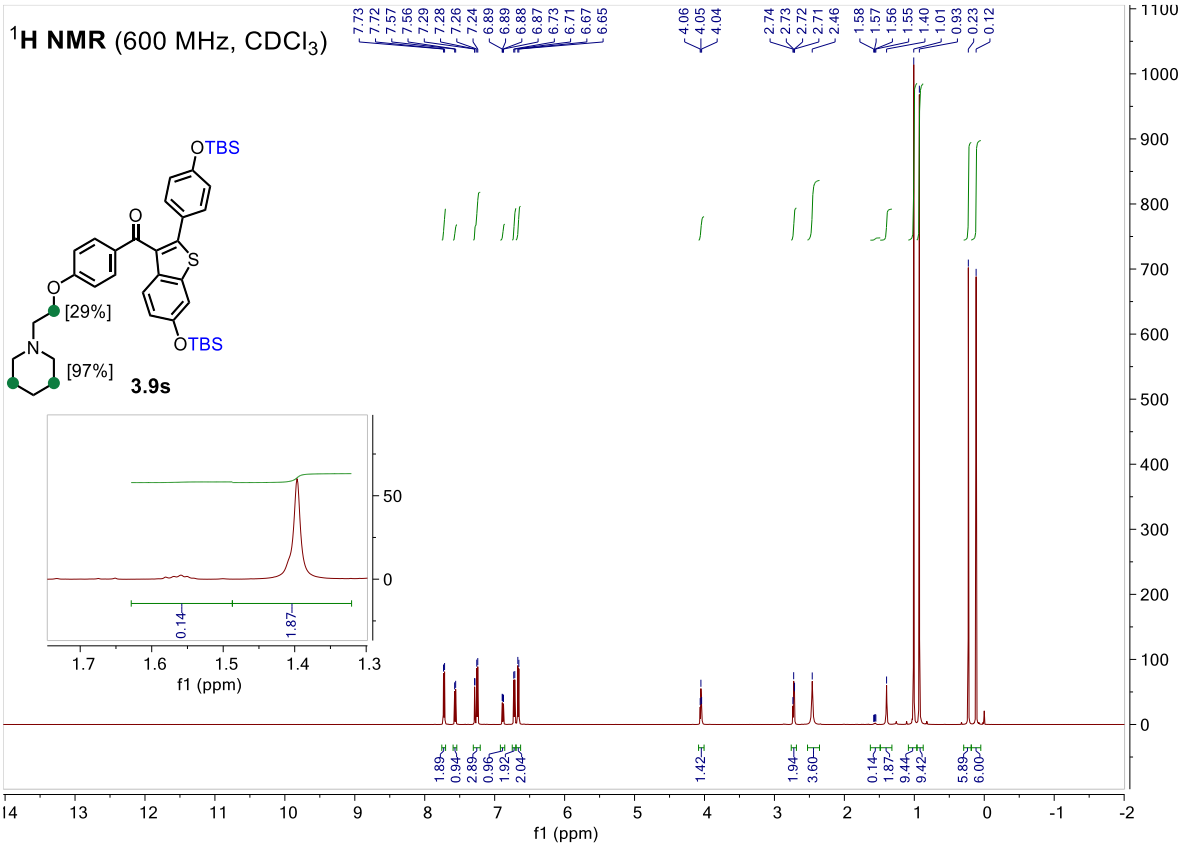
1H NMR (600 MHz, CDCl3)
OTBS
O
S
O
[29%]
N
[97%]
OTBS
3.9s
f1 (ppm)

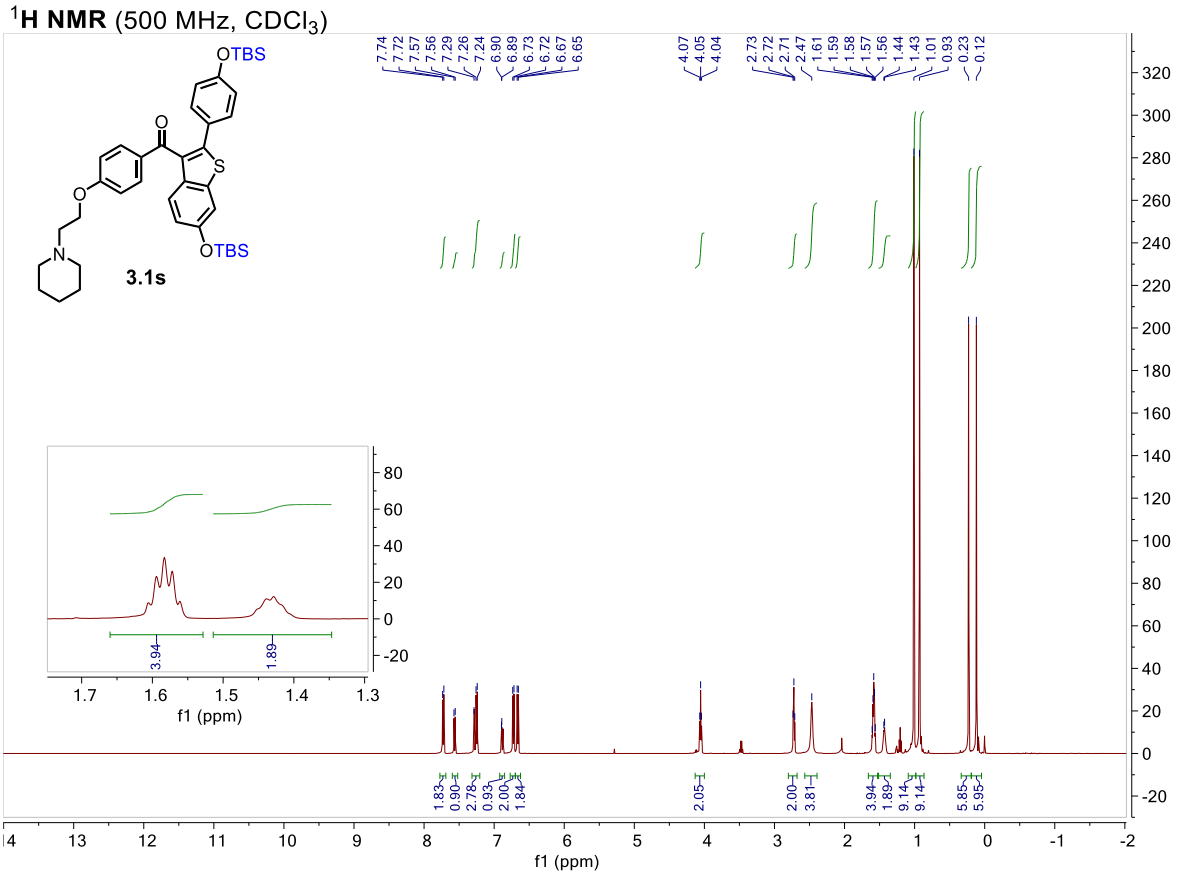
1H NMR (500 MHz, CDCl3)
OTBS
O
S
O
N
OTBS
3.1s
f1 (ppm)

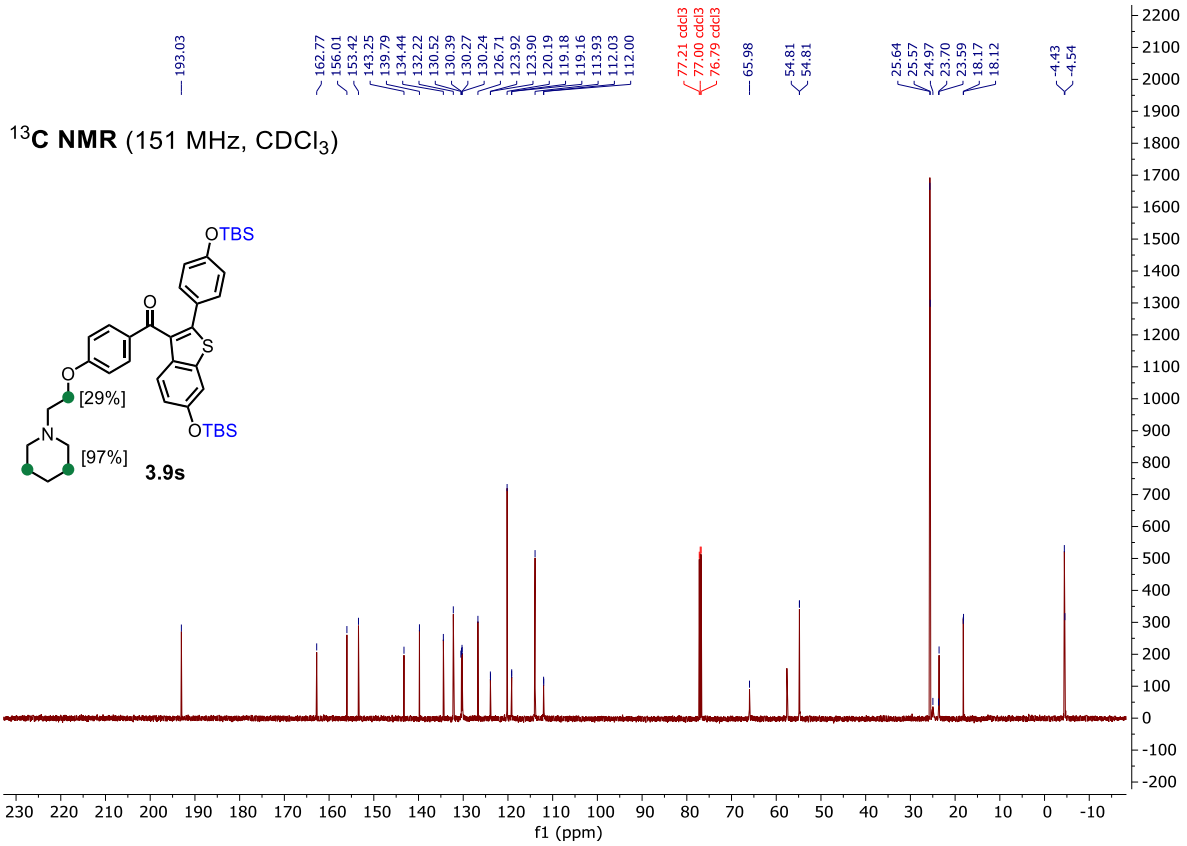
193.03
162.77
156.01
153.42
143.25
139.79
134.44
132.22
130.52
130.39
130.27
130.24
126.71
123.92
123.90
120.19
119.18
119.16
113.93
112.03
112.00
77.21 cdcl3
77.00 cdcl3
76.79 cdcl3
65.98
54.81
54.81
25.64
25.57
24.97
23.70
23.59
18.17
18.12
-4.43
-4.54
13C NMR (151 MHz, CDCl3)
OTBS
O
S
O
[29%]
N
[97%]
OTBS
3.9s
f1 (ppm)

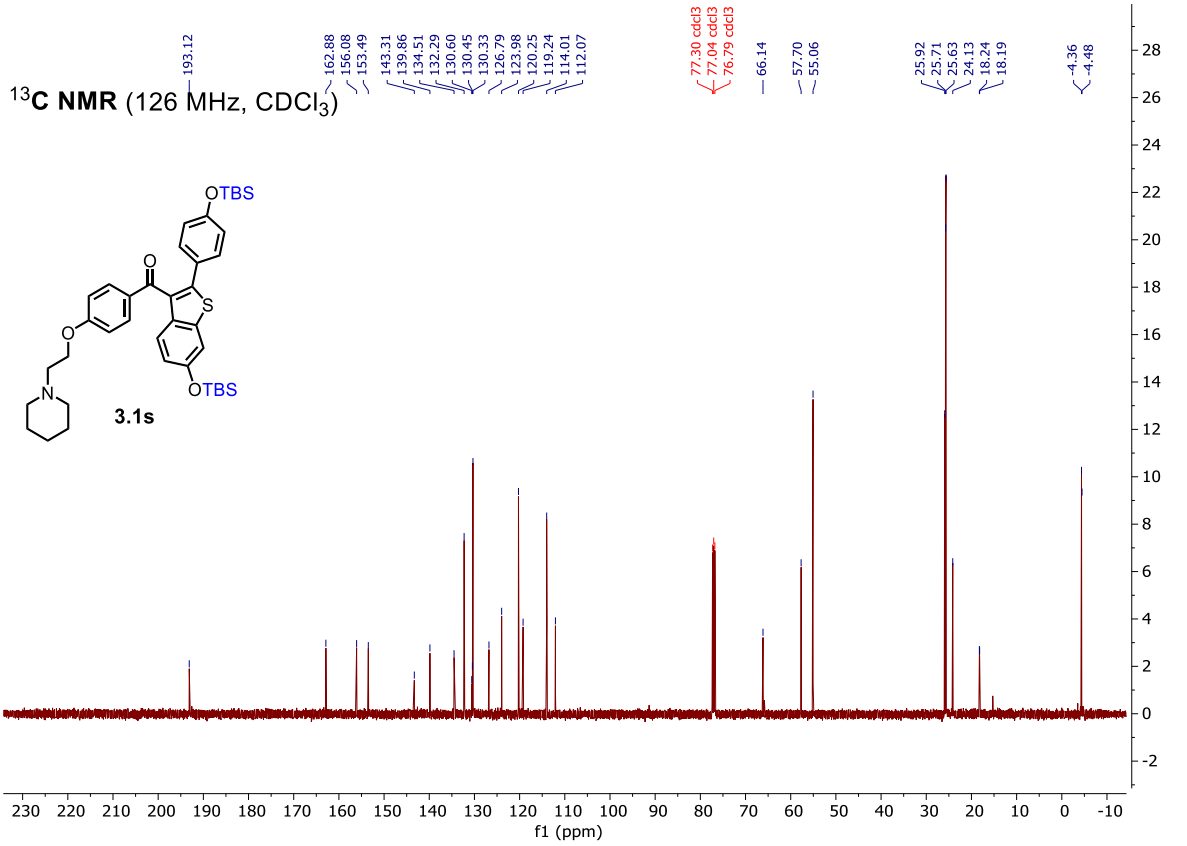
193.12
162.88
156.08
153.49
143.31
139.86
134.51
132.29
130.60
130.45
130.33
126.79
123.98
120.25
119.24
114.01
112.07
77.30 cdcl3
77.04 cdcl3
76.79 cdcl3
66.14
57.70
55.06
25.92
25.71
25.63
24.13
18.24
18.19
-4.36
-4.48
13C NMR (126 MHz, CDCl3)
OTBS
O
S
O
N
OTBS
3.1s
f1 (ppm)

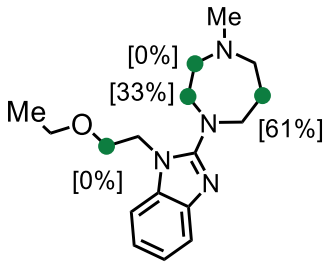

3.9t

Emedastine, 3.9t

Emedastine **3.1t** was reacted with acetone-d_6 following the General Procedure A. After purification by column chromatography (MeOH:DCM = 1:15), **3.9t** was obtained as a colorless liquid (53 mg, 88%).

Deuterium incorporation: 1.88 D/molecule (^{1}H NMR), 2.03 D/molecule [HRMS (DART)]

^{1}H NMR (500 MHz, $CDCl_3$) δ 7.53 (d, J = 7.4 Hz, 1H), 7.28 – 7.21 (m, 1H), 7.13 (ddd, J = 15.5, 7.6, 1.4 Hz, 2H), 4.19 (t, J = 6.0 Hz, 2H), 3.78 (t, J = 6.0 Hz, 2H), 3.74 – 3.68 (m, 1.33H, 33%D), 3.64 (d, J = 6.1 Hz, 2H), 3.46 (q, J = 7.0 Hz, 2H), 2.86 – 2.80 (m, 2H), 2.76 (d, J = 5.6 Hz, 2H), 2.44 (s, 3H), 2.10 – 1.98 (m, 0.78H, 61%D), 1.15 (t, J = 7.0 Hz, 3H); **^{13}C NMR** (126 MHz, $CDCl_3$) δ 159.1, 141.7, 135.5, 121.7, 120.7, 117.3, 109.1, 68.2, 66.8, 58.5, 57.3, 52.2, 51.6, 46.7, 44.8, 27.8, 15.1; **IR** (neat) 1522, 1460, 1405, 1375, 1349, 1283, 1115, 1045, 1009, 761, 741cm^{-1}.

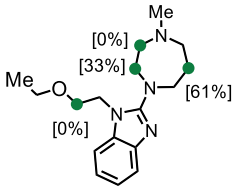
Me
[0%]
[33%]
Me
O
[61%]
[0%]
N
N

3.9t

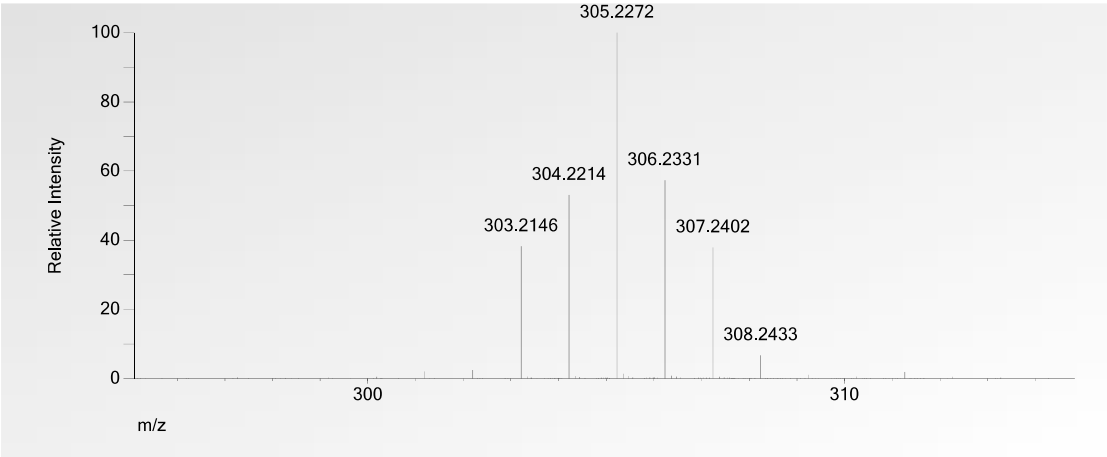
305.2272
100
80
60
40
20
0
Relative Intensity
304.2214
306.2331
303.2146
307.2402
308.2433
300
310
m/z

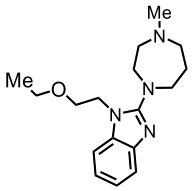
Me
Me
O
N
N
N

3.1t

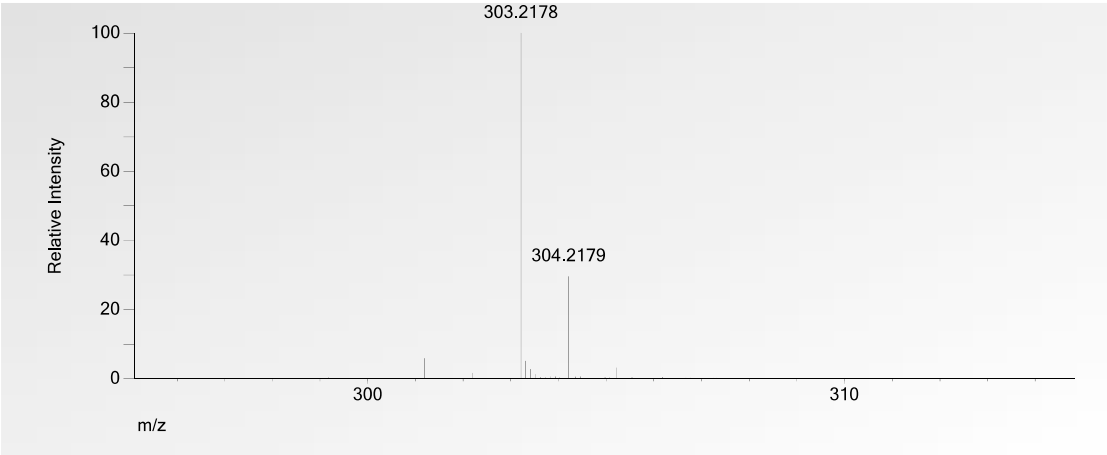
303.2178
100
80
60
40
20
0
Relative Intensity
304.2179
300
310
m/z

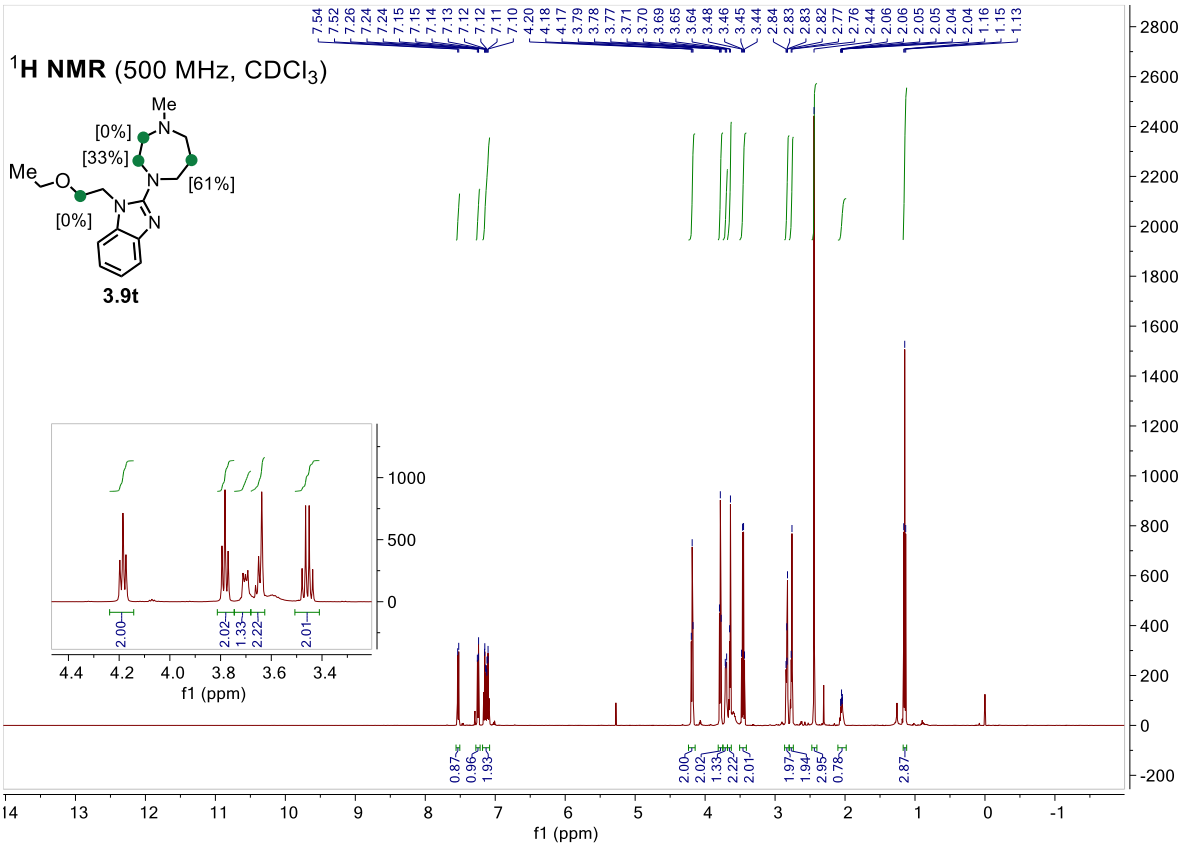
1H NMR (500 MHz, CDCl3)
Me
[0%]
[33%]
[61%]
[0%]
Me
3.9t
f1 (ppm)

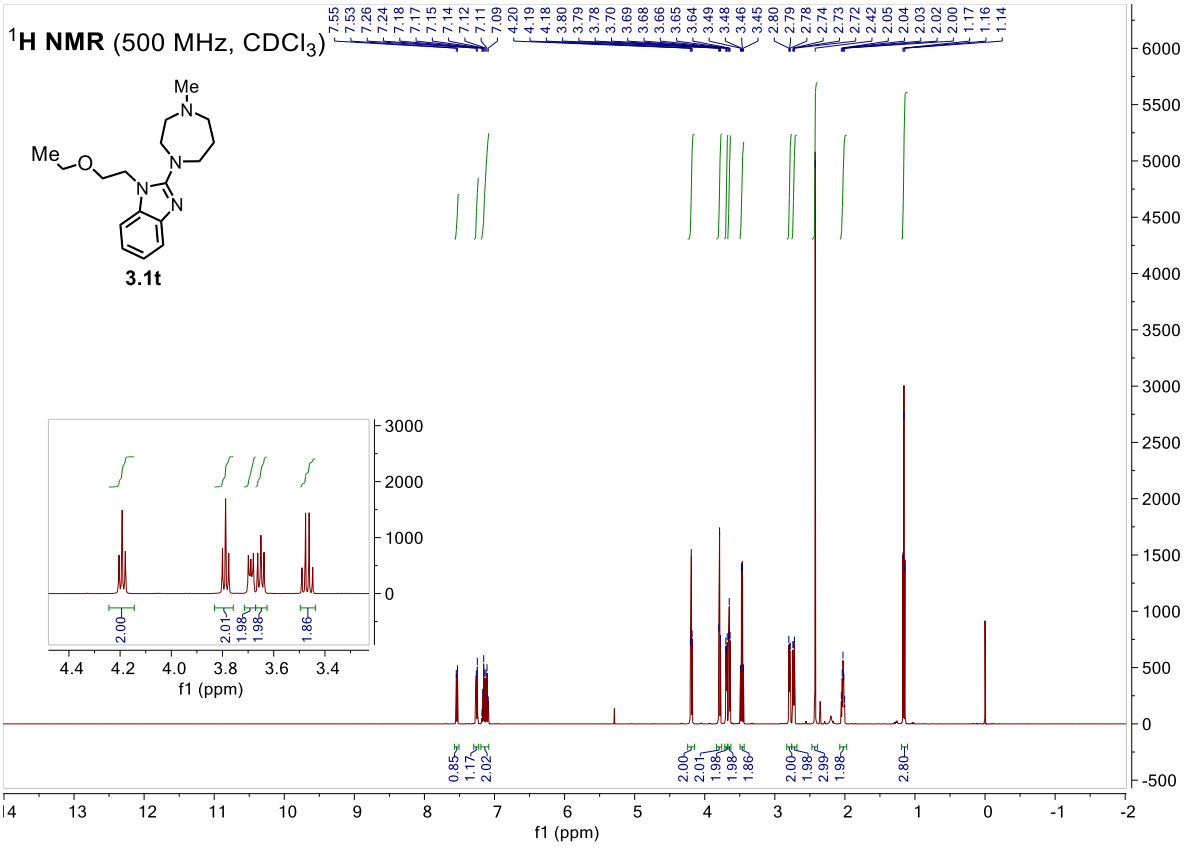
1H NMR (500 MHz, CDCl3)
Me
Me
3.1t
f1 (ppm)

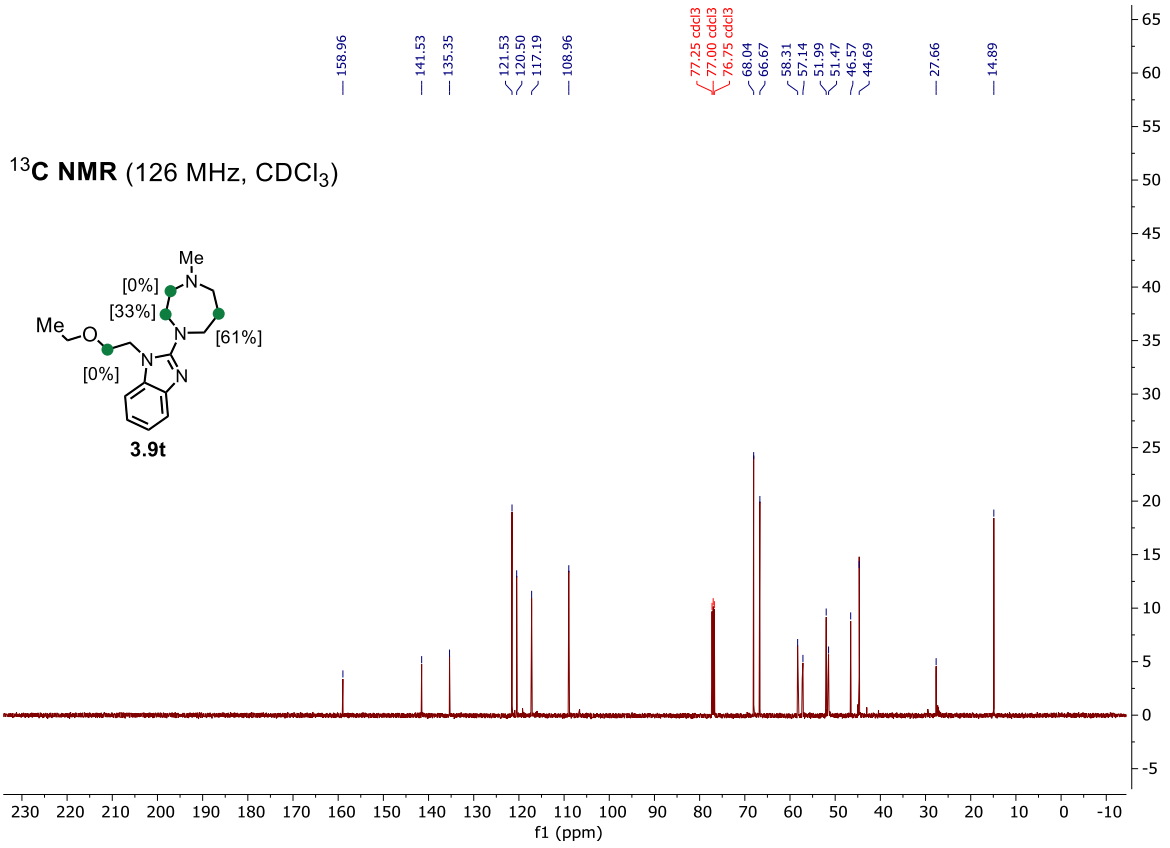
158.96
141.53
135.35
121.53
120.50
117.19
108.96
77.25 cdcl3
77.00 cdcl3
76.75 cdcl3
68.04
66.67
58.31
57.14
51.99
51.47
46.57
44.69
27.66
14.89
13C NMR (126 MHz, CDCl3)
Me
[0%]
[33%]
[61%]
Me
[0%]
3.9t
f1 (ppm)

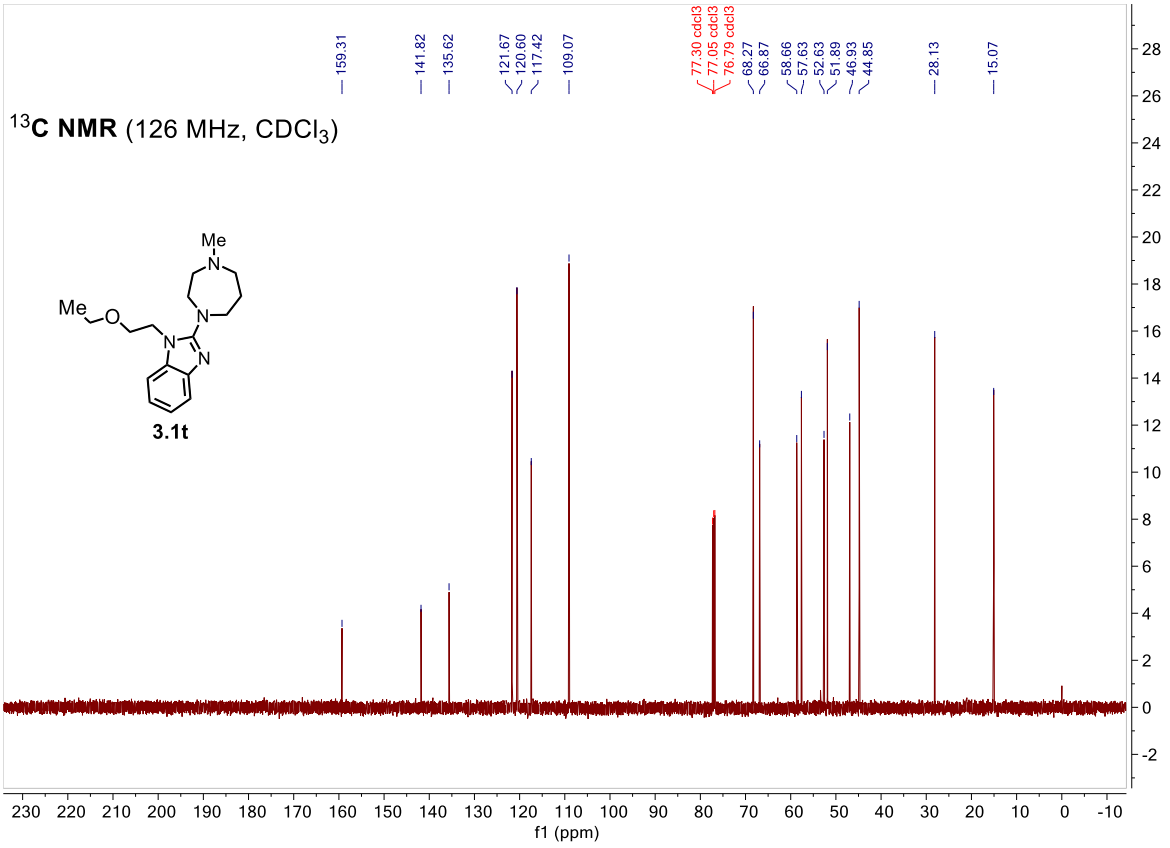
159.31
141.82
135.62
121.67
120.60
117.42
109.07
77.30 cdcl3
77.05 cdcl3
76.79 cdcl3
68.27
66.87
58.66
57.63
52.63
51.89
46.93
44.85
28.13
15.07
13C NMR (126 MHz, CDCl3)
Me
Me
3.1t
f1 (ppm)

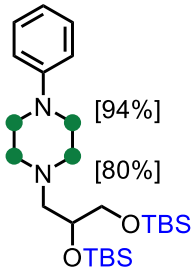

3.9u

***O*-TBS dropropizine, 3.9u**

O-TBS dropropizine **3.1u** was reacted with acetone-d_6 following the General Procedure B. After purification by column chromatography (MeOH:DCM = 1:99), **3.9u** was obtained as a yellow liquid (87 mg, 94%).

Deuterium incorporation: 6.96 D/molecule (^{1}H NMR), 7.61 D/molecule [HRMS (DART)]

^{1}H NMR (500 MHz, $CDCl_3$) δ 7.25 (dd, *J* = 8.8, 7.3 Hz, 2H), 6.91 (dt, *J* = 7.8, 1.0 Hz, 2H), 6.83 (s, 1H), 3.80 (dd, *J* = 6.0, 4.9 Hz, 1H), 3.66 – 3.57 (m, 1H), 3.53 (dd, *J* = 10.0, 5.6 Hz, 1H), 3.12 (s, 0.24H, 94%D), 2.62 (s, 0.47H, 77%D), 2.55 (s, 0.34H, 83%D), 2.50 (dd, *J* = 13.0, 4.7 Hz, 1H), 2.37 (dd, *J* = 13.0, 6.1 Hz, 1H), 0.90 (d, *J* = 4.3 Hz, 18H), 0.09 (d, *J* = 6.1 Hz, 6H), 0.06 (d, *J* = 1.6 Hz, 6H); **^{13}C NMR** (126 MHz, $CDCl_3$) δ 151.5, 129.1, 119.4, 115.8, 71.9, 66.2, 62.0, 53.2, 48.3, 26.03, 25.95, 18.4, 18.2, -4.4, -4.5, -5.2, -5.3; **IR** (neat) 2925, 2853, 1598, 1499, 1250, 1091, 1003, 830, 810, 773, 753, 689 cm^{-1}.

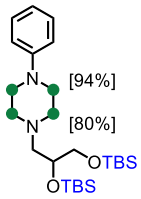
[94%]
[80%]
OTBS
OTBS

3.9u

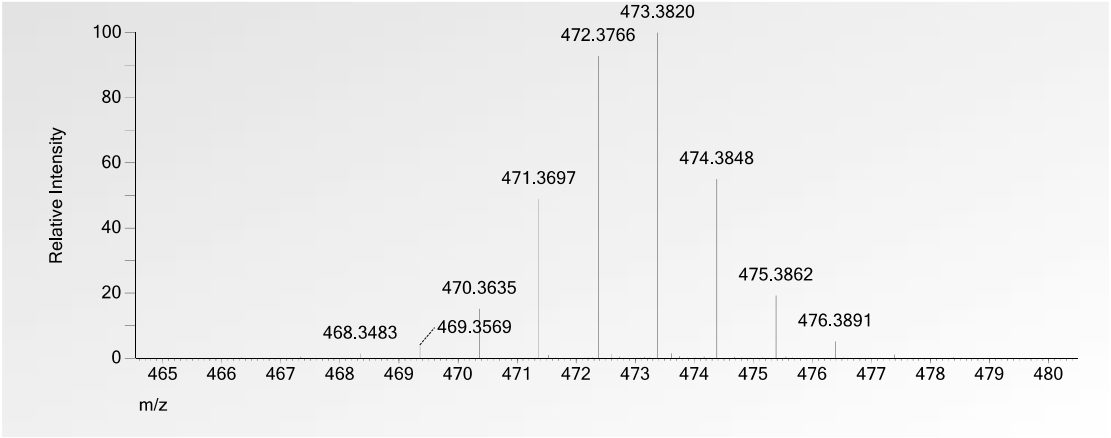
473.3820
472.3766
474.3848
471.3697
475.3862
470.3635
476.3891
468.3483
469.3569
Relative Intensity
m/z

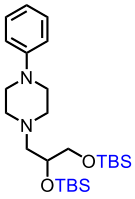
OTBS
OTBS

3.1u

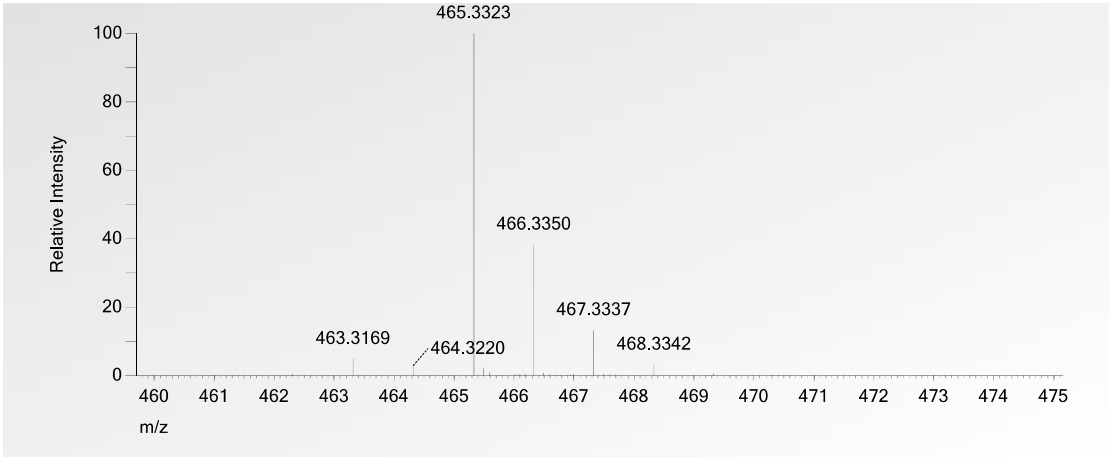
465.3323
466.3350
467.3337
463.3169
464.3220
468.3342
Relative Intensity
m/z

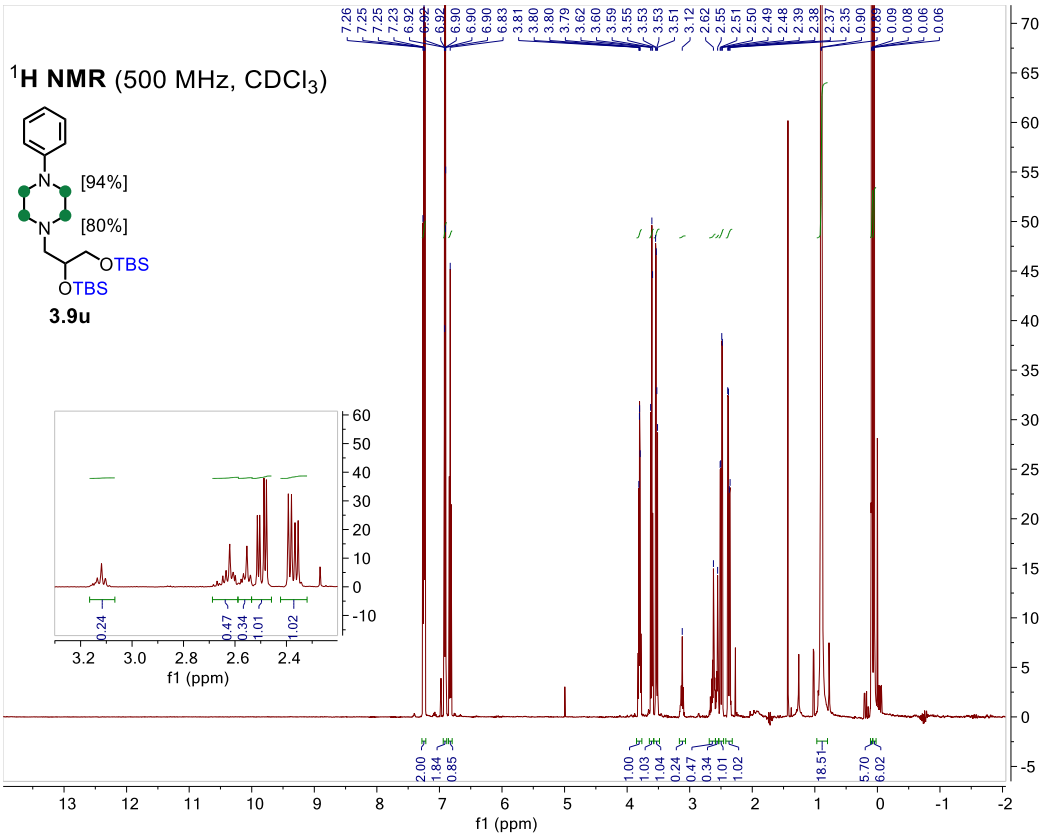
1H NMR (500 MHz, CDCl3)
[94%]
[80%]
OTBS
OTBS
3.9u
f1 (ppm)

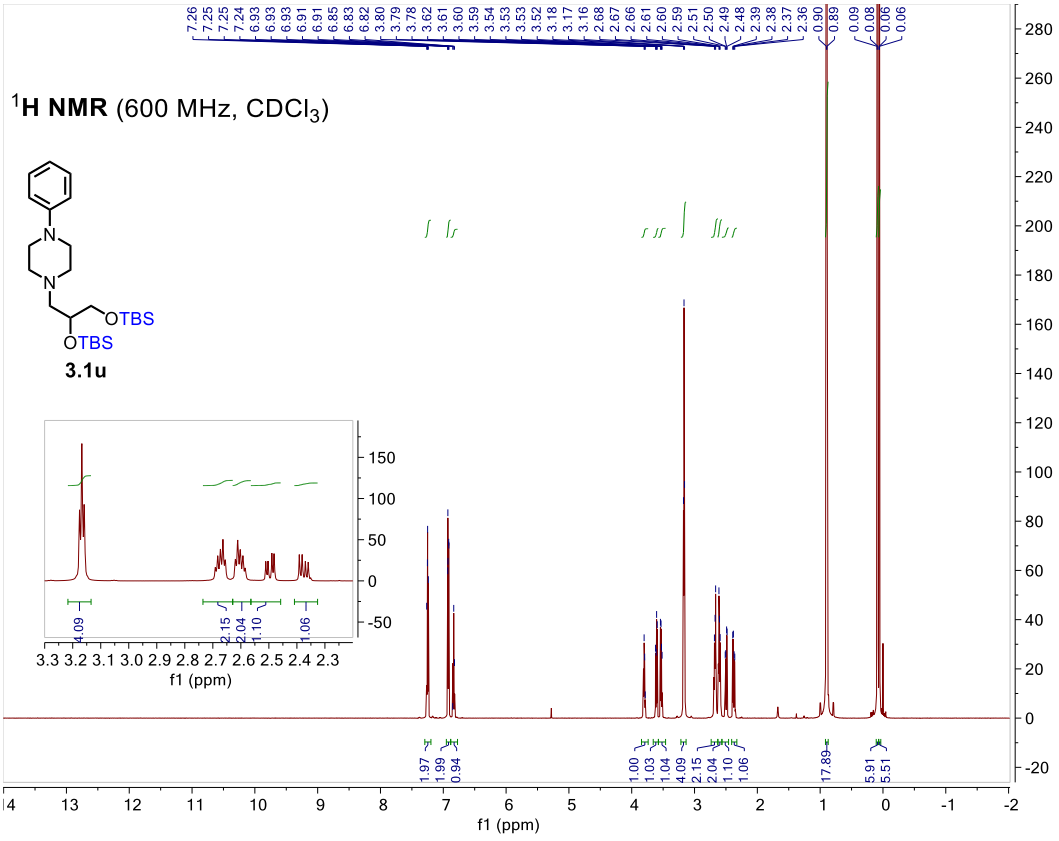
1H NMR (600 MHz, CDCl3)
OTBS
OTBS
3.1u
f1 (ppm)

^{13}**C NMR** (126 MHz, $CDCl_3$)

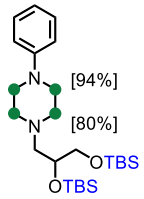

3.9u

^{13}**C NMR** (151 MHz, $CDCl_3$)

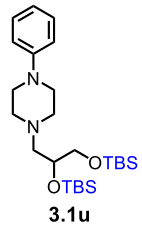

3.1u

B5. References

(1) Heinz, C.; Lutz, J. P.; Simmons, E. M.; Miller, M. M.; Ewing, W. R.; Doyle, A. G. *J. Am. Chem. Soc.* **2018**, *140*, 2292−2300.

(2) Sun, Y-H.; Sun, T-Y.; Wu, Y-D.; Zhang, X.; Rao, Y. *Chem. Sci.* **2016,** *7*, 2229–2238.

(3) Banwell, M. G.; Coster, M. J.; Harvey, M. J.; Moraes, J. *J. Org. Chem.* **2003**, *68*, 613−616.

(4) Park, C. M.; Kim, S. Y.; Park, W. K.; Choi, J. H.; Seong, C. M. *Bioorg. Med. Chem. Lett*. **2010**, *20*, 5221−5224.

(5) Liu, L-L.; Yeung, K-S.; Yu, J-Q. *Chem. Eur. J*. **2019**, *25*, 2199–2202.

(6) Nicolaou, K. C.; Claiborne, C. F.; Nantermet, P. G.; Couladouros, E. A.; Sorensen, E. J. *J. Am. Chem. Soc.***1994**, *116*, 4, 1591−1592.

(7) Lei, C.; Yip, Y. J.; Zhou, J. S. *J. Am. Chem. Soc*. **2017**, *139*, 17, 6086−6089.

(8) Chang, D.; Li, T.; Li, L.; Jakowski, J.; Huang, J.; Keum, J. K.; Lee, B.; Bonnesen, P. V.; Zhou, M.; Garashchuk, S.; Sumpter, B. G.; Hong, K. *Macromolecules* **2018**, *51*, 9393−9404.

Appendix C. Experimental for Section 3.3

General Experimental Procedures

All reactions were performed in standard, oven-dried glassware fitted with rubber septa under an inert atmosphere of nitrogen unless otherwise described. Stainless steel syringes or cannulas were used to transfer air- and moisture-sensitive liquids. Reported concentrations refer to solution volumes at room temperature. Evaporation and concentration *in vacuo* were performed using house vacuum (ca. 40 mm Hg). Column chromatography was performed with SiliaFlash® 60 (40–63 micron) silica gel from Silicycle. Thin layer chromatography (TLC) was used for reaction monitoring and product detection using pre-coated glass plates covered with 0.25 mm silica gel with fluorescent indicator; visualization by UV light (λ_{ex} = 254 nm) or $KMnO_4$ stain.

Materials

Reagents were purchased in reagent grade from commercial suppliers and used without further purification, unless otherwise described. Tris(pentafluorophenyl)borane was purchased from TCI and used without further purification. H_2O, in synthetic procedures, refers to distilled water. Chiral ligands **L1**-**L12** were prepared according to the procedures previously reported in the literature. Amines and α,β-unsaturated compounds were prepared according to the procedures reported previously.

Instrumentation

Proton nuclear magnetic resonance (^{1}H NMR) spectra and proton-decoupled carbon nuclear magnetic resonance (^{13}C {^{1}H} NMR) spectra were recorded at 25 °C (unless stated otherwise) on Inova 600 (600 MHz), Varian Unity/Inova 500 (500 MHz) or Oxford AS400 (400 MHz) spectrometers at the Boston College nuclear magnetic resonance facility. Chemical shifts for protons are reported in parts per million downfield from tetramethylsilane and are referenced to 0

ppm. Chemical shifts for carbon are reported in parts per million downfield from tetramethylsilane and are referenced to the carbon resonances of the solvent. The peak positions are quoted to one decimal place unless they are indistinguishable. The solvent peak was referenced to 77.2 ppm for ^{13}C for $CDCl_3$. Benzotrifluoride was used as an external standard for ^{19}F NMR and referenced to –63.7 ppm. Data are represented as follows: chemical shift, integration, multiplicity (br = broad, s = singlet, d = doublet, t = triplet, q = quartet, m = multiplet), coupling constants in Hertz (Hz). Infrared spectra were recorded on a Bruker FT-IR Alpha (ATR mode) spectrophotometer. Data are represented as follows: frequency of absorption (cm^{-1}). High-resolution mass spectrometry was performed on a JEOL AccuTOF-DART (positive mode) at the Mass Spectrometry Facility, Boston College.

Abbreviations used

Bn = benzyl, Boc = *tert*-butoxycarbonyl, COD = 1,5-cyclooctadiene, COSY = correlation spectroscopy, DART = direct analysis in real time, DCM = dichloromethane, DMAP = 4-dimethylaminopyridine, DMF = *N*,*N*-dimethylformamide, er = enantiomeric ratio, HPLC = high pressure liquid chromatography, Et_3N = trimethylamine, EtOAc = ethyl acetate, HR = high-resolution, HSQC = heteronuclear single quantum coherence, LC = liquid chromatography, MS = mass spectrometry, NOESY = nuclear Overhauser effect spectroscopy, OTf = triflate, PMP = *p*-methoxyphenyl, PTLC = preparatory thin-layer chromatography, TBAF = tetra-*n*-butylammonium fluoride, TBME = *tert*-butyl methyl ether, TBS = *tert*-butyldimethylsilyl, THF = tetrahydrofuran, TLC = thin-layer chromatography, TMS = trimethylsilyl, TOF = time-of-flight.

C1. Substrate Preparation

Preparation of Amine Substrates (Table S3.6)

Table S3.6A. List of Amine Substrates

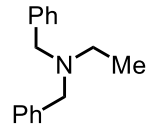

3.21a

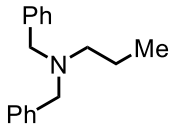

3.21b

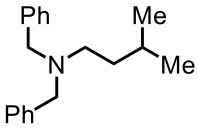

3.21c

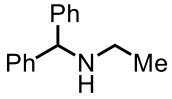

3.21d

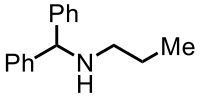

3.21e

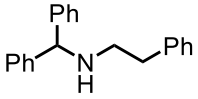

3.21f

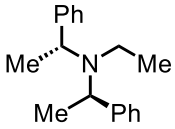

3.21g

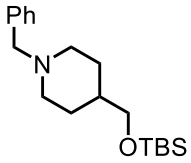

3.21h

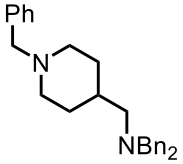

3.21i

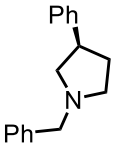

3.21j

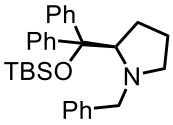

3.21k

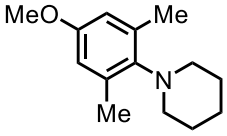

3.21l

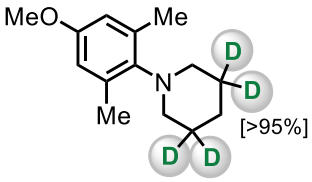

3.21l-*d*

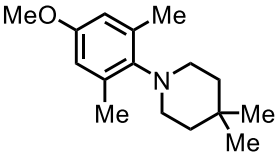

3.21m

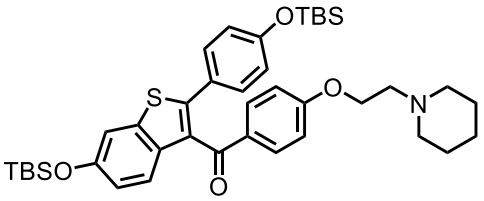

3.21n

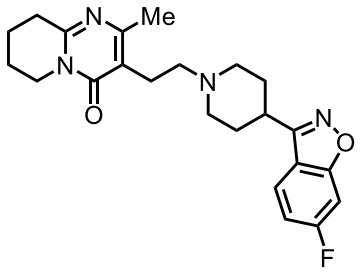

3.21o

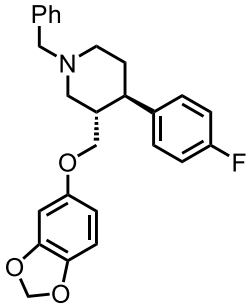

3.21p

Table S3.6B. List of Amine Substrates

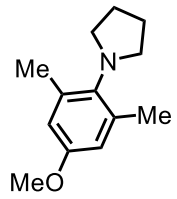	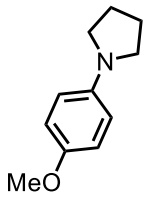	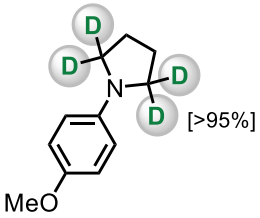
3.21q	**3.21r**	**3.21r-d_α**
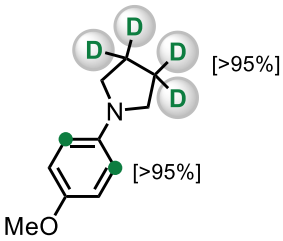	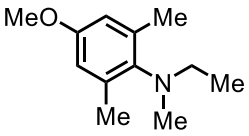	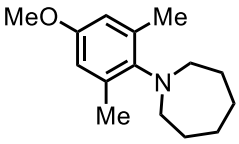
3.21r-d_β	**3.21s**	**3.21t**
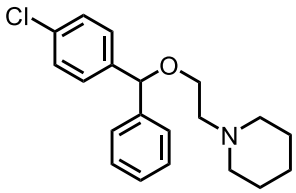	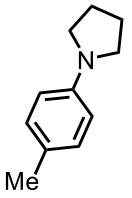	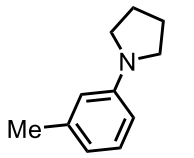	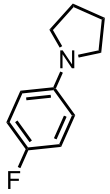
3.21u	**3.21v**	**3.21w**	**3.21x**

Substrates **3.21** were prepared according to the literature procedures. Methods used to prepare the newly synthesized amines (**3.21g-3.21i**, **3.21k, 3.21l-*d*, 3.21m, 3.21r-d_α**, and **3.21r-d_β**) and their spectroscopic data are provided below.

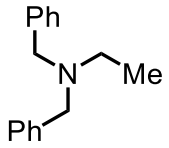

3.21a

***N*,*N*-Dibenzylethanamine (3.21a)**

N,*N*-Dibenzylethanamine was prepared following the General Procedure for the Alkylation of Amines using dibenzylamine (2.0 g, 10.1 mmol), iodoethane (1.5 equiv.) and K_2CO_3 (2 equiv.). The unpurified product was subjected to silica gel column chromatography (Et_2O:hexanes = 1:49) to afford **3.21a** as a colorless liquid (1.9 g, 83%).

^{1}H NMR (500 MHz, $CDCl_3$) δ 7.37 (d, *J* = 6.7 Hz, 4H), 7.30 (t, *J* = 7.6 Hz, 4H), 7.24 – 7.19 (m, 2H), 3.57 (s, 4H), 2.50 (q, *J* = 7.1 Hz, 2H), 1.07 (t, *J* = 7.1 Hz, 3H).

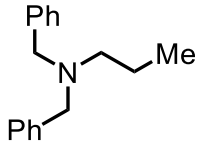

3.21b

***N*,*N*-Dibenzylpropan-1-amine (3.21b)**

N,*N*-Dibenzylpropan-1-amine was prepared following the General Procedure for the Alkylation of Amines using dibenzylamine (2.0 g, 10.1 mmol), 1-bromopropane (1.5 equiv.) and K_2CO_3 (2 equiv.). The unpurified product was subjected to silica gel column chromatography (Et_2O:hexanes = 1:49) to afford **3.21b** as a colorless liquid (1.9 g, 78%).

^{1}H NMR (400 MHz, $CDCl_3$) δ 7.37 (d, *J* = 7.5 Hz, 4H), 7.29 (t, *J* = 7.4 Hz, 4H), 7.26 – 7.17 (m, 2H), 3.55 (s, 4H), 2.42 – 2.32 (m, 2H), 1.52 (h, *J* = 7.3 Hz, 2H), 0.85 (t, *J* = 7.4 Hz, 3H).

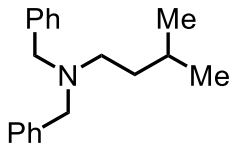

3.21c

***N*,*N*-Dibenzyl-3-methylbutan-1-amine (3.21c)**

N,*N*-Dibenzyl-3-methylbutan-1-amine was prepared following the General Procedure for the Alkylation of Amines using dibenzylamine (5.2 g, 26.1 mmol), 1-bromo-3-methylbutane (1.2 equiv.) and K_2CO_3 (2 equiv.). The unpurified product was subjected to silica gel column chromatography (Et_2O:hexanes = 1:49) to afford **3.21c** as a colorless liquid (4.3 g, 62%).

^{1}H NMR (500 MHz, $CDCl_3$) δ 7.36 (d, *J* = 6.7 Hz, 4H), 7.30 (t, *J* = 7.6 Hz, 4H), 7.22 (t, *J* = 7.3 Hz, 2H), 3.54 (s, 4H), 2.45 – 2.39 (m, 2H), 1.59 (dp, *J* = 13.3, 6.7 Hz, 1H), 1.43 – 1.36 (m, 2H), 0.78 (d, *J* = 6.6 Hz, 6H).

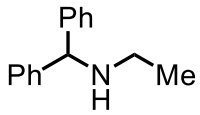

3.21d

***N*-Benzhydrylethanamine (3.21d)**

N-Benzhydrylethanamine was prepared following the General Procedure for the Alkylation of Amines using diphenylmethanamine (3.7 g, 20 mmol), iodoethane (0.9 equiv.) and K_2CO_3 (2 equiv.). The unpurified product was subjected to silica gel column chromatography (EtOAc:hexanes = 1:19) to afford **3.21d** as a colorless liquid (3.1 g, 82%).

^{1}H NMR (600 MHz, $CDCl_3$) δ 7.39 (d, *J* = 6.9 Hz, 4H), 7.29 (t, *J* = 7.7 Hz, 4H), 7.19 (t, *J* = 7.3 Hz, 2H), 4.83 (s, 1H), 2.61 (q, *J* = 7.2 Hz, 2H), 1.13 (t, *J* = 7.1 Hz, 3H).

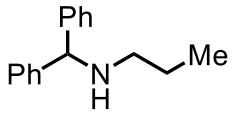

3.21e

***N*-Benzhydrylpropan-1-amine (3.21e)**

N-Benzhydrylpropan-1-amine was prepared following the General Procedure for the Alkylation of Amines using diphenylmethanamine (7.3 g, 40 mmol), 1-bromopropane (0.8 equiv.) and K_2CO_3 (1.2 equiv.). The unpurified product was subjected to silica gel column chromatography (EtOAc:hexanes = 1:19) to afford **3.21e** as a light yellow liquid (5.6 g, 78%).

^{1}H NMR (500 MHz, $CDCl_3$) δ 7.39 (d, *J* = 7.3 Hz, 4H), 7.29 (t, *J* = 7.6 Hz, 4H), 7.19 (t, *J* = 7.3 Hz, 2H), 4.81 (s, 1H), 2.54 (t, *J* = 7.1 Hz, 2H), 1.53 (h, *J* = 7.3 Hz, 2H), 1.46 (s, 1H), 0.91 (t, *J* = 7.4 Hz, 3H).

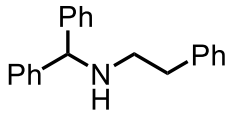

3.21f

***N*-Benzhydryl-2-phenylethan-1-amine (3.21f)**

N-Benzhydryl-2-phenylethan-1-amine was prepared following the General Procedure for the Alkylation of Amines using diphenylmethanamine (1.8 g, 10 mmol), (2-bromoethyl)benzene (0.9 equiv.) and K_2CO_3 (1.2 equiv.). The unpurified product was subjected to silica gel column chromatography (EtOAc:hexanes = 1:19) to afford **3.21f** as a colorless liquid (2.0 g, 77%).

^{1}H NMR (500 MHz, $CDCl_3$) δ 7.35 (d, *J* = 6.8 Hz, 4H), 7.27 (t, *J* = 7.6 Hz, 6H), 7.22 – 7.15 (m, 5H), 4.83 (s, 1H), 2.89 – 2.80 (m, 4H).

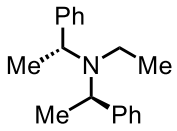

3.21g

(*R*)-*N*-Ethyl-1-phenyl-*N*-((*R*)-1-phenylethyl)ethan-1-amine (3.21g)

3.21g was prepared through the reaction of (*R*)-bis((*R*)-1-phenylethyl)amine (2.7 g, 11.8 mmol), iodoethane (1.5 equiv.) and K_2CO_3 (2.0 equiv.) in MeCN. The reaction mixture in pressure vessel was placed in an oil bath at 100 °C and was allowed to stir for 12 hours. Upon completion (monitored by TLC), the solution was allowed to cool to 22 °C. H_2O was then added and the organic material was extracted with EtOAc. The combined organic layers were dried over $MgSO_4$, filtered, and concentrated *in vacuo*. The unpurified product mixture was subjected to flash silica gel column chromatography (ethyl ether:hexanes = 1:19) to afford **3.21g** as a colorless liquid (2.1 g, 70%). **^{1}H NMR (500 MHz, $CDCl_3$):** δ 7.38 (d, *J* = 7.6 Hz, 4H), 7.29 (t, *J* = 7.6 Hz, 4H), 7.20 (t, *J* = 7.2 Hz, 2H), 4.01 (q, *J* = 6.8 Hz, 2H), 2.67 (dq, *J* = 14.1, 7.0 Hz, 1H), 2.48 (dq, *J* = 14.2, 7.1 Hz, 1H), 1.38 (d, *J* = 6.9 Hz, 6H), 0.80 (t, *J* = 7.1 Hz, 3H).

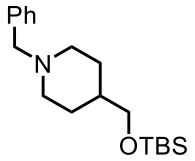

3.21h

1-Benzyl-4-(((*tert*-butyldimethylsilyl)oxy)methyl)piperidine (3.21h)

1-Benzyl-4-(((*tert*-butyldimethylsilyl)oxy)methyl)piperidine was prepared following the General Procedure for the TBS Protection of Alcohols using (1-benzylpiperidin-4-yl)methanol (10 mmol) as the alcohol. The unpurified product was subjected to silica gel column chromatography (ethyl ether:hexanes = 1:4) to afford **3.21h** as a colorless liquid (3.0 g, 94%).

^{1}H NMR (500 MHz, $CDCl_3$) δ 7.34 – 7.28 (m, 4H), 7.26 (s, 1H), 3.49 (s, 2H), 3.43 (d, *J* = 6.5 Hz, 2H), 2.88 (dt, *J* = 11.6, 3.3 Hz, 2H), 1.93 (td, *J* = 11.7, 2.5 Hz, 2H), 1.73 – 1.63 (m, 2H), 1.46 (ddd, *J* = 11.4, 7.5, 4.5 Hz, 1H), 1.28 – 1.16 (m, 2H), 0.88 (s, 9H), 0.03 (s, 6H).

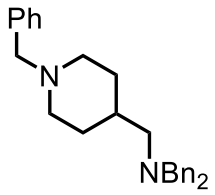

3.21i

***N*,*N*-Dibenzyl-1-(1-benzylpiperidin-4-yl)methanamine (3.21i)**

N,*N*-Dibenzyl-1-(1-benzylpiperidin-4-yl)methanamine was prepared following the General Procedure for the Alkylation of Amines using (1-benzylpiperidin-4-yl)methanamine (0.5 g, 2.5 mmol), benzyl bromide (2.0 equiv.) and K_2CO_3 (2 equiv.). The unpurified product was subjected to silica gel column chromatography (ethyl ether:hexanes = 1:4) to afford **3.21i** as a white solid (0.9 g, 92%).

^{1}H NMR (500 MHz, $CDCl_3$) δ 7.36 – 7.31 (m, 3H), 7.31 – 7.25 (m, 10H), 7.25 – 7.17 (m, 2H), 3.50 (s, 4H), 3.44 (s, 2H), 2.82 (d, *J* = 10.6 Hz, 2H), 2.23 (d, *J* = 7.3 Hz, 2H), 1.89 (td, *J* = 11.8, 2.5 Hz, 2H), 1.82 – 1.72 (m, 2H), 1.57 (s, 1H), 1.07 (qd, *J* = 12.2, 3.8 Hz, 2H).

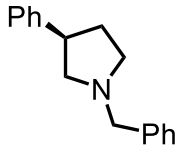

3.21j

(*R*)-1-Benzyl-3-phenylpyrrolidine (3.21j)

(*R*)-1-Benzyl-3-phenylpyrrolidine was prepared following the General Procedure for the Alkylation of Amines using (*R*)-3-phenylpyrrolidine hydrochloride (0.5 g, 2.7 mmol), benzyl bromide (1.1 equiv.) and K_2CO_3 (4 equiv.). The unpurified product was subjected to silica gel column chromatography (EtOAc:hexanes = 1:19) to afford **3.21j** as a colorless liquid (490 mg, 76%).

^{1}H NMR (500 MHz, $CDCl_3$) δ 7.36 (d, *J* = 7.4 Hz, 2H), 7.31 (t, *J* = 7.4 Hz, 2H), 7.29 – 7.22 (m, 5H), 7.21 – 7.15 (m, 1H), 3.68 (s, 2H), 3.36 (dt, *J* = 9.8, 7.5 Hz, 1H), 3.04 (t, *J* = 8.5 Hz, 1H), 2.84 (td, *J* = 8.5, 6.0 Hz, 1H), 2.69 (td, *J* = 8.9, 5.9 Hz, 1H), 2.50 (t, *J* = 8.5 Hz, 1H), 2.38 – 2.29 (m, 1H), 1.94 – 1.85 (m, 1H).

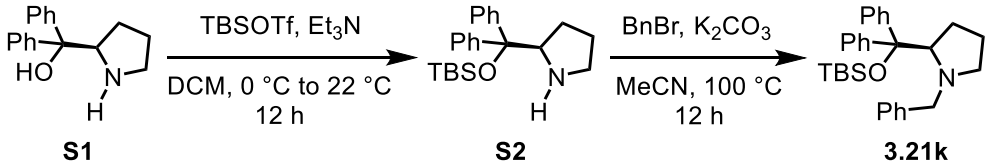

S1 **S2** **3.21k**

(*R*)-2-(((*tert*-Butyldimethylsilyl)oxy)diphenylmethyl)pyrrolidine (S2)

S2 was prepared through the TBS protection of (*R*)-diphenyl(pyrrolidin-2-yl)methanol (**S1**).

To a solution of **S7** (20 mmol) in DCM at 0 °C, Et_3N (1.3 equiv.) was added, followed by the dropwise addition of TBSOTf (1.3 equiv.). After the addition, the reaction mixture was allowed to warm to 22 °C and stirred for 12 hours. Upon completion (monitored by TLC), H_2O was added and the organic material was then extracted with DCM. The combined organic layers were dried

over $MgSO_4$, filtered, and concentrated *in vacuo*. The unpurified product mixture was subjected to flash silica gel column chromatography (ethyl ether:hexanes = 1:9) to afford **S2** as a colorless liquid (4.1 g, 56%). **^{1}H NMR (500 MHz, $CDCl_3$):** δ 7.52 (d, *J* = 7.6 Hz, 2H), 7.36 (d, *J* = 8.2 Hz, 2H), 7.32 – 7.17 (m, 6H), 4.01 (t, *J* = 7.3 Hz, 1H), 2.88 – 2.76 (m, 1H), 2.76 – 2.64 (m, 1H), 1.59 (q, *J* = 7.5 Hz, 2H), 1.55 – 1.46 (m, 1H), 1.30 – 1.12 (m, 1H), 0.95 (s, 9H), -0.21 (s, 3H), -0.46 (s, 3H).

(*R*)-1-Benzyl-2-(((*tert*-butyldimethylsilyl)oxy)diphenylmethyl)pyrrolidine (3.19o)

3.21k was prepared through the reaction of **S2** (1.5 g, 4.1 mmol), benzyl bromide (1.1 equiv.) and K_2CO_3 (4.0 equiv.) in MeCN. The reaction mixture in pressure vessel was placed in an oil bath at 100 °C and was allowed to stir for 12 hours. Upon completion (monitored by TLC), the solution was cooled to 22 °C. H_2O was then added and the organic material was extracted with EtOAc. The combined organic layers were dried over $MgSO_4$, filtered, and concentrated *in vacuo*. The unpurified product mixture was subjected to flash silica gel column chromatography (ethyl ether:hexanes = 1:19) to afford **3.21k** as a colorless liquid (1.45 g, 78%). **^{1}H NMR (500 MHz, $CDCl_3$):** δ 7.64 (dd, *J* = 7.6, 2.2 Hz, 2H), 7.55 (dd, *J* = 8.0, 1.8 Hz, 2H), 7.32 – 7.25 (m, 6H), 7.25 – 7.19 (m, 2H), 7.17 (d, *J* = 7.2 Hz, 1H), 7.11 (d, *J* = 7.4 Hz, 2H), 4.36 (d, *J* = 13.3 Hz, 1H), 4.00 (dd, *J* = 9.4, 4.1 Hz, 1H), 3.45 (d, *J* = 13.3 Hz, 1H), 2.30 (td, *J* = 6.5, 3.4 Hz, 1H), 2.12 (td, *J* = 9.2, 6.6 Hz, 1H), 1.99 (dd, *J* = 13.4, 8.9 Hz, 1H), 1.87 (dd, *J* = 8.6, 4.3 Hz, 1H), 1.39 – 1.26 (m, 1H), 0.90 (s, 9H), 0.64 – 0.54 (m, 1H), -0.39 (s, 3H), -0.43 (s, 3H).

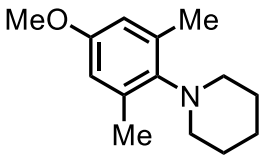

3.21l

1-(4-Methoxy-2,6-dimethylphenyl)piperidine (3.21l)

1-(4-Methoxy-2,6-dimethylphenyl)piperidine was prepared following the General Procedure for the Alkylation of Amines using 4-methoxy-2,6-dimethylaniline (1.0 g, 6.6 mmol), 1,5-dibromopentane (1.5 equiv.) and K_2CO_3 (3 equiv.). The unpurified product was subjected to silica gel column chromatography (Et_2O:hexanes = 1:49) to afford **3.21l** as a colorless liquid (1.2 g, 83%).

^{1}H NMR (500 MHz, $CDCl_3$) δ 6.52 (s, 2H), 3.74 (s, 3H), 2.98 (t, *J* = 5.1 Hz, 4H), 2.29 (s, 6H), 1.65 – 1.58 (m, 4H), 1.58 – 1.51 (m, 2H).

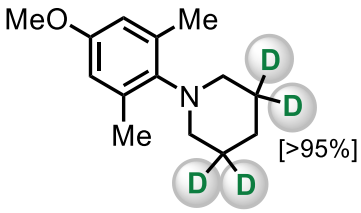

3.21l-*d*

1-(4-Methoxy-2,6-dimethylphenyl)piperidine-3,3,5,5-d_4 (3.21l-*d*)

3.21l-*d* was prepared following the previously reported literature,[12h] using 1-(4-Methoxy-2,6-dimethylphenyl)piperidine (877 mg, 4.0 mmol), acetone-d_6 (2.0 mL, 28 mmol) and $B(C_6F_5)_3$ (102 mg, 0.20 mmol). The crude reaction mixture was subjected to silica gel chromatography (ethyl ether:hexanes = 1:20) to give the product **3.21l-*d*** as a yellow liquid with 88% *d*-incorporation at the *β*-amino position. This compound was resubjected to the aforementioned reaction conditions

and after flash silica gel column chromatography (ethyl ether:hexanes = 1:20), **3.21l-*d*** was obtained with >95% *d*-incorporation level at the *β*-amino position. (0.63 g, 70%). **^{1}H NMR (500 MHz, $CDCl_3$):** δ 6.69 – 6.35 (m, 2H), 3.77 – 3.71 (m, 3H), 3.15 – 2.74 (m, 4H), 2.43 – 2.15 (m, 6H), 1.63 – 1.57 (m, 0.19H, >95%D), 1.56 – 1.47 (m, 2H).

Synthesis of 1,5-Dibromo-3,3-dimethylpentane (S5)

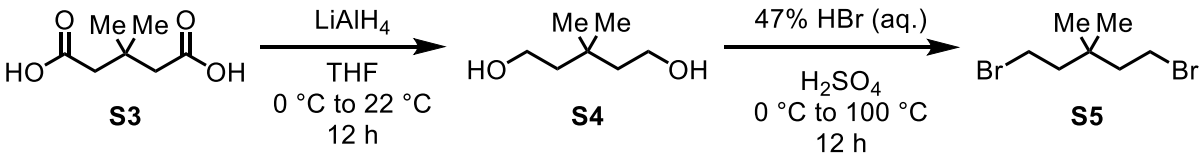

1,5-Dibromo-3,3-dimethylpentane (**S5**) was prepared following the literature previously reported.[26d]

3,3-Dimethylpentane-1,5-diol (S4)

To a solution of 3,3-dimethylpentanedioic acid **S3** (3.0 g, 18.7 mmol) in THF, $LiAlH_4$ was added portionwise at 0 °C. The reaction mixture was slowly warmed to 22 °C and was allowed to stir for 12 hours. Upon completion of the reaction (monitored by TLC), the mixture was quenched with 1.0 M NaOH (aq.) at 0 °C and extracted with EtOAc (3 x 50 mL). The organic layer was dried over $MgSO_4$, filtered, and concentrated *in vacuo*. The unpurified product was subjected to flash silica gel column chromatography (EtOAc:hexanes = 1:1) to give 3,3-dimethylpentane-1,5-diol **S4** as a colorless liquid (1.8 g, 73%). **^{1}H NMR (600 MHz, $CDCl_3$):** δ 3.74 (t, J = 7.1 Hz, 4H), 1.58 (t, J = 7.0 Hz, 4H), 0.95 (s, 6H).

1,5-Dibromo-3,3-dimethylpentane (S5)

To a solution of 3,3-dimethylpentane-1,5-diol **S4** (1.2 g, 9.4 mmol) in 47% HBr (aq.), H_2SO_4 was added dropwise at 0 °C. The reaction mixture was slowly heated to 100 °C and was allowed to stir

for 12 hours. Upon completion of the reaction (monitored by TLC), the mixture was quenched with $NaHCO_3$ (aq.) and extracted with ethyl ether (3 x 20 mL). The combined organic layers were washed with brine (30 mL), dried over $MgSO_4$, filtered and concentrated *in vacuo*. The unpurified product was then subjected to flash silica gel column chromatography (100% hexanes) to afford 1,5-dibromo-3,3-dimethylpentane **S5** as a colorless liquid (1.8 g, 75%). **^{1}H NMR (400 MHz, $CDCl_3$):** δ 3.41 – 3.33 (m, 4H), 1.90 – 1.82 (m, 4H), 0.94 (s, 6H).

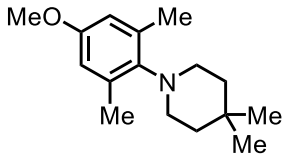

3.21m

1-(4-Methoxy-2,6-dimethylphenyl)-4,4-dimethylpiperidine (3.21m)

3.21m was prepared through the reaction of 4-methoxy-2,6-dimethylaniline (0.7 g, 4.7 mmol), 1,5-dibromo-3,3-dimethylpentane (1.5 equiv.) and K_2CO_3 (4.0 equiv.) in MeCN. The reaction mixture in pressure vessel was placed in an oil bath at 100 °C and was allowed to stir for 12 hours. Upon completion (monitored by TLC), the solution was cooled to 22 °C. H_2O was then added and the organic material was extracted with EtOAc. The combined organic layers were dried over $MgSO_4$, filtered, and concentrated *in vacuo*. The unpurified product mixture was subjected to flash silica gel column chromatography (ethyl ether:hexanes = 1:49) to afford **3.21m** as a colorless liquid (0.7 g, 61%). **^{1}H NMR (500 MHz, $CDCl_3$):** δ 6.53 (s, 2H), 3.74 (s, 3H), 3.01 – 2.94 (m, 4H), 2.30 (s, 6H), 1.47 – 1.39 (m, 4H), 0.98 (s, 6H).

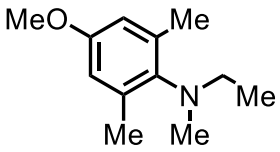

3.21s

***N*-Ethyl-4-methoxy-*N*,2,6-trimethylaniline (3.21s)**

N-Ethyl-4-methoxy-*N*,2,6-trimethylaniline was prepared following the General Procedure for the Alkylation of Amines using *N*-ethyl-4-methoxy-2,6-dimethylaniline[2] (0.5 g, 2.8 mmol), methyl iodide (1.5 equiv.) and K_2CO_3 (2.0 equiv.). The unpurified product was subjected to silica gel column chromatography (Et_2O:hexanes = 1:49) to afford **3.21s** as a colorless liquid (0.4 g, 63%). **^{1}H NMR** (400 MHz, $CDCl_3$) δ 6.54 (d, *J* = 0.5 Hz, 2H), 3.74 (s, 3H), 3.01 (q, *J* = 7.1 Hz, 2H), 2.73 (s, 3H), 2.25 (d, *J* = 0.5 Hz, 6H), 1.02 (t, *J* = 7.1 Hz, 3H).

Synthesis of 1-(4-Methoxyphenyl)pyrrolidine-2,2,3,3,4,4,5,5-*d*$_8$ (S8)

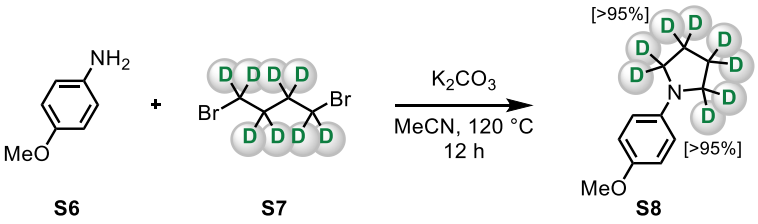

S6 **S7** **S8**

1,4-Dibromobutane-1,1,2,2,3,3,4,4-*d*$_8$ (**S7**) was prepared following the literature previously reported.[26b] **S8** was prepared through the reaction of 4-methoxyaniline (1.2 g, 10 mmol), **S7** (2.0 g, 0.9 mmol) and K_2CO_3 (4.1 g, 30 mmol) in MeCN. The reaction mixture in pressure vessel was placed in an oil bath at 120 °C and was allowed to stir for 12 hours. Upon completion (monitored by TLC), the solution cooled to 22 °C. H_2O was then added and the organic material was extracted with EtOAc. The combined organic layers were dried over $MgSO_4$, filtered, and concentrated *in vacuo*. The unpurified product mixture was subjected to flash silica gel column chromatography

(ethyl ether:hexanes = 1:20) to give the product **S8** as a white solid (1.1 g, 82%). **^{1}H NMR (400 MHz, $CDCl_3$):** δ 6.84 (d, J = 8.9 Hz, 2H), 6.53 (d, J = 9.0 Hz, 2H), 3.76 (s, 3H), 3.22 – 3.18 (m, 0.02H, >95%D), 1.96 – 1.91 (m, 0.03H, >95%D).

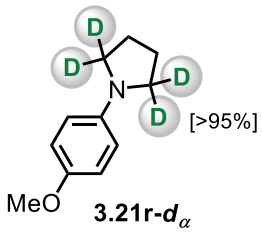

3.21r-d_α

1-(4-Methoxyphenyl)pyrrolidine-2,2,5,5-d_4 (3.21r-d_α)

3.21r-d_α was prepared following a method previously reported in the literature[12h] using **S8** (556 mg, 3.0 mmol), acetone (1.5 mL, 20.4 mmol) and $B(C_6F_5)_3$ (154 mg, 0.30 mmol). The crude reaction mixture was subjected to silica gel chromatography (ethyl ether:hexanes = 1:20) to give the product **3.21r-d_α** as a yellow liquid with >95% and 40% *d*-incorporation at the α- and β-amino position, respectively. This compound was resubjected to the aforementioned reaction conditions and after flash silica gel column chromatography (ethyl ether:hexanes = 1:20), **3.21r-d_α** was obtained with >95% and <5% *d*-incorporation level at the α- and β-amino position. (501 mg, 80%). **^{1}H NMR (600 MHz, $CDCl_3$):** δ 6.90 – 6.78 (m, 2H), 6.60 – 6.46 (m, 2H), 3.76 (s, 3H), 3.23 – 3.19 (m, 0.02H, >95%D), 2.05 – 1.88 (m, 4H).

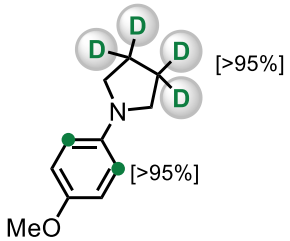

3.21r-*d*$_\beta$

1-(4-Methoxyphenyl-2,6-*d*$_2$)pyrrolidine-3,3,4,4-*d*$_4$ (3.21r-*d*$_\beta$)

3.21r-*d*$_\beta$ was prepared following a method previously reported in the literature[12h] using 1-(4-methoxyphenyl)pyrrolidine (886 mg, 5.0 mmol), acetone-d_6 (2.5 mL, 35 mmol) and $B(C_6F_5)_3$ (128 mg, 0.25 mmol). The crude reaction mixture was subjected to silica gel chromatography (ethyl ether:hexanes = 1:20) to give the product **3.21r-*d*$_\beta$** as a yellow liquid with 70% *d*-incorporation at the *β*-amino position. This compound was resubjected to the aforementioned reaction conditions and after flash silica gel column chromatography (ethyl ether:hexanes = 1:20), **3.21r-*d*$_\beta$** was obtained with >95% *d*-incorporation level at the *β*-amino position. (686 mg, 74%). **^{1}H NMR (400 MHz, $CDCl_3$):** δ 6.84 (s, 2H), 6.56 – 6.51 (m, 0.02H, >95%D), 3.76 (s, 3H), 3.33 – 3.12 (m, 4H), 1.98 – 1.93 (m, 0.15H, >95%D).

Preparation of α,β-Unsaturated Compounds (Table S3.7)

Table S3.7. List of α,β-Unsaturated Compounds

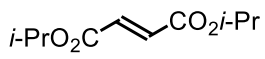	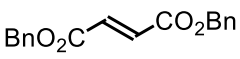	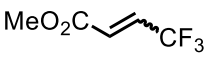
3.22a	**3.22b**	**3.22c**
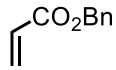	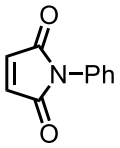	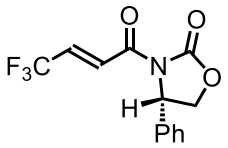
3.22d	**3.22e**	**3.25a**
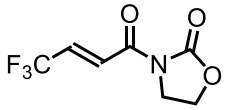	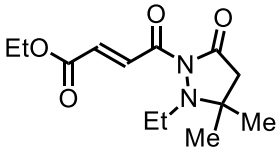	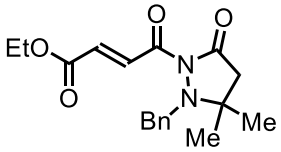
3.25b	**3.25c**	**3.25d**
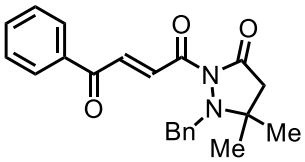	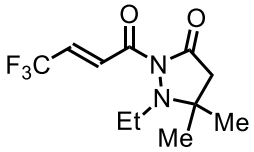	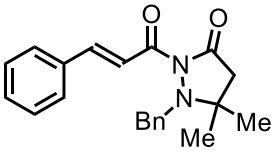
3.25e	**3.25f**	**3.25g**
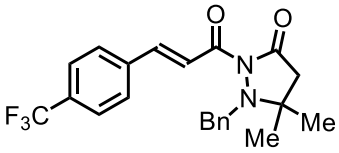	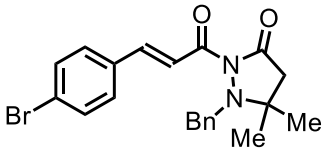	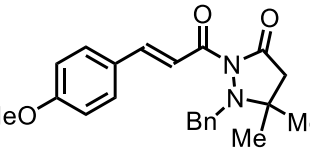
3.25h	**3.25i**	**3.25j**

α,β-Unsaturated compounds **3.22a**,[4] **3.22b**,[2] and **3.25a–3.25j**[26d-26f] were prepared according to the procedures previously reported in the literatures. Substrates **3.22c–3.22e** were obtained from commercial sources and used without further purification.

Preparation of Diisopropyl Fumarate (3.22a)

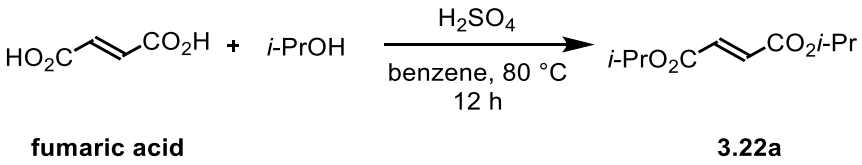

Diisopropyl fumarate was prepared according to a procedure reported previously in the literature. A mixture of fumaric acid (23.2 g, 200 mmol), isopropyl alcohol (4.0 equiv.), H_2SO_4 (2.0 mL) and benzene (25.0 mL) was heated at 80 °C and was allowed to stir for 12 hours. The reaction mixture was quenched with $NaHCO_3$ (aq.) at 0 °C and extracted with ethyl ether (3 x 25 mL). The combined organic layers were washed with brine, dried over $MgSO_4$ and concentrated *in vacuo*. The unpurified product mixture was distilled (75 °C, 40 mmHg) to give diisopropyl fumarate **3.22a** as a colorless liquid (24.0 g, 60%). **^{1}H NMR (500 MHz, $CDCl_3$):** δ 6.81 (s, 2H), 5.11 (hept, J = 6.2 Hz, 2H), 1.29 (d, J = 6.3 Hz, 12H).

Preparation of Dibenzyl Fumarate (3.22b)

Dibenzyl fumarate was prepared according to a procedure reported previously in the literature.[26d] To a solution of fumaric acid (6.0 g, 51.7 mmol) in DMF (6 mL), Et_3N (2.0 equiv) and (bromomethyl)benzene (1.9 equiv.) were added dropwise. The reaction mixture was allowed to stir at 100 °C for 12 hours. Upon completion, the reaction mixture was poured into cold water and then filtered to give a brown solid. The unpurified product was then subjected to silica gel column chromatography (EtOAc:hexanes = 3:17) and was further purified by recrystallization (EtOAc:hexanes = 1:20) to give dibenzyl fumarate **3.22b** as a white solid (8.2 g, 56%). **^{1}H NMR (600 MHz, $CDCl_3$):** δ 7.41 – 7.30 (m, 10H), 6.92 (s, 2H), 5.23 (s, 4H).

General Procedure A for Preparation of 2-Acryloylpyrazolidinone Derivatives

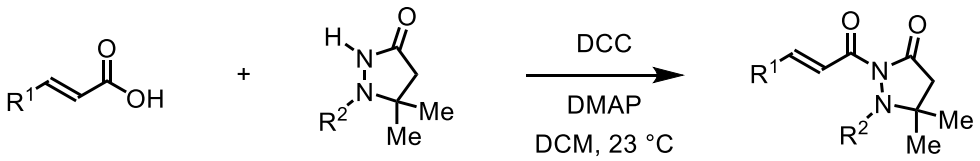

Corresponding carboxylic acid (1.0 eq.), pyrazolidinone[26e] (1.0 eq.) and 4-dimethylaminopyridine (0.1 eq) were dissolved in DCM at 22 °C. After *N*,*N*'-dicyclohexylcarbodiimide (1.1 eq) was added to the solution, it was allowed to stir overnight to afford the corresponding α,β-unsaturated compound. Upon completion, reaction mixture was filtered through Celite using DCM as solvent. The unpurified product mixture was subjected to flash silica gel column chromatography.

General Procedure B for Preparation of 2-Acryloylpyrazolidinone Derivatives

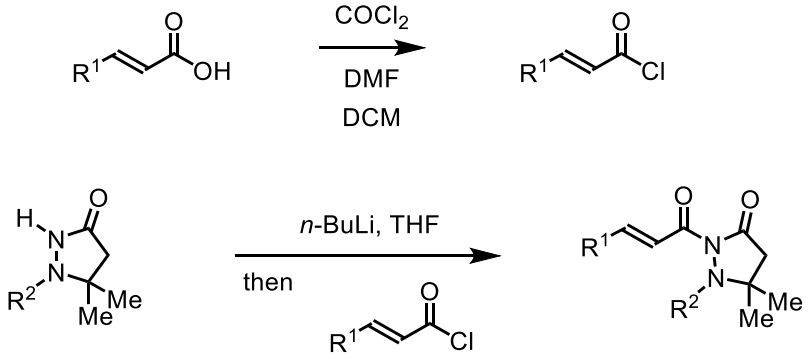

n-BuLi (1.1 eq.) was added to the appropriate pyrazolidinone in dry THF at –78 °C, and the mixture (**Mixture A**) was allowed to stir at –78 °C. Oxalyl chloride (3.0 eq.) was added dropwise into corresponding carboxylic acid (1.0 eq.) in DCM solution at 0 °C. 2 drops of DMF was added, and the mixture was allowed to stir for 1 hour. The solvent was removed under reduced pressure, and the residue was added into **Mixture A**. The mixture was stirred at –78 °C for 2-3 hours until the reaction was complete. The reaction was quenched with saturated aqueous ammonium chloride and THF was removed under reduced pressure. The residue was dissolved in DCM and washed

with sat. $NaHCO_3$ (aq.). The organic layer was washed with brine, dried over $MgSO_4$, filtered, and concentrated under reduced pressure. The unpurified product mixture was subjected to flash silica gel column chromatography.

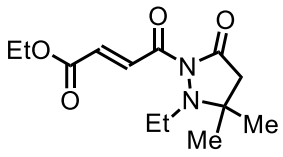

3.25c

Ethyl (*E*)-4-(2-ethyl-3,3-dimethyl-5-oxopyrazolidin-1-yl)-4-oxobut-2-enoate (3.25c)

3.25c was prepared following **General Procedure B for Preparation of 2-Acryloylpyrazolidinone Derivatives** using (*E*)-4-ethoxy-4-oxobut-2-enoic acid (3.60 g, 25.0 mmol), 1-ethyl-5,5-dimethylpyrazolidin-3-one (3.60 g, 25.0 mmol), oxalyl chloride (9.52 g, 75 mmol) and *n*-BuLi (27.5 mmol). The unpurified product was subjected to flash silica gel column chromatography (EtOAc:hexanes = 1:3) to afford **3.25c** as a yellow liquid (4.5 g, 67%). **^{1}H NMR (500 MHz, $CDCl_3$):** δ 7.93 (d, *J* = 15.6 Hz, 1H), 6.96 (d, *J* = 15.6 Hz, 1H), 4.27 (q, *J* = 7.1 Hz, 2H), 3.01 (q, *J* = 7.1 Hz, 2H), 2.60 (s, 2H), 1.35 – 1.31 (m, 9H), 1.08 (t, *J* = 7.2 Hz, 3H).

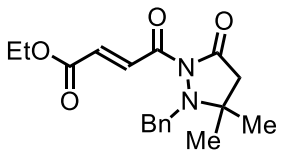

3.25d

Ethyl (*E*)-4-(2-benzyl-3,3-dimethyl-5-oxopyrazolidin-1-yl)-4-oxobut-2-enoate (3.25d)

3.25d was prepared following **General Procedure B for Preparation of 2-Acryloylpyrazolidinone Derivatives** using (*E*)-4-ethoxy-4-oxobut-2-enoic acid (5.04 g, 35.0 mmol), 1-benzyl-5,5-dimethylpyrazolidin-3-one (6.79 g, 35.0 mmol), oxalyl chloride (13.33 g,

105 mmol) and *n*-BuLi (38.5 mmol). The unpurified product was subjected to flash silica gel column chromatography (EtOAc:hexanes = 1:3) to afford **3.25d** as a yellow solid (5.0 g, 53%). **^{1}H NMR (400 MHz, $CDCl_3$):** δ 7.44 (d, *J* = 15.5 Hz, 1H), 7.29 (d, *J* = 5.0 Hz, 2H), 7.26 – 7.22 (m, 3H), 6.49 (d, *J* = 15.5 Hz, 1H), 4.21 (q, *J* = 7.1 Hz, 2H), 4.00 (s, 2H), 2.61 (s, 2H), 1.34 (s, 6H), 1.30 (t, *J* = 7.1 Hz, 3H).

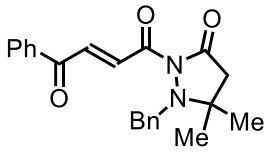

3.25e

(*E*)-1-(2-Benzyl-3,3-dimethyl-5-oxopyrazolidin-1-yl)-4-phenylbut-2-ene-1,4-dione (3.25e)

3.25e was prepared following **General Procedure A for Preparation of 2-Acryloylpyrazolidinone Derivatives** using (*E*)-4-oxo-4-phenylbut-2-enoic acid (2.64 g, 15.0 mmol), 1-benzyl-5,5-dimethylpyrazolidin-3-one (3.06 g, 15.0 mmol), *N,N′*-dicyclohexylcarbodiimide (3.30g, 16.5 mmol) and dimethylaminopyridine (0.18 g, 1.5 mmol). The unpurified product was subjected to flash silica gel column chromatography (Et_3N:EtOAc:hexanes = 1:30:90) to afford **3.25e** as a yellow solid (1.5 g, 26%). **^{1}H NMR (400 MHz, $CDCl_3$):** δ 7.92 (d, *J* = 7.8 Hz, 2H), 7.60 (t, *J* = 7.4 Hz, 1H), 7.49 (t, *J* = 7.6 Hz, 3H), 7.30 (d, *J* = 7.6 Hz, 2H), 7.25 (s, 1H), 7.19 (t, *J* = 7.5 Hz, 2H), 7.11 (t, *J* = 7.3 Hz, 1H), 4.01 (s, 2H), 2.64 (s, 2H), 1.37 (s, 6H).

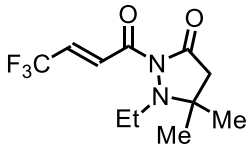

3.25f

(*E*)-1-Ethyl-5,5-dimethyl-2-(4,4,4-trifluorobut-2-enoyl)pyrazolidin-3-one (3.25f)

3.25f was prepared following **General Procedure A for Preparation of 2-Acryloylpyrazolidinone Derivatives** using (*E*)-4,4,4-trifluorobut-2-enoic acid (2.52 g, 18.0 mmol), 1-ethyl-5,5-dimethylpyrazolidin-3-one (2.66 g, 18.0 mmol), *N,N′*-dicyclohexylcarbodiimide (4.10 g, 20 mmol) and dimethylaminopyridine (0.24 g, 2.0 mmol). The unpurified product was subjected to flash silica gel column chromatography (EtOAc:hexanes = 1:3) to afford **3.25f** as a yellow liquid (3.1 g, 65%). **^{1}H NMR (400 MHz, $CDCl_3$):** δ 7.67 (d, *J* = 15.6 Hz, 1H), 6.88 (dq, *J* = 13.8, 6.7 Hz, 1H), 3.01 (q, *J* = 7.1 Hz, 2H), 2.60 (s, 2H), 1.33 (s, 6H), 1.07 (t, *J* = 7.1 Hz, 3H); **^{19}F NMR (376 MHz, $CDCl_3$):** δ -65.20 (d, *J* = 6.8 Hz).

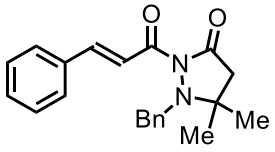

3.25g

1-Benzyl-2-cinnamoyl-5,5-dimethylpyrazolidin-3-one (3.25g)

3.25g was prepared following **General Procedure A for Preparation of 2-Acryloylpyrazolidinone Derivatives** using cinnamic acid (2.67 g, 15.0 mmol), 1-benzyl-5,5-dimethylpyrazolidin-3-one (3.05 g, 15.0 mmol), *N,N′*-dicyclohexylcarbodiimide (3.30 g, 16.5 mmol) and dimethylaminopyridine (0.18 g, 1.5 mmol). The unpurified product was subjected to flash silica gel column chromatography (EtOAc:hexanes = 1:3) to afford **3.25g** as a yellow solid (3.0 g, 60%). **^{1}H NMR (500 MHz, $CDCl_3$):** δ 7.65 (d, *J* = 15.7 Hz, 1H), 7.52 (dd, *J* = 6.6, 2.9 Hz,

2H), 7.47 – 7.35 (m, 5H), 7.29 – 7.24 (m, 3H), 7.23 – 7.18 (m, 1H), 4.12 (s, 2H), 2.61 (s, 2H), 1.34 (s, 6H).

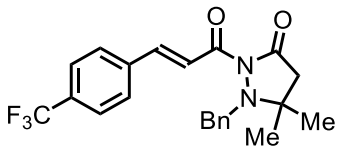

3.25h

(*E*)-1-Benzyl-5,5-dimethyl-2-(3-(4-(trifluoromethyl)phenyl)acryloyl)pyrazolidin-3-one (3.25h)

3.25h was prepared following **General Procedure A for Preparation of 2-Acryloylpyrazolidinone Derivatives** using (*E)*-3-(4-(trifluoromethyl)phenyl)acrylic acid (3.24 g, 15.0 mmol), 1-benzyl-5,5-dimethylpyrazolidin-3-one (3.05 g, 15.0 mmol), *N,N′*-dicyclohexylcarbodiimide (3.30 g, 16.5 mmol) and dimethylaminopyridine (0.18 g, 1.5 mmol). The unpurified product was subjected to flash silica gel column chromatography (EtOAc:hexanes = 1:3) to afford **3.25h** as a yellow solid (2.7 g, 45%). **^{1}H NMR (500 MHz, CDCl$_3$):** δ 7.66 – 7.54 (m, 5H), 7.50 – 7.42 (m, 1H), 7.40 (m, 2H), 7.28 – 7.23 (m, 2H), 7.20 (t, *J* = 7.3 Hz, 1H), 4.11 (s, 2H), 2.63 (s, 2H), 1.36 (s, 6H); **^{19}F NMR (470 MHz, CDCl$_3$):** δ -62.84.

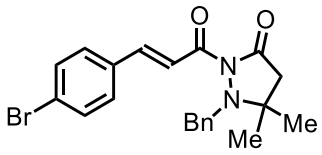

3.25i

(*E*)-1-Benzyl-2-(3-(4-bromophenyl)acryloyl)-5,5-dimethylpyrazolidin-3-one (3.25i)

3.25i was prepared following **General Procedure A for Preparation of 2-Acryloylpyrazolidinone Derivatives** using (*E*)-3-(4-bromophenyl)acrylic acid (3.39 g, 15.0

mmol), 1-benzyl-5,5-dimethylpyrazolidin-3-one (3.05 g, 15.0 mmol), *N,N′*-dicyclohexylcarbodiimide (3.30 g, 16.5 mmol) and dimethylaminopyridine (0.18 g, 1.5 mmol). The unpurified product was subjected to flash silica gel column chromatography (EtOAc:hexanes = 1:3) to afford **3.25i** as a yellow solid (1.8 g, 29%). **^{1}H NMR (500 MHz, CDCl$_3$):** δ 7.57 – 7.46 (m, 3H), 7.42 – 7.35 (m, 5H), 7.26 – 7.16 (m, 3H), 4.11 (s, 2H), 2.61 (s, 2H), 1.35 (s, 6H).

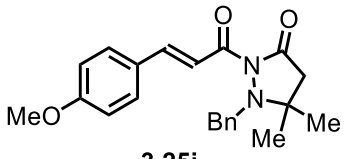

3.25j

(*E*)-1-Benzyl-2-(3-(4-methoxyphenyl)acryloyl)-5,5-dimethylpyrazolidin-3-one (3.25j)

3.25j was prepared following **General Procedure A for Preparation of 2-Acryloylpyrazolidinone Derivatives** using (*E*)-3-(4-methoxyphenyl)acrylic acid (2.67 g, 15.0 mmol), 1-benzyl-5,5-dimethylpyrazolidin-3-one (3.05 g, 15.0 mmol), *N,N′*-dicyclohexylcarbodiimide (3.30 g, 16.5 mmol) and dimethylaminopyridine (0.18 g, 1.5 mmol). The unpurified product was subjected to flash silica gel column chromatography (EtOAc:hexanes = 1:3) to afford **3.25j** as a yellow solid (2.1 g, 38%). **^{1}H NMR (500 MHz, CDCl$_3$):** δ 7.63 (d, *J* = 15.7 Hz, 1H), 7.50 – 7.46 (m, 2H), 7.43 – 7.39 (m, 2H), 7.35 (d, *J* = 15.7 Hz, 1H), 7.28 – 7.24 (m, 2H), 7.22 – 7.17 (m, 1H), 6.91 – 6.87 (m, 2H), 4.12 (s, 2H), 3.84 (s, 3H), 2.58 (s, 2H), 1.32 (s, 6H).

C2. Optimization Studies

Evaluation of Reaction Conditions for $(F_5C_6)_3B$-Catalyzed *β*-Alkylation involving *N*-Alkylamines

Experimental Procedure for the Evaluation of Solvents (Table S3.8)

To a 15 mL oven-dried pressure vessel was added *N*,*N*-dibenzylethanamine **3.21a** (0.20 mmol), $B(C_6F_5)_3$ (10 mol%), diisopropyl fumarate **3.22a** (0.30 mmol), and solvent (0.20 mL) under a nitrogen atmosphere. The reaction mixture was placed in an oil bath at 50 °C and was allowed to stir for 3 hours. After the solution was cooled to 22 °C, it was concentrated *in vacuo*. The product yield was determined by the ^{1}H NMR analysis of the unpurified product mixtures using *m*-xylene as the internal standard.

Table S3.8. Evaluation of Solvents involving Amine **3.21a**

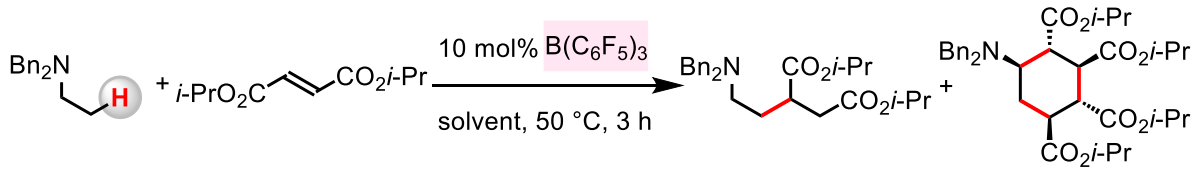

3.21a, 0.20 mmol **3.22a**, 0.30 mmol **3.23a** **3.24**

entry	solvent	yield (%) **3.23a**	**3.24**
1	*n*-hexane	75	22
2	toluene	71	21
3	DCM	70	27
4	TBME	60	27
5	Et_2O	52	36
6	THF	<5	<5

Conditions: *N*,*N*-dibenzylethanamine (**3.21a**, 0.20 mmol), diisopropyl fumarate (**3.22a**, 0.30 mmol), $B(C_6F_5)_3$ (10 mol%), solvent (0.20 mL), under N_2, 50 °C. The yield was determined by ^{1}H NMR analysis of unpurified reaction mixtures with *m*-xylene as the internal standard.

Effect of Concentration of Solution to Chemoselectivity of $(F_5C_6)_3B$-Catalyzed *β*-Alkylation involving Cyclic *N*-Alkylamines

For piperidine substrates (e.g., *N*-arylpiperidine **3.21l**, Table S3.9) that react with **3.22a** to give a mixture of products in the forms of *N*-alkylamines (e.g., **3.23o**) and enamines (e.g., **3.32**), we carried out a series of optimization studies that were aimed to selectively **3.23o** (Table S3.4). Specifically, to a 15 mL oven-dried pressure vessel were added amine **3.21l** (0.20 mmol), $B(C_6F_5)_3$ (10 mol%), diisopropyl fumarate **3.22a** (0.30 mmol), and benzene (0.20 mL or 0.80 mL) under a nitrogen atmosphere. The reaction mixture was placed in an oil bath at 50 °C and was allowed to stir for 12 hours. Upon completion, the solution was cooled down to room temperature and was concentrated *in vacuo*. The yield values for **3.23o** and **3.32** were determined by the ^{1}H NMR analysis of the unpurified product mixtures using *m*-xylene as the internal standard.

As shown in Table S**3.**4, it was found that, when the reaction was run in more dilute conditions (0.80 mL, 0.25 M in benzene) than the standard reaction conditions (0.20 mL, 1.0 M in benzene), the *N*-alkylamine product **3.23o** can be obtained more preferably over enamine **3.32**.

Furthermore, when the enamine product (e.g., **3.32**) is generated, the formation of diisopropyl succinate (**3.33**) was observed. This is likely due to the hydrogenation of **3.22a** by *in situ* generated borohydride and ammonium ion to regenerate the Lewis acid and Brønsted base catalysts. We hypothesized that if a larger quantity of **3.22a** is present in the reaction mixture to serve as a sacrificial H^+/H^- acceptor, the formation of enamine product would be favored.

To a 15 mL oven-dried pressure vessel was added 1-(4-methoxy-2,6-dimethylphenyl)-4,4-dimethylpiperidine **3.21m** (0.2 mmol), $B(C_6F_5)_3$ (10 mol%), diisopropyl fumarate **3.22a** (0.3 mmol, 1.5 equiv.) and DCM (0.1 mL) under a nitrogen atmosphere (Scheme S3.1). The reaction

Table S3.9. Evaluation of Solvent Concentration involving Amine **3.23o**

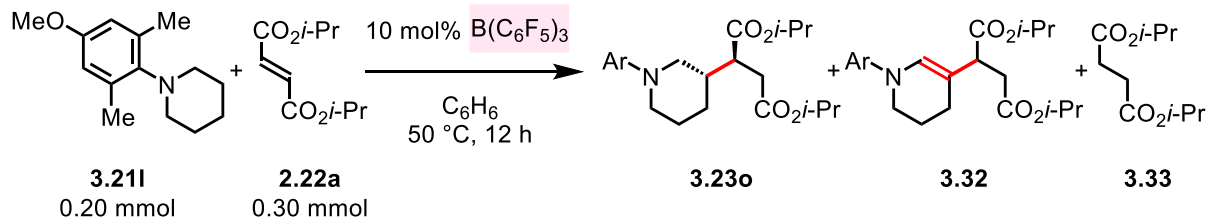

entry	solvent (mL)	yield		
		3.23o (%)	**3.32** (%)	**3.33** (mmol)
1	C_6H_6 (0.20 mL)	58	29	0.07
2	C_6H_6 (0.80 mL)	89	<5	0.02

Conditions: 1-(4-methoxy-2,6-dimethylphenyl)piperidine (**3.21l**, 0.20 mmol), diisopropyl fumarate (**2.22a**, 0.30 mmol), $B(C_6F_5)_3$ (10 mol%), solvent, under N_2, 50 °C. The yield was determined by ^1H NMR analysis of unpurified reaction mixtures with *m*-xylene as the internal standard.

Scheme S3.1. Evaluation of Reaction Conditions involving Amine **3.21m**

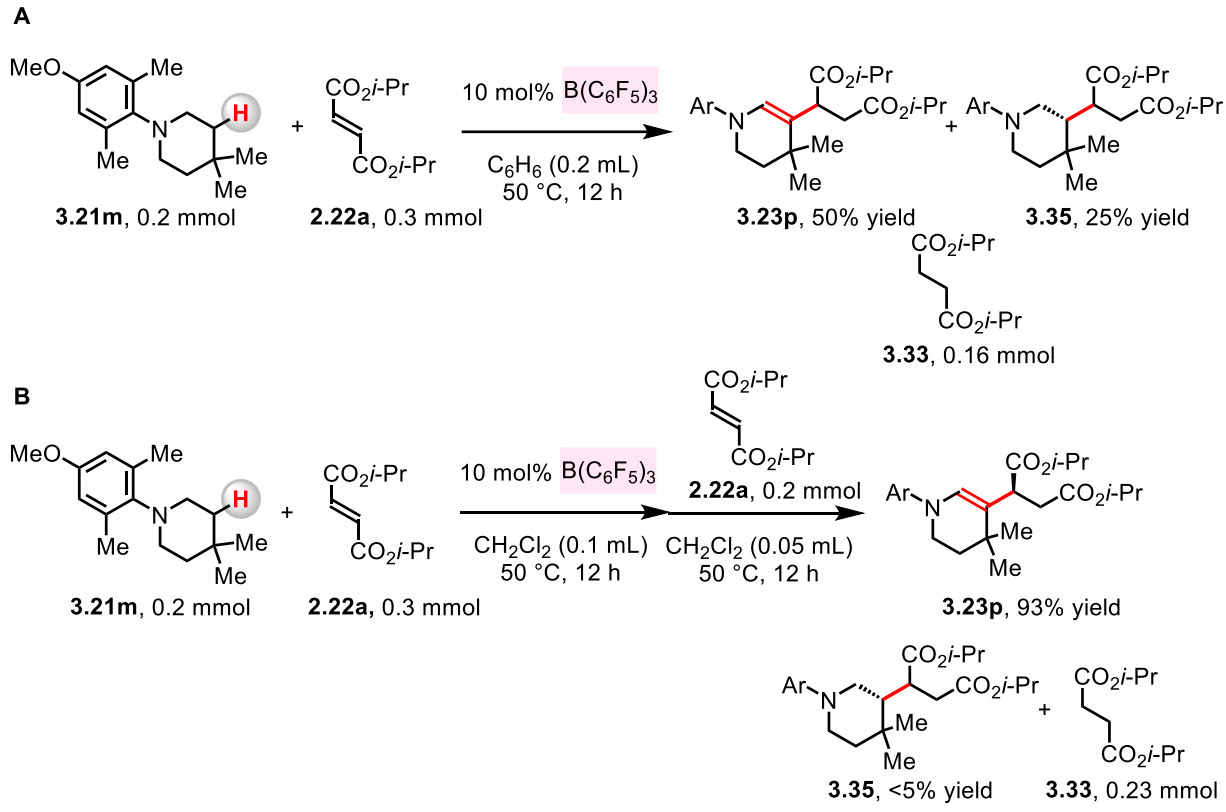

mixture was placed in an oil bath at 50 °C and was allowed to stir for 12 hours. After the solution was cooled to 22 °C, diisopropyl fumarate **2.22a** (0.2 mmol, 1.0 equiv.) and DCM (0.05 mL) were added under a nitrogen atmosphere. Then the reaction mixture was placed again in an oil bath at 50 °C and was allowed to stir for 12 hours. Upon completion, the solution was cooled to 22 °C and was concentrated *in vacuo*. The product yield was determined by the ^{1}H NMR analysis of the unpurified product mixtures using *m*-xylene as the internal standard. It was found that adding 2.5 equiv. of **2.22a** in a batchwise manner improves the product yield as well as the chemoselectivity of the reaction to yield enamine product **3.23p** (Scheme S3.1B).

Optimization Studies for Diastereoselective *β*-Alkylation

Experimental Procedure for the Optimization of Diastereoselective Reaction (Scheme 3.16)

To a 15 mL oven-dried pressure vessel were added (*R*)-1-benzyl-2-(((*tert*-butyldimethylsilyl)oxy)diphenylmethyl)pyrrolidine **3.21k** (0.10 mmol), **3.25** (0.15 mmol), $B(C_6F_5)_3$ (10 mol%), Lewis acid co-catalyst (10 mol%), HBPin (0 mol% or 70 mol%), and benzene (0.60 mL) under a nitrogen atmosphere. The reaction mixture was placed in an oil bath at 60 °C and was allowed to stir for 24 or 36 hours. Upon completion, the solution was cooled to 22 °C and concentrated *in vacuo*. The product yield and dr were determined by the ^{1}H NMR and ^{19}F NMR analyses of the unpurified product mixtures using mesitylene (for ^{1}H NMR analysis) and perfluorobenzene (for ^{19}F NMR analysis) as the internal standard.

Table S3.10. Optimization of Diastereoselective Reaction

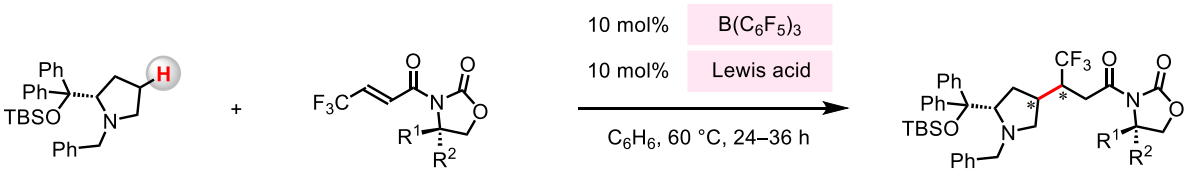

3.21k, 0.10 mmol **3.25**, 0.15 mmol **3.26**

entry	Lewis acid	R^1	R^2	time (h)	yield (%) and dr	
1	none	H	Ph	24	26	7.0:1
2	$Mg(OTf)_2$	H	Ph	24	17	2.4:1
3	$Sc(OTf)_3$	H	Ph	24	30	1.0:1
4	$Zn(OTf)_2$	H	Ph	24	56	6.0:1
5	ZnI_2	H	Ph	24	64	8.0:1
6[b]	ZnI_2	H	Ph	24	39	>20:1
7[b]	ZnI_2	H	Ph	36	65	>20:1
8[b,c]	ZnI_2	H	Ph	36	82	>20:1
9[b]	ZnI_2	H	H	36	25	7.0:1
10[b]	ZnI_2	Ph	H	36	45	>20:1
11[b]	ZnI_2	H	Bn	36	24	7.0:1
12[b]	ZnI_2	H	*i*-Pr	36	35	6.0:1

[a]Conditions: (*S*)-1-benzyl-2-(((*tert*-butyldimethylsilyl)oxy)diphenylmethyl)pyrrolidine (**3.21k**, 0.1 mmol), electrophile (**3.25**, 0.15 mmol), $B(C_6F_5)_3$ (10 mol%), Lewis acid (10 mol%), C_6H_6 (0.6 mL), under N_2, 60 °C.[b] 70 mol% HBPin was added to the reaction mixture. [c]The reaction was performed at 70°C

Studies for Enantioselective *β*-Alkylation with a Chiral Boron Lewis Acid Catalyst

Based on the hypothesis that $B(C_6F_5)_3$ is responsible for the activation of both the *N*-alkylamine and *α*,*β*-unsaturated compounds, we envisioned the use of chiral boron Lewis acid catalyst to achieve the enantioselective *β*-alkylation reaction.

N,*N*-dibenzylpropan-1-amine (**3.21b**) and benzyl acrylate (**3.22d**) were used as model substrates which afforded *β*-alkylated product **3.23w** in 75% yield (Scheme S3.2). We first examined the ability of a chiral borane catalyst to promote the C–C bond forming reaction in an enantioselective manner. No desired product was observed using less Lewis acidic Du's catalyst (Scheme S3.3A).[22] When Du's catalyst was used in combination with $B(C_6F_5)_3$, the product was obtained in 70% yield and 50:50 er (Scheme S3.3B).

Scheme S3.2. *β*-Amino C–H Alkylation Involving **3.21b** and **3.22d**

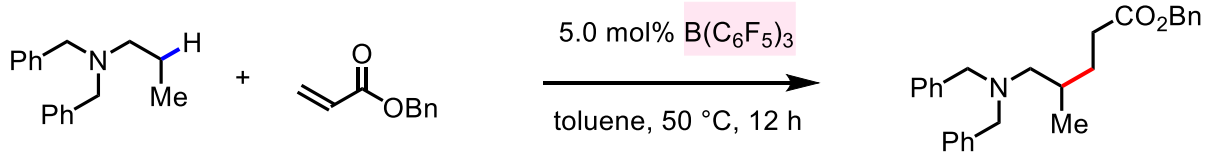

3.21b, 0.10 mmol **3.22d**, 0.15 mmol **3.23w**, 75% yield

```
Acq. Operator   : SYSTEM                          Seq. Line :   3
Acq. Instrument : Wasa_LC1                         Location :   71
Injection Date  : 1/21/2019 2:29:06 PM                 Inj :   1
                                                  Inj Volume : 4.000 µl
Method          : C:\Chem32\1\Data\JOE 2019-01-21 12-26-09\column3 1.5% IPA 98.5% hex 60min-0
                  .3ml.M (Sequence Method)
Last changed    : 1/21/2019 12:26:09 PM by SYSTEM
Additional Info : Peak(s) manually integrated
```

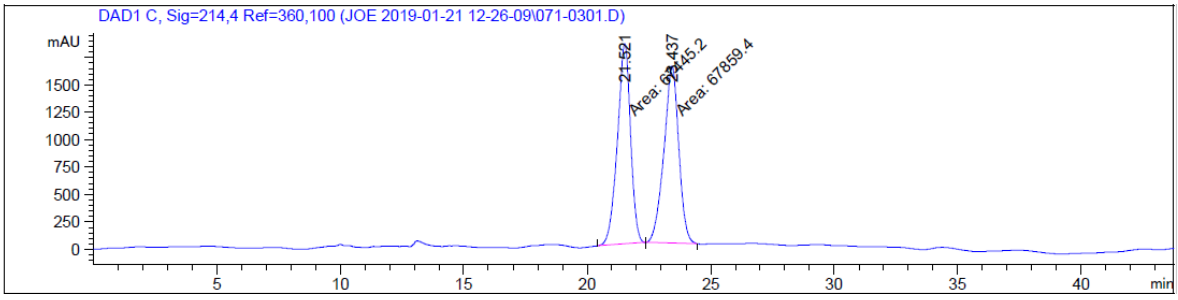

Signal 3: DAD1 C, Sig=214,4 Ref=360,100

Peak #	RetTime [min]	Type	Width [min]	Area [mAU*s]	Height [mAU]	Area %
1	21.521	MM	0.6158	6.74452e4	1825.35071	49.8470
2	23.437	MM	0.6991	6.78594e4	1617.80933	50.1530

Scheme S3.3. Evaluation of Du's Catalyst

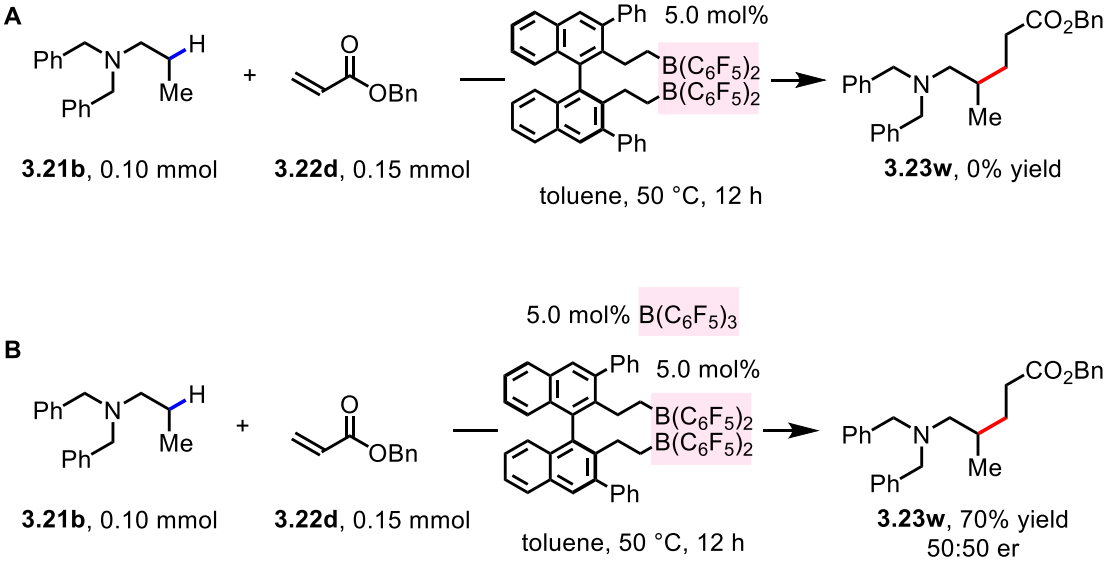

Experimental Procedure for the Evaluation of Du's Catalyst

An oven-dried sealed tube equipped with a magnetic stir bar was used. To this tube were added (*S*)-3,3'-diphenyl-2,2'-divinyl-1,1'-binaphthalene (0.005 mmol), $HB(C_6F_5)_2$ (0.01 mmol), and toluene (0.2 mL) under nitrogen atmosphere.[22] This reaction mixture was allowed to stir for 20 minutes at 22 °C to generate the chiral organoborane catalyst. To this mixture were added **3.21b** (0.10 mmol), **3.22d** (0.15 mmol), $B(C_6F_5)_3$ (0.005 mmol), and toluene (0.2 mL). The reaction mixture was placed in an oil bath at 50 °C and was allowed to stir for 12 hours. Upon completion, the reaction mixture was concentrated *in vacuo*. The product yield was determined by the ^{1}H NMR

analysis of the unpurified product mixtures using mesitylene as the internal standard. The product was isolated and purified using preparatory TLC. The er was determined by HPLC analysis of the isolated and purified product. **HPLC** (Chiralcel OD-H; 1.5%/ 98.5% isopropanol/ hexanes, 0.3 mL/min; tr = 22.0 min, 24.0 min; 50:50 er).

```
Acq. Operator   : SYSTEM                          Seq. Line :   1
Acq. Instrument : Wasa_LC1                         Location :   75
Injection Date  : 1/24/2019 12:10:00 PM                 Inj :   1
                                                 Inj Volume : 4.000 µl
Method          : C:\Chem32\1\Data\JOE 2019-01-24 12-08-54\column3 1.5% IPA 98.5% hex 40min-0
                  .3ml.M (Sequence Method)
Last changed    : 1/24/2019 12:08:54 PM by SYSTEM
```

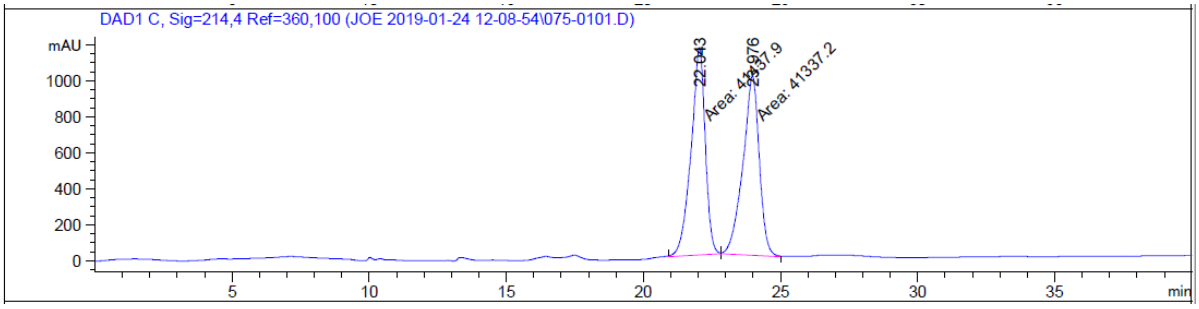


```
Signal 3: DAD1 C, Sig=214,4 Ref=360,100

Peak RetTime Type  Width     Area      Height     Area
  #   [min]        [min]   [mAU*s]     [mAU]       %
----|-------|----|-------|----------|----------|--------|
   1  22.043 MM    0.6005 4.14379e4  1150.06067  50.0608
   2  23.976 MM    0.6922 4.13372e4   995.28009  49.9392
```

Optimization Studies for Enantioselective β-Alkylation with Chiral Mg-based complex

Experimental Procedure for the Optimization of Ligand (Table S3.11)

To a 15 mL oven-dried pressure vessel was added $Mg(ClO_4)_2$ (0.01 mmol, 10 mol%), ligand (0.01 mmol, 10 mol%), benzene (0.3 mL) under nitrogen atmosphere. The mixture was allowed to stir for 20 minutes at 22 °C. Subsequently, 1-(4-methoxy-2,6-dimethylphenyl)pyrrolidine **3.21q** (0.1 mmol), (*E*)-3-(4,4,4-trifluorobut-2-enoyl)oxazolidin-2-one **3.25b** (0.15 mmol), and benzene (0.3 mL) were added to the vial under nitrogen atmosphere, and the resulting mixture was allowed to stir at 22 °C for 12 h. Upon completion, the reaction mixture was concentrated *in vacuo*. The product yield and dr were determined by the ^{1}H NMR and ^{19}F NMR analyses of the unpurified product mixtures using mesitylene (for ^{1}H NMR analysis) and perfluorobenzene (for ^{19}F NMR analysis) as the internal standard. The product was purified by preparative TLC (hexanes:EtOAc = 3:1). The er values of product **3.26b** was determined by HPLC analysis of the isolated and purified product.

Table S3.11. Optimization of Enantioselective Reaction

3.21q, 0.10 mmol + **3.25b**, 0.15 mmol → **3.26b**

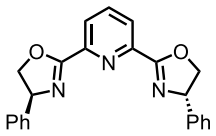

L4

3.26b, 70% yield
anti:*syn* =1.7:1
anti 82:18 er
syn 81:19 er

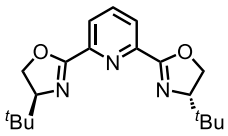

L5

3.26b, 30% yield
anti:*syn* =2.7:1
anti 30:70 er
syn 30:70 er

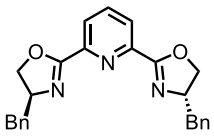

L11

3.26b, 72% yield
anti:*syn* =1.4:1
anti 85:15 er
syn 85:15 er

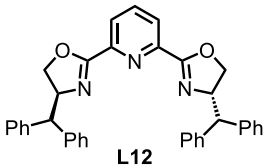

L12

3.26b, 30% yield
anti:*syn* =1.7:1
anti 53:47 er
syn 53:47 er

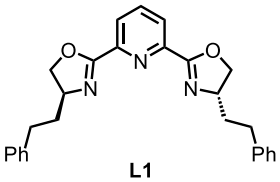

L1

3.26b, 67% yield
anti:*syn* =1.6:1
anti 90:10 er
syn 90:10er

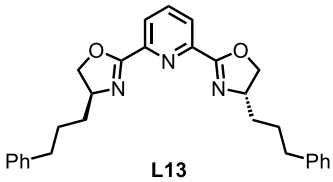

L13

3.26b, 75% yield
anti:*syn* =1.7:1
anti 80:20 er
syn 80:20 er

Evaluation of Various Auxiliaries and Chiral Lewis Acid Co-Catalysts for Enantioselective *β*-Amino C–H Alkylation

To achieve highly enantioselective *β*-alkylation of *N*-alkylamines, various combinations of chiral Lewis acid co-catalysts and electrophiles containing different auxiliaries were evaluated (Scheme S3.4).

Using achiral substrates *N*-arylpyrrolidine **3.21q** and oxazolidinone-substituted **3.25b**, we evaluated various chiral organometallic complexes to find that $Mg(ClO_4)_2$/**L1** give **3.26b** with 67% yield in up to 90:10 er. In comparison, when a chiral Zn-BOX complex was used, **3.26b** was produced in 10 % yield (10:1 dr, 50:50 er; Scheme S3.4A).

In order to identify the optimal auxiliary, we evaluated substrates **3.36**, **3.38** and **3.25f** in the presence of various chiral organometallic co-catalysts. However, the desired products were obtained in 0–30% yield and up to 69:31 er (Schemes S3.4B–D).

Scheme S3.4. Evaluation of Different Electrophiles and Chiral Lewis Acid Co-Catalysts

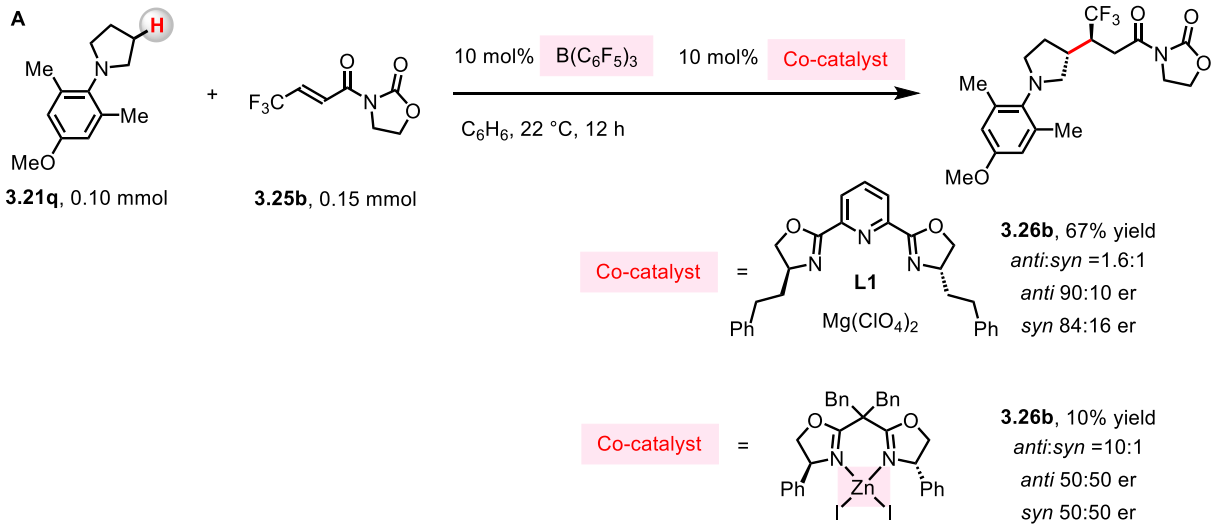

B

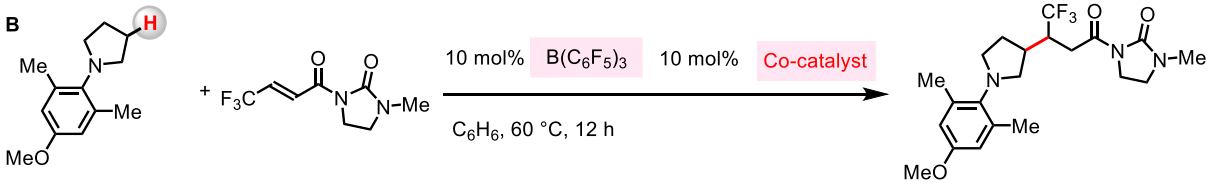

3.21q, 0.10 mmol **3.36**, 0.15 mmol

Co-catalyst = L1 + $Mg(ClO_4)_2$ — **3.37**, 30% yield, 1.0:1 dr, 69:31 er

Co-catalyst = L4 + ZnI_2 — **3.37**, 0% yield

C

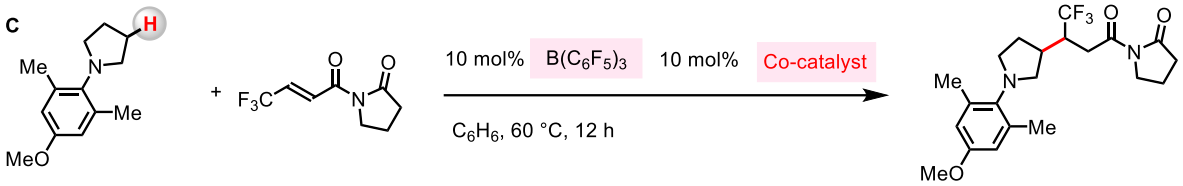

3.21q, 0.10 mmol **3.38**, 0.15 mmol

Co-catalyst = L1 + $Mg(ClO_4)_2$ — **3.39**, 0% yield

Co-catalyst = L4 + ZnI_2 — **3.39**, 0% yield

D

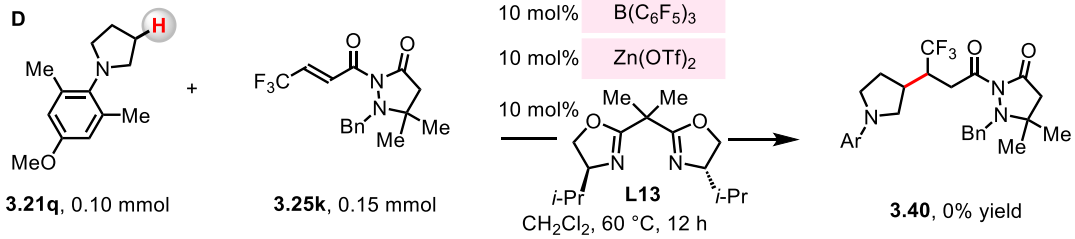

3.21q, 0.10 mmol **3.25k**, 0.15 mmol **3.40**, 0% yield

Optimization Studies for Enantioselective β-Alkylation Involving 3.25a with Chiral Lewis Acid Co-Catalysts

Experimental Procedure for the Optimization of Lewis Acid Co-Catalyst (Table S3.12)

To a 15 mL oven-dried pressure vessel was added Lewis Acid (0.010 mmol, 10 mol%), 2,6-bis((*S*)-4-isopropyl-4,5-dihydrooxazol-2-yl)pyridine **L6** (0.012 mmol, 12 mol%), and DCM (0.50 mL) under nitrogen atmosphere. The mixture was allowed to stir for 20 min at 22 °C. Subsequently, (*E*)-1-benzyl-5,5-dimethyl-2-(4,4,4-trifluorobut-2-enoyl)pyrazolidin-3-one **3.25k** (0.15 mmol), 1-(4-methoxy-2,6-dimethylphenyl)pyrrolidine **3.21q** (0.10 mmol), $B(C_6F_5)_3$ (0.010 mmol, 10 mol%) and DCM (0.50 mL) were added to the reaction vessel, and the resulting mixture was allowed to stir at 22 °C for 12 hours. Upon completion, the solution was concentrated *in vacuo*. The product yield and dr were determined by the ^{1}H NMR and ^{19}F NMR analyses of the unpurified product mixtures using mesitylene (for ^{1}H NMR analysis) and perfluorobenzene (for ^{19}F NMR analysis) as the internal standard. The product was purified by preparative TLC (EtOAc:hexanes = 1:3). The er values of product **3.40** was determined by HPLC analysis of the isolated and purified product.

Experiments for Evaluation of *N*-Aryl Substituents (Scheme S3.5)

We evaluated *N*-arylpyrrolidine with different substituents on the aromatic ring (e.g., **3.21q**, **3.21r**) in the presence of $B(C_6F_5)_3$ and **L10**–$Sc(OTf)_3$ (Scheme S3.5). The reaction between **3.21q** and **3.25f** gave **3.41** in 45% yield (6.5:1 dr, 96:4 er). When less sterically hindered *p*-methoxyphenyl (PMP)-substituted **3.21r** unit was reacted with **3.25f**, **3.26f** could be produced in 62% yield, 6.7:1 dr, and 96:4 er.

Table S3.12. Optimization of Chiral Lewis Acid Co-Catalyst

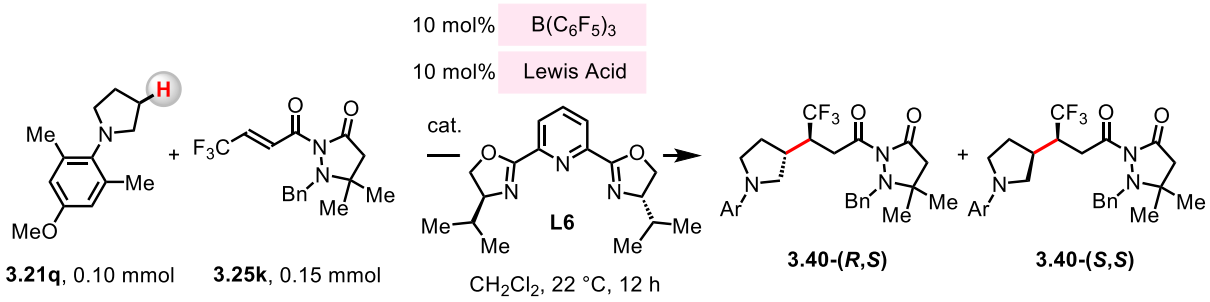

entry	Lewis Acid	yield (%) and er	
		3.40-(*R*,*S*)	**3.40-(*S*,*S*)**
1	$La(OTf)_3$	49, (50:50 er)	18, (50:50 er)
2	$Sm(OTf)_3$	38, (50:50 er)	11, (50:50 er)
3	$Eu(OTf)_3$	0	0
4	$Yb(OTf)_3$	0	0
5	$Sc(OTf)_3$	26, (96:4 er)	17, (96:4 er)

Scheme S3.5. Evaluation of *N*-Aryl Substituents

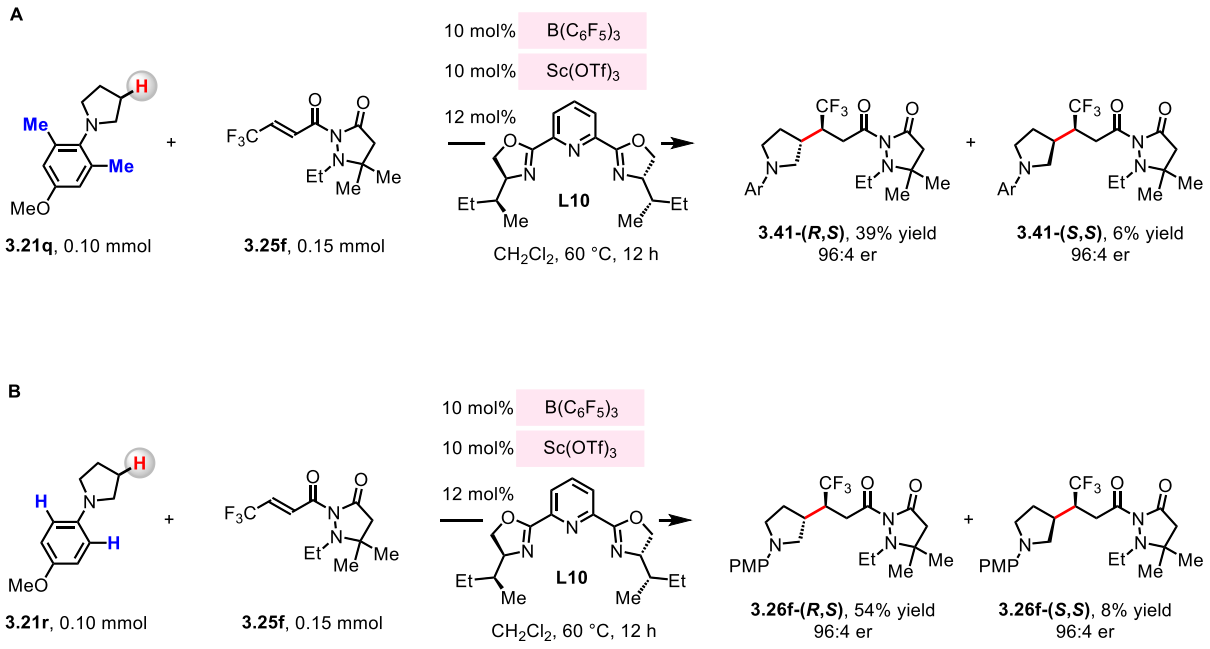

Optimization Studies for Enantioselective β-Alkylation Involving 3.25c with Chiral Sc-based Complexes

3.6.2.8.1. Evaluation of Reaction Parameters (Table S3.13)

To a 15 mL oven-dried pressure vessel was added $Sc(OTf)_3$ (0.020 mmol, 10 mol%), 2,6-bis((*S*)-4-((*S*)-sec-butyl)-4,5-dihydrooxazol-2-yl)pyridine **L10** (0.024 mmol, 12 mol%), and DCM (1.0 mL) under nitrogen atmosphere. The mixture was allowed to stir for 20 min at 22 °C. Subsequently, ethyl (*E*)-4-(2-ethyl-3,3-dimethyl-5-oxopyrazolidin-1-yl)-4-oxobut-2-enoate **3.25c** (0.30 mmol), 1-(4-methoxyphenyl)pyrrolidine **3.21r** (0.20 mmol), $B(C_6F_5)_3$ (0.020 mmol, 10 mol%) and DCM (1.0 mL) were added to the reaction vessel, and the resulting mixture was placed in an oil bath at 60 °C and was allowed to stir for 1 hour or 3 hours. Upon completion, the solution was cooled to 22 °C and concentrated *in vacuo*. The product yield and dr were determined by the ^{1}H NMR analyses of the unpurified product mixtures using as the internal standard. The product was purified by preparative TLC (EtOAc:hexanes = 1:1). The er values of product **3.26c** was determined by HPLC analysis of the isolated and purified product.

Table S3.13. Optimization of Reaction Parameters

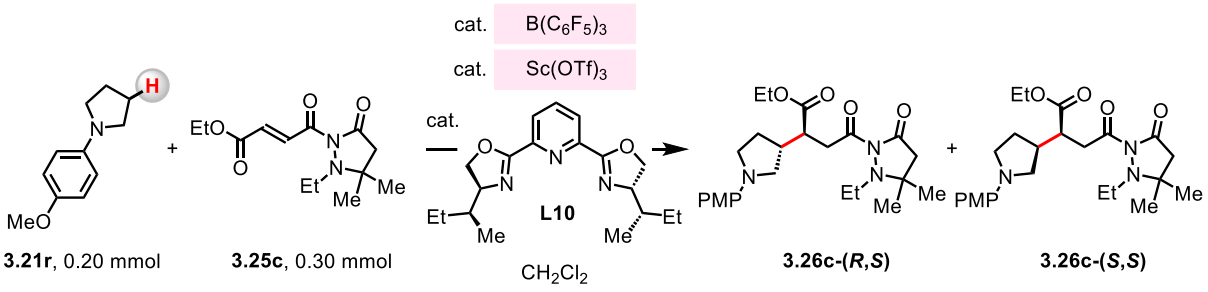

3.21r, 0.20 mmol **3.25c**, 0.30 mmol **3.26c-(*R*,*S*)** **3.26c-(*S*,*S*)**

entry	$B(C_6F_5)_3$ (mol%)	$Sc(OTf)_3$/**L10** (mol%)	time (h)	temperature (°C)	yield (%) and er **3.26c-(*R*,*S*)**	**3.26c-(*S*,*S*)**
1	10	0	3	60	0	0
2	0	10	3	60	0	0
3	10	10	3	60	51, (97:3 er)	33, (98:2 er)
4	10	10	3	22	46, (97:3 er)	24, (98:2 er)
5	10	10	1	60	56, (97:3 er)	29, (98:2 er)
6	10	5	1	60	55, (97:3 er)	30, (98:2 er)
7	5	5	1	60	32, (97:3 er)	18, (98:2 er)

General Reaction Procedure for Evaluation of Chiral Ligands (See Table 3.9)

To a 15 mL oven-dried pressure vessel was added $Sc(OTf)_3$ (0.010 mmol, 5.0 mol%), **Ligand** (0.012 mmol, 6.0 mol%), and DCM (1.0 mL) under nitrogen atmosphere. The mixture was allowed to stir for 20 min at 22 °C. Subsequently, ethyl (*E*)-4-(2-ethyl-3,3-dimethyl-5-oxopyrazolidin-1-yl)-4-oxobut-2-enoate **3.25c** (0.30 mmol), 1-(4-methoxyphenyl)pyrrolidine **3.21r** (0.20 mmol), $B(C_6F_5)_3$ (0.020 mmol, 10 mol%) and DCM (1.0 mL) were added to the reaction vessel, and the resulting mixture was placed in an oil bath at 60 °C and was allowed to stir for 1 hour. Upon completion, the solution was cooled to 22 °C and concentrated *in vacuo*. The product yield and dr were determined by the ^1H NMR analyses of the unpurified product mixtures using mesitylene as the internal standard. The product was purified by preparative TLC (EtOAc:hexanes = 1:1). The er values of product **3.26c** was determined by HPLC analysis of the isolated and purified product.

Evaluation of Acyclic Amine Substrates for Enantioselective *β*-Alkylation with Chiral Sc-based Complexes

We have evaluated several acyclic amines (**3.21**) for enantioselective *β*-amino C–H alkylation; however, the current conditions were found to be incompatible with this class of substrate (Scheme S3.6).

Scheme S3.6. Evaluation of Acyclic Amine Substrates

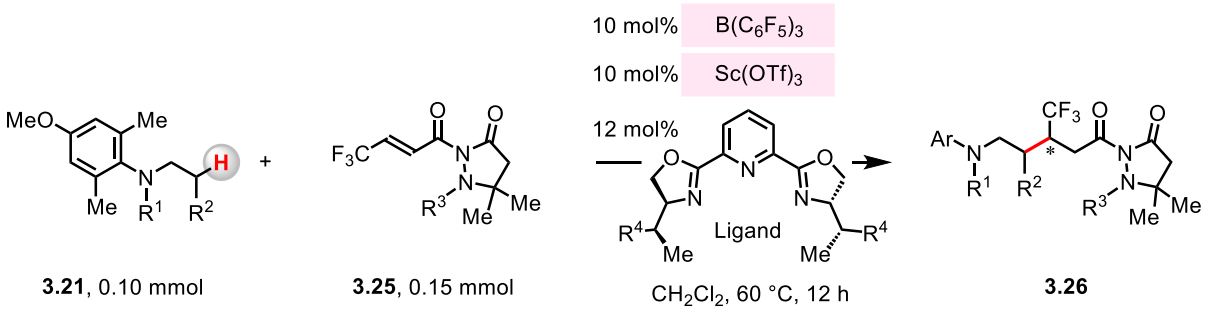

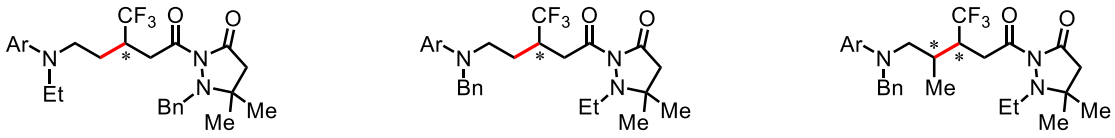

3.26t, 10% yield[b] **3.26u**, <5% yield[c] **3.26v**, <5% yield[c]

[a]Conditions: amine (**3.21**, 0.10 mmol), *α*,*β*-unsaturated compound (**3.25**, 0.15 mmol), $B(C_6F_5)_3$ (10 mol%), $Sc(OTf)_3$(10 mol%), ligand (12 mol%), CH_2Cl_2 (1.0 mL), under N_2, 60 °C.[b] **L6** (R^4=Me) was used as ligand. [c] **L10** (R^4=Et) was used as ligand.

C3. General Procedures for *β*-Alkylation of *N*-Alkylamines

General Procedure C for the *β*-Alkylation of *N*-Alkylamines (See Tables 3.6–3.9 in the Manuscript)

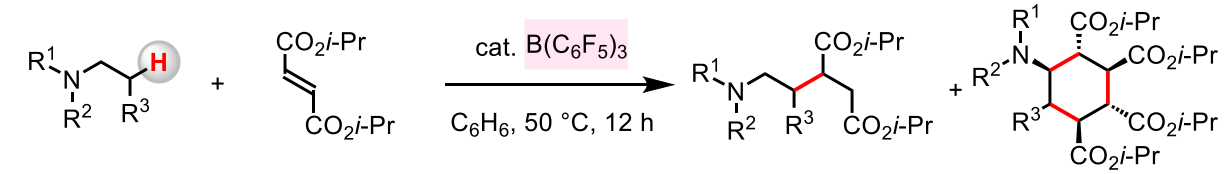

3.21, 0.20 mmol **3.22a**, 0.30 mmol **3.23** **3.24**

To a 15 mL oven-dried pressure vessel was added amine (0.20 mmol), $B(C_6F_5)_3$ (5.0 or 10 mol%), *α,β*-unsaturated compound (0.30 mmol, 1.5 equiv.) and benzene under a nitrogen atmosphere. The reaction mixture was placed in an oil bath at 50 °C and was allowed to stir for 12 hours. Upon completion, the solution was cooled to 22 °C and concentrated *in vacuo* followed by flash silica gel column chromatography.

General Procedure D for the *β*-Alkylation of *N*-Alkylamines (See Tables 3.7–3.9 in the Manuscript)

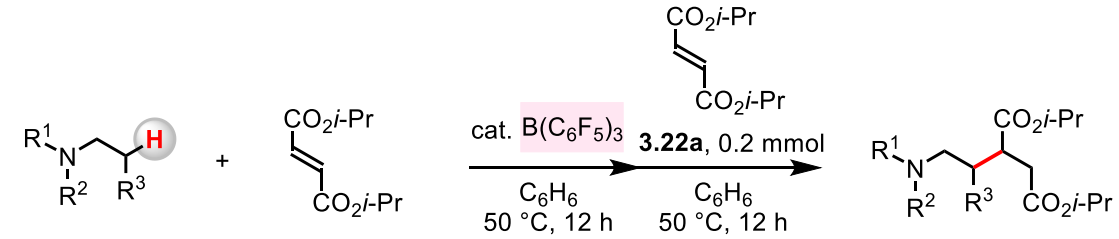

3.21, 0.20 mmol **3.22a**, 0.30 mmol **3.23**

To a 15 mL oven-dried pressure vessel was added amine (0.20 mmol), $B(C_6F_5)_3$ (5.0 or 10 mol%), *α,β*-unsaturated compound (0.30 mmol, 1.5 equiv.) and benzene (0.30 mL) under a nitrogen atmosphere. The reaction mixture was placed in an oil bath at 50 °C and was allowed to stir for 12

hours. After the solution was cooled to 22 °C, *α,β*-unsaturated compound (0.20 mmol, 1.0 equiv.) and benzene (0.10 mL) were added under a nitrogen atmosphere and the reaction mixture was again placed in an oil bath at 50 °C and was allowed to stir for 12 hours. Upon completion, the solution was cooled to 22 °C and concentrated *in vacuo* followed by flash silica gel column chromatography.

General Procedure E for the Enantioselective *β*-Alkylation of *N*-Alkylamines (See Tables 3.10-3.11 in the Manuscript)

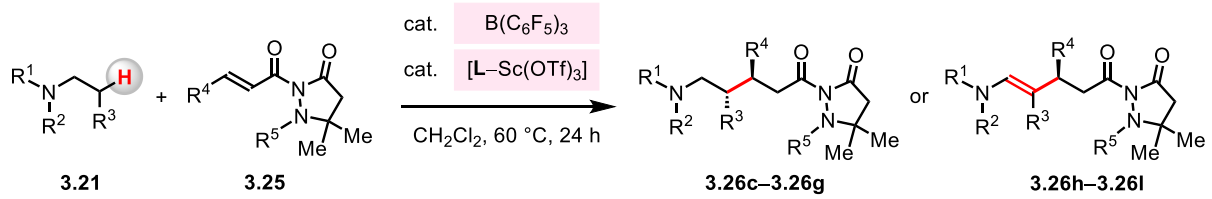

To a 15 mL oven-dried pressure vessel was added $Sc(OTf)_3$ (5.0 or 10 mol%), **ligand** (6.0 or 12 mol%), and DCM (0.50 mL) under nitrogen atmosphere. The mixture was allowed to stir for 20 min at 22 °C. Subsequently, *α,β*-unsaturated compound **3.25** (0.15 or 0.20 mmol), amine **3.21** (0.10 mmol), $B(C_6F_5)_3$ (10 or 20 mol%) and DCM (0.50 mL) were added to the reaction vessel, and the resulting mixture was placed in an oil bath at 60 °C or 80 °C and was allowed to stir for 1–36 hours. Upon completion, the solution was cooled to 22 °C and concentrated *in vacuo* followed by flash silica gel column chromatography.

Procedure for Large Scale Reaction

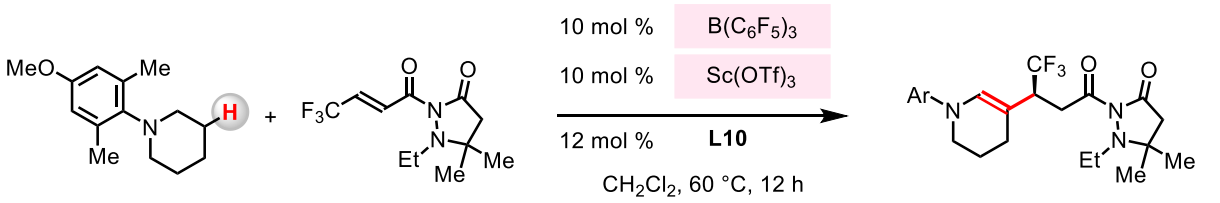

3.21l, 4.0 mmol **3.25f**, 8.0 mmol **3.26h**, >95% yield, 1.9 g, 95:5 er

To a 25 mL oven-dried sealed tube was added $Sc(OTf)_3$ (10 mol%), 2,6-bis((*S*)-4-((*S*)-sec-butyl)-4,5-dihydrooxazol-2-yl)pyridine **L10** (12 mol%), and DCM (5.0 mL) under nitrogen atmosphere. The mixture was allowed to stir for 2 hours at 22 °C. Subsequently, (*E*)-1-ethyl-5,5-dimethyl-2-(4,4,4-trifluorobut-2-enoyl)pyrazolidin-3-one **3.25f** (8.0 mmol), 1-(4-methoxy-2,6-dimethylphenyl)piperidine **3.21l** (4.0 mmol), $B(C_6F_5)_3$ (10 mol%) and DCM (1.0 mL) were added to the reaction vessel, and the resulting mixture was placed in an oil bath at 60 °C and was allowed to stir for 12 hours. Upon completion, the solvent was cooled to 22 °C and concentrated *in vacuo* followed by purification through flash silica gel column chromatography to afford the product as a light yellow oil (1.93 g, 95% yield, 95:5 er). The er value was determined by HPLC analysis of the isolated and purified product.

C4. Determination of Relative Configuration

Determination of the Relative Configuration of 3.23i-Major

The relative configurations of **3.23i-major** was determined by the X-ray crystallographic analysis of its derivative, **3.42i-major** (Scheme S3.7).

Scheme S3.7. Derivatization of **3.23i-Major** and Crystal Structure of **3.42i-Major**

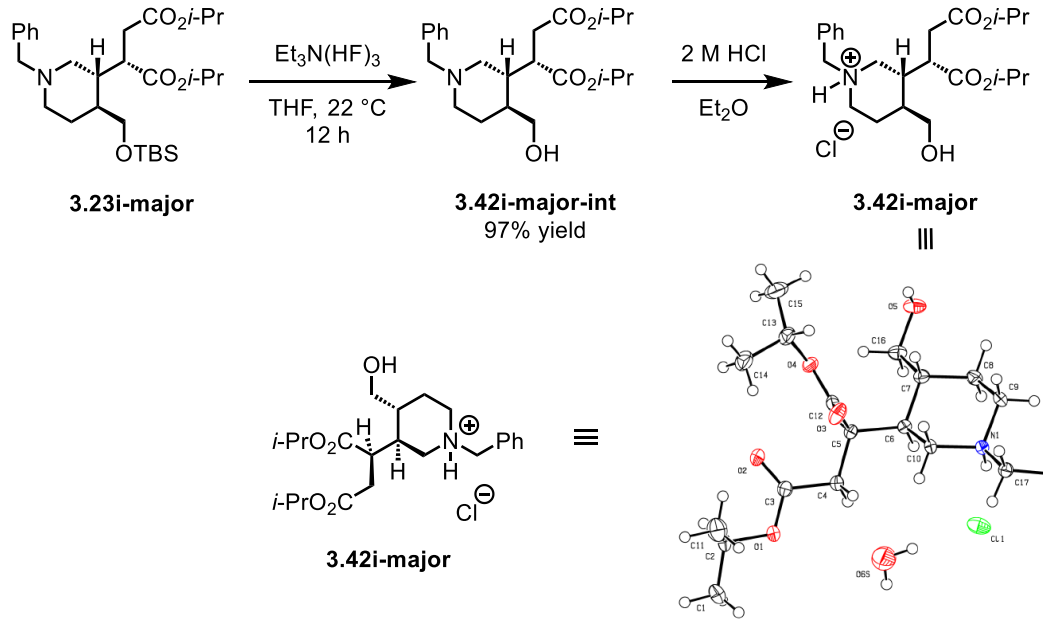

1-Benzyl-3-(1,4-diisopropoxy-1,4-dioxobutan-2-yl)-4-(hydroxymethyl)piperidin-1-ium chloride (3.42i-major)

3.42i-Major was synthesized by the following procedure. To a solution of **3.23i-major** (386 mg, 0.75 mmol) in THF (10 mL) was added $Et_3N(HF)_3$ (0.50 mL) in a dropwise manner. The reaction was allowed to stir at 22 °C for 12 hours. The reaction mixture was concentrated and filtered through a plug of Celite using DCM as solvent. The unpurified product was then subjected to flash silica gel column chromatography (EtOAc:hexanes = 9:1) to afford diisopropyl 2-(1-benzyl-4-(hydroxymethyl)piperidin-3-yl)succinate **3.42i-major-int** as a colorless oil (295 mg, 97%).

^{1}H NMR (400 MHz, $CDCl_3$): δ 7.34 – 7.20 (m, 5H), 5.01 (dp, *J* = 9.8, 6.2 Hz, 2H), 3.83 (dd, *J* =

11.5, 4.1 Hz, 1H), 3.64 (dd, *J* = 11.5, 3.2 Hz, 1H), 3.55 (d, *J* = 13.2 Hz, 1H), 3.43 (d, *J* = 13.2 Hz, 1H), 3.18 (td, *J* = 6.3, 3.3 Hz, 1H), 2.98 – 2.83 (m, 2H), 2.76 (dd, *J* = 17.3, 8.2 Hz, 1H), 2.37 (dd, *J* = 17.3, 6.3 Hz, 1H), 2.23 (s, 1H), 1.94 – 1.82 (m, 2H), 1.72 (t, *J* = 11.1 Hz, 1H), 1.63 (dd, *J* = 10.2, 3.9 Hz, 2H), 1.60 – 1.46 (m, 2H), 1.30 – 1.18 (m, 14H).

3.42i-Major-int was then diluted in ethyl ether (0.10 mL) and 2.0 M HCl in ethyl ether was added dropwise to the solution until a white precipitate was formed. The solid was allowed to precipitate out of solution, whereupon the solvent was removed *in vacuo* to afford **3.42i-major** as a white solid.

3.42i-Major was recrystallized using the vapor-vapor diffusion method, using *i*-PrOH to dissolve the product in an inner vial, and ethyl ether as the precipitant placed in the outer vial in order for slow diffusion to occur into the inner vial. The solution was cooled to 0 °C, whereupon a crystal was obtained for X-ray crystallography. The X-ray crystallographic analysis revealed that the relative configuration of **3.42i-major** is (*R,R,R*) or (*S,S,S*). The relative configuration of products **3.23k-major**, **3.23o-major**, **3.23q-major**, and **3.23s-major** were assigned in analogy.

Determination of the Relative Configuration of 3.23i-Minor

The relative configurations of **3.23i-Minor** was determined by the X-ray crystallographic analysis of its derivative, **3.42i-minor** (Scheme S3.8).

Scheme S3.8. Derivatization of **3.23i-Minor** and Crystal Structure of **3.42i-Minor**

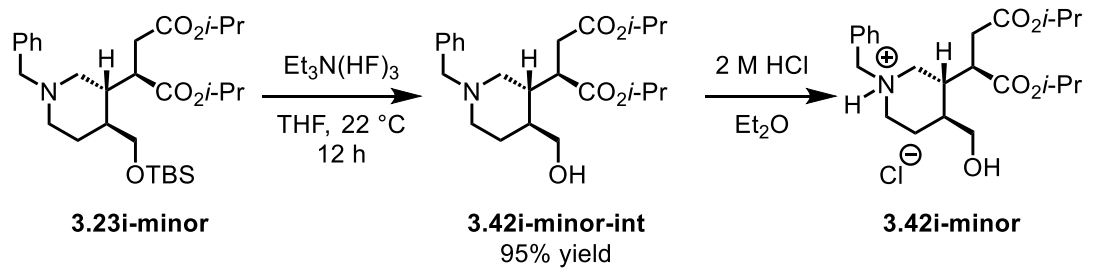

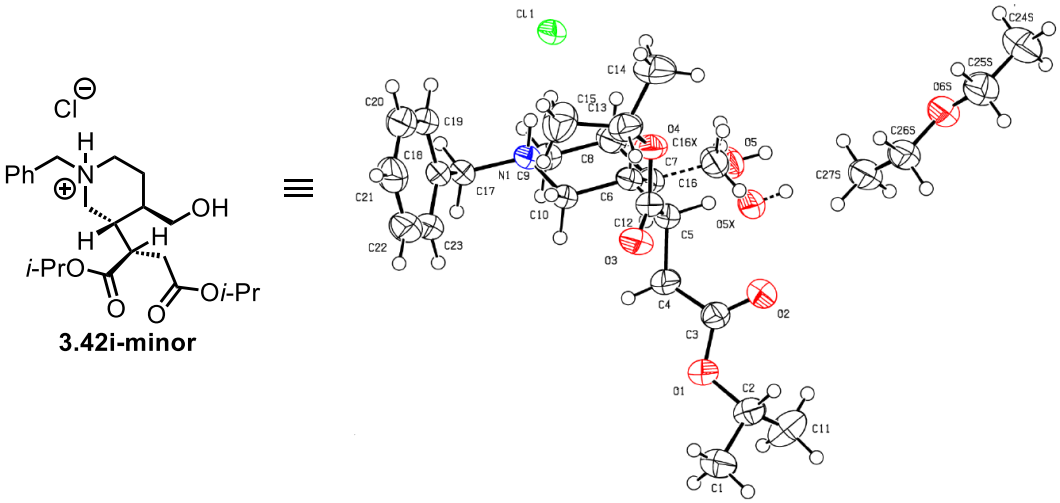

1-Benzyl-3-(1,4-diisopropoxy-1,4-dioxobutan-2-yl)-4-(hydroxymethyl)piperidin-1-ium chloride (3.42i-minor)

3.42i-Minor was synthesized by the following procedure. To a solution of **3.23i-minor** (150 mg, 0.3 mmol) in THF (10 mL) was added $Et_3N(HF)_3$ (0.3 mL), dropwise. The reaction was allowed to stir at 22 °C for 12 hours. The reaction mixture was concentrated and filtered through a plug of Celite using DCM as solvent. The unpurified product was then subjected to flash silica gel column chromatography (EtOAc:hexanes = 9:1) to afford diisopropyl 2-(1-benzyl-4-(hydroxymethyl)piperidin-3-yl)succinate **3.42i-minor-int** as a colorless oil (116 mg, 95%).

^{1}H NMR (500 MHz, $CDCl_3$): δ 7.27 (d, *J* = 4.5 Hz, 4H), 7.21 (q, *J* = 4.5 Hz, 1H), 4.98 (p, *J* = 6.3 Hz, 1H), 4.90 (p, *J* = 6.2 Hz, 1H), 3.73 (dd, *J* = 10.9, 4.4 Hz, 1H), 3.59 (dd, *J* = 10.9, 5.9 Hz, 1H), 3.50 (d, *J* = 13.1 Hz, 1H), 3.38 (d, *J* = 13.1 Hz, 1H), 3.17 (dt, *J* = 11.6, 3.7 Hz, 1H), 2.87 (d, *J* = 11.2 Hz, 1H), 2.68 – 2.48 (m, 2H), 2.32 (dd, *J* = 16.6, 3.3 Hz, 1H), 2.10 – 2.03 (m, 1H), 1.99 (t, *J* = 11.3 Hz, 1H), 1.79 (dt, *J* = 27.4, 12.1 Hz, 2H), 1.61 – 1.46 (m, 1H), 1.45 – 1.36 (m, 1H), 1.26 (t, *J* = 7.6 Hz, 1H), 1.21 (t, *J* = 6.3 Hz, 6H), 1.14 (d, *J* = 6.2 Hz, 3H), 1.04 (d, *J* = 6.2 Hz, 3H).

3.42i-Minor-int was then diluted in ethyl ether (0.10 mL) and 2.0 M HCl in ethyl ether was added dropwise to the solution until a white precipitate was formed. The solid was allowed to precipitate out of solution, whereupon the solvent was removed *in vacuo* to afford **3.42i-minor** as a white solid. **3.42i-Minor** was recrystallized using the vapor-vapor diffusion method, using *i*-PrOH to dissolve the product in an inner vial, and ethyl ether as the precipitant placed in the outer vial in order for slow diffusion to occur into the inner vial. The solution was cooled to 0 °C, whereupon a crystal was obtained for X-ray crystallography. The X-ray crystallographic analysis revealed that the relative configuration of **3.42i-minor** is (*R,R,S*) or (*S,S,R*). The relative configuration of products **3.23k-minor**, **3.23o-minor**, **3.23q-minor**, and **3.23s-minor** were assigned in analogy.

Determination of the Relative Configuration of 3.23b-Major

The relative configuration of **3.23b-major** was determined by the X-ray crystallographic analysis of **3.23bf-major.**

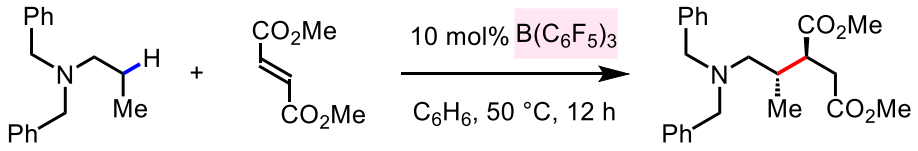

3.21b, 0.2 mmol **3.22f**, 0.3 mmol **3.23bf**, 43% yield 2.6:1 dr

To a 15 mL oven-dried pressure vessel was added dibenzylpropanamine **3.21b** (0.40 mmol), $B(C_6F_5)_3$ (10 mol%), dimethylfumarate **3.22d** (0.60 mmol) and benzene (0.40 mL) under a nitrogen atmosphere. The reaction mixture was placed in an oil bath at 50 °C and was allowed to stir for 12 hours. Upon completion, the solution was cooled to 22 °C and concentrated *in vacuo.* The ^{1}H NMR analysis of the unpurified product mixture revealed that **3.23bf** was obtained as a mixture of diastereomers in 2.6:1 ratio. After purification by flash silica gel column chromatography (ethyl ether:hexanes = 1:19), **3.23bf** was obtained as a mixture of diastereomers (66 mg, 43%). Further purification was carried out by PTLC using ethyl ether:DCM = 1:49 as the eluent to separate **3.23bf-major** and **3.23bf-minor**. The major diastereomer was isolated as a white solid (45 mg, 29% yield).

Dimethyl 2-(1-(dibenzylamino)propan-2-yl)succinate (3.23bf-major)

^{1}H NMR (600 MHz, $CDCl_3$): δ 7.34 (d, *J* = 6.7 Hz, 4H), 7.29 (t, *J* = 7.5 Hz, 4H), 7.22 (t, *J* = 7.1 Hz, 2H), 3.78 (d, *J* = 13.2 Hz, 2H), 3.67 (s, 6H), 3.38 (d, *J* = 11.9 Hz, 1H), 3.26 (d, *J* = 13.3 Hz, 2H), 2.37 (dd, *J* = 16.8, 11.5 Hz, 2H), 2.24 (t, *J* = 11.5 Hz, 1H), 2.14 (dd, *J* = 13.0, 5.5 Hz, 1H), 1.51 (dd, *J* = 16.9, 2.9 Hz, 1H), 0.71 (d, *J* = 6.9 Hz, 3H).

The major diastereomer was then recrystallized using DCM:hexanes = 1:10 to afford a crystal for the X-ray analysis. The X-ray crystallographic analysis revealed that the relative configuration of **3.23bf-major** is (*R,R*) or (*S,S*). The relative configuration of **3.23b-major** was assigned in analogy.

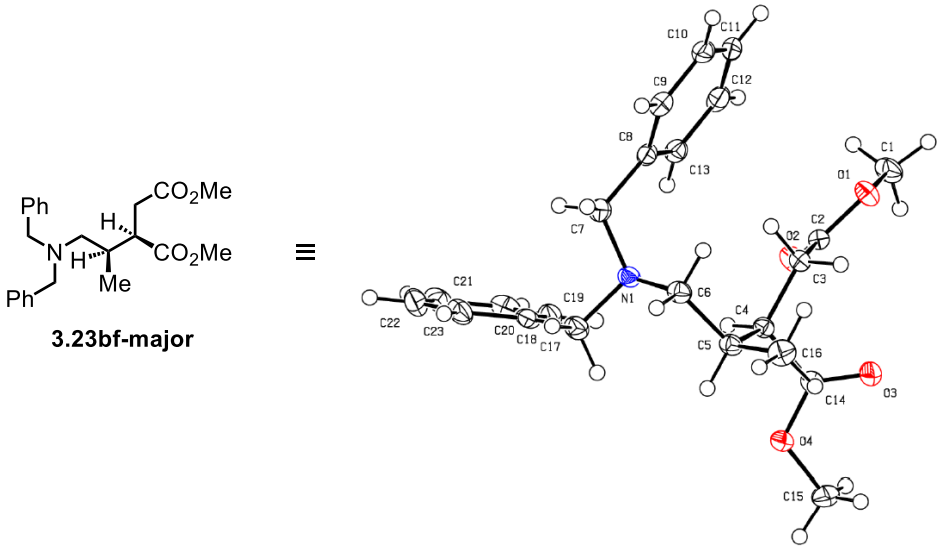

Figure S3.3. X-ray crystal structure of **3.23bf-major**

Determination of the Relative Configuration of 3.24

The relative configuration for **3.24** was determined by NOESY experiments. The following are the NOE spectrum and assignments (Figure S3.4).

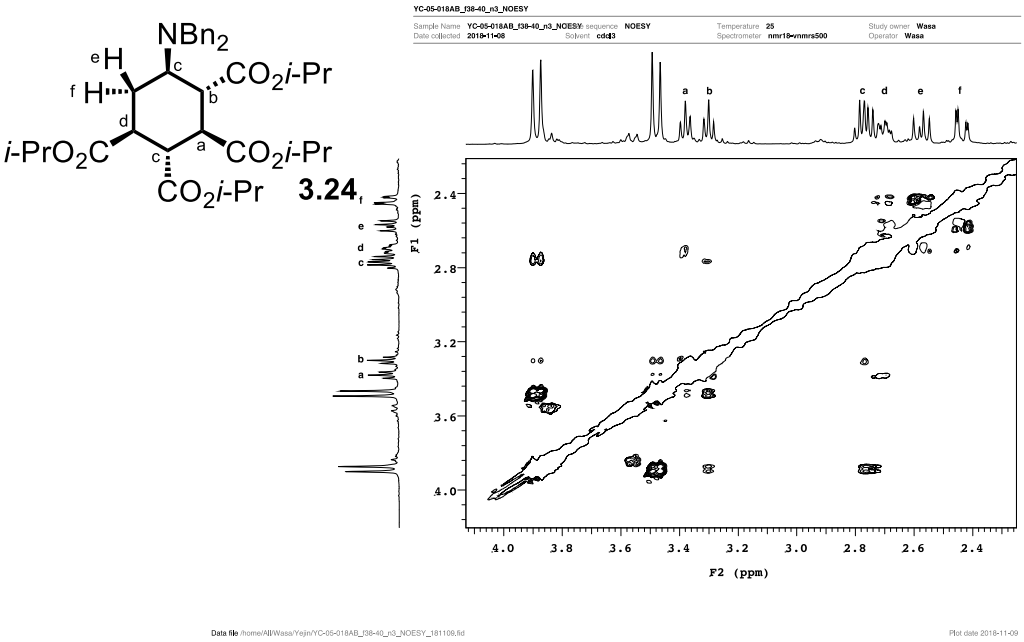

Figure S3.4. 2D NOESY spectra of **3.24**

Determination of the Relative Configuration of 3.23m-Major

The relative configuration for **3.23m-major** was determined by NOESY experiments. The following are the NOE spectrum and assignments (Figure S3.5).

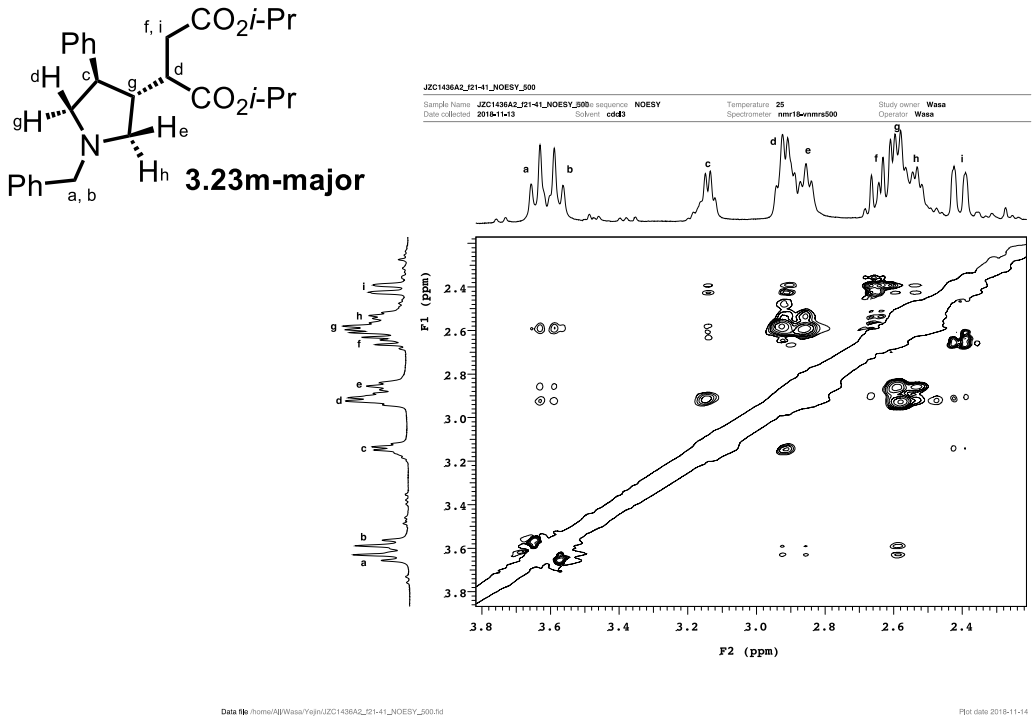

Figure S3.5. 2D NOESY spectra of **3.23m-major**

The relative configuration of the pyrrolidine substituents of **3.23m-major** was assigned to be *anti.*

C5. Determination of Absolute Configuration

Determination of the Absolute Configuration of Product 3.23h-(*R,R,R*).

We carried out the following studies in order to determine the absolute configuration of product **3.23h**.

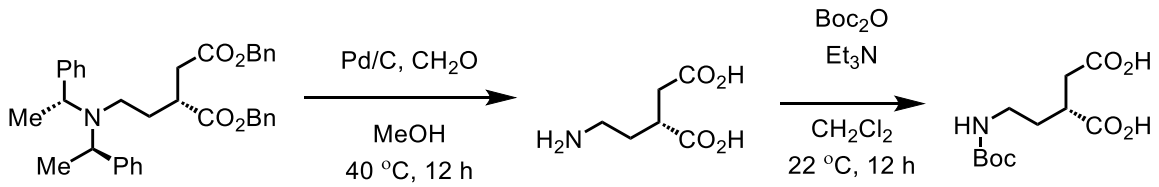

3.23h-major **3.43-major-int** **3.43-major**

The derivatization of the major diastereomer of **3.23h** was performed based on a method previously reported in the literature.[1] **3.23h-Major** (79 mg, 0.14 mmol) was dissolved in a solution of 4.4% formic acid in MeOH (3.0 mL), whereupon Pd/C (10%, 7.9 mg) was added. The reaction mixture was placed in an oil bath at 40 °C and was allowed to stir for 12 hours. After the solution was cooled down to 22 °C, the suspension was filtered through a pad of Celite using DCM as solvent and the mixture was concentrated to remove the solvent and volatile side products to obtain the product **3.43-major-int** as a colorless oil (23 mg, >95% yield).

2-(2-Aminoethyl)succinic acid **3.43-major-int** was then dissolved in DCM, whereupon Et_3N (20 μL, 0.15 mmol) and di-*tert*-butyl dicarbonate (30 μL, 0.15 mmol) were added, dropwise. The reaction mixture was allowed to stir at 22 °C for 12 hours. Upon completion, the unpurified mixture was concentrated to remove the solvent and volatile side products to obtain the product **3.43-major** as a colorless oil (25 mg, 88% yield). $[\alpha]^{25}_D$ = + 27.6° (c = 1.0, acetone). Based on the observed optical rotation value, the absolute configuration of the major diastereomer was assigned in analogy as **3.23h-(*R,R,R*)**.[28]

[1] Davies, S. G.; Epstein, S. W.; Garner, A. C.; Ichihara, O.; Smith, A. D. *Tetrahedron: Asymmetry* **2002**, *13*, 1555–1565.

Determination of the Absolute Configuration of 3.23n-(*R*,*R*,*R*)

The absolute configuration of **3.23n-(*R*,*R*,*R*)** was determined by the X-ray crystallographic analysis of **3.44-major** (Scheme S3.9).

Scheme S3.9. Derivatization of **3.23n-Major** and Crystal Structure of **3.44-Major**

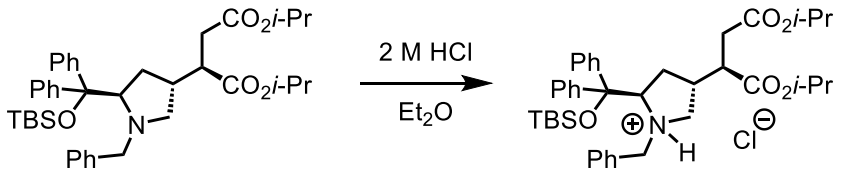

3.23n-major
3.23n-(*R*,*R*,*R*)

3.44-major

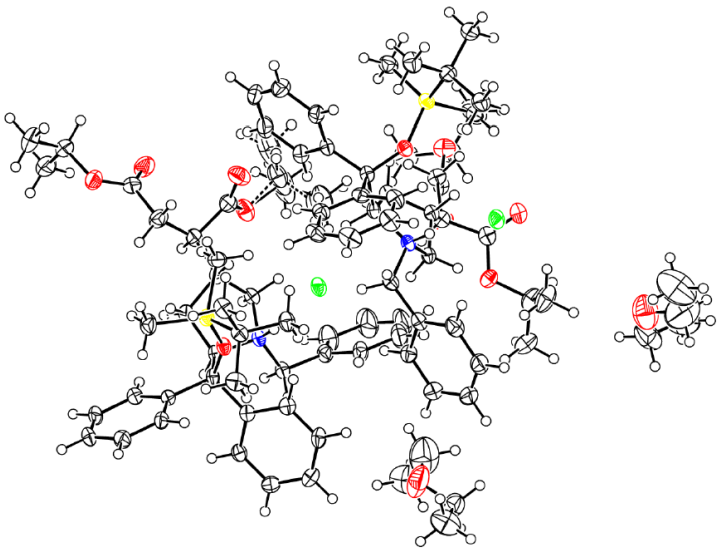

(2*R*,4*R*)-1-Benzyl-2-(((*tert*-butyldimethylsilyl)oxy)diphenylmethyl)-4-((*R*)-1,4-diisopropoxy-1,4-dioxobutan-2-yl)pyrrolidin-1-ium chloride (3.44-major)

3.44-major was synthesized by the following procedure. **3.23n-(*R*,*R*,*R*)** was diluted in ethyl ether (0.2 mL) and 2.0 M HCl in ethyl ether was added dropwise to the solution until a white precipitate was formed. The solid was allowed to precipitate out of solution, whereupon the solvent was removed *in vacuo* to afford **3.44-major** as a white solid. **3.44-Major** was then recrystallized using DCM:ethyl ether = 1:10 and cooled to 0 °C to afford a crystal for X-ray analysis. The X-ray crystallographic analysis revealed that the absolute configuration of **3.44-major** is (*R*,*R*,*R*).

Determination of the Absolute Configuration of 3.23s-(*S,S,R,S*)

The absolute configuration of **3.23s-(*S,S,R,S*)** was determined through 2D NMR studies. The following are the spectra and assignments (Figures S3.6–S3.8).

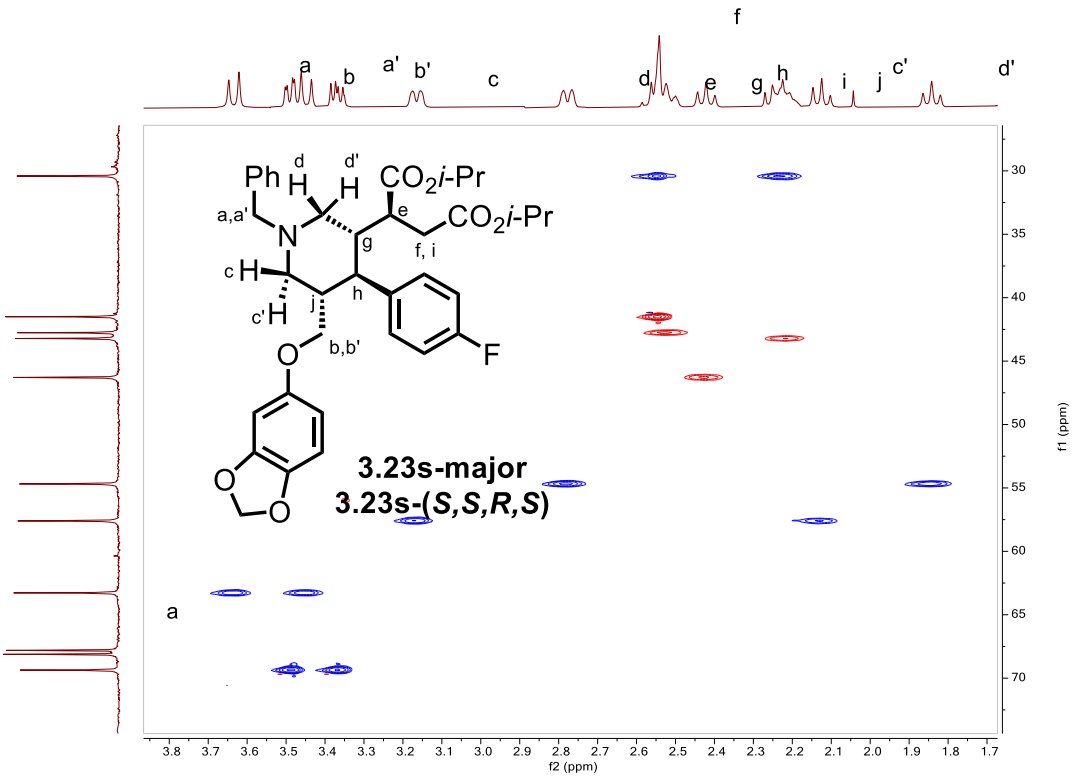

Figure S3.6. 2D HSQCAD spectra of **3.21r-major**

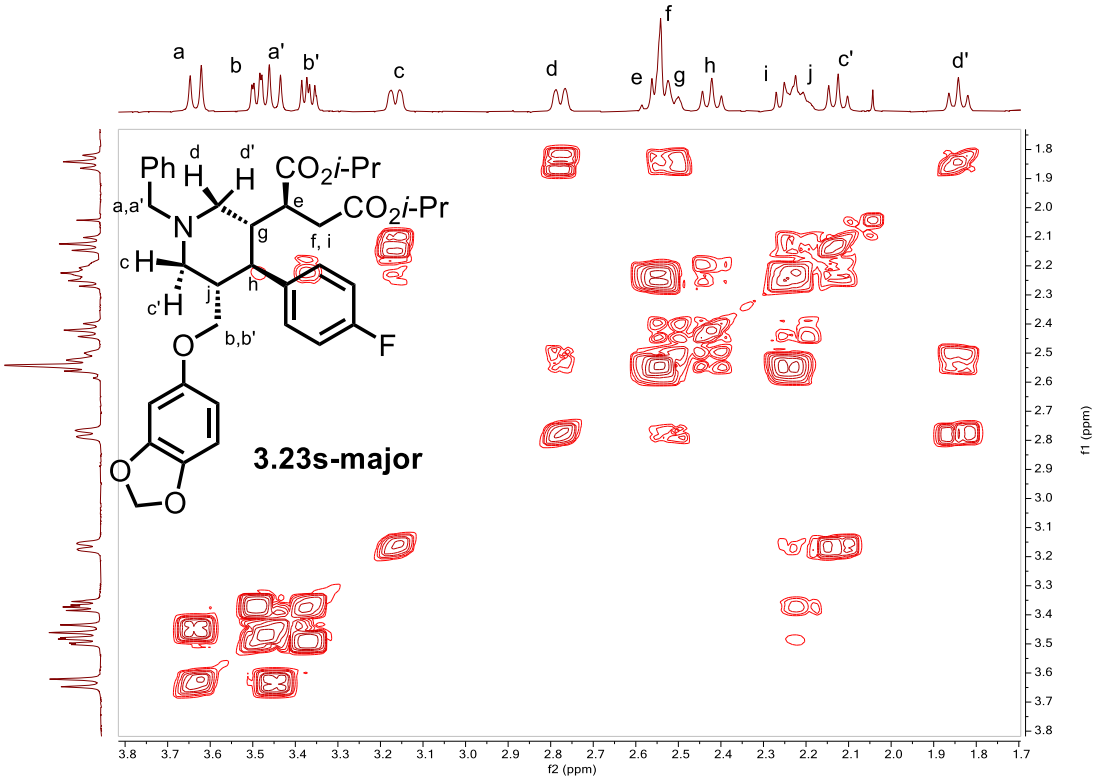

Figure S3.7. 2D COSY spectra of **3.23s-major**

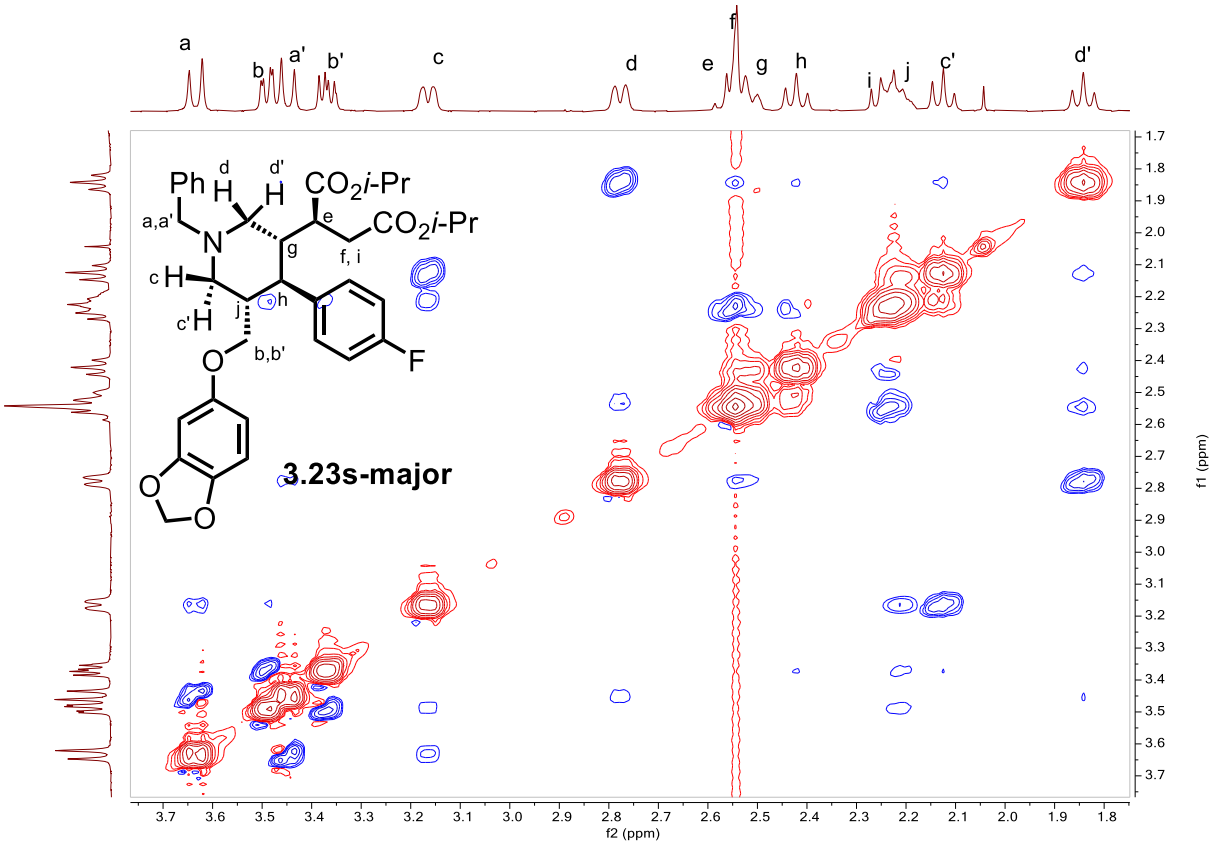

Figure S3.8. 2D NOESY spectra of **3.23s-major**

The absolute configuration of **3.23s-major** was assigned to be (*S,S,R,S*) by the 2D NMR analyses and in analogy to **3.23i-major**.

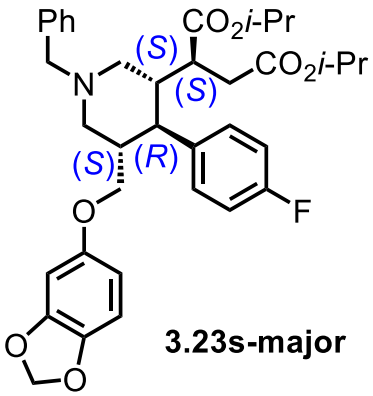

Determination of the Absolute Configuration of 3.26a-(*R,R,R,S*)

The absolute configuration of **3.26a-(*R,R,R,S*)** was determined by the X-ray crystallographic analysis of its derivative, **3.45** (Scheme S3.10).

Scheme S3.10. Derivatization of **3.26a-(*R,R,R,S*)**.

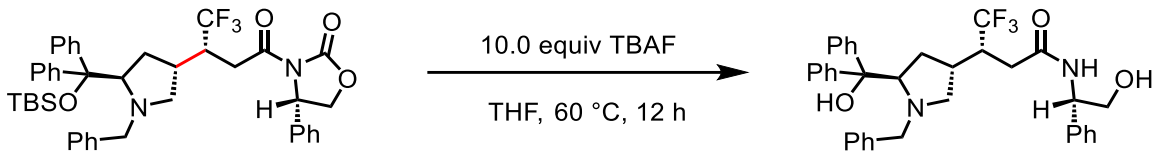

3.26a **3.45**

(*R*)-3-((3*R*,5*R*)-1-Benzyl-5-(hydroxydiphenylmethyl)pyrrolidin-3-yl)-4,4,4-trifluoro-*N*-((*S*)-2-hydroxy-1-phenylethyl)butanamide (3.45)

3.45 was synthesized by the following procedure. To a solution of **3.26a** (371 mg, 0.50 mmol) in THF (5.0 mL) was added TBAF (2.0 M, 2.5 mL), dropwise. The reaction was placed in an oil bath at 60 °C and was allowed to stir for 12 hours. After the reaction mixture was cooled down to 22 °C, it was quenched with $NaHCO_3$ (aq.) and extracted with DCM (3 x 25 mL). The combined organic layers were dried over Na_2SO_4 and concentrated *in vacuo*. The unpurified product was then subjected to flash silica gel column chromatography (EtOAc:hexanes = 1:4) to afford **3.45** as a white solid (120 mg, 40%).

^{1}H NMR (500 MHz, $CDCl_3$): δ 7.64 (d, *J* = 7.3 Hz, 2H), 7.51 (d, *J* = 7.0 Hz, 2H), 7.32 (t, *J* = 7.5 Hz, 2H), 7.29 – 7.23 (m, 5H), 7.23 – 7.07 (m, 7H), 6.97 (d, *J* = 6.2 Hz, 2H), 6.27 (d, *J* = 6.9 Hz, 1H), 4.90 (dt, *J* = 6.7, 4.8 Hz, 1H), 3.99 (dd, *J* = 10.3, 3.1 Hz, 1H), 3.77 (d, *J* = 4.9 Hz, 2H), 3.11 (d, *J* = 12.5 Hz, 1H), 3.06 (br, 1H), 2.95 (d, *J* = 12.6 Hz, 1H), 2.77 – 2.65 (m, 1H), 2.26 – 2.14 (m, 3H), 2.10 (dd, *J* = 15.9, 4.0 Hz, 1H), 1.90 (ddd, *J* = 12.5, 6.6, 3.0 Hz, 1H), 1.81 (qd, *J* = 10.2, 3.5 Hz, 1H); **^{19}F NMR (470 MHz, $CDCl_3$):** δ -69.28 (d, *J* = 8.7 Hz).

3.45 was recrystallized using the vapor-vapor diffusion method, using benzene to dissolve the product in an inner vial, and pentane as the precipitant placed in the outer vial in order for slow diffusion to occur into the inner vial. The solution was cooled to 0 °C, whereupon a crystal was obtained for X-ray crystallography (Figure S3.9). The X-ray crystallographic analysis revealed that the absolute configuration of **3.26a** is (*R,R,R,S*).

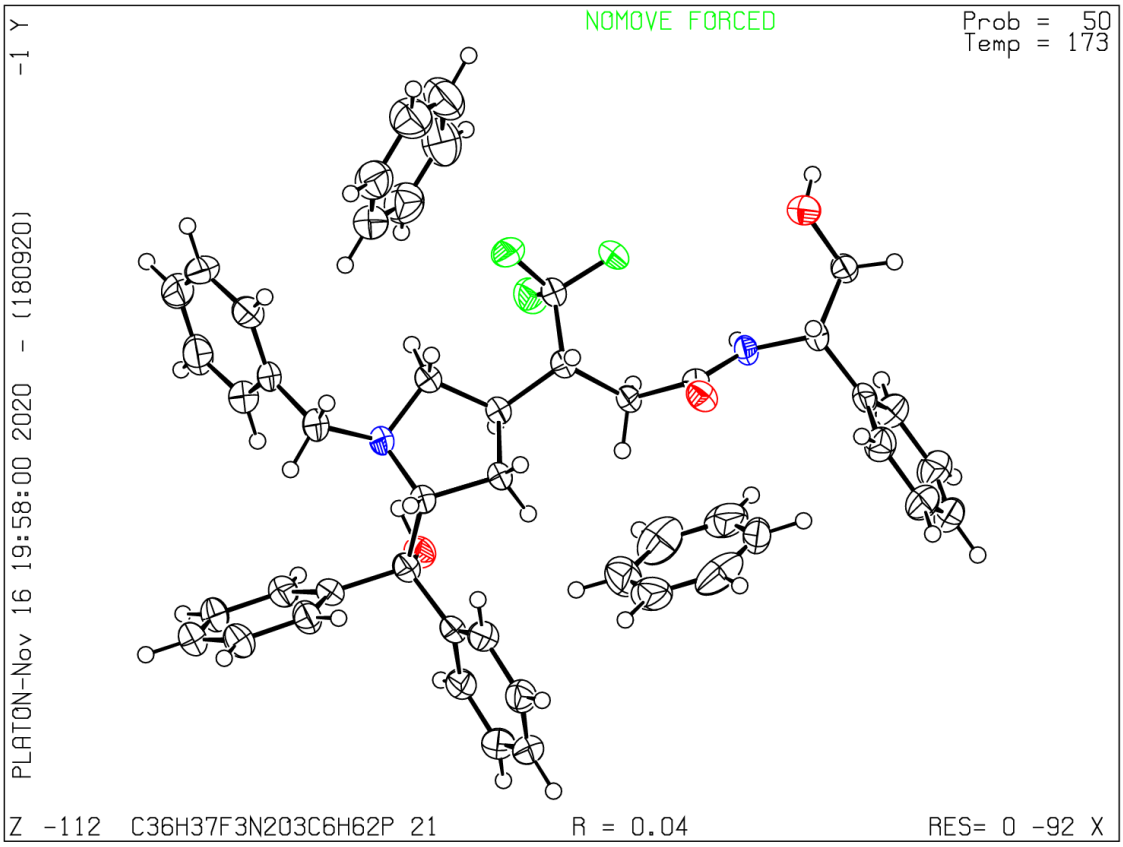

Figure S3.9. Crystal structure of **3.45**

Determination of the Absolute Configuration of 3.26f-(*R*,*S*)

The absolute configuration of **3.26f-(*R*,*S*)** was determined by X-ray crystallographic analysis of **3.29-(*R*,*S*)** (Scheme S3.11).[2]

Scheme S3.11. Derivatization of **3.26f-(*R*,*S*)** and Crystal Structure of **3.29-(*R*,*S*)**

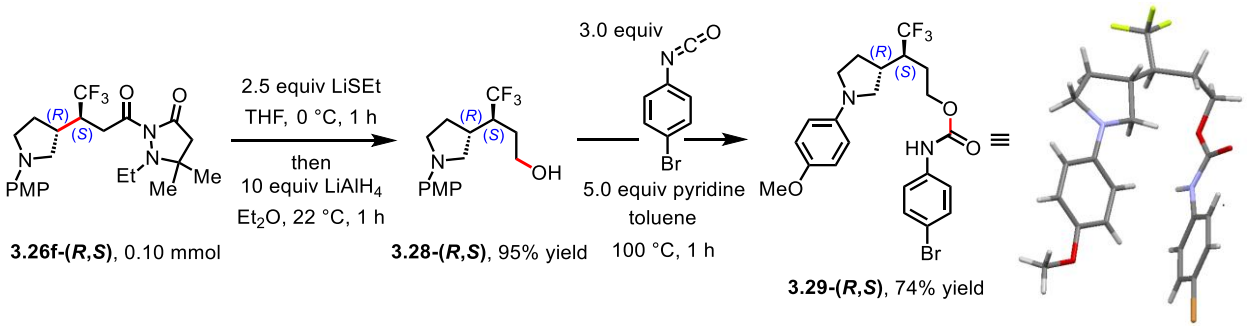

3.26f-(*R*,*S*), 0.10 mmol

3.28-(*R*,*S*), 95% yield

3.29-(*R*,*S*), 74% yield

(*S*)-4,4,4-Trifluoro-3-((*R*)-1-(4-methoxyphenyl)pyrrolidin-3-yl)butan-1-ol (3.28-(*R*,*S*))

A solution of EtSH (0.51 g, 8.2 mmol, 3.4 equiv) in THF (0.1 M) was cooled to –78 °C and treated with *n*-BuLi (3.8 mL, 6.0 mmol, 1.6 M in hexane, 2.5 equiv). The reaction was allowed to stir at 0 °C for 30 min. A solution of the **3.26f-(*R*,*S*)** (1.04 g, 2.4 mmol, 1.0 equiv) in THF (0.060 M) was then added dropwise. The reaction was allowed to stir at 0 °C until the consumption of the starting material was complete as monitored by TLC (0.5 – 1 h). The reaction was quenched with saturated NH_4Cl (aq.) and the phases separated. The aqueous layer was extracted with ethyl ether (x 3), the combined organic layers were dried over $MgSO_4$, and the solvent removed by rotary evaporation. The crude product was then dissolved in ethyl ether (0.10 M) and added to a suspension of $LiAlH_4$ (0.29 g, 7.2 mmol, 3.0 equiv) in ethyl ether at 22 °C. The mixture was stirred until the consumption of the starting material was monitored by TLC (0.5 – 2 h). The reaction was carefully quenched by the addition of water at 0 °C. The aqueous layer was then extracted with ethyl ether (x3) and the combined organic layers were dried over $MgSO_4$ and the solvents removed to yield the crude

[2] Petrone, D. A.; Isomura, M.; Franzoni, I.; Rössler, S. L.; Carreira, E. M. *J. Am. Chem. Soc.* **2018**, *140*, 4697–4704.

product, which was purified by flash silica gel column chromatography.

^{1}H NMR (500 MHz, $CDCl_3$): δ 6.85 (d, *J* = 9.0 Hz, 2H), 6.53 (d, *J* = 9.0 Hz, 2H), 3.82 (dt, *J* = 12.0, 6.4 Hz, 1H), 3.79 – 3.71 (m, 4H), 3.42 (t, *J* = 8.4 Hz, 1H), 3.36 (td, *J* = 8.7, 1.8 Hz, 1H), 3.26 (td, *J* = 9.4, 6.6 Hz, 1H), 3.06 (t, *J* = 9.1 Hz, 1H), 2.67 – 2.55 (m, 1H), 2.41 (tdd, *J* = 9.7, 6.5, 2.8 Hz, 1H), 2.22 (dt, *J* = 13.0, 6.7 Hz, 1H), 1.96 – 1.75 (m, 3H), 1.43 (s, 1H); **^{13}C NMR (126 MHz, $CDCl_3$):** δ 151.3, 142.8, 128.4 (q, *J* = 281.0 Hz), 115.2, 112.7, 60.7, 56.1, 51.6, 48.2, 42.5 (q, *J* = 24.9 Hz), 38.0, 30.3, 29.7; **^{19}F NMR (470 MHz, $CDCl_3$):** δ -68.24 (d, *J* = 9.2 Hz); **IR (neat):** ν 3385, 2933, 2831, 1514, 1485, 1371, 1239, 1158, 1126, 1039, 812 cm^{-1}; **HRMS (DART):** Calcd for $C_{15}H_{21}F_3NO_2$ (MH^+): 304.1519; found: 304.1519; **Specific Rotation $[\alpha]^{25}_D$** = -4.5° (c = 1.0, DCM).

(*S*)-4,4,4-Trifluoro-3-((*R*)-1-(4-methoxyphenyl)pyrrolidin-3-yl)butyl(4 bromophenyl)carbamate (3.29-(*R,S*))

To a solution of **3.28-(*R,S*)** (330 mg, 1.1 mmol, 1.0 equiv.) in toluene (0.035 M) were added *p*-bromophenyl isocyanate (416 mg, 3.3 mmol, 3.0 equiv.) and pyridine (434 mg, 5.5 mmol, 5.0 equiv.). The resulting heterogeneous solution was placed in an oil bath at 100 °C and was allowed to stir for 1 hour. The solution was then cooled to 22 °C and filtered through a short plug of Celite using DCM. The filtrate was concentrated and the residue was purified by flash silica gel column chromatography (EtOAc:hexanes = 1:9) to afford compound **3.29-(*R,S*)** (406 mg, 74%) as a white solid.

^{1}H NMR (600 MHz, $CDCl_3$): δ 7.41 (dd, *J* = 8.8, 1.4 Hz, 2H), 7.30 – 7.20 (m, 2H), 6.82 (d, *J* = 7.6 Hz, 2H), 6.62 (s, 1H), 6.50 (d, *J* = 7.6 Hz, 2H), 4.34 (dt, *J* = 11.8, 6.1 Hz, 1H), 4.27 – 4.16 (m, 1H), 3.75 (s, 3H), 3.42 (t, *J* = 8.4 Hz, 1H), 3.36 (t, *J* = 8.7 Hz, 1H), 3.25 (q, *J* = 8.8, 8.3 Hz, 1H),

3.05 (t, J = 8.9 Hz, 1H), 2.59 (h, J = 8.0 Hz, 1H), 2.40 – 2.28 (m, 1H), 2.22 (dt, J = 13.4, 6.8 Hz, 1H), 2.07 – 1.92 (m, 2H), 1.87 (p, J = 10.0 Hz, 1H); **^{13}C NMR (151 MHz, $CDCl_3$):** δ 153.1, 151.2, 142.6, 136.9, 132.1, 128.0 (q, J = 280.8 Hz), 120.4, 115.1, 112.6, 63.3, 56.0, 51.5, 48.0, 42.8 (q, J = 25.1 Hz), 37.9, 30.2, 26.5; **^{19}F NMR (564 MHz, $CDCl_3$):** δ -68.15 (d, J = 9.4 Hz); **IR (neat):** ν 3310, 2924, 2831, 1708, 1592, 1511, 1486, 1396, 1371, 1305, 1233, 1212, 1162, 1129, 1073, 1006, 890, 810, 764, 735, 700, 650, 626, 592, 521, 503, 458 cm^{-1}; **HRMS (DART):** Calcd for $C_{22}H_{25}BrF_3N_2O_3$ (MH^+): 501.0995; found: 501.0964; **Specific Rotation $[\alpha]^{25}_D$** = 20.0° (c = 1.0, DCM).

3.29-(*R,S*) was recrystallized using the vapor-vapor diffusion method, using *i*-PrOH to dissolve the product in an inner vial, and pentane as the precipitant placed in the outer vial in order for slow diffusion to occur into the inner vial. The solution was cooled to 0 °C, whereupon a crystal was obtained for the X-ray crystallography (Scheme S11). The X-ray crystallographic analysis revealed that the absolute configuration of **3.29** is (*R,S*).

Determination of the Absolute Configuration of 3.26g

The absolute configuration of **3.26g** was determined by analogy to **3.26f-major** and by 1D NOESY experiments. The following are the NOE spectra and assignments (**Figure S3.10**).

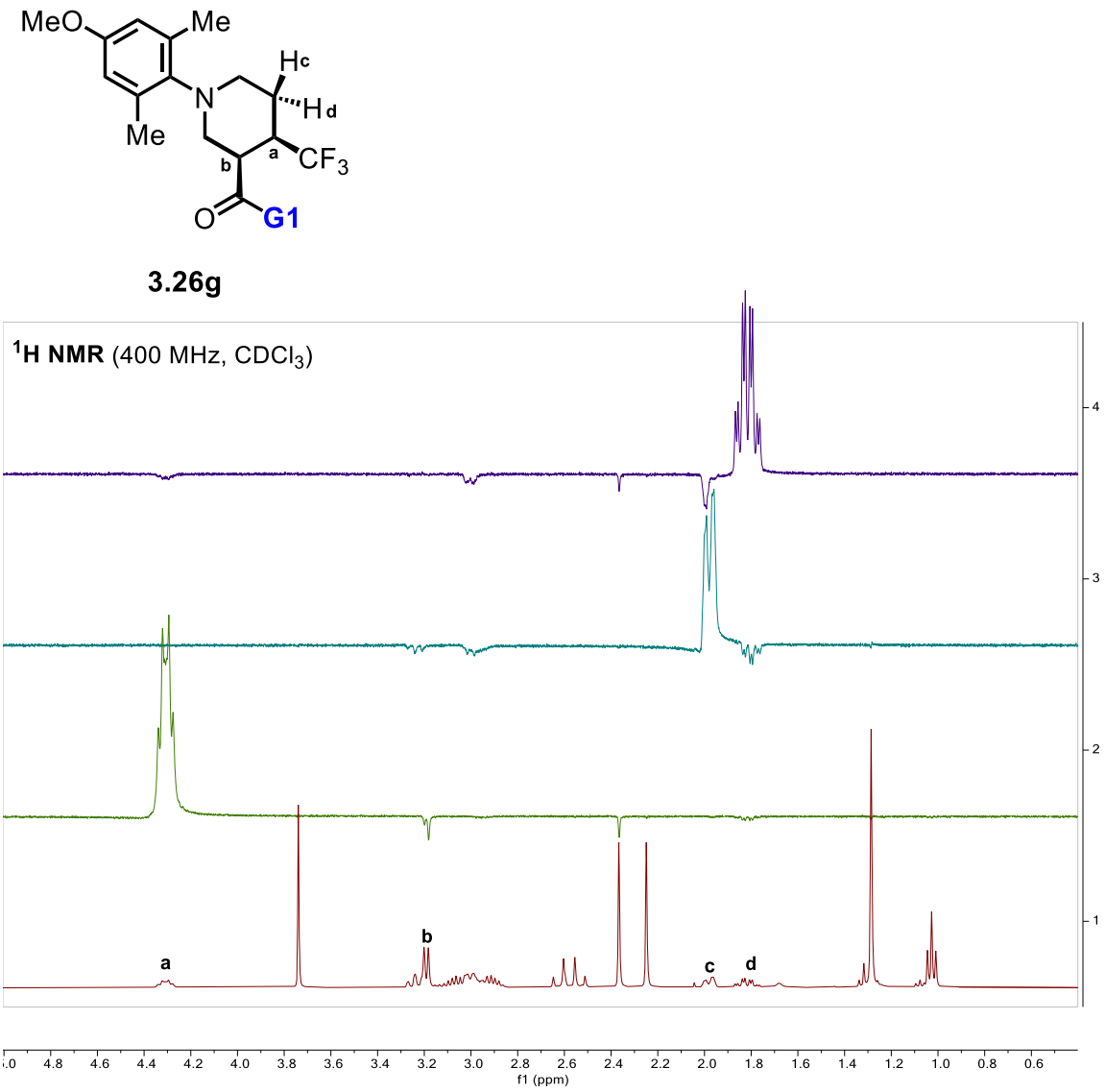

Figure S3.10. 1D NOESY spectra of **3.26g**

The NOE study revealed that the absolute configuration of **3.26g** is (*R,R*).

C6. Derivatization of β-Alkylated Amines

Hydrogenation of 3.26h

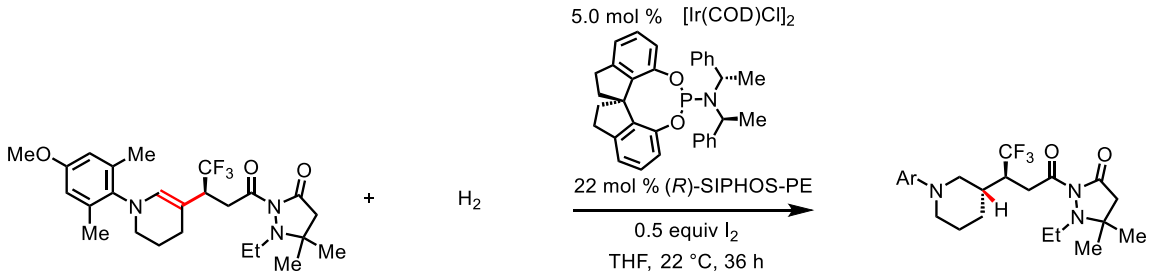

3.26h, 0.10 mmol, 95:5 er 4.0 atm H_2 **3.30**, 83% yield, 5.0:1 dr

Diastereoselective hydrogenation of enamine **3.26h** was achieved following a previously reported literature.[19] In a nitrogen filled glove box, Ir[(COD)Cl]$_2$ (3.4 mg, 5.0 mol%), (*R*)-SIPHOS-PE (11.1 mg, 22 mol%), and 1.0 mL THF were added to an oven-dried 7.0 mL vial. The mixture was allowed to stir at 22 ℃ for 30 min and then transferred to an oven-dried 100 mL Schlenk flask. Then, I_2 (12.7 mg, 0.5 equiv), **3.26h** (48.2 mg, 0.10 mmol) and 1.0 mL THF were added to the mixture and then the Schlenk flask was taken out of the glove box. The nitrogen atmosphere in the Schlenk flask was replaced by hydrogen three times and finally hydrogen gas was charged at –200 ℃. The reaction mixture was slowly warmed up to 22 ℃ and was allowed to stir for 36 hours (under 4.0 atm H_2 pressure). ^{19}F NMR analysis of the unpurified product mixture revealed that the diastereomeric ratio was 5.0:1. After purification by flash silica gel column chromatography (EtOAc:hexanes = 1:3), **3.30** was obtained as a mixture of diastereomers (40.0 mg, 83% yield). Further purification was carried out by PTLC using ethyl ether:hexanes = 2:1 as the eluent to obtain **3.30-major**.

3.30-Major. **^{1}H NMR (400 MHz, $CDCl_3$):** δ 6.58 (d, *J* = 3.0 Hz, 1H), 6.45 (d, *J* = 3.0 Hz, 1H), 3.74 (s, 3H), 3.23 (dd, *J* = 17.7, 6.2 Hz, 1H), 3.09 – 2.90 (m, 7H), 2.85 (d, *J* = 11.3 Hz, 1H), 2.63 – 2.53 (m, 2H), 2.26 (d, *J* = 13.2 Hz, 6H), 2.10 – 2.01 (m, 1H), 1.93 (d, *J* = 13.3 Hz, 1H), 1.75 –

1.61 (m, 2H), 1.31 – 1.26 (m, 7H), 1.04 (t, J = 7.1 Hz, 3H); **^{13}C NMR (101 MHz, $CDCl_3$):** δ 175.5, 168.7, 156.5, 142.5, 139.0, 137.9, 128.1 (q, J = 281.1 Hz), 114.2, 113.4, 60.7, 55.4, 54.1, 50.8, 47.2, 44.1, 41.7 (q, J = 25.1 Hz), 37.4, 32.8, 28.7, 27.1, 25.9, 25.8, 20.2, 19.7, 12.8; **^{19}F NMR (376 MHz, $CDCl_3$):** δ -66.80 (d, J = 10.1 Hz); **IR (neat):** ν 2930, 2851, 1745, 1711, 1602, 1485, 1466, 1372, 1309, 1254, 1222, 1189, 1154, 1119, 1067, 990, 855, 616 cm^{-1}; **HRMS (DART):** Calcd for $C_{25}H_{37}F_3N_3O_3$ (MH^+): 484.2782; found: 484.2785; **Specific Rotation $[\alpha]^{25}_D$** = -8.0° (c = 0.35, DCM).

3.30 (major:minor = 1:1.3). **^{1}H NMR (400 MHz, $CDCl_3$, *peaks from diastereomers are merged*):** 6.58 (d, J = 3.1 Hz, 1H), 6.45 (d, J = 3.0 Hz, 1H), 3.74 (s, 3H), 3.28 – 3.15 (m, 1H), 3.10 – 2.92 (m, 7H), 2.89 – 2.80 (m, 1H), 2.67 – 2.51 (m, 2H), 2.29 – 2.21 (m, 6H), 2.11 – 1.99 (m, 1H), 1.97 – 1.84 (m, 1H), 1.76 – 1.60 (m, 2H), 1.33 – 1.25 (m, 7H), 1.12 – 1.01 (m, 3H); **^{19}F NMR (376 MHz, $CDCl_3$):** δ -66.80 (d, J = 10.1 Hz, *major*), -67.20 (d, J = 10.2 Hz, *minor*).

Fluorocyanation of 3.26h

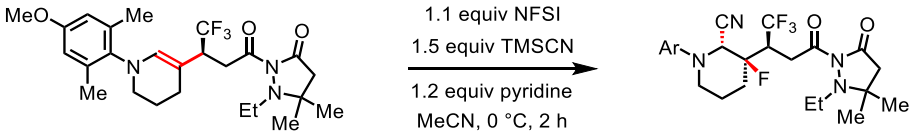

3.26h, 0.1 mmol, 95:5 er

3.31, 88% yield, 4.0:1 dr

Fluorocyanation of enamine **3.26h** was achieved following a previously reported literature.[20] To an oven-dried 10 mL round bottom flask was added NFSI (34.7 mg, 1.1 equiv), TMSCN (0.02 mL, 1.5 equiv) and 0.50 mL of MeCN. After the mixture was cooled to 0 °C, pyridine (0.01 mL, 1.2 equiv) and **3.26h** (48.2 mg, 0.10 mmol) were added. The reaction mixture was allowed to stir at 0 °C for 1 hour. Upon completion, the mixture was quenched with saturated aqueous $NaHCO_3$ and extracted with ethyl ether three times. The combined organic layer was washed with brine, dried with $MgSO_4$ and was concentrated *in vacuo*. The ^{19}F NMR analysis of the unpurified product mixture revealed that the diastereomeric ratio was 4.0:1. After purification by flash silica gel column chromatography (EtOAc:hexanes = 1:3), **3.31** was obtained as a mixture of diastereomers (46.5 mg, 88% yield). Further purification was carried out by PTLC using EtOAc:hexanes = 1:3 as the eluent to separate **3.31-major** and **3.31-minor**.

3.31-Major. **^{1}H NMR (600 MHz, $CDCl_3$):** δ 6.56 (d, *J* = 3.1 Hz, 1H), 6.50 (d, *J* = 3.1 Hz, 1H), 4.15 (d, *J* = 4.9 Hz, 1H), 3.82 – 3.70 (m, 4H), 3.64 (t, *J* = 11.6 Hz, 1H), 3.47 (ddd, *J* = 19.1, 6.4, 2.3 Hz, 1H), 3.16 (dd, *J* = 19.4, 4.3 Hz, 1H), 3.06 – 2.92 (m, 3H), 2.62 (d, *J* = 17.3 Hz, 1H), 2.55 (d, *J* = 17.3 Hz, 1H), 2.47 (s, 3H), 2.35 – 2.24 (m, 4H), 2.19 – 2.01 (m, 2H), 1.77 – 1.67 (m, 1H), 1.33 – 1.24 (m, 7H), 1.04 (t, *J* = 7.1 Hz, 3H); **^{13}C NMR (151 MHz, $CDCl_3$):** δ 175.5, 167.7, 157.4, 139.1, 138.95, 138.86, 126.4 (q, *J* = 281.9 Hz), 117.1 (d, *J* = 10.2 Hz), 114.7, 114.3, 92.3 (d, *J* = 193.6 Hz), 60.9, 58.8 (d, *J* = 29.9 Hz), 55.4, 47.5, 47.2, 44.6 (qd, *J* = 26.1, 21.4 Hz), 43.8, 31.8

(dd, *J* = 9.1, 2.6 Hz), 28.9 (dd, *J* = 22.4, 2.7 Hz), 26.1, 25.6, 21.6, 21.1, 19.5 (d, *J* = 7.0 Hz), 12.8; **^{19}F NMR (564 MHz, $CDCl_3$):** δ -63.97 – -64.00 (m), -161.94; **IR (neat):** ν 2961, 2839, 1746, 1711, 1601, 1485, 1466, 1442, 1375, 1304, 1263, 1234, 1216, 1155, 1132, 1094, 1069,992, 975, 950, 930, 898, 856, 736, 619 cm^{-1}; **HRMS (DART):** Calcd for $C_{26}H_{35}F_4N_4O_3$ (MH^+): 527.2640; found: 527.2640; **Specific Rotation $[\alpha]^{25}_D$** = +6.9° (c = 1.0, DCM).

3.31-Minor. **^{1}H NMR (400 MHz, $CDCl_3$):** δ 6.58 (d, *J* = 3.0 Hz, 1H), 6.49 (d, *J* = 3.0 Hz, 1H), 4.50 (d, *J* = 20.3 Hz, 1H), 4.10 (tt, *J* = 9.8, 5.7 Hz, 1H), 3.74 (s, 3H), 3.45 (dd, *J* = 17.8, 5.1 Hz, 1H), 3.27 (ddd, *J* = 18.0, 6.5, 2.4 Hz, 1H), 3.19 – 3.03 (m, 2H), 3.01 (q, *J* = 7.1 Hz, 2H), 2.60 (d, *J* = 3.4 Hz, 2H), 2.40 – 2.26 (m, 7H), 2.09 – 1.95 (m, 1H), 1.89 – 1.63 (m, 3H), 1.31 (d, *J* = 1.7 Hz, 6H), 1.06 (t, *J* = 7.1 Hz, 3H); **^{13}C NMR (126 MHz, $CDCl_3$):** δ 175.8, 167.0, 157.9, 140.8, 138.4, 138.1, 125.9 (q, *J* = 280.2 Hz), 114.7 (d, *J* = 1.9 Hz), 114.5, 114.0, 91.8 (d, *J* = 192.2 Hz), 60.7, 59.4 (dd, *J* = 20.1, 2.5 Hz), 55.3, 49.8, 47.1, 44.9 (p, *J* = 26.2 Hz), 44.2, 31.2 (dd, *J* = 6.7, 2.7 Hz), 29.1, 29.0, 25.9 (d, *J* = 13.1 Hz), 21.0 (d, *J* = 2.8 Hz), 19.7, 19.6, 12.7; **^{19}F NMR (470 MHz, $CDCl_3$):** δ -64.16 – -64.69 (m), -159.84; **IR (neat):** ν 2925, 2851, 1744, 1712, 1602, 1484, 1465, 1443, 1374, 1302, 1263, 1225, 1196, 1183, 1144, 1113, 1070, 1023, 992, 949, 855, 835, 796, 769, 734, 619, 458 cm^{-1}; **HRMS (DART):** Calcd for $C_{26}H_{35}F_4N_4O_3$ (MH^+): 527.2640; found: 527.2641; **Specific Rotation $[\alpha]^{25}_D$** = -8.3° (c = 0.50, DCM).

C7. Mechanistic Studies for β-Amino C–H Alkylation Reaction

We have demonstrated that cooperative functions of $B(C_6F_5)_3$ and a chiral Lewis acid co-catalyst can promote highly enantioselective union of *N*-alkylamines and α,β-unsaturated compounds. To shed light on the mechanism of this enantioselective process, we embarked on investigations that were aimed at determining its turnover-limiting step, understanding the nature of hydride and proton transfer processes, and elucidating the origin of chemoselectivity between enamine and *N*-alkylamine products.

Following are the mechanistic studies that were carried out to obtain the necessary data:

Determination of the reaction orders involving **3.25g**

Detection of the catalyst resting state involving **3.25g**

Kinetic isotope effect studies involving **3.25g**

Hammett studies

Monitoring the ratios at which different products are formed by the ^1H NMR studies.

Determination of the reaction orders involving **3.25d**

Detection of the catalyst resting state involving **3.25d**

Kinetic isotope effect studies involving **3.25d**

Mechanistic Studies Involving 3.25g

Determination of the Reaction Orders

For the *β*-C–H alkylation reaction involving 1-(4-methoxyphenyl)pyrrolidine **3.21r** and 1-benzyl-2-cinnamoyl-5,5-dimethylpyrazolidin-3-one **3.25g**, the reaction order of each reactant was studied through time course reaction monitoring by the ^{1}H NMR spectroscopic analysis.

Reaction Order of $B(C_6F_5)_3$

The reaction between **3.21r** and **3.25g** was performed using different concentrations of $B(C_6F_5)_3$ and the progress of each reaction was monitored by the ^{1}H NMR spectroscopy (Scheme S12).

Scheme S3.12. Determination of the Reaction Order of $B(C_6F_5)_3$

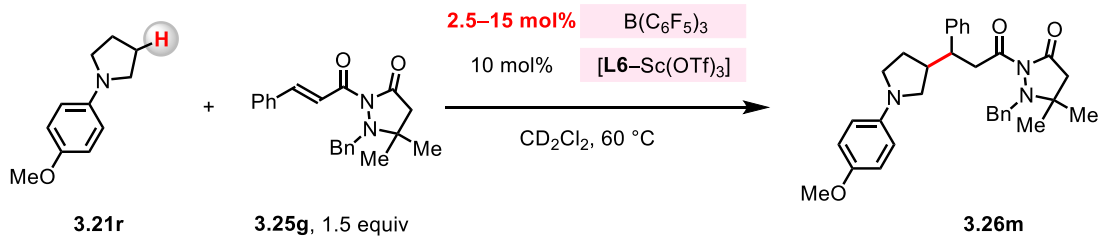

In a nitrogen-filled glove box, **L6**–$Sc(OTf)_3$ (51.4 mg, 10 mol%), **3.21r** (115.1 mg, 0.65 mmol), **3.25g** (326.1 mg, 1.5 equiv) and mesitylene (78.0 mg, 1.0 equiv) were weighed in an oven-dried 7.0 mL vial and the resulting mixture was dissolved in 3.25 mL of CD_2Cl_2 (**Stock Solution A**). In another oven-dried 7.0 mL vial, $B(C_6F_5)_3$ (30.7 mg, 0.060 mmol) was weighed and dissolved in 1.20 mL of CD_2Cl_2 (**Stock Solution B**). To each J-Young tube was added **Stock Solution A** (0.50 mL), **Stock Solution B** (0.05, 0.10, 0.15, 0.20, 0.25, or 0.30 mL) and CD_2Cl_2 (0.25, 0.20, 0.15, 0.10, 0.05 or 0 mL) to prepare the reaction samples containing different concentrations of $B(C_6F_5)_3$. After the J-Young tube was tightly capped with the Teflon plug, it was taken out of the glove box and the ^{1}H NMR spectra were acquired in the NMR spectrometer preheated at 60 °C using a pre-acquisition delay in array mode with a spectrum taken every 22 seconds for the length of the experiment. The data were processed using MestReNova software and peak integrations were

normalized using mesitylene as the internal standard.

Initial-rate kinetic analysis, which was determined based on the data points acquired in the first 600 seconds, showed that there is *second-order dependency* on $B(C_6F_5)_3$ concentration in the reaction between **3.21r** and **3.25g** (Figures S3.11, 3.12).

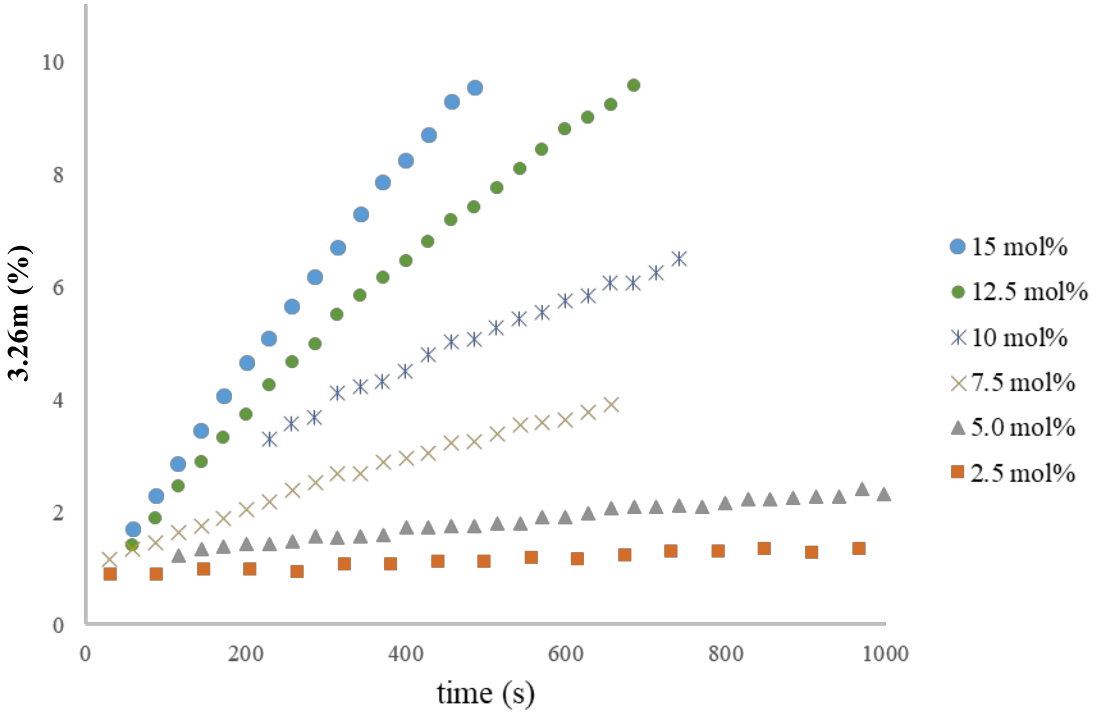

Figure S3.11. Monitoring the formation of **3.26m** under different concentrations of $B(C_6F_5)_3$

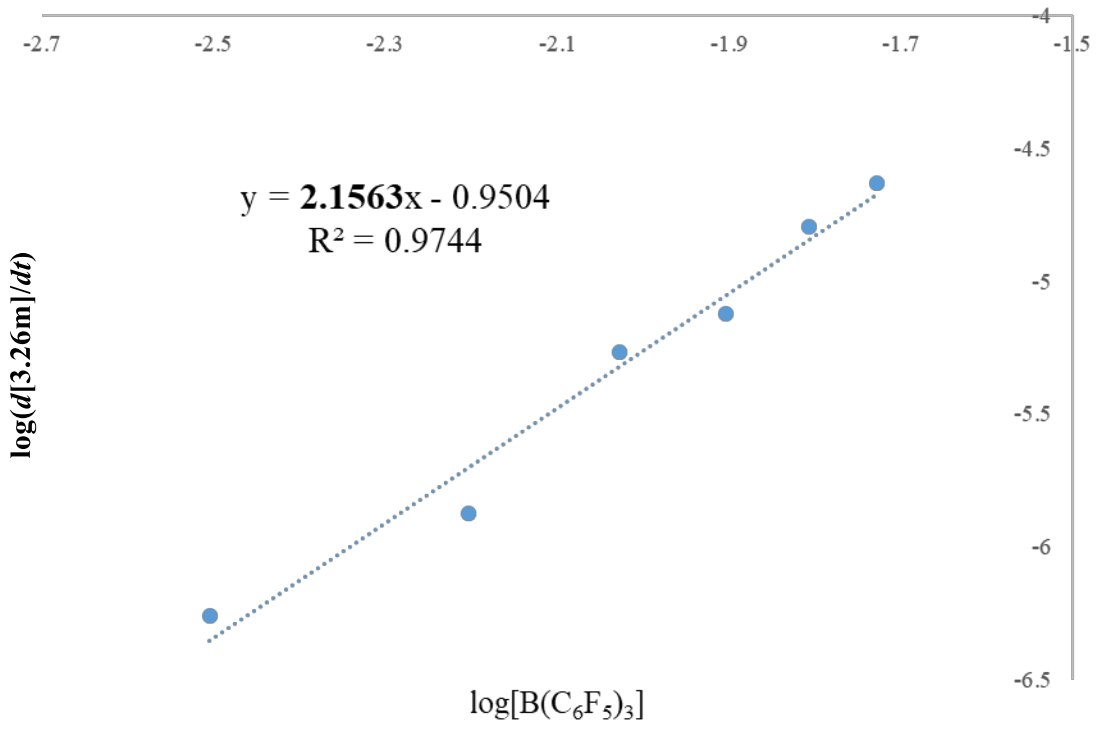

Figure S3.12. Log(rate) *vs* log[$B(C_6F_5)_3$] is employed to determine the initial reaction order for $B(C_6F_5)_3$. The result suggests that there is *second-order dependency* on $B(C_6F_5)_3$ concentration.

Reaction Order of L9–Sc(OTf)$_3$

The reaction between **3.21r** and **3.25g** was performed using different concentrations of **L6**–Sc(OTf)$_3$ and the progress of each reaction was monitored by the ^{1}H NMR spectroscopy (Scheme S3.13).

Scheme S3.13. Determination of the Reaction Order of **L6**–Sc(OTf)$_3$

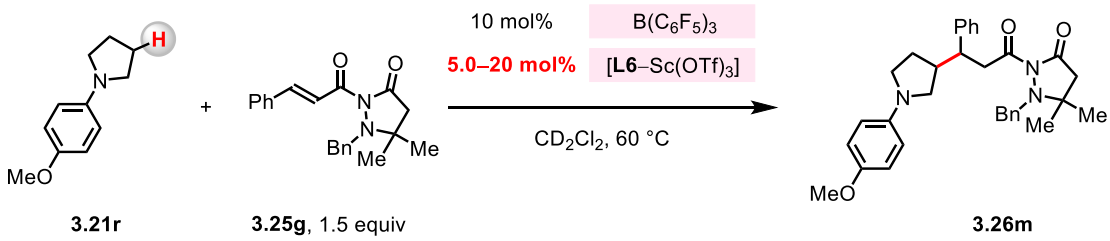

In a nitrogen-filled glove box, B(C_6F_5)$_3$ (26.6 mg, 10 mol%), **3.21r** (92.0 mg, 0.52 mmol), **3.25g** (260.8 mg, 1.5 equiv) and mesitylene (26.6 mg, 1.0 equiv) were weighed in an oven-dried 7.0 mL vial and the resulting mixture was dissolved in 2.10 mL of CD_2Cl_2 (**Stock Solution A**). In another oven-dried 7.0 mL vial, **L6**–Sc(OTf)$_3$ (47.4 mg, 0.060 mmol) was weighed and dissolved in 1.20 mL of CD_2Cl_2 (**Stock Solution B**). To each J-Young tube was added **Stock Solution A** (0.40 mL), **Stock Solution B** (0.10, 0.20, 0.30 or 0.40 mL) and neat CD_2Cl_2 (0.30, 0.20, 0.10 or 0 mL) to prepare the reaction samples containing different concentrations of **L6**–Sc(OTf)$_3$. After the J-Young tube was tightly capped with the Teflon plug, it was taken out of the glove box and ^{1}H NMR spectra were acquired in the NMR spectrometer preheated at 60 °C using a pre-acquisition delay in array mode with a spectrum taken every 22 seconds for the length of the experiment. The data were processed using MestReNova software and peak integrations were normalized using mesitylene as the internal standard.

Initial-rate kinetic analysis, which was determined based on the data points acquired in the first 1200 seconds, showed that there is *zero-order dependency* on **L6**–Sc(OTf)$_3$ concentration in the

reaction between **3.21r** and **3.25g** (Figures S3.13, S3.14).

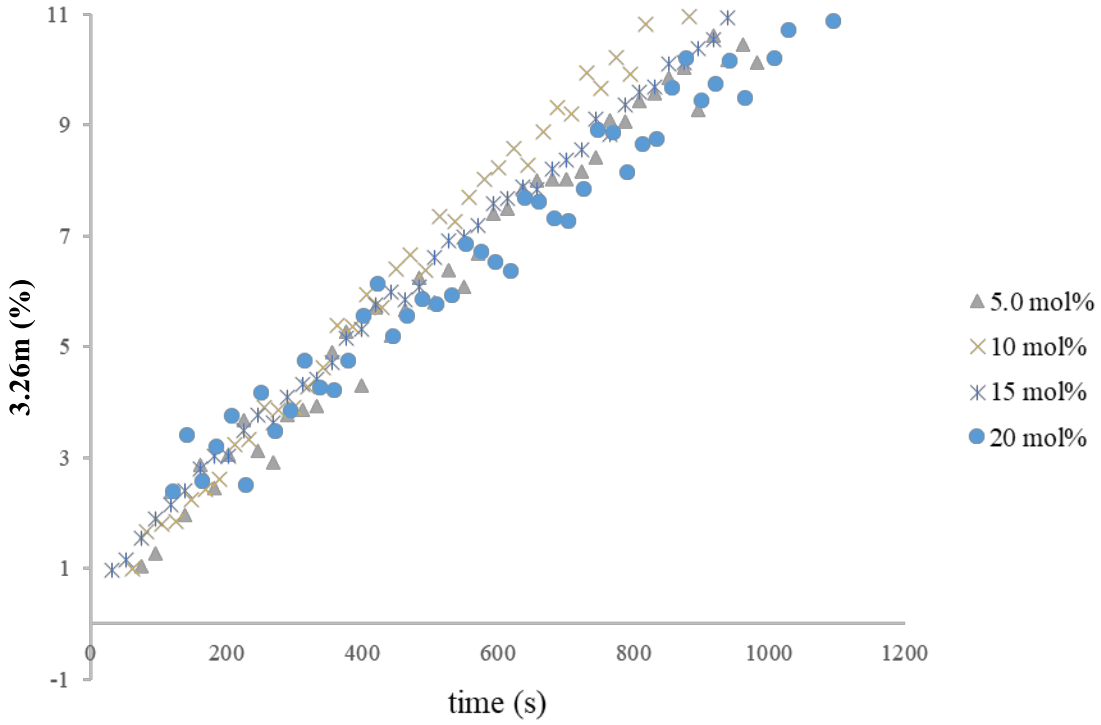

Figure S3.13. Monitoring the formation of **3.26g** under different concentrations of **L6**–$Sc(OTf)_3$

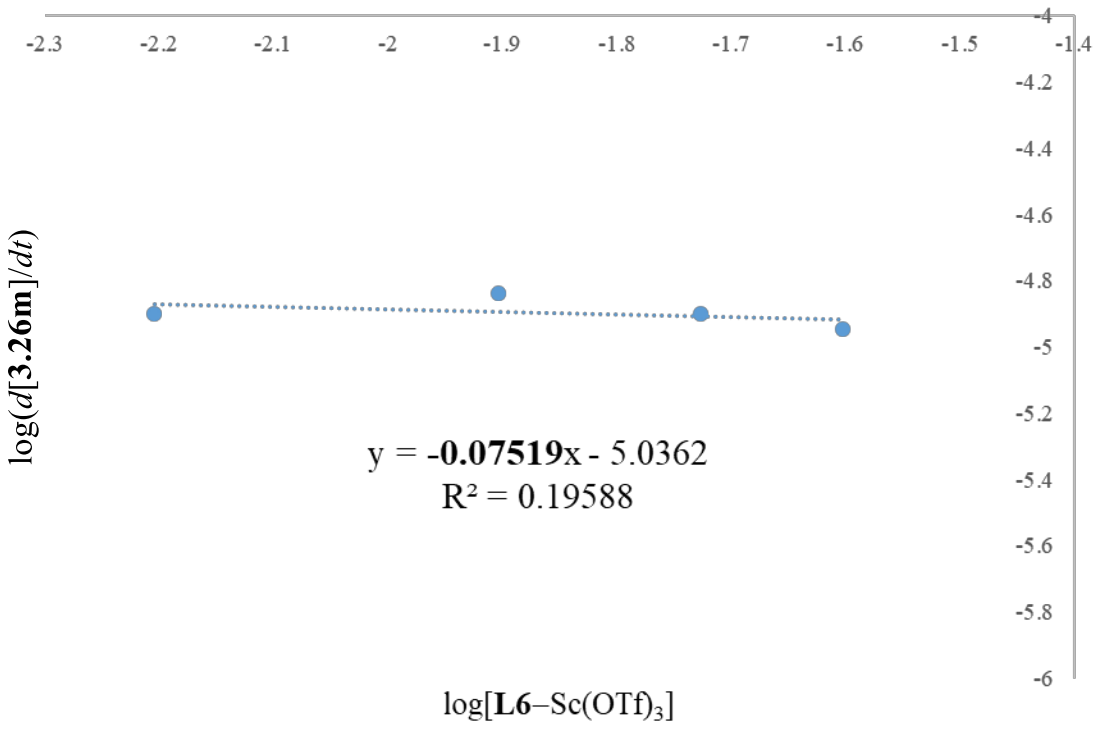

Figure S3.14. Log(rate) *vs* log[**L6**–Sc(OTf)$_3$] is employed to determine the initial reaction order for **L6**–Sc(OTf)$_3$. The result suggests that there is *zero-order dependency* on **L6**–Sc(OTf)$_3$ concentration.

Reaction Order of Amine

The reaction between **3.21r** and **3.25g** was performed using different concentrations of **3.21r** and the progress of each reaction was monitored by the ^{1}H NMR spectroscopy (Scheme S3.14).

Scheme S3.14. Determination of the Reaction Order of **3.21r**

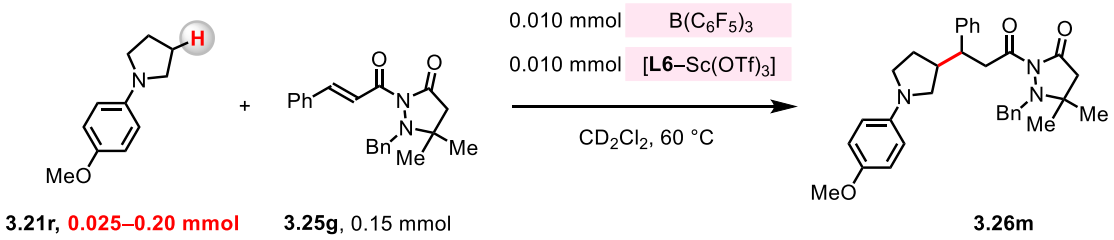

In a nitrogen-filled glove box, $B(C_6F_5)_3$ (28.2 mg, 0.055 mmol), **L6**–$Sc(OTf)_3$ (43.5 mg, 0.055 mmol), **3.25g** (275.9 mg, 0.83 mmol) and mesitylene (66.1 mg, 0.55 mmol) were weighed in an oven-dried 7.0 mL vial and the resulting mixture was dissolved in 4.40 mL of CD_2Cl_2 (**Stock Solution A**). In 5 oven-dried 7.0 mL vials were added **3.21r** (4.4 mg, 8.9 mg, 17.7 mg, 26.6 mg or 35.4 mg). To each oven-dried vial containing **3.21r** was added **Stock Solution A** (0.80 mL) to prepare the reaction samples containing different concentrations of **3.21r**. The reaction mixture was then transferred to a J-Young tube. After the J-Young tube was tightly capped with the Teflon plug, it was taken out of the glove box and ^{1}H NMR spectra were acquired in the NMR spectrometer preheated at 60 °C using a pre-acquisition delay in array mode with a spectrum taken every 22 seconds for the length of the experiment. The data were processed using MestReNova software and peak integrations were normalized using mesitylene as the internal standard.

Initial-rate kinetic analysis, which was determined based on the data points acquired in the first 600 seconds, showed that there is *first-order dependency* on amine **3.21r** concentration in the reaction between **3.21r** and **3.25g** (Figures S3.15, S3.16).

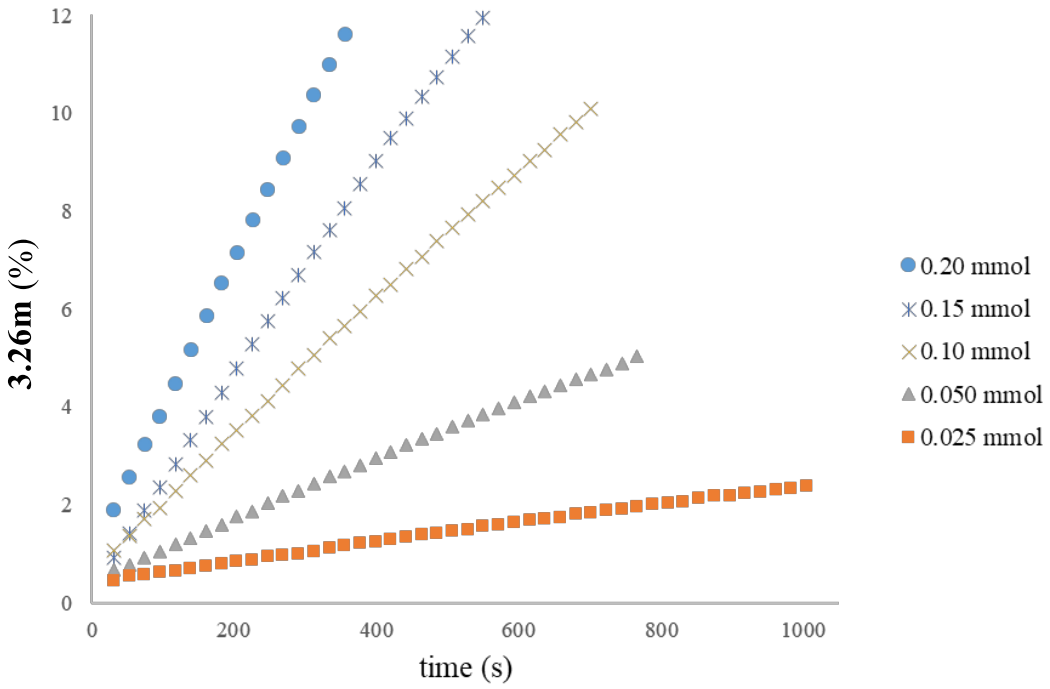

Figure S3.15. Monitoring the formation of **3.26m** under different concentrations of amine **3.21r**

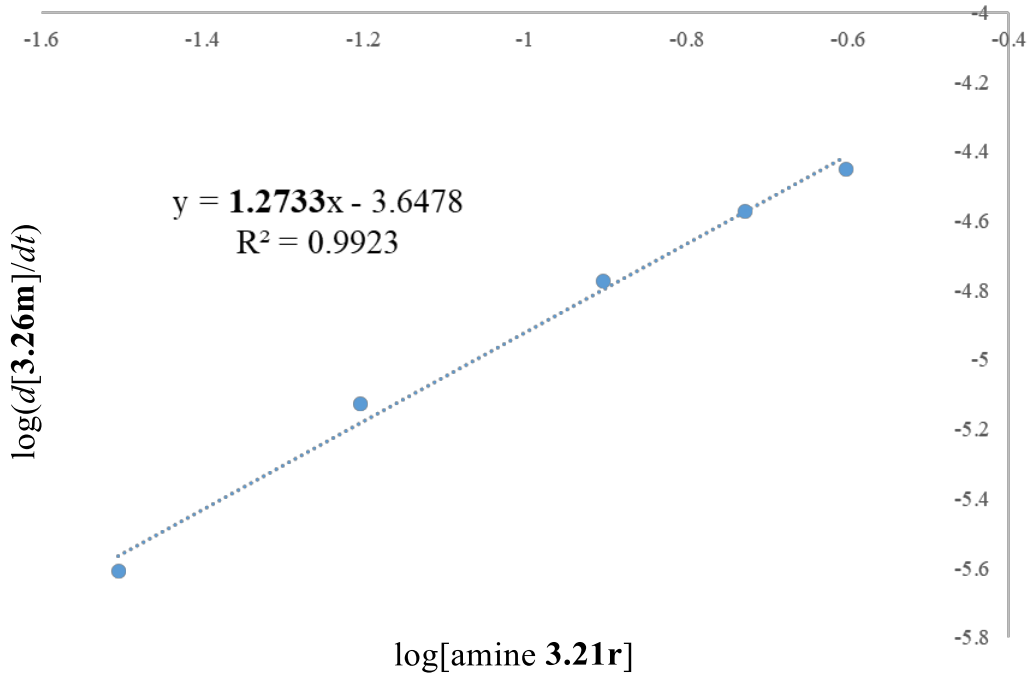

Figure S3.16. Log(rate) *vs* log[amine **3.21r**] is employed to determine the initial reaction order for amine **3.21r.** The result suggests that there is *first-order dependency* on **3.21r** concentration.

Reaction Order of *α,β*-Unsaturated Compound

The reaction between **3.21r** and **3.25g** was performed using different concentrations of **3.25g** and the progress of each reaction was monitored by the ^{1}H NMR spectroscopy (Scheme S3.15).

Scheme S3.15. Determination of the Reaction Order of **3.25g**

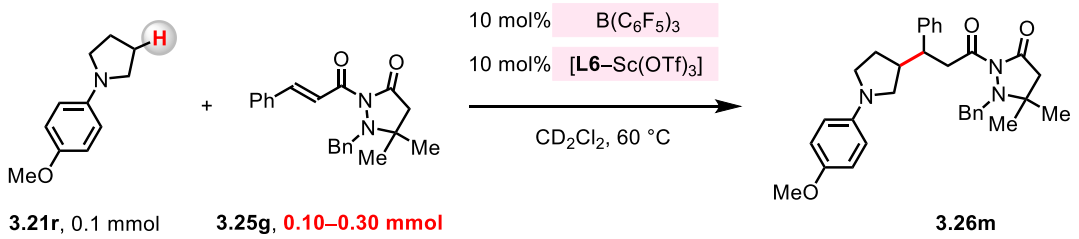

In a nitrogen-filled glove box, **L6**–Sc(OTf)$_3$ (49.0 mg, 10 mol%), **3.21r** (109.7 mg, 0.62 mmol), and mesitylene (74.4 mg, 1.0 equiv) were weighed in an oven-dried 7.0 mL vial and the resulting mixture was dissolved in 3.10 mL of CD_2Cl_2 (**Stock Solution A**). In another oven-dried 7.0 mL vial, B(C_6F_5)$_3$ (35.8mg, 0.70 mmol) was weighed and dissolved in 2.10 mL of CD_2Cl_2 (**Stock Solution B**). In 4 oven-dried 7.0 mL vials were added **3.25g** (33.4 mg, 50.2 mg, 66.9 mg, or 100.3 mg). To each oven-dried vial containing **3.25g** was added **Stock Solution A** (0.50 mL) and **Stock Solution B** (0.30 mL) to prepare the reaction samples containing different concentrations of **3.25g**. The reaction mixture was then transferred to a J-Young tube. After the J-Young tube was tightly capped with the Teflon plug, it was taken out of the glove box and ^{1}H NMR spectra were acquired in the NMR spectrometer preheated at 60 °C using a pre-acquisition delay in array mode with a spectrum taken every 22 seconds for the length of the experiment. The data were processed using MestReNova software and peak integrations were normalized using mesitylene as the internal standard.

Initial-rate kinetic analysis, which was determined based on the data points acquired in the first 600 seconds, showed that there is *–1-order dependency* on *α,β*-unsaturated compound **3.25g** concentration in the reaction between **3.21r** and **3.25g** (Figures S3.17, S3.18).

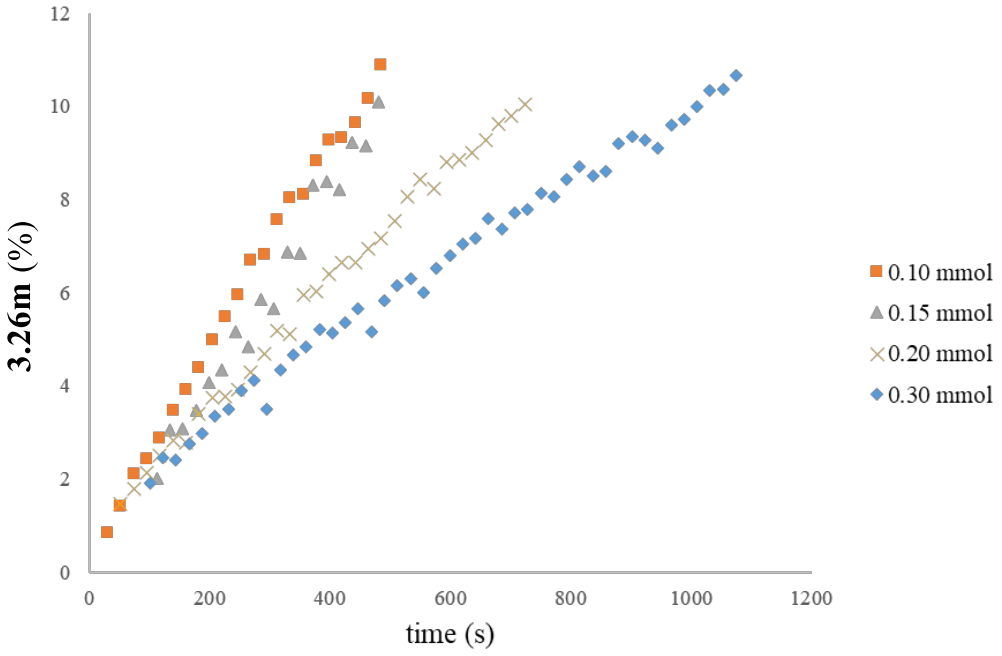

Figure S3.17. Monitoring the formation of **3.26m** under different concentrations of **3.25g**

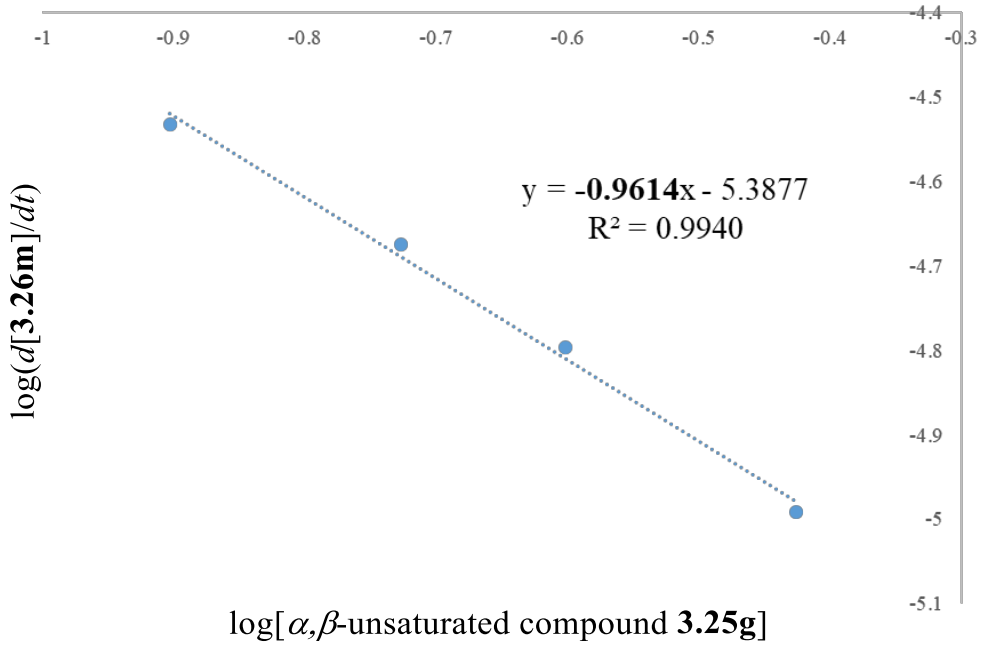

Figure S3.18. Log(rate) *vs* log[α,β-unsaturated compound **3.25g**] is employed to determine the initial reaction order for **3.25g**. The result suggests that there is *–1-order dependency* on **3.25g** concentration .

^{19}F NMR Experiments for the Detection of the Resting State

The mechanistic investigations described above revealed that the $(F_5C_6)_3B$/**L6**–$Sc(OTf)_3$ co-catalyzed *β*-amino C–H functionalization has a *–1 order dependency* with respect to the concentration of 1-benzyl-2-cinnamoyl-5,5-dimethylpyrazolidin-3-one **3.25g**. We hypothesized that **3.25g** and $B(C_6F_5)_3$ could form a resting state complex and therefore carried out the following ^{19}F NMR experiments to identify the structure of the complex (Figures S3.19, S3.20). Previously, the group of Piers has reported that $B(C_6F_5)_3$ and benzaldehyde forms an acid–base adduct, which gives characteristic ^{19}F NMR peaks at –135.3, –156.3, –164.5 ppm. We acquired the ^{19}F NMR spectrum of a sample containing 1:1 ratio of $B(C_6F_5)_3$ and **3.25g** in CD_2Cl_2 (Figures S3.19B, S3.20) and observed new ^{19}F NMR peaks at –134.8, –157.7, –164.7 ppm; based on this analysis, our spectrum is in agreement with the formation of **3.25g**–$B(C_6F_5)_3$ adduct. The resting state complex was also observed in the reaction mixture including **3.21r**, **3.25g**, $B(C_6F_5)_3$, and **L6**–$Sc(OTf)_3$ (Figure S3.19C).

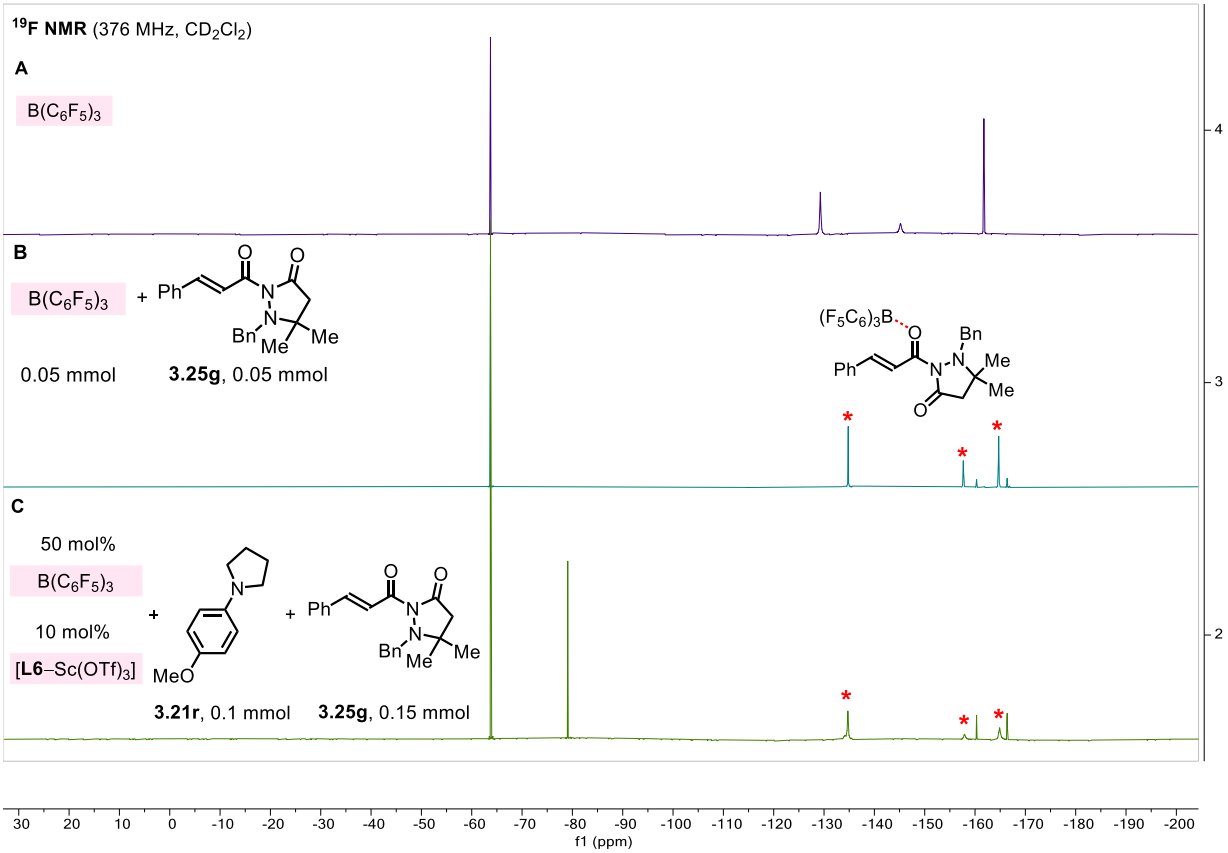

Figure S3.19. ^{19}F NMR experiments for the detection of the resting state

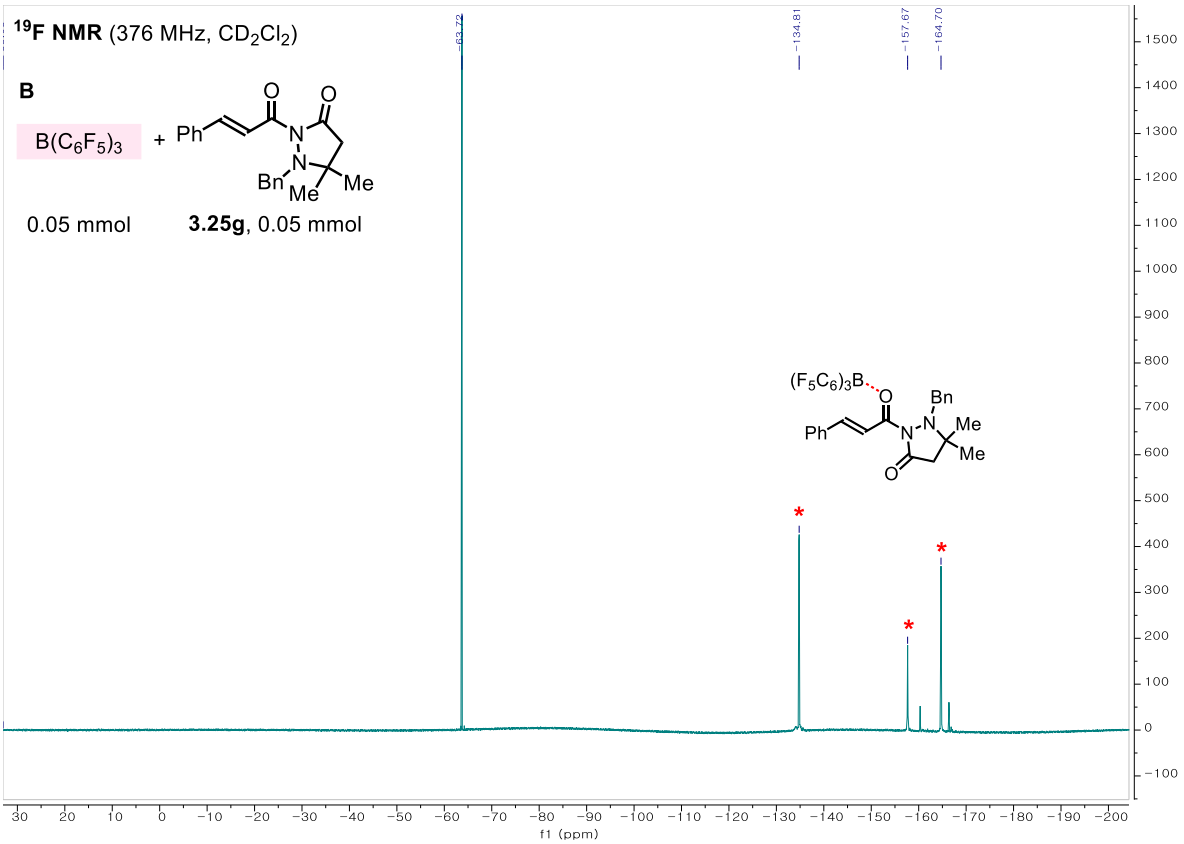

Figure S3.20. ^{19}F NMR spectrum of 3.25g–B(C$_6$F$_5$)$_3$ adduct.

Kinetic Isotope Effect Experiments

As discussed above, *zero-order dependency* with respect to concentration of **L6**–$Sc(OTf)_3$ suggests that enantioselective C–C bond forming reaction occurs after the turnover-limiting step. In order to probe whether the turnover-limiting step is the hydride abstraction or the deprotonation process, we carried out the following parallel kinetic isotope effect experiments.

Parallel KIE Measurement for *N*-Alkylamines Containing α-Amino C–H or C–D Bonds

A parallel kinetic isotope effect study was conducted through time course reaction monitoring by the ^{1}H NMR spectroscopy using internal standard to monitor the difference in initial rates of the product formation in the reaction of 1-(4-methoxyphenyl)pyrrolidine **3.21r** or 1-(4-methoxyphenyl)pyrrolidine-2,2,5,5-d_4 **3.21r-d_α** with 1-benzyl-2-cinnamoyl-5,5-dimethylpyrazolidin-3-one **3.25g** (Scheme S3.16). In a nitrogen-filled glove box, $B(C_6F_5)_3$ (20.5 mg, 0.040 mmol), **L6**–$Sc(OTf)_3$ (31.6 mg, 0.040 mmol), **3.25g** (200.8 mg, 0.60 mmol) and mesitylene (48 mg, 0.40 mmol) were weighed in an oven-dried 7.0 mL vial and the resulting mixture was dissolved in 2.00 mL of CD_2Cl_2 (**Stock Solution A**). In two oven-dried 7.0 mL vials were added **3.21r** (20.5 mg) or **3.21r-d_α** (20.9 mg). To each oven-dried vial containing **3.21r** or **3.21r-d_α** was added CD_2Cl_2 (0.30 mL) and **Stock Solution A** (0.50 mL) to prepare the reaction samples containing **3.21r** or **3.21r-d_α**. The reaction mixture was then transferred to a J-Young tube. After the J-Young tube was tightly capped with the Teflon plug, it was taken out of the glove box and ^{1}H NMR spectra were acquired in the NMR spectrometer preheated at 60 °C using a pre-acquisition delay in array mode with a spectrum taken every 22 seconds for the length of the experiment. The acquired data were processed using MestReNova software and peak integrations were normalized using mesitylene as the internal standard.

From the kinetic analysis based on the initial rates of the product formation (Figure S3.21), KIE

value of 1.28 ± 0.07 (average of two experiments) was obtained in the reaction between **3.21r** or **3.21r-*d*$_\alpha$** and **3.25g**. This suggests that the hydride abstraction step is not likely the turnover limiting process. From the ^{1}H NMR analysis of the isolated and purified **3.21r-*d*$_\alpha$** in $CDCl_3$, it was revealed that >95% of *d*-incorporation level was retained at the α-amino position (Figures S3.22–3.24). This result suggests that the borohydride reduction step may be irreversible as there was no H incorporation into the α-amino C–D bonds.

Scheme S3.16. Kinetic Isotope Effect Studies

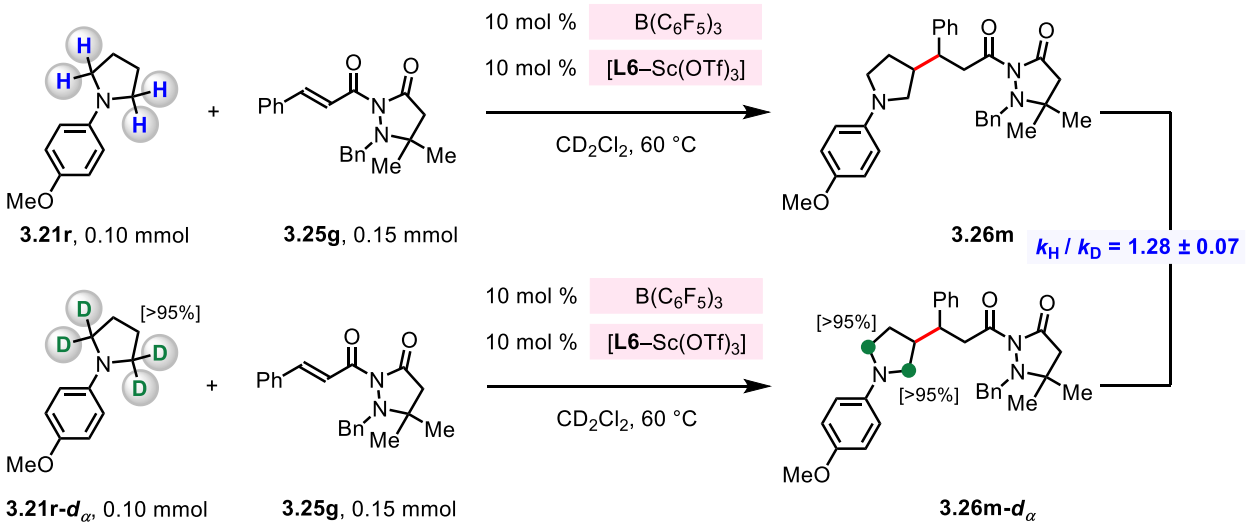

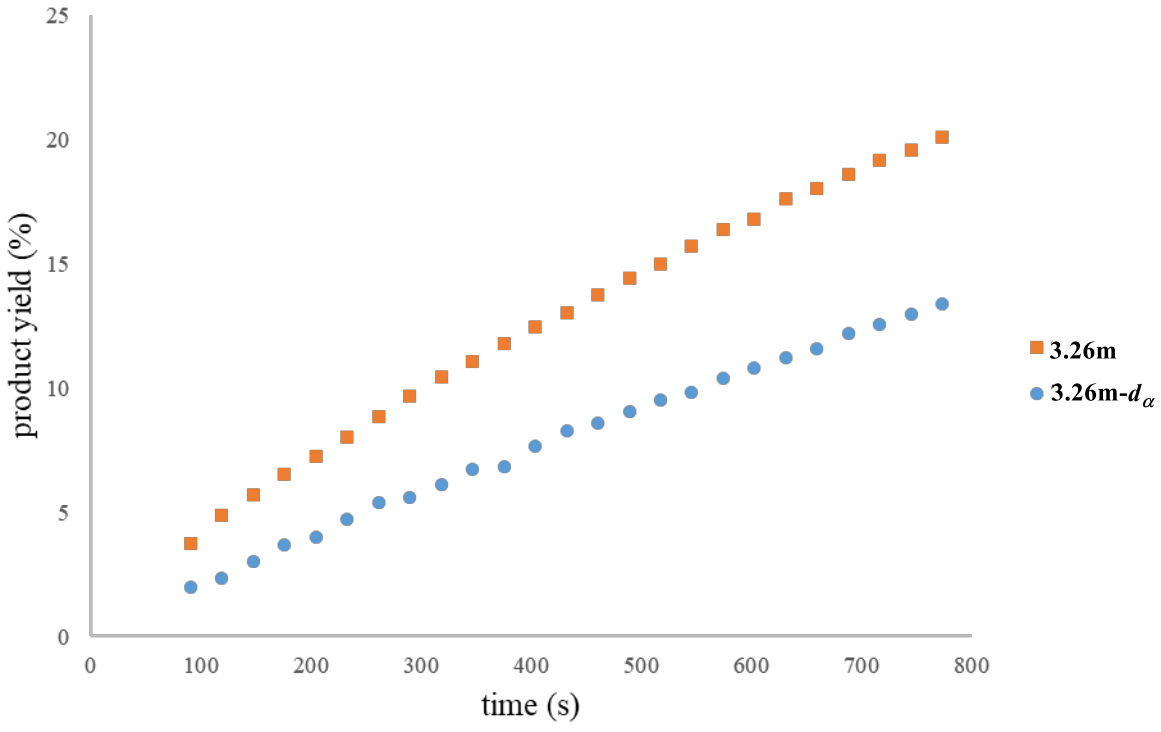

Figure S3.21. Monitoring the formation of products in parallel KIE measurements

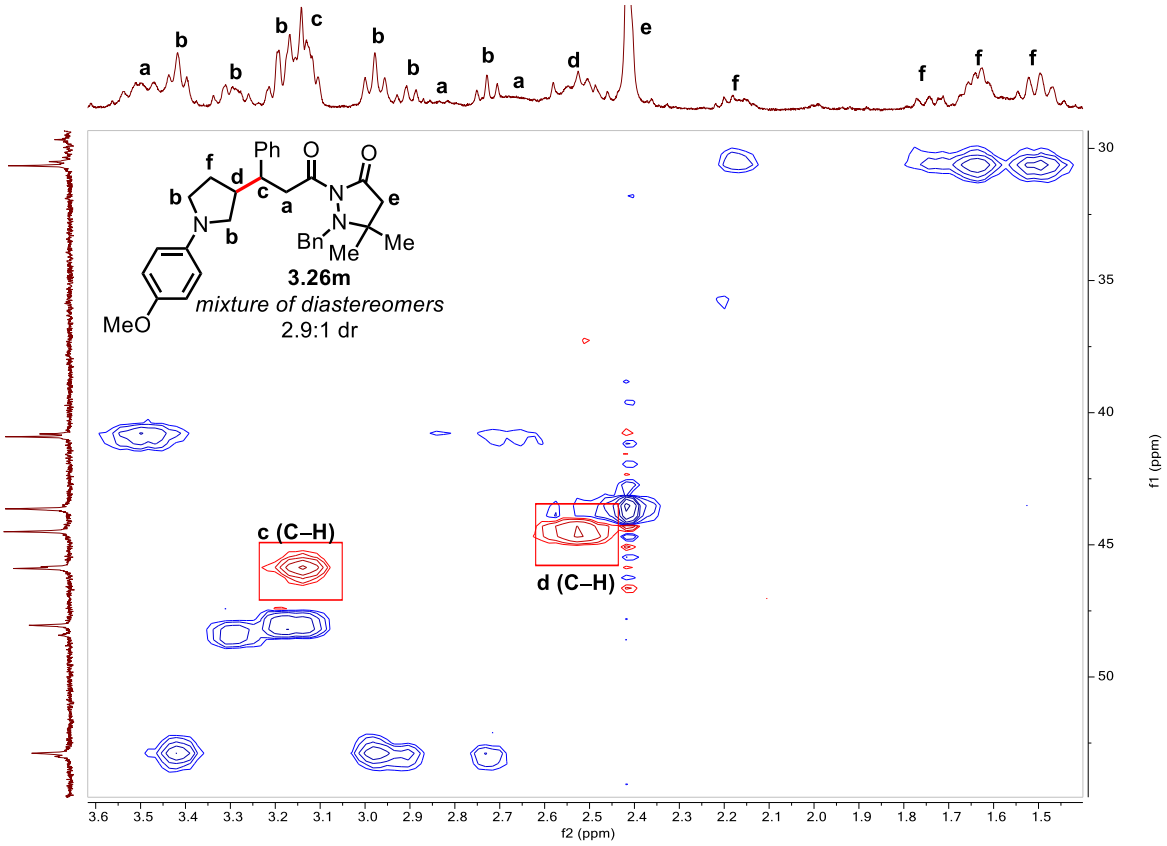

Figure S3.22. 2D HSQCAD spectra of **3.26m** in $CDCl_3$ (*for the assignment of the peaks*)

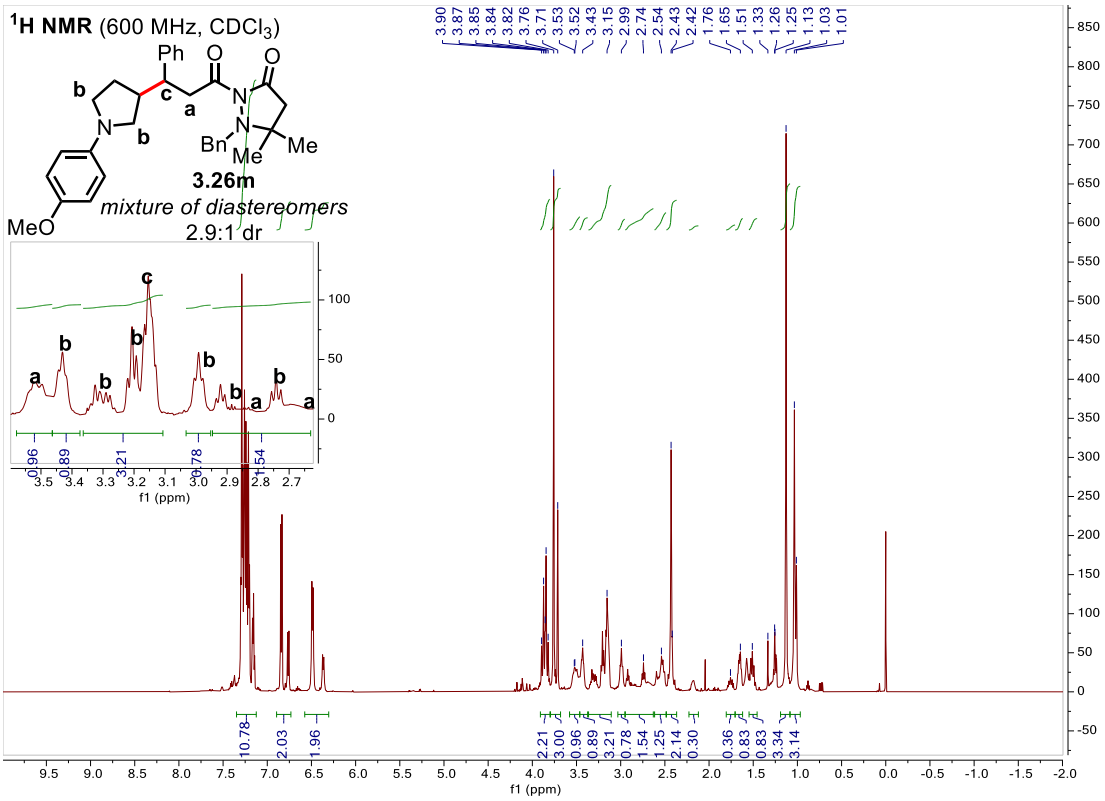

Figure S3.23. ^{1}H NMR spectrum of **3.26m**

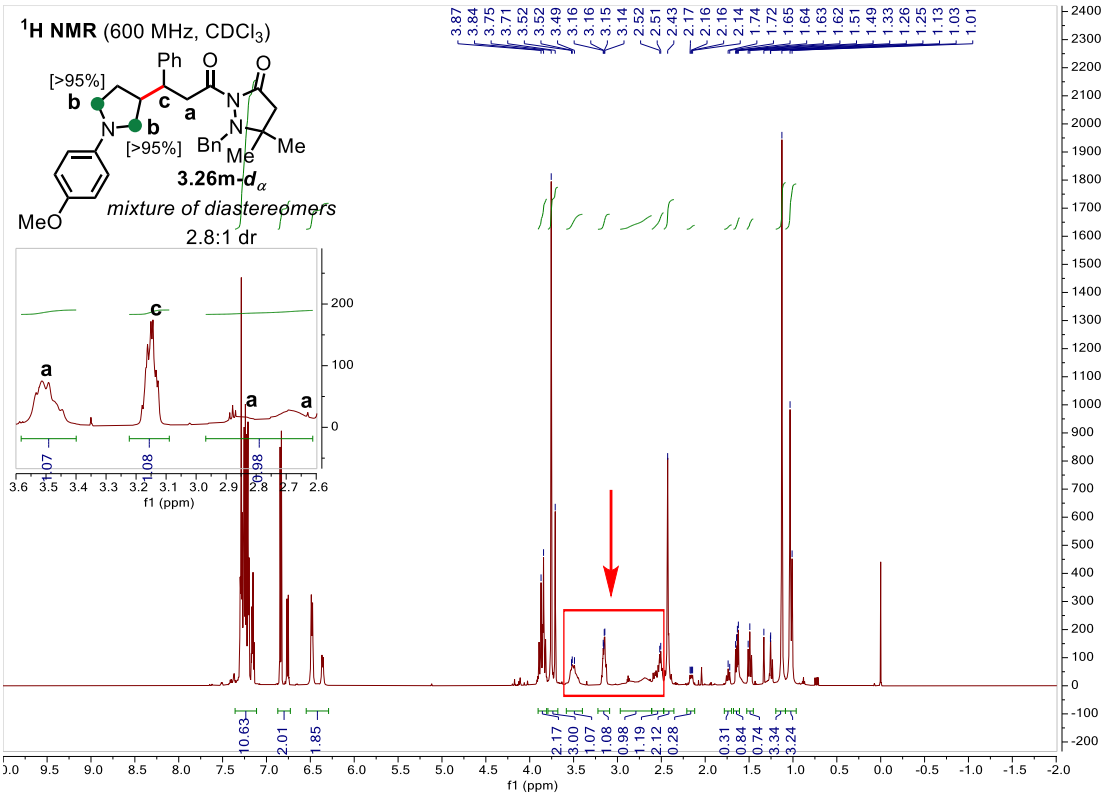

Figure S3.24. ^{1}H NMR spectrum of **3.26m-*d*$_{\alpha}$**

Parallel KIE Measurement for *N*-Alkylamines Containing *β*-Amino C–H or C–D Bonds

A parallel kinetic isotope effect study was conducted through time course reaction monitoring by the ^{1}H NMR spectroscopy using internal standard to monitor the difference in initial rates of the product formation in the reaction of 1-(4-methoxyphenyl)pyrrolidine **3.21r** or 1-(4-methoxyphenyl)pyrrolidine-3,3,4,4-d_4 **3.21r-*dβ*** with 1-benzyl-2-cinnamoyl-5,5-dimethylpyrazolidin-3-one **3.25g** (Scheme S3.17). In a nitrogen-filled glove box, $B(C_6F_5)_3$ (20.5 mg, 0.040 mmol), **L6**–$Sc(OTf)_3$ (31.6 mg, 0.040 mmol), **3.25g** (200.8 mg, 0.60 mmol) and mesitylene (48 mg, 0.40 mmol) were weighed in an oven-dried 7.0 mL vial and the resulting mixture was dissolved in 2.00 mL of CD_2Cl_2 (**Stock Solution A**). In two oven-dried 7.0 mL vials were added **3.21r** (20.5 mg) or **3.21r-*dβ*** (20.9 mg). To each oven-dried vial containing **3.21r** or **3.21r-*dβ*** was added CD_2Cl_2 (0.30 mL) and **Stock Solution A** (0.50 mL) to prepare the reaction samples containing **3.21r** or **3.21r-*dβ***. The reaction mixture was then transferred to a J-Young tube. After the J-Young tube was tightly capped with the Teflon plug, it was taken out of the glove box and ^{1}H NMR spectra were acquired in the NMR spectrometer preheated at 60 °C using a pre-acquisition delay in array mode with a spectrum taken every 22 seconds for the length of the experiment. The data were processed using MestReNova software and peak integrations were normalized using mesitylene as the internal standard.

Kinetic analysis based on the initial rates of the product formation (Figure S3.25) demonstrates that **3.21r** reacts 2.5 times faster than **3.21r-*dβ*** (k_H/k_D = 2.50 ± 0.13, average of two experiments) in the reaction between **3.21r** or **3.21r-*dβ*** and **3.25g**. This result suggests that the cleavage of *β*-amino C–H bond is likely involved in the turnover-limiting step.

From the ^{1}H NMR analysis of the isolated and purified **3.21r-*dβ*** in $CDCl_3$ and acetone-d_6, *d*-incorporation level was determined (Figures S3.26–3.30). It was found that there was a *d*-

scrambling between the substrates and the products at the β-amino C–H/D bonds and the α-carbonyl C–H/D bonds that are easily enolizable.

Scheme S3.17. Kinetic Isotope Effect Studies

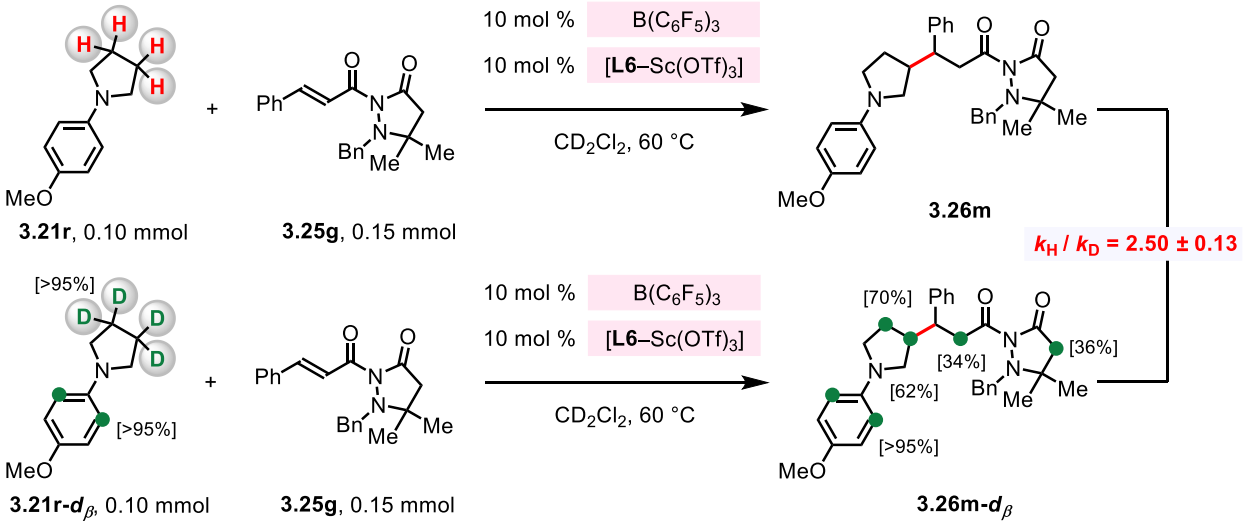

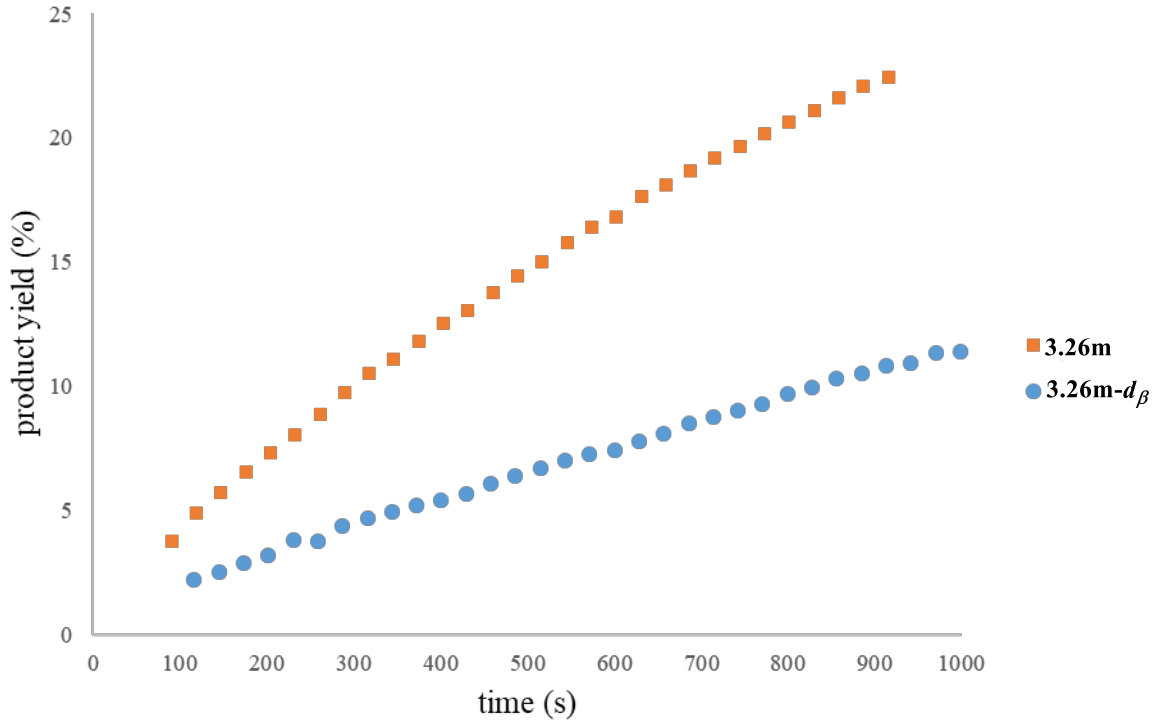

Figure S3.25. Monitoring the formation of products in parallel KIE measurements

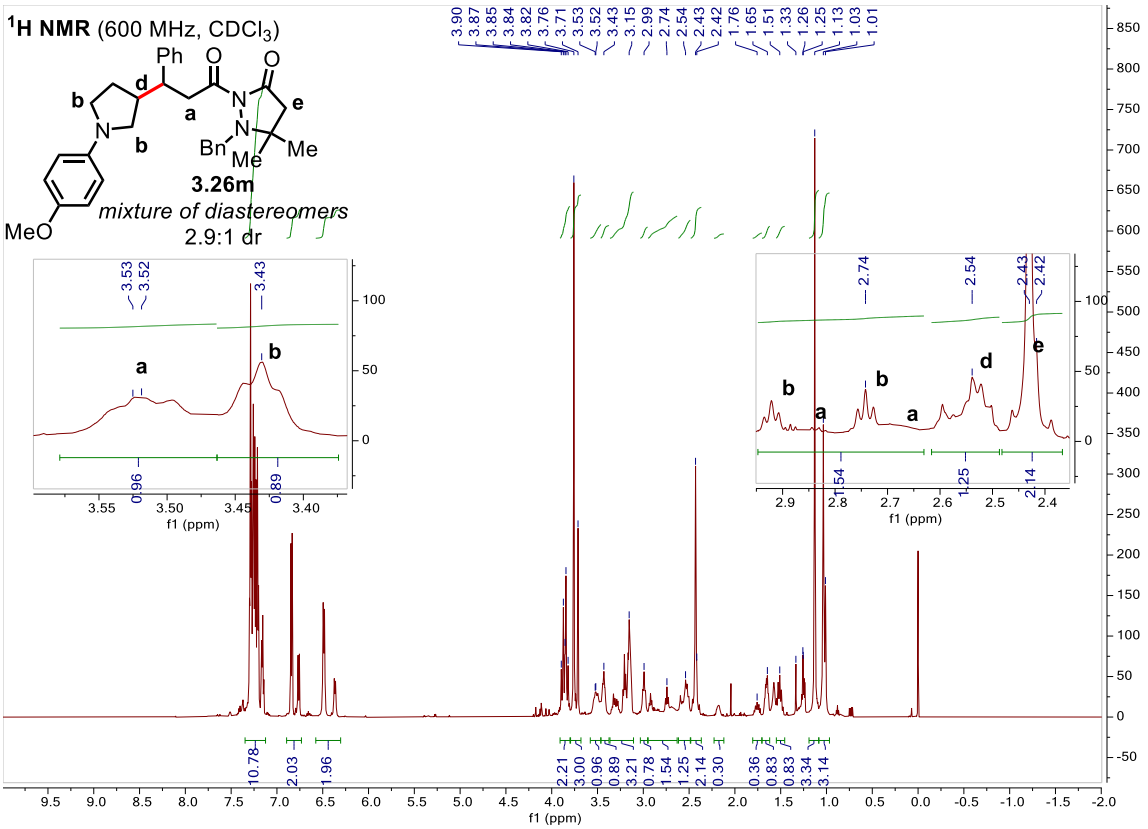

Figure S3.26. ^{1}H NMR spectrum of **3.26m** (in $CDCl_3$)

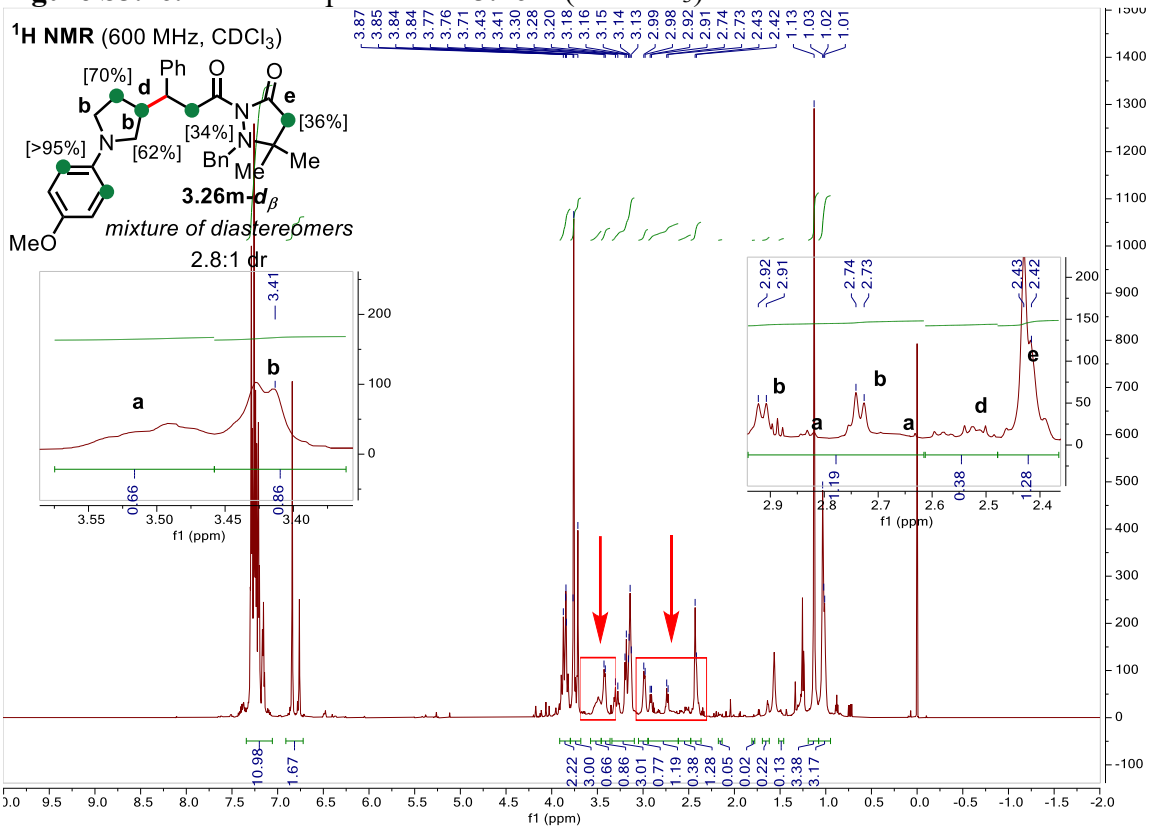

Figure S3.27. ^{1}H NMR spectrum of **3.26m-*dβ*** (in $CDCl_3$)

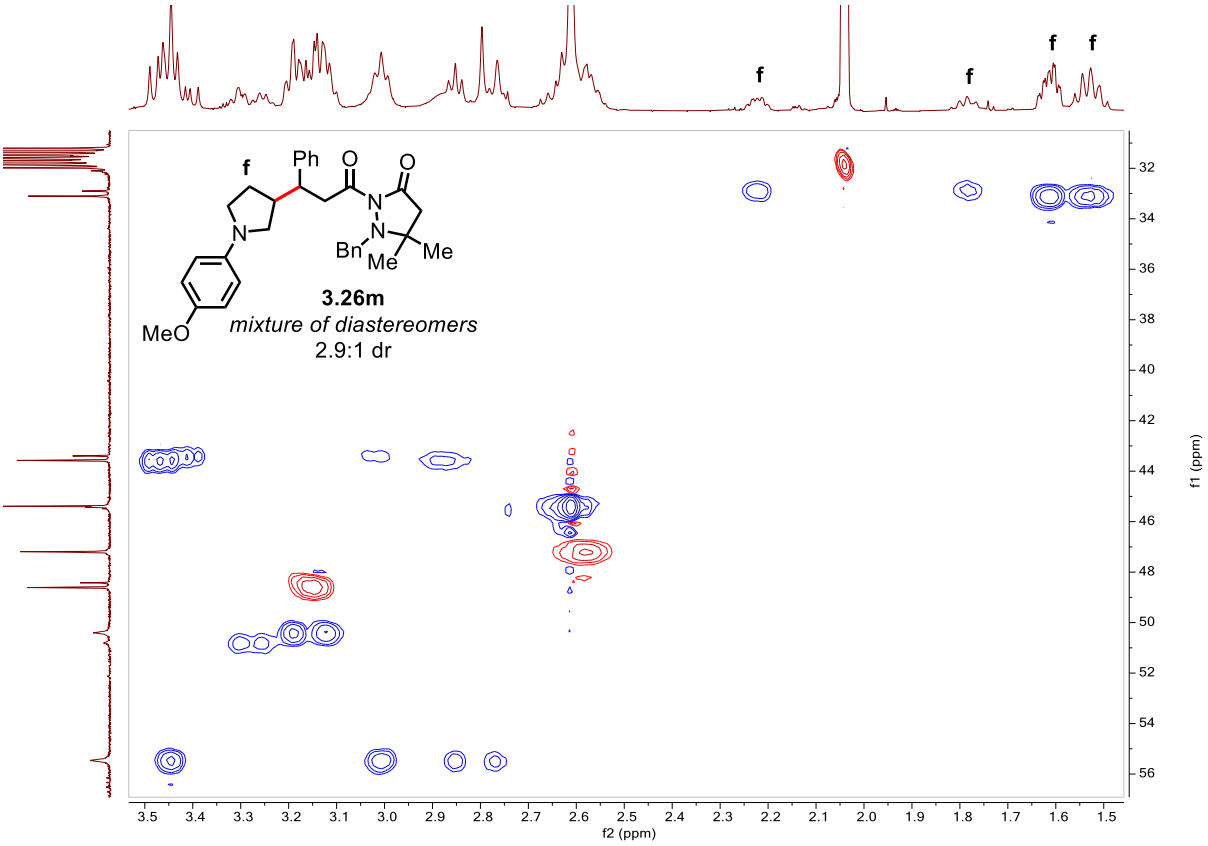

Figure S3.28. 2D HSQCAD spectra of **3.26m** in acetone-d_6 (*for the assignment of the peaks*)

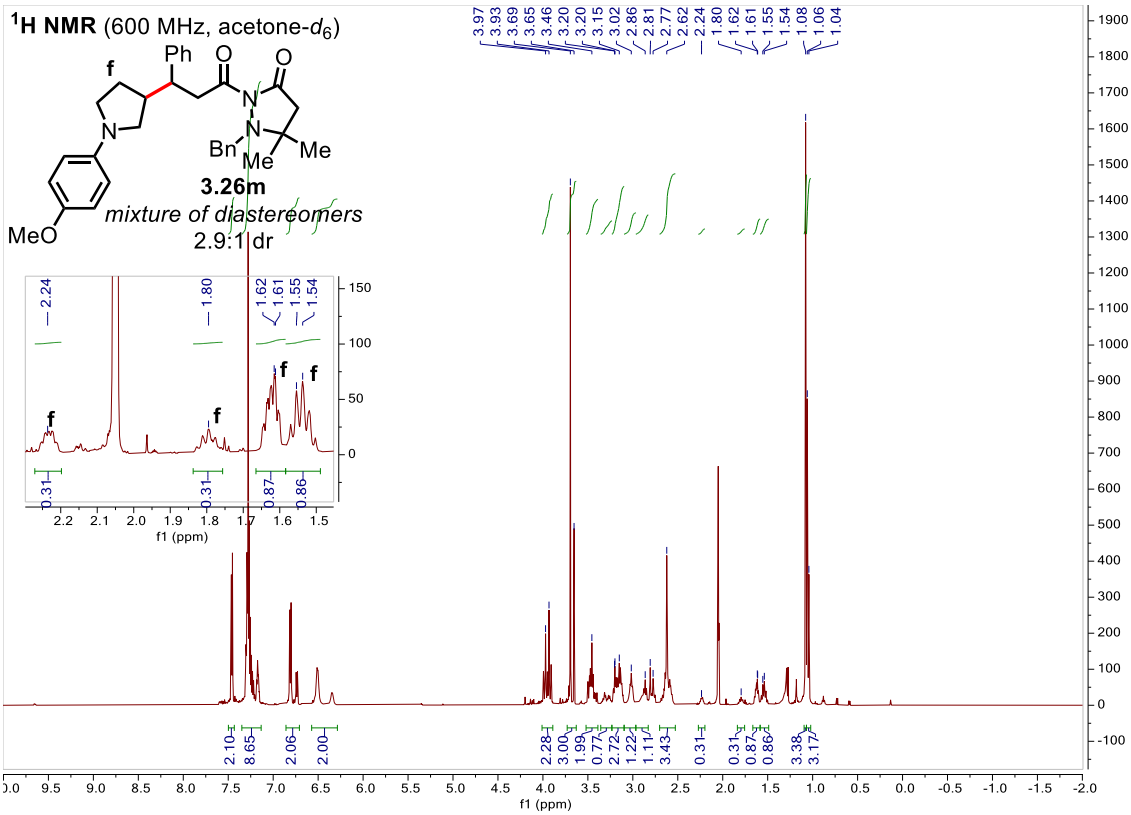

Figure S3.29. ^{1}H NMR spectrum of **3.26m** (in acetone-d_6)

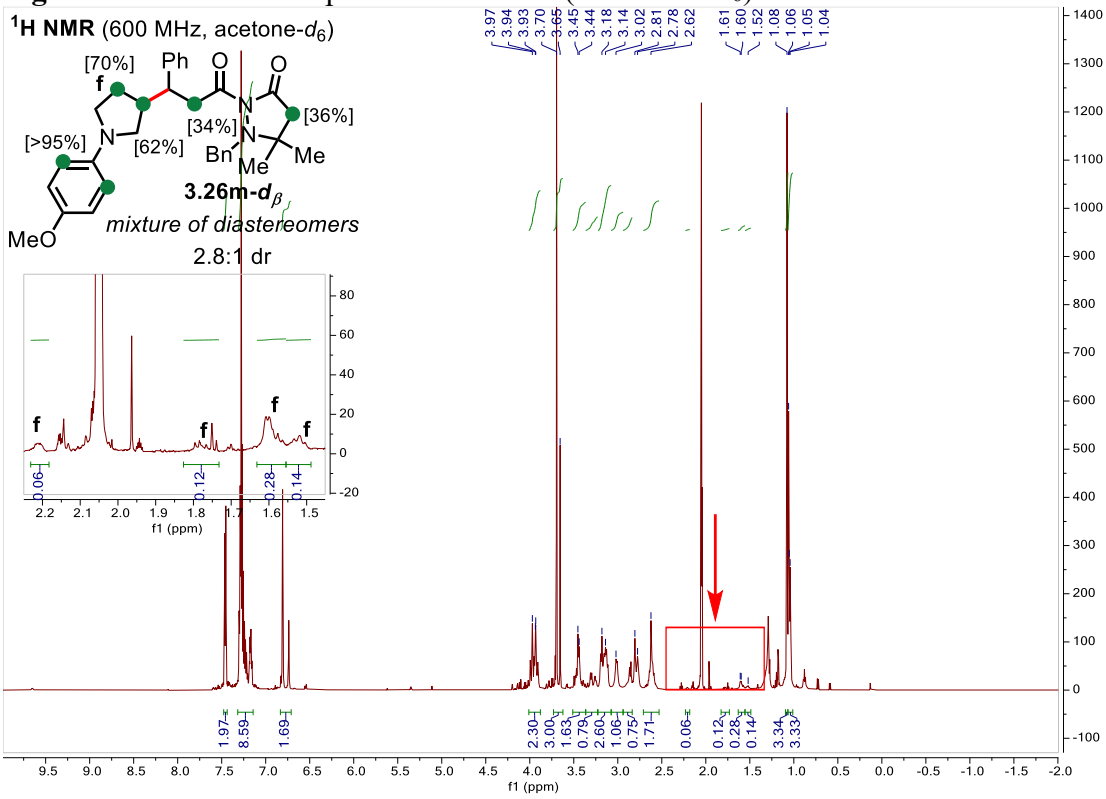

Figure S3.30. ^{1}H NMR spectrum of **3.26m-*dβ*** (in acetone-d_6)

Intermolecular Competition KIE Measurement for *N*-Alkylamines Containing *α*-Amino C–H or C–D Bonds

In order to further probe if the turnover-limiting step is the deprotonation process, we carried out the following intermolecular competition kinetic isotope effect experiments.

An intermolecular competition kinetic isotope effect study between 1-(4-methoxyphenyl)pyrrolidine **3.21r** and 1-(4-methoxyphenyl)pyrrolidine-2,2,5,5-d_4 **3.21r-*d*$_a$** with 1-benzyl-2-cinnamoyl-5,5-dimethylpyrazolidin-3-one **3.25g** was conducted (Scheme S3.18). Specifically, to a 15 mL oven-dried pressure vessel was added $B(C_6F_5)_3$ (10.2 mg, 0.020 mmol), **L6**–$Sc(OTf)_3$ (15.8 mg, 0.020 mmol), **3.25g** (100.4 mg, 0.30 mmol), **3.21r** (17.7 mg, 0.10 mmol), **3.21r-*d*$_a$** (18.1 mg, 0.10 mmol) and DCM (1.6 mL) under nitrogen atmosphere. The mixture was placed in an oil bath at 60 °C and was allowed to stir for 1 hour. Upon completion, the solution was cooled to 22 °C and concentrated *in vacuo.* The ^{1}H NMR analysis of the unpurified product mixture using mesitylene as the internal standard revealed that product **3.26m-*d*$_a$** was obtained in 27% yield (3.5:1 dr). After purification by column chromatography (EtOAc:hexanes = 1:3), **3.26m-*d*$_a$** was obtained as a light yellow liquid.

From the ^{1}H NMR analysis of the isolated and purified **3.26m-*d*$_a$** in $CDCl_3$ (Figures S3.31, S3.32), KIE value of 1.7 was obtained in the reaction between **3.21r** and **3.26m-*d*$_a$** with **3.25g**. This result is in line with the previous independent kinetic isotope effect studies and supports that the hydride abstraction step is not likely the turnover limiting process.

Scheme S3.18. Kinetic Isotope Effect Studies

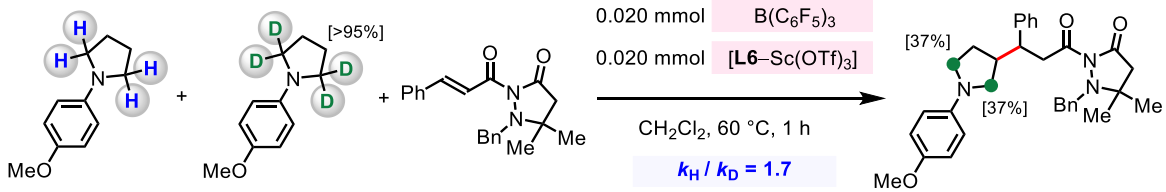

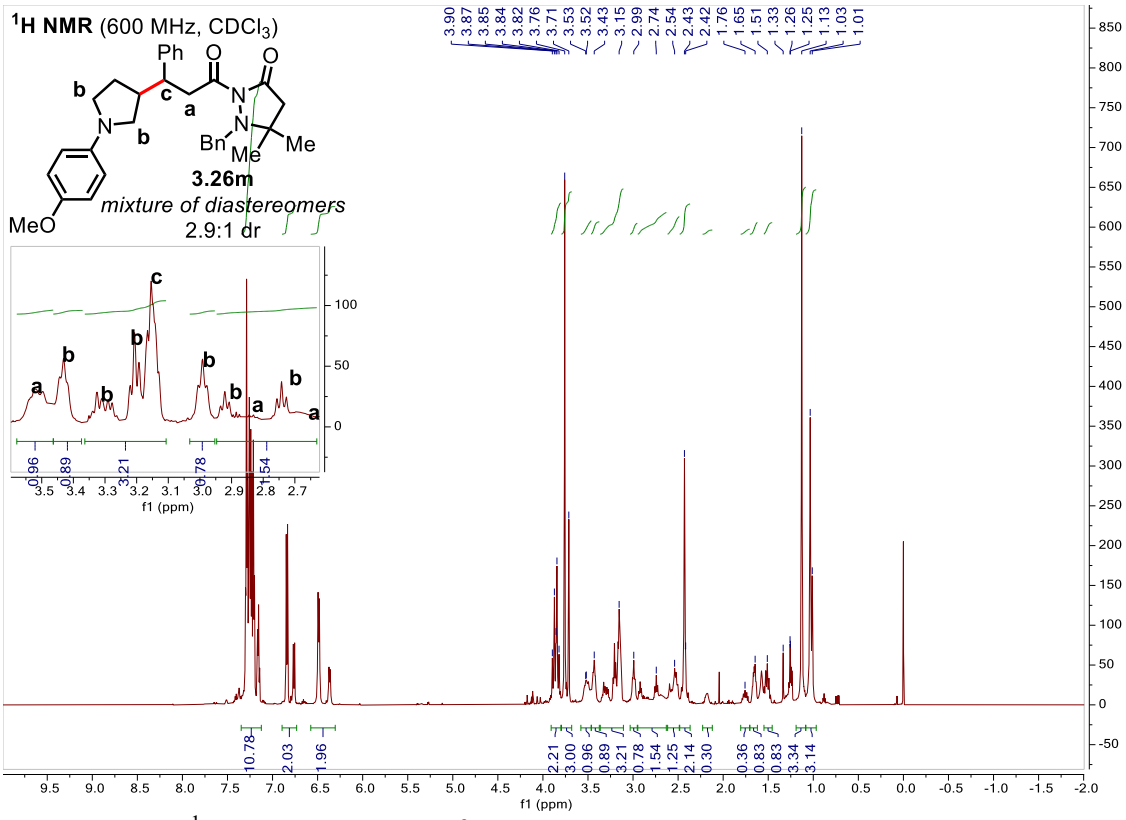

Figure S3.31. ^{1}H NMR spectrum of **3.26m**

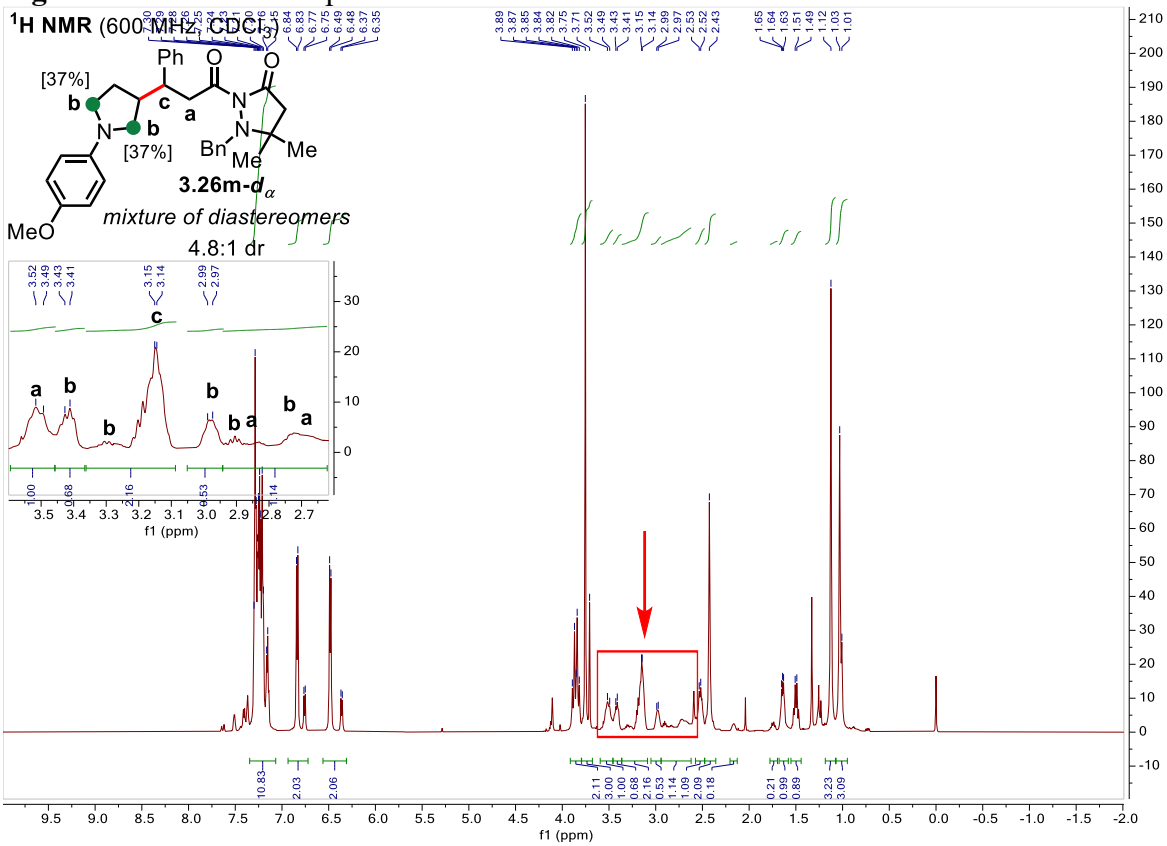

Figure S3.32. ^{1}H NMR spectrum of **3.26m-d_α**

Intermolecular Competition KIE Measurement for *N*-Alkylamines Containing *β*-Amino C–H or C–D Bonds

An intermolecular competition kinetic isotope effect study between 1-(4-methoxyphenyl)pyrrolidine **3.21r** and 1-(4-methoxyphenyl)pyrrolidine-3,3,4,4-d_4 **3.21r-*dβ*** with 1-benzyl-2-cinnamoyl-5,5-dimethylpyrazolidin-3-one **3.25g** was conducted (Scheme S3.19). Specifically, to a 15 mL oven-dried pressure vessel was added $B(C_6F_5)_3$ (10.2 mg, 0.020 mmol), **L6**–$Sc(OTf)_3$ (15.8 mg, 0.020 mmol), **3.25g** (100.4 mg, 0.30 mmol), **3.21r** (17.7 mg, 0.10 mmol), **3.21r-*dβ*** (18.1 mg, 0.10 mmol) and DCM (1.6 mL) under nitrogen atmosphere. The mixture was placed in an oil bath at 60 °C and was allowed to stir for 1 hour. Upon completion, the solution was cooled to 22 °C and concentrated *in vacuo.* The ^{1}H NMR analysis of the unpurified product mixture using mesitylene as the internal standard revealed that product **3.26m-*dβ*** was obtained in 23% yield (2.0:1 dr). After purification by column chromatography (EtOAc:hexanes = 1:3), **3.26m-*dβ*** was obtained as a light yellow liquid.

From the ^{1}H NMR analysis of the isolated and purified **3.26m-*dβ*** in $CDCl_3$ (Figures S3.33, S3.34), it was found that **3.21r** reacts 4.3 times faster than **3.21r-*dβ*** (k_H/k_D = 4.3) in the reaction between **3.21r** or **3.21r-*dβ*** and **3.26m-*dβ***. This result is in line with the previous independent kinetic isotope effect studies and supports that the cleavage of *β*-amino C–H bond is likely involved in the turnover-limiting step.

It was found that there was a *d*-scrambling between the substrates and the products at the *β*-amino C–H/D bonds and the *α*-carbonyl C–H/D bonds that are easily enolizable.

Scheme S3.19. Kinetic Isotope Effect Studies

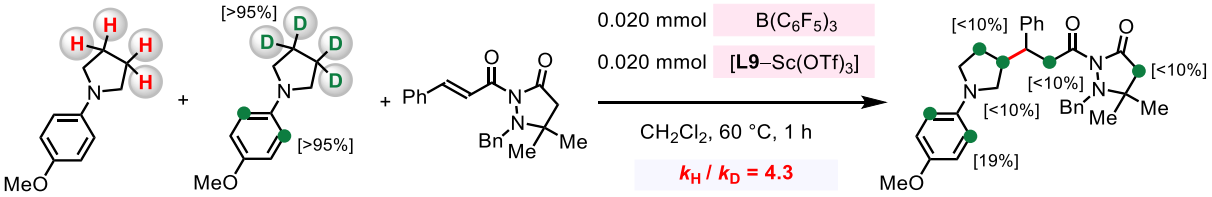

3.21r, 0.10 mmol **3.21r-*d*$_\beta$**, 0.10 mmol **3.25g**, 0.30 mmol **3.26m-*d*$_\beta$**, 23% yield

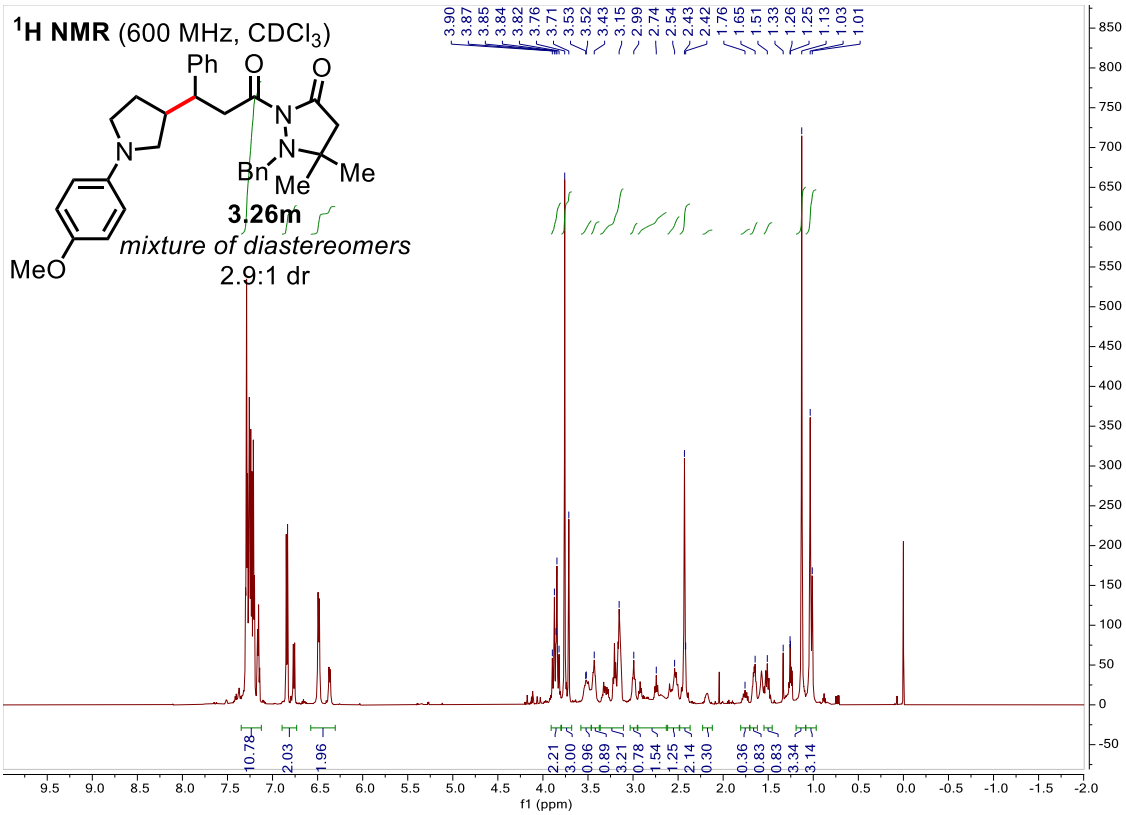

Figure S3.33. ^{1}H NMR spectrum of **3.26m** (in $CDCl_3$)

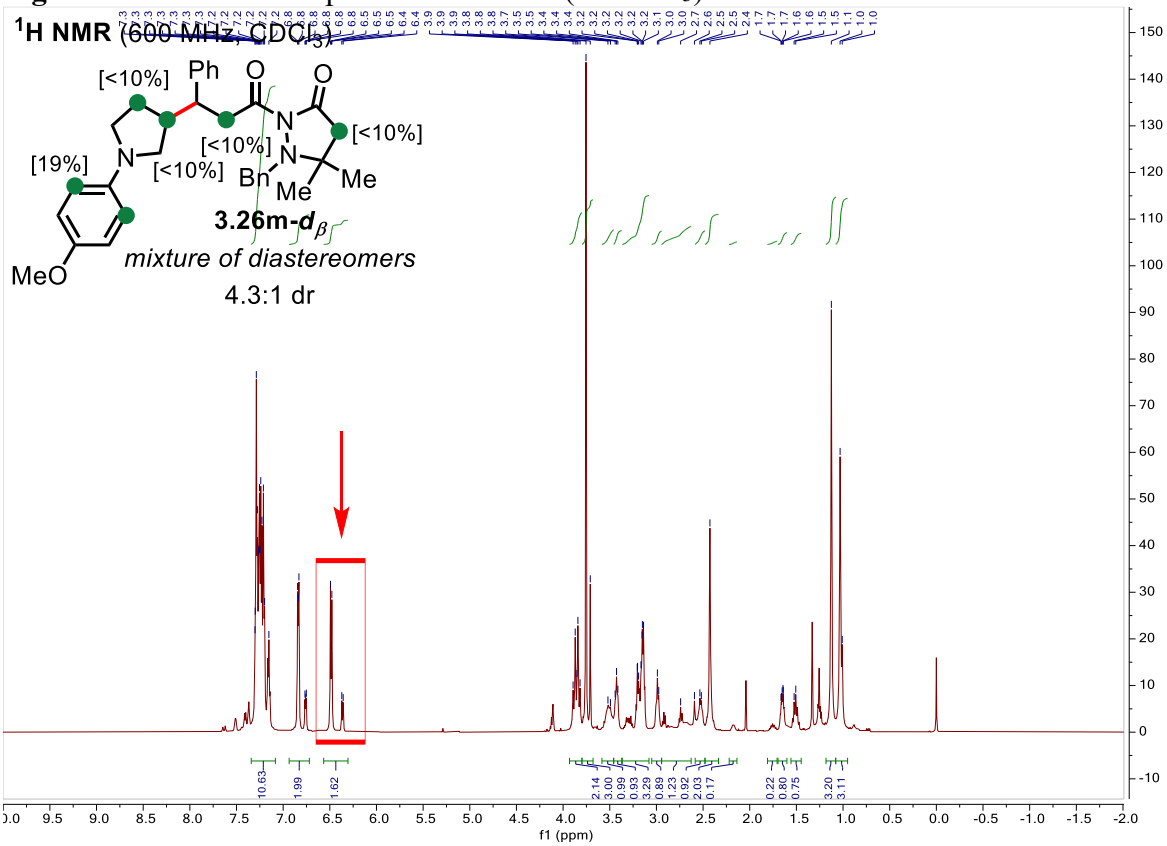

Figure S3.34. ^{1}H NMR spectrum of **3.26m-*dβ*** (in $CDCl_3$)

Hammett Studies

In order to study the effect of varying the substituents on aryl groups of *N*-alkylamine as well as α,β-unsaturated substrates on the rate of C–H alkylation, we carried out the following Hammett studies.

Determination of the Hammett ρ Value for *N*-Aryl Substituted Pyrrolidines

A Hammett ρ value for the reaction of *N*-aryl substituted pyrrolidines (**3.21r**, **3.21v**–**3.21x**) and (*E*)-1-benzyl-5,5-dimethyl-2-(3-(4-(trifluoromethyl)phenyl)acryloyl)pyrazolidin-3-one **3.25h** was determined by time course reaction monitoring by the ^{1}H NMR spectroscopy using mesitylene as an internal standard. In a nitrogen-filled glove box, **L6**–$Sc(OTf)_3$ (39.5 mg, 0.050 mmol), **3.25h** (302 mg, 0.75 mmol), mesitylene (60 mg, 0.50 mmol), and C_6F_6 (46.5 mg, 0.25 mmol) were weighed in an oven-dried 7.0 mL vial and the resulting mixture was dissolved in 2.00 mL of CD_2Cl_2 (**Stock Solution A**). In another oven-dried 7.0 mL vial, $B(C_6F_5)_3$ (30.7 mg, 0.060 mmol) was weighed and dissolved in 1.20 mL of CD_2Cl_2 (**Stock Solution B**). In 4 oven-dried 7.0 mL vials, were added 0.10 mmol of each amine. To each oven-dried vial containing amine was added **Stock Solution A** (0.40 mL), **Stock Solution B** (0.20 mL), and CD_2Cl_2 (0.20 mL) to prepare the reaction samples containing amines **3.21r**, **3.21v**, **3.21w**, or **3.21x**. The reaction mixture was then transferred to a J-Young tube. After the J-Young tube was tightly capped with the Teflon plug, it was taken out of the glove box and the ^{1}H NMR spectra were acquired in the NMR spectrometer preheated at 60 °C using a pre-acquisition delay in array mode with a spectrum taken every 22 seconds for the length of the experiment. The data were processed using MestReNova software and peak integrations were normalized using mesitylene as the internal standard.

The large negative ρ value (–4.9) obtained implies the development of positive charge at the reaction center in the transition state at or prior to the turnover-limiting step. This result thereby

supports the proposed mechanism in which $B(C_6F_5)_3$ abstracts a hydride from *N*-arylpyrrolidine to form an *N*-aryl iminium cation, and its isomerization into a positively charged enammonium species; both processes take place at or prior to the turnover-limiting step (Figure S3.35).

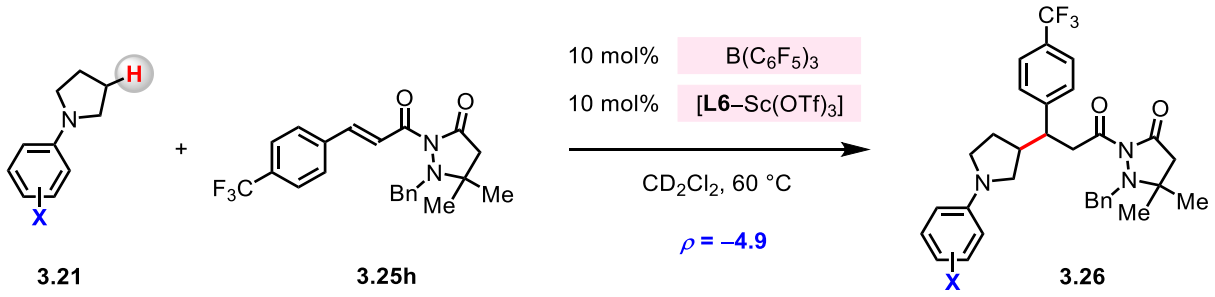

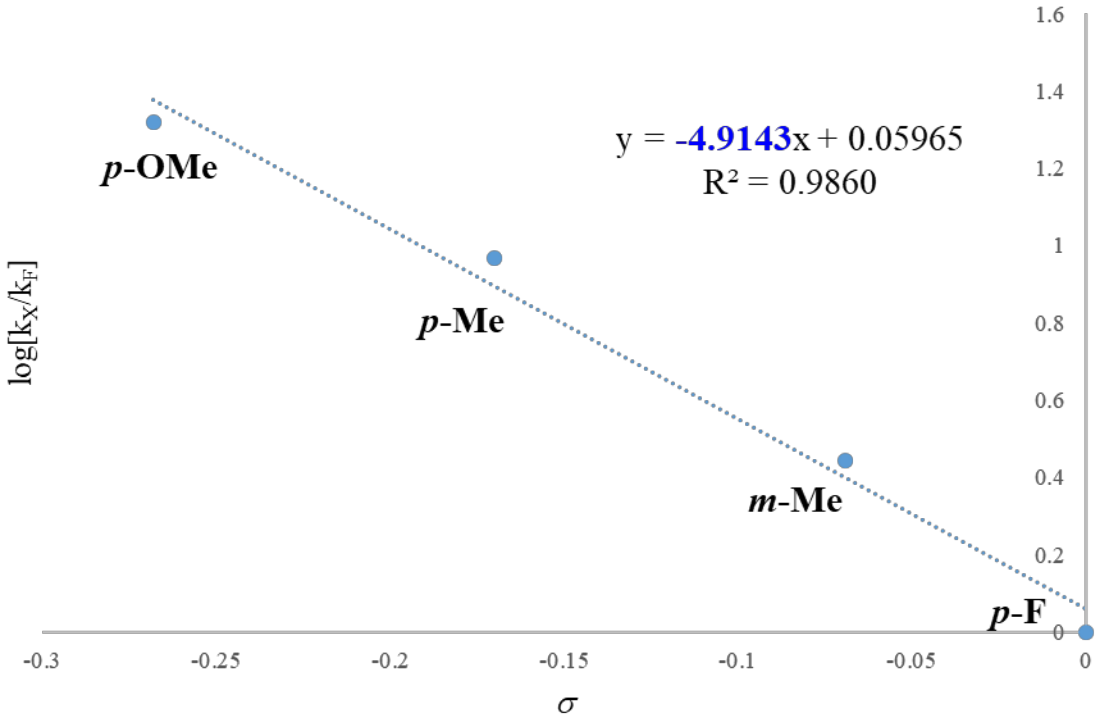

Figure S3.35. Log(k_X/k_F) *vs* σ is employed to determine the ρ value

Determination of the Hammett ρ Value for Aryl Substituted α,β-Unsaturated Compounds

A Hammett ρ value for the reaction of 1-(4-methoxyphenyl)pyrrolidine (**3.21r**) and aryl substituted α,β-unsaturated compounds (**3.25g–3.25j**) was determined by time course reaction monitoring by the ^{1}H NMR spectroscopy using mesitylene as an internal standard. In a nitrogen-filled glove box, **L6**–Sc(OTf)$_3$ (39.5 mg, 0.050 mmol), **3.21r** (88.5 mg, 0.50 mmol), and mesitylene (60 mg, 0.50 mmol) were weighed in an oven-dried 7.0 mL vial and the resulting mixture was dissolved in 2.00 mL of CD_2Cl_2 (**Stock Solution A**). In another oven-dried 7.0 mL vial, B(C_6F_5)$_3$ (30.7 mg, 0.060 mmol) was weighed and dissolved in 1.20 mL of CD_2Cl_2 (**Stock Solution B**). In 4 oven-dried 7.0 mL vials, were added 0.15 mmol of each α,β-unsaturated compounds **3.25**. To each oven-dried vial containing amine was added **Stock Solution A** (0.40 mL), **Stock Solution B** (0.20 mL), and CD_2Cl_2 (0.20 mL) to prepare the reaction samples containing α,β-unsaturated compounds **3.25g**, **3.25h**, **3.25i**, or **3.25j**. The reaction mixture was then transferred to a J-Young tube. After the J-Young tube was tightly capped with the Teflon plug, it was taken out of the glove box and the ^{1}H NMR spectra were acquired in the NMR spectrometer preheated at 60 °C using a pre-acquisition delay in array mode with a spectrum taken every 22 seconds for the length of the experiment. The data were processed using MestReNova software and peak integrations were normalized using mesitylene as the internal standard.

The σ^+ was used in the Hammett plot since the electron-donating ability of the *p*-OMe substituent was enhanced through conjugation in the α,β-unsaturated compound **3.25**. The positive ρ value (0.92) obtained implies the development of negative charge at the reaction center in the transition state at or prior to the turnover-limiting step. This result thereby supports the mechanistic hypothesis that **3.25** reacts with in situ generated [(F_5C_6)$_3$B–H]$^-$ to afford a negatively charged boron–enolate intermediate, and that this hydride transfer occurs at or prior to the turnover-limiting

step (Figure S3.36).

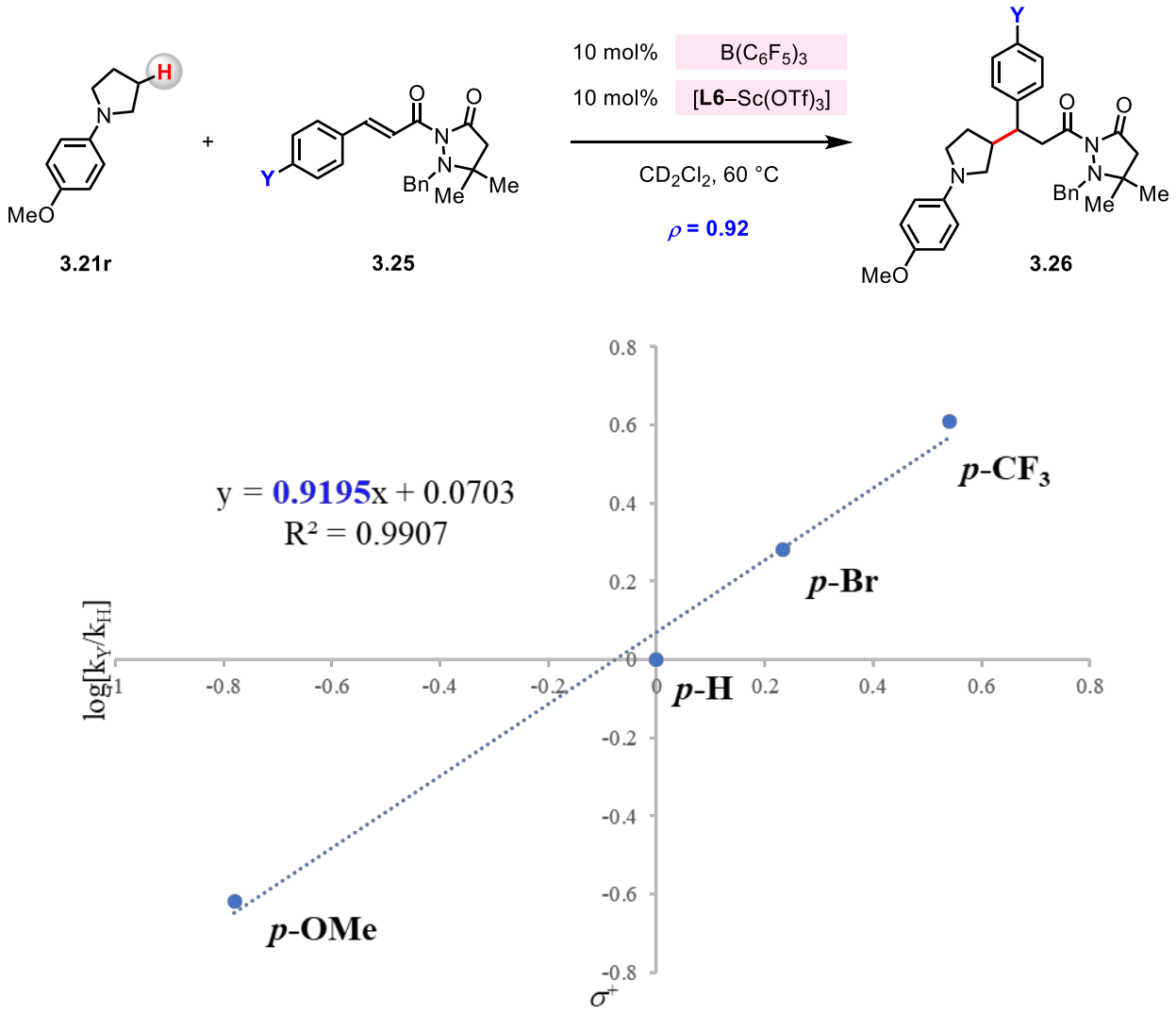

Figure S3.36. Log(k_Y/k_H) *vs* σ^+ is employed to determine the ρ value

Catalytic Cycle Consistent with the Results of Mechanistic Studies

Based on the kinetic studies as described above, we propose the following catalytic cycle (Figure S3.38). *Zero-order dependency* with respect to concentration of **L6**–$Sc(OTf)_3$ suggests that enantioselective C–C bond forming reaction between in situ generated enamine and [**L6**–$Sc(OTf)_3$]-activated **3.25g** (**XXVII → XXVIII,** Figure S3.38) occurs after the turnover-limiting step. *–1-Order dependency* on the concentration of **3.25g** suggests that the transformation has a resting state of **3.25g**–$B(C_6F_5)_3$ adduct (**XXIII**), which was suggested by ^{19}F NMR studies. Kinetic isotope effect studies demonstrate that cleavage of β-amino C–H bond is likely the turnover-limiting step. The large negative ρ value (-4.9) obtained from Hammett study of *N*-aryl substituted pyrrolidines supports the proposed mechanism that $(F_5C_6)_3B$-catalyzed hydride abstraction to generate *N*-aryl iminium cation, and its isomerization into an enammonium species taking place at or prior to the turnover-limiting step.

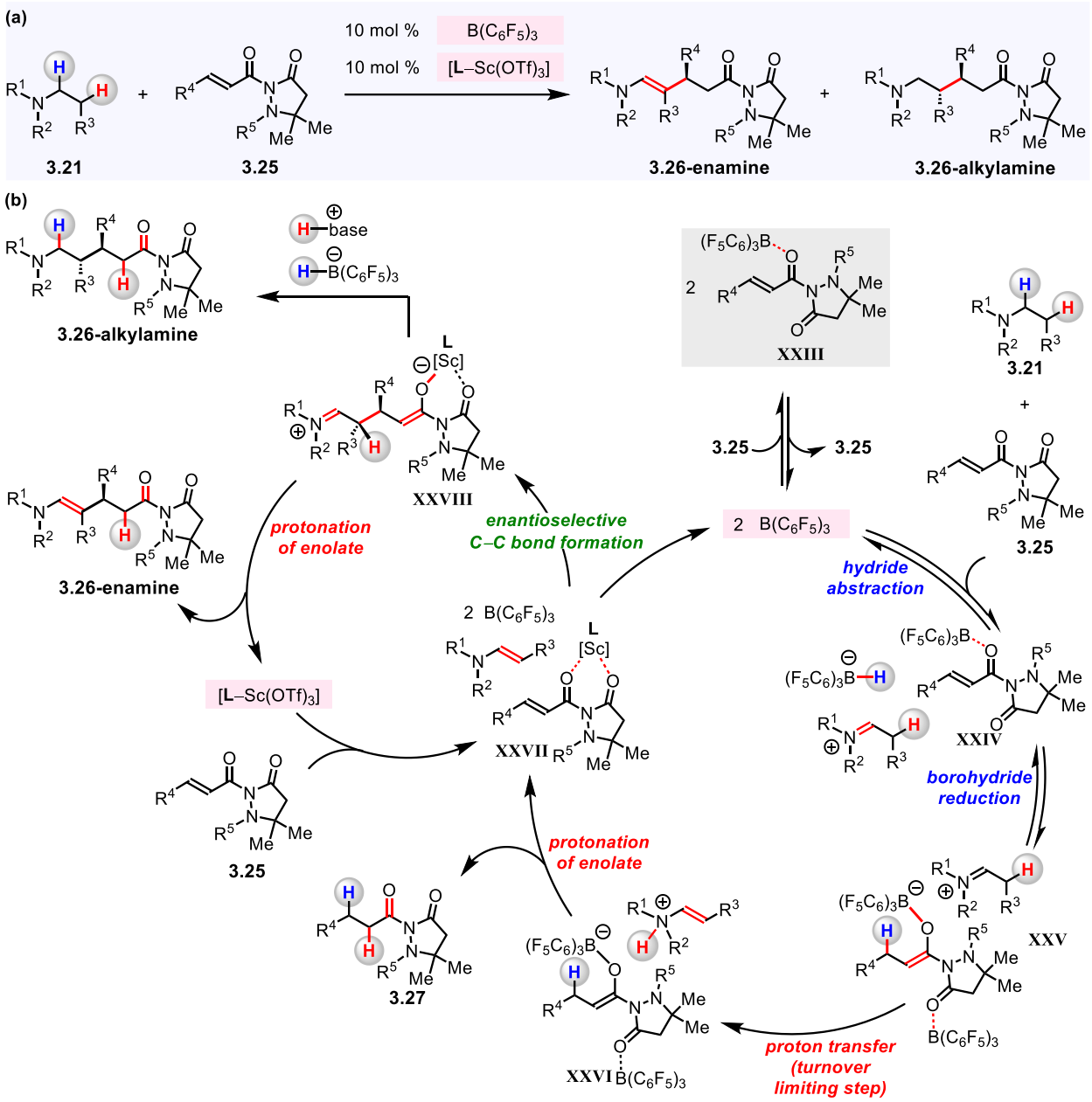

Figure S3.37. A catalytic cycle consistent with the results of the mechanistic investigation

Origin of Enamine and *N*-Alkylamine Products

In the *β*-amino C–H alkylation process, the products were obtained either as **3.26-enamine**, **3.26-alkylamine**, or a mixture of the two (Figure S3.37). We questioned if the *N*-alkylamine products were formed through transfer hydrogenation of **XXVIII** (**XXVIII→ 3.26-alkylamine**). Alternatively, **3.26-alkylamine** could be generated through reduction of **3.26-enamine** (**XXVIII → 3.26-enamine → 3.26-alkylamine**). In order to understand the origin of **3.26-enamine** and **3.26-alkylamine** products, we conducted the following experiments.

Kinetic Profile for the *β*-Alkylation of *N*-Arylpiperidine

Transfer Hydrogenation of Compound **3.21v**

Dehydrogenation of Compound **3.21i**

Kinetic Profile for the *β*-Alkylation of *N*-Arylpiperidine

As shown in Scheme 3.23 in the manuscript, the reaction of *N*-arylpiperidine **3.21l** and diisopropylfumarate **3.22a** with 10 mol% $B(C_6F_5)_3$ in benzene (1.0 M) was found to give *N*-alkylamine **3.23o** and enamine **3.32** in 57% yield and 29% yield, respectively. Since the products were obtained as a mixture of **3.23o** and **3.32**, it would be a good platform to study whether the *N*-alkylamine and enamine products are interconvertible. To determine if **3.23o** can be generated by $(F_5C_6)_3B$-catalyzed transfer hydrogenation of **3.32**, we monitored the progress of this reaction by the ^1H NMR spectroscopy (Figure S3.38). To an oven-dried 7.0 mL vial, amine **3.21l** (88 mg, 0.40 mmol), diisopropyl fumarate **3.22a** (120 mg, 0.60 mmol), mesitylene (48 mg, 0.40 mmol), $B(C_6F_5)_3$ (10 mol%) and 0.4 mL C_6D_6 were added under nitrogen atmosphere. Then, the reaction mixture was transferred to a J-Young tube which was tightly capped with the Teflon plug and taken out of the glove box. The ^1H NMR spectra were acquired in the NMR spectrometer preheated at 50 °C using a pre-acquisition delay in array mode with a spectrum taken every 22 seconds for the length of the experiment. The data were processed using MestReNova software and peak integrations were normalized using *m*-xylene as the internal standard.

As shown in Figure S36, it was found that there was minimal transformation of **3.32** into **3.23o**, evidenced by the mostly unchanged concentration of **3.32** once >85% of amine **3.21l** was consumed (after ca. 100 minutes).

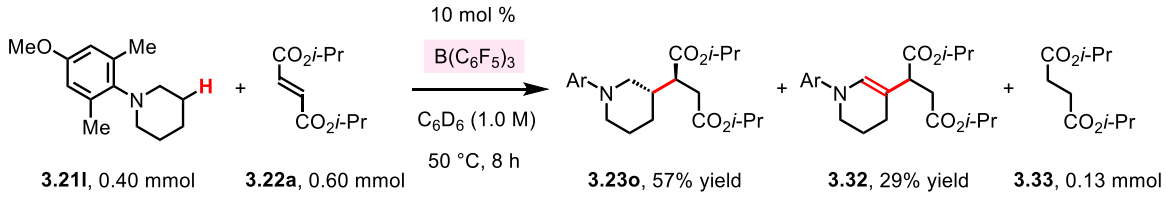

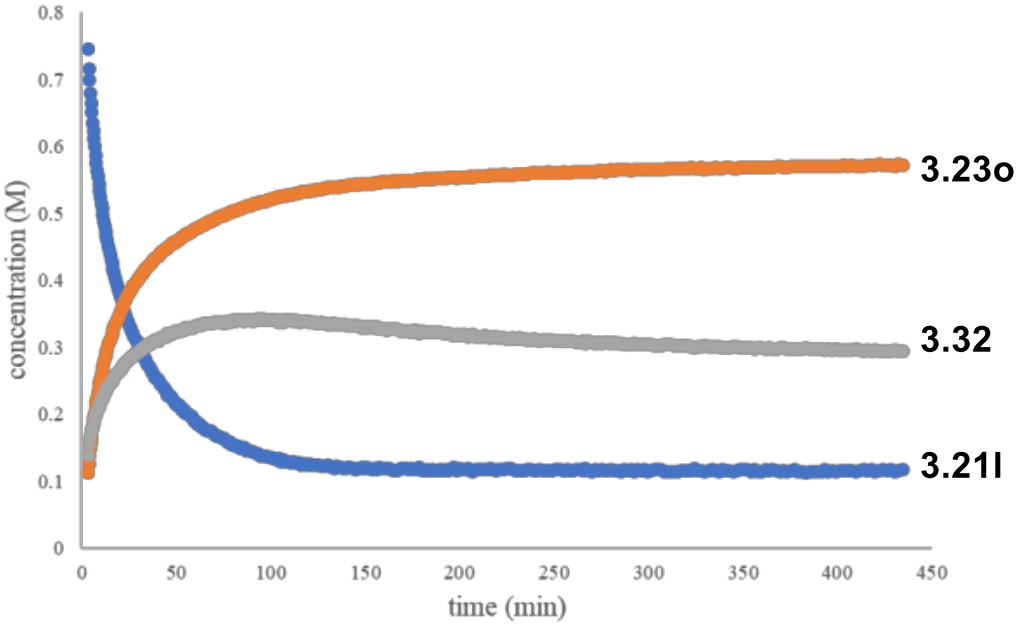

Figure S3.38. Progress of the reaction between **3.21l** and **3.22a**

Transfer Hydrogenation of Compound 3.32

As shown in Scheme 3.23 in the manuscript, transfer hydrogenation of compound **3.32** was conducted to further probe whether the enamine product can be reduced to generate the *N*-alkylamine product **3.23o**.

To a 15 mL oven-dried pressure vessel, **3.32** (0.050 mmol), $B(C_6F_5)_3$ (20 mol%) and benzene (0.20 mL) were added under a nitrogen atmosphere (Scheme S3.20). The reaction mixture was placed in an oil bath at 50 °C for 12 hours. Upon completion, the solution was cooled to 22 °C and concentrated *in vacuo*. Through the ^{1}H NMR analysis of the unpurified product mixture using mesitylene as the internal standard, it was found that **3.23o** was formed in 30% yield, together with an ionic complex of [pyridinium]$^+$[C_6F_5]$^-$ (**3.34**) which was generated in 15% yield. This experiment implies that enamine **3.32** can serve as H^+/H^- source in $(F_5C_6)_3B$-catalyzed transfer hydrogenation of **3.32** to afford *N*-alkylamine product **3.23o**.

Scheme S3.20. Transfer Hydrogenation Studies involving Compound **3.32**

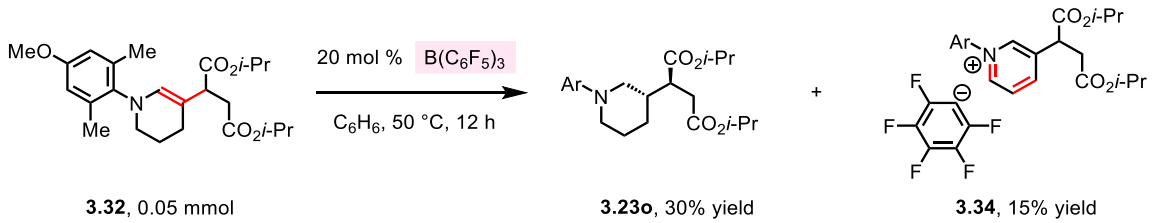

3.32, 0.05 mmol **3.23o**, 30% yield **3.34**, 15% yield

3-(1,4-Diisopropoxy-1,4-dioxobutan-2-yl)-1-(4-methoxy-2,6-dimethylphenyl)pyridin-1-ium perfluorobenzen-1-ide (3.34)

^{1}H NMR (600 MHz, $CDCl_3$): δ 8.72 (s, 1H), 8.60 (d, *J* = 8.2 Hz, 1H), 8.37 (dd, *J* = 6.0, 1.3 Hz, 1H), 8.13 – 8.08 (m, 1H), 6.80 (d, *J* = 4.2 Hz, 2H), 5.06 (dt, *J* = 12.2, 6.5 Hz, 1H), 4.88 (p, *J* = 6.7 Hz, 1H), 4.26 (dd, *J* = 8.7, 4.8 Hz, 1H), 3.87 (s, 3H), 3.10 (dd, *J* = 18.1, 4.9 Hz, 1H), 3.03 (dd, *J* =

17.7, 8.7 Hz, 1H), 1.97 (s, 3H), 1.94 (s, 3H), 1.26 (d, *J* = 5.1 Hz, 3H), 1.21 (d, *J* = 5.7 Hz, 3H), 1.18 (d, *J* = 6.2 Hz, 3H), 1.14 (d, *J* = 6.2 Hz, 3H); **^{19}F NMR (564 MHz, $CDCl_3$):** δ -137.48 (d, *J* = 23.9 Hz), -160.45 (t, *J* = 20.1 Hz), -165.00 (t, *J* = 19.4 Hz); **HRMS (DART):** Calcd for $C_{30}H_{33}F_5NO_5$ (MH^+): 582.2273; found: 582.2253.

$(F_5C_6)_3B$-catalyzed transfer hydrogenation of enamines was previously reported by Stephan and co-workers; 1-(1-cyclohexen-1-yl)-piperidine was reduced to afford 1-cyclohexylpiperidine in the presence of 20 mol% $B(C_6F_5)_3$ and large excess of $(i\text{-Pr})_2NH$ (the mixture was allowed to stir at 100 °C for 24 hours).[3] In our transformation (Figure 2), amine substrate **3.21l** may serve as H^+/H^- source in transfer hydrogenation of **3.32**. To determine if this is possible, to a 15 mL oven-dried pressure vessel were added enamine **3.32** (0.050 mmol), amine **3.21l-*d*** (0.05 mmol, 1.0 equiv), $B(C_6F_5)_3$ (20 mol%) and benzene (0.20 mL) under a nitrogen atmosphere (Scheme S3.21). The reaction mixture was placed in an oil bath at 50 °C for 12 hours. Upon completion, the solution was cooled to 22 °C and concentrated *in vacuo*. Through the ^1H NMR analysis of the unpurified product mixture using mesitylene as the internal standard, it was found that **3.23o-*d*** was formed in 50% yield with <5% of **3.34** formation when 58% of **3.19g-*d*** was recovered. Furthermore, deuterium incorporation level was determined after the isolation and purification of **3.23o-*d*** and **3.21l-*d*,** which revealed that there was *d*-scrambling at the *β*-position of **3.23o-*d*** and **3.21l-*d*** (see 1.6–2.0 ppm in Figures S3.39, S3.40) when there was no significant deuterium incorporation at the *β*-amino position of recovered **3.32**. These results imply that amine **3.21l-*d*** can serve as D^+ and H^- source in $(F_5C_6)_3B$-catalyzed transfer hydrogenation of **3.32** to afford *N*-alkylamine product **3.23o-*d***.

Scheme S3.21. Transfer Hydrogenation Studies involving Compound **3.32**

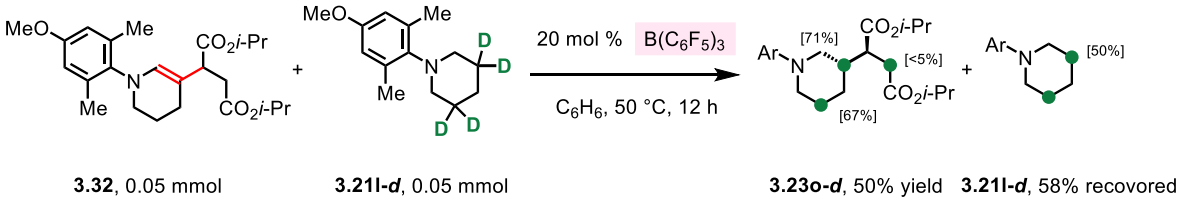

3.32, 0.05 mmol **3.21l-*d***, 0.05 mmol **3.23o-*d***, 50% yield **3.21l-*d***, 58% recovered

[3] Farrell, J. M.; Heiden, Z. M.; Stephan, D. W. *Organometallics* **2011**, *30*, 4497–4500.

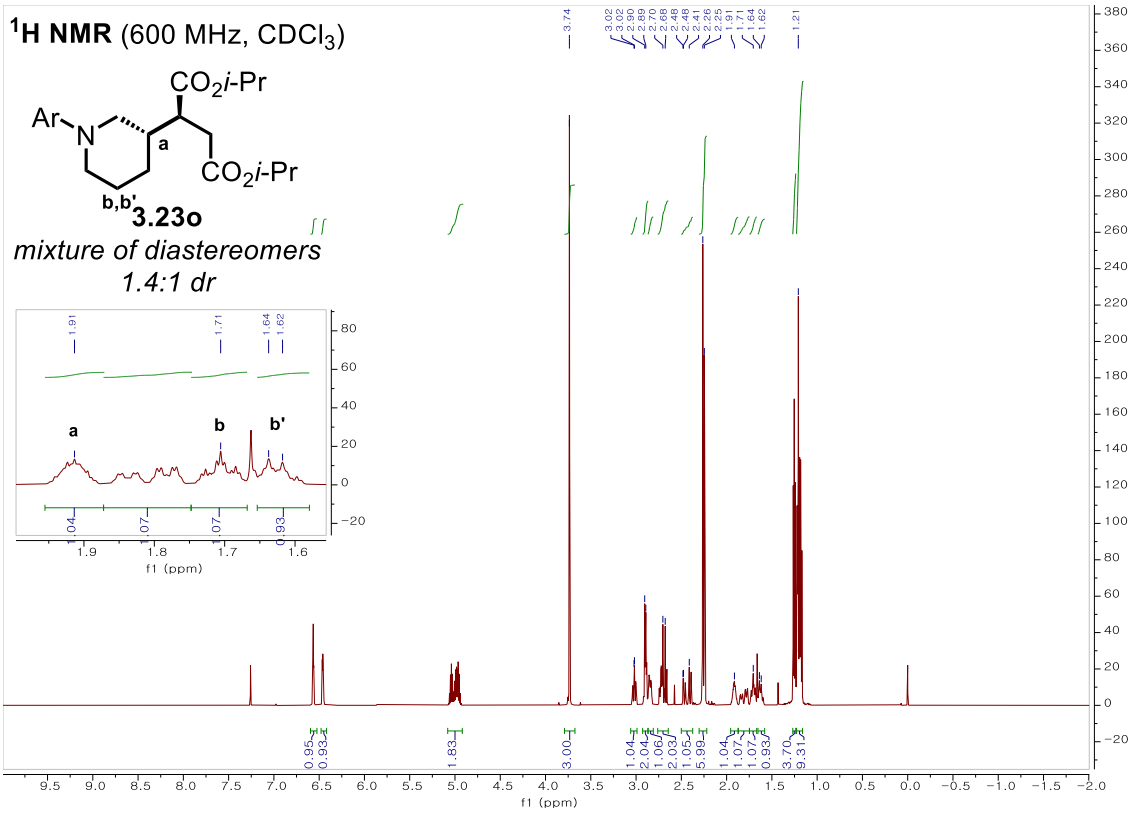

Figure S3.39. ^{1}H NMR Spectrum of **3.23o**

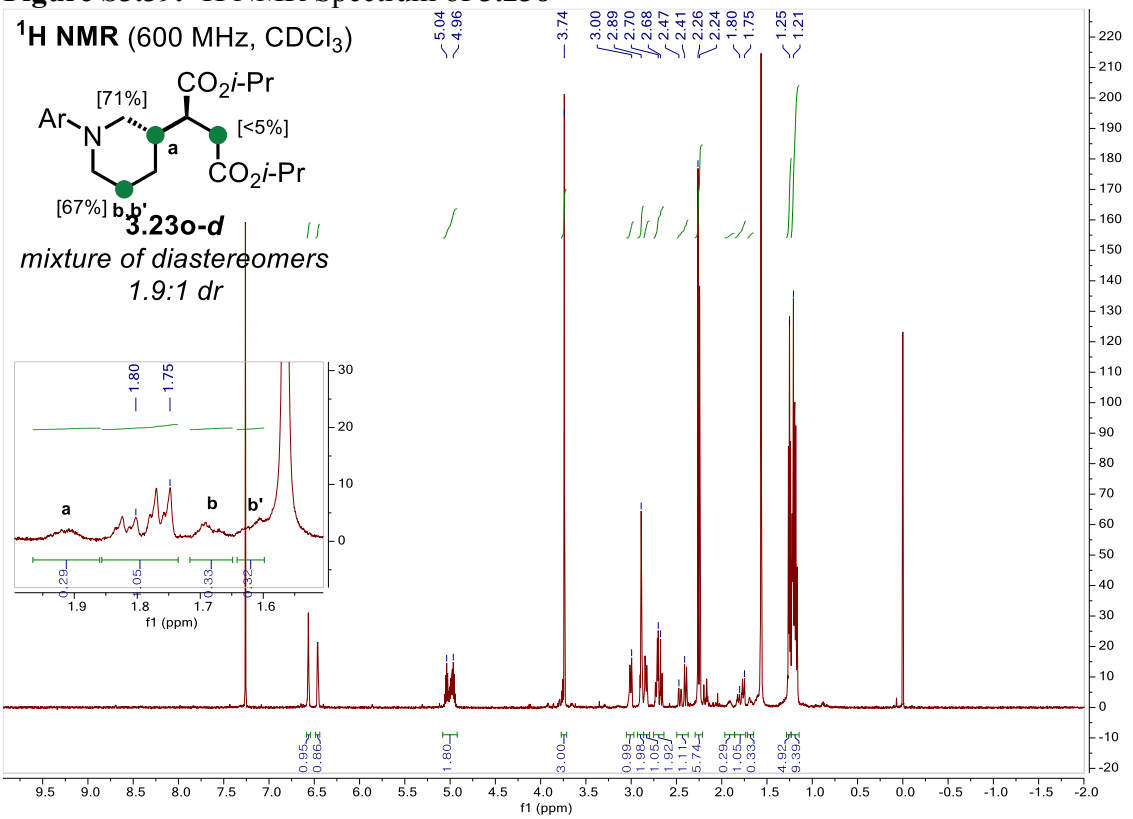

Figure S3.40. ^{1}H NMR Spectrum of **3.23o-*d***

Dehydrogenation of Compound 3.23o

As discussed in previous sections, under the standard reaction conditions, *N*-alkylamine **3.23o** is likely generated by transfer hydrogenation of **XXVIII** (Figure S3.37) without the intermediacy of enamine **3.32**. In order to probe whether enamine **3.32** can be generated from *N*-alkylamine **3.23o** through oxidation, dehydrogenation of compound **3.23o** (Schemes S3.22-S3.23) was conducted. To a 15 mL oven-dried pressure vessel was added amine **3.23o** (21 mg, 0.050 mmol), $B(C_6F_5)_3$ (20 mol%) and benzene (0.20 mL) under a nitrogen atmosphere (Scheme S3.22). The reaction mixture was placed in an oil bath at 50 °C and was allowed to stir for 12 hours. Upon completion, the reaction mixture was cooled to 22 °C and concentrated *in vacuo*. Through the ^{1}H NMR analysis of the unpurified product mixture using mesitylene as the internal standard, it was found that **3.23o** was fully recovered and formation of **3.32** was not observed.

Scheme S3.22. Dehydrogenation Studies involving Compound **3.23o**

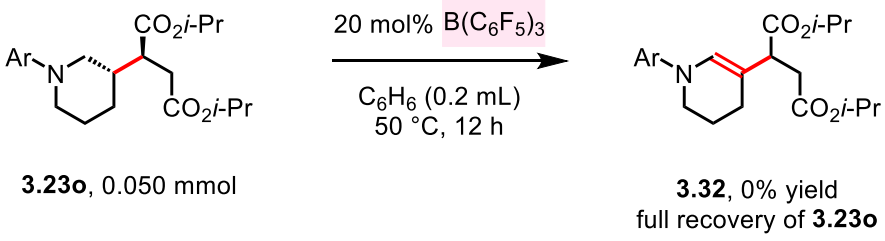

3.23o, 0.050 mmol

3.32, 0% yield
full recovery of **3.23o**

We hypothesized that in order to obtain enamine **3.32**, the presence of diisopropylfumarate **3.22a** might be necessary to serve as a H^+/H^- acceptor. Therefore, **3.22** (10 mg, 0.05 mmol, 1.0 equiv.) was added to the reaction mixture of amine **3.23o** (21 mg, 0.05 mmol), $B(C_6F_5)_3$ (20 mol%) and benzene (0.2 mL) under a nitrogen atmosphere (Scheme S3.23). The reaction mixture was placed in an oil bath at 50 °C and was allowed to stir for 12 hours. Upon completion, the reaction mixture was cooled to 22 °C and concentrated *in vacuo*. However, after ^1H NMR analysis of the unpurified product mixture using mesitylene as the internal standard, formation of **3.32** was not observed. These experiments revealed that **3.23o** cannot be readily converted to **3.32** by $B(C_6F_5)_3$, regardless of whether α,β-unsaturated compound **3.22a** is present in the reaction mixture or not. This result implies that **3.32** is generated from the deprotonation of **XXVIII** (Figure S3.37), not through the oxidation of **3.23o**. Therefore, the interconversion between **3.23o** and **3.32** under the standard reaction conditions is unlikely to take place.

Scheme S3.23. Dehydrogenation Studies involving Compound **3.23o**

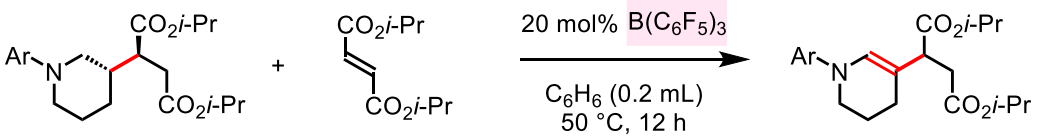

3.23o, 0.050 mmol **3.22a**, 0.050 mmol **3.32**, 0% yield

Mechanistic Studies Involving Ester Substituted α,β-Unsaturated Compound 3.25c

We performed mechanistic investigations on the reaction between *N*-alkylamine **3.21r** and ethyl ester-substituted electrophile **3.25c** to probe if the mechanism of β-C–H alkylation may be different depending on which electrophile is used (vs the processes involving aryl-substituted electrophiles).

Determination of the Reaction Orders Involving 3.25c

For the β-C–H alkylation reaction involving 1-(4-methoxyphenyl)pyrrolidine **3.21r** and **3.25c**, the reaction order of each reactant was studied through time course reaction monitoring by the ^{1}H NMR spectroscopic analysis.

Reaction Order of $B(C_6F_5)_3$

The reaction between **3.21r** and **3.25c** was performed using different concentrations of $B(C_6F_5)_3$ and the progress of each reaction was monitored by the ^{1}H NMR spectroscopy (Scheme S3.24).

Scheme S3.24. Determination of the Reaction Order of $B(C_6F_5)_3$

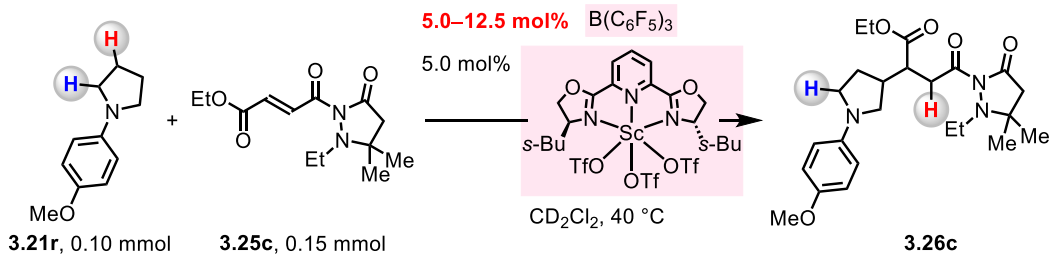

In a nitrogen-filled glove box, **L10**–$Sc(OTf)_3$ (24.6 mg, 10 mol%), **3.21r** (106.2 mg, 0.60 mmol), **3.25c** (241.2 mg, 1.5 equiv) and toluene (55.2 mg, 1.0 equiv) were weighed in an oven-dried 7.0 mL vial and the resulting mixture was dissolved in 2.40 mL of CD_2Cl_2 (**Stock Solution A**). In another oven-dried 7.0 mL vial, $B(C_6F_5)_3$ (35.8 mg, 0.070 mmol) was weighed and dissolved in 1.40 mL of CD_2Cl_2 (**Stock Solution B**). To each J-Young tube was added **Stock Solution A** (0.40 mL), **Stock Solution B** (0.10, 0.15, 0.20, or 0.25 mL) and CD_2Cl_2 (0.30, 0.25, 0.20, or 0.15 mL)

to prepare the reaction samples containing different concentrations of $B(C_6F_5)_3$. After the J-Young tube was tightly capped with the Teflon plug, it was taken out of the glove box and the ^1H NMR spectra were acquired in the NMR spectrometer preheated at 40 °C using a pre-acquisition delay in array mode with a spectrum taken every 22 seconds for the length of the experiment. The data were processed using MestReNova software and peak integrations were normalized using toluene as the internal standard.

Initial-rate kinetic analysis, which was determined based on the data points acquired in the first 600 seconds, showed that there is *fourth-order dependency* on $B(C_6F_5)_3$ concentration in the reaction between **3.21r** and **3.25c** (Figures S3.41, S3.42).

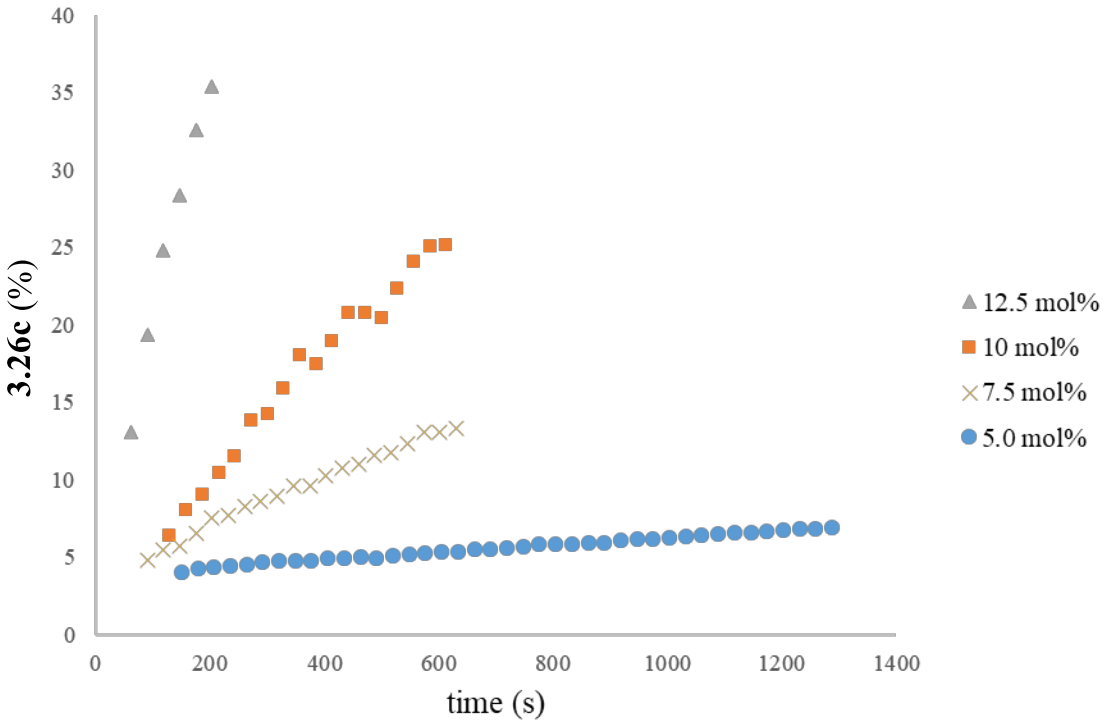

Figure S3.41. Monitoring the formation of **3.26c** under different concentrations of $B(C_6F_5)_3$

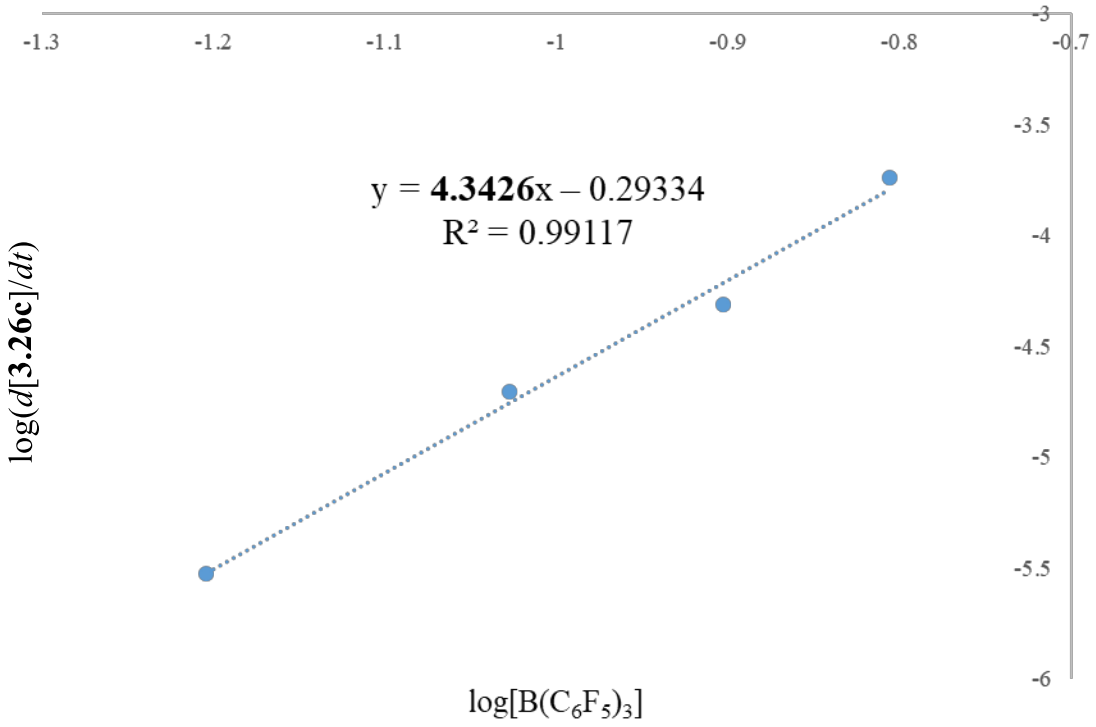

Figure S3.42. Log(rate) *vs* log[$B(C_6F_5)_3$] is employed to determine the initial reaction order for $B(C_6F_5)_3$. The result suggests that there is *fourth-order dependency* on $B(C_6F_5)_3$ concentration.

Reaction Order of L10–Sc(OTf)$_3$

The reaction between **3.21r** and **3.25c** was performed using different concentrations of **L10**–Sc(OTf)$_3$ and the progress of each reaction was monitored by the ^{1}H NMR spectroscopy (Scheme S3.25).

Scheme S3.25. Determination of the Reaction Order of **L10**–Sc(OTf)$_3$

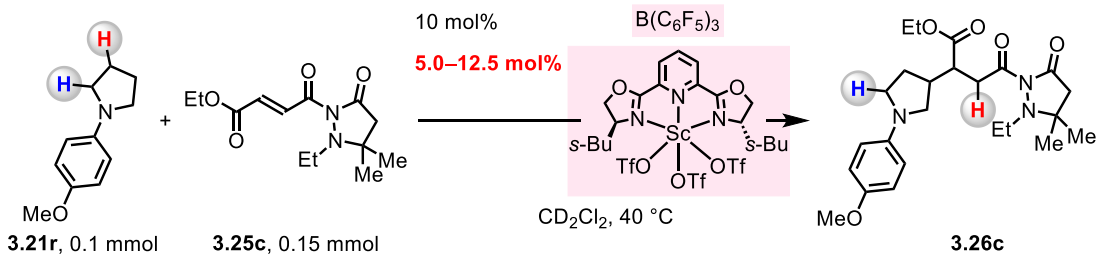

In a nitrogen-filled glove box, B(C_6F_5)$_3$ (30.7 mg, 10 mol%), **3.21r** (106.2 mg, 0.6 mmol), **3.25c** (241.2 mg, 1.5 equiv) and toluene (55.2 mg, 1.0 equiv) were weighed in an oven-dried 7.0 mL vial and the resulting mixture was dissolved in 2.40 mL of CD_2Cl_2 (**Stock Solution A**). In another oven-dried 7.0 mL vial, **L10**–Sc(OTf)$_3$ (57.4 mg, 0.070 mmol) was weighed and dissolved in 1.40 mL of CD_2Cl_2 (**Stock Solution B**). To each J-Young tube was added **Stock Solution A** (0.40 mL), **Stock Solution B** (0.10, 0.15, 0.20, or 0.25 mL) and CD_2Cl_2 (0.30, 0.25, 0.20, or 0.15 mL) to prepare the reaction samples containing different concentrations of **L10**–Sc(OTf)$_3$. After the J-Young tube was tightly capped with the Teflon plug, it was taken out of the glove box and ^{1}H NMR spectra were acquired in the NMR spectrometer preheated at 40 °C using a pre-acquisition delay in array mode with a spectrum taken every 22 seconds for the length of the experiment. The data were processed using MestReNova software and peak integrations were normalized using toluene as the internal standard.

Initial-rate kinetic analysis, which was determined based on the data points acquired in the first 1100 seconds, showed that there is *–1-order dependency* on **L10**–Sc(OTf)$_3$ concentration in the

reaction between **3.21r** and **3.25c** (Figures S3.43, S3.44).

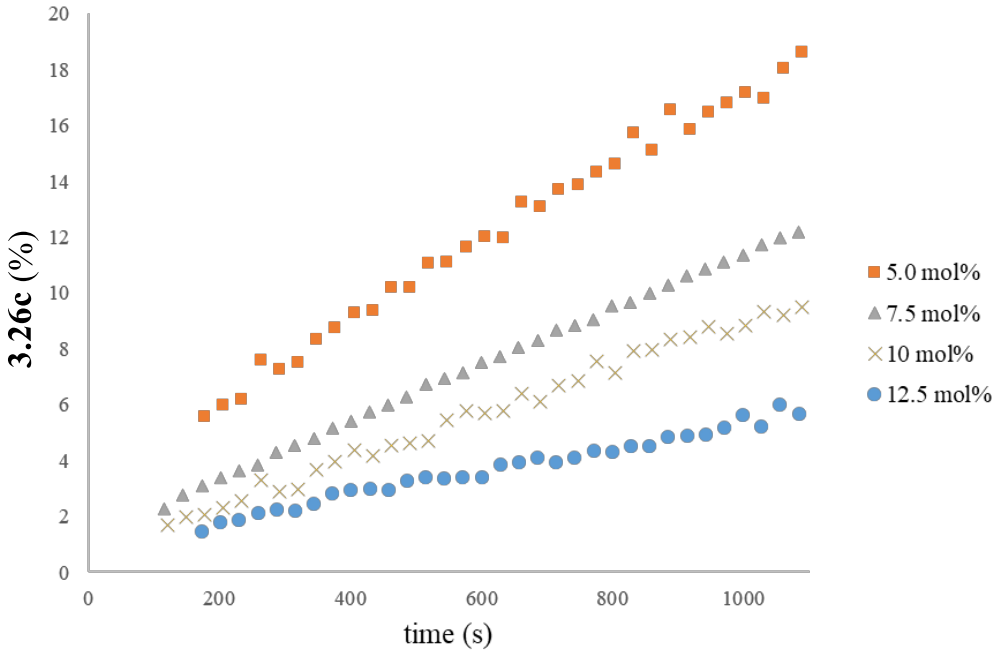

Figure S3.43. Monitoring the formation of **3.26c** under different concentrations of **L10**–Sc(OTf)$_3$

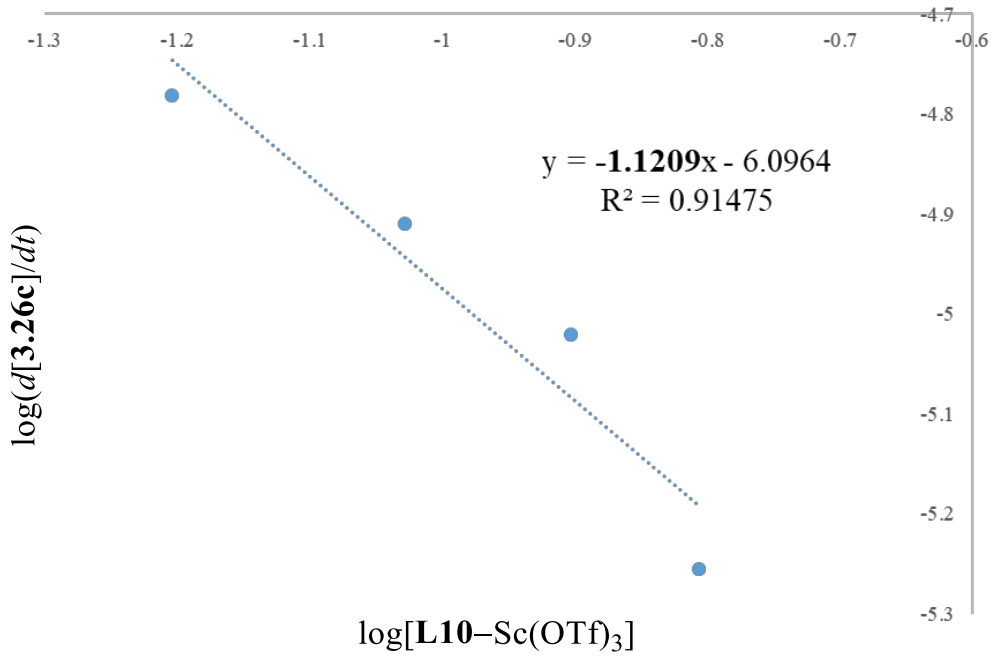

Figure S3.44. Log(rate) *vs* log[**L10**–Sc(OTf)$_3$] is employed to determine the initial reaction order for **L10**–Sc(OTf)$_3$. The result suggests that there is *–1-order dependency* on **L10**–Sc(OTf)$_3$ concentration.

Reaction Order of Amine

The reaction between **3.21r** and **3.25c** was performed using different concentrations of **3.21r** and the progress of each reaction was monitored by the ^{1}H NMR spectroscopy (Scheme S3.26).

Scheme S3.26. Determination of the Reaction Order of **3.21r**

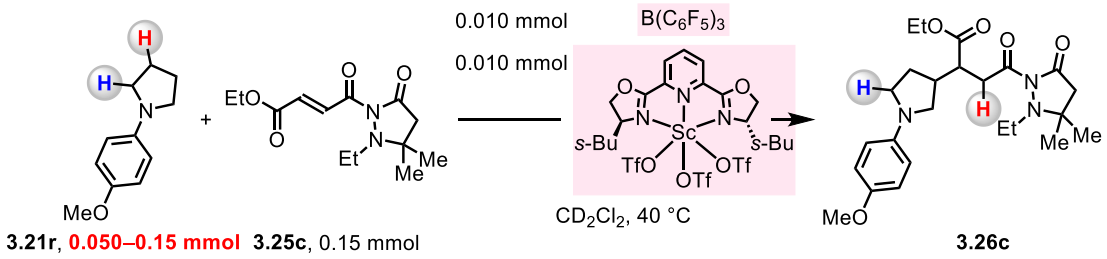

In a nitrogen-filled glove box, $B(C_6F_5)_3$ (30.7 mg, 0.060 mmol), **L10**–$Sc(OTf)_3$ (24.6 mg, 0.030 mmol), **3.25c** (241.2 mg, 0.90 mmol) and toluene (55.2 mg, 0.60 mmol) were weighed in an oven-dried 7.0 mL vial and the resulting mixture was dissolved in 3.00 mL of CD_2Cl_2 (**Stock Solution A**). In another oven-dried 7.0 mL vial, **3.21r** (177mg, 1.0 mmol) was weighed and dissolved in 1.00 mL of CD_2Cl_2 (**Stock Solution B**). To each J-Young tube was added **Stock Solution A** (0.50 mL), **Stock Solution B** (0.05, 0.07, 0.10, or 0.15 mL) and CD_2Cl_2 (0.25, 0.23, 0.20, or 0.15 mL) to prepare the reaction samples containing different concentrations of **3.21r**. The reaction mixture was then transferred to a J-Young tube. After the J-Young tube was tightly capped with the Teflon plug, it was taken out of the glove box and ^{1}H NMR spectra were acquired in the NMR spectrometer preheated at 40 °C using a pre-acquisition delay in array mode with a spectrum taken every 22 seconds for the length of the experiment. The data were processed using MestReNova software and peak integrations were normalized using toluene as the internal standard.

Initial-rate kinetic analysis, which was determined based on the data points acquired in the first 800 seconds, showed that there is *first-order dependency* on amine **3.21r** concentration in the reaction between **3.21r** and **3.25c** (Figures S3.45, S3.46).

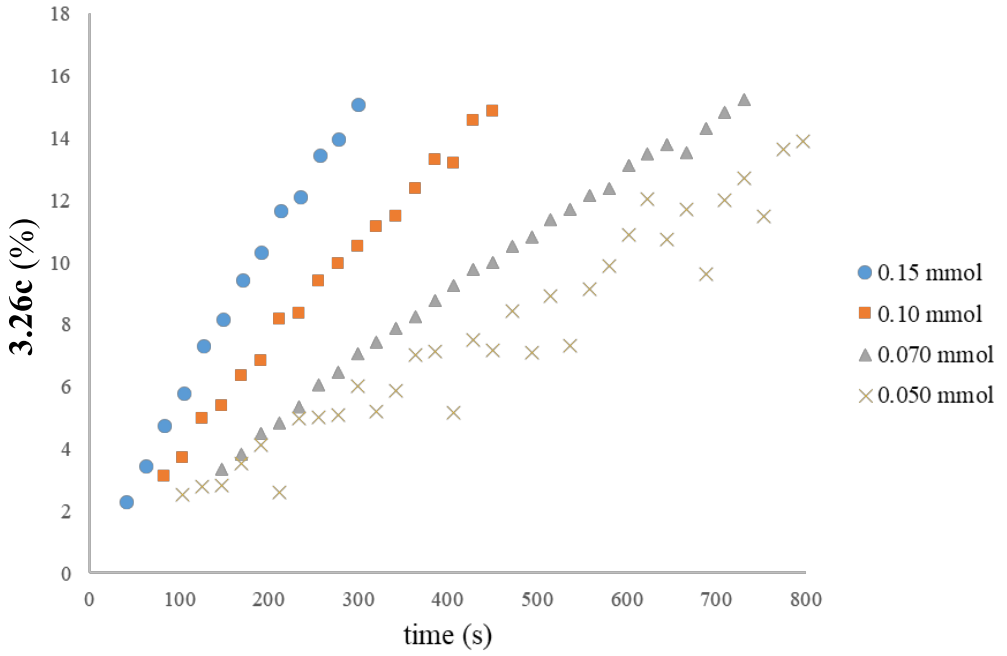

Figure S3.45. Monitoring the formation of **3.26c** under different concentrations of amine **3.21r**

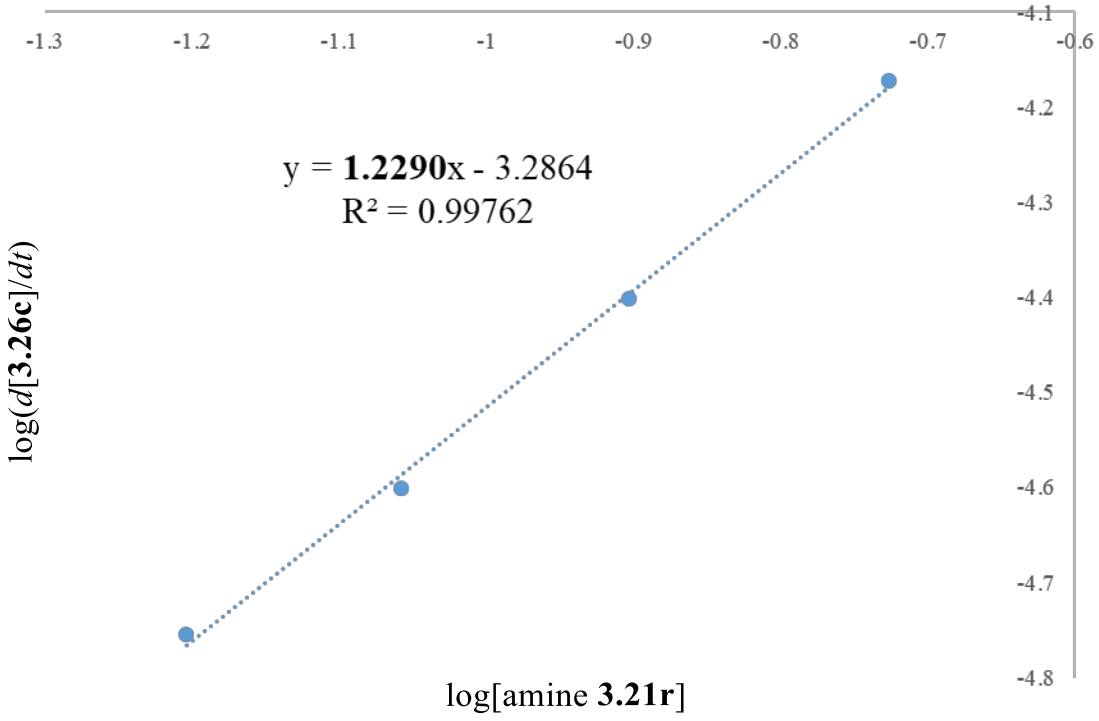

Figure S3.46. Log(rate) *vs* log[amine **3.21r**] is employed to determine the initial reaction order for amine **3.21r.** The result suggests that there is *first-order dependency* on **3.21r** concentration.

Reaction Order of α,β-Unsaturated Compound

The reaction between **3.21r** and **3.25c** was performed using different concentrations of **3.25c** and the progress of each reaction was monitored by the ^{1}H NMR spectroscopy (Scheme S3.27).

Scheme S3.27. Determination of the Reaction Order of **3.25c**

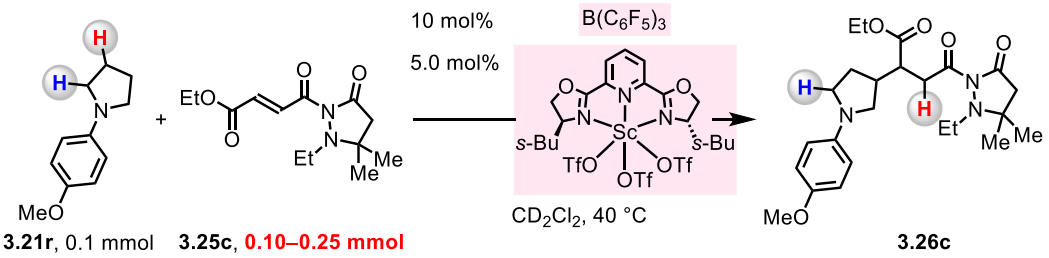

In a nitrogen-filled glove box, $B(C_6F_5)_3$ (30.7 mg, 10 mol%), **L10**–$Sc(OTf)_3$ (24.6 mg, 5.0 mol%), **3.21r** (106.2 mg, 0.60 mmol), and toluene (55.2 mg, 1.0 equiv) were weighed in an oven-dried 7.0 mL vial and the resulting mixture was dissolved in 3.00 mL of CD_2Cl_2 (**Stock Solution A**). In another oven-dried 7.0 mL vial, **3.25c** (322mg, 1.20 mmol) was weighed and dissolved in 1.20 mL of CD_2Cl_2 (**Stock Solution B**). To each J-Young tube was added **Stock Solution A** (0.50 mL), **Stock Solution B** (0.10, 0.15, 0.20, or 0.25 mL) and CD_2Cl_2 (0.20, 0.15, 0.10, or 0.05 mL) to prepare the reaction samples containing different concentrations of **3.25c**. The reaction mixture was then transferred to a J-Young tube. After the J-Young tube was tightly capped with the Teflon plug, it was taken out of the glove box and ^{1}H NMR spectra were acquired in the NMR spectrometer preheated at 40 °C using a pre-acquisition delay in array mode with a spectrum taken every 22 seconds for the length of the experiment. The data were processed using MestReNova software and peak integrations were normalized using toluene as the internal standard.

Initial-rate kinetic analysis, which was determined based on the data points acquired in the first 800 seconds, showed that there is *–3-order dependency* on α,β-unsaturated compound **3.25c** concentration in the reaction between **3.21r** and **3.25c** (Figures S3.47, S3.48).

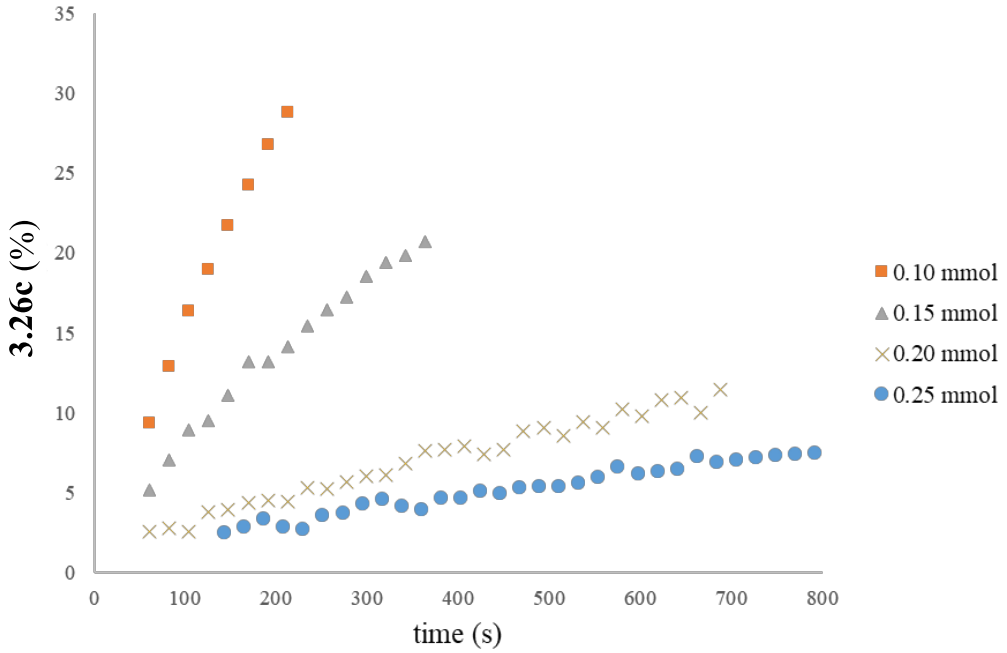

Figure S3.47. Monitoring the formation of **3.26c** under different concentrations of **3.25c**

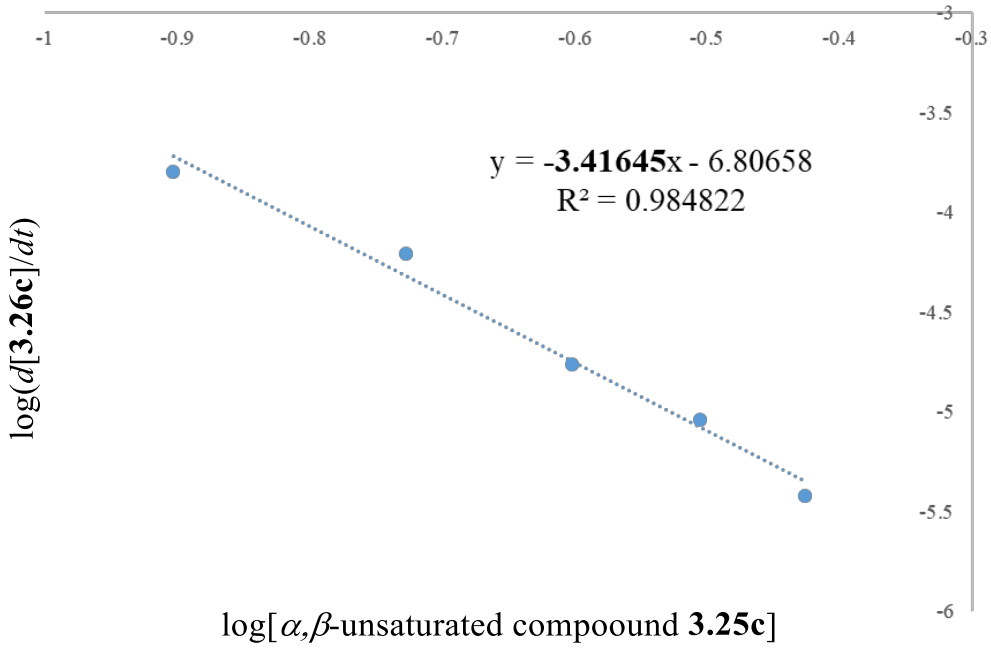

Figure S3.48. Log(rate) *vs* log[*α,β*-unsaturated compound **3.25c**] is employed to determine the initial reaction order for **3.25c**. The result suggests that there is *–3-order dependency* on **3.25c** concentration.

Kinetic Isotope Effect Experiments Involving 3.25c

In order to probe whether the turnover-limiting step involves the cleavage of α- or β-amino C–H bonds, we carried out parallel kinetic isotope effect experiments.

Parallel KIE Measurement for α-Amino C–H and C–D Bond Cleavage

A parallel kinetic isotope effect study was conducted through time course reaction monitoring by the ^{1}H NMR spectroscopy using internal standard to monitor the difference in initial rates of the product formation in the reaction of 1-(4-methoxyphenyl)pyrrolidine **3.21r** or 1-(4-methoxyphenyl)pyrrolidine-2,2,5,5-d_4 **3.21r-*d*$_\alpha$** with ethyl (*E*)-4-(2-ethyl-3,3-dimethyl-5-oxopyrazolidin-1-yl)-4-oxobut-2-enoate **3.25c** (Scheme S3.28).

In a nitrogen-filled glove box, $B(C_6F_5)_3$ (20.4 mg, 0.040 mmol), **L10**–$Sc(OTf)_3$ (16.4 mg, 0.020 mmol), **3.25c** (160.8 mg, 0.60 mmol) and toluene (36.8 mg, 0.40 mmol) were weighed in an oven-dried 7.0 mL vial and the resulting mixture was dissolved in 2.00 mL of CD_2Cl_2 (**Stock Solution A**). In two oven-dried 7.0 mL vials were added **3.21r** (17.7 mg) or **3.21r-*d*$_\alpha$** (18.1 mg). To each oven-dried vial containing **3.21r** or **3.21r-*d*$_\alpha$** was added CD_2Cl_2 (0.30 mL) and **Stock Solution A** (0.50 mL) to prepare the reaction samples containing **3.21r** or **3.21r-*d*$_\alpha$**. The reaction mixture was then transferred to a J-Young tube. After the J-Young tube was tightly capped with the Teflon plug, it was taken out of the glove box and ^{1}H NMR spectra were acquired in the NMR spectrometer preheated at 40 °C using a pre-acquisition delay in array mode with a spectrum taken every 22 seconds for the length of the experiment. The data were processed using MestReNova software and peak integrations were normalized using toluene as the internal standard.

Kinetic analysis based on the initial rates of the product formation (Figure S3.49) demonstrates that **3.21r** reacts 1.3 times faster than **3.21r-*d*$_\alpha$** (k_H/k_D = 1.34) in the reaction between **3.21r** or **3.21r-*d*$_\alpha$** and **3.25c**. From ^{1}H NMR analysis of the isolated and purified **3.26c-*d*$_\alpha$** in $CDCl_3$, it was

revealed that 94% of *d*-incorporation level was retained at the α-amino position (Figures S3.50−3.51). This result suggests that the borohydride reduction step may be irreversible as there was no H incorporation into the α-amino C−D bonds.

Scheme S3.28. Kinetic Isotope Effect Studies

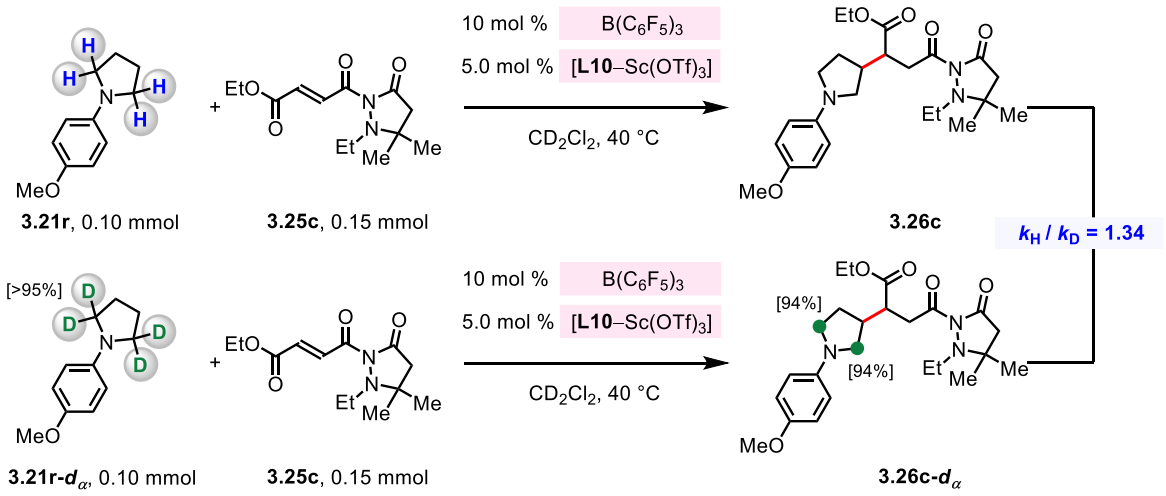

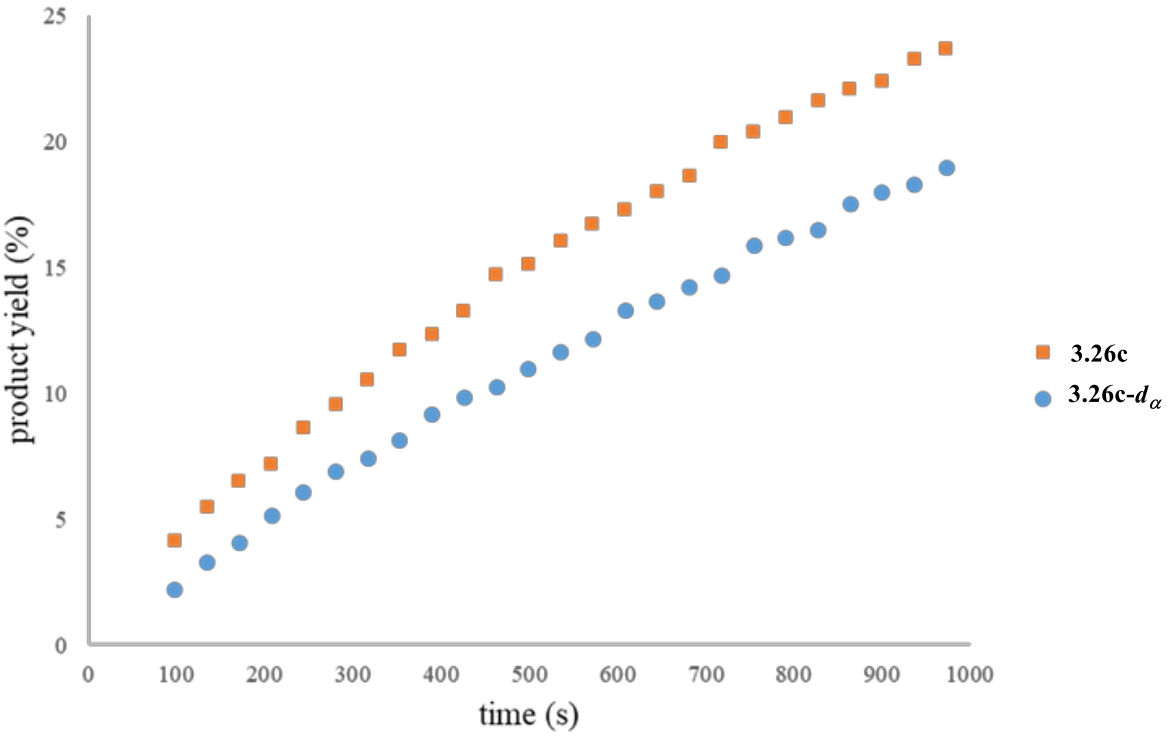

Figure S3.49. Monitoring the formation of products in parallel KIE measurements

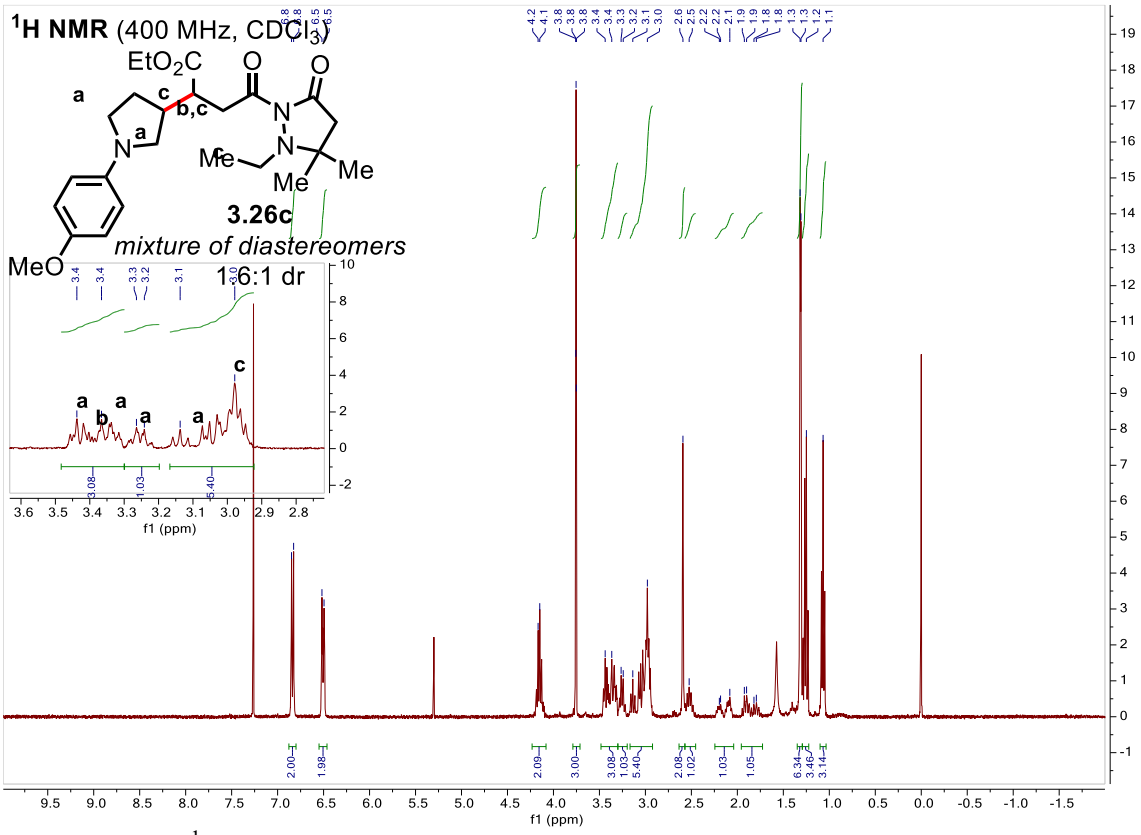

Figure S3.50. ^{1}H NMR spectrum of **3.26c** ($CDCl_3$)

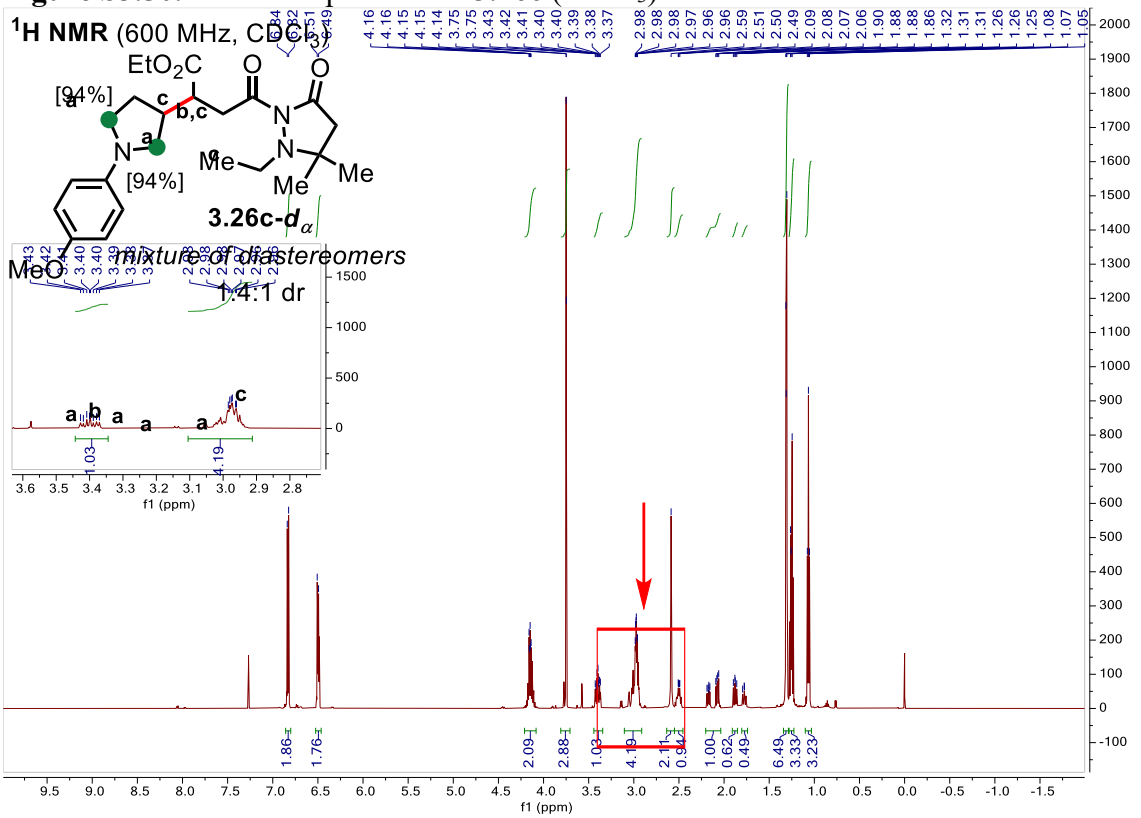

Figure S3.51. ^{1}H NMR spectrum of **3.26c-*dα*** ($CDCl_3$)

Parallel KIE Measurement for *β*-Amino C–H and C–D Bond Cleavage

A parallel kinetic isotope effect study was conducted through time course reaction monitoring by the ^{1}H NMR spectroscopy using internal standard to monitor the difference in initial rates of the product formation in the reaction of 1-(4-methoxyphenyl)pyrrolidine **3.21r** or 1-(4-methoxyphenyl)pyrrolidine-3,3,4,4-d_4 **3.21r-*dβ*** with ethyl (*E*)-4-(2-ethyl-3,3-dimethyl-5-oxopyrazolidin-1-yl)-4-oxobut-2-enoate **3.25c** (Scheme S3.29). In a nitrogen-filled glove box, $B(C_6F_5)_3$ (20.4 mg, 0.040 mmol), **L10**–$Sc(OTf)_3$ (16.4 mg, 0.020 mmol), **3.25c** (160.8 mg, 0.60 mmol) and toluene (36.8 mg, 0.40 mmol) were weighed in an oven-dried 7.0 mL vial and the resulting mixture was dissolved in 2.00 mL of CD_2Cl_2 (**Stock Solution A**). In two oven-dried 7.0 mL vials were added **3.21r** (17.7 mg) or **3.21r-*dβ*** (18.1 mg). To each oven-dried vial containing **3.21r** or **3.21r-*dβ*** was added CD_2Cl_2 (0.30 mL) and **Stock Solution A** (0.50 mL) to prepare the reaction samples containing **3.21r** or **3.21r-*dβ***. The reaction mixture was then transferred to a J-Young tube. After the J-Young tube was tightly capped with the Teflon plug, it was taken out of the glove box and ^{1}H NMR spectra were acquired in the NMR spectrometer preheated at 40 °C using a pre-acquisition delay in array mode with a spectrum taken every 22 seconds for the length of the experiment. The data were processed using MestReNova software and peak integrations were normalized using toluene as the internal standard.

Kinetic analysis based on the initial rates of the product formation (Figure S3.52) demonstrates no kinetic isotope effect (k_H/k_D = 1.00) in the reaction between **3.21r** or **3.21r-*dβ*** and **3.25c**. From ^{1}H NMR analysis of the isolated and purified **3.26c-*dβ d*** in $CDCl_3$ and acetone-d_6, *d*-incorporation level was determined (Figures S3.53–S3.56).

Scheme S3.29. Kinetic Isotope Effect Studies

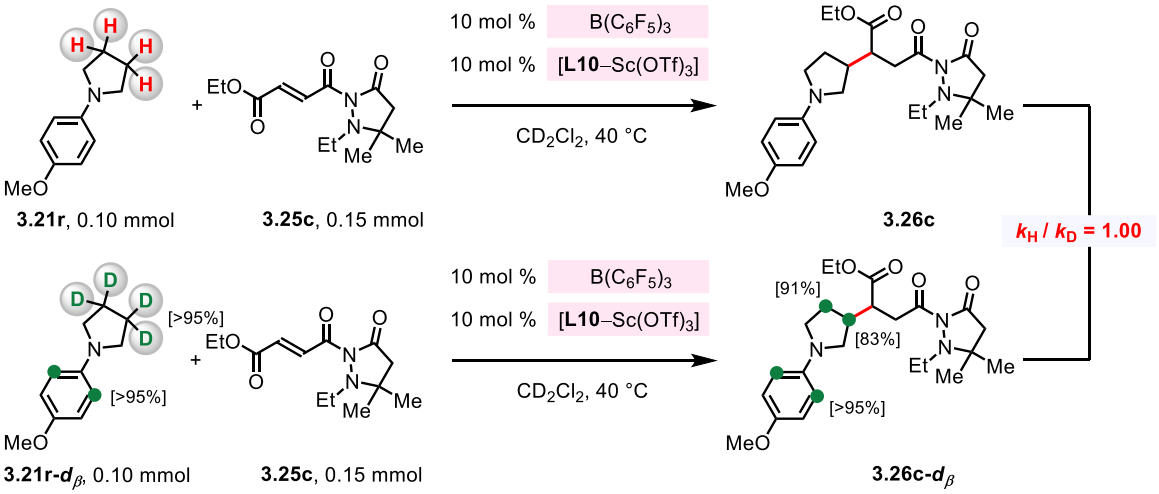

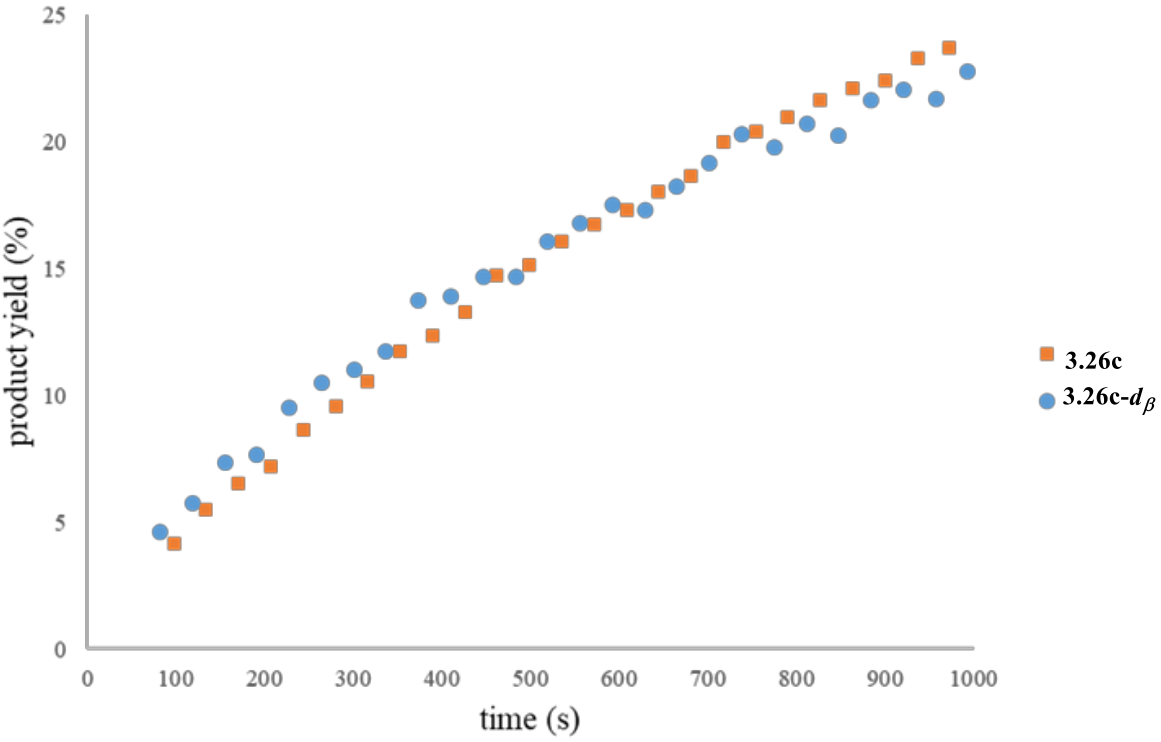

Figure S3.52. Monitoring the formation of products in parallel KIE measurements

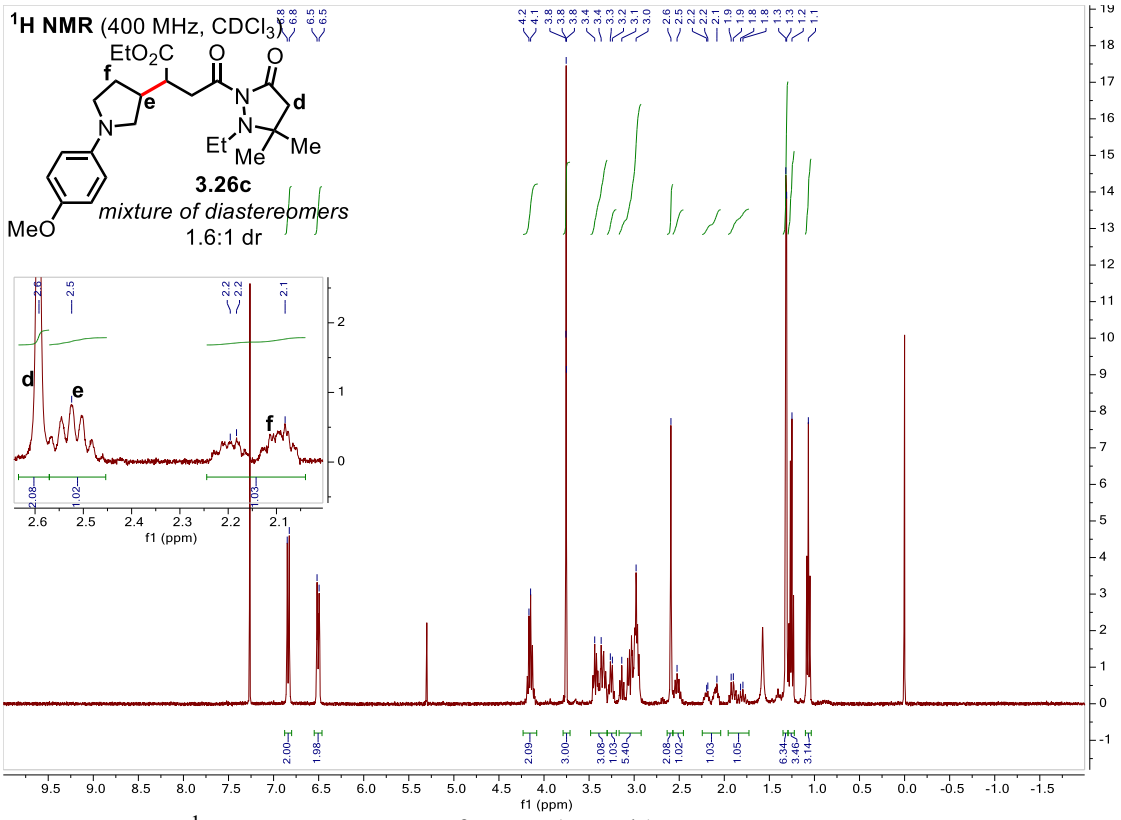

Figure S3.53. ^{1}H NMR spectrum of **3.26c** ($CDCl_3$)

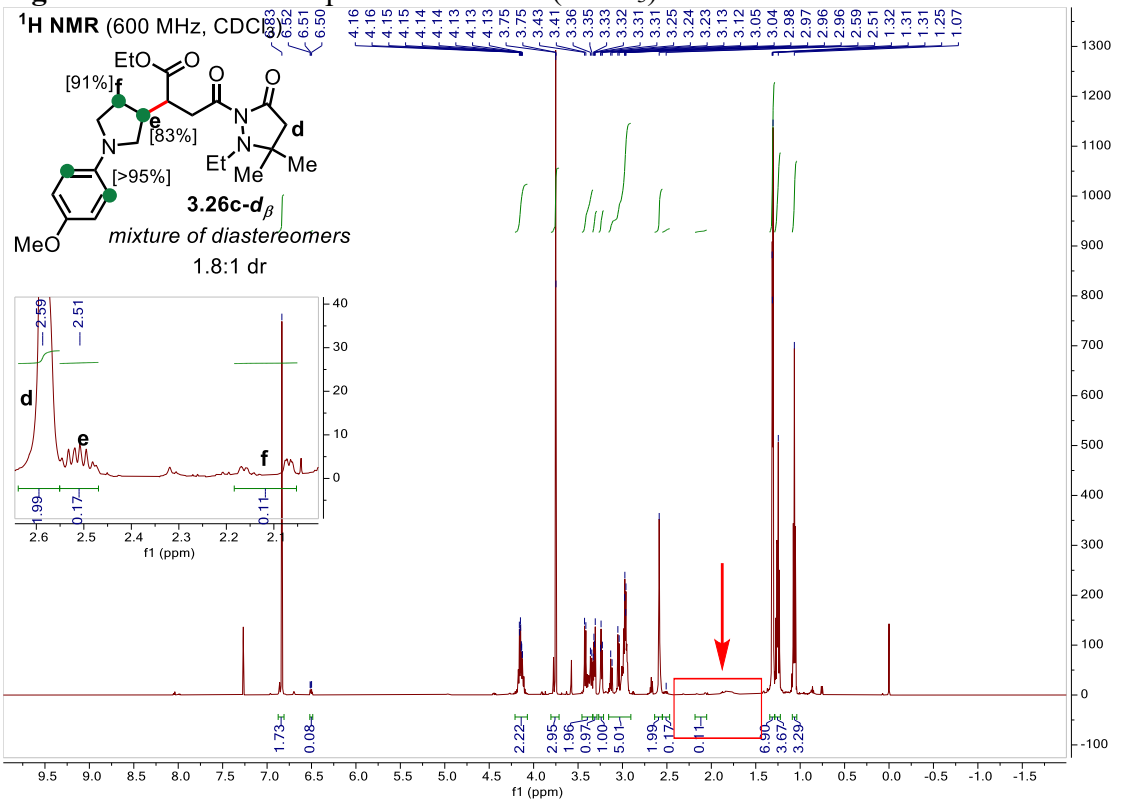

Figure S3.54. ^{1}H NMR spectrum of **3.26c-*dβ*** ($CDCl_3$)

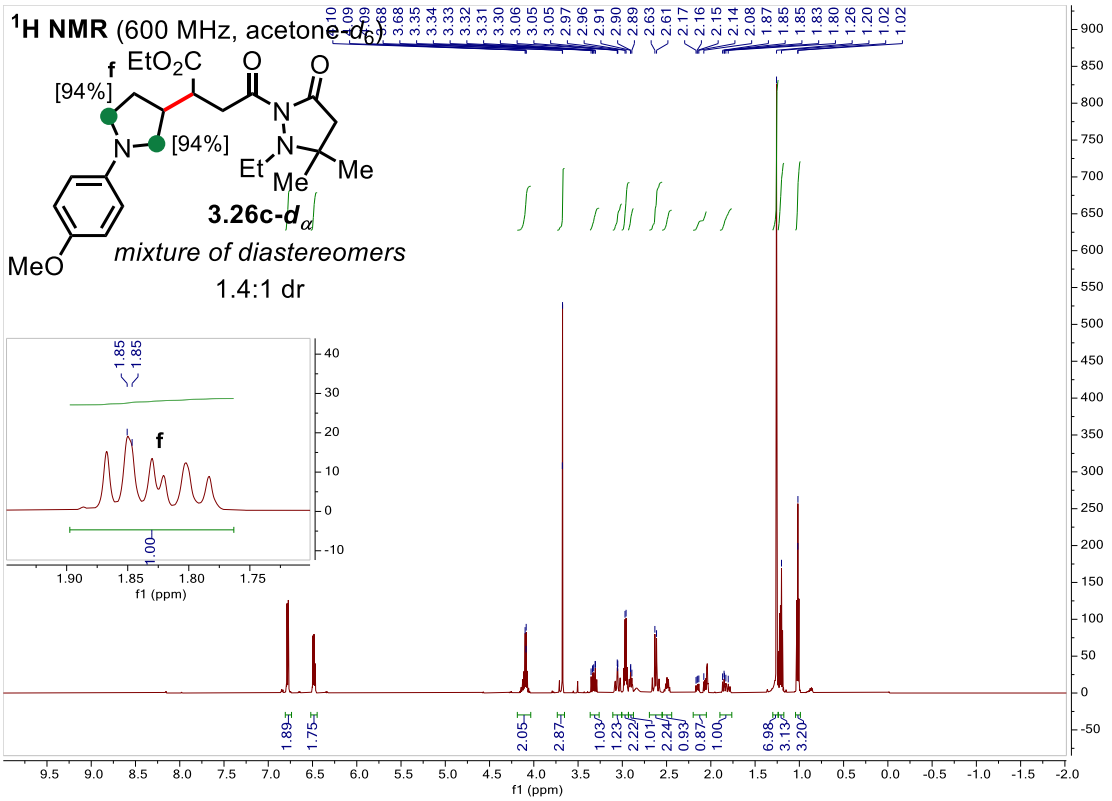

Figure S3.55. ^{1}H NMR spectrum of **3.26c-*dα*** (acetone-d_6)

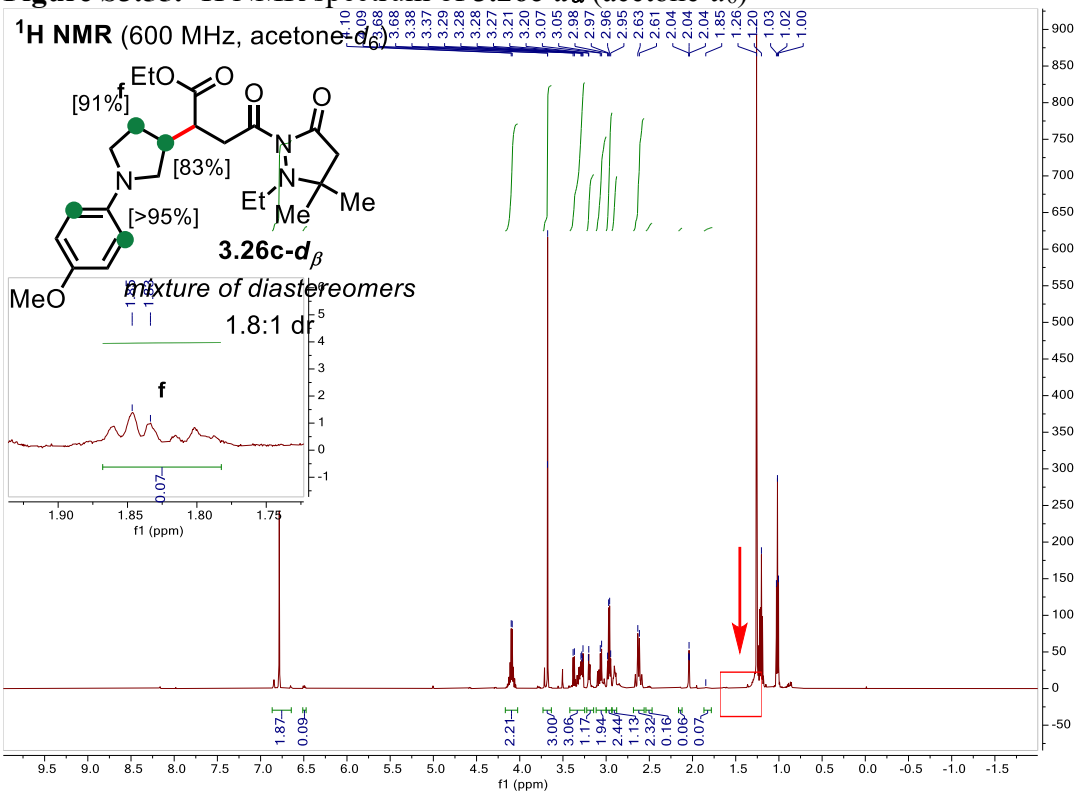

Figure S3.56. ^{1}H NMR spectrum of **3.26c-*dβ*** (acetone-d_6)

The ^{13}C NMR Experiments for Characterization of Resting State Complexes

The mechanistic investigation revealed that the $(F_5C_6)_3B$/**L10**–$Sc(OTf)_3$ co-catalyzed *β*-amino C–H functionalization has a *–1 order dependency* with respect to the concentration of **L10**–$Sc(OTf)_3$ and *–3 order dependency* with respect to the concentration of ethyl (*E*)-4-(2-ethyl-3,3-dimethyl-5-oxopyrazolidin-1-yl)-4-oxobut-2-enoate **3.25c**. We hypothesized that [**L10**–$Sc(OTf)_3$]–**3.25c**–$B(C_6F_5)_3$ adduct could be the resting state and carried out the ^{13}C NMR experiments to identify the structure of the resting state complex (Figures S3.57, S3.58). Previously, the group of Piers has reported that $B(C_6F_5)_3$ and benzaldehyde forms $(F_5C_6)_3B$–carbonyl compound adduct which showed that ^{13}C NMR peak of carbonyl moiety shifted further downfield to 199.4 ppm. We acquired the ^{13}C NMR spectra of a sample containing $B(C_6F_5)_3$ and/or **L10**–$Sc(OTf)_3$ and **3.25c** in CD_2Cl_2 (Figures S3.57, S3.58).

In the ^{13}C NMR spectrum of a reaction mixture containing **3.25c** and 50 mol% $B(C_6F_5)_3$, it was observed that the carbonyl peak of **3.25c** at 175.3 ppm has shifted to 178.1 ppm (Figure S55A, S51B. See the peak marked with a red arrow). Similar trend was observed in a mixture of **3.25c**, 50 mol% $B(C_6F_5)_3$, and 25 mol% **L10**–$Sc(OTf)_3$ showing shifted peak at 178.4 ppm (Figure S55C, S56). Furthermore, the peak at 162.5 ppm of **3.25c** shifted to 163.5 ppm, which was also detected in the solution of **3.25c** and 25 mol% **L10**–$Sc(OTf)_3$ (Figure S55C, S55D, and S56. See the peak marked with a blue arrow).

These results are in agreement with our hypothesis that Lewis acidic $B(C_6F_5)_3$ and **L10**–$Sc(OTf)_3$ coordinate to Lewis basic carbonyl functional groups of **3.25c** and form [**L10**–$Sc(OTf)_3$]–**3.25c**–$B(C_6F_5)_3$ adduct as the catalyst resting state.

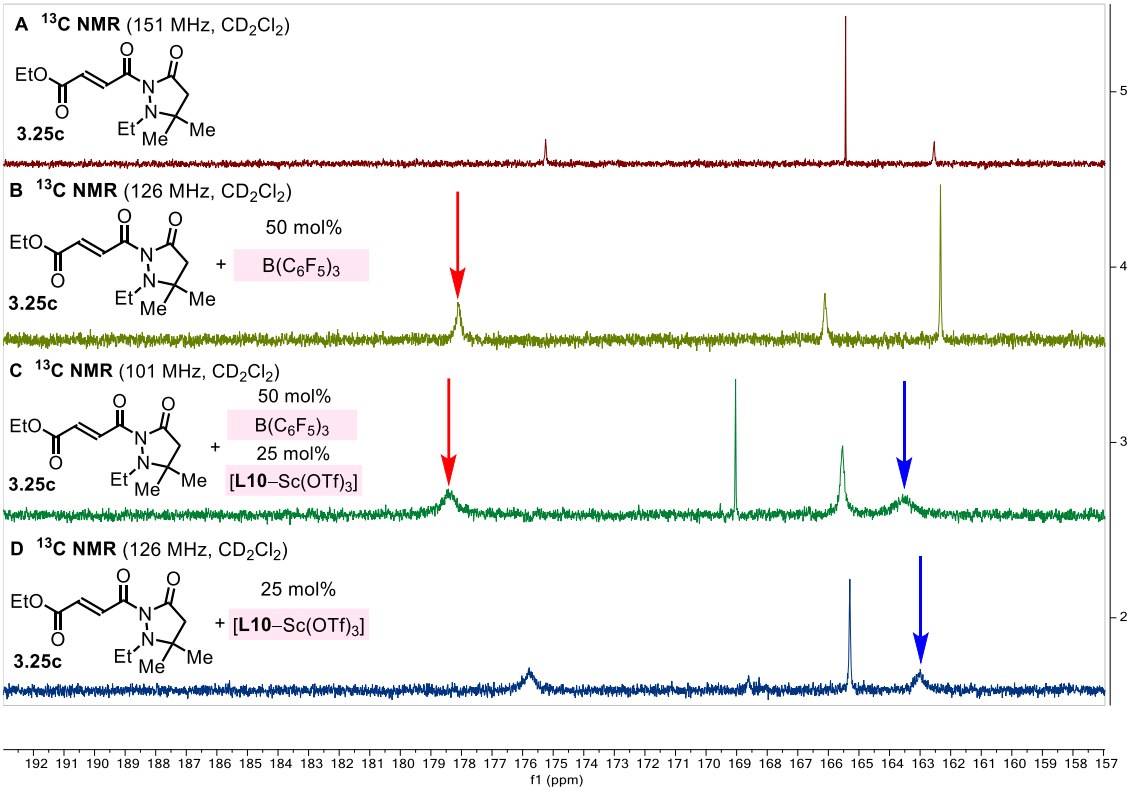

Figure S3.57. ^{13}C NMR experiments for the detection of the resting state

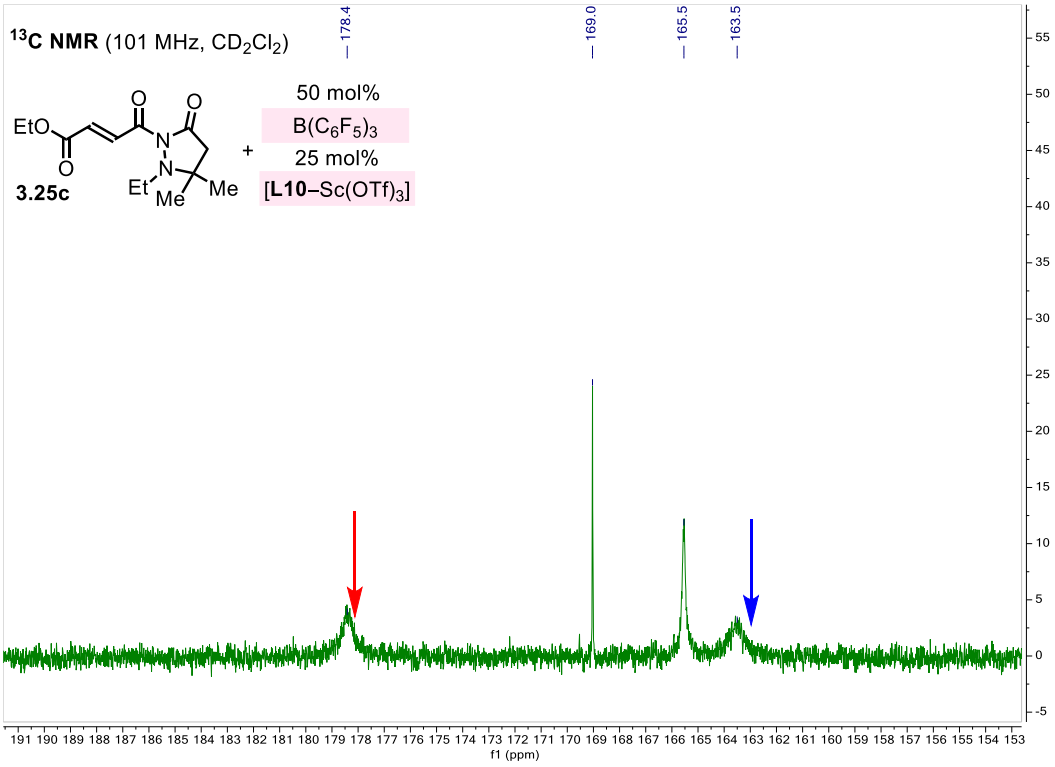

Figure S3.58. ^{13}C NMR spectrum of 3.25c, B(C_6F_5)$_3$, and L10–Sc(OTf)$_3$

Catalytic Cycle for the Enantioselective *β*-Amino C–H Functionalization Involving 3.25c

In Figure S3.59, we show the catalytic cycles that are consistent with the above-mentioned mechanistic investigations. The mechanistic studies revealed that there is *–1 order dependency* with respect to the concentration of **L10**–$Sc(OTf)_3$ and *–3 order dependency* with respect to the concentration of **3.25c**. These results suggest that there is a resting state complex comprised of [**L10**–$Sc(OTf)_3$], **3.25c**, and $B(C_6F_5)_3$ (**XXIX**) which was verified by the ^{13}C NMR studies (Figures S3.57, S3.58). $B(C_6F_5)_3$ released from **XXIX** abstracts a hydride from **3.21r** to form an ion pair consisting of iminium ion and borohydride (**XXX**). The *fourth order dependency* with respect to the concentration of $B(C_6F_5)_3$ and the kinetic isotope effect studies suggest that the borohydride reduction of $(F_5C_6)_3B$-activated **3.25c** is the turnover-limiting step (**XXX** → **XXXI**). After the protonation of enolate (**XXXI** → **XXXII**), nucleophilic enamine can undergo enantioselective C–C bond formation with [**L10**–$Sc(OTf)_3$]-activated **3.25c** to form zwitterionic **XXXIV**. We propose that **3.21r** could serve as H^+/H^- source to reduce **XXXIV** in order to afford the desired *β*-alkylation product **3.26c**.

The results from the mechanistic investigations involving **3.25c** are in similar trend with the proposed catalytic cycle that was based on the mechanistic studies involving aryl-substituted electrophile **3.25g** (Figure S3.37). However, it was found that the turnover-limiting step could be different depending on the electrophile that is used. When ethyl ester-substituted electrophile **3.25c** is involved, the borohydride reduction step (turnover-limiting) becomes irreversible as the allylic C–H bond of the boron–enolate (blue H in **XXXI**, Figure S3.59) is not as hydridic due to the electron withdrawing ester unit (vs phenyl substituent in **3.25g**).

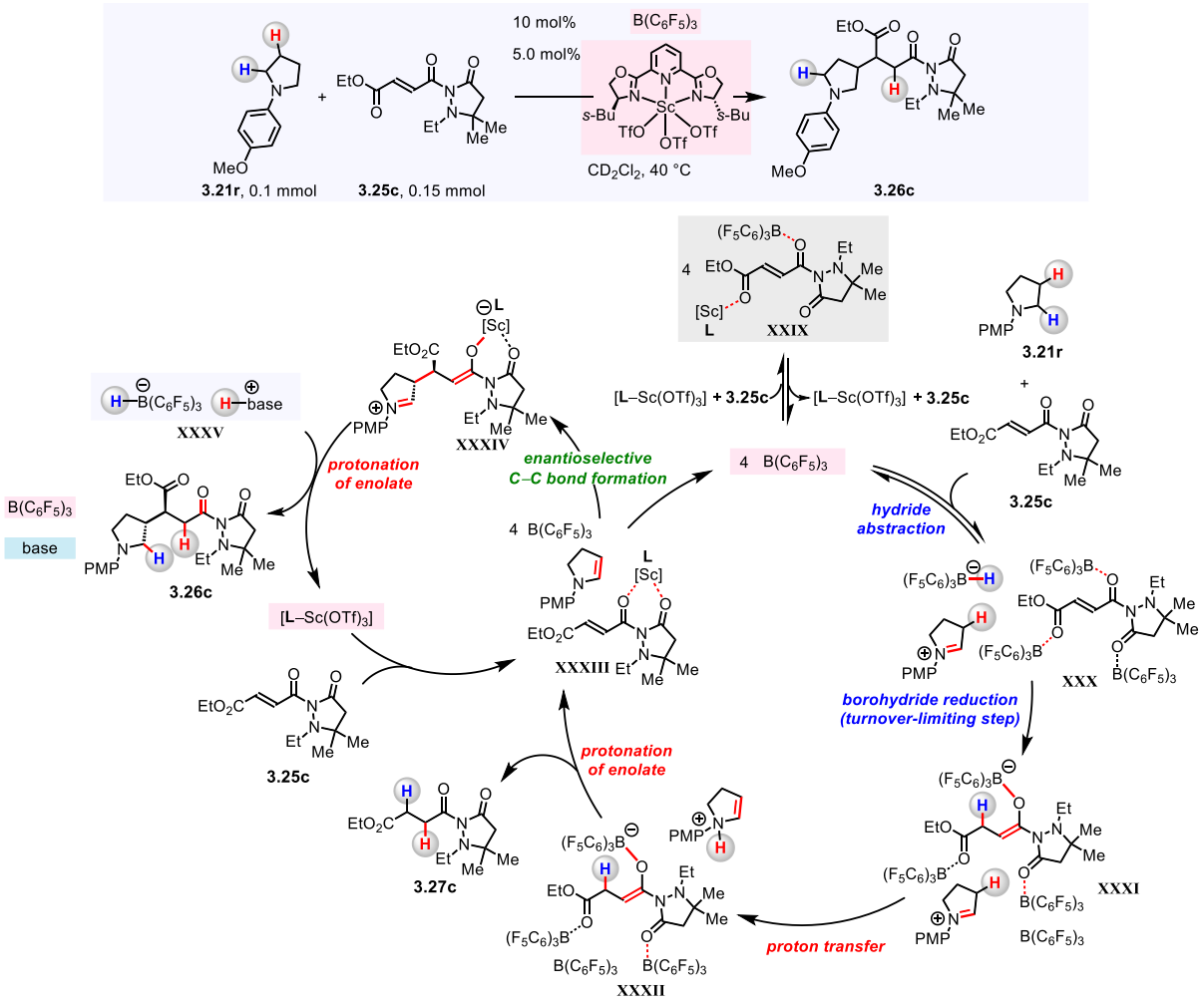

Figure S3.59. Proposed catalytic cycle for the enantioselective *β*-amino C–H functionalization involving **3.25c**

C8. Analytical Data

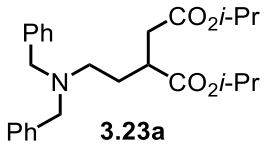

3.23a

Diisopropyl 2-(2-(dibenzylamino)ethyl)succinate (3.23a)

N,*N*-Dibenzylethanamine **3.21a** was reacted with diisopropyl fumarate **3.22a** following the **General Procedure C** using $B(C_6F_5)_3$ (10 mol%) as the Lewis acid catalyst and benzene (0.80 mL) as the solvent. After purification by column chromatography (ethyl ether:hexanes = 1:19), **3.23a** was obtained as a colorless liquid (75 mg, 88%).

^{1}H NMR (600 MHz, $CDCl_3$): δ 7.34 (d, *J* = 7.5 Hz, 4H), 7.29 (t, *J* = 7.5 Hz, 4H), 7.22 (t, *J* = 7.3 Hz, 2H), 4.95 (dp, *J* = 26.6, 6.2 Hz, 2H), 3.61 (d, *J* = 13.6 Hz, 2H), 3.46 (d, *J* = 13.5 Hz, 2H), 2.88 (dq, *J* = 12.4, 6.6 Hz, 1H), 2.51 – 2.39 (m, 3H), 2.16 (dd, *J* = 16.4, 5.1 Hz, 1H), 1.92 (dq, *J* = 14.4, 7.3 Hz, 1H), 1.61 (h, *J* = 7.3 Hz, 1H), 1.20 (d, *J* = 6.3 Hz, 6H), 1.16 (d, *J* = 6.3 Hz, 3H), 1.12 (d, *J* = 6.3 Hz, 3H); **^{13}C NMR (151 MHz, $CDCl_3$):** δ 174.3, 171.3, 139.5, 128.8, 128.2, 126.9, 67.78, 67.77, 58.3, 50.5, 39.1, 35.9, 29.0, 21.81, 21.78, 21.69, 21.65; **IR (neat):** ν 2976, 2932, 2796, 1724, 1452, 1372, 1260, 1168, 1104, 745, 698 cm^{-1}; **HRMS (ESI):** Calcd for $C_{26}H_{36}NO_4$ (MH^+): 426.2639; found: 426.2643.

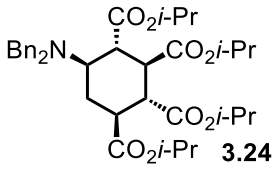

3.24

Tetraisopropyl 5-(dibenzylamino)cyclohexane-1,2,3,4-tetracarboxylate (3.24)

The relative configuration was assigned based on NOESY.

^{1}H NMR (500 MHz, $CDCl_3$): δ 7.34 – 7.27 (m, 8H), 7.22 (t, *J* = 6.6 Hz, 2H), 5.06 (hept, *J* = 6.4 Hz, 1H), 5.02 – 4.89 (m, 3H), 3.89 (d, *J* = 13.6 Hz, 2H), 3.48 (d, *J* = 13.6 Hz, 2H), 3.38 (t, *J* = 8.3 Hz, 1H), 3.30 (t, *J* = 8.3 Hz, 1H), 2.81 – 2.66 (m, 3H), 2.57 (dd, *J* = 16.7, 10.1 Hz, 1H), 2.44 (dd, *J* = 16.8, 3.6 Hz, 1H), 1.31 (d, *J* = 6.3 Hz, 3H), 1.27 (d, *J* = 6.2 Hz, 3H), 1.21 (td, *J* = 6.0, 3.7 Hz, 12H), 1.16 (d, *J* = 6.2 Hz, 3H), 1.11 (d, *J* = 6.3 Hz, 3H); **^{13}C NMR (126 MHz, $CDCl_3$):** δ 172.3, 172.2, 172.1, 171.1, 139.1, 128.9, 128.4, 127.3, 68.4, 68.3, 67.9, 60.8, 54.8, 45.3, 42.3, 41.2, 39.4, 34.2, 22.0, 21.91, 21.88, 21.87, 21.78, 21.76, 21.7; **IR (neat):** ν 2977, 2934, 1725, 1493, 1373, 1258, 1201, 1175, 1106, 748, 699 cm^{-1}; **HRMS (DART):** Calcd for $C_{36}H_{50}NO_8$ (MH^+): 624.3531; found: 624.3511.

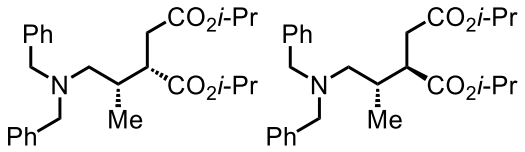

3.23b-major **3.23b-minor**

Diisopropyl 2-(1-(dibenzylamino)propan-2-yl)succinate (3.23b)

N,N-Dibenzylpropan-1-amine **3.21b** was reacted with diisopropyl fumarate **3.22a** following the **General Procedure C** using $B(C_6F_5)_3$ (10 mol%) as the Lewis acid catalyst and benzene (0.2 mL) as the solvent. ^{1}H NMR analysis of the unpurified product mixture revealed that the diastereomeric ratio was 1.3:1. After purification by column chromatography (ethyl ether:hexanes = 1:19), **3.23b** was obtained as a mixture of diastereomers (51 mg, 58%). **3.23c** was obtained as a colorless liquid (29 mg, 33%). Further purification was carried out by PTLC using ethyl ether:DCM = 1:49 as the eluent to separate **3.23b-major** and **3.23b-minor**. The relative configuration of **3.21b-major** was assigned in analogy.

3.23b-Major: ^{1}**H NMR** (600 MHz, $CDCl_3$) δ 7.35 (d, *J* = 7.1 Hz, 4H), 7.28 (t, *J* = 7.5 Hz, 4H), 7.21 (t, *J* = 7.3 Hz, 2H), 4.99 (h, *J* = 6.3 Hz, 2H), 3.75 (d, *J* = 13.3 Hz, 2H), 3.34 – 3.26 (m, 3H), 2.39 – 2.30 (m, 2H), 2.24 (dd, *J* = 12.8, 9.7 Hz, 1H), 2.14 (dd, *J* = 12.9, 6.0 Hz, 1H), 1.56 (dd, *J* = 16.7, 3.2 Hz, 1H), 1.27 – 1.19 (m, 9H), 1.16 (d, *J* = 6.2 Hz, 3H), 0.73 (d, *J* = 6.9 Hz, 3H); ^{13}**C NMR** (151 MHz, $CDCl_3$) δ 174.5, 172.0, 139.5, 129.1, 128.2, 126.9, 67.6, 67.5, 58.7, 56.8, 42.1, 32.1, 29.8, 21.9, 21.84, 21.83, 21.7, 13.9; **IR** (neat) ν 2976, 2930, 2799, 1723, 1452, 1372, 1232, 1172, 1105, 745, 698 cm^{-1}; **HRMS** (DART) Calcd for $C_{27}H_{38}NO_4$ (MH^+): 440.2795; found: 440.2789.

3.21b-Minor: **^{1}H NMR** (600 MHz, $CDCl_3$) δ 7.34 (d, *J* = 7.5 Hz, 4H), 7.29 (t, *J* = 7.5 Hz, 4H), 7.22 (t, *J* = 7.2 Hz, 2H), 4.96 (dp, *J* = 22.6, 6.3 Hz, 1H), 3.71 (d, *J* = 13.6 Hz, 2H), 3.32 (d, *J* = 13.6 Hz, 2H), 2.91 (dt, *J* = 10.7, 4.1 Hz, 1H), 2.62 (dd, *J* = 16.6, 10.7 Hz, 1H), 2.41 (dd, *J* = 12.7, 5.8 Hz, 1H), 2.32 (dd, *J* = 12.7, 8.8 Hz, 1H), 2.15 (dd, *J* = 16.6, 4.3 Hz, 1H), 1.98 (ddp, *J* = 9.8, 6.4, 3.7, 3.1 Hz, 1H), 1.21 (dd, *J* = 11.4, 6.2 Hz, 6H), 1.16 (d, *J* = 6.3 Hz, 3H), 1.06 (d, *J* = 6.3 Hz, 3H), 0.88 (d, *J* = 6.9 Hz, 3H); **^{13}C NMR** (151 MHz, $CDCl_3$) δ 173.1, 171.8, 139.5, 128.9, 128.1, 126.8, 107.3, 67.8, 59.0, 58.7, 44.3, 34.2, 33.5, 21.82, 21.79, 21.76, 21.7, 15.2; **HRMS** (DART) Calcd for $C_{27}H_{38}NO_4$ (MH^+): 440.2795; found: 440.2780.

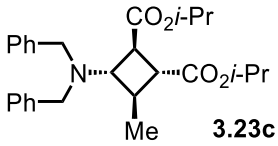

3.23c

Diisopropyl 3-(dibenzylamino)-4-methylcyclobutane-1,2-dicarboxylate (3.23c)

^{1}H NMR (600 MHz, $CDCl_3$) δ 7.33 (d, *J* = 7.6 Hz, 4H), 7.28 (t, *J* = 7.5 Hz, 4H), 7.21 (t, *J* = 7.3 Hz, 2H), 5.00 (dp, *J* = 16.7, 6.3 Hz, 2H), 3.79 (d, *J* = 14.0 Hz, 2H), 3.63 (d, *J* = 14.1 Hz, 2H), 3.30 (t, *J* = 8.7 Hz, 1H), 3.11 (t, *J* = 8.4 Hz, 1H), 2.51 – 2.36 (m, 2H), 1.27 (d, *J* = 6.2 Hz, 3H), 1.24 (d, *J* = 6.2 Hz, 3H), 1.21 (t, *J* = 6.1 Hz, 6H), 1.10 (d, *J* = 5.8 Hz, 3H); **^{13}C NMR** (151 MHz, $CDCl_3$) δ 172.7, 172.5, 139.6, 128.4, 128.2, 126.9, 67.91, 67.90, 64.2, 54.7, 43.0, 41.7, 37.3, 21.9, 21.81, 21.78, 21.76, 18.7; **IR** (neat) ν 2977, 2927, 1723, 1453, 1373, 1233, 1174, 1107, 746, 698 cm^{-1}; **HRMS** (DART) Calcd for $C_{27}H_{36}NO_4$ (MH^+): 438.2639; found: 438.2623.

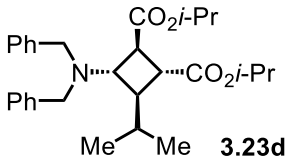

3.23d

Diisopropyl 3-(dibenzylamino)-4-isopropylcyclobutane-1,2-dicarboxylate (3.23d)

N,*N*-Dibenzyl-3-methylbutan-1-amine **3.21c** was reacted with diisopropyl fumarate **3.22a** following the **General Procedure D** using $B(C_6F_5)_3$ (10 mol%) as the Lewis acid catalyst and benzene as the solvent. ^{1}H NMR analysis of the unpurified product mixture revealed that the diastereomeric ratio was >20:1. After purification by column chromatography (ethyl ether:hexanes = 1:33), **3.23d** was obtained as a colorless liquid (64 mg, 69%). The relative configuration was assigned based on NOESY experiments.

^{1}H NMR (600 MHz, $CDCl_3$) δ 7.34 (d, *J* = 6.8 Hz, 4H), 7.29 (t, *J* = 7.6 Hz, 4H), 7.22 (t, *J* = 7.2 Hz, 2H), 5.02 (dp, *J* = 32.2, 6.3 Hz, 2H), 3.92 (d, *J* = 13.6 Hz, 2H), 3.50 (d, *J* = 13.6 Hz, 2H), 3.34 (t, *J* = 8.6 Hz, 1H), 3.26 (t, *J* = 8.7 Hz, 1H), 2.55 (t, *J* = 8.8 Hz, 1H), 2.28 (q, *J* = 8.7 Hz, 1H), 1.56 – 1.49 (m, 1H), 1.31 (d, *J* = 6.3 Hz, 3H), 1.25 (d, *J* = 6.2 Hz, 3H), 1.21 (dd, *J* = 9.3, 6.3 Hz, 6H), 0.86 (d, *J* = 6.7 Hz, 3H), 0.78 (d, *J* = 6.7 Hz, 3H); **^{13}C NMR** (151 MHz, $CDCl_3$) δ 173.4, 172.8, 139.6, 128.8, 128.2, 126.9, 68.0, 67.9, 60.9, 54.7, 48.5, 41.0, 39.1, 32.7, 21.9, 21.82, 21.80, 21.6, 20.2, 19.7; **IR** (neat) ν 2976, 2931, 1720, 1453, 1372, 1227, 1171, 1105, 747, 698 cm^{-1}; **HRMS** (DART) Calcd for $C_{29}H_{40}NO_4$ (MH^+): 466.2952; found: 466.2941.

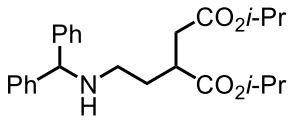

3.23e

Diisopropyl 2-(2-(benzhydrylamino)ethyl)succinate (3.23e)

N-Benzhydrylethanamine **3.21d** was reacted with diisopropyl fumarate **2.22a** following the **General Procedure D** using 10 mol% $B(C_6F_5)_3$ as the Lewis acid catalyst, benzene as the solvent. After purification by column chromatography (EtOAc:hexanes = 1:19) **3.23e** was obtained as a colorless liquid (77 mg, 93%).

^{1}H NMR (500 MHz, $CDCl_3$) δ 7.41 – 7.34 (m, 4H), 7.28 (td, *J* = 7.5, 1.5 Hz, 4H), 7.22 – 7.16 (m, 2H), 4.98 (h, *J* = 6.3 Hz, 2H), 4.78 (s, 1H), 2.91 (ddt, *J* = 8.9, 7.5, 5.8 Hz, 1H), 2.68 – 2.55 (m, 3H), 2.37 (dd, *J* = 16.4, 5.4 Hz, 1H), 1.91 – 1.80 (m, 1H), 1.77 – 1.66 (m, 1H), 1.22 (d, *J* = 2.5 Hz, 3H), 1.20 (d, *J* = 2.5 Hz, 3H), 1.19 (d, *J* = 6.2 Hz, 3H), 1.14 (d, *J* = 6.2 Hz, 3H); **^{13}C NMR** (151 MHz, $CDCl_3$) δ 174.2, 171.3, 144.0, 144.0, 128.4, 127.2, 126.4, 67.9, 67.5, 45.4, 39.5, 36.4, 32.2, 21.8, 21.74, 21.68, 21.6; **IR** (neat) ν 2977, 2933, 1727, 1452, 1373, 1265, 1173, 1105, 745, 703 cm^{-1}; **HRMS** (DART) Calcd for $C_{25}H_{34}NO_4$ (MH^+): 412.2482; found: 412.2478.

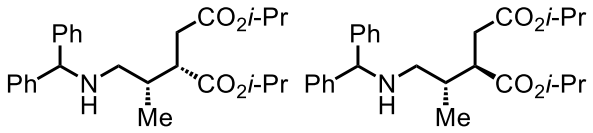

3.23f-major **3.23f-minor**

Diisopropyl 2-(1-(benzhydrylamino)propan-2-yl)succinate (3.23f)

N-Benzhydrylpropan-1-amine **3.21e** was reacted with diisopropyl fumarate **2.22a** following the **General Procedure C** using $B(C_6F_5)_3$ (10 mol%) as the Lewis acid catalyst and benzene (0.2 mL) as the solvent. ^{1}H NMR analysis of the unpurified product mixture revealed that the diastereomeric ratio was 1.1:1. After purification by column chromatography (EtOAc:hexanes = 1:19) **3.23f** was obtained as a mixture of diastereomers (56 mg, 66%). Further purification was carried out by PTLC using ethyl ether:DCM = 1:49 as the eluent to separate **3.23f-major** and **3.23f-minor**. The relative configuration of **3.23f-major** and **3.23f-minor** was assigned in analogy.

3.23f-Major: ^{1}H NMR (600 MHz, $CDCl_3$) δ 7.41 – 7.36 (m, 4H), 7.28 (q, *J* = 7.8 Hz, 4H), 7.22 – 7.17 (m, 2H), 5.00 (dq, *J* = 12.2, 6.2 Hz, 2H), 4.76 (s, 1H), 3.13 (ddd, *J* = 11.1, 4.7, 3.6 Hz, 1H), 2.58 (dd, *J* = 16.6, 11.1 Hz, 1H), 2.49 (dd, *J* = 11.9, 6.6 Hz, 1H), 2.42 (dd, *J* = 11.9, 7.4 Hz, 1H), 2.19 (dd, *J* = 16.6, 3.6 Hz, 1H), 2.13 (pd, *J* = 7.0, 4.6 Hz, 1H), 1.25 – 1.20 (m, 9H), 1.17 (d, *J* = 6.2 Hz, 3H), 0.87 (d, *J* = 6.9 Hz, 3H); **^{13}C NMR** (151 MHz, $CDCl_3$) δ 174.1, 172.0, 144.2, 144.0, 128.5, 128.4, 127.3, 127.2, 127.0, 67.8, 67.6, 51.8, 43.6, 35.3, 31.5, 21.83, 21.80, 21.78, 21.7, 14.6; **IR** (neat) ν 2976, 2930, 1725, 1452, 1373, 1260, 1173, 1105, 745, 703 cm^{-1}; **HRMS** (DART) Calcd for $C_{26}H_{36}NO_4$ (MH^+): 426.2639; found: 426.2638.

3.23f-Minor: ^{1}H NMR (500 MHz, $CDCl_3$) δ 7.38 (d, *J* = 7.3 Hz, 4H), 7.31 – 7.26 (m, 4H), 7.22 – 7.16 (m, 2H), 4.98 (pd, *J* = 6.3, 2.4 Hz, 2H), 4.75 (s, 1H), 2.97 (dt, *J* = 10.6, 4.3 Hz, 1H), 2.71 (dd, *J* = 16.6, 10.7 Hz, 1H), 2.57 (dd, *J* = 12.0, 7.0 Hz, 1H), 2.45 (dd, *J* = 12.0, 6.7 Hz, 1H), 2.27

(dd, J = 16.5, 4.2 Hz, 1H), 2.00 (qd, J = 7.0, 4.6 Hz, 1H), 1.22 (t, J = 6.2 Hz, 6H), 1.19 (d, J = 6.3 Hz, 3H), 1.13 (d, J = 6.3 Hz, 3H), 0.93 (d, J = 7.0 Hz, 3H); **^{13}C NMR** (126 MHz, $CDCl_3$) δ 173.3, 171.9, 144.2, 144.1, 128.43, 128.41, 127.3, 127.2, 126.96, 126.95, 67.8, 67.7, 51.9, 44.0, 35.8, 34.0, 21.82, 21.81, 21.77, 21.7, 15.5; **HRMS** (DART) Calcd for $C_{26}H_{36}NO_4$ (MH^+): 426.2639; found: 426.2626.

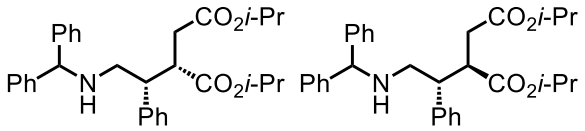

3.23g-major **3.23g-minor**

Diisopropyl 2-(2-(benzhydrylamino)-1-phenylethyl)succinate (3.23g)

N-Benzhydryl-2-phenylethan-1-amine **3.21f** was reacted with diisopropyl fumarate **2.22a** following the **General Procedure C** using $B(C_6F_5)_3$ (10 mol%) as the Lewis acid catalyst and benzene (0.2 mL) as the solvent. ^{1}H NMR analysis of the unpurified product mixture revealed that the diastereomeric ratio was 2.1:1. After purification by column chromatography (EtOAc:hexanes = 1:19), **3.23g** was obtained as a mixture of diastereomers (85 mg, 87%). Further purification was carried out by PTLC using ethyl ether:DCM = 1:49 as the eluent to separate **3.23g-major** and **3.23g-minor**. The relative configuration of **3.23g-major** and **3.23g-minor** was assigned in analogy.

3.23g-Major: ^{1}**H NMR** (600 MHz, $CDCl_3$) δ 7.30 (t, *J* = 7.4 Hz, 2H), 7.27 (d, *J* = 8.0 Hz, 2H), 7.25 – 7.19 (m, 6H), 7.19 – 7.12 (m, 4H), 4.89 (dhept, *J* = 12.5, 6.2 Hz, 2H), 4.71 (s, 1H), 3.06 (qd, *J* = 9.5, 8.5, 3.9 Hz, 2H), 2.87 (dd, *J* = 12.0, 8.5 Hz, 1H), 2.81 (dd, *J* = 12.0, 4.6 Hz, 1H), 2.47 (dd, *J* = 16.8, 10.7 Hz, 1H), 2.08 (dd, *J* = 16.7, 2.9 Hz, 1H), 1.15 (d, *J* = 6.2 Hz, 3H), 1.13 (d, *J* = 6.3 Hz, 6H), 1.04 (d, *J* = 6.3 Hz, 3H); ^{13}**C NMR** (151 MHz, $CDCl_3$) δ 173.6, 171.3, 144.0, 143.8, 140.1, 128.8, 128.40, 128.35, 127.3, 127.18, 127.16, 126.94, 126.88, 68.1, 67.9, 67.2, 50.9, 48.1, 45.5, 35.3, 21.8, 21.69, 21.66, 21.5; **IR** (neat) ν 2976, 2931, 1725, 1451, 1372, 1263, 1170, 1105, 745, 700 cm^{-1}; **HRMS** (DART) Calcd for $C_{31}H_{38}NO_4$ (MH^+): 488.2795; found: 488.2772.

3.23g-Minor: ^{1}**H NMR** (600 MHz, $CDCl_3$) δ 7.30 (d, *J* = 7.1 Hz, 2H), 7.29 – 7.19 (m, 9H), 7.19 – 7.13 (m, 4H), 4.93 (p, *J* = 6.2 Hz, 1H), 4.79 (p, *J* = 6.3 Hz, 1H), 4.74 (s, 1H), 3.21 – 3.10 (m,

2H), 2.95 – 2.85 (m, 2H), 2.60 (dd, J = 16.6, 10.4 Hz, 1H), 2.33 (dd, J = 16.6, 3.8 Hz, 1H), 1.18 (t, J = 6.9 Hz, 6H), 1.08 (d, J = 6.2 Hz, 3H), 0.91 (d, J = 6.2 Hz, 3H); **^{13}C NMR** (151 MHz, $CDCl_3$) δ 172.8, 171.4, 143.9, 140.0, 128.6, 128.43, 128.40, 127.3, 127.2, 127.1, 127.0, 126.9, 67.92, 67.88, 67.4, 49.5, 47.7, 45.5, 34.4, 21.8, 21.7, 21.6, 21.3; **HRMS** (DART) Calcd for $C_{31}H_{38}NO_4$ (MH^+): 488.2795; found: 488.2791.

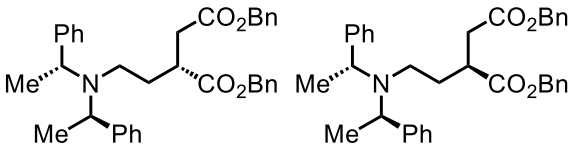

3.23h-(*R,R,R*) **3.23h-(*R,R,S*)**

Dibenzyl 2-(2-(bis((*R*)-1-phenylethyl)amino)ethyl)succinate (3.23h)

(*R*)-*N*-Ethyl-1-phenyl-*N*-((*R*)-1-phenylethyl)ethan-1-amine **3.21g** was reacted with dibenzyl fumarate **3.22b** following the **General Procedure C** using $B(C_6F_5)_3$ (10 mol%) as the Lewis acid catalyst and benzene (0.80 mL) as the solvent. ^{1}H NMR analysis of the unpurified product mixture revealed that the diastereomeric ratio was 1.4:1. After purification by column chromatography (ethyl ether:hexanes = 1:9), **3.23h** was obtained as a mixture of diastereomers (99 mg, 90% yield). Further purification was carried out by PTLC using ethyl ether:DCM = 1:49 as the eluent to separate **3.23h-(*R,R,R*)** and **3.23h-(*R,R,S*)**. The absolute configuration of product **3.23h-(*R,R,R*)** and **3.23h-(*R,R,S*)** was assigned in analogy to a previously synthesized molecule.[16]

3.23h-(*R,R,R*). ^{1}H NMR (500 MHz, $CDCl_3$): δ 7.37 – 7.21 (m, 18H), 7.20 – 7.14 (m, 2H), 5.03 (d, *J* = 12.4 Hz, 1H), 4.98 (d, *J* = 12.4 Hz, 1H), 4.94 (s, 2H), 3.93 (q, *J* = 6.8 Hz, 2H), 2.70 – 2.49 (m, 3H), 2.40 (ddd, *J* = 14.0, 10.5, 5.3 Hz, 1H), 2.19 (dd, *J* = 16.5, 4.9 Hz, 1H), 1.62 – 1.47 (m, 1H), 1.31 (d, *J* = 6.8 Hz, 6H), 1.28 – 1.15 (m, 1H); **^{13}C NMR (126 MHz, $CDCl_3$):** δ 174.3, 171.5, 144.9, 135.9, 135.7, 128.5, 128.4, 128.2, 128.1, 128.0, 127.8, 126.6, 66.33, 66.29, 57.9, 44.0, 39.2, 36.0, 33.1, 18.2; **IR (neat):** ν 3027, 2965, 1729, 1492, 1452, 1258, 1211, 1150, 971, 736, 696 cm^{-1}; **HRMS (DART):** Calcd for $C_{36}H_{40}NO_4$ (MH^+): 550.2952; found: 550.2951; **Specific Rotation** $[\alpha]^{25}_D$ = –3.1° (c = 0.9, EtOH).

3.23h-(*R*,*R*,*S*). ^{1}H NMR (600 MHz, $CDCl_3$): δ 7.37 – 7.25 (m, 14H), 7.23 (t, *J* = 7.5 Hz, 4H), 7.14 (t, *J* = 7.2 Hz, 2H), 5.04 – 4.93 (m, 4H), 3.95 (q, *J* = 7.1 Hz, 2H), 2.75 (dq, *J* = 11.4, 6.1 Hz, 1H), 2.59 (ddd, *J* = 14.2, 8.8, 5.1 Hz, 1H), 2.44 – 2.33 (m, 2H), 1.88 (dd, *J* = 16.8, 4.7 Hz, 1H), 1.57 – 1.49 (m, 1H), 1.33 (d, *J* = 6.9 Hz, 6H), 1.30 – 1.27 (m, 1H); **^{13}C NMR (126 MHz, $CDCl_3$):** δ 174.8, 171.6, 144.8, 135.9, 135.8, 128.5, 128.4, 128.2, 128.1, 128.0, 127.9, 127.8, 126.6, 66.3, 57.3, 43.0, 38.6, 35.1, 32.3, 17.3; **HRMS (DART):** Calcd for $C_{36}H_{40}NO_4$ (MH^+): 550.2952; found: 550.2967.

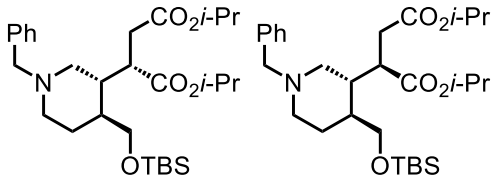

3.23i-major **3.23i-minor**

Diisopropyl 2-(1-benzyl-4-(((*tert*-butyldimethylsilyl)oxy)methyl)piperidin-3-yl)succinate (3.23i)

1-Benzyl-4-(((*tert*-butyldimethylsilyl)oxy)methyl)piperidine **3.21h** was reacted with diisopropyl fumarate **2.22a** following the **General Procedure C** using $B(C_6F_5)_3$ (10 mol%) as the Lewis acid catalyst and benzene (0.2 mL) as the solvent. ^{1}H NMR analysis of the unpurified product mixture revealed that the diastereomeric ratio was 1.1:1. After purification by column chromatography (ethyl ether:hexanes = 1:4), **3.23i** was obtained as a mixture of diastereomers (77.0 mg, 74%). Further purification was carried out by PTLC using ethyl ether:DCM = 1:6 as the eluent to separate **3. 23i-major** and **3. 23i-minor**. The relative configuration for **3. 23i-major** and **3. 23i-minor** were assigned based on X-ray crystallography data.

3.23i-Major: ^{1}**H NMR** (600 MHz, $CDCl_3$) δ 7.27 (dp, *J* = 22.0, 7.5 Hz, 5H), 4.98 (dp, *J* = 16.3, 6.4 Hz, 2H), 3.71 (dd, *J* = 10.0, 2.6 Hz, 1H), 3.65 (dd, *J* = 10.1, 5.1 Hz, 1H), 3.52 (d, *J* = 13.4 Hz, 1H), 3.41 (d, *J* = 13.4 Hz, 1H), 3.09 (dt, *J* = 11.2, 3.4 Hz, 1H), 2.82 (tt, *J* = 16.1, 10.8 Hz, 3H), 2.22 (dd, *J* = 16.7, 3.7 Hz, 1H), 1.85 (t, *J* = 11.2 Hz, 1H), 1.82 – 1.77 (m, 1H), 1.76 – 1.63 (m, 2H), 1.46 (pt, *J* = 11.9, 6.7 Hz, 2H), 1.21 (dt, *J* = 12.1, 6.0 Hz, 12H), 0.87 (d, *J* = 3.2 Hz, 9H), 0.03 (d, *J* = 2.9 Hz, 6H); ^{13}**C NMR** (151 MHz, $CDCl_3$) δ 172.7, 171.6, 138.2, 129.1, 129.0, 128.2, 128.1, 126.9, 67.91, 67.86, 64.6, 63.3, 55.4, 53.3, 40.7, 40.4, 40.0, 35.3, 29.3, 26.0, 25.9, 21.9, 21.82, 21.80, 21.75, 18.3, -5.4, -5.5; **IR** (neat) ν 2950, 2854, 1727, 1466, 1372, 1254, 1173, 1104, 834, 775 cm^{-1}; **HRMS** (DART) Calcd for $C_{29}H_{50}NO_5Si$ (MH^+): 520.3453; found: 520.3454.

3.23i-Minor: **^{1}H NMR** (500 MHz, $CDCl_3$) δ 7.31 – 7.23 (m, 4H), 7.23 – 7.17 (m, 1H), 5.03 – 4.93 (m, 1H), 4.93 – 4.84 (m, 1H), 3.61 (dd, *J* = 10.3, 4.1 Hz, 1H), 3.55 (t, *J* = 5.2 Hz, 1H), 3.50 (d, *J* = 13.2 Hz, 1H), 3.36 (d, *J* = 13.2 Hz, 1H), 3.19 (dt, *J* = 12.2, 3.6 Hz, 1H), 2.86 (d, *J* = 11.2 Hz, 1H), 2.67 – 2.50 (m, 2H), 2.35 – 2.24 (m, 1H), 2.09 (d, *J* = 11.0 Hz, 1H), 1.95 (t, *J* = 11.5 Hz, 1H), 1.70 (dd, *J* = 21.8, 11.1 Hz, 3H), 1.54 (tt, *J* = 14.2, 7.1 Hz, 1H), 1.33 (dq, *J* = 11.0, 5.3 Hz, 1H), 1.20 (dd, *J* = 10.0, 6.3 Hz, 6H), 1.13 (d, *J* = 6.3 Hz, 3H), 1.03 (d, *J* = 6.3 Hz, 3H), 0.89 (s, 9H), 0.04 (d, *J* = 5.8 Hz, 6H); **^{13}C NMR** (151 MHz, $CDCl_3$) δ 173.7, 172.0, 138.3, 129.0, 128.1, 126.9, 125.5, 67.9, 67.8, 65.0, 63.3, 54.4, 53.9, 41.3, 39.8, 39.3, 31.0, 29.0, 25.95, 25.94, 21.8, 21.74, 21.70, 21.5, 18.3, -5.5, -5.5; **HRMS** (DART) Calcd for $C_{29}H_{50}NO_5Si$ (MH^+): 520.3453; found: 520.3436.

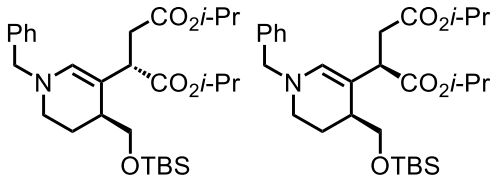

3.23j-major **3.23j-minor**

Diisopropyl 2-(1-benzyl-4-(((*tert*-butyldimethylsilyl)oxy)methyl)-1,4,5,6-tetrahydropyridin-3-yl)succinate (3.23j)

^{1}H NMR analysis of the unpurified product mixture revealed that the diastereomeric ratio of **3.23j** was 1.4:1. After purification by column chromatography (ethyl ether:hexanes = 1:9), **3.23j** was obtained as a mixture of diastereomers (26.9 mg, 26%). Further purification was carried out by PTLC using ethyl ether:DCM = 1:49 as the eluent to separate **3.23j-major** and **3.23j-minor**. The relative configuration of **3.23j-major** and **3.23j-minor** was assigned in analogy.

3.23j-Major: ^{1}H NMR (600 MHz, $CDCl_3$) δ 7.29 (t, *J* = 7.4 Hz, 2H), 7.27 – 7.21 (m, 1H), 7.19 (d, *J* = 7.5 Hz, 2H), 6.06 (s, 1H), 5.05 – 4.90 (m, 2H), 4.08 – 3.89 (m, 2H), 3.57 (dd, *J* = 10.1, 4.3 Hz, 1H), 3.29 (dd, *J* = 10.0, 5.7 Hz, 1H), 3.21 (t, *J* = 9.9 Hz, 1H), 2.87 (dd, *J* = 16.4, 10.1 Hz, 1H), 2.79 – 2.64 (m, 2H), 2.45 (dd, *J* = 16.3, 5.7 Hz, 1H), 2.37 (d, *J* = 7.8 Hz, 1H), 1.95 (dt, *J* = 13.4, 2.8 Hz, 1H), 1.65 – 1.46 (m, 1H), 1.32 – 1.11 (m, 12H), 0.86 (s, 9H), 0.06 – -0.08 (m, 6H); **^{13}C NMR** (151 MHz, $CDCl_3$) δ 173.8, 171.6, 138.4, 135.5, 128.3, 127.8, 127.1, 102.6, 67.73, 67.66, 65.0, 59.3, 44.3, 41.8, 36.4, 36.3, 26.0, 25.94, 25.90, 23.2, 21.84, 21.82, 21.77, 21.75, 21.7, 18.3, -5.2, -5.4; **IR** (neat) ν 2950, 2854, 1726, 1676, 1466, 1372, 1256, 1172, 1143, 1105, 836 cm^{-1}; **HRMS** (DART) Calcd for $C_{29}H_{48}NO_5Si$ (MH^+): 518.3296; found: 518.3284.

3.23j-Minor: ^{1}H NMR (500 MHz, $CDCl_3$) δ 7.35 – 7.20 (m, 3H), 7.20 – 7.14 (m, 2H), 6.09 (s, 1H), 5.05 – 4.88 (m, 2H), 3.99 (d, *J* = 3.7 Hz, 2H), 3.78 (dd, *J* = 10.4, 4.0 Hz, 1H), 3.26 (dd, *J* =

10.0, 5.5 Hz, 1H), 3.19 (t, *J* = 10.1 Hz, 1H), 2.87 – 2.74 (m, 2H), 2.74 – 2.62 (m, 1H), 2.48 (dd, *J* = 16.5, 5.5 Hz, 1H), 2.22 – 2.08 (m, 1H), 1.99 (dd, *J* = 13.6, 2.9 Hz, 1H), 1.67 – 1.59 (m, 1H), 1.27 – 1.16 (m, 12H), 0.88 (s, 9H), 0.03 (d, *J* = 8.5 Hz, 6H); **^{13}C NMR** (151 MHz, $CDCl_3$) δ 173.4, 171.6, 138.3, 135.5, 128.3, 127.8, 127.1, 103.0, 67.7, 67.6, 65.3, 59.3, 45.0, 41.6, 38.5, 37.6, 26.0, 23.2, 21.9, 21.8, 21.6, 18.3, -5.2, -5.4; **HRMS** (DART) Calcd for $C_{29}H_{48}NO_5Si$ (MH^+): 518.3296; found: 518.3283.

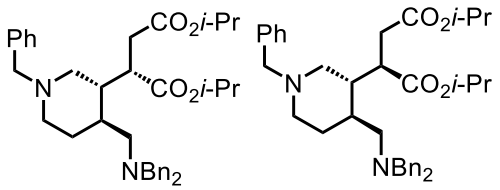

3.23k-major **3.23k-minor**

Diisopropyl 2-(1-benzyl-4-((dibenzylamino)methyl)piperidin-3-yl)succinate (3.23k)

N,N-Dibenzyl-1-(1-benzylpiperidin-4-yl)methanamine **3.21i** was reacted with diisopropyl fumarate **3.22a** following the **General Procedure A** using $B(C_6F_5)_3$ (10 mol%) as the Lewis acid catalyst and benzene (0.2 mL) as the solvent. ^{1}H NMR analysis of the unpurified product mixture revealed that the diastereomeric ratio was 1.8:1. After purification by column chromatography (ethyl ether:hexanes = 1:4), **3.23k** was obtained as a mixture of diastereomers (59.6 mg, 51%). Further purification was carried out by PTLC using ethyl ether:DCM = 3:7 as the eluent to separate **3.23k-major** and **3.23k-minor**. The relative configuration of **3.23k-major** and **3.23k-minor** was assigned in analogy.

3.23k-Major: ^{1}**H NMR** (600 MHz, $CDCl_3$) δ 7.42 – 7.32 (m, 5H), 7.32 – 7.25 (m, 5H), 7.25 – 7.17 (m, 5H), 5.09 – 4.90 (m, 2H), 3.72 (d, *J* = 13.5 Hz, 2H), 3.46 (d, *J* = 13.1 Hz, 1H), 3.44 – 3.39 (m, 1H), 3.36 (d, *J* = 13.1 Hz, 1H), 3.31 (d, *J* = 13.6 Hz, 2H), 2.77 (d, *J* = 4.3 Hz, 3H), 2.67 – 2.59 (m, 1H), 2.16 (d, *J* = 9.5 Hz, 1H), 2.11 (dd, *J* = 16.5, 4.2 Hz, 2H), 1.87 – 1.72 (m, 2H), 1.67 (t, *J* = 11.1 Hz, 1H), 1.52 – 1.44 (m, 1H), 1.22 (dd, *J* = 6.1, 1.5 Hz, 6H), 1.18 (dd, *J* = 13.0, 6.3 Hz, 6H), 1.05 (d, *J* = 10.5 Hz, 1H); ^{13}**C NMR** (151 MHz, $CDCl_3$) δ 172.9, 171.7, 139.7, 138.1, 129.2, 128.8, 128.8, 128.2, 128.13, 128.10, 127.0, 126.8, 68.0, 67.9, 63.4, 59.0, 57.6, 55.8, 53.3, 42.9, 40.6, 35.1, 35.0, 30.4, 21.91, 21.85, 21.82, 21.78; **IR** (neat) ν 2976, 2933, 2789, 1724, 1493, 1409, 1314, 1225, 1144, 745, 698 cm^{-1}; **HRMS** (DART) Calcd for $C_{37}H_{49}N_2O_4$ (MH^+): 585.3687; found: 585.3668.

3.23k-Minor: ^{1}H NMR (500 MHz, $CDCl_3$) δ 7.34 (t, *J* = 4.1 Hz, 4H), 7.32 – 7.27 (m, 4H), 7.27 – 7.15 (m, 7H), 5.09 – 4.94 (m, 1H), 4.90 – 4.76 (m, 1H), 3.64 (d, *J* = 13.4 Hz, 2H), 3.45 – 3.33 (m, 3H), 3.28 (d, *J* = 13.0 Hz, 1H), 3.23 – 3.11 (m, 1H), 2.73 – 2.60 (m, 1H), 2.58 – 2.45 (m, 2H), 2.31 (d, *J* = 11.3 Hz, 1H), 2.25 (td, *J* = 10.9, 9.4, 2.5 Hz, 1H), 2.14 (ddt, *J* = 20.0, 16.7, 3.5 Hz, 2H), 1.93 (t, *J* = 11.1 Hz, 1H), 1.79 (dt, *J* = 9.8, 4.5 Hz, 1H), 1.69 (q, *J* = 10.8, 10.1 Hz, 2H), 1.43 (d, *J* = 10.0 Hz, 1H), 1.24 (dd, *J* = 6.4, 2.3 Hz, 6H), 1.10 (dt, *J* = 6.2, 1.9 Hz, 3H), 1.01 – 0.93 (m, 3H); **^{13}C NMR** (126 MHz, $CDCl_3$) δ 173.8, 172.0, 139.5, 138.4, 129.0, 128.9, 128.8, 128.2, 128.1, 126.9, 68.0, 67.8, 63.3, 59.3, 56.9, 53.7, 53.6, 41.3, 40.8, 34.9, 31.3, 29.5, 21.9, 21.8, 21.7, 21.5 **HRMS** (DART) Calcd for $C_{37}H_{49}N_2O_4$ (MH^+): 585.3687; found: 585.3655.

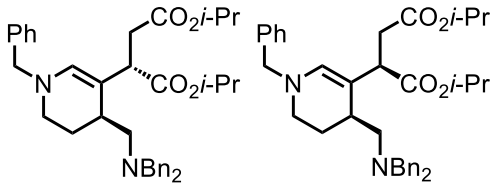

3.23l-major **3.23l-minor**

Diisopropyl 2-(1-benzyl-4-((dibenzylamino)methyl)-1,4,5,6-tetrahydropyridin-3-yl)succinate (3.23l)

^{1}H NMR analysis of the unpurified product mixture revealed that the diastereomeric ratio of **3.23l** was 1.7:1. After purification by column chromatography (ethyl ether:hexanes = 1:9), **3.23l** was obtained as a mixture of diastereomers (54.8 mg, 47%). Further purification was carried out by PTLC using ethyl ether:DCM = 1:50 as the eluent to separate **3.23l-major** and **3.23l-minor**. The relative configuration of **3.23l-major** and **3.23l-minor** was assigned in analogy.

3.23l-Major: **^{1}H NMR** (500 MHz, $CDCl_3$) δ 7.37 – 7.21 (m, 10H), 7.18 (t, *J* = 7.3 Hz, 3H), 7.07 (d, *J* = 7.2 Hz, 2H), 5.93 (s, 1H), 4.98 (dt, *J* = 12.6, 6.4 Hz, 2H), 3.85 (s, 2H), 3.83 (d, *J* = 13.3 Hz, 2H), 3.35 – 3.26 (m, 1H), 3.20 (d, *J* = 13.4 Hz, 2H), 2.85 (dd, *J* = 16.4, 10.3 Hz, 1H), 2.45 (t, *J* = 12.3 Hz, 2H), 2.37 (dd, *J* = 16.4, 5.6 Hz, 1H), 2.32 – 2.21 (m, 1H), 2.12 (t, *J* = 11.9 Hz, 1H), 2.07 – 1.87 (m, 2H), 1.49 (t, *J* = 4.9 Hz, 1H), 1.21 (d, *J* = 6.3 Hz, 9H), 1.17 (d, *J* = 6.3 Hz, 3H); **^{13}C NMR** (126 MHz, $CDCl_3$) δ 173.7, 171.6, 139.9, 138.4, 134.7, 129.0, 128.3, 128.1, 127.7, 127.0, 126.7, 104.1, 67.74, 67.66, 59.2, 58.9, 56.7, 44.2, 41.3, 36.1, 31.4, 30.3, 29.7, 24.0, 21.9, 21.84, 21.82, 21.7; **IR** (neat) ν 2975, 2927, 1724, 1647, 1493, 1320, 1295, 1144, 1074, 749, 698 cm^{-1}; **HRMS** (DART) Calcd for $C_{37}H_{47}N_2O_4$ (MH^+): 583.3530; found: 585.3540.

3.23l-Minor: **^{1}H NMR** (400 MHz, $CDCl_3$) δ 7.38 – 7.21 (m, 10H), 7.21 – 7.13 (m, 3H), 7.11 – 7.00 (m, 2H), 5.97 (s, 1H), 5.07 – 4.88 (m, 2H), 3.92 – 3.76 (m, 4H), 3.26 – 3.10 (m, 3H), 2.90 –

2.75 (m, 1H), 2.53 – 2.40 (m, 2H), 2.40 – 2.33 (m, 1H), 2.29 – 2.11 (m, 2H), 2.11 – 2.02 (m, 1H), 2.02 – 1.91 (m, 1H), 1.45 (t, J = 13.1 Hz, 1H), 1.32 – 1.18 (m, 12H); **^{13}C NMR** (151 MHz, $CDCl_3$) δ 173.4, 171.7, 139.9, 138.4, 134.8, 129.0, 128.2, 128.1, 127.7, 126.9, 126.7, 104.3, 67.7, 67.5, 59.1, 59.1, 57.2, 45.2, 41.1, 38.5, 32.4, 23.9, 21.9, 21.8, 21.7, 21.6; **HRMS** (DART) Calcd for $C_{37}H_{47}N_2O_4$ (MH^+): 583.3530; found: 585.3528.

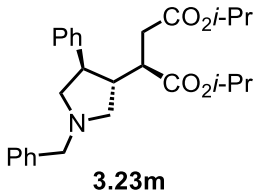

3.23m

Diisopropyl 2-((4*R*)-1-benzyl-4-phenylpyrrolidin-3-yl)succinate (3.23m)

(*R*)-1-Benzyl-3-phenylpyrrolidine **3.21j** was reacted with diisopropyl fumarate **2.22a** following the **General Procedure C** using $B(C_6F_5)_3$ (10 mol%) as the Lewis acid catalyst and benzene (0.2 mL) as the solvent. ^{1}H NMR analysis of the unpurified product mixture revealed that the diastereomeric ratio was 1.6:1. After purification by column chromatography (ethyl ether:hexanes = 1:4), **3.23m** was obtained as a mixture of diastereomers (78.7 mg, 90%). Further purification was carried out by PTLC using ethyl ether:DCM:hexanes = 2:8:3 as the eluent to separate **3.23m-(*R*,*R*,*R*)** and **3.23m-minor**. The absolute configuration of **3.23m-(*R*,*R*,*R*)** was assigned based on analogy to **3.23m-(*R*,*R*,*R*)** and by NOESY experiments.

3.23m-(*R*,*R*,*R*): **^{1}H NMR** (500 MHz, $CDCl_3$) δ 7.29 (ddt, *J* = 19.6, 15.2, 4.7 Hz, 8H), 7.23 (d, *J* = 6.9 Hz, 1H), 7.18 (d, *J* = 6.9 Hz, 1H), 4.99 – 4.82 (m, 2H), 3.64 (d, *J* = 12.9 Hz, 1H), 3.57 (d, *J* = 12.9 Hz, 1H), 3.17 – 3.10 (m, 1H), 2.96 – 2.88 (m, 2H), 2.85 (t, *J* = 8.6 Hz, 1H), 2.70 – 2.61 (m, 1H), 2.61 – 2.55 (m, 2H), 2.55 – 2.48 (m, 1H), 2.40 (dd, *J* = 16.8, 3.9 Hz, 1H), 1.21 – 1.14 (m, 9H), 1.02 (d, *J* = 6.3 Hz, 3H); **^{13}C NMR** (151 MHz, $CDCl_3$) δ 173.0, 171.5, 145.0, 139.0, 128.6, 128.5, 128.2, 127.7, 126.9, 126.3, 68.0, 67.9, 63.3, 60.2, 58.1, 48.7, 47.7, 44.7, 34.9, 21.78, 21.75, 21.7, 21.5; **IR** (neat) ν 2975, 2932, 2788, 1725, 1492, 1372, 1261, 1173, 1144, 1105, 754, 699 cm^{-1}; $[\alpha]^{25}_D$ = 5.1° (c = 0.9, EtOH); **HRMS** (DART) Calcd for $C_{27}H_{36}NO_4$ (MH^+): 438. 2639; found: 438.2627.

3.23m-Minor: **^{1}H NMR** (500 MHz, $CDCl_3$) δ 7.35 – 7.22 (m, 8H), 7.17 (q, *J* = 7.0 Hz, 2H), 4.99 – 4.91 (m, 1H), 4.82 – 4.70 (m, 1H), 3.61 (d, *J* = 7.9 Hz, 2H), 3.17 (t, *J* = 7.0 Hz, 1H), 2.88 (dq, *J* = 24.7, 8.0, 7.6 Hz, 3H), 2.69 – 2.53 (m, 3H), 2.47 (t, *J* = 8.1 Hz, 1H), 2.37 (dd, *J* = 16.9, 3.9 Hz, 1H), 1.21 – 1.16 (m, 6H), 1.12 (d, *J* = 6.3 Hz, 3H), 0.95 (d, *J* = 6.3 Hz, 3H); **HRMS** (DART) Calcd for $C_{27}H_{36}NO_4$ (MH^+): 438. 2639; found: 438.2639.

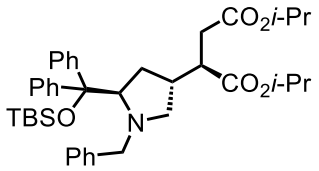

3.23n

Diisopropyl 2-((5*R*)-1-benzyl-5-(((*tert*-butyldimethylsilyl)oxy)diphenylmethyl)pyrrolidin -3-yl)succinate (3.23n)

(*R*)-1-Benzyl-2-(((*tert*-butyldimethylsilyl)oxy)diphenylmethyl)pyrrolidine **3.21k** was reacted with diisopropyl fumarate **2.22a** following the **General Procedure C** using $B(C_6F_5)_3$ (10 mol%) as the Lewis acid catalyst and benzene (0.2 mL) as the solvent. ^{1}H NMR analysis of the unpurified product mixture revealed that the diastereomeric ratio was 2.5:1. After purification by column chromatography (ethyl ether:hexanes = 1:9) **3.23n** was obtained as a mixture of diastereomers (74 mg, 56%). Further purification was carried out by PTLC using ethyl ether:DCM = 1:49 as the eluent to separate **3.23n-(*R,R,R*)** and **3.23n-minor**. The absolute configuration of **3.23n-(*R,R,R*)** was assigned based on X-ray crystallography data.

3.23n-(*R,R,R*): ^{1}H NMR (600 MHz, $CDCl_3$) δ 7.60 (s, 2H), 7.55 (d, *J* = 7.3 Hz, 2H), 7.35 – 7.26 (m, 6H), 7.19 (t, *J* = 7.4 Hz, 2H), 7.14 (t, *J* = 7.2 Hz, 1H), 7.04 (d, *J* = 7.4 Hz, 2H), 4.90 (p, *J* = 6.2 Hz, 1H), 4.78 (p, *J* = 5.9 Hz, 1H), 4.41 (br, 1H), 4.01 (d, *J* = 10.1 Hz, 1H), 3.35 (d, *J* = 12.8 Hz, 1H), 2.46 (t, *J* = 7.8 Hz, 1H), 2.39 – 2.28 (m, 2H), 2.13 (d, *J* = 14.4 Hz, 1H), 1.98 (t, *J* = 10.1 Hz, 2H), 1.66 (q, *J* = 11.6 Hz, 2H), 1.15 (t, *J* = 5.8 Hz, 6H), 1.08 (d, *J* = 6.4 Hz, 3H), 0.94 (d, *J* = 6.3 Hz, 3H), 0.88 (s, 9H), -0.41 (s, 3H), -0.45 (s, 3H); **^{13}C NMR** (151 MHz, $CDCl_3$) δ 173.1, 171.3, 143.4, 140.3, 130.1, 129.9, 128.4, 128.0, 127.4, 127.2, 127.1, 126.4, 70.6, 67.9, 67.5, 61.8, 59.1, 45.0, 38.3, 35.4, 26.3, 21.8, 21.70, 21.67, 21.4, 19.0, -2.9, -3.0; **IR** (neat) ν 2975, 2927, 2853,

1727, 1372, 1254, 1173, 1105, 1060, 833, 774, 702 cm^{-1}; $[\alpha]^{25}_{D}$ = 43.1 ° (c = 0.7, EtOH); **HRMS** (DART) Calcd for $C_{40}H_{56}NO_5Si$ (MH^+): 658.3922; found: 658.3905.

3.23n-Minor: ^{1}H NMR (600 MHz, $CDCl_3$) δ 7.63 – 7.56 (m, 2H), 7.54 (d, *J* = 6.3 Hz, 2H), 7.37 – 7.27 (m, 6H), 7.22 (t, *J* = 7.5 Hz, 2H), 7.16 (t, *J* = 7.4 Hz, 1H), 7.05 (d, *J* = 7.6 Hz, 2H), 4.90 (p, *J* = 6.3 Hz, 1H), 4.85 (p, *J* = 6.3 Hz, 1H), 4.45 (br, 1H), 4.05 (dd, *J* = 10.2, 2.6 Hz, 1H), 3.36 (d, *J* = 13.1 Hz, 1H), 2.58 (dd, *J* = 8.8, 6.4 Hz, 1H), 2.35 – 2.25 (m, 2H), 2.10 (s, 1H), 2.00 – 1.89 (m, 2H), 1.89 – 1.80 (m, 2H), 1.19 (d, *J* = 6.2 Hz, 3H), 1.15 (d, *J* = 6.3 Hz, 3H), 1.11 (d, *J* = 6.2 Hz, 3H), 1.09 (d, *J* = 6.2 Hz, 3H), 0.87 (s, 9H), -0.42 (s, 3H), -0.46 (s, 3H); **^{13}C NMR** (151 MHz, $CDCl_3$) δ 173.1, 171.2, 143.5, 140.4, 130.0, 129.9, 128.2, 128.1, 127.4, 127.2, 127.1, 126.7, 126.4, 70.8, 67.8, 67.7, 61.8, 59.5, 45.4, 38.4, 35.8, 33.5, 26.3, 21.8, 21.74, 21.70, 21.6, 18.9, -2.9, -3.0; **HRMS** (DART) Calcd for $C_{40}H_{56}NO_5Si$ (MH^+): 658.39223; found: 658.38954.

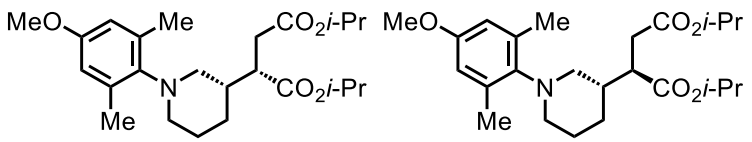

3.23o-major **3.23o-minor**

Diisopropyl 2-(1-(4-methoxy-2,6-dimethylphenyl)piperidin-3-yl)succinate (3.23o)

1-(4-Methoxy-2,6-dimethylphenyl)piperidine **3.21l** was reacted with diisopropyl fumarate **2.22a** following the **General Procedure C** using $B(C_6F_5)_3$ (5.0 mol%) as the Lewis acid catalyst and benzene (0.8 mL) as the solvent. ^{1}H NMR analysis of the unpurified product mixture revealed that the diastereomeric ratio was 1.3:1. After purification by column chromatography (ethyl ether:hexanes = 1:19) **3.23o** was obtained as a mixture of diastereomers (75 mg, 89%). Further purification was carried out by PTLC using ethyl ether:DCM = 1:49 as the eluent to separate **3.23o-major** and **3.23o-minor**. The relative configuration of **3.23o-major** and **3.23o-minor** was assigned in analogy.

3.23o-Major: ^{1}H NMR (600 MHz, $CDCl_3$) δ 6.57 (d, *J* = 3.0 Hz, 1H), 6.46 (d, *J* = 3.1 Hz, 1H), 5.04 (hept, *J* = 5.9 Hz, 1H), 4.96 (hept, *J* = 12.6, 6.3 Hz, 1H), 3.74 (s, 3H), 3.02 (td, *J* = 11.2, 2.9 Hz, 1H), 2.90 (d, *J* = 7.0 Hz, 2H), 2.85 (dt, *J* = 11.8, 3.8 Hz, 1H), 2.77 – 2.63 (m, 2H), 2.44 – 2.37 (m, 1H), 2.26 (s, 3H), 2.24 (s, 3H), 1.96 – 1.85 (m, 1H), 1.78 (dt, *J* = 13.0, 3.9 Hz, 1H), 1.72 (dt, *J* = 12.7, 3.5 Hz, 1H), 1.68 – 1.55 (m, 2H), 1.25 (t, *J* = 6.2 Hz, 6H), 1.19 (dd, *J* = 7.6, 6.2 Hz, 6H); **^{13}C NMR** (126 MHz, $CDCl_3$) δ 173.7, 171.6, 156.3, 142.4, 138.7, 137.9, 114.0, 113.3, 67.9, 67.8, 55.2, 54.6, 50.7, 44.9, 39.5, 34.5, 28.5, 26.5, 21.9, 21.8, 21.7, 19.9, 19.5; **IR** (neat) ν 2976, 2932, 1727, 1485, 1372, 1220, 1173, 1156, 1106, 1067 cm^{-1}; **HRMS** (DART) Calcd for $C_{24}H_{38}NO_5$ (MH^+): 420.2745; found: 420.2741.

3.23o-Minor: ^{1}H NMR (600 MHz, $CDCl_3$) δ 6.56 (d, *J* = 3.0 Hz, 1H), 6.45 (d, *J* = 3.1 Hz, 1H), 4.99 (dq, *J* = 11.8, 6.1 Hz, 2H), 3.74 (s, 3H), 3.02 (td, *J* = 11.2, 2.6 Hz, 1H), 2.93 – 2.86 (m, 2H), 2.84 (dt, *J* = 11.9, 3.9 Hz, 1H), 2.76 – 2.64 (m, 2H), 2.46 (dd, *J* = 15.7, 3.4 Hz, 1H), 2.26 (s, 3H), 2.24 (s, 3H), 1.92 (dq, *J* = 11.6, 6.2 Hz, 1H), 1.84 (dd, *J* = 13.1, 3.7 Hz, 1H), 1.73 – 1.56 (m, 3H), 1.25 (t, *J* = 7.0 Hz, 1H), 1.21 (dd, *J* = 6.2, 2.6 Hz, 9H), 1.17 (d, *J* = 6.5 Hz, 3H); **^{13}C NMR** (151 MHz, $CDCl_3$) δ 173.4, 171.7, 156.2, 142.5, 138.7, 137.7, 114.0, 113.2, 67.9, 67.8, 55.2, 54.7, 50.8, 45.0, 39.5, 34.5, 28.6, 26.6, 21.81, 21.80, 21.76, 20.0, 19.5; **HRMS** (DART) Calcd for $C_{24}H_{38}NO_5$ (MH^+): 420.2745; found: 420.2734.

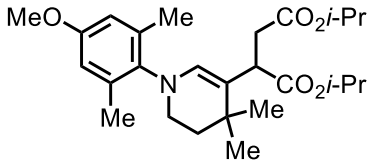

3.23p

Diisopropyl 2-(1-(4-methoxy-2,6-dimethylphenyl)-4,4-dimethylpiperidin-3-yl)succinate (3.23p)

1-(4-Methoxy-2,6-dimethylphenyl)-4,4-dimethylpiperidine **3.21m** was reacted with diisopropyl fumarate **2.22a** following the **General Procedure D** using $B(C_6F_5)_3$ (10 mol%) as the Lewis acid catalyst, DCM (0.1 mL) as the solvent, and a second batch of **2.22a** in DCM (0.05 mL) was added. After purification by column chromatography (ethyl ether:hexanes = 1:33) **3.23p** was obtained as a colorless liquid (89 mg, 93%).

^{1}H NMR (600 MHz, $CDCl_3$) δ 6.55 (d, *J* = 13.5 Hz, 2H), 5.82 (s, 1H), 4.96 (dp, *J* = 17.2, 6.3 Hz, 2H), 3.75 (s, 3H), 3.41 (dd, *J* = 10.9, 4.6 Hz, 1H), 3.22 (ddd, *J* = 12.3, 8.9, 3.7 Hz, 1H), 3.11 (ddd, *J* = 11.9, 6.4, 4.0 Hz, 1H), 2.78 (dd, *J* = 16.8, 10.9 Hz, 1H), 2.40 (dd, *J* = 16.7, 4.7 Hz, 1H), 2.18 (s, 3H), 2.13 (s, 3H), 1.76 (ddd, *J* = 12.9, 8.9, 4.0 Hz, 1H), 1.70 (ddd, *J* = 12.9, 6.4, 3.7 Hz, 1H), 1.23 (d, *J* = 6.3 Hz, 3H), 1.21 (d, *J* = 3.5 Hz, 3H), 1.20 (d, *J* = 3.5 Hz, 3H), 1.19 (s, 3H), 1.17 (d, *J* = 6.3 Hz, 3H), 1.11 (s, 3H); **^{13}C NMR** (126 MHz, $CDCl_3$) δ 174.5, 171.8, 157.3, 138.8, 138.3, 138.2, 132.0, 113.4, 113.3, 108.1, 67.6, 67.3, 55.3, 44.1, 39.9, 39.6, 39.2, 31.6, 29.1, 28.2, 21.9, 21.82, 21.80, 21.5, 18.4, 18.3; **IR** (neat) ν 2977, 2933, 1723, 1639, 1466, 1259, 1162, 1102, 1065 cm^{-1}; **HRMS** (ESI) Calcd for $C_{26}H_{40}NO_5$ (MH^+): 446.2901; found: 446.2906.

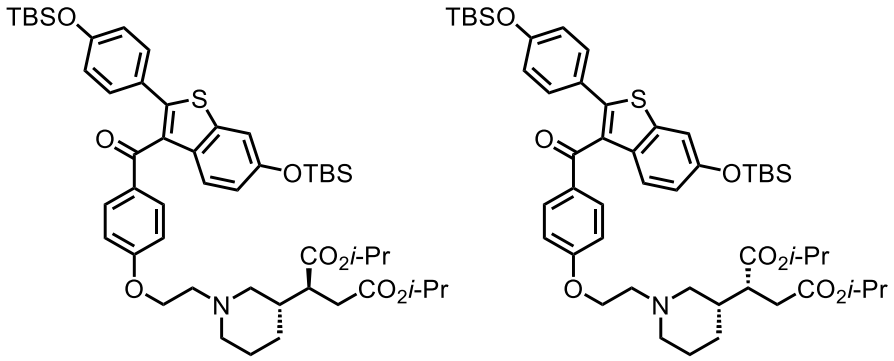

3.23q-major **3.23q-minor**

Diisopropyl 2-(1-(2-(4-(6-((*tert*-butyldimethylsilyl)oxy)-2-(4-((*tert*-butyldimethylsilyl) oxy)phenyl)benzo[*b*]thiophene-3-carbonyl)phenoxy)ethyl)piperidin-3-yl)succinate (3.23q)

(6-((*tert*-Butyldimethylsilyl)oxy)-2-(4-((*tert*-butyldimethylsilyl)oxy)phenyl)benzo[*b*]thiophen -3-yl)(4-(2-(piperidin-1-yl)ethoxy)phenyl)methanone **3.21n** (0.20 mmol) was reacted with diisopropyl fumarate **2.22a** following the **General Procedure C** using $B(C_6F_5)_3$ (10 mol%) as the Lewis acid catalyst and benzene as the solvent. ^{1}H NMR analysis of the unpurified product mixture revealed that the diastereomeric ratio was 2.5:1. After purification by column chromatography (ethyl ether:DCM = 1:4), **3.23q** was obtained as a mixture of diastereomers (145 mg, 80%). Further purification was carried out by PTLC using MeOH:DCM = 1:49 as the eluent to separate **3.23q-major** and **3.23q-minor**. The relative configuration of **3.23q-major** and **3.23q-minor** was assigned in analogy.

3.23q-major. ^{1}H NMR (500 MHz, $CDCl_3$): δ 7.73 (d, *J* = 8.9 Hz, 2H), 7.54 (d, *J* = 8.8 Hz, 1H), 7.28 (d, *J* = 2.2 Hz, 1H), 7.27 – 7.25 (m, 1H), 7.25 – 7.23 (m, 1H), 6.88 (dd, *J* = 8.8, 2.2 Hz, 1H), 6.72 (d, *J* = 8.9 Hz, 2H), 6.66 (d, *J* = 8.5 Hz, 2H), 4.99 (dp, *J* = 12.5, 6.3 Hz, 2H), 4.03 (t, *J* = 6.0 Hz, 2H), 2.87 (dd, *J* = 16.7, 9.2 Hz, 2H), 2.80 – 2.62 (m, 4H), 2.46 – 2.32 (m, 1H), 2.06 – 1.82 (m, 3H), 1.67 (dt, *J* = 16.5, 12.7 Hz, 2H), 1.54 (q, *J* = 12.8 Hz, 1H), 1.21 (td, *J* = 6.0, 1.8 Hz, 12H),

1.05 (dt, *J* = 10.5, 6.2 Hz, 1H), 1.01 (s, 9H), 0.93 (s, 9H), 0.23 (s, 6H), 0.12 (s, 6H). **^{13}C NMR (126 MHz, $CDCl_3$):** δ 193.2, 173.2, 171.6, 162.8, 156.1, 153.5, 143.2, 139.8, 134.5, 132.3, 130.6, 130.5, 130.3, 126.8, 123.9, 120.2, 119.2, 114.0, 112.1, 68.0, 67.9, 66.1, 58.3, 57.4, 54.3, 45.1, 45.0, 38.1, 34.0, 27.8, 25.7, 25.6, 25.3, 21.80, 21.79, 21.7, 18.23, 18.18, -4.4, -4.5. **HRMS (DART):** Calcd for $C_{50}H_{72}NO_8SSi_2^+$ (MH^+): 902.4512; found: 902.4522.

3.23q-minor. **^{1}H NMR (600 MHz, $CDCl_3$):** δ 7.73 (d, *J* = 8.4 Hz, 2H), 7.54 (d, *J* = 8.7 Hz, 1H), 7.28 (t, *J* = 1.8 Hz, 1H), 7.24 (d, *J* = 1.3 Hz, 1H), 6.88 (d, *J* = 8.7 Hz, 1H), 6.76 – 6.69 (m, 2H), 6.66 (d, *J* = 8.0 Hz, 2H), 5.06 – 4.93 (m, 2H), 4.03 (s, 2H), 2.93 – 2.81 (m, 2H), 2.79 – 2.66 (m, 4H), 2.37 (q, *J* = 10.0 Hz, 1H), 2.00 (t, *J* = 11.4 Hz, 1H), 1.94 (t, *J* = 10.9 Hz, 1H), 1.90 – 1.81 (m, 1H), 1.74 – 1.64 (m, 2H), 1.55 (d, *J* = 15.3 Hz, 1H), 1.20 (d, *J* = 1.7 Hz, 12H), 1.10 – 0.99 (m, 10H), 0.93 (s, 9H), 0.23 (s, 6H), 0.12 (s, 6H). **^{13}C NMR (151 MHz, $CDCl_3$):** δ 195.8, 175.9, 174.2, 165.5, 158.7, 156.1, 145.9, 142.5, 137.1, 134.9, 133.21, 133.15, 133.0, 129.4, 126.6, 122.9, 121.9, 116.7, 114.7, 70.7, 70.6, 68.7, 60.8, 60.0, 57.0, 47.6, 40.9, 36.9, 30.4, 28.34, 28.27, 27.8, 24.48, 24.45, 24.4, 20.9, 20.8, 2.6, -1.7, -1.8. **HRMS (DART):** Calcd for $C_{50}H_{72}NO_8SSi_2^+$ (MH^+): 902.4512; found: 902.4519.

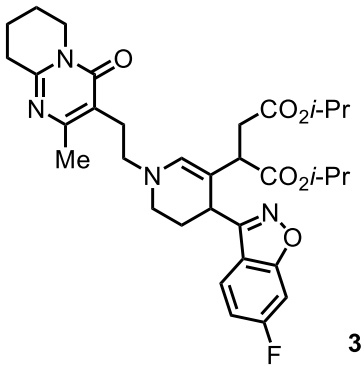

3.23r

Diisopropyl 2-(4-(6-fluorobenzo[*d*]isoxazol-3-yl)-1-(2-(2-methyl-4-oxo-6,7,8,9-tetrahydro-4*H*-pyrido[1,2-*a*]pyrimidin-3-yl)ethyl)-1,4,5,6-tetrahydropyridin-3-yl)succinate (3.23r)

3-(2-(4-(6-Fluorobenzo[*d*]isoxazol-3-yl)piperidin-1-yl)ethyl)-2-methyl-6,7,8,9-tetrahydro-4*H*-pyrido[1,2-*a*]pyrimidin-4-one **3.21o** (1g, 2.4 mmol) was reacted with diisopropyl fumarate **3.22a** following the **General Procedure C** using $B(C_6F_5)_3$ (10 mol%) as the Lewis acid catalyst and DCM as the solvent. ^{1}H NMR analysis of the unpurified product mixture revealed that the diastereomeric ratio was 1.7:1. After purification by column chromatography (methanol:DCM = 1:49), **3.23r** was obtained as a mixture of diastereomers (470 mg, 32%). Further purification was carried out by PTLC using methanol:DCM = 1:49 as the eluent to separate **3.23r-major**.

3.23r-Major. ^{1}H NMR (500 MHz, $CDCl_3$): δ 7.66 (dd, *J* = 8.8, 5.2 Hz, 1H), 7.21 (dd, *J* = 8.4, 2.1 Hz, 1H), 7.06 – 7.00 (m, 1H), 6.15 (s, 1H), 4.95 – 4.81 (m, 1H), 4.81 – 4.68 (m, 1H), 4.08 (d, *J* = 5.1 Hz, 1H), 3.94 (t, *J* = 6.3 Hz, 2H), 3.22 – 3.12 (m, 3H), 3.10 (s, 2H), 2.89 (d, *J* = 6.9 Hz, 3H), 2.74 (d, *J* = 7.6 Hz, 2H), 2.40 (dd, *J* = 16.4, 4.8 Hz, 1H), 2.30 (s, 3H), 2.19 – 2.11 (m, 1H), 2.01 (d, *J* = 7.3 Hz, 1H), 1.98 (t, *J* = 6.2 Hz, 2H), 1.93 – 1.83 (m, 2H), 1.20 – 1.09 (m, 12H); **^{13}C NMR (151 MHz, $CDCl_3$):** δ 173.0, 171.3, 163.9, 163.2, 162.5, 161.3, 158.6, 156.2, 135.7, 135.6, 122.9, 122.8, 118.2, 118.0, 112.4, 112.2, 99.1, 97.3, 97.1, 67.9, 67.84, 67.80, 67.7, 53.3, 45.7, 44.5, 42.9, 42.8, 36.1, 31.7, 31.5, 29.7, 28.7, 28.4, 25.8, 22.0, 21.8, 21.74, 21.70, 21.62, 21.55, 21.5,

21.4, 19.2; **^{19}F NMR (470 MHz, $CDCl_3$):** δ -109.99; **IR (neat):** ν 2975, 2931, 1723, 1649, 1612, 1533, 1411, 1268, 1167, 1141, 1105, 919, 830 cm^{-1}; **HRMS (DART):** Calcd for $C_{33}H_{42}FN_4O_6$ (MH^+): 609.3083; found: 609.3072.

^{1}H NMR (500 MHz, $CDCl_3$, *peaks from diastereomers are merged*): δ 7.67 (dd, *J* = 9.0, 5.1 Hz, 1H), 7.22 (t, *J* = 6.8 Hz, 1H), 7.03 (q, *J* = 9.2 Hz, 1H), 6.24 – 6.10 (m, 1H), 4.88 (dt, *J* = 12.7, 6.4 Hz, 1H), 4.81 – 4.71 (m, 1H), 4.09 (dd, *J* = 5.8, 3.1 Hz, 1H), 3.94 (q, *J* = 5.0, 4.0 Hz, 2H), 3.27 – 3.04 (m, 5H), 2.87 (dt, *J* = 23.5, 9.0 Hz, 3H), 2.74 (t, *J* = 7.7 Hz, 2H), 2.64 – 2.35 (m, 1H), 2.31 (d, *J* = 3.9 Hz, 3H), 2.21 – 2.08 (m, 1H), 2.08 – 2.02 (m, 1H), 2.02 – 1.94 (m, 2H), 1.94 – 1.83 (m, 2H), 1.20 – 1.06 (m, 12H); **^{13}C NMR (126 MHz, $CDCl_3$):** δ 172.9, 172.8, 171.22, 171.16, 164.0 (d, *J* = 250.3 Hz), 164.0 (d, *J* = 250.3 Hz), 163.9, 163.8, 163.7, 162.4, 161.7, 161.2, 158.51, 158.47, 156.11, 156.07, 135.9, 135.6, 123.4 (d, *J* = 10.9 Hz), 122.8 (d, *J* = 11.0 Hz), 118.07, 118.05, 117.9, 117.6, 112.16 (d, *J* = 25.2 Hz), 112.22 (d, *J* = 25.1 Hz), 98.9, 98.5, 97.2 (d, *J* = 26.7 Hz). 97.1 (d, *J* = 26.7 Hz), 67.8, 67.7, 67.6, 53.2, 53.0, 45.6, 44.4, 42.9, 42.8, 42.6, 37.0, 36.0, 31.6, 31.38, 31.37, 31.1, 28.6, 28.4, 25.70, 25.67, 21.9, 21.7, 21.64, 21.61, 21.59, 21.53, 21.45, 21.4, 21.3, 19.2, 19.1.

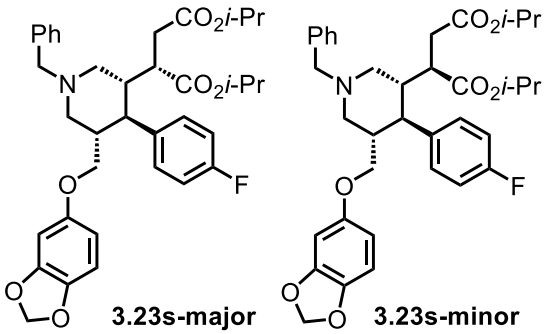

Diisopropyl 2-((4*R*,5*S*)-5-((benzo[*d*][1,3]dioxol-5-yloxy)methyl)-1-benzyl-4-(4-fluorophenyl)piperidin-3-yl)succinate (3.23s)

For 0.2 mmol scale:

(3*S*,4*R*)-3-((Benzo[*d*][1,3]dioxol-5-yloxy)methyl)-1-benzyl-4-(4-fluorophenyl)piperidine **3.21p** was reacted with diisopropyl fumarate **2.22a** following the **General Procedure D** using $B(C_6F_5)_3$ (10 mol%) as the Lewis acid catalyst and benzene as the solvent. ^{1}H NMR analysis of the unpurified product mixture revealed that the diastereomeric ratio of **3.23s** was 2.3:1. After purification by column chromatography (ethyl ether:hexanes = 3:2), **3.23s** was obtained as a mixture of diastereomers (48 mg, 39%). The relative configuration of **3.23s-major** and **3.23s-minor** was assigned in analogy.

3.23s-Major: **^{1}H NMR** (500 MHz, $CDCl_3$) δ 7.38 – 7.19 (m, 5H), 7.00 (s, 2H), 6.61 (d, *J* = 8.4 Hz, 1H), 6.31 (d, *J* = 2.5 Hz, 1H), 6.09 (dd, *J* = 8.5, 2.5 Hz, 1H), 5.88 (s, 2H), 4.94 – 4.76 (m, 2H), 3.64 (d, *J* = 13.1 Hz, 1H), 3.48 (d, *J* = 2.6 Hz, 1H), 3.45 (d, *J* = 13.1 Hz, 1H), 3.41 – 3.33 (m, 1H), 3.20 – 3.13 (m, 1H), 2.83 – 2.74 (m, 1H), 2.61 – 2.48 (m, 3H), 2.42 (t, *J* = 11.2 Hz, 1H), 2.29 – 2.17 (m, 2H), 2.13 (t, *J* = 11.1 Hz, 1H), 1.84 (t, *J* = 11.1 Hz, 1H), 1.15 (d, *J* = 6.2 Hz, 6H), 1.08 (d, *J* = 6.3 Hz, 3H), 1.02 (d, *J* = 6.2 Hz, 3H); **^{13}C NMR** (151 MHz, $CDCl_3$) δ 173.3, 171.4, 161.8 (d, J_{C-F} = 245.3 Hz), 154.2, 148.1, 141.6, 137.9, 136.4, 136.3, 129.1, 128.2, 127.1, 115.8, 107.8, 105.6,

101.1, 97.9, 69.4, 68.1, 67.8, 63.3, 57.6, 54.7, 46.3, 43.2, 42.8, 41.5, 30.4, 21.71, 21.67, 21.6, 21.5; **^{19}F NMR** (470 MHz, $CDCl_3$) δ -115.52, -115.53, -115.54, -115.55, -115.56, -115.58; **IR** (neat) ν 2978, 2917, 2870, 1724, 1508, 1502, 1486, 1224, 1182, 1104, 1037, 779 cm^{-1}; $[\alpha]^{25}_D$ = – 22.1° (c = 1.0, EtOH); **HRMS** (DART) Calcd for $C_{36}H_{43}FNO_7$ (MH^+): 620.3018; found: 620.3004.

3.23s-Minor: **^{1}H NMR** (500 MHz, $CDCl_3$) δ 7.42 – 7.29 (m, 4H), 7.29 – 7.23 (m, 1H), 7.20 (t, *J* = 7.0 Hz, 2H), 6.98 (s, 2H), 6.60 (dd, *J* = 8.5, 1.7 Hz, 1H), 6.27 (t, *J* = 2.1 Hz, 1H), 6.06 (dt, *J* = 8.6, 2.1 Hz, 1H), 5.87 (d, *J* = 1.8 Hz, 2H), 4.97 (td, *J* = 6.3, 1.7 Hz, 1H), 4.88 (td, *J* = 6.2, 1.7 Hz, 1H), 3.58 (q, *J* = 13.2 Hz, 2H), 3.45 (dt, *J* = 9.4, 2.2 Hz, 1H), 3.40 – 3.23 (m, 1H), 3.19 – 3.09 (m, 1H), 3.09 – 2.97 (m, 1H), 2.83 – 2.64 (m, 2H), 2.64 – 2.51 (m, 1H), 2.25 – 2.08 (m, 3H), 2.05 (d, *J* = 11.1 Hz, 1H), 1.83 (t, *J* = 11.4 Hz, 2H), 1.30 (dd, *J* = 6.2, 1.7 Hz, 3H), 1.23 (dd, *J* = 6.3, 1.7 Hz, 3H), 1.15 (dt, *J* = 5.6, 2.3 Hz, 6H); **^{13}C NMR** (126 MHz, $CDCl_3$) δ 172.1, 171.2, 161.7 (d, J_{C-F} = 244.8 Hz), 154.3, 148.1, 141.5, 137.8, 137.04, 137.02, 129.0, 128.3, 127.1, 115.5, 107.8, 105.4, 101.0, 97.8, 69.3, 68.1, 67.9, 63.3, 57.1, 55.6, 46.3, 44.2, 43.1, 40.9, 35.2, 22.0, 21.9, 21.73, 21.72; **^{19}F NMR** (470 MHz, $CDCl_3$) δ -115.96, -115.98, -115.99, -116.00, -116.02; **HRMS** (DART) Calcd for $C_{36}H_{43}FNO_7$ (MH^+): 620.3018; found: 620.3001.

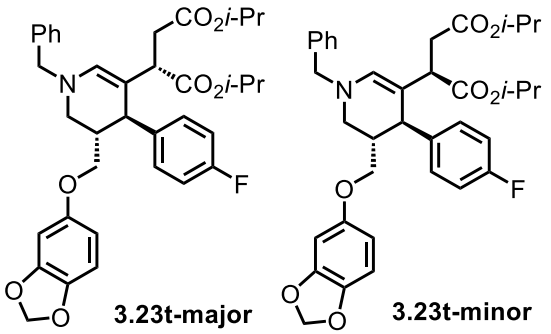

Diisopropyl 2-((4*R*,5*S*)-5-((benzo[*d*][1,3]dioxol-5-yloxy)methyl)-1-benzyl-4-(4-fluorophenyl)-1,4,5,6-tetrahydropyridin-3-yl)succinate (3.23t)

From 0.2 mmol of *N*-Bn paroxetine (3.23t): ^{1}H NMR analysis of the unpurified product mixture revealed that the diastereomeric ratio of **3.23t** was 1.9:1. After purification by column chromatography (ethyl ether:hexanes = 1:4), **3.23t** was obtained as a mixture of diastereomers (19 mg, 14%). The relative configuration of **3.23t-major** and **3.23t-minor** was assigned in analogy.

3.23t-Major: **^{1}H NMR** (500 MHz, $CDCl_3$) δ 7.35 – 7.24 (m, 4H), 7.24 – 7.19 (m, 2H), 7.07 (s, 2H), 6.89 (s, 2H), 6.69 (d, J = 8.4 Hz, 1H), 6.43 (d, J = 2.4 Hz, 1H), 6.35 (s, 1H), 6.27 (dd, J = 8.5, 2.5 Hz, 1H), 5.91 (s, 2H), 5.00 – 4.83 (m, 2H), 4.17 – 3.99 (m, 2H), 3.78 (d, J = 23.9 Hz, 2H), 3.31 (s, 1H), 3.22 (dd, J = 10.3, 4.9 Hz, 1H), 2.81 – 2.67 (m, 2H), 2.56 (dd, J = 16.9, 10.3 Hz, 1H), 2.17 (dd, J = 16.9, 4.9 Hz, 1H), 2.09 – 1.99 (m, 1H), 1.21 (d, J = 6.2 Hz, 3H), 1.19 – 1.12 (m, 9H); **^{13}C NMR** (151 MHz, $CDCl_3$) δ 173.0, 171.4, 161.5 (d, J_{C-F} = 244.4 Hz), 154.4, 148.2, 141.5 (d, J_{C-F} = 2.9 Hz), 137.6, 134.9, 129.9 (d, J_{C-F} = 7.7 Hz), 128.4, 128.1, 127.4, 114.8 (d, J_{C-F} = 21.1 Hz), 107.9, 105.9, 101.10, 101.07, 98.2, 70.2, 67.9, 67.8, 59.3, 45.9, 42.0, 40.8, 40.4, 37.4, 21.84, 21.78, 21.75, 21.7, 21.6; **^{19}F NMR** (470 MHz, $CDCl_3$) δ -117.23, -117.24, -117.25, -117.26, -117.27, -117.28, -117.29; **IR** (neat) ν 2977, 2927, 2872, 1721, 1649, 1502, 1486, 1372, 1219, 1180, 1137,

1104, 817, 788, 701 cm^{-1}; $[\alpha]^{25}_{D}$ = – 84.8° (c = 1.0, EtOH); **HRMS** (DART) Calcd for $C_{36}H_{41}FNO_7$ (MH^+): 618.2861; found: 618.2847.

3.23t-Minor: **^{1}H NMR** (600 MHz, $CDCl_3$) δ 7.38 – 7.15 (m, 5H), 7.06 (dd, *J* = 8.3, 5.4 Hz, 2H), 6.89 (t, *J* = 8.5 Hz, 2H), 6.68 (d, *J* = 8.4 Hz, 1H), 6.43 (d, *J* = 2.4 Hz, 1H), 6.30 (s, 1H), 6.26 (dd, *J* = 8.5, 2.5 Hz, 1H), 5.98 – 5.84 (m, 2H), 4.92 (q, *J* = 6.3 Hz, 1H), 4.67 (q, *J* = 6.2 Hz, 1H), 4.09 (q, *J* = 14.6 Hz, 2H), 3.82 (dd, *J* = 9.1, 6.6 Hz, 1H), 3.75 (t, *J* = 8.3 Hz, 1H), 3.46 (s, 1H), 3.12 (dd, *J* = 10.5, 5.1 Hz, 1H), 2.90 (dd, *J* = 16.5, 10.6 Hz, 1H), 2.83 – 2.69 (m, 2H), 2.34 (dd, *J* = 16.5, 5.1 Hz, 1H), 2.07 (dd, *J* = 6.9, 3.8 Hz, 1H), 1.17 (d, *J* = 6.3 Hz, 6H), 1.10 (dd, *J* = 10.2, 6.3 Hz, 6H); **^{13}C NMR** (151 MHz, $CDCl_3$) δ 173.1, 171.3, 161.5 (d, $J_{C\text{-}F}$ = 244.5 Hz), 154.4, 148.2, 141.6, 140.9 (d, $J_{C\text{-}F}$ = 3.1 Hz), 137.6, 134.7, 129.8 (d, $J_{C\text{-}F}$ = 7.7 Hz), 128.5, 128.1, 127.5, 114.9 (d, $J_{C\text{-}F}$ = 21.0 Hz), 107.9, 105.8, 101.8, 101.1, 98.2, 70.2, 68.0, 67.9, 59.5, 44.8, 42.4, 41.4, 40.5, 36.6, 21.79, 21.75, 21.60, 21.56; **^{19}F NMR** (470 MHz, $CDCl_3$) δ -117.14, -117.15, -117.16, -117.17, -117.18, -117.19, -117.20 **HRMS** (DART) Calcd for $C_{36}H_{41}FNO_7$ (MH^+): 618.2861; found: 618.2859.

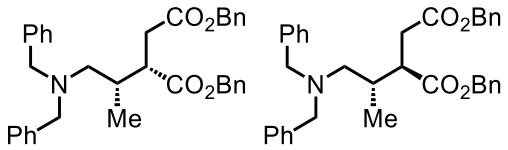

Dibenzyl 2-(1-(dibenzylamino)propan-2-yl)succinate (3.23u)

N,*N*-Dibenzylpropan-1-amine **3.21b** was reacted with dibenzyl fumarate **3.22b** following the **General Procedure A** using $B(C_6F_5)_3$ (10 mol%) as the Lewis acid catalyst and benzene (0.8 mL) as the solvent. ^{1}H NMR analysis of the unpurified product mixture revealed that the diastereomeric ratio was 2.5:1. After purification by column chromatography (ethyl ether:hexanes = 1:33) **3.23u** was obtained as a mixture of diastereomers (85 mg, 79%). Further purification was carried out by PTLC using ethyl ether:DCM = 1:49 as the eluent to separate **3.23u-major** and **3.23u-minor**. The relative configuration of **3.23u-major** and **3.23u-minor** was assigned by analogy.

3.23u-Major: ^{1}H NMR (500 MHz, $CDCl_3$) δ 7.39 – 7.25 (m, 14H), 7.20 (t, *J* = 7.4 Hz, 4H), 7.14 (t, *J* = 7.3 Hz, 2H), 5.17 – 5.00 (m, 4H), 3.75 (d, *J* = 13.2 Hz, 2H), 3.49 (d, *J* = 12.1 Hz, 1H), 3.21 (d, *J* = 13.2 Hz, 2H), 2.49 – 2.34 (m, 2H), 2.22 (dd, *J* = 12.9, 10.3 Hz, 1H), 2.11 (dd, *J* = 13.0, 5.5 Hz, 1H), 1.56 (dd, *J* = 16.8, 2.9 Hz, 1H), 0.67 (d, *J* = 6.9 Hz, 3H); **^{13}C NMR** (151 MHz, $CDCl_3$) δ 175.0, 172.2, 139.3, 136.1, 136.0, 129.1, 128.5, 128.4, 128.23, 128.18, 128.0, 126.9, 66.2, 58.69, 58.65, 56.6, 41.79, 41.77, 32.1, 29.2, 13.7; **IR** (neat) ν 3027, 2956, 1730, 1494, 1453, 1254, 1154, 976, 747, 697 cm^{-1}; **HRMS** (DART) Calcd for $C_{35}H_{38}NO_4$ (MH^+): 536.2795; found: 536.2799.

3.23u-Minor: ^{1}H NMR (600 MHz, $CDCl_3$) δ 7.39 – 7.26 (m, 13H), 7.26 – 7.24 (m, 3H), 7.24 – 7.21 (m, 2H), 7.20 (t, *J* = 7.0 Hz, 2H), 5.08 (d, *J* = 12.4 Hz, 1H), 5.02 (d, *J* = 10.6 Hz, 2H), 4.94 (d, *J* = 12.2 Hz, 1H), 3.54 (d, *J* = 13.6 Hz, 2H), 3.34 (d, *J* = 13.6 Hz, 2H), 3.08 (dt, *J* = 10.8, 4.0

Hz, 1H), 2.70 (dd, *J* = 16.8, 10.7 Hz, 1H), 2.38 (dd, *J* = 12.7, 6.7 Hz, 1H), 2.25 – 2.15 (m, 2H), 2.03 (qd, *J* = 7.1, 4.0 Hz, 1H), 0.81 (d, *J* = 6.9 Hz, 3H); **^{13}C NMR** (151 MHz, $CDCl_3$) δ 173.5, 172.1, 139.3, 135.8, 129.0, 128.50, 128.46, 128.4, 128.2, 128.1, 126.9, 66.4, 66.3, 58.9, 58.4, 44.0, 33.3, 15.6; **HRMS** (DART) Calcd for $C_{35}H_{38}NO_4$ (MH^+): 536.2795; found: 536.2789.

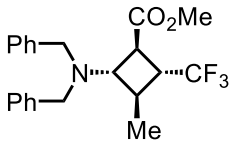

3.23v

Methyl 2-(dibenzylamino)-3-methyl-4-(trifluoromethyl)cyclobutane-1-carboxylate (3.23v)

N,*N*-Dibenzylpropan-1-amine **3.21b** was reacted with methyl 4,4,4-trifluorobut-2-enoate **3.22c** following the **General Procedure B** using $B(C_6F_5)_3$ (10 mol%) as the Lewis acid catalyst and benzene as the solvent. ^{1}H NMR analysis of the unpurified product mixture revealed that the diastereomeric ratio was >20:1. After purification by column chromatography (ethyl ether:hexanes = 1:49) **3.23v** was obtained as a colorless liquid (58 mg, 74%). The relative configuration of **3.23v** was assigned by analogy.

^{1}H NMR (600 MHz, $CDCl_3$) δ 7.37 – 7.27 (m, 8H), 7.25 – 7.20 (m, 2H), 3.80 (d, J = 13.9 Hz, 2H), 3.72 (s, 3H), 3.61 (d, J = 13.9 Hz, 2H), 3.20 (t, J = 8.6 Hz, 1H), 3.14 (t, J = 8.6 Hz, 1H), 2.51 – 2.44 (m, 1H), 2.44 – 2.36 (m, 1H), 1.09 (d, J = 6.4 Hz, 3H); **^{13}C NMR** (151 MHz, $CDCl_3$) δ 172.6, 139.1, 128.4, 128.3, 127.1, 64.1, 54.7, 52.1, 40.6 (q, J_{C-F} = 30.7 Hz), 39.9, 33.40, 33.38, 18.2; **^{19}F NMR** (470 MHz, $CDCl_3$) δ -71.84; **IR** (neat) ν 2923, 2800, 1709, 1498, 1378, 1178, 747, 697 cm^{-1}; **HRMS** (DART) Calcd for $C_{22}H_{25}NO_2F_3$ (MH^+): 392.1832; found: 392.1824.

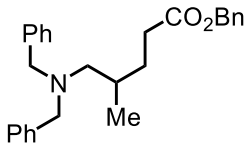

3.23w

Benzyl 5-(dibenzylamino)-4-methylpentanoate (3.23w)

N,*N*-Dibenzylpropan-1-amine **3.21b** was reacted with benzyl acrylate **3.22d** following the **General Procedure A** using $B(C_6F_5)_3$ (5.0 mol%) as the Lewis acid catalyst and benzene (0.8 mL) as the solvent. After purification by column chromatography (ethyl ether:hexanes = 1:33) **3.23w** was obtained as a colorless liquid (60 mg, 75%).

^{1}H NMR (600 MHz, $CDCl_3$) δ 7.34 (d, *J* = 5.4 Hz, 9H), 7.28 (t, *J* = 7.5 Hz, 4H), 7.20 (t, *J* = 7.3 Hz, 2H), 5.10 (s, 2H), 3.48 (s, 4H), 2.33 – 2.25 (m, 2H), 2.23 (dd, *J* = 12.4, 7.3 Hz, 1H), 2.14 (dd, *J* = 12.5, 7.3 Hz, 1H), 1.86 – 1.79 (m, 1H), 1.79 – 1.71 (m, 1H), 1.40 – 1.31 (m, 1H), 0.84 (d, *J* = 6.6 Hz, 3H); **^{13}C NMR** (151 MHz, $CDCl_3$) δ 173.8, 139.8, 136.1, 128.9, 128.5, 128.2, 128.14, 128.10, 126.7, 66.1, 60.3, 58.8, 31.7, 30.4, 29.7, 17.8; **IR** (neat) ν 2951, 2926, 1733, 1493, 1452, 1256, 1167, 746, 697 cm^{-1}; **HRMS** (DART) Calcd for $C_{27}H_{32}NO_2$ (MH^+): 402.2428; found: 402.2427.

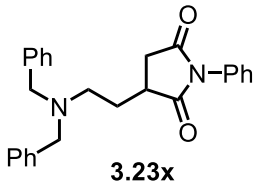

3.23x

3-(2-(dibenzylamino)ethyl)-1-phenylpyrrolidine-2,5-dione (3.23x)

N,*N*-Dibenzylethanamine **3.21a** was reacted with 1-phenyl-1*H*-pyrrole-2,5-dione **3.22e** following the **General Procedure B** using $B(C_6F_5)_3$ (10 mol%) as the Lewis acid catalyst and benzene as the solvent. After purification by column chromatography (ethyl ether:hexanes = 1:33) **3.23x** was obtained as a colorless liquid (39 mg, 49%).

^{1}H NMR (600 MHz, $CDCl_3$) δ 7.45 (dd, *J* = 8.4, 7.2 Hz, 2H), 7.40 – 7.36 (m, 1H), 7.35 – 7.29 (m, 8H), 7.29 – 7.22 (m, 4H), 3.73 (d, *J* = 13.3 Hz, 2H), 3.43 (d, *J* = 13.4 Hz, 2H), 3.11 (tdd, *J* = 9.5, 5.3, 3.8 Hz, 1H), 2.56 (dd, *J* = 7.6, 5.2 Hz, 2H), 2.47 (dd, *J* = 18.5, 9.3 Hz, 1H), 2.33 (dtd, *J* = 14.0, 7.7, 4.0 Hz, 1H), 2.20 (dd, *J* = 18.5, 5.3 Hz, 1H), 1.63 (ddt, *J* = 14.1, 10.3, 5.2 Hz, 1H); **^{13}C NMR** (126 MHz, $CDCl_3$) δ 179.3, 175.7, 139.2, 132.0, 129.1, 129.0, 128.5, 128.3, 127.2, 126.4, 58.6, 50.0, 38.0, 34.1, 29.1; **IR** (neat) ν 2922, 2801, 1707, 1498, 1452, 1377, 1177, 747, 697 cm^{-1}; **HRMS** (DART) Calcd for $C_{26}H_{27}N2O_2$ (MH^+): 399.2067; found: 399.2071.

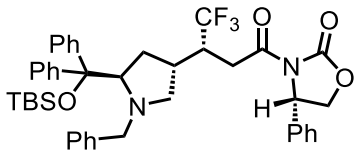

3.26a

(*S*)-3-((*R*)-3-((3*R*,5*R*)-1-Benzyl-5-(((*tert*-butyldimethylsilyl)oxy)diphenylmethyl) pyrrolidin-3-yl)-4,4,4-trifluorobutanoyl)-4-phenyloxazolidin-2-one (3.26a)

To a 15 mL oven-dried pressure vessel was added (*R*)-1-benzyl-2-(((*tert*-butyldimethylsilyl)oxy)diphenylmethyl)pyrrolidine **3.21k** (0.10 mmol), (*S,E*)-4-phenyl-3-(4,4,4-trifluorobut-2-enoyl)oxazolidin-2-one **3.25a** (0.15 mmol), $B(C_6F_5)_3$ (10 mol%), ZnI_2 (10 mol%), HBpin (70 mol%) and benzene (0.60 mL) under a nitrogen atmosphere. The reaction mixture was allowed to heat for 36 hours at 70 °C. Upon completion, the reaction mixture was concentrated *in vacuo*. After purification by column chromatography (EtOAc:hexanes = 1:6), **3.26a** was obtained as a white solid (61 mg, 82%). The absolute configuration of **3.26a-(*R,R,R,S*)** was assigned based on X-ray crystallography data of **3.29**.

^{1}H NMR (600 MHz, $CDCl_3$): δ 7.59 (d, *J* = 8.3 Hz, 2H), 7.54 (d, *J* = 6.6 Hz, 2H), 7.37 – 7.27 (m, 9H), 7.21 (t, *J* = 7.3 Hz, 4H), 7.15 (t, *J* = 7.2 Hz, 1H), 7.04 (d, *J* = 7.4 Hz, 2H), 5.33 (dd, *J* = 8.8, 4.1 Hz, 1H), 4.65 (t, *J* = 8.8 Hz, 1H), 4.46 (br, 1H), 4.25 (dd, *J* = 9.0, 4.0 Hz, 1H), 4.02 (d, *J* = 9.8 Hz, 1H), 3.40 (d, *J* = 13.3 Hz, 1H), 3.02 (dd, *J* = 18.4, 6.2 Hz, 1H), 2.80 (dd, *J* = 18.4, 5.0 Hz, 1H), 2.63 (t, *J* = 7.8 Hz, 1H), 2.59 – 2.51 (m, 1H), 1.96 – 1.84 (m, 2H), 1.69 (q, *J* = 11.7 Hz, 1H), 1.33 – 1.18 (m, 1H), 0.87 (s, 9H), -0.44 (d, *J* = 17.4 Hz, 6H); **^{13}C NMR (151 MHz, $CDCl_3$):** δ 170.2, 153.6, 143.2, 140.3, 138.6, 130.2, 130.1, 130.1, 129.4, 129.0, 128.3, 128.2, 128.2, 127.7, 127.4, 127.2 (q, *J* = 266.8 Hz), 127.1, 126.6, 125.8, 70.2, 69.8, 61.7, 59.0, 58.1, 40.7 (q, *J* = 26.3 Hz), 35.4, 33.1, 29.9, 26.5, 19.1, -2.7, -2.9; **^{19}F NMR (376 MHz, $CDCl_3$):** δ -69.82 (d, *J* = 9.3 Hz); **IR**

(neat): ν 2952, 2926, 2892, 2853, 1783, 1710, 1493, 1452, 1384, 1359, 1326, 1252, 1197, 1155, 1120, 1095, 1061, 854, 834, 774, 702 cm^{-1}; **HRMS (DART):** Calcd for $C_{43}H_{50}F_3N_2O_4Si$ (MH^+): 743.3486; found: 743.3486; **Specific Rotation:** $\boldsymbol{[\alpha]^{25}_D}$ = -6.9° (c = 0.88, DCM).

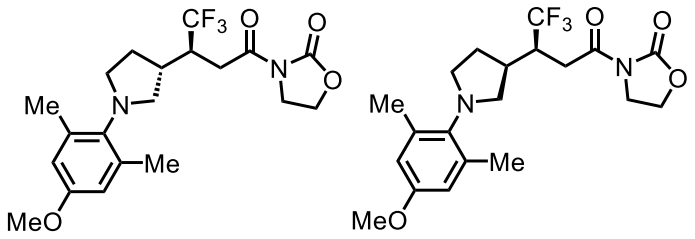

3.26b-*anti* **3.26b-*syn***

3-((*S*)-4,4,4-Trifluoro-3-(1-(4-methoxy-2,6-dimethylphenyl)pyrrolidin-3-yl)butanoyl)oxazolidin-2-one (3.26b)

To a 15 mL oven-dried pressure vessel was added $Mg(ClO_4)_2$ (0.010 mmol, 10 mol%), **L1** (0.010 mmol, 10 mol%), benzene (0.30 mL) under nitrogen atmosphere. The mixture was allowed to stir for 20 minutes at 22 °C. Subsequently, 1-(4-methoxy-2,6-dimethylphenyl)pyrrolidine **3.21q** (0.10 mmol), (*E*)-3-(4,4,4-trifluorobut-2-enoyl)oxazolidin-2-one **3.25b** (0.15 mmol), and benzene (0.30 mL) were added to the vial under nitrogen atmosphere, and the resulting mixture was allowed to stir at 22 °C for 12 h. Upon completion, the reaction mixture was concentrated *in vacuo*. ^{1}H NMR and ^{19}F NMR analyses of the unpurified product mixture using mesitylene and perfluorobenzene as the internal standard revealed that the diastereomeric ratio was 1.6:1. After purification by column chromatography (EtOAc:hexanes = 1:3), **3.26b** was obtained as a colorless liquid (28 mg, 67%). Further purification was carried out by PTLC using ethyl EtOAc:hexanes = 1:2 as the eluent to separate **3.26b-*anti*** and **3.26b-*syn***.

3.26b-*anti*. ^{1}H NMR (400 MHz, $CDCl_3$): δ 6.55 (s, 2H), 4.41 (t, *J* = 7.9 Hz, 2H), 4.09 – 3.93 (m, 2H), 3.73 (s, 3H), 3.41 (dd, *J* = 18.5, 7.2 Hz, 1H), 3.28 (q, *J* = 8.7 Hz, 1H), 3.22 – 3.09 (m, 3H), 3.08 – 2.92 (m, 2H), 2.65 (h, *J* = 8.3 Hz, 1H), 2.36 – 2.12 (m, 7H), 1.85 (p, *J* = 10.3 Hz, 1H); **^{13}C NMR (101 MHz, $CDCl_3$):** δ 170.6, 157.0, 153.6, 139.8, 137.5, 127.8 (q, *J* = 280.5 Hz), 113.7, 62.3, 55.3, 53.9, 50.4, 42.8, 41.4 (q, *J* = 25.7 Hz), 39.0, 33.1, 33.0, 31.6, 19.0; **^{19}F NMR (376 MHz,**

$CDCl_3$): δ -69.12 (d, *J* = 9.3 Hz); **IR (neat):** ν 2921, 2837, 1778, 1701, 1601, 1480, 1387, 1363, 1319, 1280, 1222, 1194, 1124, 1067, 1040, 956, 856, 709, 671, 626 cm^{-1}; **HRMS (DART):** Calcd for $C_{20}H_{26}F_3N_2O_4$ (MH^+): 415.1839; found: 415.1819; **HPLC** (CHIRACPAK IA-3; 5%/ 95% isopropanol/ hexanes, 0.5 mL/min; tr = 25.7 min (minor), 36.0 min (major); 90:10 er); **Specific Rotation:** $[\alpha]^{25}_D$ = -6.0° (c = 1.0, DCM).

```
Acq. Operator    : SYSTEM                          Seq. Line :   2
Acq. Instrument  : Wasa_LC1                         Location :   86
Injection Date   : 8/23/2020 6:12:31 PM                 Inj :   1
                                                  Inj Volume : 4.000 µl
Method           : C:\Chem32\1\Data\JOE 2020-08-23 17-39-20\column6 5%IPA 95% hexane 60min-0.
                   5mL.M (Sequence Method)
Last changed     : 8/23/2020 5:39:26 PM by SYSTEM
Method Info      : Column6 60min-5.0% iPrOH 95% hexane-0.5mL
```

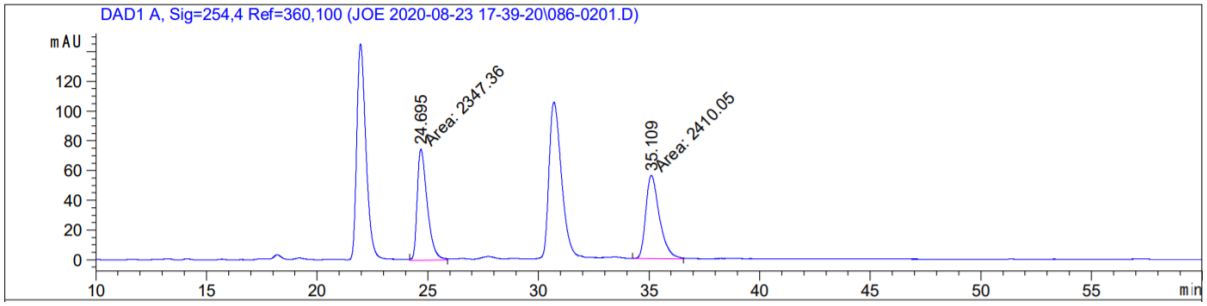

Signal 1: DAD1 A, Sig=254,4 Ref=360,100

Peak #	RetTime [min]	Type	Width [min]	Area [mAU*s]	Height [mAU]	Area %
1	24.695	MM	0.5242	2347.36230	74.63573	49.3412
2	35.109	MM	0.7172	2410.04810	56.00684	50.6588
Totals :				4757.41040	130.64258	

```
Acq. Operator   : SYSTEM                          Seq. Line :   3
Acq. Instrument : Wasa_LC1                         Location :   87
Injection Date  : 8/23/2020 7:13:29 PM                 Inj :   1
                                                 Inj Volume : 4.000 µl
Method          : C:\Chem32\1\Data\JOE 2020-08-23 17-39-20\column6 5%IPA 95% hexane 60min-0.
                  5mL.M (Sequence Method)
Last changed    : 8/23/2020 5:39:26 PM by SYSTEM
Method Info     : Column6 60min-5.0% iPrOH 95% hexane-0.5mL
```

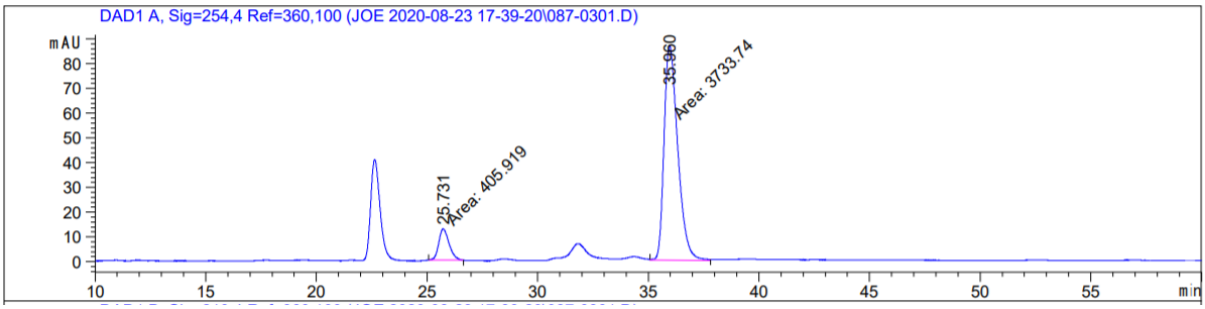

Signal 1: DAD1 A, Sig=254,4 Ref=360,100

Peak #	RetTime [min]	Type	Width [min]	Area [mAU*s]	Height [mAU]	Area %
1	25.731	MM	0.5377	405.91949	12.58177	9.8056
2	35.960	MM	0.7167	3733.73560	86.82920	90.1944
Totals :				4139.65509	99.41098	

3.26b-*syn*. **^{1}H NMR (400 MHz, $CDCl_3$):** δ 6.55 (s, 2H), 4.44 (t, *J* = 8.1 Hz, 2H), 4.09 – 4.00 (m, 2H), 3.73 (s, 3H), 3.45 – 3.34 (m, 1H), 3.32 – 3.19 (m, 2H), 3.19 – 3.10 (m, 3H), 3.07 (t, *J* = 8.8 Hz, 1H), 2.62 (dq, *J* = 16.7, 7.9 Hz, 1H), 2.21 (s, 6H), 2.10 – 2.01 (m, 1H), 1.79 (p, *J* = 10.2 Hz, 1H); **^{19}F NMR (470 MHz, $CDCl_3$):** δ -69.62 (d, *J* = 9.2 Hz); **IR (neat):** ν 2920, 2852, 1780, 1701, 1660, 1602, 1480, 1466, 1388, 1364, 1318, 1261, 1223, 1194, 1157, 1126, 1066, 1039 cm^{-1}; **HRMS (DART):** Calcd for $C_{20}H_{26}F_3N_2O_4$ (MH^+): 415.1839; found: 415.1837. **HPLC** (CHIRACPAK IA-3; 5%/ 95% isopropanol/ hexanes, 0.5 mL/min; tr = 22.0 min (major), 30.7 min (minor); 84:16 er); **Specific Rotation $[\alpha]^{25}_D$** = -5.3° (c = 0.15, DCM).

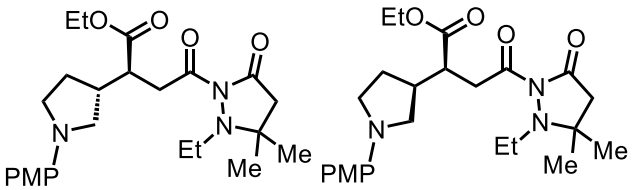

3.26c-(*R*,*S*) **3.26c-(*S*,*S*)**

Ethyl (*S*)-4-(2-ethyl-3,3-dimethyl-5-oxopyrazolidin-1-yl)-2-(1-(4-methoxyphenyl) pyrrolidin-3-yl)-4-oxobutanoate (3.26c)

1-(4-Methoxy-2,6-dimethylphenyl)pyrrolidine **3.21r** was reacted with ethyl (*E*)-4-(2-ethyl-3,3-dimethyl-5-oxopyrazolidin-1-yl)-4-oxobut-2-enoate **3.25c** following the **General Procedure E** for 1 hour using $B(C_6F_5)_3$ (10 mol%), $Sc(OTf)_3$ (5.0 mol%), **L10** (6.0 mol%) and DCM as the solvent. ^{1}H NMR analysis of the unpurified product mixture using mesitylene as the internal standard revealed that the diastereomeric ratio was 2.0:1. After purification by column chromatography (EtOAc:hexanes = 1:2), **3.26c** was obtained as a colorless liquid (36 mg, 80%). Further purification was carried out by PTLC using ethyl EtOAc:hexanes = 1:2 as the eluent to separate **3.26c-(*R*,*S*)** and **3.26c-(*S*,*S*)**. The absolute configuration for this product was assigned in analogy to that determined for product **3.26f**.

3.26c-(*R*,*S*). ^{1}H NMR (500 MHz, $CDCl_3$): δ 6.84 (d, *J* = 9.0 Hz, 2H), 6.51 (d, *J* = 9.0 Hz, 2H), 4.22 – 4.08 (m, 2H), 3.75 (s, 3H), 3.46 – 3.37 (m, 2H), 3.33 (td, *J* = 8.7, 2.7 Hz, 1H), 3.29 – 3.21 (m, 1H), 3.05 (t, *J* = 8.7 Hz, 1H), 3.03 – 2.93 (m, 4H), 2.59 (s, 2H), 2.51 (q, *J* = 8.4 Hz, 1H), 2.14 – 2.05 (m, 1H), 1.90 (dq, *J* = 12.2, 8.9 Hz, 1H), 1.31 (d, *J* = 5.1 Hz, 6H), 1.25 (t, *J* = 7.1 Hz, 3H), 1.07 (t, *J* = 7.1 Hz, 3H); **^{13}C NMR (126 MHz, $CDCl_3$):** δ 175.5, 174.3, 169.6, 151.1, 142.8, 115.2, 112.6, 60.88, 60.85, 56.1, 52.3, 48.1, 47.3, 44.3, 43.9, 40.9, 37.9, 29.7, 26.1, 25.8, 14.4, 12.9; **IR (neat):** ν 2968, 2929, 2829, 1727, 1514, 1485, 1465, 1370, 1302, 1238, 1176, 1128, 1095, 1038, 812 cm^{-1}; **HRMS (DART):** Calcd for $C_{24}H_{36}N_3O_5$ (MH^+): 446.2650; found: 446.2656; **HPLC**

(CHIRACPAK IA-3; 10%/ 90% isopropanol/ hexanes, 1.0 mL/min; tr = 15.6 min (minor), 21.7 min (major); 97:3 er); **Specific Rotation $[\alpha]^{25}_{D}$** = -10.5° (c = 0.33, DCM).

```
Acq. Operator   : SYSTEM                          Seq. Line :   2
Acq. Instrument : Wasa_LC1                        Location :   11
Injection Date  : 8/14/2020 10:18:07 PM               Inj :   1
                                                 Inj Volume : 4.000 µl
Acq. Method     : C:\Chem32\1\Data\JOE 2020-08-14 21-30-51\column6 10% IPA 90% hex 45min-1.
                  0ml.M
Last changed    : 8/14/2020 9:30:57 PM by SYSTEM
Analysis Method : C:\Chem32\1\Data\JOE 2020-08-14 21-30-51\column6 10% IPA 90% hex 45min-1.
                  0ml.M (Sequence Method)
Last changed    : 12/18/2020 6:35:43 PM by SYSTEM
                  (modified after loading)
Method Info     : Column 6 10% IPA/90% hexane 1.0 mL/min 45 min
```

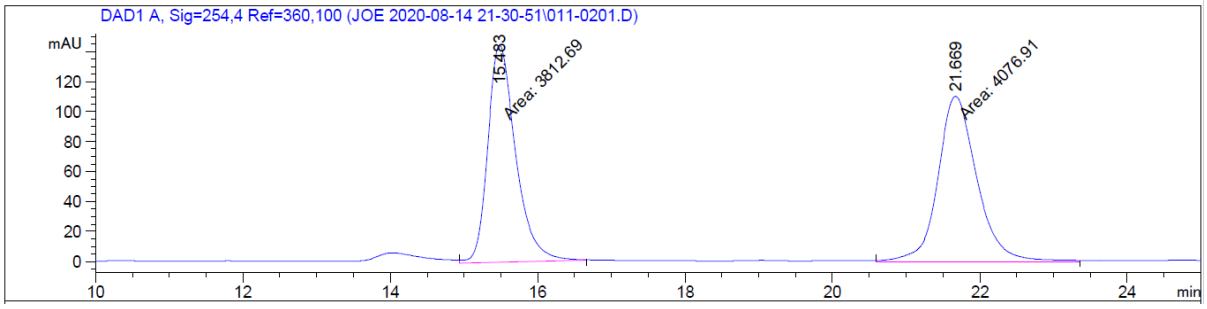

Signal 1: DAD1 A, Sig=254,4 Ref=360,100

Peak #	RetTime [min]	Type	Width [min]	Area [mAU*s]	Height [mAU]	Area %
1	15.483	MM	0.4381	3812.68506	145.06230	48.3255
2	21.669	MM	0.6154	4076.91406	110.41205	51.6745
Totals :				7889.59912	255.47435	

```
Acq. Operator   : SYSTEM                          Seq. Line :   2
Acq. Instrument : Wasa_LC1                         Location :   46
Injection Date  : 12/15/2020 7:39:45 PM                Inj :   1
                                                 Inj Volume : 4.000 µl
Acq. Method     : C:\Chem32\1\Data\JOE 2020-12-15 18-21-35\column6 10% IPA 90% hex 45min-1.
                  0ml.M
Last changed    : 12/15/2020 6:21:41 PM by SYSTEM
Analysis Method : C:\Chem32\1\Data\JOE 2020-12-15 18-21-35\column6 10% IPA 90% hex 45min-1.
                  0ml.M (Sequence Method)
Last changed    : 12/18/2020 6:41:56 PM by SYSTEM
                  (modified after loading)
Method Info     : Column 6 10% IPA/90% hexane 1.0 mL/min 45 min
```

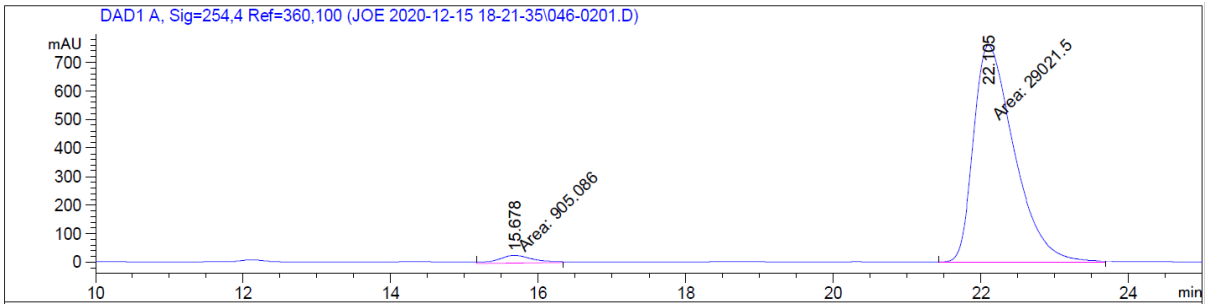

Signal 1: DAD1 A, Sig=254,4 Ref=360,100

Peak #	RetTime [min]	Type	Width [min]	Area [mAU*s]	Height [mAU]	Area %
1	15.678	MM	0.5507	905.08649	27.39032	3.0244
2	22.105	MM	0.6368	2.90215e4	759.58032	96.9756
Totals :				2.99265e4	786.97065	

3.26c-(*S*,*S*). ^{1}H NMR (600 MHz, $CDCl_3$): δ 6.82 (d, *J* = 8.9 Hz, 2H), 6.49 (d, *J* = 9.0 Hz, 2H), 4.14 (q, *J* = 7.1 Hz, 2H), 3.74 (s, 3H), 3.44 – 3.29 (m, 3H), 3.28 – 3.20 (m, 1H), 3.12 (t, *J* = 8.8 Hz, 1H), 3.03 (dd, *J* = 18.0, 3.7 Hz, 1H), 3.02 – 2.90 (m, 3H), 2.58 (s, 2H), 2.56 – 2.48 (m, 1H), 2.18 (ddd, *J* = 12.6, 7.7, 5.3 Hz, 1H), 1.83 – 1.71 (m, 1H), 1.30 (d, *J* = 3.7 Hz, 6H), 1.25 (t, *J* = 7.1 Hz, 3H), 1.05 (t, *J* = 7.1 Hz, 3H); **IR (neat):** ν 2969, 2924, 2849, 1727, 1513, 1485, 1464, 1371, 1302, 1238, 1177, 1127, 1095, 1034, 813 cm^{-1}; **HRMS (DART):** Calcd for $C_{24}H_{36}N_3O_5$ (MH^+): 446.2650; found: 446.2643; **HPLC** (CHIRACPAK IA-3; 10%/ 90% isopropanol/ hexanes, 1.0 mL/min; tr = 29.0 min (major), 38.5 min (minor); 98:2 er); **Specific Rotation $[\alpha]^{25}_D$** = -2.0° (c = 0.10, DCM).

```
Acq. Operator   : SYSTEM                          Seq. Line :   2
Acq. Instrument : Wasa_LC1                         Location :   11
Injection Date  : 8/14/2020 10:18:07 PM               Inj :   1
                                                  Inj Volume : 4.000 µl
Acq. Method     : C:\Chem32\1\Data\JOE 2020-08-14 21-30-51\column6 10% IPA 90% hex 45min-1.
                  0ml.M
Last changed    : 8/14/2020 9:30:57 PM by SYSTEM
Analysis Method : C:\Chem32\1\Data\JOE 2020-08-14 21-30-51\column6 10% IPA 90% hex 45min-1.
                  0ml.M (Sequence Method)
Last changed    : 12/18/2020 6:34:05 PM by SYSTEM
                  (modified after loading)
Method Info     : Column 6 10% IPA/90% hexane 1.0 mL/min 45 min
```

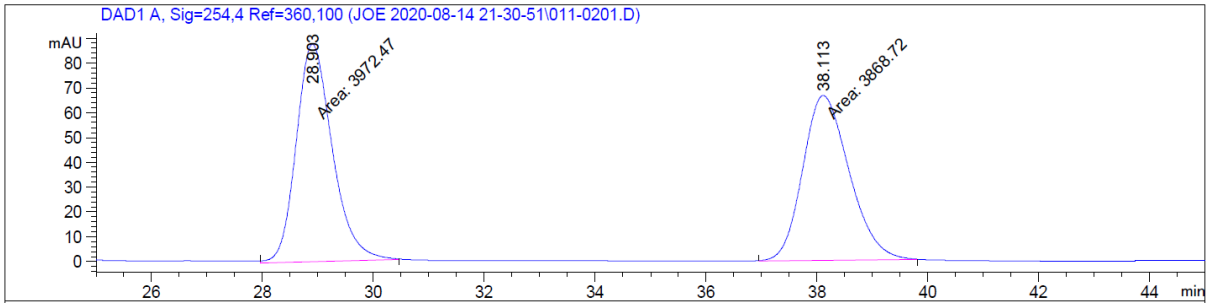

Signal 1: DAD1 A, Sig=254,4 Ref=360,100

Peak #	RetTime [min]	Type	Width [min]	Area [mAU*s]	Height [mAU]	Area %
1	28.903	MM	0.7563	3972.46875	87.54141	50.6616
2	38.113	MM	0.9717	3868.71851	66.35892	49.3384
Totals :				7841.18726	153.90034	

```
Acq. Operator   : SYSTEM                          Seq. Line :   4
Acq. Instrument : Wasa_LC1                         Location :   37
Injection Date  : 8/14/2020 11:50:00 PM                Inj :   1
                                                 Inj Volume : 4.000 µl
Acq. Method     : C:\Chem32\1\Data\JOE 2020-08-14 21-30-51\column6 10% IPA 90% hex 45min-1.
                  0ml.M
Last changed    : 8/14/2020 9:30:57 PM by SYSTEM
Analysis Method : C:\Chem32\1\Data\JOE 2020-08-14 21-30-51\column6 10% IPA 90% hex 45min-1.
                  0ml.M (Sequence Method)
Last changed    : 12/18/2020 6:40:33 PM by SYSTEM
                  (modified after loading)
Method Info     : Column 6 10% IPA/90% hexane 1.0 mL/min 45 min
```

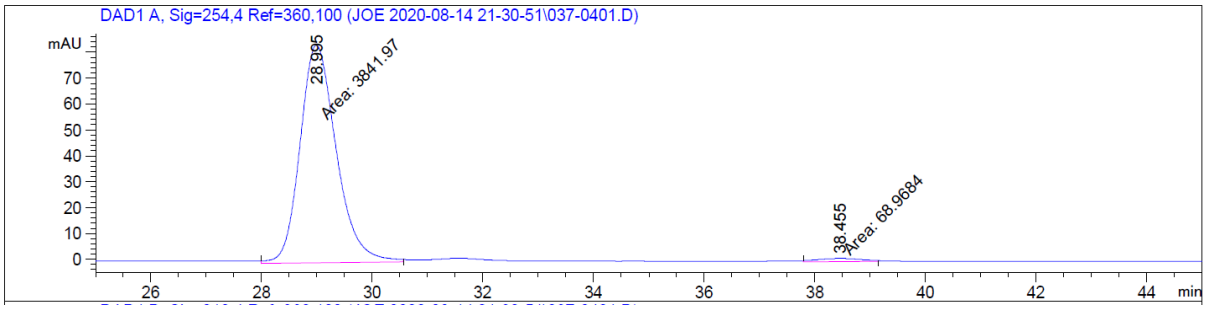

Signal 1: DAD1 A, Sig=254,4 Ref=360,100

Peak #	RetTime [min]	Type	Width [min]	Area [mAU*s]	Height [mAU]	Area %
1	28.995	MM	0.7602	3841.96606	84.22824	98.2365
2	38.455	MM	0.9488	68.96841	1.21147	1.7635
Totals :				3910.93448	85.43971	

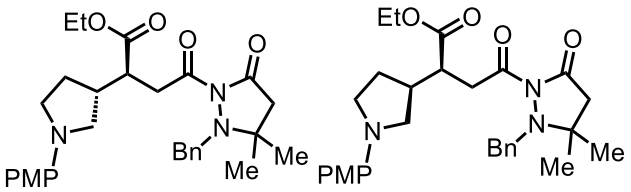

3.26d-(*R,S*) **3.26d-(*S,S*)**

Ethyl (*S*)-4-(2-benzyl-3,3-dimethyl-5-oxopyrazolidin-1-yl)-2-(1-(4-methoxyphenyl) pyrrolidin-3-yl)-4-oxobutanoate (3.26d)

1-(4-Methoxy-2,6-dimethylphenyl)pyrrolidine **3.21r** was reacted with ethyl (*E*)-4-(2-benzyl-3,3-dimethyl-5-oxopyrazolidin-1-yl)-4-oxobut-2-enoate **3.25d** following the **General Procedure E** for 1 hour using $B(C_6F_5)_3$ (10 mol%), $Sc(OTf)_3$ (10 mol%), **L6** (12 mol%) and DCM as the solvent. ^{1}H NMR analysis of the unpurified product mixture using mesitylene as the internal standard revealed that the diastereomeric ratio was 3.0:1. After purification by column chromatography (ether:hexanes = 3:2), **3.26d** was obtained as a colorless liquid (42 mg, 83%). Further purification was carried out by PTLC using ethyl ether:hexanes = 3:2 as the eluent to obtain **3.26d-(*R,S*)**. The absolute configuration for this product was assigned in analogy to that determined for product **3.26f**.

3.26d-(*R,S*). ^{1}H NMR (600 MHz, $CDCl_3$): δ 7.39 (d, *J* = 7.4 Hz, 2H), 7.30 (t, *J* = 7.4 Hz, 2H), 7.26 (d, *J* = 7.3 Hz, 1H), 6.83 (d, *J* = 8.9 Hz, 2H), 6.49 (d, *J* = 8.8 Hz, 2H), 4.11 (qd, *J* = 7.2, 2.0 Hz, 2H), 4.06 (d, *J* = 13.6 Hz, 1H), 3.99 (d, *J* = 13.9 Hz, 1H), 3.75 (s, 3H), 3.38 – 3.26 (m, 2H), 3.21 (td, *J* = 8.7, 6.5 Hz, 2H), 2.91 (t, *J* = 7.0 Hz, 1H), 2.79 (t, *J* = 10.0 Hz, 1H), 2.70 – 2.47 (m, 3H), 2.42 (q, *J* = 8.4 Hz, 1H), 2.06 – 2.01 (m, 1H), 1.81 (p, *J* = 9.5 Hz, 1H), 1.27 (d, *J* = 6.5 Hz, 6H), 1.21 (t, *J* = 7.1 Hz, 3H); **^{13}C NMR (151 MHz, $CDCl_3$):** δ 174.6, 174.2, 169.1, 151.1, 142.8, 137.3, 129.6, 128.6, 127.8, 115.2, 112.6, 61.4, 60.8, 57.0, 56.1, 52.3, 48.1, 44.0, 43.6, 40.8, 37.5, 29.8, 29.7, 26.5, 26.0, 14.4; **IR (neat):** ν 2924, 2851, 1771, 1728, 1702, 1513, 1370, 1301, 1238,

1176, 1125, 1038, 812 cm^{-1}; **HRMS (DART):** Calcd for $C_{29}H_{38}N_3O_5$ (MH^+): 508.2806; found: 508.2805; **HPLC** (CHIRACPAK IA-3; 5%/ 95% isopropanol/ hexanes, 0.45 mL/min; tr = 82.9 min (major), 91.3 min (minor); 95:5 er); **Specific Rotation** $[\alpha]^{25}_D$ = -3.0° (c = 0.20, DCM).

```
Acq. Operator   : SYSTEM                          Seq. Line :   7
Acq. Instrument : Wasa_LC1                        Location :   51
Injection Date  : 8/15/2020 1:57:58 AM                 Inj :   1
                                                Inj Volume : 4.000 µl
Acq. Method     : C:\Chem32\1\Data\JOE 2020-08-14 21-30-51\column6 5.0%IPA 95% hexane 240min-
                  0.45mL.M
Last changed    : 8/14/2020 9:30:57 PM by SYSTEM
Analysis Method : C:\Chem32\1\Data\JOE 2020-08-14 21-30-51\column6 5.0%IPA 95% hexane 240min-
                  0.45mL.M (Sequence Method)
Last changed    : 12/18/2020 6:46:00 PM by SYSTEM
                  (modified after loading)
Method Info     : Column6 240min-5.0% iPrOH 95% hexane-0.45mL
```

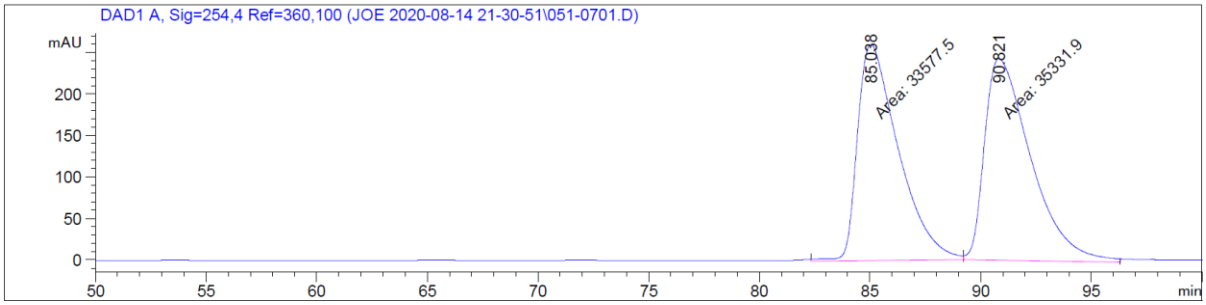

Signal 1: DAD1 A, Sig=254,4 Ref=360,100

Peak #	RetTime [min]	Type	Width [min]	Area [mAU*s]	Height [mAU]	Area %
1	85.038	MM	2.1427	3.35775e4	261.18115	48.7270
2	90.821	MM	2.4172	3.53319e4	243.61862	51.2730
Totals :				6.89095e4	504.79977	

```
Acq. Operator   : SYSTEM                          Seq. Line :   9
Acq. Instrument : Wasa_LC1                         Location :   14
Injection Date  : 8/15/2020 9:59:52 AM                 Inj :   1
                                                 Inj Volume : 4.000 µl
Acq. Method     : C:\Chem32\1\Data\JOE 2020-08-14 21-30-51\column6 5.0%IPA 95% hexane 240min-
                  0.45mL.M
Last changed    : 8/14/2020 9:30:57 PM by SYSTEM
Analysis Method : C:\Chem32\1\Data\JOE 2020-08-14 21-30-51\column6 5.0%IPA 95% hexane 240min-
                  0.45mL.M (Sequence Method)
Last changed    : 12/18/2020 6:47:49 PM by SYSTEM
                  (modified after loading)
Method Info     : Column6 240min-5.0% iPrOH 95% hexane-0.45mL
```

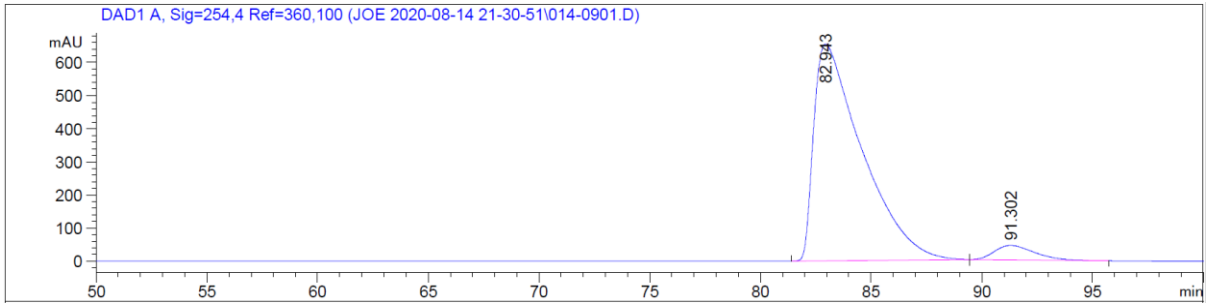

Signal 1: DAD1 A, Sig=254,4 Ref=360,100

Peak #	RetTime [min]	Type	Width [min]	Area [mAU*s]	Height [mAU]	Area %
1	82.943	BB	2.1274	9.92032e4	655.57562	94.7781
2	91.302	BB	1.8391	5465.65527	43.52220	5.2219
Totals :				1.04669e5	699.09782	

3.26d ((*R*,*S*):(*S*,*S*)= 2.3:1). **^{1}H NMR (600 MHz, $CDCl_3$, *peaks from diastereomers are merged*):** δ 7.40 (dd, *J* = 7.4, 2.3 Hz, 2H), 7.35 – 7.29 (m, 2H), 7.29 – 7.23 (m, 1H), 6.89 – 6.79 (m, 2H), 6.55 – 6.44 (m, 2H), 4.20 – 4.09 (m, 2H), 4.09 – 4.03 (m, 1H), 4.03 – 3.95 (m, 1H), 3.83 – 3.70 (m, 3H), 3.39 – 3.27 (m, 2H), 3.27 – 3.14 (m, 2H), 3.09 – 2.87 (m, 1H), 2.87 – 2.75 (m, 1H), 2.74 – 2.36 (m, 4H), 2.13 – 1.98 (m, 1H), 1.86 – 1.63 (m, 1H), 1.31 – 1.25 (m, 6H), 1.25 – 1.19 (m, 3H); **^{13}C NMR (151 MHz, $CDCl_3$):** δ 174.51, 174.47, 174.1, 173.9, 169.0 (*overlapped*), 151.01, 151.00, 142.8, 142.7, 137.3, 137.2, 129.5, 129.4, 128.51, 128.48, 127.7, 127.6, 115.0 (*overlapped*), 112.5 (*overlapped*), 61.3, 61.2, 60.72, 60.70, 56.84, 56.80, 56.00, 55.99, 52.15, 52.13, 48.0, 47.9, 44.0, 43.9, 43.5, 43.4, 40.6, 40.4, 37.4, 37.0, 29.8, 29.6, 26.4 (*overlapped*), 25.9 (*overlapped*), 14.30, 14.26; **HPLC** (CHIRACPAK IA-3; 5%/ 95% isopropanol/ hexanes, 0.45 mL/min; tr = 107.5 min (major), 191.0 min (minor); 95:5 er).

```
Acq. Operator   : SYSTEM                          Seq. Line :   7
Acq. Instrument : Wasa_LC1                         Location :   51
Injection Date  : 8/15/2020 1:57:58 AM                  Inj :   1
                                                Inj Volume : 4.000 µl
Acq. Method     : C:\Chem32\1\Data\JOE 2020-08-14 21-30-51\column6 5.0%IPA 95% hexane 240min-
                  0.45mL.M
Last changed    : 8/14/2020 9:30:57 PM by SYSTEM
Analysis Method : C:\Chem32\1\Data\JOE 2020-08-14 21-30-51\column6 5.0%IPA 95% hexane 240min-
                  0.45mL.M (Sequence Method)
Last changed    : 12/18/2020 6:44:29 PM by SYSTEM
                  (modified after loading)
Method Info     : Column6 240min-5.0% iPrOH 95% hexane-0.45mL
```

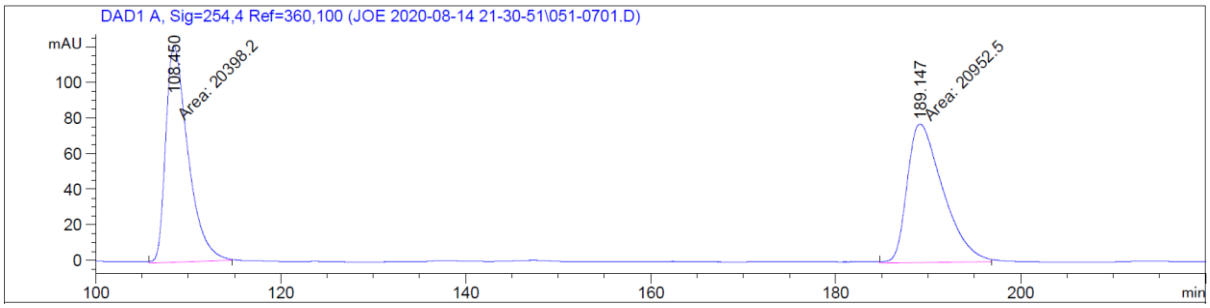

Signal 1: DAD1 A, Sig=254,4 Ref=360,100

Peak #	RetTime [min]	Type	Width [min]	Area [mAU*s]	Height [mAU]	Area %
1	108.450	MM	2.7896	2.03982e4	121.87206	49.3298
2	189.147	MM	4.4886	2.09525e4	77.79833	50.6702
Totals :				4.13507e4	199.67039	

```
Acq. Operator   : SYSTEM                          Seq. Line :   9
Acq. Instrument : Wasa_LC1                         Location :   14
Injection Date  : 8/15/2020 9:59:52 AM                Inj :   1
                                                Inj Volume : 4.000 µl
Acq. Method     : C:\Chem32\1\Data\JOE 2020-08-14 21-30-51\column6 5.0%IPA 95% hexane 240min-
                  0.45mL.M
Last changed    : 8/14/2020 9:30:57 PM by SYSTEM
Analysis Method : C:\Chem32\1\Data\JOE 2020-08-14 21-30-51\column6 5.0%IPA 95% hexane 240min-
                  0.45mL.M (Sequence Method)
Last changed    : 12/18/2020 6:48:54 PM by SYSTEM
                  (modified after loading)
Method Info     : Column6 240min-5.0% iPrOH 95% hexane-0.45mL
```

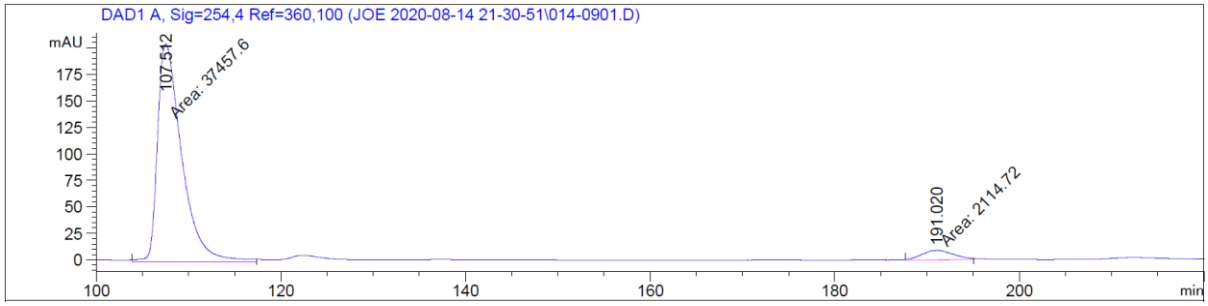

Signal 1: DAD1 A, Sig=254,4 Ref=360,100

Peak #	RetTime [min]	Type	Width [min]	Area [mAU*s]	Height [mAU]	Area %
1	107.512	MM	3.0369	3.74576e4	205.56982	94.6561
2	191.020	MM	3.9514	2114.71851	8.91960	5.3439
Totals :				3.95723e4	214.48942	

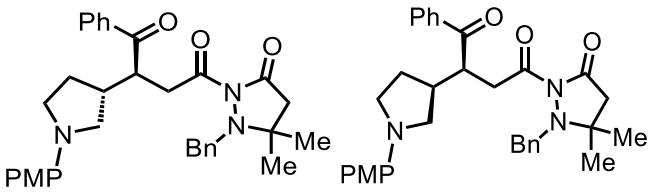

3.26e-(*R,S*) **3.26e-(*S,S*)**

(*S*)-4-(2-Benzyl-3,3-Dimethyl-5-oxopyrazolidin-1-yl)-2-(1-(4-methoxyphenyl) pyrrolidin-3-yl)-1-phenylbutane-1,4-dione (3.26e)

1-(4-Methoxy-2,6-dimethylphenyl)pyrrolidine **3.21r** was reacted with (*E*)-1-(2-benzyl-3,3-dimethyl-5-oxopyrazolidin-1-yl)-4-phenylbut-2-ene-1,4-dione **3.25e** following the **General Procedure E** for 12 hours using $B(C_6F_5)_3$ (10 mol%), $Sc(OTf)_3$ (10 mol%), **L6** (12 mol%) and DCM as the solvent. ^{1}H NMR analysis of the unpurified product mixture using mesitylene as the internal standard revealed that the diastereomeric ratio was 3.5:1. After purification by column chromatography (ethyl ether:hexanes = 3:2), **3.26e** was obtained as a colorless liquid (42 mg, 78%). Further purification was carried out by PTLC using ethyl ether:hexanes = 3:2 as the eluent to separate **3.26e-(*R,S*)** and **3.26e-(*S,S*)**. The absolute configuration for this product was assigned in analogy to that determined for product **3.26f**.

3.26e-(*R,S*). **^{1}H NMR (600 MHz, $CDCl_3$):** δ 7.97 (d, *J* = 7.7 Hz, 2H), 7.52 (t, *J* = 7.4 Hz, 1H), 7.42 (t, *J* = 7.6 Hz, 2H), 7.35 (d, *J* = 8.1 Hz, 2H), 7.30 (t, *J* = 7.4 Hz, 2H), 7.29 – 7.22 (m, 1H), 6.83 (d, *J* = 8.6 Hz, 2H), 6.45 (d, *J* = 8.7 Hz, 2H), 4.04 (d, *J* = 13.3 Hz, 1H), 3.94 (d, *J* = 13.6 Hz, 1H), 3.91 – 3.82 (m, 1H), 3.75 (s, 3H), 3.57 – 3.40 (m, 1H), 3.32 – 3.23 (m, 1H), 3.20 (td, *J* = 8.6, 2.3 Hz, 1H), 3.11 (q, *J* = 8.6 Hz, 1H), 2.97 – 2.87 (m, 1H), 2.59 (d, *J* = 17.1 Hz, 1H), 2.49 (d, *J* = 17.2 Hz, 1H), 2.47 – 2.37 (m, 1H), 1.86 – 1.77 (m, 1H), 1.62 – 1.53 (m, 2H), 1.31 – 1.23 (m, 7H); **^{13}C NMR (151 MHz, $CDCl_3$):** δ 203.3, 174.6, 169.7, 151.1, 142.7, 138.1, 137.1, 133.0, 129.8, 128.8, 128.63, 128.60, 127.8, 115.1, 112.5, 61.5, 57.1, 56.1, 52.2, 48.1, 44.3, 43.4, 41.4, 38.0, 30.1,

26.7, 25.8; **IR** (neat) ν 2924, 2850, 1742,1674, 1511, 1464, 1446, 1359, 1300, 1234, 1178, 1001, 957, 811, 729, 700, 595, 564 cm^{-1}; **HRMS (DART):** Calcd for $C_{33}H_{38}N_3O_4$ (MH^+): 540.2857; found: 540.2856; **HPLC** (CHIRACPAK IA-3; 10%/ 90% isopropanol/ hexanes, 1.0 mL/min; tr = 23.8 min (minor), 28.5 min (major); 95:5 er); **Specific Rotation** $[\alpha]^{25}_D$ = +35.0° (c = 0.40, DCM).

```
Acq. Operator   : SYSTEM                          Seq. Line :   2
Acq. Instrument : Wasa_LC1                        Location :   13
Injection Date  : 8/19/2020 9:32:51 PM                 Inj :   1
                                                 Inj Volume : 4.000 µl
Acq. Method     : C:\Chem32\1\Data\JOE 2020-08-19 20-35-32\column6 10% IPA 90% hex 55min-1.
                  0ml.M
Last changed    : 8/19/2020 8:35:37 PM by SYSTEM
Analysis Method : C:\Chem32\1\Data\JOE 2020-08-19 20-35-32\column6 10% IPA 90% hex 55min-1.
                  0ml.M (Sequence Method)
Last changed    : 8/21/2020 3:27:04 PM by SYSTEM
                  (modified after loading)
Method Info     : Column 6 10% IPA/90% hexane 1.0 mL/min 55 min
```

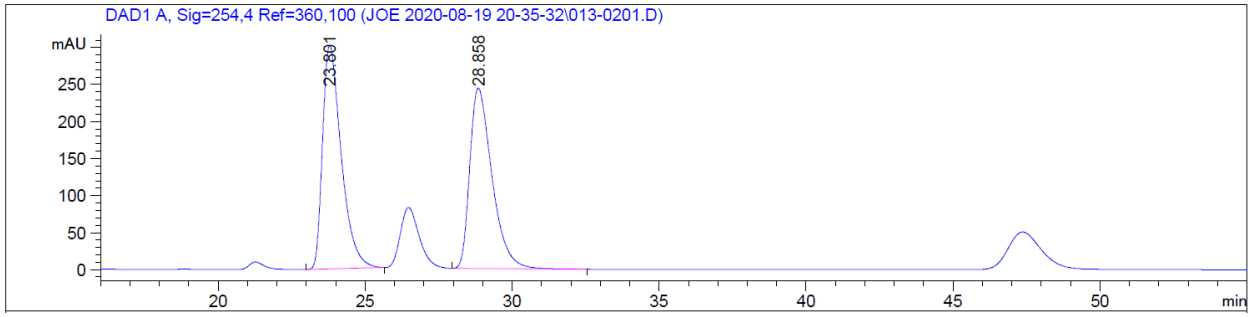

Signal 1: DAD1 A, Sig=254,4 Ref=360,100

Peak #	RetTime [min]	Type	Width [min]	Area [mAU*s]	Height [mAU]	Area %
1	23.801	BB	0.6694	1.33297e4	301.72205	51.0074
2	28.858	BB	0.8069	1.28032e4	243.70734	48.9926
Totals :				2.61330e4	545.42938	

```
Acq. Operator   : SYSTEM                          Seq. Line :   5
Acq. Instrument : Wasa_LC1                         Location :   44
Injection Date  : 12/11/2020 9:00:47 PM               Inj :   1
                                                 Inj Volume : 4.000 µl
Acq. Method     : C:\Chem32\1\Data\JOE 2020-12-11 17-49-52\column6 10% IPA 90% hex 55min-1.
                  0ml.M
Last changed    : 12/11/2020 5:49:59 PM by SYSTEM
Analysis Method : C:\Chem32\1\Data\JOE 2020-12-11 17-49-52\column6 10% IPA 90% hex 55min-1.
                  0ml.M (Sequence Method)
Last changed    : 12/16/2020 10:46:36 AM by SYSTEM
                  (modified after loading)
Method Info     : Column 6 10% IPA/90% hexane 1.0 mL/min 55 min
```

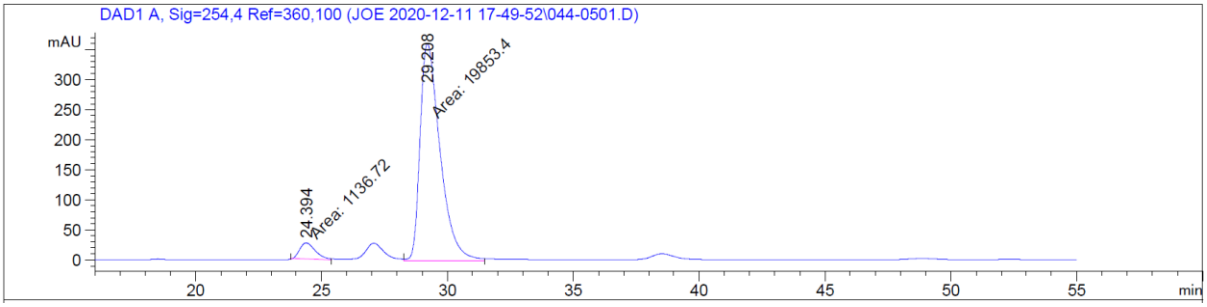

Signal 1: DAD1 A, Sig=254,4 Ref=360,100

Peak #	RetTime [min]	Type	Width [min]	Area [mAU*s]	Height [mAU]	Area %
1	24.394	MM	0.7122	1136.71631	26.60268	5.4155
2	29.208	MM	0.9164	1.98534e4	361.08331	94.5845
Totals :				2.09901e4	387.68599	

3.26e-(*S*,*S*). ^{1}H NMR (600 MHz, $CDCl_3$): δ 7.96 (d, *J* = 6.7 Hz, 2H), 7.54 (t, *J* = 7.4 Hz, 1H), 7.43 (t, *J* = 7.7 Hz, 2H), 7.34 (d, *J* = 7.1 Hz, 2H), 7.28 (d, *J* = 7.3 Hz, 2H), 7.22 (t, *J* = 7.1 Hz, 1H), 6.77 (d, *J* = 9.0 Hz, 2H), 6.35 (d, *J* = 9.0 Hz, 2H), 4.02 (d, *J* = 13.4 Hz, 1H), 3.99 – 3.90 (m, 2H), 3.72 (s, 3H), 3.53 – 3.38 (m, 1H), 3.27 (td, *J* = 8.7, 2.8 Hz, 1H), 3.17 (q, *J* = 8.8 Hz, 1H), 3.13 (t, *J* = 8.3 Hz, 1H), 2.83 (t, *J* = 8.6 Hz, 1H), 2.57 (d, *J* = 17.0 Hz, 1H), 2.54 – 2.45 (m, 2H), 2.08 – 1.99 (m, 1H), 1.75 – 1.62 (m, 1H), 1.31 – 1.23 (m, 7H); **^{13}C NMR (151 MHz, $CDCl_3$):** δ 202.9, 182.3, 174.6, 151.1, 142.7, 137.6, 137.1, 133.1, 129.7, 128.75, 128.67, 128.6, 127.8, 115.1, 112.6, 61.4, 57.0, 56.1, 52.2, 47.9, 44.3, 43.5, 41.1, 37.4, 29.5, 26.6, 25.9; **IR (neat):** ν 2922, 2850, 1744,1676, 1513, 1484, 1447, 1364, 1301, 1237, 1179, 1038, 812, 699 cm^{-1}; **HRMS (DART):** Calcd for $C_{33}H_{38}N_3O_4$ (MH^+): 540.2857; found: 540.2828; **HPLC** (CHIRACPAK IA-3; 10%/ 90% isopropanol/ hexanes, 1.0 mL/min; tr = 26.2 min (minor), 47.0 min (major); 95:5 er); **Specific Rotation $[\alpha]^{25}_D$** = +12.0° (c = 0.20, DCM).

```
Acq. Operator   : SYSTEM                          Seq. Line :   2
Acq. Instrument : Wasa_LC1                         Location :   13
Injection Date  : 8/19/2020 9:32:51 PM                Inj :   1
                                                  Inj Volume : 4.000 µl
Acq. Method     : C:\Chem32\1\Data\JOE 2020-08-19 20-35-32\column6 10% IPA 90% hex 55min-1.
                  0ml.M
Last changed    : 8/19/2020 8:35:37 PM by SYSTEM
Analysis Method : C:\Chem32\1\Data\JOE 2020-08-19 20-35-32\column6 10% IPA 90% hex 55min-1.
                  0ml.M (Sequence Method)
Last changed    : 8/21/2020 3:27:04 PM by SYSTEM
                  (modified after loading)
Method Info     : Column 6 10% IPA/90% hexane 1.0 mL/min 55 min
```

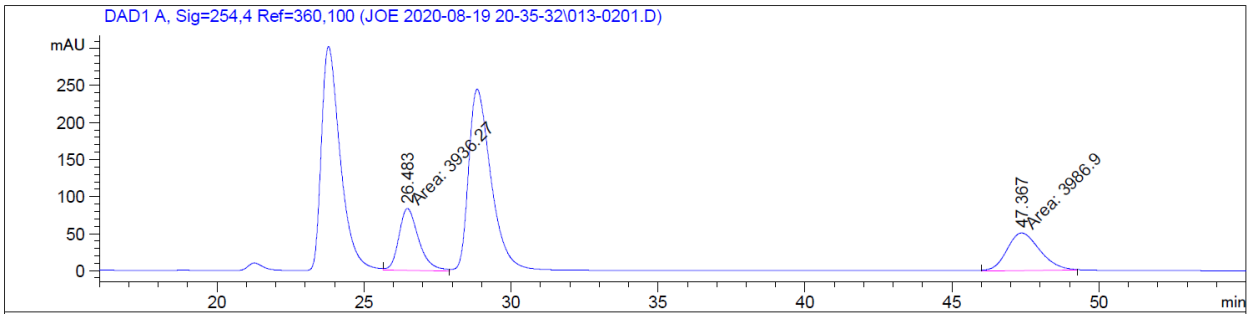

Signal 1: DAD1 A, Sig=254,4 Ref=360,100

Peak #	RetTime [min]	Type	Width [min]	Area [mAU*s]	Height [mAU]	Area %
1	26.483	MM	0.7830	3936.26709	83.78169	49.6805
2	47.367	MM	1.3058	3986.90332	50.88859	50.3195
Totals :				7923.17041	134.67028	

```
Acq. Operator   : SYSTEM                          Seq. Line :   3
Acq. Instrument : Wasa_LC1                         Location :   14
Injection Date  : 8/19/2020 10:28:47 PM                Inj :   1
                                                 Inj Volume : 4.000 µl
Acq. Method     : C:\Chem32\1\Data\JOE 2020-08-19 20-35-32\column6 10% IPA 90% hex 55min-1.
                  0ml.M
Last changed    : 8/19/2020 8:35:37 PM by SYSTEM
Analysis Method : C:\Chem32\1\Data\JOE 2020-08-19 20-35-32\column6 10% IPA 90% hex 55min-1.
                  0ml.M (Sequence Method)
Last changed    : 8/21/2020 3:27:04 PM by SYSTEM
                  (modified after loading)
Method Info     : Column 6 10% IPA/90% hexane 1.0 mL/min 55 min
```

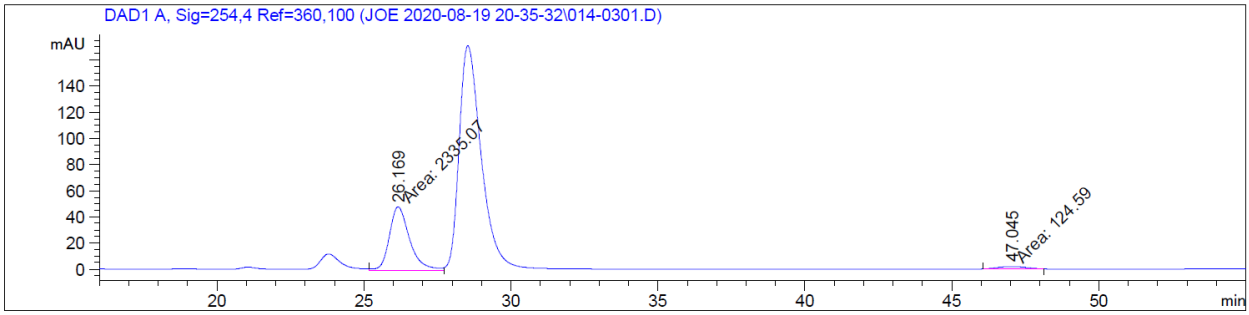

Signal 1: DAD1 A, Sig=254,4 Ref=360,100

Peak #	RetTime [min]	Type	Width [min]	Area [mAU*s]	Height [mAU]	Area %
1	26.169	MM	0.8005	2335.06763	48.61831	94.9347
2	47.045	MM	1.0958	124.58971	1.89503	5.0653
Totals :				2459.65733	50.51335	

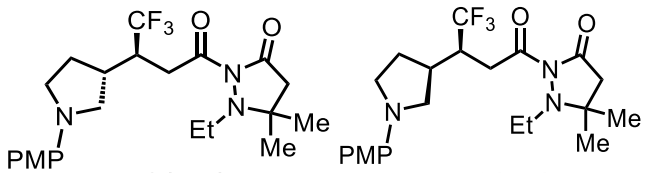

3.26f-(*R,S*) **3.26f-(*S,S*)**

1-Ethyl-5,5-dimethyl-2-((*S*)-4,4,4-trifluoro-3-(1-(4-methoxyphenyl)pyrrolidin-3-yl)butanoyl)pyrazolidin-3-one (3.26f)

1-(4-Methoxy-2,6-dimethylphenyl)pyrrolidine **3.21r** was reacted with (*E*)-1-ethyl-5,5-dimethyl-2-(4,4,4-trifluorobut-2-enoyl)pyrazolidin-3-one **3.25f** following the **General Procedure E** for 3 hours using $B(C_6F_5)_3$ (10 mol%), $Sc(OTf)_3$ (10 mol%), **L10** (12 mol%) and DCM as the solvent. ^{1}H NMR and ^{19}F NMR analyses of the unpurified product mixture using mesitylene and perfluorobenzene as the internal standard revealed that the diastereomeric ratio was 6.7:1. After purification by column chromatography (EtOAc:hexanes = 1:2), **3.26f** was obtained as a colorless liquid (27 mg, 62%). Further purification was carried out by PTLC using EtOAc:hexanes = 1:2 as the eluent to separate **3.26f-(*R,S*)** and **3.26f-(*S,S*)**. The absolute configuration of product was assigned based on X-ray crystallography data of **3.29**.

3.26f-(*R,S*). **^{1}H NMR (500 MHz, $CDCl_3$):** δ 6.83 (d, *J* = 8.9 Hz, 2H), 6.50 (d, *J* = 9.0 Hz, 2H), 3.75 (s, 3H), 3.41 (dd, *J* = 18.3, 6.9 Hz, 1H), 3.38 – 3.32 (m, 2H), 3.31 – 3.22 (m, 2H), 3.09 (t, *J* = 9.1 Hz, 1H), 3.02 (qd, *J* = 6.9, 2.7 Hz, 2H), 2.89 (dd, *J* = 18.4, 4.3 Hz, 1H), 2.69 – 2.54 (m, 3H), 2.23 (dt, *J* = 13.0, 7.3 Hz, 1H), 1.83 (p, *J* = 10.3 Hz, 1H), 1.32 (s, 6H), 1.09 (t, *J* = 7.1 Hz, 3H); **^{13}C NMR (101 MHz, $CDCl_3$):** δ 175.5, 168.4, 151.3, 142.6, 127.8 (q, *J* = 280.4 Hz), 115.1, 112.7, 60.8, 56.1, 51.3, 48.1, 47.2, 44.0, 40.9 (q, *J* = 26.0 Hz), 37.8, 33.2, 30.2, 26.1, 25.7, 12.9; **^{19}F NMR (470 MHz, $CDCl_3$):** δ -69.19 (d, *J* = 9.5 Hz); **IR (neat):** ν 2974, 2934, 2853, 2833, 1745, 1709, 1514, 1373, 1303, 1260, 1238, 1159, 1125, 1038, 813, 690 cm^{-1}; **HRMS (DART):** Calcd for

$C_{22}H_{31}F_3N_3O_3$ (MH^+): 442.2312; found: 442.2305; **HPLC** (CHIRACPAK IA-3; 5%/ 95% isopropanol/ hexanes, 1.0 mL/min; tr = 15.8 min (major), 31.5 min (minor); 96:4 er); **Specific Rotation** $[\alpha]^{25}_D$ = -7.3° (c = 0.20, DCM).

```
Acq. Operator   : SYSTEM                          Seq. Line :   4
Acq. Instrument : Wasa_LC1                         Location :   94
Injection Date  : 11/11/2020 11:10:16 PM               Inj :   1
                                                 Inj Volume : 4.000 µl
Acq. Method     : C:\Chem32\1\Data\JOE 2020-11-11 21-05-19\column6 5%IPA 95% hexane 40min-1.
                  0mL.M
Last changed    : 11/11/2020 9:05:25 PM by SYSTEM
Analysis Method : C:\Chem32\1\Data\JOE 2020-11-11 21-05-19\column6 5%IPA 95% hexane 40min-1.
                  0mL.M (Sequence Method)
Last changed    : 11/12/2020 7:05:24 PM by SYSTEM
                  (modified after loading)
Method Info     : Column6 40min-5% iPrOH 95% hexane-1.0mL
```

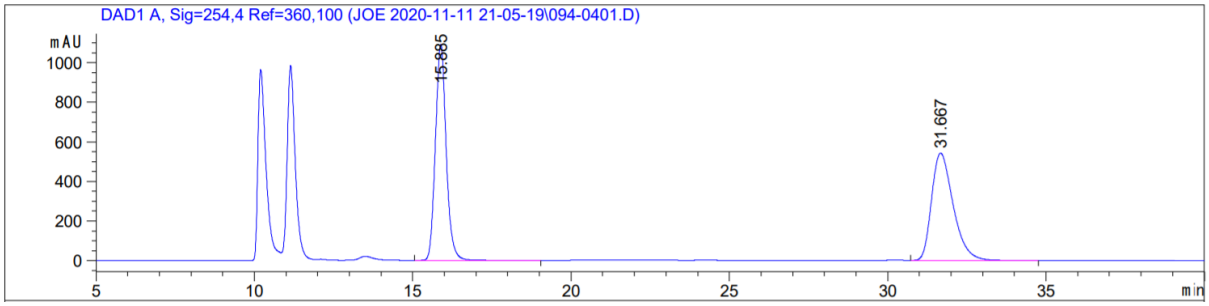

Signal 1: DAD1 A, Sig=254,4 Ref=360,100

Peak #	RetTime [min]	Type	Width [min]	Area [mAU*s]	Height [mAU]	Area %
1	15.885	BB	0.3654	2.57801e4	1092.16479	50.1031
2	31.667	BB	0.7264	2.56739e4	542.24054	49.8969
Totals :				5.14540e4	1634.40533	

```
Acq. Operator   : SYSTEM                          Seq. Line :   2
Acq. Instrument : Wasa_LC1                         Location :   41
Injection Date  : 12/15/2020 10:27:38 PM               Inj :   1
                                                 Inj Volume : 4.000 µl
Acq. Method     : C:\Chem32\1\Data\JOE 2020-12-15 20-45-20\column6 5%IPA 95% hexane 40min-1.
                  0mL.M
Last changed    : 12/15/2020 8:45:26 PM by SYSTEM
Analysis Method : C:\Chem32\1\Data\JOE 2020-12-15 20-45-20\column6 5%IPA 95% hexane 40min-1.
                  0mL.M (Sequence Method)
Last changed    : 12/16/2020 11:06:35 AM by SYSTEM
                  (modified after loading)
Method Info     : Column6 40min-5% iPrOH 95% hexane-1.0mL
```

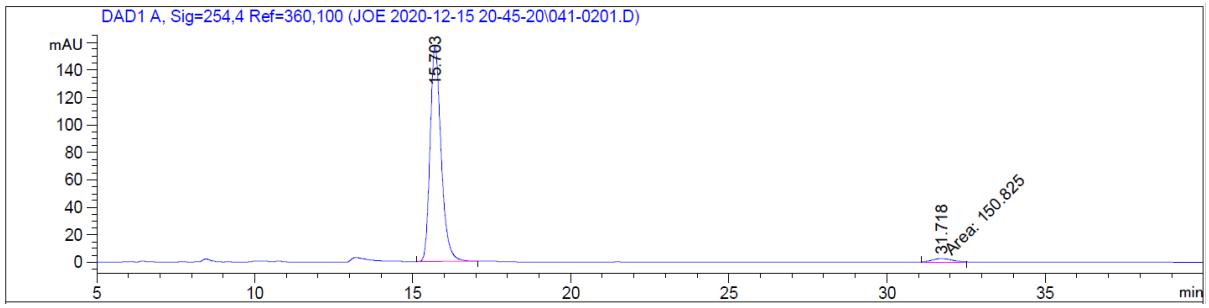

Signal 1: DAD1 A, Sig=254,4 Ref=360,100

Peak #	RetTime [min]	Type	Width [min]	Area [mAU*s]	Height [mAU]	Area %
1	15.703	BB	0.3699	3790.19409	156.84543	96.1729
2	31.718	MM	0.8379	150.82510	2.99991	3.8271
Totals :				3941.01920	159.84534	

3.26f ((*R*,*S*):(*S*,*S*)= 1:4.7). **^{1}H NMR (600 MHz, $CDCl_3$, *peaks from diastereomers are merged*):** δ 6.86 – 6.81 (m, 2H), 6.53 – 6.48 (m, 2H), 3.77 – 3.73 (m, 3H), 3.50 – 3.39 (m, 1H), 3.39 – 3.30 (m, 2H), 3.30 – 3.20 (m, 2H), 3.11 – 2.86 (m, 4H), 2.67 – 2.54 (m, 3H), 2.27 – 2.06 (m, 1H), 1.84 (p, *J* = 10.4 Hz, 1H), 1.33 – 1.28 (m, 6H), 1.11 – 1.05 (m, 3H); **^{19}F NMR (470 MHz, $CDCl_3$):** δ -69.18 (d, *J* = 9.6 Hz, **7f-(*S*,*S*)**), -69.48 (d, *J* = 9.2 Hz, **3.26d-(*R*,*S*)**); **HRMS** (DART) Calcd for $C_{22}H_{31}F_3N_3O_3$ (MH^+): 442.2312; found: 442.2305; **HPLC** (CHIRACPAK IA-3; 5%/ 95% isopropanol/ hexanes, 1.0 mL/min; tr = 10.2 min (major), 11.3 min (minor); 95:5 er).

```
Acq. Operator   : SYSTEM                          Seq. Line :   4
Acq. Instrument : Wasa_LC1                         Location :   94
Injection Date  : 11/11/2020 11:10:16 PM               Inj :   1
                                                  Inj Volume : 4.000 µl
Acq. Method     : C:\Chem32\1\Data\JOE 2020-11-11 21-05-19\column6 5%IPA 95% hexane 40min-1.
                  0mL.M
Last changed    : 11/11/2020 9:05:25 PM by SYSTEM
Analysis Method : C:\Chem32\1\Data\JOE 2020-11-11 21-05-19\column6 5%IPA 95% hexane 40min-1.
                  0mL.M (Sequence Method)
Last changed    : 11/12/2020 7:05:24 PM by SYSTEM
                  (modified after loading)
Method Info     : Column6 40min-5% iPrOH 95% hexane-1.0mL
```

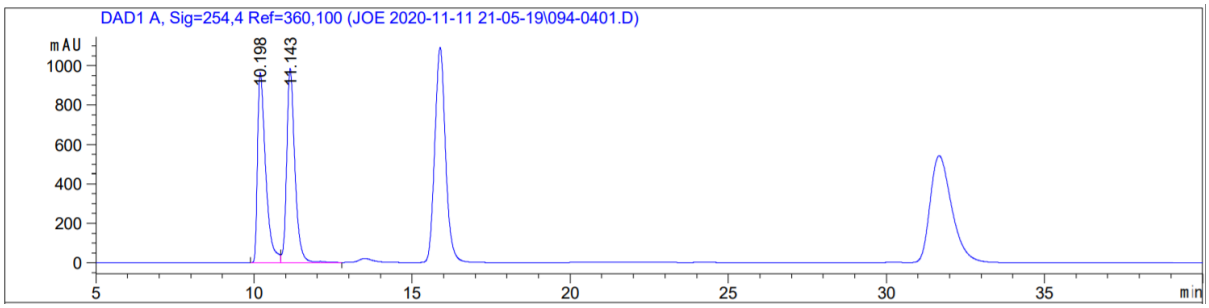

Signal 1: DAD1 A, Sig=254,4 Ref=360,100

Peak #	RetTime [min]	Type	Width [min]	Area [mAU*s]	Height [mAU]	Area %
1	10.198	BV	0.2712	1.72915e4	964.19971	49.4346
2	11.143	VV R	0.2701	1.76871e4	985.10260	50.5654
Totals :				3.49786e4	1949.30231	

```
Acq. Operator   : SYSTEM                          Seq. Line :   3
Acq. Instrument : Wasa_LC1                         Location :   6
Injection Date  : 8/27/2020 11:44:28 PM                Inj :   1
                                                 Inj Volume : 4.000 µl
Acq. Method     : C:\Chem32\1\Data\JOE 2020-08-27 22-21-10\column6 5%IPA 95% hexane 40min-1.
                  0mL.M
Last changed    : 8/27/2020 10:21:17 PM by SYSTEM
Analysis Method : C:\Chem32\1\Data\JOE 2020-08-27 22-21-10\column6 5%IPA 95% hexane 40min-1.
                  0mL.M (Sequence Method)
Last changed    : 8/28/2020 10:27:11 AM by SYSTEM
                  (modified after loading)
Method Info     : Column6 40min-5% iPrOH 95% hexane-1.0mL
```

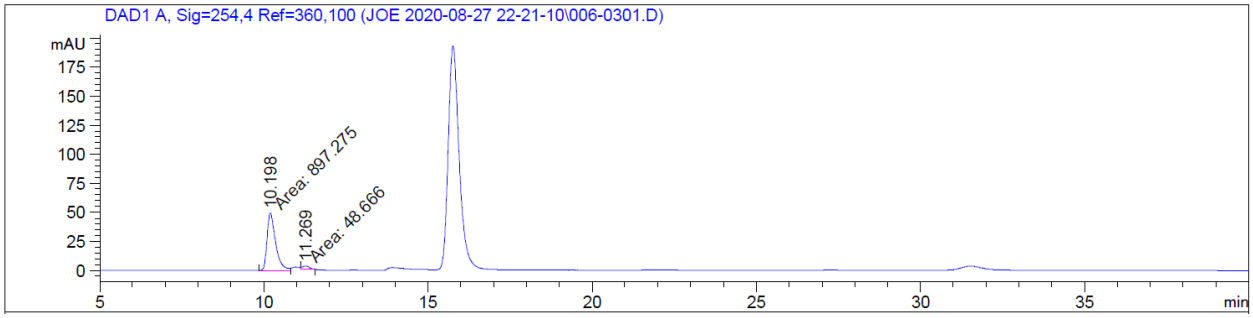

Signal 1: DAD1 A, Sig=254,4 Ref=360,100

Peak #	RetTime [min]	Type	Width [min]	Area [mAU*s]	Height [mAU]	Area %
1	10.198	MM	0.3023	897.27521	49.46244	94.8553
2	11.269	MM	0.2722	48.66601	2.97946	5.1447
Totals :				945.94122	52.44190	

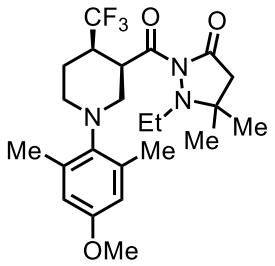

3.26g

1-Ethyl-2-((3*R*,4*R*)-1-(4-methoxy-2,6-dimethylphenyl)-4-(trifluoromethyl)piperidine-3-carbonyl)-5,5-dimethylpyrazolidin-3-one (3.26g)

N-Ethyl-4-methoxy-*N*,2,6-trimethylaniline **3.21s** was reacted with (*E*)-1-ethyl-5,5-dimethyl-2-(4,4,4-trifluorobut-2-enoyl)pyrazolidin-3-one **3.25f** following the **General Procedure E** for 24 hours using $B(C_6F_5)_3$ (10 mol%), $Sc(OTf)_3$ (20 mol%), **L10** (24 mol%) and DCM as the solvent. After purification by column chromatography (Et_3N:ethyl ether:hexanes = 1:50:50), **3.26g** was obtained as a single diastereomer and as colorless liquid (31 mg, 67%). The absolute configuration for this product was assigned in analogy to that determined for product **3.26f**.

^{1}H NMR (600 MHz, $CDCl_3$): δ 6.61 (d, *J* = 3.0 Hz, 1H), 6.46 (d, *J* = 3.0 Hz, 1H), 4.38 – 4.23 (m, 1H), 3.74 (s, 3H), 3.24 (td, *J* = 12.1, 2.6 Hz, 1H), 3.19 (d, *J* = 7.3 Hz, 2H), 3.07 (dq, *J* = 14.2, 7.2 Hz, 1H), 3.04 – 2.93 (m, 2H), 2.91 (dq, *J* = 13.8, 7.1 Hz, 1H), 2.62 (d, *J* = 17.3 Hz, 1H), 2.54 (d, *J* = 17.3 Hz, 1H), 2.37 (s, 3H), 2.25 (s, 3H), 1.98 (dd, *J* = 12.8, 4.3 Hz, 1H), 1.82 (qd, *J* = 12.4, 4.6 Hz, 1H), 1.29 (s, 6H), 1.03 (t, *J* = 7.1 Hz, 3H); **^{13}C NMR (126 MHz, $CDCl_3$):** δ 175.3, 169.9, 157.0, 141.3, 139.5, 138.1, 127.5 (q, *J* = 280.2 Hz), 114.2, 113.5, 60.2, 55.4, 53.4, 48.9, 46.9, 44.4, 41.9, 41.1 (q, *J* = 26.0 Hz), 26.4, 25.3, 25.1, 20.0, 19.7, 12.7; **^{19}F NMR (376 MHz, $CDCl_3$):** δ -70.88 (d, *J* = 7.7 Hz); **IR (neat):** ν 2960, 2836, 1742,1701, 1601, 1485, 1467, 1443, 1388, 1373, 1303, 1227, 1191, 1151, 1130, 1085, 1034, 999, 855, 731, 619 cm^{-1}; **HRMS (DART):** Calcd for $C_{23}H_{32}F_3N_3O_3$ (MH^+): 456.2468; found: 456.2460; **HPLC** (CHIRACPAK IA-3; 5%/ 95%

isopropanol/ hexanes, 0.5 mL/min; tr = 12.5 min (minor), 16.0 min (major); 95:5 er); **Specific Rotation** $[\alpha]^{25}_{D}$ = +7.0° (c = 0.40, DCM).

```
Acq. Operator    : SYSTEM                          Seq. Line :   2
Acq. Instrument  : Wasa_LC1                         Location :   61
Injection Date   : 8/27/2020 12:10:12 PM                Inj :   1
                                                  Inj Volume : 4.000 µl
Acq. Method      : C:\Chem32\1\Data\JOE 2020-08-27 11-37-07\column6 5%IPA 95% hexane 30min-0.
                   5mL.M
Last changed     : 8/27/2020 11:37:13 AM by SYSTEM
Analysis Method  : C:\Chem32\1\Data\JOE 2020-08-27 11-37-07\column6 5%IPA 95% hexane 30min-0.
                   5mL.M (Sequence Method)
Last changed     : 8/28/2020 10:32:40 AM by SYSTEM
                   (modified after loading)
Method Info      : Column6 30min-5.0% iPrOH 95% hexane-0.5mL
```

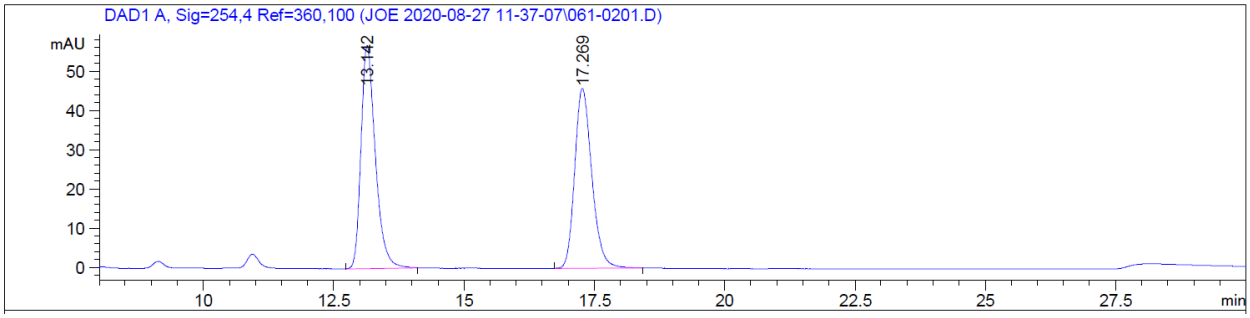

Signal 1: DAD1 A, Sig=254,4 Ref=360,100

Peak #	RetTime [min]	Type	Width [min]	Area [mAU*s]	Height [mAU]	Area %
1	13.142	BB	0.2887	1084.45898	56.82304	50.9372
2	17.269	BB	0.3497	1044.55127	45.87325	49.0628
Totals :				2129.01025	102.69629	

```
Acq. Operator   : SYSTEM                          Seq. Line :   3
Acq. Instrument : Wasa_LC1                         Location :   62
Injection Date  : 8/27/2020 12:41:09 PM                Inj :   1
                                                 Inj Volume : 4.000 µl
Acq. Method     : C:\Chem32\1\Data\JOE 2020-08-27 11-37-07\column6 5%IPA 95% hexane 30min-0.
                  5mL.M
Last changed    : 8/27/2020 11:37:13 AM by SYSTEM
Analysis Method : C:\Chem32\1\Data\JOE 2020-08-27 11-37-07\column6 5%IPA 95% hexane 30min-0.
                  5mL.M (Sequence Method)
Last changed    : 8/28/2020 10:32:40 AM by SYSTEM
                  (modified after loading)
Method Info     : Column6 30min-5.0% iPrOH 95% hexane-0.5mL
```

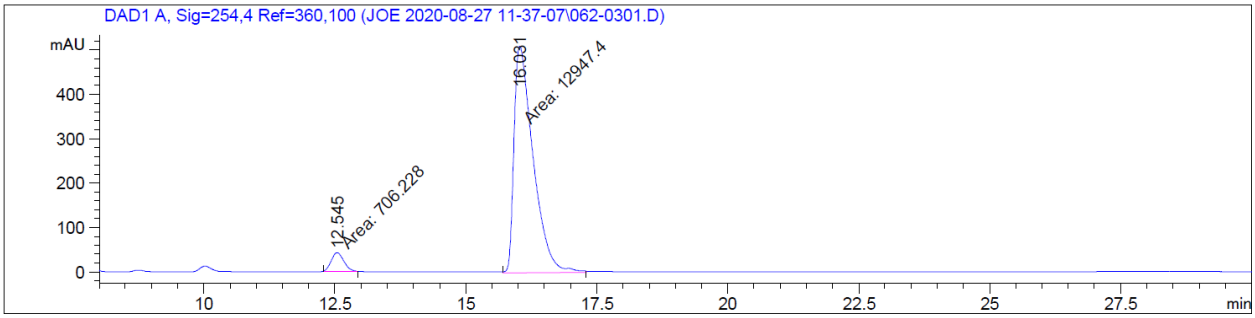

Signal 1: DAD1 A, Sig=254,4 Ref=360,100

Peak #	RetTime [min]	Type	Width [min]	Area [mAU*s]	Height [mAU]	Area %
1	12.545	MM	0.2768	706.22766	42.52583	5.1724
2	16.031	MM	0.4221	1.29474e4	511.25565	94.8276
Totals :				1.36537e4	553.78147	

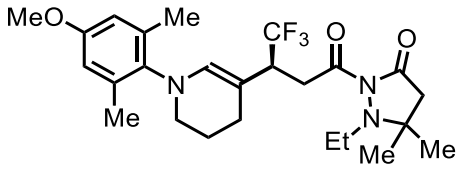

3.26h

(*S*)-1-Ethyl-5,5-dimethyl-2-(4,4,4-trifluoro-3-(1-(4-methoxy-2,6-dimethylphenyl)-1,4,5,6-tetrahydropyridin-3-yl)butanoyl)pyrazolidin-3-one (3.26h)

1-(4-Methoxy-2,6-dimethylphenyl)piperidine **3.21l** was reacted with (*E*)-1-ethyl-5,5-dimethyl-2-(4,4,4-trifluorobut-2-enoyl)pyrazolidin-3-one **3.25f** following the **General Procedure E** for 12 hours using $B(C_6F_5)_3$ (10 mol%), $Sc(OTf)_3$ (10 mol%), **L10** (12 mol%) and DCM as the solvent. After purification by column chromatography (ethyl ether:hexane = 1:1), **3.26h** was obtained as a colorless liquid (46 mg, 95%). The absolute configuration for this product was assigned in analogy to that determined for product **3.26f**.

^{1}H NMR (400 MHz, $CDCl_3$): δ 6.55 (s, 2H), 5.91 (s, 1H), 3.75 (s, 3H), 3.43 – 3.29 (m, 2H), 3.20 – 3.07 (m, 3H), 2.96 (q, *J* = 7.0 Hz, 2H), 2.57 (s, 2H), 2.29 – 2.10 (m, 8H), 2.05 – 1.83 (m, 2H), 1.29 (s, 6H), 1.06 (t, *J* = 7.1 Hz, 3H); **^{13}C NMR (126 MHz, $CDCl_3$):** δ 175.3, 168.2, 157.5, 138.8, 138.38, 138.37, 135.6, 127.7 (q, *J* = 280.9 Hz), 113.53, 113.50, 95.9, 60.6, 55.4, 47.3, 47.2, 44.8 (q, *J* = 27.0 Hz), 44.0, 34.32, 34.30, 25.9, 25.8, 23.2, 22.7, 18.44, 18.41, 13.0; **^{19}F NMR (376 MHz, $CDCl_3$):** δ -70.18 (d, *J* = 9.3 Hz); **IR (neat):** ν 2925, 2840, 1743, 1708, 1654, 1602, 1487, 1467, 1442, 1374, 1319, 1301, 1274, 1152, 1099, 1068, 999, 857, 616 cm^{-1}; **HRMS (DART):** $C_{25}H_{35}F_3N_3O_3$ (MH^+): 482.2625; found: 482.2617; **HPLC** (CHIRACPAK IA-3; 2.5%/ 97.5% isopropanol/ hexanes, 0.5 mL/min; tr = 15.4 min (minor), 38.7 min (major); 95:5 er); **Specific Rotation $[\alpha]^{25}_D$** = +12.9° (c = 1.0, DCM).

```
Acq. Operator   : SYSTEM                          Seq. Line :   4
Acq. Instrument : Wasa_LC1                         Location :   11
Injection Date  : 8/13/2020 2:42:49 PM                Inj :   1
                                                 Inj Volume : 4.000 µl
Method          : C:\Chem32\1\Data\JOE 2020-08-13 12-18-34\column6 2.5%IPA 97.5% hexane 60min
                  -0.5mL.M (Sequence Method)
Last changed    : 8/13/2020 12:18:40 PM by SYSTEM
Method Info     : Column6 60min-2.5% iPrOH 99% hexane-0.5mL
```

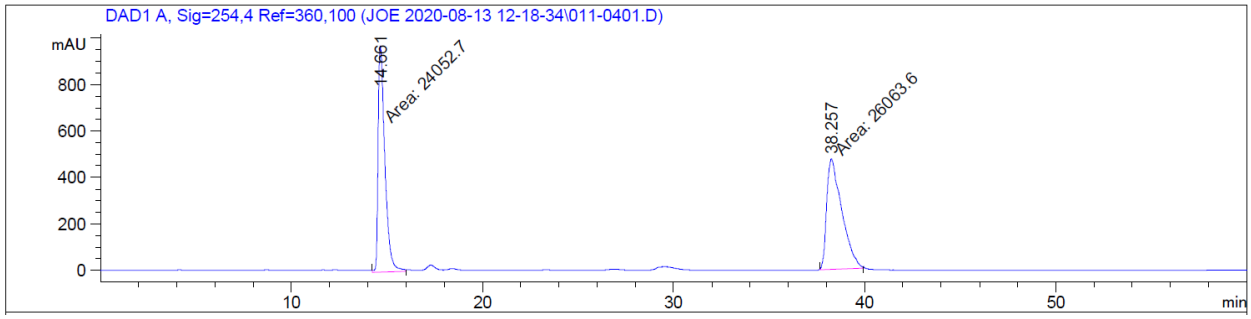

Signal 1: DAD1 A, Sig=254,4 Ref=360,100

Peak #	RetTime [min]	Type	Width [min]	Area [mAU*s]	Height [mAU]	Area %
1	14.661	MM	0.4109	2.40527e4	975.62061	47.9938
2	38.257	MM	0.9147	2.60636e4	474.88654	52.0062
Totals :				5.01163e4	1450.50714	

```
Acq. Operator   : SYSTEM                          Seq. Line :   5
Acq. Instrument : Wasa_LC1                         Location :   12
Injection Date  : 8/13/2020 3:43:44 PM                Inj :   1
                                                 Inj Volume : 4.000 µl
Method          : C:\Chem32\1\Data\JOE 2020-08-13 12-18-34\column6 2.5%IPA 97.5% hexane 60min
                  -0.5mL.M (Sequence Method)
Last changed    : 8/13/2020 12:18:40 PM by SYSTEM
Method Info     : Column6 60min-2.5% iPrOH 99% hexane-0.5mL
```

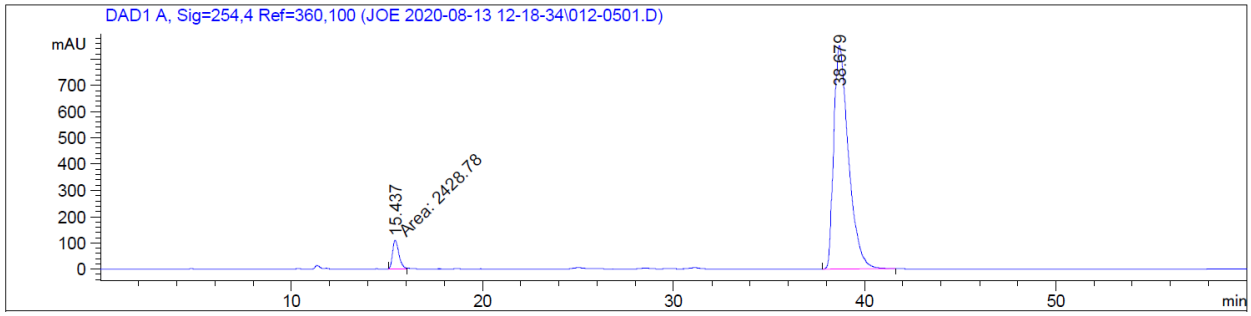

Signal 1: DAD1 A, Sig=254,4 Ref=360,100

Peak #	RetTime [min]	Type	Width [min]	Area [mAU*s]	Height [mAU]	Area %
1	15.437	MM	0.3751	2428.77881	107.90679	5.0724
2	38.679	BB	0.7134	4.54539e4	850.64508	94.9276
Totals :				4.78826e4	958.55187	

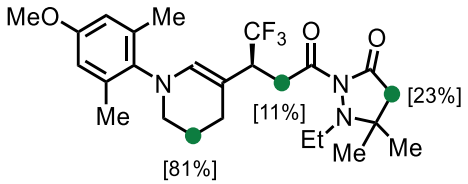

3.26h-*d*

(*S*)-1-Ethyl-5,5-dimethyl-2-(4,4,4-trifluoro-3-(1-(4-methoxy-2,6-dimethylphenyl)-1,4,5,6-tetrahydropyridin-3-yl-5,5-d_2)butanoyl)pyrazolidin-3-one (3.26h-*d*)

1-(4-Methoxy-2,6-dimethylphenyl)piperidine-3,3,5,5-d_4 **3.21l-*d*** was reacted with (*E*)-1-ethyl-5,5-dimethyl-2-(4,4,4-trifluorobut-2-enoyl)pyrazolidin-3-one **3.25f** following the **General Procedure E** for 12 hours using $B(C_6F_5)_3$ (10 mol%), $Sc(OTf)_3$ (10 mol%), **L10** (12 mol%) and DCM as the solvent. After purification by column chromatography (ethyl ether:hexanes = 1:1), **3.26h-*d*** was obtained as a colorless liquid (41 mg, 84%). The absolute configuration for this product was assigned in analogy to that determined for product **3.26f**.

^{1}H NMR (500 MHz, $CDCl_3$): δ 6.55 (s, 2H), 5.91 (s, 1H), 3.75 (s, 3H), 3.42 – 3.30 (m, 1.78H, 11%D), 3.22 – 3.08 (m, 3H), 2.97 (q, *J* = 7.2 Hz, 2H), 2.60 – 2.50 (m, 1.53H, 23%D), 2.20 – 2.08 (m, 8H), 1.98 – 1.87 (m, 0.32H, 81%D), 1.29 (s, 6H), 1.06 (t, *J* = 7.1 Hz, 3H); **^{13}C NMR (126 MHz, $CDCl_3$):** δ 175.3, 168.2, 157.5, 138.8, 138.41, 138.40, 135.6, 127.7 (q, *J* = 281.0 Hz), 113.55, 113.52, 96.0, 60.63, 60.56, 55.4, 47.3, 47.22, 47.20, 44.8 (q, *J* = 27.0 Hz), 44.0, 34.3, 25.9, 23.0, 18.5, 18.4, 13.0; **^{19}F NMR (564 MHz, $CDCl_3$):** δ -70.18 (d, *J* = 8.6 Hz); **IR (neat):** ν 2971, 2934, 2840, 1744, 1707, 1655, 1601, 1486, 1467, 1374, 1319, 1155, 1102, 856, 616 cm^{-1}; **HRMS** (DART) Calcd for $C_{25}H_{33}D_2F_3N_3O_3$ (MH^+): 484.5804; found: 484.2746; **HPLC** (CHIRACPAK IA-3; 2.5%/ 97.5% isopropanol/ hexanes, 0.5 mL/min; tr = 12.8 min (minor), 33.6 min (major); 95:5 er); **Specific Rotation $[\alpha]^{25}_D$** = +2.1° (c = 0.53, DCM).

Acq. Operator : SYSTEM Seq. Line : 5
Acq. Instrument : Wasa_LC1 Location : 1
Injection Date : 8/25/2020 6:55:01 PM Inj : 1
Inj Volume : 4.000 µl
Method : C:\Chem32\1\Data\JOE 2020-08-25 16-19-49\column6 2.5%IPA 97.5% hexane 60min -0.5mL.M (Sequence Method)
Last changed : 8/25/2020 4:19:54 PM by SYSTEM
Method Info : Column6 60min-2.5% iPrOH 99% hexane-0.5mL

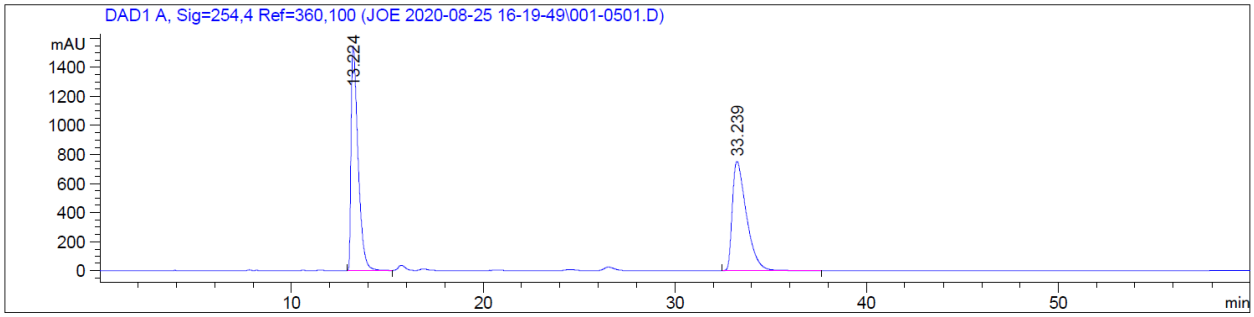

Signal 1: DAD1 A, Sig=254,4 Ref=360,100

Peak #	RetTime [min]	Type	Width [min]	Area [mAU*s]	Height [mAU]	Area %
1	13.224	BB	0.3820	3.92641e4	1547.81995	50.5224
2	33.239	BB	0.7726	3.84521e4	751.87958	49.4776
Totals :				7.77162e4	2299.69952	

```
Acq. Operator   : SYSTEM                          Seq. Line :   6
Acq. Instrument : Wasa_LC1                         Location :   2
Injection Date  : 8/25/2020 7:55:57 PM                Inj :   1
                                                Inj Volume : 4.000 µl
Method          : C:\Chem32\1\Data\JOE 2020-08-25 16-19-49\column6 2.5%IPA 97.5% hexane 60min
                  -0.5mL.M (Sequence Method)
Last changed    : 8/25/2020 4:19:54 PM by SYSTEM
Method Info     : Column6 60min-2.5% iPrOH 99% hexane-0.5mL
```

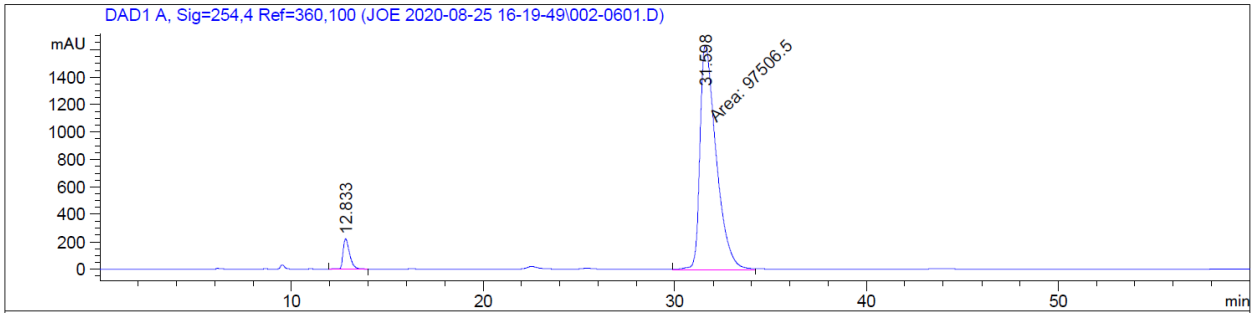

Signal 1: DAD1 A, Sig=254,4 Ref=360,100

Peak #	RetTime [min]	Type	Width [min]	Area [mAU*s]	Height [mAU]	Area %
1	12.833	VB R	0.3650	5260.93115	219.42328	5.1193
2	31.598	MM	0.9911	9.75065e4	1639.71899	94.8807
Totals :				1.02767e5	1859.14227	

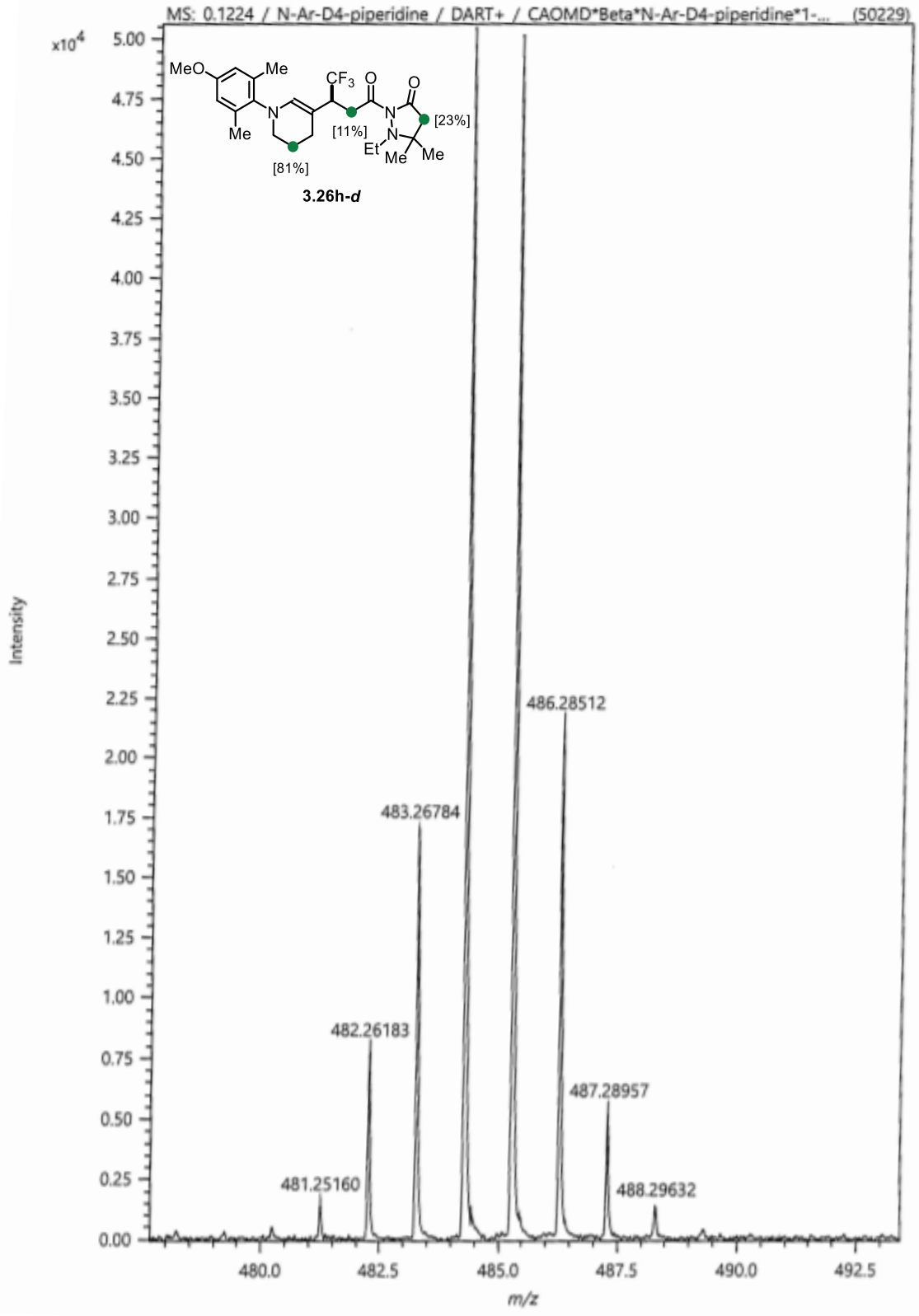
MS: 0.1224 / N-Ar-D4-piperidine / DART+ / CAOMD*Beta*N-Ar-D4-piperidine*1-... (50229)
x10^4
Intensity
MeO
Me
Me
CF3
O
O
N
N
Et
Me
Me
[81%]
[11%]
[23%]
3.26h-d
5.00
4.75
4.50
4.25
4.00
3.75
3.50
3.25
3.00
2.75
2.50
2.25
2.00
1.75
1.50
1.25
1.00
0.75
0.50
0.25
0.00
486.28512
483.26784
482.26183
487.28957
481.25160
488.29632
480.0
482.5
485.0
487.5
490.0
492.5
m/z

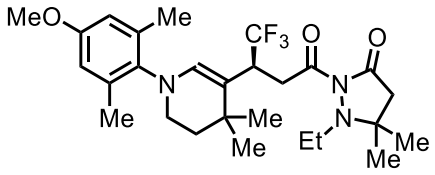

3.26i

(*S*)-1-Ethyl-5,5-dimethyl-2-(4,4,4-trifluoro-3-(1-(4-methoxy-2,6-dimethylphenyl)-4,4-dimethyl-1,4,5,6-tetrahydropyridin-3-yl)butanoyl)pyrazolidin-3-one (3.26i)

1-(4-Methoxy-2,6-dimethylphenyl)-4,4-dimethylpiperidine **3.21m** was reacted with (*E*)-1-ethyl-5,5-dimethyl-2-(4,4,4-trifluorobut-2-enoyl)pyrazolidin-3-one **3.25f** following the **General Procedure E** for 36 hours using $B(C_6F_5)_3$ (10 mol%), $Sc(OTf)_3$ (10 mol%), **L10** (12 mol%) and DCM as the solvent at 80 °C. After purification by column chromatography (EtOAc:DCM = 1:16), **3.26i** was obtained as a colorless liquid (38 mg, 74%). The absolute configuration for this product was assigned in analogy to that determined for product **3.26f**.

^{1}H NMR (500 MHz, $CDCl_3$): δ 6.58 (s, 2H), 5.97 (s, 1H), 3.76 (s, 3H), 3.70 (dt, *J* = 9.8, 6.7 Hz, 1H), 3.34 (dd, *J* = 17.4, 6.2 Hz, 1H), 3.25 – 3.08 (m, 3H), 2.97 (q, *J* = 7.1 Hz, 2H), 2.60 – 2.48 (m, 2H), 2.17 (d, *J* = 9.7 Hz, 6H), 1.72 (t, *J* = 5.8 Hz, 2H), 1.29 (s, 6H), 1.14 (d, *J* = 9.1 Hz, 6H), 1.05 (t, *J* = 7.1 Hz, 3H); **^{13}C NMR (126 MHz, $CDCl_3$):** δ 175.2, 168.4, 157.6, 138.80, 138.75, 138.1, 134.2, 127.7 (q, *J* = 280.1 Hz), 113.63, 113.56, 104.9, 60.6, 55.4, 47.2, 44.3, 44.1, 39.2, 38.5, 37.6 (q, *J* = 26.9 Hz), 31.5, 29.0, 28.7, 26.0, 25.7, 18.4, 18.3, 12.9; **^{19}F NMR (376 MHz, $CDCl_3$):** δ -69.40 (d, *J* = 9.5 Hz); **IR (neat):** ν 2959, 2927, 2842, 1744, 1711, 1637, 1466, 1442, 1374, 1302, 1250, 1228, 1150, 1123, 1096, 856, 670 cm^{-1}; **HRMS (DART):** Calcd for $C_{27}H_{39}F_3N_3O_3$ (MH^+): 510.2938; found: 510.2922; **HPLC** (CHIRACPAK IA-3; 2.5%/ 97.5% isopropanol/ hexanes, 0.2 mL/min; tr = 24.3 min (major), 28.8 min (minor); 94:6 er); **Specific Rotation $[\alpha]^{25}_D$** = -4.6° (c = 0.62, DCM).

```
Acq. Operator   : SYSTEM                          Seq. Line :   9
Acq. Instrument : Wasa_LC1                         Location :   3
Injection Date  : 8/27/2020 12:36:56 AM                Inj :   1
                                                 Inj Volume : 4.000 µl
Method          : C:\Chem32\1\Data\JOE 2020-08-26 19-27-55\column6 2.5%IPA 97.5% hexane 60min
                  -0.2mL.M (Sequence Method)
Last changed    : 8/26/2020 7:28:01 PM by SYSTEM
Method Info     : Column6 60min-2.5% iPrOH 99% hexane-0.2mL
```

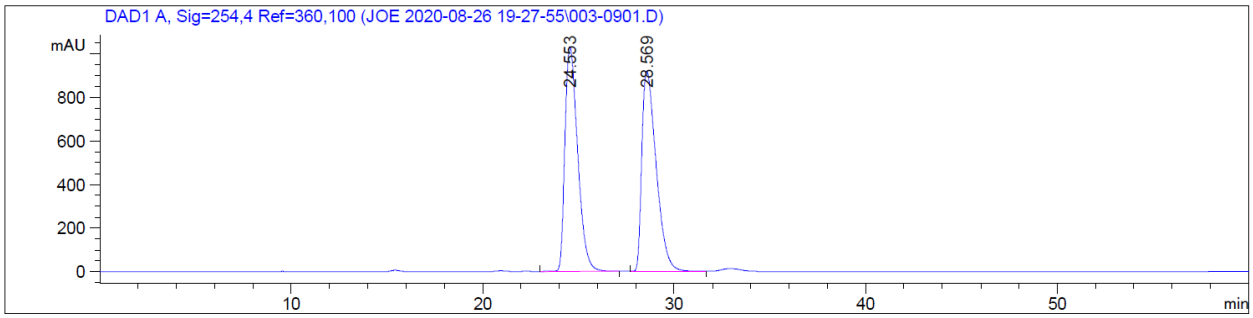

Signal 1: DAD1 A, Sig=254,4 Ref=360,100

Peak #	RetTime [min]	Type	Width [min]	Area [mAU*s]	Height [mAU]	Area %
1	24.553	BB	0.7190	4.76944e4	1032.41467	50.0168
2	28.569	BB	0.8025	4.76623e4	919.91980	49.9832
Totals :				9.53567e4	1952.33447	

```
Acq. Operator   : SYSTEM                          Seq. Line :  10
Acq. Instrument : Wasa_LC1                         Location :   4
Injection Date  : 8/27/2020 1:37:52 AM                Inj :   1
                                                 Inj Volume : 4.000 µl
Method          : C:\Chem32\1\Data\JOE 2020-08-26 19-27-55\column6 2.5%IPA 97.5% hexane 60min
                  -0.2mL.M (Sequence Method)
Last changed    : 8/26/2020 7:28:01 PM by SYSTEM
Method Info     : Column6 60min-2.5% iPrOH 99% hexane-0.2mL
```

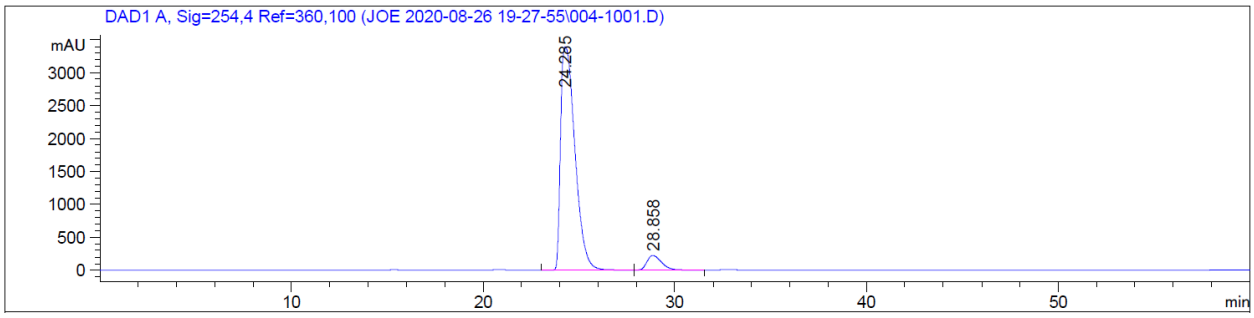

Signal 1: DAD1 A, Sig=254,4 Ref=360,100

Peak #	RetTime [min]	Type	Width [min]	Area [mAU*s]	Height [mAU]	Area %
1	24.285	BB	0.8178	1.76359e5	3396.43530	93.7370
2	28.858	BB	0.8209	1.17834e4	222.13094	6.2630
Totals :				1.88143e5	3618.56624	

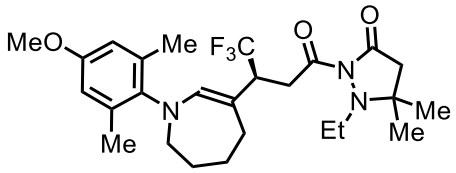

3.26j

(*S*)-1-Ethyl-5,5-dimethyl-2-(4,4,4-trifluoro-3-(1-(4-methoxy-2,6-dimethylphenyl)-4,5,6,7-tetrahydro-1*H*-azepin-3-yl)butanoyl)pyrazolidin-3-one (3.26j)

1-(4-Methoxy-2,6-dimethylphenyl)azepane **3.21t** was reacted with (*E*)-1-ethyl-5,5-dimethyl-2-(4,4,4-trifluorobut-2-enoyl)pyrazolidin-3-one **3.25f** following the **General Procedure E** for 24 hours using $B(C_6F_5)_3$ (10 mol%), $Sc(OTf)_3$ (10 mol%), **L10** (12 mol%) and DCM as the solvent. After purification by column chromatography (ethyl ether:hexanes = 1:1) **3.26j** was obtained as a colorless liquid (39 mg, 78%). The absolute configuration for this product was assigned in analogy to that determined for product **3.26f**.

^{1}H NMR (600 MHz, $CDCl_3$): δ 6.55 (s, 2H), 5.84 (s, 1H), 3.75 (s, 3H), 3.40 – 3.22 (m, 4H), 3.15 (d, *J* = 12.8 Hz, 1H), 3.01 – 2.90 (m, 2H), 2.61 – 2.50 (m, 2H), 2.41 – 2.25 (m, 2H), 2.20 (d, *J* = 4.3 Hz, 6H), 1.84 – 1.70 (m, 4H), 1.28 (d, *J* = 3.6 Hz, 6H), 1.04 (t, *J* = 7.1 Hz, 3H); **^{13}C NMR (151 MHz, $CDCl_3$):** δ 175.4, 168.1, 157.4, 141.8, 140.5, 138.1, 137.9, 127.7 (q, *J* = 280.8 Hz), 113.6, 113.5, 104.1, 60.6, 55.4, 54.7, 47.2, 46.7 (q, *J* = 26.7 Hz), 44.0, 34.5, 30.5, 29.3, 26.8, 25.9, 18.9, 18.8, 13.0; **^{19}F NMR (470 MHz, $CDCl_3$):** δ -70.17 (d, *J* = 9.1 Hz); **IR (neat):** ν 2925, 2849, 1744, 1709, 1648, 1602, 1485, 1466, 1442, 1374, 1308, 1261, 1207, 1152, 1104, 1066, 1031, 895, 732, 701, 618 cm^{-1}; **HRMS (DART):** Calcd for $C_{26}H_{37}F_3N_3O_3$ (MH^+): 496.2782; found: 496.2774; **HPLC** (CHIRACPAK IA-3; 5%/ 95% isopropanol/ hexanes, 1.0 mL/min; tr = 4.2 min (minor), 11.0 min (major); 94:6 er); **Specific Rotation $[\alpha]^{25}_D$** = -17.3° (c = 0.47, DCM).

```
Acq. Operator   : SYSTEM                          Seq. Line :   7
Acq. Instrument : Wasa_LC1                         Location :   48
Injection Date  : 8/10/2020 3:57:11 PM                 Inj :   1
                                                 Inj Volume : 4.000 µl
Method          : C:\Chem32\1\Data\JOE 2020-08-10 09-49-00\column6 5%IPA 95% hexane 35min-1.
                  0mL.M (Sequence Method)
Last changed    : 8/10/2020 9:49:05 AM by SYSTEM
Method Info     : Column6 35min-5% iPrOH 95% hexane-1.0mL
```

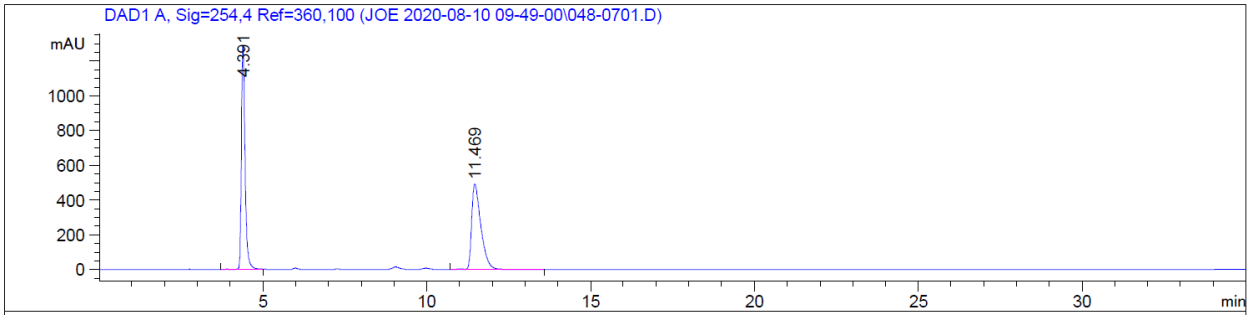

Signal 1: DAD1 A, Sig=254,4 Ref=360,100

Peak #	RetTime [min]	Type	Width [min]	Area [mAU*s]	Height [mAU]	Area %
1	4.391	VB R	0.1184	1.00388e4	1293.51587	50.9692
2	11.469	VB R	0.2963	9656.99121	491.59241	49.0308
Totals :				1.96957e4	1785.10828	

```
Acq. Operator   : SYSTEM                          Seq. Line :  14
Acq. Instrument : Wasa_LC1                         Location :  59
Injection Date  : 8/23/2020 9:50:57 AM                 Inj :  1
                                                 Inj Volume : 4.000 µl
Method          : C:\Chem32\1\Data\JOE 2020-08-22 21-25-56\column6 5%IPA 95% hexane 35min-1.
                  0mL.M (Sequence Method)
Last changed    : 8/22/2020 9:26:02 PM by SYSTEM
Method Info     : Column6 35min-5% iPrOH 95% hexane-1.0mL
```

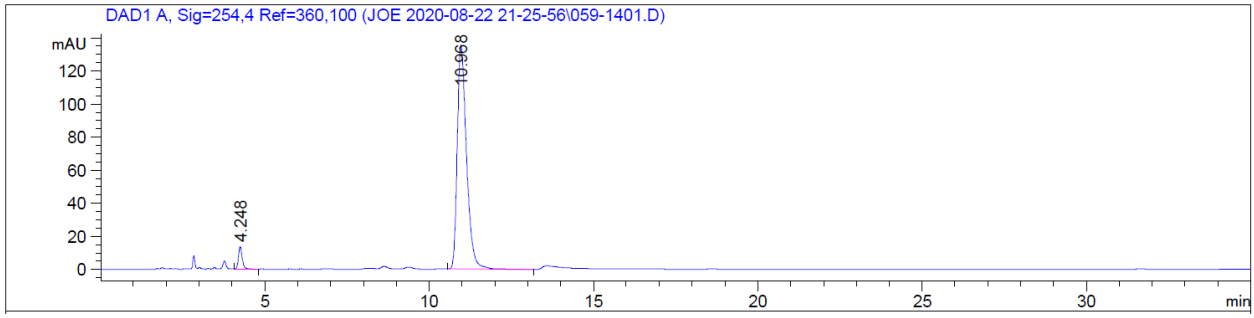

Signal 1: DAD1 A, Sig=254,4 Ref=360,100

Peak #	RetTime [min]	Type	Width [min]	Area [mAU*s]	Height [mAU]	Area %
1	4.248	VB	0.1245	108.70381	13.42023	3.9333
2	10.968	BB	0.2970	2654.95752	135.25128	96.0667
Totals :				2763.66133	148.67151	

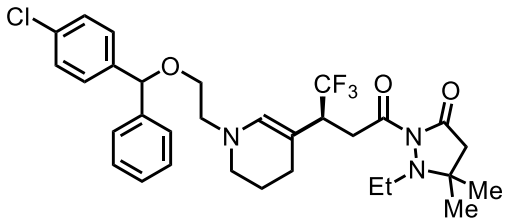

3.26k

2-((3*S*)-3-(1-(2-((4-Chlorophenyl)(phenyl)methoxy)ethyl)-1,4,5,6-tetrahydropyridin-3-yl)-4,4,4-trifluorobutanoyl)-1-ethyl-5,5-dimethylpyrazolidin-3-one (3.26k)

1-(2-((4-Chlorophenyl)(phenyl)methoxy)ethyl)piperidine **3.21u** was reacted with (*E*)-1-ethyl-5,5-dimethyl-2-(4,4,4-trifluorobut-2-enoyl)pyrazolidin-3-one **3.25f** following the **General Procedure General Procedure E** for 24 hours using $B(C_6F_5)_3$ (20 mol%), $Sc(OTf)_3$ (10 mol%), **L8** (12 mol%) and DCM as the solvent at 80 °C. ^{1}H NMR and ^{19}F NMR analysis of the unpurified product mixture using mesitylene and perfluorobenzene as the internal standard revealed that the diastereomeric ratio was 1.0:1. After purification by column chromatography (EtOAc:hexanes = 1:4), **3.26k** was obtained as an inseparable mixture of diastereomers (31 mg, 53%). The absolute configuration for this product was assigned in analogy to that determined for product **3.26f**.

^{1}H NMR (400 MHz, $CDCl_3$, *peaks from diastereomers are merged*): δ 7.33 – 7.20 (m, 8H), 5.96 (s, 1H), 5.27 (s, 1H), 3.48 – 3.40 (m, 2H), 3.39 – 3.27 (m, 2H), 3.14 – 2.83 (m, 7H), 2.61 – 2.48 (m, 2H), 2.03 (t, J = 6.2 Hz, 2H), 1.83 – 1.67 (m, 2H), 1.25 (d, J = 9.6 Hz, 6H), 1.01 (t, J = 7.1 Hz, 3H); **^{13}C NMR (126 MHz, $CDCl_3$):** δ 175.3, 168.3, 141.88, 141.87, 141.0, 136.9, 133.3, 128.7, 128.6, 128.34, 128.31, 127.8, 127.6 (q, J = 281.3 Hz), 127.00, 126.96, 97.8, 83.4, 67.55, 67.53, 60.6, 55.0, 47.2, 47.0, 45.0 (q, J = 27.1 Hz), 44.1, 34.2, 26.0, 25.7, 22.8, 22.6, 12.9; **^{19}F NMR (470 MHz, $CDCl_3$):** δ -69.70 – -69.87 (m); **IR (neat):** ν 2919, 2849, 1742, 1710, 1654, 1513, 1488, 1465, 1450, 1373, 1337, 1303, 1256, 1237, 1177, 1138, 1096, 1038, 812, 757, 718, 616 cm^{-1};

HRMS (DART): Calcd for $C_{31}H_{38}ClF_3N_3O_3$ (MH^+): 592.2548; found: 592.2542; **HPLC** (CHIRACPAK AD-H; 5%/ 95% isopropanol/ hexanes, 0.2 mL/min; tr = 49.2 min (major1), 53.6 min (major2), 61.7 min (minor1), 65.5 min (minor2); 90:10 er); **Specific Rotation** $[\alpha]^{25}_D$ = +2.0° (c = 0.50, DCM).

```
Acq. Operator   : SYSTEM                          Seq. Line :   8
Acq. Instrument : Wasa_LC1                        Location :   5
Injection Date  : 9/20/2020 11:01:30 PM               Inj :   1
                                                 Inj Volume : 4.000 µl
Acq. Method     : C:\Chem32\1\Data\JOE 2020-09-20 17-02-28\column1 5% IPA 95% hexane 80min-0.
                  2mL.M
Last changed    : 9/20/2020 5:02:34 PM by SYSTEM
Analysis Method : C:\Chem32\1\Data\JOE 2020-09-20 17-02-28\column1 5% IPA 95% hexane 80min-0.
                  2mL.M (Sequence Method)
Last changed    : 9/21/2020 10:31:35 AM by SYSTEM
                  (modified after loading)
Method Info     : 80min-5% iPrOH 95% hexane-0.2mL
```

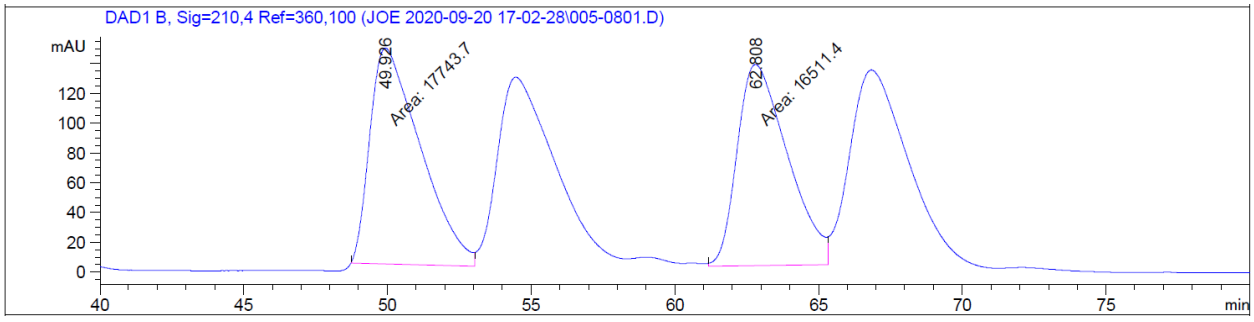

Signal 2: DAD1 B, Sig=210,4 Ref=360,100

Peak #	RetTime [min]	Type	Width [min]	Area [mAU*s]	Height [mAU]	Area %
1	49.926	MM	2.0423	1.77437e4	144.79956	51.7986
2	62.808	MM	2.0391	1.65114e4	134.95860	48.2014
Totals :				3.42551e4	279.75816	

```
Acq. Operator   : SYSTEM                          Seq. Line :  10
Acq. Instrument : Wasa_LC1                         Location :   9
Injection Date  : 9/21/2020 1:43:24 AM                 Inj :   1
                                                 Inj Volume : 4.000 µl
Acq. Method     : C:\Chem32\1\Data\JOE 2020-09-20 17-02-28\column1 5% IPA 95% hexane 80min-0.
                  2mL.M
Last changed    : 9/20/2020 5:02:34 PM by SYSTEM
Analysis Method : C:\Chem32\1\Data\JOE 2020-09-20 17-02-28\column1 5% IPA 95% hexane 80min-0.
                  2mL.M (Sequence Method)
Last changed    : 9/21/2020 10:31:35 AM by SYSTEM
                  (modified after loading)
Method Info     : 80min-5% iPrOH 95% hexane-0.2mL
```

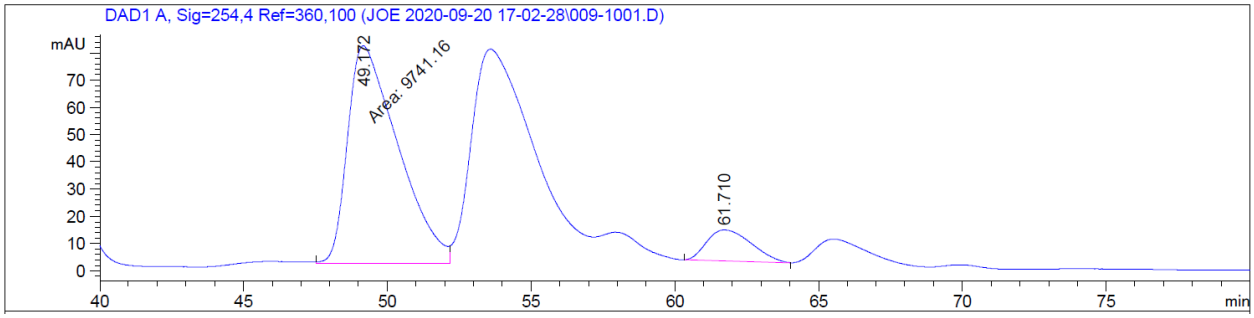

Signal 1: DAD1 A, Sig=254,4 Ref=360,100

Peak #	RetTime [min]	Type	Width [min]	Area [mAU*s]	Height [mAU]	Area %
1	49.172	MM	2.0318	9741.15723	79.90520	88.8697
2	61.710	BB	1.2890	1220.00977	11.37721	11.1303
Totals :				1.09612e4	91.28240	

```
Acq. Operator   : SYSTEM                          Seq. Line :   8
Acq. Instrument : Wasa_LC1                         Location :   5
Injection Date  : 9/20/2020 11:01:30 PM                Inj :   1
                                                Inj Volume : 4.000 µl
Acq. Method     : C:\Chem32\1\Data\JOE 2020-09-20 17-02-28\column1 5% IPA 95% hexane 80min-0.
                  2mL.M
Last changed    : 9/20/2020 5:02:34 PM by SYSTEM
Analysis Method : C:\Chem32\1\Data\JOE 2020-09-20 17-02-28\column1 5% IPA 95% hexane 80min-0.
                  2mL.M (Sequence Method)
Last changed    : 9/21/2020 10:31:35 AM by SYSTEM
                  (modified after loading)
Method Info     : 80min-5% iPrOH 95% hexane-0.2mL
```

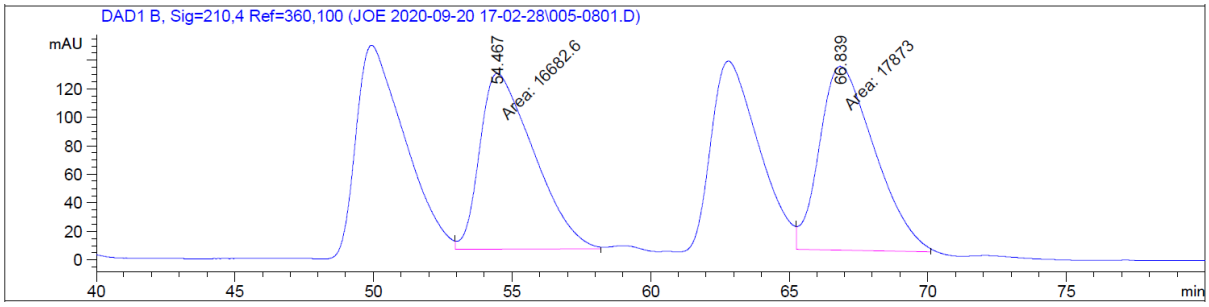

Signal 2: DAD1 B, Sig=210,4 Ref=360,100

Peak #	RetTime [min]	Type	Width [min]	Area [mAU*s]	Height [mAU]	Area %
1	54.467	MM	2.2531	1.66826e4	123.40290	48.2776
2	66.839	MM	2.3115	1.78730e4	128.87001	51.7224
Totals :				3.45555e4	252.27291	

```
Acq. Operator   : SYSTEM                          Seq. Line :  10
Acq. Instrument : Wasa_LC1                         Location :   9
Injection Date  : 9/21/2020 1:43:24 AM                Inj :   1
                                                 Inj Volume : 4.000 µl
Acq. Method     : C:\Chem32\1\Data\JOE 2020-09-20 17-02-28\column1 5% IPA 95% hexane 80min-0.
                  2mL.M
Last changed    : 9/20/2020 5:02:34 PM by SYSTEM
Analysis Method : C:\Chem32\1\Data\JOE 2020-09-20 17-02-28\column1 5% IPA 95% hexane 80min-0.
                  2mL.M (Sequence Method)
Last changed    : 9/21/2020 10:31:35 AM by SYSTEM
                  (modified after loading)
Method Info     : 80min-5% iPrOH 95% hexane-0.2mL
```

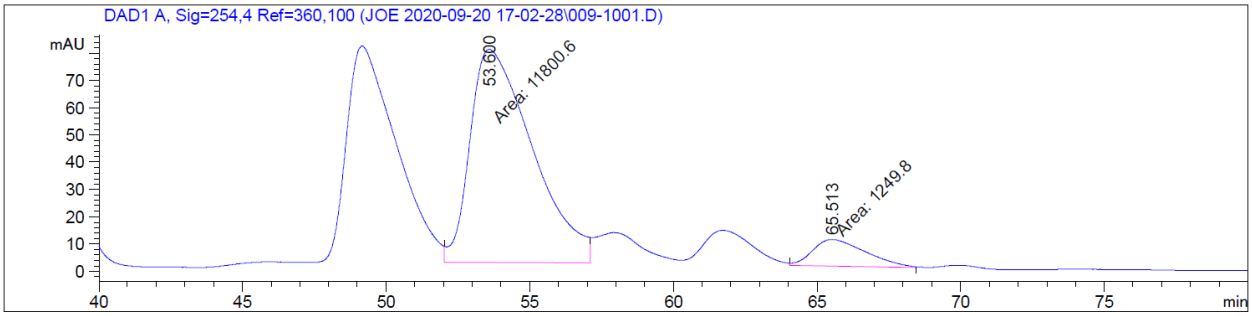

Signal 1: DAD1 A, Sig=254,4 Ref=360,100

Peak #	RetTime [min]	Type	Width [min]	Area [mAU*s]	Height [mAU]	Area %
1	53.600	MM	2.5154	1.18006e4	78.18829	90.4233
2	65.513	MM	2.1369	1249.79602	9.74771	9.5767
Totals :				1.30504e4	87.93600	

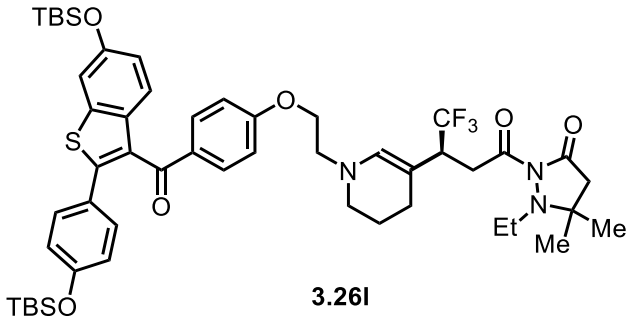

3.26l

(*S*)-2-(3-(1-(2-(4-(6-((*tert*-Butyldimethylsilyl)oxy)-2-(4-((*tert*-butyldimethylsilyl)oxy) phenyl)benzo[*b*]thiophene-3-carbonyl)phenoxy)ethyl)-1,4,5,6-tetrahydropyridin-3-yl)-4,4,4-trifluorobutanoyl)-1-ethyl-5,5-dimethylpyrazolidin-3-one (3.26l)

(6-((*tert*-Butyldimethylsilyl)oxy)-2-(4-((*tert*-butyldimethylsilyl)oxy)phenyl)benzo[*b*]thiophen -3-yl)(4-(2-(piperidin-1-yl)ethoxy)phenyl)methanone **3.21n** was reacted with (*E*)-1-ethyl-5,5-dimethyl-2-(4,4,4-trifluorobut-2-enoyl)pyrazolidin-3-one **3.25f** following the **General Procedure General Procedure E** for 24 hours using $B(C_6F_5)_3$ (20 mol%), $Sc(OTf)_3$ (10 mol%), **L8** (12 mol%) and DCM as the solvent at 80 °C. After purification by column chromatography (EtOAc:hexanes = 1:4), **3.26l** was obtained as a white solid (55 mg, 57%). The absolute configuration for this product was assigned in analogy to that determined for product **3.26f**.

^{1}H NMR (500 MHz, $CDCl_3$): δ 7.72 (d, *J* = 8.9 Hz, 2H), 7.54 (d, *J* = 8.7 Hz, 1H), 7.29 – 7.22 (m, 3H), 6.87 (dd, *J* = 8.8, 2.3 Hz, 1H), 6.70 (d, *J* = 9.0 Hz, 2H), 6.66 (d, *J* = 8.6 Hz, 2H), 5.95 (s, 1H), 3.93 (t, *J* = 5.6 Hz, 2H), 3.40 – 3.30 (m, 2H), 3.22 – 3.12 (m, 2H), 3.11 – 3.03 (m, 1H), 3.00 – 2.93 (m, 2H), 2.91 (q, *J* = 7.1 Hz, 2H), 2.59 – 2.48 (m, 2H), 2.01 (t, *J* = 6.3 Hz, 2H), 1.85 – 1.69 (m, 2H), 1.25 (d, *J* = 10.2 Hz, 6H), 1.02 – 0.98 (m, 12H), 0.92 (s, 9H), 0.22 (s, 6H), 0.11 (s, 6H); **^{13}C NMR (101 MHz, $CDCl_3$):** δ 193.3, 175.3, 168.3, 162.8, 156.2, 153.6, 143.4, 140.0, 136.5, 134.6, 132.4, 130.7, 130.6, 130.4, 127.5 (q, *J* = 281.1 Hz), 126.9, 124.0, 120.4, 119.4, 114.1, 112.2, 99.3, 66.6, 60.6, 54.1, 47.2, 47.1, 44.9 (q, *J* = 27.2 Hz), 43.9, 34.2, 30.4, 29.8, 25.8, 25.7, 22.7, 22.5,

18.4, 18.3, 12.9, -4.2, -4.4; **^{19}F NMR (376 MHz, $CDCl_3$):** δ -69.86 (d, *J* = 9.2 Hz); **IR (neat):** ν 2952, 2927, 2856, 1744, 1710, 1655, 1597, 1530, 1465, 1304, 1255, 1165, 1137, 1038, 942, 909, 838, 642 cm^{-1}; **HRMS (DART):** Calcd for $C_{51}H_{69}F_3N_3O_6SSi_2$ (MH^+): 964.4392; found: 964.4392; **HPLC** (CHIRACPAK IA-3; 5%/ 95% isopropanol/ hexanes, 1.0 mL/min; tr = 11.8 min (minor), 15.7 min (major); 95:5 er); **Specific Rotation $[\alpha]^{25}_D$** = -4.6° (c = 0.82, DCM).

```
Acq. Operator   : SYSTEM                          Seq. Line :   1
Acq. Instrument : Wasa_LC1                         Location :   31
Injection Date  : 8/10/2020 5:33:46 PM                 Inj :   1
                                                 Inj Volume : 4.000 µl
Acq. Method     : C:\Chem32\1\Data\JOE 2020-08-10 17-32-29\column6 5%IPA 95% hexane 35min-1.
                  0mL.M
Last changed    : 8/10/2020 5:55:51 PM by SYSTEM
                  (modified after loading)
Analysis Method : C:\Chem32\1\Data\JOE 2020-08-10 17-32-29\column6 5%IPA 95% hexane 35min-1.
                  0mL.M (Sequence Method)
Last changed    : 9/1/2020 12:41:57 PM by SYSTEM
                  (modified after loading)
Method Info     : Column6 35min-5% iPrOH 95% hexane-1.0mL
```

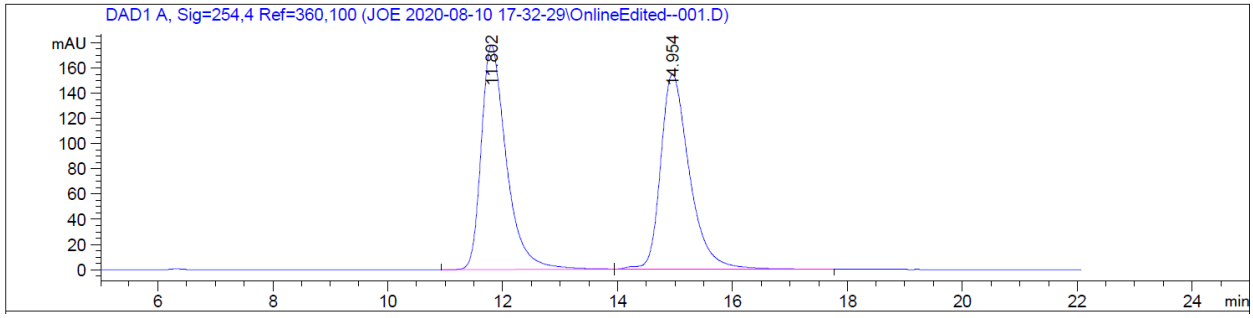

Signal 1: DAD1 A, Sig=254,4 Ref=360,100

Peak #	RetTime [min]	Type	Width [min]	Area [mAU*s]	Height [mAU]	Area %
1	11.802	BB	0.4620	5396.38525	177.85497	50.0678
2	14.954	BB	0.5279	5381.77783	154.66997	49.9322
Totals :				1.07782e4	332.52493	

```
Acq. Operator   : SYSTEM                          Seq. Line :   2
Acq. Instrument : Wasa_LC1                         Location :   84
Injection Date  : 8/20/2020 10:21:48 PM                Inj :   1
                                                 Inj Volume : 4.000 µl
Acq. Method     : C:\Chem32\1\Data\JOE 2020-08-20 21-53-45\column6 5%IPA 95% hexane 25min-1.
                  0mL.M
Last changed    : 8/20/2020 9:53:51 PM by SYSTEM
Analysis Method : C:\Chem32\1\Data\JOE 2020-08-20 21-53-45\column6 5%IPA 95% hexane 25min-1.
                  0mL.M (Sequence Method)
Last changed    : 9/1/2020 12:43:11 PM by SYSTEM
                  (modified after loading)
Method Info     : Column6 25min-5% iPrOH 95% hexane-1.0mL
```

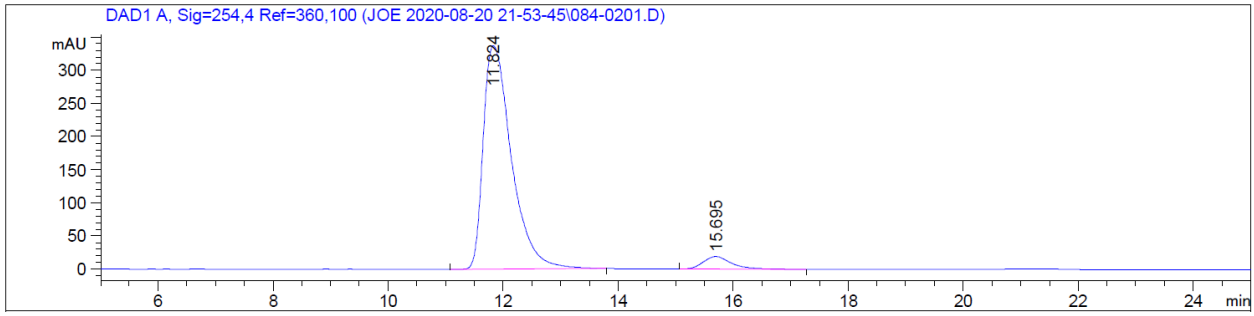

Signal 1: DAD1 A, Sig=254,4 Ref=360,100

Peak #	RetTime [min]	Type	Width [min]	Area [mAU*s]	Height [mAU]	Area %
1	11.824	BB	0.4976	1.14902e4	337.18747	94.7035
2	15.695	BB	0.4999	642.61816	19.03380	5.2965
Totals :				1.21328e4	356.22127	

C9. Reference

(1) Tse, M. D.; Bhor, S.; Klawonn, M.; Anilkumar, G.; Jiao, H.; Döbler, C.; Spannenberg, A.; Mägerlein, W.; Hugl, H.; Beller, M. Ruthenium–Catalyzed Asymmetric Epoxidation of Olefins Using H_2O_2, Part I: Synthesis of New Chiral *N*,*N*,*N*–Tridentate Pybox and Pyboxazine Ligands and Their Ruthenium Complexes. *Chem*. *Eur*. *J*. **2006**, *12*, 1855–1874.

(2) Thorhauge, J.; Roberson, M.; Hazell, R. G.; Jørgensen, K. A. On the Intermediates in Chiral Bis(oxazoline)copper(II)-Catalyzed Enantioselective Reactions–Experimental and Theoretical Investigations. *Chem*. *Eur*. *J*. **2002**, *8*, 1888–1898.

(3) Desimoni, G.; Faita, G.; Jørgensen, K. A. C_2-Symmetric Chiral Bis(oxazoline) Ligands in Asymmetric Catalysis. *Chem*. *Rev*. **2011**, *111*, 284–437.

(4) Itoh, K.; Sibi, M. P. Dibenzofuran-4,6-bis (oxazoline)(DBFOX). A novel *trans*-chelating bis(oxazoline) Ligand for asymmetric reactions. *Org*. *Biomol*. *Chem*. **2018**, *16*, 5551–5565.

(5) Shang, M.; Chan, J. Z.; Cao, M.; Chang, Y.; Wang, Q.; Cook, B.; Torker, S.; Wasa, M. C–H Functionalization of Amines via Alkene-Derived Nucleophiles through Cooperative Action of Chiral and Achiral Lewis Acid Catalysts: Applications in Enantioselective Synthesis**.** *J. Am. Chem. Soc.* **2018**, *140*, 10593–10601.

(6) Chan, J. Z.; Chang, Y.; Wasa, M. $B(C_6F_5)_3$-Catalyzed C–H Alkylation of *N*-alkylamines Using Silicon Enolates without External Oxidant. *Org. Lett.* **2019**, *21*, 984–988.

(7) Chang, Y.; Yesilcimen, A.; Cao, M.; Zhang, Y.; Zhang, B.; Chan, J. Z.; Wasa, M. Catalytic Deuterium Incorporation within Metabolically Stable *β*-Amino C–H Bonds of Drug Molecules. *J. Am. Chem. Soc.* **2019**, *141*, 14570–14575.

(8) Chan, J. Z.; Yesilcimen, A.; Cao, M.; Zhang, Y.; Zhang, B.; Wasa, M. Direct Conversion of

N-Alkylamines to *N*-Propargylamines through C–H Activation Promoted by Lewis Acid/Organocopper Catalysis: Application to Late-Stage Functionalization of Bioactive Molecules. *J. Am. Chem. Soc.* **2020**, *142*, 16493−16505.

(9) Takasu, N.; Oisaki, K.; Kanai, M. Iron-Catalyzed Oxidative C(3)–H Functionalization of Amines. *Org. Lett*. **2013**, *15*, 1918−1921.

(10) Kawamoto, K.; Zhong, M.; Wang, R.; Olsen, B. D.; Johnson, J. A. Loops versus Branch Functionality in Model Click Hydrogels. *Macromolecules* **2015**, *48*, 8980–8988.

(11) Schmidt, W.; Vögtle, F.; Poetsch, E. Spiro Units as Building Blocks in Thermotropic Liquid Crystals: Synthesis and Physical Properties of Terminally Substituted Spiro[5.5]undecanes. *Liebigs Ann.* **1995**, 1319−1326.

(12) Lecomte, P. Stereoselective synthesis of cyclopropane derivatives by reaction of organometallic functionalized α-carbonyls heterosubstituted on α,β-unsaturation; Application for the synthesis of deltamethrin, a powerful insecticide. Departement de Chimie Facultes Universitaires Notre-Dame de la Paix, **1993**.

(13) Jiang, X.; Wei, X.; Lin, F.; Zhang, Z.; Yao, G.; Yang, S.; Zhao, W.; Zhao, C.; Xu, H. Substrate-Controlled [5+1] Annulation of 5-Amino-1*H*-phenylpyrazoles with Alkenes: Divergent Synthesis of Multisubstituted 4,5-Dihydropyrazolo[1,5-a] quinazolines. *Eur. J. Org. Chem*. **2020**, 3997–4003.

(14) Sibi, M. P.; Ma, Z.; Jasperse, C. P. Exo Selective Enantioselective Nitrone Cycloadditions. *J. Am. Chem. Soc.* **2004**, *126*, 718−719.

(15) Ruiz Espelt, L.; McPherson, I. S.; Wiensch, E. M.; Yoon, T. P. Enantioselective Conjugate Additions of α-Amino Radicals via Cooperative Photoredox and Lewis Acid Catalysis. *J. Am. Chem. Soc.* **2015**, *137*, 2452−2455.

(16) Davies, S. G.; Epstein, S. W.; Garner, A. C.; Ichihara, O.; Smith, A. D. Asymmetric synthesis of α-amino carbonyl derivatives using lithium (*R*)-*N*-benzyl-*N*-α-methylbenzylamide. *Tetrahedron: Asymmetry* **2002**, *13*, 1555–1565.

(17) Petrone, D. A.; Isomura, M.; Franzoni, I.; Rössler, S. L.; Carreira, E.M. Allenylic Carbonates in Enantioselective Iridium-Catalyzed Alkylations. *J. Am. Chem. Soc.* **2018**, *140*, 4697–4704.

(18) Hou, G. H.; Xie, J. H.; Yan, P. C.; Zhou, Q. L. Iridium-Catalyzed Asymmetric Hydrogenation of Cyclic Enamines. *J. Am. Chem. Soc.* **2009**, *131*, 1366–1367.

(19) Dilman, A. D.; Belyakov, P. A.; Struchkova, M. I.; Arkhipov, D. E.; Korlyukov, A. A.; Tartakovsky, V. A. Fluorocyanation of Enamines. *J. Org. Chem*, **2010**, *75*, 5367–5370.

(20) Parks, D. J.; Piers, W. E. Tris(pentafluorophenyl)boron-Catalyzed Hydrosilation of Aromatic Aldehydes, Ketones, and Esters. *J. Am. Chem. Soc.* **1996**, *118*, 9440–9441.

(21) Farrell, J. M.; Heiden, Z. M.; Stephan, D. W. Metal-Free Transfer Hydrogenation Catalysis by $B(C_6F_5)_3$. *Organometallics* **2011**, *30*, 4497–4500.

(22) Liu, Y.; Du, H. Chiral dienes as "Ligands" for borane-catalyzed metal-free asymmetric hydrogenation of imines. *J. Am. Chem. Soc*. **2013**, *135*, 6810-6813.

C10. NMR Spectra for New Compounds

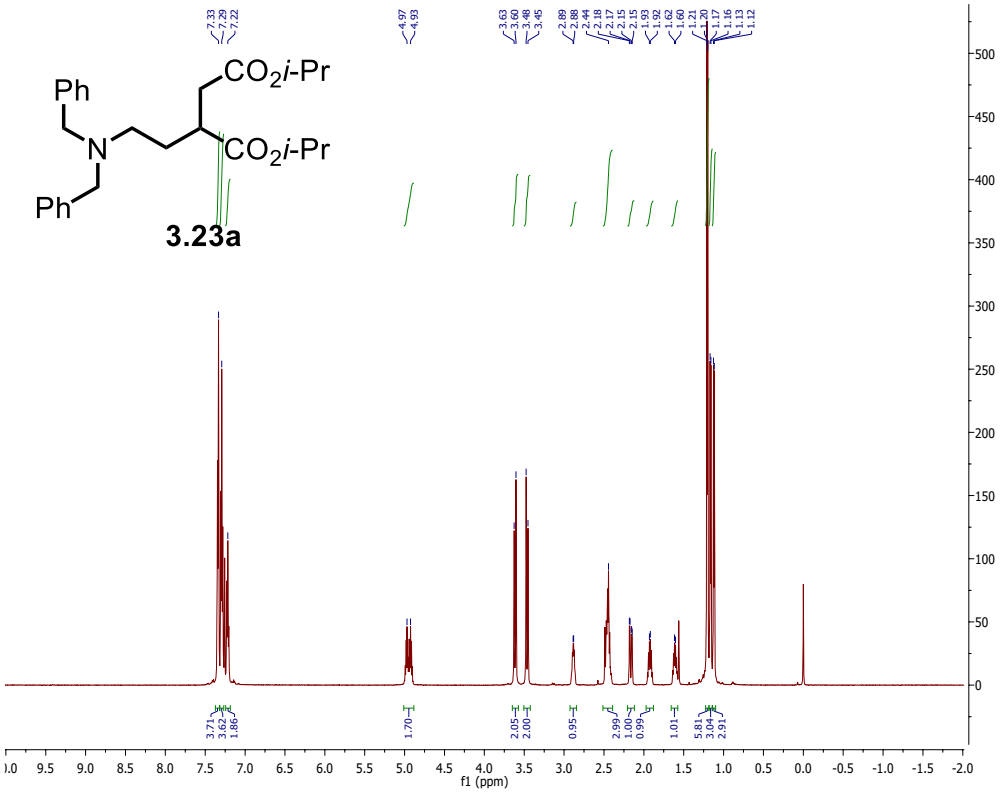

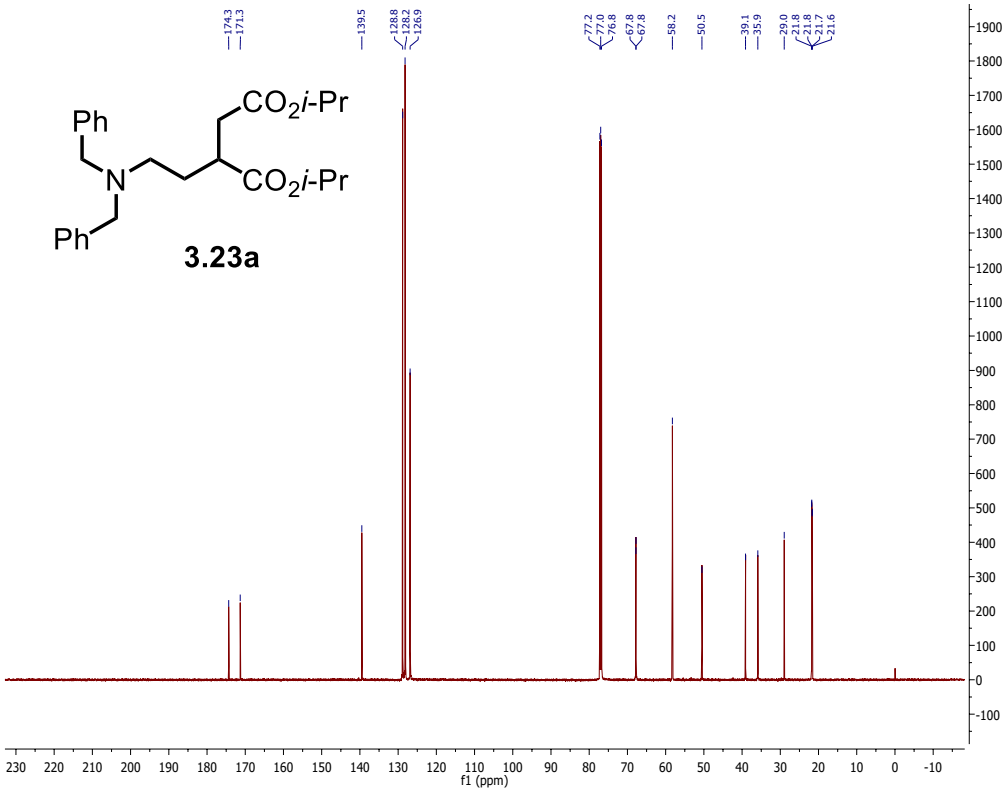

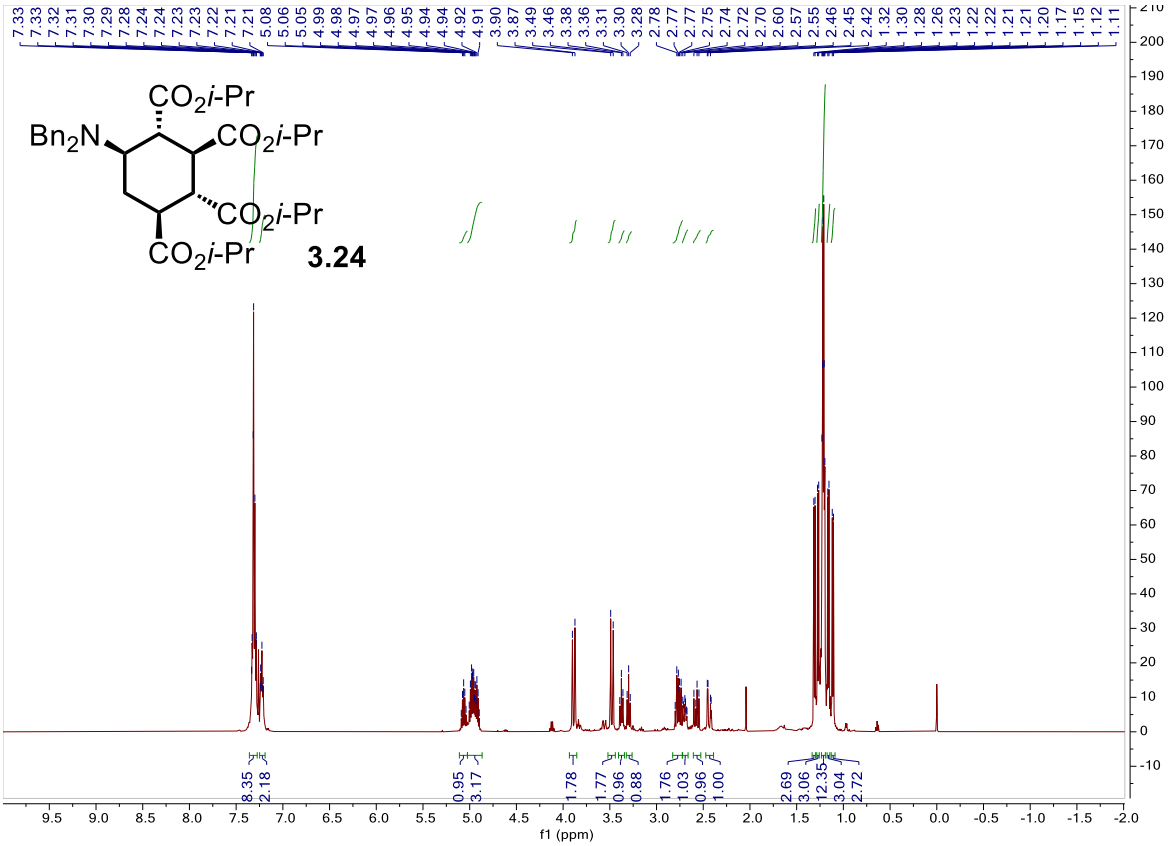
CO2i-Pr
Bn2N
CO2i-Pr
CO2i-Pr
CO2i-Pr
3.24
f1 (ppm)

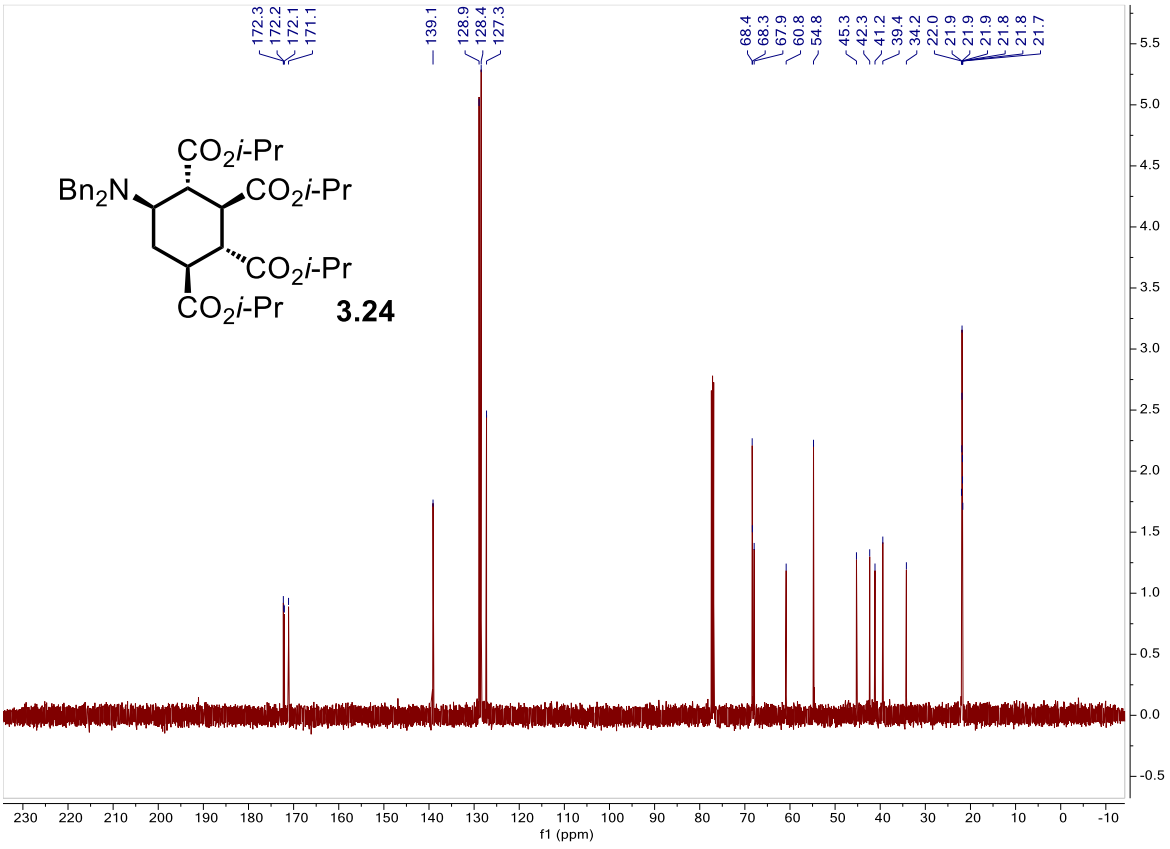
CO2i-Pr
Bn2N
CO2i-Pr
CO2i-Pr
CO2i-Pr
3.24
f1 (ppm)

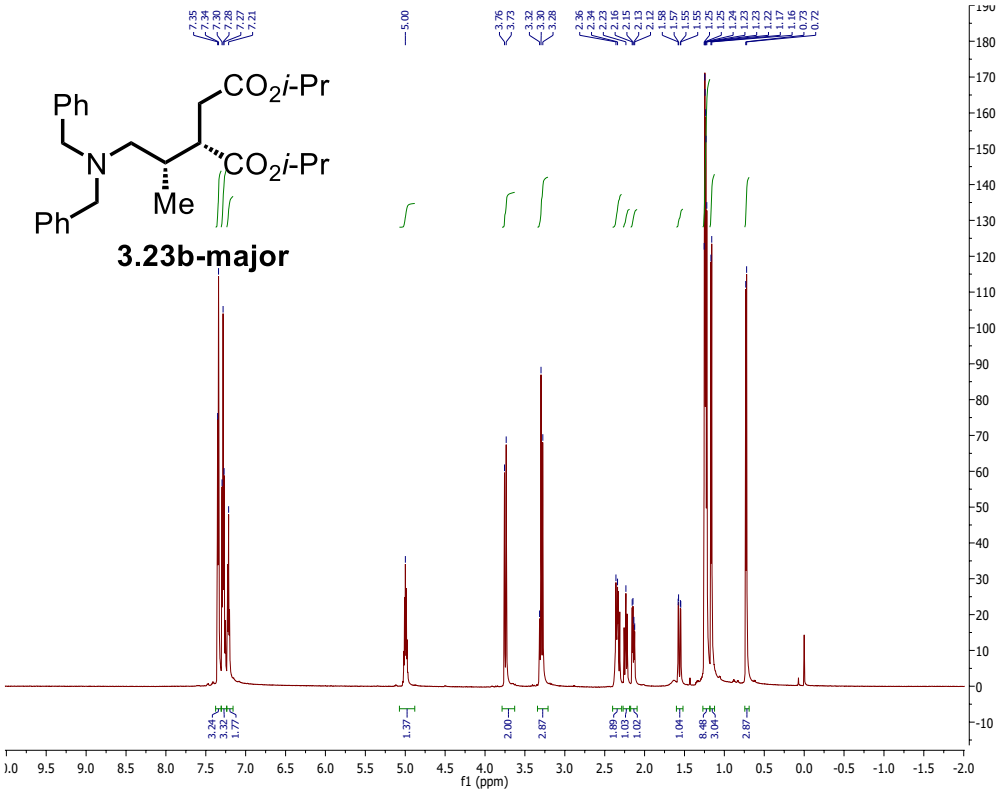
Ph
N
Ph
Me
CO2i-Pr
CO2i-Pr
3.23b-major
f1 (ppm)

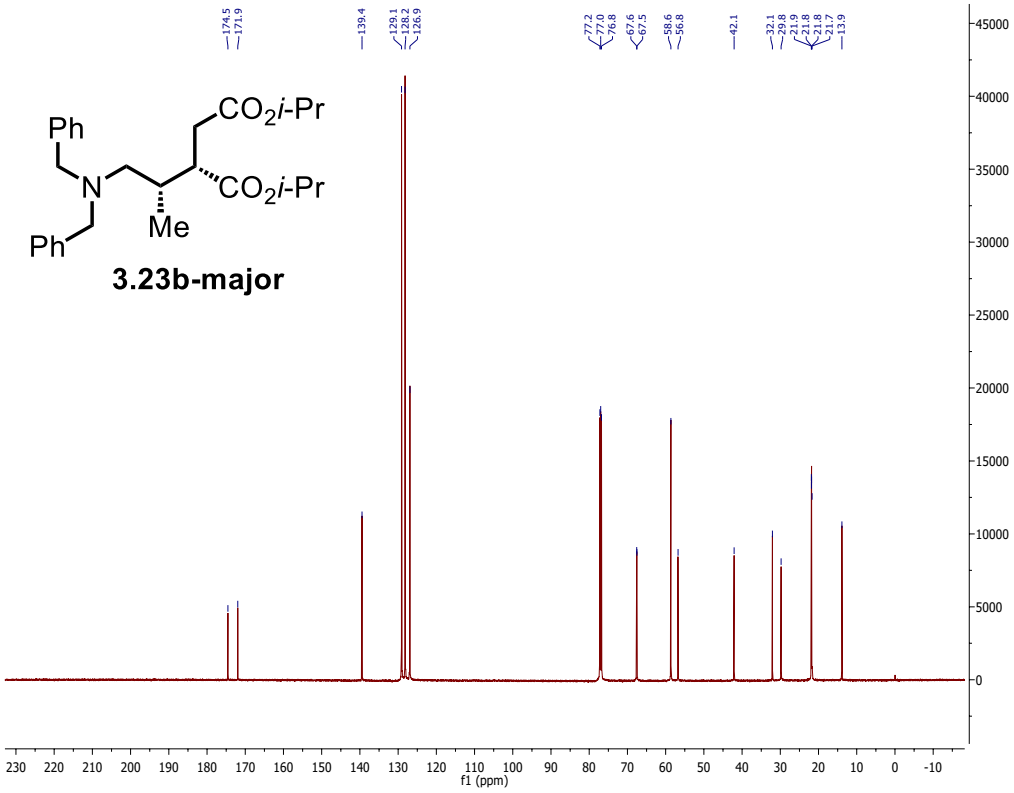
Ph
N
Ph
Me
CO2i-Pr
CO2i-Pr
3.23b-major
f1 (ppm)

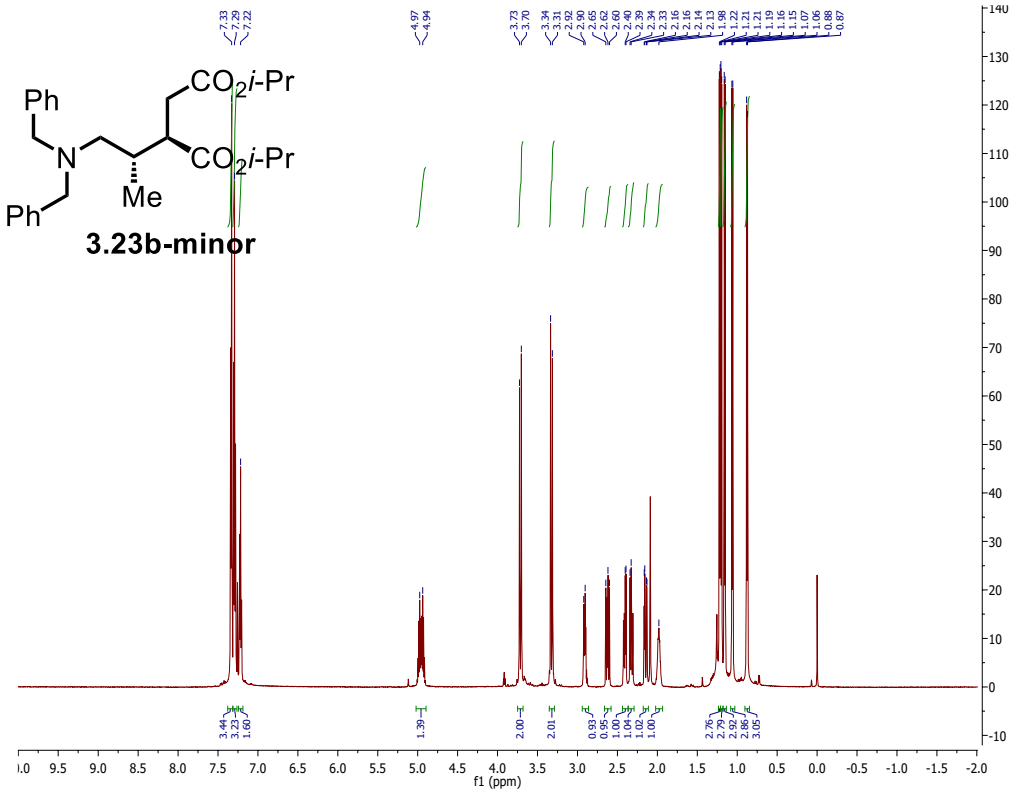
Ph
N
Ph
Me
CO2i-Pr
CO2i-Pr
3.23b-minor
f1 (ppm)

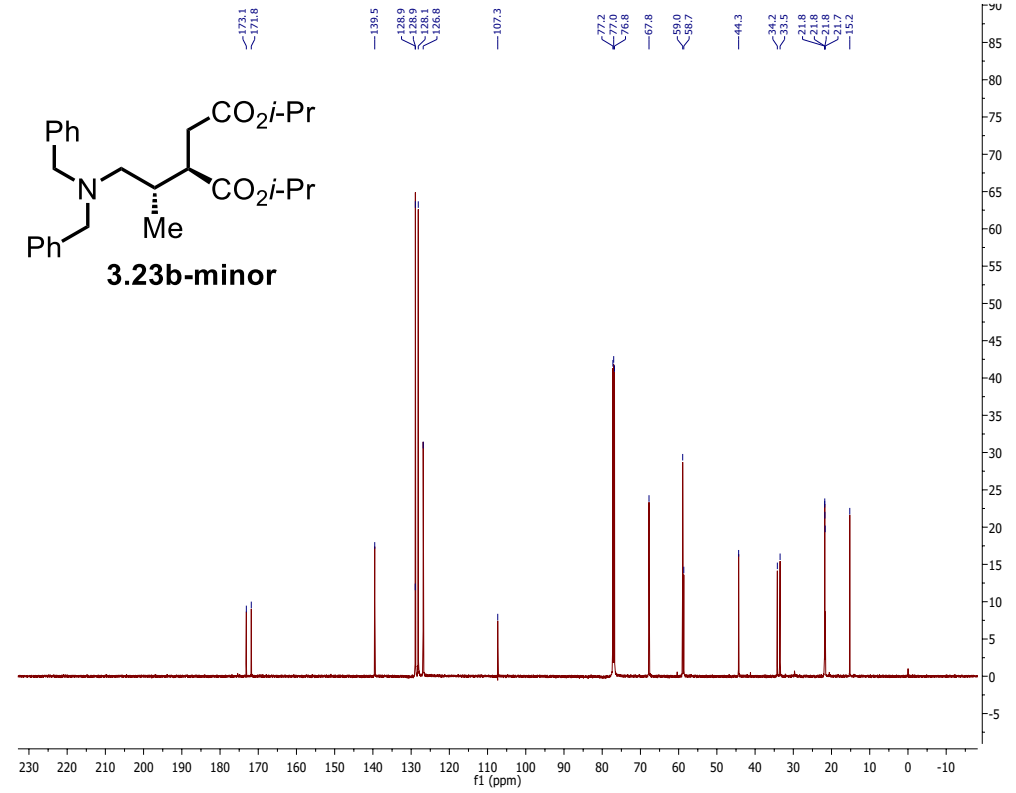
Ph
N
Ph
Me
CO2i-Pr
CO2i-Pr
3.23b-minor
f1 (ppm)

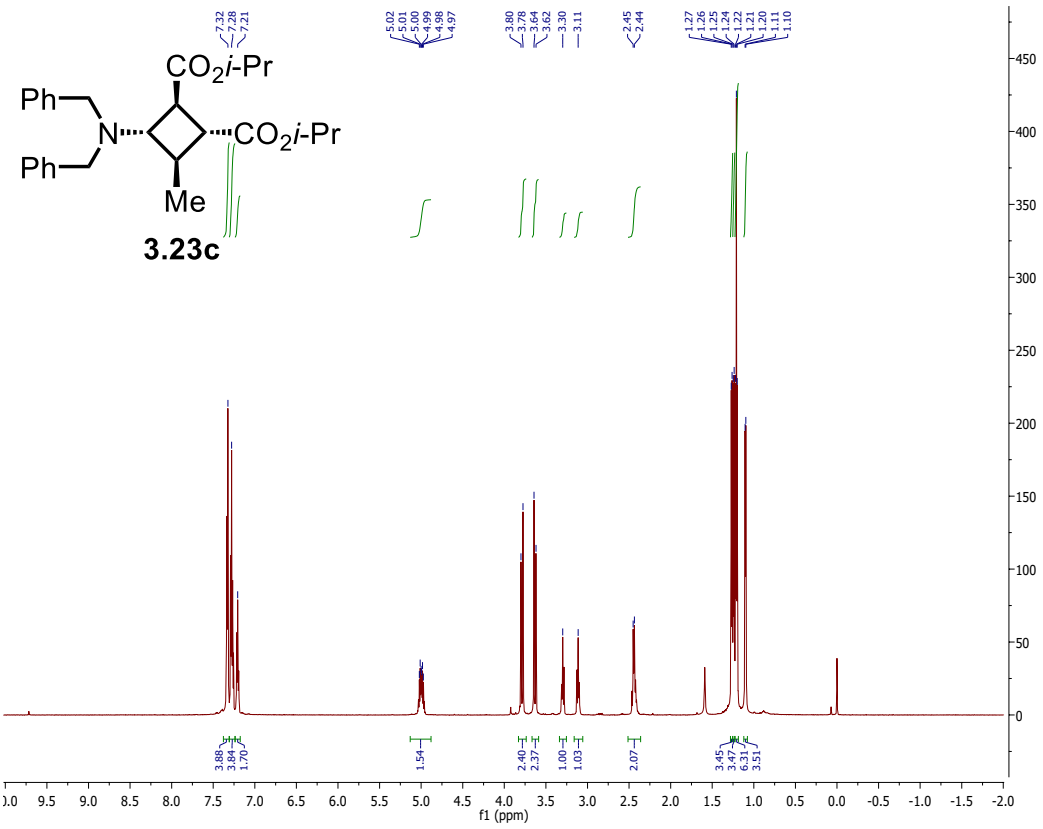
CO2i-Pr
Ph
N
Ph
CO2i-Pr
Me
3.23c
f1 (ppm)

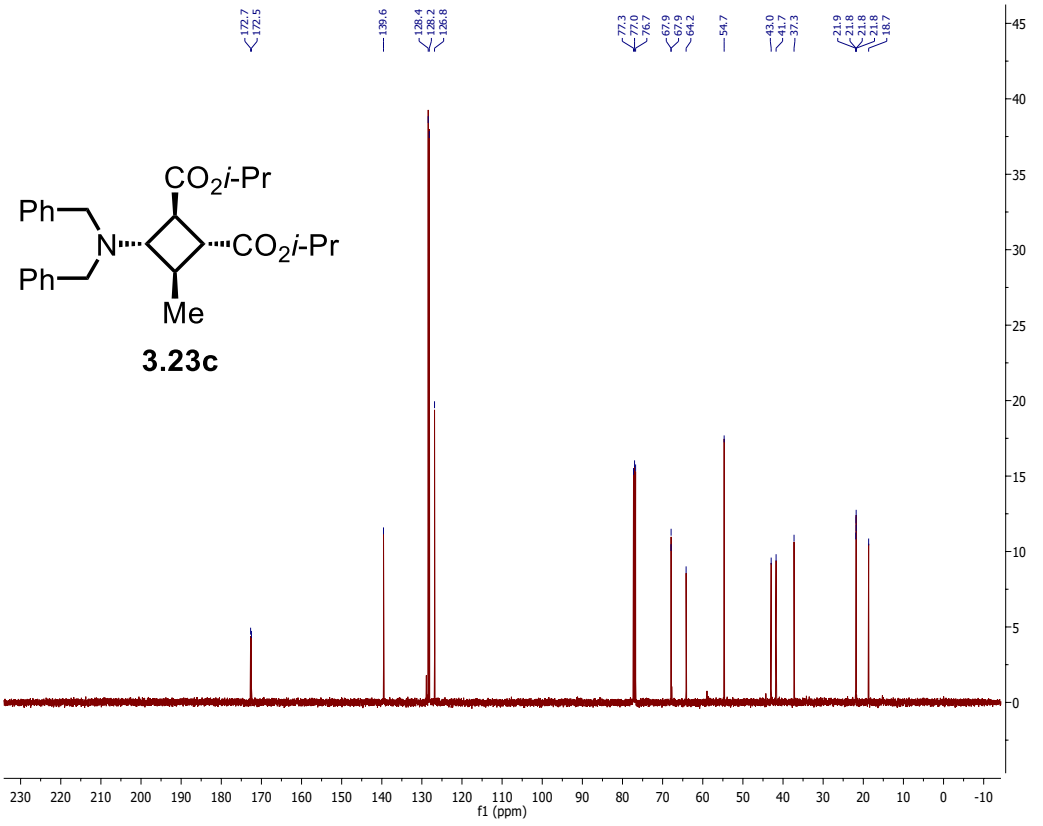
CO2i-Pr
Ph
N
Ph
CO2i-Pr
Me
3.23c
f1 (ppm)

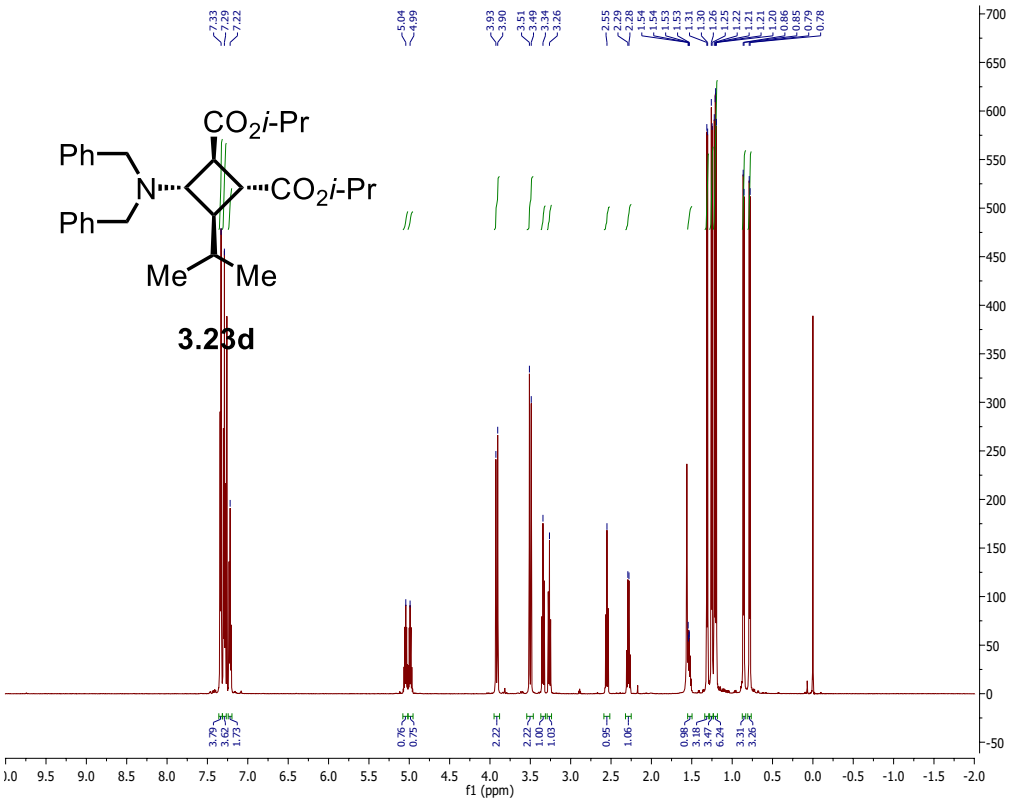
CO2i-Pr
Ph
N
CO2i-Pr
Ph
Me
Me
3.23d
f1 (ppm)

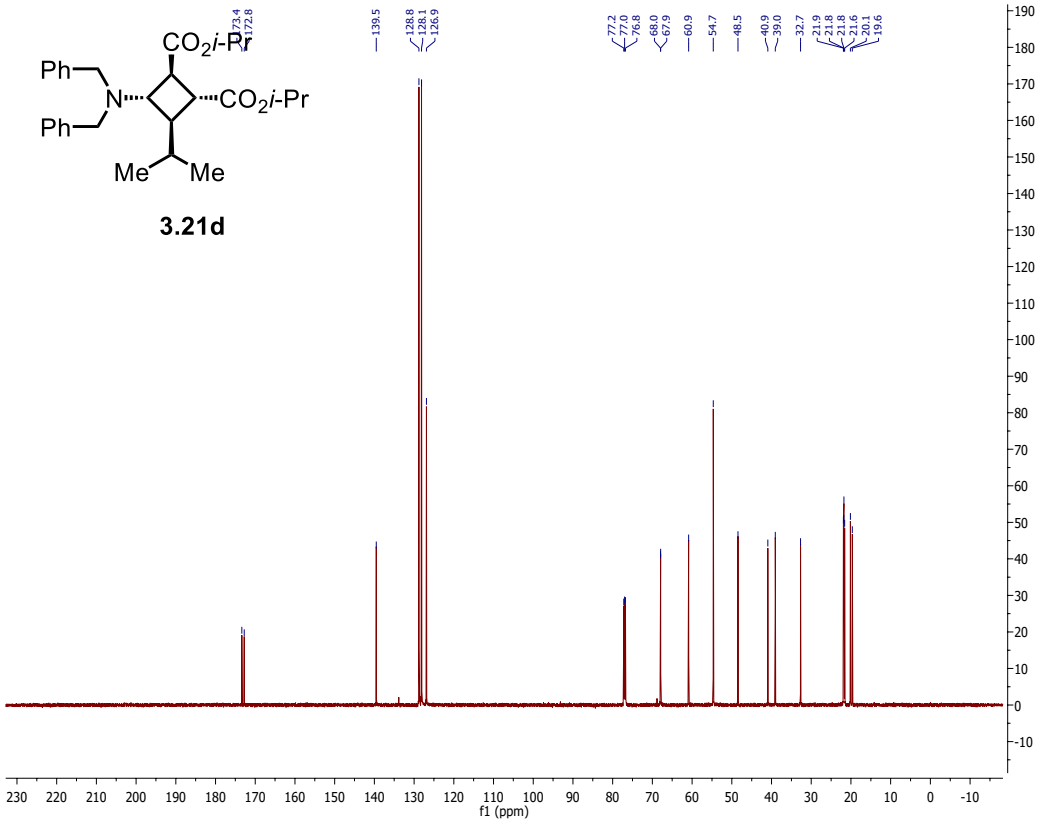
CO2i-Pr
Ph
N
CO2i-Pr
Ph
Me
Me
3.21d
f1 (ppm)

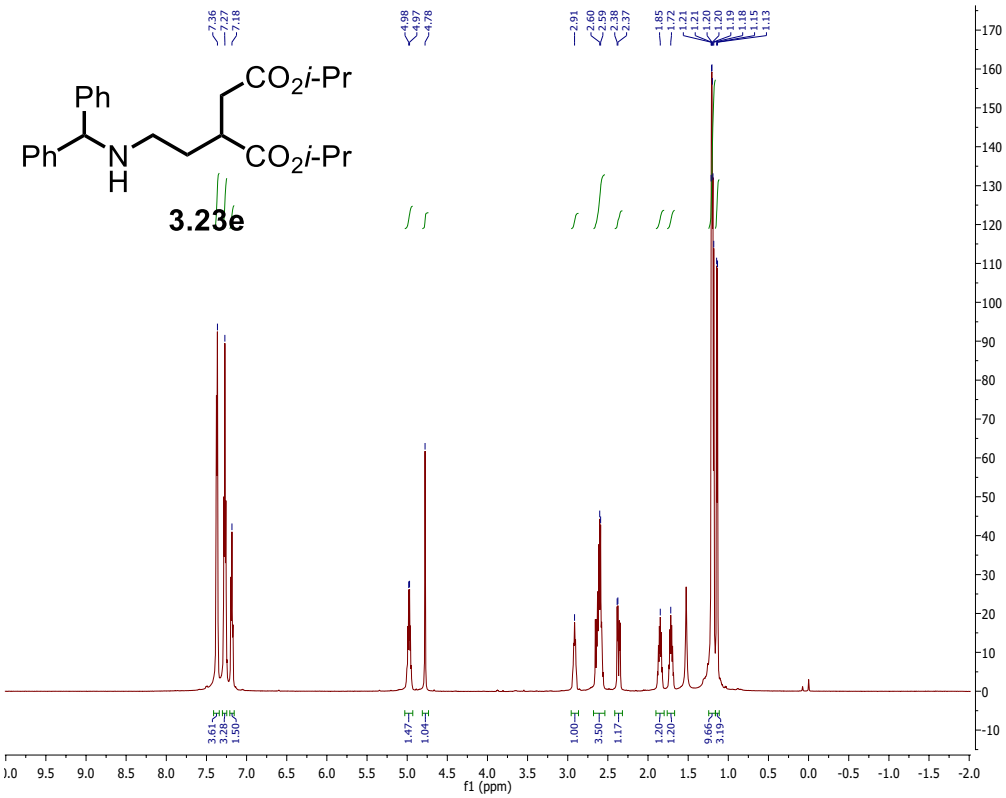
Ph
Ph
N
H
CO2i-Pr
CO2i-Pr
3.23e
f1 (ppm)

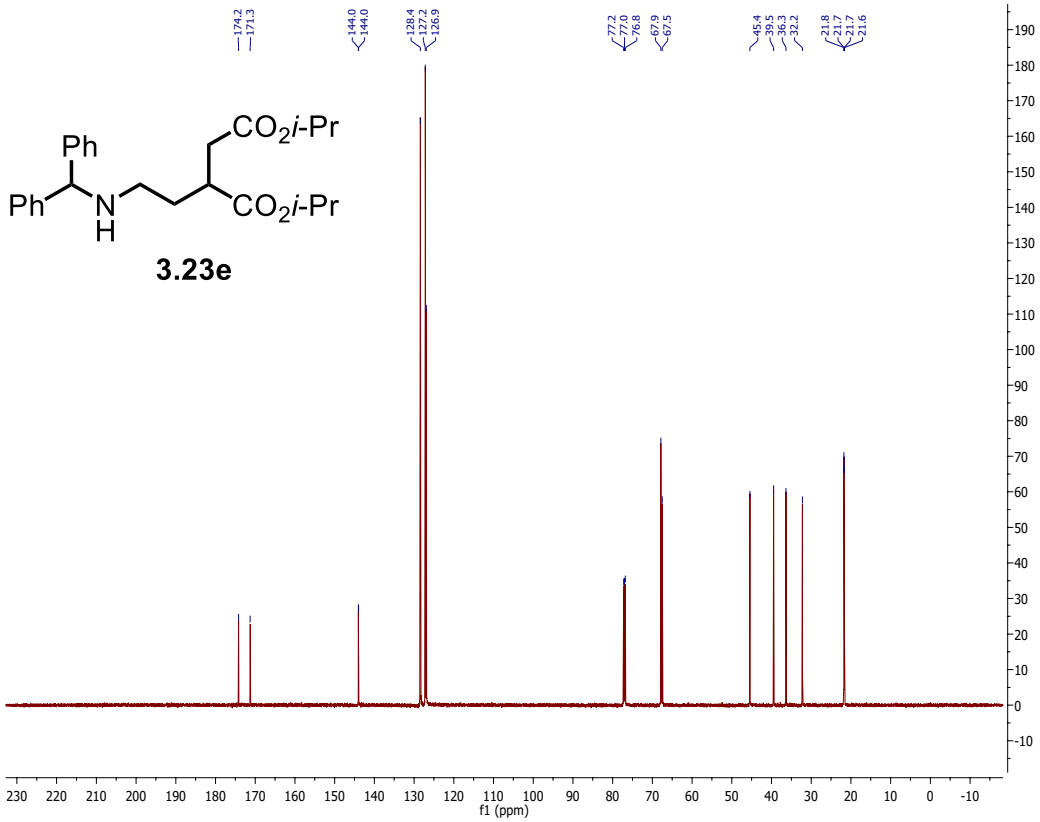
Ph
Ph
N
H
CO2i-Pr
CO2i-Pr
3.23e
f1 (ppm)

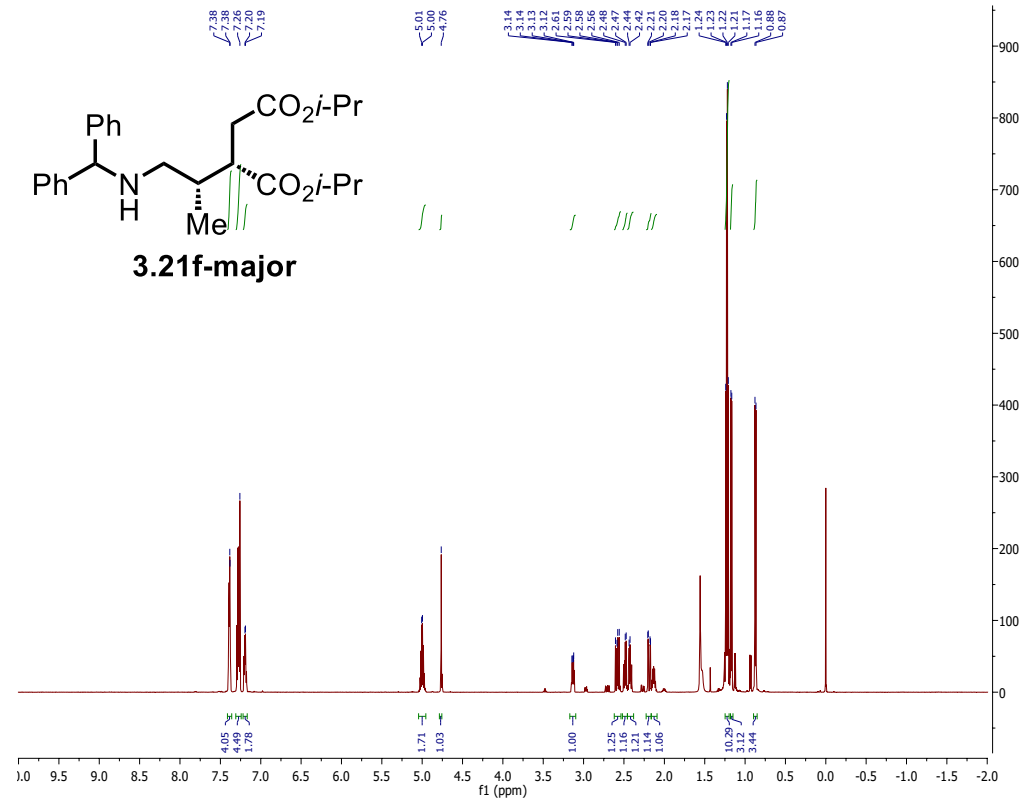
Ph
Ph
N
H
Me
CO2i-Pr
CO2i-Pr
3.21f-major
f1 (ppm)

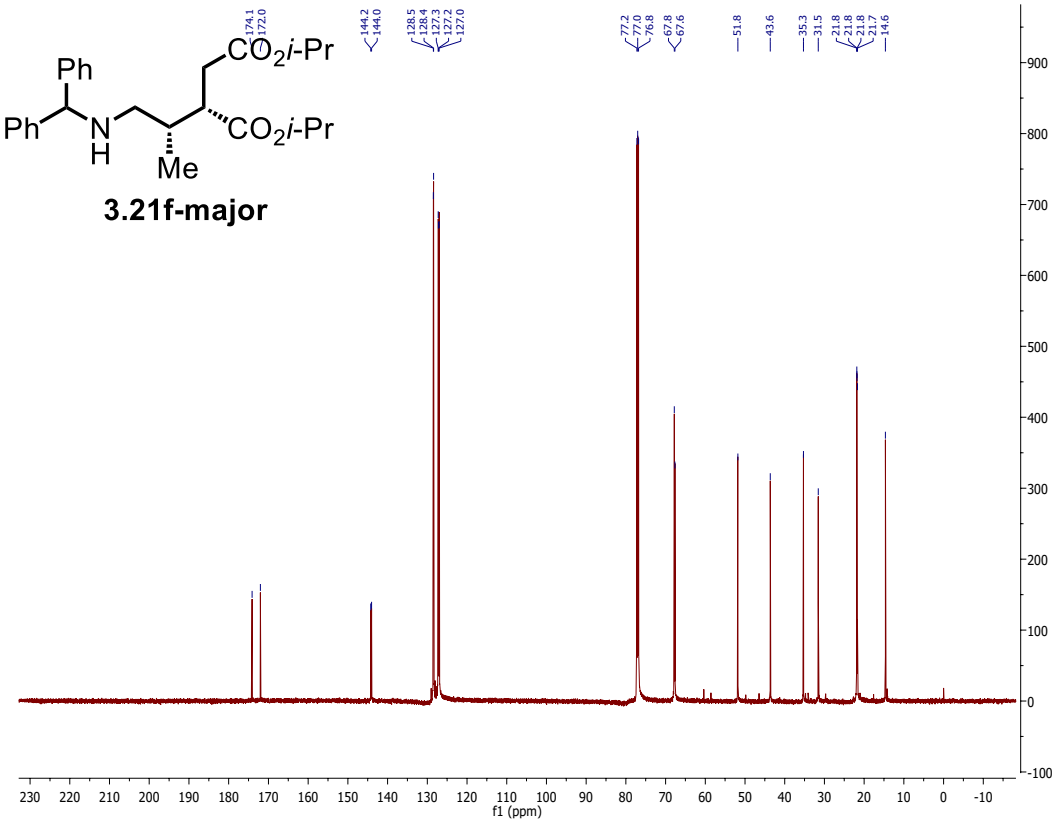
Ph
Ph
N
H
Me
CO2i-Pr
CO2i-Pr
3.21f-major
f1 (ppm)

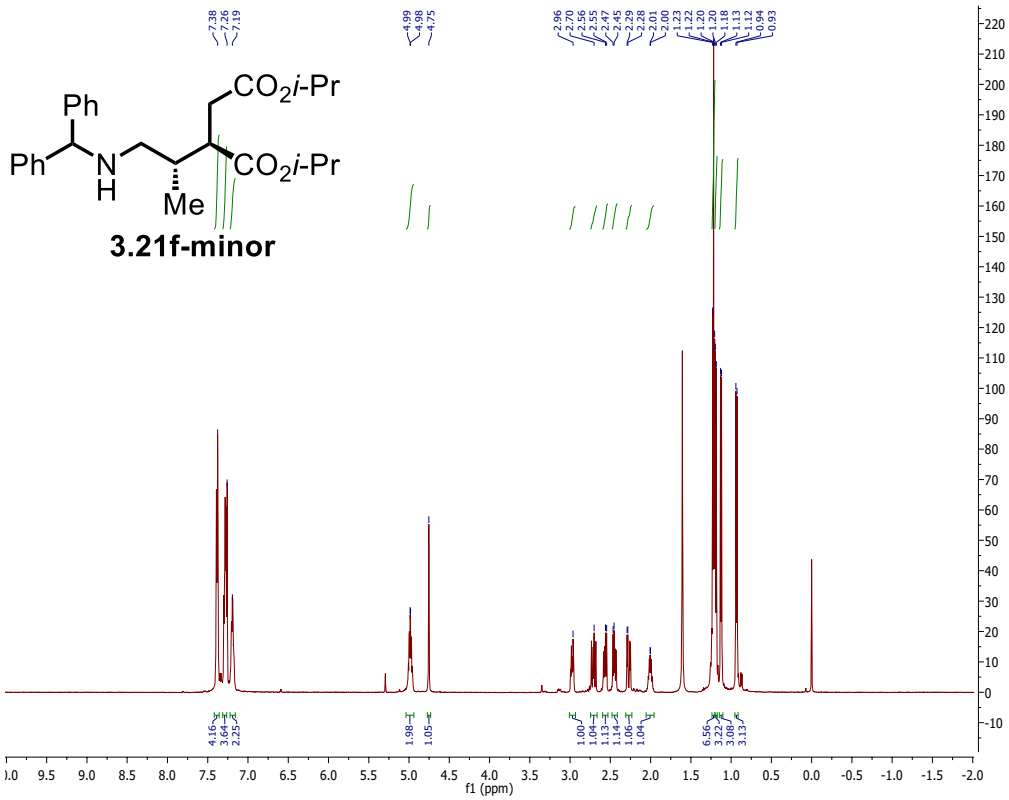
Ph
Ph
N
H
Me
CO2i-Pr
CO2i-Pr
3.21f-minor
f1 (ppm)

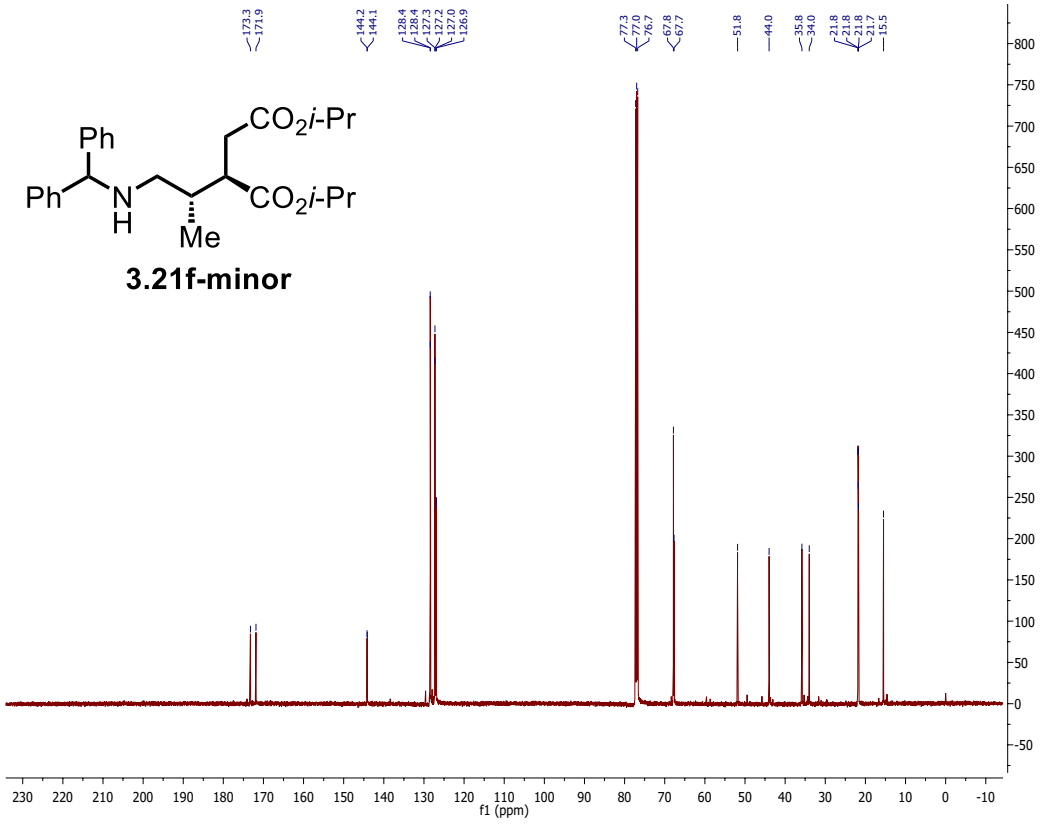
Ph
Ph
N
H
Me
CO2i-Pr
CO2i-Pr
3.21f-minor
f1 (ppm)

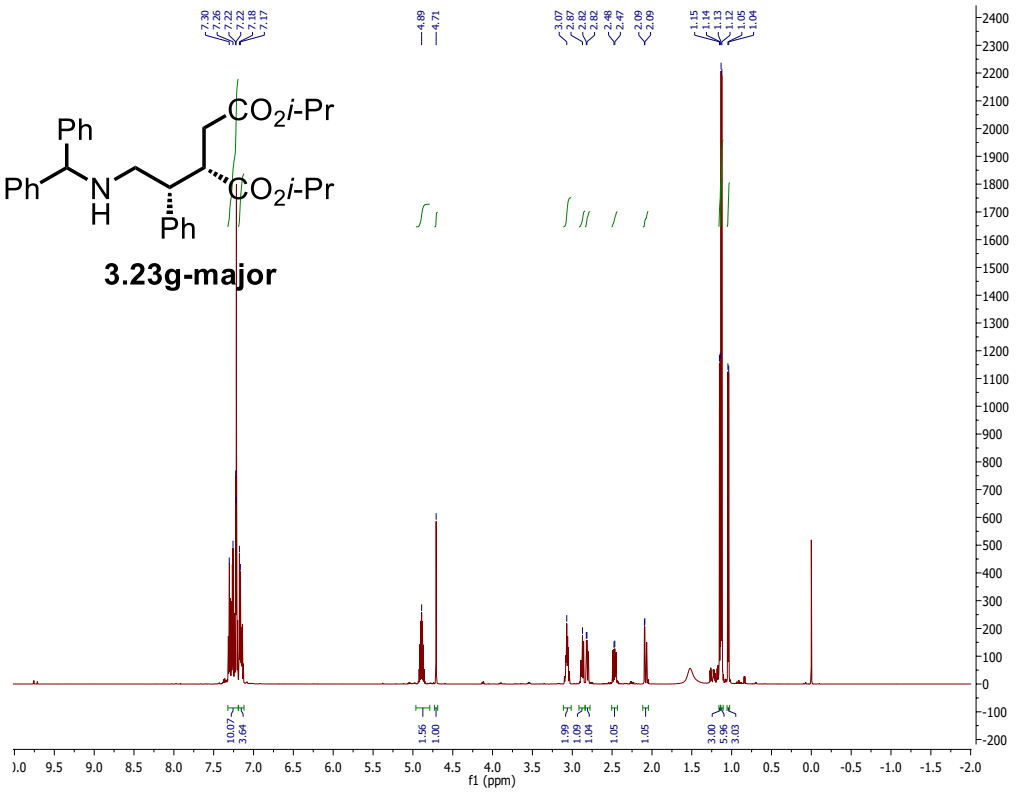
Ph
Ph
N
H
Ph
CO2i-Pr
CO2i-Pr
3.23g-major
f1 (ppm)

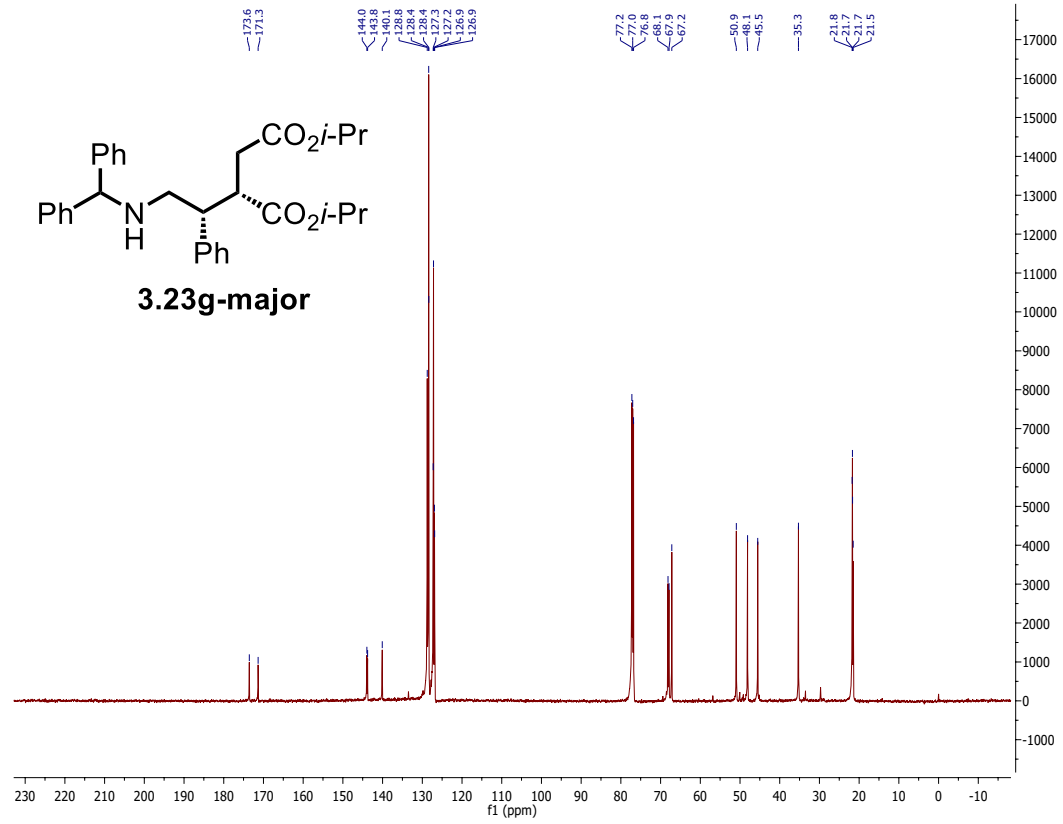
Ph
Ph
N
H
Ph
CO2i-Pr
CO2i-Pr
3.23g-major
f1 (ppm)

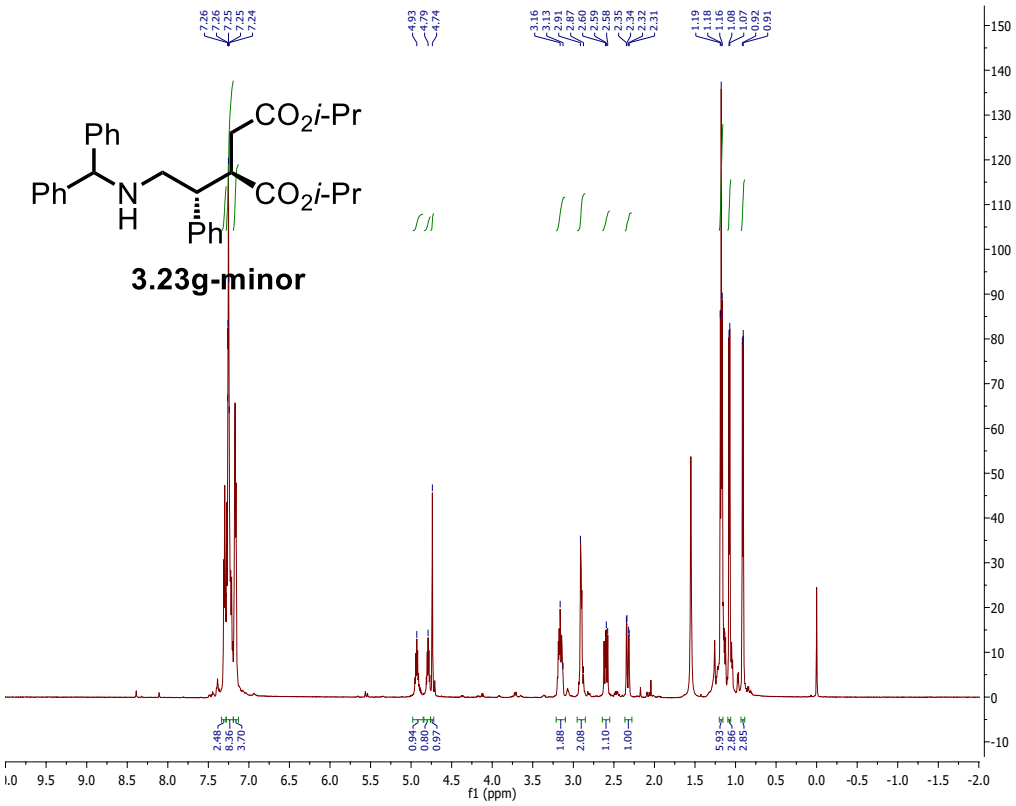
7.26
7.26
7.25
7.25
7.25
7.24
4.93
4.79
4.74
3.16
3.13
2.91
2.87
2.60
2.59
2.58
2.35
2.34
2.32
2.31
1.19
1.18
1.16
1.08
1.07
0.92
0.91
Ph
Ph
N
H
Ph
CO2i-Pr
CO2i-Pr
3.23g-minor
2.48
8.45
3.70
0.94
0.80
0.97
1.88
2.08
1.10
1.00
5.93
2.86
2.85
f1 (ppm)

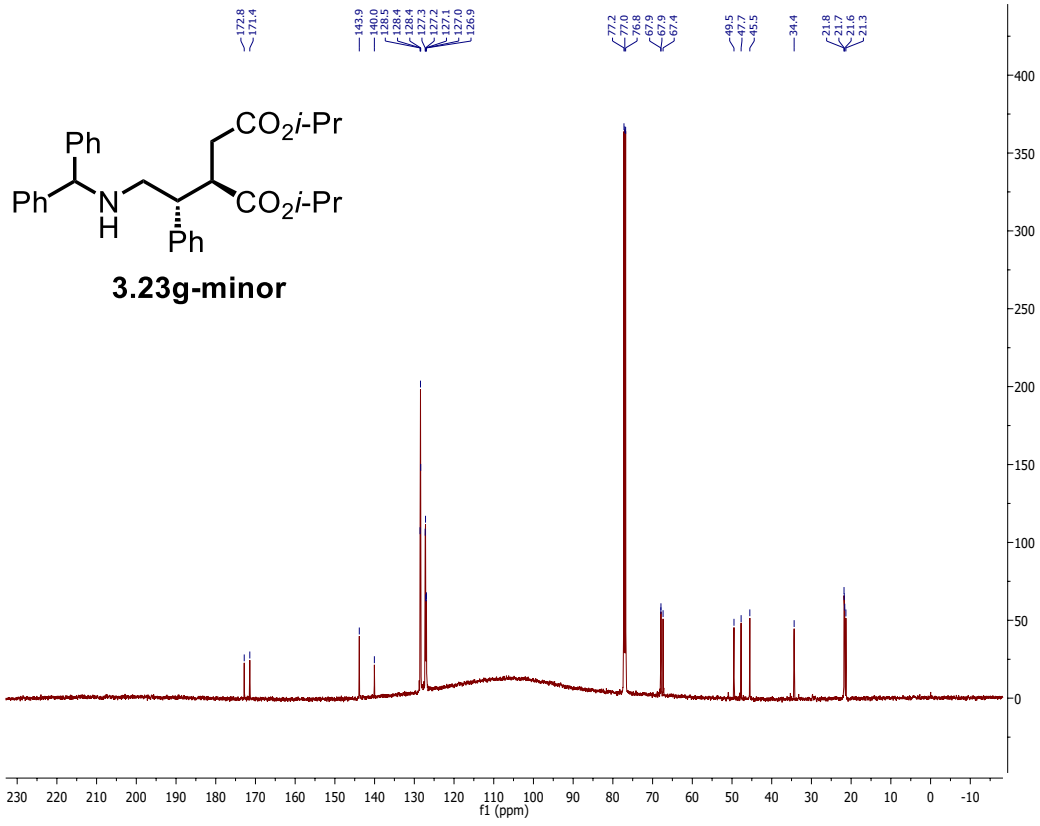
172.8
171.4
143.9
140.0
128.5
128.4
128.4
127.3
127.2
127.1
127.0
126.9
77.2
77.0
76.8
67.9
67.9
67.9
67.4
49.5
47.7
45.5
34.4
21.8
21.7
21.6
21.3
Ph
Ph
N
H
Ph
CO2i-Pr
CO2i-Pr
3.23g-minor
f1 (ppm)

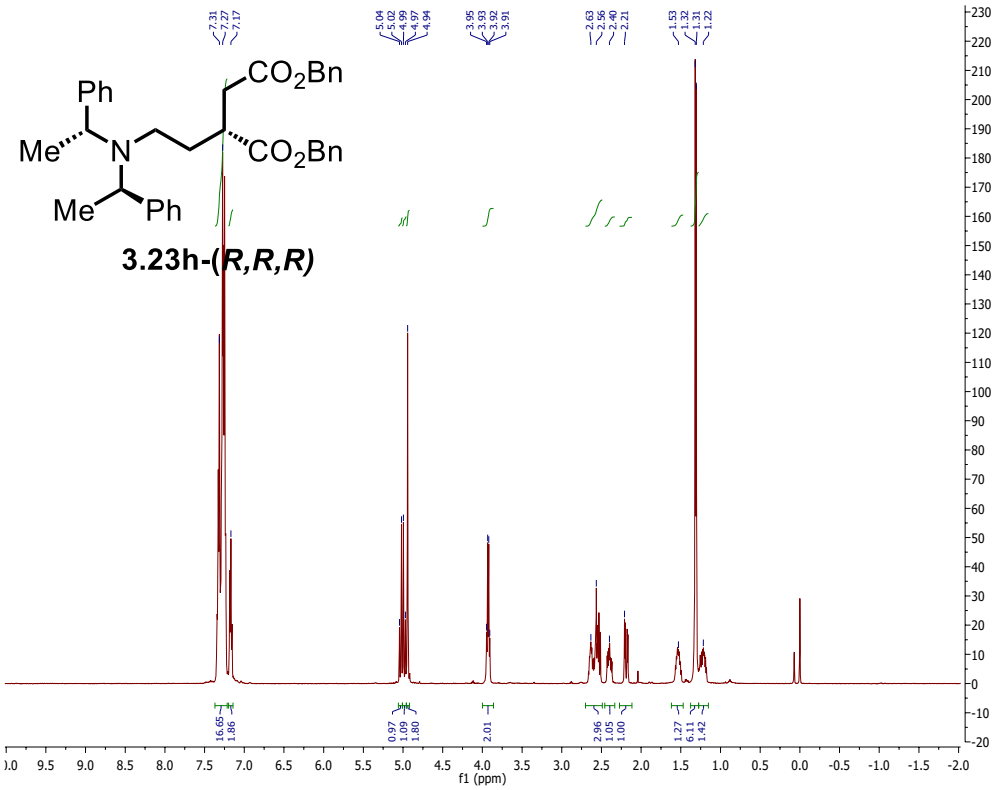
Ph
Me
N
Me
Ph
CO2Bn
CO2Bn
3.23h-(R,R,R)
f1 (ppm)

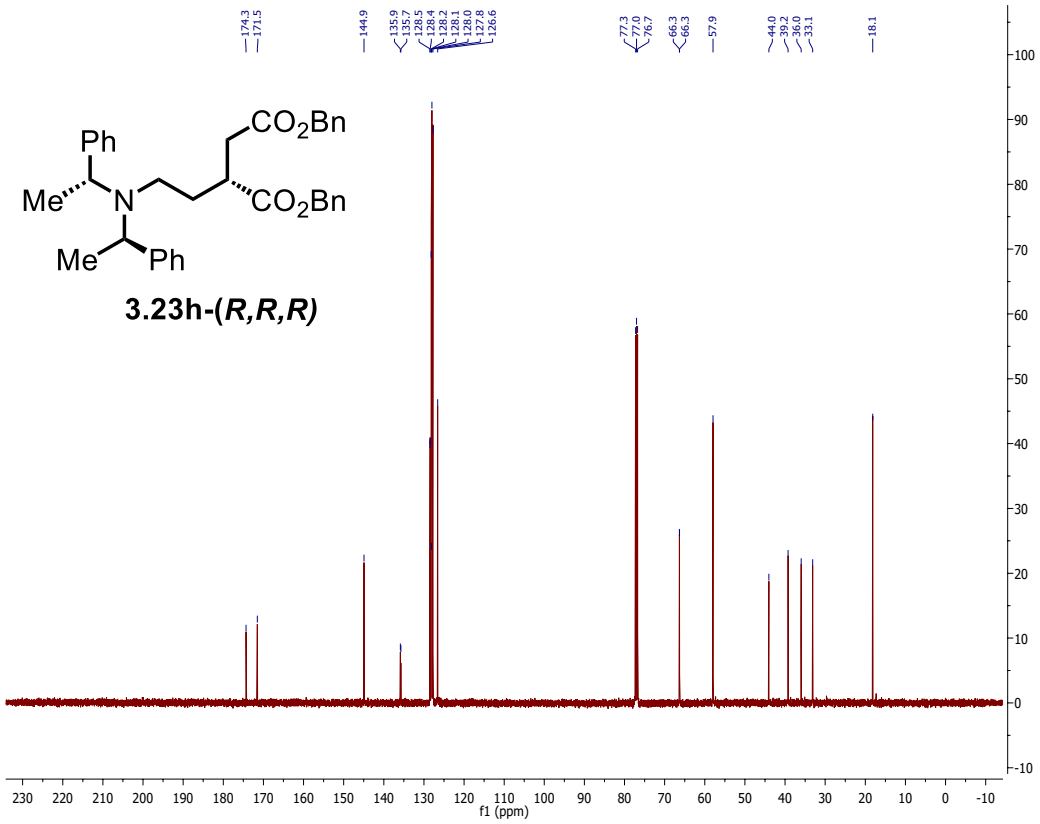
Ph
Me
N
Me
Ph
CO2Bn
CO2Bn
3.23h-(R,R,R)
f1 (ppm)

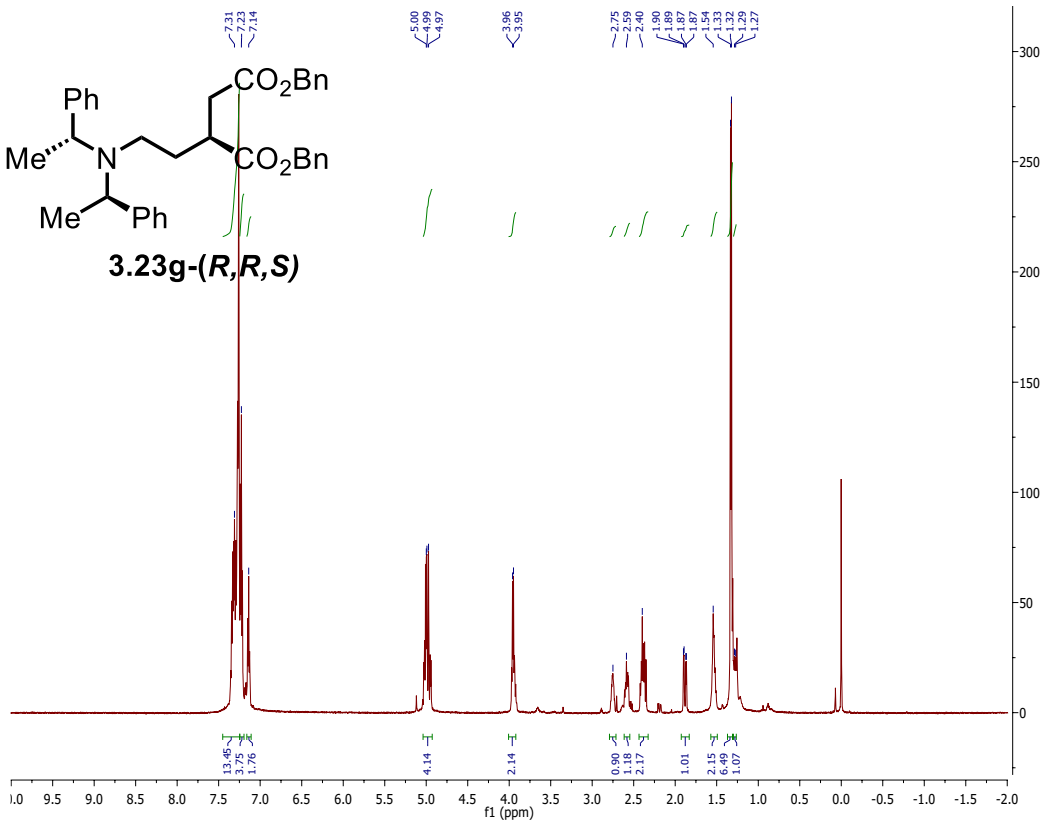
Ph
Me
N
Me
Ph
CO2Bn
CO2Bn
3.23g-(R,R,S)
f1 (ppm)

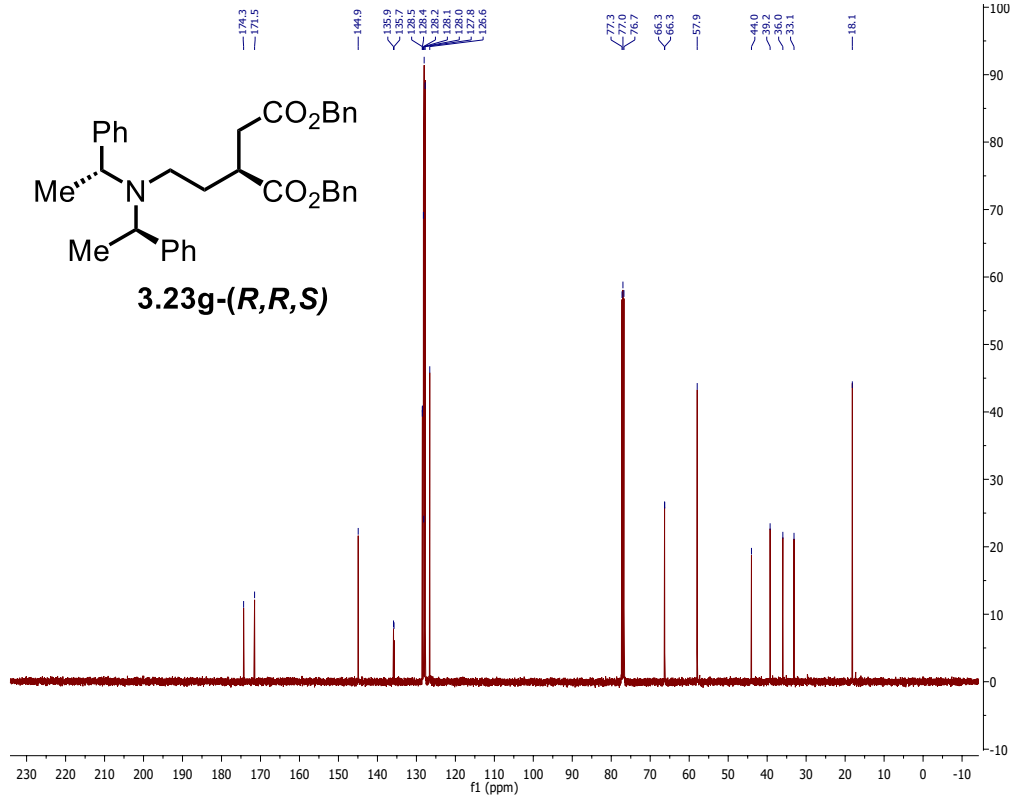
Ph
Me
N
Me
Ph
CO2Bn
CO2Bn
3.23g-(R,R,S)
f1 (ppm)

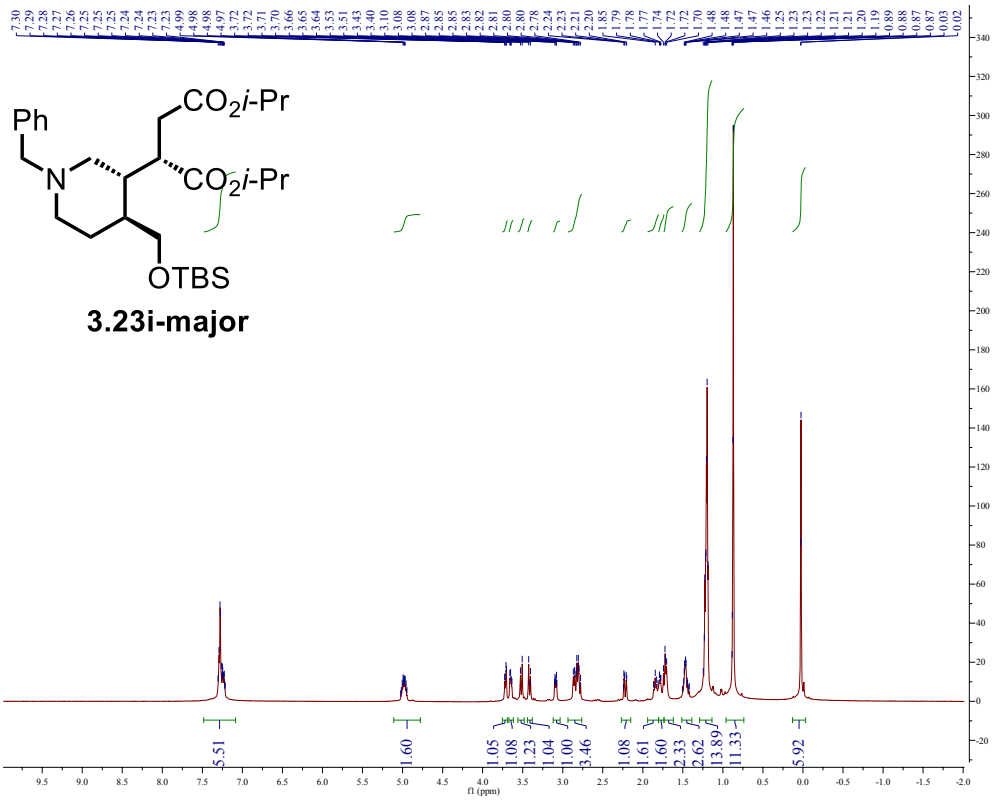
Ph
N
CO2i-Pr
CO2i-Pr
OTBS
3.23i-major
5.51
1.60
1.05
1.08
1.23
1.04
1.00
3.46
1.08
1.61
1.60
2.33
2.62
13.89
11.33
5.92
f1 (ppm)

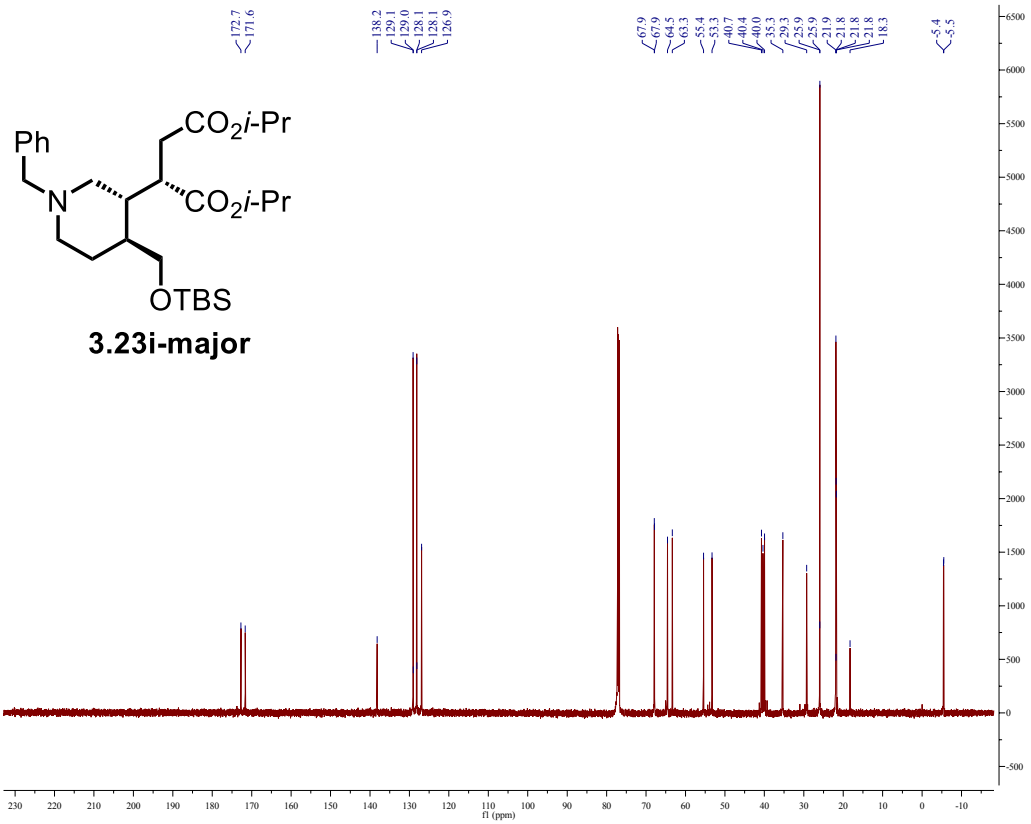
Ph
N
CO2i-Pr
CO2i-Pr
OTBS
3.23i-major
f1 (ppm)

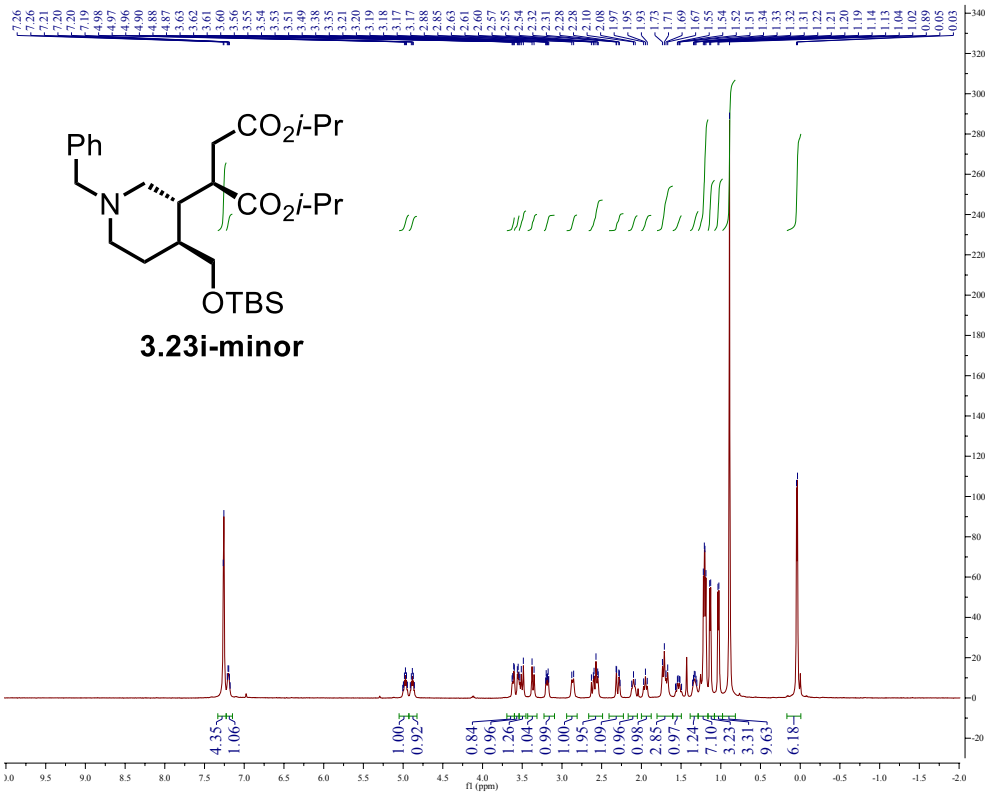
Ph
N
CO2i-Pr
CO2i-Pr
OTBS
3.23i-minor

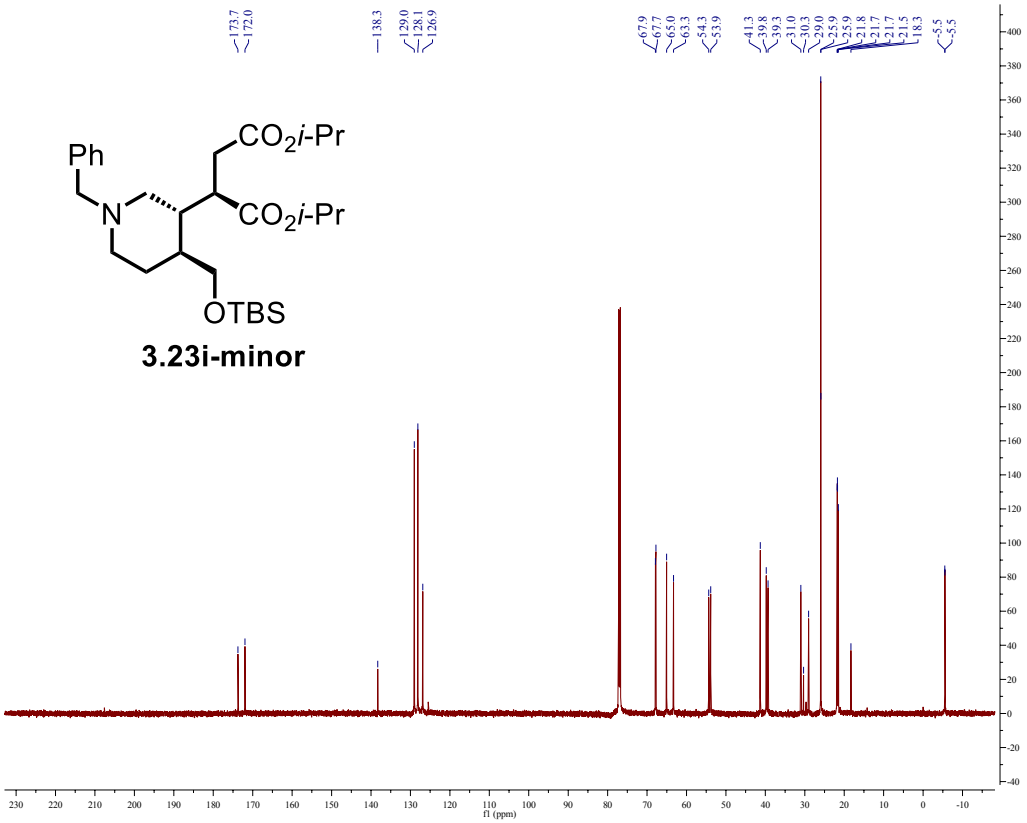
Ph
N
CO2i-Pr
CO2i-Pr
OTBS
3.23i-minor

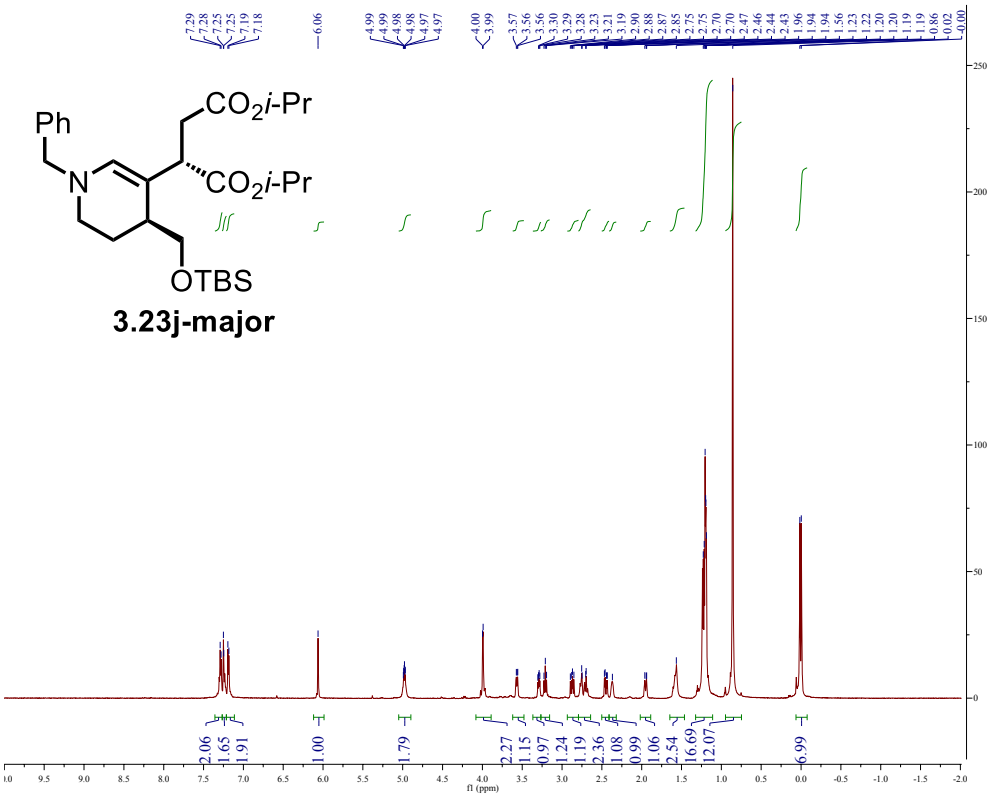
Ph
N
CO2i-Pr
CO2i-Pr
OTBS
3.23j-major

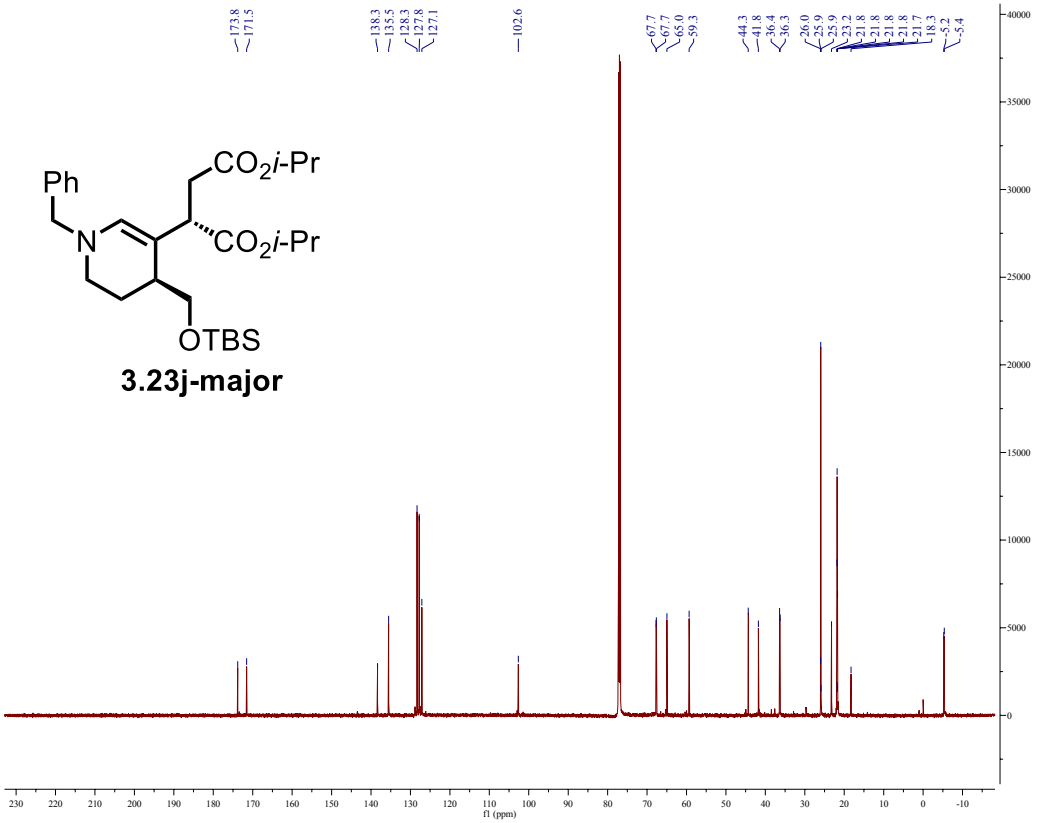
Ph
N
CO2i-Pr
CO2i-Pr
OTBS
3.23j-major

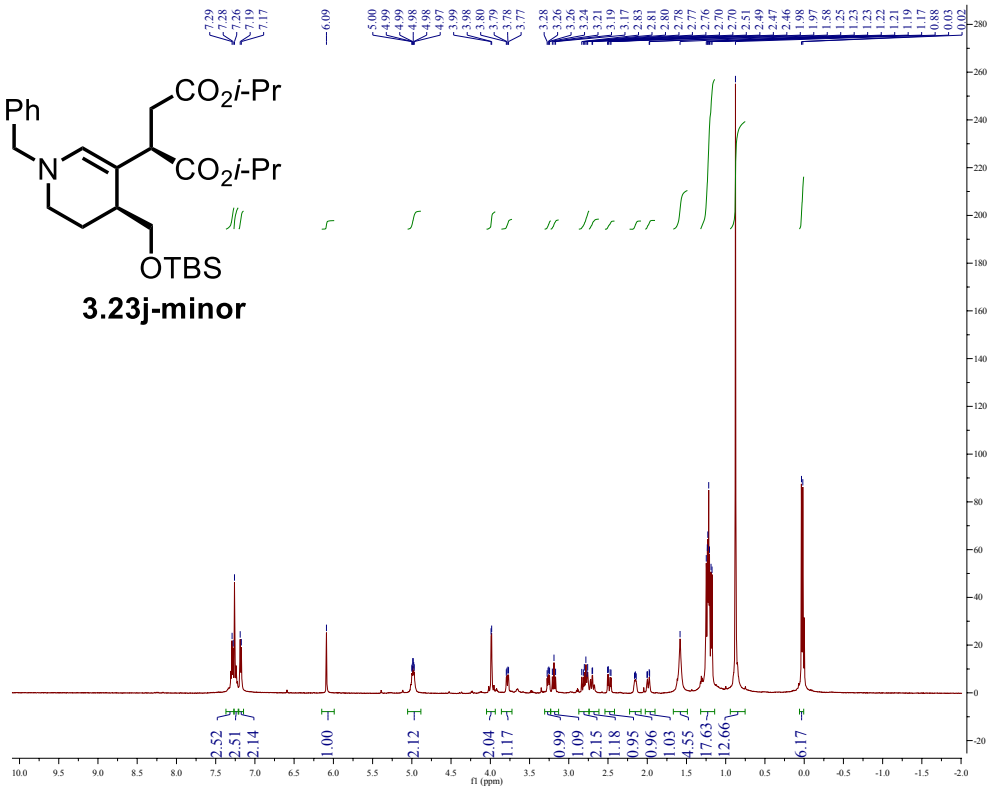
Ph
N
CO2i-Pr
CO2i-Pr
OTBS
3.23j-minor

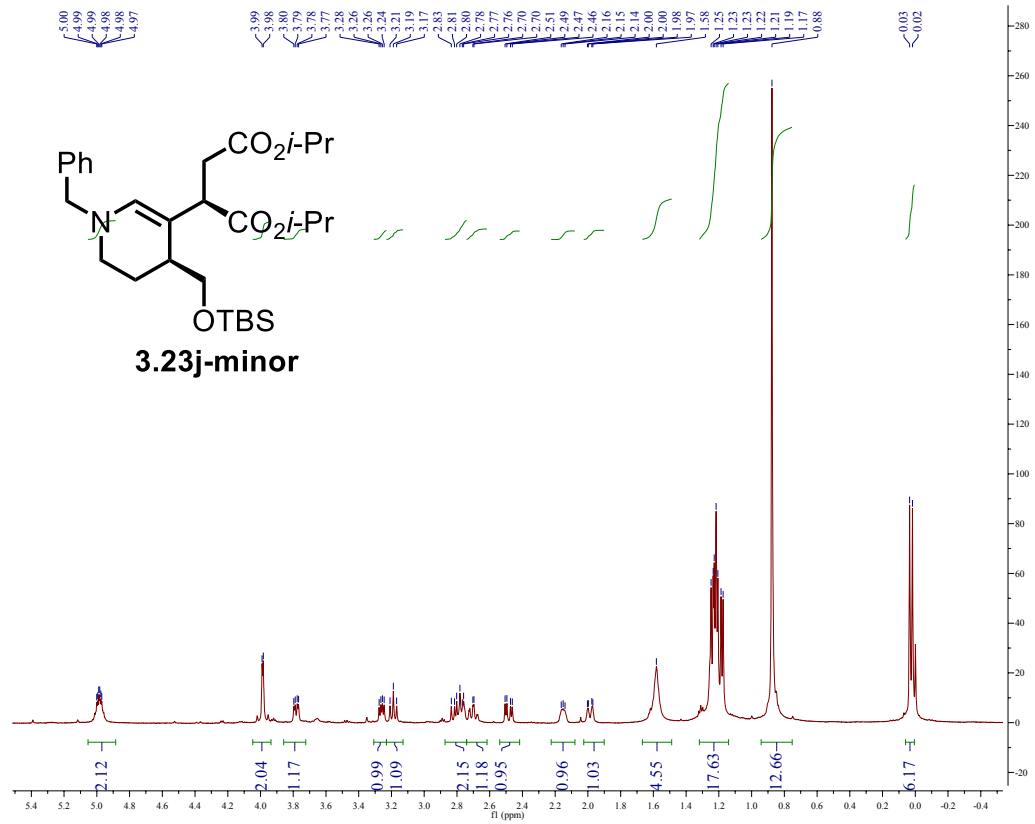
Ph
N
CO2i-Pr
CO2i-Pr
OTBS
3.23j-minor

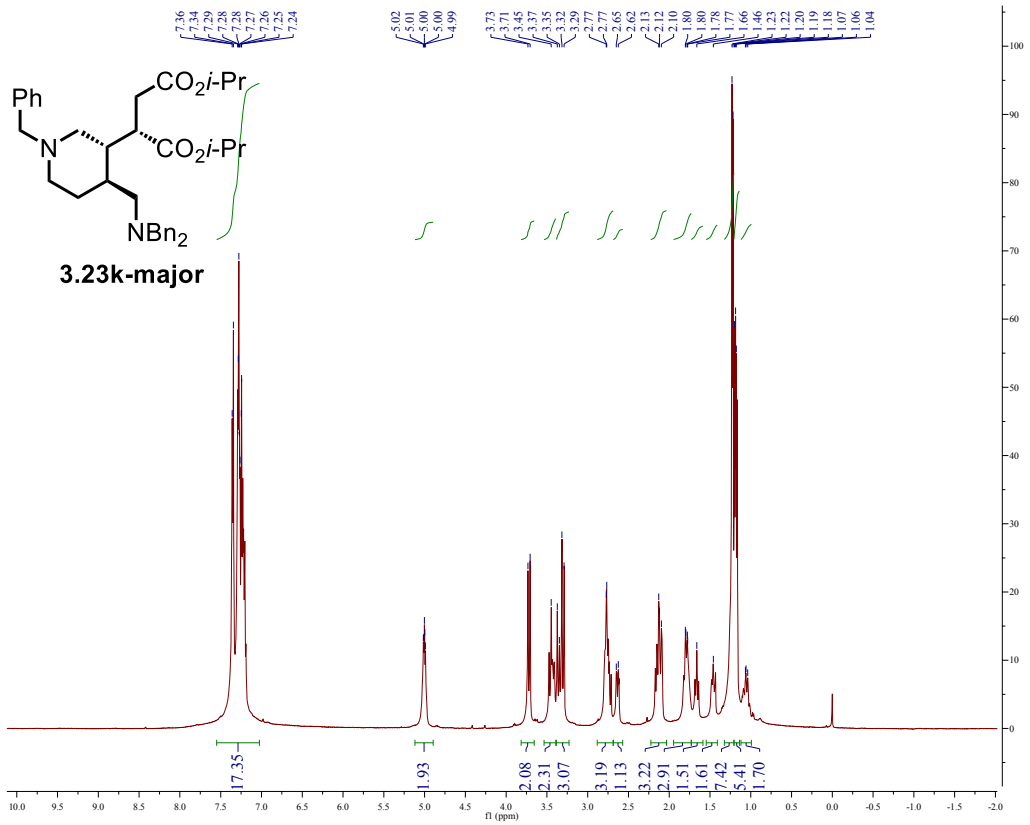
Ph
N
CO2i-Pr
CO2i-Pr
NBn2
3.23k-major
f1 (ppm)

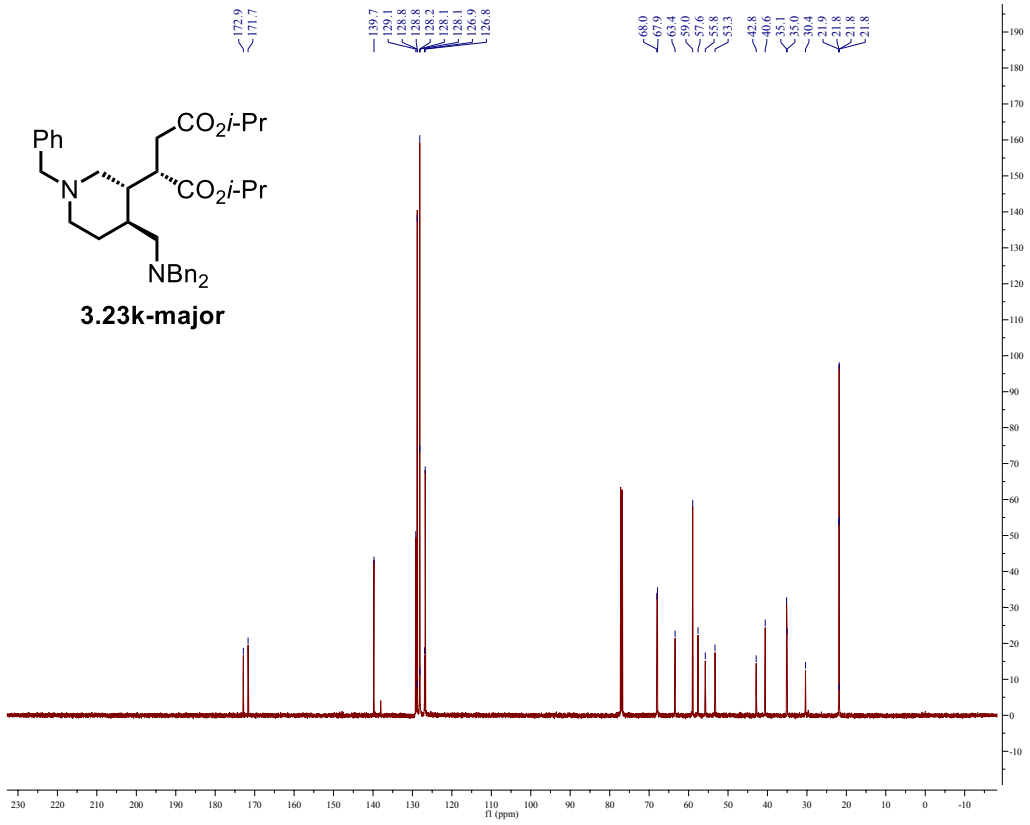
Ph
N
CO2i-Pr
CO2i-Pr
NBn2
3.23k-major
f1 (ppm)

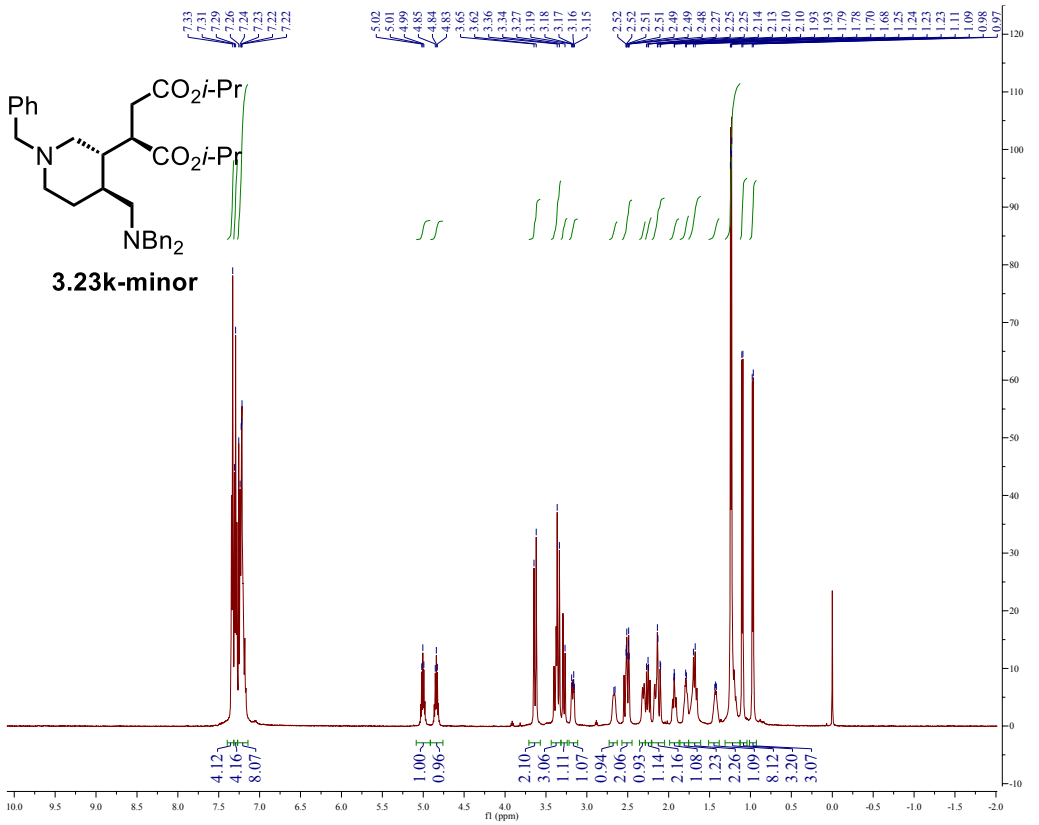
Ph
N
CO2i-Pr
CO2i-Pr
NBn2
3.23k-minor
f1 (ppm)

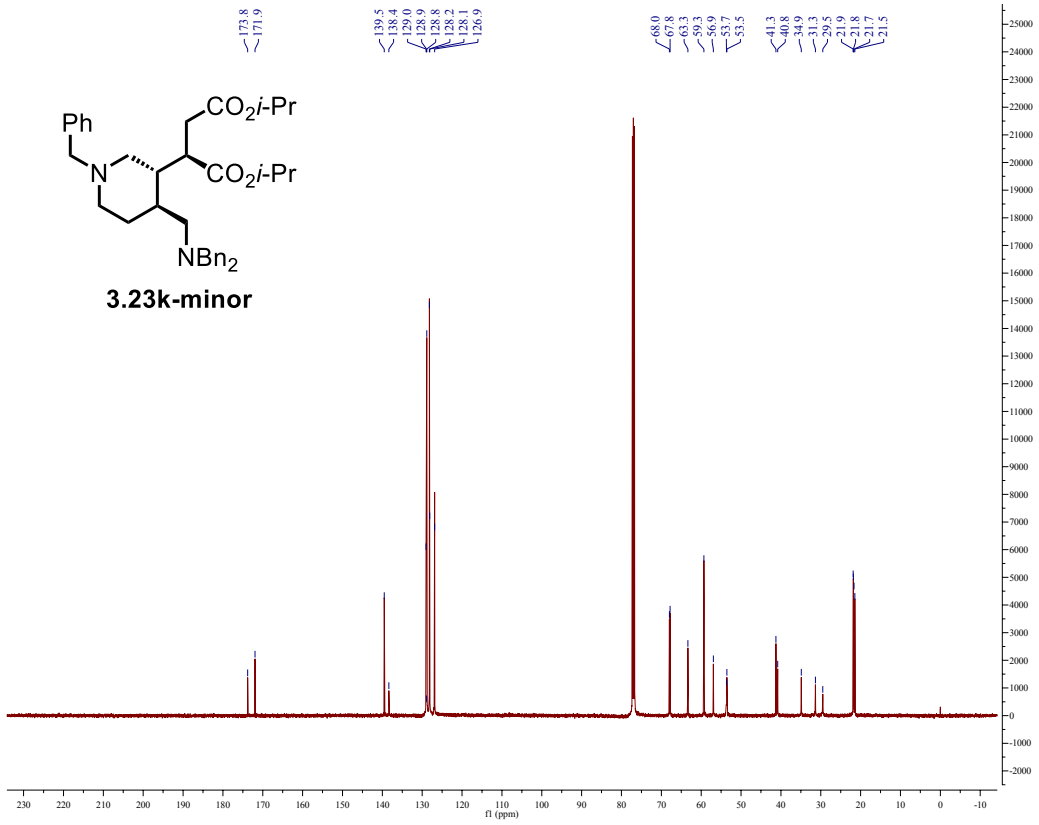
Ph
N
CO2i-Pr
CO2i-Pr
NBn2
3.23k-minor
f1 (ppm)

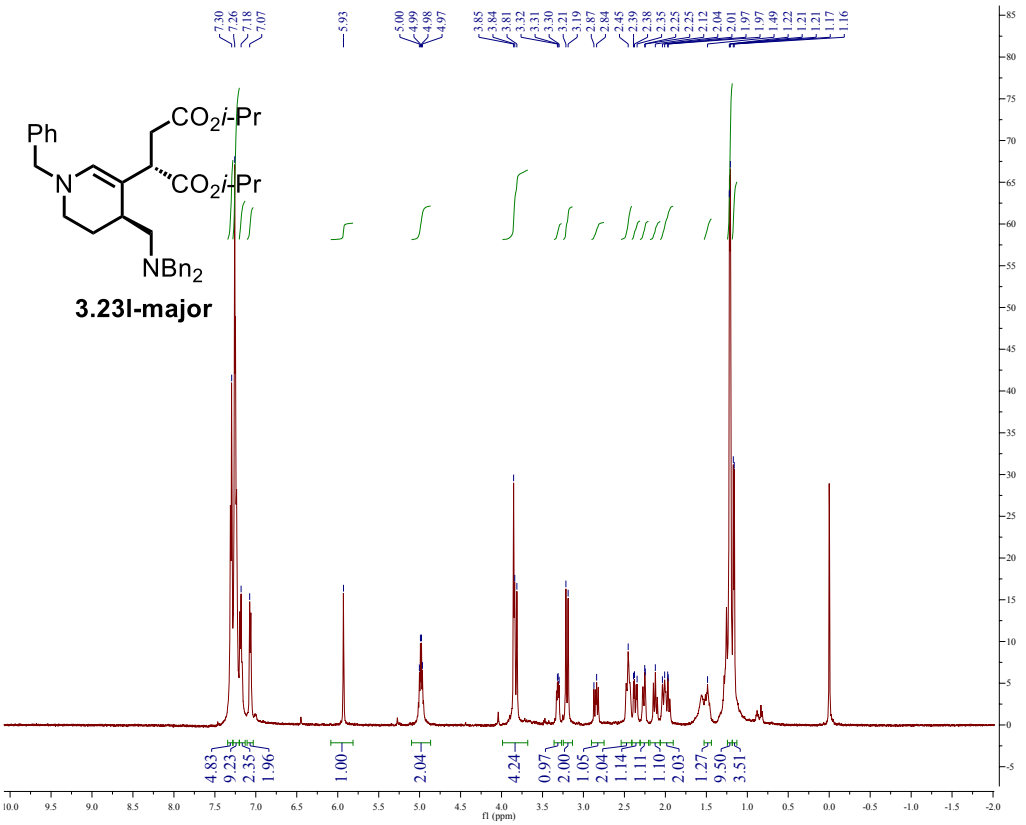
Ph
N
CO2i-Pr
CO2i-Pr
NBn2
3.23l-major

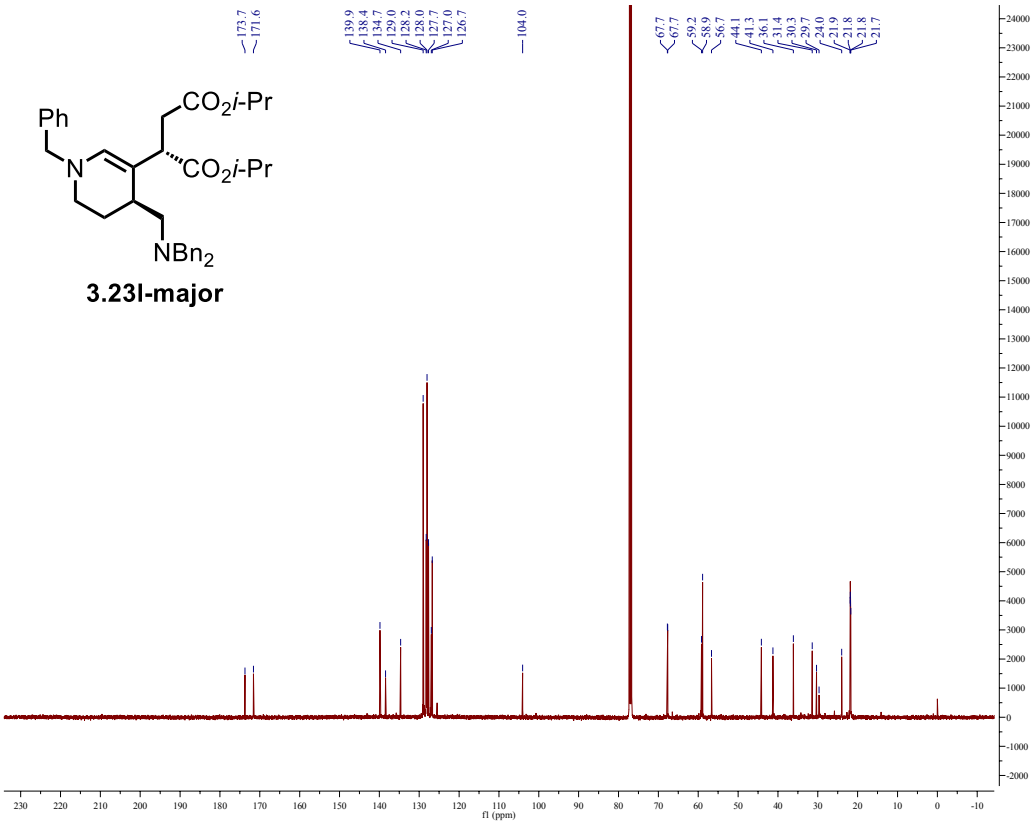
Ph
N
CO2i-Pr
CO2i-Pr
NBn2
3.23l-major

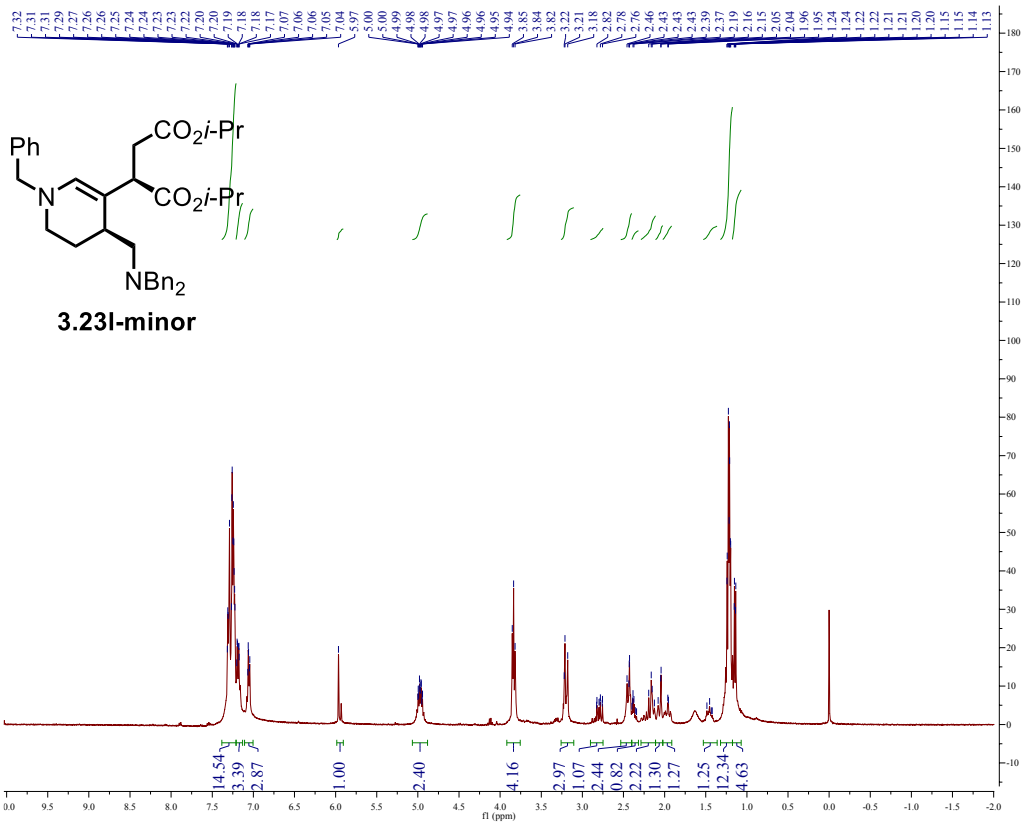

3.23l-minor

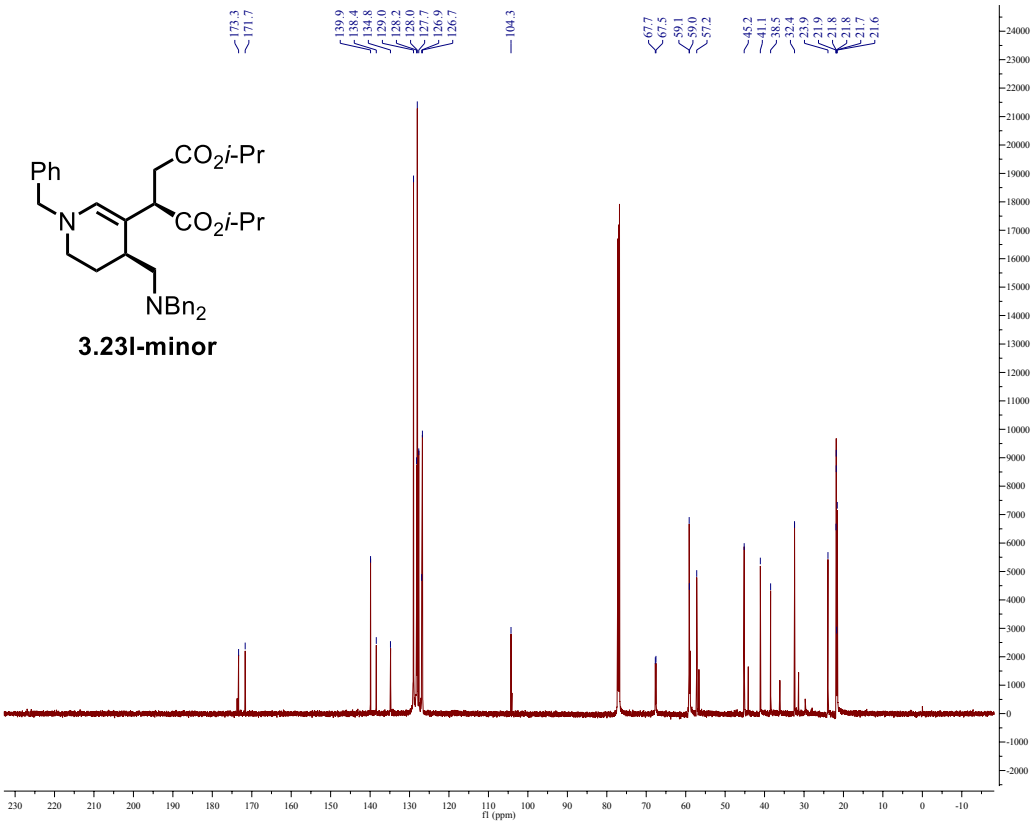

3.23l-minor

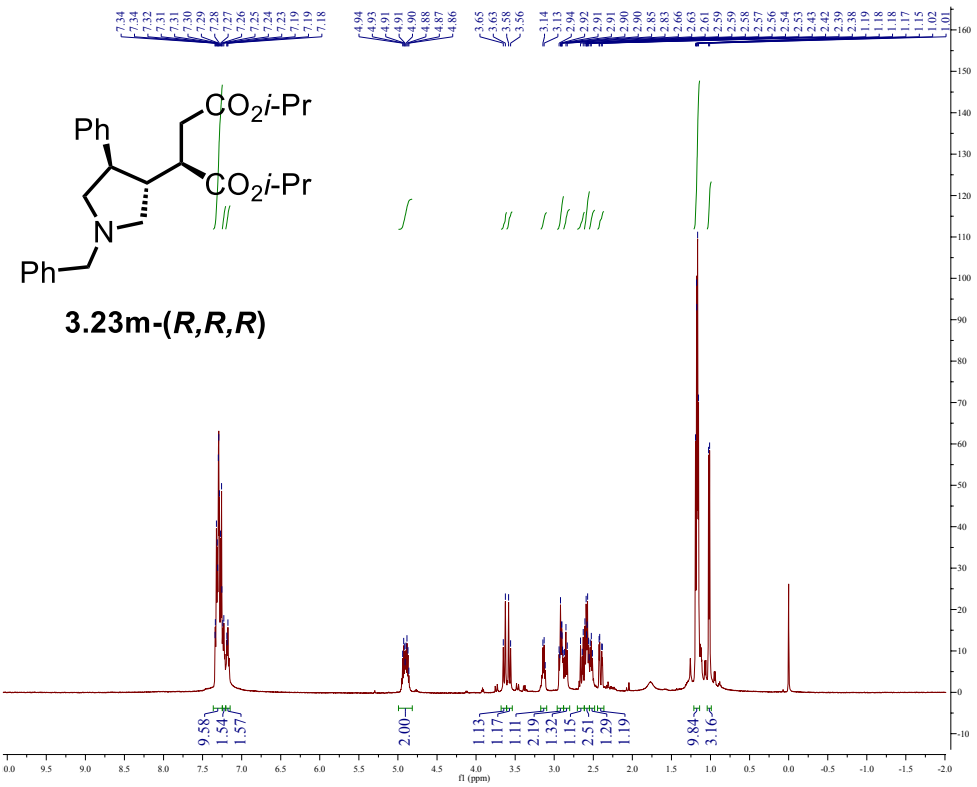
Ph
CO2i-Pr
CO2i-Pr
N
Ph
3.23m-(R,R,R)
fl (ppm)

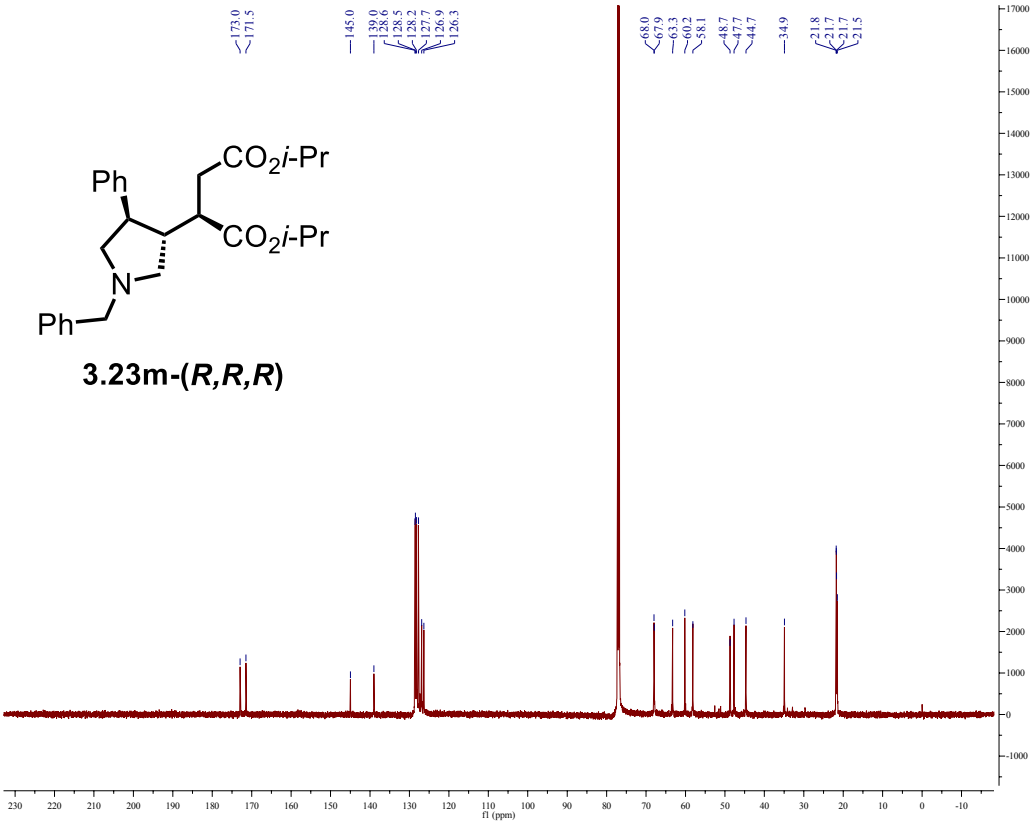
Ph
CO2i-Pr
CO2i-Pr
N
Ph
3.23m-(R,R,R)
fl (ppm)

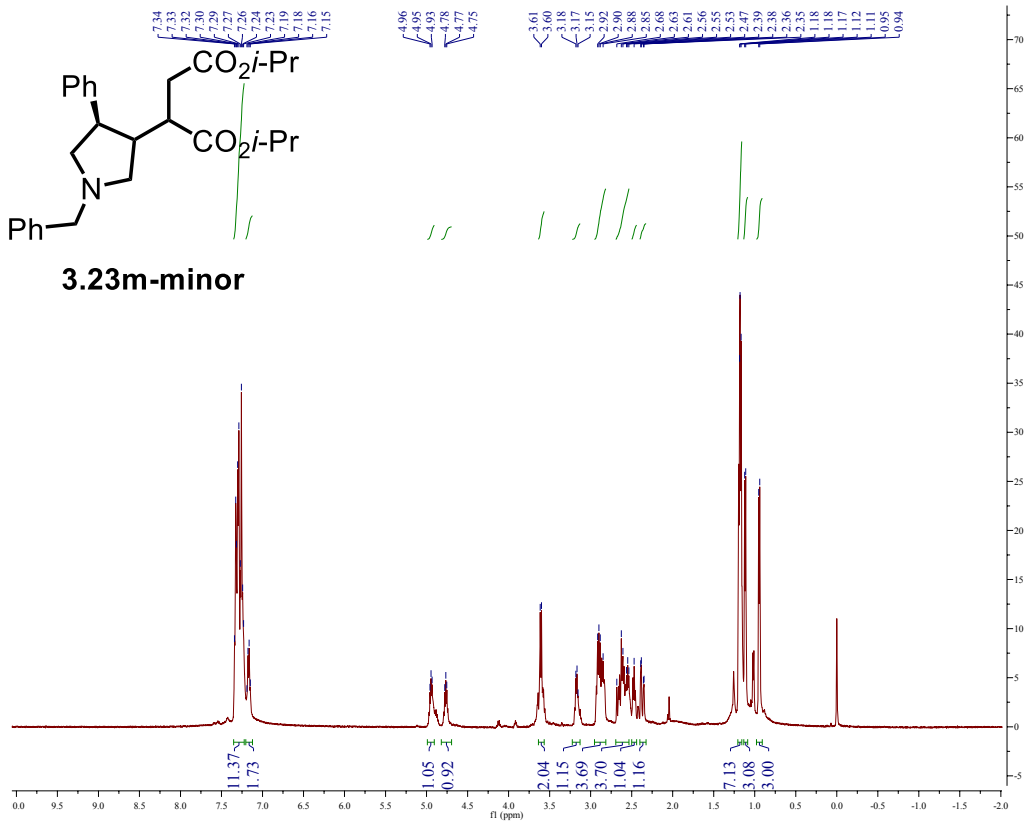
Ph
CO2i-Pr
CO2i-Pr
N
Ph
3.23m-minor
f1 (ppm)

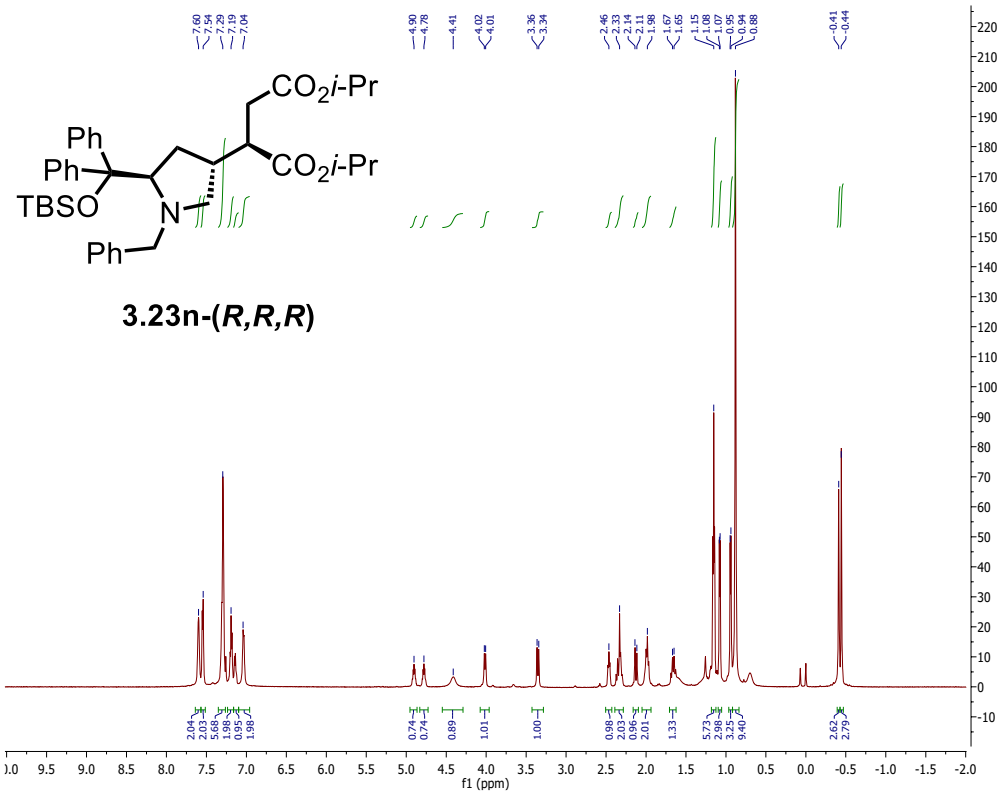

3.23n-(*R,R,R*)

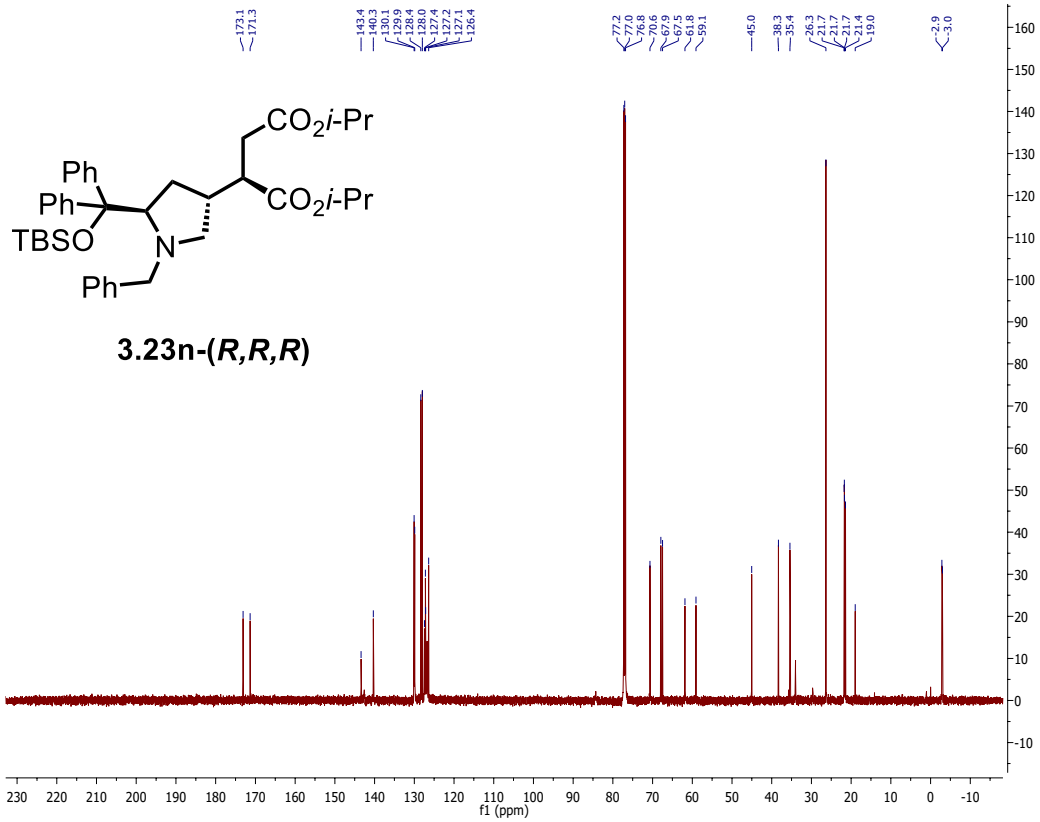

3.23n-(*R,R,R*)

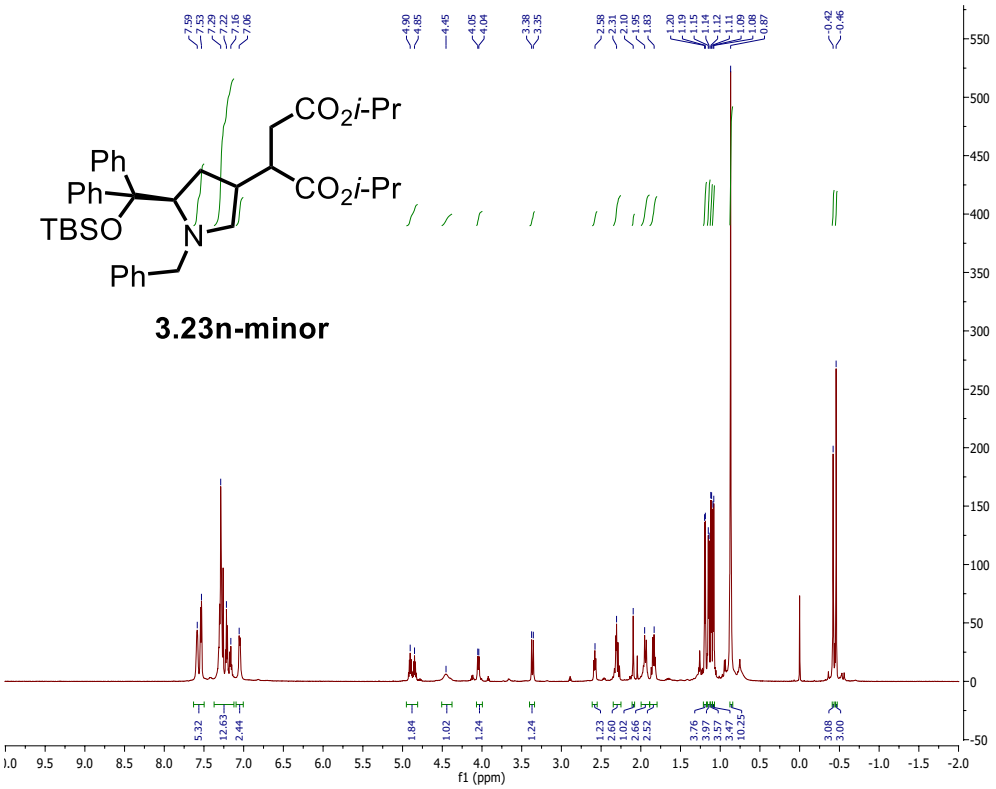
CO2i-Pr
CO2i-Pr
Ph
Ph
TBSO
N
Ph
3.23n-minor
f1 (ppm)

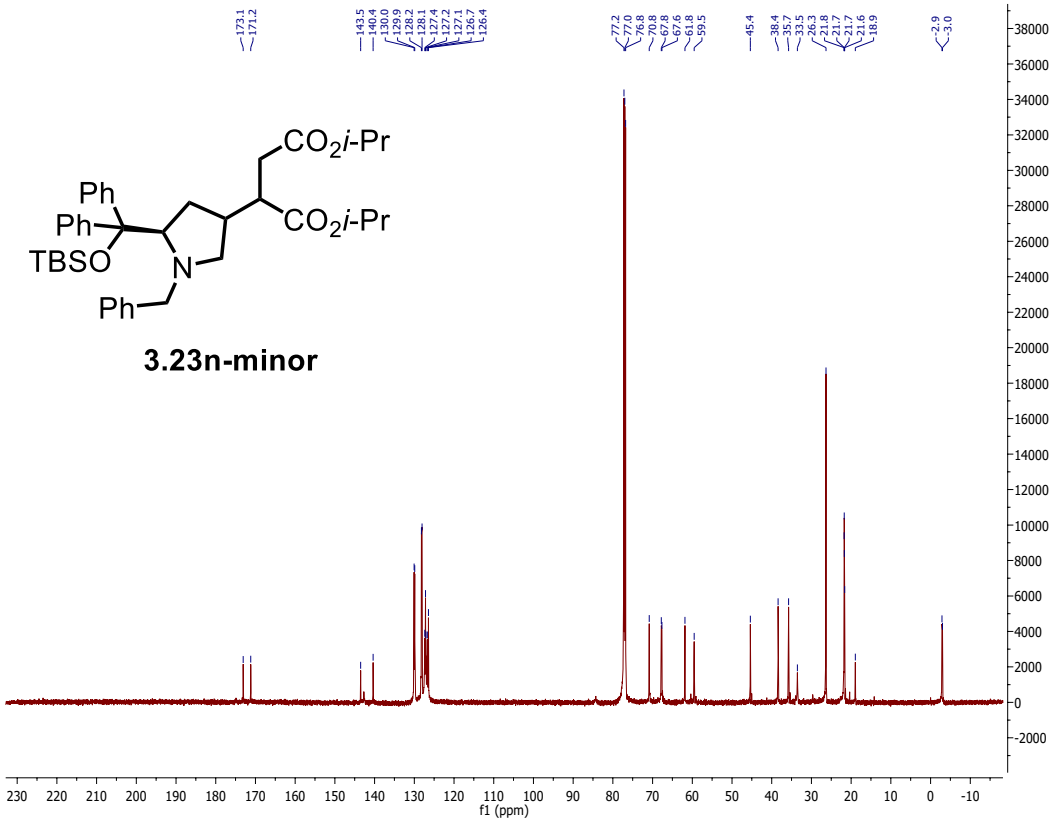
CO2i-Pr
CO2i-Pr
Ph
Ph
TBSO
N
Ph
3.23n-minor
f1 (ppm)

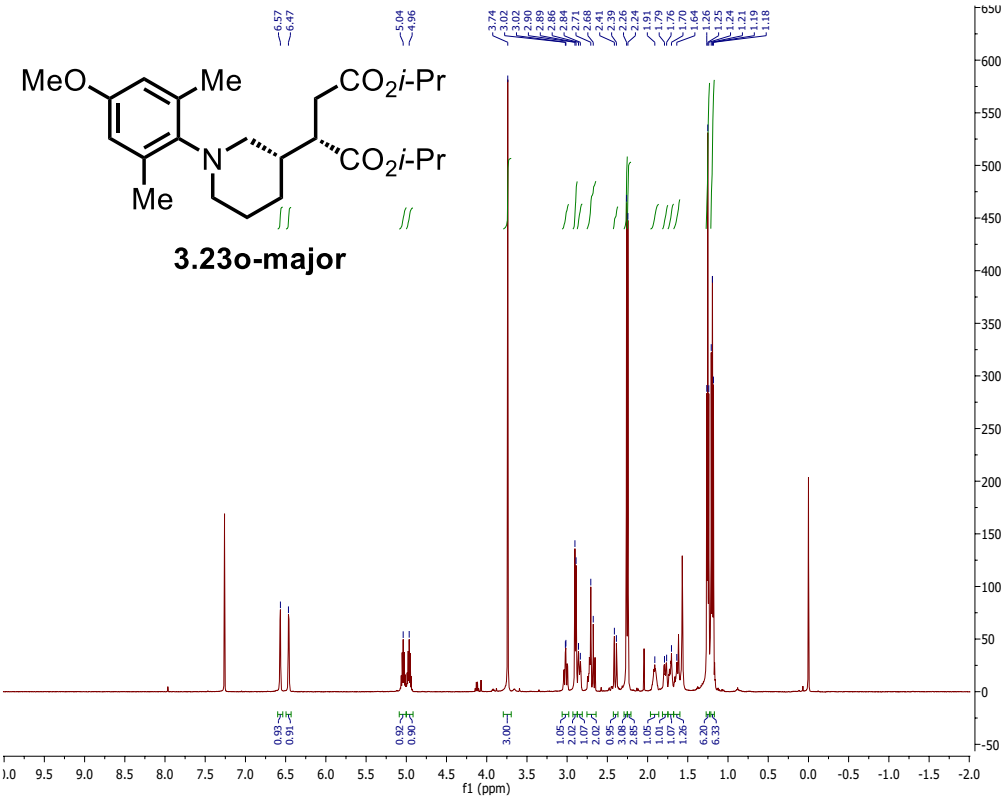
MeO
Me
CO2i-Pr
CO2i-Pr
N
Me
3.23o-major
f1 (ppm)

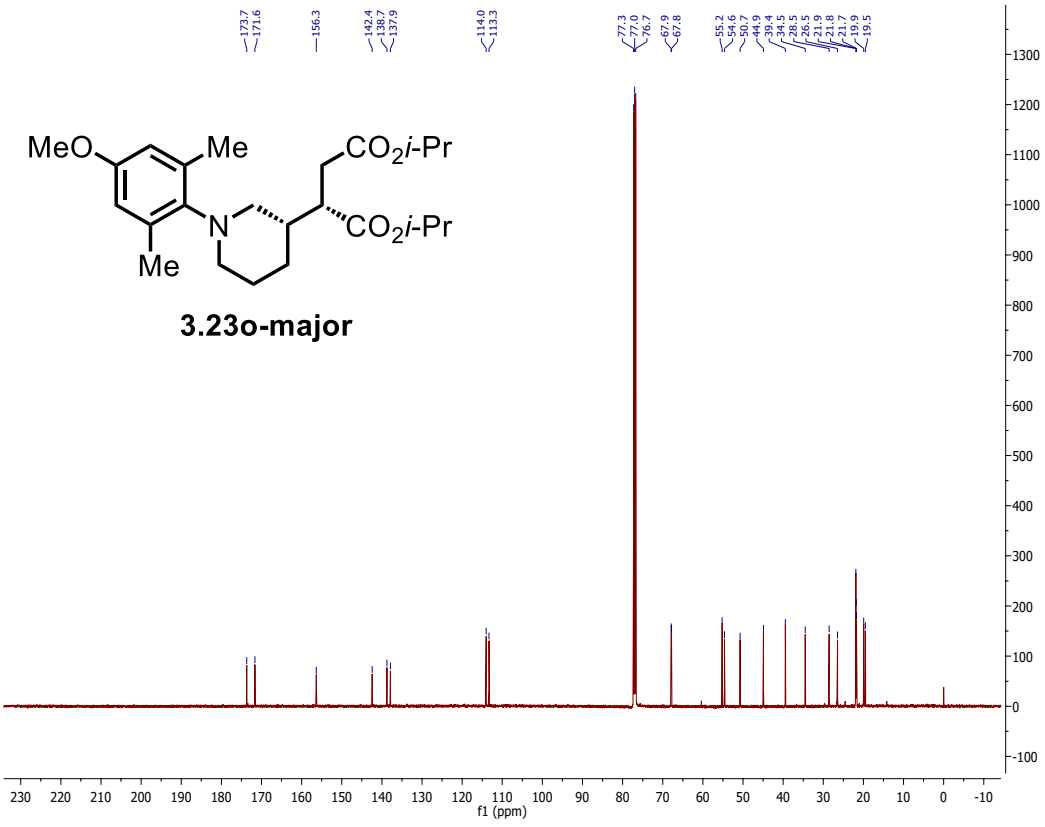
MeO
Me
CO2i-Pr
CO2i-Pr
N
Me
3.23o-major
f1 (ppm)

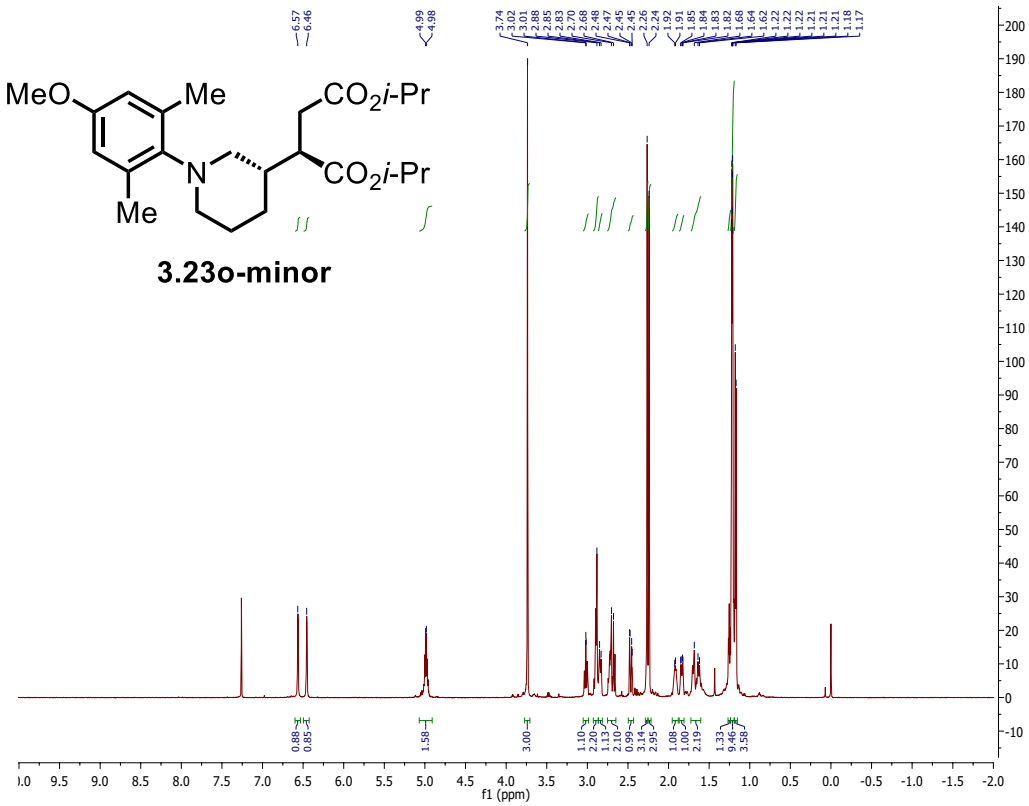
MeO
Me
Me
N
CO2i-Pr
CO2i-Pr
3.23o-minor
f1 (ppm)

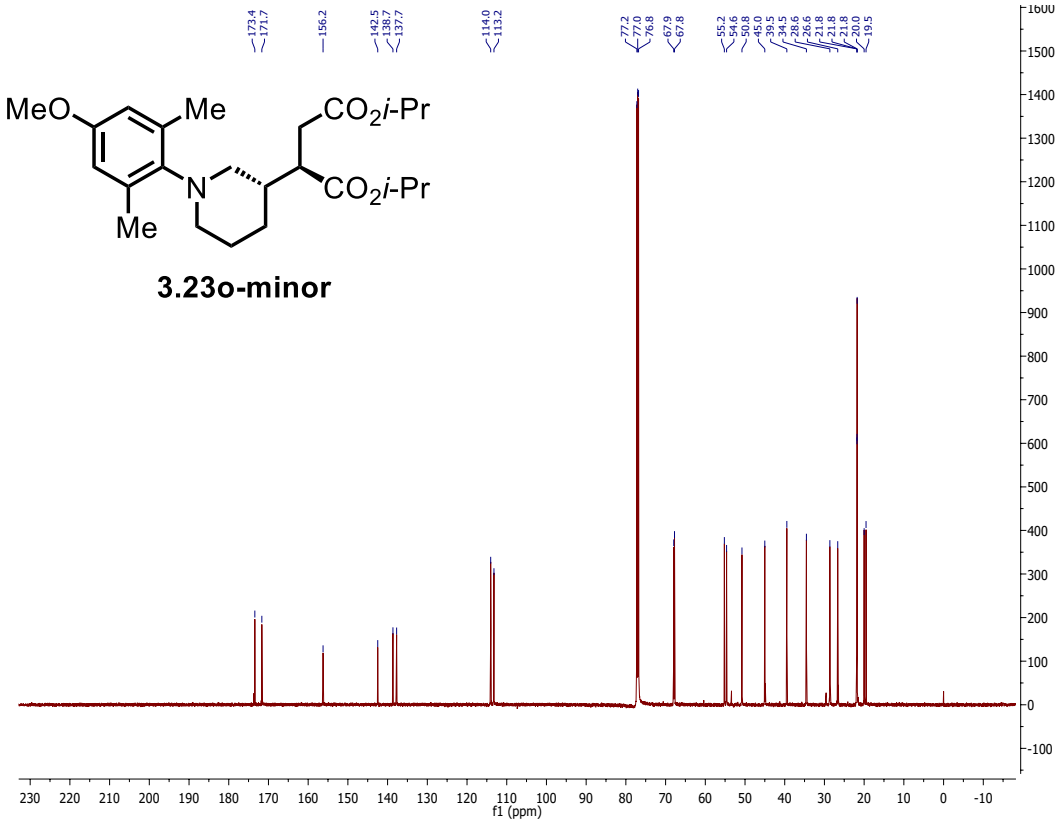
MeO
Me
Me
N
CO2i-Pr
CO2i-Pr
3.23o-minor
f1 (ppm)

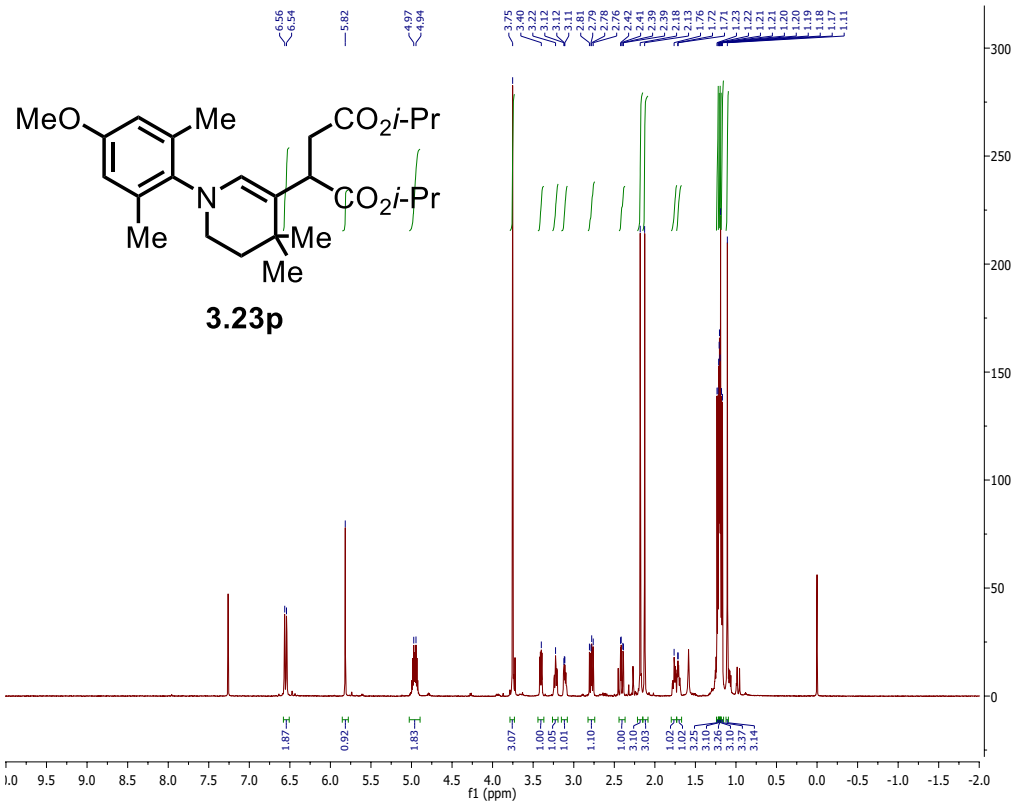
MeO
Me
CO2i-Pr
CO2i-Pr
N
Me
Me
Me
f1 (ppm)

3.23p

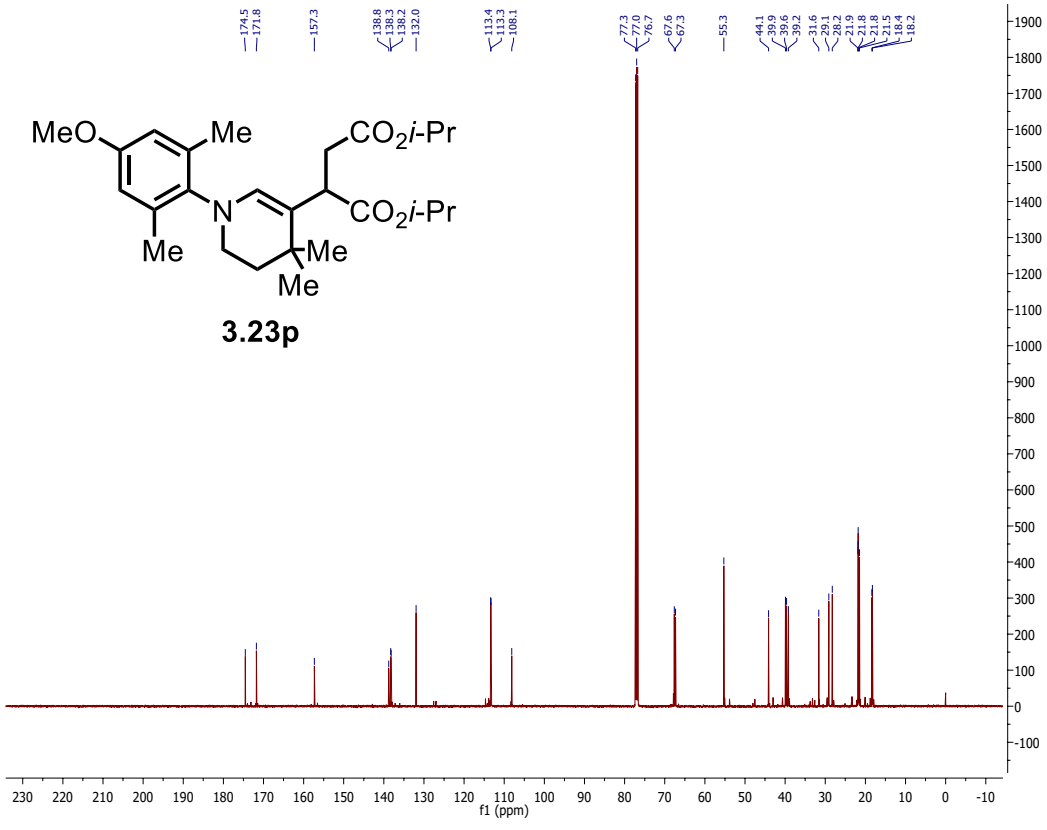
MeO
Me
CO2i-Pr
CO2i-Pr
N
Me
Me
Me
f1 (ppm)

3.23p

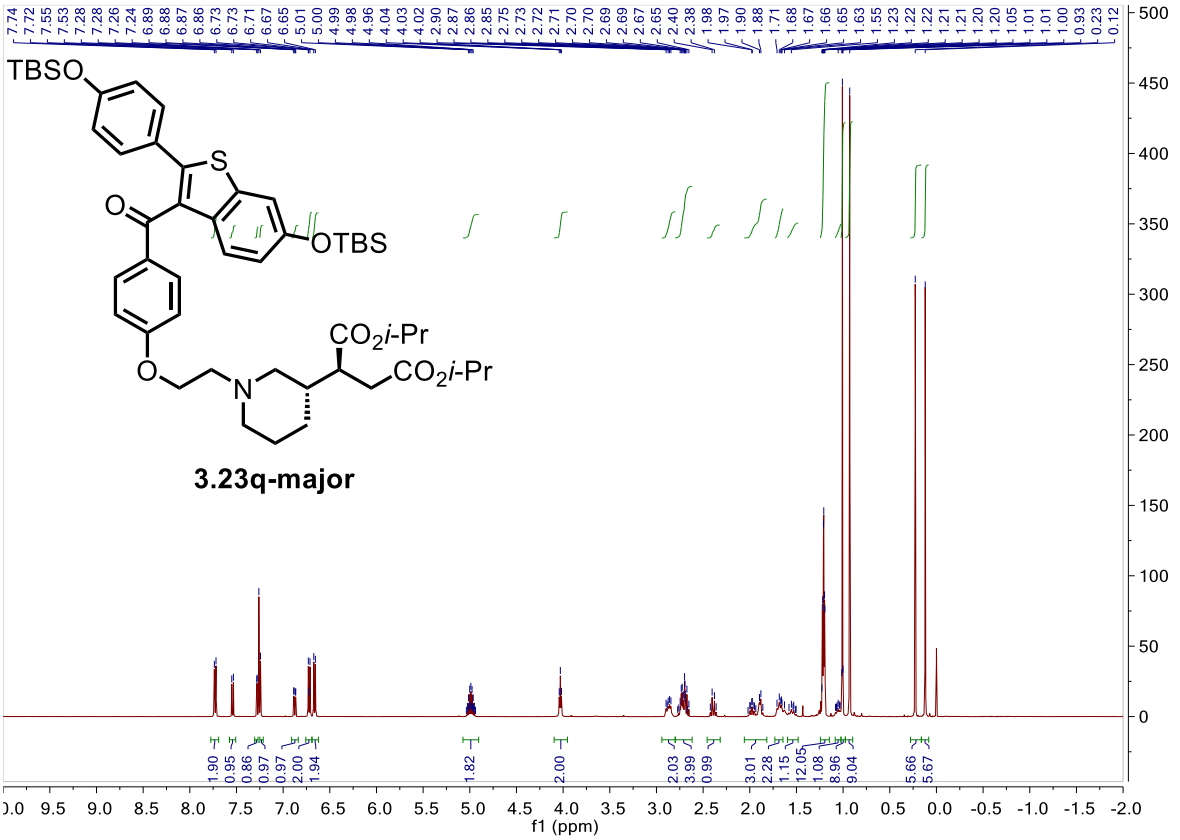
TBSO
S
O
OTBS
O
N
CO2i-Pr
CO2i-Pr
3.23q-major
f1 (ppm)

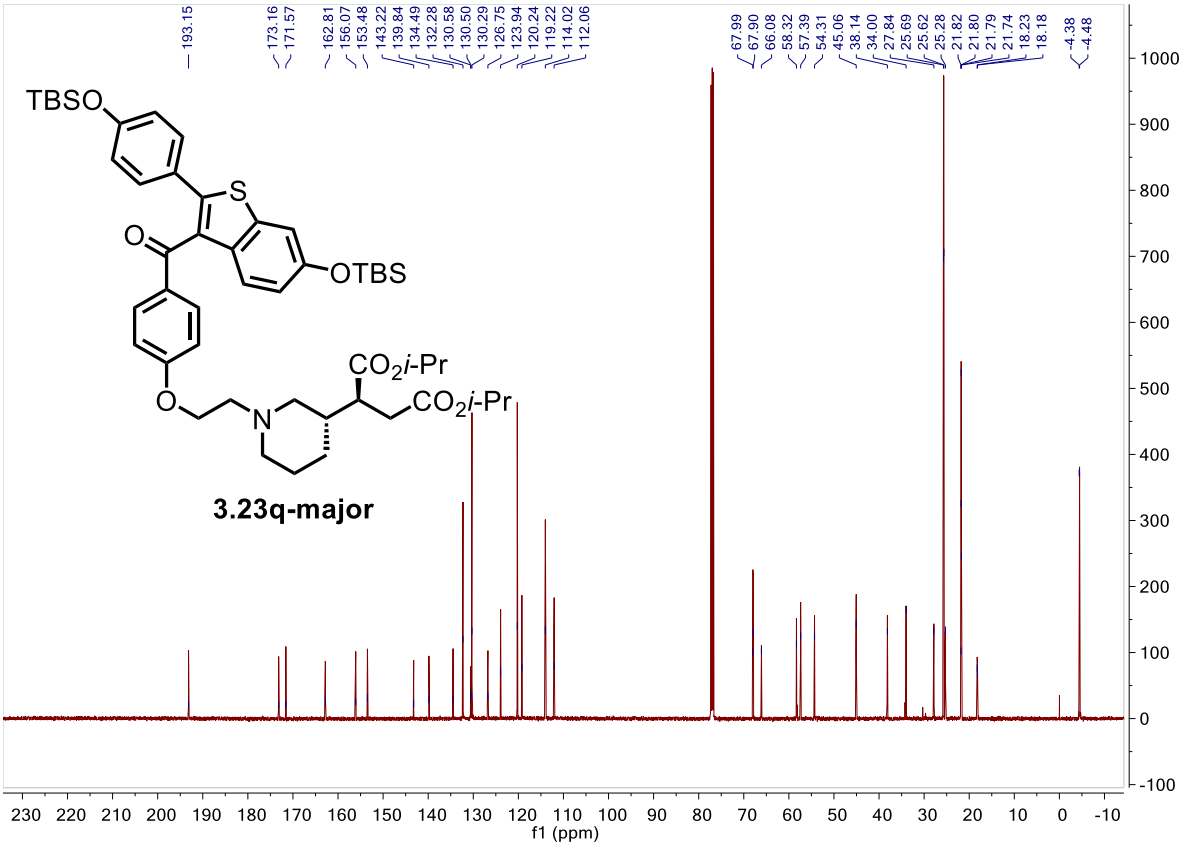
TBSO
S
O
OTBS
O
N
CO2i-Pr
CO2i-Pr
3.23q-major
f1 (ppm)

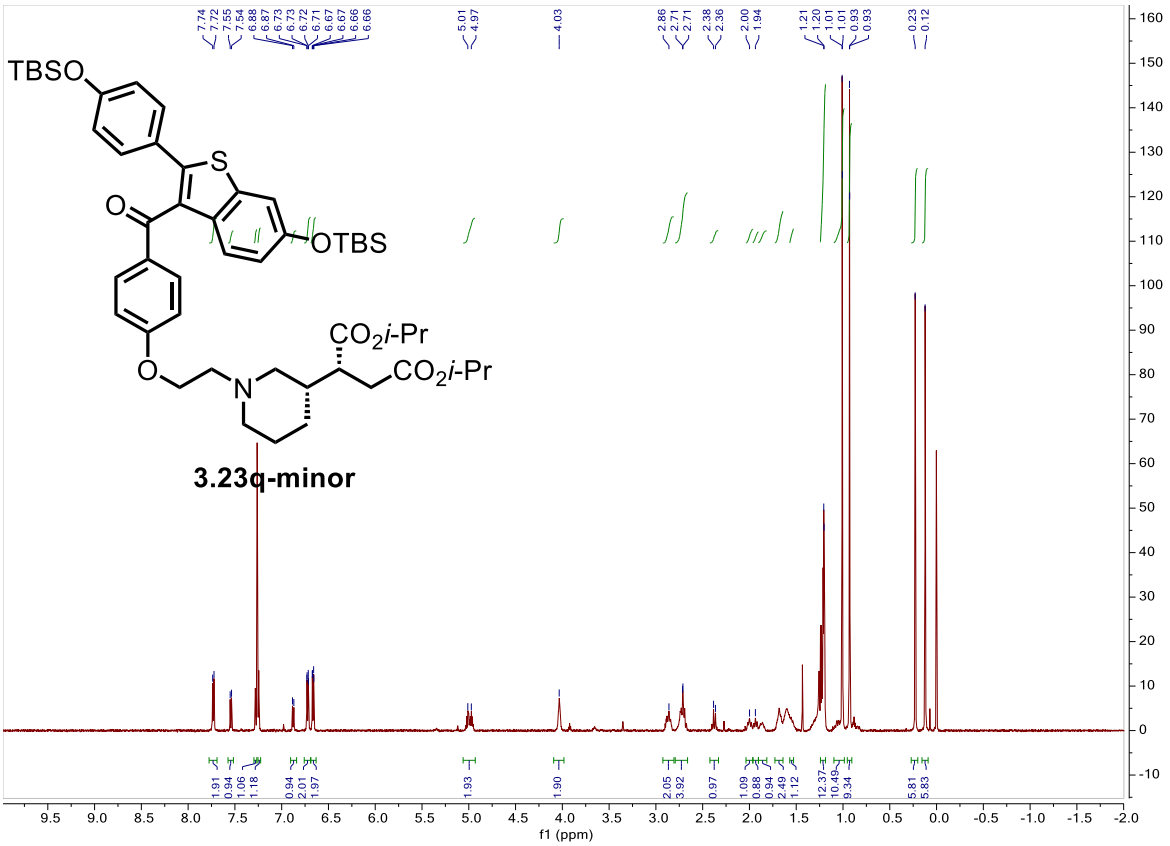
TBSO
S
O
OTBS
O
N
CO2i-Pr
CO2i-Pr
3.23q-minor
f1 (ppm)

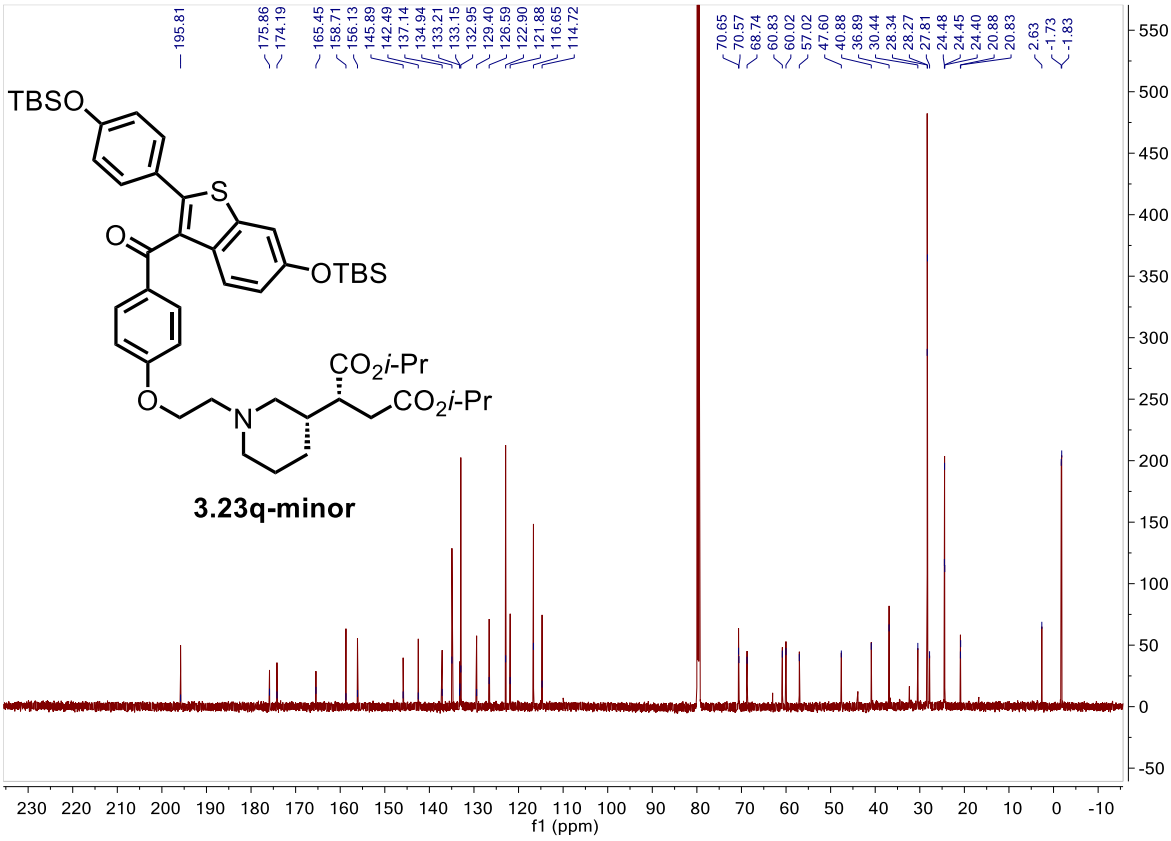
TBSO
S
O
OTBS
O
N
CO2i-Pr
CO2i-Pr
3.23q-minor
f1 (ppm)

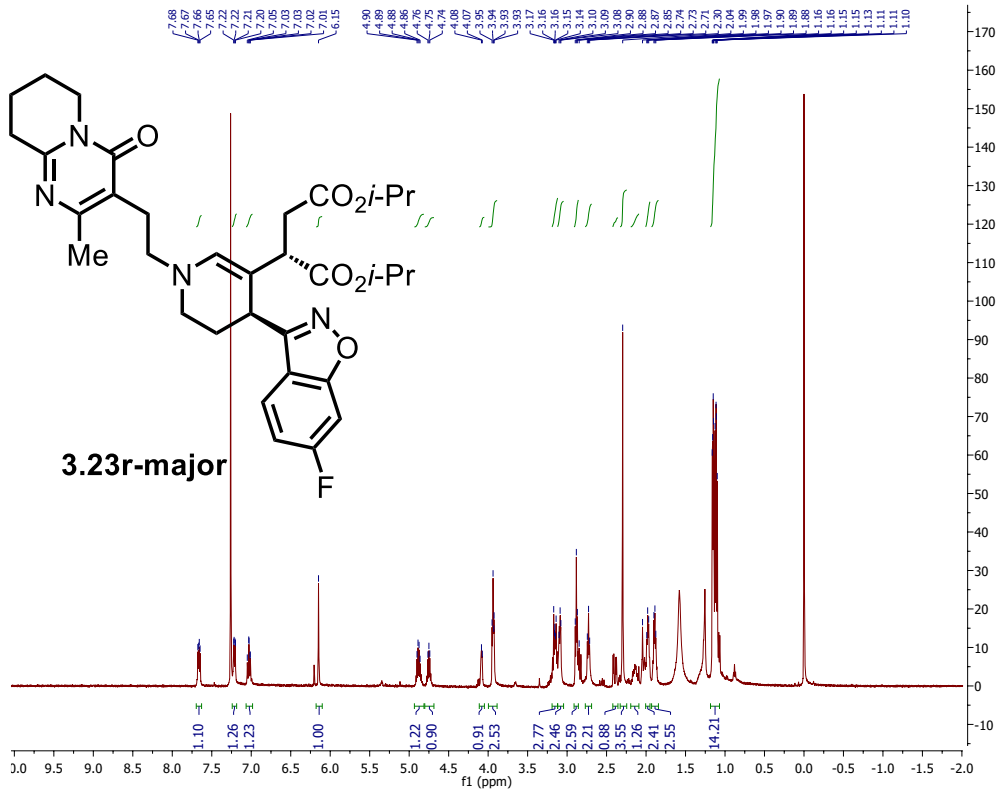
3.23r-major
CO2i-Pr
CO2i-Pr
Me
F
f1 (ppm)

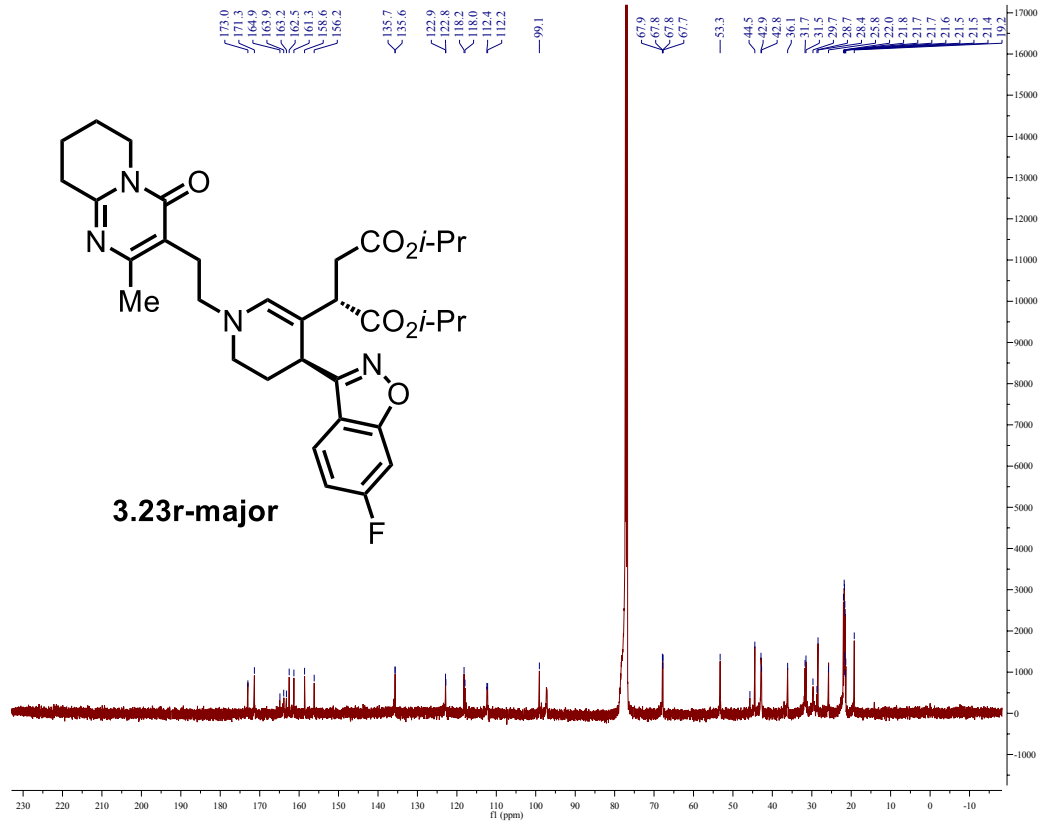
3.23r-major
CO2i-Pr
CO2i-Pr
Me
F
f1 (ppm)

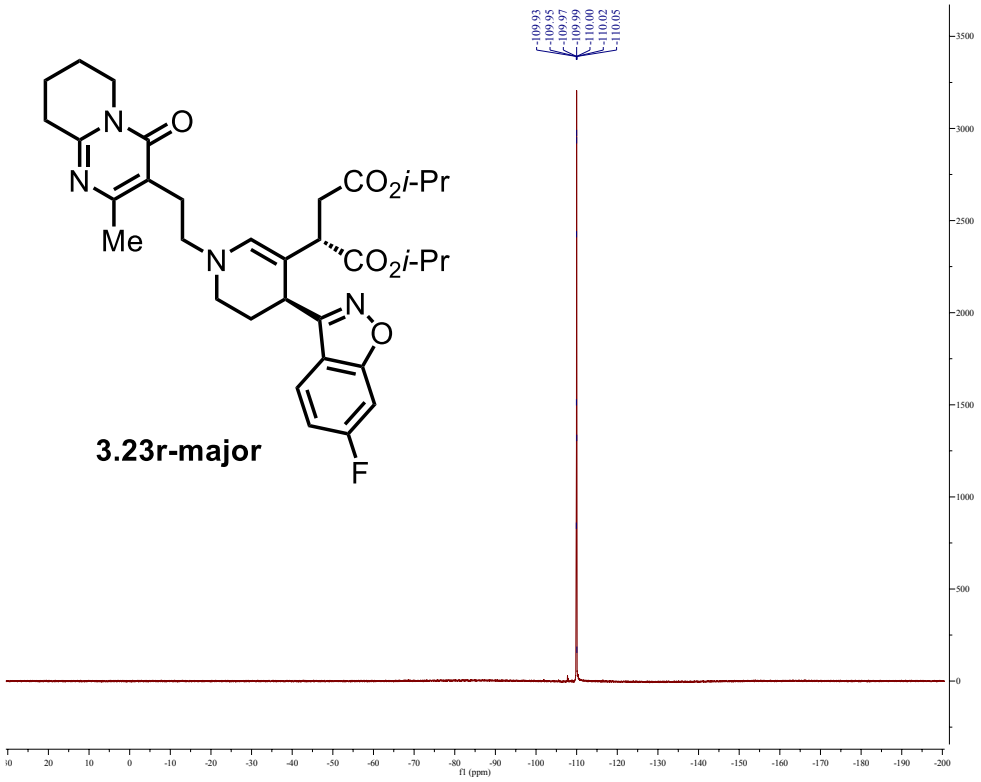
-109.93
-109.95
-109.97
-109.99
-110.00
-110.02
-110.05
N
O
N
Me
N
CO2i-Pr
CO2i-Pr
N
O
F
3.23r-major
f1 (ppm)

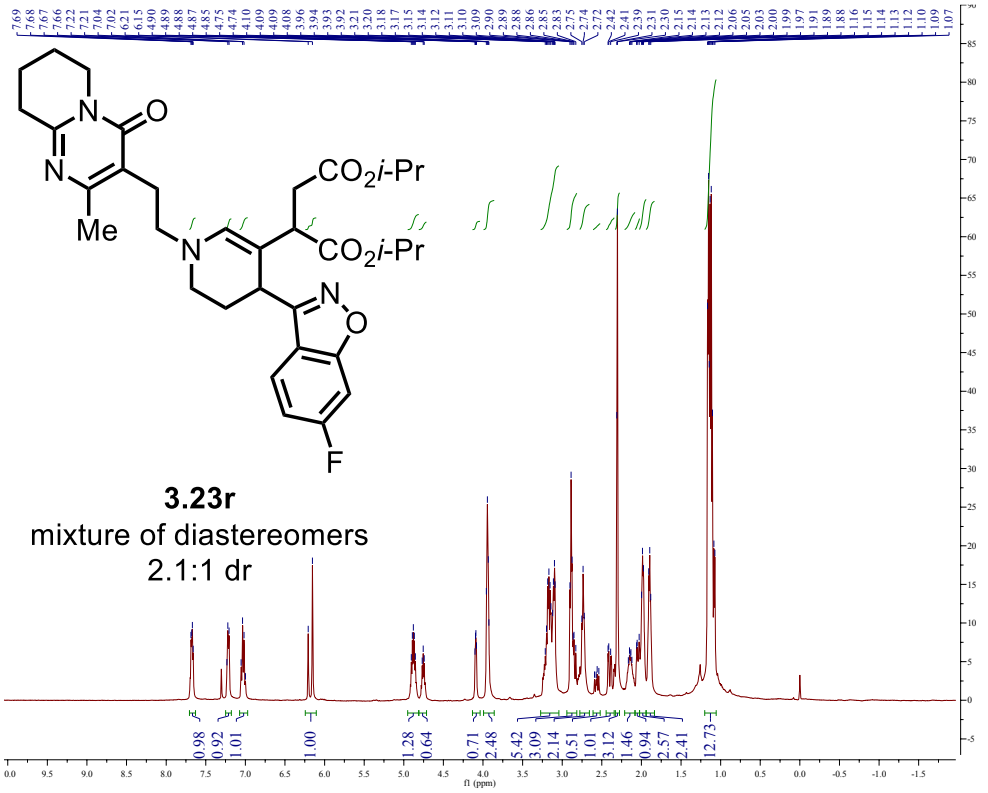
Me
CO2i-Pr
CO2i-Pr
F
3.23r
mixture of diastereomers
2.1:1 dr

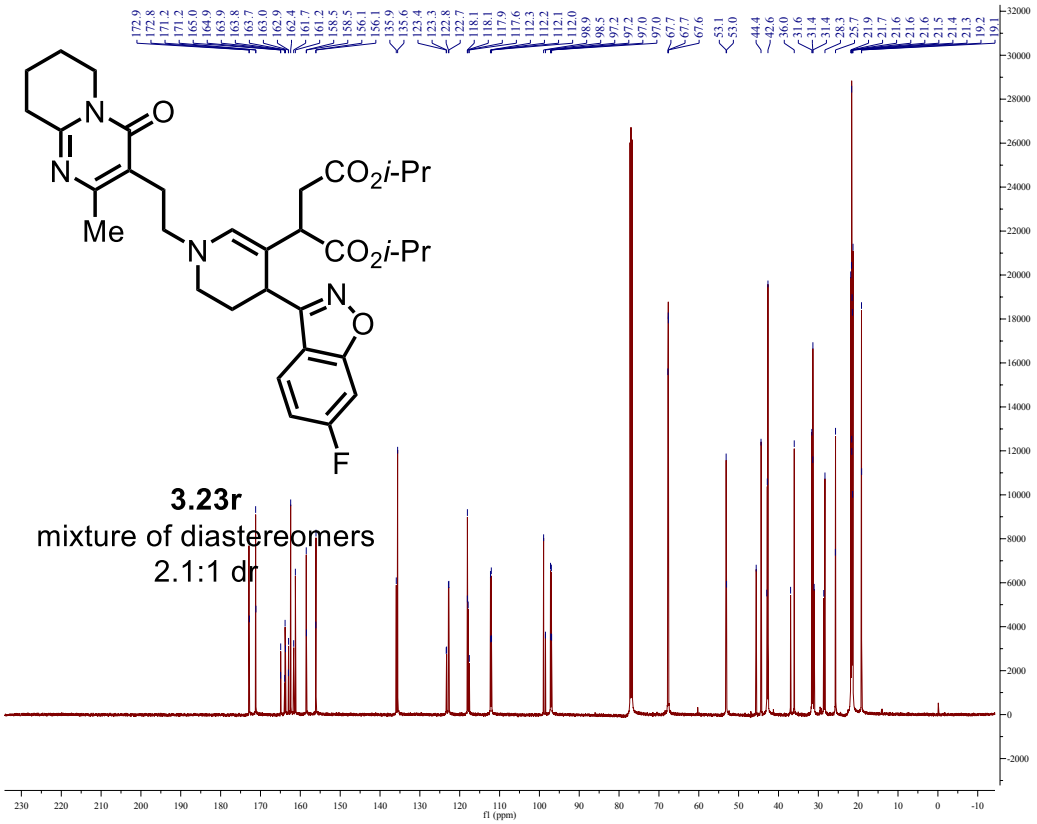
Me
CO2i-Pr
CO2i-Pr
F
3.23r
mixture of diastereomers
2.1:1 dr

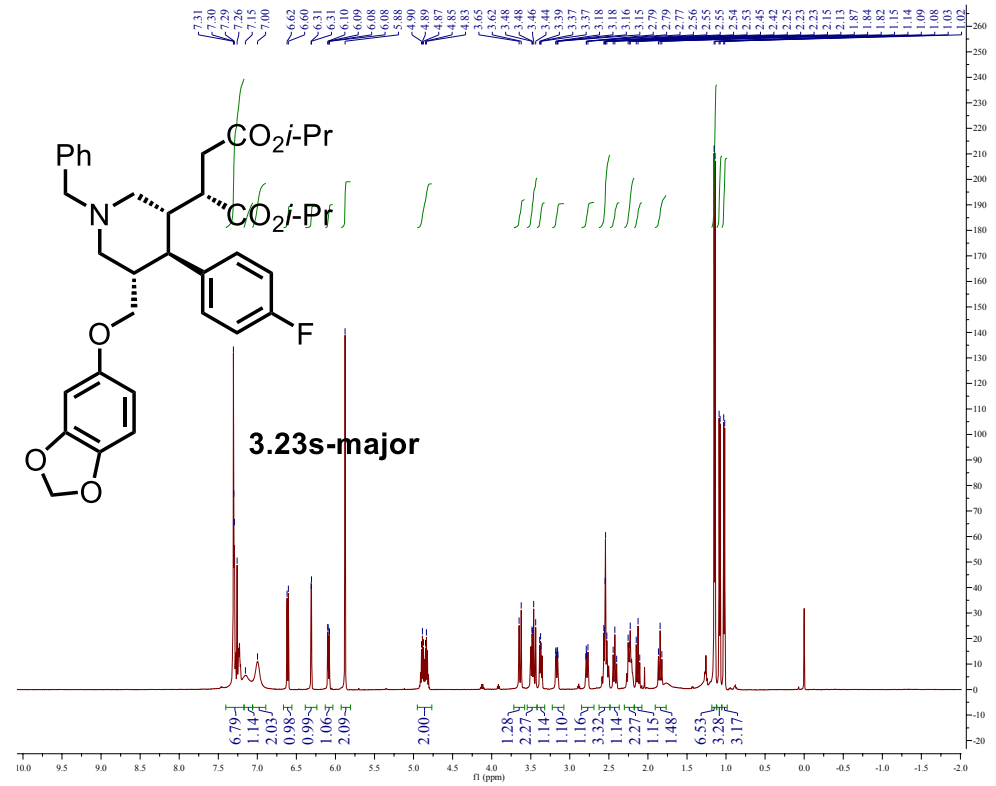
Ph
N
CO2i-Pr
CO2i-Pr
F
O
O
O
3.23s-major
f1 (ppm)

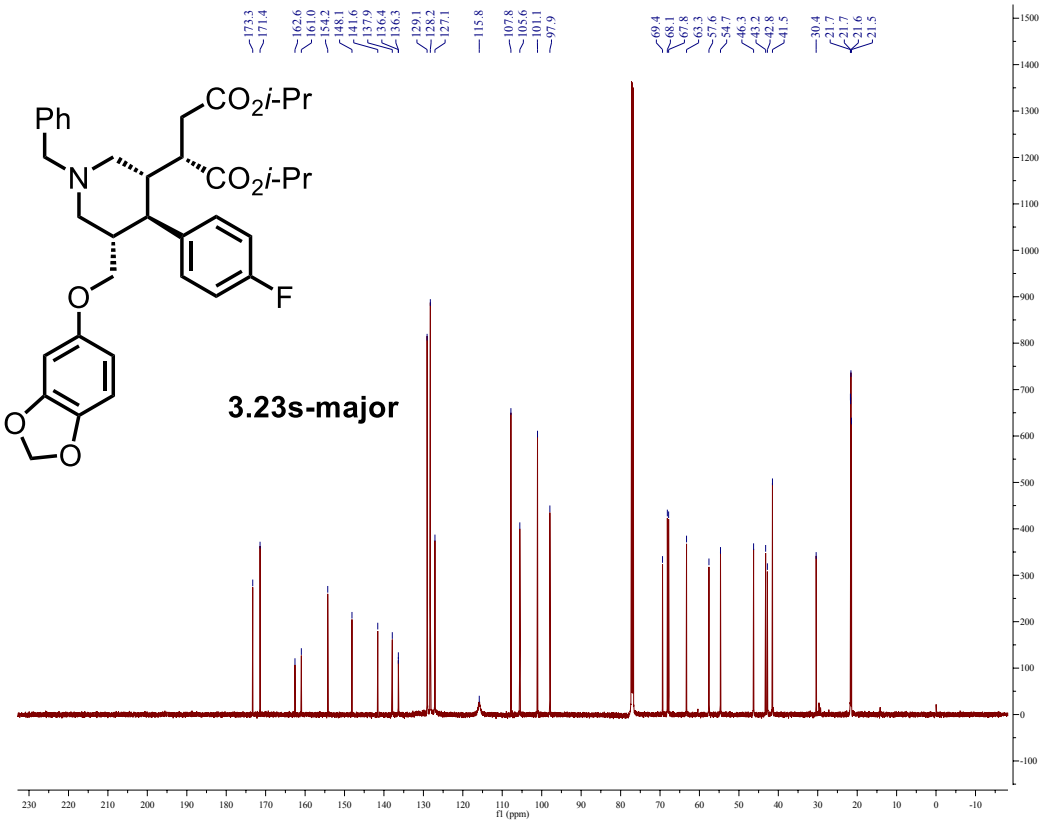
Ph
N
CO2i-Pr
CO2i-Pr
F
O
O
O
3.23s-major
f1 (ppm)

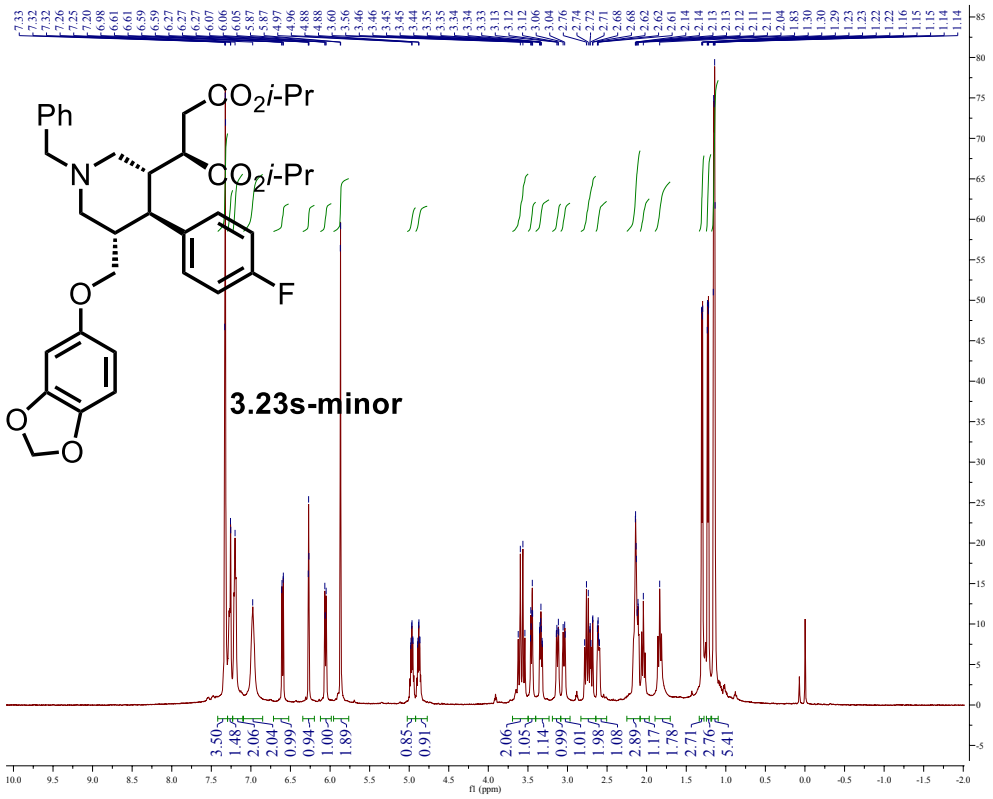
Ph
N
CO2i-Pr
CO2i-Pr
O
F
O
O
O
3.23s-minor
f1 (ppm)

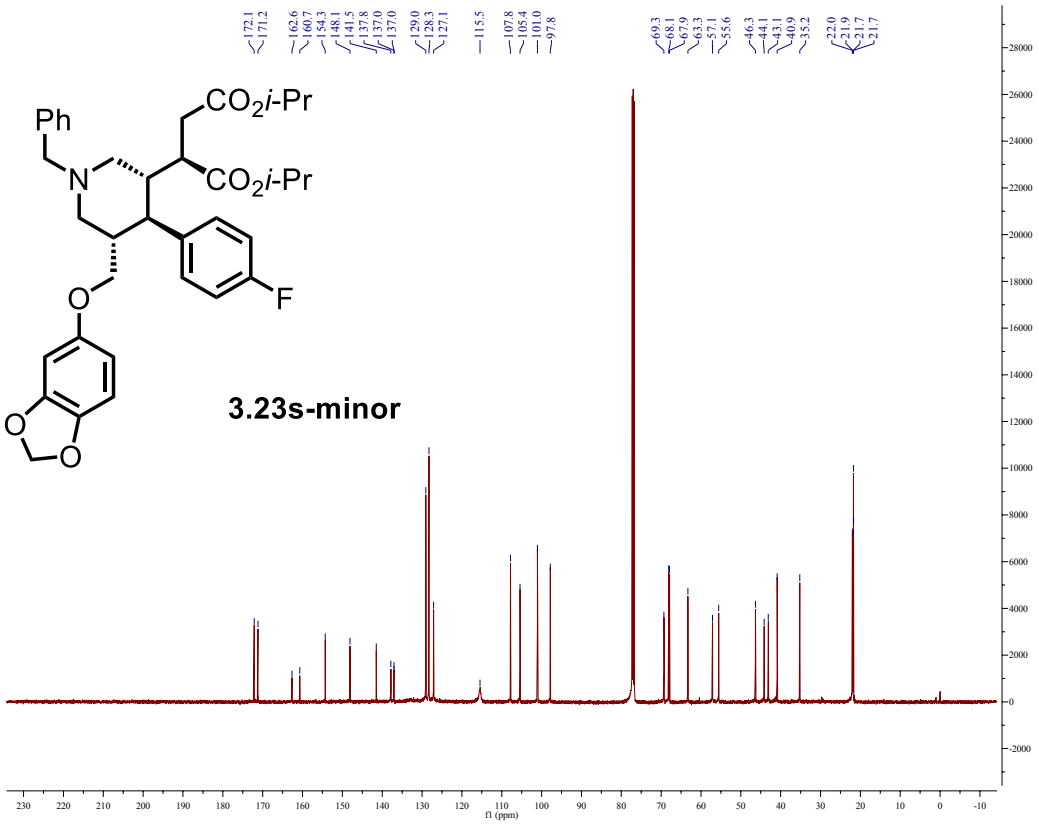
Ph
N
CO2i-Pr
CO2i-Pr
O
F
O
O
O
3.23s-minor
f1 (ppm)

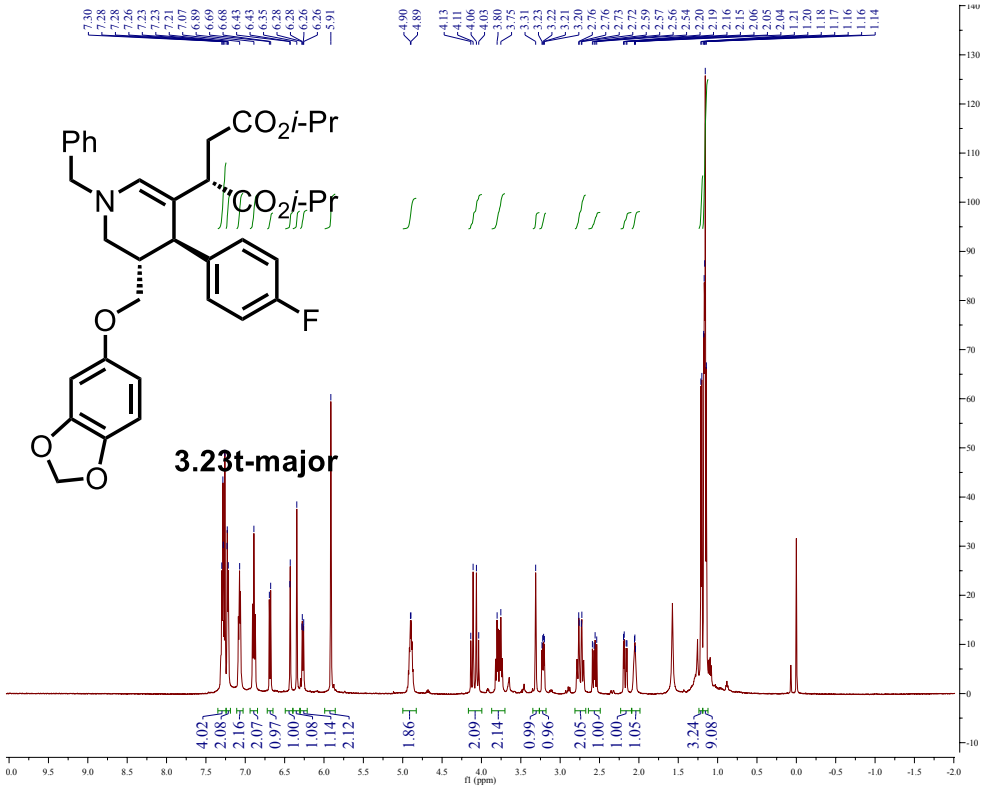
Ph
N
CO2i-Pr
CO2i-Pr
O
F
O
O
O
3.23t-major

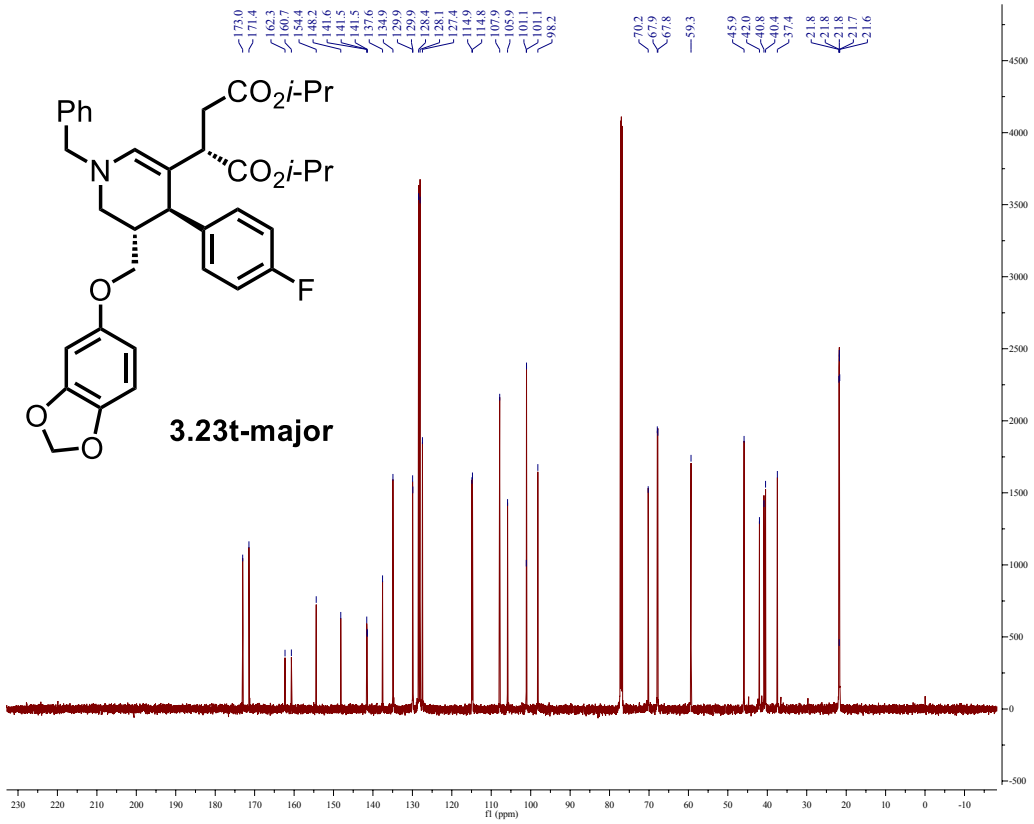
Ph
N
CO2i-Pr
CO2i-Pr
O
F
O
O
O
3.23t-major

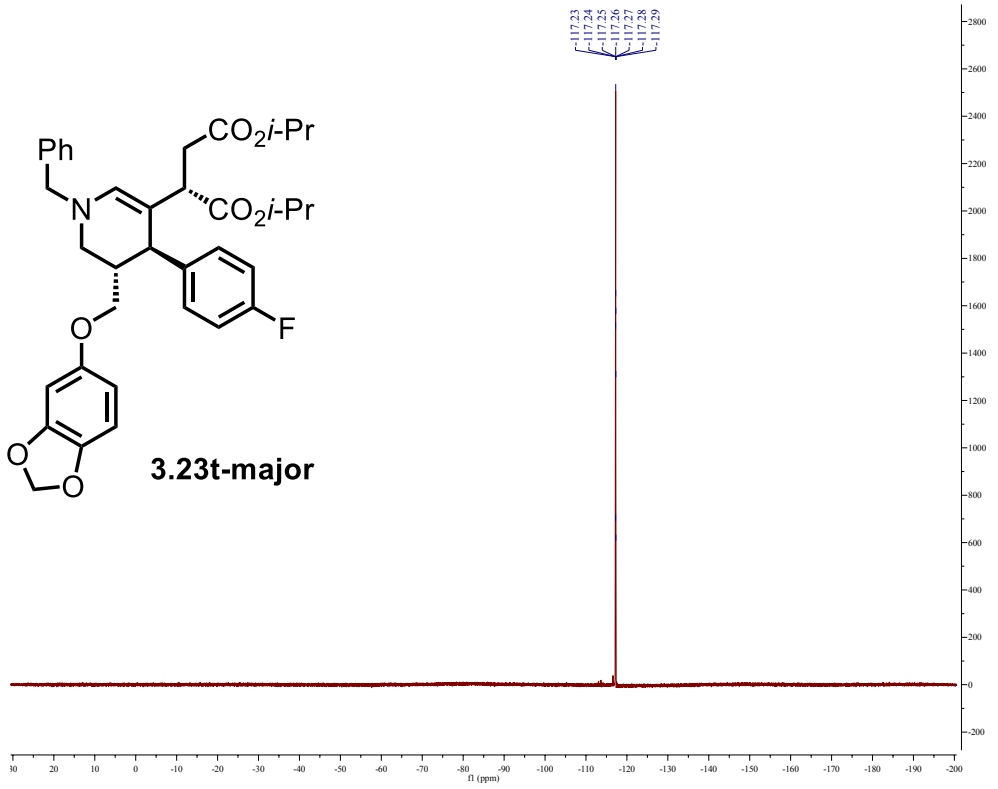
Ph
N
CO2i-Pr
CO2i-Pr
F
O
O
O
3.23t-major
f1 (ppm)

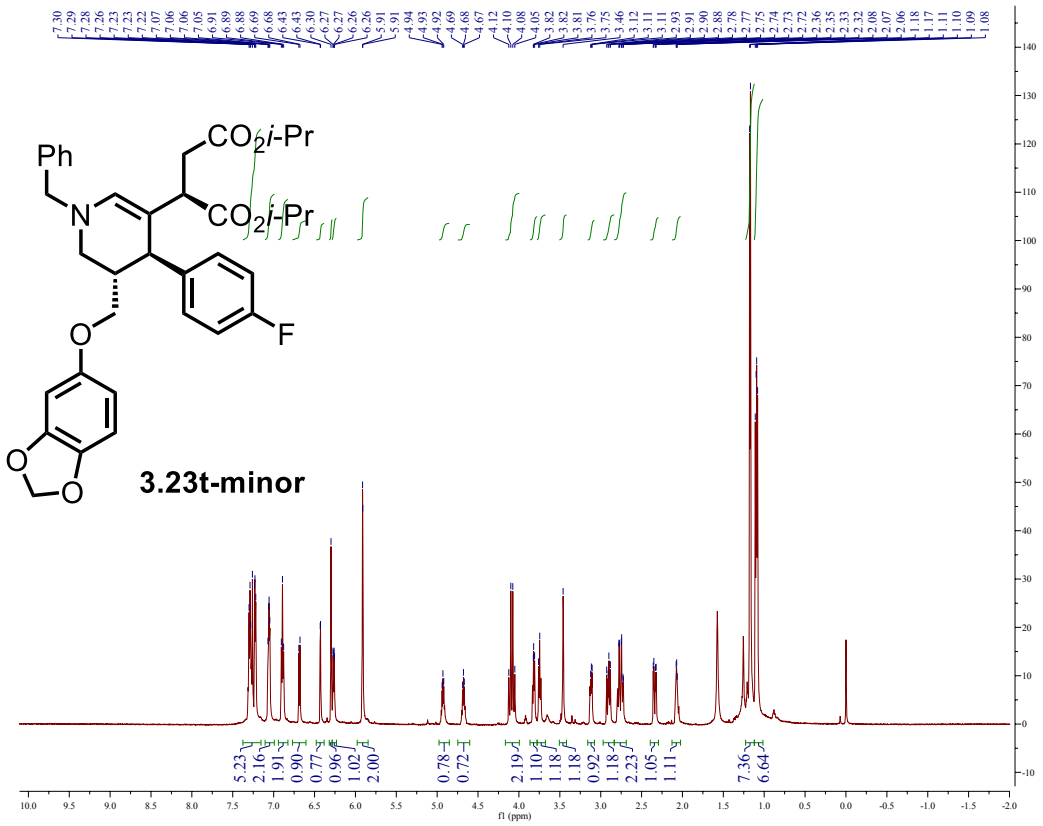
Ph
N
CO2i-Pr
CO2i-Pr
F
O
O
O
3.23t-minor
f1 (ppm)

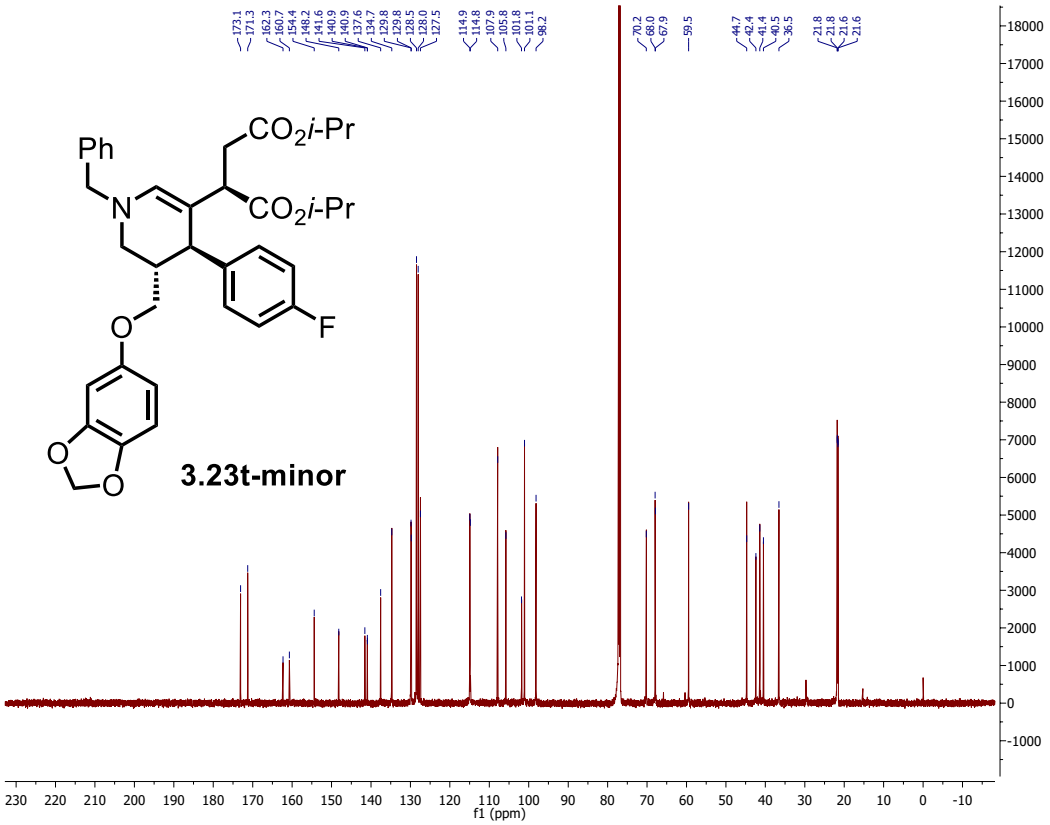
Ph
N
CO2i-Pr
CO2i-Pr
O
F
O
O
3.23t-minor
173.1
171.3
162.3
160.7
154.4
148.2
141.6
140.9
140.9
137.6
134.7
129.8
129.8
128.5
128.0
127.5
114.9
114.8
107.9
105.8
101.8
101.1
98.2
70.2
68.0
67.9
59.5
44.7
42.4
41.4
40.5
36.5
21.8
21.8
21.6
21.6
f1 (ppm)

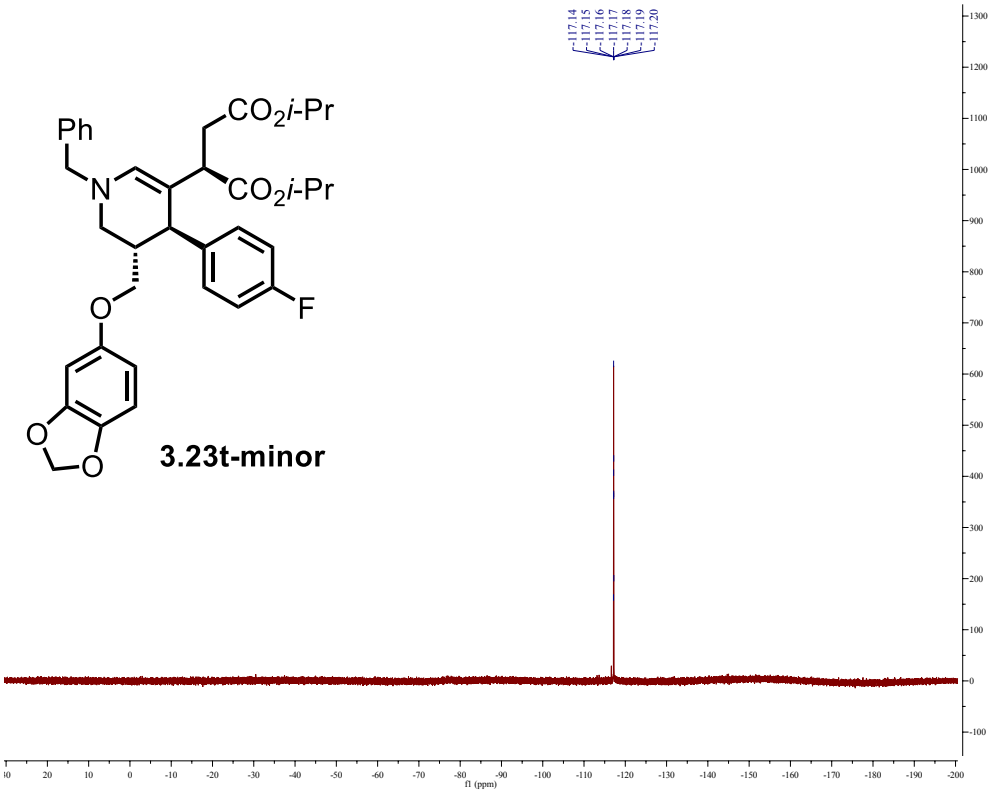
Ph
N
CO2i-Pr
CO2i-Pr
O
F
O
O
3.23t-minor
117.14
117.15
117.16
117.17
117.18
117.19
117.20
f1 (ppm)

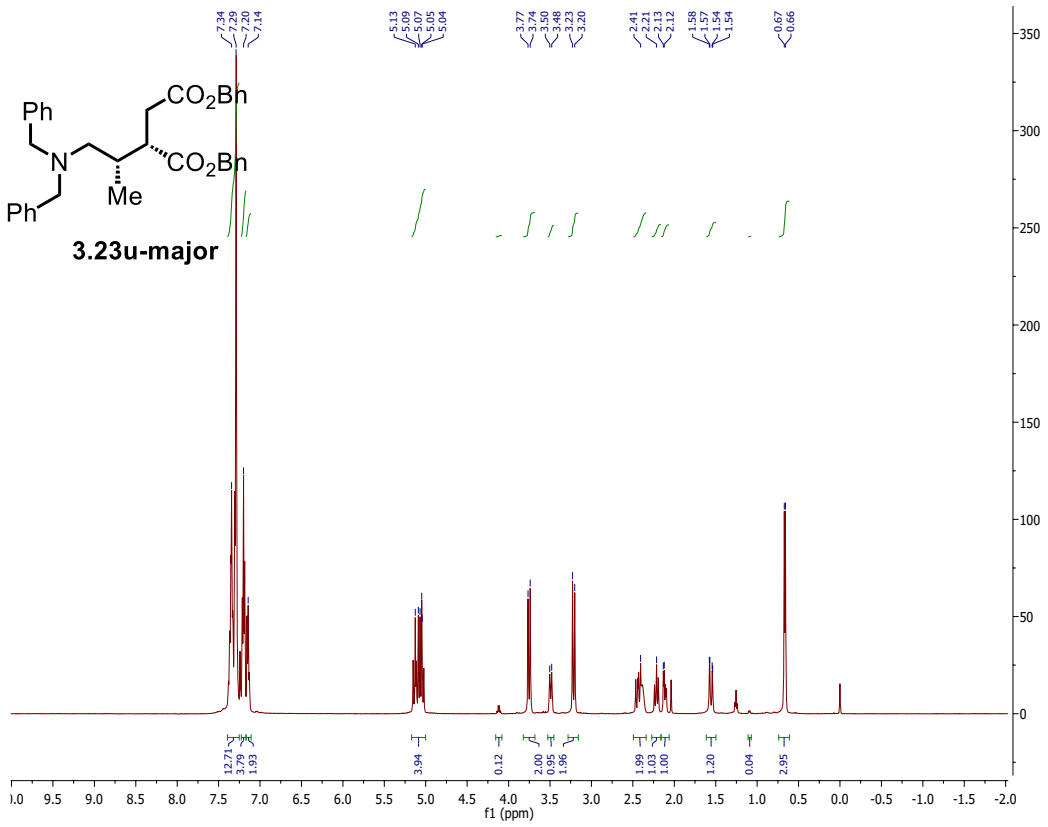
Ph
N
Ph
Me
CO2Bn
CO2Bn
3.23u-major
f1 (ppm)

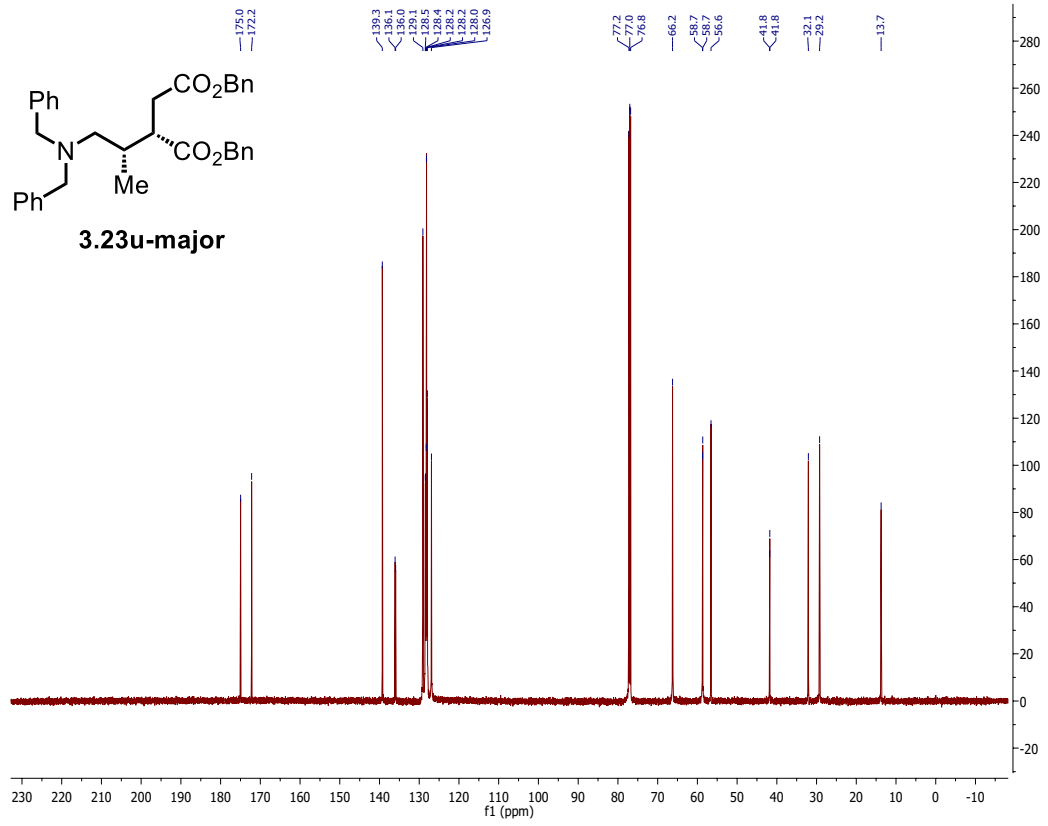
Ph
N
Ph
Me
CO2Bn
CO2Bn
3.23u-major
f1 (ppm)

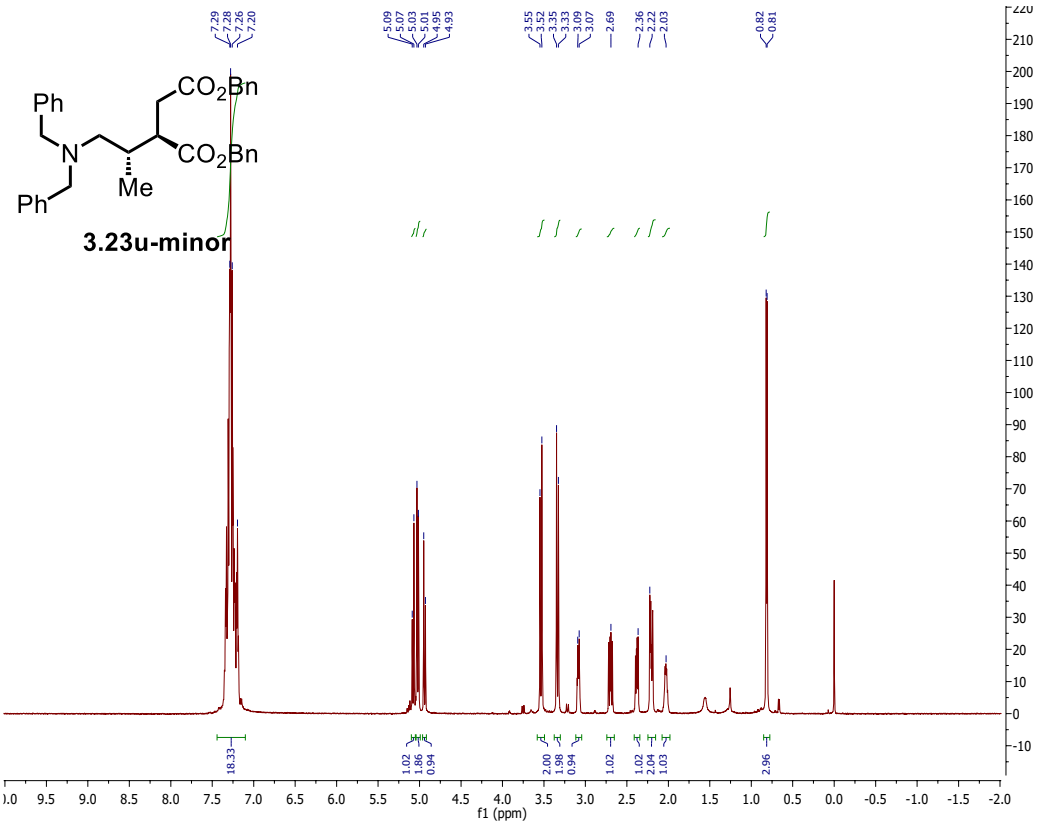
Ph
N
Ph
Me
CO2Bn
CO2Bn
3.23u-minor
f1 (ppm)

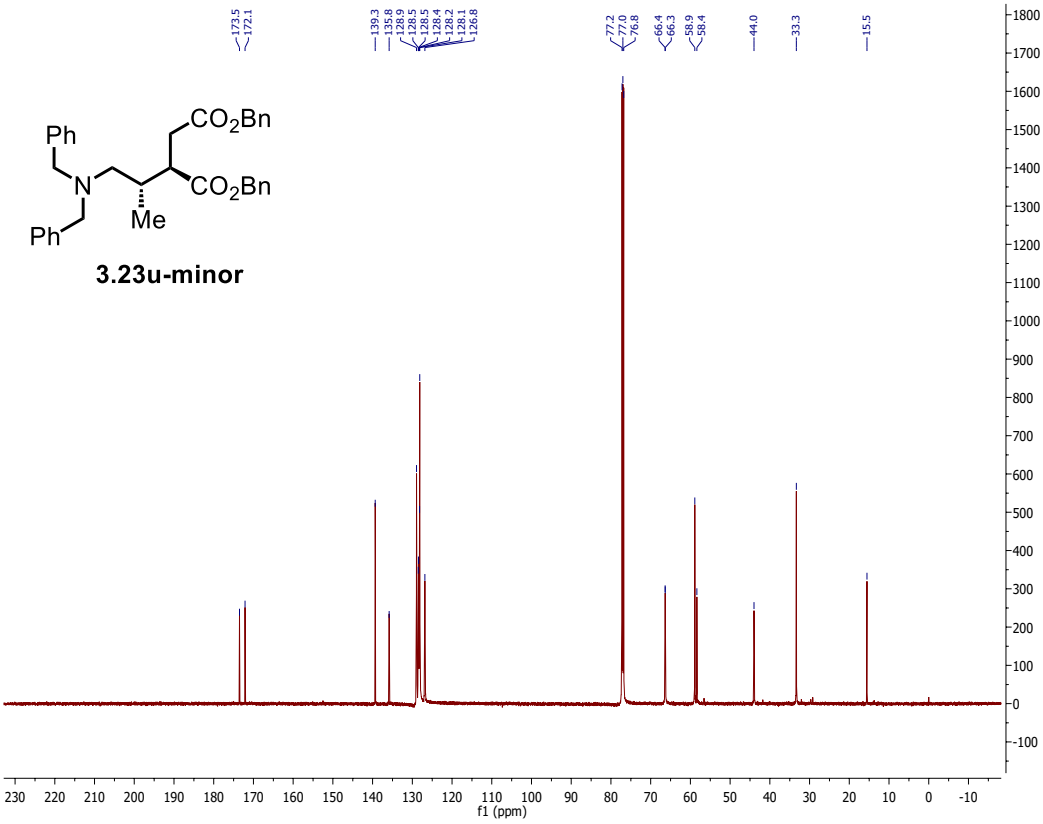
Ph
N
Ph
Me
CO2Bn
CO2Bn
3.23u-minor
f1 (ppm)

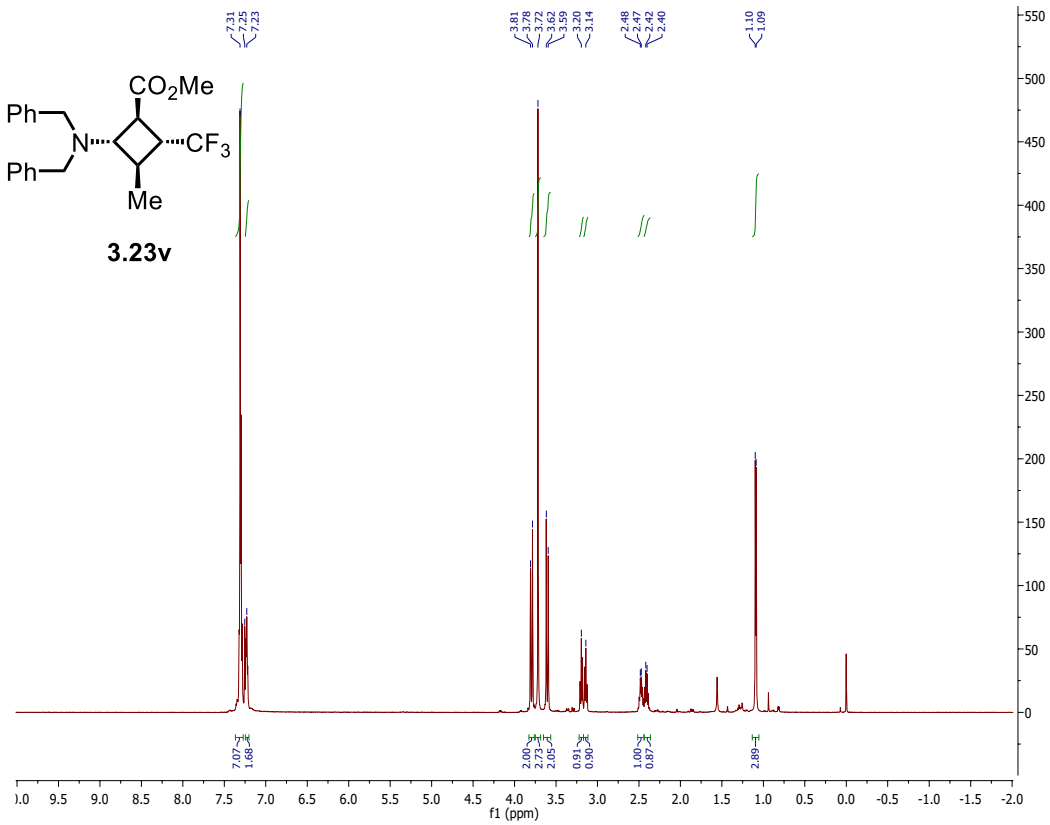
CO2Me
Ph
N
CF3
Ph
Me
3.23v
f1 (ppm)

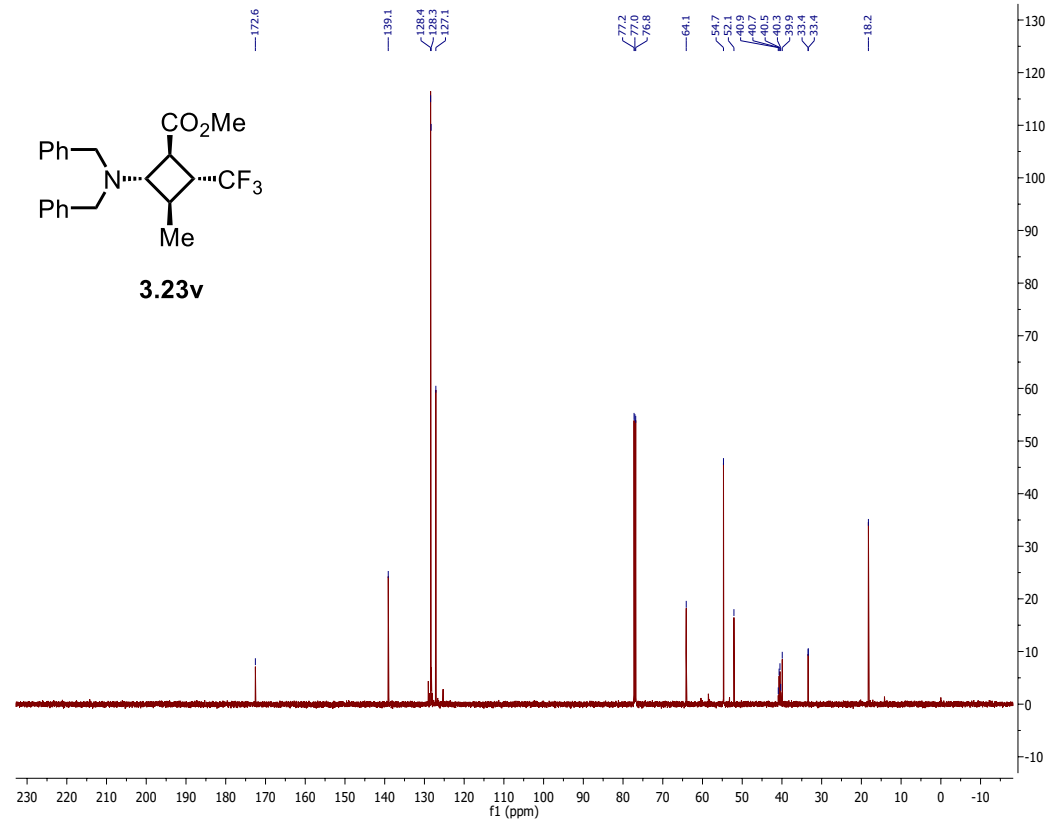
CO2Me
Ph
N
CF3
Ph
Me
3.23v
f1 (ppm)

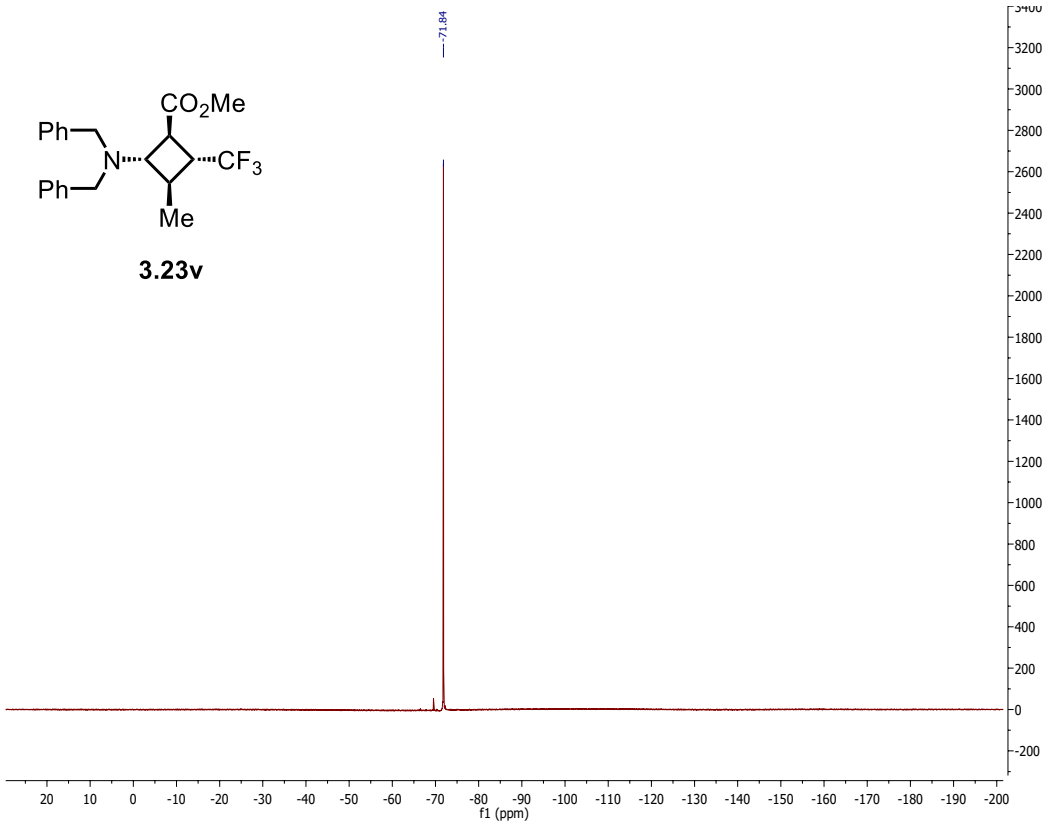
CO2Me
Ph
N
CF3
Ph
Me
-71.84
3200
3000
2800
2600
2400
2200
2000
1800
1600
1400
1200
1000
800
600
400
200
0
-200
20 10 0 -10 -20 -30 -40 -50 -60 -70 -80 -90 -100 -110 -120 -130 -140 -150 -160 -170 -180 -190 -200
f1 (ppm)

3.23v

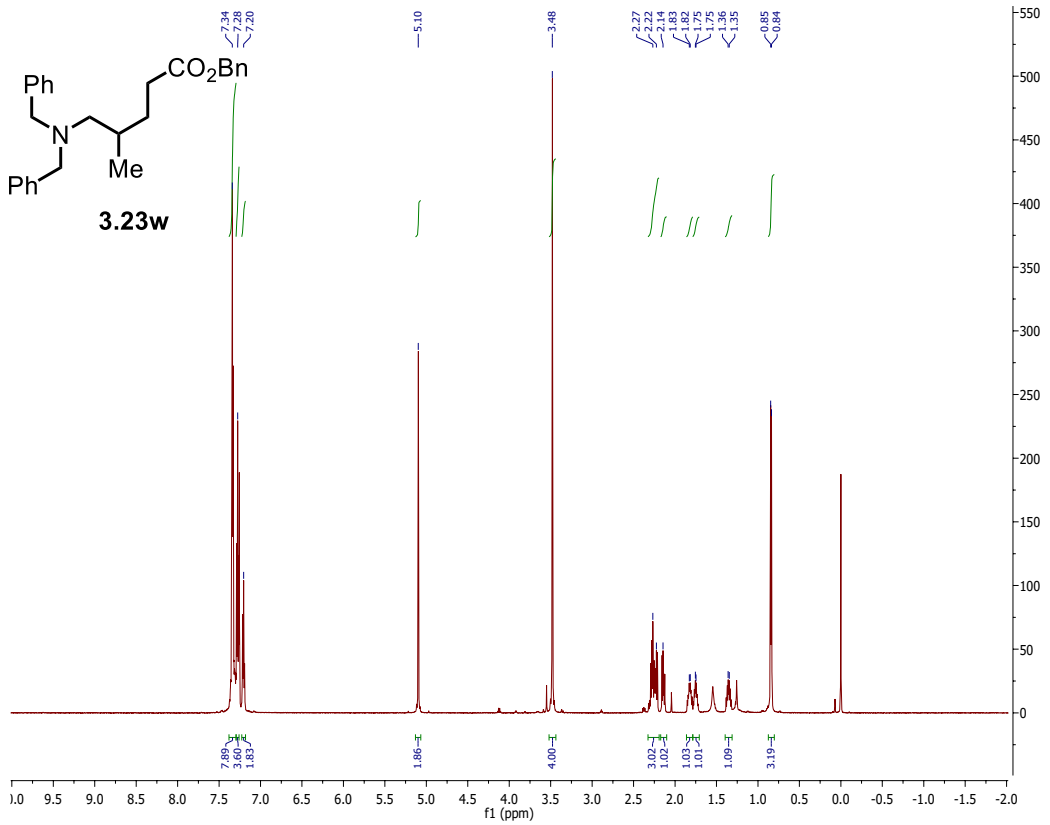
Ph
N
Ph
Me
CO2Bn
3.23w
7.34
7.28
7.20
5.10
3.48
2.27
2.22
2.14
1.83
1.82
1.75
1.75
1.36
1.35
0.85
0.84
7.89
3.60
1.83
1.86
4.00
3.02
1.02
1.03
1.01
1.09
3.19
f1 (ppm)

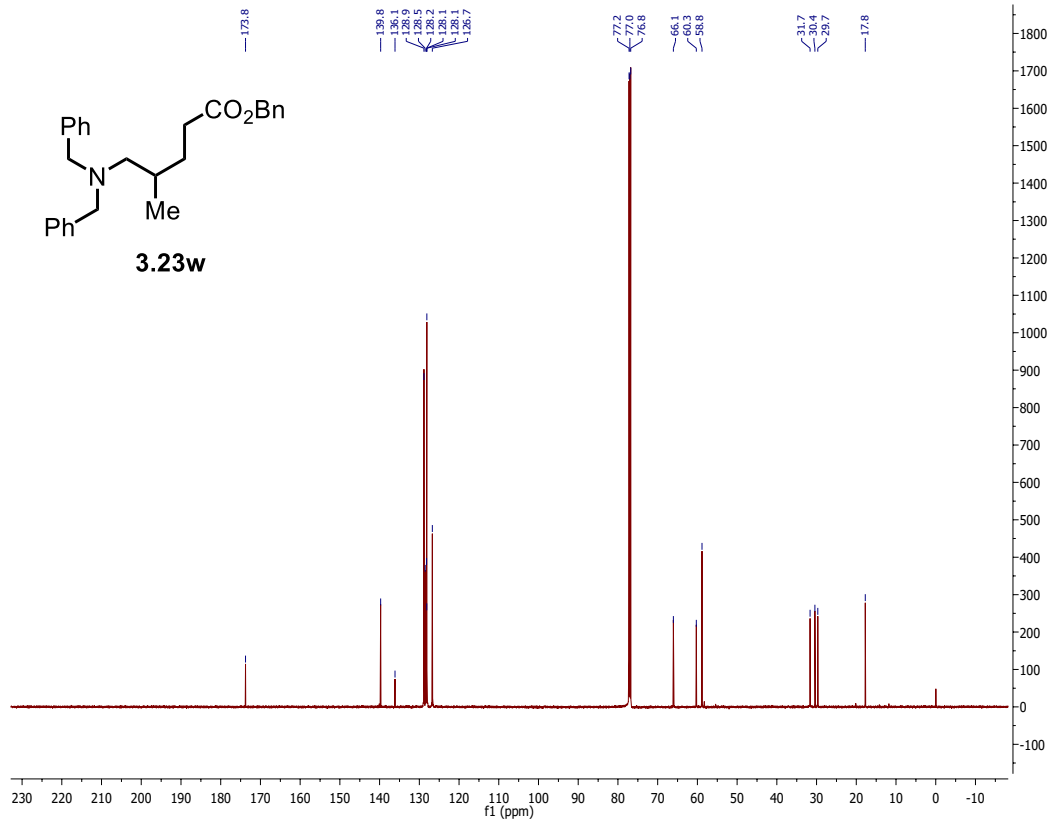
Ph
N
Ph
Me
CO2Bn
3.23w
173.8
139.8
136.1
128.9
128.5
128.2
128.1
128.1
126.7
77.2
77.0
76.8
66.1
60.3
58.8
31.7
30.4
29.7
17.8
f1 (ppm)

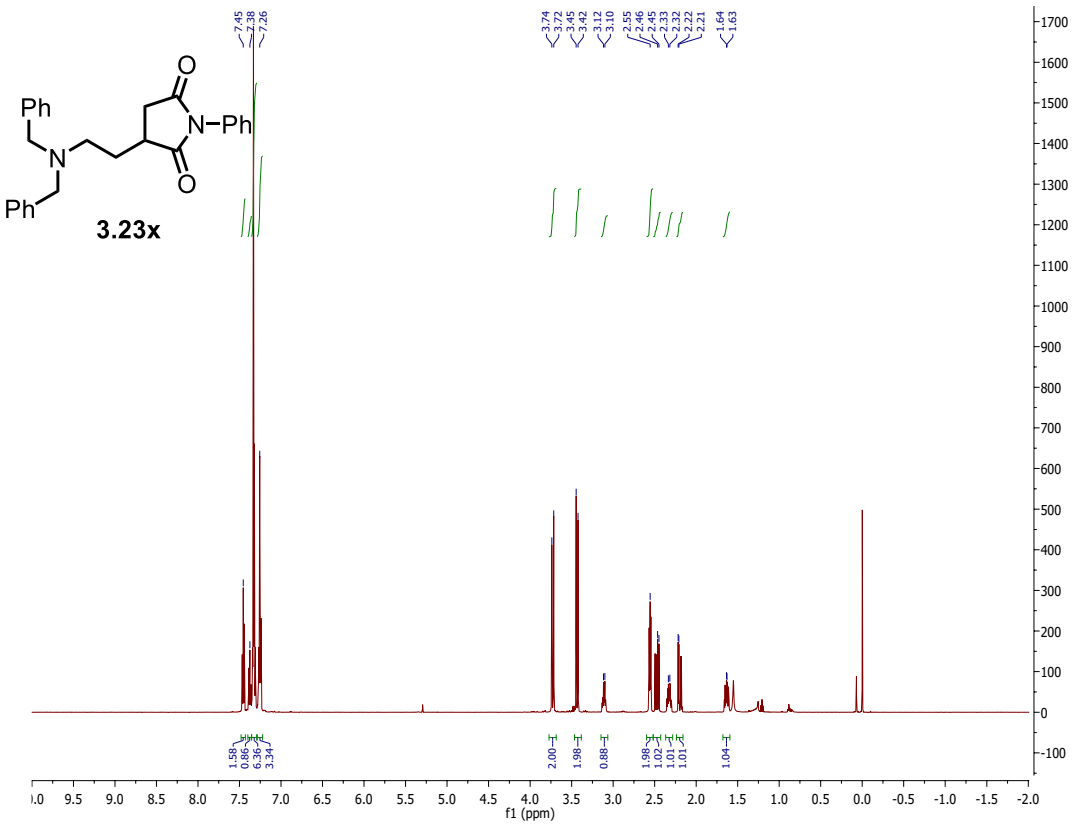
Ph
N
Ph
O
N–Ph
O
3.23x
7.45
7.38
7.26
3.74
3.72
3.45
3.42
3.12
3.10
2.55
2.46
2.45
2.33
2.32
2.22
2.21
1.64
1.63
1.58
0.86
6.36
3.34
2.00
1.98
0.88
1.98
1.02
1.01
1.01
1.04
f1 (ppm)

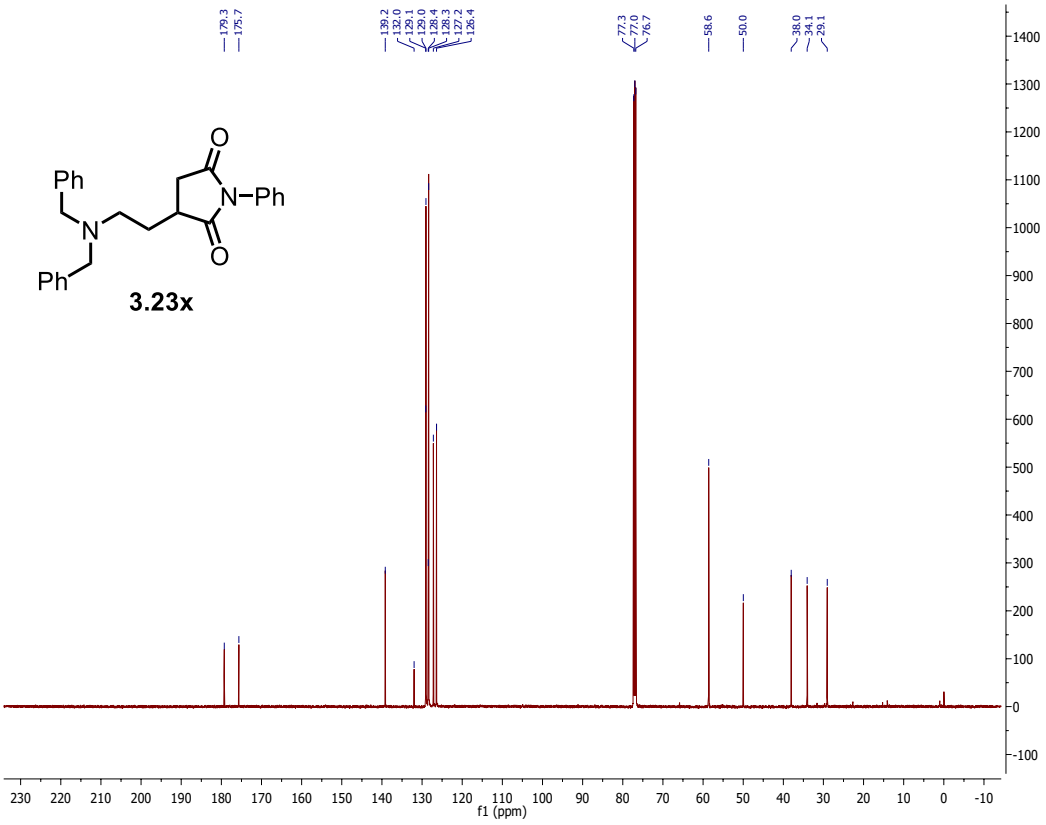
Ph
N
Ph
O
N–Ph
O
3.23x
179.3
175.7
139.2
132.0
129.1
129.0
128.4
128.3
127.2
126.4
77.3
77.0
76.7
58.6
50.0
38.0
34.1
29.1
f1 (ppm)

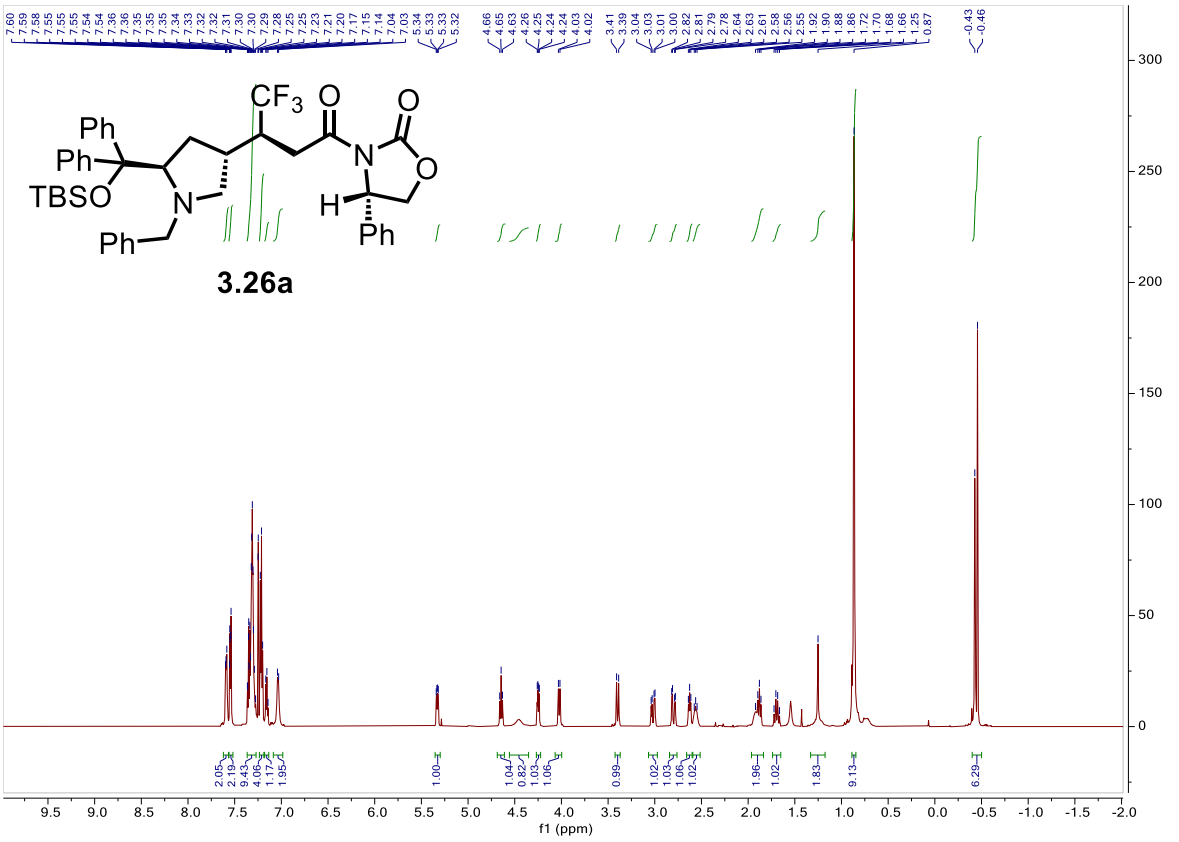
CF3
O
O
Ph
Ph
TBSO
N
N
O
H
Ph
Ph
3.26a
f1 (ppm)

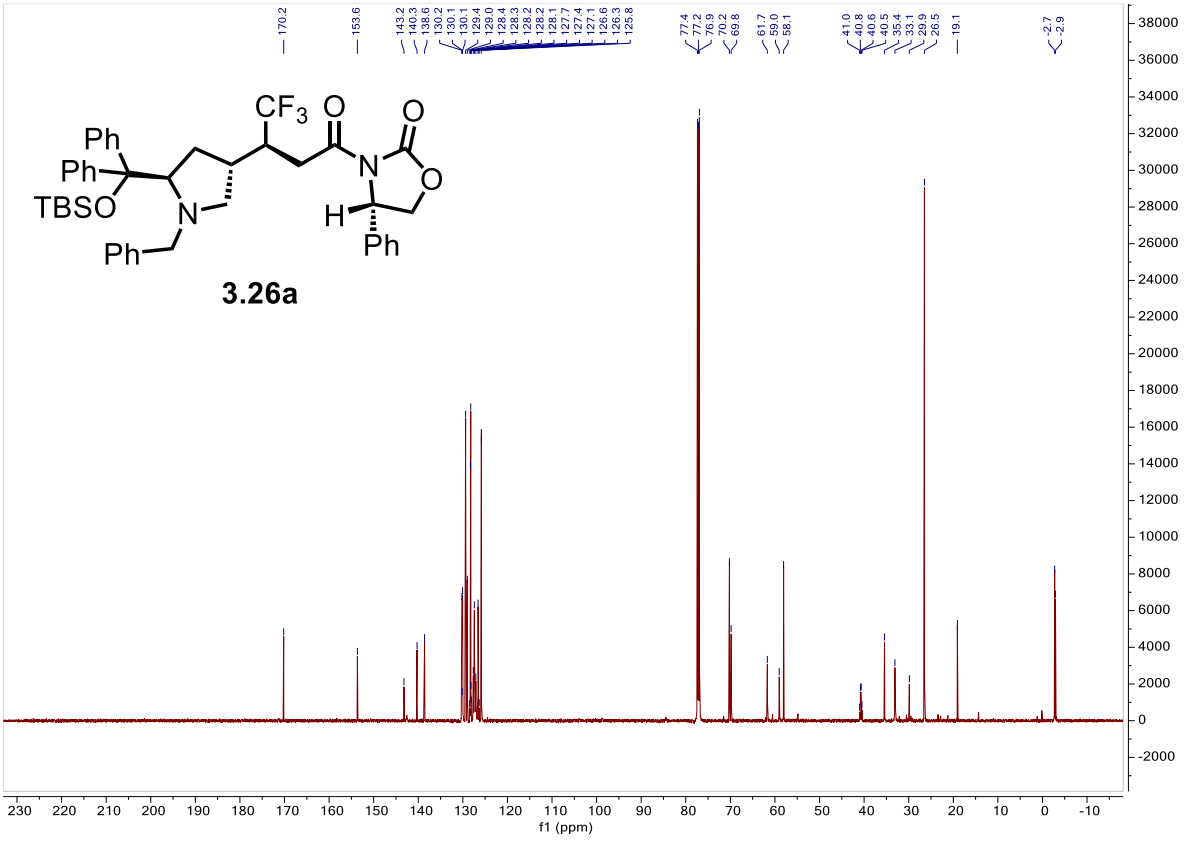
CF3
O
O
Ph
Ph
TBSO
N
N
O
H
Ph
Ph
3.26a
f1 (ppm)

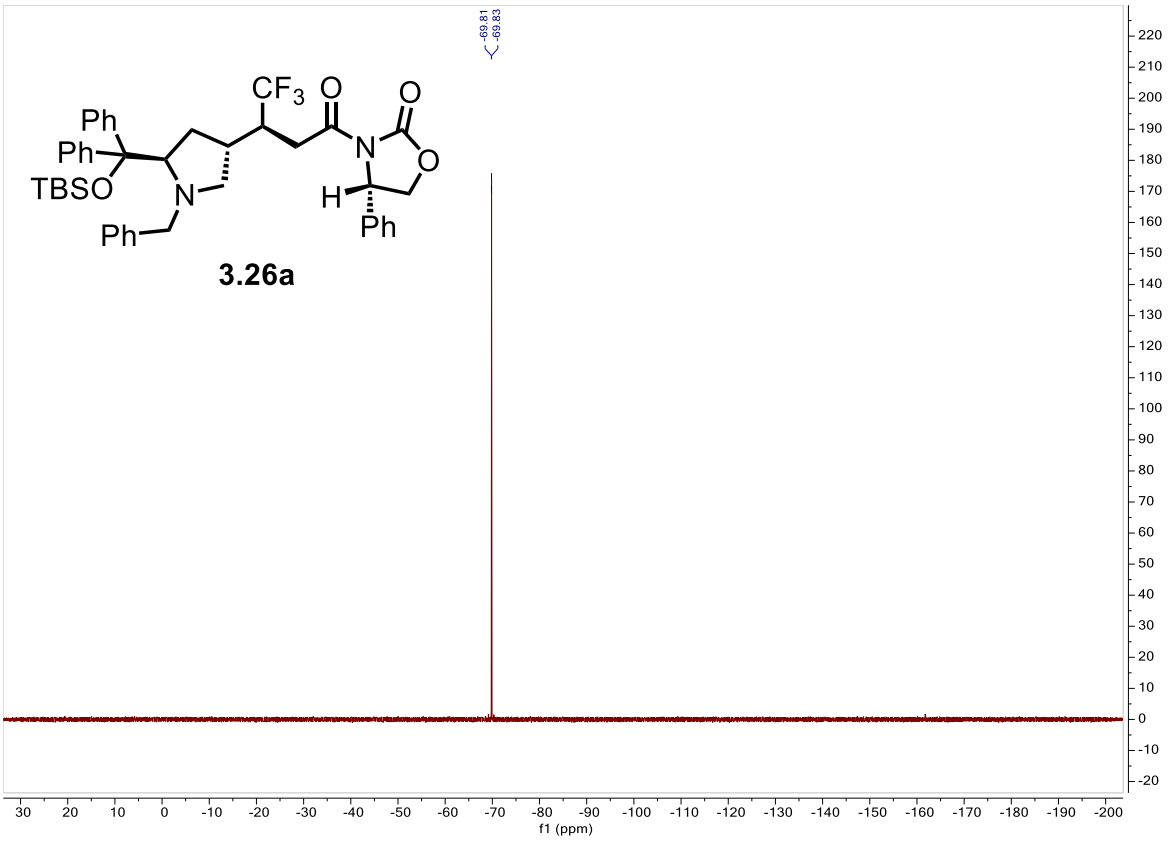
-69.81
-69.83
CF3
O
O
Ph
Ph
TBSO
N
N
O
H
Ph
Ph
3.26a
220
210
200
190
180
170
160
150
140
130
120
110
100
90
80
70
60
50
40
30
20
10
0
-10
-20
30 20 10 0 -10 -20 -30 -40 -50 -60 -70 -80 -90 -100 -110 -120 -130 -140 -150 -160 -170 -180 -190 -200
f1 (ppm)

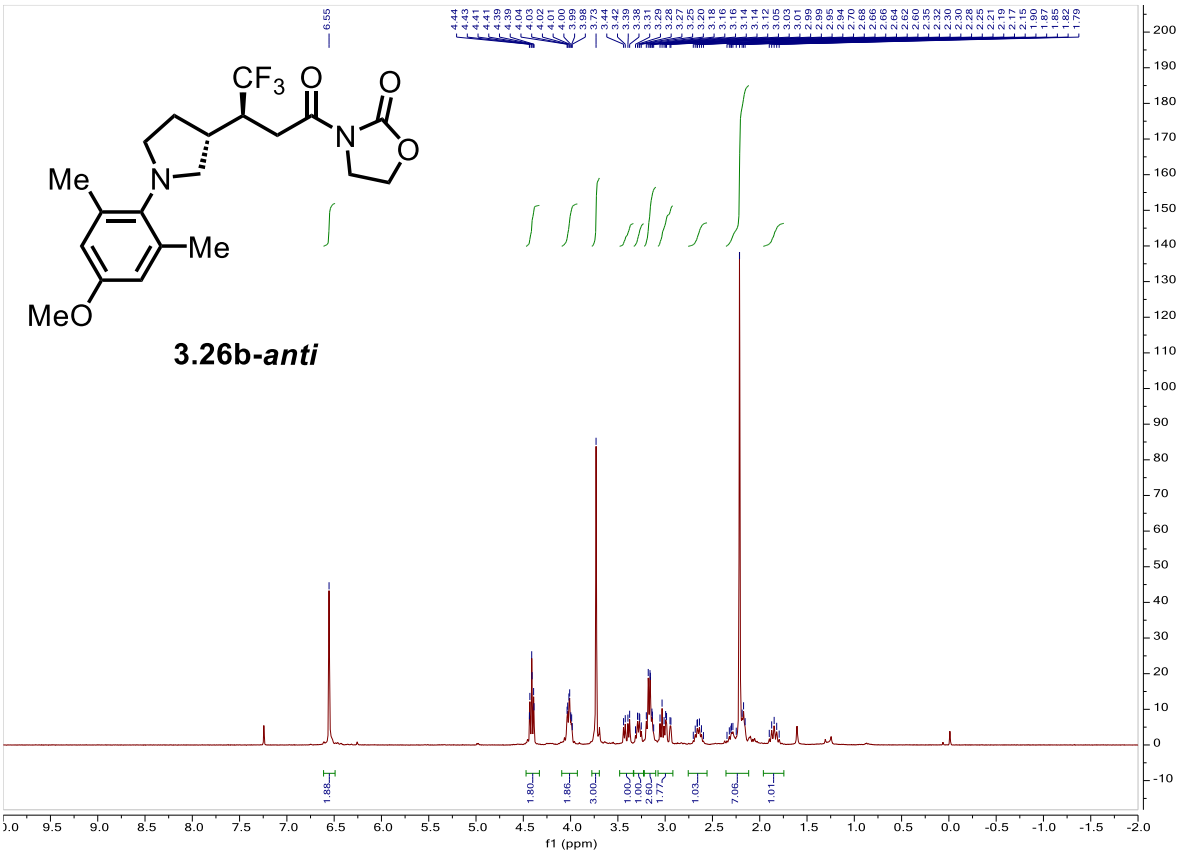
CF3
O
O
N
O
Me
N
Me
MeO
3.26b-*anti*
f1 (ppm)

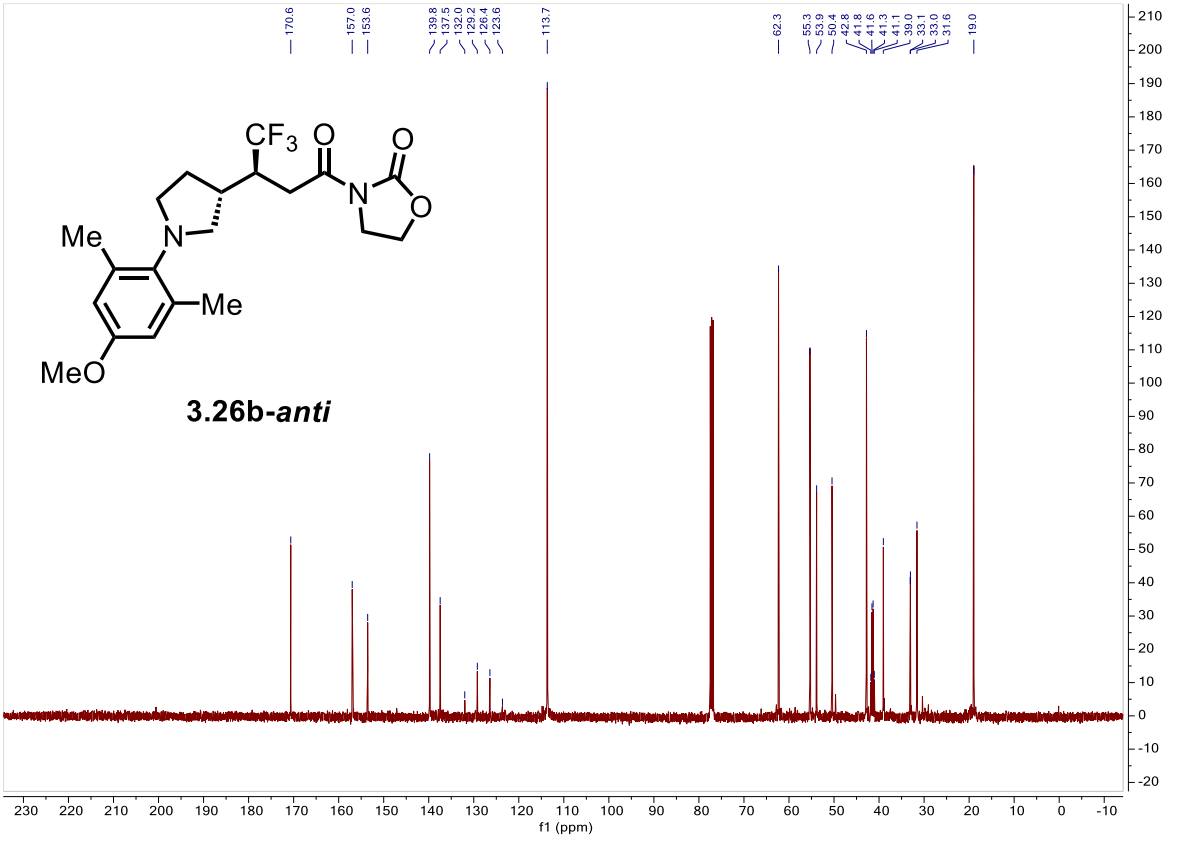
CF3
O
O
N
O
Me
N
Me
MeO
3.26b-*anti*
f1 (ppm)

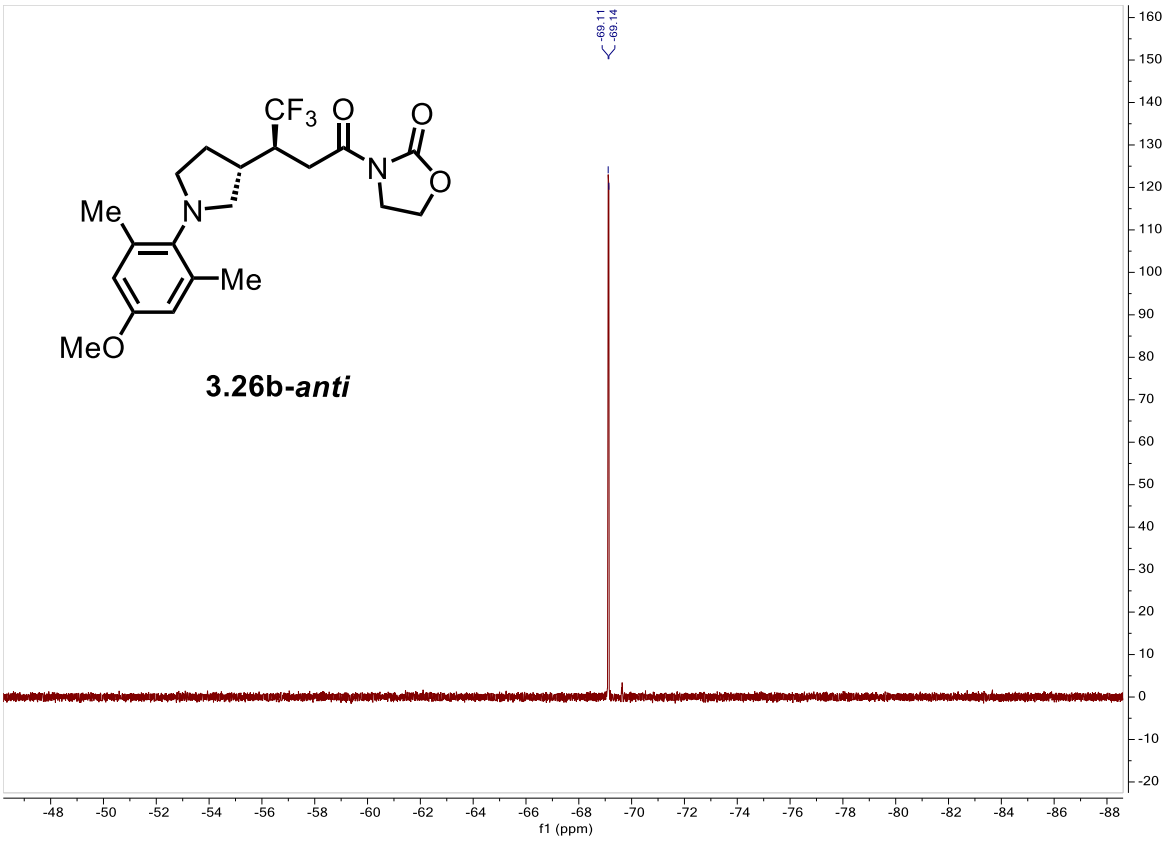
-69.11
-69.14
CF3
O
O
N
O
Me
N
Me
MeO
3.26b-anti
160
150
140
130
120
110
100
90
80
70
60
50
40
30
20
10
0
-10
-20
-48
-50
-52
-54
-56
-58
-60
-62
-64
-66
-68
-70
-72
-74
-76
-78
-80
-82
-84
-86
-88
f1 (ppm)

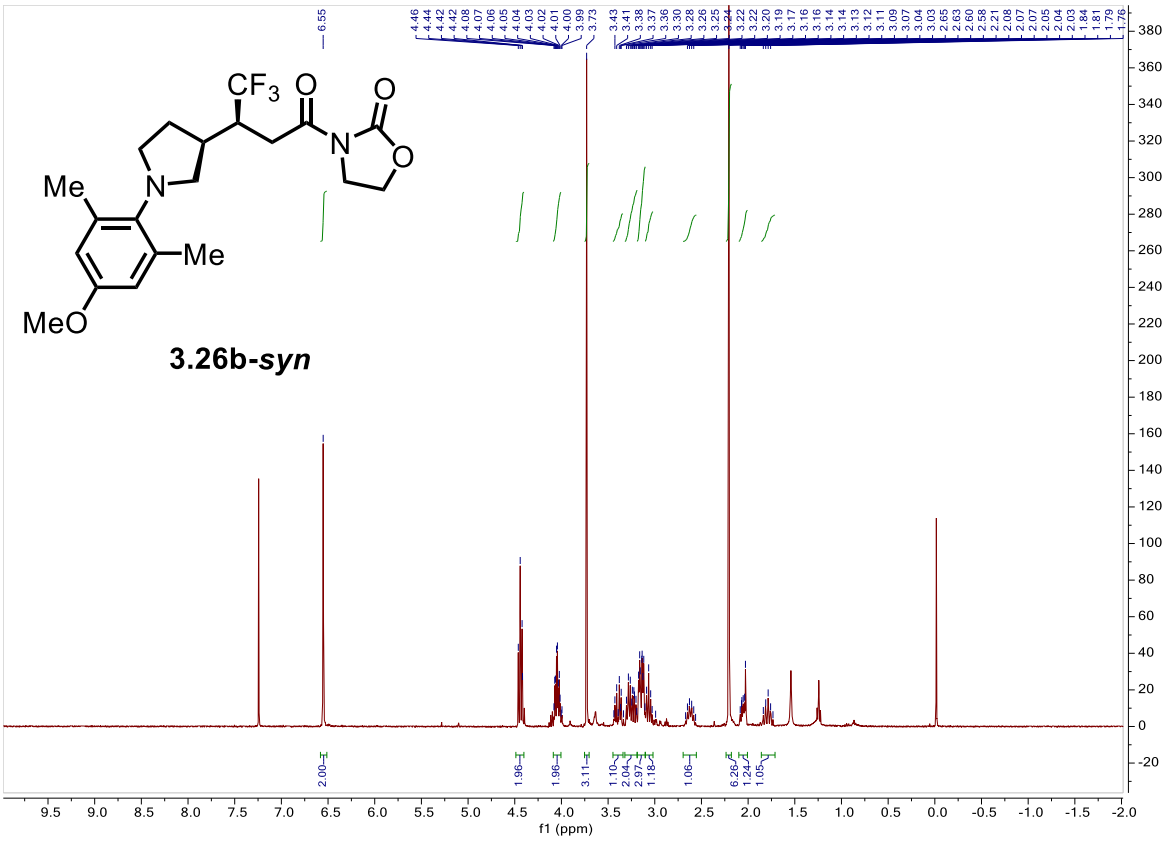
CF3
O
O
N
O
Me
N
Me
MeO
3.26b-*syn*
f1 (ppm)

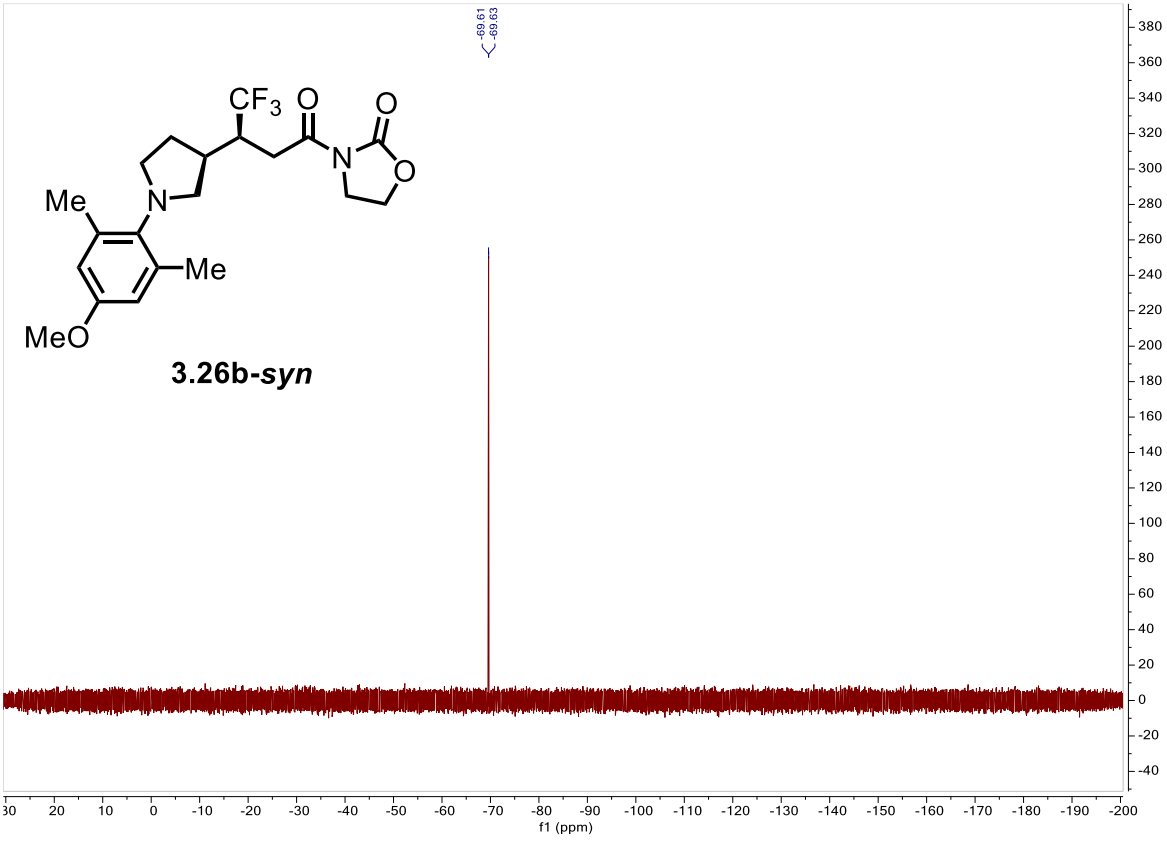
-69.61
-69.63
CF3
O
O
N
O
Me
N
Me
MeO
3.26b-*syn*
f1 (ppm)

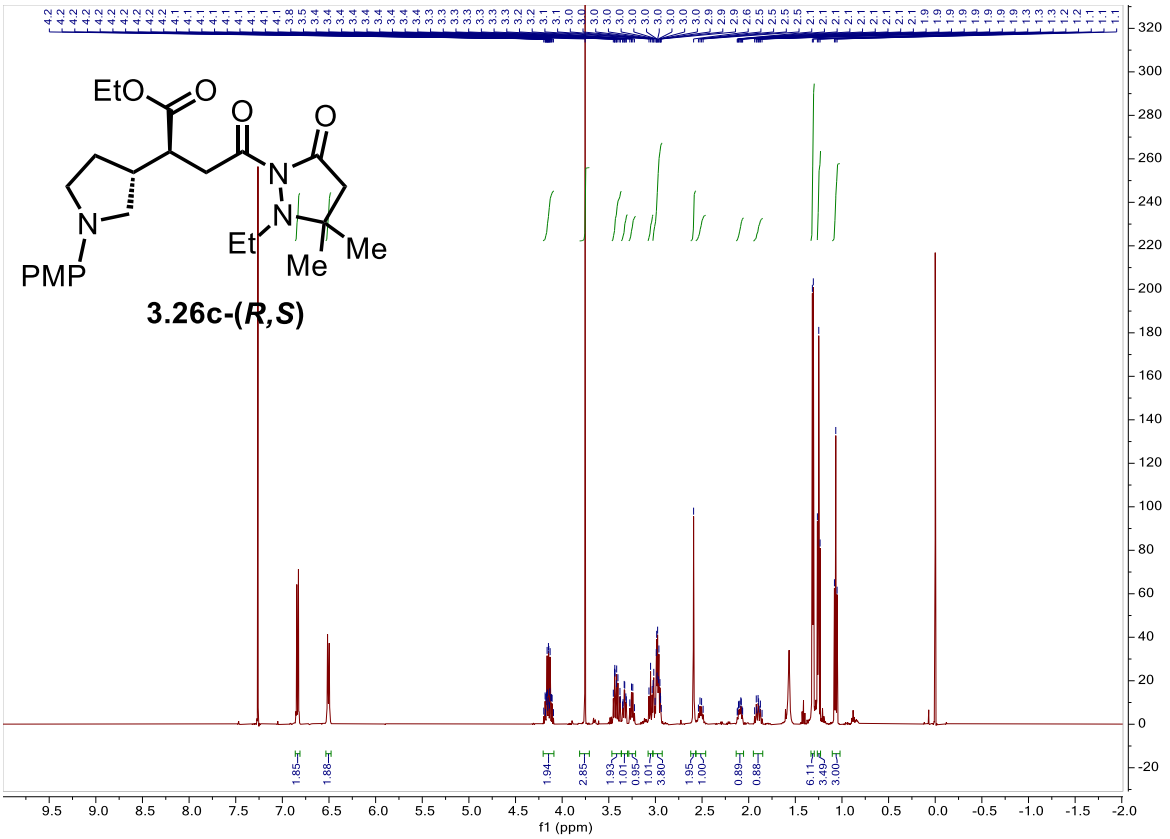
EtO
O
O
O
N
N
N
Et
Me
Me
PMP
3.26c-(R,S)
f1 (ppm)

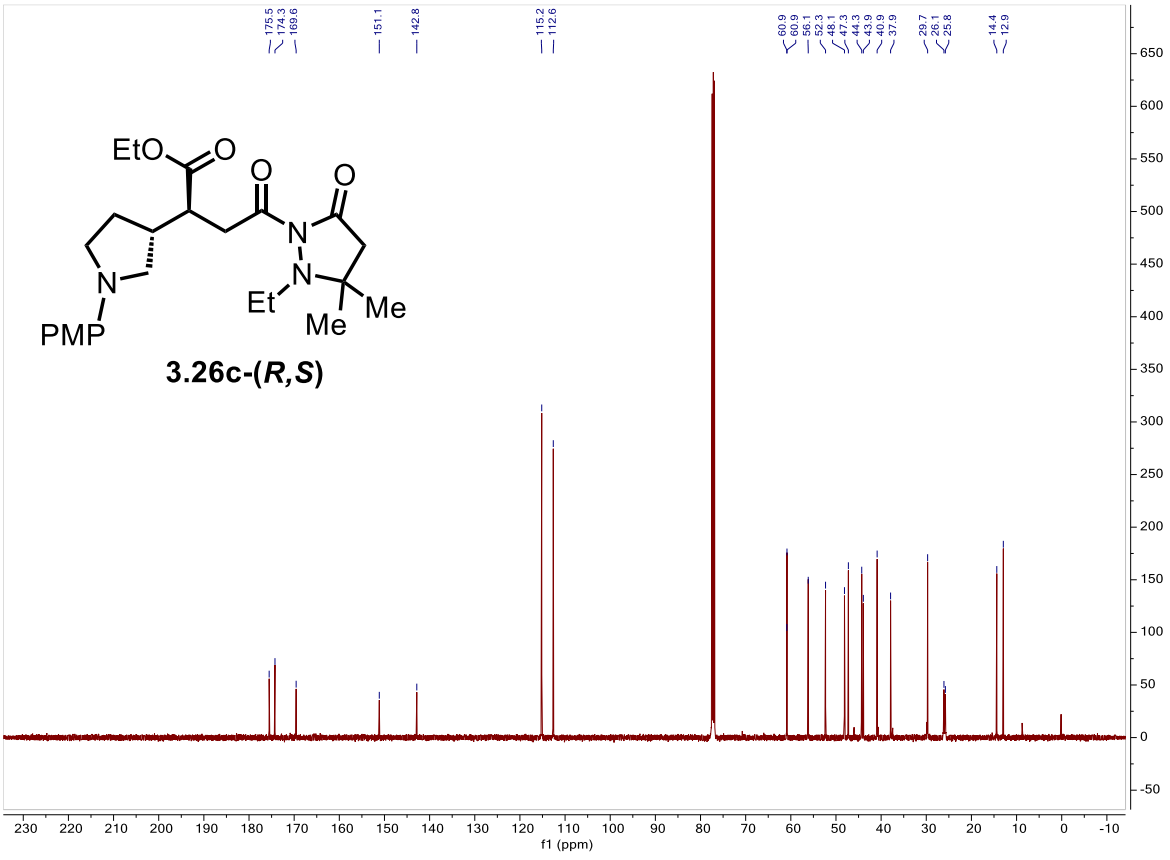
EtO
O
O
O
N
N
N
Et
Me
Me
PMP
3.26c-(R,S)
f1 (ppm)

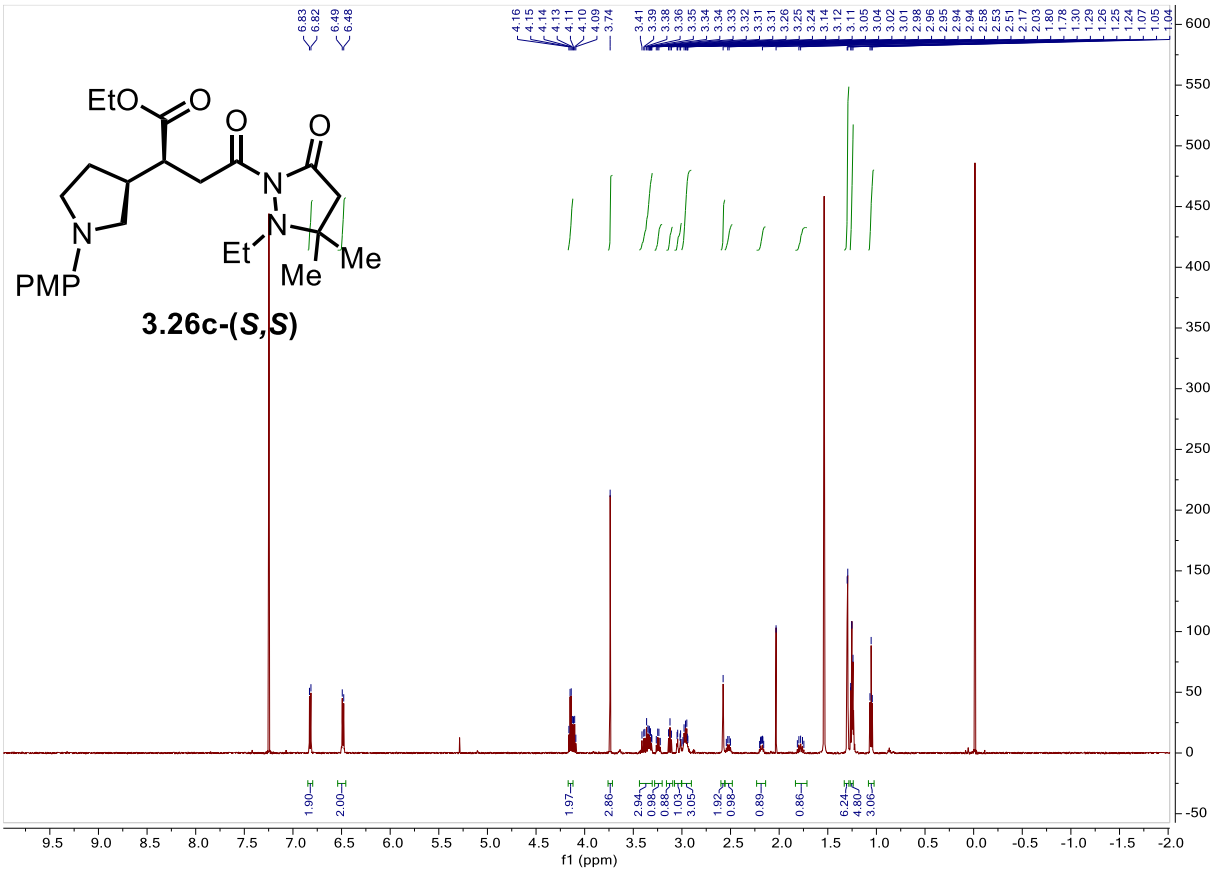
EtO
O
O
O
N
N
N
PMP
Et
Me
Me
3.26c-(S,S)
f1 (ppm)

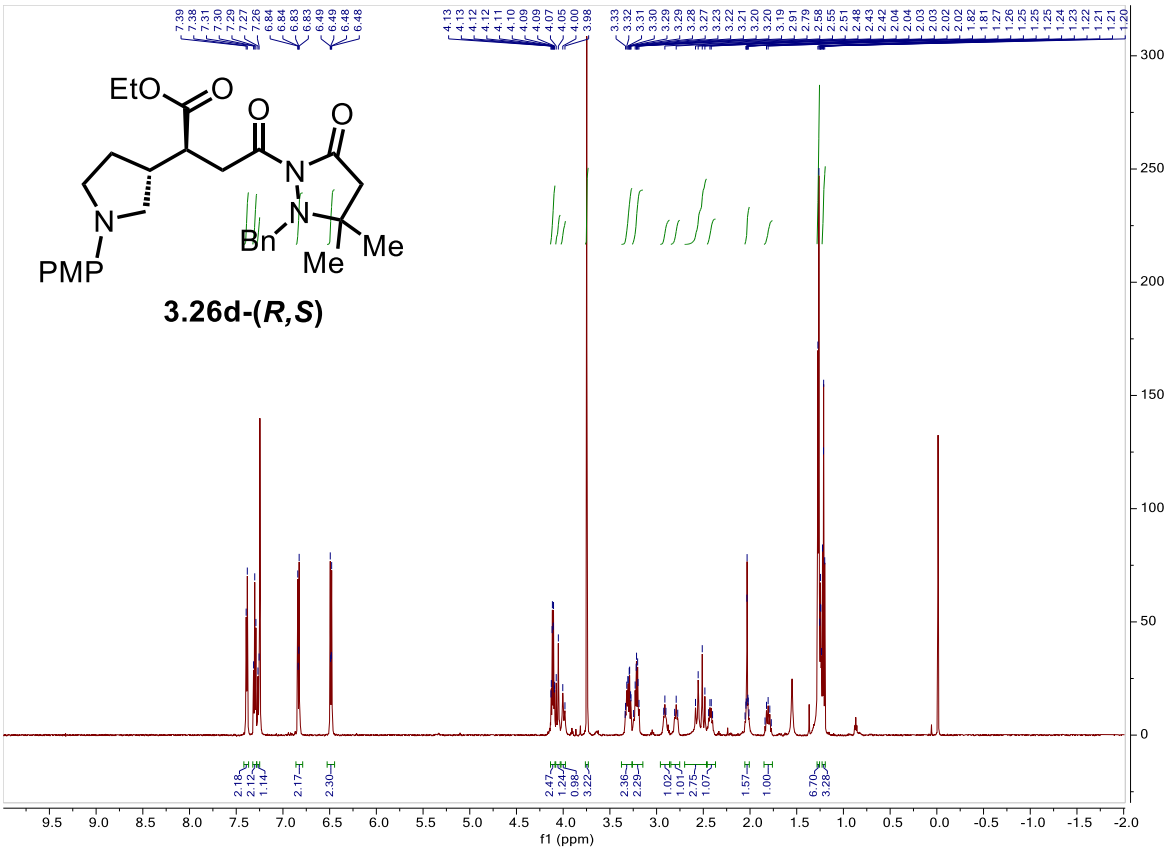
EtO
O
O
O
N
N
N
Bn
Me
Me
PMP
3.26d-(R,S)
f1 (ppm)

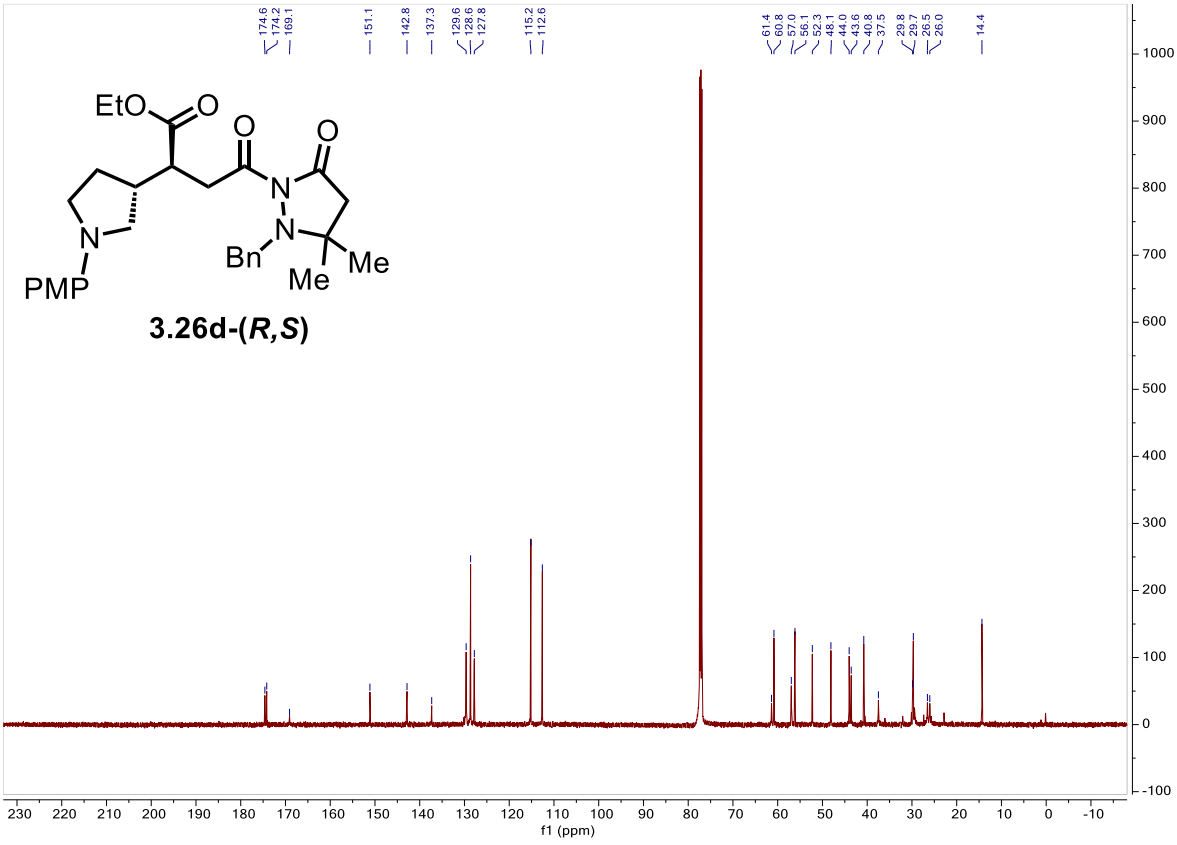
EtO
O
O
O
N
N
N
Bn
Me
Me
PMP
3.26d-(R,S)
f1 (ppm)

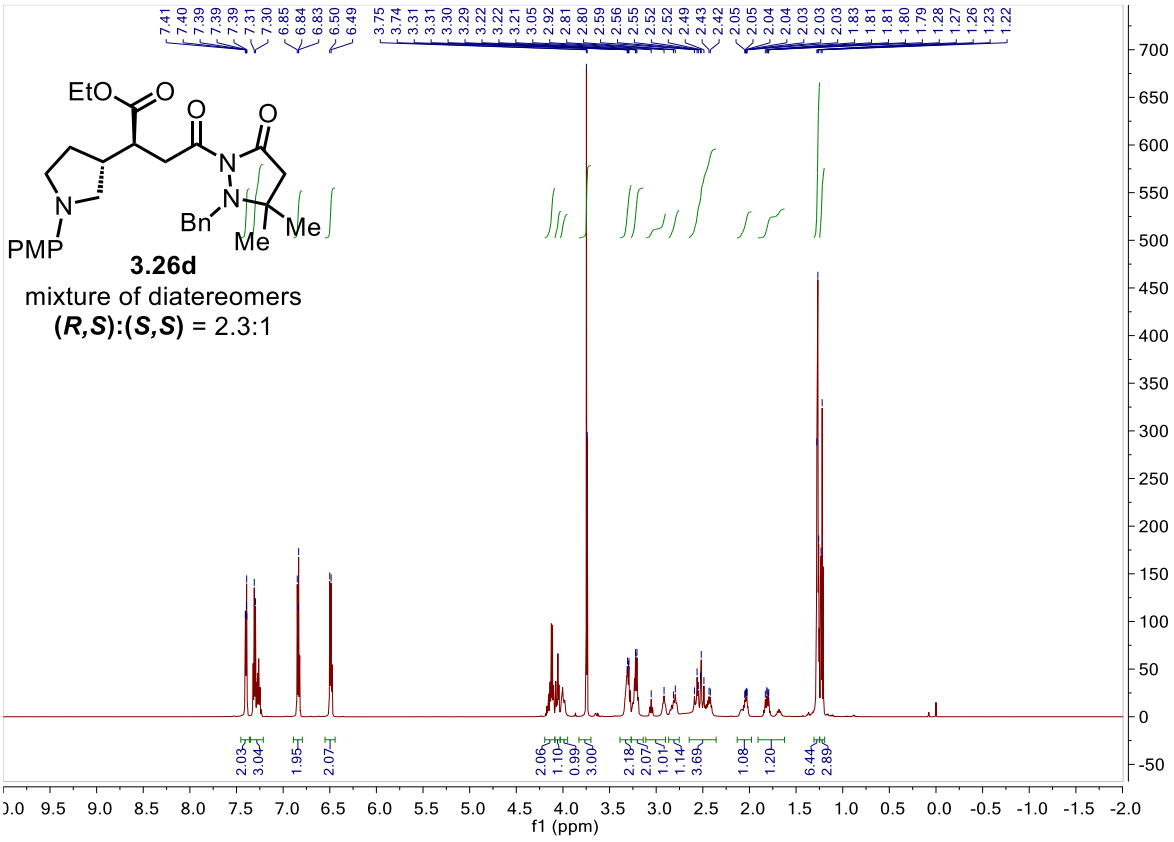
EtO
O
O
O
N
N
Bn
Me
Me
N
PMP
3.26d
mixture of diatereomers
(R,S):(S,S) = 2.3:1
f1 (ppm)

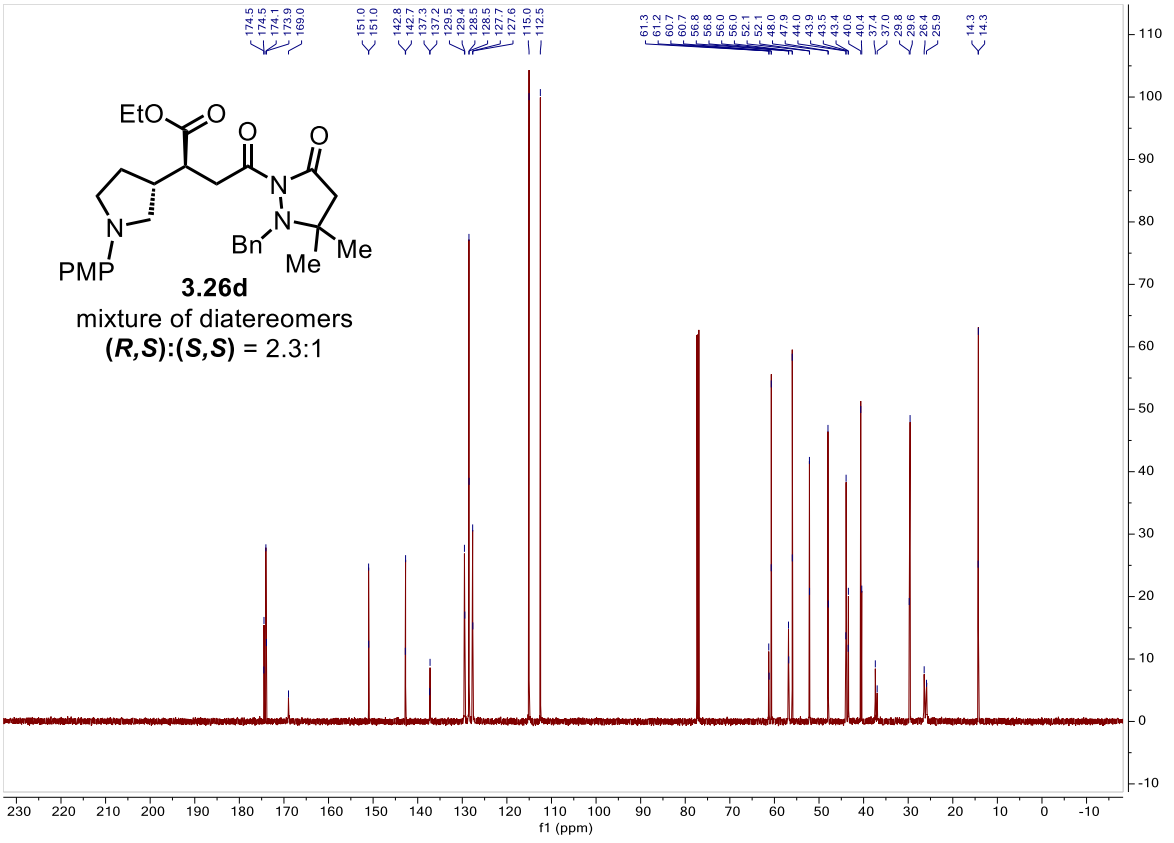
EtO
O
O
O
N
N
Bn
Me
Me
N
PMP
3.26d
mixture of diatereomers
(R,S):(S,S) = 2.3:1
f1 (ppm)

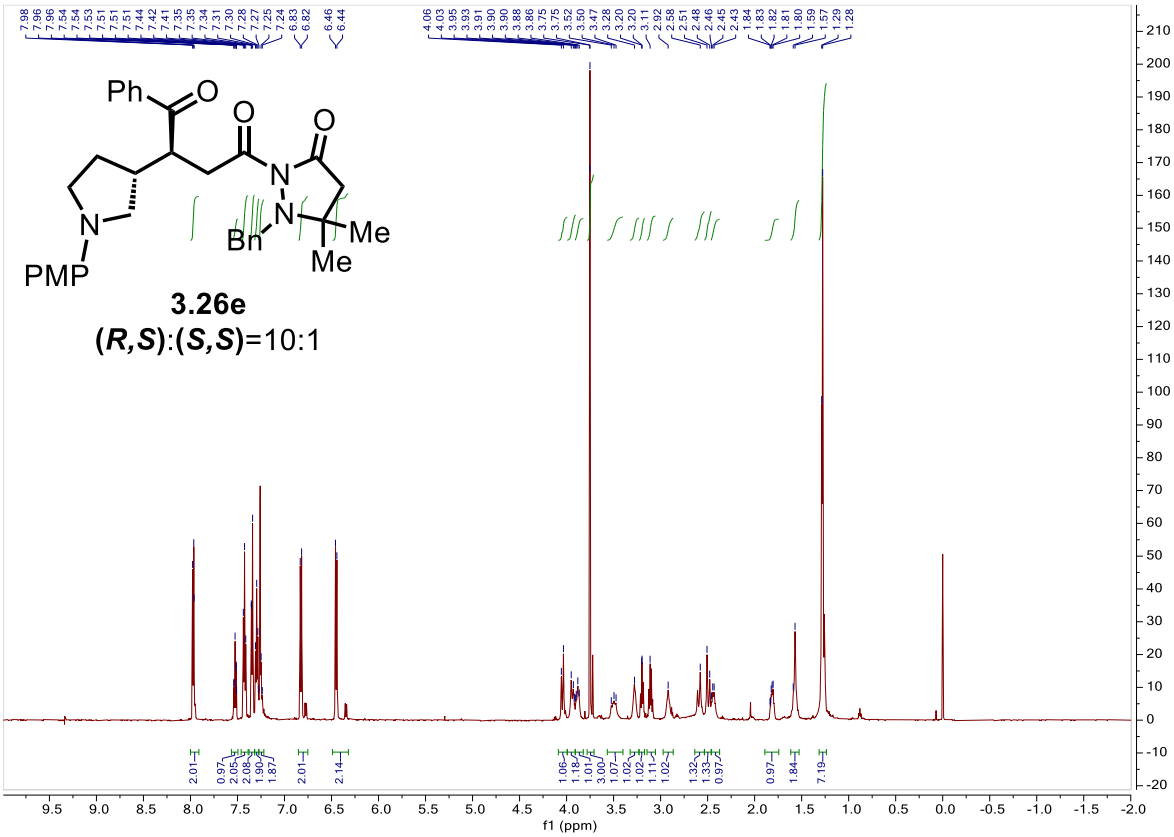
Ph
O
O
O
N
N
N
Bn
Me
Me
PMP
3.26e
(R,S):(S,S)=10:1
f1 (ppm)

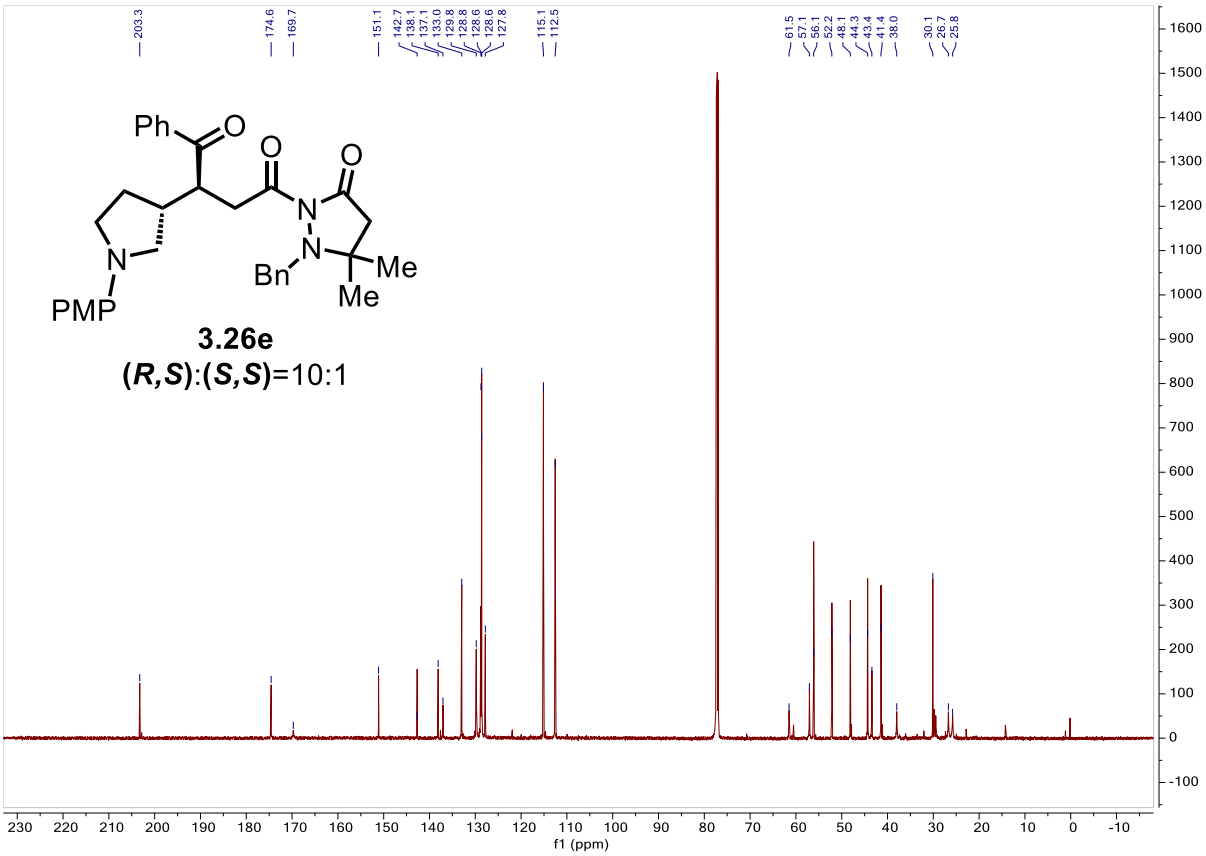
Ph
O
O
O
N
N
N
Bn
Me
Me
PMP
3.26e
(R,S):(S,S)=10:1
f1 (ppm)

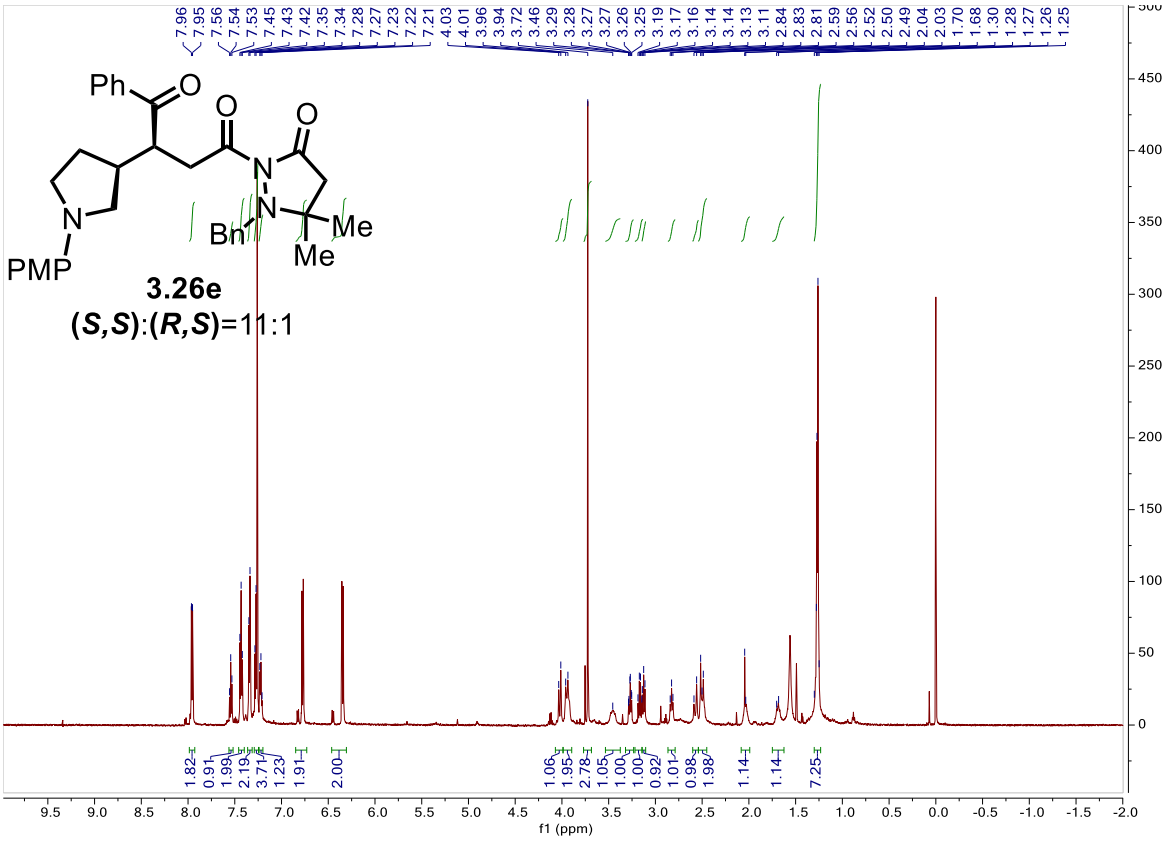
Ph
O
O
O
N
N
Bn
Me
Me
N
PMP
3.26e
(S,S):(R,S)=11:1
f1 (ppm)

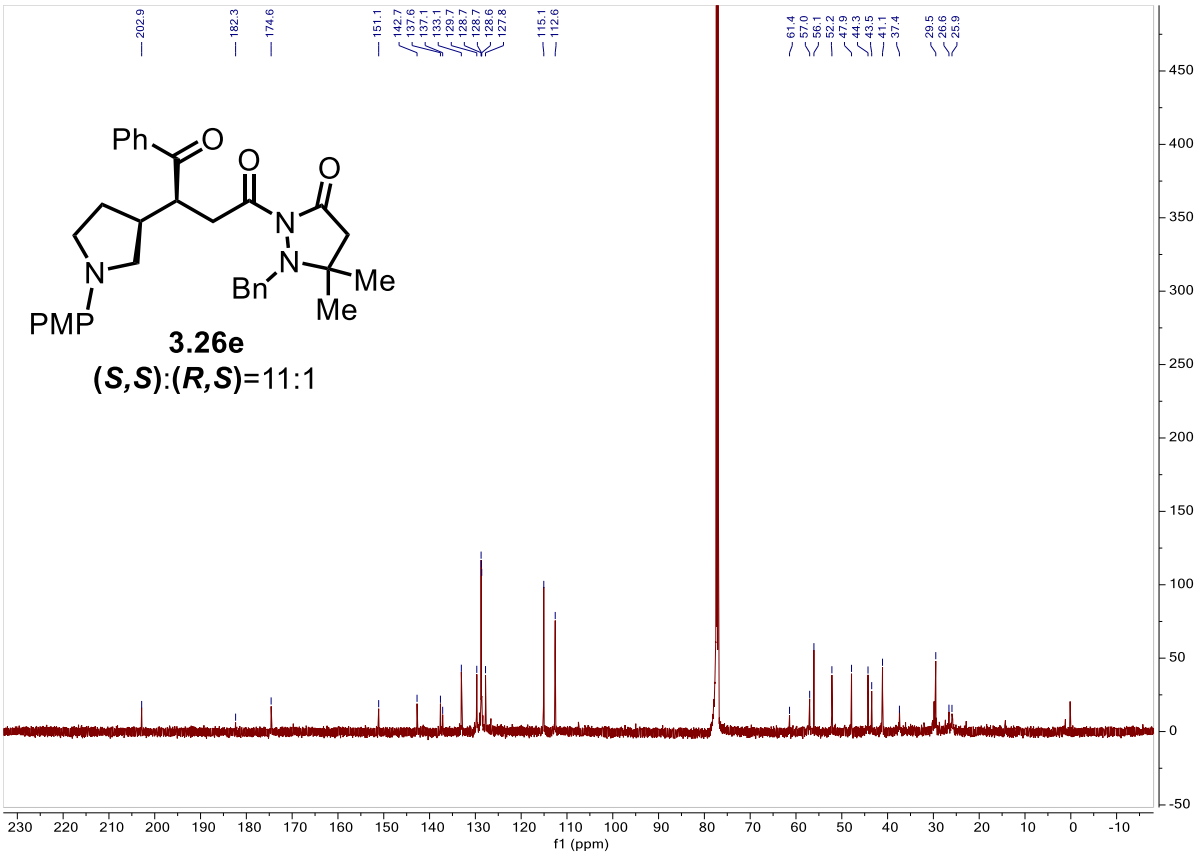
Ph
O
O
O
N
N
Bn
Me
Me
N
PMP
3.26e
(S,S):(R,S)=11:1
f1 (ppm)

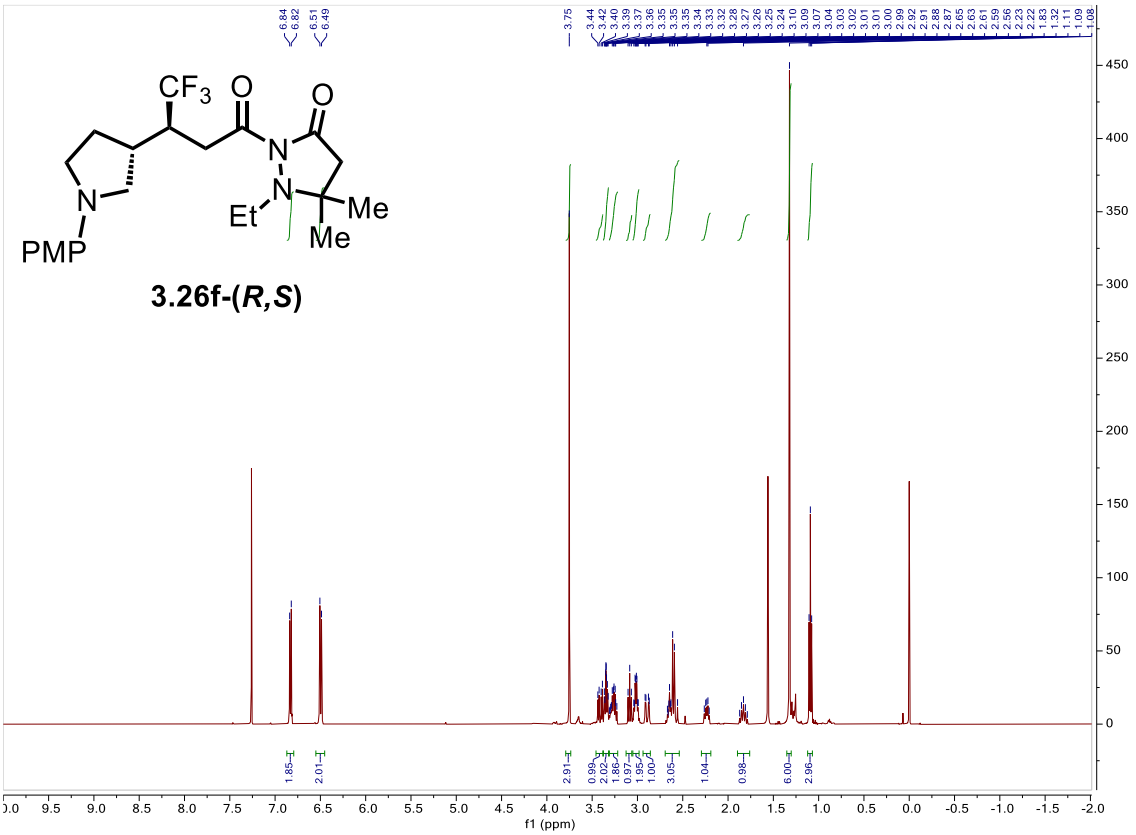
CF3
O
O
N
N
N
Et
Me
Me
PMP
3.26f-(R,S)
f1 (ppm)

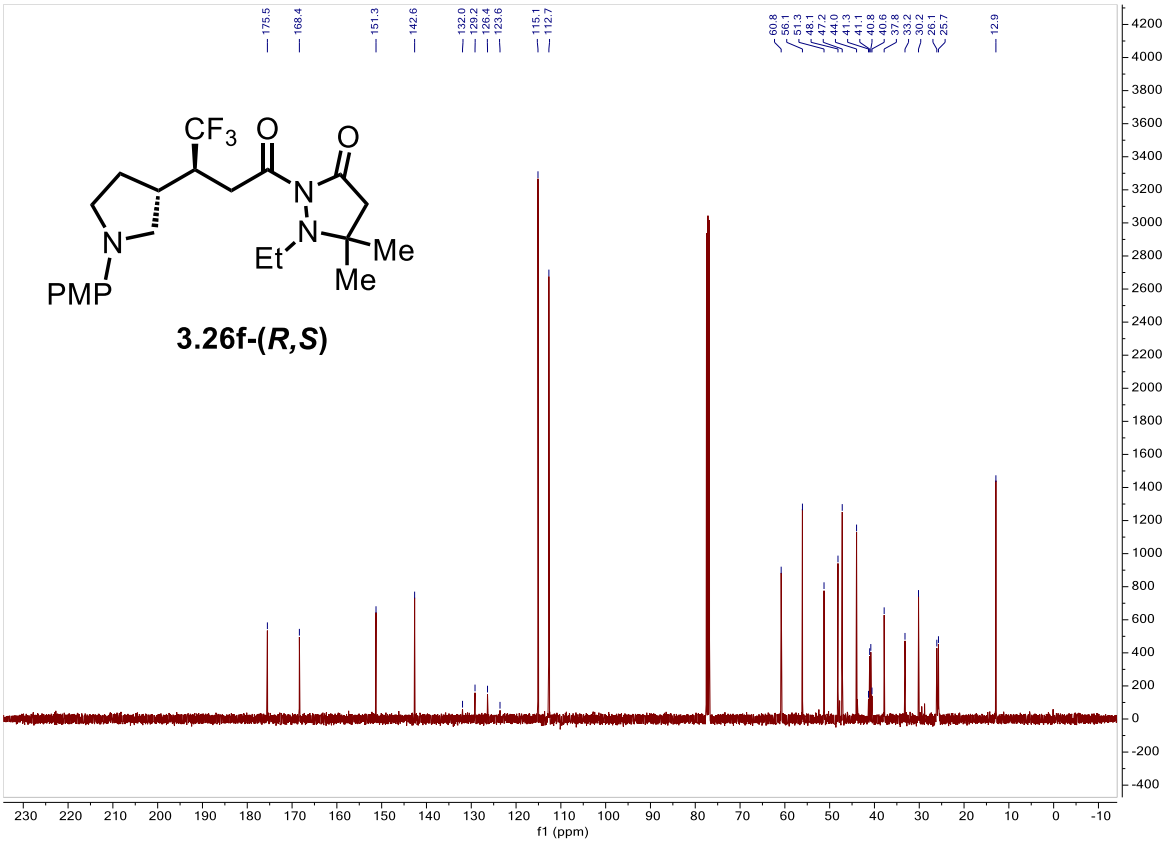
CF3
O
O
N
N
N
Et
Me
Me
PMP
3.26f-(R,S)
f1 (ppm)

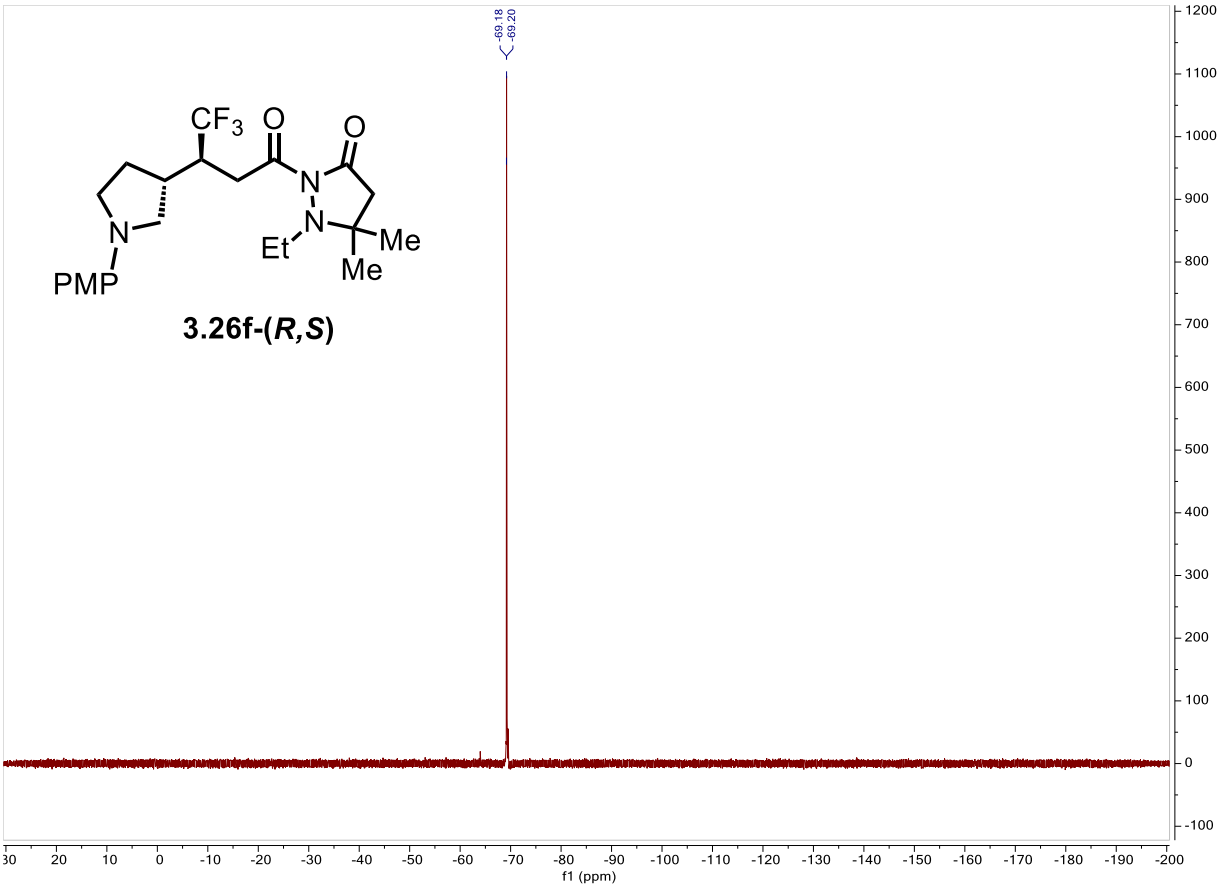
-69.18
-69.20
CF3
O
O
N
N
Et
Me
Me
N
PMP
1200
1100
1000
900
800
700
600
500
400
300
200
100
0
-100
30
20
10
0
-10
-20
-30
-40
-50
-60
-70
-80
-90
-100
-110
-120
-130
-140
-150
-160
-170
-180
-190
-200
f1 (ppm)

3.26f-(*R*,*S*)

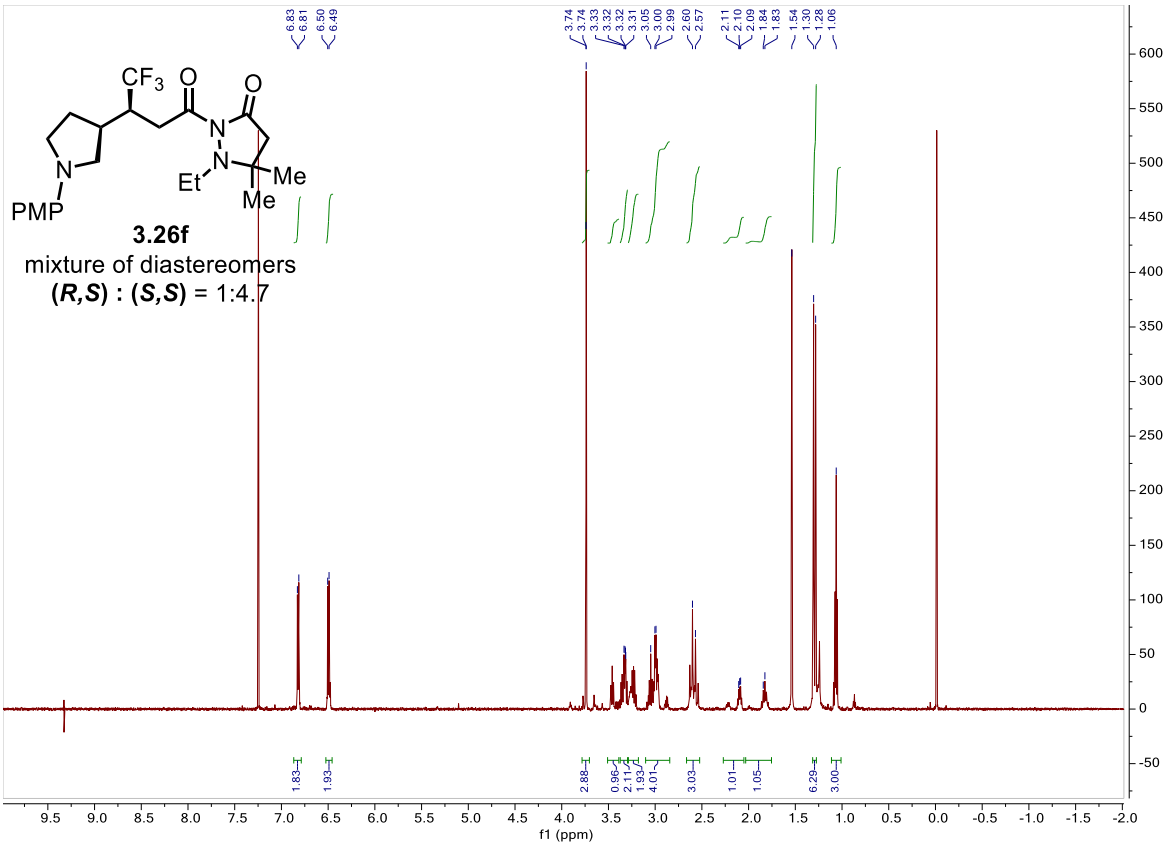
CF3
O
O
N
N
Et
Me
Me
PMP
3.26f
mixture of diastereomers
(R,S) : (S,S) = 1:4.7
f1 (ppm)

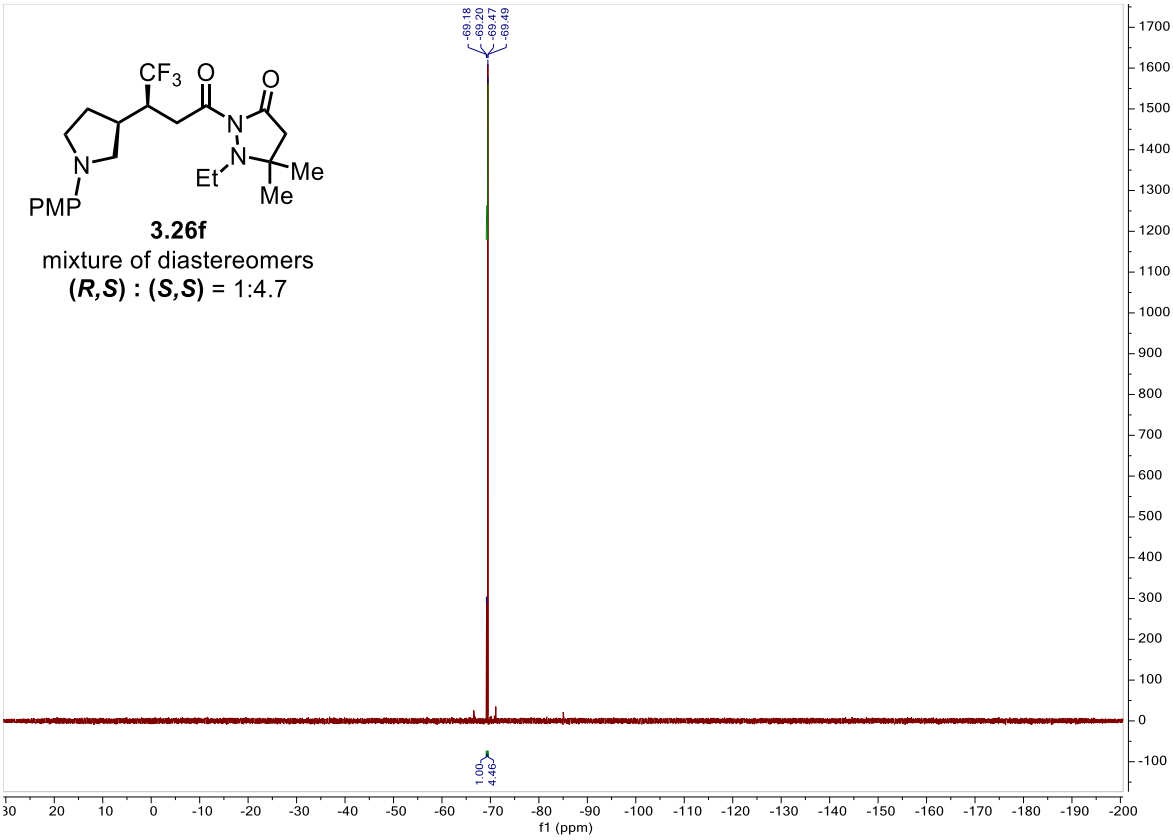
CF3
O
O
N
N
Et
Me
Me
PMP
3.26f
mixture of diastereomers
(R,S) : (S,S) = 1:4.7
f1 (ppm)

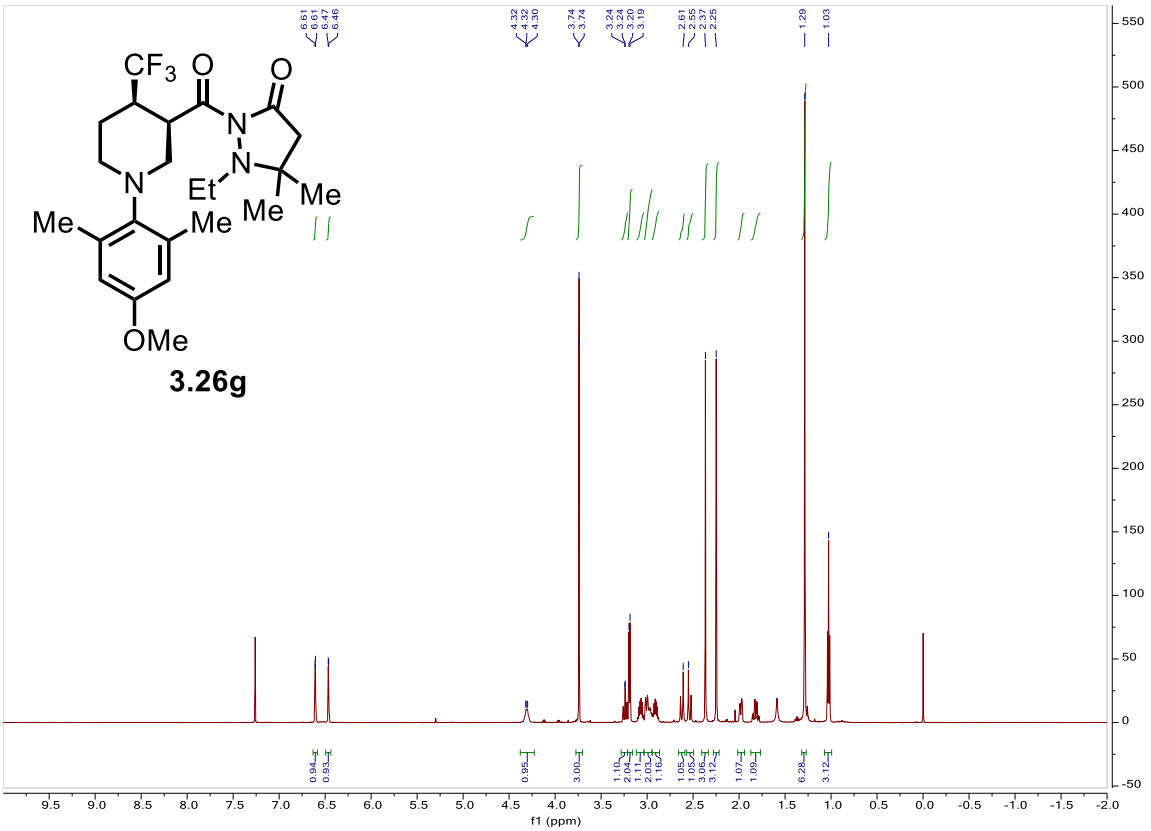
CF3
O
O
N
N
Et
Me
Me
Me
Me
N
OMe
3.26g
6.61
6.61
6.47
6.46
4.32
4.32
4.30
3.74
3.74
3.24
3.24
3.20
3.19
2.61
2.55
2.37
2.25
1.29
1.03
0.94
0.93
0.95
3.00
1.10
2.04
1.11
2.03
1.16
1.05
1.00
3.06
3.12
1.07
1.09
6.28
3.12
f1 (ppm)

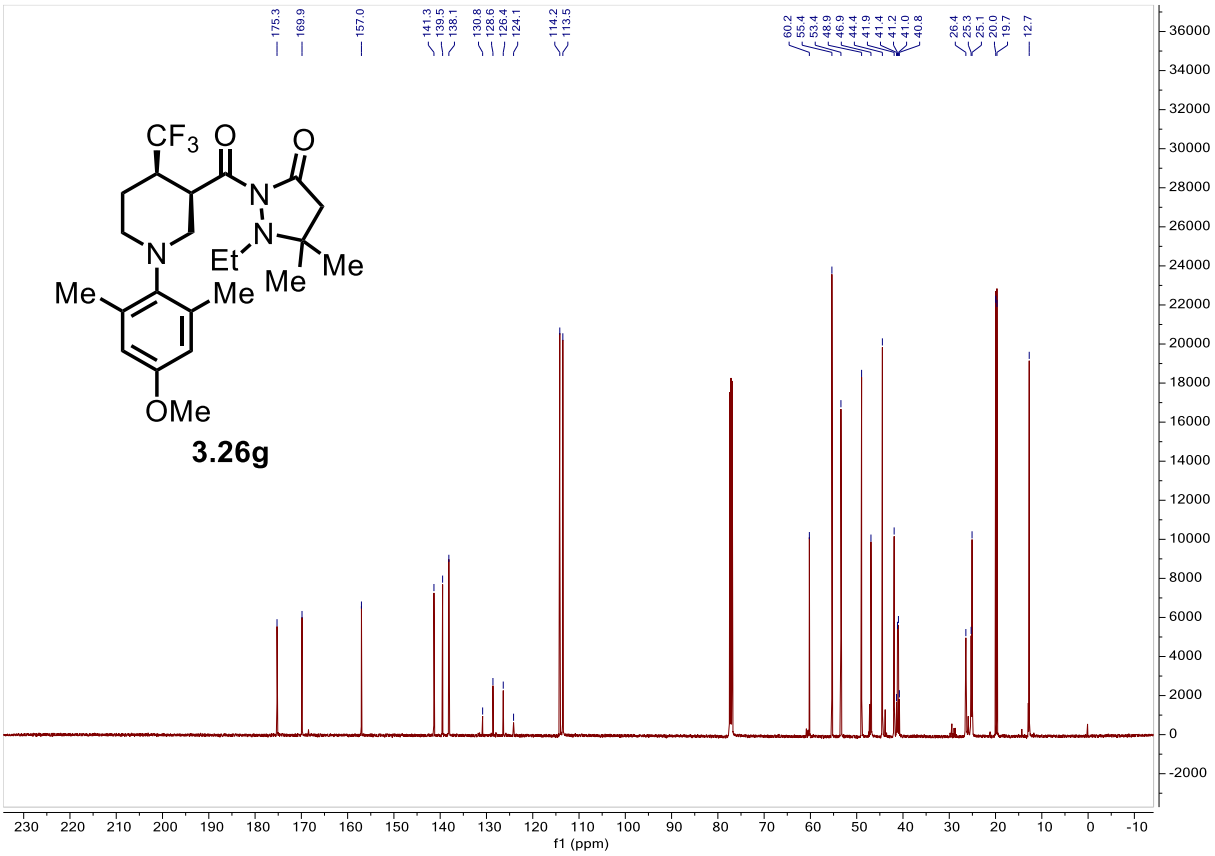
CF3
O
O
N
N
Et
Me
Me
Me
Me
N
OMe
3.26g
175.3
169.9
157.0
141.3
139.5
138.1
130.8
128.6
126.4
124.1
114.2
113.5
60.2
55.4
53.4
48.9
46.9
44.4
41.9
41.4
41.2
41.0
40.8
26.4
25.3
25.1
20.0
19.7
12.7
f1 (ppm)

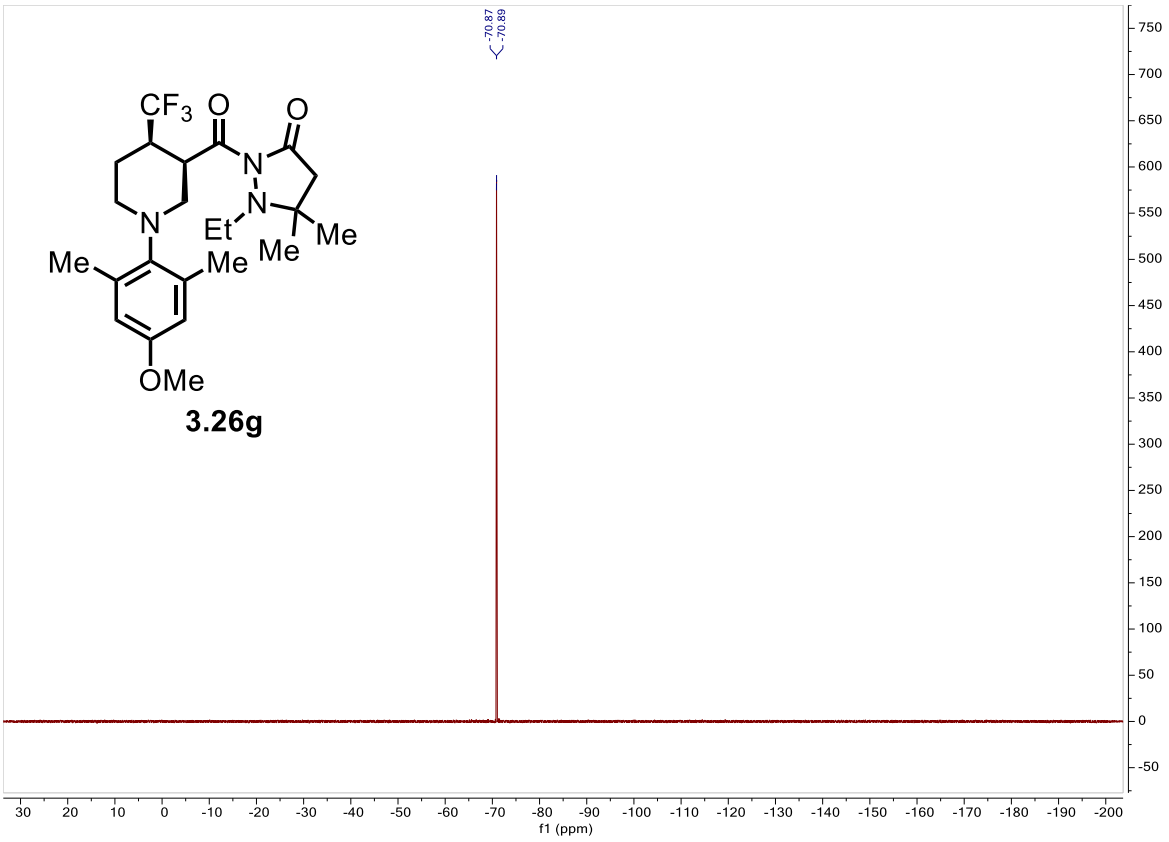
-70.87
-70.89
CF3
O
O
N
N
Et
Me
Me
N
Me
Me
OMe
3.26g
750
700
650
600
550
500
450
400
350
300
250
200
150
100
50
0
-50
30 20 10 0 -10 -20 -30 -40 -50 -60 -70 -80 -90 -100 -110 -120 -130 -140 -150 -160 -170 -180 -190 -200
f1 (ppm)

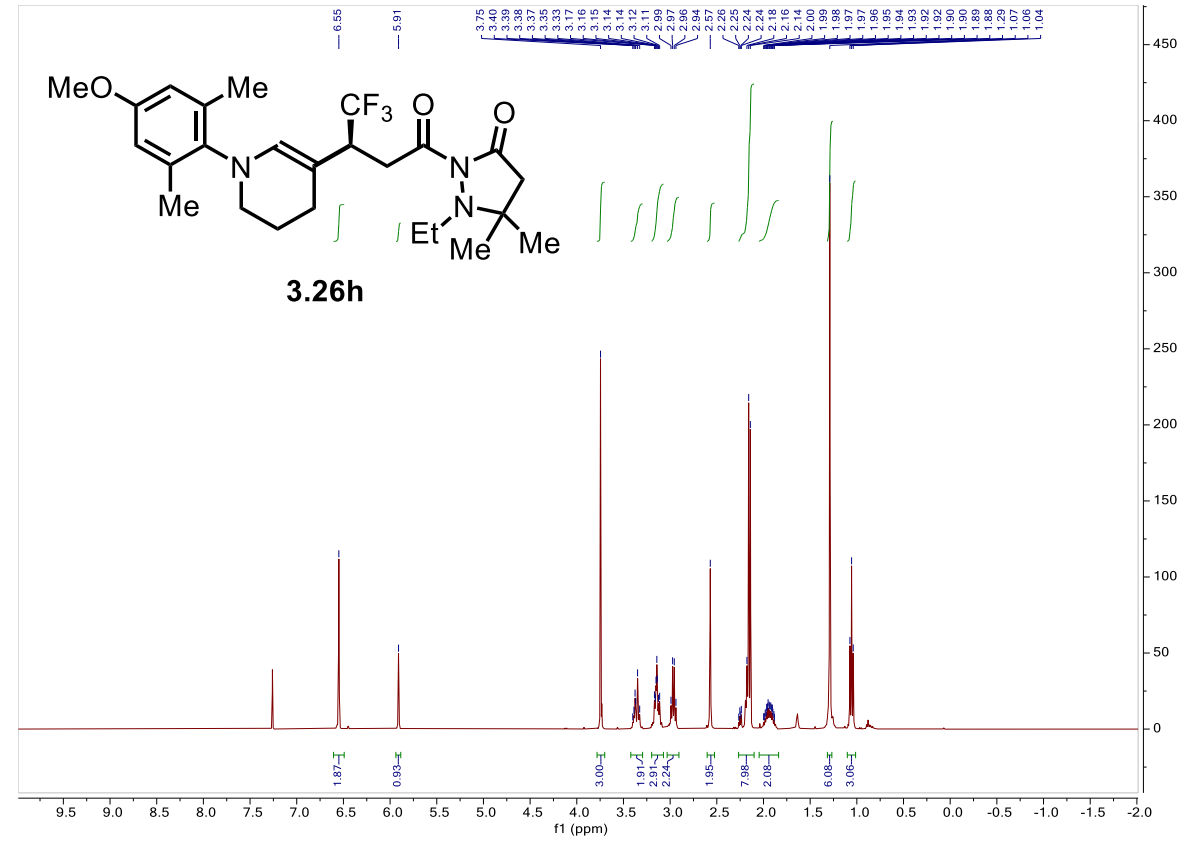
MeO
Me
Me
N
CF3
O
O
N
N
Et
Me
Me
3.26h
f1 (ppm)

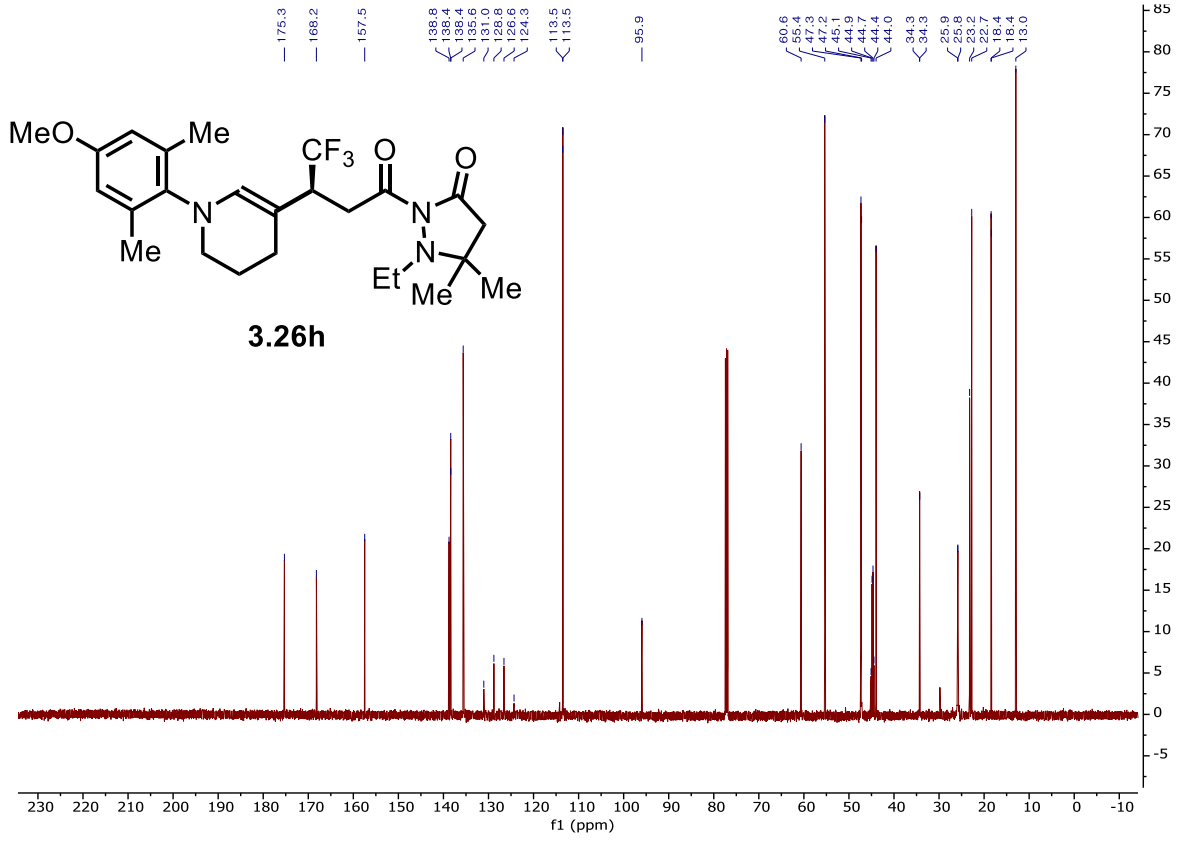
MeO
Me
Me
N
CF3
O
O
N
N
Et
Me
Me
3.26h
f1 (ppm)

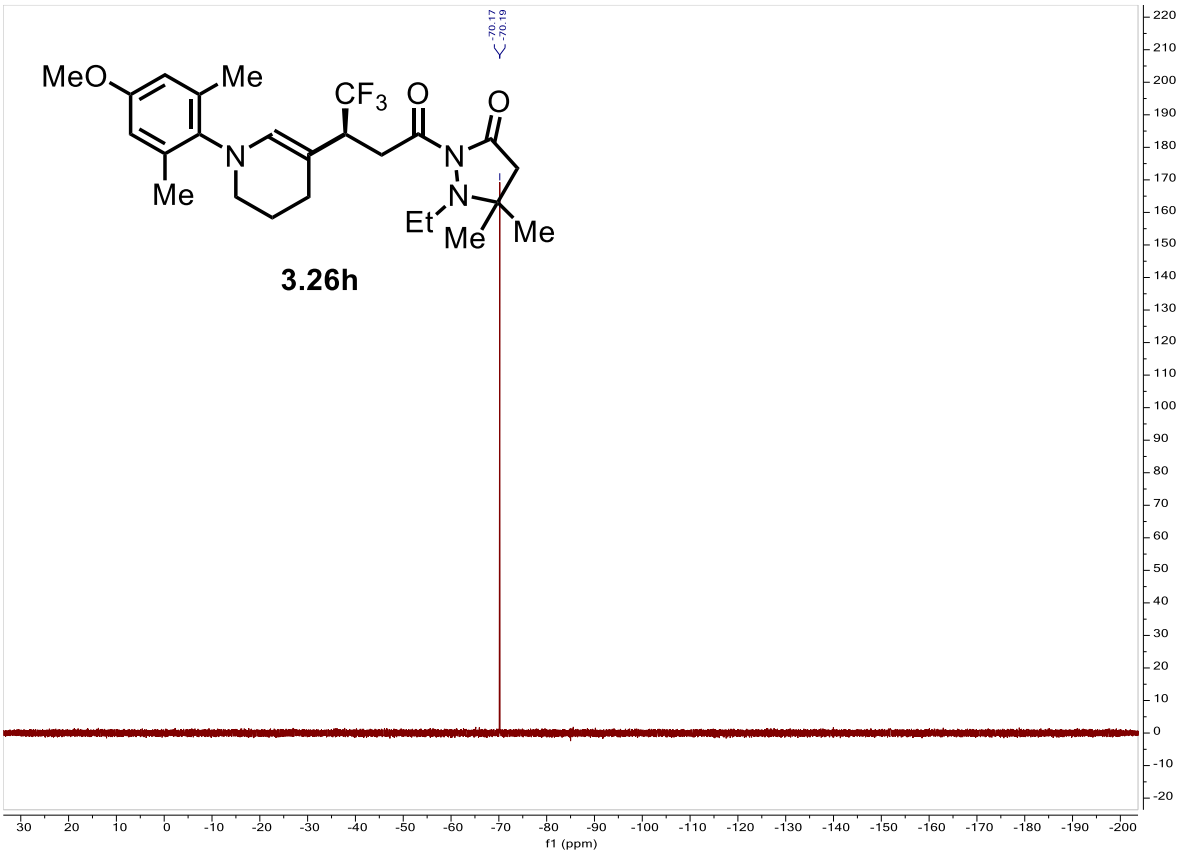
-70.17
-70.19
MeO
Me
Me
N
CF3
O
O
N
N
Et
Me
Me
3.26h
f1 (ppm)

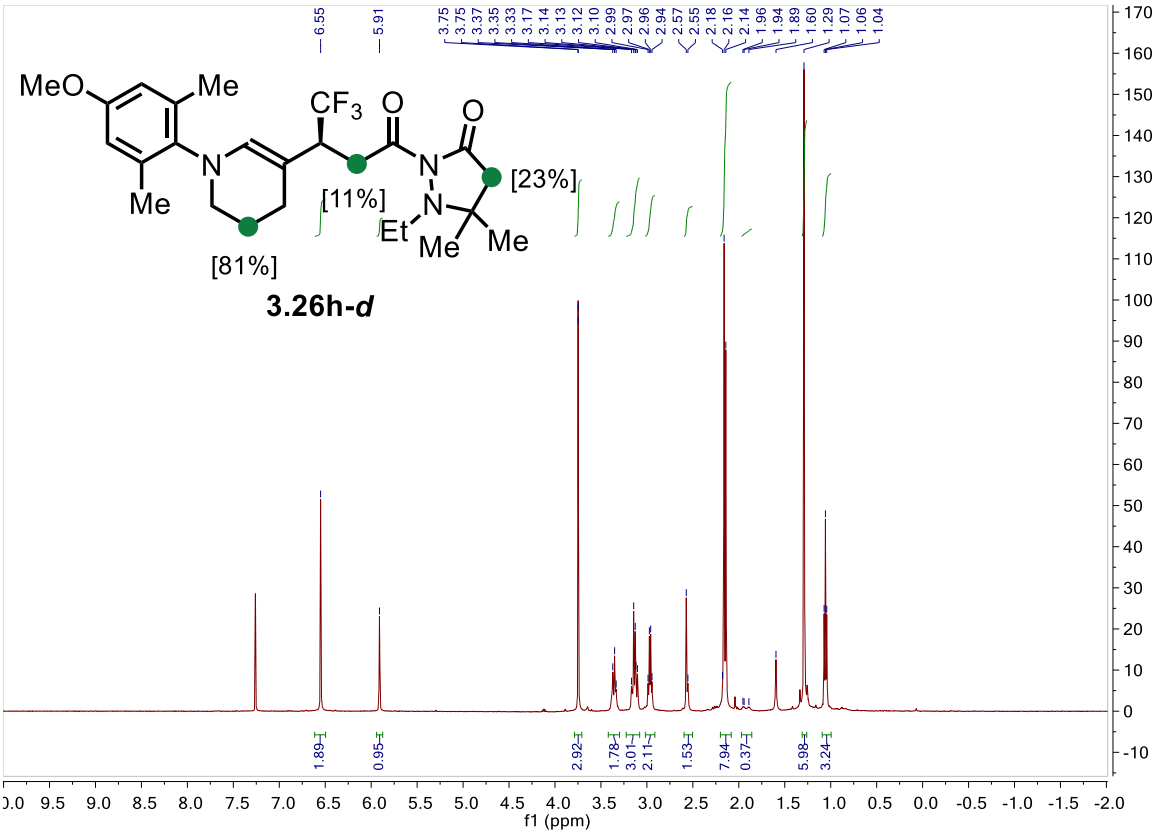
MeO
Me
Me
N
CF3
O
O
N
N
Et
Me
Me
[23%]
[11%]
[81%]
3.26h-d
f1 (ppm)

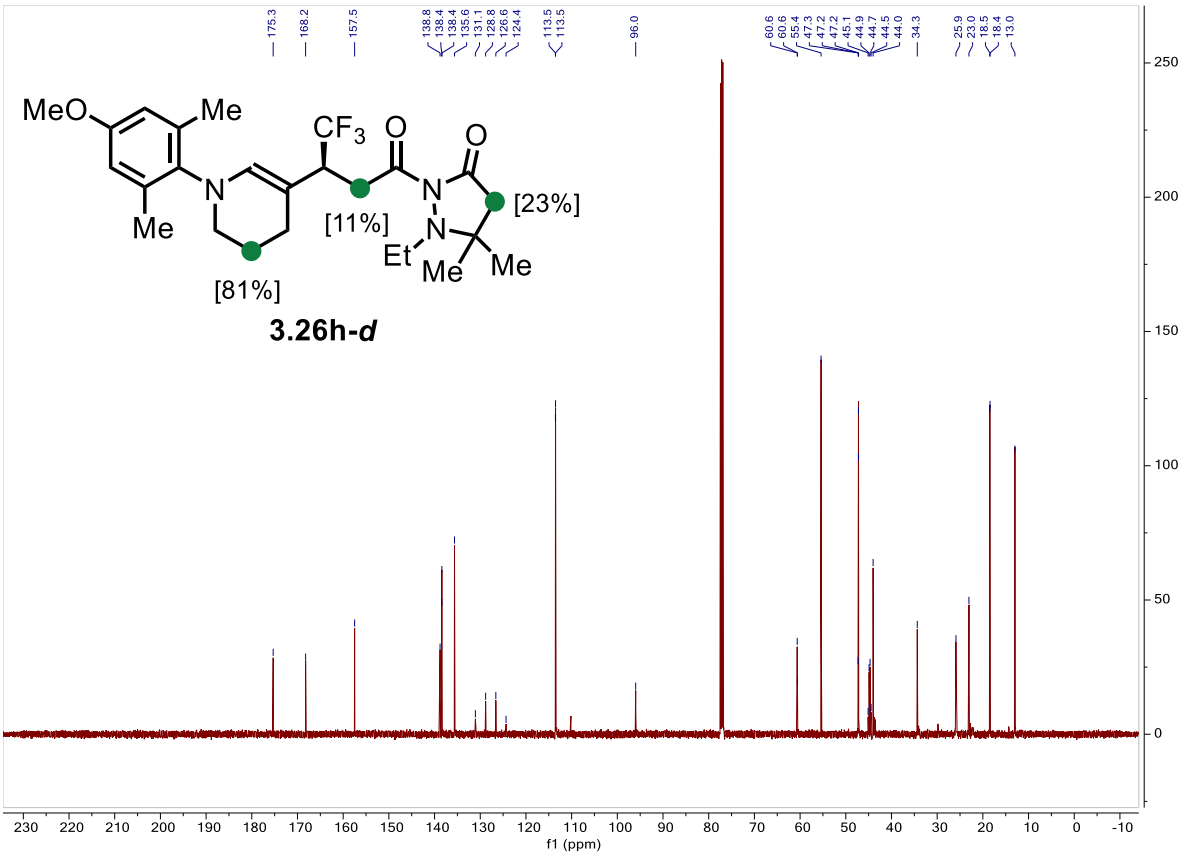
MeO
Me
Me
N
CF3
O
O
N
N
Et
Me
Me
[23%]
[11%]
[81%]
3.26h-d
f1 (ppm)

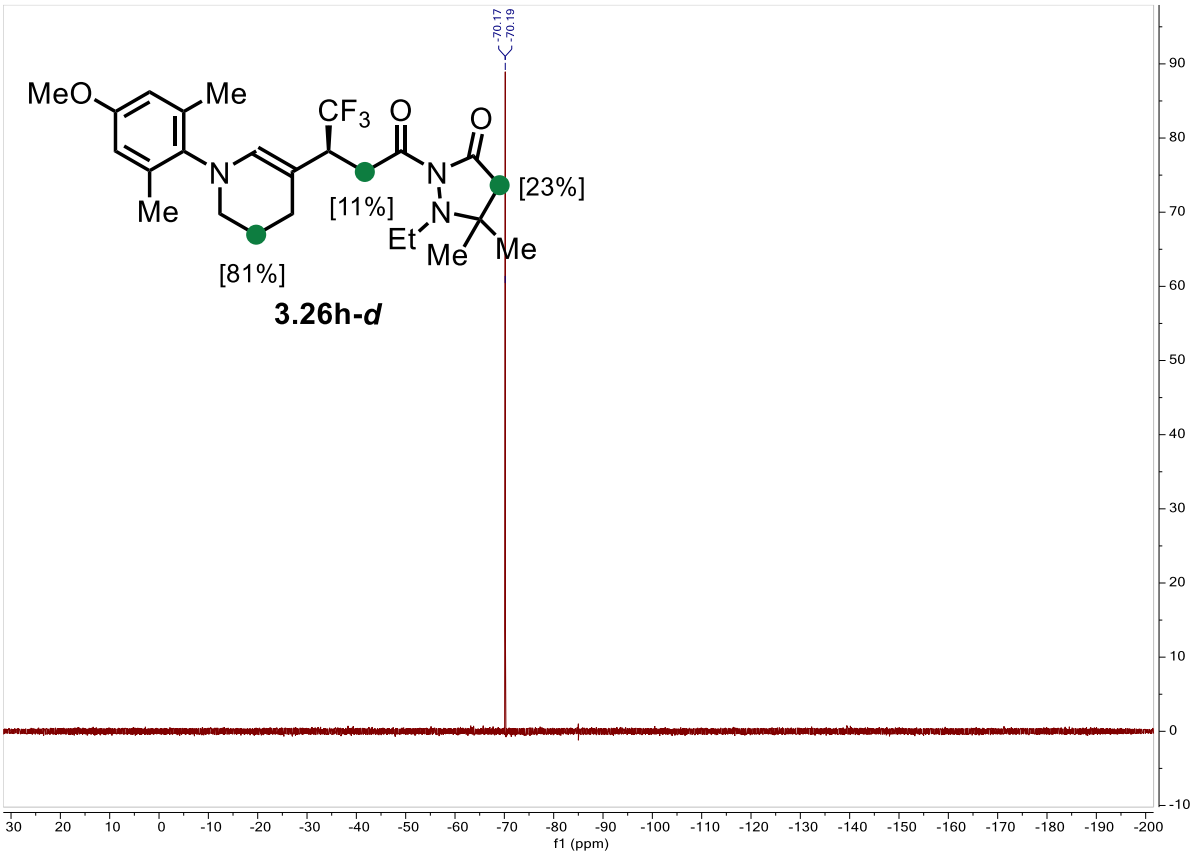
-70.17
-70.19
MeO
Me
Me
N
CF3
O
O
N
N
Et
Me
Me
[11%]
[23%]
[81%]
3.26h-d
90
80
70
60
50
40
30
20
10
0
-10
30 20 10 0 -10 -20 -30 -40 -50 -60 -70 -80 -90 -100 -110 -120 -130 -140 -150 -160 -170 -180 -190 -200
f1 (ppm)

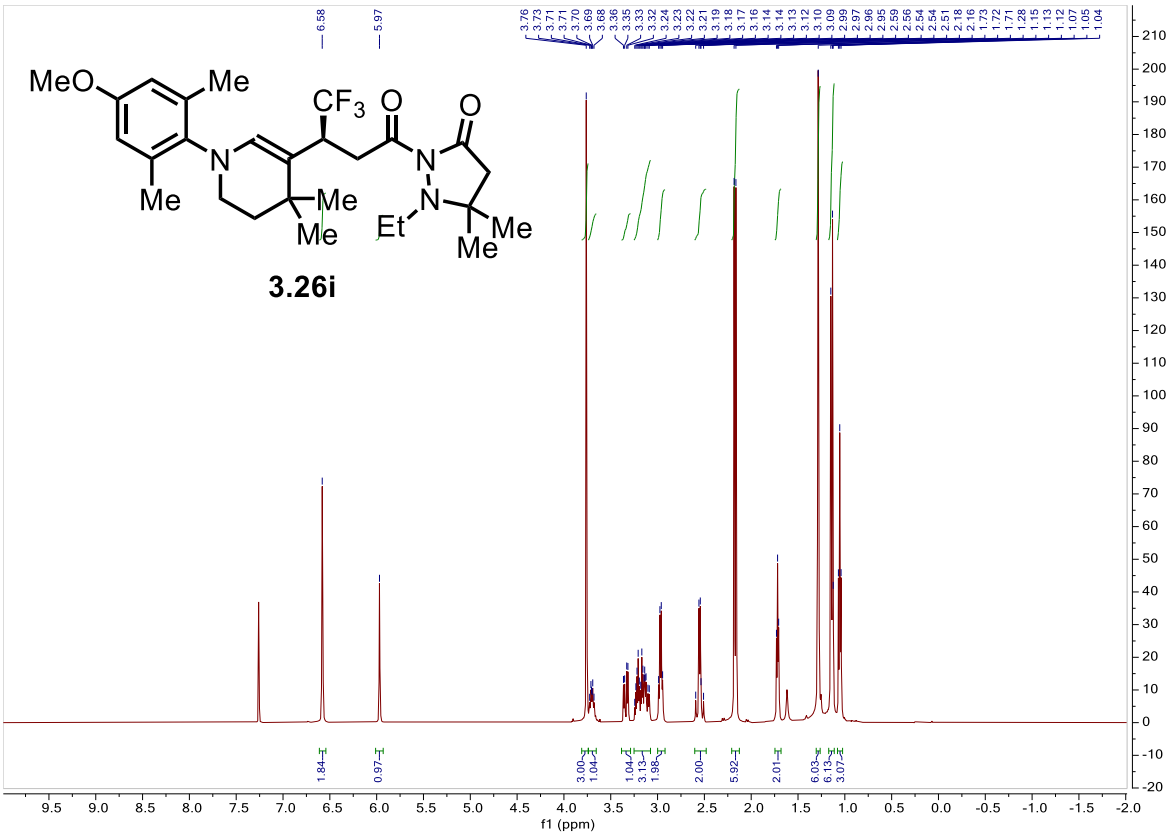
MeO
Me
CF3
O
O
N
N
N
Me
Me
Me
Et
Me
Me
3.26i
f1 (ppm)

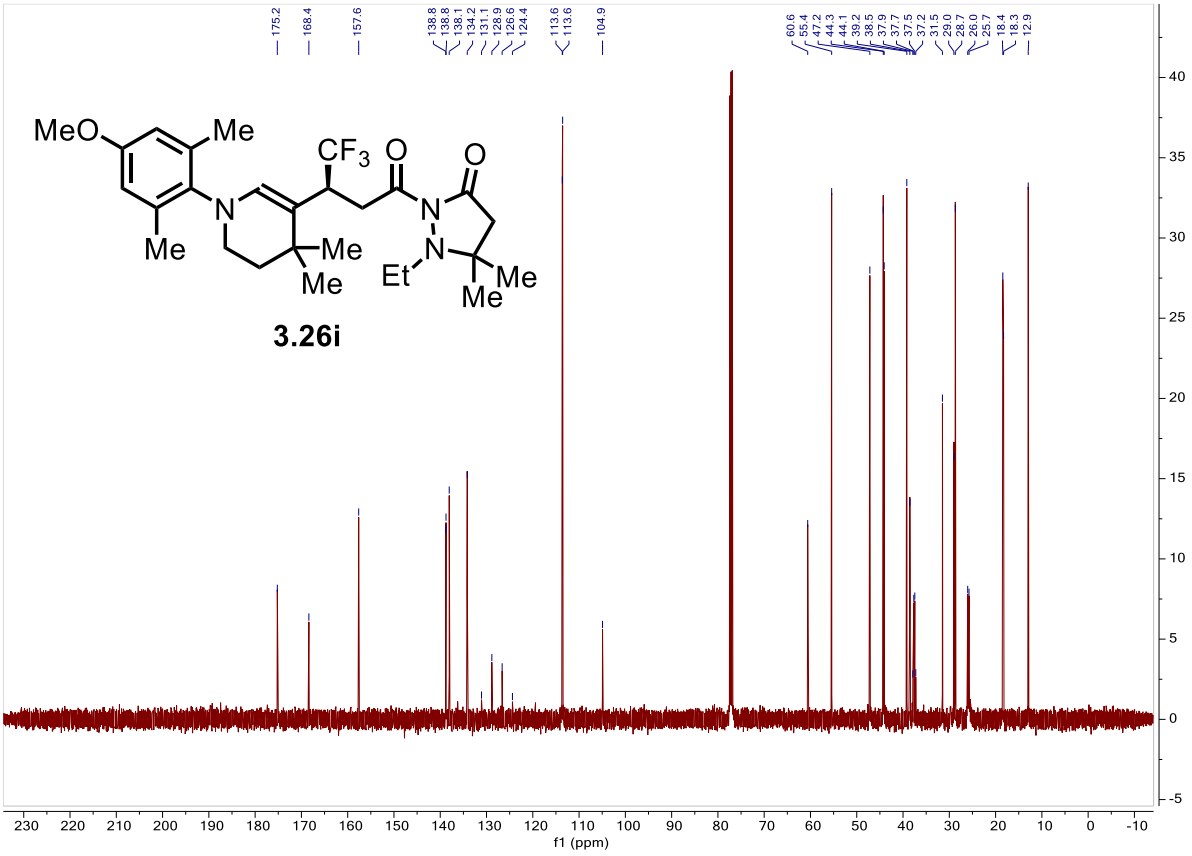
MeO
Me
CF3
O
O
N
N
N
Me
Me
Me
Et
Me
Me
3.26i
f1 (ppm)

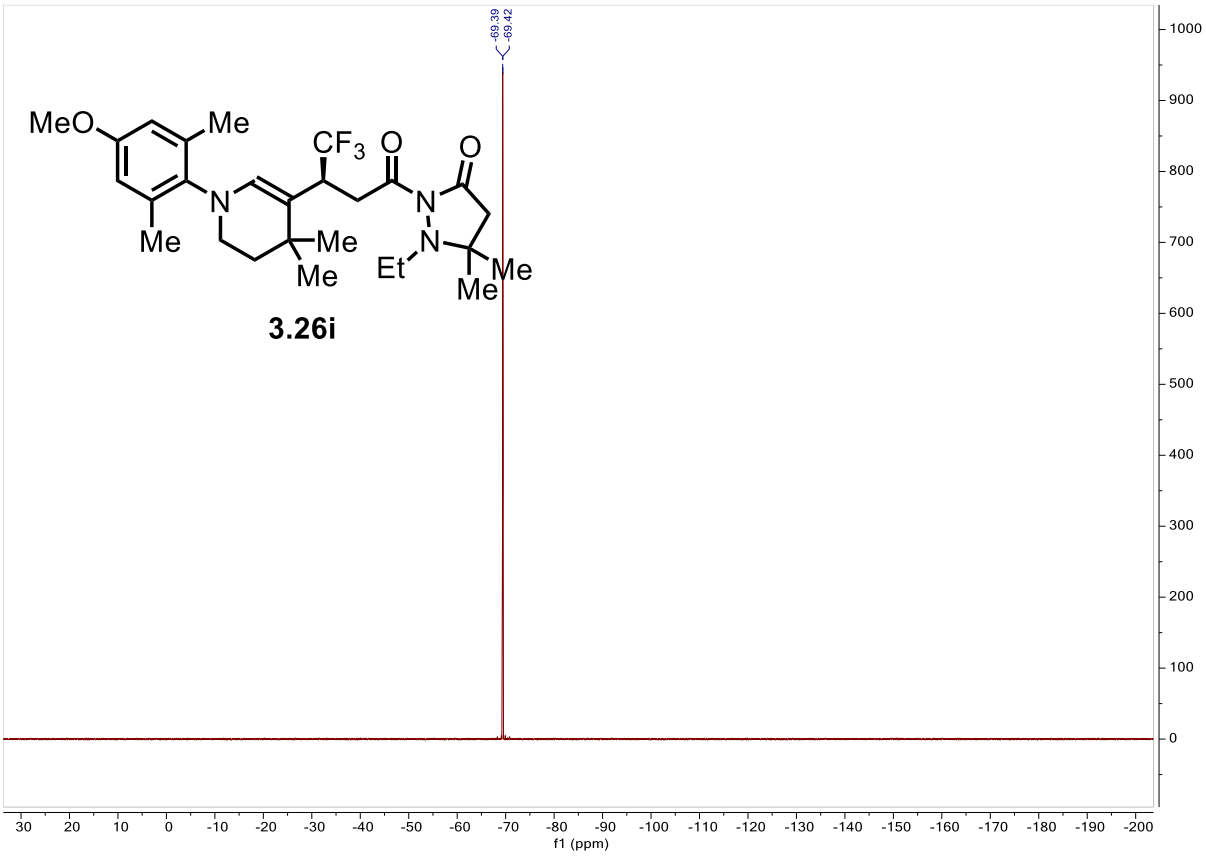
-69.39
-69.42
MeO
Me
CF3
O
O
N
N
N
Et
Me
Me
Me
Me
Me
1000
900
800
700
600
500
400
300
200
100
0
30
20
10
0
-10
-20
-30
-40
-50
-60
-70
-80
-90
-100
-110
-120
-130
-140
-150
-160
-170
-180
-190
-200
f1 (ppm)

3.26i

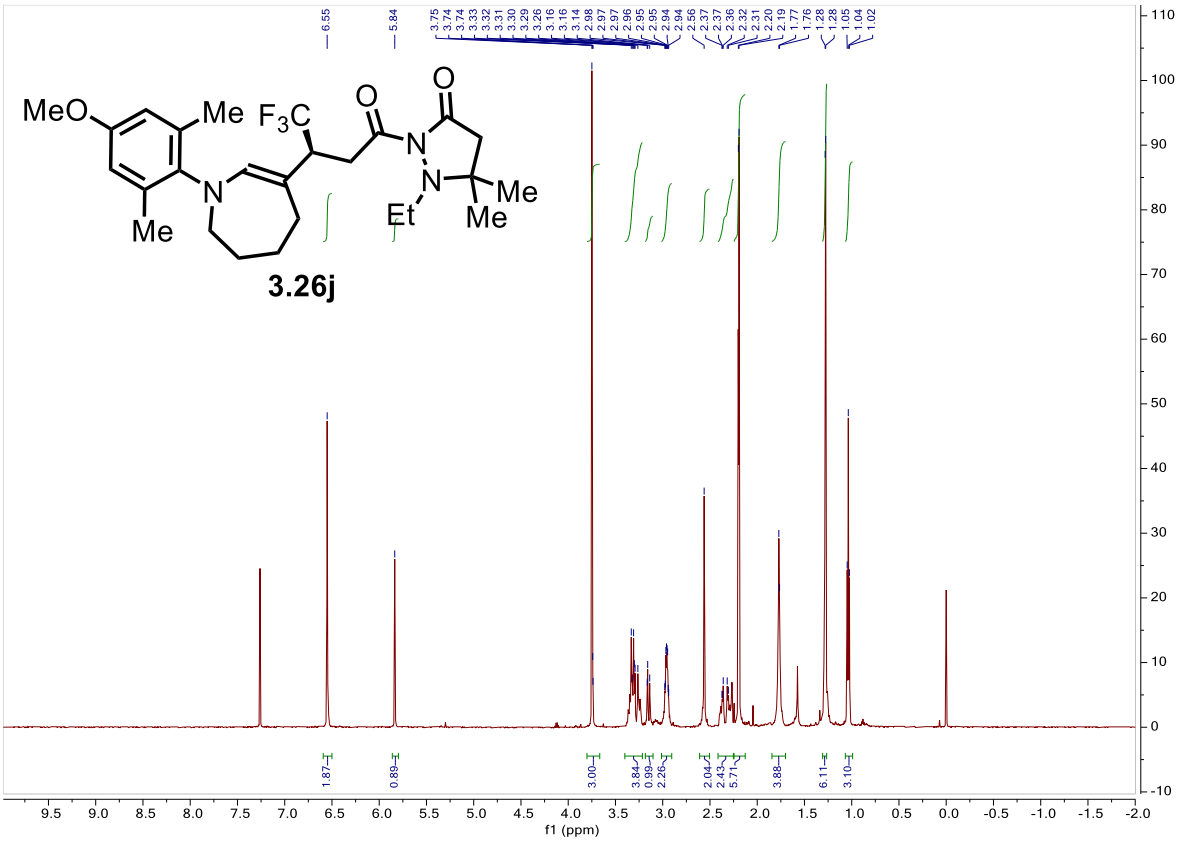
MeO
Me
F3C
O
O
N
N
Me
Me
Et
Me
Me
N
3.26j
f1 (ppm)

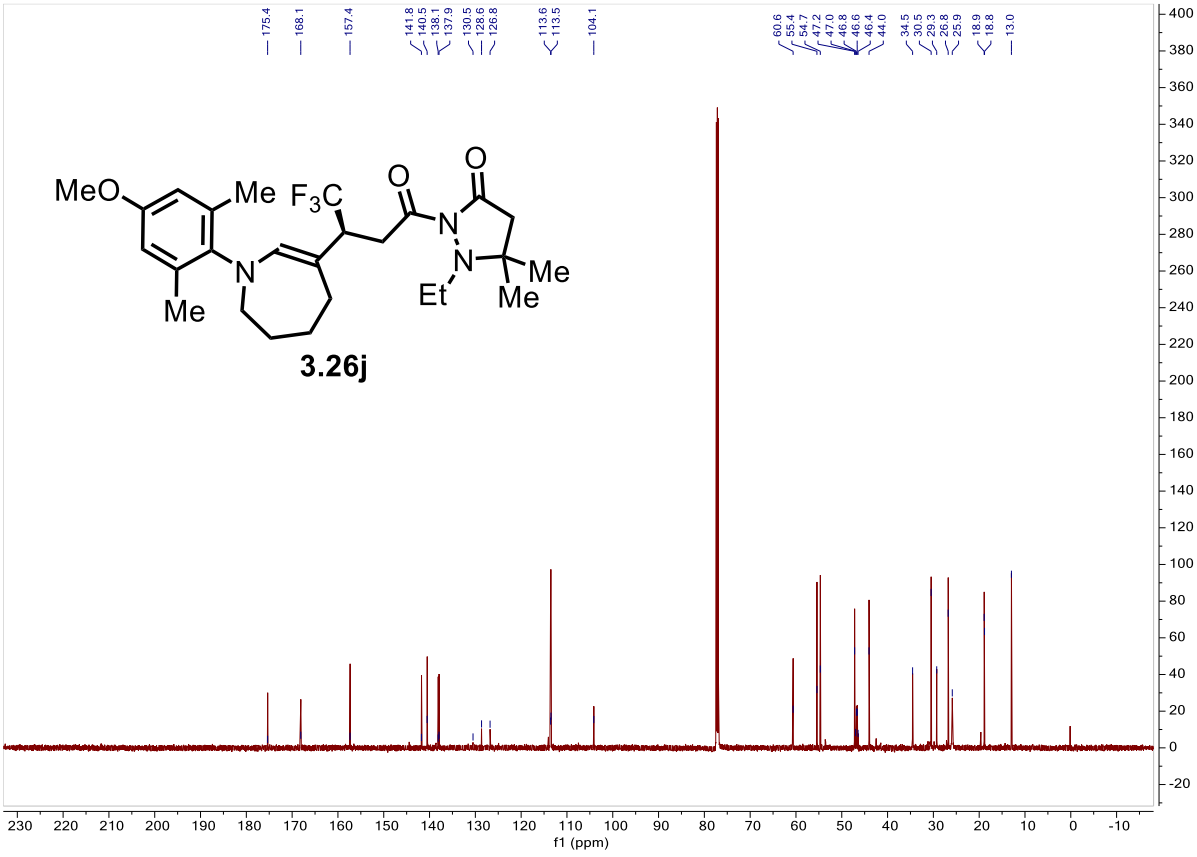
MeO
Me
F3C
O
O
N
N
Me
Me
Et
Me
Me
N
3.26j
f1 (ppm)

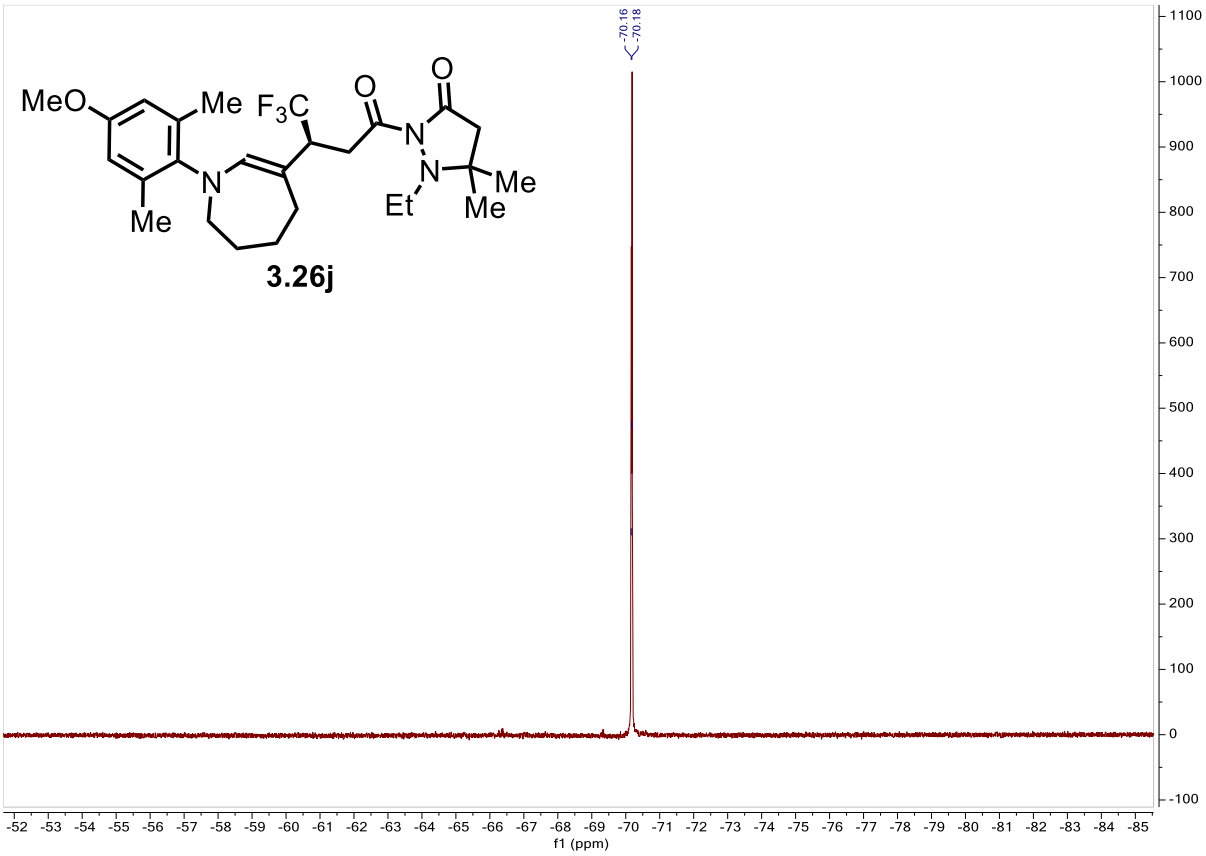
MeO
Me
F3C
O
O
N
N
Me
Et
Me
Me
N
3.26j
-70.16
-70.18
1100
1000
900
800
700
600
500
400
300
200
100
0
-100
-52 -53 -54 -55 -56 -57 -58 -59 -60 -61 -62 -63 -64 -65 -66 -67 -68 -69 -70 -71 -72 -73 -74 -75 -76 -77 -78 -79 -80 -81 -82 -83 -84 -85
f1 (ppm)

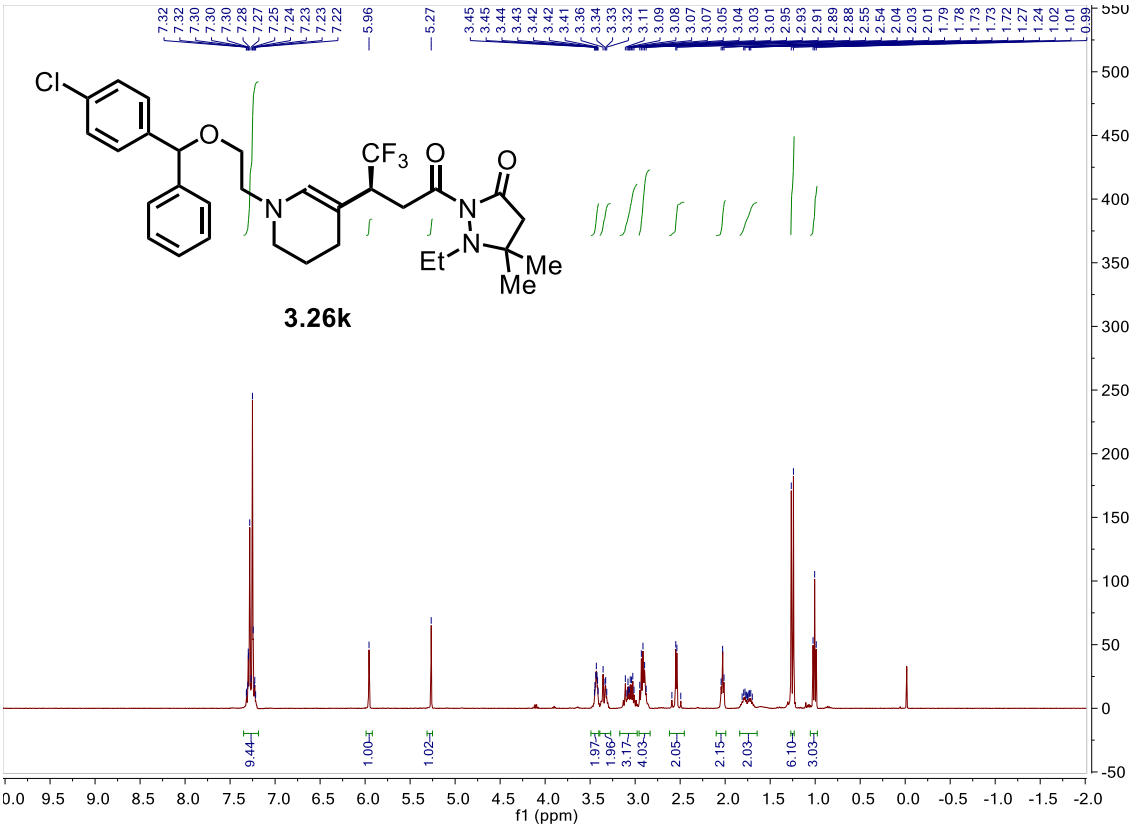
Cl
O
N
CF3
O
O
N
N
Et
Me
Me
3.26k
f1 (ppm)

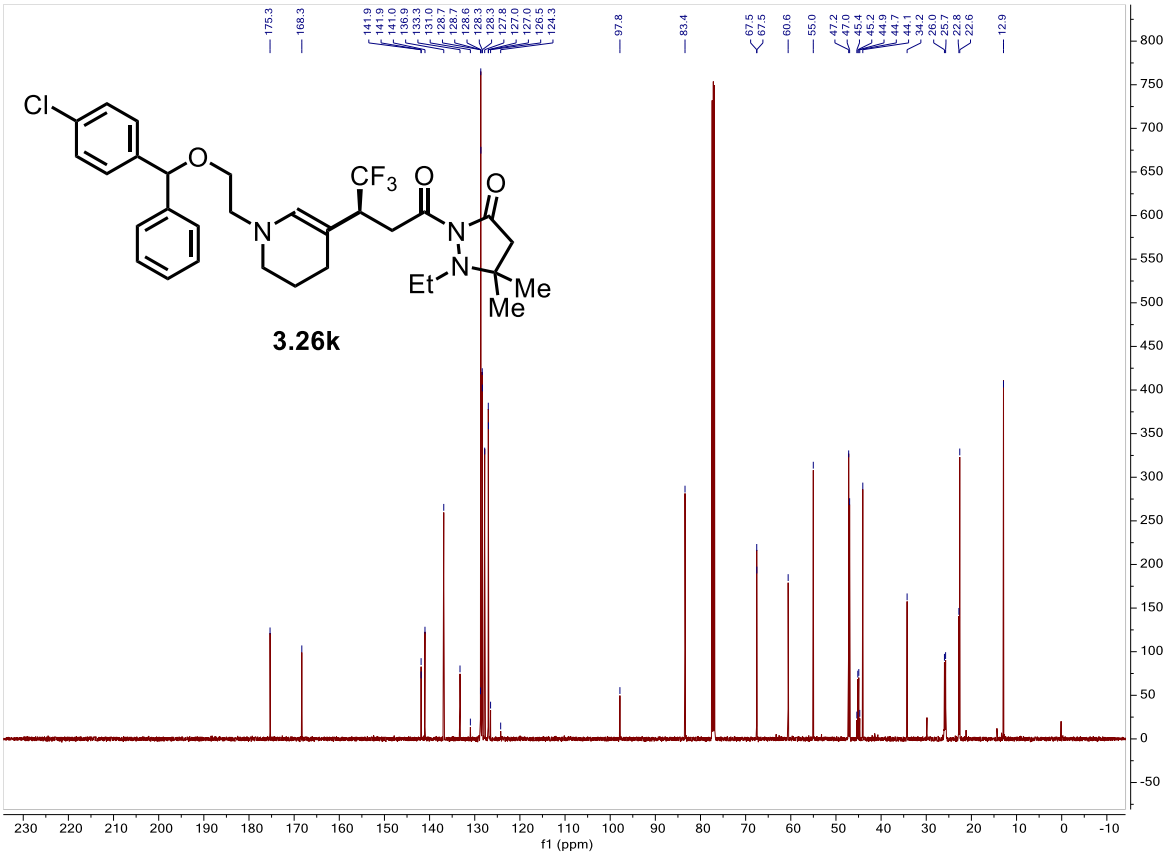
Cl
O
N
CF3
O
O
N
N
Et
Me
Me
3.26k
f1 (ppm)

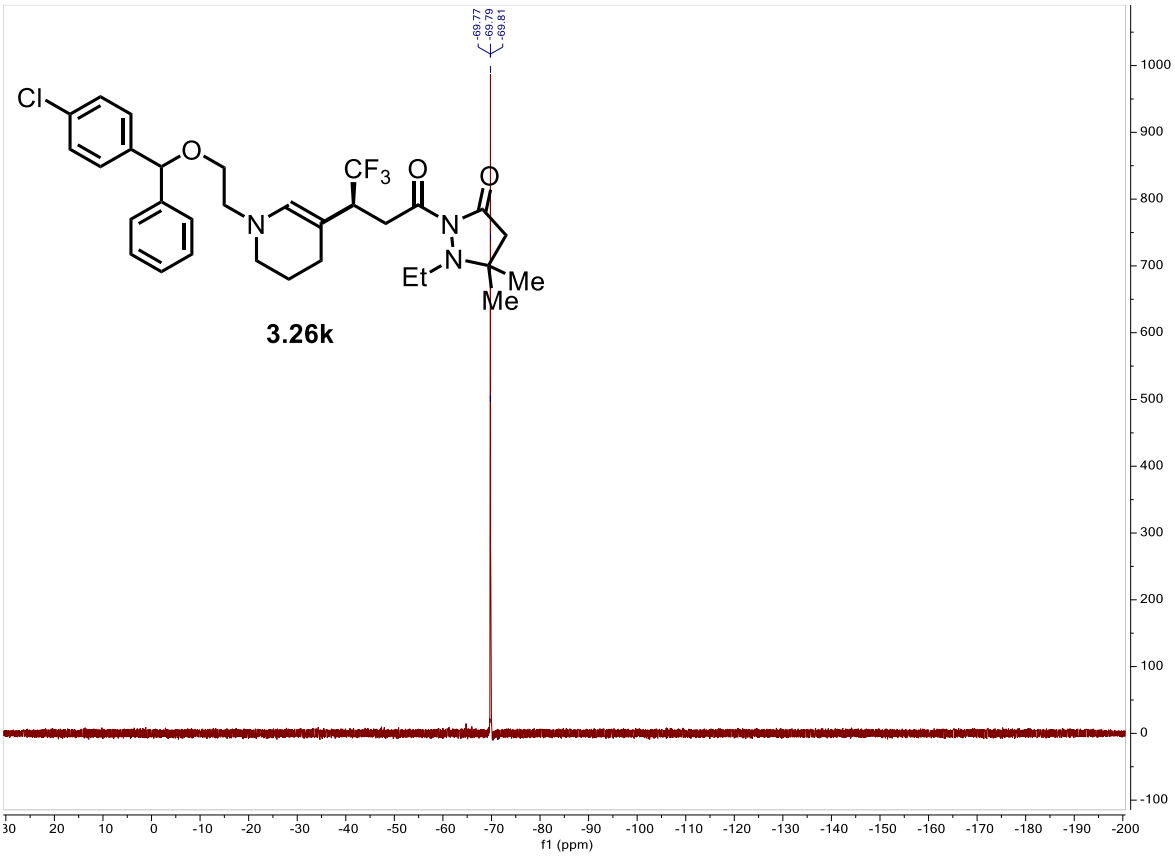
-69.77
-69.79
-69.81
Cl
O
CF3
O
O
N
N
N
Et
Me
Me
3.26k
1000
900
800
700
600
500
400
300
200
100
0
-100
30 20 10 0 -10 -20 -30 -40 -50 -60 -70 -80 -90 -100 -110 -120 -130 -140 -150 -160 -170 -180 -190 -200
f1 (ppm)

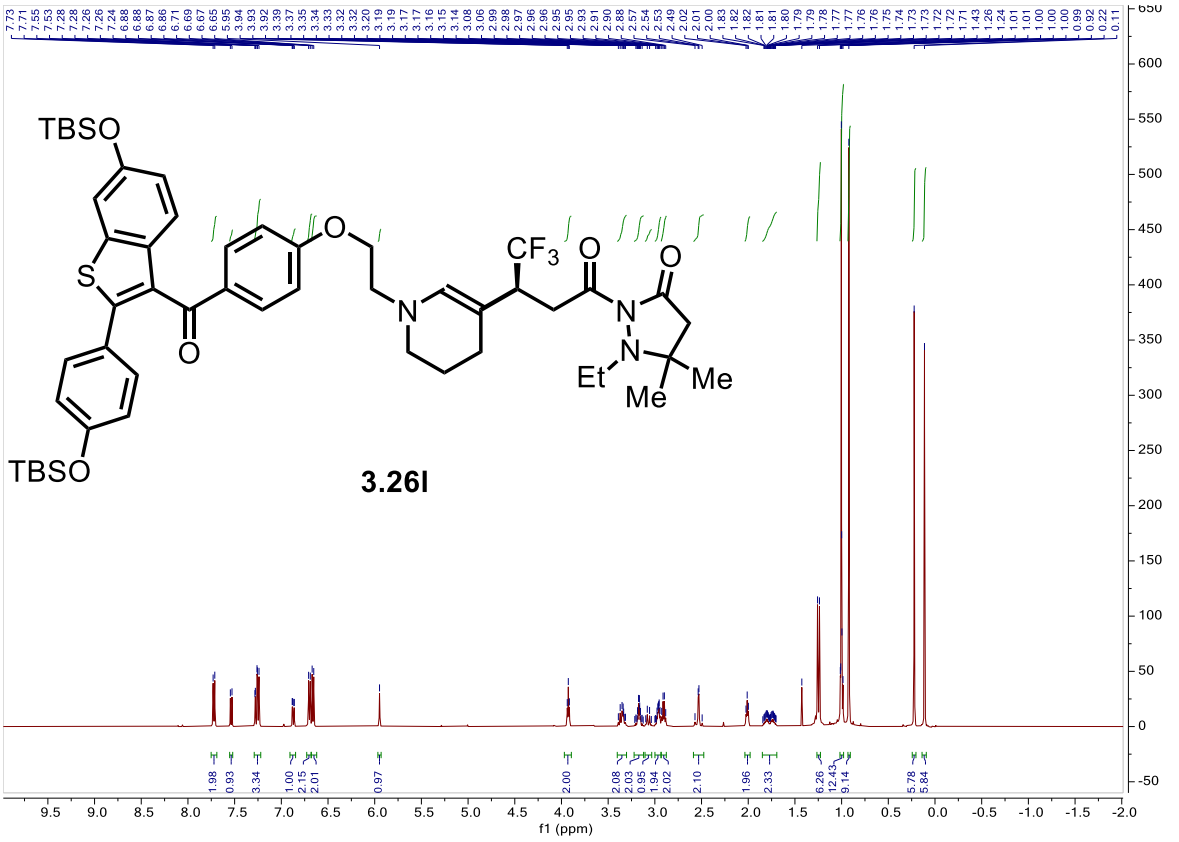
TBSO
TBSO
S
O
O
N
CF3
O
O
N
N
Et
Me
Me
3.26l
f1 (ppm)

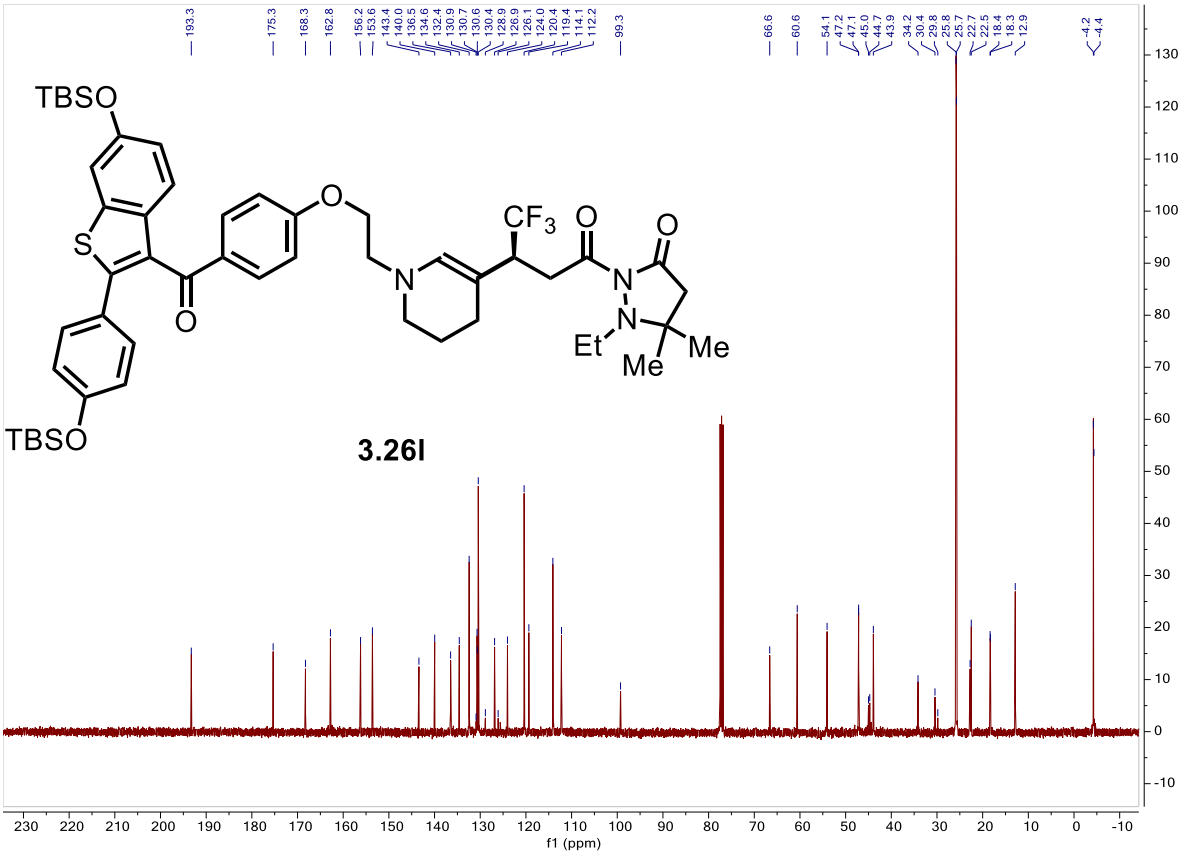
TBSO
TBSO
S
O
O
N
CF3
O
O
N
N
Et
Me
Me
3.26l
f1 (ppm)

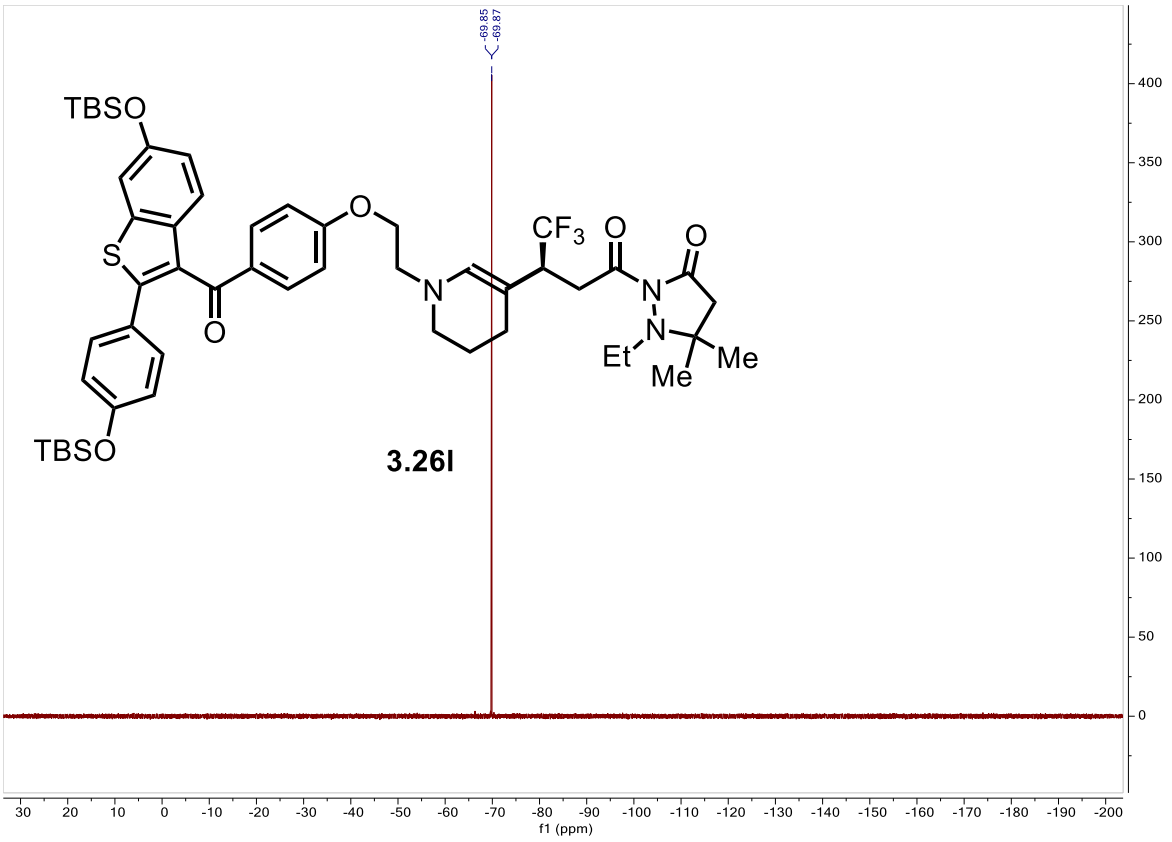
-69.85
-69.87
TBSO
S
O
O
N
CF3
O
O
N
N
Et
Me
Me
TBSO
3.26l
400
350
300
250
200
150
100
50
0
30 20 10 0 -10 -20 -30 -40 -50 -60 -70 -80 -90 -100 -110 -120 -130 -140 -150 -160 -170 -180 -190 -200
f1 (ppm)

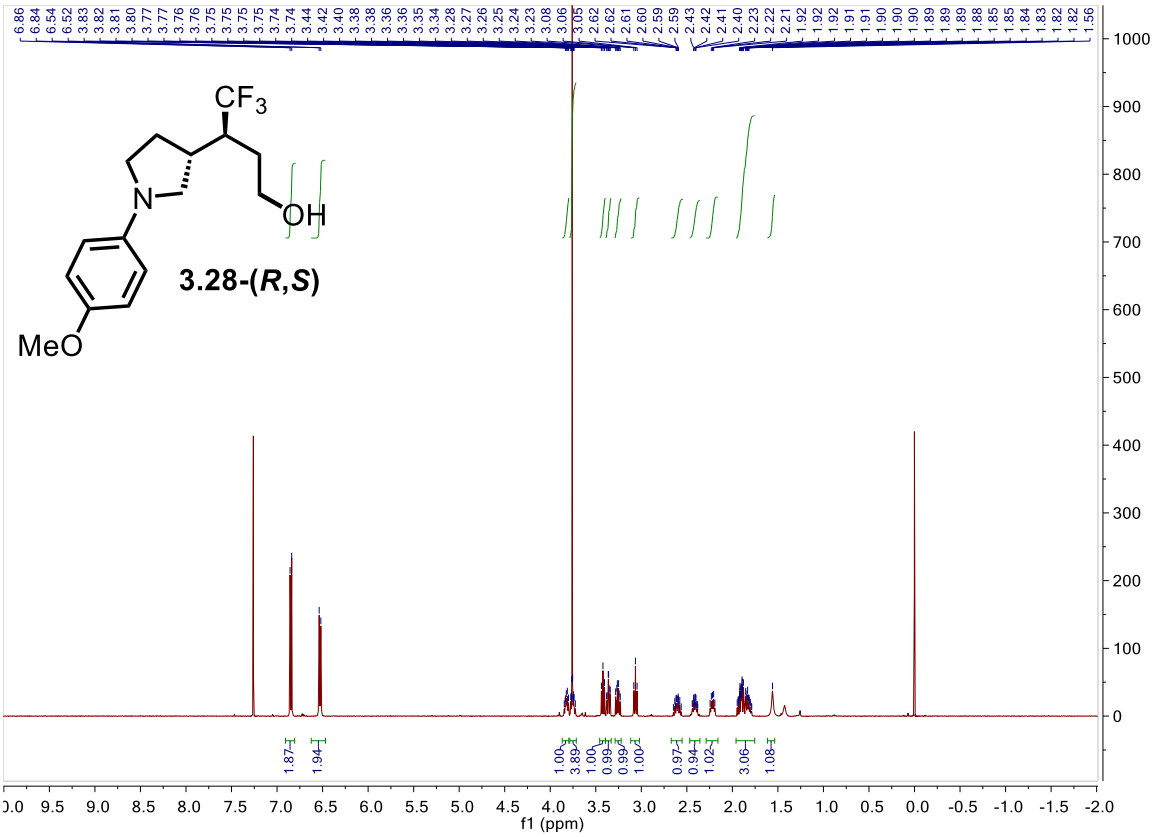
CF3
N
OH
MeO
3.28-(R,S)
f1 (ppm)

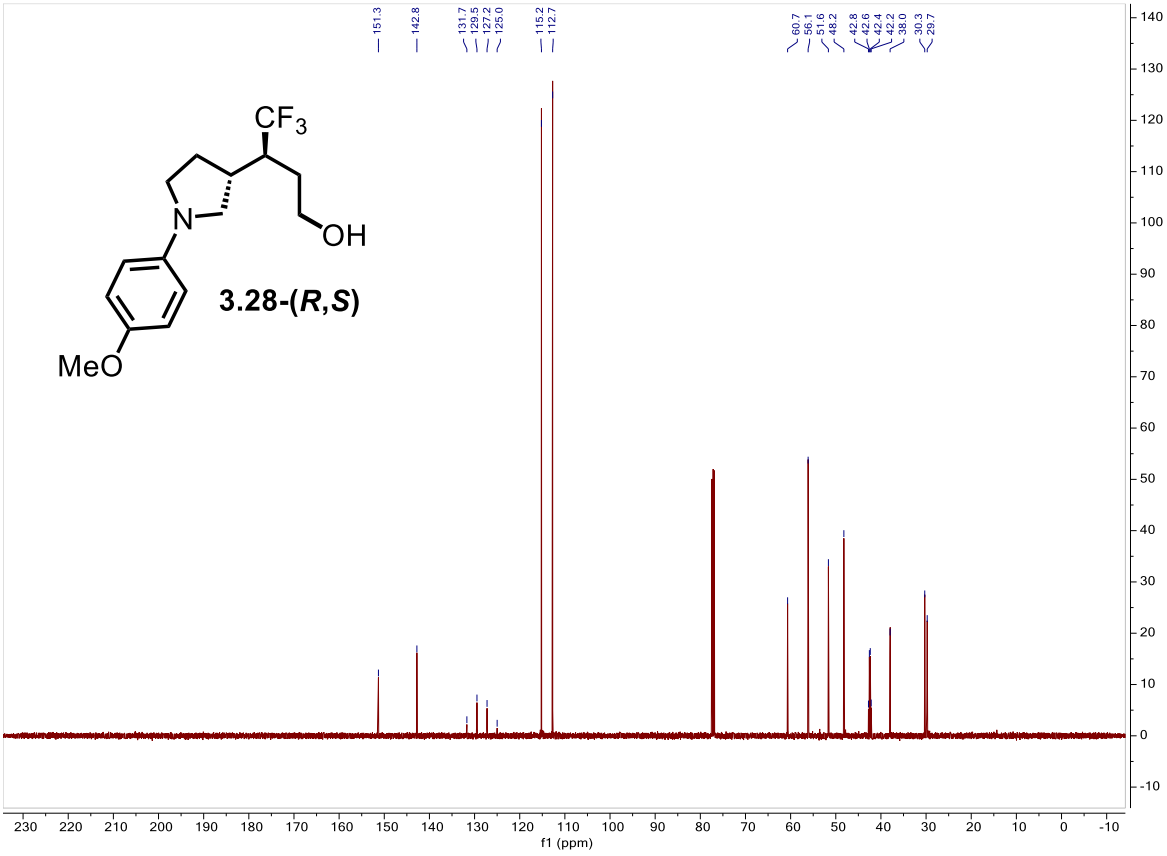
CF3
N
OH
MeO
3.28-(R,S)
f1 (ppm)

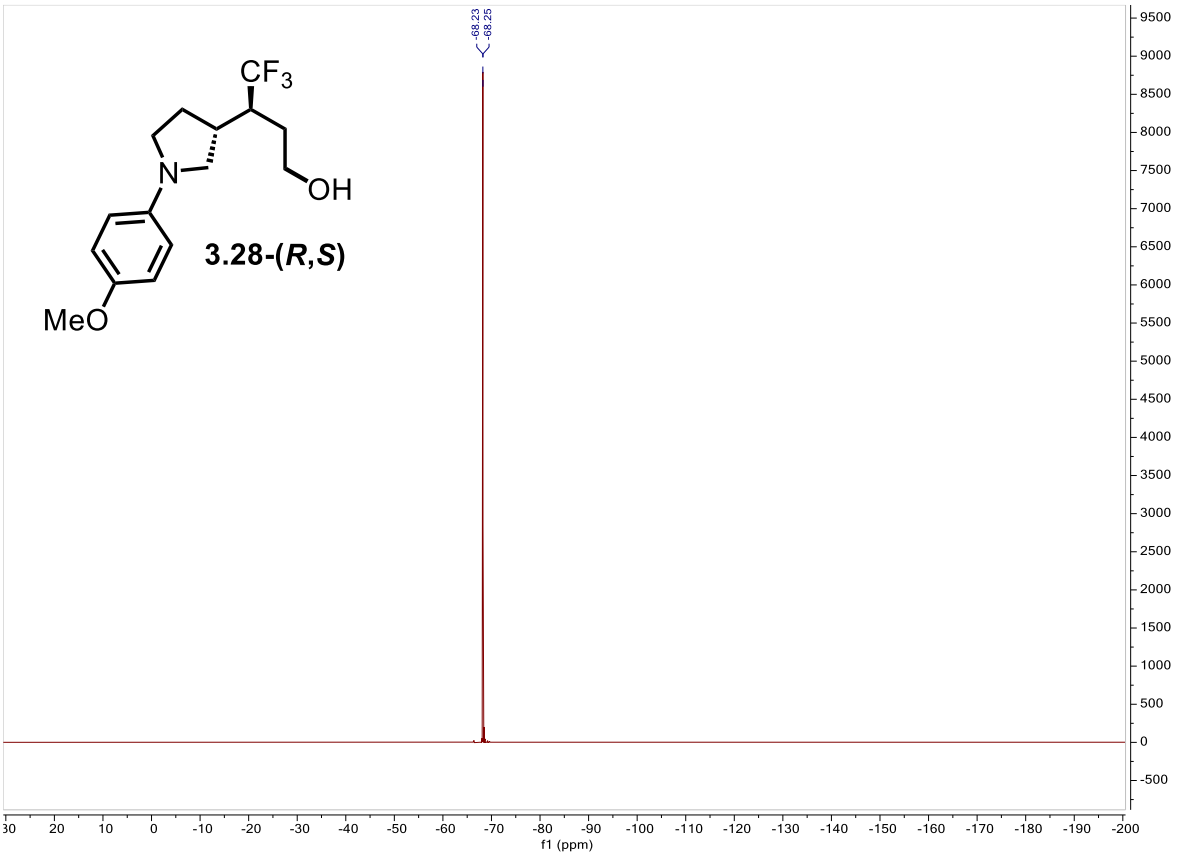
CF3
N
OH
MeO
3.28-(R,S)
-68.23
-68.25
f1 (ppm)

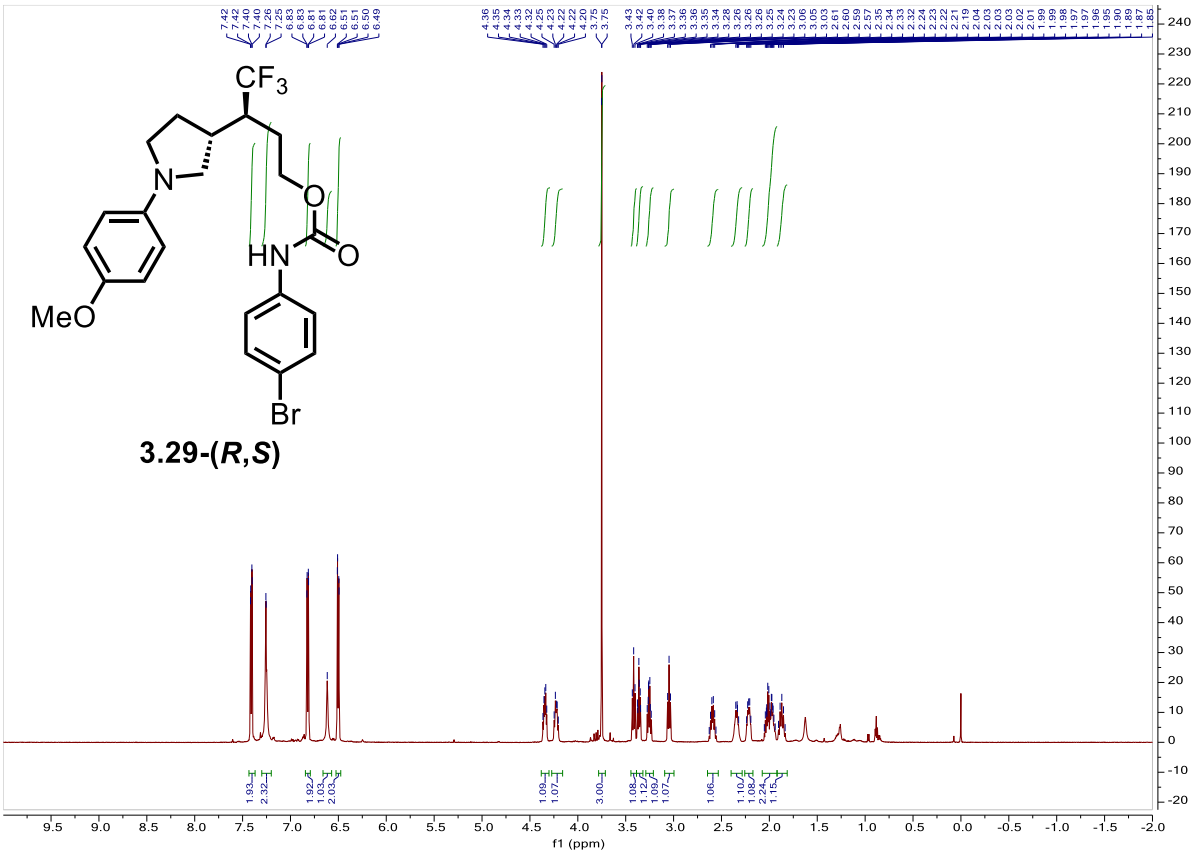
CF3
N
O
HN
O
MeO
Br
3.29-(R,S)
f1 (ppm)

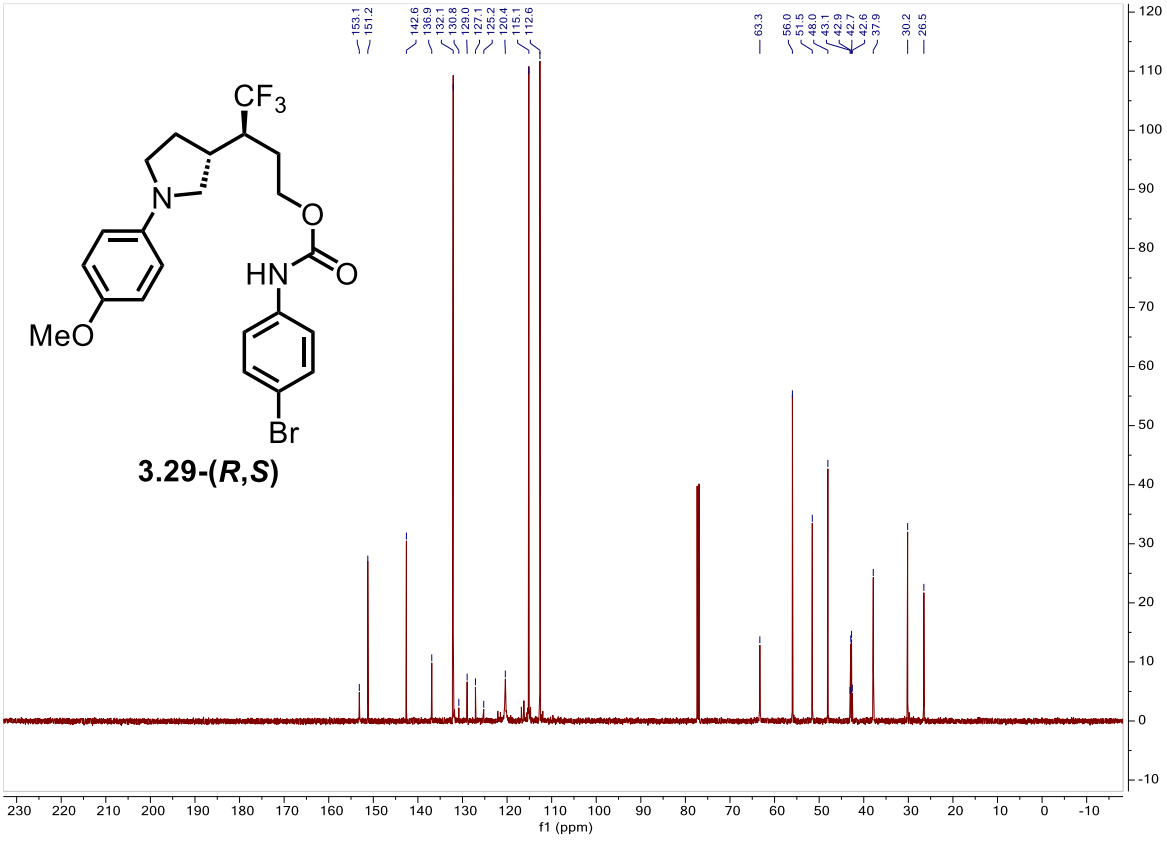
CF3
N
O
HN
O
MeO
Br
3.29-(R,S)
f1 (ppm)

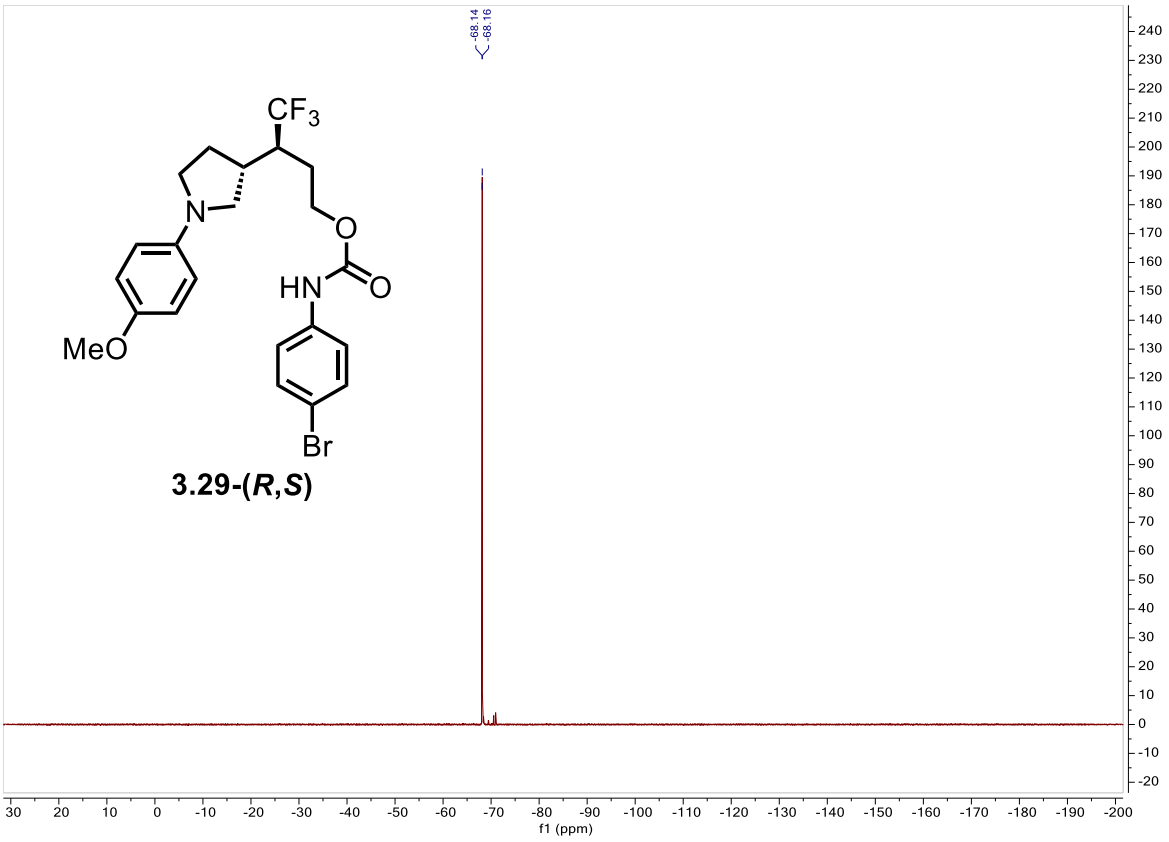
-68.14
-68.16
CF3
N
O
HN
O
MeO
Br
3.29-(R,S)
240
230
220
210
200
190
180
170
160
150
140
130
120
110
100
90
80
70
60
50
40
30
20
10
0
-10
-20
30 20 10 0 -10 -20 -30 -40 -50 -60 -70 -80 -90 -100 -110 -120 -130 -140 -150 -160 -170 -180 -190 -200
f1 (ppm)

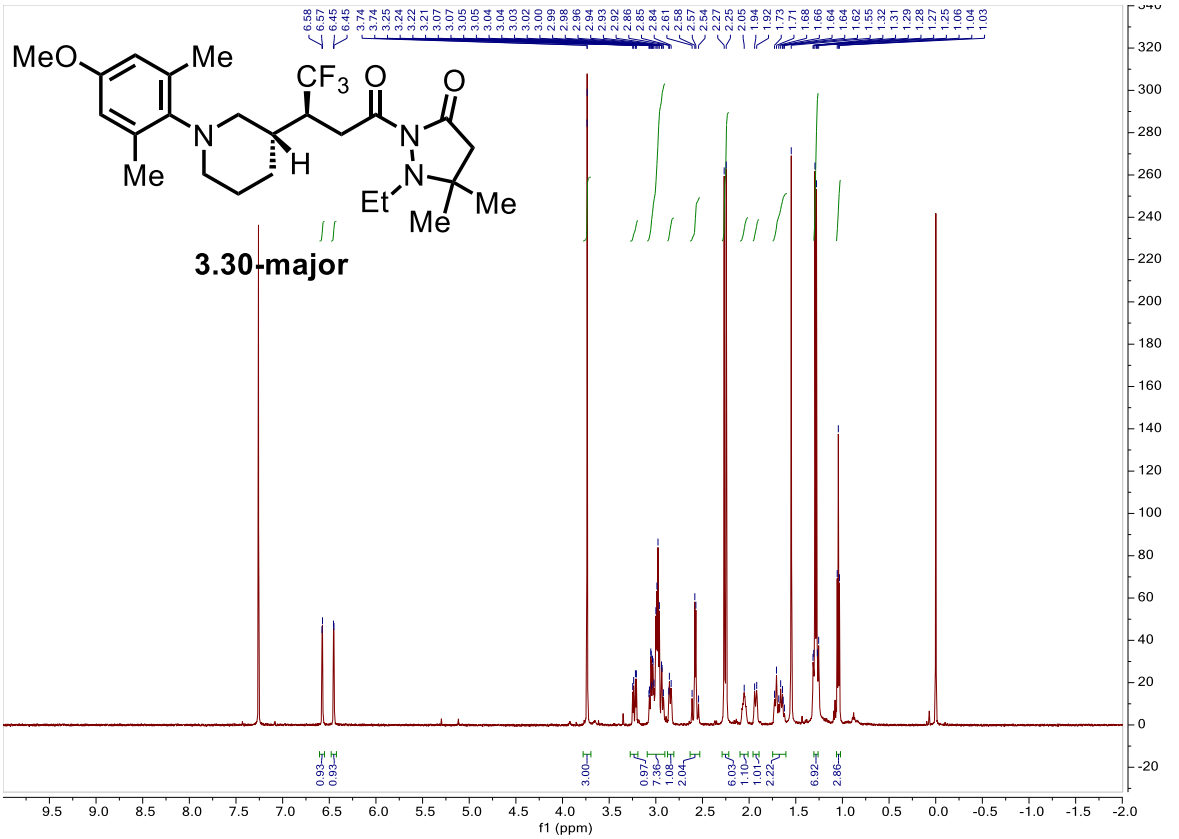
MeO
Me
CF3
O
O
N
N
H
Me
Et
N
Me
Me
3.30-major
f1 (ppm)

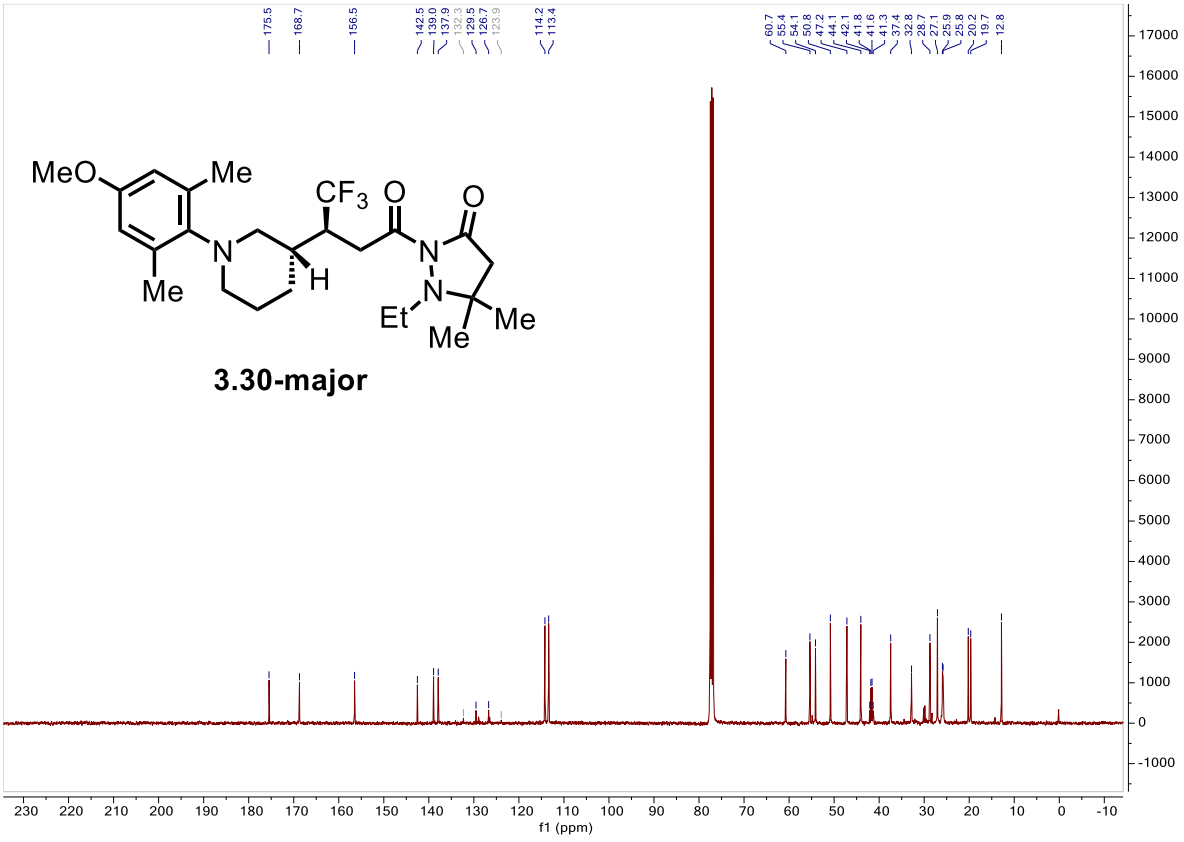
MeO
Me
CF3
O
O
N
N
H
Me
Et
N
Me
Me
3.30-major
f1 (ppm)

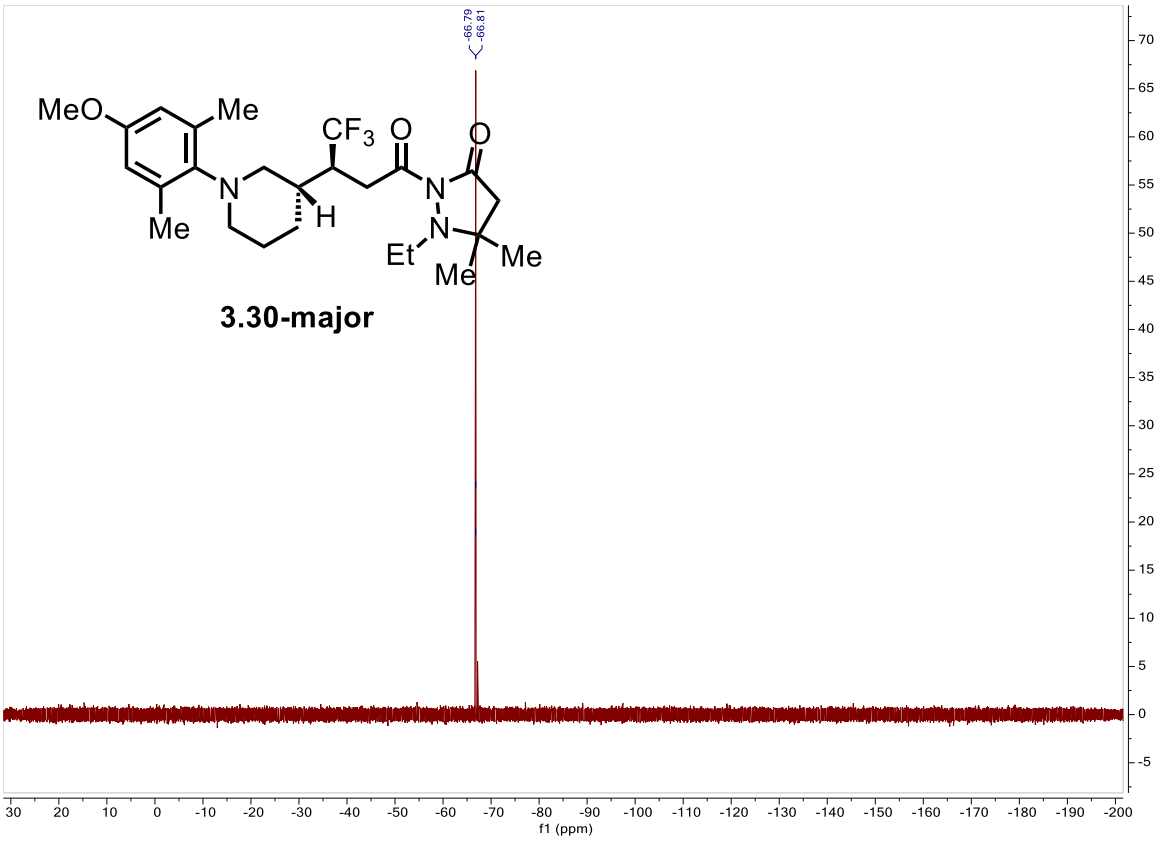
-66.79
-66.81
MeO
Me
Me
N
CF3
O
H
O
N
N
Et
Me
Me
3.30-major
70
65
60
55
50
45
40
35
30
25
20
15
10
5
0
-5
30 20 10 0 -10 -20 -30 -40 -50 -60 -70 -80 -90 -100 -110 -120 -130 -140 -150 -160 -170 -180 -190 -200
f1 (ppm)

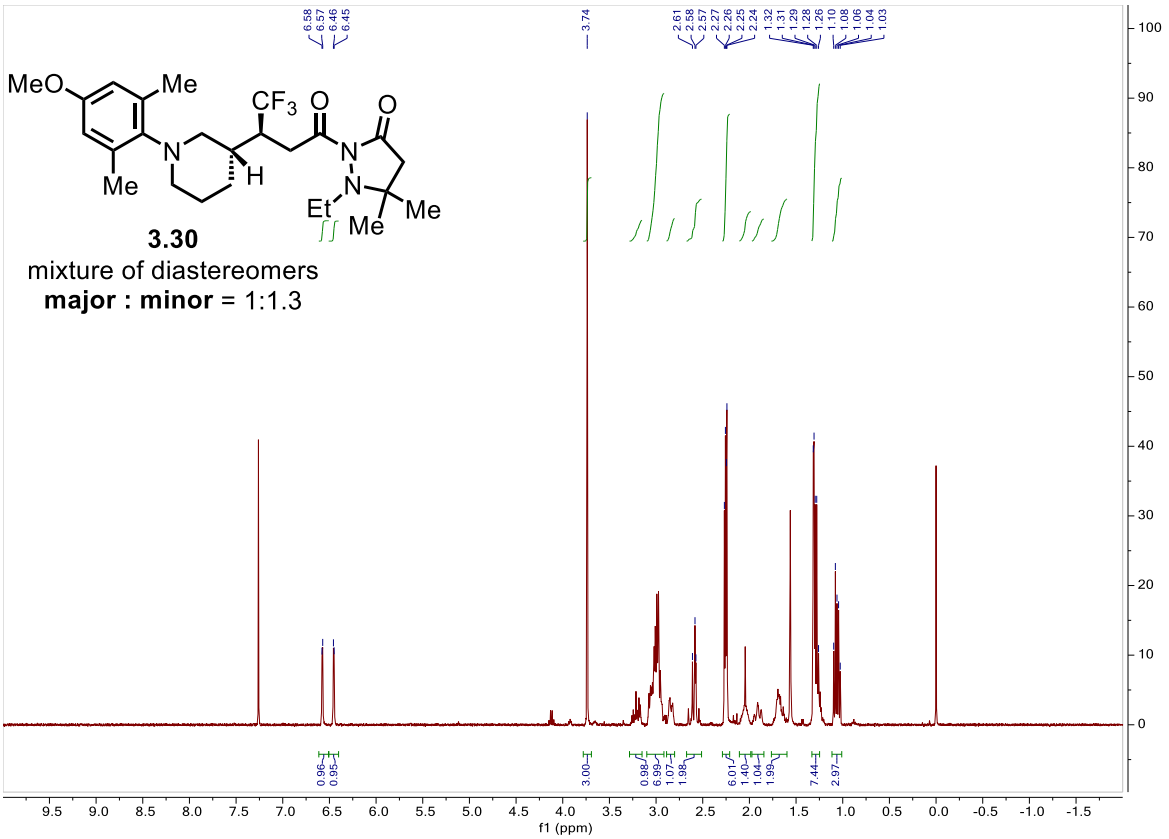
MeO
Me
Me
CF3
O
O
N
N
H
N
Et
Me
Me
3.30
mixture of diastereomers
major : minor = 1:1.3
f1 (ppm)

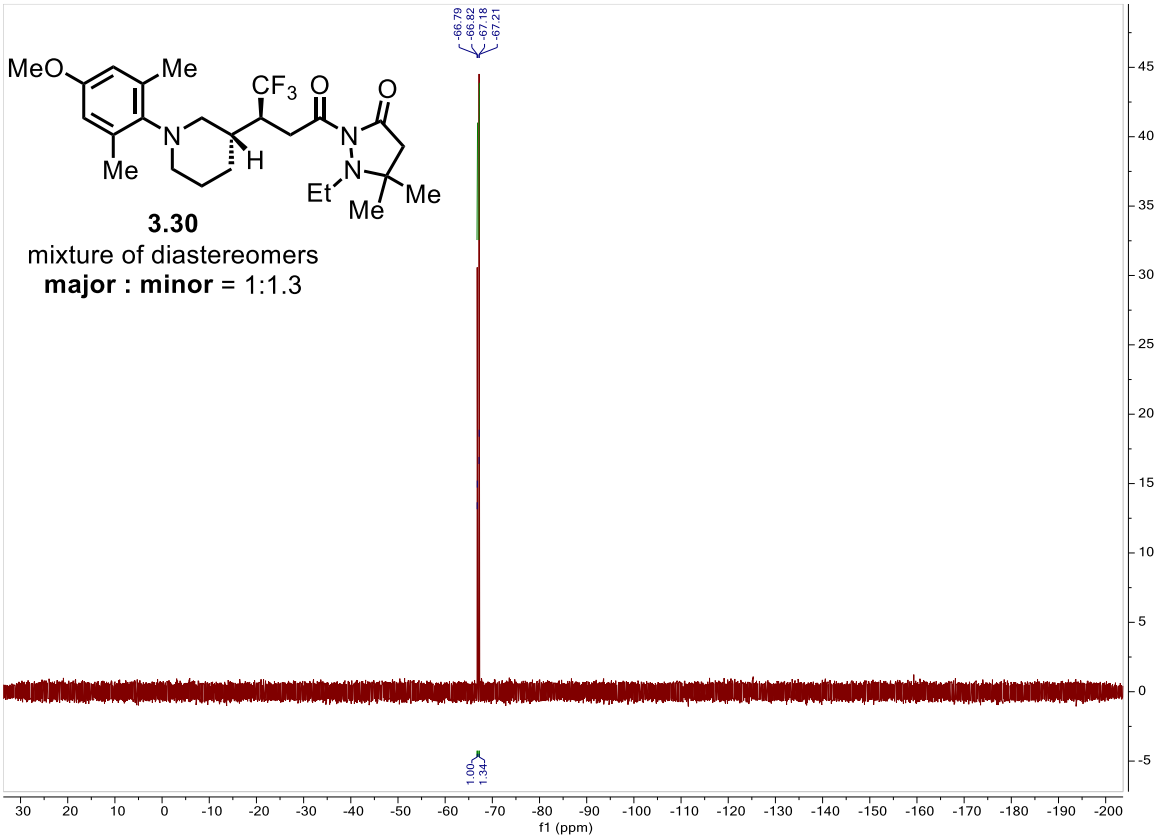
MeO
Me
Me
CF3
O
O
N
N
H
N
Et
Me
Me
3.30
mixture of diastereomers
major : minor = 1:1.3
f1 (ppm)

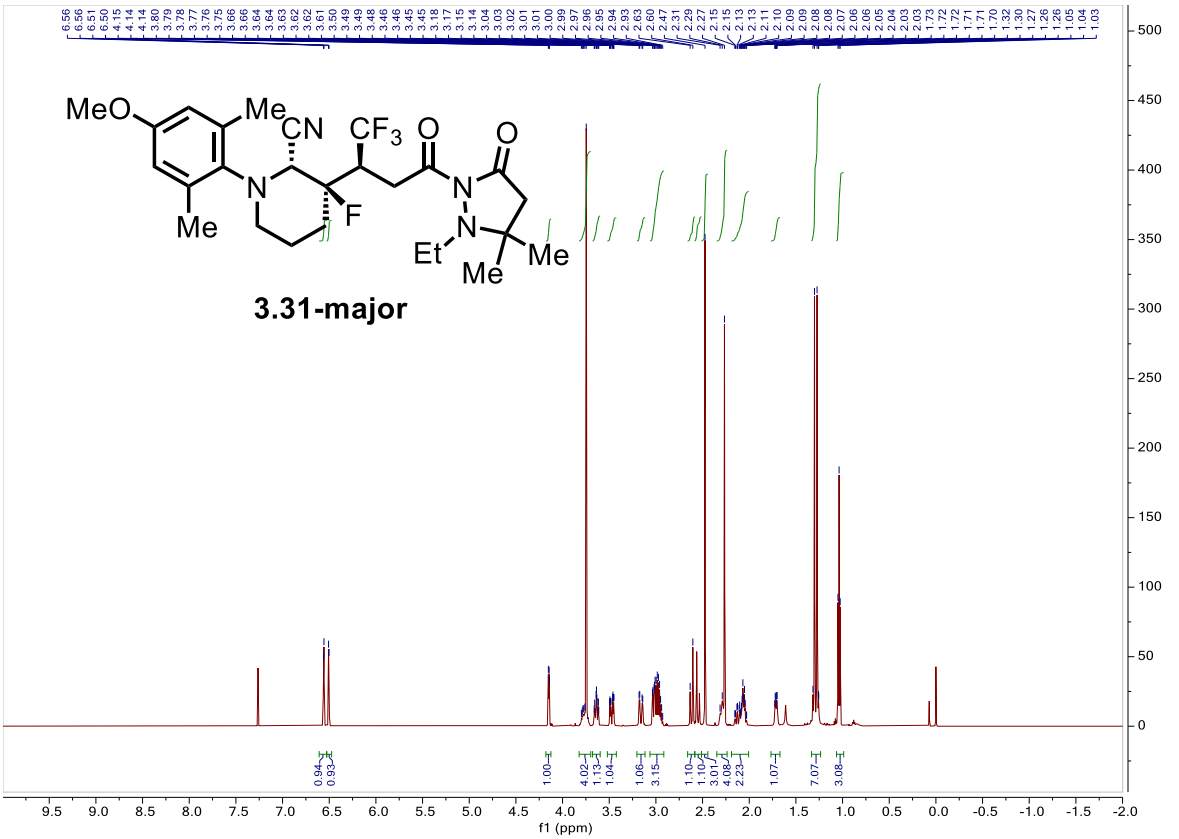
MeO
Me
CN
CF3
O
O
N
N
F
N
Me
Et
Me
Me
3.31-major
f1 (ppm)

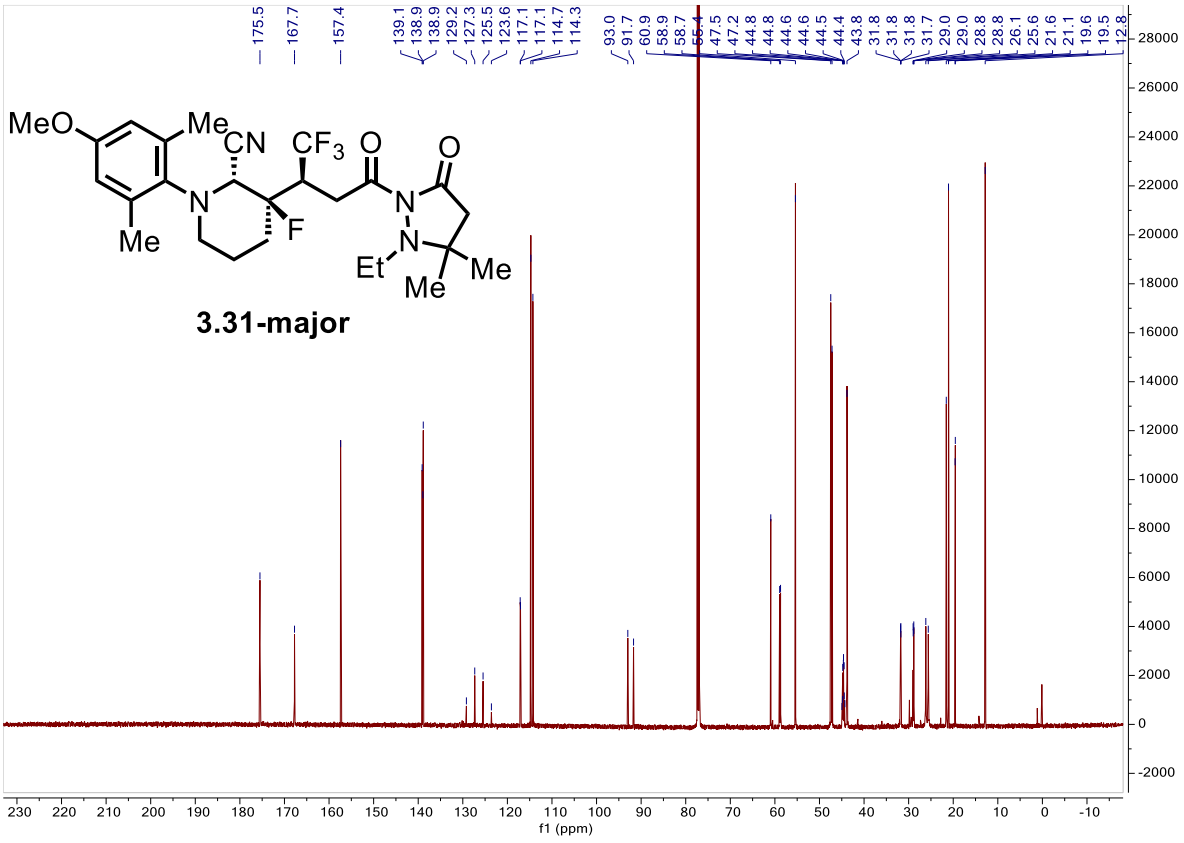
MeO
Me
CN
CF3
O
O
N
N
F
N
Me
Et
Me
Me
3.31-major
f1 (ppm)

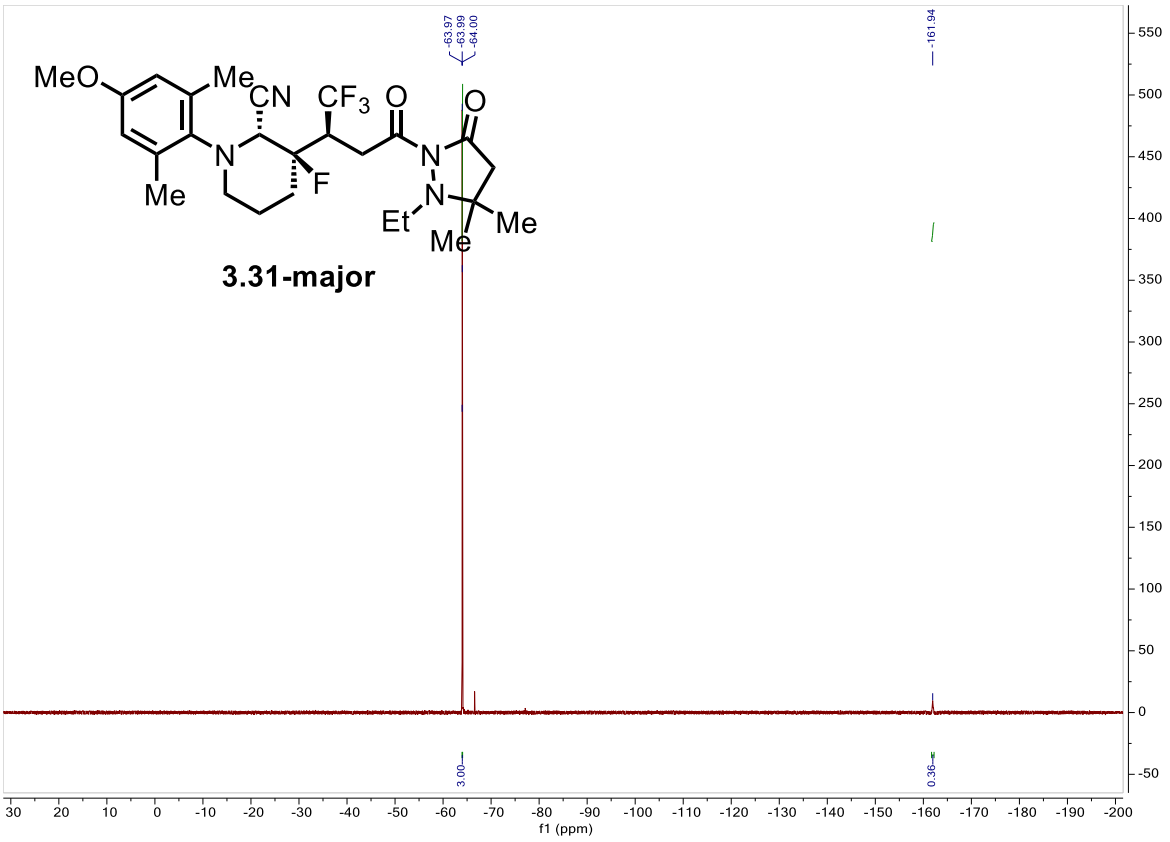
MeO
Me
CN
CF3
O
O
N
N
F
Me
Et
N
Me
Me
3.31-major
-63.97
-63.99
-64.00
-161.94
3.00
0.36
f1 (ppm)

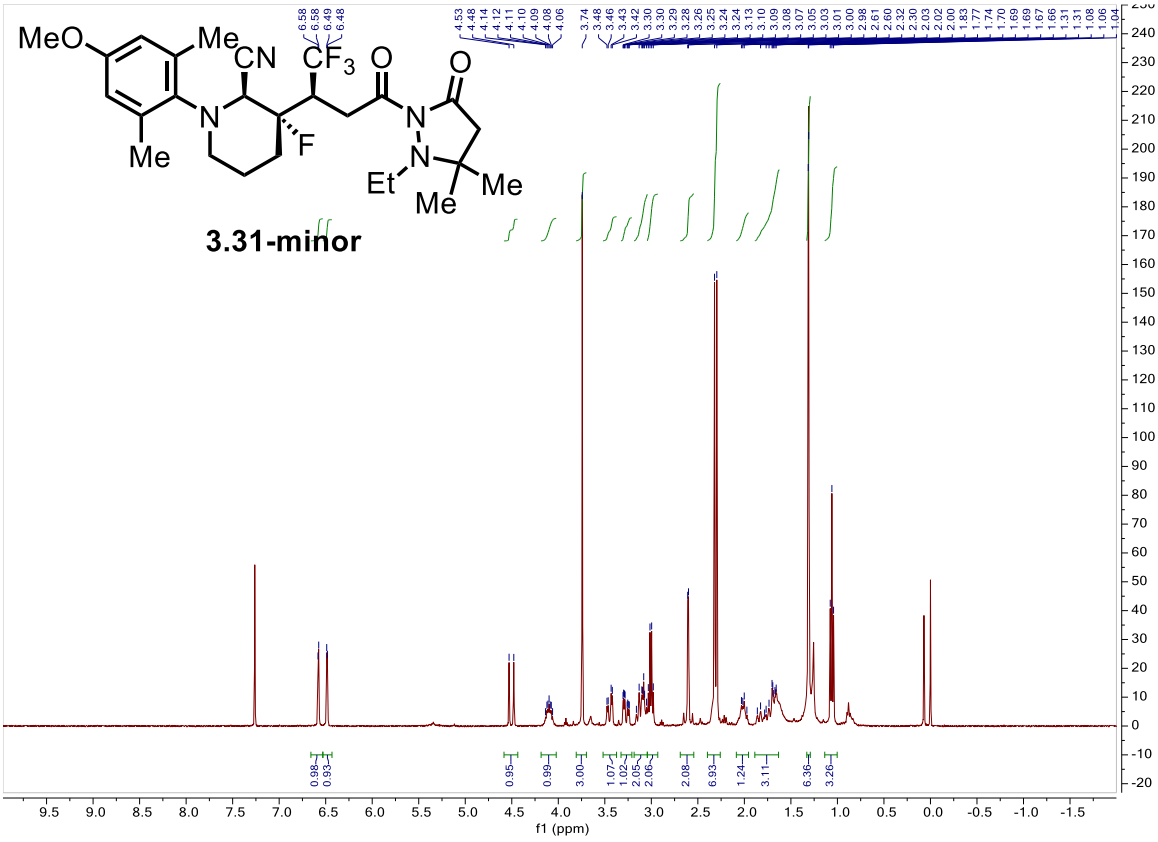
MeO
Me
CN
CF3
O
O
N
N
F
Me
Et
N
Me
Me
3.31-minor
f1 (ppm)

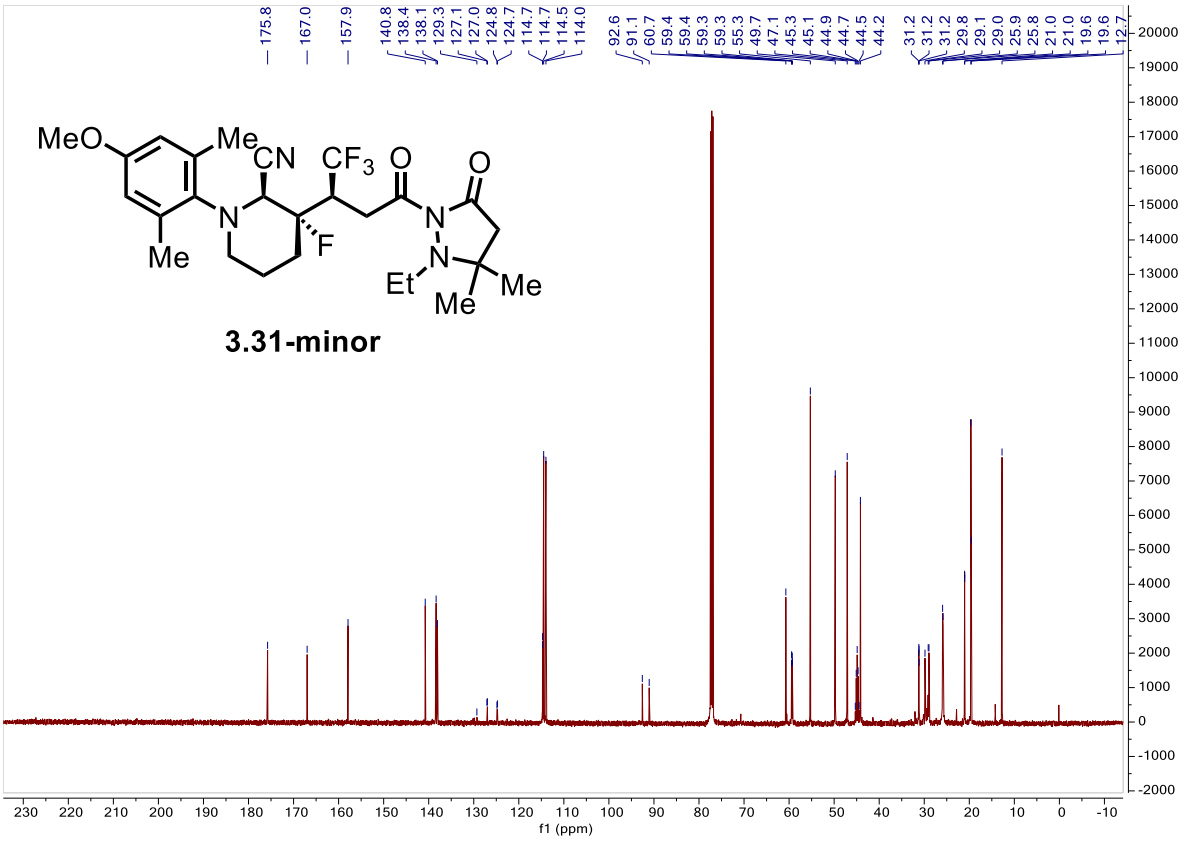
175.8
167.0
157.9
140.8
138.4
138.1
129.3
127.1
127.0
124.8
124.7
114.7
114.7
114.5
114.0
92.6
91.1
60.7
59.4
59.4
59.3
59.3
55.3
49.7
47.1
45.3
45.1
44.9
44.7
44.5
44.2
31.2
31.2
31.2
29.8
29.1
29.0
25.9
25.8
21.0
21.0
19.6
19.6
12.7
MeO
Me
CN
CF3
O
O
N
N
F
N
Me
Et
Me
Me
3.31-minor
f1 (ppm)

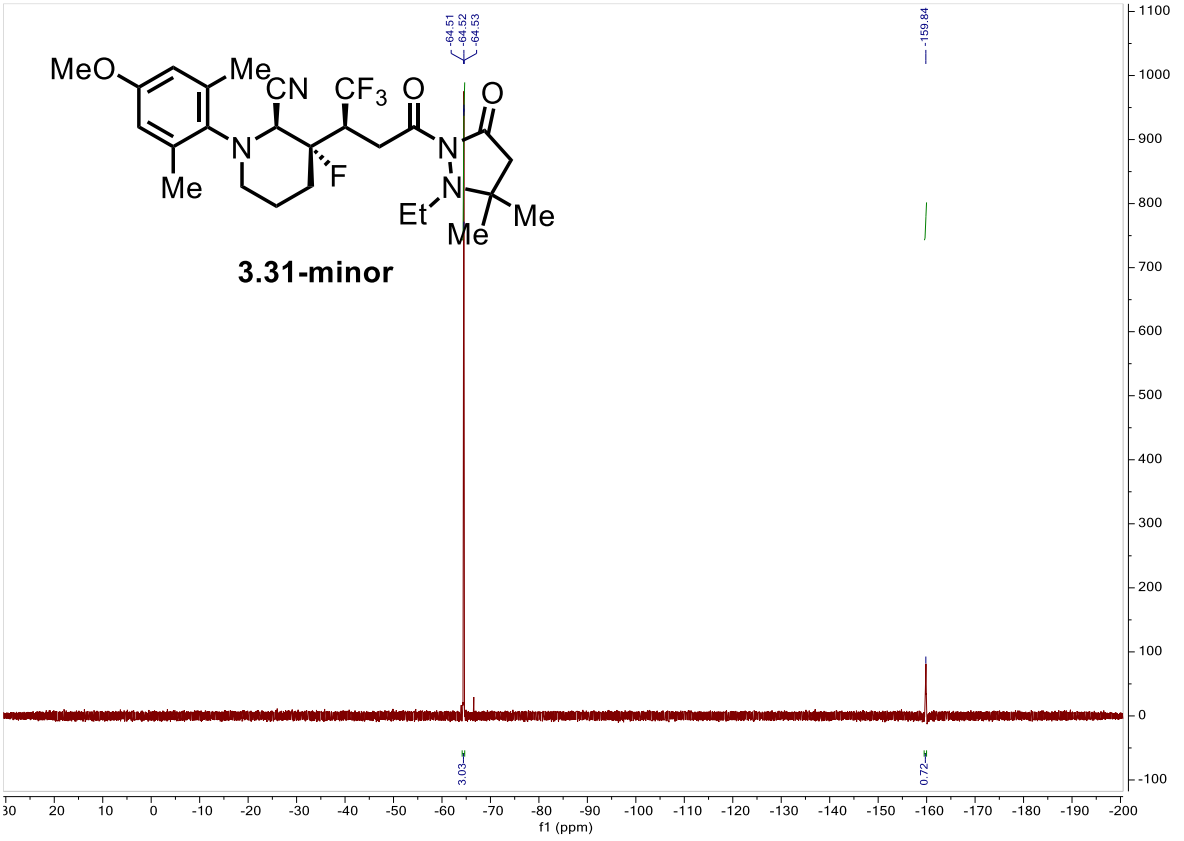
-64.51
-64.52
-64.53
-159.84
MeO
Me
CN
CF3
O
O
N
N
F
N
Me
Et
Me
Me
3.31-minor
3.03
0.72
f1 (ppm)

C11. X-Ray Crystallography Data

X-Ray Crystallography Data of 3.42i-major

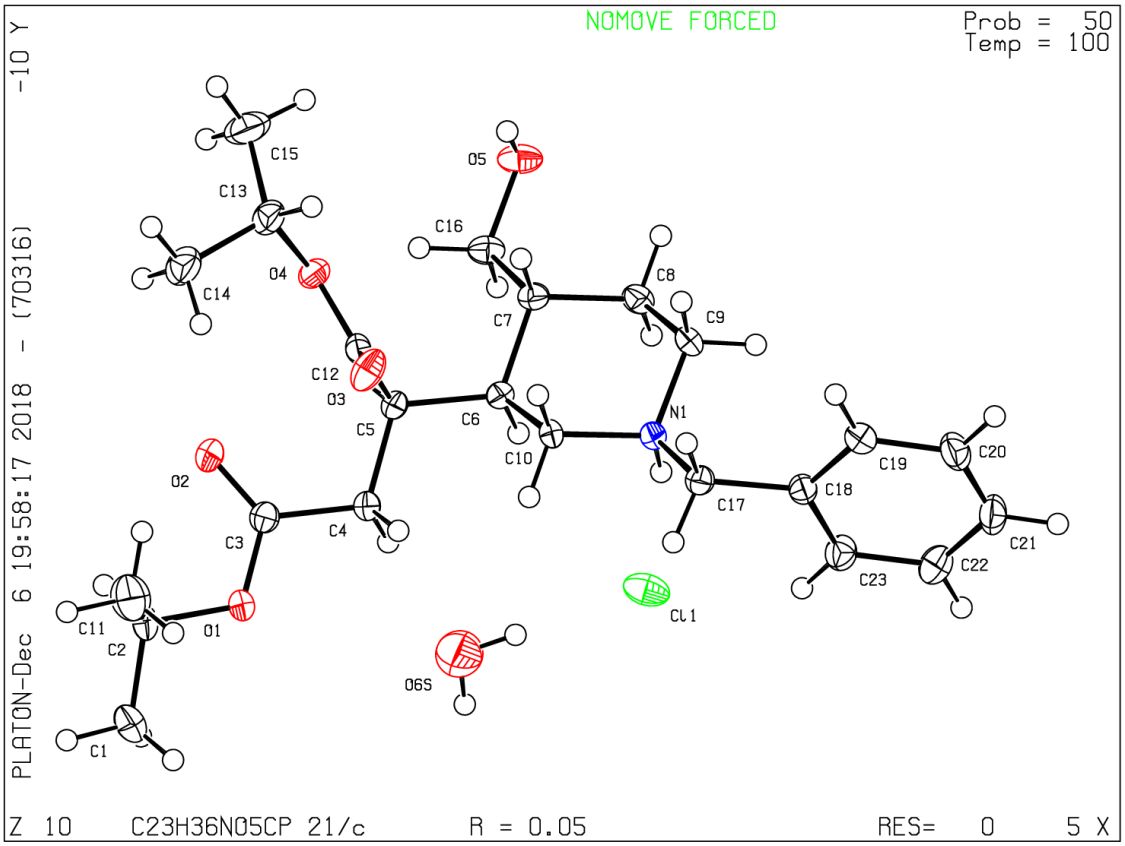

Table S3.7. Crystal data and structure refinement for $C_{23}H_{36}NO_5$+Cl-.

Identification code	C23H36NO5+Cl-
Empirical formula	C23 H37 Cl N O5.50
Formula weight	450.98
Temperature	100(2) K
Wavelength	1.54178 Å
Crystal system	Monoclinic
Space group	$P2_1/c$

Unit cell dimensions	a = 15.0369(10) Å	α= 90°.
	b = 15.1361(9) Å	β= 109.486(2)°.
	c = 11.4130(7) Å	γ = 90°.
Volume	2448.8(3) $Å^3$	
Z	4	
Density (calculated)	1.223 Mg/m^3	
Absorption coefficient	1.662 mm^{-1}	
F(000)	972	
Crystal size	0.570 x 0.250 x 0.220 mm^3	
Theta range for data collection	4.273 to 66.688°.	
Index ranges	-17<=h<=17, -17<=k<=18, -13<=l<=13	
Reflections collected	26897	
Independent reflections	4324 [R(int) = 0.0346]	
Completeness to theta = 66.688°	99.6 %	
Absorption correction	Semi-empirical from equivalents	
Max. and min. transmission	0.7528 and 0.5887	
Refinement method	Full-matrix least-squares on F^2	
Data / restraints / parameters	4324 / 4 / 296	
Goodness-of-fit on F^2	1.145	
Final R indices [I>2sigma(I)]	R1 = 0.0506, wR2 = 0.1303	
R indices (all data)	R1 = 0.0511, wR2 = 0.1306	
Extinction coefficient	n/a	
Largest diff. peak and hole	0.409 and -0.389 $e.Å^{-3}$	

X-Ray Crystallography Data of 3.42i-Minor

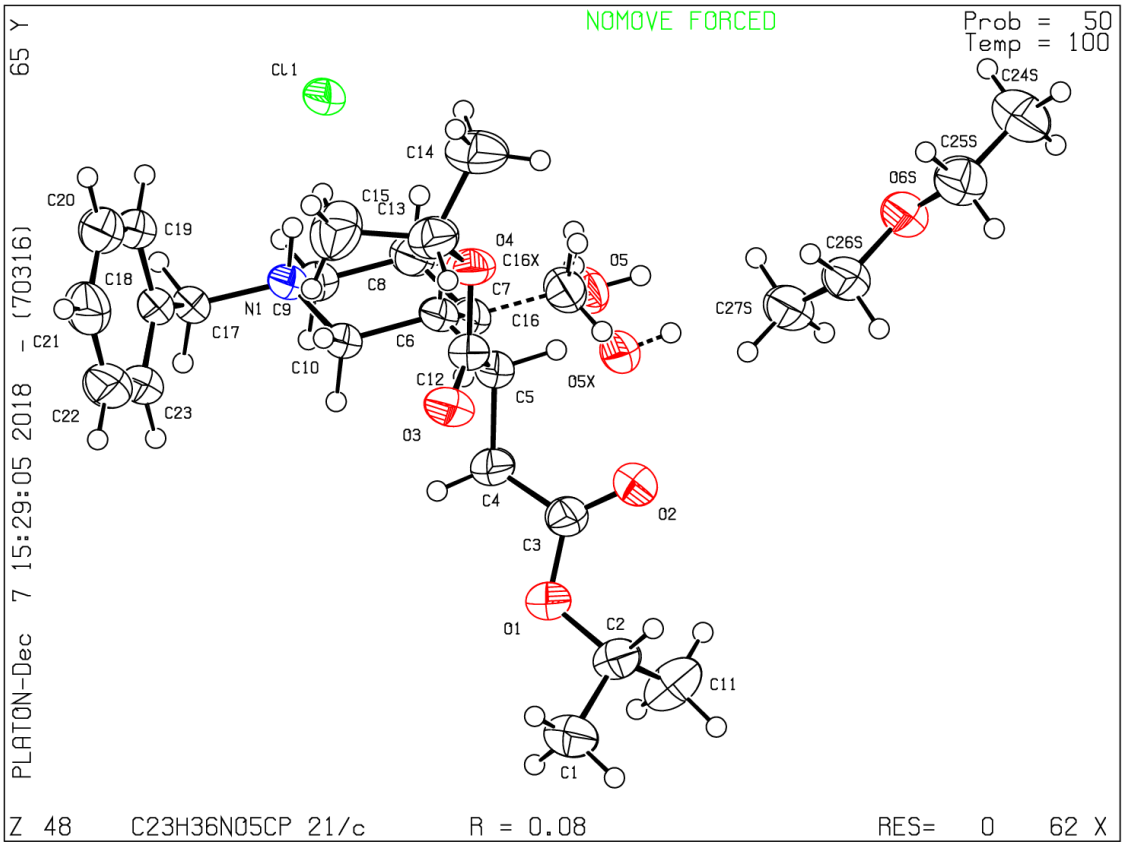

Table S3.8. Crystal data and structure refinement for $C_{23}H_{36}NO_5$+Cl-.

Identification code	(C23H36NO5)+Cl-
Empirical formula	C27 H46 Cl N O6
Formula weight	516.10
Temperature	100(2) K
Wavelength	1.54178 Å
Crystal system	Monoclinic
Space group	$P2_1/c$
Unit cell dimensions	a = 12.7945(13) Å a= 90°.

	b = 16.9523(16) Å b= 90.019(5)°.
	c = 13.6116(13) Å g = 90°.
Volume	2952.3(5) $Å^3$
Z	4
Density (calculated)	1.161 Mg/m^3
Absorption coefficient	1.449 mm^{-1}
F(000)	1120
Crystal size	0.600 x 0.280 x 0.220 mm^3
Theta range for data collection	3.454 to 66.915°.
Index ranges	-15<=h<=15, -20<=k<=0, -16<=l<=16
Reflections collected	9581
Independent reflections	5139 [R(int) = 0.0569]
Completeness to theta = 66.915°	97.8 %
Absorption correction	Semi-empirical from equivalents
Max. and min. transmission	0.7528 and 0.5470
Refinement method	Full-matrix least-squares on F^2
Data / restraints / parameters	5139 / 1 / 335
Goodness-of-fit on F2	1.065
Final R indices [I>2sigma(I)]	R1 = 0.0789, wR2 = 0.2343
R indices (all data)	R1 = 0.0836, wR2 = 0.2389
Extinction coefficient	n/a
Largest diff. peak and hole	1.050 and -0.299 $e.Å^{-3}$

X-Ray Crystallography Data of 3.23bf-Major

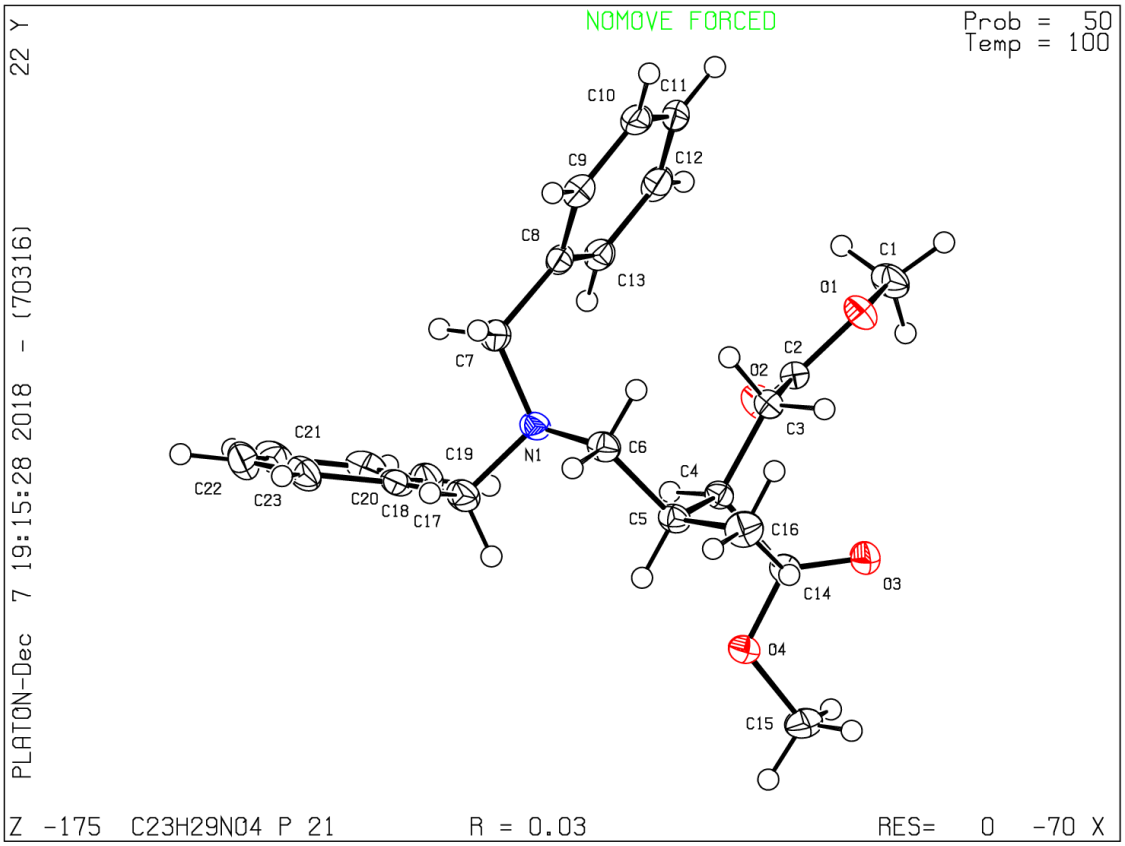

Table S3.9. Crystal data and structure refinement for $C_{23}H_{29}NO_4$.

Identification code	C23H29NO4
Empirical formula	C23 H29 N O4
Formula weight	383.47
Temperature	100(2) K
Wavelength	1.54178 Å
Crystal system	Monoclinic
Space group	$P2_1$
Unit cell dimensions	a = 10.2867(8) Å α= 90°.

	b = 7.8024(7) Å β= 94.248(4)°.
	c = 13.1792(10) Å γ = 90°.
Volume	1054.87(15) $Å^3$
Z	2
Density (calculated)	1.207 Mg/m^3
Absorption coefficient	0.659 mm^{-1}
F(000)	412
Crystal size	0.600 x 0.320 x 0.220 mm^3
Theta range for data collection	3.363 to 66.626°.
Index ranges	-9<=h<=12, -9<=k<=7, -15<=l<=15
Reflections collected	6116
Independent reflections	2950 [R(int) = 0.0250]
Completeness to theta = 66.626°	99.0 %
Absorption correction	Semi-empirical from equivalents
Max. and min. transmission	0.7528 and 0.5979
Refinement method	Full-matrix least-squares on F^2
Data / restraints / parameters	2950 / 1 / 255
Goodness-of-fit on F^2	1.076
Final R indices [I>2sigma(I)]	R1 = 0.0275, wR2 = 0.0732
R indices (all data)	R1 = 0.0276, wR2 = 0.0734
Extinction coefficient	n/a
Largest diff. peak and hole	0.170 and -0.145 $e.Å^{-3}$

X-Ray Crystallography Data of 3.44-Major

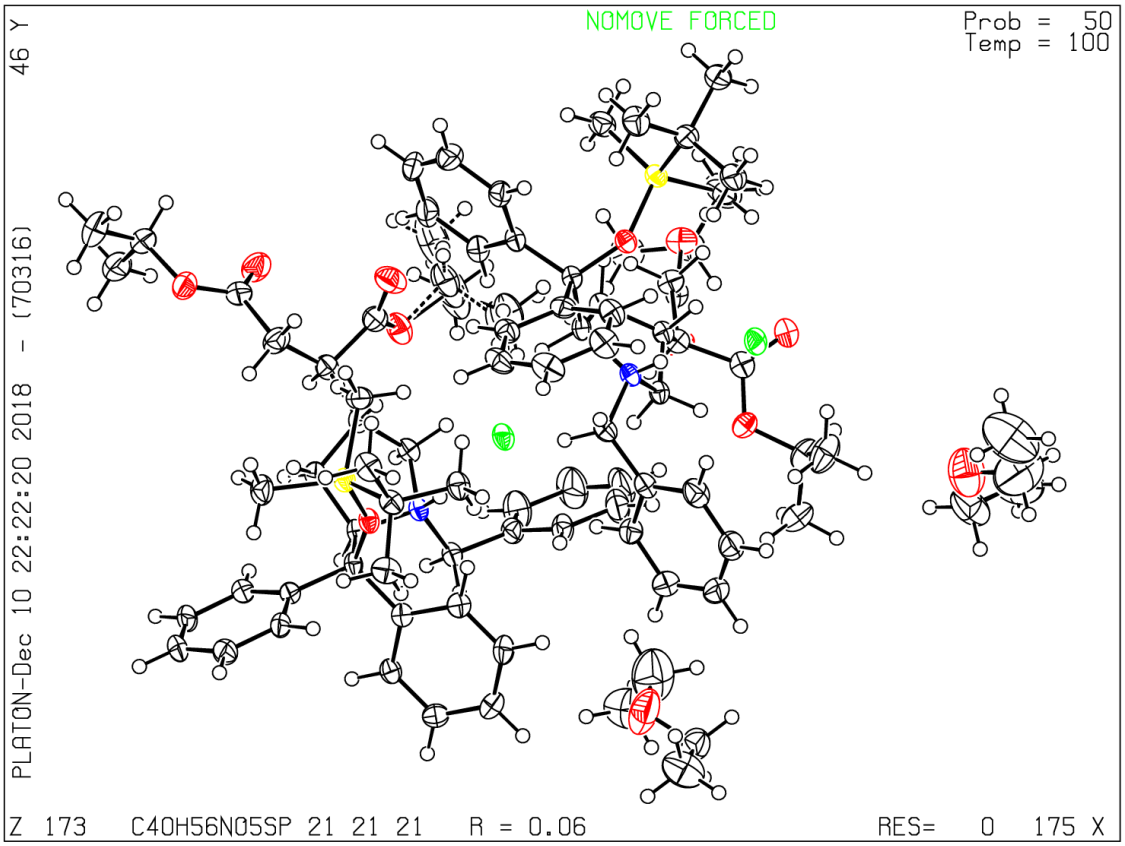

Table S3.10. Crystal data and structure refinement for $(C_{40}H_{56}NO_5Si)+Cl-$

Identification code	(C40H56NO5Si)+Cl-
Empirical formula	C44 H66 Cl N O6 Si
Formula weight	768.51
Temperature	100(2) K
Wavelength	1.54178 Å
Crystal system	Orthorhombic
Space group	$P2_12_12_1$
Unit cell dimensions	a = 13.8219(7) Å α= 90°.

	b = 25.0250(14) Å β= 90°.
	c = 26.0978(14) Å γ = 90°.
Volume	9027.0(8) $Å^3$
Z	8
Density (calculated)	1.131 Mg/m^3
Absorption coefficient	1.348 mm^{-1}
F(000)	3328
Crystal size	0.540 x 0.100 x 0.080 mm^3
Theta range for data collection	2.446 to 66.712°.
Index ranges	-15<=h<=16, -29<=k<=29, -31<=l<=25
Reflections collected	46423
Independent reflections	15586 [R(int) = 0.0733]
Completeness to theta = 66.712°	99.2 %
Absorption correction	Semi-empirical from equivalents
Max. and min. transmission	0.7528 and 0.5629
Refinement method	Full-matrix least-squares on F^2
Data / restraints / parameters	15586 / 793 / 965
Goodness-of-fit on F^2	1.050
Final R indices [I>2sigma(I)]	R1 = 0.0642, wR2 = 0.1605
R indices (all data)	R1 = 0.0698, wR2 = 0.1646
Absolute structure parameter	0.037(7)
Extinction coefficient	n/a
Largest diff. peak and hole	0.742 and -0.534 $e.Å^{-3}$

X-Ray Crystallography Data of 3.45

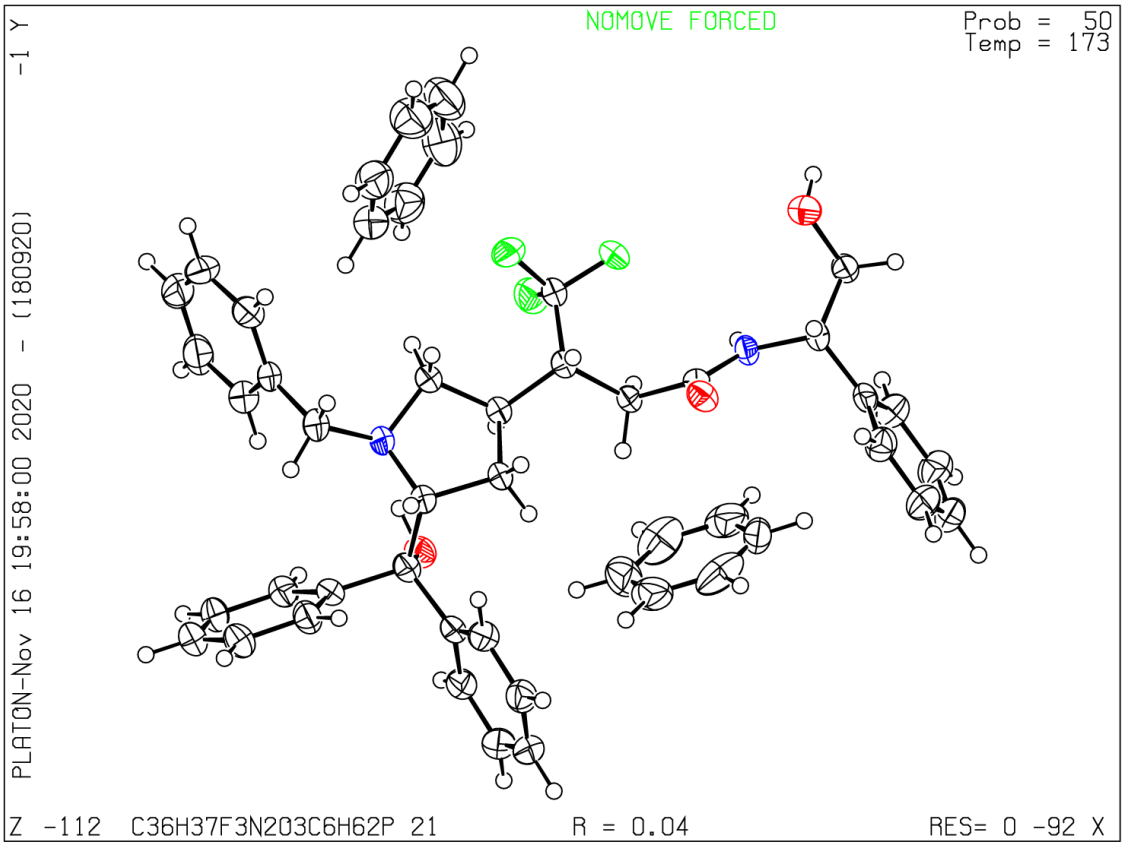

Table S3.11. Crystal data and structure refinement for $C_{36}H_{37}F_3N_2O_3(C_6H_6)_2$.

Identification code	C36H37F3N2O3(C6H6)2
Empirical formula	C48 H49 F3 N2 O3
Formula weight	758.89
Temperature	173(2) K
Wavelength	1.54178 Å
Crystal system	Monoclinic
Space group	$P2_1$
Unit cell dimensions	a = 13.7584(15) Å α= 90°.

	b = 6.1841(7) Å β= 100.009(6)°.
	c = 24.281(3) Å γ = 90°.
Volume	2034.4(4) $Å^3$
Z	2
Density (calculated)	1.239 Mg/m^3
Absorption coefficient	0.698 mm^{-1}
F(000)	804
Crystal size	0.360 x 0.180 x 0.120 mm^3
Theta range for data collection	1.848 to 67.096°.
Index ranges	-16<=h<=16, -7<=k<=7, -28<=l<=28
Reflections collected	52023
Independent reflections	7082 [R(int) = 0.0633]
Completeness to theta = 67.096°	98.1 %
Absorption correction	Semi-empirical from equivalents
Max. and min. transmission	0.7528 and 0.6627
Refinement method	Full-matrix least-squares on F^2
Data / restraints / parameters	7082 / 33 / 514
Goodness-of-fit on F^2	1.061
Final R indices [I>2sigma(I)]	R1 = 0.0399, wR2 = 0.0896
R indices (all data)	R1 = 0.0503, wR2 = 0.0949
Absolute structure parameter	-0.06(8)
Extinction coefficient	n/a
Largest diff. peak and hole	0.143 and -0.173 $e.Å^{-3}$

X-Ray Crystallography Data of 3.29

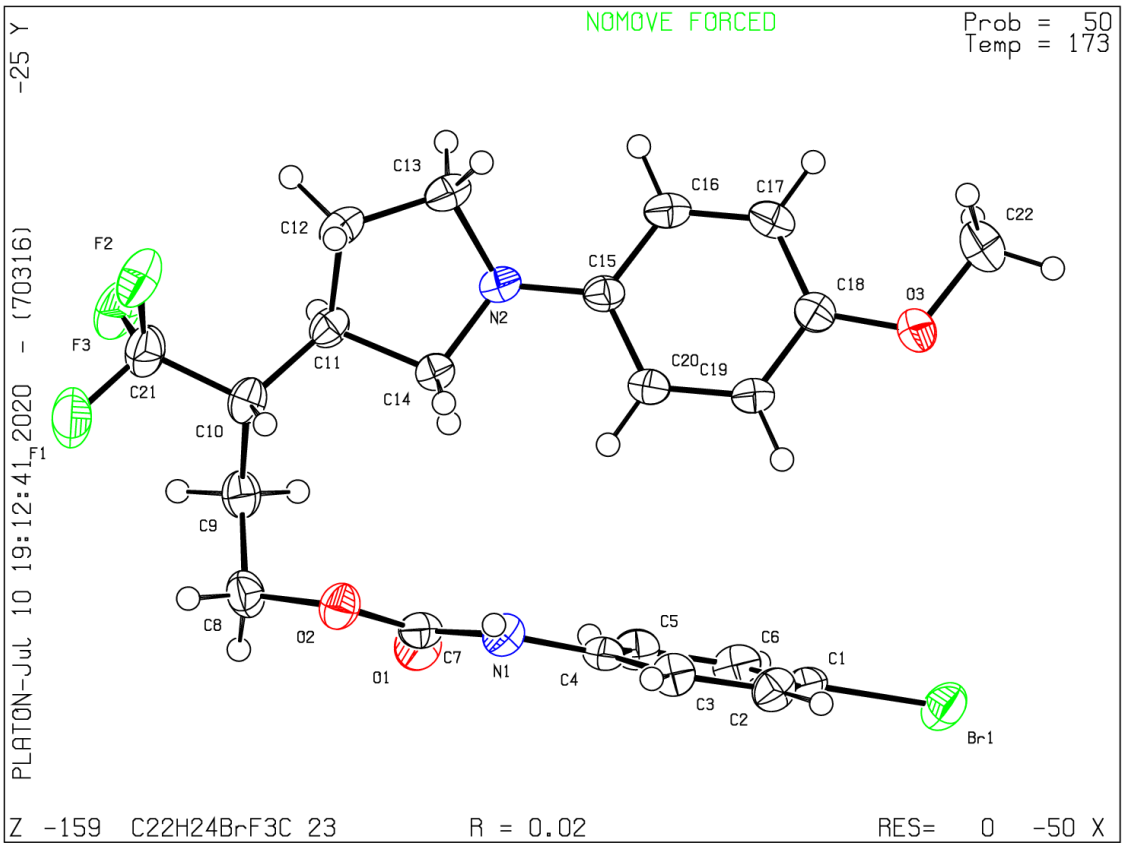

Table S3.12. Crystal data and structure refinement for $C_{22}H_{24}BrF_3N_2O_3$.

Identification code	C22H24BrF3N2O3
Empirical formula	C22 H24 Br F3 N2 O3
Formula weight	501.34
Temperature	173(2) K
Wavelength	1.54178 Å
Crystal system	Monoclinic
Space group	C2
Unit cell dimensions	a = 46.369(4) Å α= 90°.

	b = 5.7157(5) Å β= 91.434(2)°.
	c = 7.9867(7) Å γ = 90°.
Volume	2116.0(3) $Å^3$
Z	4
Density (calculated)	1.574 Mg/m^3
Absorption coefficient	3.128 mm^{-1}
F(000)	1024
Crystal size	0.560 x 0.380 x 0.160 mm^3
Theta range for data collection	3.814 to 66.565°.
Index ranges	-54<=h<=54, -6<=k<=6, -9<=l<=9
Reflections collected	32823
Independent reflections	3675 [R(int) = 0.0304]
Completeness to theta = 66.565°	98.4 %
Absorption correction	Semi-empirical from equivalents
Max. and min. transmission	0.7528 and 0.4622
Refinement method	Full-matrix least-squares on F^2
Data / restraints / parameters	3675 / 1 / 280
Goodness-of-fit on F^2	1.059
Final R indices [I>2sigma(I)]	R1 = 0.0218, wR2 = 0.0587
R indices (all data)	R1 = 0.0218, wR2 = 0.0587
Absolute structure parameter	-0.007(7)
Extinction coefficient	n/a
Largest diff. peak and hole	0.388 and -0.506 $e.Å^{-3}$